

DO NOT MICROFILM
COVER

NUREG/CR-3314
EPRI NP-3268
WCAP-10307

PWR FLECHT SEASET 163-Rod Bundle Flow Blockage

Task Data Report
NRC/EPRI/Westinghouse Report No. 13

Prepared by M. J. Loftus, L. E. Hochreiter, M. F. McGuire,
M. M. Valkovic

Jointly Sponsored by
USNRC, EPRI, and Westinghouse

Prepared for
U.S. Nuclear Regulatory
Commission

MASTER

DISTRIBUTION OF THIS DOCUMENT IS UNLIMITED

NOTICE

This report was prepared as an account of work sponsored by an agency of the United States Government. Neither the United States Government nor any agency thereof, or any of their employees, makes any warranty, expressed or implied, or assumes any legal liability of responsibility for any third party's use, or the results of such use, of any information, apparatus, product or process disclosed in this report, or represents that its use by such third party would not infringe privately owned rights.

Availability of Reference Materials Cited in NRC Publications

Most documents cited in NRC publications will be available from one of the following sources:

1. The NRC Public Document Room, 1717 H Street, N.W.
Washington, DC 20555
2. The NRC/GPO Sales Program, U.S. Nuclear Regulatory Commission,
Washington, DC 20555
3. The National Technical Information Service, Springfield, VA 22161

Although the listing that follows represents the majority of documents cited in NRC publications, it is not intended to be exhaustive.

Referenced documents available for inspection and copying for a fee from the NRC Public Document Room include NRC correspondence and internal NRC memoranda; NRC Office of Inspection and Enforcement bulletins, circulars, information notices, inspection and investigation notices; Licensee Event Reports; vendor reports and correspondence; Commission papers; and applicant and licensee documents and correspondence.

The following documents in the NUREG series are available for purchase from the NRC/GPO Sales Program: formal NRC staff and contractor reports, NRC-sponsored conference proceedings, and NRC booklets and brochures. Also available are Regulatory Guides, NRC regulations in the *Code of Federal Regulations*, and *Nuclear Regulatory Commission Issuances*.

Documents available from the National Technical Information Service include NUREG series reports and technical reports prepared by other federal agencies and reports prepared by the Atomic Energy Commission, forerunner agency to the Nuclear Regulatory Commission.

Documents available from public and special technical libraries include all open literature items, such as books, journal and periodical articles, and transactions. *Federal Register* notices, federal and state legislation, and congressional reports can usually be obtained from these libraries.

Documents such as theses, dissertations, foreign reports and translations, and non-NRC conference proceedings are available for purchase from the organization sponsoring the publication cited.

Single copies of NRC draft reports are available free upon written request to the Division of Technical Information and Document Control, U.S. Nuclear Regulatory Commission, Washington, DC 20555.

Copies of industry codes and standards used in a substantive manner in the NRC regulatory process are maintained at the NRC Library, 7920 Norfolk Avenue, Bethesda, Maryland, and are available there for reference use by the public. Codes and standards are usually copyrighted and may be purchased from the originating organization or, if they are American National Standards, from the American National Standards Institute, 1430 Broadway, New York, NY 10018.

NOTICE

This report was prepared as an account of work sponsored by an agency of the United States Government. Neither the United States Government nor any agency thereof, or any of their employees, makes any warranty, expressed or implied, or assumes any legal liability of responsibility for any third party's use, or the results of such use, of any information, apparatus, product or process disclosed in this report, or represents that its use by such third party would not infringe privately owned rights.

Availability of Reference Materials Cited in NRC Publications

Most documents cited in NRC publications will be available from one of the following sources:

1. The NRC Public Document Room, 1717 H Street, N.W.
Washington, DC 20555
2. The NRC/GPO Sales Program, U.S. Nuclear Regulatory Commission,
Washington, DC 20555
3. The National Technical Information Service, Springfield, VA 22161

Although the listing that follows represents the majority of documents cited in NRC publications, it is not intended to be exhaustive.

Referenced documents available for inspection and copying for a fee from the NRC Public Document Room include NRC correspondence and internal NRC memoranda; NRC Office of Inspection and Enforcement bulletins, circulars, information notices, inspection and investigation notices; Licensee Event Reports; vendor reports and correspondence; Commission papers; and applicant and licensee documents and correspondence.

The following documents in the NUREG series are available for purchase from the NRC/GPO Sales Program: formal NRC staff and contractor reports, NRC-sponsored conference proceedings, and NRC booklets and brochures. Also available are Regulatory Guides, NRC regulations in the *Code of Federal Regulations*, and *Nuclear Regulatory Commission Issuances*.

Documents available from the National Technical Information Service include NUREG series reports and technical reports prepared by other federal agencies and reports prepared by the Atomic Energy Commission, forerunner agency to the Nuclear Regulatory Commission.

Documents available from public and special technical libraries include all open literature items, such as books, journal and periodical articles, and transactions. *Federal Register* notices, federal and state legislation, and congressional reports can usually be obtained from these libraries.

Documents such as theses, dissertations, foreign reports and translations, and non-NRC conference proceedings are available for purchase from the organization sponsoring the publication cited.

Single copies of NRC draft reports are available free upon written request to the Division of Technical Information and Document Control, U.S. Nuclear Regulatory Commission, Washington, DC 20555.

Copies of industry codes and standards used in a substantive manner in the NRC regulatory process are maintained at the NRC Library, 7920 Norfolk Avenue, Bethesda, Maryland, and are available there for reference use by the public. Codes and standards are usually copyrighted and may be purchased from the originating organization or, if they are American National Standards, from the American National Standards Institute, 1430 Broadway, New York, NY 10018.

DISCLAIMER

This report was prepared as an account of work sponsored by an agency of the United States Government. Neither the United States Government nor any agency Thereof, nor any of their employees, makes any warranty, express or implied, or assumes any legal liability or responsibility for the accuracy, completeness, or usefulness of any information, apparatus, product, or process disclosed, or represents that its use would not infringe privately owned rights. Reference herein to any specific commercial product, process, or service by trade name, trademark, manufacturer, or otherwise does not necessarily constitute or imply its endorsement, recommendation, or favoring by the United States Government or any agency thereof. The views and opinions of authors expressed herein do not necessarily state or reflect those of the United States Government or any agency thereof.

DISCLAIMER

Portions of this document may be illegible in electronic image products. Images are produced from the best available original document.

FLECHT SEASET Program
NRC/EPRI/Westinghouse Report No. 13
NUREG/CR-3314
EPRI NP-3268
WCAP-10307

NUREG/CR--3314

DE84 900702

PWR FLECHT SEASET
163-ROD BUNDLE FLOW BLOCKAGE
TASK DATA REPORT

Manuscript Completed: September 1983
Date Published: October 1983

M. J. Loftus M. F. McGuire
L. E. Hochreiter M. M. Valkovic

Prepared for

Division of Accident Evaluation
Office of Nuclear Regulatory Research
U.S. Nuclear Regulatory Commission
Washington, D.C. 20555

Electric Power Research Institute
3412 Hillview Avenue
Palo Alto, California 94304

and

Westinghouse Electric Corporation
Nuclear Energy Systems
P.O. Box 355
Pittsburgh, Pennsylvania 15230

by

Westinghouse Electric Corporation

Under

Contract No. NRC-04-77-127, EPRI Project No. RP959-1

Program Management Group
NRC - R. Lee
EPRI - A. Singh
Westinghouse - H. B. Rosenblatt

FIN B6204

NOTICE

PORTIONS OF THIS REPORT ARE ILLEGIBLE

**It has been reproduced from the best
available copy to permit the broadest
possible availability.**

gth
DISTRIBUTION OF THIS DOCUMENT IS UNLIMITED

NOTICE

This report was prepared as an account of work sponsored by the U.S. Nuclear Regulatory Commission, the Electric Power Research Institute, Inc., and the Westinghouse Electric Corporation. Neither the United States government nor any agency thereof, nor the Institute or members thereof, nor the Westinghouse Electric Corporation, nor any of their employees, makes any warranty, express or implied, or assumes any legal liability or responsibility for any third party's use or the results of such use of any information, apparatus, product, or process disclosed in this report or represents that its use by such third party would not infringe privately owned rights.

ABSTRACT

This report presents data from the 163-Rod Bundle Flow Blockage Task of the Full-Length Emergency Cooling Heat Transfer Systems Effects and Separate Effects Test Program (FLECHT SEASET). The task consisted of forced and gravity reflooding tests utilizing electrical heater rods with a cosine axial power profile to simulate PWR nuclear core fuel rod arrays. These tests were designed to determine effects of flow blockage and flow bypass on reflooding behavior and to aid in the assessment of computational models in predicting the reflooding behavior of flow blockage in rod bundle arrays.

ACKNOWLEDGMENTS

The authors acknowledge the efforts of the following Westinghouse Nuclear Energy Systems contributors:

NTD PROJECTS
H. Rosenblatt
J. Cohen

SAFEGUARDS ENGINEERING
M. Y. Young
N. Lee
F. F. Cadek
E. R. Rosal
D. P. Kitzmiller
K. F. McNamee
D. P. Remlinger
D. W. Sklarsky

TEST ENGINEERING
C. E. Conway
J. T. Martin
B. R. Sinwell

TEST OPERATIONS
P. F. Orangio
A. C. Toth
J. Carovac
J. Kalo
J. Latta
W. Hamilton

NUCLEAR FUEL DIVISION
D. L. Burman
P. Heasely
A. H. Wenzel

PUBLICATION PROGRAMS
J. G. Nagle

The work of the following members of the Program Management Group, their colleagues, and their consultants is hereby acknowledged:

EPRI - K. H. Sun, R. B. Duffey
NRC-NRR - W. Hodges, D. A. Powers, N. Lauben, H. Balukjian
ORNL - R. W. McCulloch, S. D. Snyder
NRC-RSR - M. L. Picklesimer, L. H. Sullivan, R. Lee

GLOSSARY

This glossary explains definitions, acronyms, and symbols included in the text which follows.

Axial peaking factor -- ratio of the peak-to-average power for a given power profile

Blocked -- a situation in which the flow area in the rod bundle or single tube is purposely obstructed at selected locations so as to restrict the flow

Bottom of core recovery (BOCR) -- a condition at the end of the refill period in which the lower plenum is filled with injected ECC water as the water is about to flood the core

Carryout rate fraction -- the fraction of the inlet flooding flow rate which flows out the rod bundle exit by upflowing steam

Carryover -- the process in which the liquid is carried in a two-phase mixture out of a control volume, that is, the test bundle

Core rod geometry (CRG) -- a nominal rod-to-rod pitch of 12.6 mm (0.496 in.) and outside nominal diameter of 9.50 mm (0.374 in.) representative of various nuclear fuel vendors' new fuel assembly geometries (commonly referred to as the 17 x 17 or 16 x 16 assemblies)

Cosine axial power profile -- the axial power distribution of the heater rods in the CRG bundle that contains the maximum (peak) linear power at the midplane of the active heated rod length. This axial power profile will be used on all FLECHT SEASET tests as a fixed parameter.

ECC -- emergency core cooling

Entrainment -- the process by which liquid, typically in droplet form, is carried in a flowing stream of gas or two-phase mixture.

Fallback -- the process whereby the liquid in a two-phase mixture flows countercurrent to the gas phase

FLECHT -- Full-Length Emergency Core Heat Transfer test program

FLECHT SEASET -- Full-Length Emergency Core Heat Transfer Systems Effects and Separate Effects Tests

Loss-of-coolant accident -- a break in the pressure boundary integrity resulting in loss of core cooling water

PMG -- Program Management Group

Separation -- the process whereby the liquid in a two-phase mixture is separated and detached from the gas phase

Silicon-controlled rectifier (SCR) -- a rectifier control system used to supply dc current to the bundle heater rods

Spacer grids -- the metal matrix assembly (egg crate design) used to support and space the heater rods in a bundle array

TABLE OF CONTENTS

Section	Title	Page
1	SUMMARY	1-1
2	INTRODUCTION	2-1
	2-1. Background	2-1
	2-2. Task Objectives	2-4
	2-3. Test Facility	2-5
	2-4. Reference Reflood Test Conditions	2-6
	2-5. Gravity Reflood Test Description	2-8
	2-6. Test Matrix	2-11
3	BLOCKAGE CONFIGURATION	3-1
	3-1. Introduction	3-1
	3-2. Blockage Shapes	3-2
	3-3. Noncoplanar Blockage Distribution	3-3
	3-4. Mean and Variation of Local Temperature	3-7
	3-5. Flow Bypass Region	3-10
	3-6. Bulge Directions for Nonconcentric Sleeves	3-15
4	SYSTEM DESCRIPTION	4-1
	4-1. Introduction	4-1
	4-2. Forced Reflood Tests	4-2
	4-3. Gravity Reflood Tests	4-2
	4-4. Facility Component Description	4-5
	4-5. Heater Rod Bundle	4-5
	4-6. Flow Blockage Sleeves	4-9
	4-7. Test Section	4-11
	4-8. Carryover Vessel	4-14
	4-9. Entrainment Separator	4-14
	4-10. Exhaust Line	4-16
	4-11. Coolant Injection System	4-16
	4-12. Downcomer and Crossover Leg	4-17

TABLE OF CONTENTS (cont)

Section	Title	Page
	4-13. Facility Heating Boiler	4-18
4-14.	Data Acquisition and Processing System	4-18
	4-15. Computer Data Acquisition System	4-18
	4-16. Fluke Data Logger	4-19
	4-17. Multiple-Pen Stripchart Recorders	4-19
4-18.	Instrumentation	4-21
	4-19. Loop Instrumentation	4-22
	4-20. Bundle Instrumentation	4-38
	4-21. Heater Rod Thermocouples	4-38
	4-22. Steam Temperature and Thimble Wall Instrumentation	4-38
	4-23. Differential Pressure Measurements	4-40
	4-24. Power Measurements	4-40
	4-25. Upper Plenum Instrumentation	4-41
	4-26. Lower Plenum Instrumentation	4-42
4-27.	Facility Operation	4-42
4-28.	Key Facility Operating Limitations and Safety Features	4-43
4-29.	Photographic Studies	4-45
 5	 TEST RESULTS	 5-1
5-1	Introduction	5-1
5-2.	Data Reduction	5-1
	5-3. FFLWS Program and Results	5-2
	5-4. QUENCH Program and Results	5-11
	5-5. DATAR Program and Results	5-11
	5-6. COMPARE Program Results	5-16
	5-7. Initial Heater Rod Radial Temperature Distribution	5-16
	5-8. Symmetry of Heater Rod Temperatures	5-24
	5-9. Data Repeatability	5-28

TABLE OF CONTENTS (cont)

Section	Title	Page
	5-10. Summary of Run Conditions and Hot Rod Test Results for Reflood Tests	5-33
	5-11. Gravity Reflood Test Results	5-34
	5-12. Rod Bundle Geometry	5-39
	5-13. Flow Bypass Effects	5-42
6	CONCLUSIONS	6-1
Appendix A	BLOCKAGE SLEEVE SELECTION	A-1
Appendix B	THIMBLE AND GRID EFFECTS ON BURST	B-1
Appendix C	FACILITY DRAWINGS	C-1
Appendix D	INVESTIGATION OF LOW ISOLATION RESISTANCE IN HEATER ROD THERMOCOUPLES	D-1
Appendix E	BUNDLE STEAM PROBE RESPONSE	E-1
Appendix F	BUNDLE INSTRUMENTATION	F-1
Appendix G	HIGH-SPEED DROPLET MOVIE RESULTS	G-1
Appendix H	DATA TABLES AND PLOTS	H-1
Appendix I	INSTRUMENTATION ERROR ANALYSIS	I-1
Appendix J	CALCULATION TECHNIQUES	J-1
Appendix K	BUNDLE GEOMETRY ANALYSIS	K-1



LIST OF ILLUSTRATIONS

Figure	Title	Page
2-1	Decay Power Curve (1971 ANS + 20%) for Reflood	2-7
2-2	Cosine Axial Power Profile	2-9
2-3	Variable Flooding Rate	2-12
3-1	Shape of Nonconcentric Sleeve	3-5
3-2	Westinghouse Mean Temperature Distribution	3-9
3-3	Blockage Sleeve Distribution, Blockage Island Locations, and Bulge Orientations	3-12
3-4	Blockage Island Axial Blockage Distribution	3-13
4-1	Forced and Gravity Reflood Configuration Flow Diagram	4-3
4-2	Heater Rod Bundle Cross Section	4-6
4-3	Grid and Filler Rod in Bundle Assembly	4-10
4-4	Blockage Sleeves Attached to Heater Rod	4-12
4-5	FLECHT SEASET Upper Plenum Baffle	4-15
4-6	FLECHT SEASET Computer Hardware Interface for 163-Rod Blocked Bundle Facility	4-20
4-7	163-Rod Blocked Bundle Task Loop Instrumentation	4-23
4-8	Bundle Instrumentation Locations	4-39
5-1	Mass Balance, Reference Run (Run 61106)	5-9
5-2	Mass Imbalance at End of Injection for All Tests	5-10
5-3	Temperature History of Hottest Rod, Run 61106	5-12
5-4	Quench Front Curve With Associated Thermocouple Quench Times, Run 61106	5-13
5-5	Quench Front Curve With Associated Quench Front Velocity, Run 61106	5-14
5-6	Heat Transfer Coefficient for Rod 10I at 2.03 m (80 in.) for 25.4 mm/sec (1 in./sec) Flooding Rate Test	5-15
5-7	Smoothed and Unsmoothed Heat Transfer Coefficient for Rod 10I at 2.03 m (80 in.)	5-17

LIST OF ILLUSTRATIONS (cont)

Figure	Title	Page
5-8	Heat Transfer Coefficient Error Analysis for 161-Rod Blocked Bundle	5-18
5-9	Initial Heater Rod Radial Temperature Distribution, Run 61106, 1.90 m (75 in.) Elevation	5-20
5-10	Midplane Radial Temperature Distribution, 161-Rod Unblocked Bundle, Run 31504, 1.83 m (72 in.) Elevation	5-21
5-11	Radial Temperature Distribution Immediately Upstream and Downstream of Blockage, Run 61106 (2 sheets)	5-22
5-12	Initial Heater Rod Radial Temperature Distribution, Run 62117, 1.70 and 2.03 m (67 and 80 in.) Elevations (2 sheets)	5-25
5-13	Heater Rod Symmetrical Instrumentation	5-27
5-14	Temperature Measurement Differences at Symmetrical Locations, Runs 61005 and 61607	5-29
5-15	Temperature Measurement Differences at Symmetrical Locations, Runs 61916 and 62605	5-30
5-16	Heater Rod Temperature Comparison for Three Repeat Tests	5-31
5-17	Quench Front Comparison for Three Repeat Tests	5-32
5-18	Downcomer Fluid Levels	5-35
5-19	Hot Rod Temperature Response for Gravity Reflood Tests With Low (Run 62919) and High (Run 62819) Mass Injection	5-36
5-20	Quench Times at 1.98 m (78 in.), Run 62819	5-37
5-21	Comparison of Heater Rod Temperatures, Rod 9E, Runs 63018 (163-Rod Blocked Bundle) and 33436 (161-Rod Unblocked Bundle), 1.98 m (78 in.) Elevation	5-38
5-22	Quench Times at 1.98 m (78 in.), Run 63018	5-40
5-23	Integral of Time-Temperature Curve for Hottest Rod in 163-Rod Blocked Bundle	5-41
5-24	Maximum Temperature Rise Difference Comparison With and Without Flow Bypass	5-44
5-25	Transient Temperature Rise Comparison With and Without Flow Bypass, 1.98 m (78 in.) Elevation	5-47

LIST OF TABLES

Table	Title	Page
2-1	Comparison of PWR Vendors' Fuel Rod Geometries	2-6
2-2	Reference and Range of Test Conditions for 163-Rod Bundle Flow Blockage Task	2-10
2-3	163-Rod Blocked Bundle Test Matrix	2-13
3-1	Mean Temperature Distribution	3-11
4-1	Thermophysical Properties of Heater Rod Materials	4-7
4-2	163-Rod Bundle Flow Area	4-13
4-3	Bundle Instrumentation Locations and Computer Channels	4-25
5-1	Summary of Run Conditions and Hot Rod Test Results	5-3
5-2	Unblocked and Blocked Bundle Tests for Comparison of Flow Bypass Effects	5-43

SECTION 1

SUMMARY

As part of the NRC/EPRI/Westinghouse FLECHT SEASET reflood heat transfer and hydraulic test program,⁽¹⁾ a series of forced flow and gravity feed reflooding tests with flow blockage were conducted on a 163-rod bundle whose dimensions were typical of current PWR fuel rod arrays. The purpose of this program was to test the flow blockage configuration which provided the least favorable heat transfer characteristics in the 21-rod bundle tests,⁽²⁾ in order to evaluate the additional effect of flow bypass. The 21-rod bundle data will be utilized to develop a blockage heat transfer model, and this model will be assessed through comparison and analysis of the 163-rod blocked bundle data.

In this particular test program, a new facility was built to accept a 163-rod bundle⁽³⁾ whose dimensions are typical of the PWR fuel rod sizes currently in use by PWR and PWR fuel vendors. This test facility was very similar to the facility used in the 161-rod unblocked bundle task.⁽⁴⁾ The instrumentation plan was developed such that local thermal-hydraulic parameters could be calculated from the experimental data. Also, sufficient instrumentation was installed in the test facility to perform mass and energy balances from the data.

1. Conway, C. E., et al., "PWR FLECHT Separate Effects and Systems Effects Test (SEASET) Program Plan," NRC/EPRI/Westinghouse-1, December 1977.
2. Loftus, M. J., et al., "PWR FLECHT SEASET 21-Rod Bundle Flow Blockage Task: Data and Analysis Report," NRC/EPRI/Westinghouse-11, June 1982.
3. The 161-rod bundle was changed to a 163-rod bundle by substituting two heater rods for two thimbles in order to provide better comparison with the 21-rod bundle, as discussed in section 3.
4. Loftus, M. J., et al., "PWR FLECHT SEASET Unblocked Bundle, Forced and Gravity Reflood Task Data Report," NRC/EPRI/Westinghouse-7, June 1980.

The forced reflood tests examined the two-phase flow effects of flow blockage and bypass on system pressure, rod power, flooding rate, coolant subcooling, initial clad temperature, and variable flooding rate.

Data obtained in tests which met the specified conditions are reported herein, including clad temperature, turnaround and quench times, heat transfer coefficients, mass flow rates, mass balance, bundle differential pressures and calculated void fractions, steam temperatures, thimble temperatures, and housing temperatures. All the valid data are available from the NRC Data Bank.

SECTION 2

INTRODUCTION

2-1. BACKGROUND

The flow blockage tasks in the FLECHT SEASET program are intended to provide sufficient data and resulting analysis such that the existing Appendix K, 10CFR50.46, flow blockage and steam cooling rule used in PWR safety analyses can be reassessed and replaced by a suitably conservative but more physically realistic safety analysis model.

The Appendix K rule requires that any effect of fuel rod flow blockage must be explicitly accounted for in safety analysis calculations when the core re-flooding rate drops below 25 mm/sec (1 in./sec). The rule also requires that a steam cooling calculation be performed in this case. To comply with this requirement, PWR vendors have developed semiempirical methods of treating fuel rod flow blockage and steam cooling. Experimental data on single- and multi-rod burst test behavior have been correlated into a burst criterion which yields a worst-case planar blockage, given the burst temperature and internal rod pressure of the average power rod in the hot assembly. The test data used to establish this burst criterion indicate that rod burst is random and noncoplanar, and is distributed over some axial length within the hot zone. When calculating the flow redistribution due to flow blockage, PWR vendors used multichannel codes to obtain the blocked channel flow.

Simpler models developed by Gambill⁽¹⁾ have also been used for flow redistribution calculations. In its ECCS evaluation model, Westinghouse modeled noncoplanar blockage as a series of planar blockages distributed axially over the region of interest, with each plane representing a given percentage of blockage. The flow distribution effect was then calculated from a series of

1. Gambill, W. R., "Estimate of Effect of Localized Flow Blockages on PWR Clad Temperatures During the Reflood," CONF-730304-4, 1973.
2. Chelemer, H., et al., "An Improved Thermal-Hydraulic Analysis Method for Rod Bundle Cores," Nucl. Eng. Des. 41, 219-229 (1977).

proprietary THINC-IV⁽²⁾ computer runs and correlated into a simple expression for flow redistribution. The hot assembly was used as the unit cell in these calculations so that the individual subchannel flow redistribution effects generated by the noncoplanar blockage at a given plane are averaged and each subchannel has the same flow reduction. However, it should be remembered that the percentage of blockage simulated in these calculations was derived by examination of noncoplanar multirod burst data.

The resulting flow redistribution is then used to calculate a hot assembly enthalpy rise as part of the steam cooling calculation. The resulting fluid sink temperature and a radial conduction fuel rod model are then used to predict the clad peak temperature. Again, the flow redistribution or blockage effects and the steam cooling calculation are only used when the core flooding rate drops below 25 mm/sec (1 in./sec). Above 25 mm/sec (1 in./sec), the unblocked FLECHT heat transfer data are used.

A review of flow blockage literature^(1,2,3,4) indicates that there are four primary heat transfer effects which need to be examined for both forced and gravity reflooding:

- o Flow redistribution effects due to blockage and their effect on the enthalpy rise of the steam behind the blockage. Bypass of steam flow could result in increased superheating of the remaining steam flow behind the blockage region. The higher the downstream steam temperature, the lower the rod heat flux and resulting heat transfer behind the blockage.

1. Gambill, W. R., "Estimate of Effect of Localized Flow Blockages on PWR Clad Temperatures During the Reflood," CONF-730304-4, 1973.
2. Davis, P. R., "Experimental Studies of the Effect of Flow Restrictions in a Small Rod Bundle Under Emergency Core Coolant Injection Conditions," Nucl. Technol. 11, 551-556 (1971).
3. Rowe, D. S., et al., "Experimental Study of Flow and Pressure in Rod Bundle Subchannels Containing Blockages," BNWL-1771, September 1973.
4. Hall, P. C., and Duffey, R. B., "A Method of Calculating the Effect of Clad Ballooning on Loss-of-Coolant Accident Temperature Transients," Nucl. Sci. Eng. 58, 1-20 (1975).

- o Effect of blockage downstream of the blockage zone and the resulting mixing of the steam and droplet breakup behind the blockage. The breakup of the entrained water droplets will increase the liquid surface area so that the drops will become a more effective heat sink for the steam. The breakup should desuperheat the steam; this would result in greater rod heat transfer behind the blockage zone in the wake of the blockage.
- o The heat transfer effects in the immediate blockage zone due to droplet impact, breakup, mixing, and cooling due to increased slip, as well as the increased steam velocity due to blockage flow area changes. The droplet breakup is a localized effect primarily caused by the blockage geometry; it will influence the amount of steam generation which can occur farther downstream of the blockage.
- o Effect of blockage on the upstream region of the blockage zone due to steam bypass, droplet velocities, and sizes

In summary, the flow blockage heat transfer effects are a combination of two key thermal-hydraulic phenomena:

- o A flow bypass effect, which reduces the mass flow in the blocked region and consequently tends to decrease the heat transfer
- o A flow blockage effect, which can cause flow acceleration, droplet breakup, improved mixing, steam desuperheating, and establishment of new boundary layers, and consequently tends to increase the heat transfer

These two effects are dependent on blockage geometry and distribution and counteract each other such that it is not evident which effect dominates over a range of flow conditions.

The FLECHT SEASET flow blockage test program has been coordinated with the programs conducted in Germany's FEBA tests⁽¹⁾ and Japan's SCTF tests.⁽²⁾ The FEBA tests have been conducted on a 1 x 5 rod bundle and a 5 x 5 rod bundle with 62 percent and 90 percent blockages, with and without flow

1. Ihle, P., et al., "FEBA - Flooding Experiments with Blocked Arrays - Heat Transfer in Partly Blocked 25-Rod Bundle," presented at 19th National Heat Transfer Conference, Orlando, FL, July 27, 1980.
2. Adachi, H., "SCTF - Core-1 Test Results," presented at Ninth Water Reactor Safety Research Information Meeting, Gaithersburg, MD, October 26-30, 1981.

bypass. The Japanese Slab Core Tests were conducted on eight full-size simulated fuel rod bundles arranged in a row with two adjacent bundles blocked 62 percent in a coplanar fashion. The combination of all three programs provides a comprehensive data base with which to evaluate flow blockage heat transfer effects.

The FLECHT SEASET flow blockage program is specifically oriented to provide data and analysis such that the steam cooling/flow blockage section of the Appendix K rule can be reassessed and replaced by a conservative but physically based method. Other experiments, such as the Karlsruhe FEBA Tests and the Japanese Slab Core Tests, along with other smaller experiments will form, with the FLECHT SEASET tests, a comprehensive flow blockage data base. The benefits of revising the current flow blockage/steam cooling section of the Appendix K rule to the industry and NRC are as follows:

- o The heat transfer models for flooding rates less than 25 mm/sec (1 in./sec) would be more physically based, compared to the current artificially conservative models.
- o It is expected that the resulting data and analysis will show that the heat transfer of blocked rod arrays is not degraded below that of unblocked arrays for flooding rates typical of reactor safety analyses.

It is expected that the current section of the Appendix K rule will be clearly shown to be conservative and thus should be modified. The resulting modifications should give most PWR reactors additional LOCA margin, which will increase the utilities' flexibility in utilization of their particular plants.

2-2. TASK OBJECTIVES

The primary objectives of the 163-rod bundle tests were twofold:

- o To obtain, evaluate, and analyze thermal hydraulic data using a 163-rod bundle to determine the effects of flow blockage and flow bypass on the reflood heat transfer
- o To assess an analytical or empirical method for use in analyzing the blocked bundle heat transfer data

The 163-rod blocked bundle task examined the reflooding phenomenon in a large bundle with ample flow bypass. The effects of blockage on heat transfer can be attributed to two counteracting phenomena: flow depletion in the blockage zone due to flow bypass and increased turbulence in the blocked area due to the flow disturbance. Bypass flow is expected to reduce heat transfer in the blocked region because of the coolant depletion; however, the increased turbulence and possible droplet disintegration may enhance heat transfer in the blocked zone. Therefore, it is necessary to determine the dominant effect under various thermal-hydraulic conditions for a clear understanding of the blockage effect on heat transfer. This test series will study these effects to determine the relative importance of flow bypass and local disturbance. This large-bundle test was specifically designed to maximize the usefulness of the small-bundle (21-rod) test results.

2-3. TEST FACILITY

The tests performed in the 163-rod bundle task are classified as separate effects tests. In this case, the bundle is isolated from the system and the thermal-hydraulic conditions are prescribed at the bundle entrance and exit. Within the bundle, the dimensions are full scale (compared to a PWR), with the exception of overall radial dimension. The low-mass housing used in this test series was designed to minimize the wall effects such that the rods more than two rows away from the housing were unaffected by the housing. To preserve proper thermal scaling of the FLECHT facility with respect to a PWR, the power-to-flow area ratio was made to be nearly the same as that of a PWR fuel assembly.

The tests in the 163-rod bundle flow blockage task utilized a core rod geometry, CRG,⁽¹⁾ that is typified by the Westinghouse 17 x 17 fuel rod design, as shown in table 2-1. This CRG is representative of all current vendors' PWR fuel assembly geometries.

1. The CRG is defined in this program as a nominal rod-to-rod pitch of 12.6 mm (0.496 in.) and outside nominal diameter of 9.50 mm (0.374 in.), representative of various nuclear fuel vendors' new fuel assembly geometries and commonly referred to as the 17 x 17 or 16 x 16 assemblies.

TABLE 2-1
COMPARISON OF PWR VENDORS' FUEL
ROD GEOMETRIES

Vendor	Rod Diameter [mm (in.)]	Rod Pitch [mm (in.)]
Westinghouse	9.50 (0.374)	12.6 (0.496)
Babcock & Wilcox	9.63 (0.379)	12.8 (0.502)
Combustion Engineering	9.70 (0.382)	12.9 (0.506)
Exxon	9.45 (0.372)	12.6 (0.496)

2-4. REFERENCE REFLOOD TEST CONDITIONS

Most of the tests in the 163-rod bundle test matrix were constant forced flooding reflood tests. The test conditions represent typical safety evaluation model assumptions and initial conditions.

The reflood phase of the PWR design basis LOCA transient is calculated to start approximately 30 seconds after initiation of a hypothetical break. At this time, the lower plenum (which had emptied during the blowdown) has refilled to the bottom of the core. The applicable reference assumptions for the reflood transient for a worst-case analysis of a hypothetical LOCA typical of a Westinghouse 17 x 17 four-loop PWR or other PWR vendor plant are as follows:

- o The core hot assembly was simulated in terms of peak linear power and initial temperature at the time of core recovery.
- o Decay power was ANS + 20 percent, as specified by Appendix K of 10CFR50.46 and shown in figure 2-1.
- o The initial rod clad temperature is primarily dependent on the full-power linear heating rate at the time of the accident and the subsequent cooling during the blowdown phase. Typical calculations yield an initial clad temperature in the hot assembly of 871°C (1600°F) at core recovery.

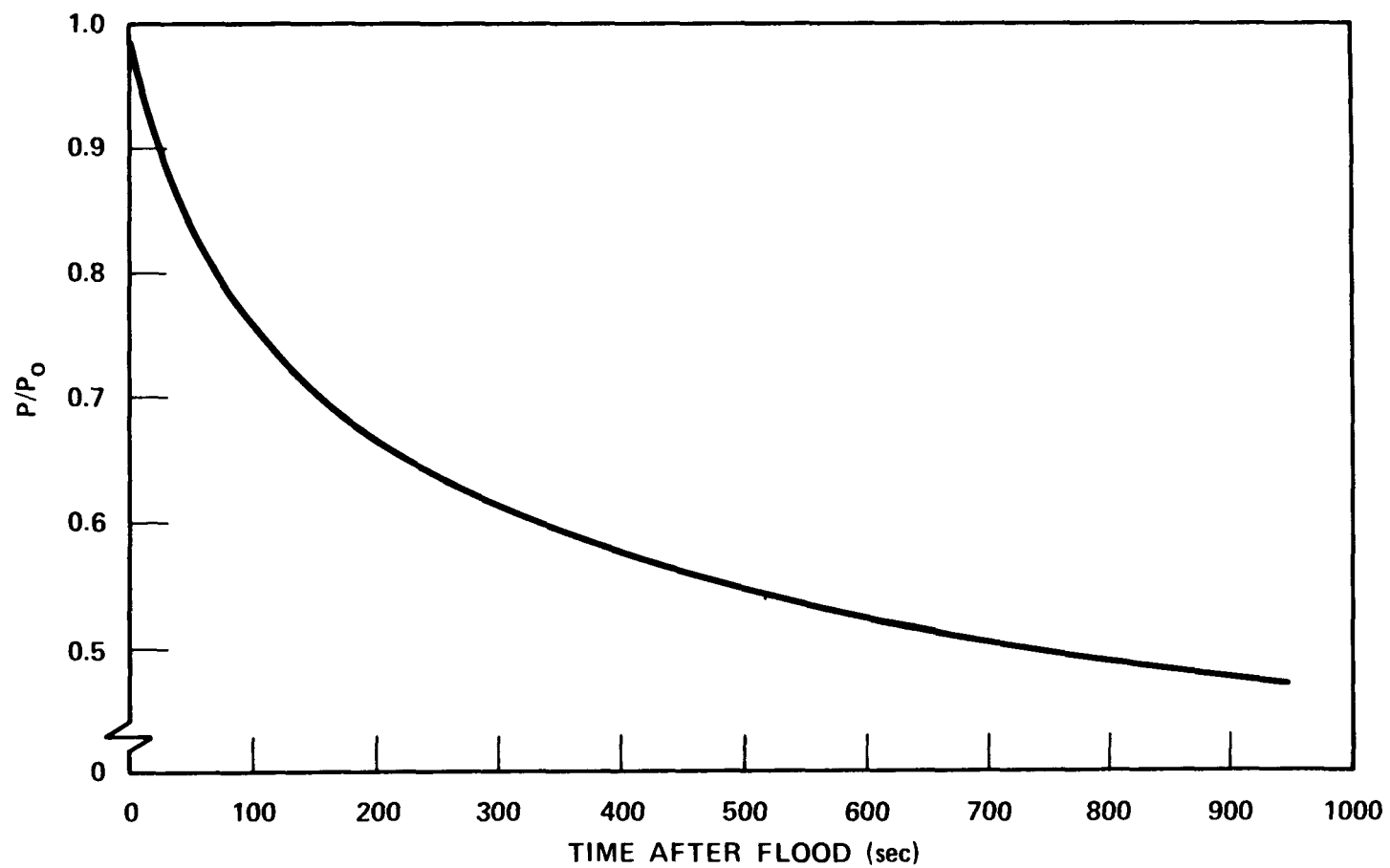


Figure 2-1. Decay Power Curve (1971 ANS + 20%) for Reflood

- o Coolant temperature was selected to maintain a constant sub-cooling to facilitate the determination of parametric effects.
- o Coolant was injected directly into the test section lower plenum for the forced flooding rate tests, and into the bottom of the downcomer for the gravity reflood tests. Injection into the bottom of the downcomer was used for better test facility pressure control.
- o Upper plenum pressure at the end of blowdown is approximately 0.14 MPa (20 psia) constant for an ice condenser plant, and about 0.28 MPa (40 psia) for a dry containment plant.
- o The tests were performed with a uniform radial power profile, except for one test with hot and cold simulated channels.
- o The axial power shape built into the heater rod was the modified cosine with a power peak-to-average ratio of 1.66, as shown in figure 2-2.

The use of the 1.66 axial profile will allow comparisons with the 161-rod unblocked and the 21-rod bundle test data, since the bundle sizes constitute the primary difference among these tests.

The initially proposed reference test conditions and range of test conditions are listed in table 2-2, based on the above reference assumptions.

2-5. GRAVITY REFLOOD TEST DESCRIPTION

The gravity reflood tests were conducted to provide a simulation of the conditions expected to occur in reflooding the core after a LOCA. Coolant was injected into the simulated downcomer at scaled flow rates which are representative of the nuclear power plant accumulators.⁽¹⁾ The downcomer was attached to the test facility lower plenum by the crossover leg, which was designed to provide a pressure loss coefficient equivalent to that of a reactor lower plenum and core inlet, or a value of approximately 11. The system pressure was controlled downstream of the test facility in the simulated containment and the reactor coolant system flow resistance (approximately 32.5) was simulated by a orifice plate upstream of the simulated containment.

1. Waring, J. P., et al., "PWR FLECHT-SET Phase B1 Data Report," WCAP-8431, December 1974.

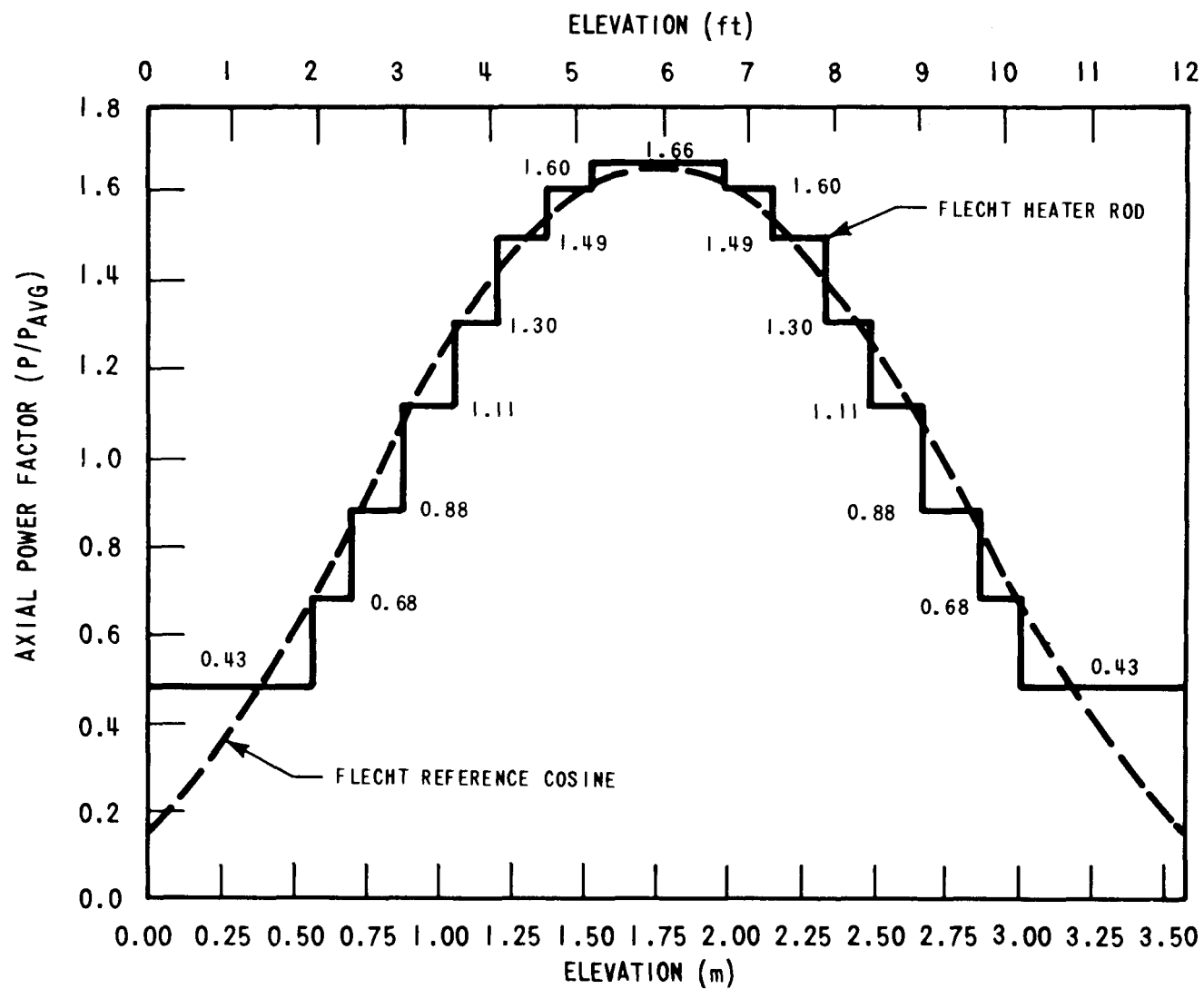


Figure 2-2. Cosine Axial Power Profile

TABLE 2-2
REFERENCE AND RANGE OF TEST CONDITIONS FOR
163-ROD BUNDLE FLOW BLOCKAGE TASK

Parameter	Initial Condition	Range of Conditions
Initial clad temperature (1600°F)	871°C (500°F - 1600°F)	260°C - 871°C
Peak power (0.7 kw/ft)	2.3 kw/m (0.4 - 1.0 kw/ft)	1.31 - 3.3 kw/m
Upper plenum pressure (40 psia)	0.28 MPa (20 - 60 psia)	0.14 - 0.42 MPa
Flooding rate:		
o Constant	25 mm/sec (1 in./sec)	15 - 152 mm/sec (0.6 - 6 in./sec)
o Variable in steps	--	152 to 20 mm/sec (6.0 to 0.8 in./sec)
o Continuously variable	--	36 to 17 mm/sec (1.4 to 0.65 in./sec)
Injection rate (gravity reflood) - variable in steps	--	5.80 to 0.785 kg/sec (12.8 to 1.73 lb/sec)
Coolant ΔT subcooling (140°F)	78°C (15°F - 140°F)	8°C - 78°C

2-8. TEST MATRIX

The original test matrix as developed in the task plan⁽¹⁾ consisted of 20 tests grouped into seven parametric series. However, prior to the test program, several modifications and/or additions were made to the test matrix, as discussed in the following paragraphs. This revised test matrix was sent to the PWR fuel manufacturers (Exxon, Combustion Engineering, and Babcock & Wilcox) for their review. This test matrix was designed to investigate the effects of initial clad temperature, flooding rate, pressure, power, subcooling, variable flow, hot/cold channels, and gravity reflood.

The two low-flooding-rate tests [10.1 mm/sec (0.4 in./sec)] originally planned to be conducted at pressures of 0.14 and 0.28 MPa (20 and 40 psia) were not run because these two tests were expected to be conducted at a high temperature [above 1093°C (2000°F)], which could cause heater rod distortion, and because there were no valid replicate tests from the unblocked bundle to provide data comparisons (valid in the sense that there was not any significant rod bundle distortion in the unblocked bundle). These two low-flow tests were replaced with tests which were expected to be conducted at a low temperature [below 982°C (1800°F)] and for which comparable tests had been run in the unblocked bundle. Two of the three hot/cold channel tests were replaced with a high-power [3.2 kW/m (1 kW/ft)] test which had a comparable unblocked bundle test and a variable forced flow test. This variable forced flow test was conducted according to the specifications provided by Exxon Nuclear Company, as shown in figure 2-3.

To provide a good data comparison between the blocked bundle and the unblocked bundle, the boundary and initial conditions from the unblocked bundle were repeated in the blocked bundle, as much as experimentally possible. The test matrix for the 163-rod bundle is shown in table 2-3, along with the corresponding 161-rod unblocked bundle test numbers. The actual test conditions achieved in the 163-rod bundle are tabulated in section 5, table 5-1.

1. Hochreiter, L. E., et al., "PWR FLECHT SEASET 161-Rod Bundle Flow Blockage Task: Task Plan Report," NRC/EPRI/Westinghouse-6, September 1980.

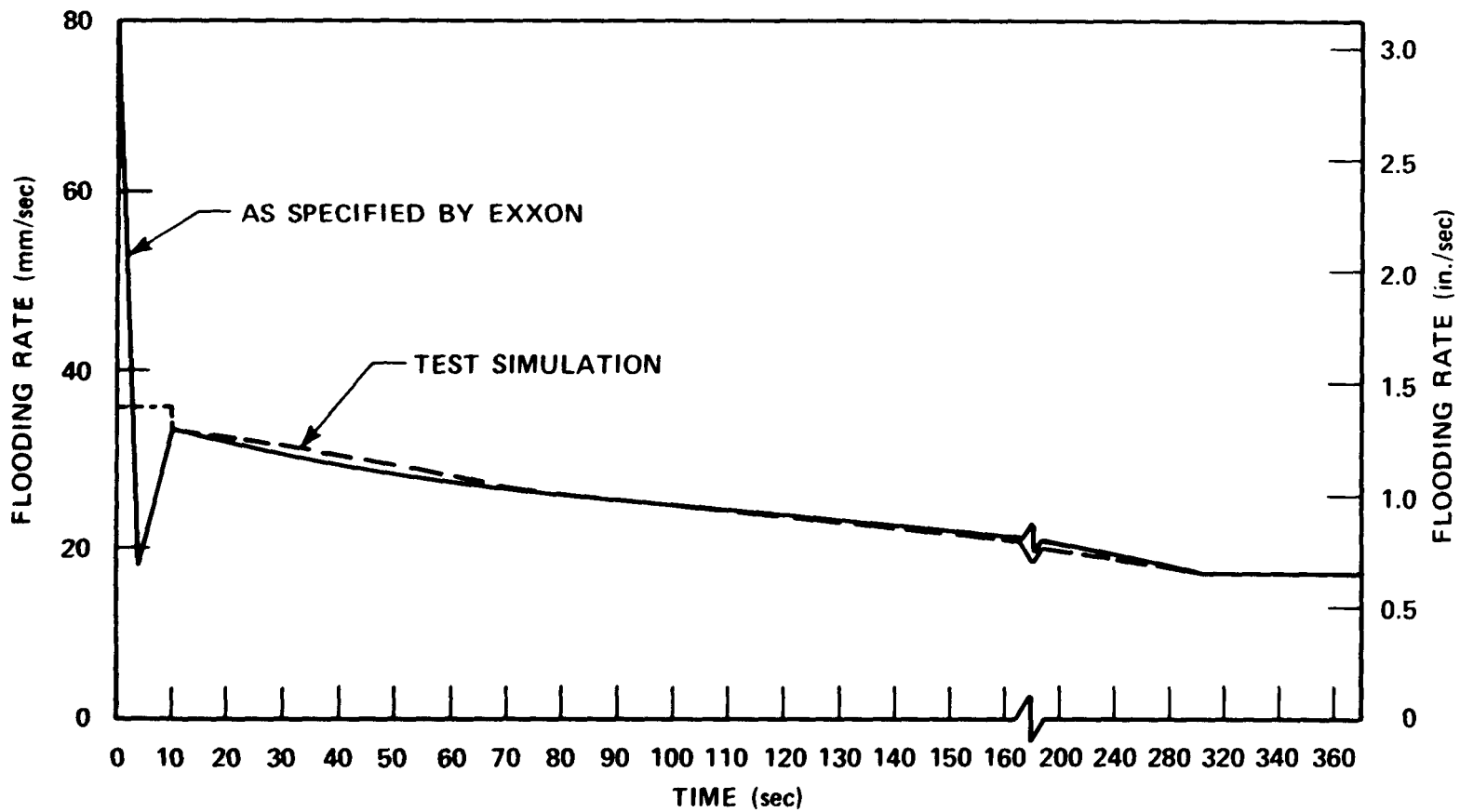


Figure 2-3. Variable Flooding Rate

TABLE 2-3
163-ROD BLOCKED BUNDLE TEST MATRIX

Test No.	Pressure [MPa (psia)]	Clad Initial Temperature [°C (°F)]	Rod Peak Power [kw/m (kw/ft)]	Flooding Rate [mm/sec (in./sec)]	High-Speed Movies	Inlet Fluid Temperature [°C (°F)]	161-Rod Bundle Replicate Test	Parameter
01	0.28 (40.1)	263 (505)	2.3 (0.70)	38.6 (1.52)	Yes	52.2 (126)	30518	Initial clad temperature effect
02	0.27 (39.3)	538 (1000)	2.3 (0.70)	38.6 (1.52)	No	53.3 (128)	30817	Flooding rate effect
03	0.28 (40)	871 (1600)	2.3 (0.70)	33.0-16.5 (1.30-0.65) in 300 sec	No	52.8 (127)		
04	0.28 (40)	885 (1625)	2.3 (0.70)	157.5 (6.2)	Yes	52.8 (127)	31701	
05	0.27 (39.5)	871 (1600)	2.3 (0.70)	38.6 (1.52)	Yes	52.8 (127)	31203	
06	0.28 (40.2)	885 (1625)	2.3 (0.70)	24.9 (0.98)	Yes	52.8 (127)	31504	
07	0.28 (40)	877 (1610)	2.3 (0.70)	20 (0.81)	Yes	52.8 (127)	31805	
08	0.27 (39)	874 (1605)	1.3 (0.4)	15 (0.60)	No	52.8 (127)	34006	

TABLE 2-3 (cont)
163-ROD BLOCKED BUNDLE TEST MATRIX

Matrix No.	Pressure [MPa (psia)]	Clad Initial Temperature [°C (°F)]	Rod Peak Power [kw/m (kw/ft)]	Flooding Rate [mm/sec (in./sec)]	High-Speed Movies	Inlet Fluid Temperature [°C (°F)]	161-Rod Bundle Replicate Test	Parameter
09	0.14 (20)	877 (1610)	2.4 (0.72)	26.9 (1.06)	Yes	34 (93)	34209	Pressure effect
10	0.134 (19.5)	871 (1600)	1.38 (0.422)	17 (0.65)	No	33 (92)	34711	
11	0.137 (19.9)	271 (1600)	1.3 (0.40)	28 (1.1) for 30sec	No	34 (93)	31922	
12	0.411 (59.6)	874 (1605)	2.3 (0.70)	26.9 (1.06) onward 25 (0.98) for 120 sec 26 (1.04) onward	Yes	66.7 (152)	32013	
13	0.28 (40)	871 (1600)	3.28 (1.00)	38 (1.5)	Yes	54.4 (130)	34524	Peak power effect
14	0.273 (39.6)	877 (1610)	1.3 (0.40)	38.6 (1.52)	No	52.2 (126)	31021	
15	0.277 (40.2)	877 (1610)	2.3 (0.70)	25 (0.98) for 60 sec 27.4 (1.08) for 140 sec 30.0 (1.18) onward	Yes	122.2 (252)	32114	Subcooling effect

TABLE 2-3 (cont)
163-ROD BLOCKED BUNDLE TEST MATRIX

Matrix No.	Pressure [MPa (psia)]	Clad Initial Temperature [°C (°F)]	Rod Peak Power [kw/m (kw/ft)]	Flooding Rate [mm/sec (in./sec)]	High-Speed Movies	Inlet Fluid Temperature [°C (°F)]	161-Rod Bundle Replicate Test	Parameter
16	0.277 (40.2)	877 (1610)	2.3 (0.70)	160 (6.3) for 5 sec 20 (0.8) onward	Yes	52.8 (127)	32333	Stepped flow effect
17	0.28 (40)	871/260 (1600/500)	2.3/1.3 (0.7/0.4)	20 (0.8)	Yes	52.8 (127)	--	Hot/cold channel effect
				Injection Rate [kg/sec (lb/sec)]				
18	0.28 (40)	871 (1600)	2.3 (0.7)	5.80 (12.8) for 15 sec 0.785 (1.73) onward	No	51.7 (125)	33436	Gravity reflood
19	0.14 (20)	871 (1600)	2.3 (0.7)	5.80 (12.8) for 15 sec 0.785 (1.73) onward	No	31 (88)	--	

SECTION 3

BLOCKAGE CONFIGURATION

3-1. INTRODUCTION

The high internal pressure and temperature of fuel rods during a postulated PWR LOCA are expected to cause the fuel rods to swell and burst. The resulting rod deformation, referred to as a blockage shape, would reduce the fluid flow area in the rod array. The flow area reduction is governed by the shapes and spatial distribution of blockage. Therefore, blockage shapes and their spatial distribution were chosen to simulate the thermal-hydraulic conditions of the fluid flow in the blocked rod array. The spatial blockage distribution was chosen to represent realistic situations and to provide fundamental understanding of blockage effects on the local heat transfer. The simulated rod swelling represents the blockage just prior to burst, such that no tearing of the cladding, or burst "lips," are simulated. The initial testing plans for the 21-rod bundle had included a configuration with burst lips, but the burst lips were expected to act as fins to enhance heat transfer and did not make a significant contribution to the flow restriction because of the small cross-sectional area.

The results of several single- and multirod burst tests, as well as discussions with NRC and EPRI, were used to define the blockage shapes simulated in the 21-rod bundle blockage task, as described in paragraph 3-2. The sleeve shape used in the 163-rod bundle task was chosen from the blockage configurations used in the 21-rod bundle blockage test.⁽¹⁾ The method of distributing the blockage sleeves is discussed in paragraphs 3-3 and 3-4. A geometric similarity between the 21-rod and 163-rod bundles was designed into the 163-rod bundle, as discussed in paragraph 3-5. This similarity was expected to provide a better basis for data analysis and understanding of bypass effects.

1. Loftus, M. J., et al., "PWR FLECHT SEASET 21-Rod Bundle Flow Blockage Task: Data and Analysis Report," NRC/EPRI/Westinghouse-11, September 1982.

3-2. BLOCKAGE SHAPES

Several out-of-pile and in-pile burst tests were conducted to aid in the understanding of rod burst phenomena during a LOCA. Out-of-pile tests employed several heating methods to simulate rod heatup during a reflooding period. The heating methods included a stiff internal heater rod (continuous rigid heating element) method, external radiant heating, and direct resistance heating. The external radiant heating and direct resistance heating are believed to distort the thermal response of the clad during its deformation. The internal heater rod may reduce the clad temperature nonuniformity; this reduction is expected in the real situation of stacked fuel pellets. Although an out-of-pile test method is not ideal, it is generally agreed that an internal heater method is most representative of the real situation. Therefore, the results from the tests using internal heater rod methods were reviewed in the 21-rod bundle flow blockage task to provide a basis for defining blockage shapes. The limited amount of in-pile test results were also reviewed.⁽¹⁾

The available results from several rod burst tests showed that there were two distinctive rod swelling patterns, depending on the burst temperature. This is due to the existence of two phases of Zircaloy, whose material properties are quite different from each other. Zircaloy is in the alpha phase at temperatures of less than 830°C (1529°F) and in a mixed phase of alpha and beta types between 830°C and 970°C (1529°F and 1779°F). Above 970°C (1779°F), Zircaloy is in the beta phase. Alpha phase Zircaloy has anisotropic strain properties. Therefore, the resulting deformation of alpha phase Zircaloy is very sensitive to minor temperature irregularities in both circumferential and axial directions. This anisotropic property causes rod bowing, in addition to swelling and burst. Although the burst phenomenon in the mixed phase is not well understood, this burst range can be treated essentially as alpha phase burst because of the nonisotropic property of alpha phase. Beta phase Zircaloy has an isotropic strain property which causes somewhat uniform clad swelling. Thus the property of alpha phase Zircaloy is different from that of beta phase Zircaloy. This difference provides a different clad swelling

1. Loftus, M. J., et al., "PWR FLECHT SEASET 21-Rod Bundle Flow Blockage Task: Data and Analysis Report," NRC/EPRI/Westinghouse-11, September 1982.

phenomenon for each phase. That is, alpha phase swelling has a long nonconcentric shape in contrast to the beta phase swelling of a relatively short concentric shape. Therefore, two typical blockage shapes representing alpha and beta phase swelling were chosen to be simulated in the 21-rod tests. Detailed explanations of the choices are given in the 21-rod bundle flow blockage task plan.⁽¹⁾

The 21-rod bundle task was designed to compare the blockage effects of the two sleeves and screen out the blockage shape which provided the least favorable heat transfer characteristics within and downstream of the blockage zone. The blockage shape which was selected to provide the least favorable heat transfer (appendix A) and subsequently used in the 163-rod bundle was the long, nonconcentric sleeve, shown in figure 3-1. The maximum strain was increased from 36 percent to 44 percent to provide more flow blockage in the 163-rod bundle, and therefore more flow bypass.

3-3. NONCOPLANAR BLOCKAGE DISTRIBUTION

A noncoplanar blockage test configuration requires a method to axially distribute the blockage sleeves, as described in the following paragraphs. The objective was to locate blockage sleeves in the bundle in such a manner that the statistics of the location coincided with the expected deformation and bursts of a PWR. The basis of this approach was the following statement from the ORNL multirod burst test results: "Posttest deformation measurements showed excellent correlation with the axial temperature distribution, with deformation being extremely sensitive to small temperature variations."⁽²⁾

1. Hochreiter, L. E., et al., "PWR FLECHT SEASET 21-Rod Bundle Flow Blockage Task: Task Plan Report," NRC/EPRI/Westinghouse-5, March 1980.
2. Chapman, R. H., "Significant Results From Single-Rod and Multirod Burst Tests in Steam With Transient Heating," paper presented at Fifth Water Reactor Safety Research Information Meeting, Gaithersburg, MD, November 7-10, 1977.

Burman and Olson⁽¹⁾ have studied temperature distribution on rods in a bundle and their method can be employed to determine the statistics of burst locations in the bundle.

The burst locations so determined were selected without considering the grid effect on burst location which was observed in the German REBEKA tests.⁽²⁾

It was found that rod burst locations were shifted toward the fluid flow direction because of the downward fluid flow at the time. Burst at the end of blowdown may not be affected by fluid flow because there is virtually no flow. During the refill and reflood phases, rod bursts would occur at locations shifted upward.

Fuel rods in a PWR can burst at any phase of a LOCA transient, depending on power distribution, operating life, type of break, material strength uncertainties, and the like. Therefore, the hydraulic effect can be incorporated into the determination of burst locations in several ways. However, the primary objective in the present study is local heat transfer under a typical blockage distribution; such an objective can be achieved without considering a preburst hydraulic effect.

To determine burst locations, it is assumed that all rods to be deformed have the same or similar temperature distribution. The ORNL multirod burst tests showed that there were no interactions among rods during burst, so it may be assumed that each rod in a bundle bursts independently. Then the characteristics of one rod may be used to infer the behavior of the rod bundle.

A rod is divided into several sections with the same interval. Burman and Olson computed the probability that a certain section (say, the i -th increment) of a fuel rod is at the highest temperature in the rod, as follows:

-
1. Burman, D. L., and Olson, C. A., "Temperature and Cladding Burst Distributions in a PWR Core During LOCA," Specialists Meeting on the Behaviour of Water Reactor Fuel Elements Under Accident Conditions, Norway, September 13 1976, p. 73-77.
 2. Wiehr, K., et al., "Fuel Rod Behavior in the Refill and Flooding Phase of a Loss-of-Coolant Accident," CONF-771252-5, December 1977.

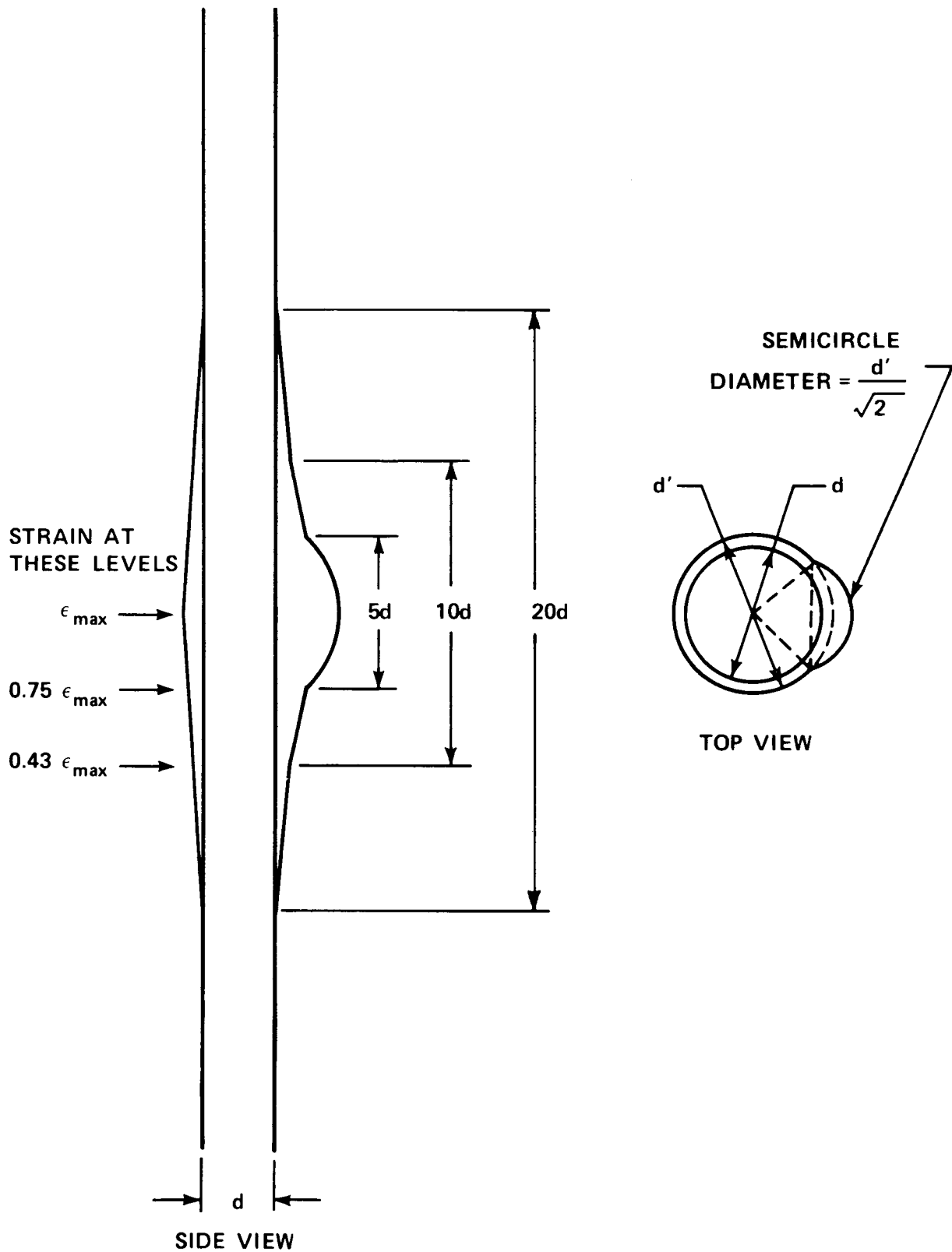


Figure 3-1. Shape of Nonconcentric Sleeve

$$\int_0^{\infty} \left\{ \frac{1}{\sigma_T \sqrt{2\pi}} \exp \left[\frac{(\mu_i - T)^2}{2\sigma_T^2} \right] \sum_{j=1}^{j=1, N} \frac{1}{\sigma_T \sqrt{2\pi}} \int_0^T \exp \left[\frac{-(\mu_i - t)^2}{2\sigma_T^2} \right] dt \right\} dT \quad (3-1)$$

Here σ_T and μ_i are the standard deviation of local temperature and mean temperature at the i -th increment, respectively. It can be seen that these two characteristics (σ_T and μ_i) must be known to compute the local probability of highest temperature. As ORNL showed, this highest-temperature location can be interpreted as the burst location.

The mean temperature distribution required in equation (3-1) is the axial mean temperature of a nuclear fuel rod at the time of rod burst. The standard deviation of local temperature is included to account for the local temperature fluctuation. Burman and Olson assumed that the fluctuation is normally distributed.

The local temperature can be divided into two components:

$$T_{local} = \bar{T}_{local} + T'_{local}$$

where \bar{T}_{local} and T'_{local} are the mean and variation of local temperature, respectively. The mean temperature is obtained from the axial mean temperature distribution. The local temperature variation is a function of the following effects:

o Manufacturing effect

- Initial fuel pellet density
- Fuel pellet diameter
- Fuel enrichment
- Manufacturing variables which affect fuel densification
- Clad local ovality
- Fuel pellet chemical bounding

o In-pile effect

- Fuel pellet radial offset within clad
- Fuel pellet cracking
- Fuel densification

Burst probabilities at each increment of rod can be computed by equation (3-1) with the inputs of σ_T and μ_i .

Multiplying the probabilities by the total rod number gives theoretical burst numbers at the corresponding axial increments. These numbers are usually not integers. Therefore, for practical purpose, these numbers are transformed to integers to satisfy the requirements that the total burst number is the same as the total rod number. These integer numbers indicate how many sleeves should be located at specific axial increments. An increment (i-th) is then selected at random. Since it is known from the above calculation that N_i rods have bursts at this increment, N_i rods are selected at random. Each of these selected rods has a sleeve on the i-th increment. Then another increment and corresponding rods are selected at random. This procedure is repeated until all the axial increments where bursts occur have been considered.

A computer program was written to execute this procedure for selection of sleeve locations. This program, called COFARR (Coolant Flow Area Reduction), calculates subchannel blockage with given input strain information of the blockage sleeve. This program and relevant details are described in detail in the 21-rod bundle task plan.⁽¹⁾

3-4. MEAN AND VARIATION OF LOCAL TEMPERATURE

The mean temperature distribution at time of burst and local temperature fluctuation data were required to compute burst probability from equation (3-1). In addition, strain information was required to compute actual blockage distribution and subchannel area. Westinghouse received relevant information to

1. Hochreiter, L. E., et al., "PWR FLECHT SEASET 21-Rod Bundle Flow Blockage Task: Task Plan Report," NRC/EPRI/Westinghouse-5, March 1980.

calculate a noncoplanar blockage distribution from the three other PWR fuel vendors (Babcock & Wilcox, Combustion Engineering, and Exxon).

Westinghouse calculated a mean temperature distribution at the time of burst as shown in figure 3-2 by analyzing a LOCA. Burst was calculated to occur at the end of blowdown. Babcock & Wilcox⁽¹⁾ calculated an axial temperature distribution for its plant (15 x 15 fuel) for a 0.794 m² (8.55 ft²) double-ended cold leg break. Babcock & Wilcox also analyzed a plant with 17x17 fuel for the same accident case. Clad rupture was calculated to occur during blowdown. Combustion Engineering⁽²⁾ analyzed its 16 x 16 fuel assembly for a worst-case temperature distribution using LOCA licensing analysis codes and input data. Exxon⁽³⁾ also used its WREM ECCS model to calculate a mean temperature distribution for a 15 x 15 fuel assembly at the time of rod rupture. Comparisons of the available mean temperature data reveal that Westinghouse and Babcock & Wilcox plants are expected to have the most peaked axial temperature distributions. The Westinghouse temperature distribution was chosen to be a reference case. Detailed discussion of this analysis can be found in the task plan.⁽⁴⁾

Manufacturing quality assurance records were reviewed by Burman and Olson to determine the realistic distribution for pellet parameters which would have an effect on local temperature variation, such as enrichment (negligible), initial density, sintering characteristics, diameter, and surface roughness. The variations thus obtained were input into Westinghouse standard design codes to determine their effect on operating temperature. Perturbation studies were analyzed to determine the effect of small variations in initial power

1. Personal communication from J. J. Cudlin, Babcock & Wilcox, to H. W. Massie, Jr., Westinghouse, April 5, 1978.
2. Personal communication from J. H. Holderness, Combustion Engineering, to H. W. Massie, Jr., Westinghouse, April 11, 1978.
3. Personal communication from R. E. Collingham, Exxon Nuclear, to M. W. Hodges, USNRC, August 3, 1978.
4. Hochreiter, L. E., et al., "PWR FLECHT SEASET 21-Rod Bundle Flow Blockage Task: Task Plan Report," NRC/EPRI/Westinghouse-5, March 1980.

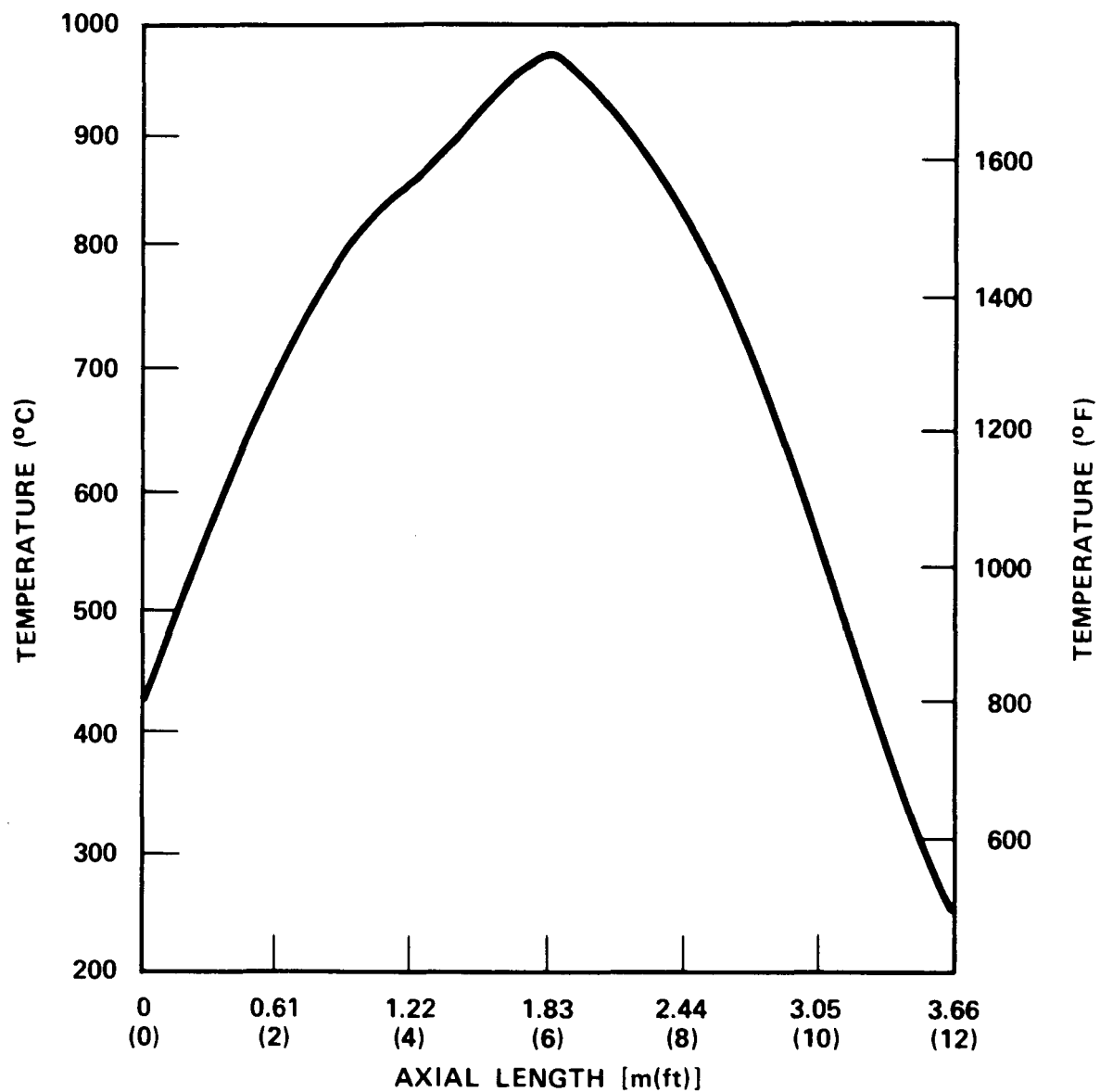


Figure 3-2. Westinghouse Mean Temperature Distribution

and temperature on the clad temperature at the time of burst, for cases in which burst occurred during refill. The initial temperature distributions were then modified to account for these effects. The resulting responses were statistically combined to obtain the overall temperature uncertainty just prior to the accident due to manufacturing variables. The resulting standard deviation in temperature was found to be approximately 9.78°C (17.6°F).

Of the various uncertainties in pellet temperature due to in-pile effects, only the standard deviation in pellet temperature due to pellet offset was analyzed. Using a finite difference program, the effect of pellet eccentricity on pellet average temperature during normal operation was calculated, assuming various degrees of pellet clad eccentricity. The resulting temperature distribution was convoluted with that arising from manufacturing uncertainties and the convoluted sum corrected to account for the temperature variability at burst time for a given temperature variability at power. This variation was determined to be 9.11°C (16.4°F). When statistically combined with the uncertainties due to manufacturing variables, the total standard deviation in local temperature becomes 13°C (24°F) at the time of blowdown, or 6.7°C (12°F) at the time of burst.

In summary, the mean temperature distribution of Westinghouse as shown in figure 3-2 and table 3-1 with the correction of grid effect as shown by Burman (appendix B), and a standard deviation of 6.7°C (12°F) were chosen to calculate a noncoplanar blockage distribution. With these inputs, the COFARR code calculated the blockage sleeve distribution as indicated in figure 3-3. The percent flow blockage for each 21-rod bundle island is shown in figure 3-4 as a function of elevation.

3-5. FLOW BYPASS REGION

The large 163-rod bundle was blocked to investigate the flow bypass effects on the reflood heat transfer in the simulated fuel rod assembly. The arrangement of the blockage in the bundle had to be set up so as to not force fluid through the blocked zone. Several methods could be used to produce a sufficient bypass area in the bundle. However, the following limitations affect how the blockage should be arranged radially:

TABLE 3-1

MEAN TEMPERATURE DISTRIBUTION

Axial Height [m(in.)]	Temperature [°C(°F)]	Axial Height [m(in.)]	Temperature [°C(°F)]
1.57 (62)	914 (1678)	1.83 (72)	949 (1741)
1.60 (63)	920 (1688)	1.85 (73)	948 (1738)
1.63 (64)	925 (1697)	1.88 (74)	946 (1735)
1.65 (65)	930 (1706)	1.90 (75)	938 (1721)
1.68 (66)	934 (1713)	1.93 (76)	933 (1712)
1.70 (67)	938 (1720)	1.96 (77)	929 (1705)
1.73 (68)	942 (1727)	1.98 (78)	927 (1701)
1.75 (69)	944 (1732)	2.01 (79)	925 (1698)
1.78 (70)	947 (1736)	2.03 (80)	923 (1693)
1.80 (71)	947 (1737)	2.06 (81)	918 (1684)

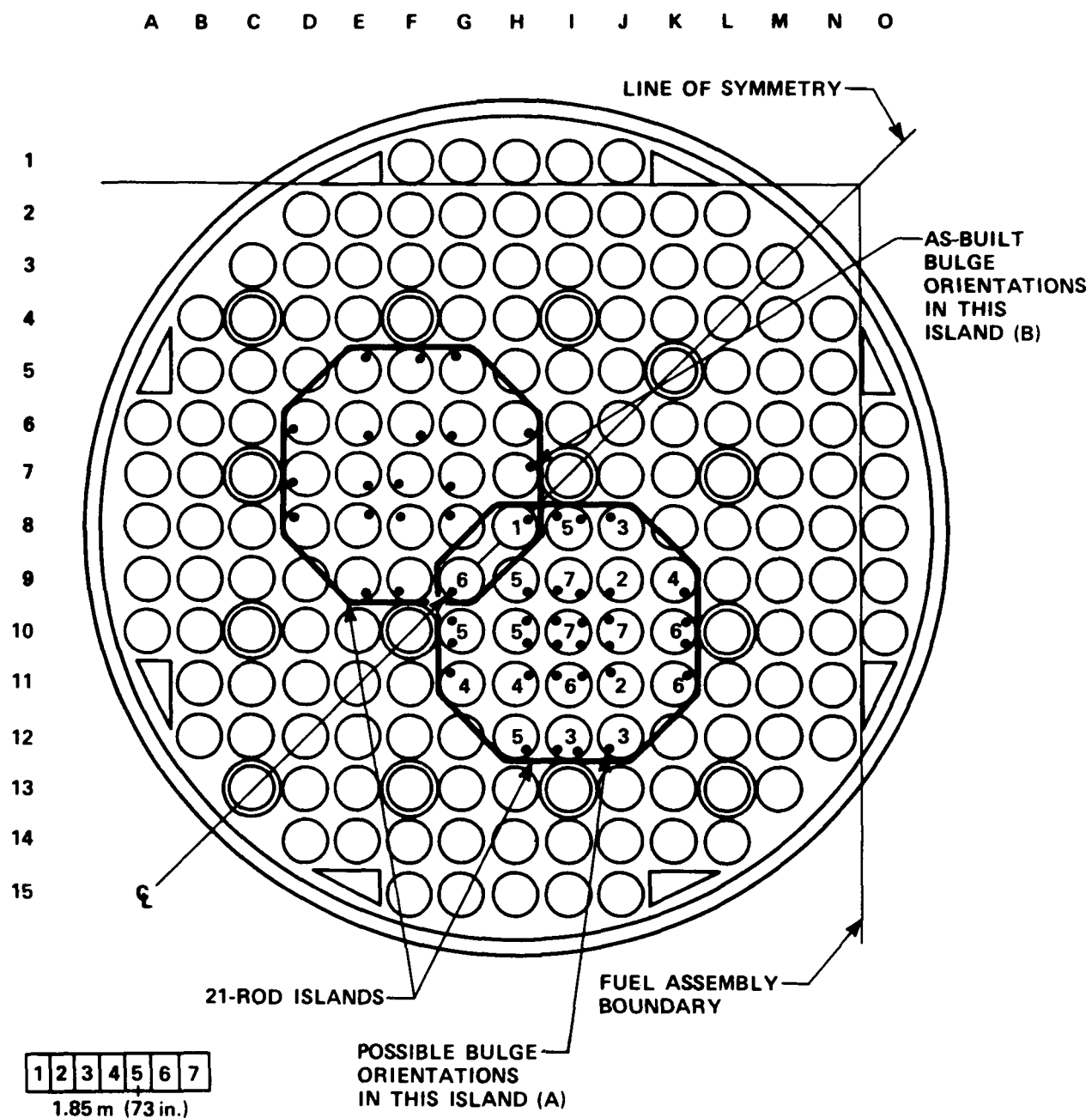


Figure 3-3. Blockage Sleeve Distribution, Blockage Island Locations, and Bulge Orientations

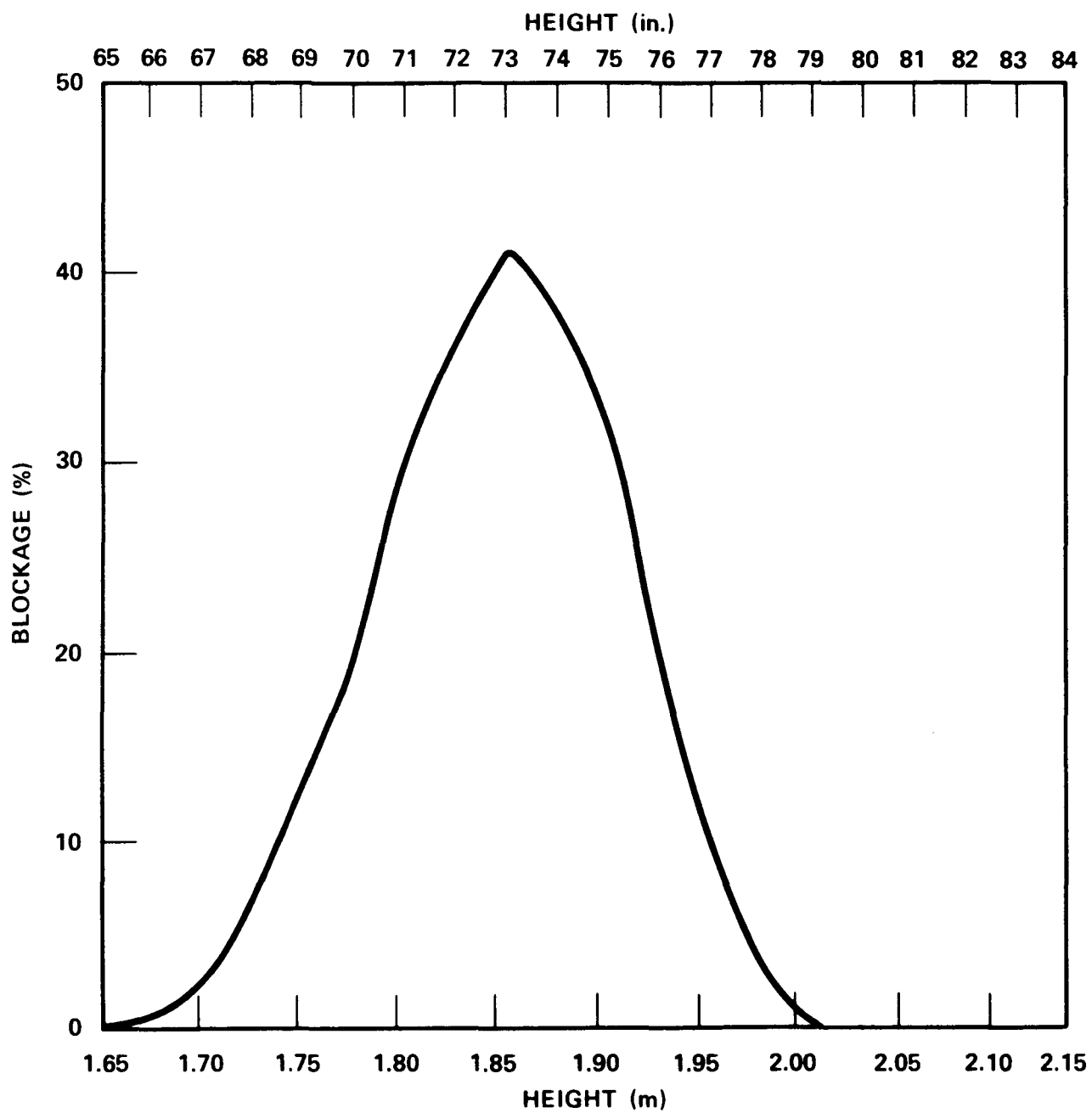


Figure 3-4. Blockage Island Axial Blockage Distribution

- o The large bundle has only one symmetry line because of thimble locations, as shown in figure 3-3.
- o The large-bundle test should be linked to the small-bundle test (21-rod) to better utilize information.
- o Lateral symmetry in the blocked bundle for the bypass area and blockage zone is desirable in view of possible data scattering and computer time for flow calculations.
- o The blockage zone must be large enough to provide a detectable flow field distortion and a maximum flow depletion in the blocked zone.

Thus, the following two blockage flow bypass configurations were considered, as discussed in the blocked bundle task plan:⁽¹⁾

- o Block one-half of the bundle
- o Block an island of rods in the center of the bundle

The first configuration has an advantage of direct data comparison between blocked and unblocked subchannels in the same bundle, using the bundle symmetry. However, COBRA calculations showed that when half of the bundle is blocked, the fluid near the wall on the blocked half of the bundle tends to be trapped in the blockage zone. Therefore, the flow in the blockage zone is higher than in the scheme where there is no wall; this blockage-bypass configuration is therefore unacceptable.

In the second configuration, the rods are divided in the large bundle into two 21-rod bundle islands. For this configuration, the rods in the islands are blocked exactly as in the 21-rod bundle. This blockage configuration has a higher bypass area because of the smaller and isolated blockage zone.

Comparisons of the two blockage configurations were made by calculating flow rates in subchannels by COBRA-IV-I. These results show that the two 21-rod bundle islands have lower flow rates in the blocked zone, and the flow depletion in the zone is almost comparable to that of the half-bundle blockage.

1. Hochreiter, L. E., et al., "PWR FLECHT SEASET 161-Rod Bundle Flow Blockage Task: Task Plan Report," NRC/EPRI/Westinghouse-6, September 1980.

3-6. BULGE DIRECTIONS FOR NONCONCENTRIC SLEEVES

Data from Westinghouse multirod burst tests⁽¹⁾ showed a thimble effect on circumferential burst location (appendix B). The burst locations were not random, and were usually directed away from thimbles. This indicated that the thimbles were good heat sinks, causing nonuniform circumferential temperature distributions on neighboring rods. It must be noted that a burst occurs at the hottest point of a rod; however, the major flow blockage due to the non-concentric bulge is on the opposite side of the burst location.

Observations from the Westinghouse tests indicate that burst can occur toward either adjacent subchannel or rods. It was proposed that bursts be restricted to occur only toward adjacent subchannels for the following reasons:

- o Blockage tests were not intended to investigate detailed variations in a subchannel but to determine average subchannel behavior.
- o The additional parameter of burst orientation makes data analysis complicated without an apparent improvement of understanding.
- o There were physical limitations in installing the blockage sleeves on the rods.

The above proposal provided the basis for selecting bulge directions of the nonconcentric sleeves in the 21-rod bundle. First it was necessary to find the hottest subchannel out of the four subchannels surrounding each rod. Then the bulge direction was the opposite side of the hottest point.

Since an effort had been made to couple the 21-rod bundle to the 163-rod bundle to maximize data utilization,⁽¹⁾ it was better to consider the relative location of the 21-rod island in a fuel assembly in applying the present method to the small bundle, as shown in figure 3-3. For this case it was straightforward to determine the hottest subchannel (or subchannels) associated with each rod, because of the unique distribution of the thimbles.

1. Schreiber, R. E., et al., "Performance of Zircaloy-Clad Fuel Rods During a Simulated Loss-of-Coolant Accident -- Multirod Burst Tests," WCAP-7495-L, April 1970.

The above arguments were used to determine the possible bulge directions in the 21-rod bundle, as indicated by dots in the island A of figure 3-3. The bulge directions of some rods were determined uniquely; others had several possible locations. Bulge directions of the rods with multiple choices could be chosen from the possible locations so that the four center subchannels had high blockages. The locations of the peripheral rods with multiple choices could be chosen arbitrarily from the possible locations. The resulting bulge directions are shown in the island B of figure 3-3.

-
1. L. E. Hochreiter, et al., "PWR FLECHT SEASET 161-Rod Bundle Flow Blockage Task: Task Plan Report," NRC/EPRI/Westinghouse-6, September 1980.

SECTION 4

SYSTEM DESCRIPTION

4-1. INTRODUCTION

The FLECHT SEASET 163-rod bundle test facility was designed and built specifically for conducting flow blockage tests following the 21-rod bundle flow blockage test program.⁽¹⁾ A new test facility was required since the facility previously utilized for the 161-rod unblocked bundle tests⁽²⁾ was being utilized to perform natural circulation systems effect tests. A schematic diagram of the facility is shown in figure 4-1.

The 163-rod blocked bundle test facility, like the 21-rod and 161-rod unblocked bundle test facilities, was designed with the following major components:

- o A heater rod bundle
- o A low mass housing coupled directly to an upper plenum and a lower plenum
- o A coolant injection system and a steam heating system
- o A phase separation and liquid collection system
- o A downcomer and crossover leg

All the above components were thoroughly instrumented to measure flow blockage effects within the bundle and respective boundary conditions at the bundle inlet and outlet.

The volumes of the upper and lower plenums, downcomer, crossover leg, and steam separator tanks were essentially the same as in the 161-rod unblocked

1. Loftus, M. J., et al., "PWR FLECHT SEASET 21-Rod Bundle Flow Blockage Task: Data and Analysis Report," NRC/EPRI/Westinghouse-11, September 1982.
2. Loftus, M. J., et al., "PWR FLECHT SEASET Unblocked Bundle, Forced and Gravity Reflood Task: Data Report," NRC/EPRI/Westinghouse-7, June 1980.

bundle facility. The carryover tank volume was increased to accommodate additional water capacity.

Both forced flooding and gravity reflood tests were performed in the 163-rod blocked bundle test facility similar to those performed in the 21-rod bundle test facility.

4-2. FORCED REFLOOD TESTS

The forced reflood tests were performed to measure the two-phase flow heat transfer effects of the flow blockage and flow bypass during forced flow injection. These tests utilized all the major facility components, with the exception of the downcomer and the crossover leg.

During forced reflood test operation, coolant flow from the 1.52 m³ (400 gal) capacity water supply accumulators entered the test section housing through a series of hand valves, pneumatically operated control valves, and solenoid valves. Coolant flow was measured by a turbine meter located in the injection line. Orifice plate flowmeters were used for redundant flow measurement. Test section pressure was established initially by a steam boiler connected to the upper plenum of the test section. During the reflood test run, the boiler was isolated from the system and pressure was maintained by a pneumatically operated control valve located in the exhaust line. Liquid effluent leaving the test section was separated in the upper plenum and collected in a close-coupled carryover tank. An entrainment separator located in the exhaust line was used to separate any remaining entrained liquid in the vapor. Dry steam flow leaving the separator was measured by an orifice plate flowmeter before it was exhausted to the atmosphere. A more detailed explanation of forced reflood facility operation is presented in paragraph 4-26.

4-3. GRAVITY REFLOOD TESTS

The gravity reflood tests were performed to measure the two-phase flow heat transfer effects of the flow blockage and flow bypass during the PWR-simulated gravity flow injection. The PWR accumulator injection flow into the downcomer

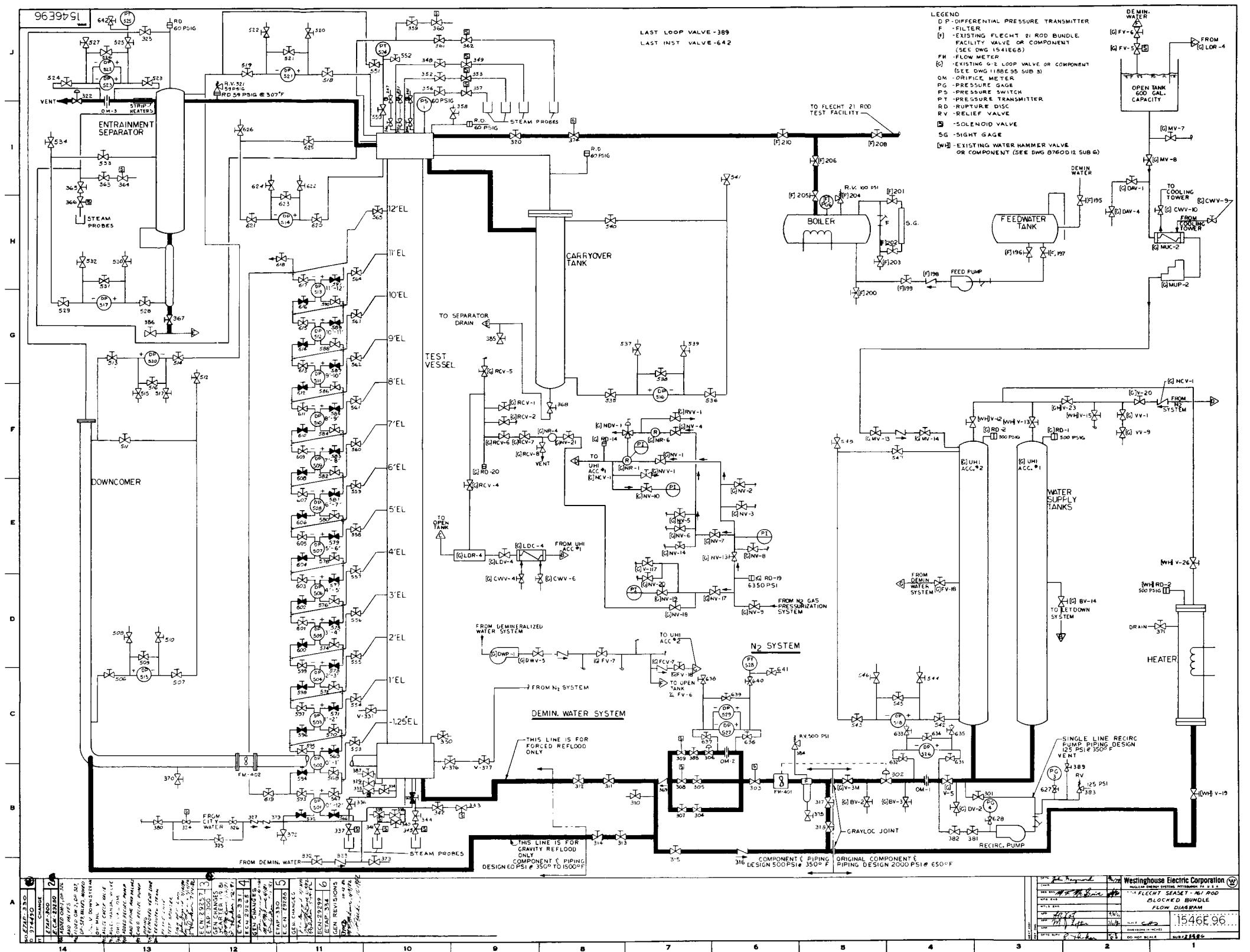


Figure 4-1. Forced and Gravity Reflood Configuration Flow Diagram



was simulated for the first 15 seconds and the safety injection pump flow was simulated thereafter.

A downcomer and crossover leg were connected to the test section lower plenum. Coolant was then injected into the test section through the downcomer. An orifice plate (beta ratio of 0.522) was installed in the exhaust line immediately upstream of the separator for these tests to simulate the PWR hot leg flow resistance of approximately 32.5. A vent path was also established between the top of the downcomer and the entrainment separator to prevent overpressurization in the downcomer. Facility operation was essentially the same as that in forced reflood tests.

Since neither the steam generators nor the upper plenum liquid fallback are simulated, the bundle and downcomer response is expected to be similar to but not exactly the same as that in a systems effect test.

4-4. FACILITY COMPONENT DESCRIPTION

The various components of the 163-rod blocked bundle test facility are described in paragraphs 4-5 through 4-13. Detailed drawings of the various components are shown in appendix C. The data acquisition systems and instrumentation are described in paragraphs 4-14 through 4-26.

4-5. Heater Rod Bundle

As shown by the cross-section in figure 4-2, the bundle was composed of 163 heater rods (101 uninstrumented and 62 instrumented), 14 thimbles (13 instrumented), 8 solid triangular filler rods (figure C-1), 8 FLECHT-type grids (figure C-2), and 40 blockage sleeves.

The heater rod design was essentially identical to the design successfully used for configurations E and F in the 21-rod bundle test program. Details of the heater rod design are shown in figure C-3. A minor change was incorporated by chamfering the rod sheath at the ends to facilitate installing the O-ring seals over the rods. The thermophysical properties of the heater rod materials are listed in table 4-1.

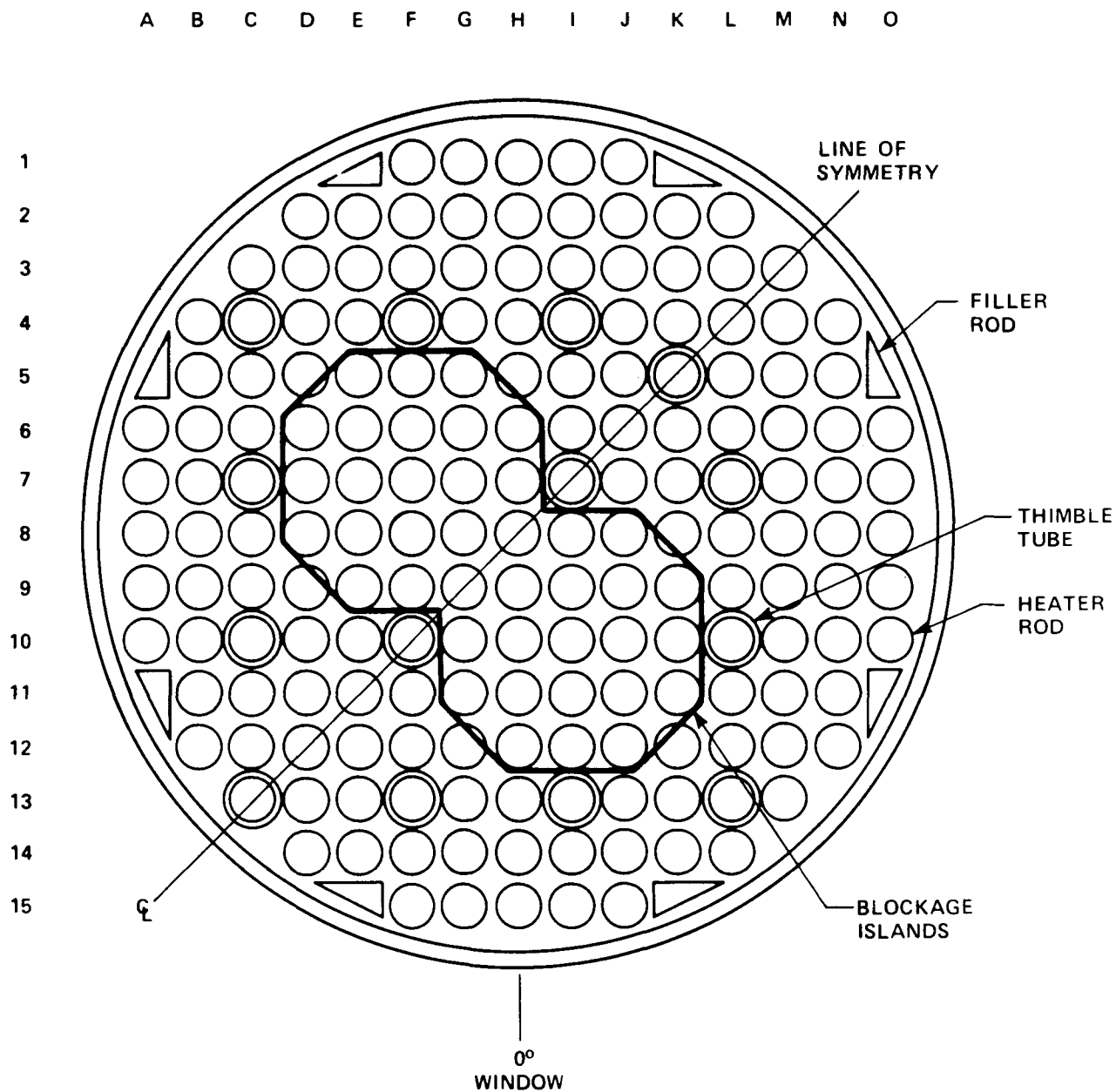


Figure 4-2. Heater Rod Bundle Cross Section

TABLE 4-1
THERMOPHYSICAL PROPERTIES OF HEATER ROD MATERIALS

Material	Density [kg/m ³ (lbm/ft ³)]	Specific Heat [J/kg-°C (Btu/lbm-°F)]	Thermal Conductivity [W/m-°C (Btu/hr-ft-°F)]
Kanthal	2898.70 (180.96)	$456.36 + 0.45674 T$ for $T \leq 649^{\circ}\text{C}$ $(0.109 + 0.000059 T)$ for $T \leq 1200^{\circ}\text{F}$ $4161.68 - 3.843 T$ for $649^{\circ}\text{C} < T < 871^{\circ}\text{C}$ $(0.994 - 0.00051 T)$ for $1200^{\circ}\text{F} < T < 1600^{\circ}\text{F}$ $664.86 + 0.0904 T$ for $T \geq 871^{\circ}\text{C}$ $(0.1588 + 0.000012 T)$ for $T \geq 1600^{\circ}\text{F}$	$16.784 + 0.0134 T$ ($9.7 + 0.0043 T$)
Boron nitride	2212.15 (138.1)	$2017.74 - 1396.26 e^{-0.00245 T}$ [$0.48193 - 0.33492 e^{0.0013611 T}$]	$25.571 - 0.00276 T$ ($14.7778 - 0.0008889 T$)
Stainless	8025.25 (501.0)	$443.8 + 0.2888 T$ for $T < 315^{\circ}\text{C}$ $(0.106 + 3.833 \times 10^{-5} T)$ for $T < 599.25^{\circ}\text{F}$ $484.4 + 0.1668 T$ for $T \geq 315^{\circ}\text{C}$ $(0.1157 + 2.2143 \times 10^{-5} T)$ for $T \geq 599.25^{\circ}\text{F}$	$14.535 + 0.01308 T$ ($8.4 + 0.0042 T$)

A major improvement over the 161-rod unblocked bundle heater rod design was the incorporation of larger diameter [1.0 mm (0.040 in.)] thermocouples. This helped to minimize the possibility of thermocouple damage due to handling and thus minimized thermocouple failures during testing. To accommodate this change, the heater element coil diameter and wire diameter were decreased so that heater element electrical isolation could be maintained.

As in the 21-rod bundle test program, all heater rods were annealed after manufacture at low temperatures [450°C (842°F) for 60 hours] to remove the residual stresses. The annealing process was believed to reduce premature thermocouple failure by counteracting grain structure embrittlement caused by cold working of the thermocouples during the manufacturing process.⁽¹⁾ An infrared scan of each heater rod was also performed by Oak Ridge National Laboratory (ORNL) to check heater coil integrity and density of boron nitride insulation. These two procedures were incorporated into the 163-rod blocked bundle test program, as in the 21-rod bundle test program, to eliminate the heater rod failures and thermocouple failures which had occurred in the 161-rod unblocked bundle tests. An additional problem concerning the low isolation resistance in the rod thermocouples was discovered and resolved during heater rod inspection for the 163-rod bundle, as described in appendix D. These procedures were successful; heater rod thermocouple failures were minimal (approximately 3.5 percent) during the test program.

Although one heater rod was found to be defective after bundle installation, the cause of the defect is not believed to have been related to anything detectable by ORNL infrared scan. The rod in question was an uninstrumented dual-diameter heater rod located next to a filler rod at the outer periphery of the bundle (location A-10 in figure 4-2). The rod exhibited low isolation resistance, which was most likely due to moisture penetration at one end where the seal plug was found to be defective. The rod was disconnected for all matrix tests to preclude the possibility of a catastrophic failure which might damage other nearby rods or the housing pressure boundary. Since the rod was

1. McCulloch, R. W., et al., Proceedings of the International Symposium on Fuel Rod Simulators - Development and Application, Gatlinburg, TN, October 1980, pp 435-439.

located at the periphery of the bundle, the effect of disconnecting the rod was negligible.

The eight triangular filler rods in the bundle were split and pin-connected to each other midway between grids to accommodate thermal growth, and welded to the grids to maintain the proper grid location. The filler rods reduced the amount of excess flow area in the housing and also supported test bundle instrumentation leads. The excess flow area was approximately 4.7 percent with the fillers (9.3 percent without the fillers). Bundle assembly and filler rod details are shown in figures C-4 and C-1.

The grid design used in the 163-rod blocked bundle was similar to that utilized in the 161-rod unblocked bundle. In the 163-rod bundle, the grid straps were lengthened slightly and notched (figure C-2, section A-A) to accommodate routing of unshielded and self-aspirating steam probe thermocouple leads. The grid design and filler rod design are shown in a photograph of the bundle during assembly (figure 4-3).

The 12.0 mm (0.474 in.) diameter thimbles and steam probes (figures C-5 through C-9) were modified somewhat from the 161-rod unblocked bundle design. The wall thickness was increased from 0.56 mm (0.022 in.) to 0.76 mm (0.030 in.) to provide a thicker wall to which to weld the thermocouples. A split collar was incorporated to simplify retention of the thimbles in the upper seal plate. The thimble tube aspirating steam probe which aspirates through the bottom of the bundle was redesigned to prevent thermocouple wetting (appendix E). Increased flexibility was provided in the thimble design such that a single thimble was capable of containing both an aspirating steam probe and several wall thermocouples (figures C-5 and C-6).

4-6. Flow Blockage Sleeves

The long nonconcentric blockage sleeve was selected for use in the 163-rod blocked bundle, based on the results of the 21-rod blocked bundle test program.⁽¹⁾ This sleeve was projected to provide the poorest heat transfer

1. Loftus, M. J., et al., "PWR FLECHT SEASET 21-Rod Bundle Flow Blockage Task Data and Analysis Report," NRC/EPRI/Westinghouse-11, September 1982.

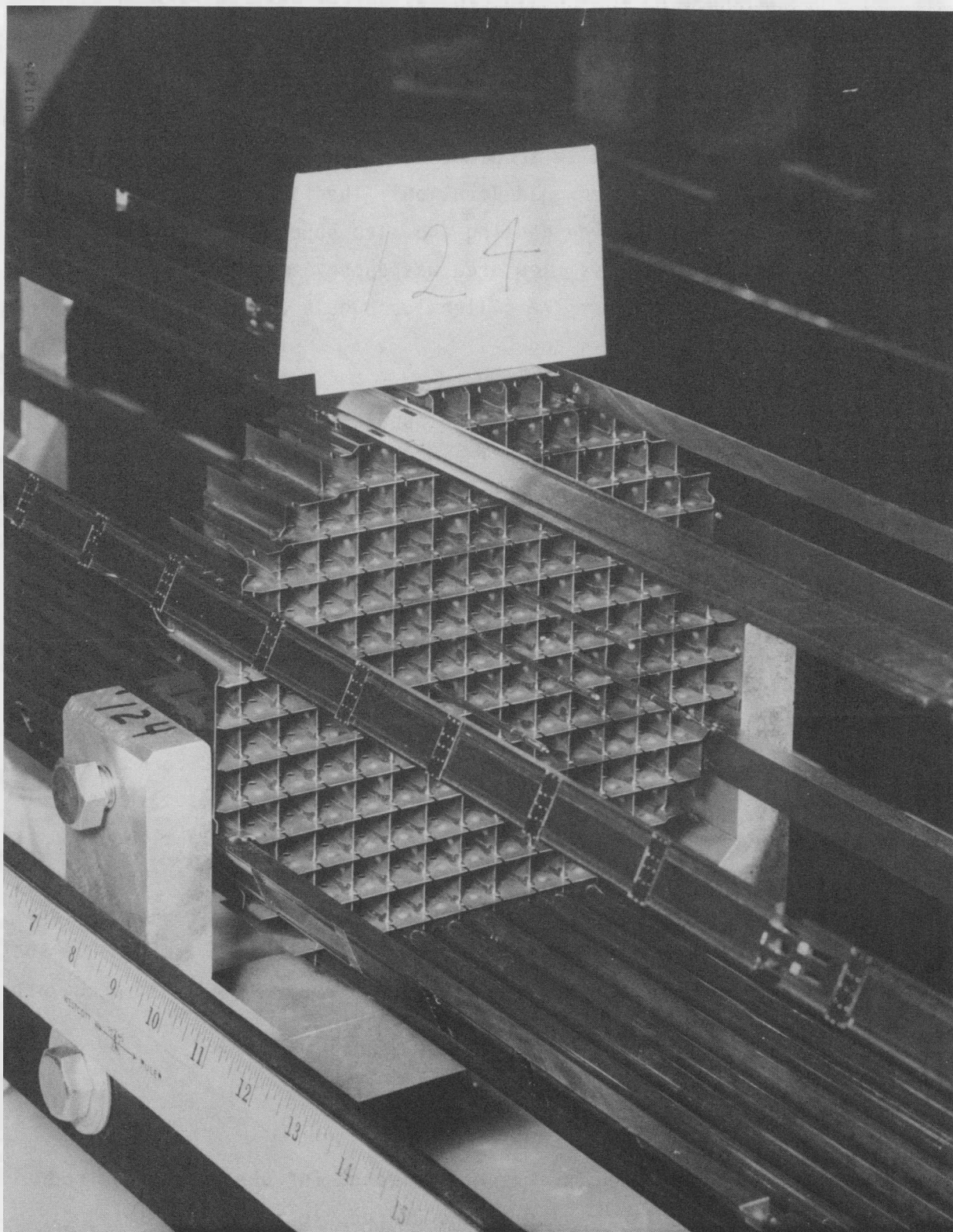


Figure 4-3. Grid and Filler Rod in Bundle Assembly

in the large blocked bundle (appendix A). The strain for the blockage sleeve utilized in the 163-rod bundle test, as shown in figure C-10, was 44 percent. The sleeves were manufactured by hydroforming (hydraulic expansion) 0.76 mm (0.030 in.) thick tubing into a mold. As with the heater rods, the blockage sleeves were annealed after hydroforming to remove residual stresses which might cause them to warp under thermal cycling.

Sleeves were attached to the rods by applying a weld bead to the heater rod sheath through a hole predrilled in the sleeve wall at the downstream end. The weld bead was high enough so that the sleeve could not slide over it. Figure 4-4 shows the blockage sleeves attached to the heater rods.

4-7. Test Section

The low mass housing, together with the lower and upper plenum, constituted the test section (figure C-11). The low mass housing (figure C-12) was a cylindrical vessel with a nominal inside diameter of 0.1937 m (7.625 in.) and a 5.1 mm (0.20 in.) wall, constructed of 304 stainless steel rated for 0.41 MPa (60 psi) at 815°C (1500°F). The wall thickness was the minimum allowed by the ASME pressure vessel code so that the housing would absorb, and hence release, the minimum amount of heat compared with the rod bundle. The inside diameter of the housing was made as close to the rod bundle outer dimensions as possible to minimize excess flow area. The excess flow area was further reduced by the solid triangular fillers. Volumetric checks were performed on the test section with the rod bundle in place to determine the flow area, as shown in table 4-2. The housing had two commercially manufactured sight glasses located 180 degrees apart at the 0.91, 1.83, and 2.74 m (36, 72, and 108 in.) elevations for viewing and photographic studies. The sight glass configuration allowed backlighting for photographic studies. The sight glasses were fitted with clamp-on heaters to raise the quartz temperature to approximately 260°C (500°F); this prevented formation of a liquid film on the windows during a test run.

To help eliminate thermal buckling and distortion, the test section was supported from the upper plenum to permit the housing to freely expand downward

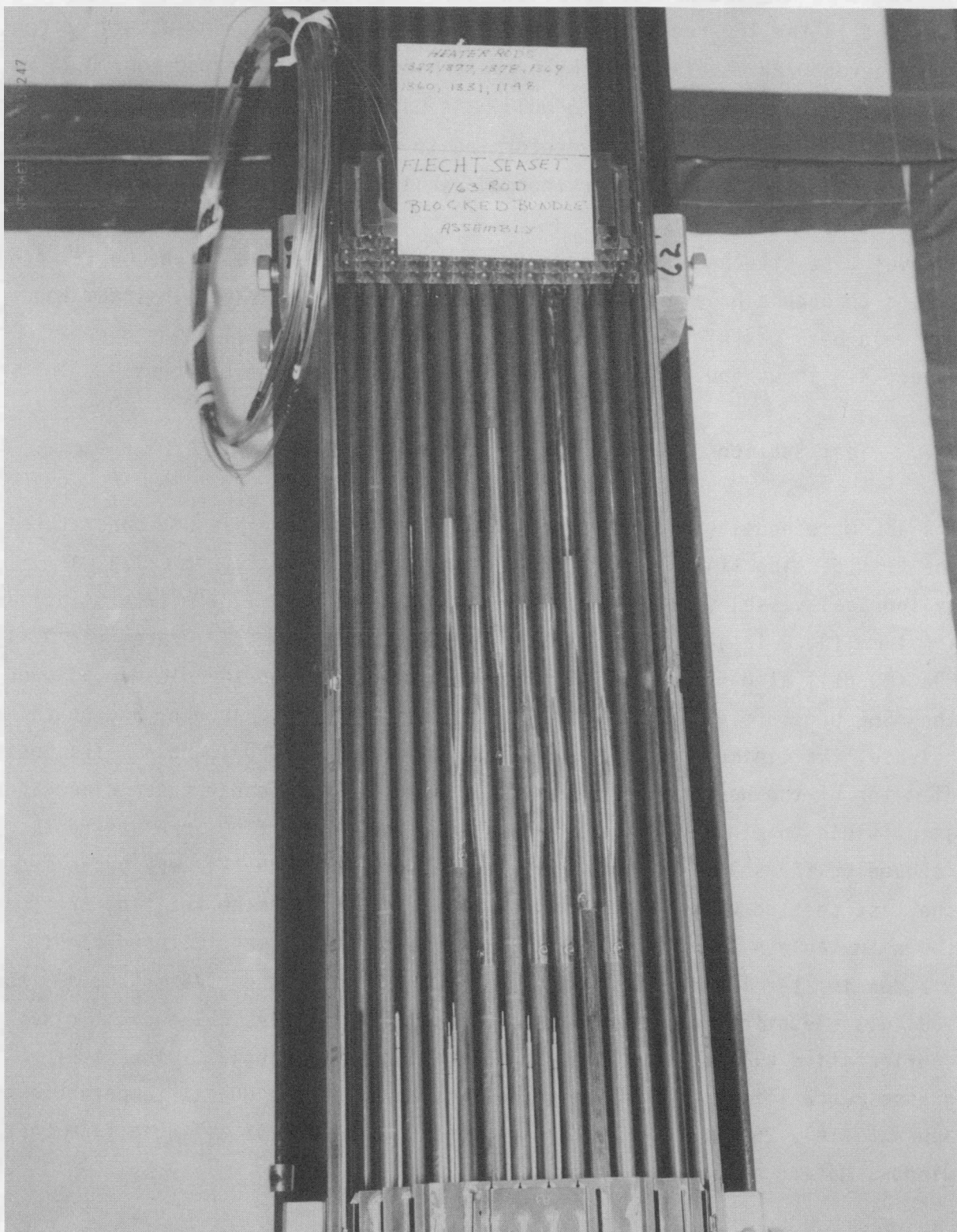


Figure 4-4. Blockage Sleeves Attached to Heater Rod

TABLE 4-2

163-ROD BUNDLE FLOW AREA

Nominal Elevation [m (in.)]	Actual Elevation [m (in.)]	Volume Collected (ml)	Flow Area [m ² (in. ²)]
0-0 30 (0-12)	0.038 (1.5)	4480	0.01534 (23.77)
0.30-0.61 (12-24)	0.599 (23.6)	5000	0.01627 (25.21)
0.61-0.91 (24-36)	0.904 (35.6)	5050	0.01657 (25.68)
0.91-1.22 (36-48)	1.21 (47.6)	4922	0.01615 (25.03)
1.22-1.52 (48-60)	1.52 (59.7)	4933	0.01605 (24.88)
1.52-1.83 (60-72)	1.82 (71.6)	4835	0.01599 (24.79)
1.83-2.13 (72-84)	2.12 (83.6)	4650	0.01525 (23.64)
2.13-2.44 (84-96)	2.43 (95.6)	4927	0.01616 (25.05)
2.44-2.74 (96-108)	2.733 (107.6)	4860	0.01594 (24.71)
2.74-3.05 (108-120)	3.035 (119.5)	4855	0.01606 (24.89)
3.05-3.35 (120-132)	3.343 (131.6)	4690	0.01526 (23.65)
3.35-3.57 (132-140.4)	3.564 (140.3)	3456	0.01564 (24.24)
		AVERAGE	0.01588 (24.62)

as it heated up. A lateral support structure (figure C-13) was installed to restrict housing bowing.

The stainless steel upper plenum (figure C-14) provided the initial phase separation for the two-phase flow exiting the heater rod bundle, as shown in figure 4-5. The flow expansion from the bundle flow area of approximately 0.0159 m^2 (24.6 in.^2) to the upper plenum cross-sectional area of 0.274 m^2 (424 in.^2) decelerated the two-phase flow such that the water droplets could no longer be suspended. The water was collected at the bottom of the upper plenum and prevented from flowing back into the bundle by the upper plenum housing extension (figure C-11). A flow hole in the bottom of the upper plenum allowed water to drain into the carryover tank. The two-phase flow was further separated by means of the upper plenum baffle.

Flow was injected into the stainless steel lower plenum (figure C-15) and entered the housing through the lower plenum housing extension (figure C-11), which contained 162 9.7 mm (0.38 in.) diameter holes to provide a uniform flow distribution into the rod bundle.

4-8. Carryover Vessel

The function of the carryover vessel was to collect liquid which flowed out of the bundle and was deentrained in the upper plenum. The vessel was fabricated from 0.15 m (6 in.) diameter carbon steel pipe and fittings (figure C-16). Its capacity was increased by 22 percent over that of the unblocked facility vessel, which was undersized, to accommodate additional water carryover volume.

4-9. Entrainment Separator

The entrainment (steam) separator was designed to remove any remaining water droplets in the two-phase flow exiting the upper plenum so that a meaningful single-phase flow measurement could be obtained by an orifice plate flowmeter located downstream of the separator. The separator was the same vessel utilized in the 161-rod unblocked bundle test program (figure C-17). It was fabricated from 0.30 m (12 in.) diameter standard weight carbon steel pipe with a volume of 0.22 m^3 (7.8 ft^3). The separator utilized centrifugal action to

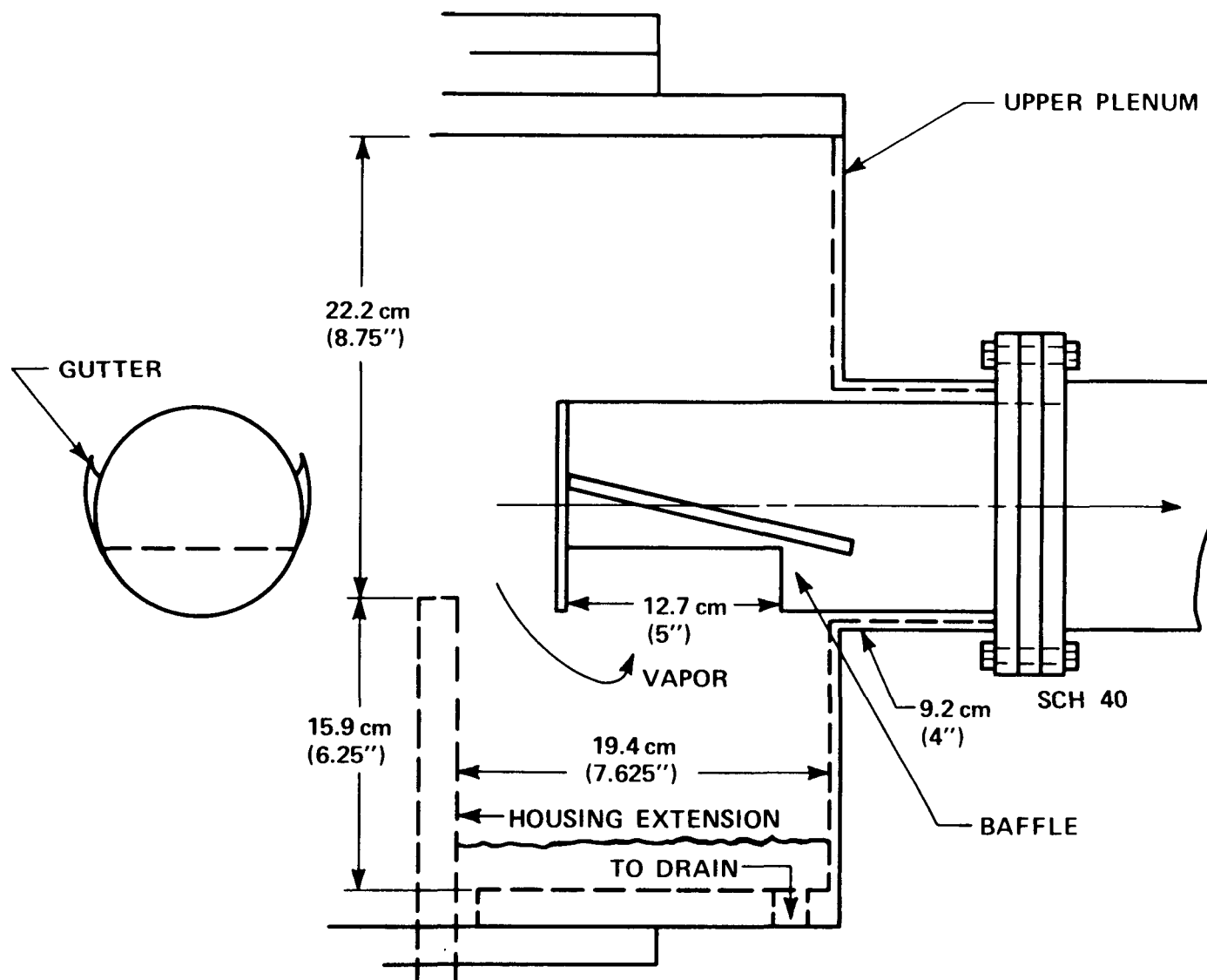


Figure 4-5. FLECHT SEASET Upper Plenum Baffle

force the heavier moisture against the wall. The water was collected in a drain tank connected to the bottom of the separator. The drain tank was fabricated from 0.76 m (3 in.) diameter standard weight pipe with a volume of approximately 0.01 m^3 (0.36 ft^3).

4-10. Exhaust Line

Test section effluent discharged to the atmosphere through the exhaust line piping. A 0.13 m (5 in.) diameter flanged nozzle penetration on the upper plenum provided the attachment point for the exhaust line piping. Sandwiched between the two mating flanges was a 13 mm (0.5 in.) thick plate which served as a structural attachment for an internal 0.76 m (3 in.) diameter baffle pipe assembly (figure 4-5). The baffle served to improve liquid carryout separation and minimize liquid entrainment into the exhaust vapor. After passing through the upper plenum baffle pipe, the vapor and remaining water droplets were separated in the entrainment separator and the exhaust vapor flowed through a 0.10 m (4 in.) diameter flanged orifice section before exhausting to the atmosphere through an air-operated backpressure control valve. Piping upstream of the orifice section was heated with clamp-on strip heaters to assure single-phase steam flow measurement at the orifice plate. Steam probes were located in the exhaust line immediately upstream and downstream of the entrainment separator.

Although the exhaust line components were similar to those used in the 161-rod unblocked bundle facility, the piping size and arrangement was changed to ensure adequate flow capacity and avoid restraints imposed by the new facility location. Exhaust piping details are shown in figure C-18.

4-11. Coolant Injection System

The coolant injection system provided reflood water to quench the heater rod bundle. In brief, coolant injection water was supplied by two 0.757 m^3 (200 gal) water supply vessels through a series of flowmeters and valves. Nitrogen overpressure on the water supply tanks provided the necessary driving head to attain the required injection rates. A recirculation pump and immersion heater vessel were used to bring the water and injection piping to the

uniform specified temperature prior to testing. The two water supply tanks and an immersion heater vessel were existing components; piping from these components was modified to suit facility requirements.

Constant or stepped injection flow was accomplished by the proper sequencing of solenoid valves, which were located in a piping manifold arrangement. Flow to the test section was controlled by means of an air-operated valve, programmed through a demand signal from the computer with feedback supplied by the turbine flowmeter. Two turbine meters were used for flow measurement, one whose range was 3.8×10^{-5} to $3.8 \times 10^{-3} \text{ m}^3/\text{sec}$ (0.6 to 60 gal/min) for forced flooding tests, and one whose range was 9.5×10^{-5} to $9.5 \times 10^{-3} \text{ m}^3/\text{sec}$ (1.5 to 150 gal/min) for gravity reflood tests. A $1.27 \times 10^{-2} \text{ m}^3/\text{sec}$ (200 gal/min) bidirectional turbo-probe was installed in the downcomer crossover leg for gravity reflood tests to measure flow into the test section; however, the meter was found to be defective and could not be repaired prior to testing. Instead, flow into the test section was determined from a mass inventory in the downcomer and the known flooding rate into the downcomer.

4-12. Downcomer and Crossover Leg

The downcomer and crossover leg were connected to the test section lower plenum for gravity reflood tests. The downcomer and crossover leg were fabricated from 0.13 m (5 in.) diameter stainless steel pipe with a 90-degree-long radius elbow, a specially designed spool piece for insertion of the turbo-probe flowmeter, and a flexible stainless steel expansion joint. The expansion joint connected the crossover leg to the lower plenum and allowed for thermal growth of the test section relative to the downcomer. The horizontal crossover leg was 2.29 m (90 in.) long and the vertical downcomer was approximately 6.10 m (240 in.). A 0.38 m (1.5 in.) diameter nozzle located in the elbow of the downcomer was used to inject the coolant water from the water supply system. The downcomer and crossover leg piping are shown in figure C-19.

4-13. Facility Heating Boiler

The boiler was a Reimers Electric steam boiler with a steam capacity of approximately 1.51×10^{-3} kg/sec (125 lb/hr) at 100°C (212°F). The boiler was used to pressurize the facility and pretest facility heatup. This was accomplished by valving the boiler into the upper plenum of the test section.

A solenoid valve was used to isolate the boiler from the test facility at initiation of testing, at which time the steam generated in the test section in combination with the control valve in the exhaust line was sufficient to maintain facility pressure. The same boiler was used for the 21-rod bundle test program.

4-14. DATA ACQUISITION AND PROCESSING SYSTEM

Three types of systems monitored the instrumentation and recorded data on the FLECHT SEASET 163-rod blocked bundle test facility: a Computer Data Acquisition System (CDAS), the Fluke Data Logger, and five Texas Instruments strip-chart pen recorders.

4-15. Computer Data Acquisition System

The CDAS, the primary data collecting system used on the FLECHT SEASET facility, consisted of an SEL 32/77 minicomputer and A/D front end converters. The system could monitor, control, and record 576 channels of analog input data representing bundle and system temperatures, bundle powers, flows, and absolute and differential pressures.

The important control function included initiation and control of reflood flow and bundle power by means of D/A converter and computer contact closure outputs, termination of bundle power in the event of a heater rod overtemperature or bundle overpower condition, and termination of test when all thermocouples had reached a designated termination temperature.

Typically, each data channel was recorded once every second until flood, then once every half-second for 200 seconds, and then back to once every second

thereafter to a maximum of 2300 seconds. The computer was capable of storing approximately 2500 data scans for each of the 576 analog input channels.

The computer software had the following features:

- o A calibration file to convert raw data into engineering units
- o Local as well as remote (at the test loop) CRT console display capabilities which provided critical loop parameters during testing, such as hottest rod temperature, test section level, flooding rate, and bundle power
- o A preliminary data reduction program (DASTP.P) which transferred the raw data stored on disk to a magnetic tape, in a format compatible for entry into the Control Data Corporation 7600 computer
- o Posttest data reduction for analyzing and determining immediately whether a test performed according to specifications. Among these programs were a system mass balance program (MASBAL.B), a data validation program (DATVAL.B) which provided statistical information on key data channels, and a print/plot program (PRTPLT.P) which could either print or plot any desired data channel in engineering units.

Figure 4-6 shows the hardware interfaces of the CDAS.

4-16. Fluke Data Logger

The Fluke data logger had 60 channels of analog input used for monitoring loop heatup and to aid in equipment troubleshooting. The unit served primarily as backup to the computer and meters on the operator instrument and control console. The Fluke was utilized infrequently during the 163-rod blocked bundle test program.

4-17. Multiple-Pen Stripchart Recorders

Five Texas Instruments stripchart recorders were used to record bundle power; selected bundle steam probe and heater rod thermocouple readings; reflood turbine meter flows; accumulator, separator drain tank, housing, and carryover tank levels; and exhaust orifice and differential pressures. These recorders

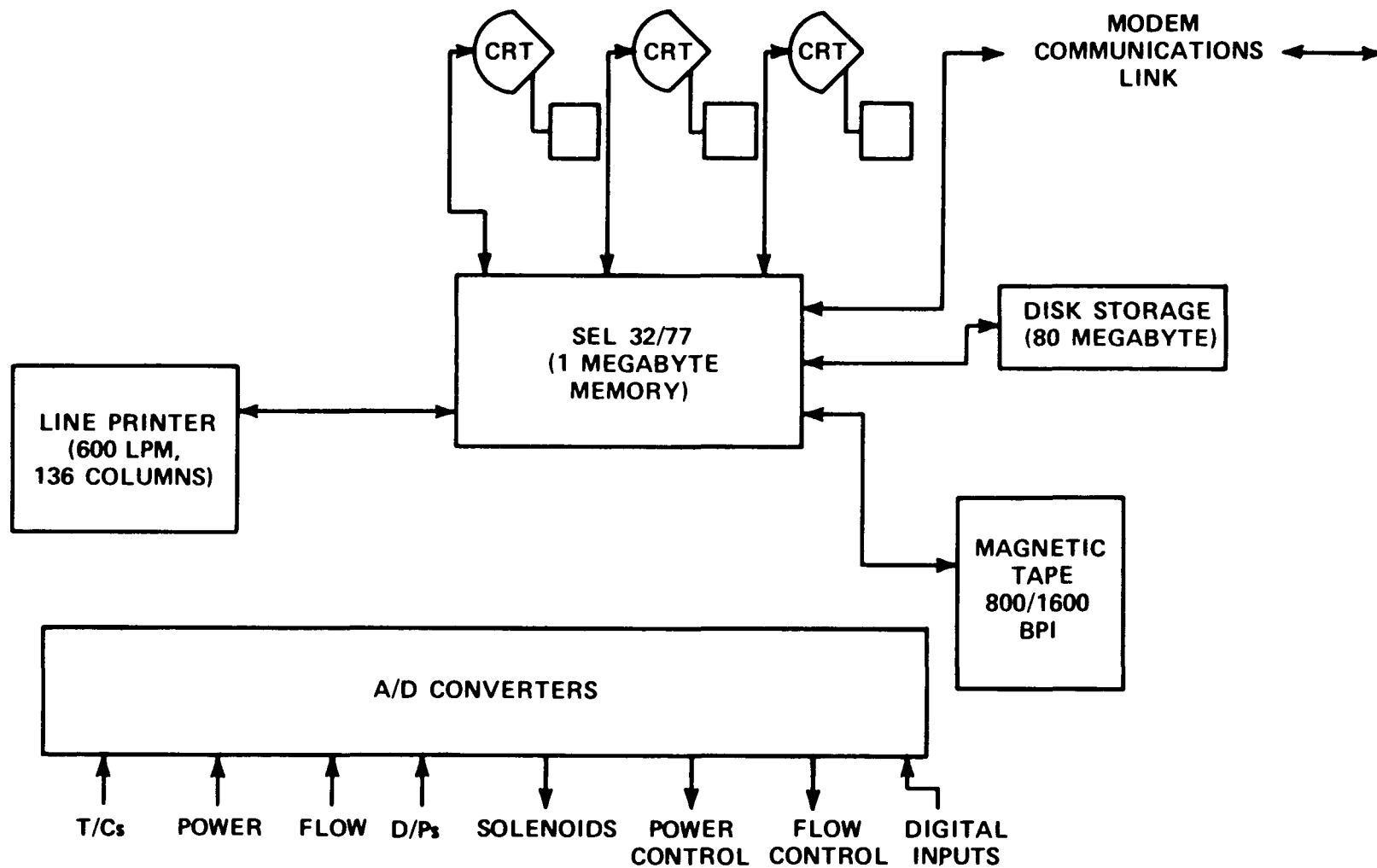


Figure 4-6. FLECHT SEASET Computer Hardware Interface for 163-Rod Blocked Bundle Facility

gave the loop operators and test directors immediate information on test progress and warning in the event of system anomalies. A single recorder indicating selected bundle aspirating steam probe temperatures was utilized during testing to indicate when thermocouples quenched, so that vent lines to ambient could be closed. The stripchart recorders were also utilized during facility heatup when the computer was not available.

4-18. INSTRUMENTATION

The instrumentation on the 163-rod blocked bundle facility was designed to measure temperature, power, flow, fluid level, and pressure. The temperature data were measured by type K, Chromel-Alumel, ungrounded thermocouples using 66°C (150°F) reference junctions.

Power input to the bundle heater rods was measured by Hall-effect watt transducers, which produced a direct current electrical output proportional to power input. The voltage and current input to the watt transducers was scaled down by transformers so that the range of the watt transducers matched the bundle power. The scaling factor of the transformers was accounted for when the raw data (millivolts) were converted to engineering units.

Reflood injection flow was measured by turbine meters. The turbine meter was connected to a preamplifier and flow rate monitor for conversion of turbine blade pulses into flow rate in engineering units. Calibration of the turbine meter by the manufacturer provided for data conversion to volumetric flows for the turbine meter analog signal.

System static and differential pressures were measured with Rosemount model 1151 pressure transmitters. The differential pressure transmitters measured water level in the vessels, bundle pressure drops, and pressure drops across orifice sections and other system components.

Standard thermocouple calibration table entries and the corresponding coefficients were used to compute the temperature values. All other channel calibration files were straight-line interpolations of calibration data. The slope, intercept, and zero for the least-squares fit of a straight line to the

equipment calibration data were computed for each channel and entered into its calibration file. The CDAS software used this straight-line formula to convert millivolts to engineering units.

4-19. Loop Instrumentation

Figure 4-7 shows schematically the forced and gravity reflood test loop instrumentation arrangement. Forty-seven computer channels were assigned to the collection of temperature, flow, and pressure data throughout the loop, exclusive of the instrumentation found in the upper and lower plenums and bundle.

The loop instrumentation, as listed in table 4-3 starting at channel 503, included 11 fluid and vapor thermocouples, 19 wall thermocouples, 3 turbine meters, 11 differential pressure cells, and 3 absolute pressure cells.

The 11 fluid thermocouples were placed in the water supply systems (channels 534 and 535), the injection line (channel 536), the exhaust line (channel 533), the carryover tank (channel 522), the steam separator (channel 526), the steam separator drain tank (channel 524), and in gravity reflood tests, the downcomer (channel 538) and the crossover leg (channel 537). The fluid thermocouples were utilized to measure the temperature of either stored or injected flow. Two thermocouples (channels 528 and 530) were utilized in aspirating steam probes placed in the elbows of the exhaust line on either side of the steam separator. These steam probes were designed to measure vapor nonequilibrium in the test section exit and the desuperheating effect of the steam separator. This steam probe was similar to that used in the 21-rod bundle test series.

The 19 wall thermocouples monitored by the computer were placed on the carryover tank (channel 523), steam separator (channel 527), steam separator drain tank (channel 525), exhaust line (channels 529, 531, and 532), and housing, and in gravity reflood tests, the crossover leg (channel 539). This instrumentation was utilized to control the heatup period such that initial component wall temperatures were at saturation and to estimate the heat release from the fluid to the loop components during the test. Nine housing wall thermocouples (channels 503-511) and three housing insulation thermocouples

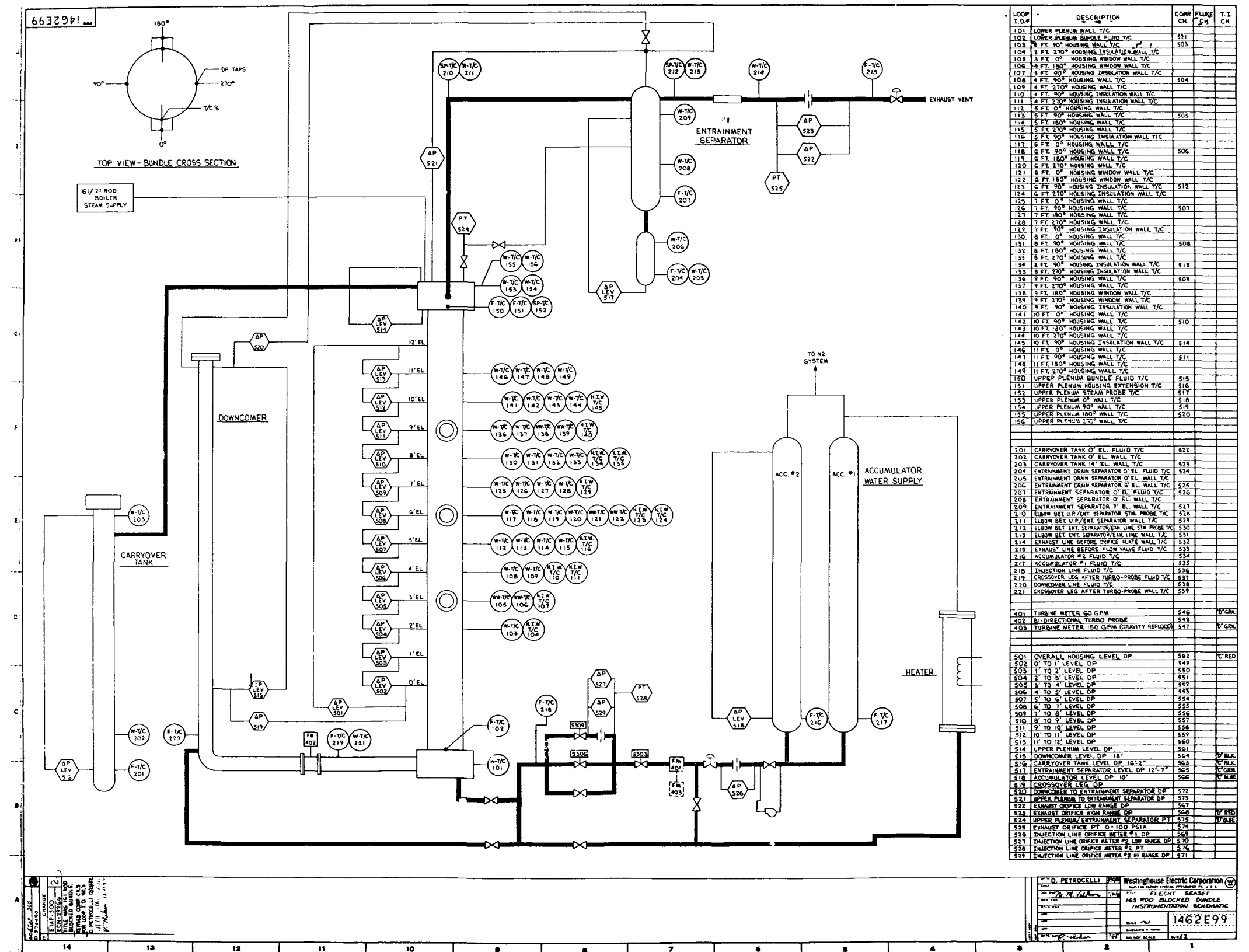


Figure 4-7. 163-Rod Blocked Bundle Task Loop Instrumentation



TABLE 4-3

BUNDLE INSTRUMENTATION LOCATIONS AND COMPUTER CHANNELS

1	BUNDLE	HEATER ROD	TEMPERATURE	HR-T/C	12.00	5J
2	BUNDLE	HEATER ROD	TEMPERATURE	HR-T/C	12.00	7B
3	BUNDLE	HEATER ROD	TEMPERATURE	HR-T/C	12.00	9G
4	BUNDLE	HEATER ROD	TEMPERATURE	HR-T/C	24.00	3J
5	BUNDLE	HEATER ROD	TEMPERATURE	HR-T/C	24.00	7B
6	BUNDLE	HEATER ROD	TEMPERATURE	HR-T/C	24.00	10H
7	BUNDLE	HEATER ROD	TEMPERATURE	HR-T/C	39.00	4J
8	BUNDLE	HEATER ROD	TEMPERATURE	HR-T/C	39.00	9C
9	BUNDLE	HEATER ROD	TEMPERATURE	HR-T/C	39.00	9G
10	BUNDLE	HEATER ROD	TEMPERATURE	HR-T/C	39.00	12F
11	BUNDLE	HEATER ROD	TEMPERATURE	HR-T/C	48.00	3J
12	BUNDLE	HEATER ROD	TEMPERATURE	HR-T/C	48.00	7H
13	BUNDLE	HEATER ROD	TEMPERATURE	HR-T/C	48.00	8K
14	BUNDLE	HEATER ROD	TEMPERATURE	HR-T/C	48.00	8N
15	BUNDLE	HEATER ROD	TEMPERATURE	HR-T/C	48.00	9L
16	BUNDLE	HEATER ROD	TEMPERATURE	HR-T/C	48.00	6E
17	BUNDLE	HEATER ROD	TEMPERATURE	HR-T/C	48.00	12D
18	BUNDLE	HEATER ROD	TEMPERATURE	HR-T/C	60.00	3H
19	BUNDLE	HEATER ROD	TEMPERATURE	HR-T/C	60.00	4J
20	BUNDLE	HEATER ROD	TEMPERATURE	HR-T/C	60.00	5E
21	BUNDLE	HEATER ROD	TEMPERATURE	HR-T/C	60.00	7G
22	BUNDLE	HEATER ROD	TEMPERATURE	HR-T/C	60.00	8D
23	BUNDLE	HEATER ROD	TEMPERATURE	HR-T/C	60.00	8K
24	BUNDLE	HEATER ROD	TEMPERATURE	HR-T/C	60.00	9G
25	BUNDLE	HEATER ROD	TEMPERATURE	HR-T/C	60.00	11I
26	BUNDLE	HEATER ROD	TEMPERATURE	HR-T/C	60.00	12F
27	BUNDLE	HEATER ROD	TEMPERATURE	HR-T/C	60.00	12L
28	BUNDLE	HEATER ROD	TEMPERATURE	HR-T/C	67.00	2I
29	BUNDLE	HEATER ROD	TEMPERATURE	HR-T/C	67.00	3H
30	BUNDLE	HEATER ROD	TEMPERATURE	HR-T/C	67.00	3J
31	BUNDLE	HEATER ROD	TEMPERATURE	HR-T/C	67.00	3K
32	BUNDLE	HEATER ROD	TEMPERATURE	HR-T/C	67.00	4J
33	BUNDLE	HEATER ROD	TEMPERATURE	HR-T/C	67.00	5E
34	BUNDLE	HEATER ROD	TEMPERATURE	HR-T/C	67.00	5F
35	BUNDLE	HEATER ROD	TEMPERATURE	HR-T/C	67.00	5H
36	BUNDLE	HEATER ROD	TEMPERATURE	HR-T/C	67.00	5H
37	BUNDLE	HEATER ROD	TEMPERATURE	HR-T/C	67.00	5I
38	BUNDLE	HEATER ROD	TEMPERATURE	HR-T/C	67.00	5M
39	BUNDLE	HEATER ROD	TEMPERATURE	HR-T/C	67.00	6D
40	BUNDLE	HEATER ROD	TEMPERATURE	HR-T/C	67.00	7B
41	BUNDLE	HEATER ROD	TEMPERATURE	HR-T/C	67.00	7D
42	BUNDLE	HEATER ROD	TEMPERATURE	HR-T/C	67.00	7G
43	BUNDLE	HEATER ROD	TEMPERATURE	HR-T/C	67.00	7K
44	BUNDLE	HEATER ROD	TEMPERATURE	HR-T/C	67.00	8E
45	BUNDLE	HEATER ROD	TEMPERATURE	HR-T/C	67.00	8G
46	BUNDLE	HEATER ROD	TEMPERATURE	HR-T/C	67.00	9G
47	BUNDLE	HEATER ROD	TEMPERATURE	HR-T/C	67.00	9K
48	BUNDLE	HEATER ROD	TEMPERATURE	HR-T/C	67.00	11I

TABLE 4-3 (cont)

BUNDLE INSTRUMENTATION LOCATIONS AND COMPUTER CHANNELS

49	BUNDLE	HEATER ROD	TEMPERATURE	HR-T/C	67.00	11K
50	BUNDLE	HEATER ROD	TEMPERATURE	HR-T/C	69.00	6J
51	BUNDLE	HEATER ROD	TEMPERATURE	HR-T/C	69.00	9F
52	BUNDLE	HEATER ROD	TEMPERATURE	HR-T/C	69.00	9H
53	BUNDLE	HEATER ROD	TEMPERATURE	HR-T/C	69.00	12F
54	BUNDLE	HEATER ROD	TEMPERATURE	HR-T/C	69.00	5J
55	BUNDLE	HEATER ROD	TEMPERATURE	HR-T/C	69.00	11J
56	BUNDLE	HEATER ROD	TEMPERATURE	HR-T/C	69.00	13H
57	BUNDLE	HEATER ROD	TEMPERATURE	HR-T/C	70.00	3K
58	BUNDLE	HEATER ROD	TEMPERATURE	HR-T/C	70.00	6L
59	BUNDLE	HEATER ROD	TEMPERATURE	HR-T/C	70.00	7G
60	BUNDLE	HEATER ROD	TEMPERATURE	HR-T/C	70.00	11C
61	BUNDLE	HEATER ROD	TEMPERATURE	HR-T/C	70.00	13G
62	BUNDLE	HEATER ROD	TEMPERATURE	HR-T/C	71.00	7F
63	BUNDLE	HEATER ROD	TEMPERATURE	HR-T/C	71.00	10J
64	BUNDLE	HEATER ROD	TEMPERATURE	HR-T/C	71.00	4G
65	BUNDLE	HEATER ROD	TEMPERATURE	HR-T/C	71.00	11C
66	BUNDLE	HEATER ROD	TEMPERATURE	HR-T/C	72.00	7M
67	BUNDLE	HEATER ROD	TEMPERATURE	HR-T/C	72.00	2I
68	BUNDLE	HEATER ROD	TEMPERATURE	HR-T/C	72.00	3H
69	BUNDLE	HEATER ROD	TEMPERATURE	HR-T/C	72.00	3J
70	BUNDLE	HEATER ROD	TEMPERATURE	HR-T/C	72.00	5D
71	BUNDLE	HEATER ROD	TEMPERATURE	HR-T/C	72.00	5H
72	BUNDLE	HEATER ROD	TEMPERATURE	HR-T/C	72.00	5I
73	BUNDLE	HEATER ROD	TEMPERATURE	HR-T/C	72.00	5M
74	BUNDLE	HEATER ROD	TEMPERATURE	HR-T/C	72.00	6J
75	BUNDLE	HEATER ROD	TEMPERATURE	HR-T/C	72.00	6L
76	BUNDLE	HEATER ROD	TEMPERATURE	HR-T/C	72.00	9D
77	BUNDLE	HEATER ROD	TEMPERATURE	HR-T/C	72.00	9K
78	BUNDLE	HEATER ROD	TEMPERATURE	HR-T/C	72.00	9M
79	BUNDLE	HEATER ROD	TEMPERATURE	HR-T/C	72.00	10I
80	BUNDLE	HEATER ROD	TEMPERATURE	HR-T/C	72.00	11E
81	BUNDLE	HEATER ROD	TEMPERATURE	HR-T/C	72.00	12L
82	BUNDLE	HEATER ROD	TEMPERATURE	HR-T/C	73.00	5L
83	BUNDLE	HEATER ROD	TEMPERATURE	HR-T/C	73.00	7B
84	BUNDLE	HEATER ROD	TEMPERATURE	HR-T/C	73.00	7D
85	BUNDLE	HEATER ROD	TEMPERATURE	HR-T/C	73.00	8K
86	BUNDLE	HEATER ROD	TEMPERATURE	HR-T/C	73.00	8N
87	BUNDLE	HEATER ROD	TEMPERATURE	HR-T/C	73.00	11F
88	BUNDLE	HEATER ROD	TEMPERATURE	HR-T/C	73.00	3K
89	BUNDLE	HEATER ROD	TEMPERATURE	HR-T/C	73.00	4J
90	BUNDLE	HEATER ROD	TEMPERATURE	HR-T/C	73.00	7K
91	BUNDLE	HEATER ROD	TEMPERATURE	HR-T/C	73.00	9D
92	BUNDLE	HEATER ROD	TEMPERATURE	HR-T/C	73.00	12D
93	BUNDLE	HEATER ROD	TEMPERATURE	HR-T/C	73.00	4G
94	BUNDLE	HEATER ROD	TEMPERATURE	HR-T/C	73.00	11C
95	BUNDLE	HEATER ROD	TEMPERATURE	HR-T/C	73.00	11J
96	BUNDLE	HEATER ROD	TEMPERATURE	HR-T/C	74.00	7M

TABLE 4-3 (cont)
BUNDLE INSTRUMENTATION LOCATIONS AND COMPUTER CHANNELS

97	BUNDLE	HEATER ROD	TEMPERATURE	HR-T/C	74.00	8H
98	BUNDLE	HEATER ROD	TEMPERATURE	HR-T/C	74.00	3J
99	BUNDLE	HEATER ROD	TEMPERATURE	HR-T/C	74.00	5H
100	BUNDLE	HEATER ROD	TEMPERATURE	HR-T/C	74.00	5J
101	BUNDLE	HEATER ROD	TEMPERATURE	HR-T/C	74.00	5M
102	BUNDLE	HEATER ROD	TEMPERATURE	HR-T/C	74.00	6G
103	BUNDLE	HEATER ROD	TEMPERATURE	HR-T/C	74.00	6L
104	BUNDLE	HEATER ROD	TEMPERATURE	HR-T/C	74.00	9D
105	BUNDLE	HEATER ROD	TEMPERATURE	HR-T/C	74.00	9E
106	BUNDLE	HEATER ROD	TEMPERATURE	HR-T/C	74.00	9J
107	BUNDLE	HEATER ROD	TEMPERATURE	HR-T/C	74.00	11E
108	BUNDLE	HEATER ROD	TEMPERATURE	HR-T/C	74.00	13G
109	BUNDLE	HEATER ROD	TEMPERATURE	HR-T/C	74.00	13H
110	BUNDLE	HEATER ROD	TEMPERATURE	HR-T/C	74.00	4G
111	BUNDLE	HEATER ROD	TEMPERATURE	HR-T/C	75.00	8H
112	BUNDLE	HEATER ROD	TEMPERATURE	HR-T/C	75.00	9C
113	BUNDLE	HEATER ROD	TEMPERATURE	HR-T/C	75.00	11F
114	BUNDLE	HEATER ROD	TEMPERATURE	HR-T/C	75.00	12D
115	BUNDLE	HEATER ROD	TEMPERATURE	HR-T/C	75.00	3K
116	BUNDLE	HEATER ROD	TEMPERATURE	HR-T/C	75.00	4J
117	BUNDLE	HEATER ROD	TEMPERATURE	HR-T/C	75.00	6E
118	BUNDLE	HEATER ROD	TEMPERATURE	HR-T/C	75.00	6H
119	BUNDLE	HEATER ROD	TEMPERATURE	HR-T/C	75.00	7K
120	BUNDLE	HEATER ROD	TEMPERATURE	HR-T/C	75.00	8J
121	BUNDLE	HEATER ROD	TEMPERATURE	HR-T/C	75.00	9D
122	BUNDLE	HEATER ROD	TEMPERATURE	HR-T/C	75.00	9L
123	BUNDLE	HEATER ROD	TEMPERATURE	HR-T/C	75.00	9M
124	BUNDLE	HEATER ROD	TEMPERATURE	HR-T/C	75.00	4G
125	BUNDLE	HEATER ROD	TEMPERATURE	HR-T/C	75.00	5M
126	BUNDLE	HEATER ROD	TEMPERATURE	HR-T/C	75.00	6D
127	BUNDLE	HEATER ROD	TEMPERATURE	HR-T/C	75.00	11C
128	BUNDLE	HEATER ROD	TEMPERATURE	HR-T/C	75.00	11J
129	BUNDLE	HEATER ROD	TEMPERATURE	HR-T/C	75.00	12L
130	BUNDLE	HEATER ROD	TEMPERATURE	HR-T/C	60.00	5I
131	BUNDLE	HEATER ROD	TEMPERATURE	HR-T/C	76.00	6G
132	BUNDLE	HEATER ROD	TEMPERATURE	HR-T/C	76.00	8N
133	BUNDLE	HEATER ROD	TEMPERATURE	HR-T/C	76.00	10I
134	BUNDLE	HEATER ROD	TEMPERATURE	HR-T/C	76.00	11H
135	BUNDLE	HEATER ROD	TEMPERATURE	HR-T/C	76.00	12D
136	BUNDLE	HEATER ROD	TEMPERATURE	HR-T/C	76.00	2I
137	BUNDLE	HEATER ROD	TEMPERATURE	HR-T/C	76.00	3H
138	BUNDLE	HEATER ROD	TEMPERATURE	HR-T/C	76.00	5D
139	BUNDLE	HEATER ROD	TEMPERATURE	HR-T/C	76.00	5I
140	BUNDLE	HEATER ROD	TEMPERATURE	HR-T/C	76.00	5J
141	BUNDLE	HEATER ROD	TEMPERATURE	HR-T/C	76.00	6J
142	BUNDLE	HEATER ROD	TEMPERATURE	HR-T/C	76.00	8J
143	BUNDLE	HEATER ROD	TEMPERATURE	HR-T/C	76.00	9D
144	BUNDLE	HEATER ROD	TEMPERATURE	HR-T/C	76.00	11E

TABLE 4-3 (cont)

BUNDLE INSTRUMENTATION LOCATIONS AND COMPUTER CHANNELS

145	BUNDLE	HEATER ROD	TEMPERATURE	HR-T/C	76.00	13G
146	BUNDLE	HEATER ROD	TEMPERATURE	HR-T/C	77.00	6L
147	BUNDLE	HEATER ROD	TEMPERATURE	HR-T/C	77.00	7D
148	BUNDLE	HEATER ROD	TEMPERATURE	HR-T/C	77.00	8E
149	BUNDLE	HEATER ROD	TEMPERATURE	HR-T/C	77.00	8H
150	BUNDLE	HEATER ROD	TEMPERATURE	HR-T/C	77.00	9C
151	BUNDLE	HEATER ROD	TEMPERATURE	HR-T/C	77.00	9K
152	BUNDLE	HEATER ROD	TEMPERATURE	HR-T/C	77.00	11G
153	BUNDLE	HEATER ROD	TEMPERATURE	HR-T/C	77.00	12I
154	BUNDLE	HEATER ROD	TEMPERATURE	HR-T/C	77.00	3J
155	BUNDLE	HEATER ROD	TEMPERATURE	HR-T/C	77.00	5D
156	BUNDLE	HEATER ROD	TEMPERATURE	HR-T/C	77.00	5H
157	BUNDLE	HEATER ROD	TEMPERATURE	HR-T/C	48.00	8E
158	BUNDLE	HEATER ROD	TEMPERATURE	HR-T/C	77.00	6G
159	BUNDLE	HEATER ROD	TEMPERATURE	HR-T/C	77.00	6H
160	BUNDLE	HEATER ROD	TEMPERATURE	HR-T/C	77.00	7H
161	BUNDLE	HEATER ROD	TEMPERATURE	HR-T/C	77.00	8D
162	BUNDLE	HEATER ROD	TEMPERATURE	HR-T/C	77.00	8J
163	BUNDLE	HEATER ROD	TEMPERATURE	HR-T/C	77.00	9D
164	BUNDLE	HEATER ROD	TEMPERATURE	HR-T/C	77.00	9E
165	BUNDLE	HEATER ROD	TEMPERATURE	HR-T/C	77.00	9J
166	BUNDLE	HEATER ROD	TEMPERATURE	HR-T/C	77.00	9M
167	BUNDLE	HEATER ROD	TEMPERATURE	HR-T/C	77.00	4G
168	BUNDLE	HEATER ROD	TEMPERATURE	HR-T/C	77.00	6D
169	BUNDLE	HEATER ROD	TEMPERATURE	HR-T/C	77.00	11C
170	BUNDLE	HEATER ROD	TEMPERATURE	HR-T/C	77.00	11J
171	BUNDLE	HEATER ROD	TEMPERATURE	HR-T/C	78.00	7M
172	BUNDLE	HEATER ROD	TEMPERATURE	HR-T/C	78.00	9H
173	BUNDLE	HEATER ROD	TEMPERATURE	HR-T/C	78.00	11F
174	BUNDLE	HEATER ROD	TEMPERATURE	HR-T/C	78.00	8H
175	BUNDLE	HEATER ROD	TEMPERATURE	HR-T/C	78.00	8N
176	BUNDLE	HEATER ROD	TEMPERATURE	HR-T/C	78.00	9F
177	BUNDLE	HEATER ROD	TEMPERATURE	HR-T/C	78.00	9K
178	BUNDLE	HEATER ROD	TEMPERATURE	HR-T/C	78.00	10H
179	BUNDLE	HEATER ROD	TEMPERATURE	HR-T/C	78.00	11H
180	BUNDLE	HEATER ROD	TEMPERATURE	HR-T/C	78.00	12I
181	BUNDLE	HEATER ROD	TEMPERATURE	HR-T/C	78.00	2I
182	BUNDLE	HEATER ROD	TEMPERATURE	HR-T/C	78.00	3H
183	BUNDLE	HEATER ROD	TEMPERATURE	HR-T/C	78.00	3K
184	BUNDLE	HEATER ROD	TEMPERATURE	HR-T/C	78.00	5D
185	BUNDLE	HEATER ROD	TEMPERATURE	HR-T/C	78.00	5E
186	BUNDLE	HEATER ROD	TEMPERATURE	HR-T/C	78.00	5F
187	BUNDLE	HEATER ROD	TEMPERATURE	HR-T/C	78.00	6J
188	BUNDLE	HEATER ROD	TEMPERATURE	HR-T/C	78.00	6L
189	BUNDLE	HEATER ROD	TEMPERATURE	HR-T/C	78.00	7E
190	BUNDLE	HEATER ROD	TEMPERATURE	HR-T/C	78.00	7H
191	BUNDLE	HEATER ROD	TEMPERATURE	HR-T/C	78.00	7K
192	BUNDLE	HEATER ROD	TEMPERATURE	HR-T/C	78.00	8J

TABLE 4-3 (cont)
BUNDLE INSTRUMENTATION LOCATIONS AND COMPUTER CHANNELS

193	BUNDLE	HEATER	ROD	TEMPERATURE	HR-T/C	78.00	9D
194	BUNDLE	HEATER	ROD	TEMPERATURE	HR-T/C	78.00	9E
195	BUNDLE	HEATER	ROD	TEMPERATURE	HR-T/C	78.00	9J
196	BUNDLE	HEATER	ROD	TEMPERATURE	HR-T/C	78.00	9L
197	BUNDLE	HEATER	ROD	TEMPERATURE	HR-T/C	78.00	11K
198	BUNDLE	HEATER	ROD	TEMPERATURE	HR-T/C	78.00	12L
199	BUNDLE	HEATER	ROD	TEMPERATURE	HR-T/C	78.00	13G
200	BUNDLE	HEATER	ROD	TEMPERATURE	HR-T/C	78.00	11J
201	BUNDLE	HEATER	ROD	TEMPERATURE	HR-T/C	79.00	5L
202	BUNDLE	HEATER	ROD	TEMPERATURE	HR-T/C	79.00	6G
203	BUNDLE	HEATER	ROD	TEMPERATURE	HR-T/C	79.00	7D
204	BUNDLE	HEATER	ROD	TEMPERATURE	HR-T/C	79.00	8E
205	BUNDLE	HEATER	ROD	TEMPERATURE	HR-T/C	79.00	8G
206	BUNDLE	HEATER	ROD	TEMPERATURE	HR-T/C	79.00	8K
207	BUNDLE	HEATER	ROD	TEMPERATURE	HR-T/C	79.00	9C
208	BUNDLE	HEATER	ROD	TEMPERATURE	HR-T/C	79.00	9F
209	BUNDLE	HEATER	ROD	TEMPERATURE	HR-T/C	79.00	9G
210	BUNDLE	HEATER	ROD	TEMPERATURE	HR-T/C	79.00	9K
211	BUNDLE	HEATER	ROD	TEMPERATURE	HR-T/C	79.00	10H
212	BUNDLE	HEATER	ROD	TEMPERATURE	HR-T/C	79.00	11G
213	BUNDLE	HEATER	ROD	TEMPERATURE	HR-T/C	79.00	11H
214	BUNDLE	HEATER	ROD	TEMPERATURE	HR-T/C	79.00	12D
215	BUNDLE	HEATER	ROD	TEMPERATURE	HR-T/C	79.00	12F
216	BUNDLE	HEATER	ROD	TEMPERATURE	HR-T/C	79.00	12I
217	BUNDLE	HEATER	ROD	TEMPERATURE	HR-T/C	79.00	5F
218	BUNDLE	HEATER	ROD	TEMPERATURE	HR-T/C	79.00	6E
219	BUNDLE	HEATER	ROD	TEMPERATURE	HR-T/C	79.00	9L
220	BUNDLE	HEATER	ROD	TEMPERATURE	HR-T/C	79.00	11I
221	BUNDLE	HEATER	ROD	TEMPERATURE	HR-T/C	79.00	13H
222	BUNDLE	HEATER	ROD	TEMPERATURE	HR-T/C	79.00	6D
223	BUNDLE	HEATER	ROD	TEMPERATURE	HR-T/C	79.00	11C
224	BUNDLE	HEATER	ROD	TEMPERATURE	HR-T/C	80.00	7M
225	BUNDLE	HEATER	ROD	TEMPERATURE	HR-T/C	80.00	9H
226	BUNDLE	HEATER	ROD	TEMPERATURE	HR-T/C	60.00	11E
227	BUNDLE	HEATER	ROD	TEMPERATURE	HR-T/C	80.00	7F
228	BUNDLE	HEATER	ROD	TEMPERATURE	HR-T/C	80.00	9F
229	BUNDLE	HEATER	ROD	TEMPERATURE	HR-T/C	80.00	10J
230	BUNDLE	HEATER	ROD	TEMPERATURE	HR-T/C	80.00	2I
231	BUNDLE	HEATER	ROD	TEMPERATURE	HR-T/C	80.00	3H
232	BUNDLE	HEATER	ROD	TEMPERATURE	HR-T/C	80.00	3J
233	BUNDLE	HEATER	ROD	TEMPERATURE	HR-T/C	80.00	5F
234	BUNDLE	HEATER	ROD	TEMPERATURE	HR-T/C	80.00	5H
235	BUNDLE	HEATER	ROD	TEMPERATURE	HR-T/C	80.00	5M
236	BUNDLE	HEATER	ROD	TEMPERATURE	HR-T/C	80.00	6H
237	BUNDLE	HEATER	ROD	TEMPERATURE	HR-T/C	80.00	6J
238	BUNDLE	HEATER	ROD	TEMPERATURE	HR-T/C	80.00	7E
239	BUNDLE	HEATER	ROD	TEMPERATURE	HR-T/C	80.00	7G
240	BUNDLE	HEATER	ROD	TEMPERATURE	HR-T/C	80.00	8D

TABLE 4-3 (cont)
BUNDLE INSTRUMENTATION LOCATIONS AND COMPUTER CHANNELS

241	BUNDLE	HEATER	ROD	TEMPERATURE	HR-T/C	80.00	9D
242	BUNDLE	HEATER	ROD	TEMPERATURE	HR-T/C	80.00	9E
243	BUNDLE	HEATER	ROD	TEMPERATURE	HR-T/C	80.00	9J
244	BUNDLE	HEATER	ROD	TEMPERATURE	HR-T/C	80.00	9M
245	BUNDLE	HEATER	ROD	TEMPERATURE	HR-T/C	80.00	10I
246	BUNDLE	HEATER	ROD	TEMPERATURE	HR-T/C	80.00	11K
247	BUNDLE	HEATER	ROD	TEMPERATURE	HR-T/C	80.00	12L
248	BUNDLE	HEATER	ROD	TEMPERATURE	HR-T/C	80.00	13H
249	BUNDLE	HEATER	ROD	TEMPERATURE	HR-T/C	81.00	5E
250	BUNDLE	HEATER	ROD	TEMPERATURE	HR-T/C	81.00	5L
251	BUNDLE	HEATER	ROD	TEMPERATURE	HR-T/C	81.00	6L
252	BUNDLE	HEATER	ROD	TEMPERATURE	HR-T/C	81.00	7D
253	BUNDLE	HEATER	ROD	TEMPERATURE	HR-T/C	81.00	7F
254	BUNDLE	HEATER	ROD	TEMPERATURE	HR-T/C	81.00	8G
255	BUNDLE	HEATER	ROD	TEMPERATURE	HR-T/C	81.00	8N
256	BUNDLE	HEATER	ROD	TEMPERATURE	HR-T/C	81.00	10J
257	BUNDLE	HEATER	ROD	TEMPERATURE	HR-T/C	81.00	11G
258	BUNDLE	HEATER	ROD	TEMPERATURE	HR-T/C	81.00	11I
259	BUNDLE	HEATER	ROD	TEMPERATURE	HR-T/C	81.00	12I
260	BUNDLE	HEATER	ROD	TEMPERATURE	HR-T/C	84.00	9H
261	BUNDLE	HEATER	ROD	TEMPERATURE	HR-T/C	84.00	4G
262	BUNDLE	HEATER	ROD	TEMPERATURE	HR-T/C	84.00	4J
263	BUNDLE	HEATER	ROD	TEMPERATURE	HR-T/C	84.00	5M
264	BUNDLE	HEATER	ROD	TEMPERATURE	HR-T/C	84.00	7E
265	BUNDLE	HEATER	ROD	TEMPERATURE	HR-T/C	84.00	7G
266	BUNDLE	HEATER	ROD	TEMPERATURE	HR-T/C	84.00	7K
267	BUNDLE	HEATER	ROD	TEMPERATURE	HR-T/C	84.00	9L
268	BUNDLE	HEATER	ROD	TEMPERATURE	HR-T/C	84.00	11E
269	BUNDLE	HEATER	ROD	TEMPERATURE	HR-T/C	84.00	12I
270	BUNDLE	HEATER	ROD	TEMPERATURE	HR-T/C	84.00	13G
271	BUNDLE	HEATER	ROD	TEMPERATURE	HR-T/C	86.00	7D
272	BUNDLE	HEATER	ROD	TEMPERATURE	HR-T/C	86.00	8G
273	BUNDLE	HEATER	ROD	TEMPERATURE	HR-T/C	86.00	9C
274	BUNDLE	HEATER	ROD	TEMPERATURE	HR-T/C	86.00	10H
275	BUNDLE	HEATER	ROD	TEMPERATURE	HR-T/C	86.00	11J
276	BUNDLE	HEATER	ROD	TEMPERATURE	HR-T/C	86.00	2I
277	BUNDLE	HEATER	ROD	TEMPERATURE	HR-T/C	86.00	3H
278	BUNDLE	HEATER	ROD	TEMPERATURE	HR-T/C	86.00	5E
279	BUNDLE	HEATER	ROD	TEMPERATURE	HR-T/C	86.00	5F
280	BUNDLE	HEATER	ROD	TEMPERATURE	HR-T/C	86.00	5I
281	BUNDLE	HEATER	ROD	TEMPERATURE	HR-T/C	86.00	6D
282	BUNDLE	HEATER	ROD	TEMPERATURE	HR-T/C	86.00	6H
283	BUNDLE	HEATER	ROD	TEMPERATURE	HR-T/C	86.00	7F
284	BUNDLE	HEATER	ROD	TEMPERATURE	HR-T/C	86.00	7H
285	BUNDLE	HEATER	ROD	TEMPERATURE	HR-T/C	86.00	8N
286	BUNDLE	HEATER	ROD	TEMPERATURE	HR-T/C	86.00	9E
287	BUNDLE	HEATER	ROD	TEMPERATURE	HR-T/C	86.00	9F
288	BUNDLE	HEATER	ROD	TEMPERATURE	HR-T/C	86.00	9H

TABLE 4-3 (cont)

BUNDLE INSTRUMENTATION LOCATIONS AND COMPUTER CHANNELS

289	BUNDLE	HEATER ROD	TEMPERATURE	HR-T/C	86.00	9J
290	BUNDLE	HEATER ROD	TEMPERATURE	HR-T/C	86.00	9M
291	BUNDLE	HEATER ROD	TEMPERATURE	HR-T/C	86.00	10I
292	BUNDLE	HEATER ROD	TEMPERATURE	HR-T/C	86.00	10J
293	BUNDLE	HEATER ROD	TEMPERATURE	HR-T/C	86.00	11C
294	BUNDLE	HEATER ROD	TEMPERATURE	HR-T/C	86.00	11G
295	BUNDLE	HEATER ROD	TEMPERATURE	HR-T/C	86.00	3H
296	BUNDLE	HEATER ROD	TEMPERATURE	HR-T/C	86.00	3H
297	BUNDLE	HEATER ROD	TEMPERATURE	HR-T/C	90.00	2I
298	BUNDLE	HEATER ROD	TEMPERATURE	HR-T/C	90.00	3H
299	BUNDLE	HEATER ROD	TEMPERATURE	HR-T/C	90.00	3K
300	BUNDLE	HEATER ROD	TEMPERATURE	HR-T/C	90.00	4G
301	BUNDLE	HEATER ROD	TEMPERATURE	HR-T/C	90.00	4J
302	BUNDLE	HEATER ROD	TEMPERATURE	HR-T/C	90.00	5F
303	BUNDLE	HEATER ROD	TEMPERATURE	HR-T/C	90.00	5I
304	BUNDLE	HEATER ROD	TEMPERATURE	HR-T/C	90.00	6D
305	BUNDLE	HEATER ROD	TEMPERATURE	HR-T/C	90.00	6E
306	BUNDLE	HEATER ROD	TEMPERATURE	HR-T/C	90.00	6G
307	BUNDLE	HEATER ROD	TEMPERATURE	HR-T/C	90.00	6H
308	BUNDLE	HEATER ROD	TEMPERATURE	HR-T/C	90.00	6J
309	BUNDLE	HEATER ROD	TEMPERATURE	HR-T/C	90.00	7D
310	BUNDLE	HEATER ROD	TEMPERATURE	HR-T/C	90.00	7E
311	BUNDLE	HEATER ROD	TEMPERATURE	HR-T/C	90.00	7F
312	BUNDLE	HEATER ROD	TEMPERATURE	HR-T/C	90.00	7G
313	BUNDLE	HEATER ROD	TEMPERATURE	HR-T/C	90.00	7K
314	BUNDLE	HEATER ROD	TEMPERATURE	HR-T/C	90.00	8E
315	BUNDLE	HEATER ROD	TEMPERATURE	HR-T/C	90.00	8G
316	BUNDLE	HEATER ROD	TEMPERATURE	HR-T/C	90.00	8J
317	BUNDLE	HEATER ROD	TEMPERATURE	HR-T/C	90.00	9C
318	BUNDLE	HEATER ROD	TEMPERATURE	HR-T/C	90.00	9E
319	BUNDLE	HEATER ROD	TEMPERATURE	HR-T/C	90.00	9G
320	BUNDLE	HEATER ROD	TEMPERATURE	HR-T/C	90.00	9H
321	BUNDLE	HEATER ROD	TEMPERATURE	HR-T/C	90.00	9J
322	BUNDLE	HEATER ROD	TEMPERATURE	HR-T/C	90.00	9K
323	BUNDLE	HEATER ROD	TEMPERATURE	HR-T/C	90.00	10H
324	BUNDLE	HEATER ROD	TEMPERATURE	HR-T/C	90.00	10J
325	BUNDLE	HEATER ROD	TEMPERATURE	HR-T/C	90.00	11E
326	BUNDLE	HEATER ROD	TEMPERATURE	HR-T/C	90.00	11F
327	BUNDLE	HEATER ROD	TEMPERATURE	HR-T/C	90.00	11G
328	BUNDLE	HEATER ROD	TEMPERATURE	HR-T/C	90.00	11H
329	BUNDLE	HEATER ROD	TEMPERATURE	HR-T/C	90.00	11I
330	BUNDLE	HEATER ROD	TEMPERATURE	HR-T/C	90.00	12D
331	BUNDLE	HEATER ROD	TEMPERATURE	HR-T/C	90.00	12I
332	BUNDLE	HEATER ROD	TEMPERATURE	HR-T/C	96.00	3K
333	BUNDLE	HEATER ROD	TEMPERATURE	HR-T/C	96.00	4G
334	BUNDLE	HEATER ROD	TEMPERATURE	HR-T/C	96.00	5D
335	BUNDLE	HEATER ROD	TEMPERATURE	HR-T/C	96.00	5F
336	BUNDLE	HEATER ROD	TEMPERATURE	HR-T/C	96.00	5I

TABLE 4-3 (cont)

BUNDLE INSTRUMENTATION LOCATIONS AND COMPUTER CHANNELS

337	BUNDLE	HEATER	ROD	TEMPERATURE	HR-T/C	96.00	5L
338	BUNDLE	HEATER	ROD	TEMPERATURE	HR-T/C	96.00	6D
339	BUNDLE	HEATER	ROD	TEMPERATURE	HR-T/C	96.00	6G
340	BUNDLE	HEATER	ROD	TEMPERATURE	HR-T/C	96.00	6L
341	BUNDLE	HEATER	ROD	TEMPERATURE	HR-T/C	96.00	7D
342	BUNDLE	HEATER	ROD	TEMPERATURE	HR-T/C	96.00	7E
343	BUNDLE	HEATER	ROD	TEMPERATURE	HR-T/C	96.00	7F
344	BUNDLE	HEATER	ROD	TEMPERATURE	HR-T/C	96.00	7G
345	BUNDLE	HEATER	ROD	TEMPERATURE	HR-T/C	96.00	7H
346	BUNDLE	HEATER	ROD	TEMPERATURE	HR-T/C	96.00	7K
347	BUNDLE	HEATER	ROD	TEMPERATURE	HR-T/C	96.00	7M
348	BUNDLE	HEATER	ROD	TEMPERATURE	HR-T/C	96.00	8D
349	BUNDLE	HEATER	ROD	TEMPERATURE	HR-T/C	96.00	8E
350	BUNDLE	HEATER	ROD	TEMPERATURE	HR-T/C	96.00	8N
351	BUNDLE	HEATER	ROD	TEMPERATURE	HR-T/C	96.00	9E
352	BUNDLE	HEATER	ROD	TEMPERATURE	HR-T/C	96.00	9H
353	BUNDLE	HEATER	ROD	TEMPERATURE	HR-T/C	96.00	9J
354	BUNDLE	HEATER	ROD	TEMPERATURE	HR-T/C	96.00	9K
355	BUNDLE	HEATER	ROD	TEMPERATURE	HR-T/C	96.00	9L
356	BUNDLE	HEATER	ROD	TEMPERATURE	HR-T/C	96.00	9M
357	BUNDLE	HEATER	ROD	TEMPERATURE	HR-T/C	96.00	10H
358	BUNDLE	HEATER	ROD	TEMPERATURE	HR-T/C	96.00	10I
359	BUNDLE	HEATER	ROD	TEMPERATURE	HR-T/C	96.00	10J
360	BUNDLE	HEATER	ROD	TEMPERATURE	HR-T/C	96.00	11C
361	BUNDLE	HEATER	ROD	TEMPERATURE	HR-T/C	96.00	11F
362	BUNDLE	HEATER	ROD	TEMPERATURE	HR-T/C	96.00	11J
363	BUNDLE	HEATER	ROD	TEMPERATURE	HR-T/C	96.00	12D
364	BUNDLE	HEATER	ROD	TEMPERATURE	HR-T/C	96.00	12I
365	BUNDLE	HEATER	ROD	TEMPERATURE	HR-T/C	96.00	13G
366	BUNDLE	HEATER	ROD	TEMPERATURE	HR-T/C	102.00	5J
367	BUNDLE	HEATER	ROD	TEMPERATURE	HR-T/C	102.00	6E
368	BUNDLE	HEATER	ROD	TEMPERATURE	HR-T/C	102.00	7B
369	BUNDLE	HEATER	ROD	TEMPERATURE	HR-T/C	102.00	7H
370	BUNDLE	HEATER	ROD	TEMPERATURE	HR-T/C	102.00	8D
371	BUNDLE	HEATER	ROD	TEMPERATURE	HR-T/C	102.00	8G
372	BUNDLE	HEATER	ROD	TEMPERATURE	HR-T/C	102.00	8J
373	BUNDLE	HEATER	ROD	TEMPERATURE	HR-T/C	102.00	9L
374	BUNDLE	HEATER	ROD	TEMPERATURE	HR-T/C	102.00	11H
375	BUNDLE	HEATER	ROD	TEMPERATURE	HR-T/C	102.00	11K
376	BUNDLE	HEATER	ROD	TEMPERATURE	HR-T/C	102.00	12F
377	BUNDLE	HEATER	ROD	TEMPERATURE	HR-T/C	111.00	3J
378	BUNDLE	HEATER	ROD	TEMPERATURE	HR-T/C	111.00	4J
379	BUNDLE	HEATER	ROD	TEMPERATURE	HR-T/C	111.00	5E
380	BUNDLE	HEATER	ROD	TEMPERATURE	HR-T/C	111.00	5F
381	BUNDLE	HEATER	ROD	TEMPERATURE	HR-T/C	111.00	5H
382	BUNDLE	HEATER	ROD	TEMPERATURE	HR-T/C	111.00	6G
383	BUNDLE	HEATER	ROD	TEMPERATURE	HR-T/C	111.00	7E
384	BUNDLE	HEATER	ROD	TEMPERATURE	HR-T/C	111.00	7F

TABLE 4-3 (cont)

BUNDLE INSTRUMENTATION LOCATIONS AND COMPUTER CHANNELS

385	BUNDLE	HEATER ROD	TEMPERATURE	HR-T/C	111.00	8D
386	BUNDLE	HEATER ROD	TEMPERATURE	HR-T/C	111.00	8E
387	BUNDLE	HEATER ROD	TEMPERATURE	HR-T/C	111.00	8H
388	BUNDLE	HEATER ROD	TEMPERATURE	HR-T/C	111.00	8K
389	BUNDLE	HEATER ROD	TEMPERATURE	HR-T/C	111.00	9C
390	BUNDLE	HEATER ROD	TEMPERATURE	HR-T/C	111.00	9E
391	BUNDLE	HEATER ROD	TEMPERATURE	HR-T/C	111.00	9F
392	BUNDLE	HEATER ROD	TEMPERATURE	HR-T/C	111.00	9G
393	BUNDLE	HEATER ROD	TEMPERATURE	HR-T/C	111.00	9J
394	BUNDLE	HEATER ROD	TEMPERATURE	HR-T/C	111.00	11F
395	BUNDLE	HEATER ROD	TEMPERATURE	HR-T/C	111.00	11I
396	BUNDLE	HEATER ROD	TEMPERATURE	HR-T/C	111.00	11J
397	BUNDLE	HEATER ROD	TEMPERATURE	HR-T/C	111.00	11K
398	BUNDLE	HEATER ROD	TEMPERATURE	HR-T/C	111.00	12I
399	BUNDLE	HEATER ROD	TEMPERATURE	HR-T/C	111.00	13G
400	BUNDLE	HEATER ROD	TEMPERATURE	HR-T/C	111.00	13H
401	BUNDLE	HEATER ROD	TEMPERATURE	HR-T/C	120.00	3K
402	BUNDLE	HEATER ROD	TEMPERATURE	HR-T/C	120.00	5D
403	BUNDLE	HEATER ROD	TEMPERATURE	HR-T/C	120.00	5J
404	BUNDLE	HEATER ROD	TEMPERATURE	HR-T/C	120.00	5L
405	BUNDLE	HEATER ROD	TEMPERATURE	HR-T/C	120.00	5M
406	BUNDLE	HEATER ROD	TEMPERATURE	HR-T/C	120.00	6D
407	BUNDLE	HEATER ROD	TEMPERATURE	HR-T/C	120.00	6L
408	BUNDLE	HEATER ROD	TEMPERATURE	HR-T/C	120.00	7B
409	BUNDLE	HEATER ROD	TEMPERATURE	HR-T/C	120.00	7F
410	BUNDLE	HEATER ROD	TEMPERATURE	HR-T/C	120.00	7G
411	BUNDLE	HEATER ROD	TEMPERATURE	HR-T/C	120.00	7H
412	BUNDLE	HEATER ROD	TEMPERATURE	HR-T/C	120.00	8D
413	BUNDLE	HEATER ROD	TEMPERATURE	HR-T/C	120.00	8E
414	BUNDLE	HEATER ROD	TEMPERATURE	HR-T/C	120.00	8G
415	BUNDLE	HEATER ROD	TEMPERATURE	HR-T/C	120.00	8H
416	BUNDLE	HEATER ROD	TEMPERATURE	HR-T/C	120.00	8J
417	BUNDLE	HEATER ROD	TEMPERATURE	HR-T/C	120.00	8K
418	BUNDLE	HEATER ROD	TEMPERATURE	HR-T/C	120.00	8N
419	BUNDLE	HEATER ROD	TEMPERATURE	HR-T/C	120.00	9F
420	BUNDLE	HEATER ROD	TEMPERATURE	HR-T/C	120.00	9K
421	BUNDLE	HEATER ROD	TEMPERATURE	HR-T/C	120.00	9M
422	BUNDLE	HEATER ROD	TEMPERATURE	HR-T/C	120.00	10H
423	BUNDLE	HEATER ROD	TEMPERATURE	HR-T/C	120.00	10I
424	BUNDLE	HEATER ROD	TEMPERATURE	HR-T/C	120.00	11G
425	BUNDLE	HEATER ROD	TEMPERATURE	HR-T/C	120.00	11H
426	BUNDLE	HEATER ROD	TEMPERATURE	HR-T/C	120.00	11K
427	BUNDLE	HEATER ROD	TEMPERATURE	HR-T/C	120.00	12F
428	BUNDLE	HEATER ROD	TEMPERATURE	HR-T/C	120.00	13H
429	BUNDLE	HEATER ROD	TEMPERATURE	HR-T/C	132.00	6H
430	BUNDLE	HEATER ROD	TEMPERATURE	HR-T/C	132.00	6J
431	BUNDLE	HEATER ROD	TEMPERATURE	HR-T/C	132.00	9G
432	BUNDLE	HEATER ROD	TEMPERATURE	HR-T/C	132.00	11E

TABLE 4-3 (cont)

BUNDLE INSTRUMENTATION LOCATIONS AND COMPUTER CHANNELS

433	BUNDLE	HEATER ROD	TEMPERATURE	HR-T/C	132.00	11G
434	BUNDLE	HEATER ROD	TEMPERATURE	HR-T/C	132.00	11I
435	BUNDLE	HEATER ROD	TEMPERATURE	HR-T/C	132.00	11K
436	BUNDLE	HEATER ROD	TEMPERATURE	HR-T/C	138.00	5J
437	BUNDLE	HEATER ROD	TEMPERATURE	HR-T/C	138.00	7B
438	BUNDLE	HEATER ROD	TEMPERATURE	HR-T/C	138.00	8J
439	BUNDLE	HEATER ROD	TEMPERATURE	HR-T/C	138.00	9F
440	BUNDLE	HEATER ROD	TEMPERATURE	HR-T/C	138.00	12F
441	BUNDLE	ASPIRATING STEAM PROBE	VAPOR	TEMPERATURE	ASP-T/C	39.00 10C
442	BUNDLE	ASPIRATING STEAM PROBE	VAPOR	TEMPERATURE	ASP-T/C	48.00 13F
443	BUNDLE	ASPIRATING STEAM PROBE	VAPOR	TEMPERATURE	ASP-T/C	60.00 4I
444	BUNDLE	ASPIRATING STEAM PROBE	VAPOR	TEMPERATURE	ASP-T/C	72.00 7I
445	BUNDLE	ASPIRATING STEAM PROBE	VAPOR	TEMPERATURE	ASP-T/C	72.00 10L
446	BUNDLE	ASPIRATING STEAM PROBE	VAPOR	TEMPERATURE	ASP-T/C	78.00 7L
447	BUNDLE	ASPIRATING STEAM PROBE	VAPOR	TEMPERATURE	ASP-T/C	78.00 4F
448	BUNDLE	ASPIRATING STEAM PROBE	VAPOR	TEMPERATURE	ASP-T/C	90.00 7C
449	BUNDLE	ASPIRATING STEAM PROBE	VAPOR	TEMPERATURE	ASP-T/C	90.00 13I
450	BUNDLE	ASPIRATING STEAM PROBE	VAPOR	TEMPERATURE	ASP-T/C	96.00 4F
451	BUNDLE	ASPIRATING STEAM PROBE	VAPOR	TEMPERATURE	ASP-T/C	96.00 10L
452	BUNDLE	ASPIRATING STEAM PROBE	VAPOR	TEMPERATURE	ASP-T/C	111.00 7I
453	BUNDLE	ASPIRATING STEAM PROBE	VAPOR	TEMPERATURE	ASP-T/C	111.00 10F
454	BUNDLE	ASPIRATING STEAM PROBE	VAPOR	TEMPERATURE	ASP-T/C	120.00 7C
455	BUNDLE	ASPIRATING STEAM PROBE	VAPOR	TEMPERATURE	ASP-T/C	120.00 13I
456	BUNDLE	ASPIRATING STEAM PROBE	VAPOR	TEMPERATURE	ASP-T/C	132.00 10F
457	BUNDLE	ASPIRATING STEAM PROBE	VAPOR	TEMPERATURE	ASP-T/C	138.00 5K
458	BUNDLE	BARE FLUID	VAPOR	TEMPERATURE	BF-T/C	58.00 L/M
459	BUNDLE	BARE FLUID	VAPOR	TEMPERATURE	BF-T/C	58.00 J/K
460	BUNDLE	BARE FLUID	VAPOR	TEMPERATURE	BF-T/C	58.00 F/G
461	BUNDLE	BARE FLUID	VAPOR	TEMPERATURE	BF-T/C	58.00 H/I
462	BUNDLE	BARE FLUID	VAPOR	TEMPERATURE	BF-T/C	78.00 L/M
463	BUNDLE	BARE FLUID	VAPOR	TEMPERATURE	BF-T/C	78.00 H/I
464	BUNDLE	BARE FLUID	VAPOR	TEMPERATURE	BF-T/C	78.00 J/K
465	BUNDLE	BARE FLUID	VAPOR	TEMPERATURE	BF-T/C	78.00 F/G
466	BUNDLE	BARE FLUID	VAPOR	TEMPERATURE	BF-T/C	78.00 I/J
467	BUNDLE	BARE FLUID	VAPOR	TEMPERATURE	BF-T/C	78.00 H/I
468	BUNDLE	BARE FLUID	VAPOR	TEMPERATURE	BF-T/C	78.00 G/H
469	BUNDLE	BARE FLUID	VAPOR	TEMPERATURE	BF-T/C	78.00 J/K
470	BUNDLE	BARE FLUID	VAPOR	TEMPERATURE	BF-T/C	96.00 J/K
471	BUNDLE	STEAM PROBE	VAPOR	TEMPERATURE	SP-T/C	96.00 L/M
472	BUNDLE	STEAM PROBE	VAPOR	TEMPERATURE	SP-T/C	96.00 H/I
473	BUNDLE	STEAM PROBE	VAPOR	TEMPERATURE	SP-T/C	96.00 J/K
474	BUNDLE	STEAM PROBE	VAPOR	TEMPERATURE	SP-T/C	96.00 I/J
475	BUNDLE	STEAM PROBE	VAPOR	TEMPERATURE	SP-T/C	96.00 H/I
476	BUNDLE	BARE FLUID	VAPOR	TEMPERATURE	BF-T/C	120.00 H/I
477	BUNDLE	STEAM PROBE	VAPOR	TEMPERATURE	SP-T/C	120.00 J/K
478	BUNDLE	STEAM PROBE	VAPOR	TEMPERATURE	SP-T/C	120.00 L/M
479	BUNDLE	STEAM PROBE	VAPOR	TEMPERATURE	SP-T/C	120.00 J/K
480	BUNDLE	STEAM PROBE	VAPOR	TEMPERATURE	SP-T/C	120.00 I/J

TABLE 4-3 (cont)

BUNDLE INSTRUMENTATION LOCATIONS AND COMPUTER CHANNELS

481 BUNDLE	STEAM PROBE	VAPOR TEMPERATURE	SP-T/C	120.00	H/I
482 BUNDLE	THIMBLE	WALL TEMPERATURE	TH-T/C	48.00	4I
483 BUNDLE	THIMBLE	WALL TEMPERATURE	TH-T/C	48.00	7L
484 BUNDLE	THIMBLE	WALL TEMPERATURE	TH-T/C	60.00	7L
485 BUNDLE	THIMBLE	WALL TEMPERATURE	TH-T/C	72.00	5K
486 BUNDLE	THIMBLE	WALL TEMPERATURE	TH-T/C	72.00	10C
487 BUNDLE	THIMBLE	WALL TEMPERATURE	TH-T/C	72.00	13F
488 BUNDLE	THIMBLE	WALL TEMPERATURE	TH-T/C	78.00	5K
489 BUNDLE	THIMBLE	WALL TEMPERATURE	TH-T/C	78.00	10C
490 BUNDLE	THIMBLE	WALL TEMPERATURE	TH-T/C	78.00	13F
491 BUNDLE	THIMBLE	WALL TEMPERATURE	TH-T/C	90.00	10C
492 BUNDLE	THIMBLE	WALL TEMPERATURE	TH-T/C	90.00	5K
493 BUNDLE	THIMBLE	WALL TEMPERATURE	TH-T/C	90.00	13L
494 BUNDLE	THIMBLE	WALL TEMPERATURE	TH-T/C	96.00	4C
495 BUNDLE	THIMBLE	WALL TEMPERATURE	TH-T/C	96.00	5K
496 BUNDLE	THIMBLE	WALL TEMPERATURE	TH-T/C	96.00	10C
497 BUNDLE	THIMBLE	WALL TEMPERATURE	TH-T/C	111.00	10C
498 BUNDLE	THIMBLE	WALL TEMPERATURE	TH-T/C	111.00	13L
499 BUNDLE	THIMBLE	WALL TEMPERATURE	TH-T/C	120.00	5K
500 BUNDLE	THIMBLE	WALL TEMPERATURE	TH-T/C	120.00	4C
501 BUNDLE	THIMBLE	WALL TEMPERATURE	TH-T/C	120.00	13F
502 BUNDLE	THIMBLE	WALL TEMPERATURE	TH-T/C	132.00	13L
503 HOUSING		WALL TEMPERATURE	W-T/C	24.00	90
504 HOUSING		WALL TEMPERATURE	W-T/C	48.00	90
505 HOUSING		WALL TEMPERATURE	W-T/C	60.00	90
506 HOUSING		WALL TEMPERATURE	W-T/C	72.00	90
507 HOUSING		WALL TEMPERATURE	W-T/C	84.00	90
508 HOUSING		WALL TEMPERATURE	W-T/C	96.00	90
509 HOUSING		WALL TEMPERATURE	W-T/C	108.00	90
510 HOUSING		WALL TEMPERATURE	W-T/C	120.00	90
511 HOUSING		WALL TEMPERATURE	W-T/C	132.00	90
512 HOUSING INSULATION		WALL TEMPERATURE	I-T/C	72.00	90
513 HOUSING INSULATION		WALL TEMPERATURE	I-T/C	96.00	90
514 HOUSING INSULATION		WALL TEMPERATURE	I-T/C	120.00	90
515 UPPER PLENUM		FLUID TEMPERATURE	F-T/C		
516 UPPER PLENUM HOUSING EXTENSION		FLUID TEMPERATURE	F-T/C		
517 UPPER PLENUM STEAM PROBE		VAPOR TEMPERATURE	SP-T/C		
518 UPPER PLENUM		WALL TEMPERATURE	W-T/C		0
519 UPPER PLENUM		WALL TEMPERATURE	W-T/C		90
520 UPPER PLENUM		WALL TEMPERATURE	W-T/C		180
521 LOWER PLENUM		FLUID TEMPERATURE	F-T/C		
522 CARRYOVER TANK		FLUID TEMPERATURE	F-T/C	000.00	
523 CARRYOVER TANK		WALL TEMPERATURE	TW-T/C	168.00	
524 SEPARATOR DRAIN TANK		FLUID TEMPERATURE	F-T/C		
525 SEPARATOR DRAIN TANK		WALL TEMPERATURE	W-T/C	72.00	
526 SEPARATOR		FLUID TEMPERATURE	F-T/C	00.00	
527 SEPARATOR		WALL TEMPERATURE	W-T/C	84.00	
528 UPPER PLENUM/SEPARATOR STEAM PROBE		VAPOR TEMPERATURE	SP-T/C		

TABLE 4-3 (cont)
BUNDLE INSTRUMENTATION LOCATIONS AND COMPUTER CHANNELS

529	UPPER PLENUM/SEPARATOR	WALL TEMPERATURE	W-T/C	
530	SEPARATOR/EXHAUST LINE STEAM PROBE	VAPOR TEMPERATURE	SP-T/C	
531	SEPARATOR/EXHAUST LINE	WALL TEMPERATURE	W-T/C	
532	EXHAUST LINE UPSTREAM	WALL TEMPERATURE	W-T/C	
533	EXHAUST LINE DOWNSTREAM	FLUID TEMPERATURE	F-T/C	
534	ACCUMULATOR NO.2	FLUID TEMPERATURE	F-T/C	
535	ACCUMULATOR NO.1	FLUID TEMPERATURE	F-T/C	
536	INJECTION LINE	FLUID TEMPERATURE	F-T/C	
537	CROSSOVER LEG DOWNSTREAM	FLUID TEMPERATURE	F-T/C	
538	DOWNCOMER	FLUID TEMPERATURE	F-T/C	
539	CROSSOVER LEG DOWNSTREAM	WALL TEMPERATURE	W-T/C	
540	POWER PRIMARY ZONE A	POWER	SCR	
541	POWER SECONDARY ZONE A	POWER	SCR	
542	POWER PRIMARY ZONE B	POWER	SCR	
543	POWER SECONDARY ZONE B	POWER	SCR	
544	POWER PRIMARY ZONE C	POWER	SCR	
545	POWER SECONDARY ZONE C	POWER	SCR	
546	INJECTION LINE- 60 GPM	FLOW	TM	
547	INJECTION LINE-150 GPM	FLOW	TM	
548	CROSSOVER LEG BI-DIRCT TURBOPROBE	FLOW	TM	
549	HOUSING	DFRNTL PRESSURE	H2O	0
550	HOUSING	DFRNTL PRESSURE	H2O	12
551	HOUSING	DFRNTL PRESSURE	H2O	24
552	HOUSING	DFRNTL PRESSURE	H2O	36
553	HOUSING	DFRNTL PRESSURE	H2O	48
554	HOUSING	DFRNTL PRESSURE	H2O	60
555	HOUSING	DFRNTL PRESSURE	H2O	72
556	HOUSING	DFRNTL PRESSURE	H2O	84
557	HOUSING	DFRNTL PRESSURE	H2O	96
558	HOUSING	DFRNTL PRESSURE	H2O	108
559	HOUSING	DFRNTL PRESSURE	H2O	120
560	HOUSING	DFRNTL PRESSURE	H2O	132
561	UPPER PLENUM	DFRNTL PRESSURE	H2O	
562	HOUSING OVERALL	DFRNTL PRESSURE	H2O	0
563	CARRYOVER TANK LEVEL	DFRNTL PRESSURE	H2O	194.00
564	DOWNCOMER	DFRNTL PRESSURE	H2O	216.00
565	SEPARATOR	DFRNTL PRESSURE	H2O	151.00
566	ACCUMULATOR	DFRNTL PRESSURE	H2O	120.00
567	EXHAUST ORIFICE LOW RANGE	DFRNTL PRESSURE	D/P	
568	EXHAUST ORIFICE HIGH RANGE	DFRNTL PRESSURE	D/P	
569	INJECTION LINE ORIFICE METER 1	DFRNTL PRESSURE	D/P	
570	INJECTION LINE ORIFICE METER 2 LO	DFRNTL PRESSURE	D/P	
571	INJECTION LINE ORIFICE METER 2 HI	DFRNTL PRESSURE	D/P	
572	DOWNCOMER TO SEPARATOR	DFRNTL PRESSURE	D/P	
573	UPPER PLENUM TO SEPARATOR	DFRNTL PRESSURE	D/P	
574	EXHAUST ORIFICE	PRESSURE	PT	
575	UPPER PLENUM/SEPARATOR	PRESSURE	PT	
576	INJECTION LINE ORIFICE METER	PRESSURE	PT	

(channels 512-514) were utilized to compute housing heat release as part of the overall mass and energy balance analysis.

Three turbine meters were utilized to measure the flow rate of injected water in forced flooding and gravity reflooding tests. One turbine meter was used to measure the injected flow for the forced flooding tests (channel 546), and two turbine meters, one in the injection line (channel 547) and one in the crossover leg (channel 548), were used to measure flow for the gravity reflooding tests. The turbine meter in the crossover leg was bidirectional; however, this meter did not perform satisfactorily.

The 11 differential pressure cells were used to measure loop pressure drops, flow, or water level. The water supply tanks had a differential pressure cell (channel 566) which was utilized to measure fluid level in the tanks during filling operations and testing. Three differential pressure cells (channels 569, 570, and 571) were utilized with orifice plates in the water injection system as redundant flow measuring devices to the injection line turbine flowmeter. The storage tanks on the downstream side of the bundle, the carryover tank (channel 563), the steam separator, and the steam separator drain tank (channel 565) were instrumented with differential pressure cells to measure liquid accumulation. The exit steam flow was measured downstream of the steam separator utilizing an orifice plate with a differential pressure cell (channels 567 and 563), fluid thermocouple, and a pressure cell. Three additional differential pressure cells were utilized in the gravity reflood tests to measure mass accumulated in the downcomer (channel 564), and to measure differential pressures between the upper plenum and steam separator (channel 573), and between the top of the downcomer and the steam separator (channel 572).

The three loop pressure cells were utilized to measure the absolute pressure at the orifice plates on the bundle inlet (channel 576) and outlet (channel 574), and in the upper plenum for forced reflood tests or in the steam separator for the gravity reflood tests (channel 575).

4-20. Bundle Instrumentation

The bundle instrumentation consisted of heater rod thermocouples, steam temperature measurements, plenum temperature measurements, differential pressure cells, and power measurements.

The locations of the heater rod thermocouples, steam probes, and thimble wall thermocouples are listed in table 4-3. Appendix F provides a detailed layout of the bundle instrumentation.

4-21. Heater Rod Thermocouples

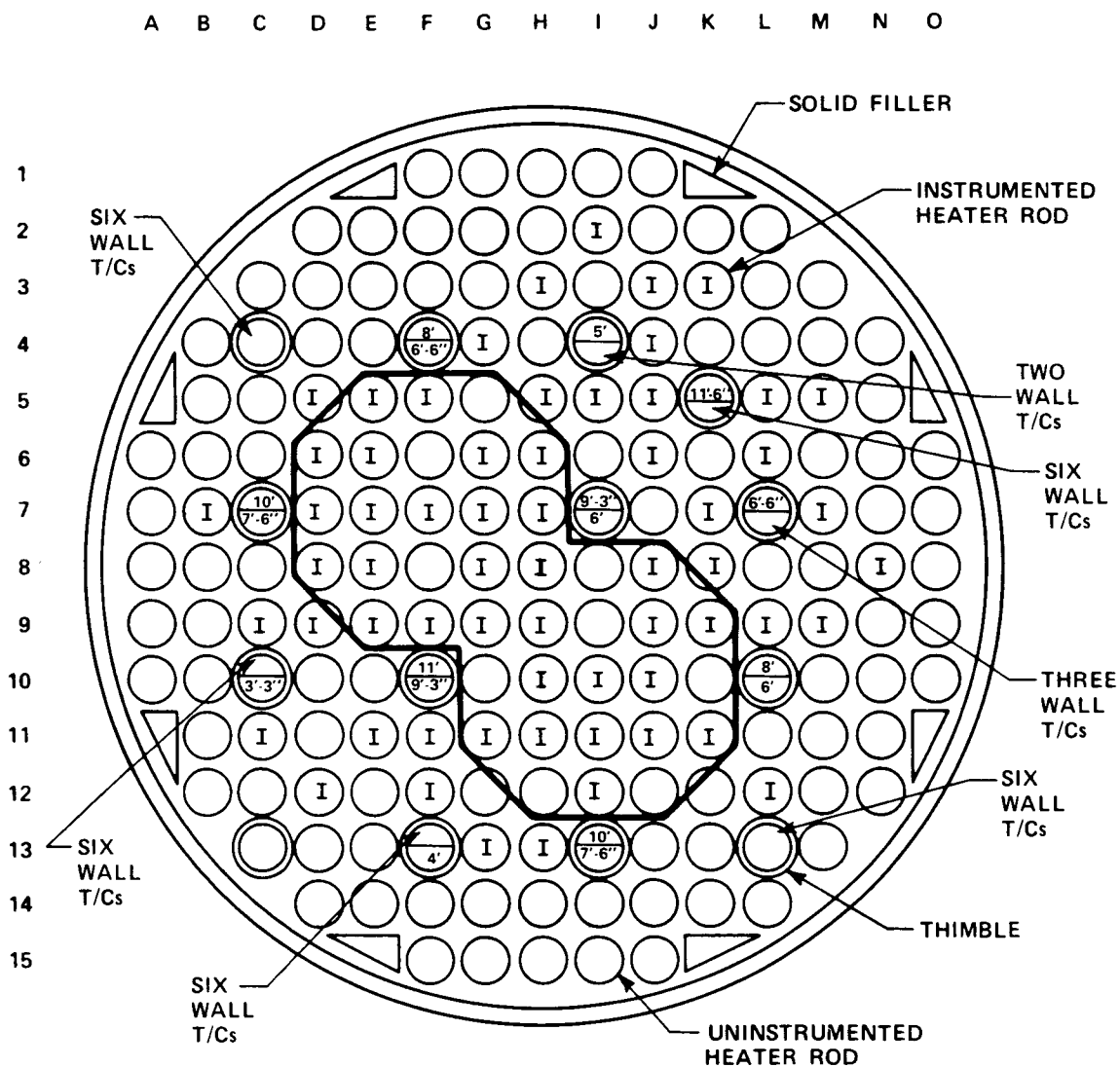
Sixty-two of the 163 heater rods in the large blocked bundle were instrumented with up to eight thermocouples each. A total of 440 bundle heater rod thermocouples were connected and recorded by the Computer Data Acquisition System. Some spare thermocouples were available for hookup to the computer in the event of rod thermocouple failures during testing; however, the number of failures was low and therefore the spares were never utilized.

Figure 4-8 shows the radial location of the 62 instrumented heater rods in the bundle as well as their orientation with respect to the two blockage islands. The placement of the instrumented heater rod thermocouples was based on the following criteria:

- o Maximizing direct comparisons with data from the 21-rod bundle and the 161-rod unblocked bundle
- o Achieving a radial distribution such that both the flow blockage region and flow bypass region were adequately instrumented
- o Achieving an axial distribution similar to that in the 21-rod and 161-rod unblocked bundles
- o Achieving a sufficient number of thermocouples upstream and downstream of the blockage zone to determine axial effect of blockage sleeves

4-22. Steam Temperature and Thimble Wall Instrumentation

The steam temperature, which was required for data analysis and evaluation, was measured by means of an aspirating steam probe located within the thimble



ELEVATION (m)	0.99	1.22	1.52	1.83	1.98	2.29	2.44	2.82	3.05	3.35	3.51
ELEVATION (in.)	39	48	60	72	78	90	96	111	120	132	138
NUMBER OF THIMBLE TUBE ASPIRATING STEAM PROBES	1	1	1	2	2	2	2	2	2	1	1
NUMBER OF THIMBLE WALL THERMOCOUPLES	3	3	4	4	4	3	4	4	4	2	-

Figure 4-8. Bundle Instrumentation Locations

tube, a self-aspirating steam probe placed in the subchannel, and an unshielded thermocouple also located in the subchannel.

The subchannel vapor temperature instruments and thimble tube steam probes provided data for evaluating mass and energy balances, nonequilibrium vapor properties, radial and axial vapor temperature variations, and blockage effects.

The thimble tube steam probe utilized the same general design as that in the 161-rod unblocked bundle. Two-phase flow was aspirated into the probe, water was separated prior to measuring the vapor temperature, and steam was subsequently condensed, measured, and collected on the outside of the test section. Figures C-5 through C-9 show the details of construction of the bundle thimble tubes. Figures 4-8 and C-20 show the bundle locations of the thimble steam probes as well as the thimble wall thermocouples. The thimble wall thermocouples were used to evaluate subcooling in the bottom of the bundle shortly after quenching, and radiation heat transfer between surfaces in the upper half of the bundle. Because of limited data acquisition system capacity, not all thimble wall thermocouples were recorded.

The self-aspirating steam probes and unshielded thermocouples were placed immediately upstream and downstream of the blockage zone of the 1.65 to 2.01 m (65 to 79 in.) elevation to supplement data obtained from the thimble tube aspirating steam probes and to measure radial vapor temperature distribution. Details of construction and bundle locations for the self-aspirating steam probes and unshielded thermocouples are shown in figure C-21.

Appendix E provides detailed test data comparisons of the three types of steam temperature instrumentation for a range of forced reflood test conditions.

4-23. Differential Pressure Measurements

Differential pressure measurements were made every 0.30 m (12 in.) along the length of the bundle to determine mass accumulation in the bundle during reflood tests (channels 549-560). Differential pressure transmitters [± 3.7 MPa

(± 15 in. H_2O) were utilized to obtain an accurate mass accumulation measurement representative of an average across the bundle. An additional cell measured the overall pressure drop from the bottom to the top of the heated length (channel 562).

4-24. Power Measurements

Six instrumentation channels were devoted to measurement of power into the bundle. Three were used as a primary measurement (channels 540, 542, and 544) from which power was controlled by the computer software. Three independent power measurements (channels 541, 543, and 545) were used for data reduction purposes for forced and gravity reflood tests. The power to the 59 peripheral heater rods was measured by channel 541, power to the 69 rods in the bypass zone by channel 593, and power to the 40 rods in the blockage islands by channel 595.

4-25. Upper Plenum Instrumentation

The upper plenum, an important component of the FLECHT SEASET test loop, was utilized to separate the liquid and steam phases in close proximity to the test section so that accurate mass and energy balances could be accomplished. A differential pressure cell connected between the top and bottom of the upper plenum (channel 561) was used to measure liquid accumulation within this component. Liquid collected at the bottom of the upper plenum before draining into the carryover tank. System pressure was controlled by a pressure transmitter located in the upper plenum for all tests except gravity reflood tests. The same pressure transmitter was connected to the computer for measuring system pressure (channel 575).

Two upper plenum thermocouples were designed to measure the fluid temperatures at the upper plenum exit (channel 515) and in the upper plenum extension (channel 516). These thermocouples indicated the location and presence of liquid in the upper plenum and housing extension. An aspirating steam probe located in the upper plenum (channel 517) at the bundle exit was utilized to measure vapor nonequilibrium temperature. Three wall thermocouples were used

to ensure that the plenum was at a uniform temperature prior to and during testing (channels 518-520).

4-26. Lower Plenum Instrumentation

The lower plenum was instrumented with a fluid thermocouple (channel 521) located in the center of the lower plenum extension for measuring inlet sub-cooling as cooling water flooded with bundle.

4-27. FACILITY OPERATION

The 163-rod blocked bundle facility operation for forced reflood testing was similar to the operation of the 161-rod unblocked and 21-rod bundle test facilities. The following general procedure was used to conduct a typical reflood test:

- (1) Fill accumulator with water and heat to desired coolant temperature [53°C (127°F) nominal].
- (2) Turn on heatup boiler and bring the pressure up to 0.62 MPa (75 psig) nominal gage pressure.
- (3) Heat and pressurize the carryover vessel, entrainment separator, separator drain tank, test section, and test section outlet piping (located before the entrainment separator) to the saturation conditions corresponding to the test run pressure. Using clamp-on heaters, heat the exhaust line between the separator and exhaust orifice and housing windows to 260°C (500°F). Heat the test section lower plenum and injection piping (filled with water) to the temperature of the bundle coolant in the water supply tanks.
- (4) Scan all instrumentation channels by the computer to check for defective instrumentation. The differential pressure and static pressure cell zero readings are taken and entered into the computer calibration file. These zero readings are compared with the component calibration zero reading. The straight-line conversion to engineering units is changed to the new zero when the raw data are converted to engineering units. This zero shift process accounts for errors due to transmitter zero shifts and compensates for transmitter reference leg levels, enabling the engineering units to start with an empty or "zeroed" reading.
- (5) Apply power to the test bundle at a peak rate of 1.3 kw/m (0.4 kw/ft) and allow rods to heat up. When the temperature in any

two bundle thermocouples between the 1.70 m (67 in.) and the 2.06 (81 in.) elevations reaches 815°C (1500°F), the power is stepped to the specified peak rate [typically 2.3 kw/m (0.7 kw/ft)] until the desired test flood temperature is achieved [nominally 871°C (1600°F)], at which time the computer automatically activates flood and controls power decay. The exhaust control valve regulates the system pressure at the preset value by releasing steam to the atmosphere. The thimble tube steam probes are vented until rod temperature reaches 760°C (1400°F) and subsequently closed until rod temperature reaches 871°C (1600°F) to help maintain system pressure. The system pressure is maintained prior to flood by the heatup boiler, which has a capacity of 1.57×10^{-2} kg/sec (125 lb/hr).

- (6) Ascertain that all designated thermocouples have quenched (indicated by the computer printout of bundle quench).
- (7) Cut power to heaters, terminate coolant injection, and depressurize the entire system.
- (8) Drain and weigh water from all components.

At the end of the forced reflood tests, the facility was modified to conduct gravity reflood tests; however, the same procedure was used to conduct these tests.

4-28. KEY FACILITY OPERATING LIMITATIONS AND SAFETY FEATURES

All vessels in the FLECHT SEASET 163-rod bundle facility were designed and built to the ASME Boiler and Pressure Vessel Code. Facility piping conformed to the latest edition of the Code for Power Piping, ANSI B31.1. Facility operating limits were set by design criteria and/or component material limitations. Primary loop (test section and exhaust piping and components) design pressure was limited to 0.52 MPa (60 psig) because of the thin-walled low mass housing design, which was rated at 0.52 MPa (60 psig) with an 815°C (1500°) midplane temperature. This temperature was a maximum material limitation set by the ASME Code. All 163-rod bundle facility tests were run at or below 0.41 MPa (45 psig).

The water injection system piping and components were designed for 3.5 MPa (500 psig) and a temperature of 177°C (350°F). The system was operated well within these design limits.

Heater rod O-ring seals were made of ethylene propylene, which limited the test section upper seal plate temperature to 172°C (350°F) during testing.

The Kanthal heater rod element material limited operation of the test bundle heater rods to 1232°C (2250°F).

Personnel safety as well as facility protection were prime considerations in the design of the FLECHT SEASET 163-rod bundle facility. Accordingly, the following safety devices and/or features were designed into the facility:

- o Test section: Rupture disk with a burst pressure of 0.52 MPa (60 psig) at 22°C (72°F)
- o Exhaust piping: Combination rupture disk and relief valve set for 0.52 MPa (60 psig) at 153°C (307°F)
- o Carryover tank: Rupture disk with a burst pressure of 0.52 MPa (60 psig) at 22°C (72°F)
- o Entrainment separator: Rupture disk with a burst pressure of 0.52 MPa (60 psig) at 22°C (72°F)
- o Facility heating boiler: Relief valve set at 0.79 MPa (100 psig)
- o Water supply vessels: Rupture disks with a burst pressure of 3.5 MPa (500 psig) at 22°C (72°F)
- o Heater rod bundle:
 - Overcurrent limit to protect rods from failure due to an overpowered SCR by shutting off bundle power and sounding alarm
 - Computer-monitored and activated overtemperature trip set to shut off bundle power and sound alarm at 1232°C (2250°F)
 - Provision for shutting off bundle power and sounding alarm in case of computer power failure
 - Circuitry designed to shut off bundle power in case of control panel voltage (110 v) failure
 - Provision in computer software for signalling an incorrect power setting

4-29. PHOTOGRAPHIC STUDIES

The 163-rod bundle housing was equipped with three pairs of quartz windows located at the 0.91, 1.83, and 2.74 m (36, 72, and 108 in.) elevations. These windows were used to make visual observations and high-speed motion pictures of two-phase flow regimes and quench front progression. Droplet size and velocity was the key information sought from the movies. To provide this information, the camera focal distance was established so that droplets between the third and seventh rod rows would appear in sharp focus. High-intensity back lighting was utilized such that the water droplets would appear in silhouette in the flow channels between rod rows. Good visibility through the quartz windows was a prerequisite for quality movies. In previous FLECHT SEASET tests, a liquid film which formed on the inside of the glass obstructed the viewing area. In the FLECHT SEASET bundle tests, heaters were placed on the outside of the window housing and the window temperatures were monitored at both the computer and operator control console. The heaters raised the inner surface of the quartz to approximately 260°C (500°F) prior to initiation of test. At this time, the heaters were turned off and the windows maintained their temperature because of heat input from the rods.

High-speed movies were taken at both the 0.91 and 2.74 m (36 and 108 in.) elevation windows. The 1.83 m (72 in.) elevation window was used for visual observation only, as the flow blockage sleeves prevented backlighting of the flow channels and thus prevented motion picture filming.

The movies at the 0.91 and 2.74 m (36 and 108 in.) elevation windows were taken with identical Redlake Corporation Hycam model 42-001 high-speed, 16mm motion picture cameras. Both cameras utilized 366 m (1200 ft) rolls of Tri-X reversal (black and white) film. Movies were shot at 2000 frames per second at the 0.91 m (36 in.) elevation window and 2000 to 2500 frames per second at the 2.74 m (108 in.) window. Because of the high film speed and limited camera film capacity, only about 22.5 seconds of the test run could be filmed at a speed of 2000 frames per second, or 18 seconds at 2500 frames per second. The initial plan called for shooting at three intermittent time intervals;

however, frequent film breakage because of the high start and stop acceleration forces required that most of the filming be shot in a single time interval.

Movies were shot at specified preselected times during the first 46 seconds of the test run. Clock timers, started at flood initiation, were used to indicate when to activate the movie cameras.

Prior to testing, two measuring scales were positioned at right angles and filmed with one of the test movie cameras at the same focal length as the droplets in the test run movies. This film was then projected on a screen and used to establish a scale for determining droplet size and velocity in the test run movies.

Appendix G provides detailed results obtained from reducing the information contained in the high-speed droplet movies.

SECTION 5

TEST RESULTS

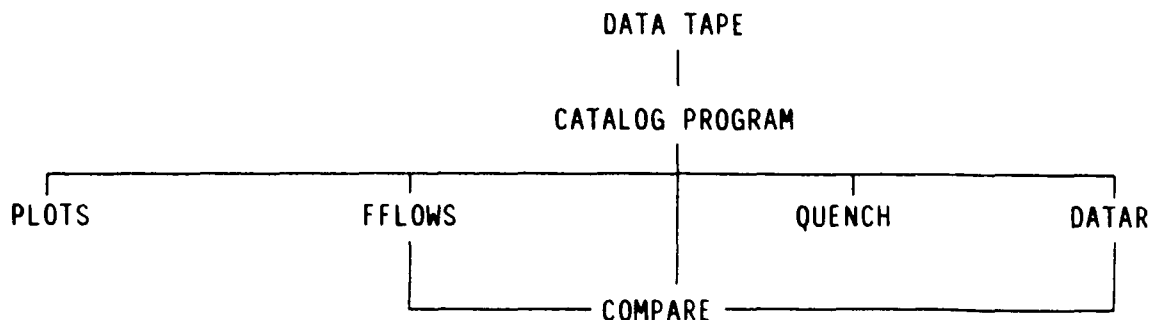
5-1. INTRODUCTION

The data from 20 forced reflood and three gravity reflood tests performed during the FLECHT SEASET 163-rod bundle test program met the specified test conditions and are reported herein. This section contains examples of key data and appendix H contains a large sampling of data for each of the 23 reflood tests.

The FLECHT SEASET test numbers comprise five characters each. The first character, 6, refers to the 163-rod bundle test program, the second and third refer to the sequential bundle cycle numbers, and the fourth and fifth are the test matrix number. For example, run 60701 is matrix test number 01 in the seventh cycle.

5-2. DATA REDUCTION

Data collected for each run at the test site were compiled on a binary magnetic tape in engineering units by the CDAS. This magnetic tape was processed by a CDC-7600 computer and the following series of data reduction programs were utilized for forced and gravity reflood tests:



The CATALOG program converted the data to a form compatible with the CDC computer and printed all the data as a function of time. The PLOTS program simply plotted all the recorded data as a function of time.

The following paragraphs describe the other four reflood programs and provide an example of the reduced data. The as-run test conditions for the reflood tests are shown in table 5-1. The instrumentation error analysis associated with the recorded data is discussed in appendix I.

5-3. FFLOWS Program and Results

The FFLOWS program was utilized primarily to calculate the mass balance for each reflood test. The mass balance was calculated by the following formulation:

$$\text{percent mass imbalance} = \frac{\text{mass difference}}{\text{mass injected}} \times 100$$

where mass difference = injected mass - (upper plenum mass + carryover tank mass + steam separator mass + mass in bundle + steam mass out + steam probe mass).

A mass balance plot for the reference run (run 61106) is shown in figure 5-1. The percent mass imbalances at the end of injection for all the reflood tests are shown in figure 5-2. The average mass imbalance was found to be approximately 2.6 percent at the end of injection for all forced reflood tests, and approximately 0.4 percent for all gravity reflood tests. Only one test (run 62304) had a mass imbalance greater than 5 percent at the end of injection; this may be attributed to the high injection rate of 157 mm/sec (6.2 in./sec). The mass balance plot for each test is shown in appendix H.

The FFLOWS program was also utilized to calculate the void fractions along the length of the bundle. The differential pressure measurements located every 0.30 m (12 in.) were used to calculate the void fraction by accounting for frictional and acceleration pressure drops. The bundle differential pressure and void fraction plots for each test are shown in appendix H. The mass flow rate into the bundle, the carryover tank, and the separator, as well as the steam flow out of the test section are also plotted in appendix H for each test. The details of the mass balance and void fraction calculations in the FFLOWS program are provided in appendix J.

TABLE 5-1

SUMMARY OF RUN CONDITIONS AND HOT ROD TEST RESULTS

Matrix Test	Run No.	Actual As-Run Conditions						Hot Rod Test Results							
		Upper Plenum Pressure [MPa (psia)]	Rod Initial Temperature [°C(°F)]	Peak Power [kw/m (kw/ft)]	Flooding Rate [mm/sec (in./sec)]	Coolant Temperature [°C(°F)]	Radial Power Distribution	Rod T/C and Elevation [m(in.)]	Initial Temperature [°C(°F)]	Maximum Temperature [°C(°F)]	Temperature Rise [°C(°F)]	Turn-around Time (sec)	Quench Time (sec)	Bundle Quench Time (sec)	Disconnected Rod Location
INITIAL CLAD TEMPERATURE EFFECT															
01	60701	0.277 (40.2)	264.6 (508.2)	2.3 (0.7)	38.6 (1.52)	52.2 (126)	Uniform	7F-2.44 (96.00)	226.6 (439.9)	638.7 (1181.7)	412.1 (741.8)	139.8	321.2	404.1	Rod 10A
02	60802	0.271 (39.3)	538.8 (1001.9)	2.3 (0.7)	38.6 (1.52)	53.9 (129)	Uniform	7D-2.29 (90.0)	483.3 (901.9)	817.4 (1503.4)	334.1 (601.5)	124.0	294.7	393	Rod 10A
	60902	0.2703 (39.20)	538.8 (1001.9)	2.3 (0.7)	38.6 (1.52)	53.3 (128)	Uniform	6E-2.29 (90.00)	498.9 (930.0)	821.1 (1510.0)	304.4 (580.0)	113.5	276.0	432	Rod 10A
FLOODING RATE EFFECT															
03	62503	0.274 (39.7)	871.6 (1600.9)	2.3 (0.7)	Variable	52.8 (127)	Uniform	7F-2.44 (96.00)	742.2 (1368.0)	1109.5 (2029.1)	367.3 (661.0)	250.1	623.7	782.7	Rod 10A
04	62304	0.277 (40.2)	877.1 (1610.8)	2.3 (0.7)	155 (6.1)	53.3 (128)	Uniform	8N-1.98 (78.00)	877.1 (1610.8)	900.9 (1653.7)	23.8 (42.8)	4.0	73.5	112.5	Rod 10A
05	61005	0.271 (39.3)	871.6 (1600.9)	2.3 (0.7)	38.6 (1.52)	51.7 (125)	Uniform	8N-1.98 (78.00)	862.0 (1583.6)	1001.9 (1835.4)	139.9 (251.8)	66.0	257.1	452.4	Rod 10A
	61705	0.273 (39.6)	873.5 (1604.3)	2.3 (0.7)	38.1 (1.50)	52.2 (126)	Uniform	9D-2.03 (80.00)	836.7 (1538.1)	1013.8 (1856.9)	177.1 (318.8)	82.5	266.5	421.3	Rod 10A
	62605	0.272 (39.5)	872.2 (1602.0)	2.3 (0.7)	38.6 (1.52)	52.2 (126)	Uniform	3H-2.03 (80.00)	835.2 (1548.9)	1010.4 (1850.1)	167.3 (301.2)	70.5	260.2	409.2	Rod 10A
06	61106	0.277 (40.2)	885.7 (1626.2)	2.3 (0.7)	24.9 (0.981)	52.8 (127)	Uniform	10I-2.03 (80.00)	855.6 (1571.6)	1144.4 (2089.9)	270.0 (518.0)	143.5	384	678	Rod 10A
07	61607	0.276 (40.1)	877.7 (1611.9)	2.3 (0.7)	21 (0.81)	52.8 (127)	Uniform	11G-2.01 (79.00)	856.0 (1572.8)	1198.2 (2188.7)	324.4 (616.0)	204.1	434.8	725	Rod 10A
08	61208	0.2689 (39.00)	871.0 (1599.8)	1.3 (0.4)	15 (0.60)	51.1 (124)	Uniform	9H-2.29 (90.00)	812.2 (1494.0)	1095.0 (2003.0)	265.0 (509.0)	212	420	541	Rod 10A



TABLE 5-1 (cont)

SUMMARY OF RUN CONDITIONS AND HOT ROD TEST RESULTS

Matrix Test	Run No.	Actual As-Run Conditions						Hot Rod Test Results							
		Upper Plenum Pressure [MPa (psia)]	Rod Initial Temperature [°C(°F)]	Peak Power [kw/m (kw/ft)]	Flooding Rate [mm/sec (in./sec)]	Coolant Temperature [°C(°F)]	Radial Power Distribution	Rod T/C and Elevation [m(in.)]	Initial Temperature [°C(°F)]	Maximum Temperature [°C(°F)]	Temperature Rise [°C(°F)]	Turn-around Time (sec)	Quench Time (sec)	Bundle Quench Time (sec)	Disconnected Rod Location
SYSTEM PRESSURE EFFECT															
09	61509	0.140 (20.1)	876.5 (1609.7)	2.4 (0.72)	26.9 (1.06)	35 (95)	Uniform	7E-2.03 (80.00)	852.9 (1567.3)	1125.1 (2057.2)	254.4 (489.9)	217.1	532.9	854.1	Rod 10A
10	61810	0.1358 (19.70)	871.6 (1600.9)	1.4 (0.42)	17 (0.65)	33.9 (93)	Uniform	7G-2.03 (80.00)	850.0 (1561.9)	1085.0 (1984.9)	235.0 (423.0)	198.5	489.6	729.2	Rod 10A
11	62211	0.137 (19.9)	871.0 (1599.8)	1.4 (0.4)	28(1.1) for 30 sec 26.9 (1.06) onward	33.9 (94)	Uniform	8N-1.98 (78.00)	871.1 (1599.8)	942.8 (1728.9)	71.7 (129.0)	52.0	294.0	467.2	Rod 10A
12	61412	0.404 (58.6)	874.7 (1606.4)	2.3 (0.69)	24.6 (0.968) for 120 sec 26.2 (1.03) onward	63.9 (147)	Uniform	9D-2.03 (80.00)	831.3 (1528.3)	1125.1 (2057.2)	293.8 (528.9)	132.5	296.9	471.0	Rod 10A
PEAK POWER EFFECT															
13	62413	0.276 (40.0)	875.9 (1608.6)	3.3 (1.0)	38 (1.5)	53.8 (129)	Uniform	8N-1.98 (78.00)	875.9 (1608.6)	1136.8 (2078.2)	260.9 (469.6)	78.5	331.6	564(a)	Rod 10A
14	61314	0.274 (39.7)	876.5 (1609.7)	1.30 (0.397)	38.6 (1.52)	51.7 (125)	Uniform	8N-1.98 (78.00)	875.9 (1608.6)	910.1 (1670.2)	16.4 (61.5)	35	179	274.1	Rod 10A
SUBCOOLING EFFECT															
15	62015	0.277 (40.2)	877.1 (1610.8)	2.30 (0.702)	24.9 (0.980) for 60 sec 27.7 (1.09) for 140 sec 29.7 (1.17) onward	119.4 (247)	Uniform	9D-2.03 (80.00)	835.6 (1536.0)	1085.0 (1985.0)	231.7 (449.0)	115	462	672	Rod 10A
STEPPED FLOW EFFECT															
16	61916	0.277 (40.2)	877.1 (1610.8)	2.3 (0.7)	154 (6.07) for 7 sec 20.6 (0.810) onward	52.2 (126)	Uniform	9H-2.29 (90.00)	818.9 (1505.6)	1119.4 (2046.6)	300.5 (541.1)	234.1	508.6	658.1	Rod 10A

a. Terminated prior to bundle quench



TABLE 5-1 (cont)

SUMMARY OF RUN CONDITIONS AND HOT ROD TEST RESULTS

Matrix Test	Run No.	Actual As-Run Conditions						Hot Rod Test Results							
		Upper Plenum Pressure [MPa (psia)]	Rod Initial Temperature [°C(°F)]	Peak Power [kw/m (kw/ft)]	Flooding Rate [mm/sec (in./sec)]	Coolant Temperature [°C(°F)]	Radial Power Distribution	Rod T/C and Elevation [m(in.)]	Initial Temperature [°C(°F)]	Maximum Temperature [°C(°F)]	Temperature Rise [°C(°F)]	Turn-around Time (sec)	Quench Time (sec)	Bundle Quench Time (sec)	Disconnected Rod Location
HOT/COLD CHANNEL EFFECT															
17	62117	0.277 (40.2)	871.6 (1600.9)	2.3/1.3 (0.7/0.4)	20 (0.79)	53 (127)	Hot/cold channels	9H-2.29 (90.0)	832.5 (1530.5)	1210.2 (2210.4)	377.7 (679.9)	163.0	324.4	440.1	Rod 10A
GRAVITY REFLOOD															
					Injection Rate [kg/sec (lb/sec)]										
18	63018	0.276 (40.0)	871.7 (1601.0)	2.3 (0.70)	5.76 (12.7) for 14 sec 0.780 (1.72)	52.2 (126)	Uniform	8N-1.98 (78.00)	869.8 (1597.7)	893.0 (1639.4)	23.2 (41.7)	9	172.2	277.1	Rod 10A
19	62819	0.140 (20.3)	(871.6) (1600.9)	2.3 (0.70)	5.76 (12.7) for 14 sec 0.780 (1.72)	73.2 (91)	Uniform	8N-1.98 (78.0)	1578.8 (1596.6)	1695.4 (1713.2)	64.6 (116.7)	83.5	252.4	413.1	Rod 10A
	62919	0.139 (20.1)	871.6 (1600.9)	2.3 (0.70)	5.62 (12.4) for 4.5 sec 0.594 (1.31)	32.2 (90)	Uniform	11E-1.93 (76.00)	849.3 (1560.8)	1119.2 (2046.6)	269.9 (485.8)	117.5	349	593.1	Rod 10A



5-5

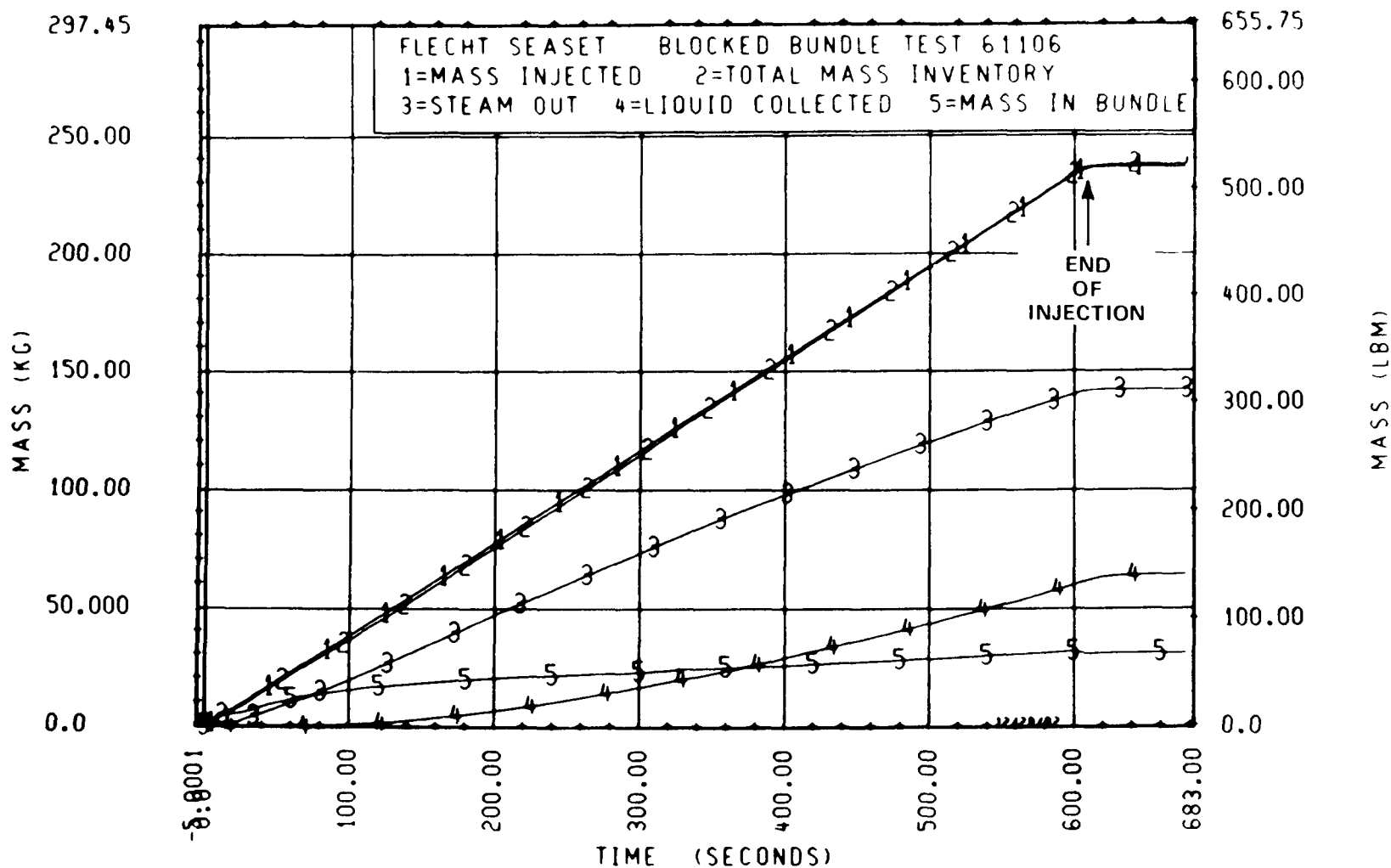


Figure 5-1. Mass Balance, Reference Run (Run 61106)

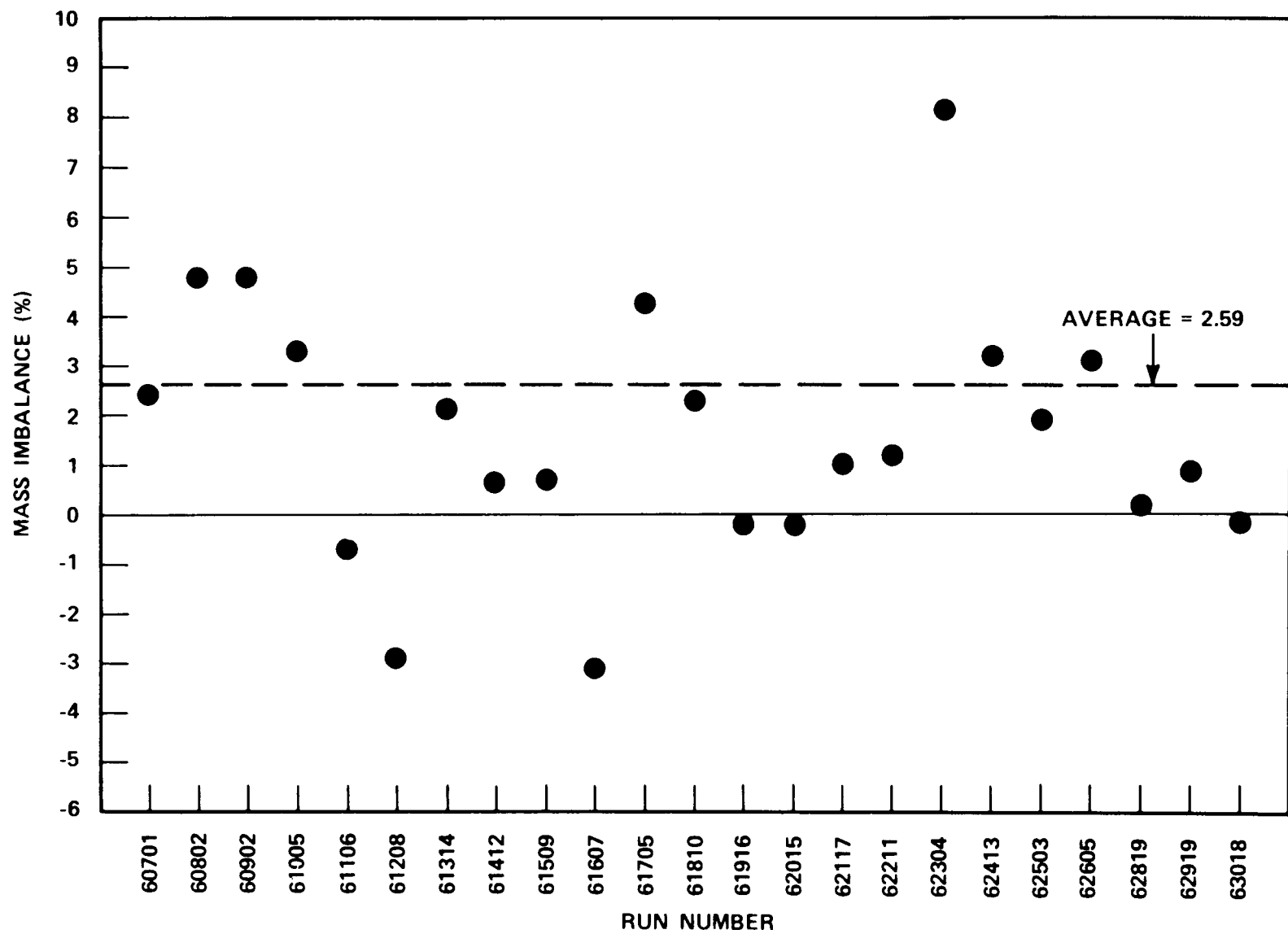


Figure 5-2. Mass Imbalance at End of Injection for All Tests

5-4. QUENCH Program and Results

The heater rod and housing thermocouple data for reflood tests were reduced by the QUENCH program. The QUENCH program was designed to determine the characteristics of temperature histories of the thermocouple data. These characteristics include the initial temperature, maximum temperature, quench temperature, turnaround time, and quench time. The temperature history of the hottest rod thermocouple for the reference run (run 61106) is shown in figure 5-3 with the actual data points chosen by the QUENCH program. A tabulation of the hot rod characteristics from the QUENCH program for all gravity and forced reflood tests is provided in table 5-1. The QUENCH program calculates the statistics of these characteristics for each instrumentation elevation, such as average turnaround time. These statistics are tabulated for each reflood test in appendix H.

The QUENCH program also calculates a quench front curve (from a cubic spline curve fit) from the average of the thermocouple quench times at a given elevation, and subsequently calculates a quench front velocity which is utilized in the FLEMB code for calculating an energy balance. Examples of the calculated quench curve with the associated thermocouple quench times and quench front velocity are shown in figures 5-4 and 5-5, respectively, for run 61106.

The details of the criteria used for choosing quench time and temperature are provided in appendix J.

5-5. DATAR Program and Results

The DATAR program was used to calculate the heat transfer coefficients for the reflood tests. The program employs a finite difference method to solve the inverse conduction problem utilizing the measured rod power, temperature, and physical dimensions to calculate the rod heat flux. The calculated heat transfer coefficient is referenced to the measured saturation temperature. The heat transfer coefficient for the hottest rod thermocouple from run 61106 is shown in figure 5-6.

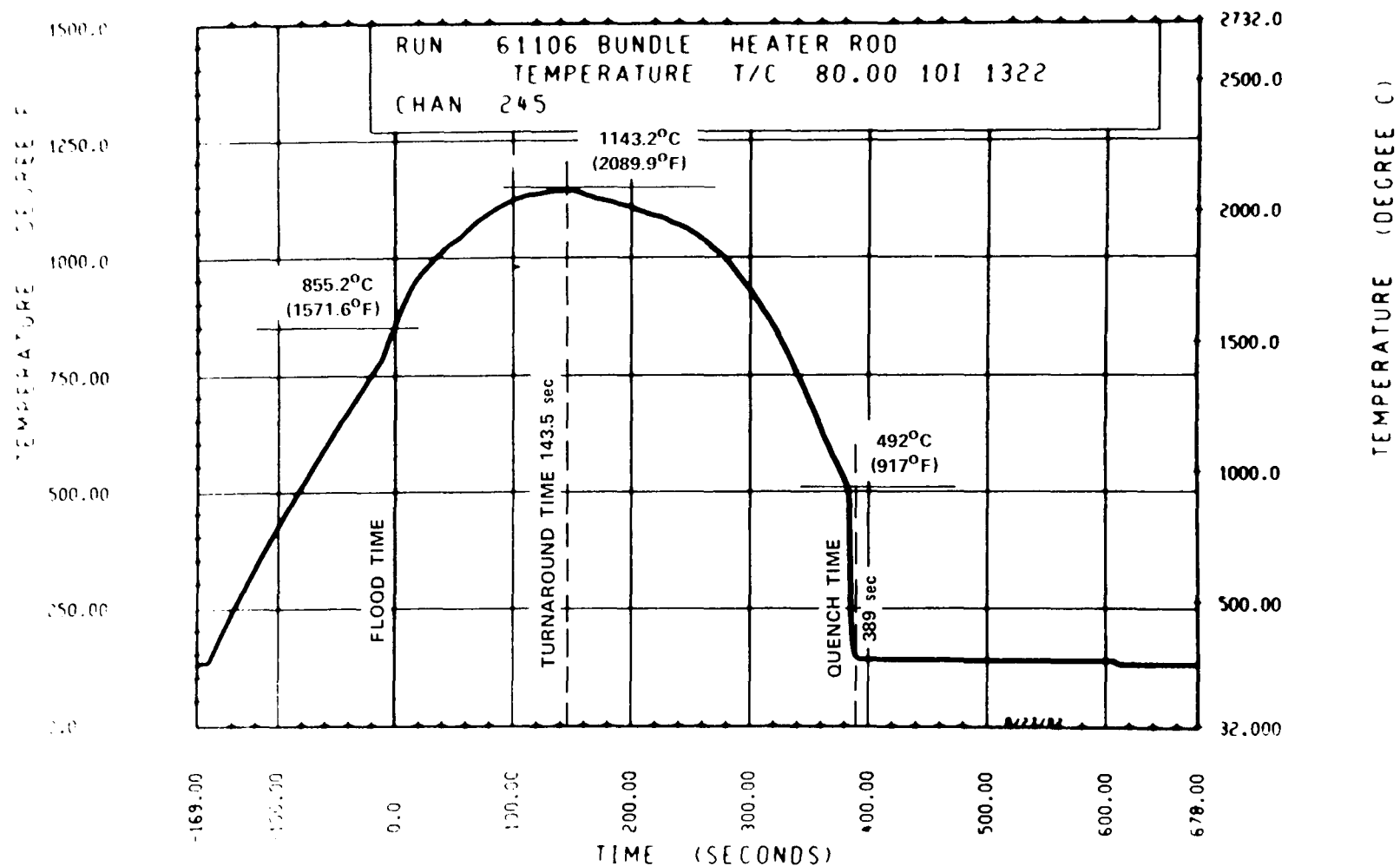


Figure 5-3. Temperature History of Hottest Rod, Run 61106

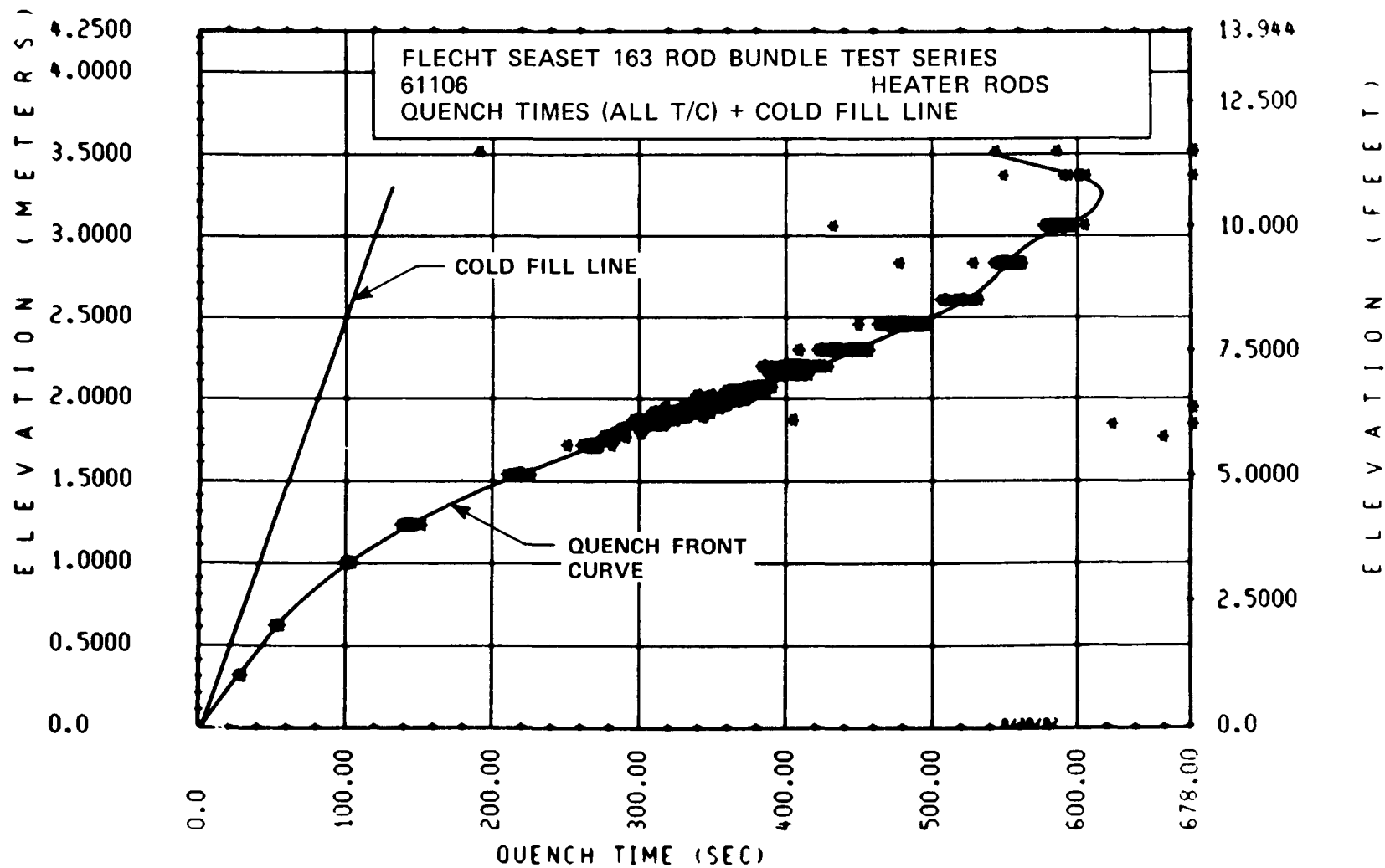


Figure 5-4. Quench Front Curve With Associated Thermocouple Quench Times, Run 61106

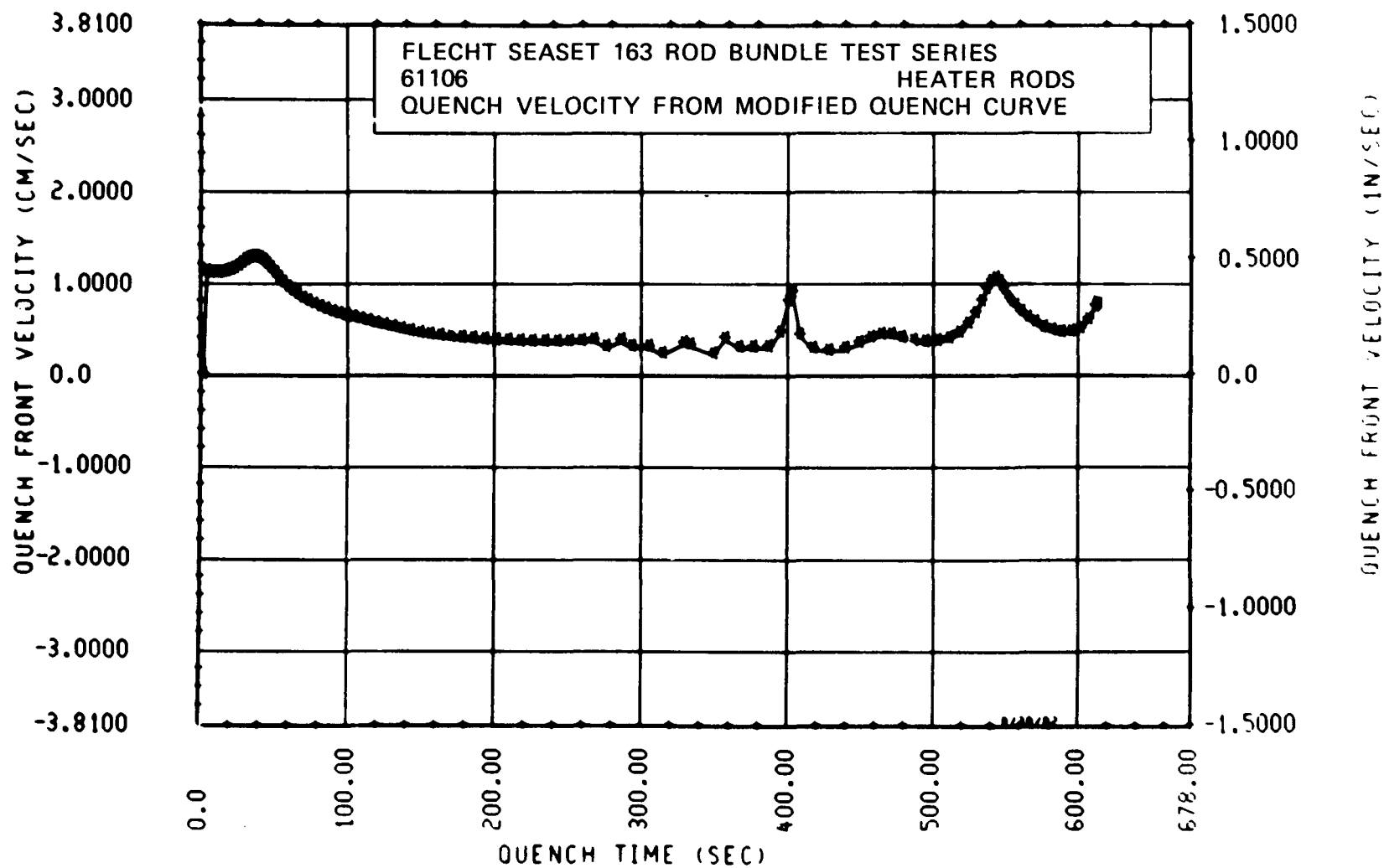


Figure 5-5. Quench Front Curve With Associated Quench Front Velocity, Run 61106

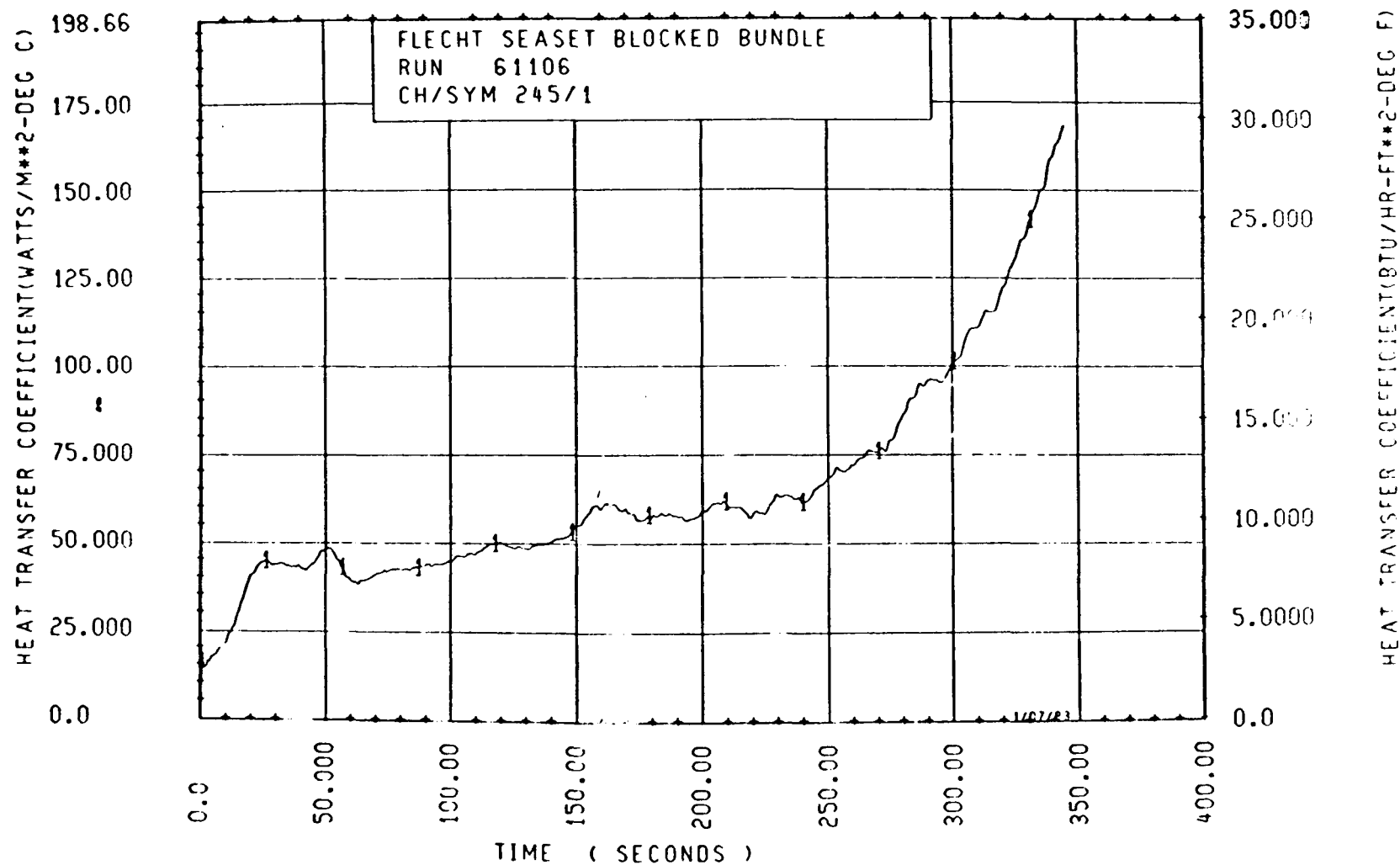


Figure 5-6. Heat Transfer Coefficient for Rod 10I at 2.03 m (80 in.) for 25.4 mm/sec (1 in./sec) Flooding Rate Test

To provide heat transfer coefficient data more suitable for analysis and evaluation, the data were smoothed (or averaged) over a total time of 10 seconds. This smoothing technique consisted of replacing each data point with an average value of the original data point and a specified number of points before and after the time of interest. An example of the original data and smoothed data is shown in figure 5-7 for the hottest rod thermocouple from run 61106.

The details of the DATAR program calculations, as well as the details on the data smoothing technique, are given in appendix J.

The heat transfer coefficient error analysis as previously performed for the 161-rod unblocked bundle, as shown in (figure 5-8), is applicable to the 163-rod bundle, since the heater rod materials are exactly the same and the rod dimensions are approximately the same as in the 161-rod unblocked bundle. In the 163-rod bundle, the thermocouple diameter was increased to 1.0 mm (0.040 in.) from 0.64 mm (0.025 in.), and the heating coil diameter was subsequently reduced from 4.44 to 3.43 mm (0.175 to 0.135 in.), but it is believed that the errors associated with these changes are negligible.

5-6. COMPARE Program and Results

The COMPARE program was utilized to compare data within a test run, between test runs, and/or between test series by plotting the respective data as a function of time, elevation (ZPLOT), or radial location (RPLLOT). The automated comparison of data provided for quick and efficient validation of tests and thorough analysis of large quantities of data. The following paragraphs describe some of the data results utilizing this program. Appendix H provides comparisons of the 163-rod blocked and 161-rod unblocked bundle measured rod temperatures and the calculated heat transfer coefficients. Axial temperature distributions as a function of time for the vapor, thimbles, and housing are also provided in appendix H, as well as loop temperatures and component fluid levels.

5-7. Initial Heater Rod Radial Temperature Distribution -- In the 163-rod bundle, the addition of the 40 flow blockage sleeves affected the initial

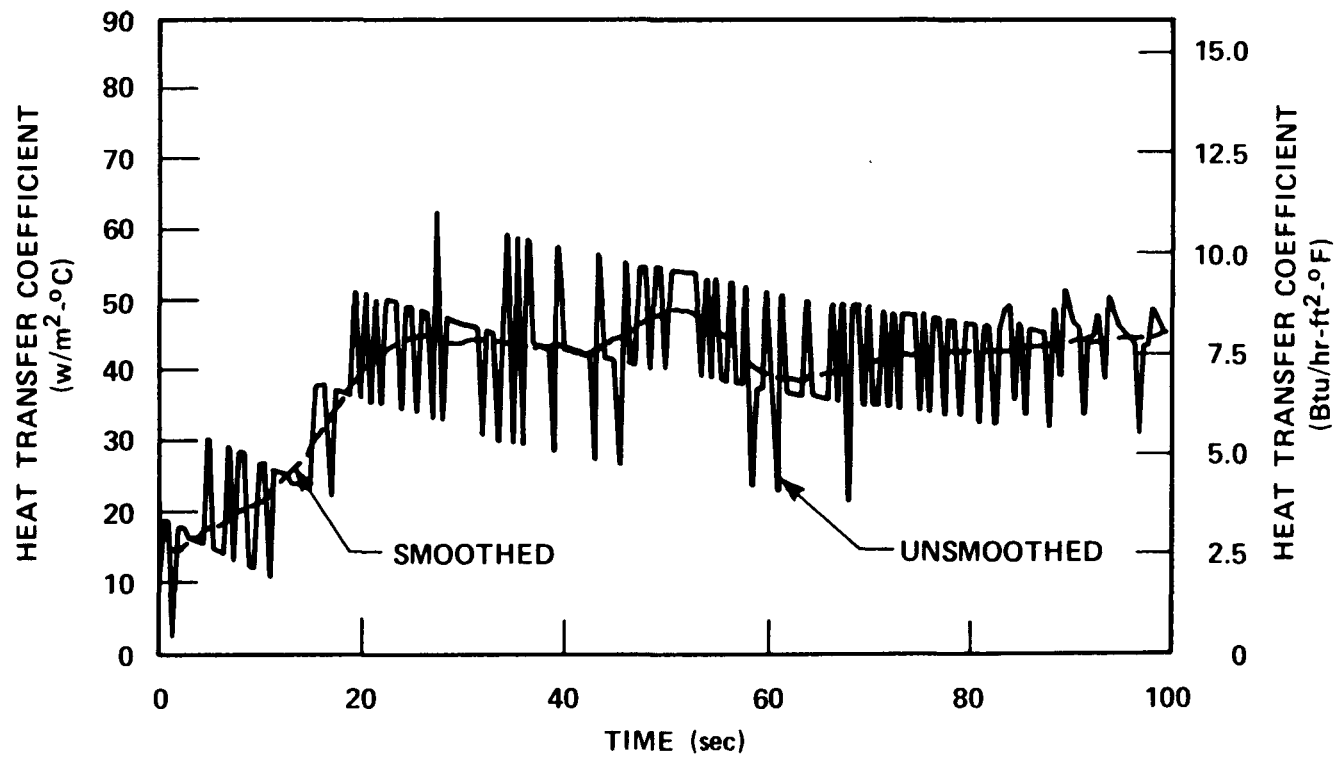


Figure 5-7. Smoothed and Unsmoothed Heat Transfer Coefficient for Rod 10I at 2.03 m (80 in.)

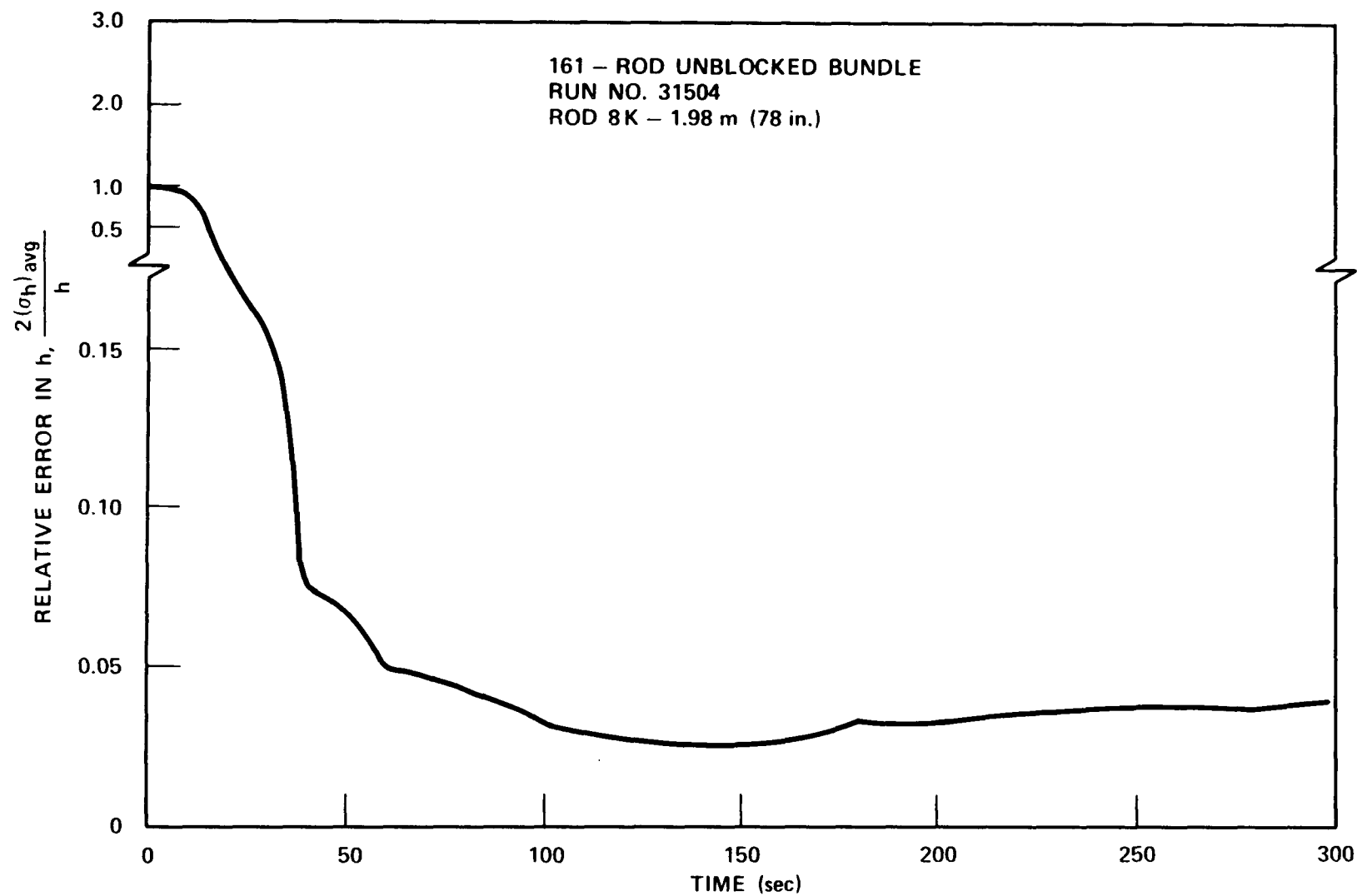


Figure 5-8. Heat Transfer Coefficient Error Analysis for 161-Rod Unblocked Bundle

heater rod radial temperature distribution, as shown in figure 5-9 at the 1.90 m (75 in.) elevation for run 61106. This figure shows the measured rod temperature as a function of radial position from the center of the blockage island. The reduction in the temperature of the heater rods in and near the blockage islands was attributed to the blockage sleeves. The radiation heat transfer between the "cold" sleeves and the hot rods was increased, thereby reducing the temperature of the adjacent heater rods. The convection heat transfer from the rods to the steam was increased because of the flow acceleration through the blockage. Also, the blockage sleeves, which represent approximately 30 percent of the mass of the heater rod per unit length, stored energy which otherwise would have been stored in the heater rod. In contrast, the midplane radial temperature distribution for the 161-rod unblocked bundle, as shown in figure 5-10 for the 1.83 m (72 in.) elevation for run 31504, indicates a radial temperature gradient which was higher in the center of the bundle. At elevations immediately upstream [1.70 m (67 in.)] and downstream [2.03 m (80 in.)] of the blockage for run 61106, a fairly uniform radial temperature distribution was achieved, as shown in figure 5-11, signifying the localized effect of the blockage sleeves on the heater rod temperature distribution.

Since the midplane radial temperatures were significantly different between the unblocked and blocked bundles, bundle flood was initiated in the blocked bundle at a time when the average midplane temperature was approximately the same as in the unblocked bundle. In this manner, it was believed that the overall thermal response would be approximately the same for the two bundles, although the radial distribution would be different. However, it was found that the initial temperatures in both the lower and upper halves of the bundle were generally higher in the blocked bundle than the corresponding unblocked bundle tests. Consequently, the quench front for the blocked bundle was approximately 20 to 40 seconds slower than that of the unblocked bundle.

All the 163-rod bundle tests provided approximately the same initial radial temperature distribution except for the hot/cold channel test (run 62117). In this test, the 40 blockage island rods were powered at 2.3 kw/m (0.7 kw/ft) and the other 123 rods were powered at 1.3 kw/m (0.4 kw/ft); flood was initiated when the hottest thermocouple reached 871°C (1600°F). The initial radial

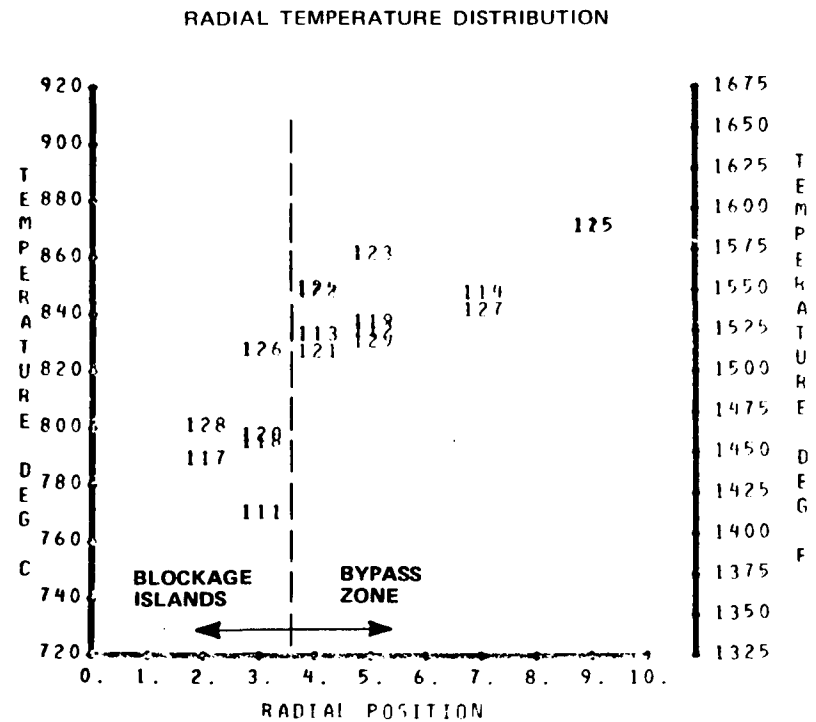
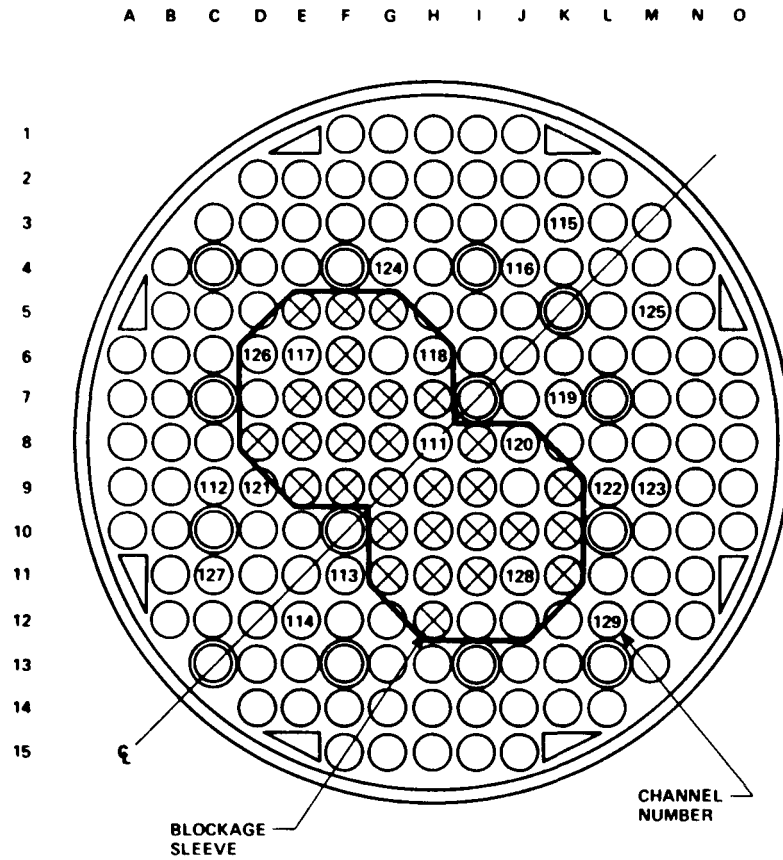


Figure 5-9. Initial Heater Rod Radial Temperature Distribution, Run 61106, 1.90 m (75 in.) Elevation

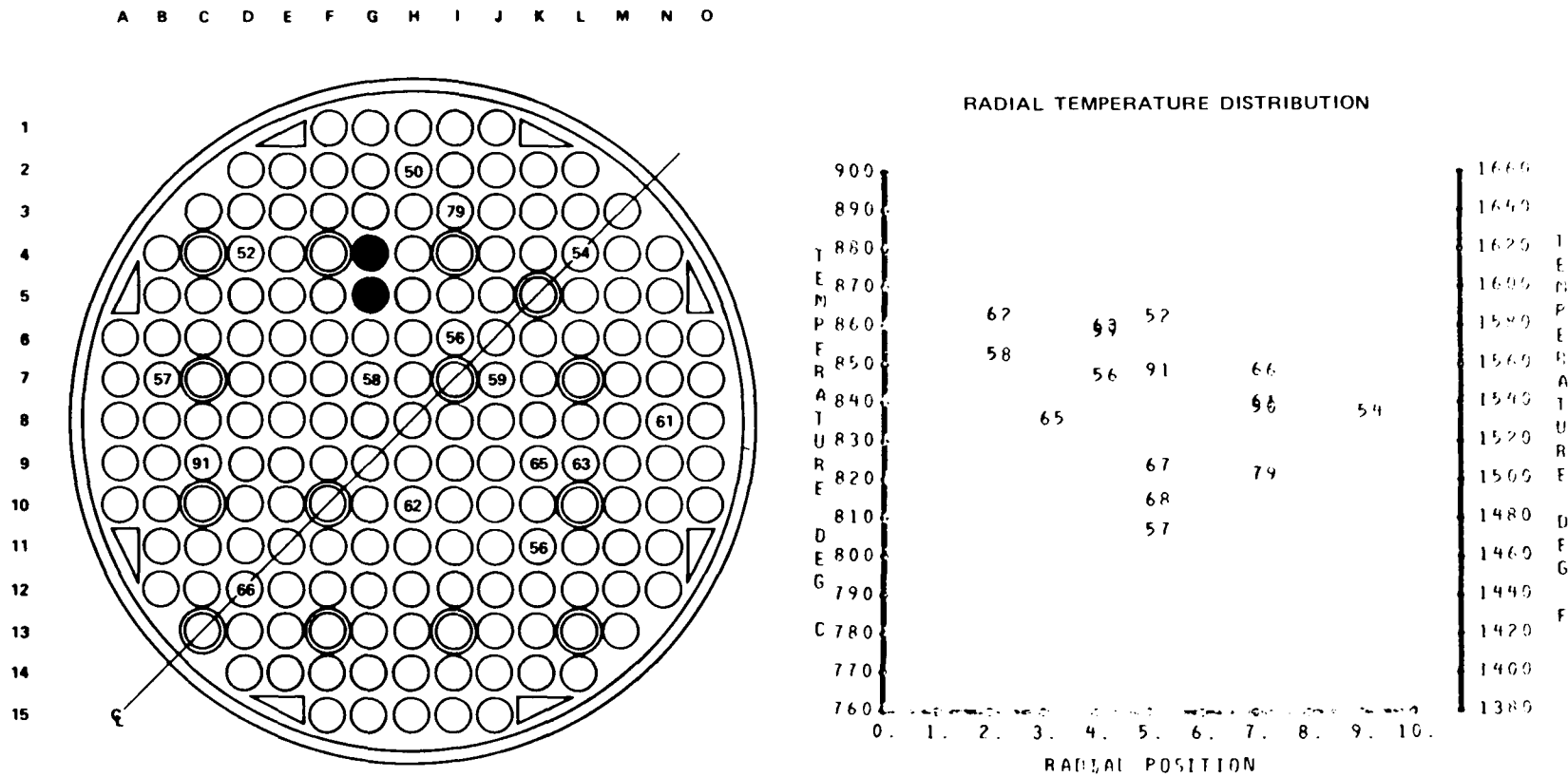


Figure 5-10. Midplane Radial Temperature Distribution, 161-Rod Unblocked Bundle, Run 31504, 1.83 m (72 in.) Elevation

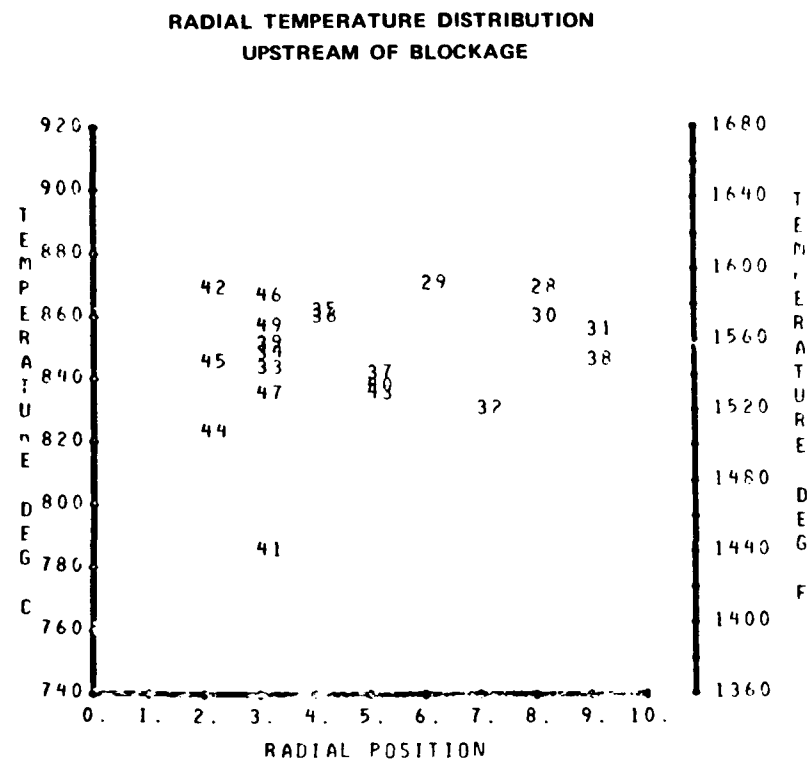
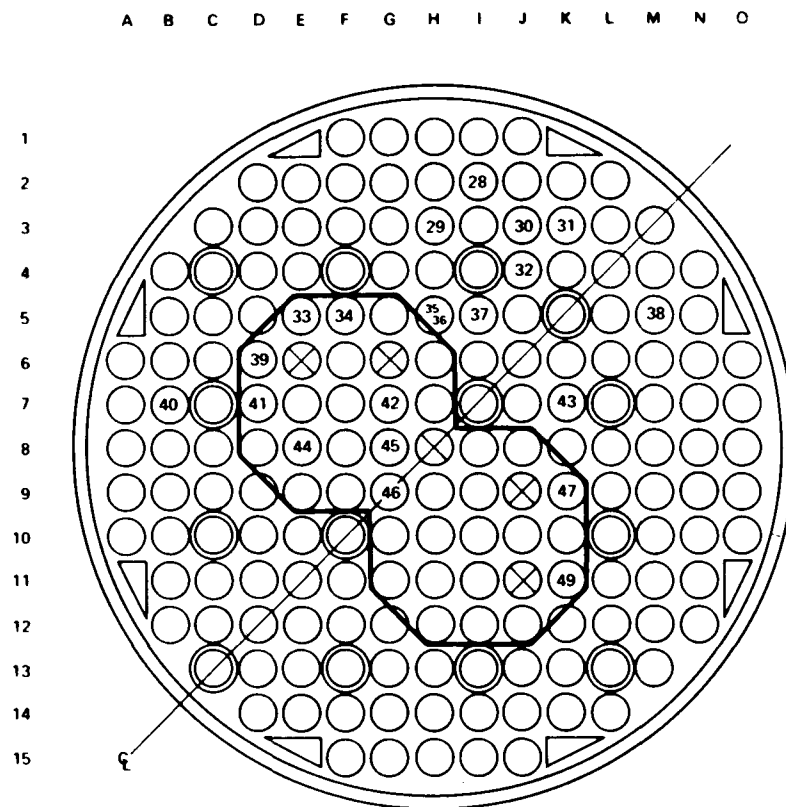
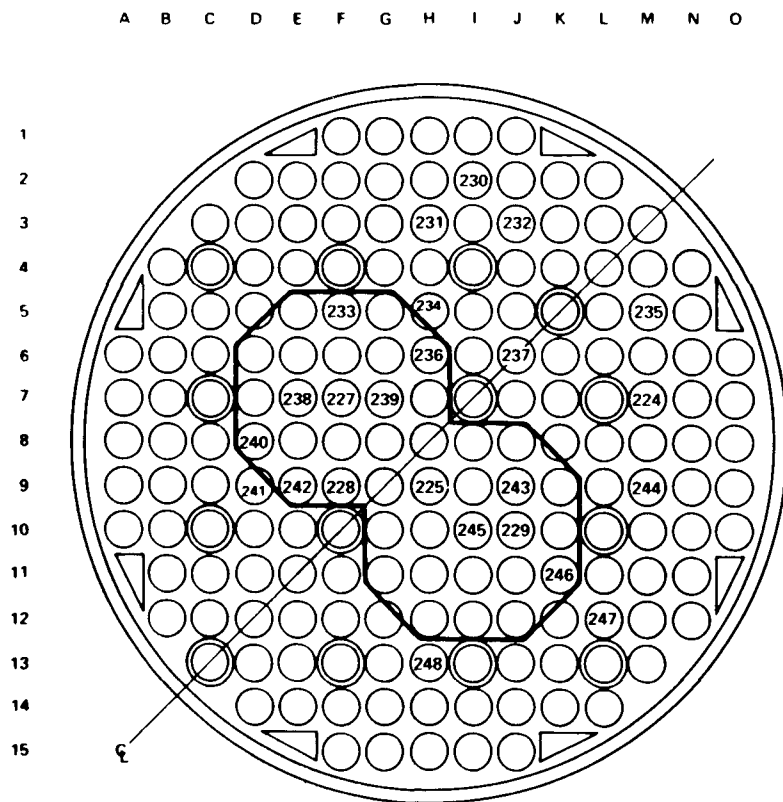


Figure 5-11. Radial Temperature Distribution Immediately Upstream and Downstream of Blockage, Run 61106 (sheet 1 of 2)



RADIAL TEMPERATURE DISTRIBUTION DOWNSTREAM OF BLOCKAGE

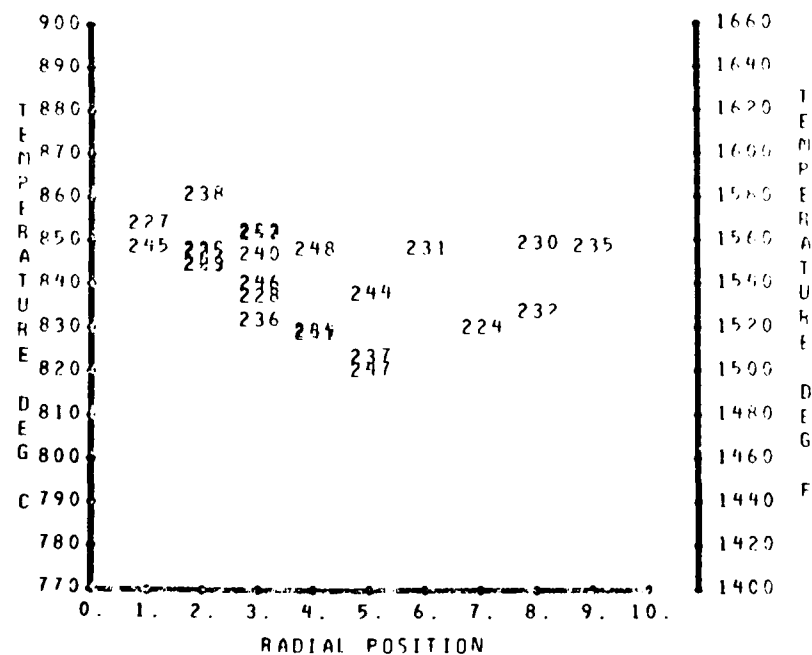


Figure 5-11. Radial Temperature Distribution Immediately Upstream and Downstream of Blockage, Run 61106 (sheet 2 of 2)

temperature distribution at the 1.70 and 2.03 m (67 and 80 in.) elevations are shown in figure 5-12. The average rod temperature for the two blockage islands was approximately 816°C (1500°F) and for the other rods was approximately 593°C (1100°F).

- 5-8. Symmetry of Heater Rod Temperatures -- In the 163-rod blocked bundle, there was only one line of symmetry, as previously discussed in paragraph 3-5 and illustrated in figure 5-13. To determine the symmetry of the heater rod temperature, there were 42 pairs of thermocouples symmetrically located in the bundle between the elevations of 1.70 m (67 in.) and 3.05 m (120 in.) distributed axially and radially as tabulated below:

Elevation [m (in.)]	Number and Location of Symmetrical Thermocouples
1.70 (67)	6 (4 in bypass and 2 in blockage islands)
1.88 (74)	2 (in blockage islands)
1.90 (75)	8 (4 in bypass and 4 in blockage islands)
1.96 (77)	8 (in blockage islands)
1.98 (78)	4 (in blockage islands)
2.01 (79)	4 (in blockage islands)
2.03 (80)	2 (in blockage islands)
2.06 (81)	2 (in blockage islands)
2.13 (84)	2 (in bypass region)
2.18 (86)	6 (in blockage islands)
2.29 (90)	14 (in blockage islands)
2.44 (96)	10 (4 in bypass and 6 in blockage islands)
2.82 (111)	10 (4 in bypass and 6 in blockage islands)
3.05 (120)	6 (2 in bypass and 4 in blockage islands)
TOTAL	84 (20 in bypass and 64 in blockage islands)

Comparison of the temperatures from the above symmetrical heater rod thermocouples as a function of time showed that the rod temperatures were fairly symmetrical at all elevations. Even in tests conducted later in the program,

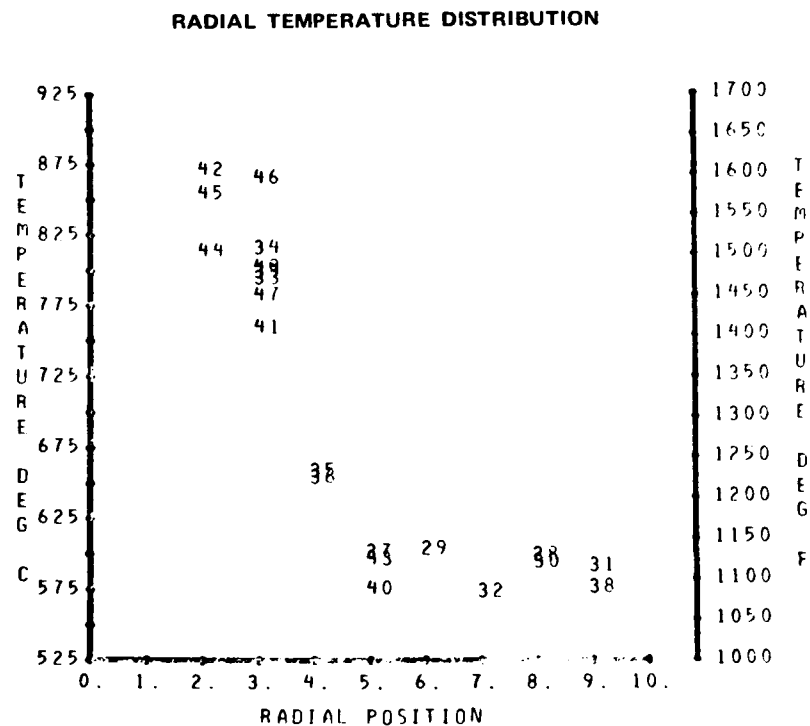
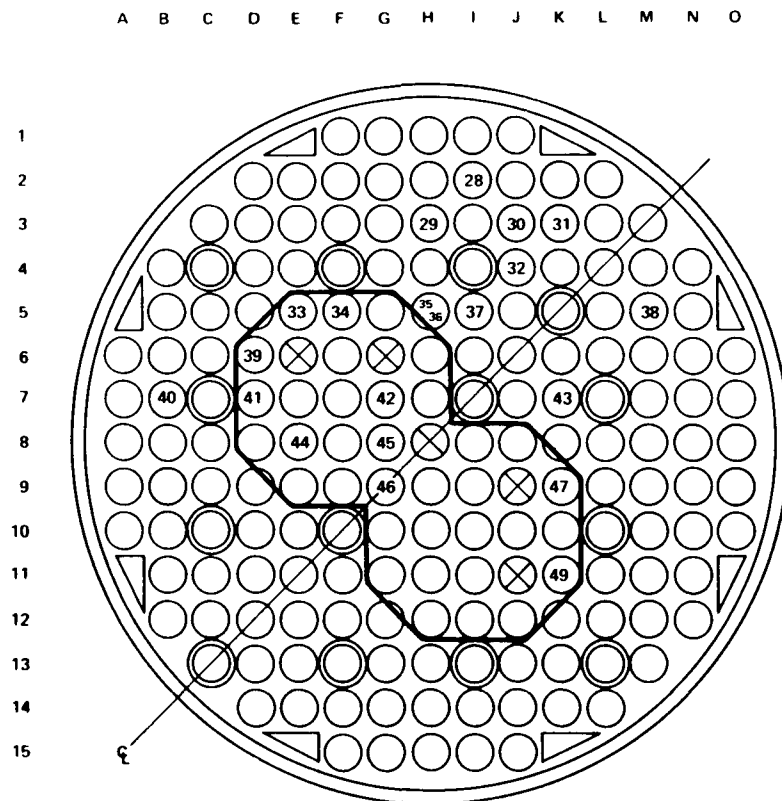


Figure 5-12. Initial Heater Rod Radial Temperature Distribution, Run 62117, 1.70 and 2.03 m (67 and 80 in.) Elevations (sheet 1 of 2)

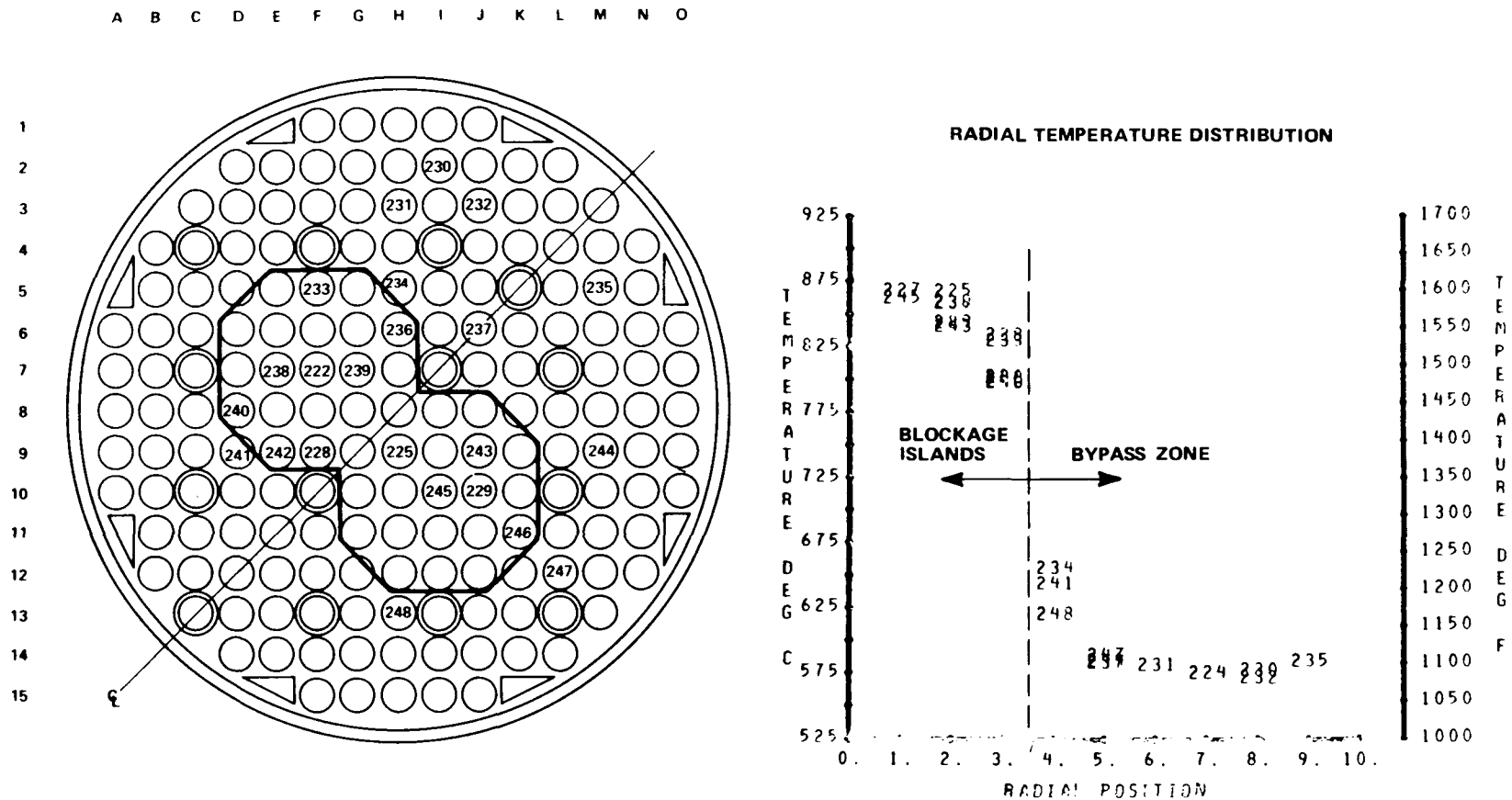


Figure 5-12. Initial Heater Rod Radial Temperature Distribution, Run 62117, 1.70 and 2.03 m (67 and 80 in.) Elevations (sheet 2 of 2)

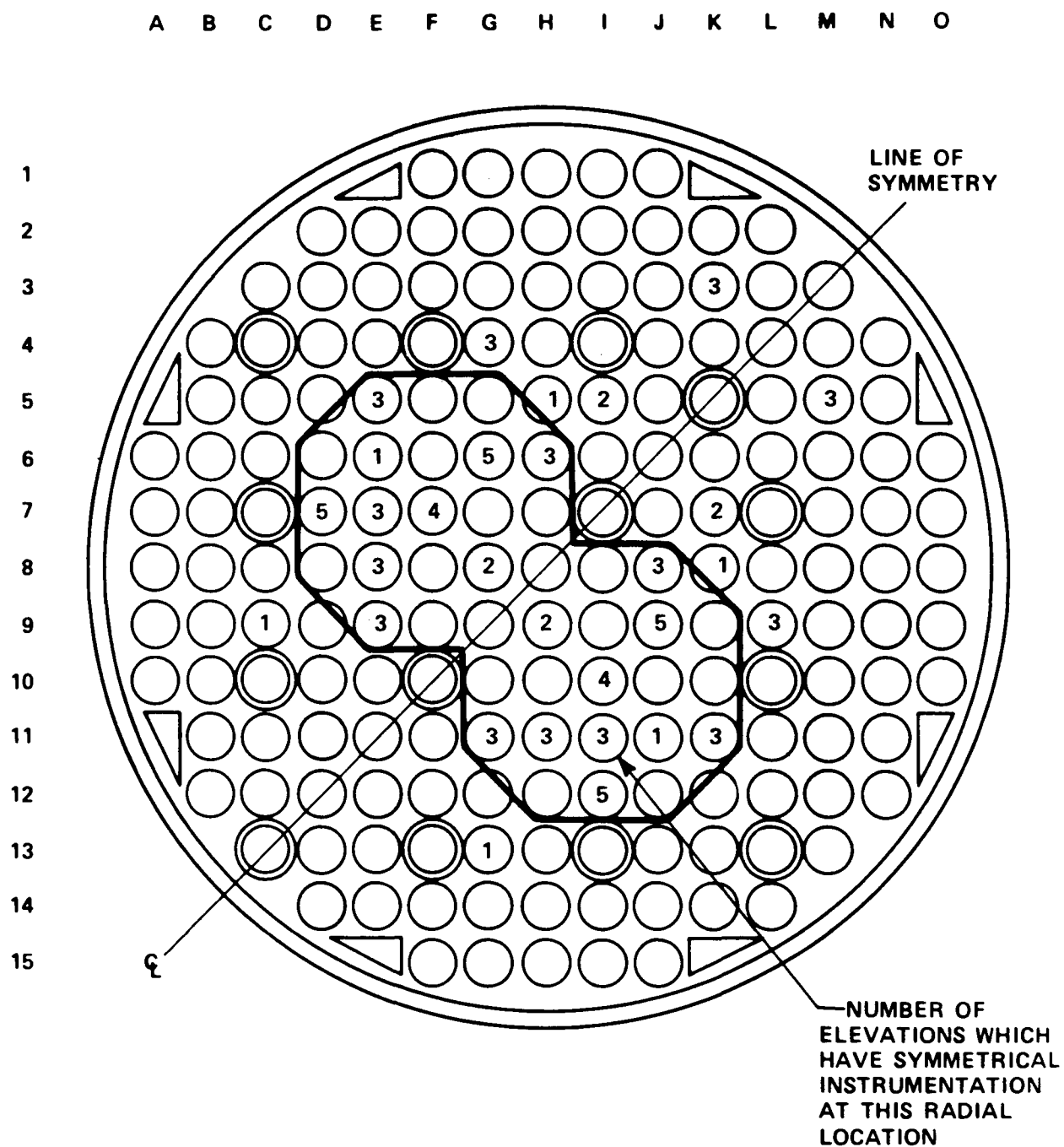


Figure 5-13. Heater Rod Symmetrical Instrumentation

there were insignificant differences in the temperature measurements at symmetrical locations, as shown in figures 5-14 and 5-15 for runs 61005, 61607, 61916, and 62605.

5-9. Data Repeatability -- The repeatability of the data was measured by conducting three test runs at the same exact conditions (as much as experimentally possible) at approximately equal intervals in the testing program. These were runs 61005, 61705, and 62605. There were no successive repeat tests; therefore, effects such as rod bow and surface degradation could have affected the measured rod temperature data. The nominal test conditions for each of the repeat tests were as follows:

- o 38.6 mm/sec (1.52 in./sec) flooding rate
- o 2.30 kW/m (0.7 kW/ft) peak initial linear power
- o 871°C (1600°F) initial clad temperature
- o 0.272 MPa (39.5 psia) system pressure
- o 52.7°C (127°F) inlet fluid temperature

The hot rod characteristics for each of the three repeat tests were found to be somewhat different (table 5-1). However, the hot rod maximum temperatures of 1002°C to 1014°C (1835°F to 1857°F) provide the only basis for that comparison. Subsequently, the temperature rise, turnaround time, and quench time for the hot rod should not be compared since the respective hot rod location varied from test to test (rods 8N, 9D, and 3H). A better evaluation of the data repeatability was achieved by comparing the same thermocouple location from test to test.

The heater rod temperature data repeated fairly well up through and past turnaround time, as shown in figure 5-16. However, there were temperature differences late in the reflood transient, with a resulting difference in the quench time. A comparison of the average quench front is shown in figure 5-17 for each of the three repeat tests. The quench front is approximately the same up to the 1.65 m (65 in.) elevation, which is just upstream of the blockage. The differences in quench times between test runs 61005 and 62605 at the 1.91 m (75 in.) elevation are shown in the inset in figure 5-17. The

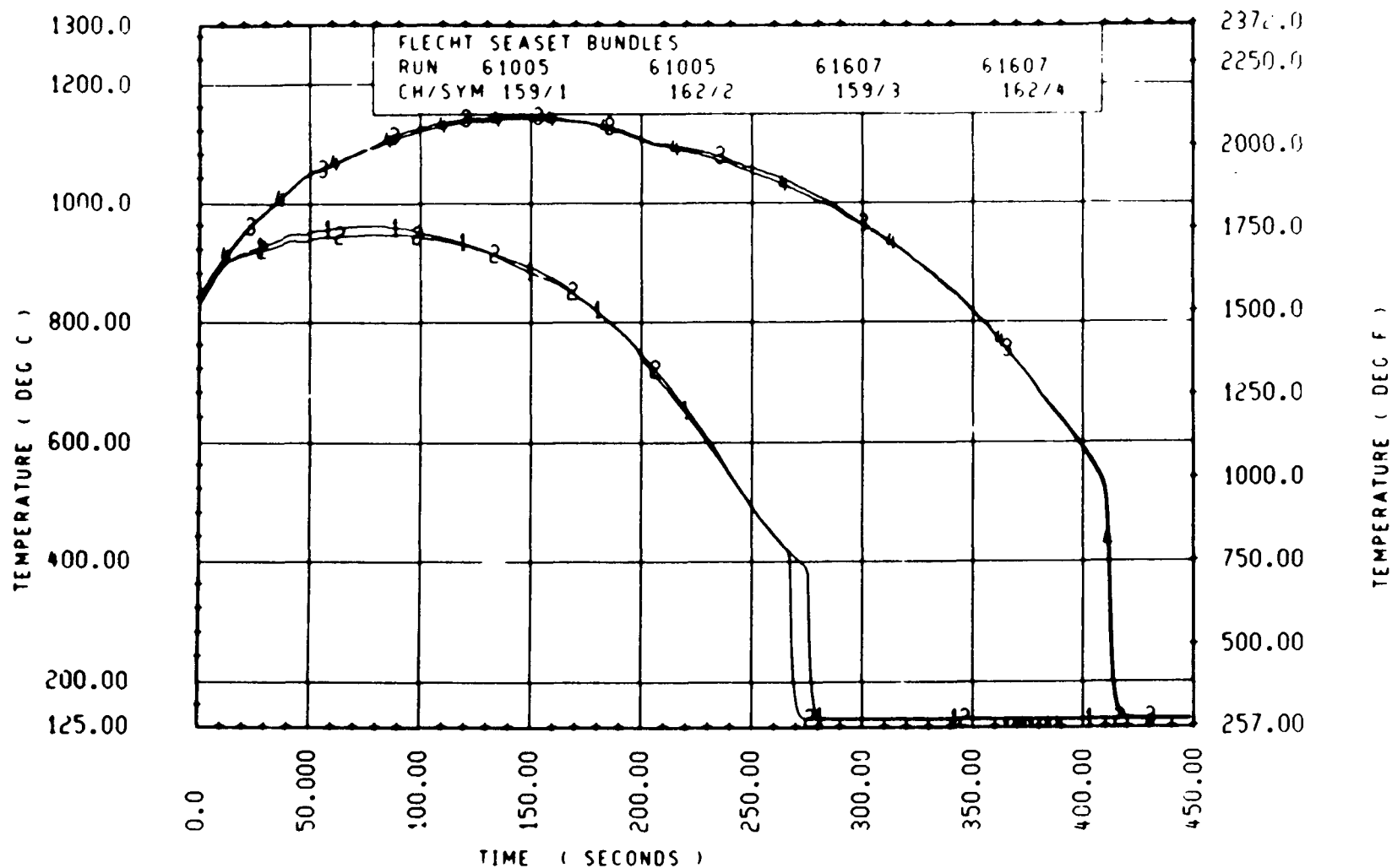


Figure 5-14. Temperature Measurement Differences at Symmetrical Locations, Runs 61005 and 61607

05-5

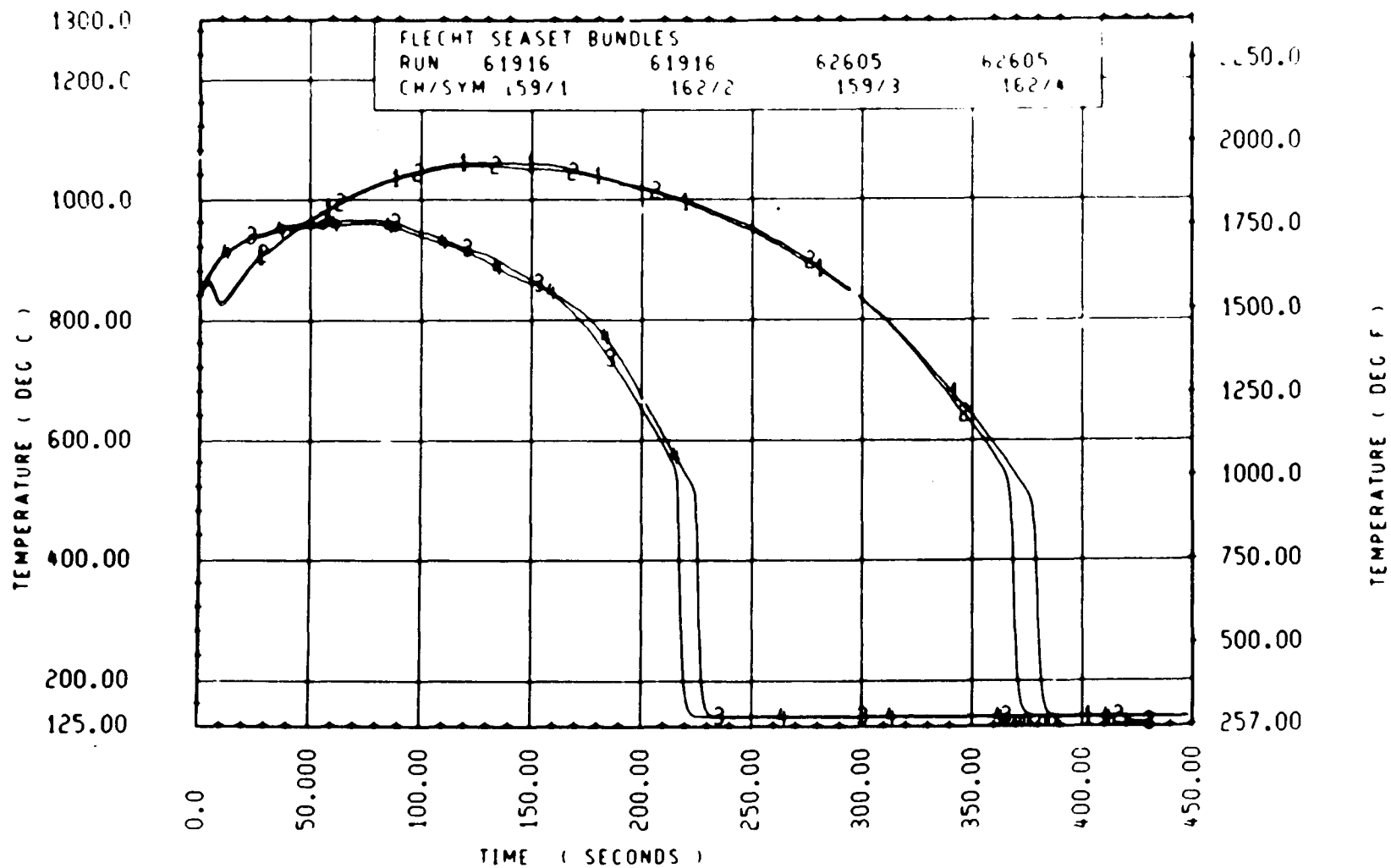


Figure 5-15. Temperature Measurement Differences at Symmetrical Locations, Runs 61916 and 62605

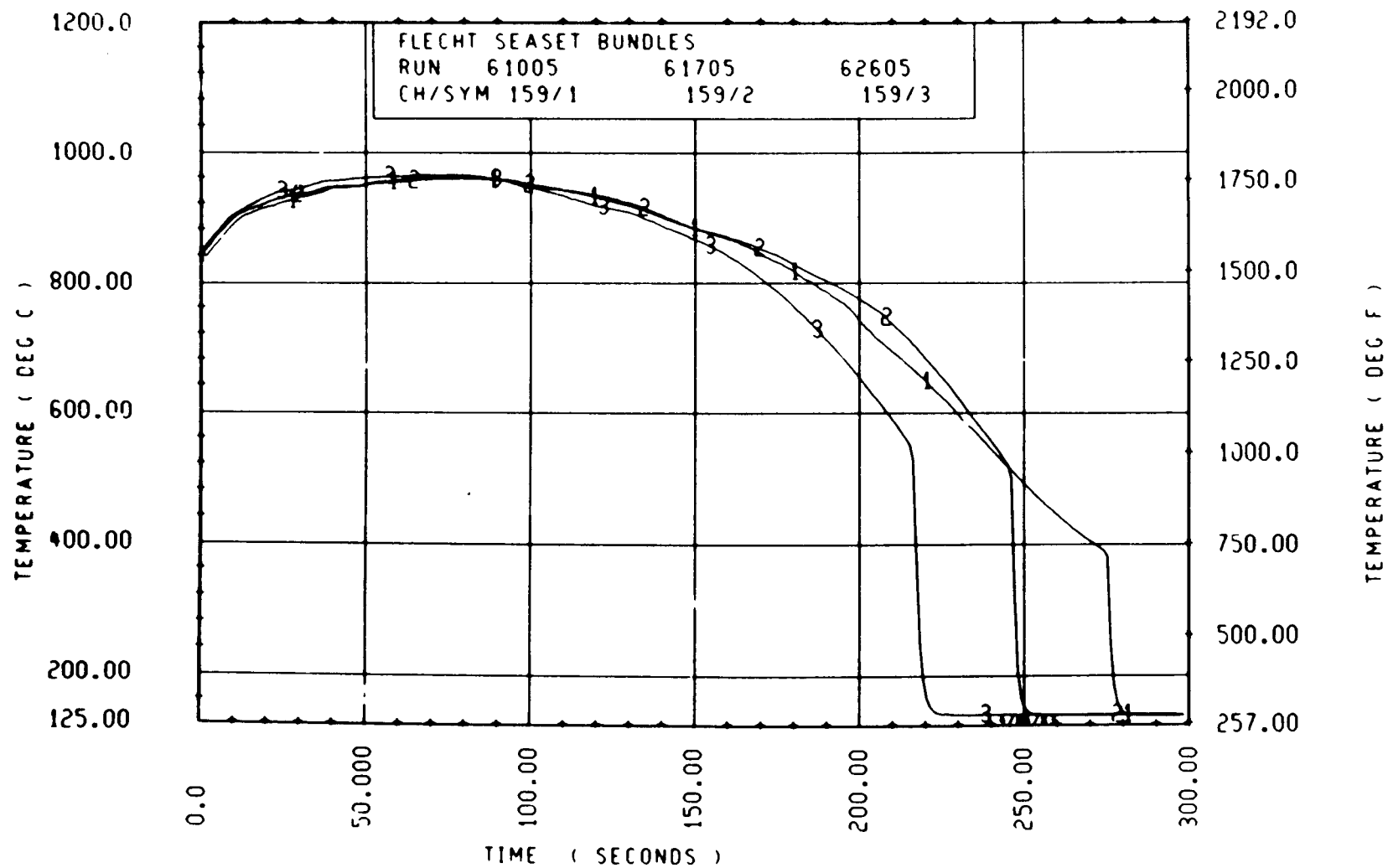


Figure 5-16. Heater Rod Temperature Comparison for Three Repeat Tests

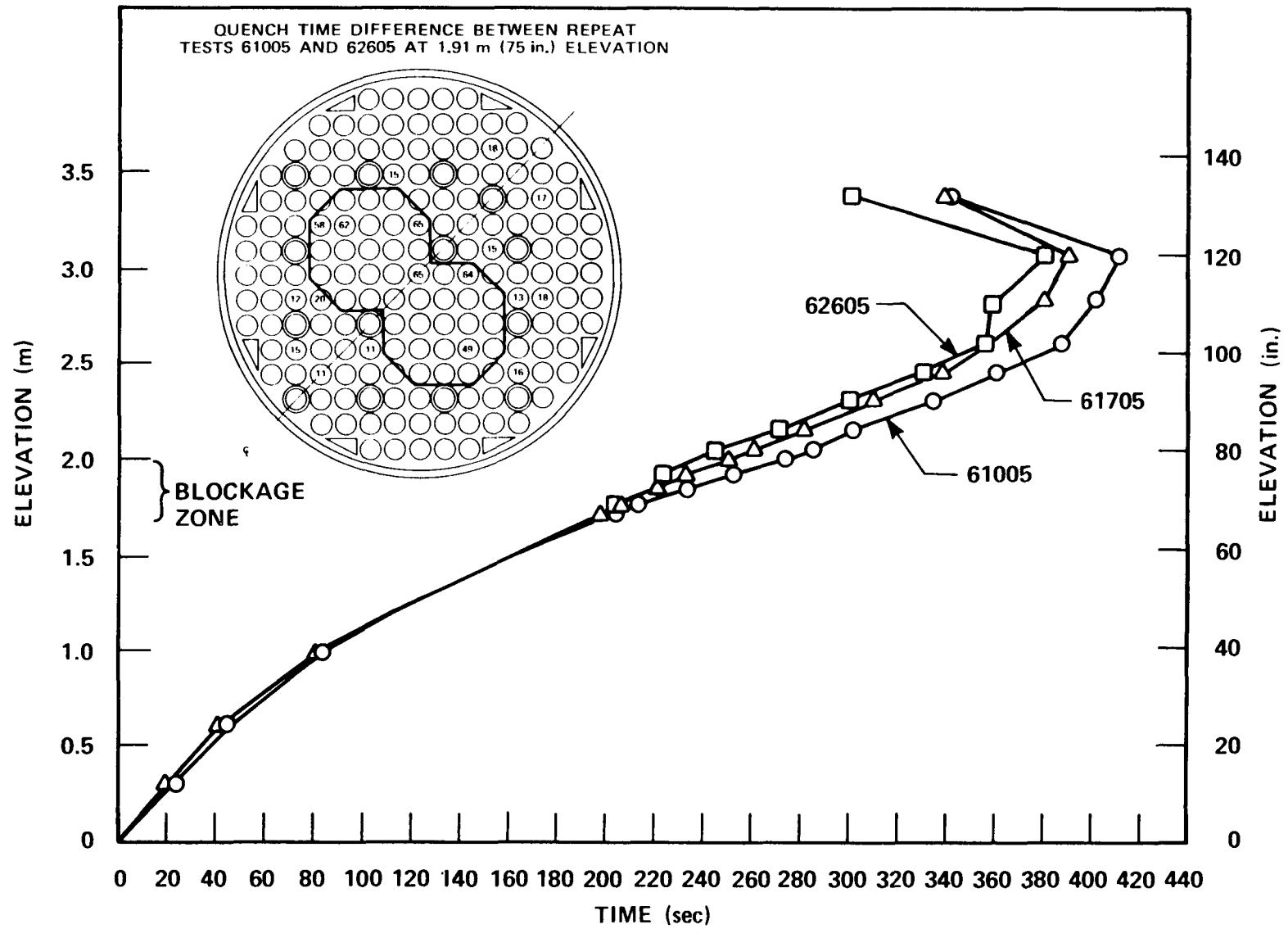


Figure 5-17. Quench Front Comparison for Three Repeat Tests

thermocouples in the blockage islands quenched approximately 60 seconds earlier in run 62605 than in run 61005; the thermocouples in the bypass region quenched only 15 seconds earlier in run 62605 than in run 61005. However, these results are consistent with those measured in the 21-rod bundle repeat tests, as shown below:

21-Rod Bundle Test Repeat	Quench Time at Indicated Elevation (sec)	
	1.52 m (60 in.) (upstream of blockage)	1.98 m (78 in.) (downstream of blockage)
41807F	231.4	352.2
42215F	230.3	354.6
42915F	220.4	330.5
43915F	230.7	316.8
44015F	219.9	302.9

These results indicate the heat transfer improvement near the quench front as the surface of the heater rods and blockage sleeves oxidized.

5-10. SUMMARY OF RUN CONDITIONS AND HOT ROD TEST RESULTS FOR REFLOOD TESTS

The as-run conditions and the hot-rod results for the reflood tests are listed in table 5-1.

The summary results for the forced and gravity reflood tests include the following information:

- o Location of the hottest temperature recorded during the test, which is characterized by the radial location of the rod in the bundle and the thermocouple nominal elevation with respect to the bottom of the heated length
- o Initial and maximum temperatures of the hot rod
- o Turnaround time, which is the time after the start of flooding at which the hot rod maximum temperature was recorded

- o Hottest rod quench time, which is the time after the start of flooding at which the temperature of the hottest rod started to decrease very rapidly
- o Bundle quench time, which is the time after start of flooding at which all thermocouples in the bundle had quenched

5-11. GRAVITY REFLOOD TEST RESULTS

In the first gravity reflood test (run 62819), conducted at 0.14 MPa (20 psia), the downcomer filled to 5.49 m (216 in.) within approximately 20 seconds of initiation of mass injection. The downcomer subsequently remained filled through most of the test, as shown by the measured liquid level in figure 5-18. To prevent the downcomer from filling, the mass injection rate was reduced in run 62919 as tabulated below:

Run	Injection Flow [kg/sec (lb/sec)]
62819	5.80 (12.8) for 15 seconds, 0.785 (1.73) onward
62919	5.80 (12.8) for 5 seconds, 0.594 (1.31) onward

As a result of the decreased mass injection rate, a significantly different downcomer hydraulic response and bundle thermal response was achieved in run 62919. As shown in figure 5-18, the downcomer initially filled to the 1.22 m (48 in.) elevation and continued to fill for approximately 200 seconds to the 4.57 m (180 in.) elevation, at which time the downcomer began to empty. The hot rod temperature responses for the two tests are shown in figure 5-19. Since there were no comparable 161-rod unblocked bundle tests for runs 62819 and 62919, data comparisons were not performed. However, a comparison of the quench times at the 1.98 m (78 in.) elevation for run 62819 in figure 5-20 indicates that the blockage island thermocouples quenched approximately 87 seconds earlier than the bypass region thermocouples. This result signifies the improved heat transfer downstream of the blockage relative to the flow bypass region, although approximately 45 seconds of this time differential may be attributed to the surface oxidation differences between the bypass zone and the blockage zone, as shown in paragraph 5-9.

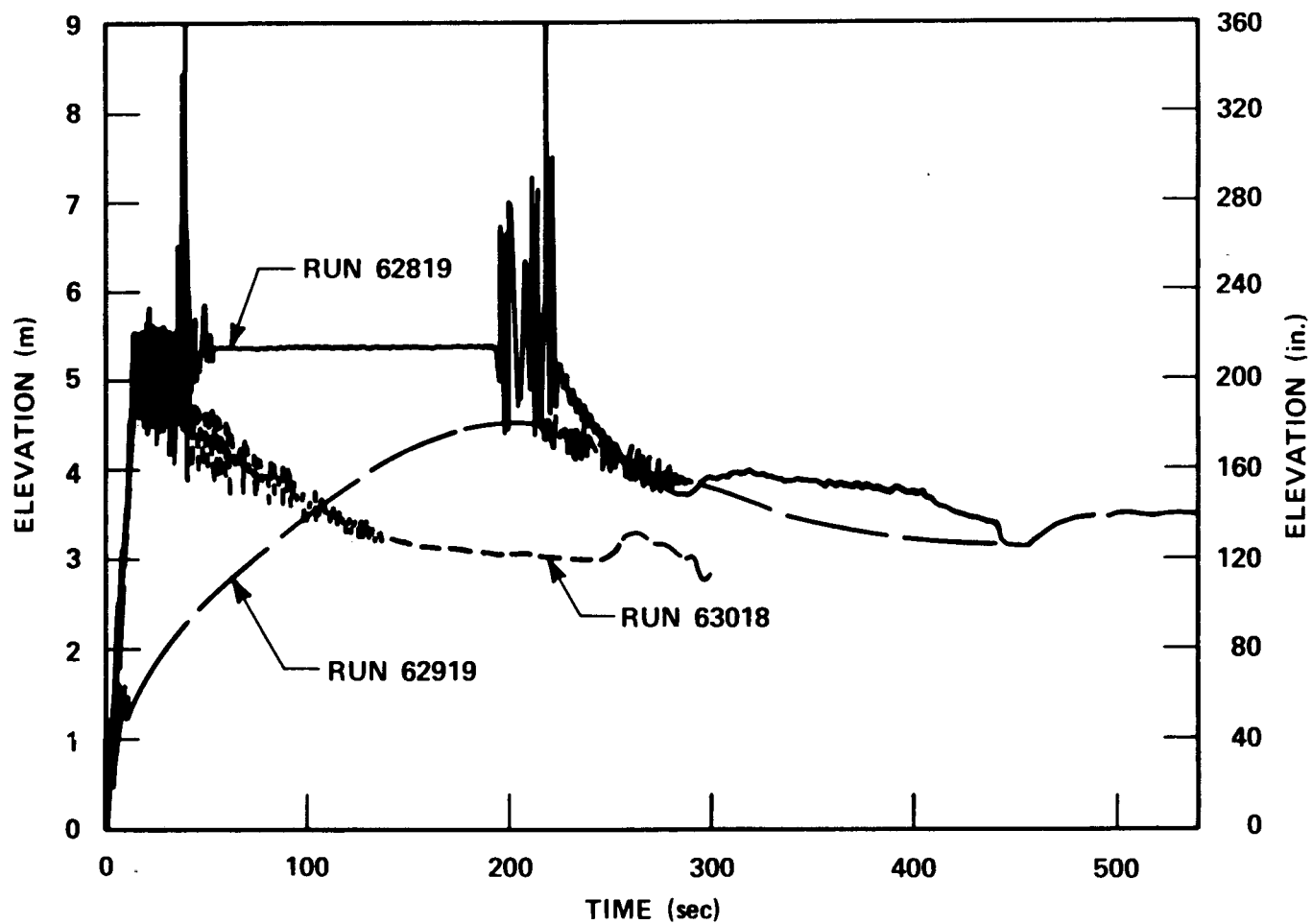


Figure 5-18. Downcomer Fluid Levels

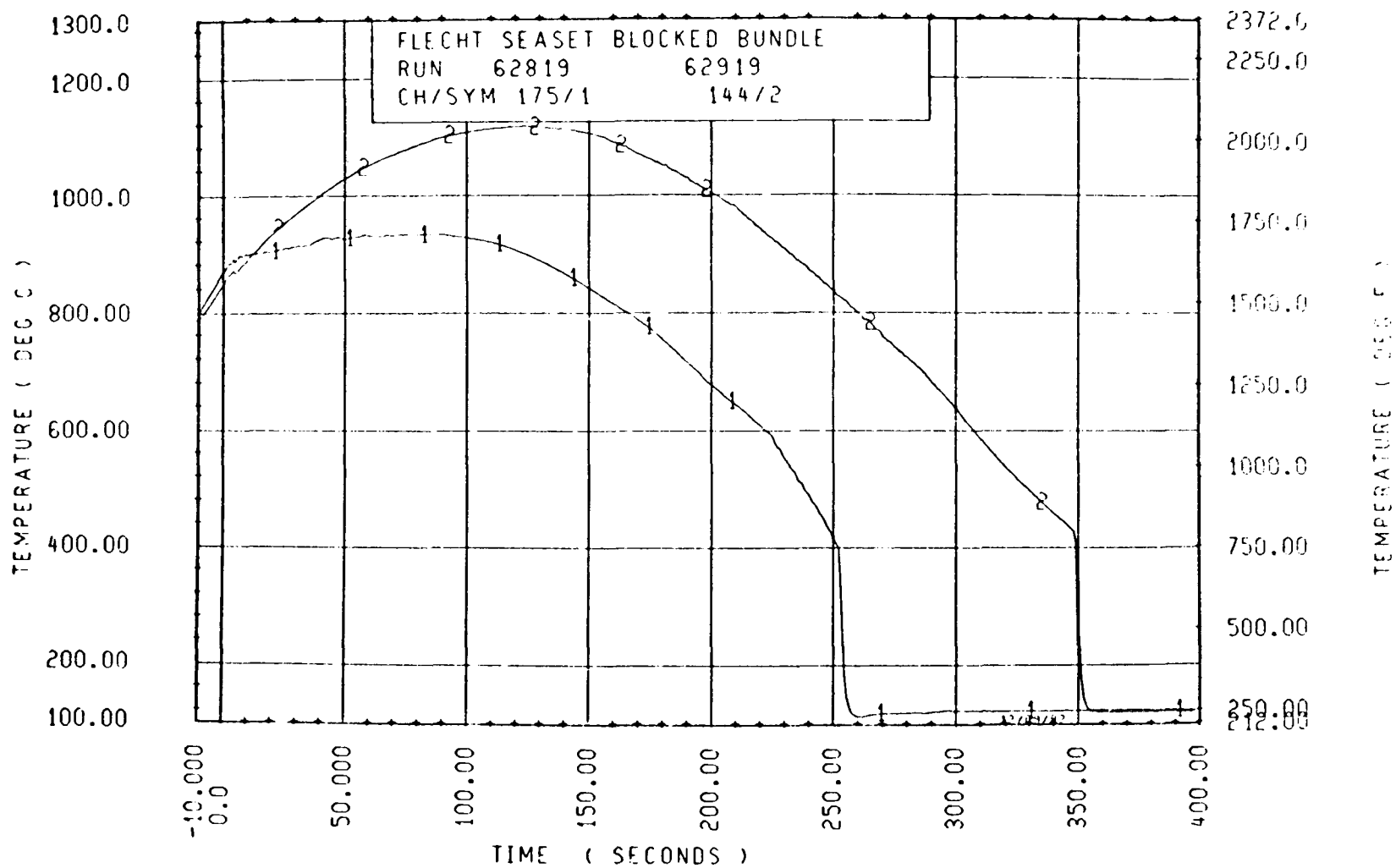


Figure 5-19. Hot Rod Temperature Response for Gravity Reflood Tests with Low (Run 62919) and High (Run 62819) Mass Injection

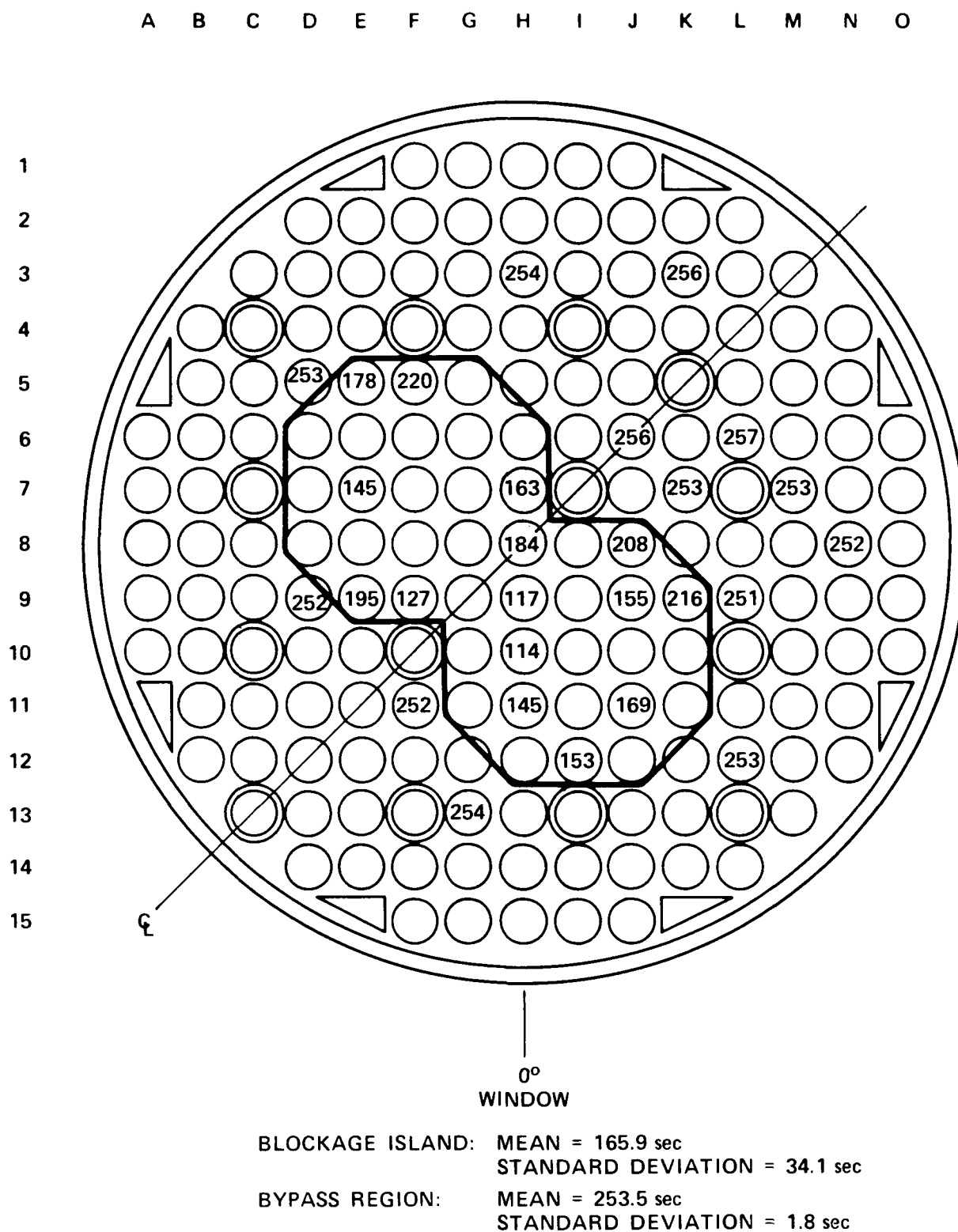


Figure 5-20. Quench Times at 1.98 m (78 in.), Run 62819

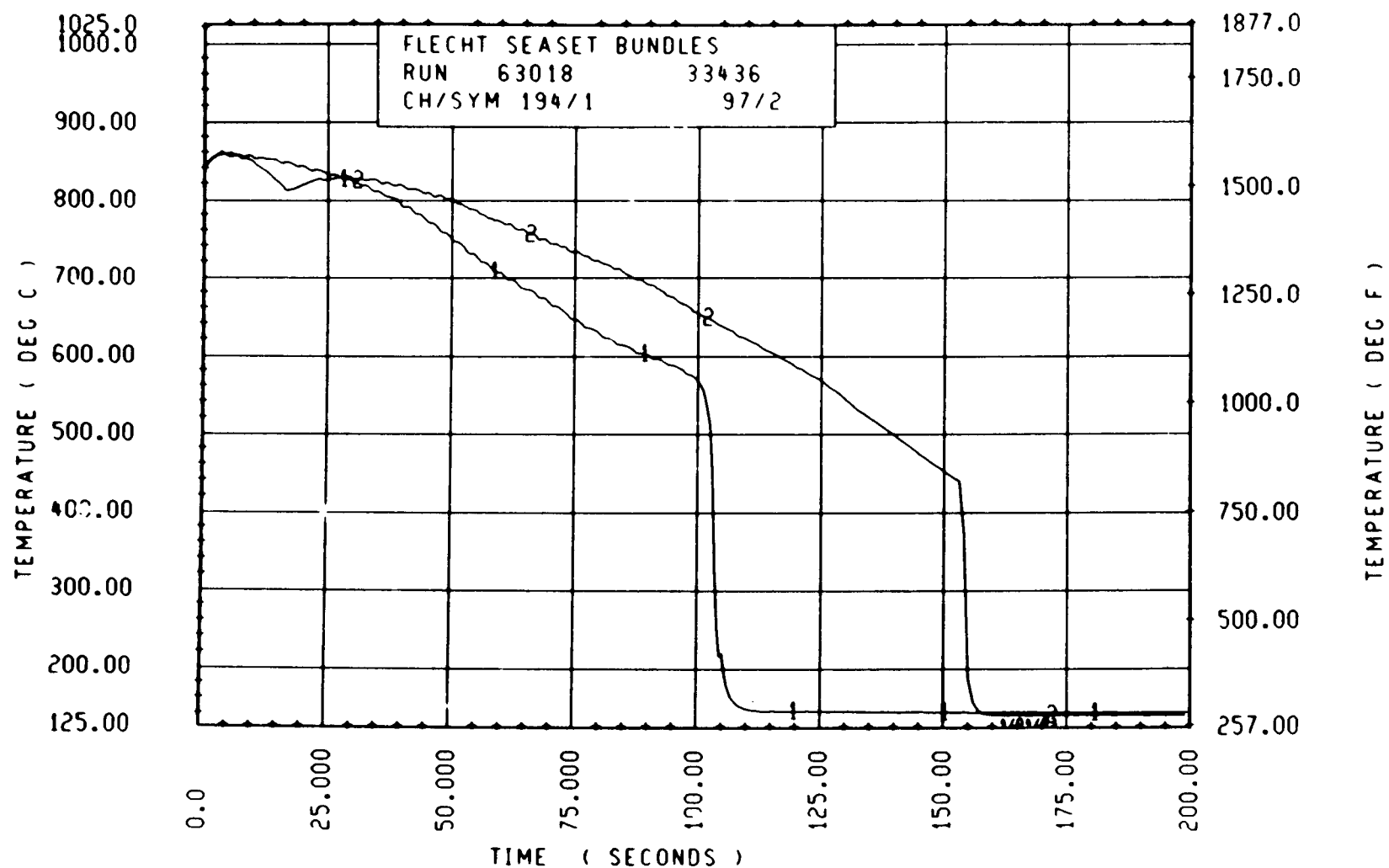


Figure 5-21. Comparison of Heater Rod Temperatures, Rod 9E, Runs 63018 (163-Rod Blocked Bundle) and 33436 (161-Rod Unblocked Bundle), 1.98 m (78 in.) Elevation

The third gravity reflood test (run 63018) was conducted at 0.28 MPa (40 psia) utilizing the same injection rate as in run 62819. In this test, as shown in figure 5-18, the downcomer filled to approximately 4.88 m (192 in.) within 15 seconds after injection and slowly decreased to a level of 3.05 m (120 in.) by the end of the test. A comparison of the measured heater rod temperatures from the blocked bundle and the 161-rod unblocked bundle (run 33436) for rod 9E at the 1.98 m (78 in.) elevation is shown in figure 5-21. A comparison of the quench times at the 1.98 m (78 in.) elevation for run 63018 in figure 5-22 also indicates that the blockage island thermocouples quenched approximately 76 seconds earlier than the bypass region thermocouples.

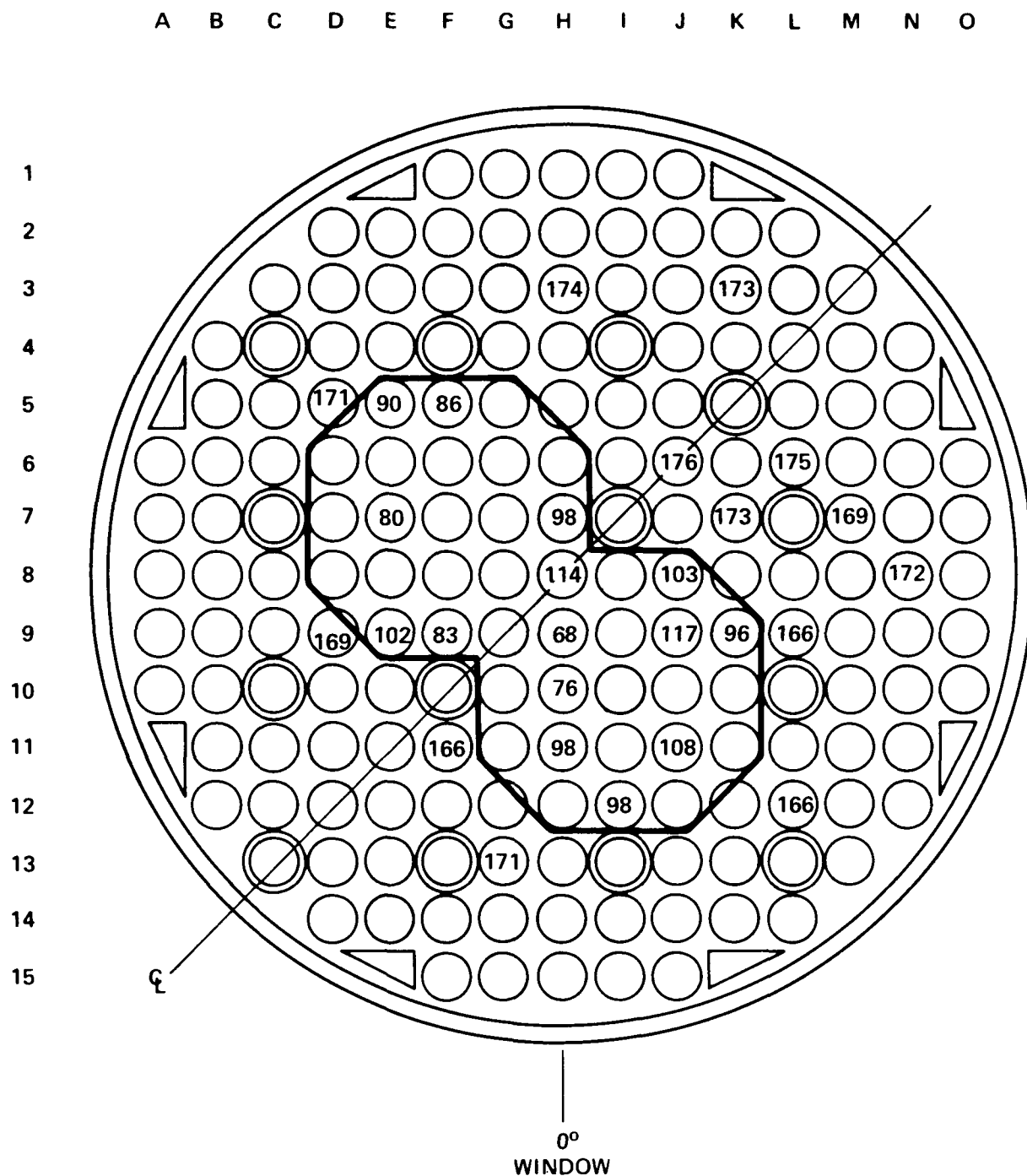
5-12. ROD BUNDLE GEOMETRY

A major concern in conducting the 163-rod bundle tests was the severe rod bundle distortion which had previously occurred in the 161-rod unblocked bundle. This bundle distortion was attributed to the thermal cycling imposed on the heater rods and the filler rods. The following design changes were incorporated in the 163-rod bundle to alleviate the distortion:

- o Heater rods were annealed to remove residual stresses and thus reduce rod bowing.
- o The height of the dimples on the grids was reduced to allow thermal growth of the heater rods through the grids.
- o Filler rods were split and pin-connected to each other to allow thermal growth of the filler rods.

A simple and quantitative indication of the thermal cycling imposed on the heater rod bundle was the time at temperature. The integral of the time-temperature curve for the hot thermocouple at times when the temperature was above 816°C (1500°F) was calculated for each 163-rod bundle test, as shown in figure 5-23. In the 161-rod unblocked bundle, severe rod distortion was calculated to occur by test run 34711, as discussed in appendix G of the 161-rod bundle data report.⁽¹⁾ The summation of the integral of the time-

1. Loftus, M. J., et al., "PWR FLECHT-SEASET Unblocked Bundle, Forced and Gravity Reflood Task Data Report," NRC/EPRI/Westinghouse-7, June 1980.



BLOCKAGE ISLAND: MEAN = 94.5 sec
STANDARD DEVIATION = 13.9 sec

BYPASS REGION: MEAN = 170.8 sec
STANDARD DEVIATION = 3.4 sec

Figure 5-22. Quench Times at 1.98 m (78 in.), Run 63018

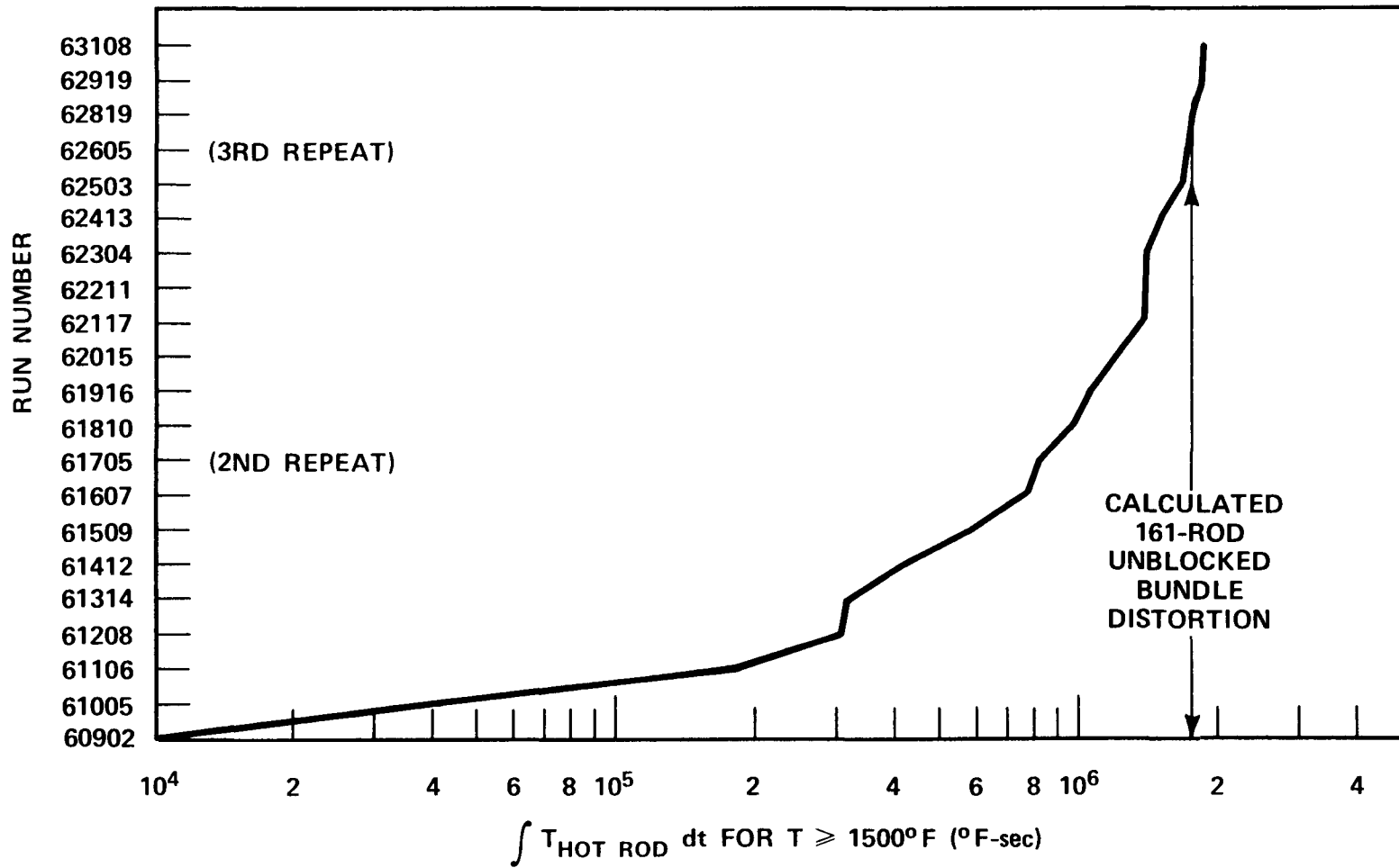


Figure 5-23. Integral of Time-Temperature Curve for Hottest Rod in 163-Rod Blocked Bundle

temperature curve for the 161-rod unblocked bundle tests up to and including run 34711 was $0.97 \times 10^6 \text{ }^\circ\text{C-sec}$ ($1.75 \times 10^6 \text{ }^\circ\text{F-sec}$), as also indicated in figure 5-23. The respective value for the 163-rod blocked bundle tests was $1.03 \times 10^6 \text{ }^\circ\text{C-sec}$ ($1.86 \times 10^6 \text{ }^\circ\text{F-sec}$), which is insignificantly greater than that for the unblocked bundle.

The heater rod bundle was removed from the test facility and thoroughly inspected. There was minimal rod distortion in the center of the bundle, as shown in appendix K.

5-13. FLOW BYPASS EFFECTS

To provide a comprehensive, yet simple, comparison of the flow blockage results to qualify the effects of flow bypass, the temperature rise difference between the blocked and unblocked bundles was calculated as a function of elevation and flooding rate. The temperature rise reflects the integrated heat transfer effect of the flow blockage and bypass. The unblocked-to-blocked temperature rise difference is defined as

$$(\Delta T_{\text{rise}})_{\text{unblocked}} - (\Delta T_{\text{rise}})_{\text{blocked}} \quad (5-3)$$

$$(T_{\text{MAX}} - T_{\text{INIT}})_{\text{unblocked}} - (T_{\text{MAX}} - T_{\text{INIT}})_{\text{blocked}} \quad (5-4)$$

If the initial clad temperatures were the same in the two bundles, the above relationships would simply reduce to the difference between the respective maximum temperatures at the turnaround time,

$$(T_{\text{MAX}})_{\text{unblocked}} - (T_{\text{MAX}})_{\text{blocked}}$$

The unblocked and blocked bundle tests which were compared are shown in table 5-2. The elevations selected for these comparisons were 1.98 m (78 in.), which is immediately downstream of the blockage, and 2.44 and 3.05 m (96 and 120 in.), which are located in the next two grid spans. To provide the most appropriate comparisons between the 21-rod bundle and the 163-rod/161-rod bundles, only the heater rods in the two 21-rod blockage islands of the 163-rod bundle were utilized.

TABLE 5-2
UNBLOCKED AND BLOCKED BUNDLE TESTS
FOR COMPARISON OF FLOW BYPASS EFFECTS

Bundle	Blockage Description	Test Conditions		Power/Flow
		Flooding Rate [m/sec (in./sec)]	Peak Power [kw/m (kw/ft)]	
21-rod unblocked	Not applicable	0.02 (0.9)	2.44 (0.745)	0.87
		0.028 (1.1)	2.44 (0.745)	0.71
21-rod blocked	Long, nonconcentric sleeves distributed noncoplanar on all 21 heater rods	0.038 (1.5)	2.3 (0.70)	0.46
		0.2 (6)	2.3 (0.70)	0.12
161-rod unblocked	Not applicable	0.02 (0.8)	2 (0.7)	0.87
		0.025 (1.0)	2.3 (0.70)	0.71
163-rod blocked	Long, nonconcentric sleeves distributed noncoplanar on two 21-rod islands	0.038 (1.5)	2.3 (0.70)	0.46
		0.038 (1.5)	1.3 (0.40)	0.27
		0.2 (6)	2.3 (0.70)	0.12

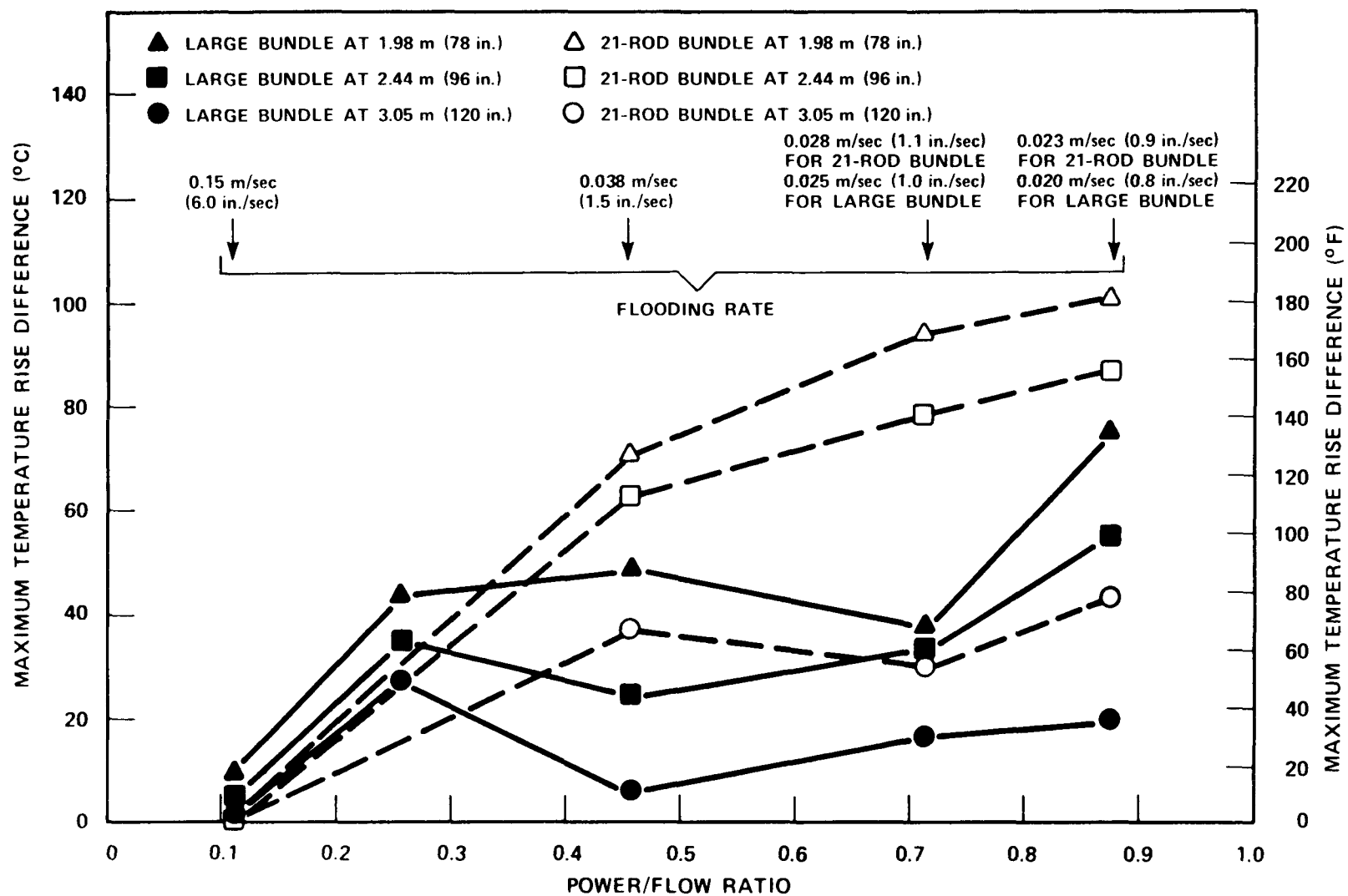


Figure 5-24. Maximum Temperature Rise Difference Comparison With and Without Flow Bypass

The results of these calculations, as shown in figure 5-24, generally indicate the following effects:

- o The temperature rise difference is greater for the 21-rod bundle than for the large blocked bundle. This is attributed to the flow bypass effect in the large bundle, which decreases the flow through the blockage region. However, even with the flow bypass effect, the blocked bundle maximum temperature is less than that for the unblocked bundle.
- o As the flooding rate decreases, the temperature rise difference between the unblocked and blocked bundles increases. This indicates that the maximum temperature in the blocked bundle decreases. The maximum temperature in the blocked bundle decreases because of the improved heat transfer downstream of the blockage. The amount of the heat transfer improvement is affected by the absolute level of the heat transfer. As the flooding rate decreases, the overall heat transfer level decreases; therefore any improvement in the heat transfer significantly affects the measured rod temperature. Also, with reduced flooding rate, the period of two-phase dispersed flow is increased with respect to time, which means that the droplet breakup effect is increased.
- o As the distance downstream of the blockage increases, the temperature rise difference between the unblocked and blocked bundles decreases. This indicates that the maximum temperature in the blocked bundle increases with distance from the blockage. However, the blocked bundle maximum temperature is still less than that for the unblocked bundle. This axial effect downstream of the blockage is similar to a thermal entry region for a tube and has been observed downstream of a grid⁽¹⁾ and other blockages.⁽²⁾

-
1. Yao, S. C., et al., "Heat Transfer Augmentation in Rod Bundles Near Grid Spans," presented at ASME Winter Annual Meeting in Chicago, IL, November 16-21, 1980.
 2. Ihle, P., and Rust, K., "FEBA - Flooding Experiments With Blocked Arrays - Influence of Blockage Shape," Trans. American Nuclear Society 31, 399-400 (1979).

The temperature rise difference as a function of time is shown in figure 5-25 for the tests with the highest power-to-flow ratio at the 1.98 m (78 in.) elevation.) This figure indicates a consistently larger difference in the temperature rise as the reflood transient progresses through 120 seconds. This difference is greater [approximately 44°C (80°F)] than that shown previously in figure 5-24 [approximately 25°C (45°F)], since the turnaround time for the blocked bundle with flow bypass is longer than that for the blocked bundle without flow bypass.

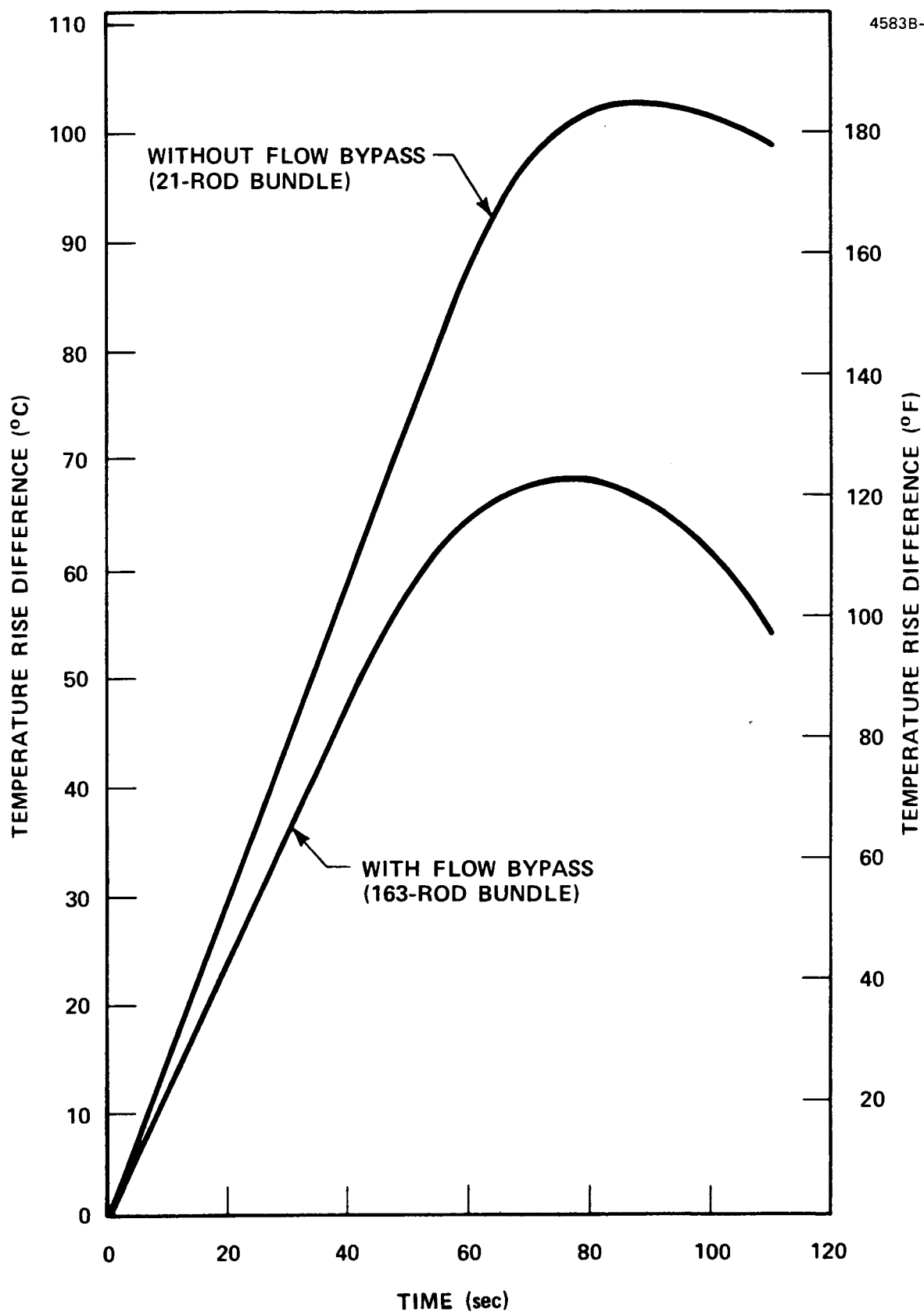


Figure 5-25. Transient Temperature Rise Comparison With and Without Flow Bypass, 1.98 m (78 in.) Elevation

SECTION 6

CONCLUSIONS

The objectives of the 163-rod blocked bundle test program were judged to have been successfully met. Thermal-hydraulic data from 20 forced reflood tests and three gravity reflood tests were obtained, and all test data were found to be valid. The 163-rod blocked bundle data, which cover a wide range of thermal-hydraulic conditions, provide a basis for assessment of the flow blockage model to be developed from the 21-rod bundle test data. The flow blockage model evaluation report will be issued in 1984.

In the 163-rod bundle, the peak measured rod temperatures in and downstream of the blockage islands were less than the corresponding rod temperatures in the 161-rod unblocked bundle for all conditions tested. Although more tests would have provided a larger data base, it is believed that the tests which were conducted would adequately address the NRC Appendix K, 10CFR50.46, steam cooling and flow blockage rule.

APPENDIX A
BLOCKAGE SLEEVE SELECTION

A-1. INTRODUCTION

Paragraphs A-2 and A-3 are reprinted from appendix C of the 21-rod bundle data and analysis report,⁽¹⁾ which details the selection of the long, nonconcentric sleeve for use in the 163-rod blocked bundle. The blockage sleeve selection was based on the test data from the following four 21-rod bundle configurations:

- o Configuration A - unblocked
- o Configuration C - 21-rods blocked coplanar, short sleeves
- o Configuration D - 21-rods blocked noncoplanar, short sleeves
- o Configuration E - 21-rods blocked noncoplanar, long sleeves, 36-percent peak strain

The sleeve selection was also based on the COBRA code flow redistribution calculations for the two 21-rod bundle blockage islands, as illustrated in figure A-1. The following paragraphs describe the COBRA results, the projected heat transfer in the 163-rod blocked bundle, and the estimated rod temperature rise in the 163-rod blocked bundle.

The long, nonconcentric blockage sleeve with 36-percent peak strain was found to provide the highest temperature rise in the large blocked bundle. However, to provide more flow blockage in the 163-rod bundle, the PMG agreed to increase the peak strain for the nonconcentric sleeve to 44 percent. To provide test data for the 44-percent peak strain sleeve without flow bypass, a sixth 21-rod bundle configuration (F) was subsequently tested.

1. Loftus, M. J., et al., "PWR FLECHT SEASET 21-Rod Bundle Flow Blockage Task Data and Analysis Report," NRC/EPRI/Westinghouse-11, September 1982.

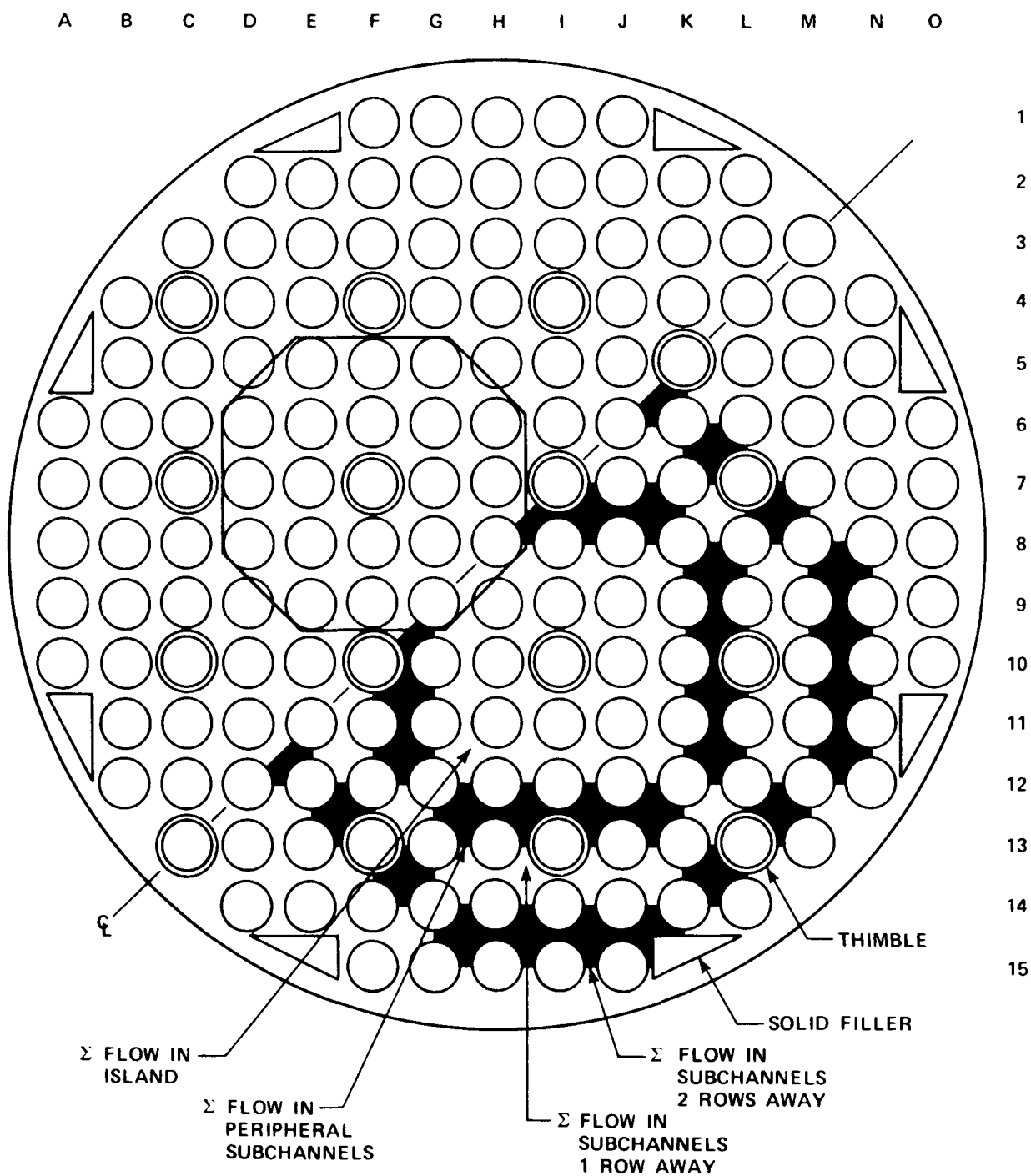


Figure A-1. 21-Rod Island in Large Blocked Bundle

A-2. FLOW DIVERSION IN 163-ROD BUNDLE WITH BLOCKAGE

The sleeve choice should be based on resulting heat transfer in tests with enough bypass flow area to allow fluid bypass. The tests of the 21-rod bundle do not provide bypass flow area. Therefore, flow diversions in the large bundle with blockage islands (figure A-1) were calculated using COBRA-IV-1 to estimate the heat transfer coefficients in the large bundle as described below. COBRA simulations of this large bundle were performed on half of the bundle to take advantage of bundle symmetry. All the simulation conditions were the same as those of the 21-rod bundle except for the channel and gap addresses. There were also slight changes in flow blockage factors for the peripheral subchannels of the blockage islands, since there was excess flow area in the peripheral subchannels of the 21-rod bundle.

The results, shown in figures A-2 through A-5, show clearly that flow diversion from the blockage islands is important. Figure A-2 shows the total flow rate ratios in the blocked island, figure A-3 shows the total flow rate ratios just outside the blocked island, and figures A-4 and A-5 show the total flow rate ratios one and two rows away from the blocked islands, respectively.

A-3. ESTIMATION OF HEAT TRANSFER COEFFICIENTS IN THE LARGE BUNDLE

The heat transfer coefficients in the large bundle with the partial blockages can be estimated using the following relationship:

$$\frac{h_{(1,Z,x,163)}}{h_{(1,Z,A,163)}} = Ne \left(\frac{U_{(1,Z,x,163)}}{U_{(1,Z,A,163)}} \right)^m \quad (A-1)$$

where

- 1 = rod identification
- Z = axial elevation
- x = type of blockage
 - C - coplanar short sleeve
 - D - noncoplanar short sleeve
 - E - noncoplanar long sleeve

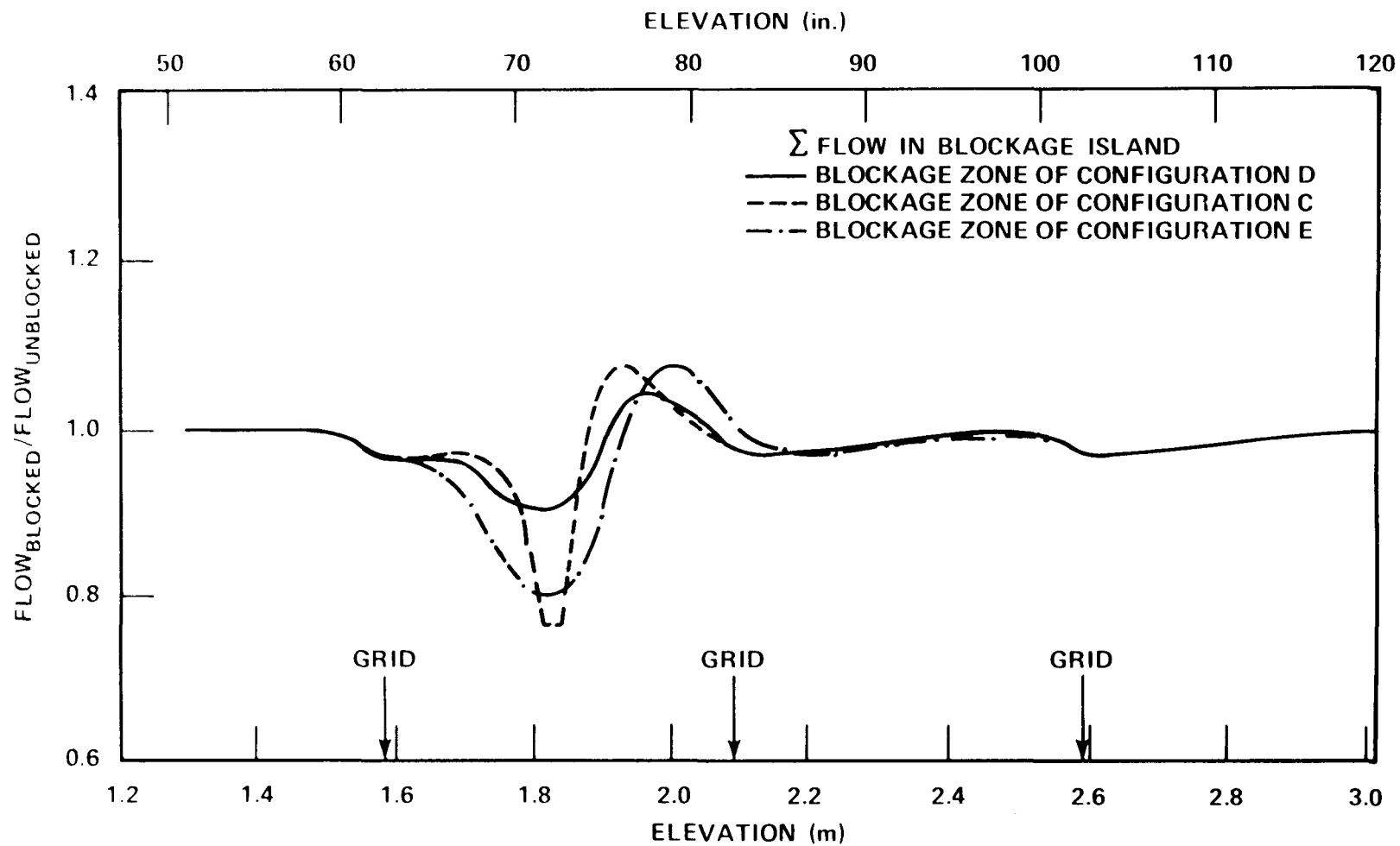


Figure A-2. Integrated Flow Diversion in Blocked Island of Large Bundle

A-5

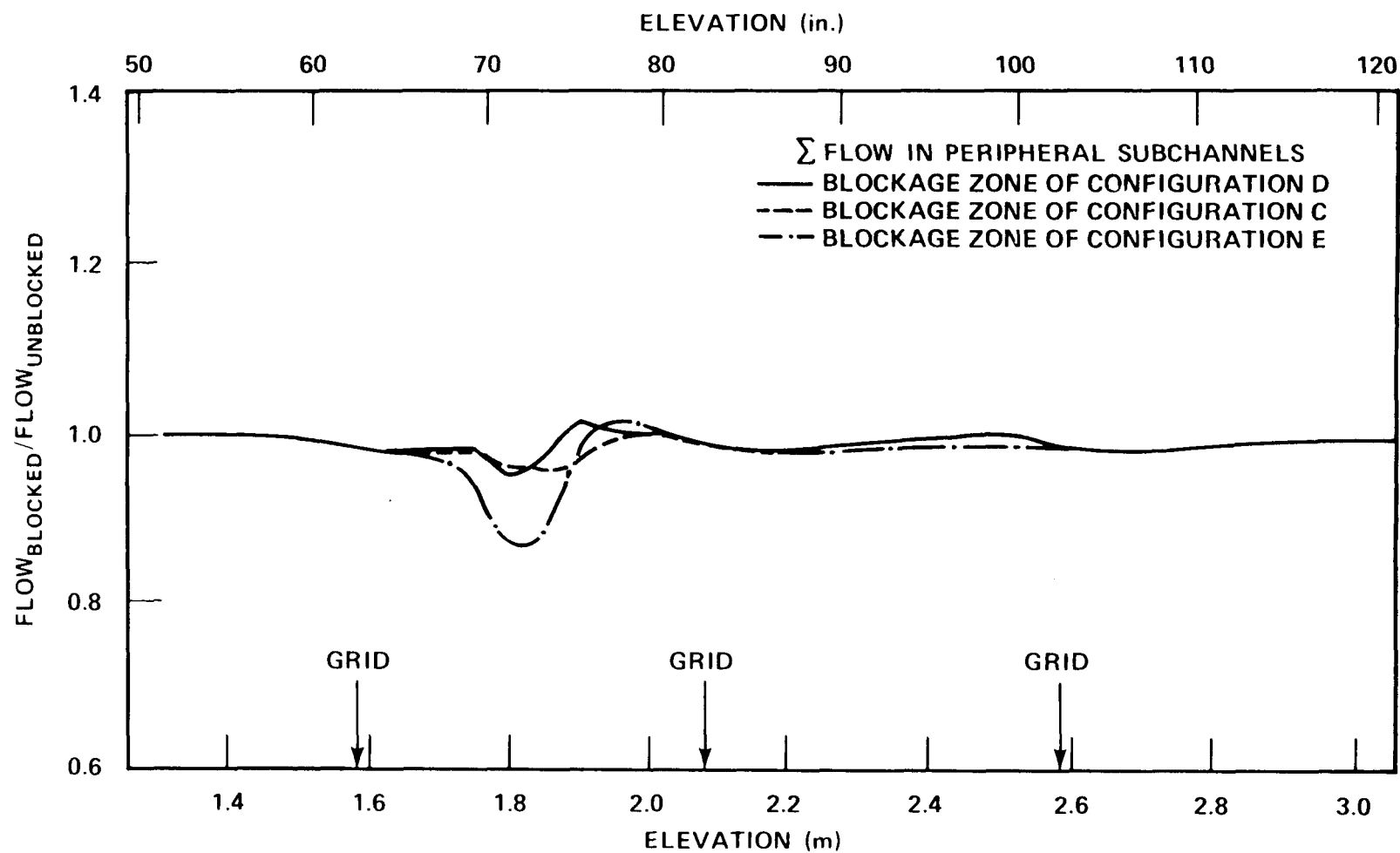


Figure A-3. Integrated Flow Diversion in Peripheral Subchannels of Blocked Island in Large Bundle

A-6

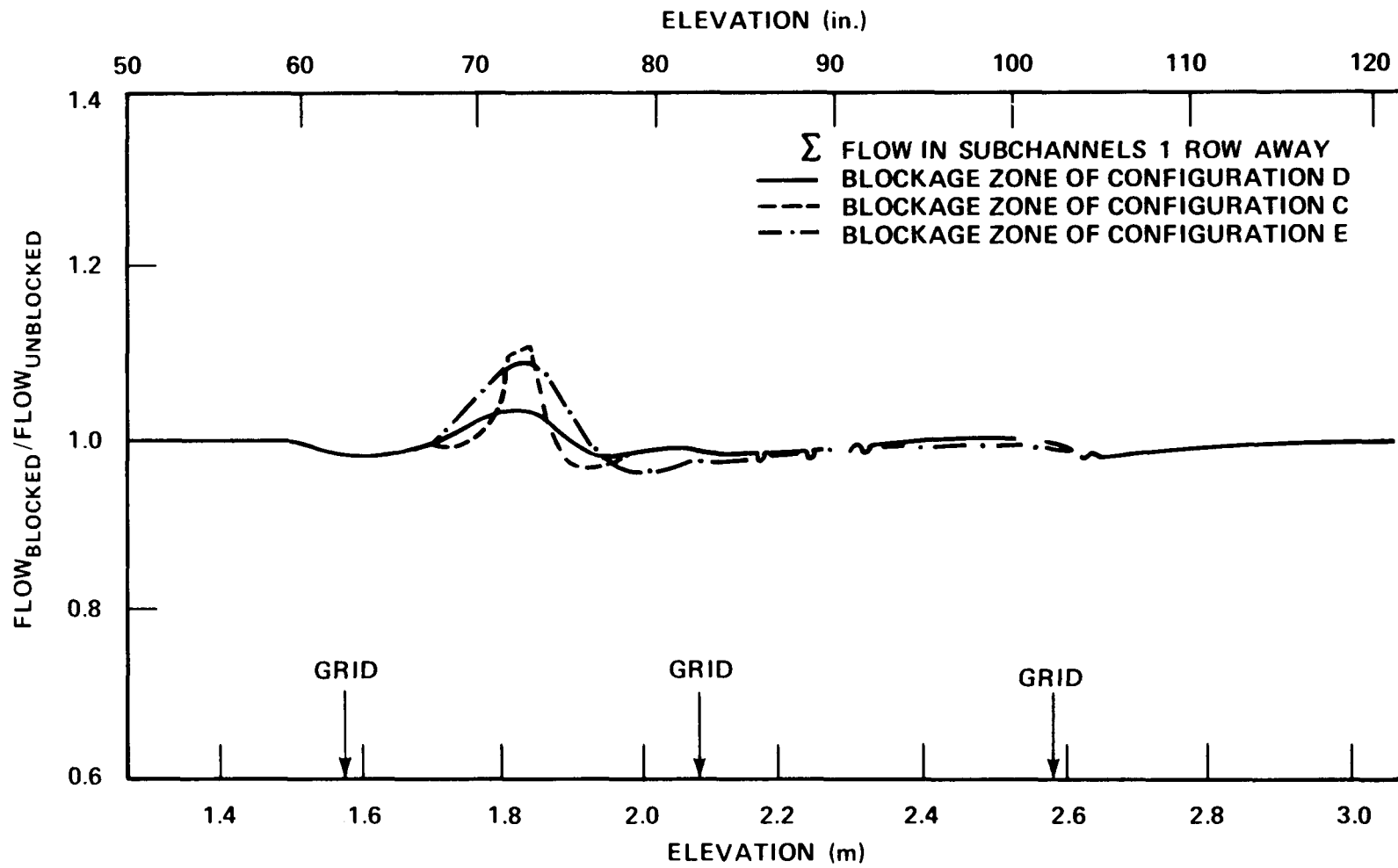


Figure A-4. Integrated Flow Diversion in Channels One Row Away From Blocked Island in Large Bundle

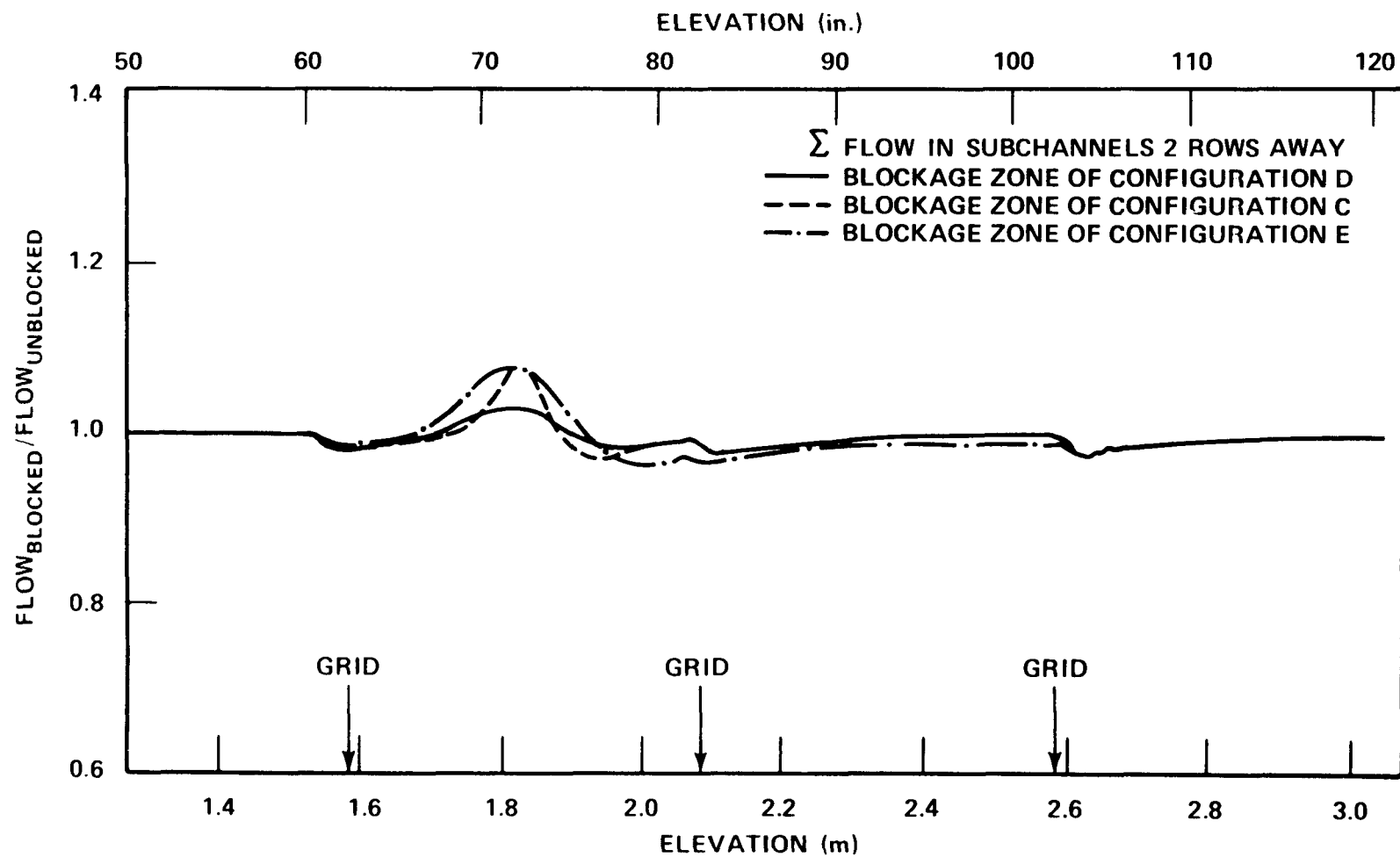


Figure A-5. Integrated Flow Diversion in Channels Two Rows Away From Blocked Island in Large Bundle

A = unblocked bundle
 163 = 163-rod bundle
 h = heat transfer coefficient
 Ne = enhancement factor
 U = velocity
 m = exponent (0.6-0.8)

The velocities in equation (A-1) are calculated by COBRA and the enhancement factor can be calculated from the 21-rod bundle test data, assuming that the factor is the same for both bundles. That is,

$$\begin{aligned}
 Ne_{(1,Z,x,163)} &= Ne_{(1,Z,x,21)} \\
 &= \left[\frac{h_{(1,Z,x,21)}}{h_{(1,Z,A,21)}} \bigg/ \frac{U_{(1,Z,x,21)}}{h_{(1,Z,A,21)}} \right]^m
 \end{aligned}
 \tag{A-2}$$

Since the heat transfer coefficients in the unblocked large bundle are available, equation (A-1) permits calculation of the expected heat transfer coefficients in the large bundle with blockages. A schematic diagram of the procedure used to obtain the heat transfer ratios is shown in figure A-6.

Some of the results of the reference tests using the constant 0.8 as the exponent m are shown in figure A-7 for the blockage islands corresponding to bundle configurations C, D, and E. (Configuration C is considered to discern the sleeve distribution effect.) The figures show that the enhancement factors reach a peak during the first 20 to 30 seconds and then decrease to a fairly uniform value. It appears that the blockage effects on heat transfer during these two periods are different from each other. Comparisons of heat transfer among the three bundles at early and late times in the test are shown in table A-1. The comparisons of the heat transfer are summarized as follows:

- o For later times (>30 sec), below 1.98 m (78 in.), configuration E is the lowest for all inner thermocouples (thermocouples on the inner nine rods). Configuration E is generally the lowest for outer thermocouples, in most cases.
- o For early times (<30 seconds), many cases show $D < E$.

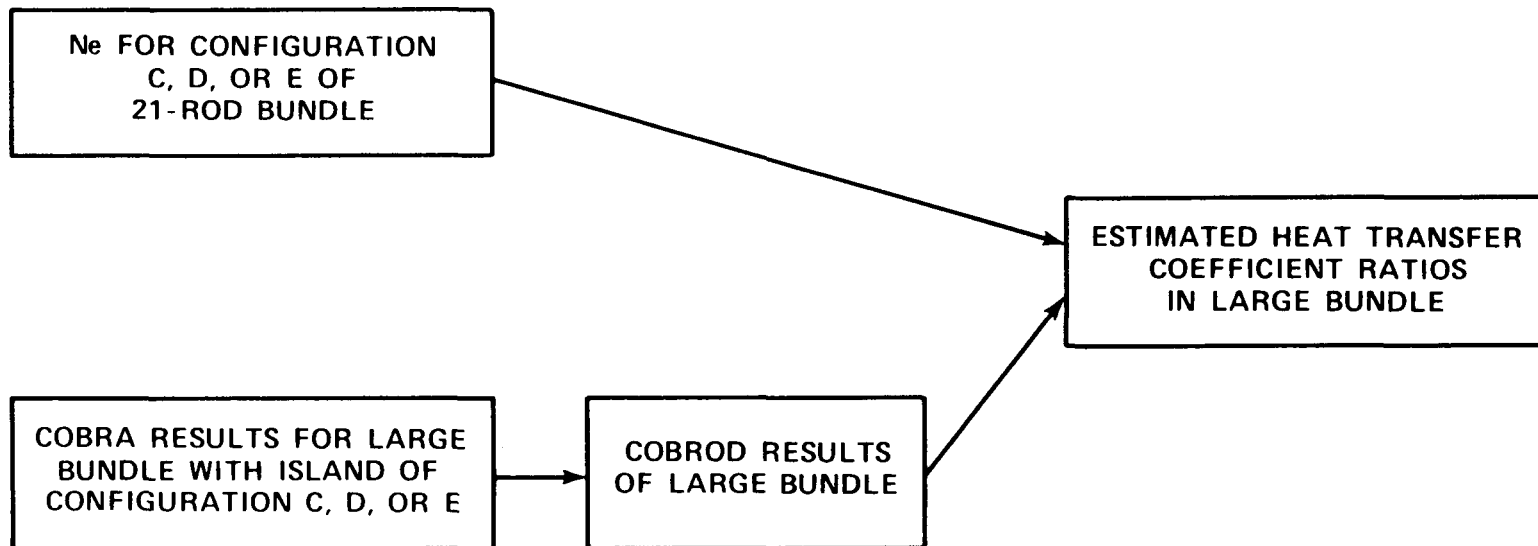


Figure A-6. Estimation of Heat Transfer Coefficient Ratios

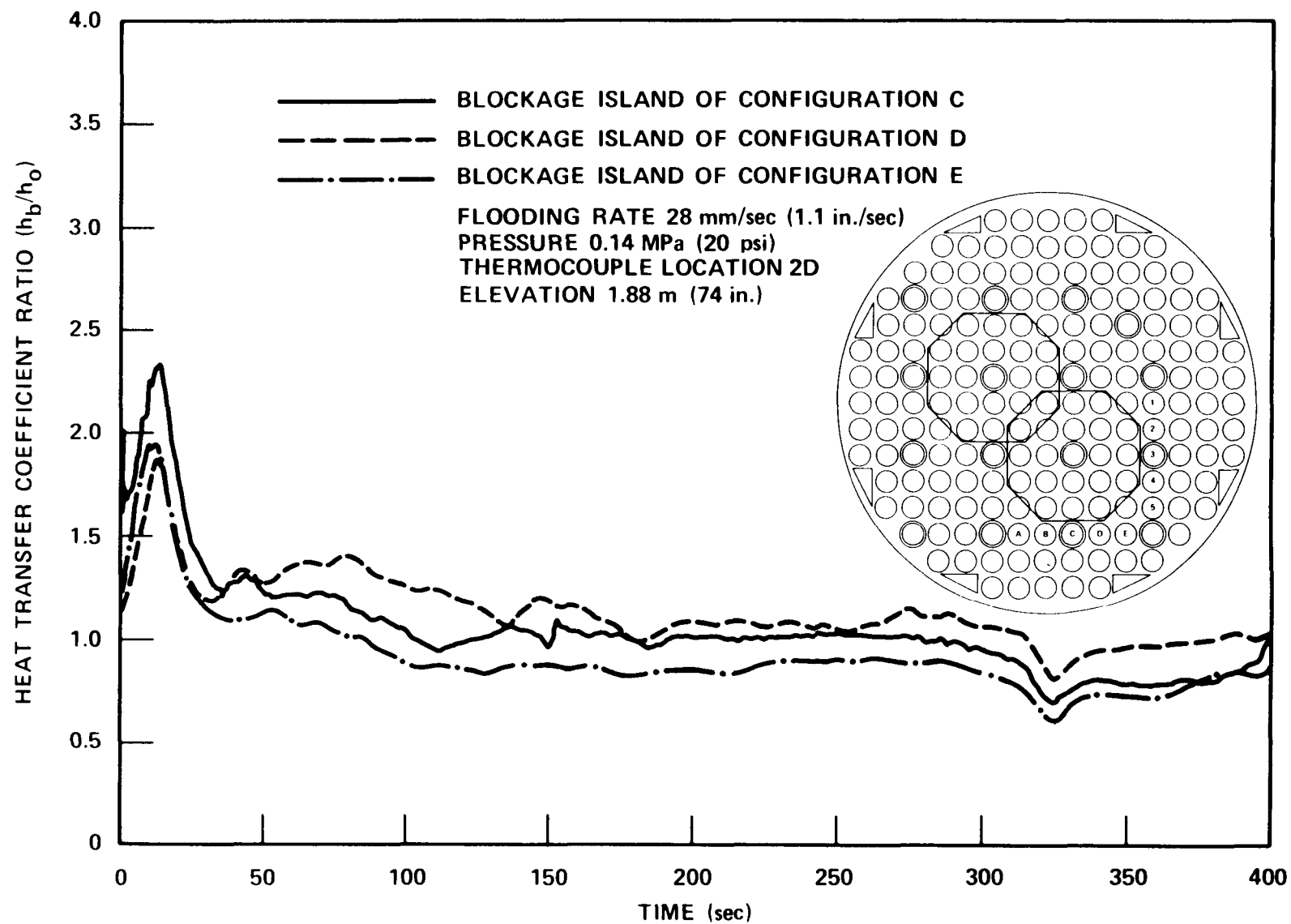


Figure A-7. Estimated Heat Transfer Coefficient Ratios (sheet 1 of 3)

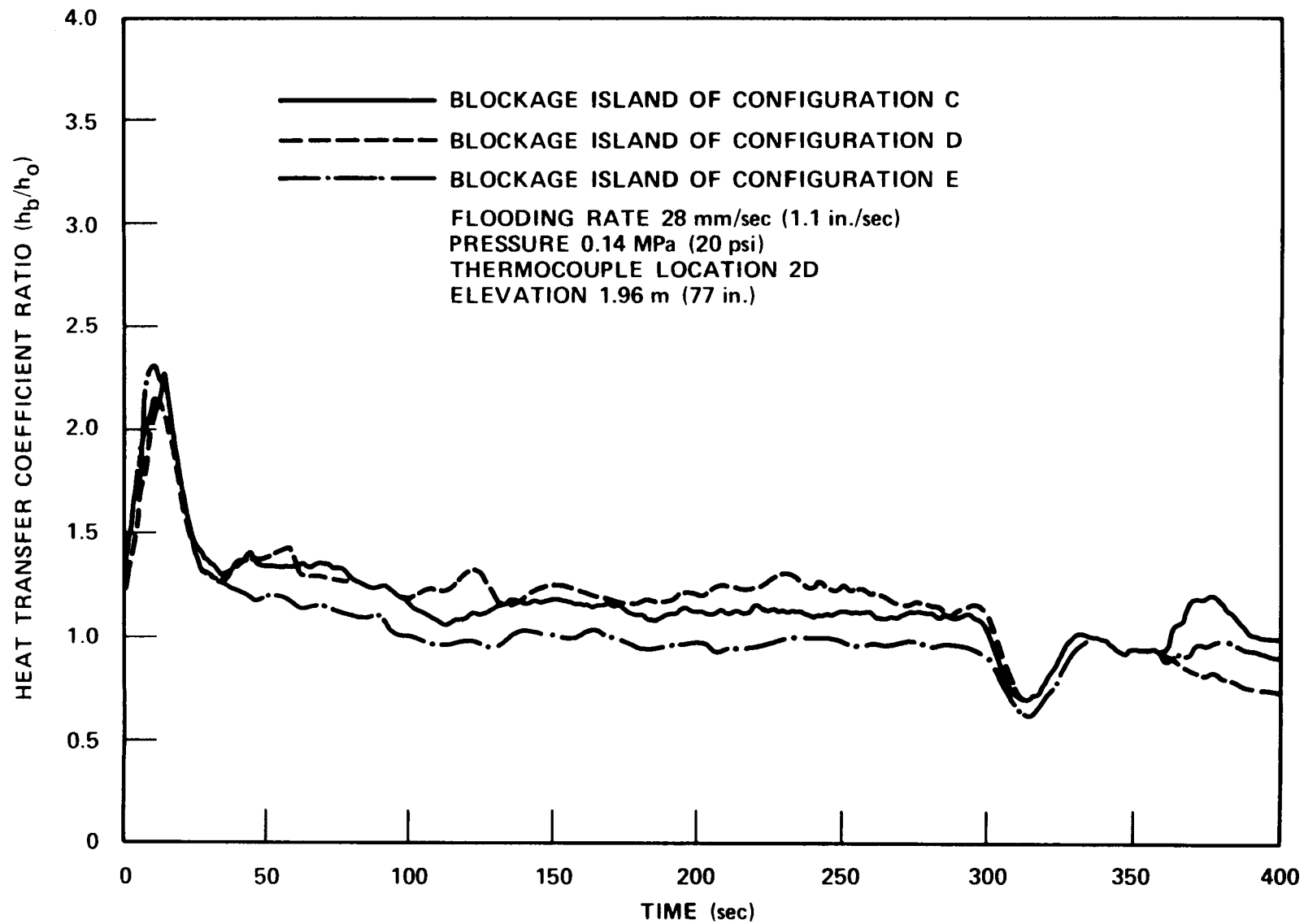


Figure A-7. Estimated Heat Transfer Coefficient Ratios (sheet 2 of 3)

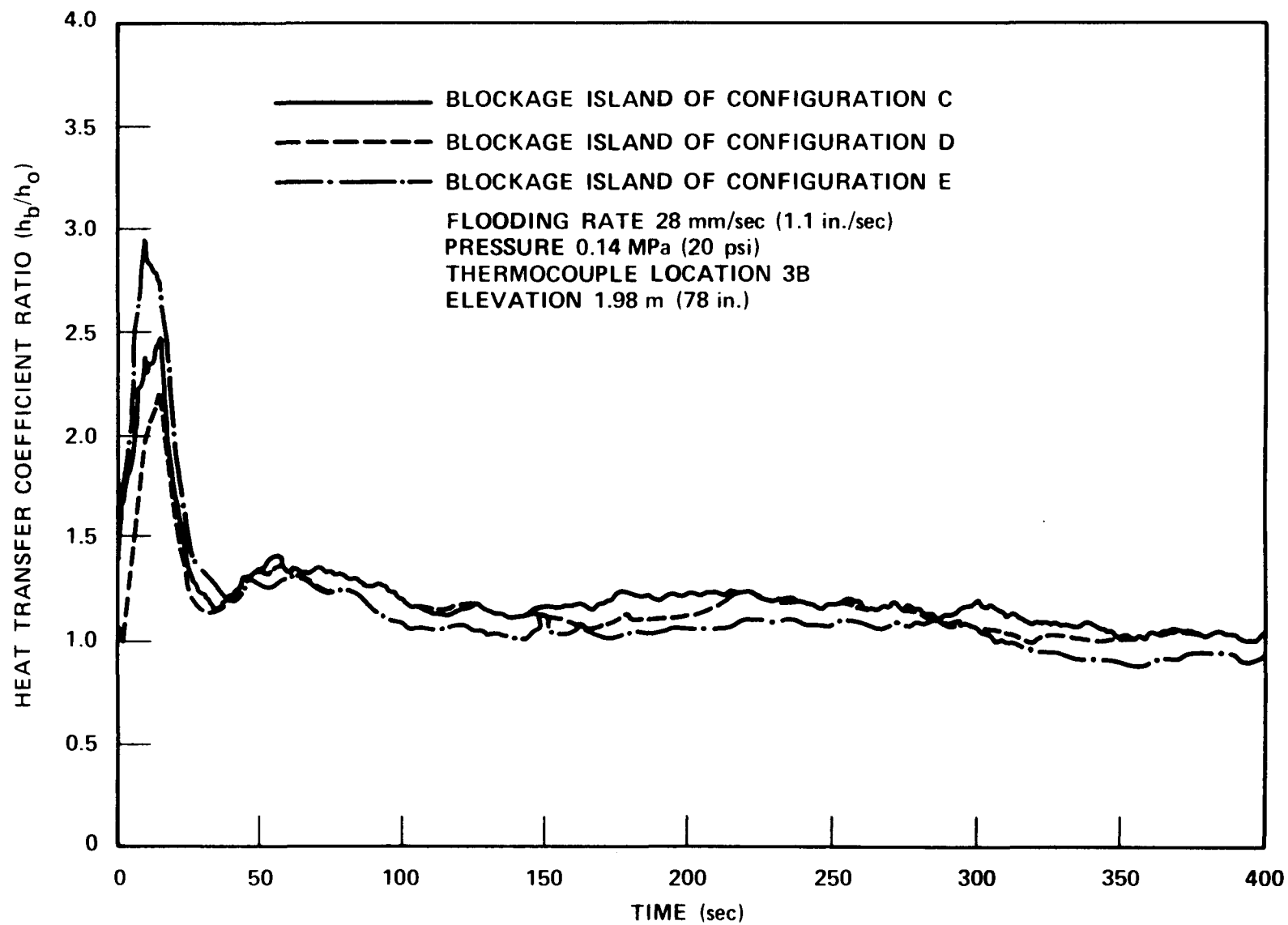


Figure A-7. Estimated Heat Transfer Coefficient Ratios (sheet 3 of 3)

TABLE A-1
CALCULATED HEAT TRANSFER COMPARISONS

Rod	Elevation [m (in.)]	Run 42430A 28 mm/sec (1.1 in./sec) 0.28 MPa (40 psi)		Run 42606A 23 mm/sec (0.91 in./sec) 0.28 MPa (40 psi)		Run 43112A 28 mm/sec (1.1 in./sec) 0.14 MPa (20 psi)		Run 42804A 12 mm/sec (0.52 in./sec) 0.28 MPa (40 psi)	
		Early	Later	Early	Later	Early	Later	Early	Later
2D	1.88(74)	E≈D<C	E<D≈C	E<D<C	E<D<C	D≈E<C	E<C<D	E<D<C	E<C<D
2D	1.96(77)	E≈D≈C	E<D≈C	E≈D≈C	E<D<C	D≈C≈E	E<C<D	E≈D<C	E<D≈C
4C	1.98(78)	--	E<D<C	--	E<D<C	--	E<D<C	--	E<D≈C
3B	1.98(78)	C≈D<E	E<D<C	D<C<E	E<D<C	D<C<E	E<D<C	E≈D≈C	E≈D≈C
3C	1.98(78)	C<D≈E	E<D<C	D≈C≈E	E<D<C	D≈C≈E	E<D<C	C<D≈E	E<C≈D
3D	2.13(84)	C≈D<E	E<D≈C	D<C<E	?	D<C<E	E<C<D	C≈D<E	C<E≈D
2C	2.29(90)	D<C≈E	D≈C≈E	D<E<C	C<E≈D	D<C<E	D≈C≈E	D<C≈E	D<C<E
3B	2.29(90)	C<D≈E	E<D<C	D<C<E	D<E<C	D≈C<E	D≈C≈E	E<D≈C	E<D<C
3B	2.44(96)	--	E<D<C	--	E<D<C	--	E<C<D	--	E=C=D
5C	2.44(96)	C≈D≈E	C≈D≈E	D≈C≈E	D≈C≈E	C≈D<E	E<C<D	--	E≈C≈D
1C	2.59(102)	--	E<C<D	--	E<C<D	--	E<C<D	--	E≈C≈D
3D	2.82(111)	--	D≈C≈E	--	D≈C≈E	--	D≈C≈E	--	C≈E≈D
4C	2.82(111)	--	E≈D<C	--	D<E<C	--	E<D<C	--	C≈E≈D
1D	1.90(75)	E≈D≈C	E<C<D	--	E<D<C	E≈C≈D	E<C<D	E<C<D	E<C<D
5D	1.90(75)	D<C<E	E<C<D	D≈C<E	E<D<C	D<C<E	E<C<D	E<C<D	E<D<C
4A	1.93(76)	C<D<E	E≈C<D	C<D<E	E≈D≈C	C<D<E	E≈C<D	E<C≈D	E<D≈C

TABLE A-1 (cont)
CALCULATED HEAT TRANSFER COMPARISONS

Rod	Elevation [m (in.)]	Run 42430A		Run 42606A		Run 43112A		Run 42804A	
		Early	Later	Early	Later	Early	Later	Early	Later
1D	1.96(77)	C<D<E	E≈C≈D	E<D<C	E≈C≈D	D≈C<E	E≈C<D	C<D≈E	E<D<C
2D	1.96(77)	E≈D≈C	E<D<C	D<E<C	E<D<C	D≈C≈E	E<C<D	D≈E<C	E<D<C
5D	1.96(77)	C<D<E	E≈C<D	C<D<E	E≈D<C	C≈D<E	C≈E≈D	E≈D<C	E≈D≈C
4A	1.98(78)	C<D<E	C<E<D	C<D<E	C≈E≈D	C<D<E	C<E<D	C<D<E	C<D<E
4E	1.98(78)	C<E	E<C	C<E	E<C	C<E	C≈E	C<E	C<E
1C	2.13(84)	C<E<D	D<E<C	E≈C	E≈C	C<E	E≈C	C<E	C<E
2B	2.13(84)	C<E	E≈C	D<C<E	--	D≈C≈E	D<C≈E	D<C<E	D<C<E
4D	2.13(84)	E≈C	E<C	E≈C	E<C	C<E	E<C	--	--
5B	2.13(84)	C≈E≈D	E≈C<D	--	E<D<C	D<C<E	E<C<D	D≈E<C	D≈C≈E
2E	2.29(90)	C<E<D	E≈C≈D	C<D<E	--	C<D<E	C<E<D	C<D≈E	C<E<D
3A	2.29(90)	C≈D	C≈D	--	--	C≈D	C≈D	C<D	D<C
3D	2.29(90)	E≈C	E<C	E≈C	C<E	C<E	C≈E	C<E	C<E
4B	2.29(90)	D<C<E	E<D<C	D<C<E	E≈D<C	D<C<E	E<D≈C	D<C<E	--
5C	2.29(90)	C≈D<E	E<C<D	E≈D≈C	E≈D≈C	C≈D<E	C≈E<D	C<E≈D	C≈E≈D
3E	2.29(90)	C<E<D	C<E<D	E<D	E<D	D<E	E<D	E<D	E<D
1C	2.44(96)	C<D<E	E<C<D	C≈D≈E	C≈D≈E	C≈E≈D	C≈E<D	C<E≈D	C<D<E
2E	2.44(96)	C<E<D	C<E<D	C<E<D	C<E<D	C<E<D	C<E<D	C<D≈E	C≈E<D
3D	2.44(96)	E≈C≈D	E≈C≈D	E≈D≈C	C<D<E	D<C<E	C≈E<D	E<C<D	C<D≈E
4D	2.44(96)	--	--	--	C<E	C≈E	C≈E	--	E≈C

TABLE A-1 (cont)
CALCULATED HEAT TRANSFER COMPARISONS

Rod	Elevation [m (in.)]	Run 42430A		Run 42606A		Run 43112A		Run 42804A	
		Early	Later	Early	Later	Early	Later	Early	Later
5B	2.44(96)	D<E<C	D<E<C	E≈D<C	D≈E<C	D<E<C	E<C<D	D<E<C	D<C<E
1D	2.59(102)	--	D<E<C	--	D<E<C	D<E<C	D≈E<C	--	D<C<E
2C	2.59(102)	--	E<D	--	E<D	--	E<D	--	E≈D
4B	2.59(102)	--	E<D<C	--	E<C≈D	--	E<C<D	--	C≈E≈D
5B	2.59(102)	--	E≈D	--	E<D	--	E<D	--	E<D
5D	2.59(102)	--	--	D<C<E	--	--	E≈C≈D	--	E<C≈D
2A	2.82(111)	E<D	E<D	E<D	E<D	E<D	E<D	--	--
4E	2.82(111)	C<E	C<E	C<E	C<E	C<E	C<E	--	C≈E
1C	3.05(120)	--	D<C<E	--	D<E≈C	--	D≈C≈E	--	--
1D	3.05(120)	--	E<D<C	--	E<D<C	--	D<E<C	--	--
2C	3.05(120)	--	C<E<D	--	C≈D≈E	--	C≈E<D	--	--
4B	3.05(120)	--	--	--	E<D<C	--	E<C<D	--	--
5B	3.05(120)	--	C<D<E	--	--	--	--	--	--
5D	3.05(120)	--	--	--	--	--	C<D<E	--	--

- o At 1.88 m (74 in.), where all cases have blockage, E is the lowest even during the early time.
- o At 1.96 m (77 in.), usually $D \approx E$ for the early time period.
- o During the early period above 2.59 m (102 in.), the ratios oscillate. This is possible due to small-magnitude errors in the heat transfer coefficient.
- o At the later time for 2.59 m (102 in.), E is the lowest except at rod 1D.
- o At 2.82 and 3.05 m (111 and 120 in.), trends are mixed.

Because of the observed contradictory behavior between the two periods, it was not immediately clear which sleeve should be chosen. To resolve this difficulty, it was necessary to learn the effect of the early-period behavior on the peak clad temperature up to the turnaround time, because this is the most important period. This can be done by calculation of the clad temperatures or temperature rises by constructing expected temperature histories in the large bundle, as discussed below. In the following discussion, only blockage configurations D and E are considered, since it was found that configuration C blockage usually did not give poorer heat transfer.

A-3. ESTIMATION OF TEMPERATURE HISTORY IN LARGE BUNDLE

Assuming that each rod is homogeneous radially, for simplicity, a one-dimensional heat balance equation can be written as

$$A \rho C_p \frac{dT}{dt} = Q' - hS (T - T_{sat}) \quad (A-3)$$

where

A	=	rod cross-sectional area
ρ	=	rod density
C_p	=	rod heat capacity
T	=	temperature
t	=	time
Q	=	heat generation rate

h = heat transfer coefficient at rod surface
 S = rod peripheral length
 T_{sat} = saturation temperature

The terms A , C_p and S can be estimated using the rod design information and Q' from the rod design and power decay factor curve. The heat transfer coefficient can be estimated by

$$h(t) = (h_b)_{163} = \frac{h_b}{h_o} \quad 161 \quad (h_o) \quad (A-4)$$

where h_o is the heat transfer coefficient in an unblocked bundle. In equation (A-4), h_o should ideally be taken from the large unblocked test, but unfortunately there were only two overlapping test conditions at a flooding rate of approximately 25 mm/sec (1 in./sec). For these two cases, $h(t)$ was estimated by using $(h_o)_{161}$. Four other cases were also studied using the heat transfer coefficient obtained from the 21-rod bundle, configuration A test. The results are compared in table A-2. Actual temperature rise information is provided in tables A-3 through A-8.

These results show that, in most cases, blockage in configuration E will give a higher temperature rise in the large bundle. Therefore, the long nonconcentric sleeve is expected to provide poorer heat transfer than the short concentric sleeve.

Figure A-8 plots the measured turnaround time versus the flooding rates. As expected, the lower the flooding rate, the longer the turnaround time. The longer turnaround time means more significant contribution of the later period effect, in which configuration E consistently showed poorer heat transfer.

Therefore, it is concluded that the long nonconcentric sleeve should be used for the large bundle tests.

TABLE A-2
SUMMARY OF TEMPERATURE RISE COMPARISONS
FOR LARGE BUNDLE WITH PARTIAL BLOCKAGE

Flooding Rate [mm/sec]	Pressure	Source of h_o (bundle)	Number of Thermocouples Where ΔT_E $> \Delta T_D$	Number of Thermocouples Where ΔT_D $> \Delta T_E$	Number of Thermocouples Where ΔT_D $\sim \Delta T_E$ (a)
1.1	0.28 (40)	161 ^(b)	11	1	3
1.1	0.14 (20)	161 ^(b)	11	0	1
1.1	0.28 (40)	21	9	3	3
1.1	0.14 (20)	21	4	5	6
0.9	0.28 (40)	21	11	3	1
0.5	0.28 (40)	21	8	3	4

a. Within 11°C (20°F)

b. Considering 21-rod island corresponding to 21-rod bundle tests

TABLE A-3
CALCULATED TEMPERATURE RISES,
CASE 1^(a)

Rod	Elevation [m (in.)]	D Island		E Island	
		Channel	ΔT [°C(°F)]	Channel	ΔT [°C(°F)]
2D	1.88 (74)	50	238.1 (428.7)	39	342.6 (616.8)
1D	1.90 (75)	61	305.2 (549.4)	44	353.2 (635.9)
5D	1.90 (75)	68	295.0 (531.1)	46	323.0 (581.4)
4A	1.93 (76)	78	257.6 (463.7)	51	286.4 (515.5)
1D	1.96 (77)	82	268.5 (483.4)	58	297.6 (535.7)
2D	1.96 (77)	84	176.2 (317.2)	61	272.2 (490.0)
5D	1.96 (77)	89	266.5 (479.7)	66	274.8 (494.7)
3B	1.98 (78)	96	210.5 (379.0)	71	234.6 (422.4)
3C	1.98 (78)	97	190.1 (356.6)	72	262.5 (472.6)
4A	1.98 (78)	100	257.1 (462.9)	73	257.4 (463.4)
3D	2.13 (84)	115	266.5 (479.7)	98	292.7 (527.0)
5B	2.13 (84)	117	220.6 (397.2)	103	322.1 (579.9)
2C	2.29 (90)	122	367.4 (661.3)	111	341.1 (614.1)
2E	2.29 (90)	123	375.0 (675.0)	113	395.4 (711.8)
3B	2.29 (90)	125	344.2 (619.6)	115	350.1 (630.3)
SUMMARY					
$(\Delta T)_E > (\Delta T)_D$		$(\Delta T)_D > (\Delta T)_E$		$(\Delta T)_D \approx (\Delta T)_E$	
11		1		3	

a. $(h_o)_{161}$
27.9 mm/sec (1.1 in./sec) flooding rate
0.28 MPa (40 psi) pressure

TABLE A-4
CALCULATED TEMPERATURE RISES,
CASE 2^(a)

Rod	Elevation [m (in.)]	D Island		E Island	
		Channel	ΔT [°C(°F)]	Channel	ΔT [°C(°F)]
2D	1.88 (74)	50	179.1 (322.4)	39	317.5 (571.6)
1D	1.90 (75)	61	283.3 (510.0)	44	393.2 (707.9)
5D	1.90 (75)	68	310.4 (558.7)	46	369.4 (664.9)
4A	1.93 (76)	78	262.8 (473.1)	51	291.6 (525.0)
1D	1.96 (77)	82	179.6 (323.4)	58	--
2D	1.96 (77)	84	132.4 (238.4)	61	168.0 (302.4)
5D	1.96 (77)	89	213.2 (416.2)	66	293.0 (527.5)
3B	1.98 (78)	96	148.7 (267.6)	71	--
3C	1.98 (78)	97	129.4 (232.9)	72	--
4A	1.98 (78)	100	210.0 (378.0)	73	240.1 (432.2)
3D	2.13 (84)	115	197.1 (355.9)	98	246.1 (443.0)
5B	2.13 (84)	117	160.2 (288.3)	103	275.5 (499.6)
2C	2.29 (90)	122	250.5 (450.9)	111	262.9 (473.3)
3E	2.29 (90)	123	274.7 (494.5)	113	390.1 (702.3)
3B	2.29 (90)	125	255.1 (405.2)	115	364.2 (655.6)
SUMMARY					
$(\Delta T)_E > (\Delta T)_D$		$(\Delta T)_D > (\Delta T)_E$		$(\Delta T)_D \approx (\Delta T)_E$	
11		0		1	

a. $(h_o)_{161}$
27.9 mm/sec (1.1 in./sec) flooding rate
0.14 MPa (20 psi) pressure

TABLE A-5
CALCULATED TEMPERATURE RISES,
CASE 3^(a)

Rod	Elevation [m (in.)]	D Island		E Island	
		Channel	ΔT [°C(°F)]	Channel	ΔT [°C(°F)]
2D	1.88 (74)	50	141.3 (254.3)	39	215.1 (387.2)
1D	1.90 (75)	61	152.8 (275.1)	44	302.4 (364.3)
5D	1.90 (75)	68	164.3 (295.7)	46	189.0 (340.2)
4A	1.93 (76)	78	135.2 (243.3)	51	149.4 (269.0)
1D	1.96 (77)	82	147.9 (266.3)	58	171.3 (308.4)
2D	1.96 (77)	84	109.7 (197.4)	61	171.3 (308.3)
5D	1.96 (77)	89	161.9 (291.5)	66	158.7 (285.7)
3B	1.98 (78)	96	153.9 (277.0)	71	145.7 (262.2)
3C	1.98 (78)	97	161.1 (290.0)	72	188.9 (340.0)
4A	1.98 (78)	100	158.8 (285.8)	73	137.8 (248.0)
3D	2.13 (84)	115	169.0 (304.2)	98	147.8 (266.1)
5B	2.13 (84)	117	135.4 (243.8)	103	157.3 (283.1)
2C	2.29 (90)	122	212.4 (382.3)	111	179.3 (322.7)
2E	2.29 (90)	123	147.7 (265.8)	113	180.5 (324.9)
3B	2.29 (90)	125	184.0 (331.2)	115	189.0 (340.2)
SUMMARY					
$(\Delta T)_E > (\Delta T)_D$		$(\Delta T)_D > (\Delta T)_E$		$(\Delta T)_D \approx (\Delta T)_E$	
9		3		3	

a. $(h_o)_{161}$
27.9 mm/sec (1.1 in./sec) flooding rate
0.28 MPa (40 psi) pressure

TABLE A-6
CALCULATED TEMPERATURE RISES,
CASE 4^(a)

Rod	Elevation [m (in.)]	D Island		E Island	
		Channel	ΔT [°C(°F)]	Channel	ΔT [°C(°F)]
2D	1.88 (74)	50	127.6 (229.7)	39	182.9 (329.3)
1D	1.90 (75)	61	143.0 (257.4)	44	188.6 (339.6)
5D	1.90 (75)	68	165.0 (297.0)	46	166.8 (300.2)
4A	1.93 (76)	78	134.5 (242.2)	51	140.9 (253.6)
1D	1.96 (77)	82	139.7 (251.5)	58	148.0 (266.5)
2D	1.96 (77)	84	130.2 (234.4)	61	145.0 (261.0)
5D	1.96 (77)	89	162.7 (292.8)	66	134.4 (242.0)
3B	1.98 (78)	96	148.4 (267.1)	71	118.6 (213.5)
3C	1.98 (78)	97	154.6 (278.3)	72	154.2 (277.5)
4A	1.98 (78)	100	154.9 (278.9)	73	125.0 (225.0)
3D	2.13 (84)	115	135.4 (243.7)	98	91.6 (164.9)
5B	2.13 (84)	117	125.0 (225.1)	103	119.9 (215.8)
2C	2.29 (90)	122	161.0 (289.8)	111	109.8 (197.7)
2E	2.29 (90)	123	126.2 (227.1)	113	126.2 (227.1)
3B	2.29 (90)	125	144.0 (259.3)	115	171.3 (308.4)
SUMMARY					
$(\Delta T)_E > (\Delta T)_D$		$(\Delta T)_D > (\Delta T)_E$	$(\Delta T)_D \approx (\Delta T)_E$		
4		5	6		

a. $(h_o)_{21}$
27.9 mm/sec (1.1 in./sec) flooding rate
0.14 MPa (20 psi) pressure

TABLE A-7
CALCULATED TEMPERATURE RISES,
CASE 5^(a)

Rod	Elevation [m (in.)]	D Island		E Island	
		Channel	ΔT [°C(°F)]	Channel	ΔT [°C(°F)]
2D	1.88 (74)	50	200.1 (360.2)	39	305.2 (549.5)
1D	1.90 (75)	61	213.1 (383.7)	44	285.6 (514.2)
5D	1.90 (75)	68	224.4 (400.4)	46	295.1 (531.3)
4A	1.93 (76)	78	188.5 (339.3)	51	224.0 (403.3)
1D	1.96 (77)	82	196.0 (352.8)	58	328.1 (590.6)
2D	1.96 (77)	84	191.6 (344.9)	61	178.9 (322.1)
5D	1.96 (77)	89	215.4 (387.7)	66	288.6 (519.5)
3B	1.98 (78)	96	210.5 (379.0)	71	173.8 (312.9)
3C	1.98 (78)	97	222.2 (400.0)	72	160.8 (289.5)
4A	1.98 (78)	100	215.7 (388.3)	73	238.5 (429.4)
3D	2.13 (84)	115	259.8 (467.6)	98	282.6 (508.8)
5B	2.13 (84)	117	204.3 (367.8)	103	314.7 (566.6)
2C	2.29 (90)	122	309.1 (556.5)	111	218.5 (393.4)
2E	2.29 (90)	123	210.6 (379.2)	113	232.1 (417.9)
3B	2.29 (90)	125	269.3 (484.7)	115	288.2 (518.8)
SUMMARY					
$(\Delta T)_E > (\Delta T)_D$		$(\Delta T)_D > (\Delta T)_E$		$(\Delta T)_D \approx (\Delta T)_E$	
11		3		1	

a. $(h_o)_{21}$
23 mm/sec (0.9 in./sec) flooding rate
0.28 MPa (40 psi) pressure

TABLE A-8
CALCULATED TEMPERATURE RISES,
CASE 6^(a)

Rod	Elevation [m (in.)]	D Island		E Island	
		Channel	ΔT [°C(°F)]	Channel	ΔT [°C(°F)]
2D	1.88 (74)	50	80.8 (145.4)	39	131.2 (236.2)
1D	1.90 (75)	61	84.3 (151.7)	44	114.8 (206.7)
5D	1.90 (75)	68	82.3 (148.2)	46	105.2 (189.3)
4A	1.93 (76)	78	63.2 (113.8)	51	82.9 (149.3)
1D	1.96 (77)	82	81.5 (146.7)	58	86.3 (155.3)
2D	1.96 (77)	84	77.1 (138.8)	61	93.3 (168.0)
5D	1.96 (77)	89	76.9 (138.5)	66	78.9 (142.0)
3B	1.98 (78)	96	81.4 (146.5)	71	81.1 (146.0)
3C	1.98 (78)	97	85.8 (154.4)	72	101.2 (182.2)
4A	1.98 (78)	100	85.2 (153.4)	73	69 (125)
3D	2.13 (84)	115	171.3 (308.3)	98	147.1 (264.8)
5B	2.13 (84)	117	136.0 (244.8)	103	136.9 (246.4)
2C	2.29 (90)	122	177.8 (320.0)	111	145.8 (262.4)
2E	2.29 (90)	123	158.5 (285.4)	113	171.1 (308.1)
3B	2.29 (90)	125	155.7 (280.2)	115	219.3 (394.7)
SUMMARY					
$(\Delta T)_E > (\Delta T)_D$		$(\Delta T)_D > (\Delta T)_E$		$(\Delta T)_D \approx (\Delta T)_E$	
8		3		4	

a. $(h_o)_{21}$
23 mm/sec (0.9 in./sec) flooding rate
0.28 MPa (40 psi) pressure

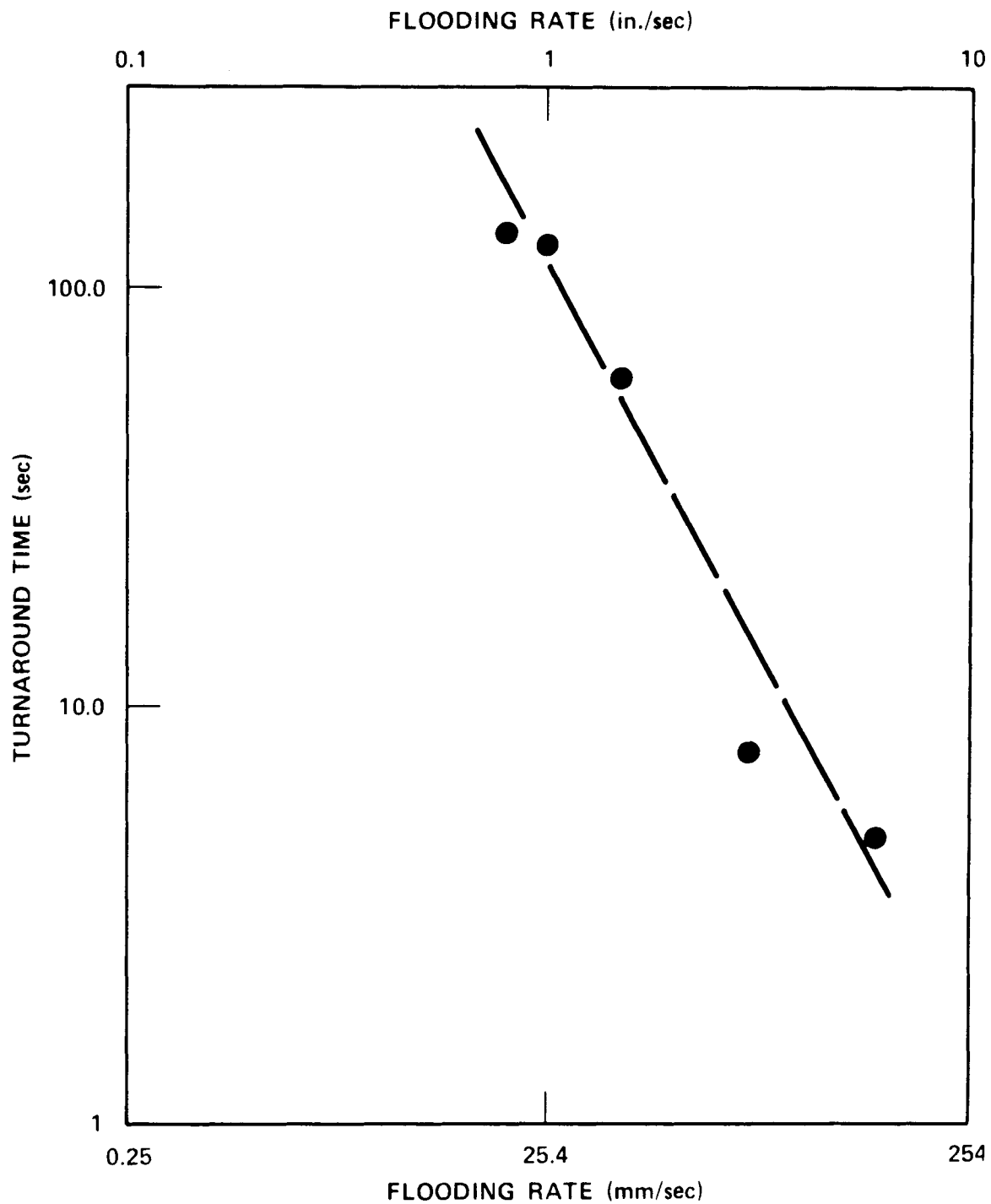


Figure A-8. Relationships Between Turnaround Time and Flooding Rate

APPENDIX B
THIMBLE AND GRID EFFECTS ON BURST

B-1. GENERAL

This appendix provides the analyses of Westinghouse multirod burst tests⁽¹⁾ and the grid effect on the Westinghouse mean temperature calculation.

B-2. EFFECT OF HEATING METHOD ON BURST AND BALLOONING SHAPES IN
OUT-OF-PILE LOCA SIMULATIONS

It has been well established by ANL⁽²⁾ and others that local temperature differences are extremely important in determining the size and shape of rod ballooning and burst under LOCA conditions.

In a reactor, local temperature variations result from many sources, such as pellet enrichment differences, local gap average differences, random cracking and radial redistribution, and pellet radial offset. In addition to these rod internal effects, external heat transfer considerations are also important. Among these are local crud patches and radiant losses to relatively cold sinks, such as control rod thimbles.

To properly simulate these effects out of pile is very difficult and requires compromises. Three principal methods have been used by various investigators:

- o Direct heating of the clad by electrical resistance or induction heating with or without internal mandrels or pellet columns
- o External radiant heating of the clad with internal mandrels or pellet columns
- o Internal electrical heaters with or without annular pellets between the heater and clad

1. Schreiber, R.E., et al., "Performance of Zircaloy-Clad Fuel Rods During a Simulated Loss-of-Coolant Accident -- Multirod Burst Tests," WCAP-7495-L, April 1970.
2. "Light-Water-Reactor Safety Research Program: Quarterly Progress Report -- January-March 1977," ANL-77-34, June 1977.

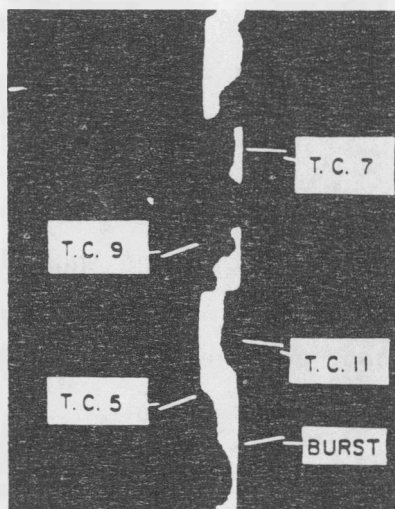
Direct heating of the clad by induction or resistance heating has a temperature smoothing effect not typical of nuclear-heated rods. That is, the local heat deposition is a function of the mass of the clad, whereas heat loss to the environment is a function of surface area. If a hot spot develops in a joule-heated rod and the clad swells locally, the wall thickness decreases, thus increasing local resistance and shunting the electrical current to the cooler, less deformed side of the rod. At the same time, the increased surface area of the bulge is radiating more heat to the environment. The net result is a negative feedback function which produces a more uniform clad temperature distribution and thus larger strains.

The net effect of induction heating is the same as that of joule heating, although the reason for power shifting is different.

External radiant heating does not have the same problems as direct clad heating; however, for this type of heating, the only sink for temperature is the internal mandrel or pellet. These heat sinks are also available to the direct-heated clad and produce the same results. If pellets are used, the random stacking will produce significant and very localized clad temperature differences in both the axial and circumferential directions.⁽¹⁾ This is well illustrated by figure B-1 (taken from ANL-77-34). If an internal mandrel is used and it is slightly nonconcentric to the cladding, the heat loss from the cladding to the mandrel will be greater on the side with minimum clad-to-mandrel gap. This will produce a circumferential temperature gradient in the cladding. Below about 900°C (1650°F), Zircaloy strains anisotropically and will bow because of the greater strain on the hot side. The direction of the bow will be concave on the hot side. The hot side will thus move toward the mandrel, increasing heat loss on that side. This is a stabilizing mechanism and results in larger strains, at least in the lower temperature range.

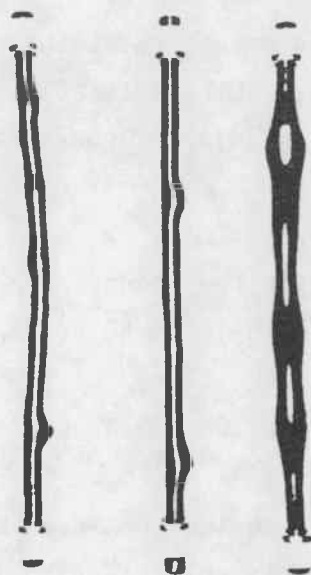
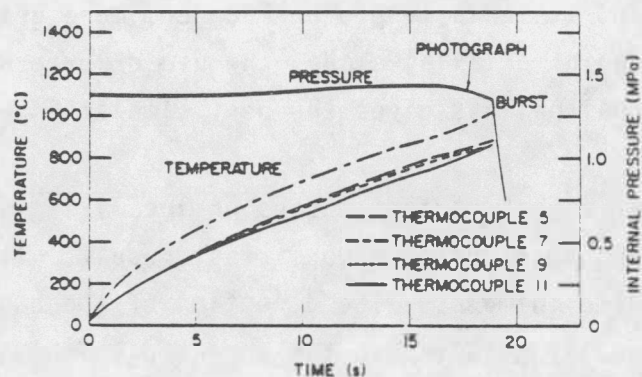
The randomness of pellet stacks and thus clad hot spots prevents gross bowing for tests using pellet stacks. Hence, this mechanism is not present to the same degree for those tests with pellet stacks.

1. Motley, F.E., et al., "The Effect of 17x17 Fuel Assembly Geometry on Interchannel Thermal Mixing," WCAP-8299, March 1974.



Nonuniform Brightness of Cladding Specimen Containing Al_2O_3 Pellets due to Axial and Circumferential Temperature Variations during Heating at 45°C/s .

Temperature and Internal Pressure as a Function of Time for Cladding Specimen Described in Fig. III.37.



Cladding Constrained by Pellets after Burst. Multiple ballooning regions and irregular bends are a result of temperature nonuniformity.

Figure B-1. Effects of Random Pellet Stacking

If rigid internal heaters are used in burst tests, they act in a manner similar to mandrels except that the heat flow is from mandrel to clad. Clad hot spots will tend to coincide with minimum gaps. The concave bowing of alpha Zircaloy will then reduce the gap on the hot side, creating a self-enhancing reaction.

This results in large circumferential temperature variations and thus low swelling and burst strains; however, the alignment of the hot side close to the heater promotes axial extension of the ballooning, since there is less probability of cold ligaments to localize straining.

Although it is believed that of all the test methods described, the use of internal heaters produces the most prototypical amount of circumferential strain, it tends to produce longer, more gradual axial shapes. From the standpoint of axial shape, the use of externally radiant-heated rods with internal pellets gives the best simulation of nuclear heating.

The effect of radiant losses on localizing strain was examined by reviewing Westinghouse multirod burst test results. The 4x4 test bundles contained two unheated thimbles. The direction of the burst of rods which were laterally or diagonally adjacent to the unheated thimbles was evaluated. Of 68 bursts observed, only three burst in a direction within 45 degrees of the thimbles. For random direction bursting, the expected number would be 17. A frequency this low has a probability of about 7×10^{-6} . This demonstrates that the heat transfer between thimbles and adjacent rods is a significant factor in determining circumferential temperature distribution in adjacent rods and thus in both the magnitude and direction of the strain.

In a Westinghouse 17x17 assembly, 68 percent of the fuel rods are adjacent to a thimble. In a Westinghouse 15x15 assembly, the ratio is 60 percent.

B-3. EFFECT OF GRID ON AXIAL TEMPERATURE DISTRIBUTION DURING LOCA

The axial temperature distribution for a fuel rod during LOCA determines the location of blockage due to rod bursting. This axial distribution is affected

by the presence of spacer grids, because of local power depressions and hydraulic effects.

For Westinghouse Inconel grids, the power depression has been determined near the peak power locations by analysis of gamma scans from irradiated commercial fuel rods.

For a large-break LOCA in which fuel rods are calculated to burst shortly after the end of blowdown, the perturbation in local clad temperature due to a perturbation in local power has been determined to be 6°C (11°F) per percent $\Delta p/p$ for a 17x17 three-loop plant.

The following shows the perturbation in power and the corresponding temperature perturbation as a function of distance from the center of a grid:

Distance From Grid Center		ΔT
[cm (in.)]	% $\Delta p/p$	[°C (°F)]
0 (0)	8	49 (88)
2.5 (1)	5	31 (55)
5.1 (2)	2	12 (22)
7.6 (3)	0.5	3.1 (5.5)
10 (4)	0	0 (0)

APPENDIX C
FACILITY DRAWINGS

Drawings applicable to the 163-rod blocked bundle facility are listed below and, except for figures 4-1 and 4-7, are reproduced on the following pages.

Figure No.	Title
Figure 4-1	Forced and Gravity Reflood Configuration Flow Diagram
Figure 4-7	163-Rod Blocked Bundle Task Loop Instrumentation
Figure C-1	FLECHT SEASET 163-Rod Blocked Bundle Filler Strips (2 sheets)
Figure C-2	FLECHT SEASET Grid Strap Assembly
Figure C-3	FLECHT SEASET Blocked Bundle Heater Rod
Figure C-4	FLECHT SEASET 163-Rod Blocked Bundle Assembly (3 sheets)
Figure C-5	FLECHT SEASET 163-Rod Blocked Bundle Steam Probe (4 sheets)
Figure C-6	FLECHT SEASET 163-Rod Blocked Bundle Thimble
Figure C-7	FLECHT SEASET 21-Rod Test (44-Percent Strain) Nonconcentric Flow Blockage Sleeve
Figure C-8	FLECHT SEASET Low Mass Housing Assembly
Figure C-9	FLECHT SEASET 161-Rod Blocked Bundle Low Mass Housing
Figure C-10	FLECHT SEASET 161-Rod Blocked Bundle Facility Housing Lateral Brace
Figure C-11	FLECHT SEASET 161-Rod Blocked Bundle Facility Upper Plenum
Figure C-12	FLECHT SEASET 161-Rod Blocked Bundle Facility Lower Plenum
Figure C-13	FLECHT SEASET 161-Rod Blocked Bundle Facility Carryover Tank
Figure C-14	FLECHT SEASET Facility Modified 0.1 m (4 in.) Type T Steam Separator

- Figure C-15 FLECHT SEASET 161-Rod Blocked Bundle Piping
Details
- Figure C-16 FLECHT SEASET 161-Rod Blocked Bundle
Downcomer and Crossover Leg Piping
- Figure C-17 FLECHT SEASET 163-Rod Blocked Bundle Heater
Rod and Instrumentation Thimble Arrangement
- Figure C-18 FLECHT SEASET 163-Rod Blocked Bundle
Instrumentation Components (2 sheets)

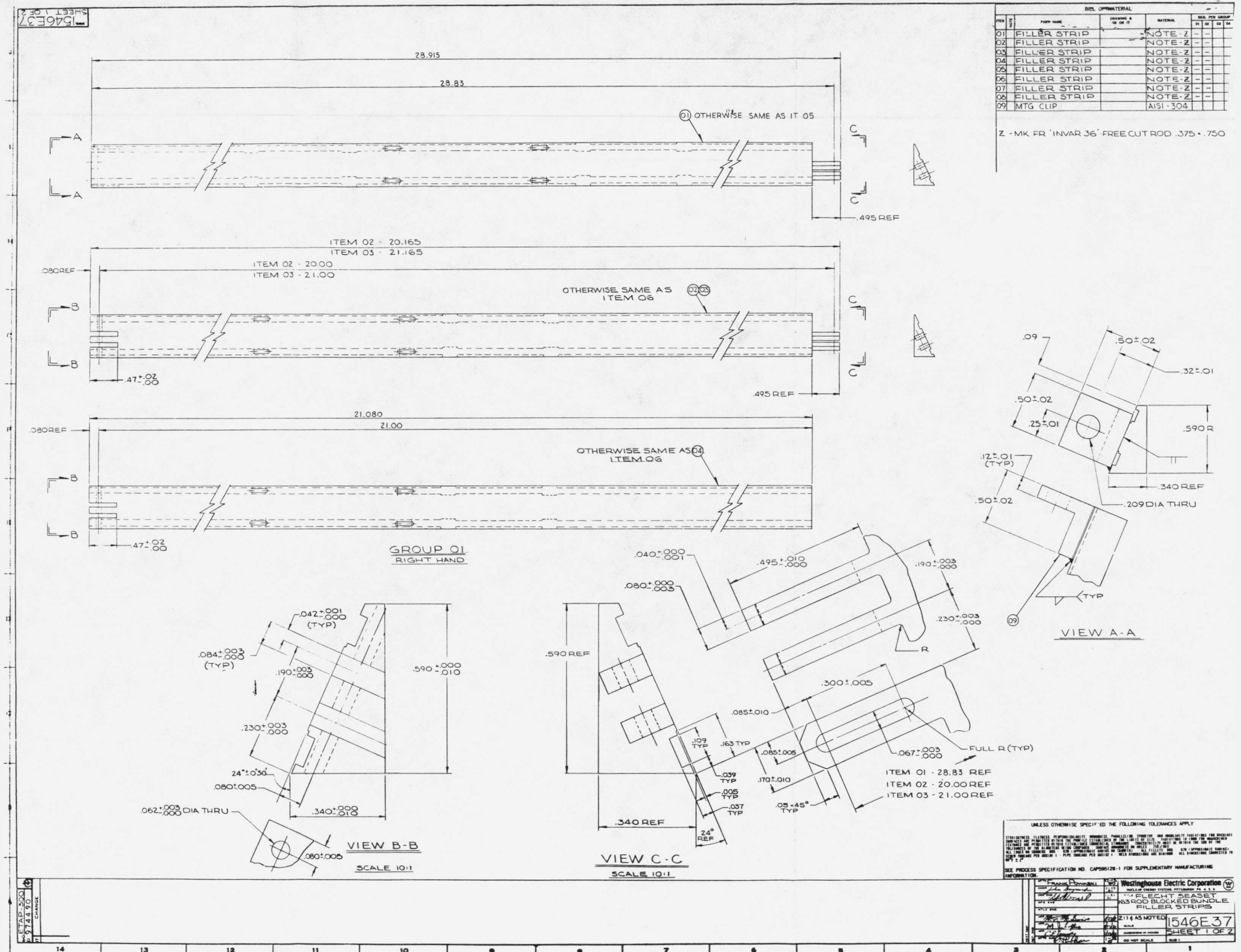
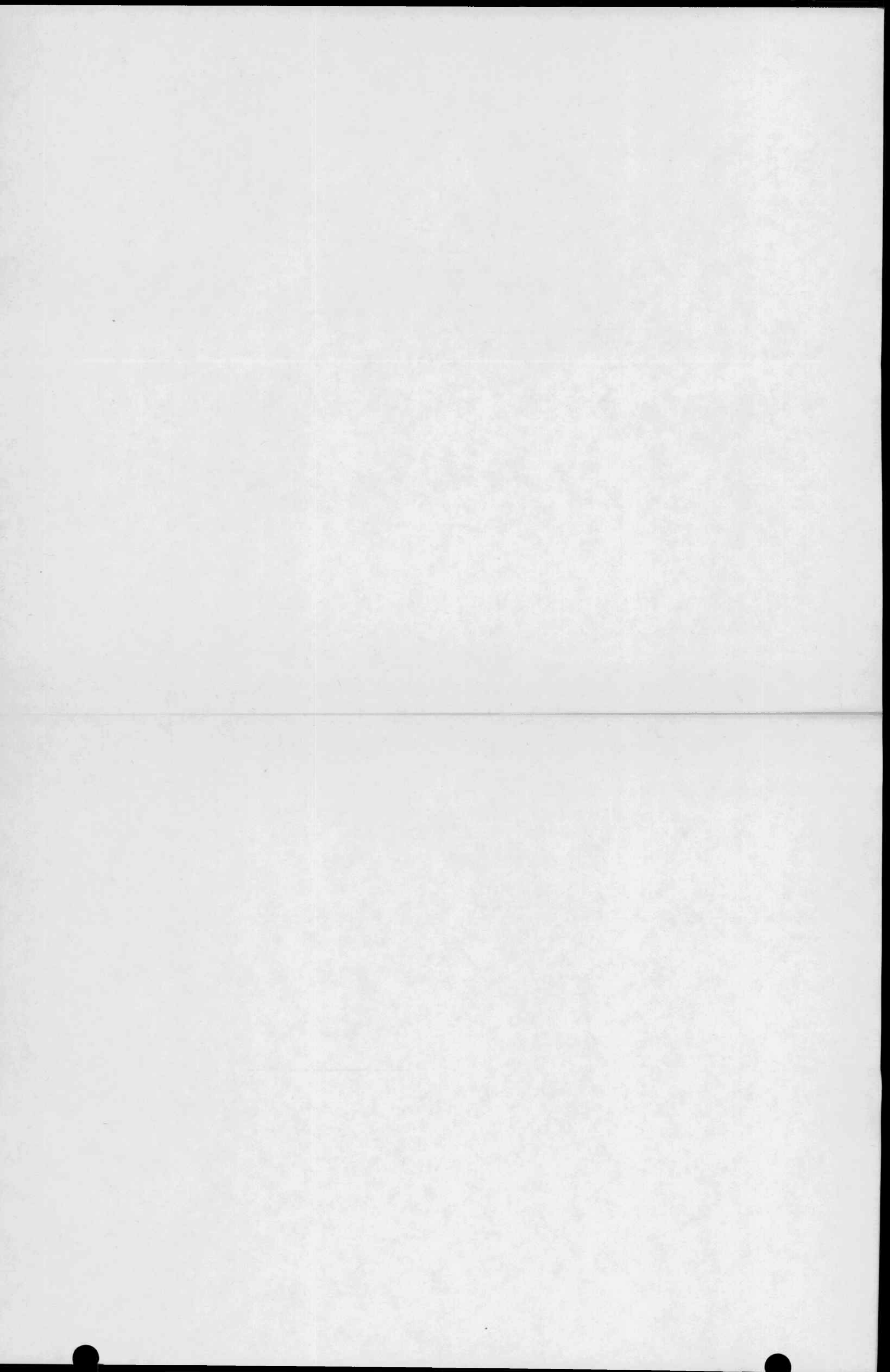


Figure C-1. FLECHT SEASET 163-Rod Blocked Bundle Filler Strips (sheet 1 of 2)



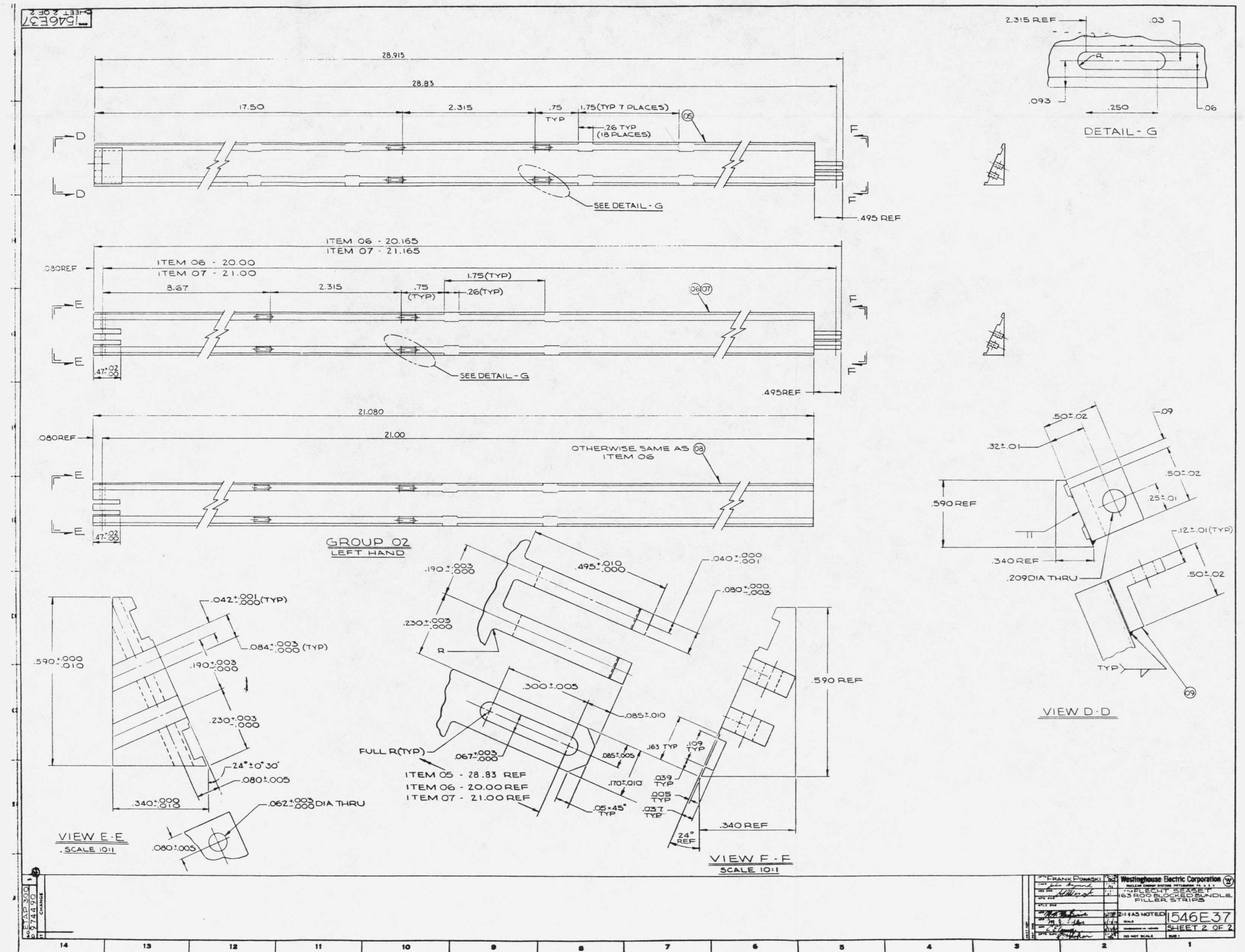
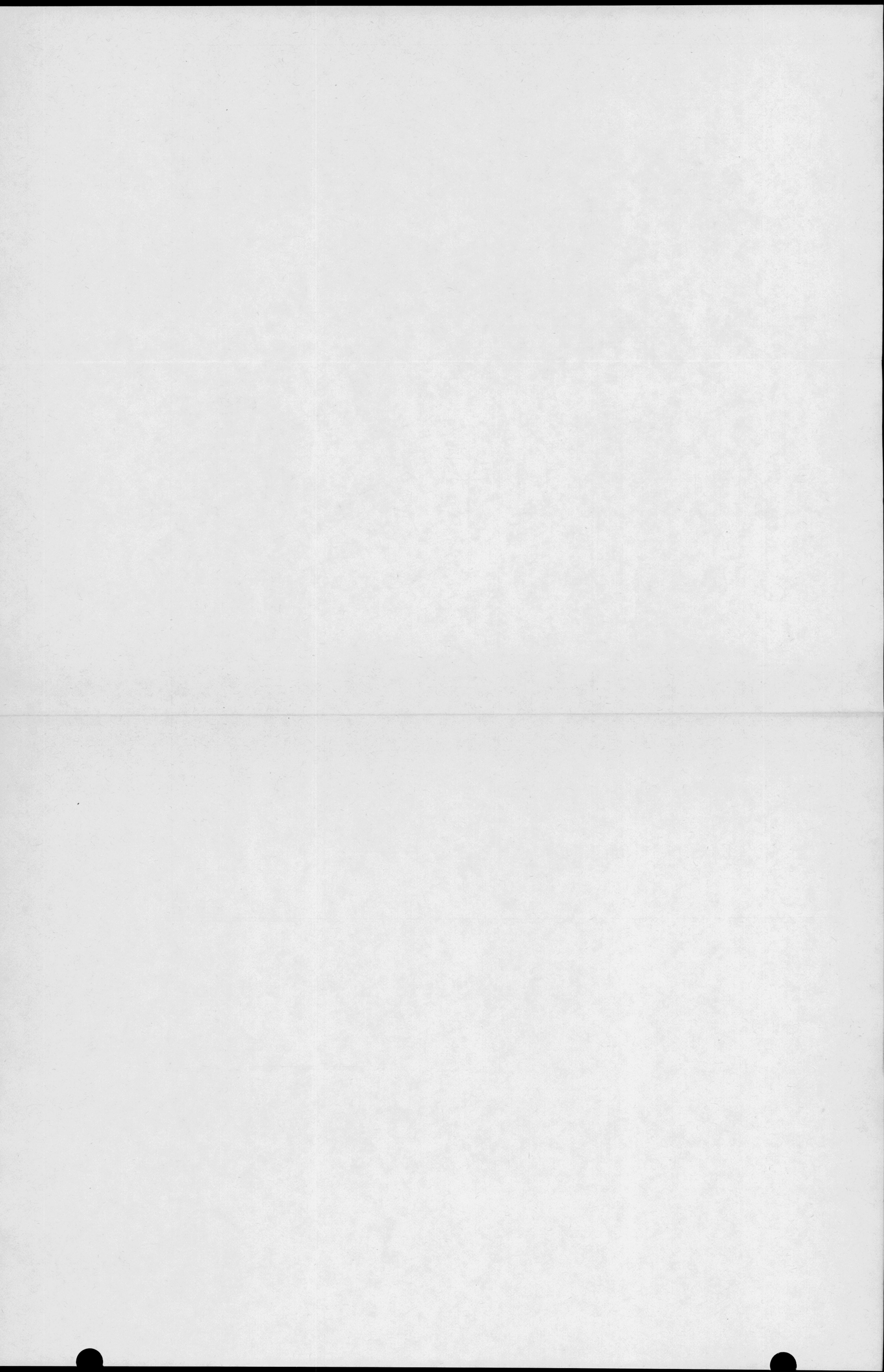


Figure C-1. FLECHT SEASET 163-Rod Blocked Bundle Filler Strips (sheet 2 of 2)



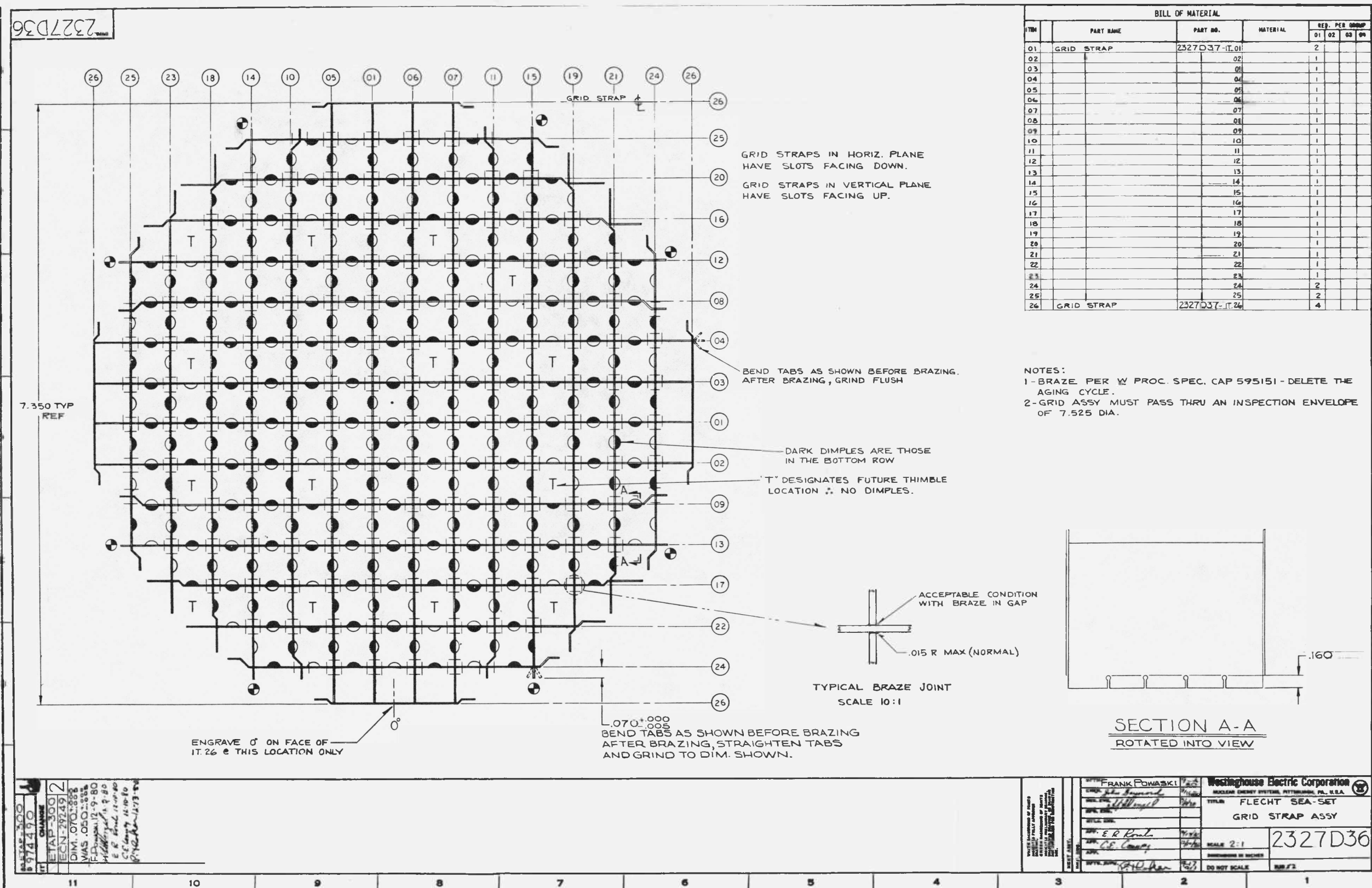
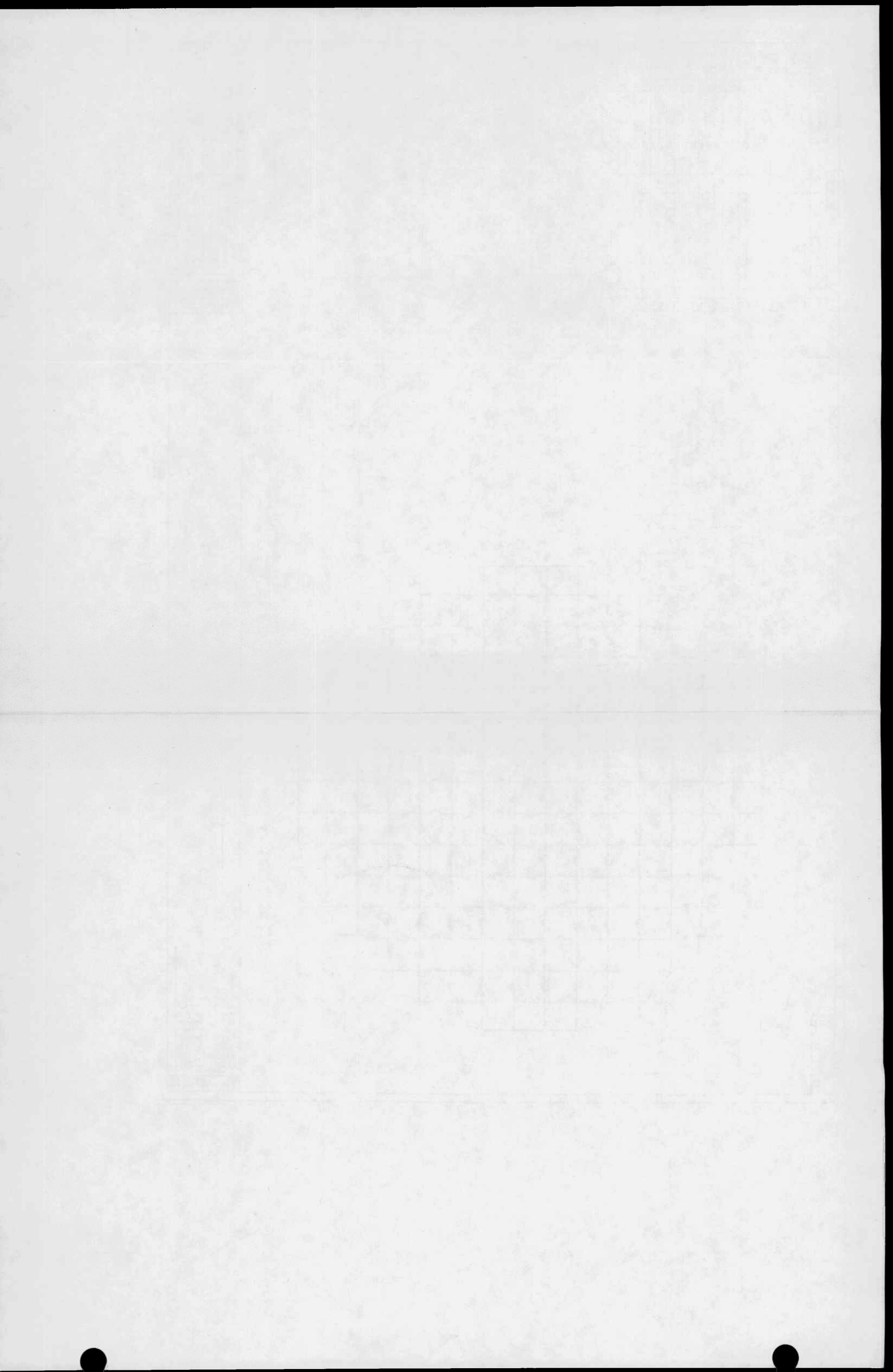


Figure C-2. FLECHT SEASET Grid Strap Assembly



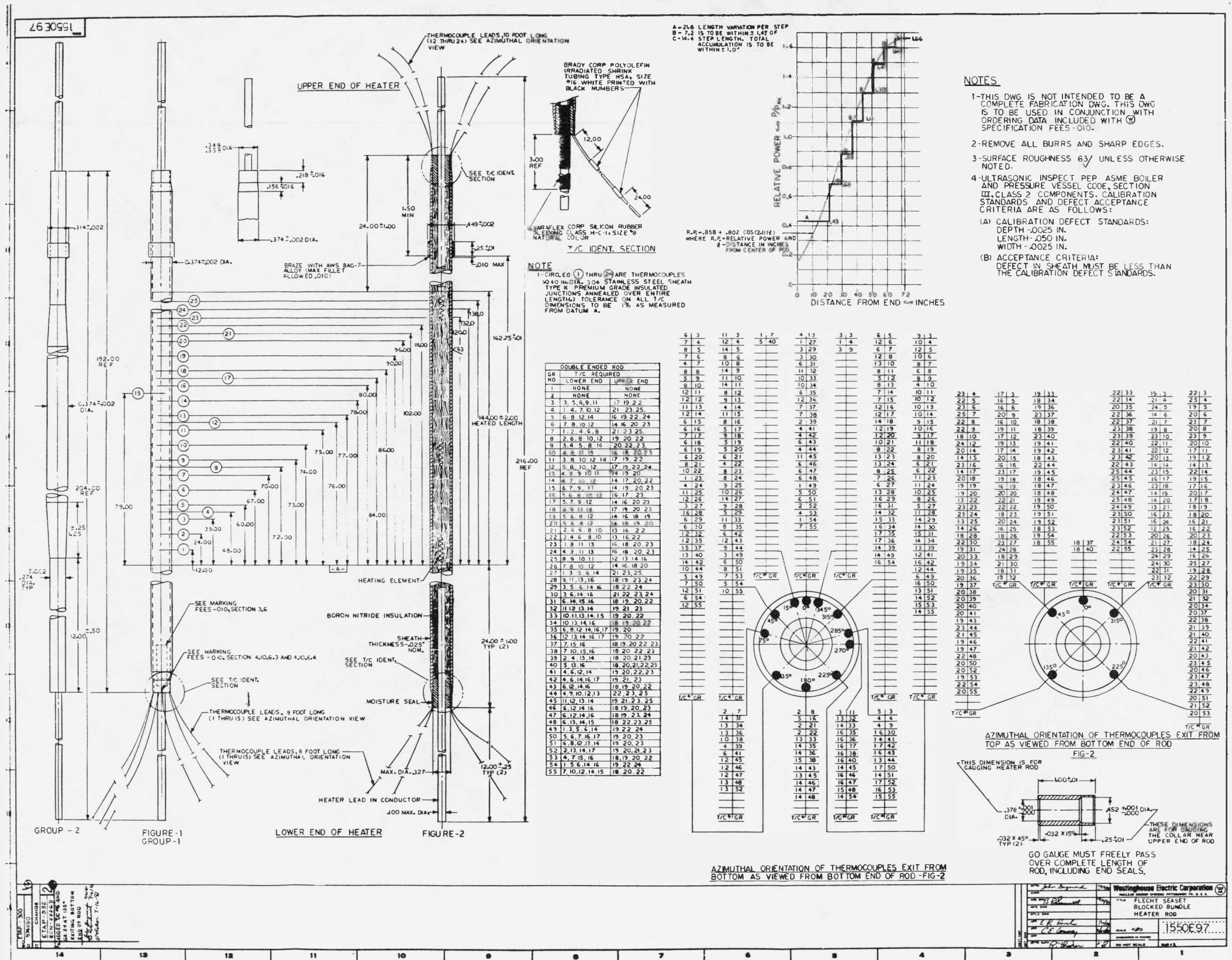
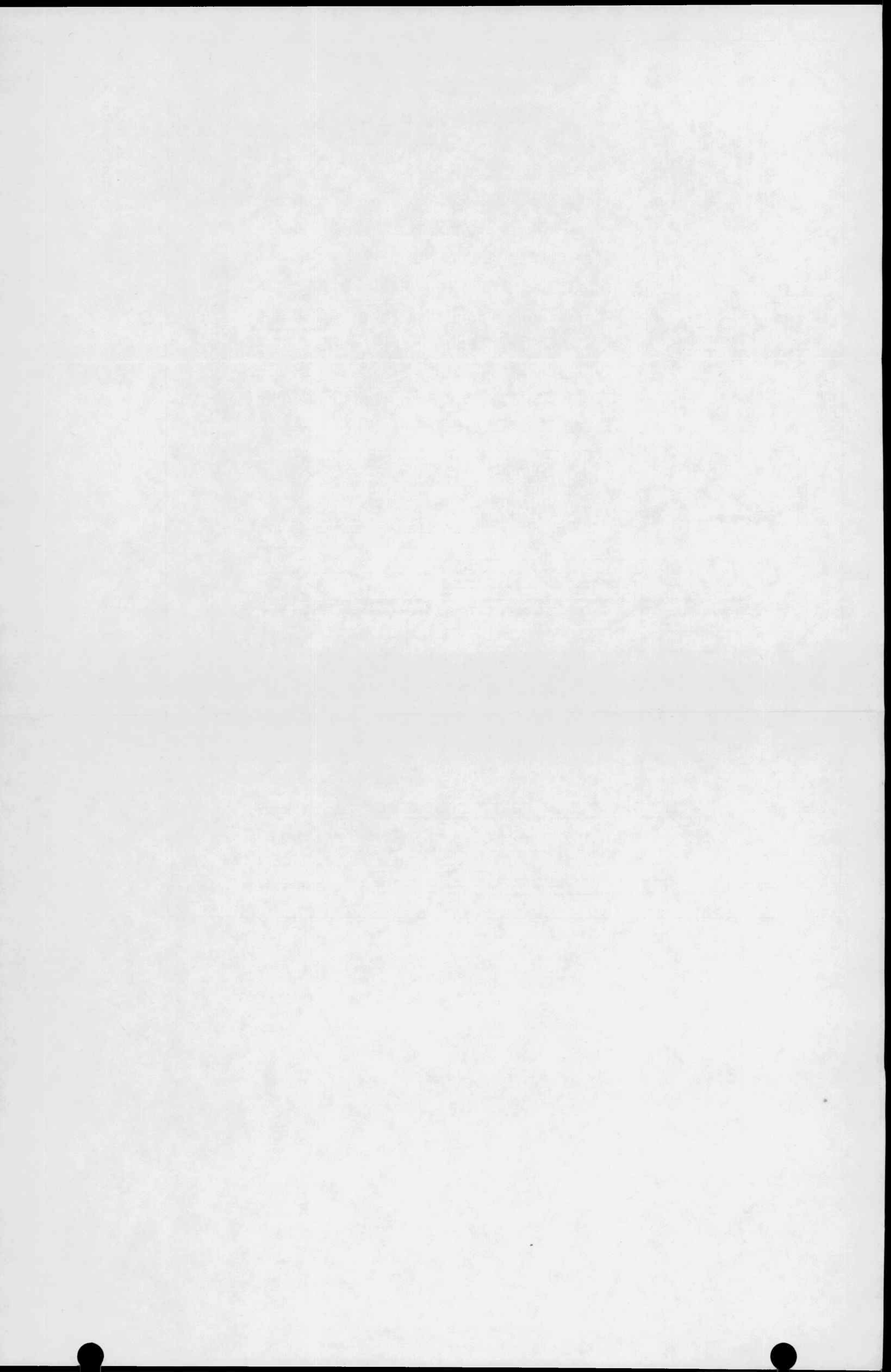
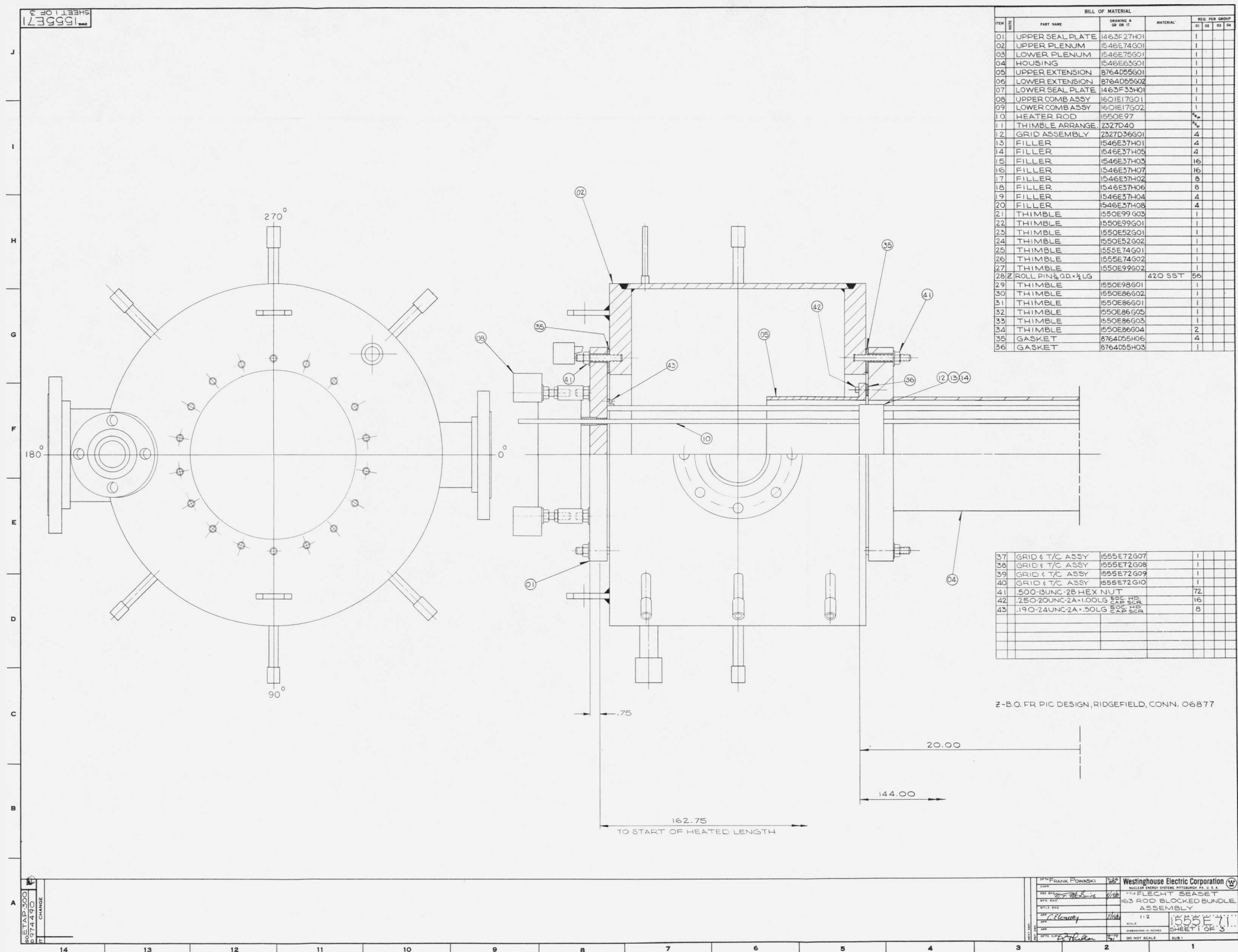
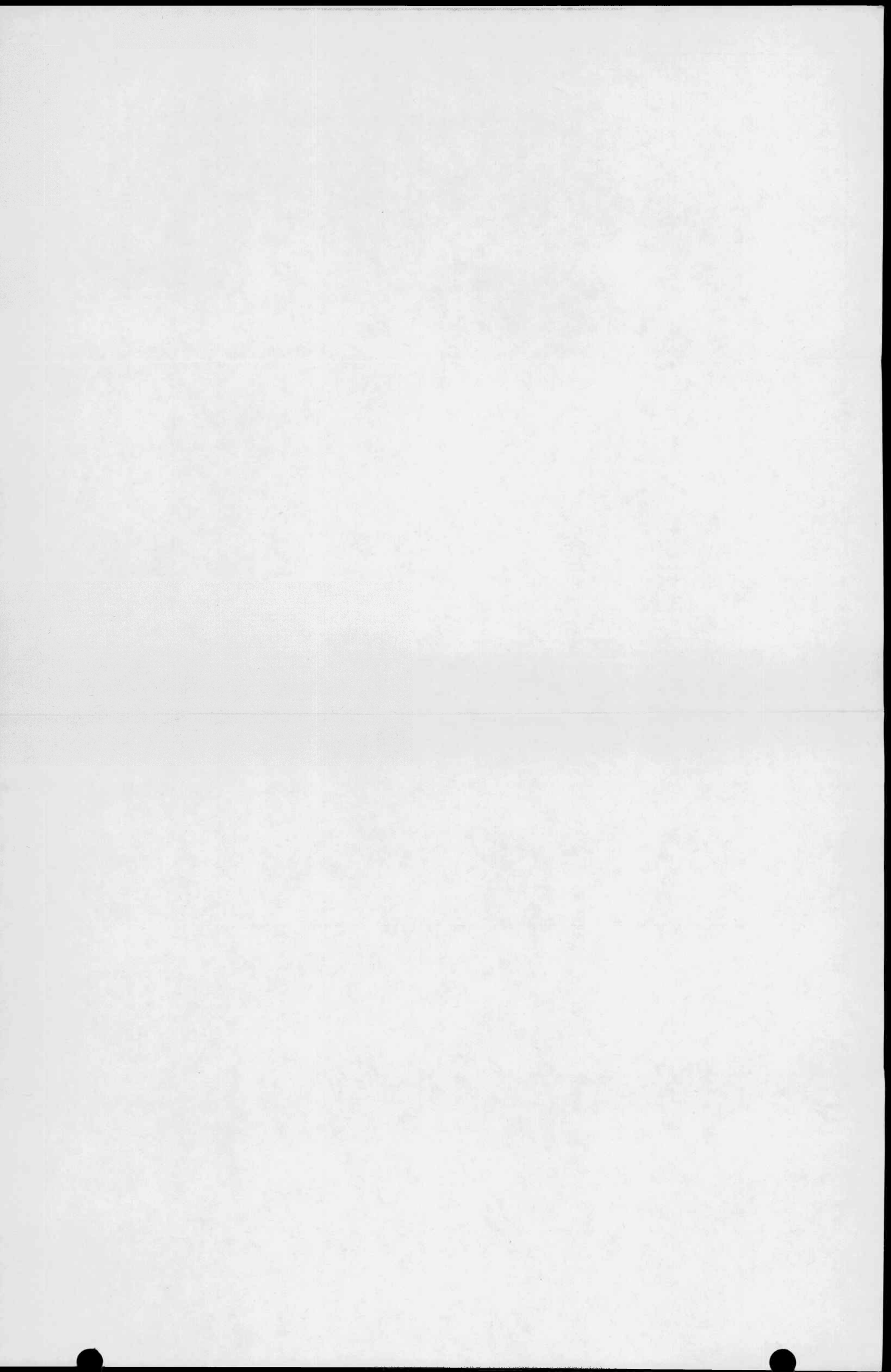


Figure C-3. FLECHT SEASET Blocked Bundle Heater Rod







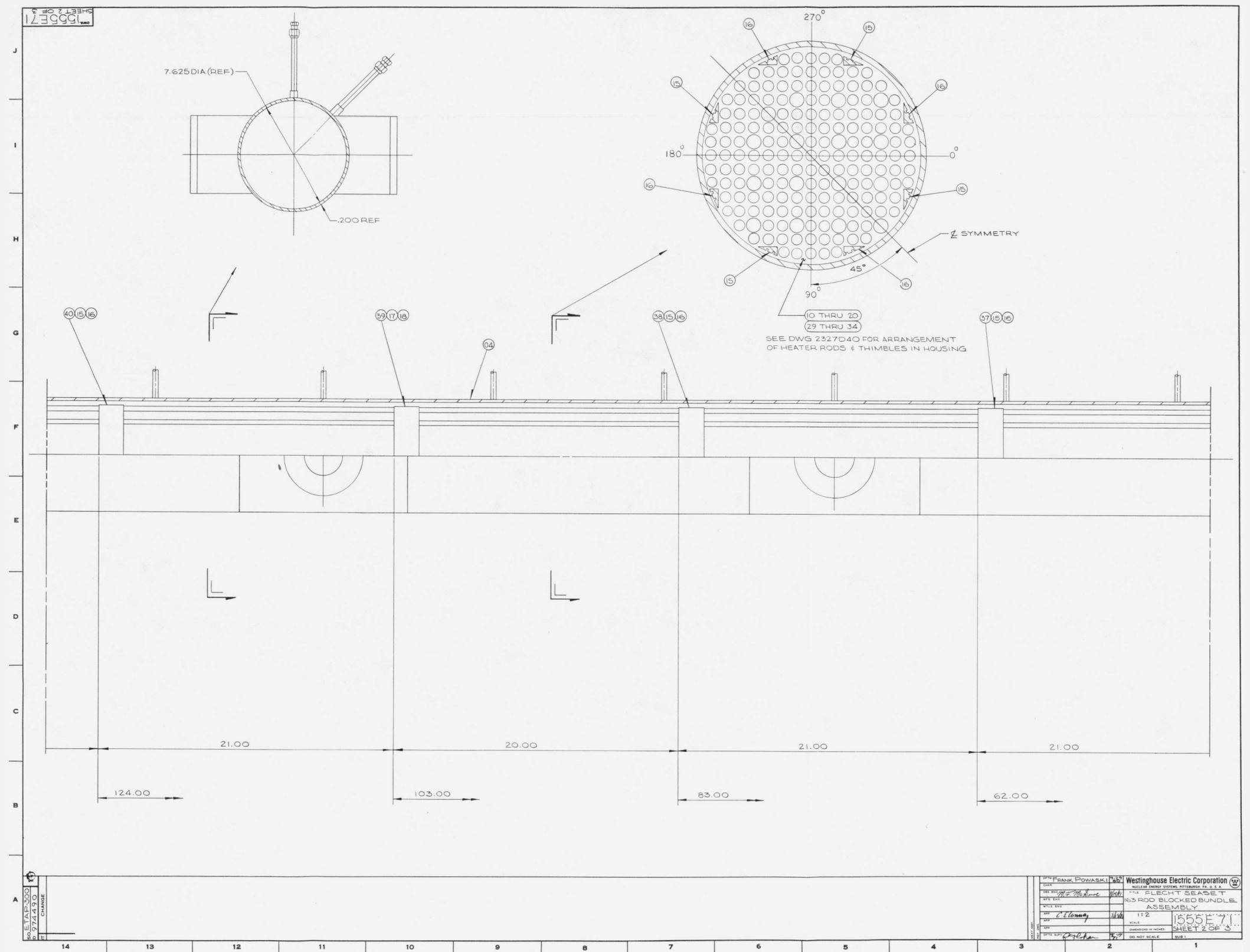
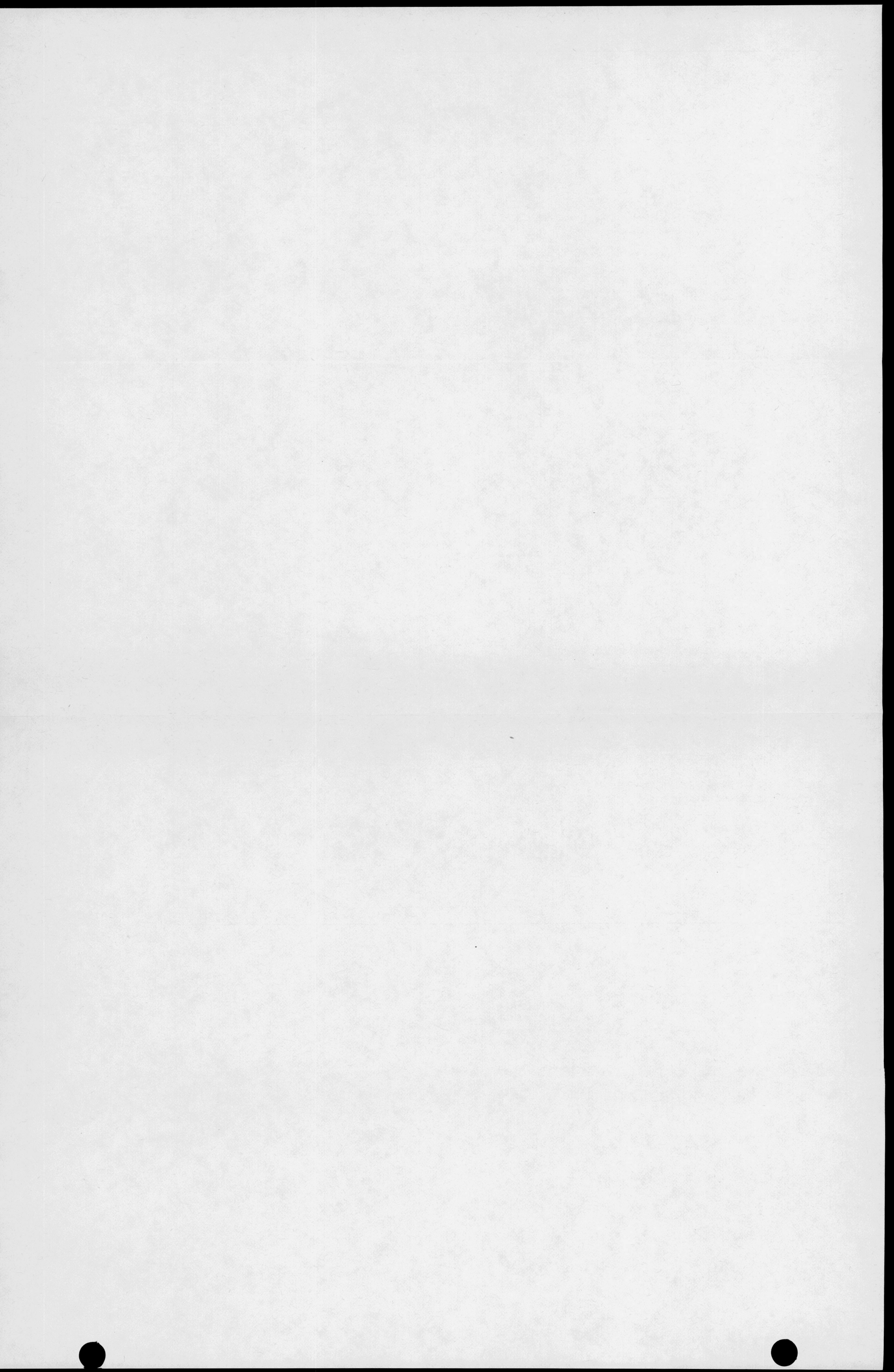


Figure C-4. FLECHT SEASET 163-Rod Blocked Bundle Assembly (sheet 2 of 3)



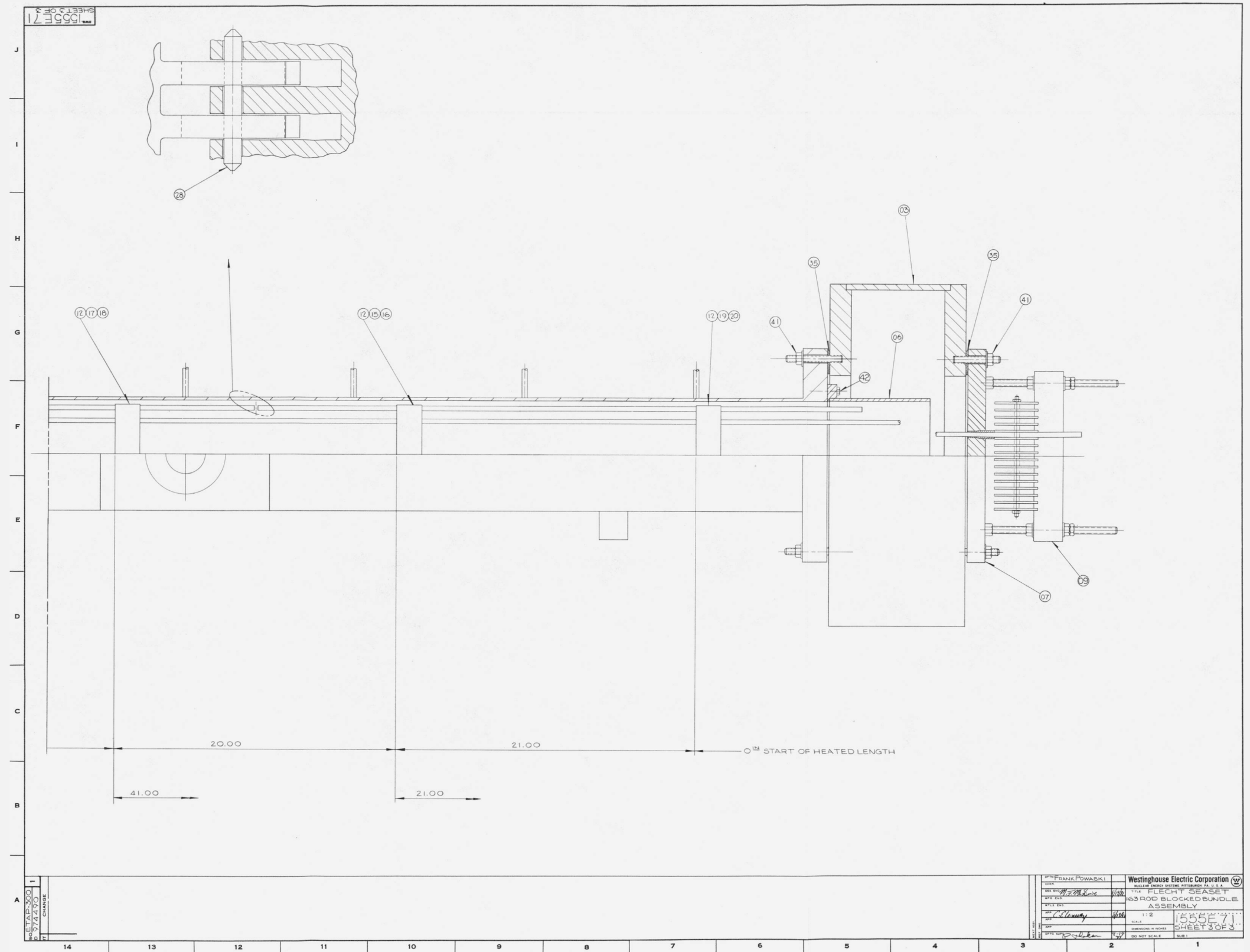
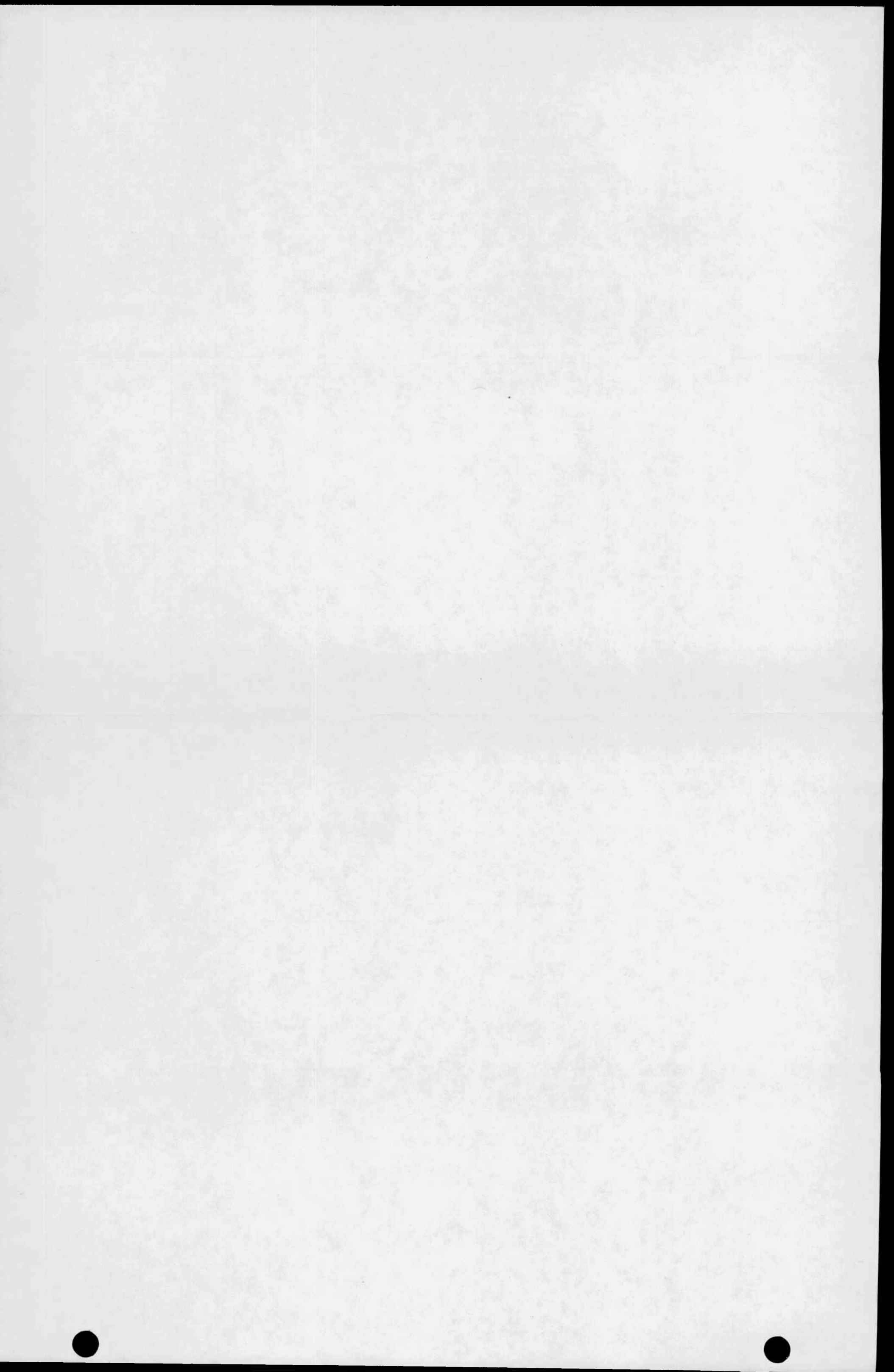


Figure C-4. FLECHT SEASET 163-Rod Blocked Bundle Assembly (sheet 3 of 3)



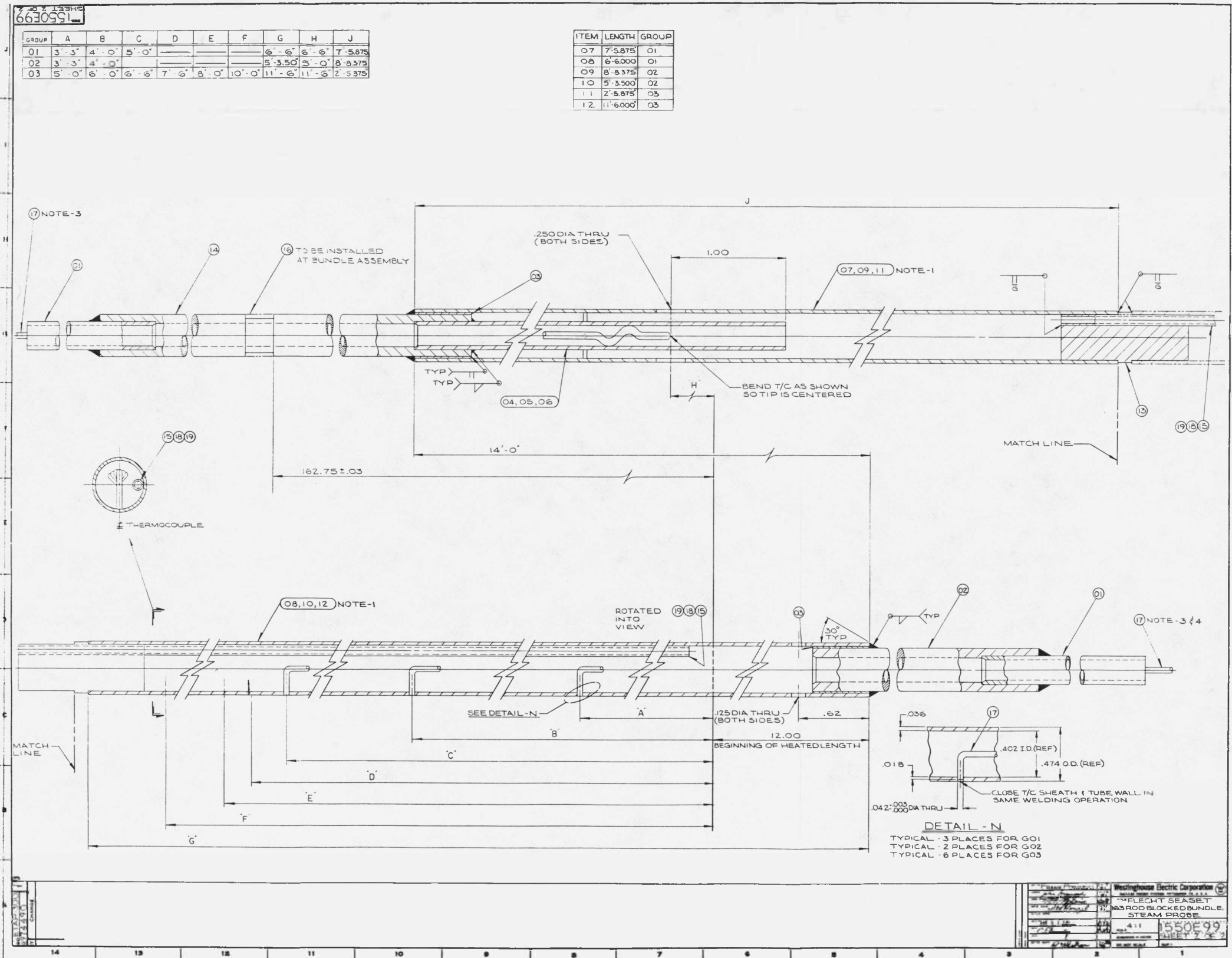
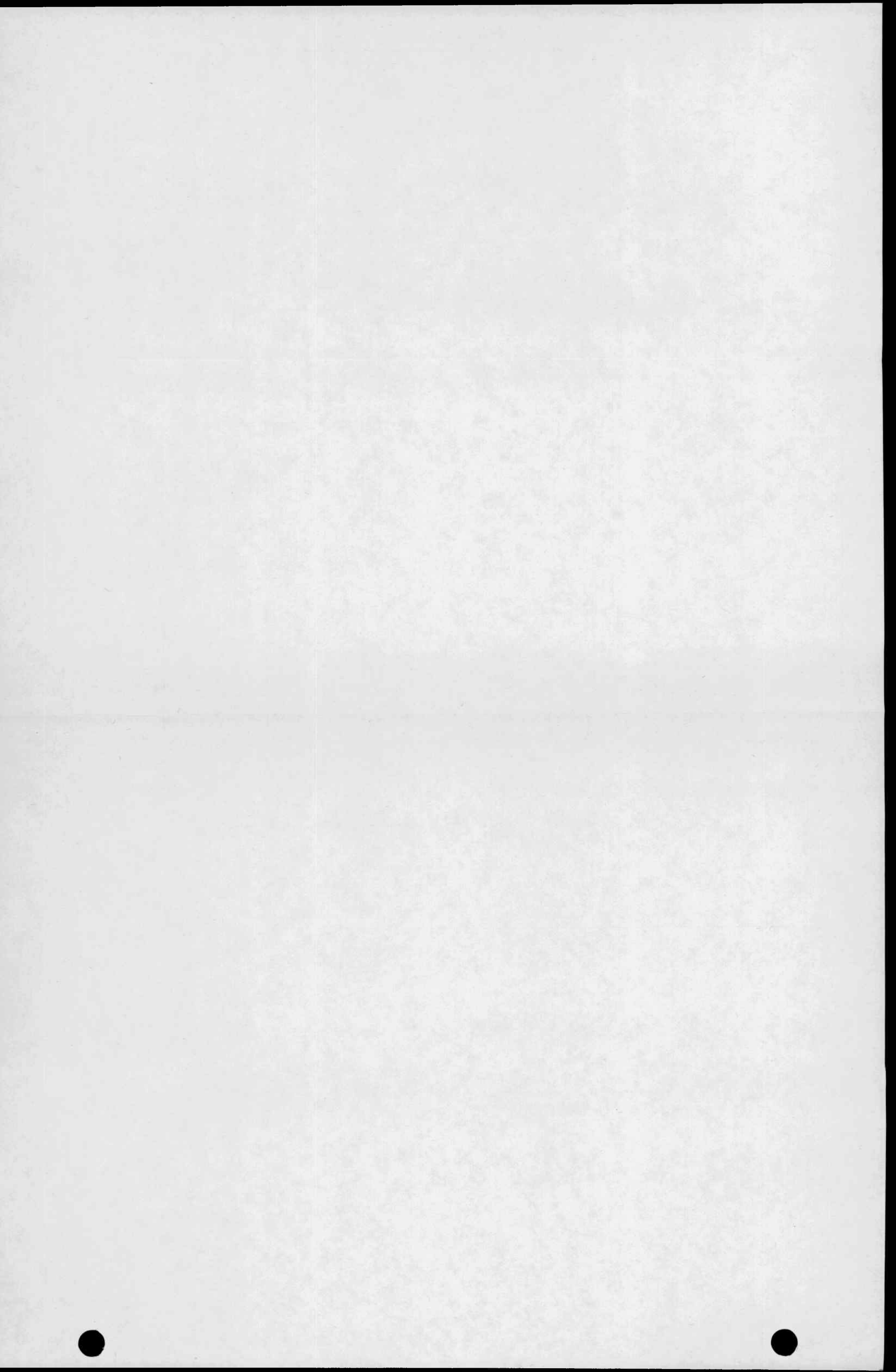
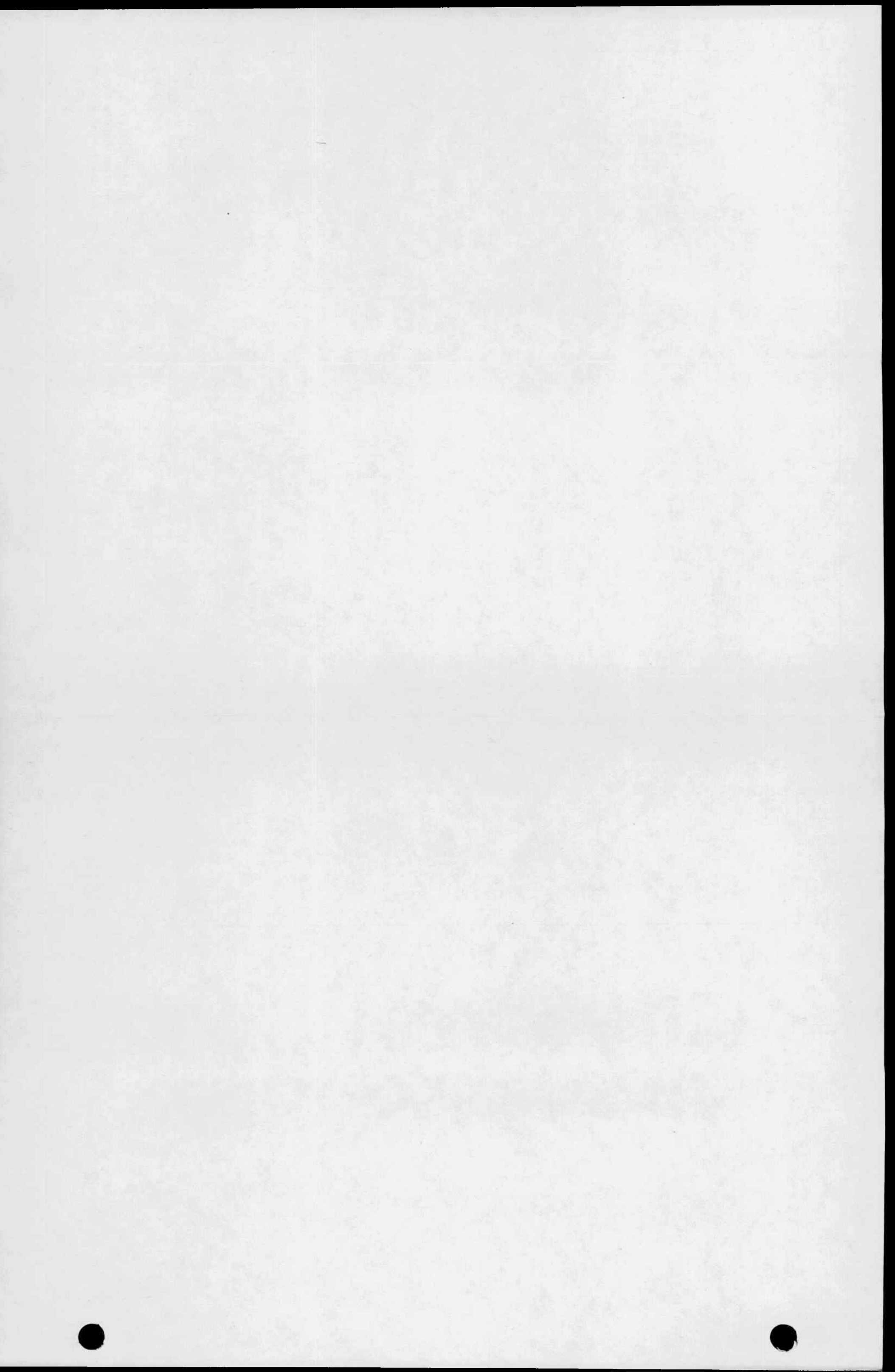


Figure C-5. FLECHT SEASET 163-Rod Blocked Bundle Steam Probe (sheet 1 of 4)







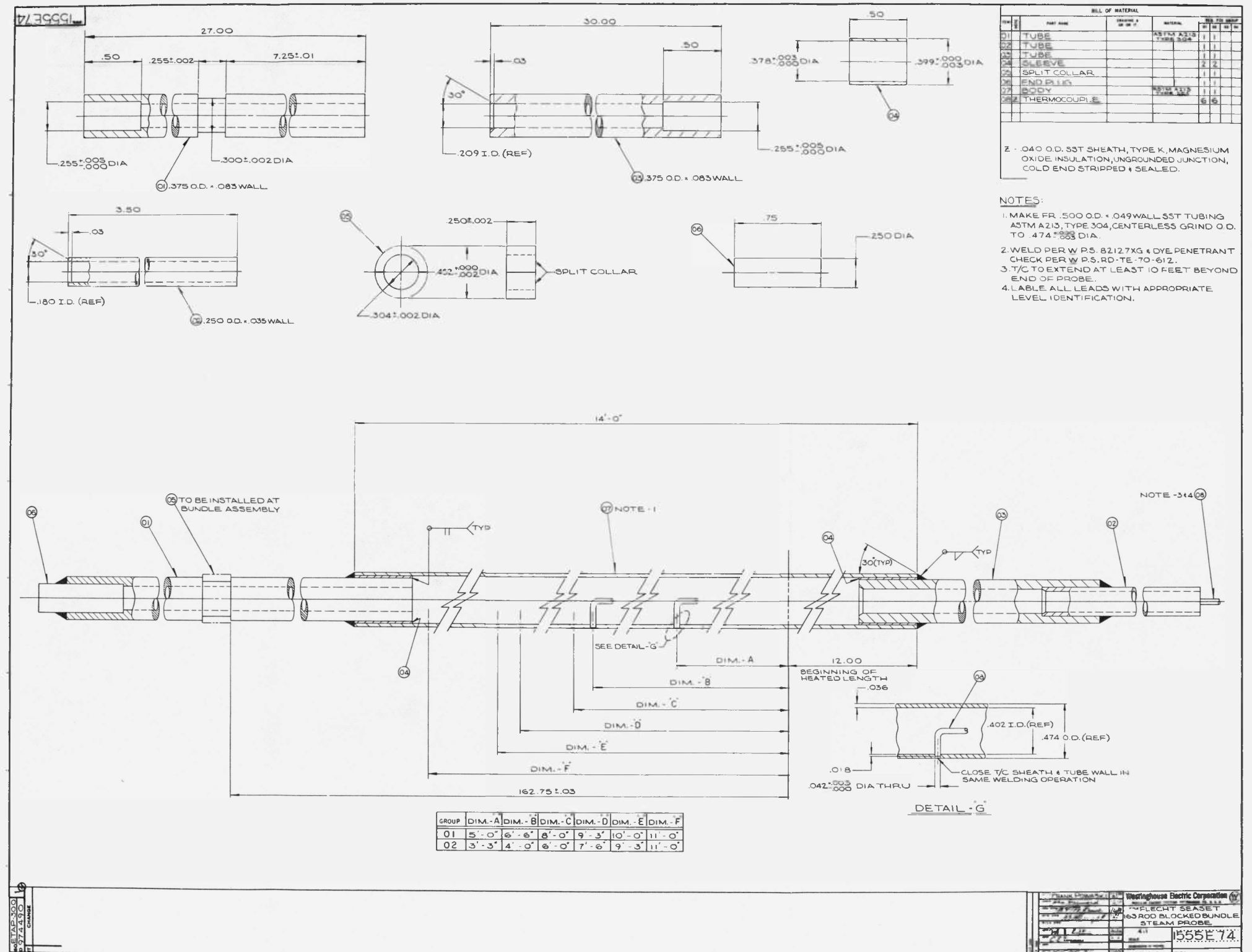
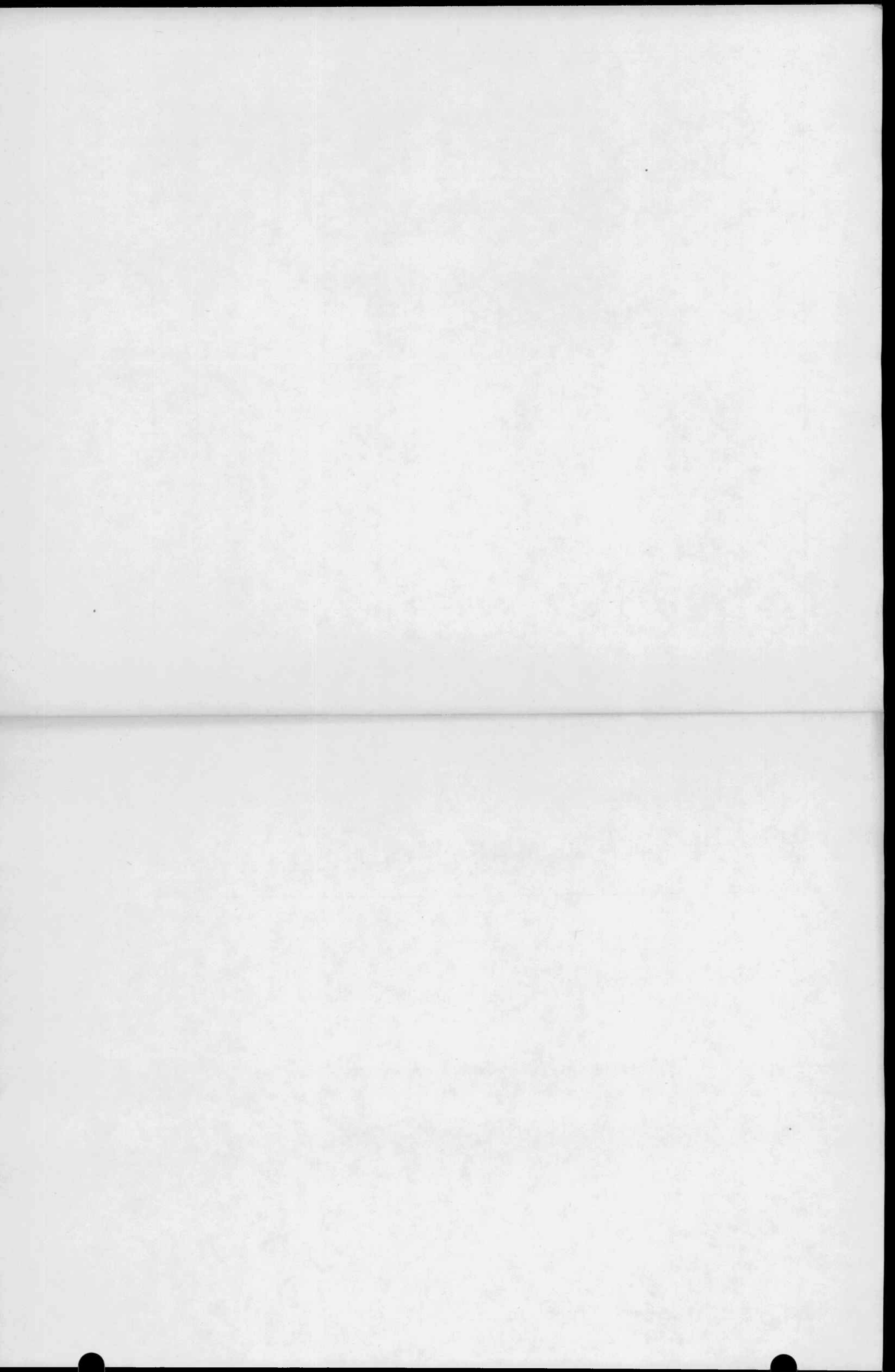
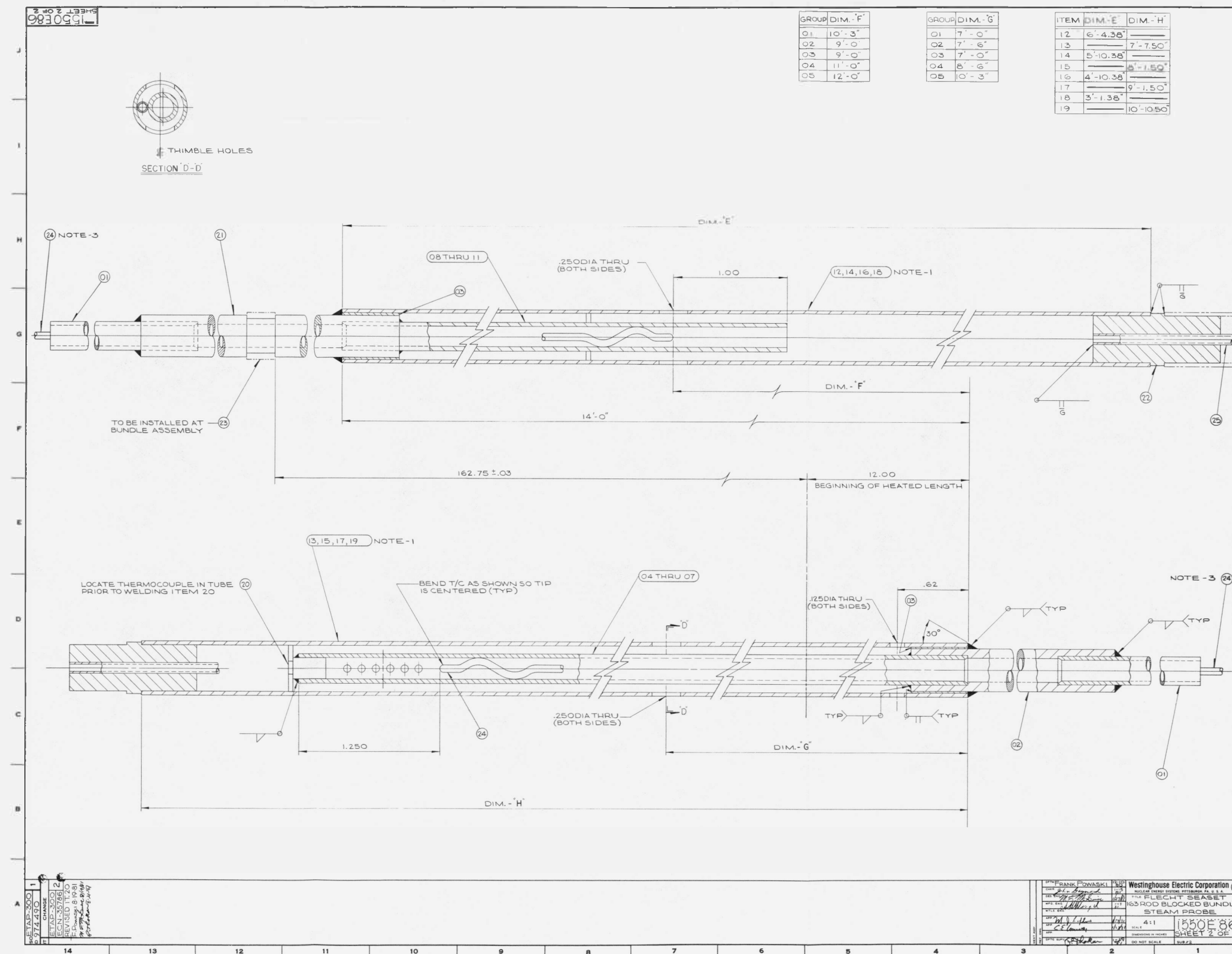


Figure C-5. FLECHT SEASET 163-Rod Blocked Bundle Steam Probe (sheet 3 of 4)





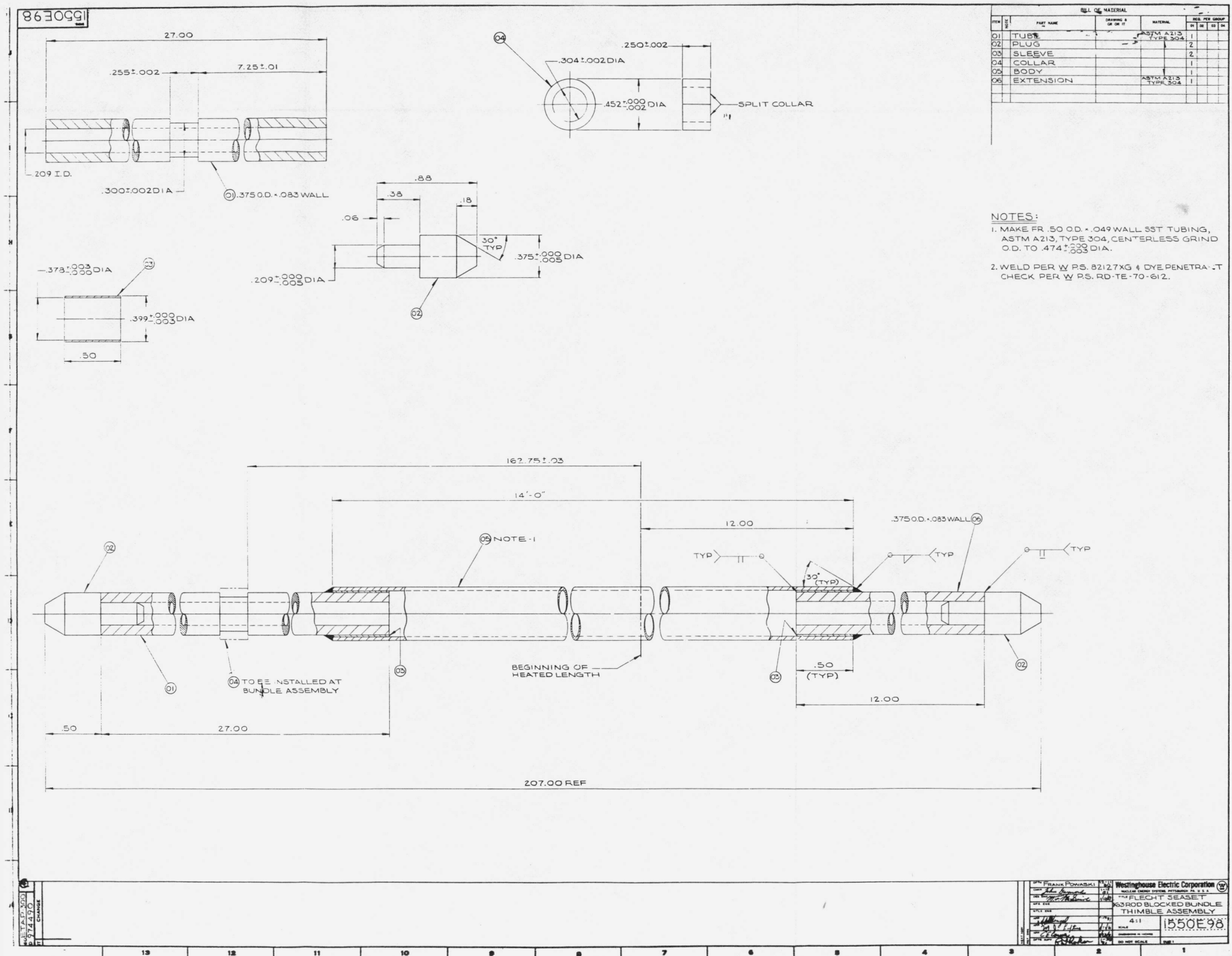
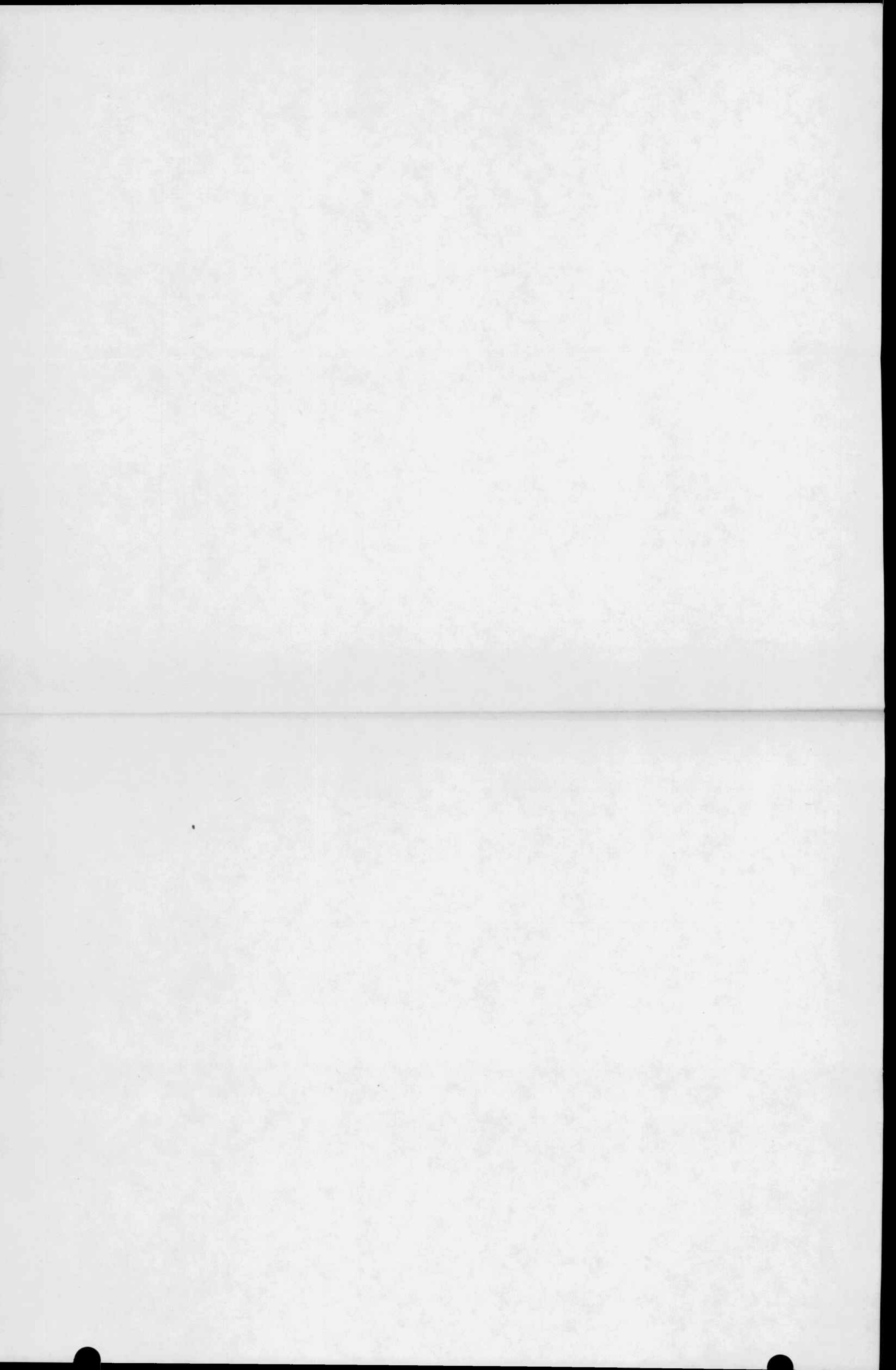


Figure C-6. FLECHT SEASET 163-Rod Blocked Bundle Thimble



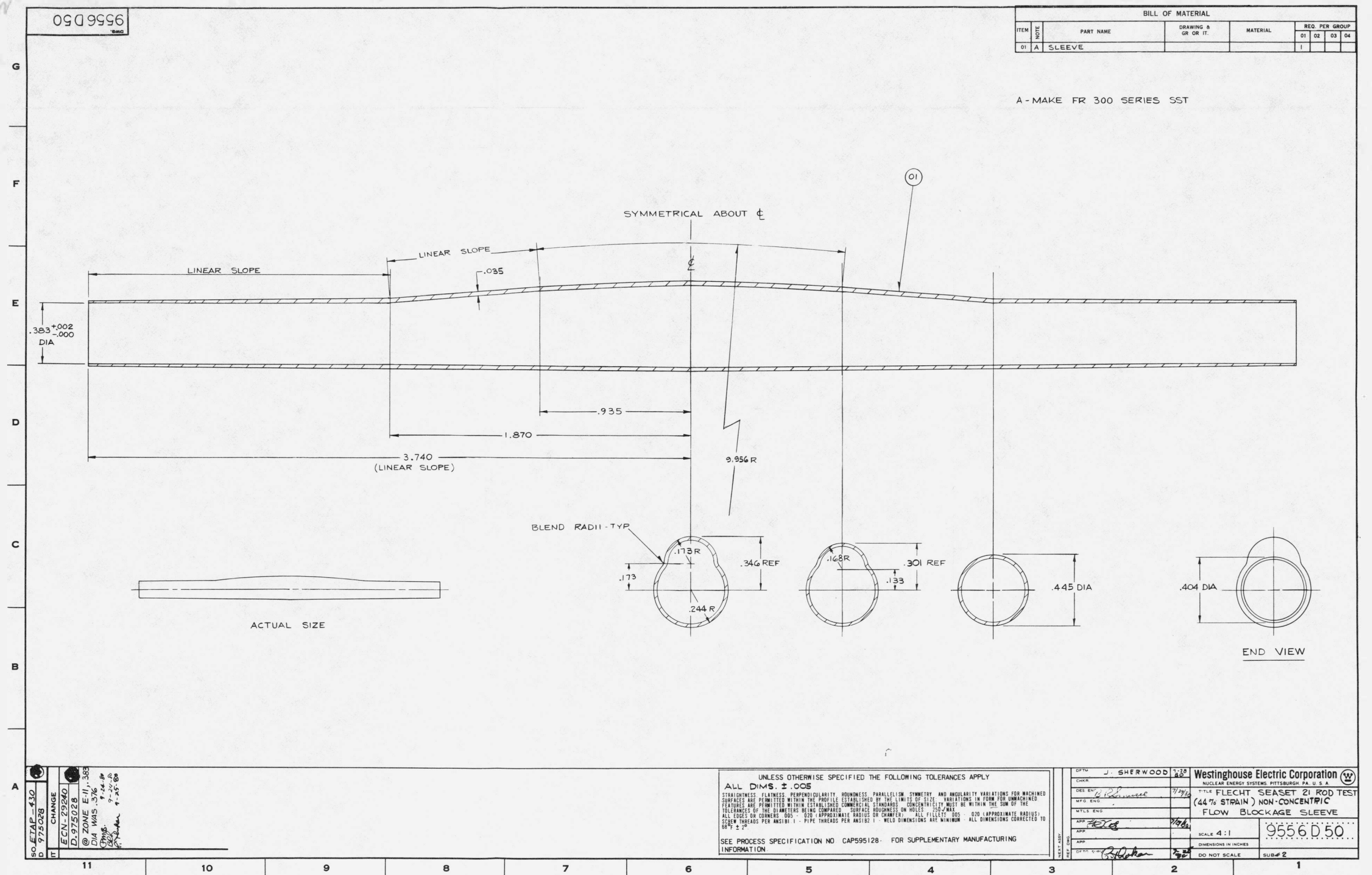
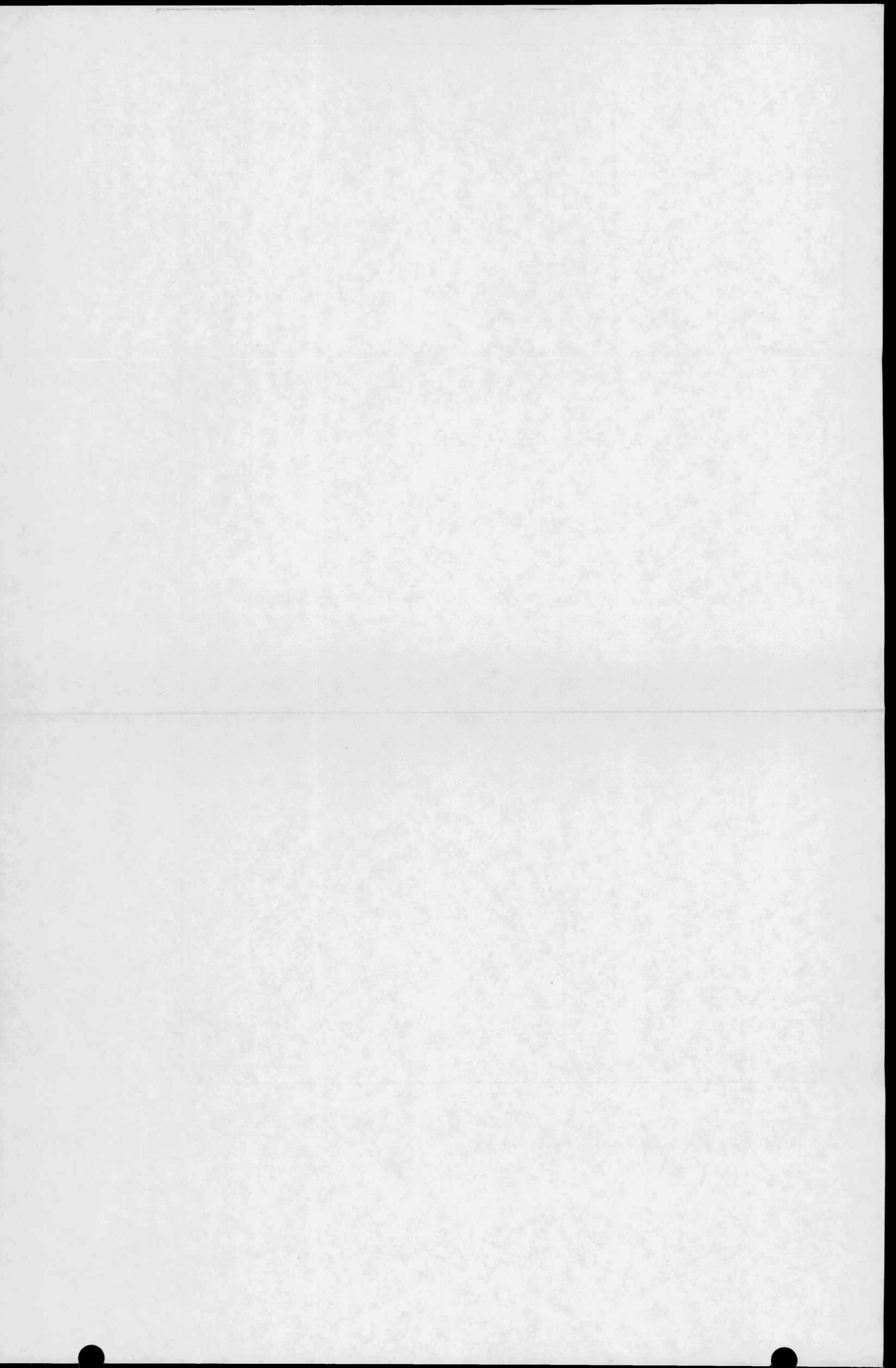


Figure C-7. FLECHT SEASET 21-Rod Test (44-Percent Strain) Nonconcentric Flow Blockage Sleeve



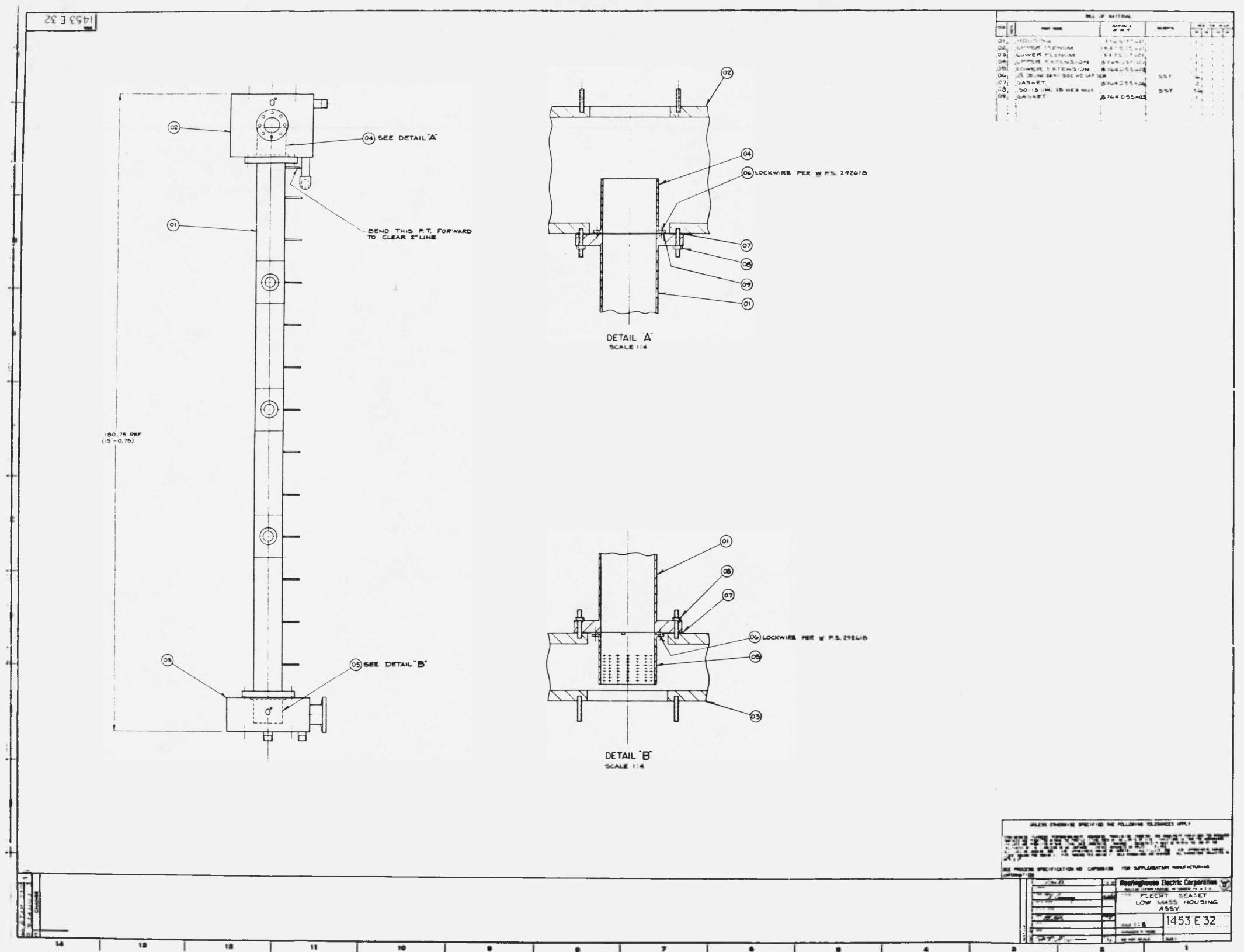
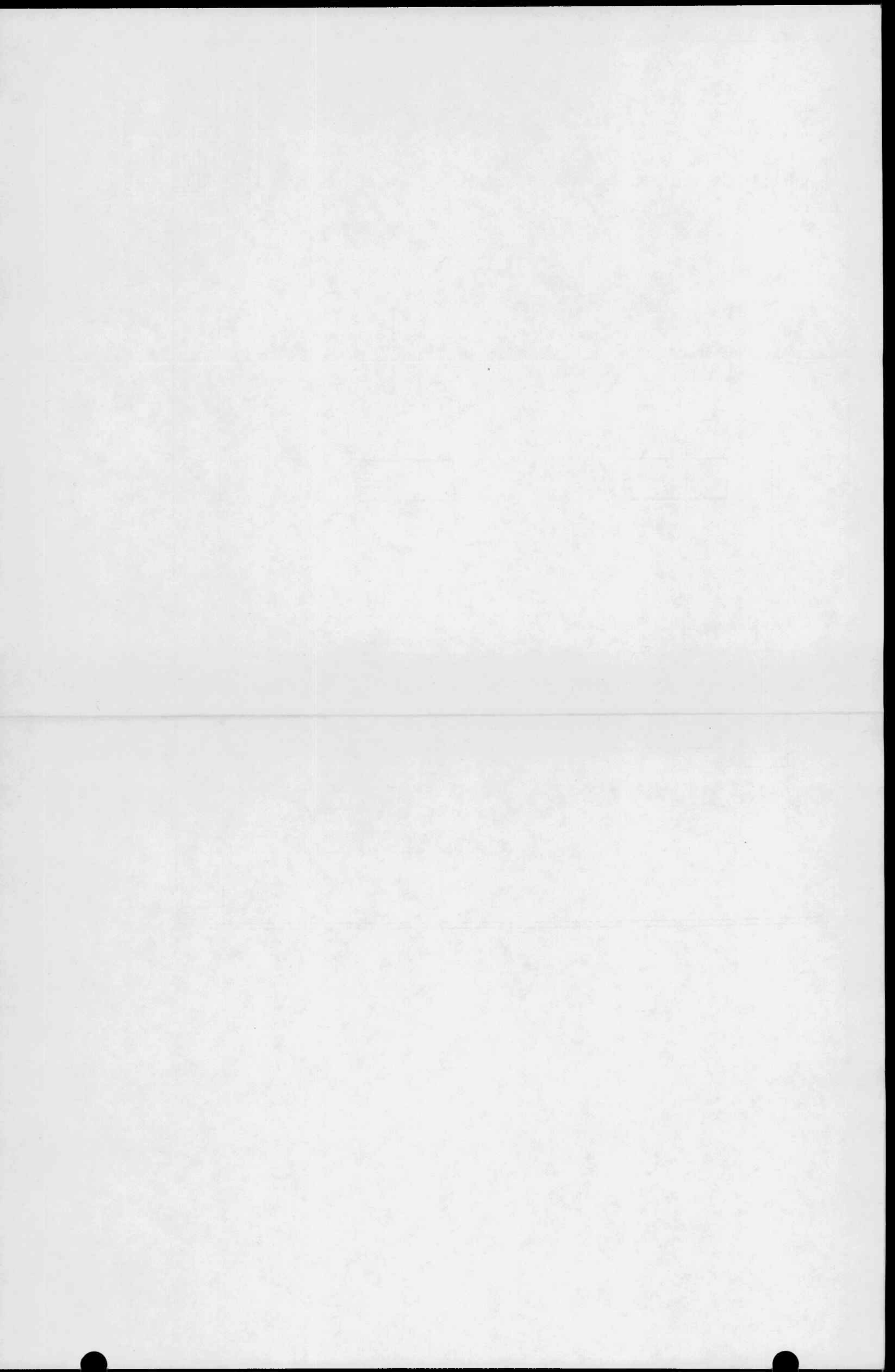
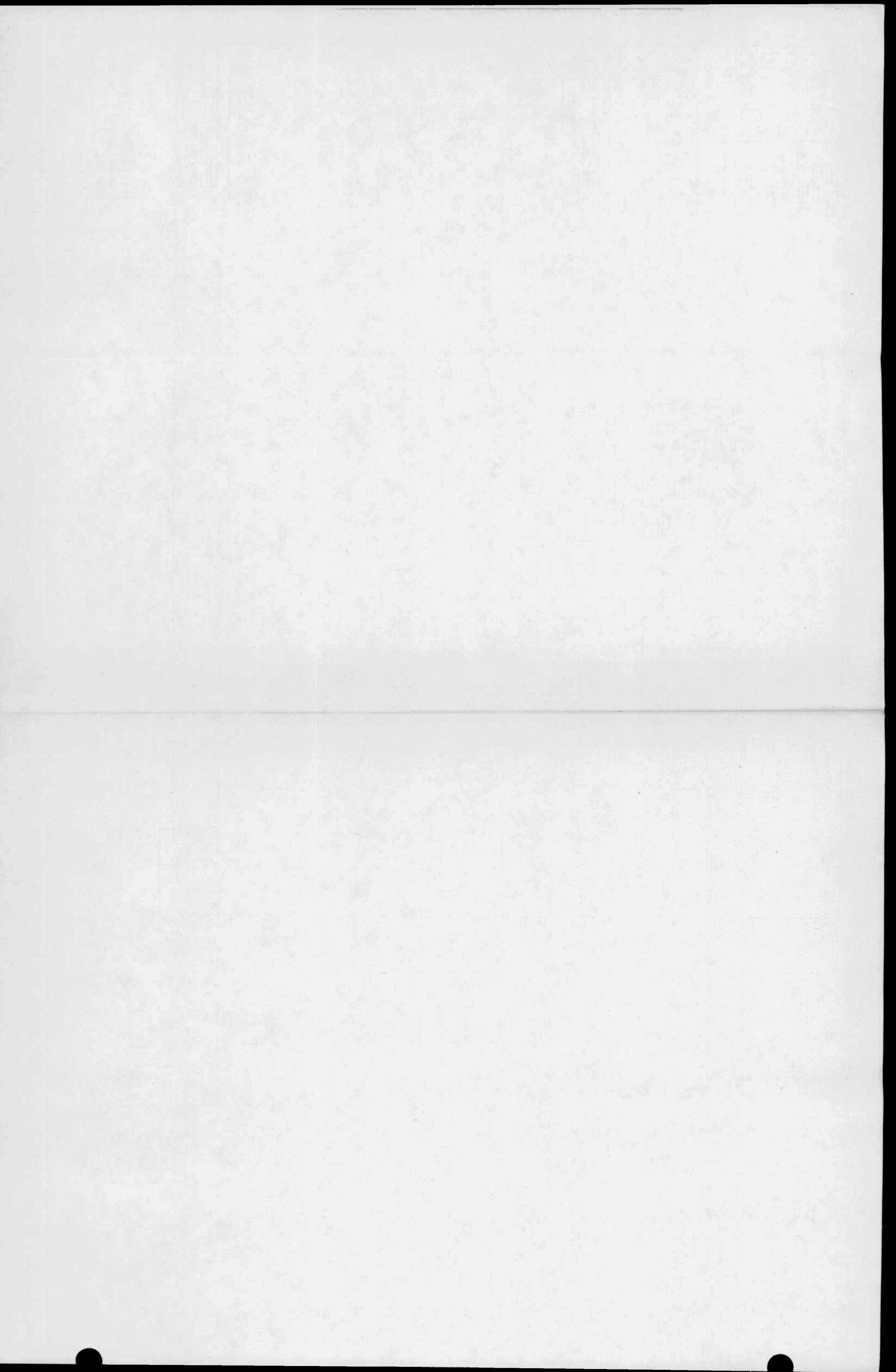
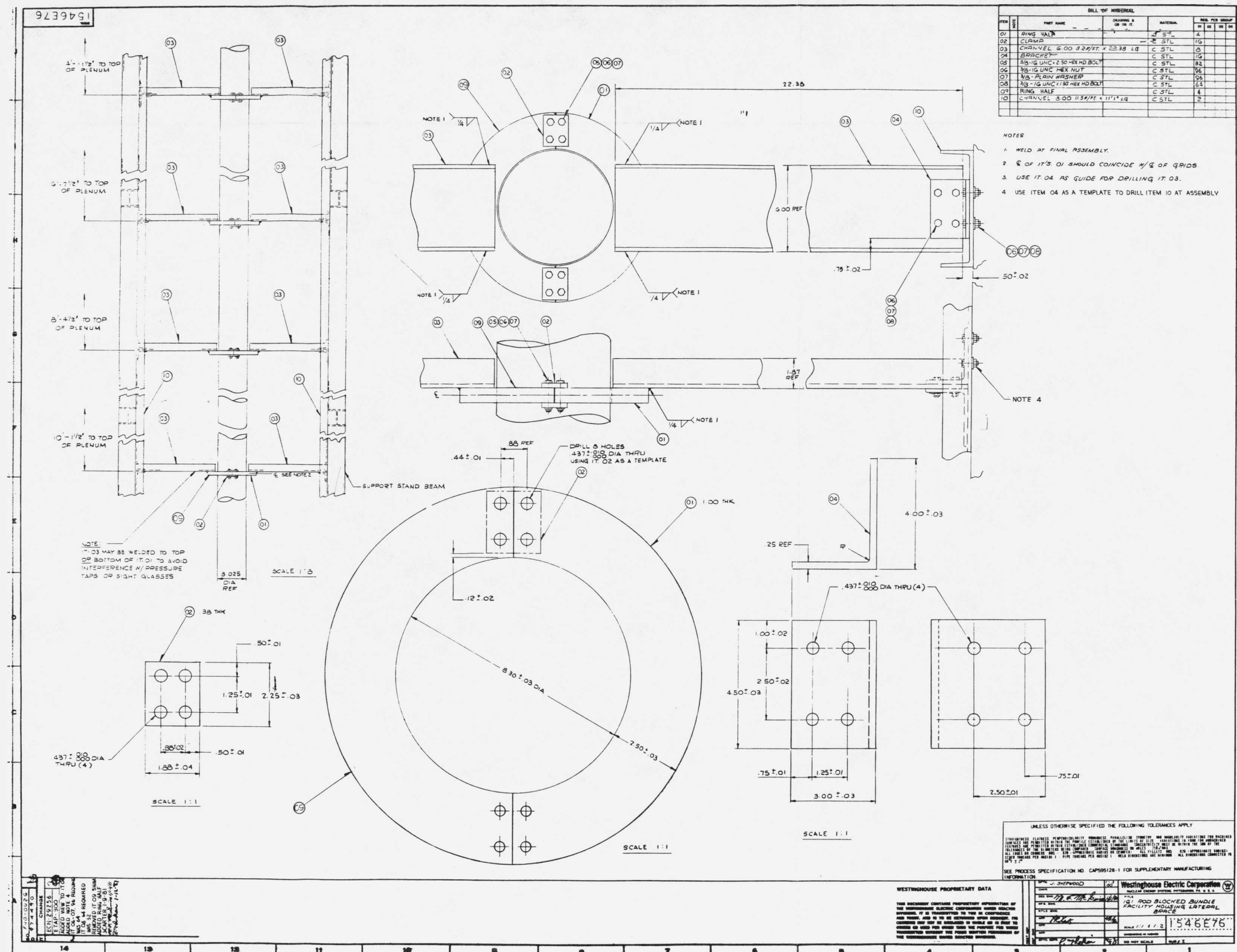


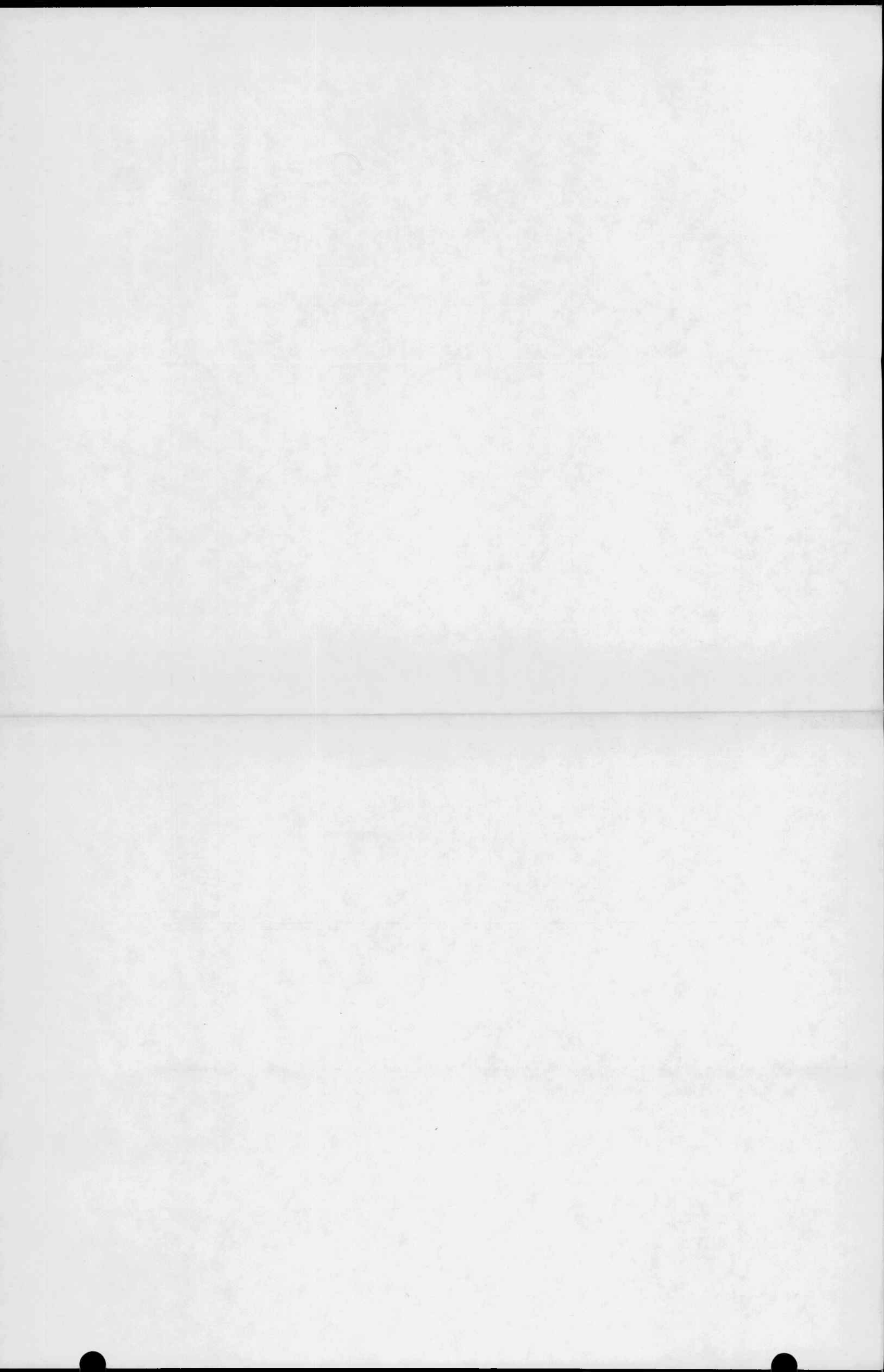
Figure C-8. FLECHT SEASET Low Mass Housing Assembly











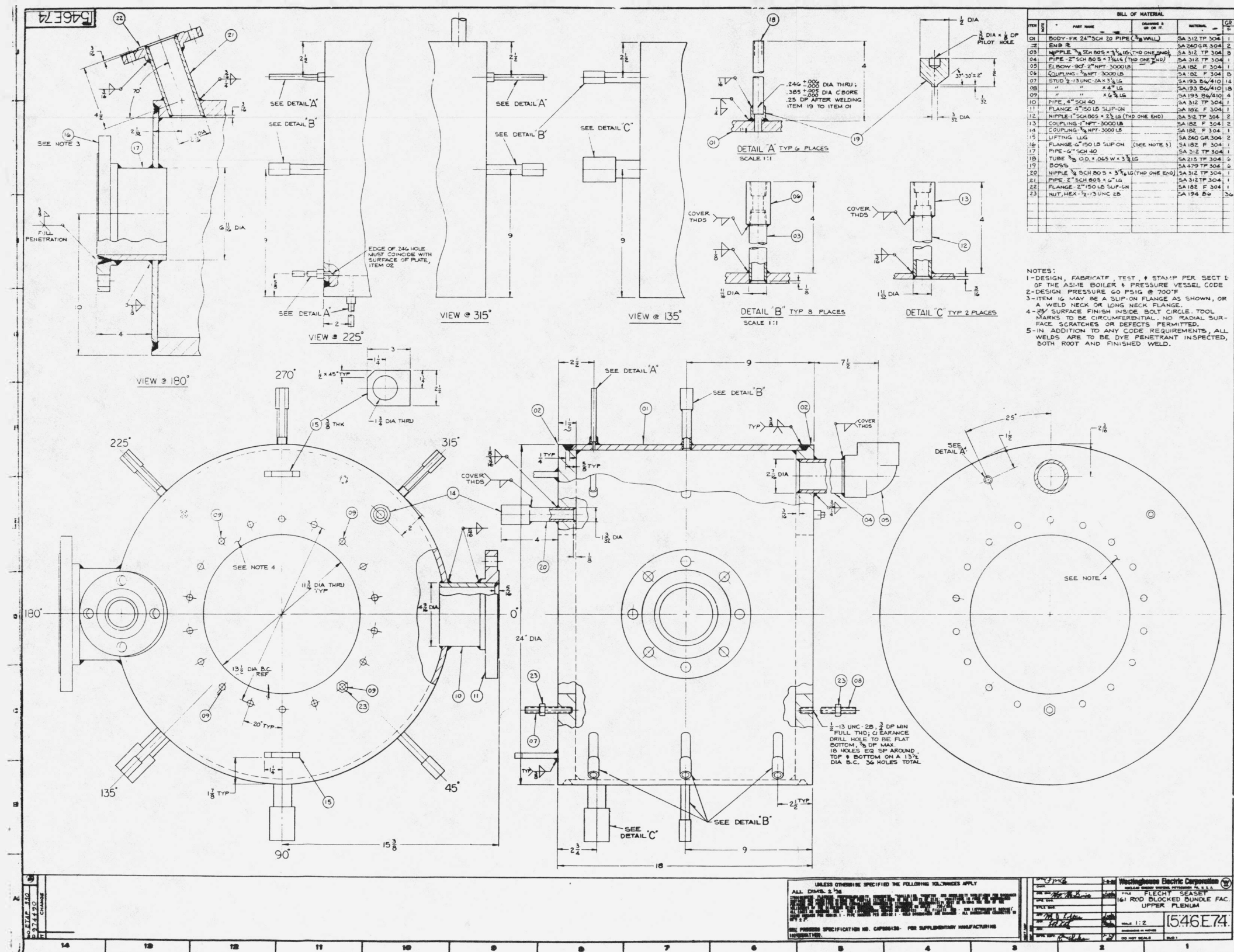


Figure C-11. FLECHT SEASET 161-Rod
Blocked Bundle Facility
Upper Plenum

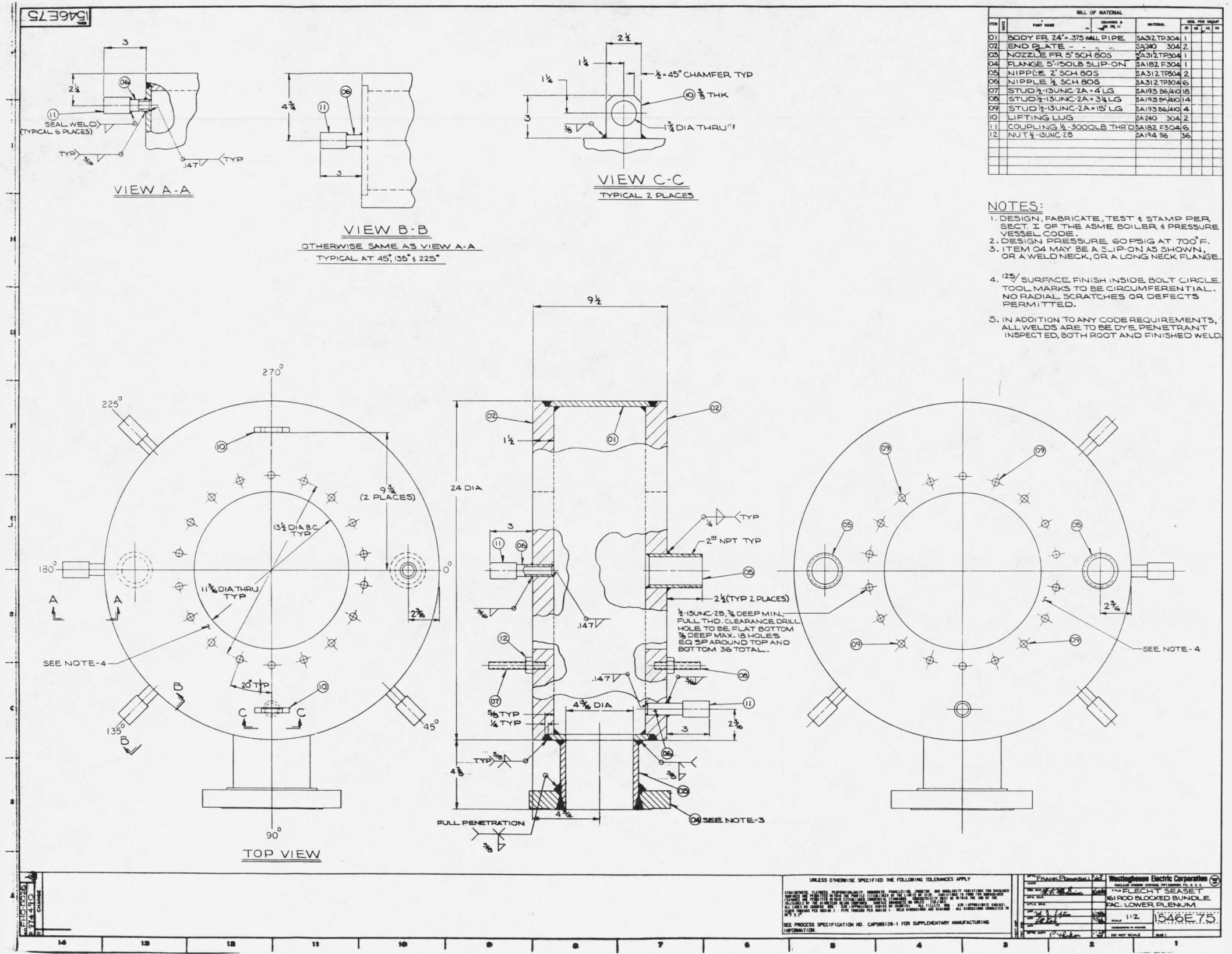
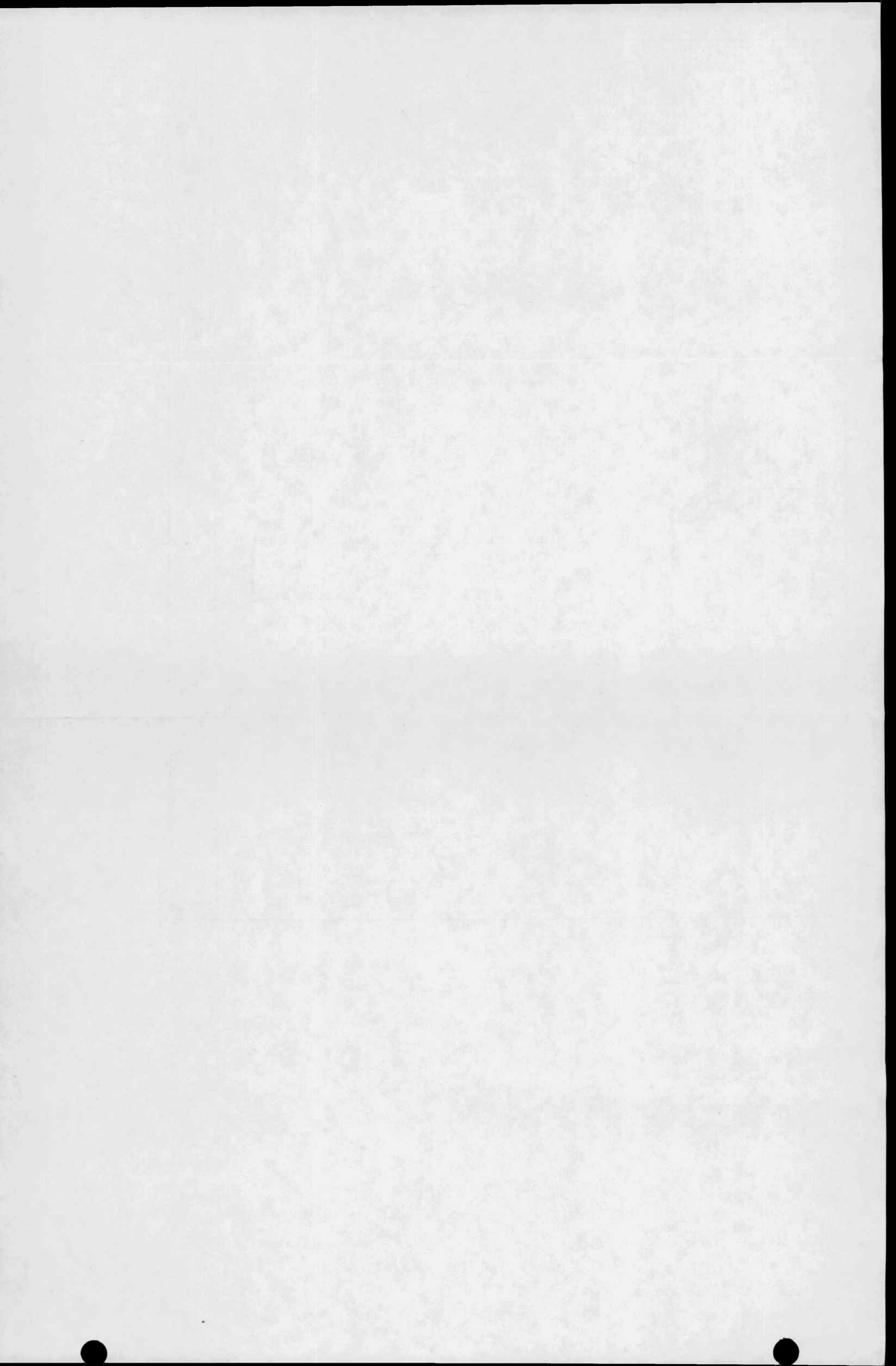


Figure C-12. FLECHT SEASET 161-Rod Blocked Bundle Facility Lower Plenum



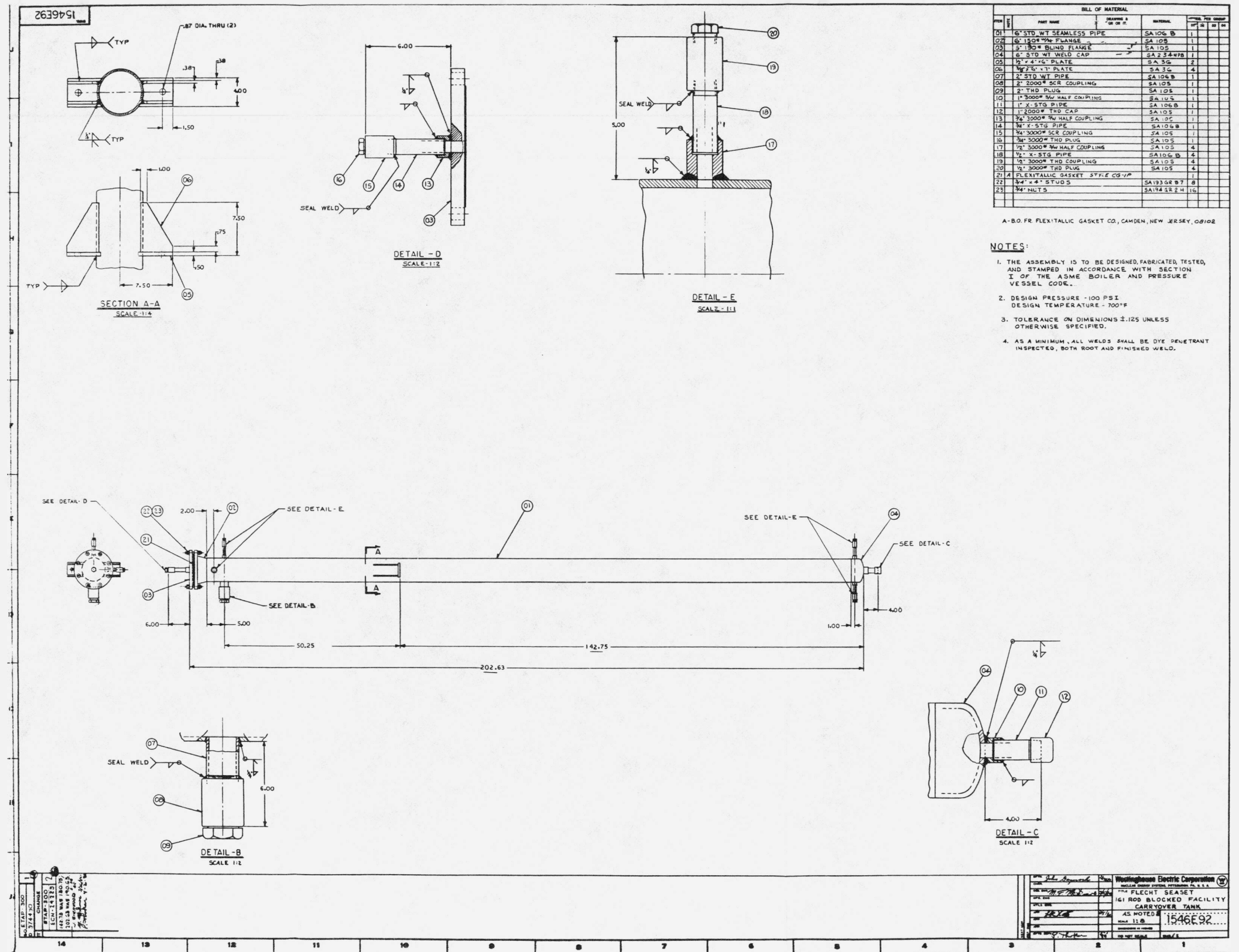
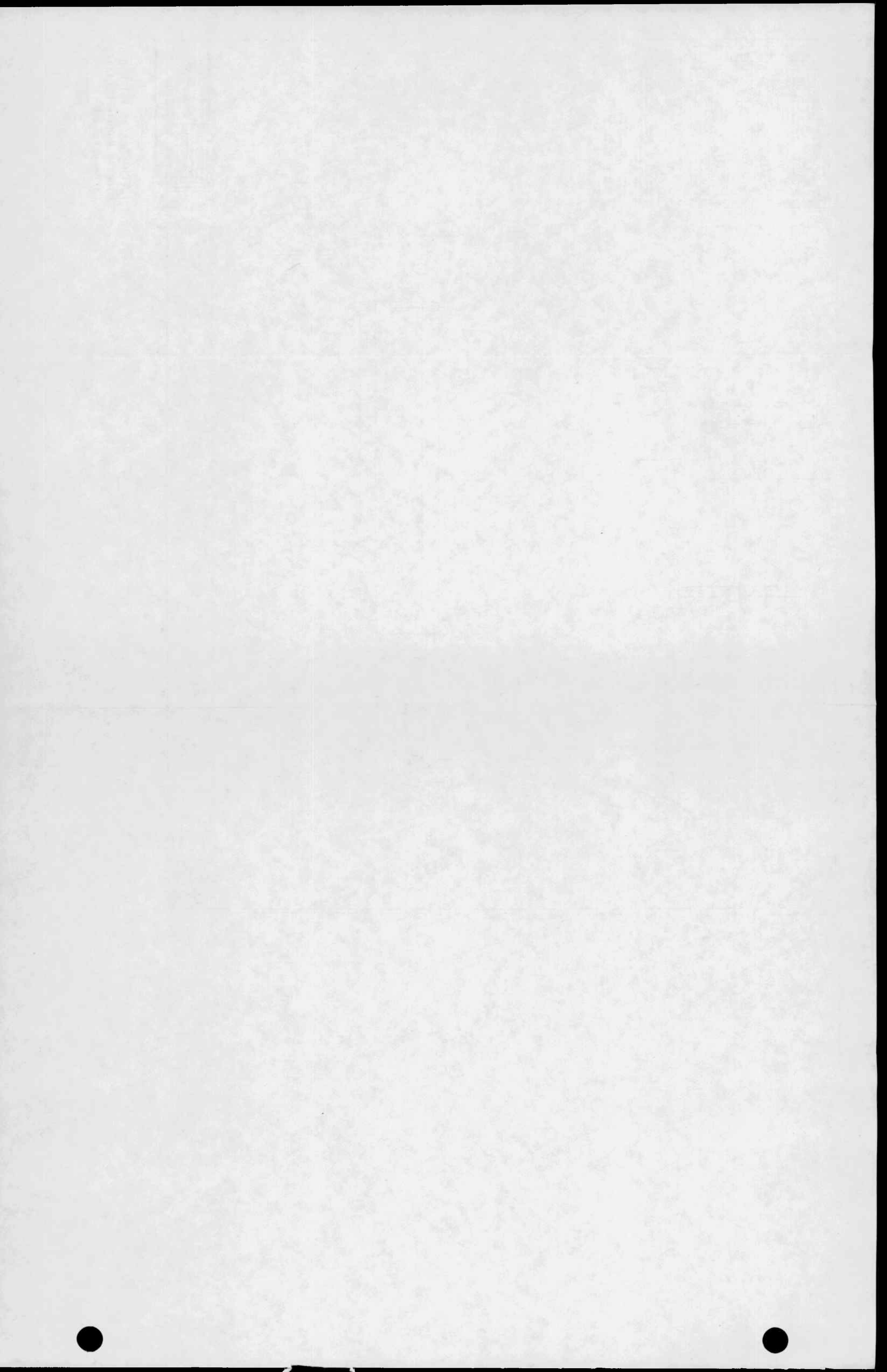
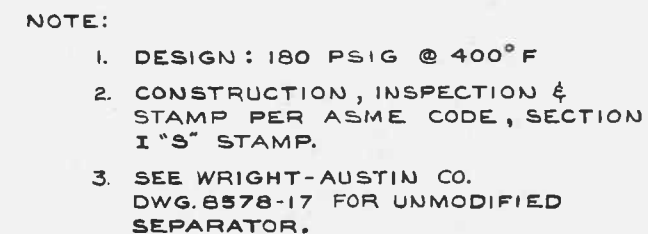


Figure C-13. FLECHT SEASET 161-Rod Blocked Bundle Facility Carryover Tank

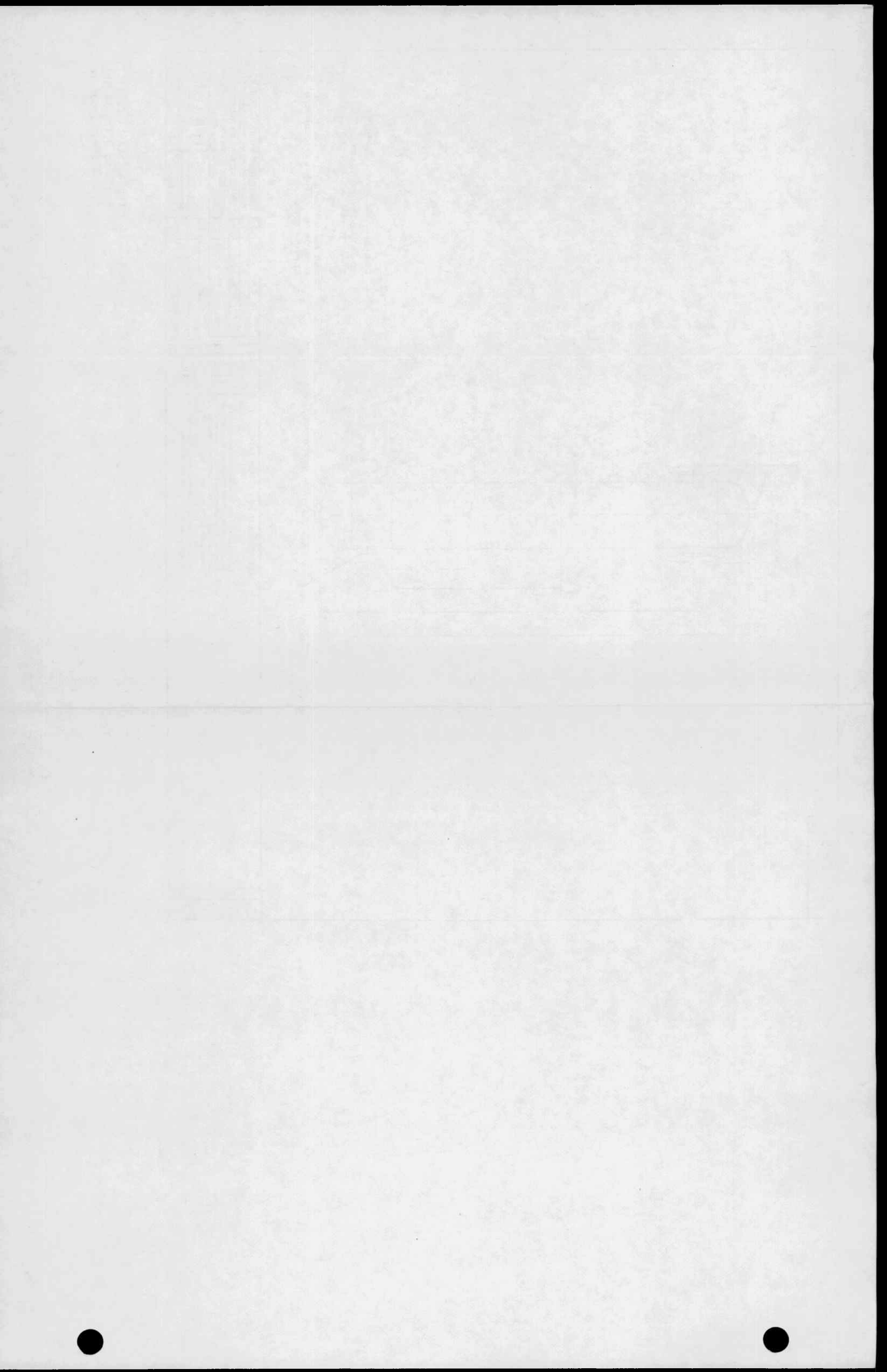


100%



1	WESTINGHOUSE PROPRIETARY DATA	<p>THIS DOCUMENT CONTAINS PROPRIETARY INFORMATION OF THE WESTINGHOUSE ELECTRIC CORPORATION WATER REACTOR DIVISIONS. IT IS TRANSMITTED TO YOU IN CONFIDENCE AND TRUST, AND IS TO BE RETURNED UPON REQUEST. ITS CONTENTS MAY NOT BE DISCLOSED IN WHOLE OR IN PART TO OTHERS OR USED FOR OTHER THAN THE PURPOSE FOR WHICH TRANSMITTED WITHOUT THE PRIOR WRITTEN PERMISSION OF THE WESTINGHOUSE WATER REACTOR DIVISIONS.</p>	<p>UNITED STATES GOVERNMENT PRINTING OFFICE: 1964 O 561-741 <small>THIS DOCUMENT IS UNCLASSIFIED DATE 08-14-2011 BY 60322 UCBAW</small></p>	<p>DFTM. R CRALLE 3-25-77</p>	<p>Westinghouse Electric Corporation <small>NUCLEAR ENERGY SYSTEMS, PITTSBURGH, PA., U.S.A.</small></p>
				<p>CHKR.</p>	<p>TITLE: FLECHT FACILITY MODIFIED 4" TYPE 'T' STEAM SEPARATOR</p>
<p>DES. ENG. C.E. Conway 11/6/77</p>				<p>SCALE</p>	<p>1683C19</p>
<p>INFO. ENG.</p>				<p>DIMENSIONS IN INCHES</p>	
<p>INTL. ENG.</p>				<p>DO NOT SCALE</p>	<p>SUB 1</p>
<p>APP. [Signature] 11/5/77</p>					
<p>APP.</p>					
<p>APP.</p>					
<p>APP. [Signature] 4-1</p>					

Figure C-14. FLECHT SEASET Facility
Modified 0.1 m (4 in.)
Type T Steam Separator



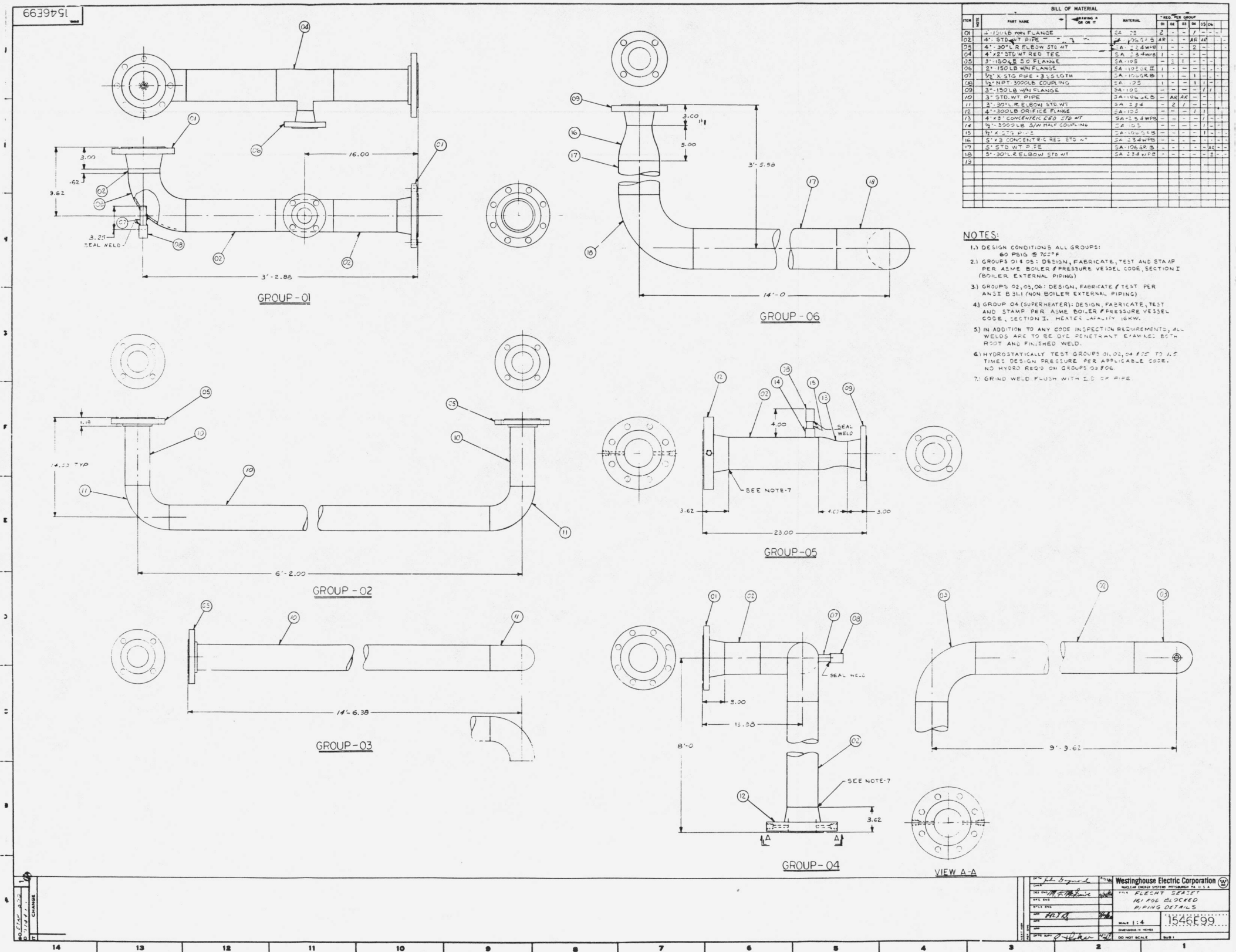
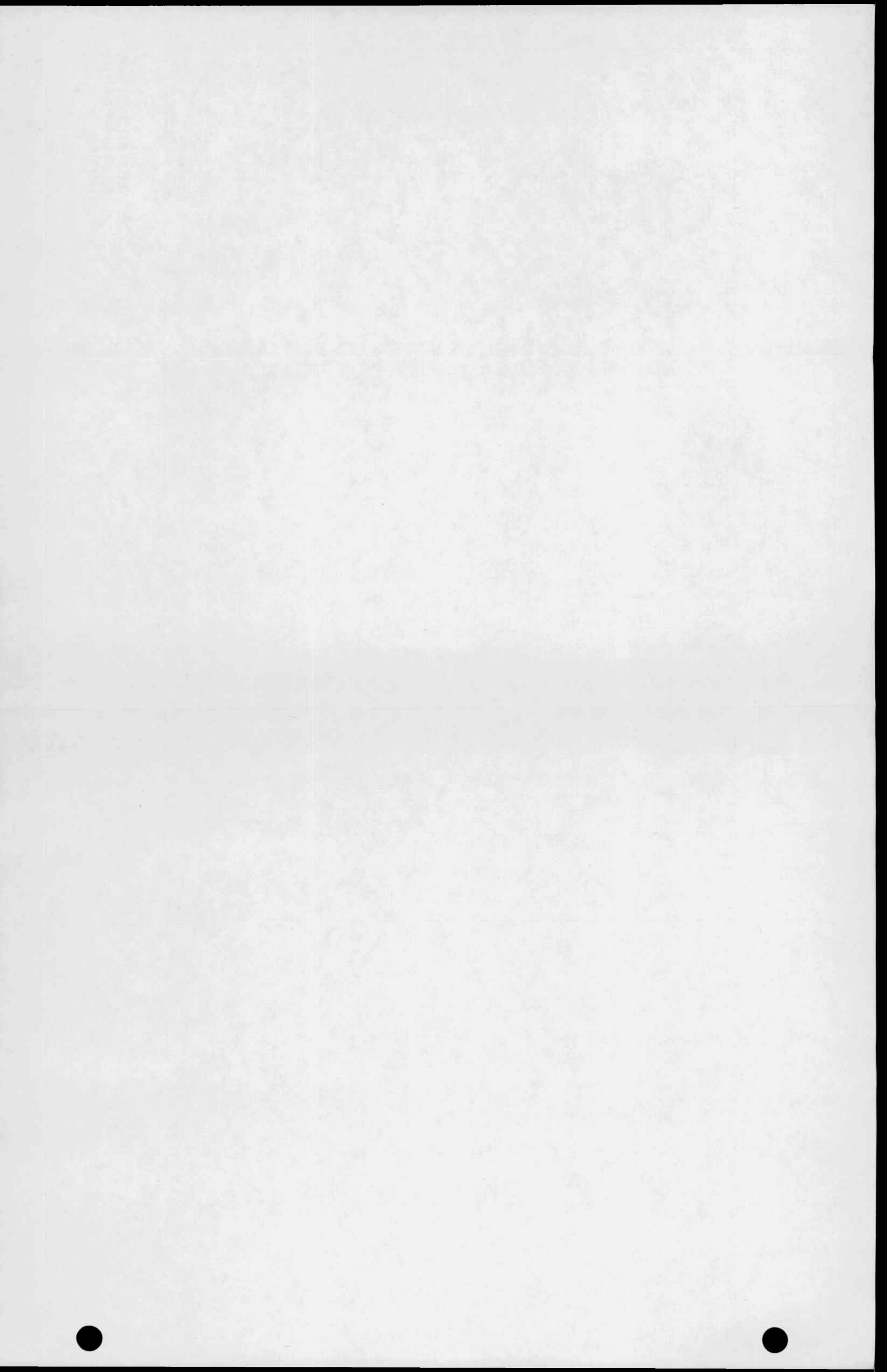


Figure C-15. FLECHT SEASET 161-Rod Blocked Bundle Piping Details



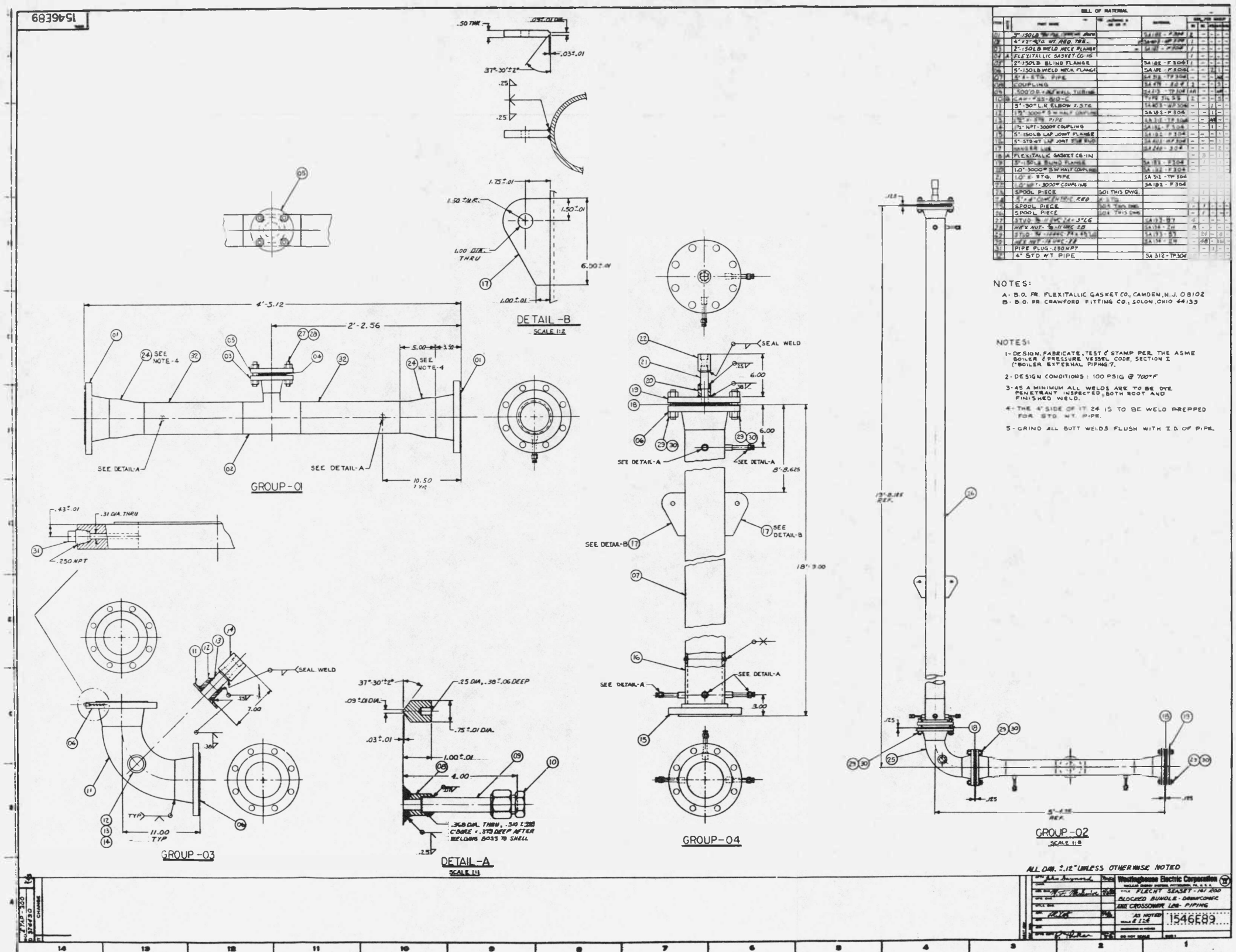
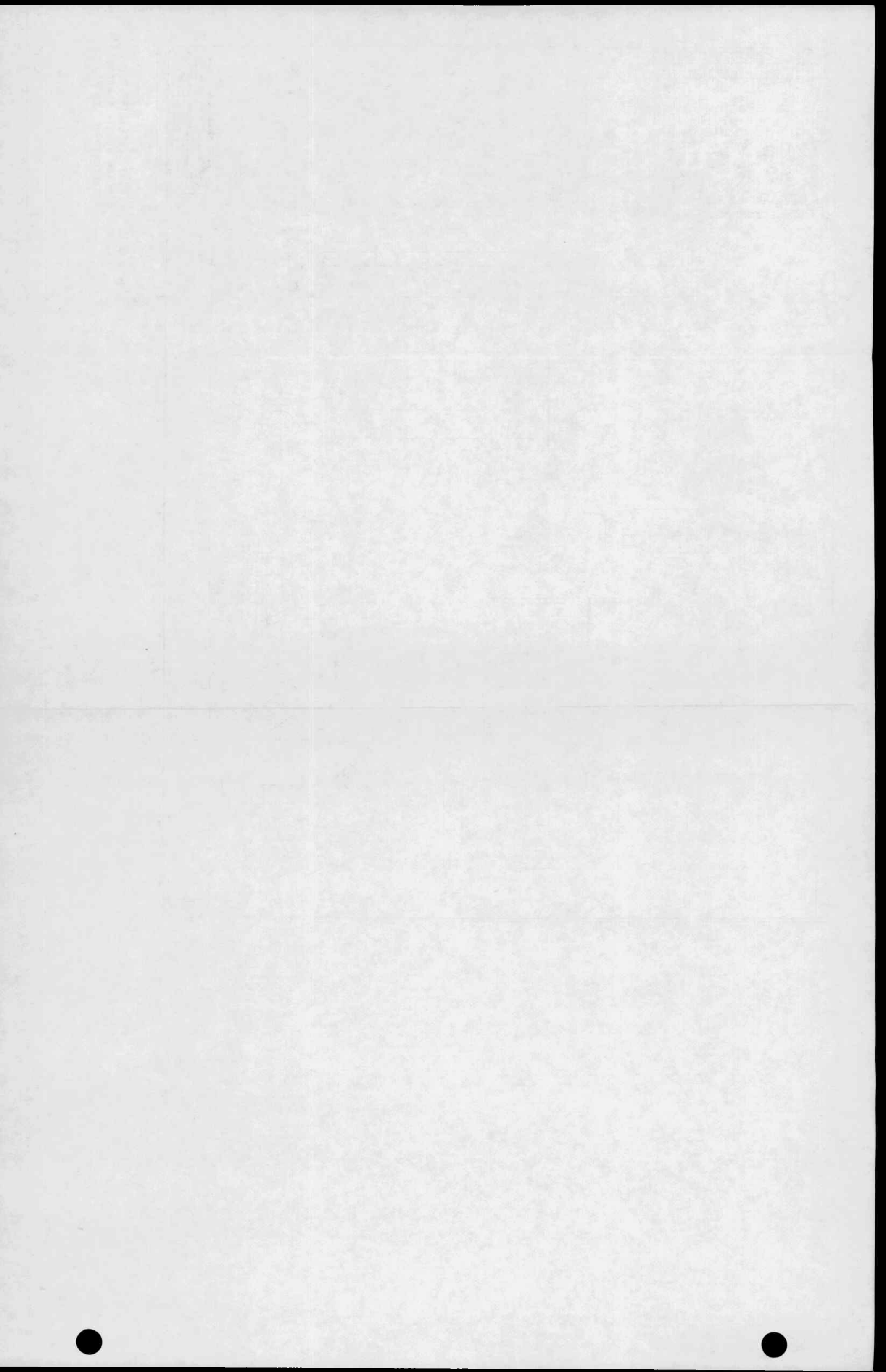
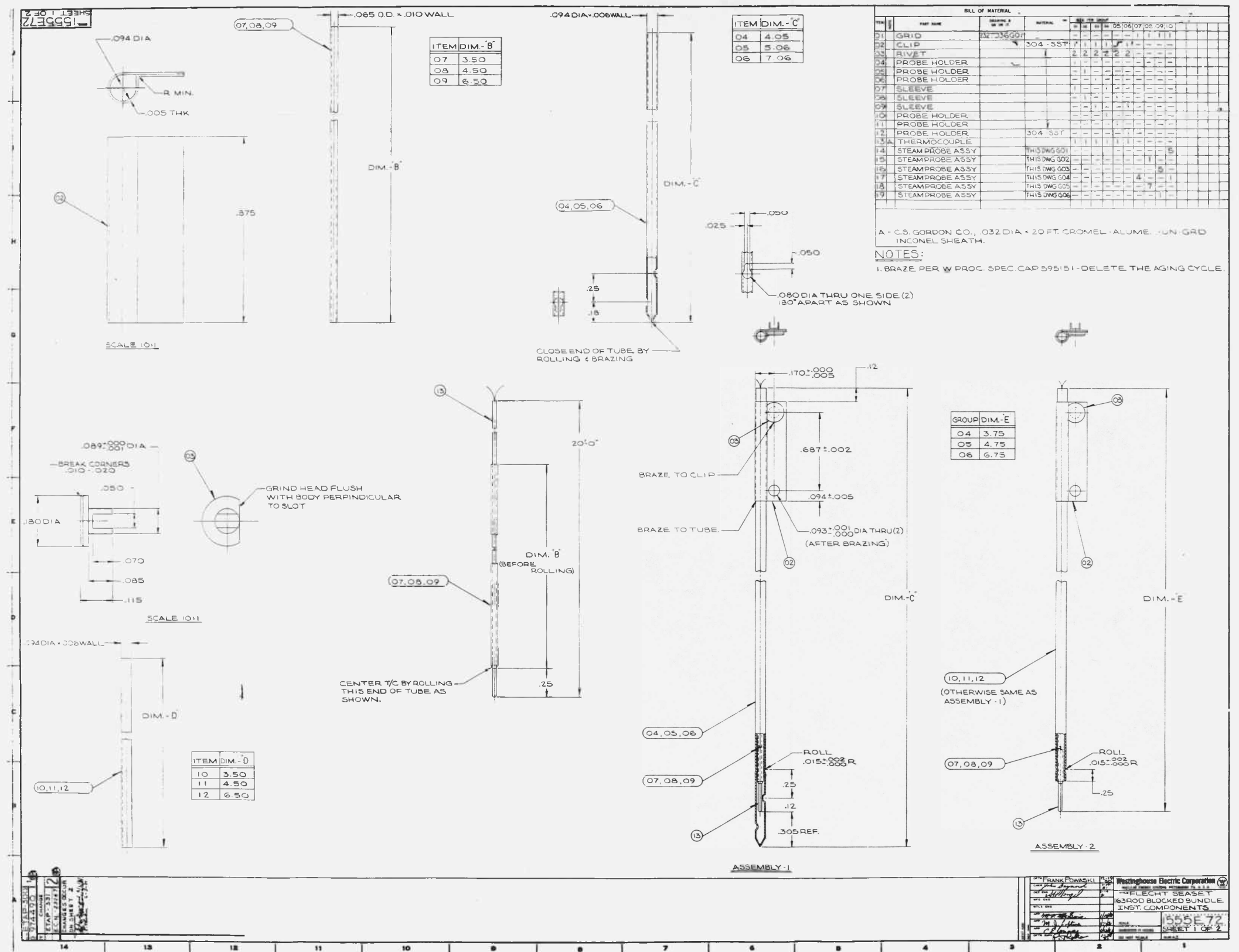
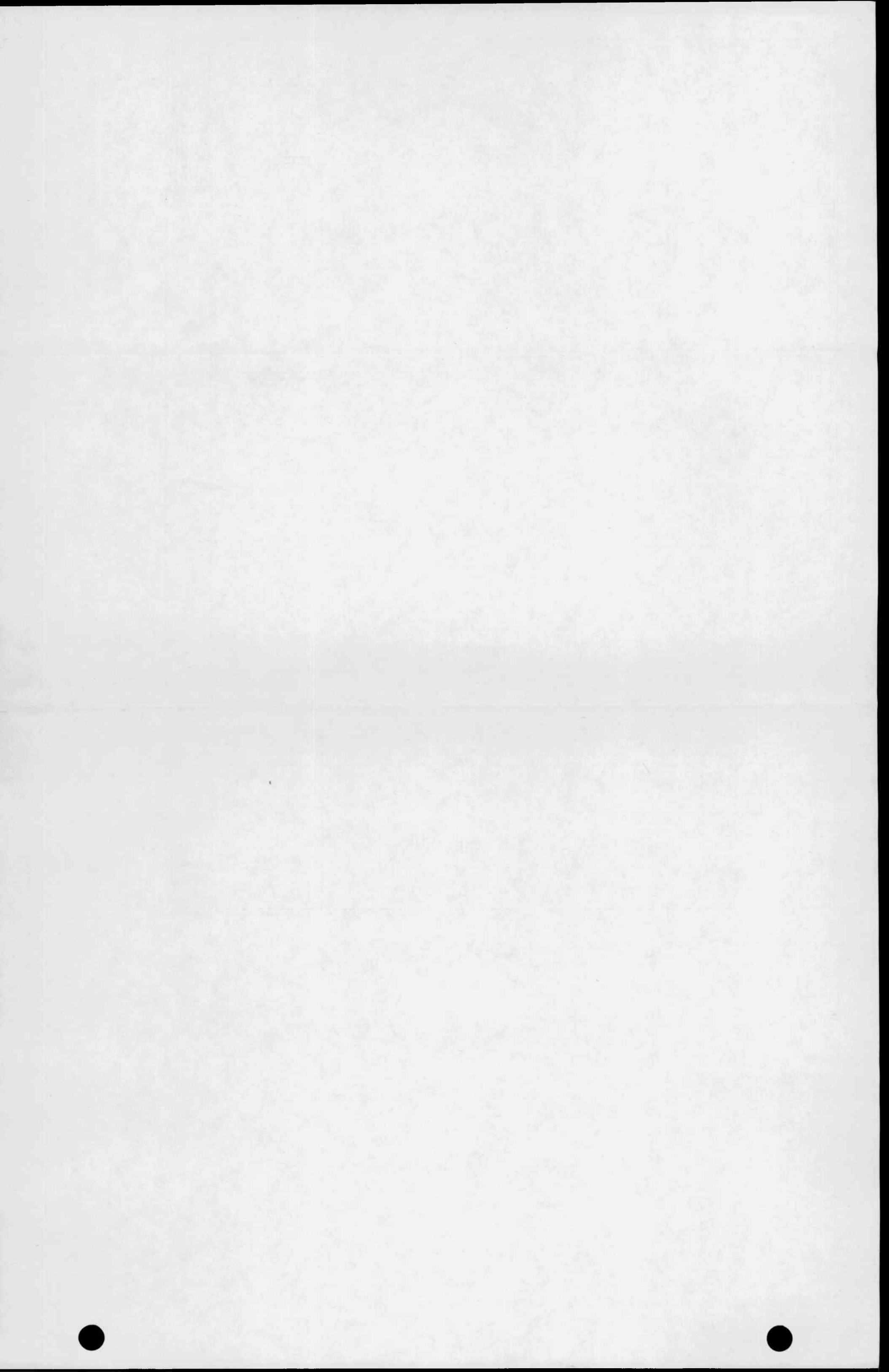
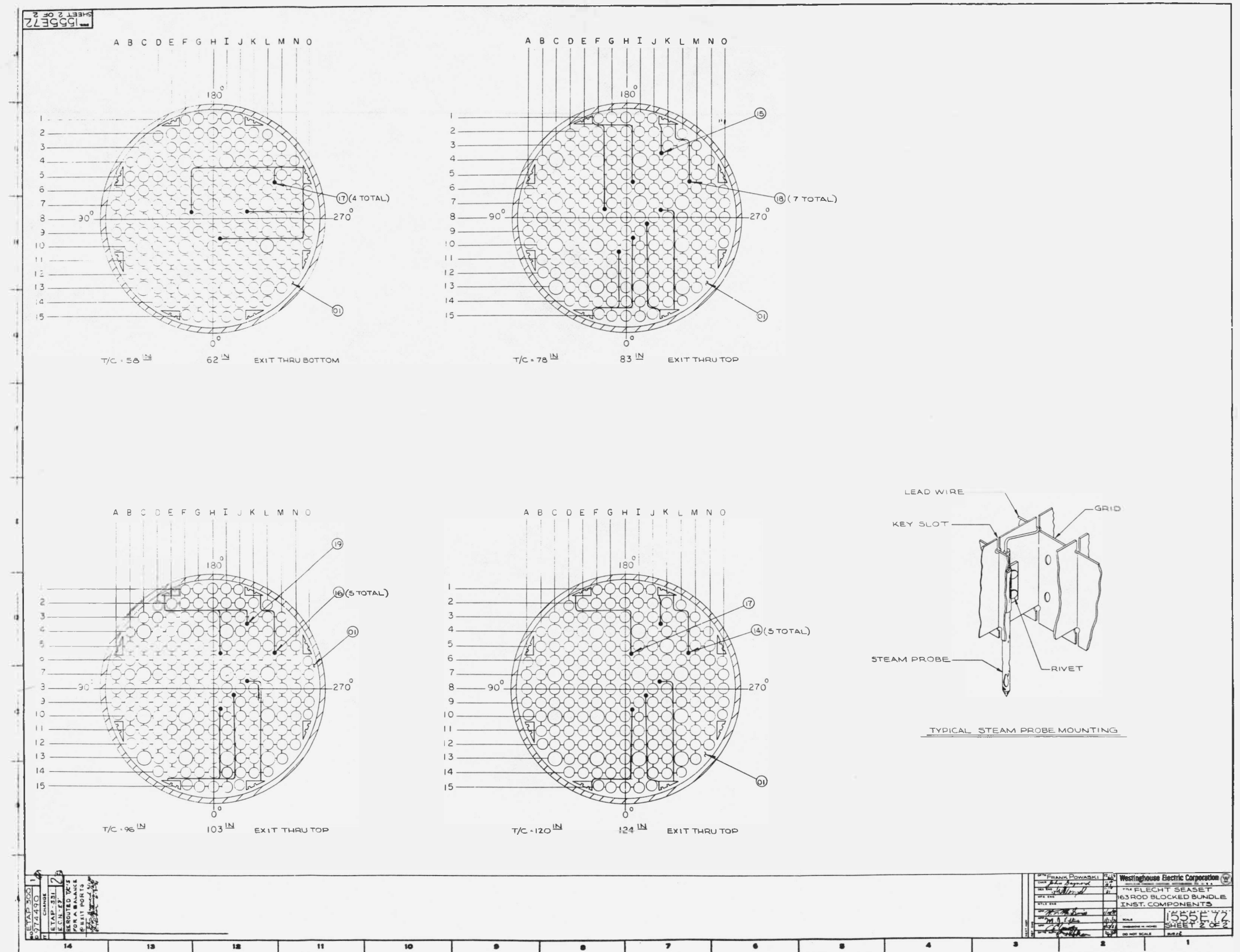


Figure C-16. FLECHT SEASET 161-Rod Blocked Bundle Downcomer and Crossover Leg Piping









APPENDIX D
INVESTIGATION OF LOW ISOLATION RESISTANCE
IN HEATER ROD THERMOCOUPLES

During the initial Westinghouse inspection of the FLECHT SEASET 163-rod blocked bundle heater rods, it was determined that approximately half the instrumented rods had thermocouples with lead-to-sheath isolation resistances less than the minimum specified 1 megohm. Since this condition had not been found in earlier 21-rod bundle heater rods, there was concern over how it would affect thermocouple failure rate in the blocked bundle.

The low isolation resistance was believed to have been caused by improper application of sealant material to the ends of the thermocouple leads by the heater rod manufacturer, in conjunction with exposure of the heater rods to environments of higher than normal humidity during handling and storage. This situation allowed moisture to penetrate the end seal and migrate through the magnesium oxide insulation material, and resulted in the low lead-to-sheath resistance.

Attempts to dry out the thermocouple leads with a heat gun and reseal the thermocouple ends met with limited success. A number of thermocouples which exhibited satisfactory isolation resistance after dryout again showed low resistance (less than 1 megohm) when rechecked at a later date. This prompted an investigation into the thermocouple sealant materials. The results of the investigation showed that Sealstik, manufactured by Cole Parmer, outperformed Duco cement, Micro Measurements M-Coat D and A, and Hardman Epoweld 8173 fast-drying epoxy. M-Coat D had been utilized by Westinghouse. Conversations with both the heater rod manufacturer and the thermocouple manufacturer (Claud S. Gordon Company) confirmed Westinghouse experience that, after a period of time, all sealants will admit some moisture. Seal welding of the cold end is the only way to prevent moisture migration into the thermocouple.

The Claud S. Gordon Company's specification for isolation resistance, at time of manufacturing, is 5 megohm at 50 vdc. The Westinghouse specification for thermocouple isolation resistance (1 megohm) was based on past experience, and

was readily obtainable by the heater rod manufacturer after assembly of the rod. Both the heater rod manufacturer and the thermocouple manufacturer were consulted on low isolation resistance in thermocouples due to the presence of moisture. Although no minimum thermocouple isolation resistance was specified, the consensus was that thermocouple life would not be decreased by the presence of moisture in the MgO insulation and in their opinions, the thermocouples would dry out as they were heated during testing.

Based on the above findings, no further prebundle assembly dryout work was performed on the heater rod thermocouples. However, after bundle installation in the test section, thermocouple isolation resistance was measured prior to installing connector plugs. If resistance was low, the thermocouple was cut back until isolation resistance improved to at least 0.2 megohm. All pretest heater rod thermocouple isolation resistance measurements were recorded. A 10-percent posttest sampling was selected and final thermocouple isolation resistances were recorded. (Only 10 percent of the thermocouples were chosen, since the thermocouple failure rate was only approximately 3 percent.) Table D-1 shows the comparison between pretest and posttest thermocouple isolation resistances of the sampled heater rods. A review of the data shows that, in general, the isolation resistance of the thermocouples increased over the course of the test program, a fact which confirmed the assumption that bundle-generated heat does tend to drive moisture from the thermocouples. An average increase of approximately 1 megohm was seen between pretest and posttest readings; however, there were notable exceptions to this trend (see data for rod 3J).

Of the thermocouples examined (table D-1), two were considered to have failed during the course of the test program [rod 6D, 2.03 m (80 in.) and 2.44 m (96 in.) elevation thermocouples]. A thermocouple was considered to have failed when it did not respond to changes in temperature or when it exhibited exceptionally noisy, erratic, or atypical behavior. When a thermocouple was considered failed, its input to the computer data acquisition system was shorted so that data were not misinterpreted and erroneous safety trips did not occur.

Neither of these failures can be attributed to low isolation resistance, since both thermocouples had initial readings greater than 1 megohm and exhibited an

increased isolation resistance after testing. Furthermore, of the 13 heater rod thermocouples that failed during testing (3 percent of the total), the average pretest isolation resistance was 5.7 megohms. (The lowest reading was 0.75 megohm.) This would indicate that the failure was probably due to high temperature cyclic fatigue, as expected, and not to low initial isolation resistance caused by moisture in the thermocouples.

In conclusion, based on pre- and posttest thermocouple isolation resistance measurements and the low number of thermocouple failures experienced during the blocked bundle test program, it is judged that thermocouple isolation resistances as low as 0.2 megohm can be tolerated without significantly increasing the heater rod thermocouple failure rate.

TABLE D-1
SAMPLE PRETEST AND POSTTEST THERMOCOUPLE ISOLATION RESISTANCE COMPARISON

Thermocouple Elevation [m (in.)]	Isolation Resistance at Indicated Rod Location (mΩ)											
	9C		3J		10I		6D		9G		12F	
	Pretest	Posttest	Pretest	Posttest	Pretest	Posttest	Pretest	Posttest	Pretest	Posttest	Pretest	Posttest
0.30 (12)					0.55	0.17			1.70	0.50	2.20	0.80
0.60 (24)			>20	0.78								
0.91 (39)	0.28	0.61							1.26	0.74	1.10	0.55
1.22 (48)			>20	0.85								
1.52 (60)									1.30	0.34	1.30	0.60
1.70 (67)			0.29	0.17			0.71	9.50	0.74	0.52		
1.83 (72)			0.36	0.20	1.14	0.20						
1.88 (74)	0.50	3.60	0.47	1.13								
1.90 (75)					1.17	0.39						
1.93 (76)	0.39	1.80					1.28	9.10				
1.96 (77)			2.50	2.00								
1.99 (78)	0.31	0.96					0.78	1.80	5.50	0.68	2.10	1.02
2.03 (80)			1.85	1.80	1.37	2.60	1.77	>20				
2.13 (84)	0.80	1.90										
2.18 (86)					0.83	1.70	0.77	0.92				
2.29 (90)	1.43	1.60					1.59	1.44	2.80	1.65		
2.44 (96)					0.72	2.60	1.30	1.98				
2.59 (102)											1.18	1.88
2.82 (111)	0.76	1.40	4.12	>20					2.10	1.38		
3.05 (120)					7.30	>20	1.48	1.28			2.60	0.94
3.35 (132)									2.00	1.24		
3.51 (138)											1.80	2.12

APPENDIX E

BUNDLE STEAM PROBE RESPONSE

E-1. INTRODUCTION

The following three types of instruments were utilized in the 163-rod blocked bundle to measure the nonequilibrium vapor temperatures:

- o 17 thimble tube aspirating steam probes
- o 10 subchannel self-aspirating steam probes
- o 14 subchannel unshielded thermocouples

The thermal response of each of the instruments is addressed in paragraphs E-2 and E-3. The data from the following three tests with various peak power to flow ratios is shown:

Test Run	Conditions	Peak Power/Flow
61314	39.1 mm/sec (1.54 in./sec) at 1.3 kw/m (0.4 kw/ft)	0.266
61005	38.9 mm/sec (1.53 in./sec) at 2.30 kw/m (0.7 kw/ft)	0.467
61607	20.6 mm/sec (0.81 in./sec) at 2.30 kw/m (0.7 kw/ft)	0.875 (maximum)

E-2. THIMBLE TUBE ASPIRATING STEAM PROBES

To maximize the quantity of thimble tube aspirating steam probes in the bundle, the probes aspirated through both the top and the bottom of the bundle as in the 161-rod unblocked bundle. The design of the probe which aspirated through the top of the bundle was used successfully in previous FLECHT SEASET tests.⁽¹⁾ The design of the probe which aspirated through the bottom of the bundle was different from that utilized unsuccessfully in the 161-rod unblocked bundle. It was believed that the tortuous flow path in the unblocked

1. Loftus, M. J., et al., "PWR FLECHT SEASET Unblocked Bundle, Forced and Gravity Reflood Task Data Report," NRC/EPRI/Westinghouse-7, June, 1980.

bundle bottom probe caused significant flow mixing between the high-temperature steam and the entrained water droplets. Thus, the design was modified in the blocked bundle, as shown by the schematic diagram in figure E-1.

Comparisons of the following top and bottom steam temperature measurements at the same elevations are shown in figures E-2 and E-3 for the test with the maximum power-to-flow ratio:

Figure	Elevation [m (in.)]	Top Steam Probe	Bottom Steam Probe
E-2	1.98 m (78 in.)	Channel 446, 7K	Channel 447, 4F
E-3	2.82 m (111 in.)	Channel 452, 7I	Channel 453, 10F

These two figures clearly show the difference between the bottom and top steam probes. The bottom steam probe measures approximately the same vapor temperature as the top probe during the early single-phase flow period prior to and immediately after flood. However, modification of the design of the bottom steam probe did not improve the response of the probe during the two-phase flow period relative to that measured in the unblocked bundle. The vapor and the entrained droplets are apparently mixed within the probe; this subsequently desuperheats the steam.

The amount of vapor aspirated through the bottom steam probes was reduced in run 61106 to decrease the amount of entrained droplets; however, this change resulted in minimal effect on the probe thermal response. All the probes exiting the bottom of the bundle responded in the same manner for the entire test series.

It is recommended that the probes exiting the bottom of the bundle not be utilized as measurements of vapor temperature. The steam probes which aspirated through the bottom and top of the bundle were as follows:

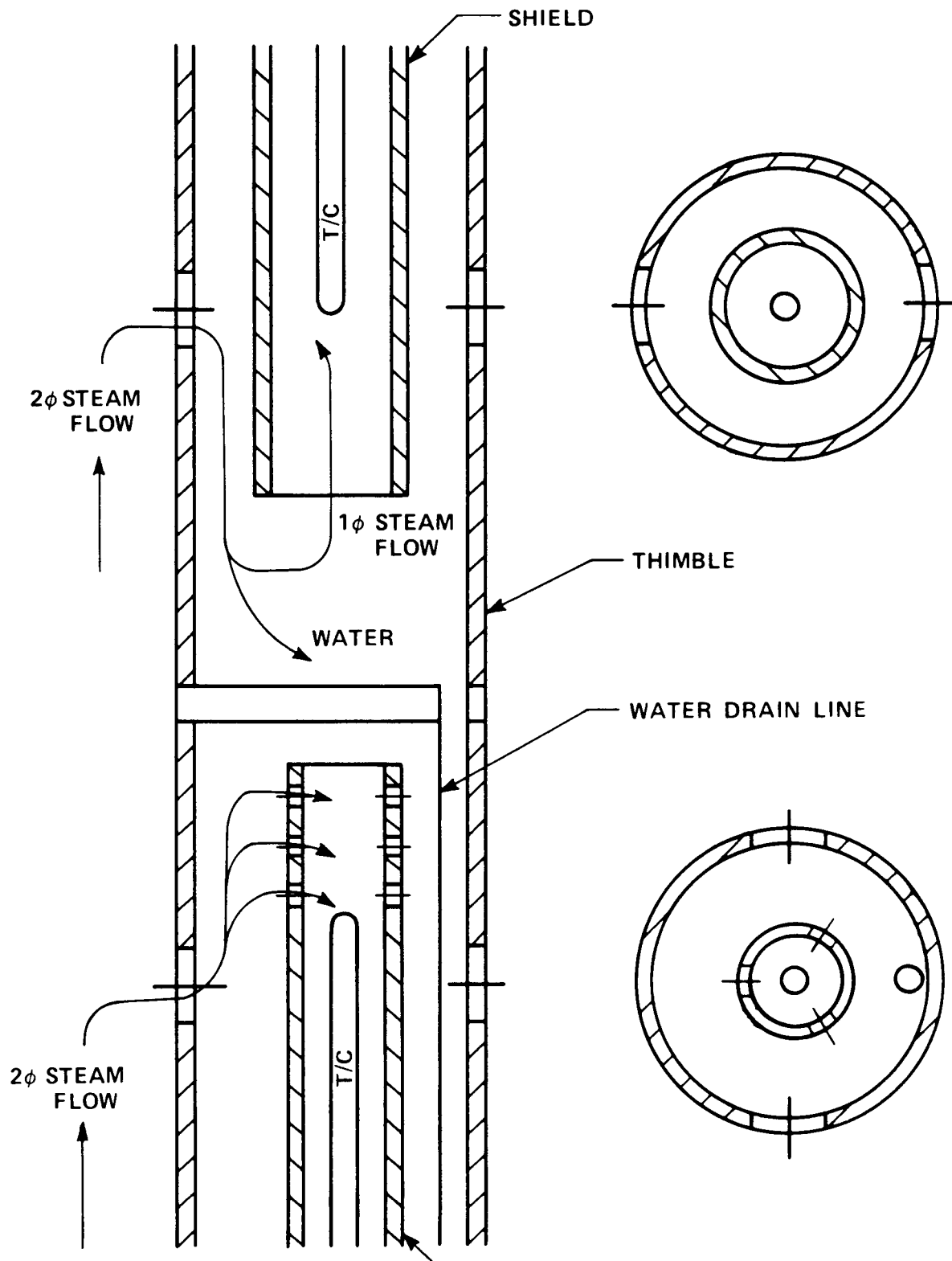


Figure E-1. Steam Probe Design

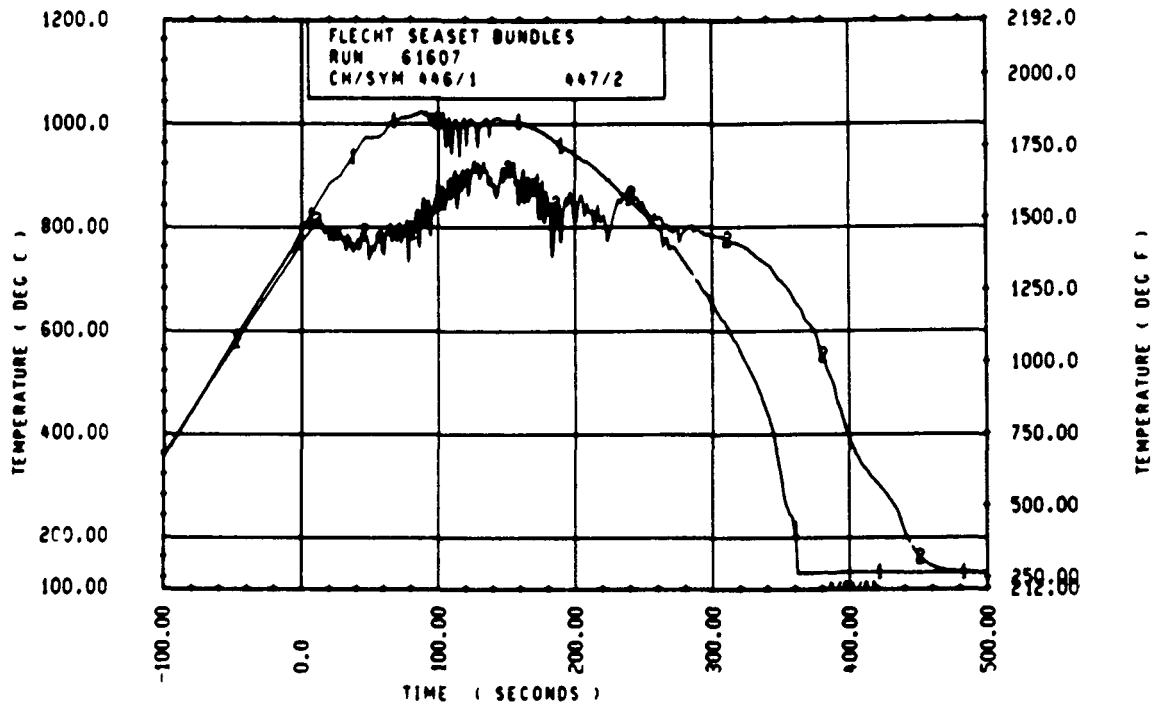


Figure E-2. Comparison of Top and Bottom Steam Probe Measurements, Run 61607, 1.98 m (78 in.) Elevation

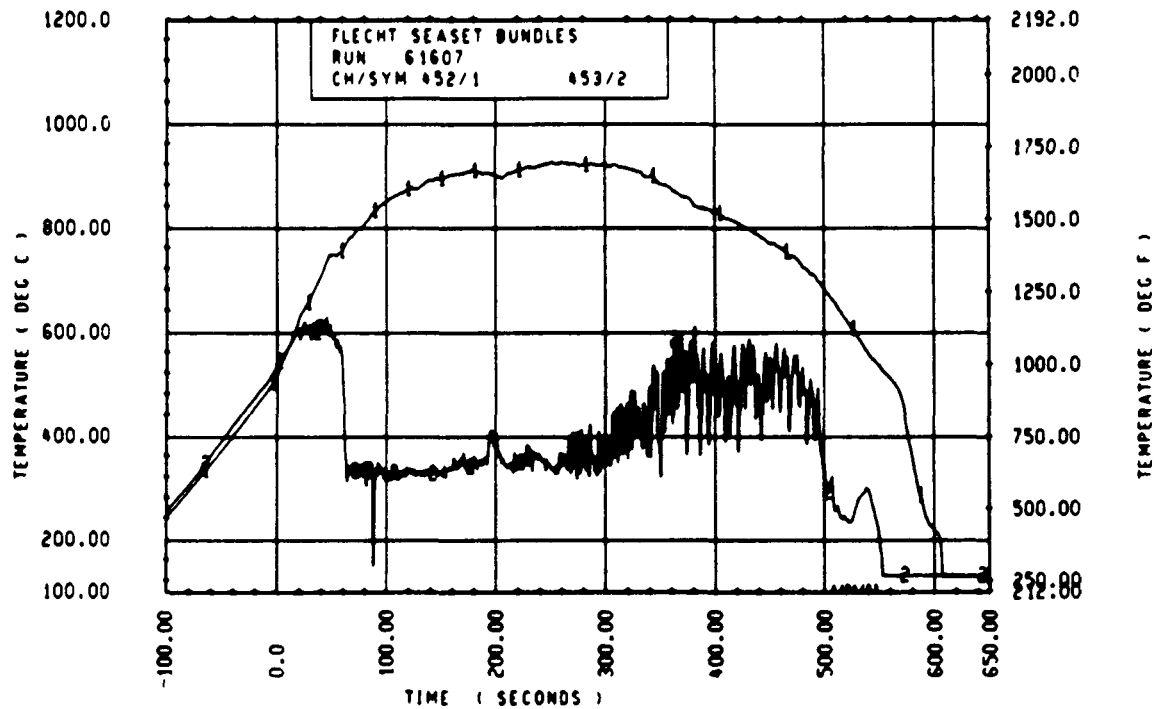


Figure E-3. Comparison of Top and Bottom Steam Probe Measurements, Run 61607, 2.82 m (111 in.) Elevation

Elevation [m (in.)]	Top Steam Probe	Bottom Steam Probe
0.99 (39)	--	Channel 441, 10C
1.22 (48)	--	Channel 442, 13F
1.52 (60)	Channel 443, 4I	--
1.83 (72)	--	Channel 444, 7I Channel 445, 10L
1.98 (78)	Channel 446, 7L	Channel 447, 4F
2.29 (90)	--	Channel 448, 7C Channel 449, 13I
2.44 (96)	Channel 450, 4F Channel 451, 10L	--
2.82 (111)	Channel 452, 7I	Channel 453, 10F
3.05 (120)	Channel 454, 7C Channel 455, 13I	--
3.35 (132)	Channel 456, 10F	--
3.51 (139)	Channel 457, 5K	--

E-3. SUBCHANNEL SELF-ASPIRATING STEAM PROBES AND UNSHIELDED THERMOCOUPLES

The subchannel steam probes and thermocouples were utilized in the blocked bundle primarily to measure the radial vapor temperature distribution at elevations immediately upstream [1.47 m (58 in.)] and downstream [1.98, 2.44, and 3.05 m (78, 96, and 120 in.)] of the blockage. Comparisons of the following subchannel and thimble tube temperature measurements are shown in figures E-4 through E-21 for all three of the previously tabulated tests:

Figure	Elevation [m (in.)]	Subchannel Instrument	Thimble Tube Probes
E-4,5,6	1.52 (60)	Channels 458, 459	Channel 443, 4I
E-7,8,9	1.98 (78)	Channels 462, 464	Channel 446, 7L

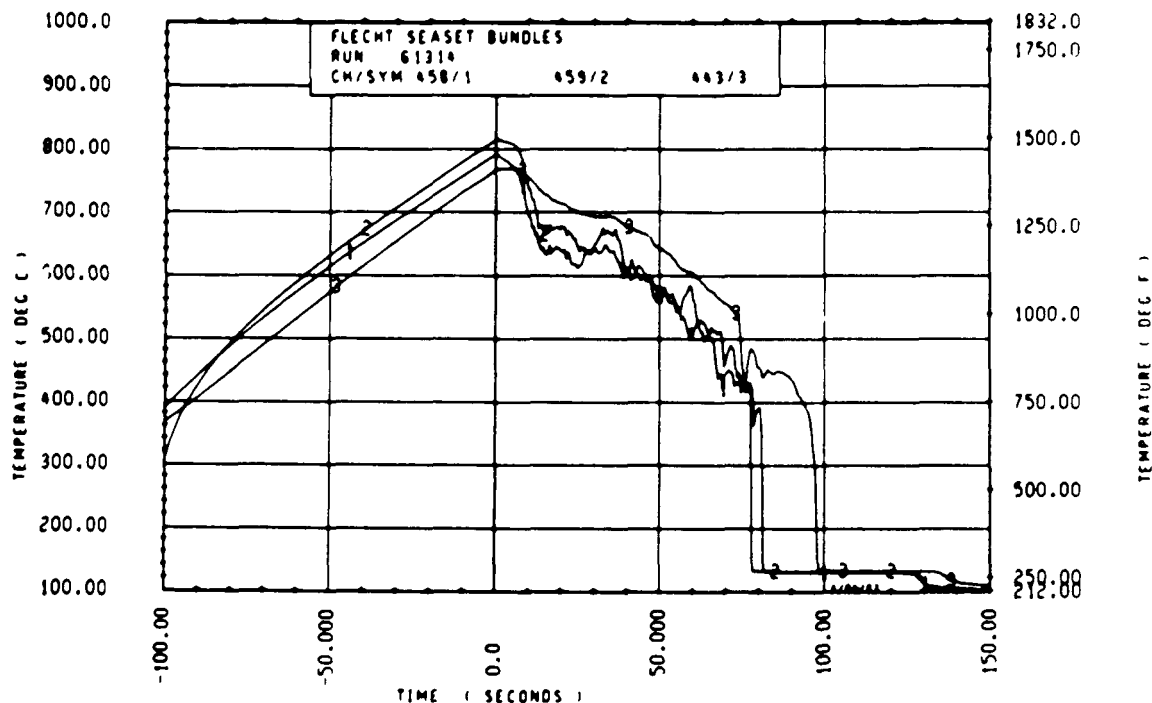


Figure E-4. Comparison of Radial Vapor Temperature Distribution Measurements, Run 61314, 1.52 m (60 in.) Elevation

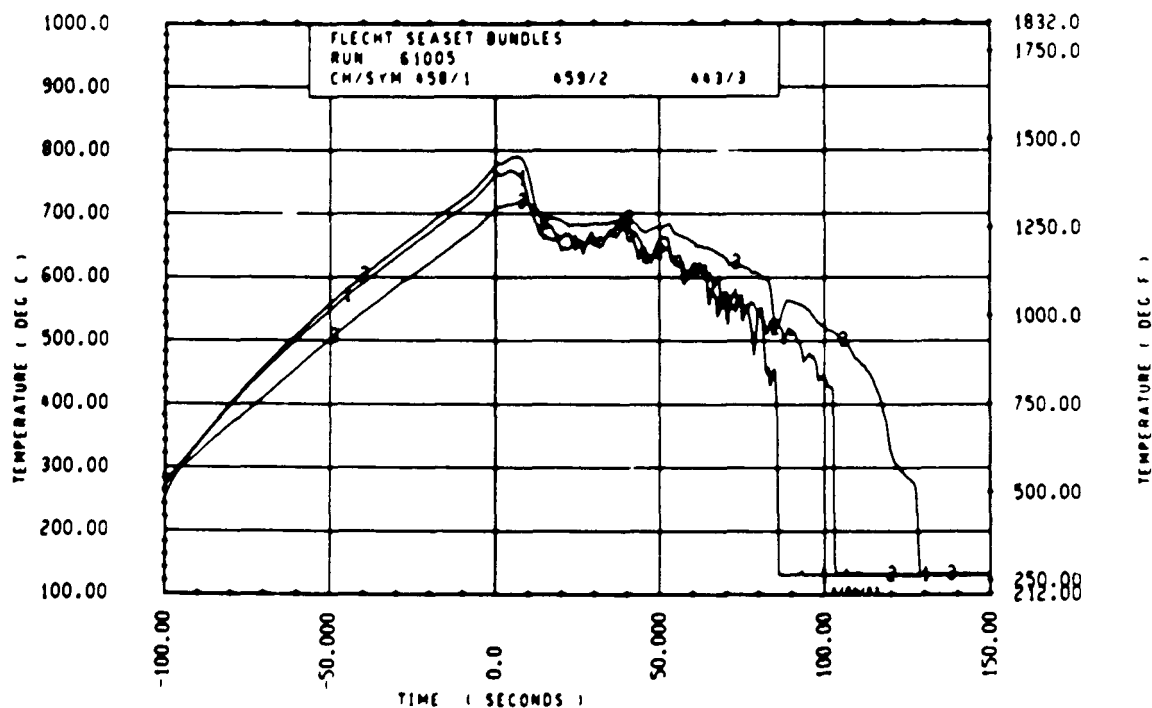


Figure E-5. Comparison of Radial Vapor Temperature Distribution Measurements, Run 61005, 1.52 m (60 in.) Elevation

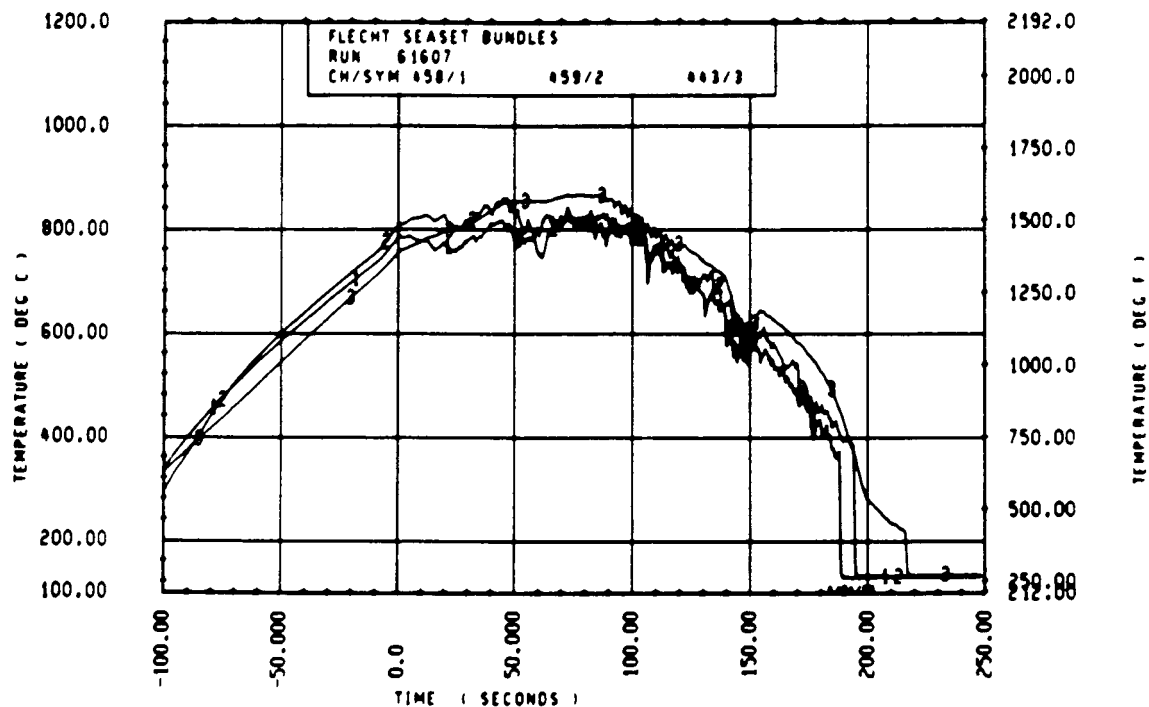


Figure E-6. Comparison of Radial Vapor Temperature Distribution Measurements, Run 61607, 1.52 m (60 in.) Elevation

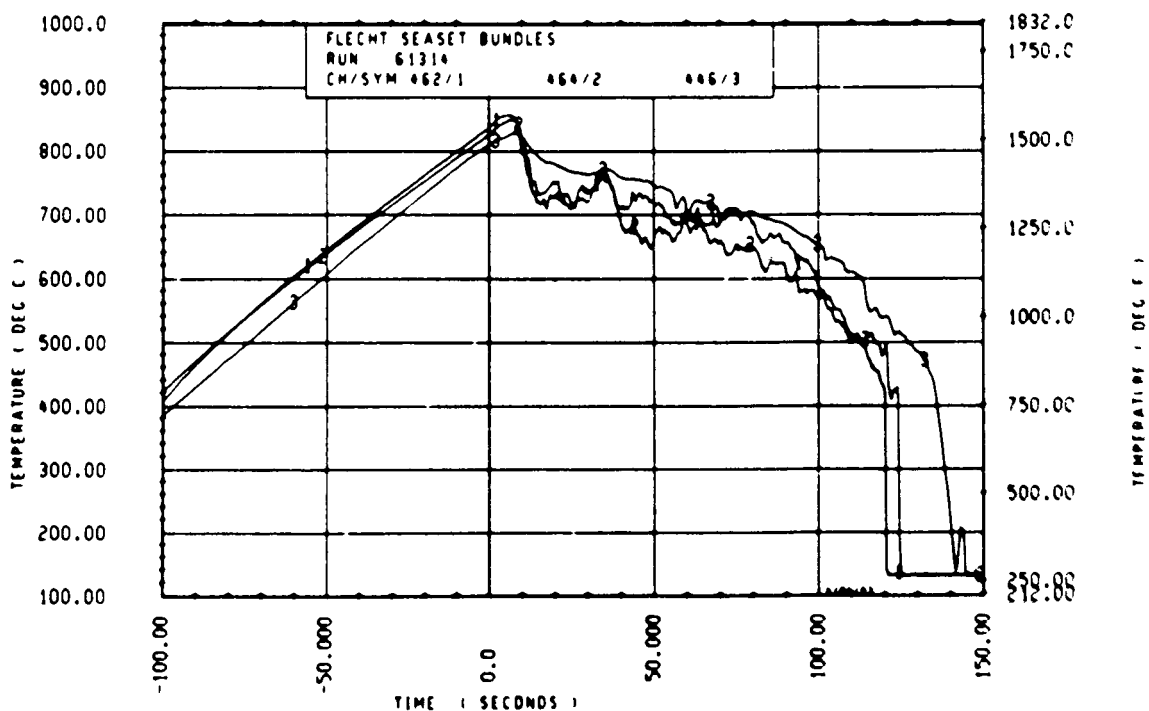


Figure E-7. Comparison of Radial Vapor Temperature Distribution Measurements, Run 61314, 1.98 m (78 in.) Elevation

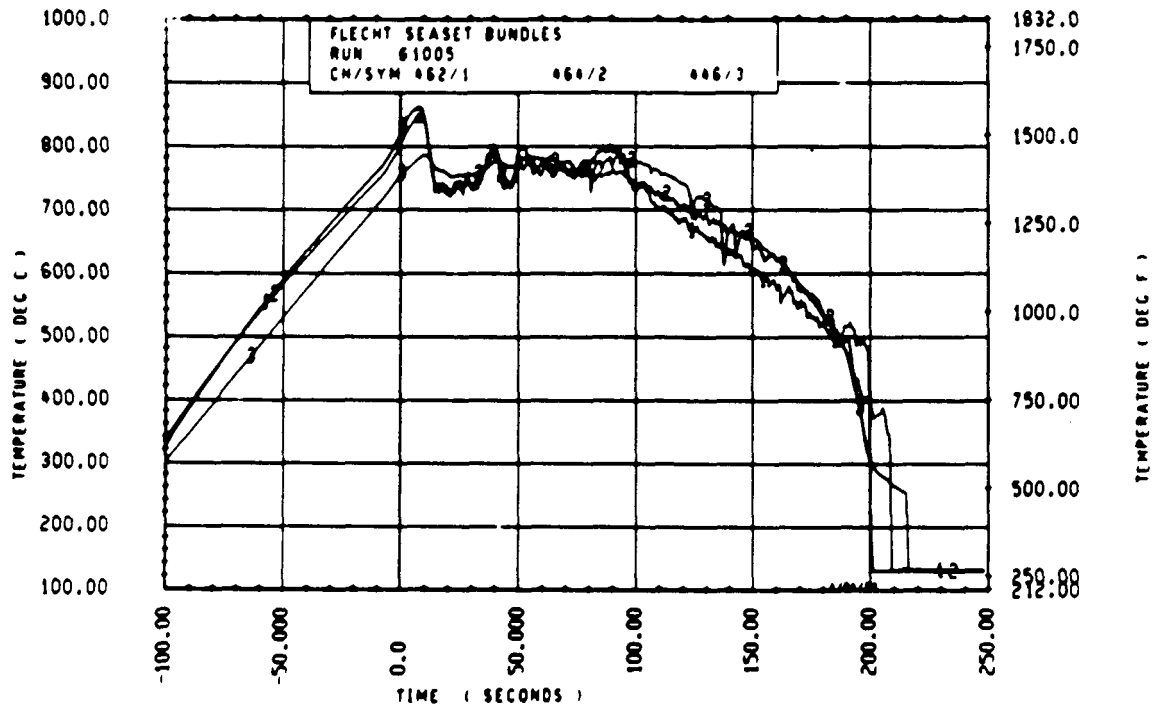


Figure E-8. Comparison of Radial Vapor Temperature Distribution Measurements, Run 61005, 1.98 m (78 in.) Elevation

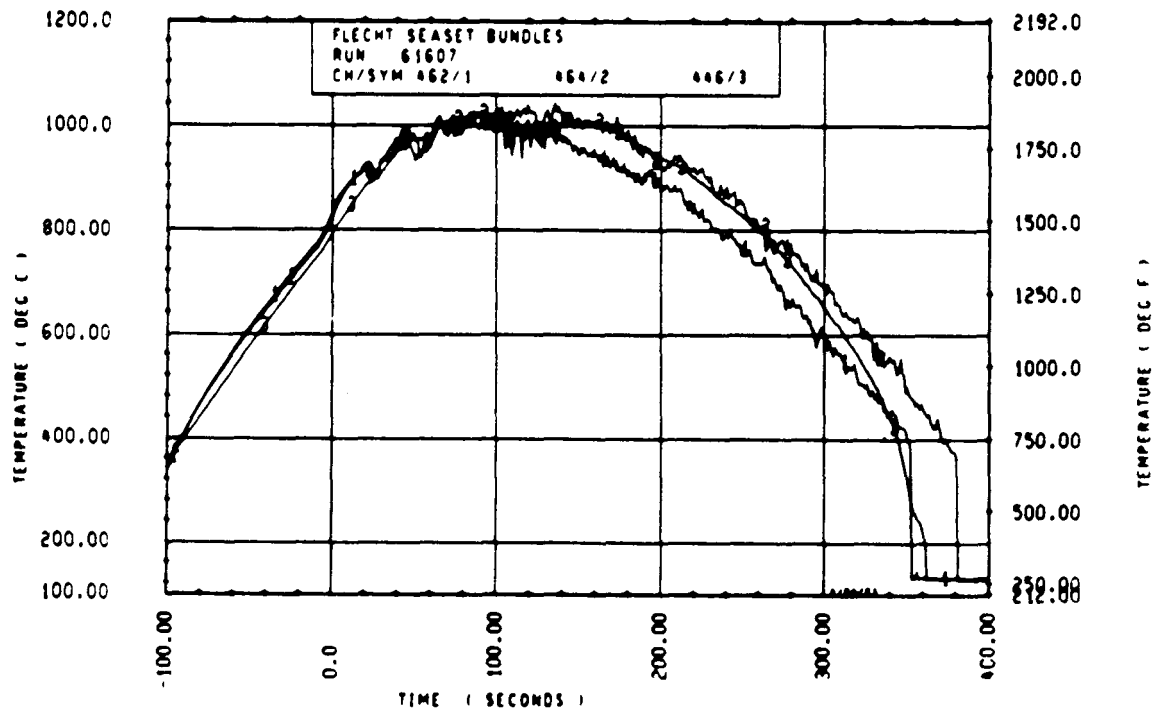


Figure E-9. Comparison of Radial Vapor Temperature Distribution Measurements, Run 61607, 1.98 m (78 in.) Elevation

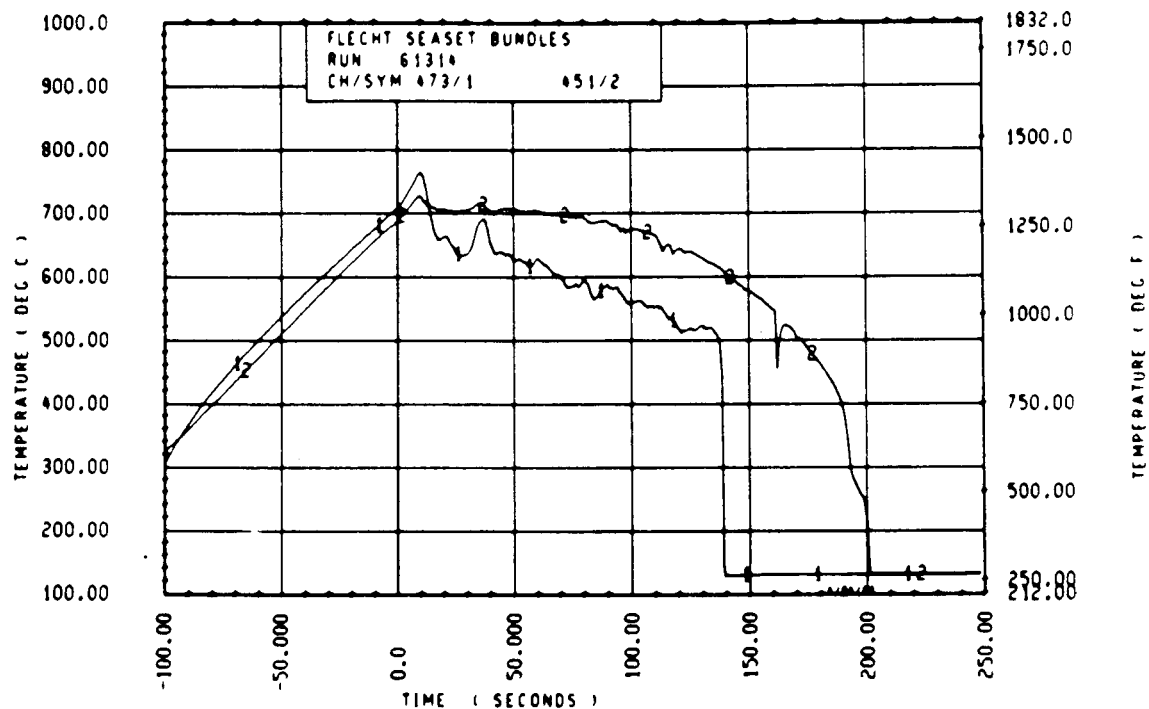


Figure E-10. Comparison of Radial Vapor Temperature Distribution Measurements, Run 61314, 2.44 m (96 in.) Elevation, Rod 10L

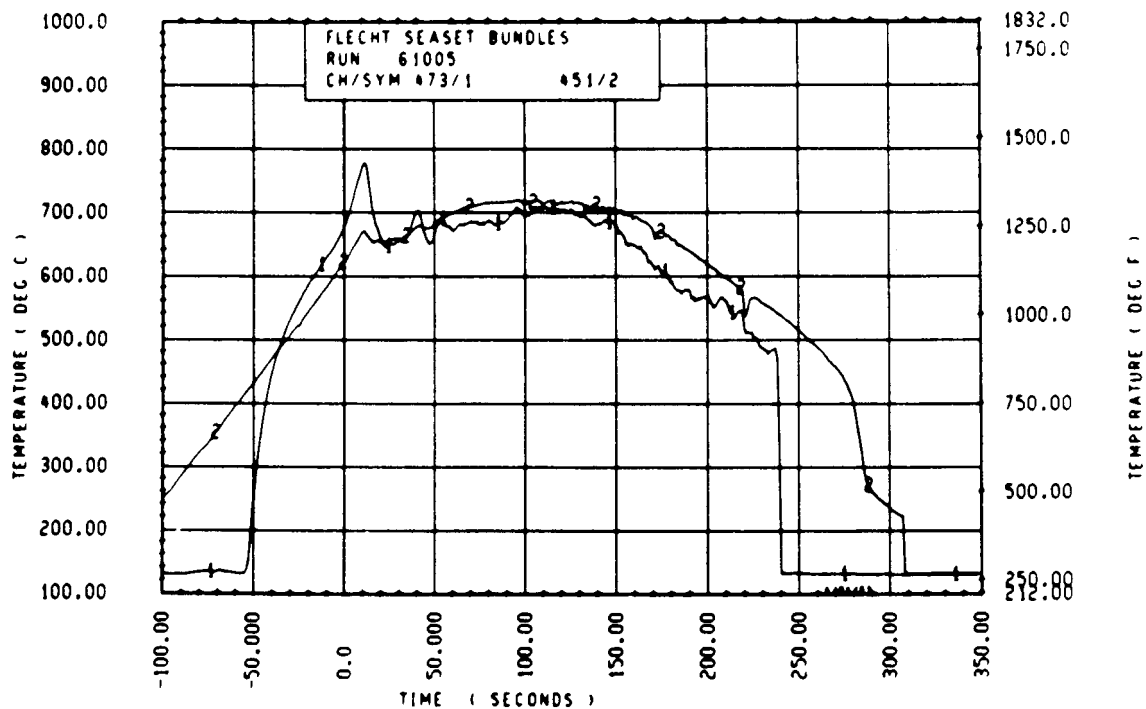


Figure E-11. Comparison of Radial Vapor Temperature Distribution Measurements, Run 61005, 2.44 m (96 in.) Elevation, Rod 10L

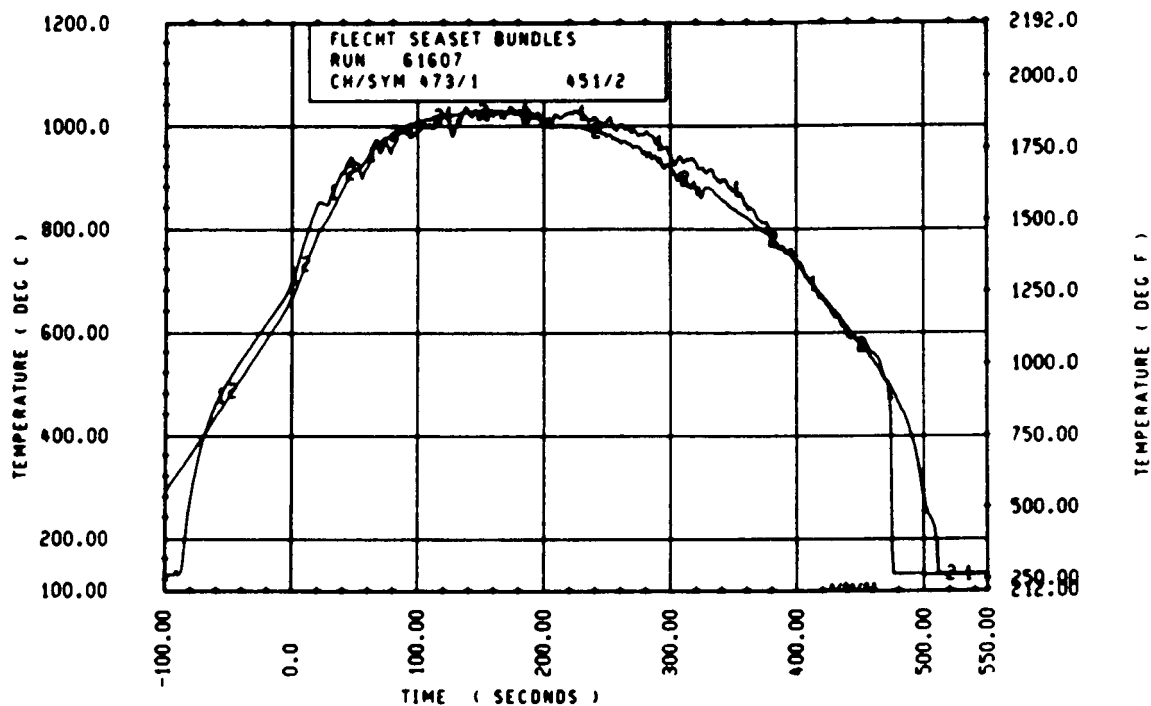


Figure E-12. Comparison of Radial Vapor Temperature Distribution Measurements, Run 61607, 2.44 m (96 in.) Elevation, Rod 10L

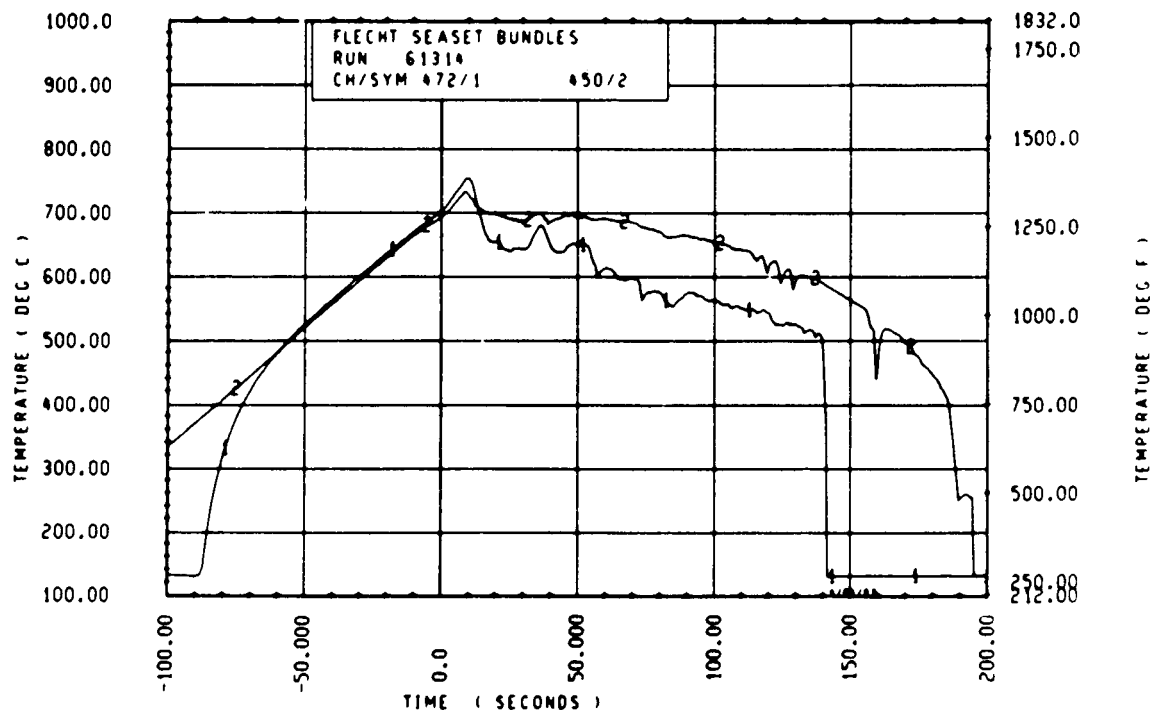


Figure E-13. Comparison of Radial Vapor Temperature Distribution Measurements, Run 61314, 2.44 m (96 in.) Elevation, Rod 4F

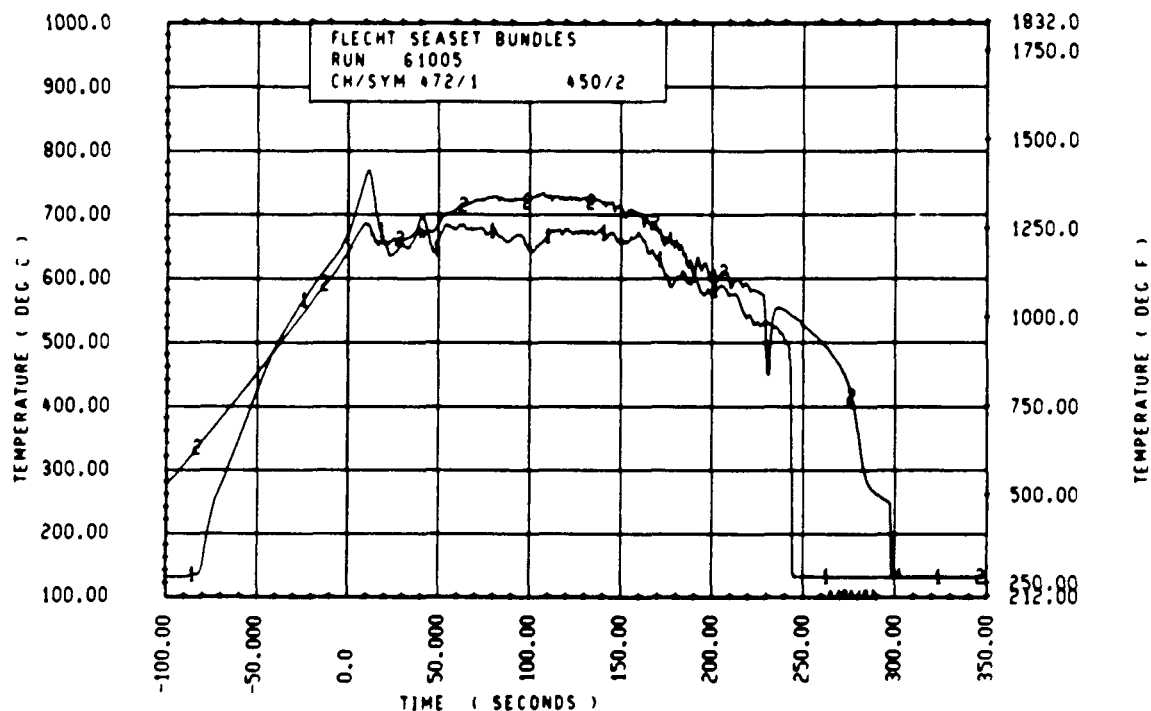


Figure E-14. Comparison of Radial Vapor Temperature Distribution Measurements, Run 61005, 2.44 m (96 in.) Elevation, Rod 4F

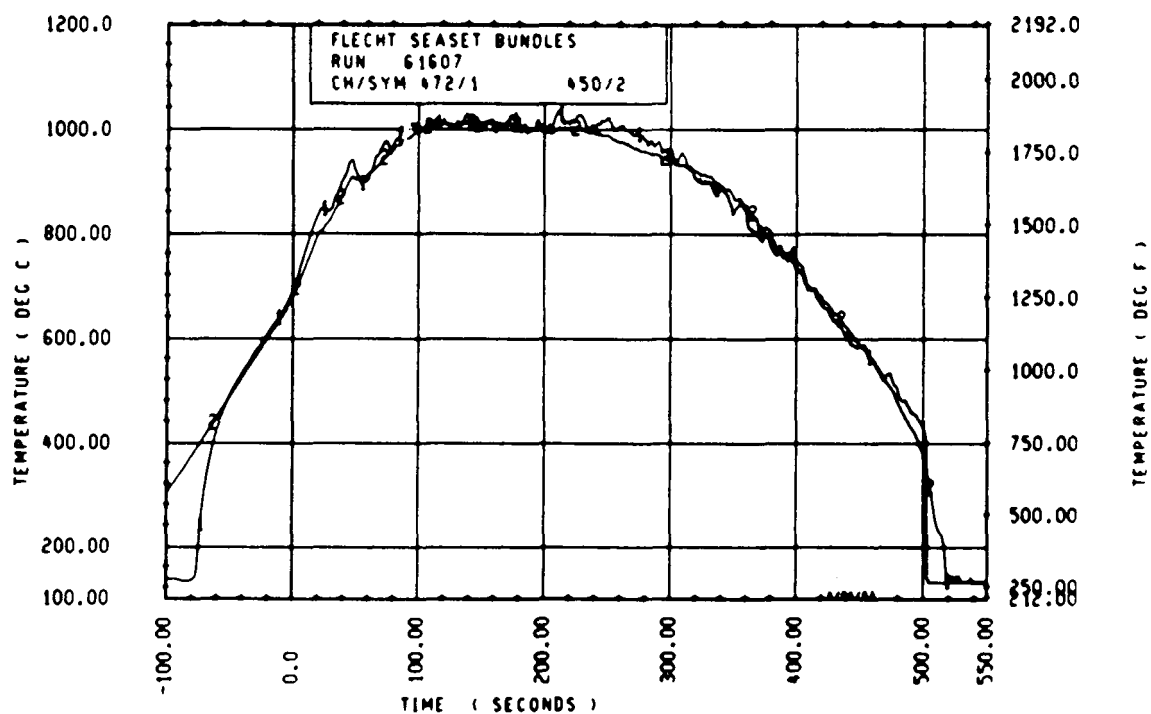


Figure E-15. Comparison of Radial Vapor Temperature Distribution Measurements, Run 61607, 2.44 m (96 in.) Elevation, Rod 4F

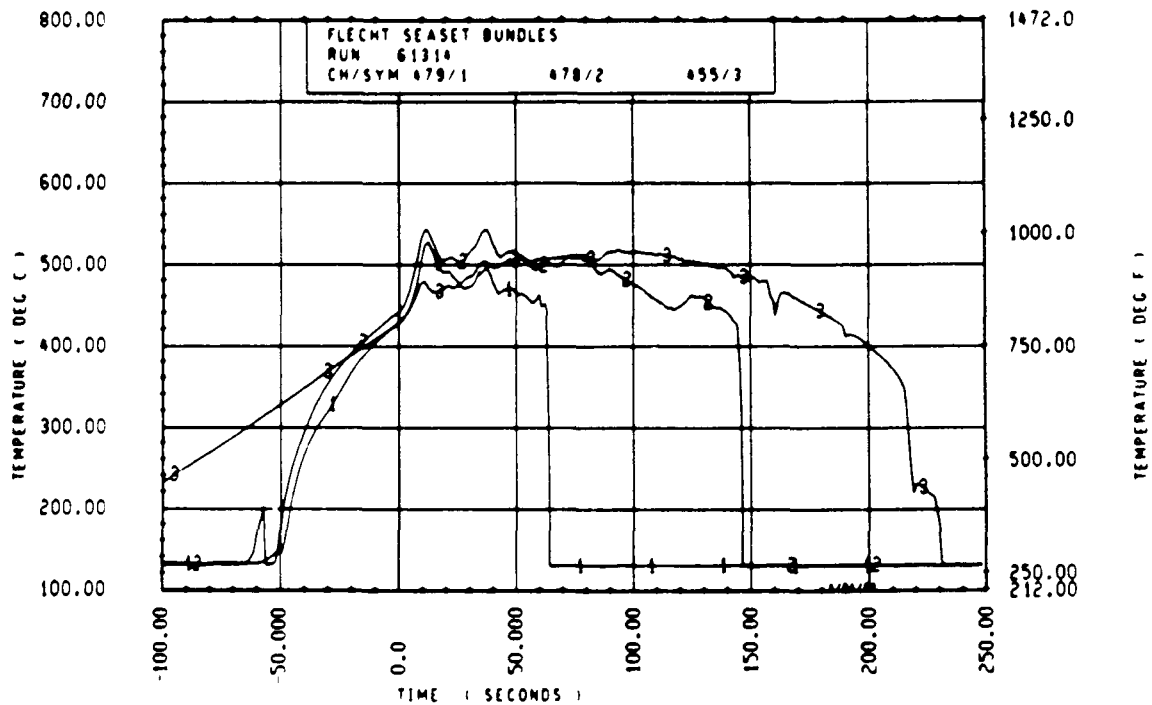


Figure E-16. Comparison of Radial Vapor Temperature Distribution Measurements, Run 61314, 3.05 m (120 in.) Elevation, Rod 13I

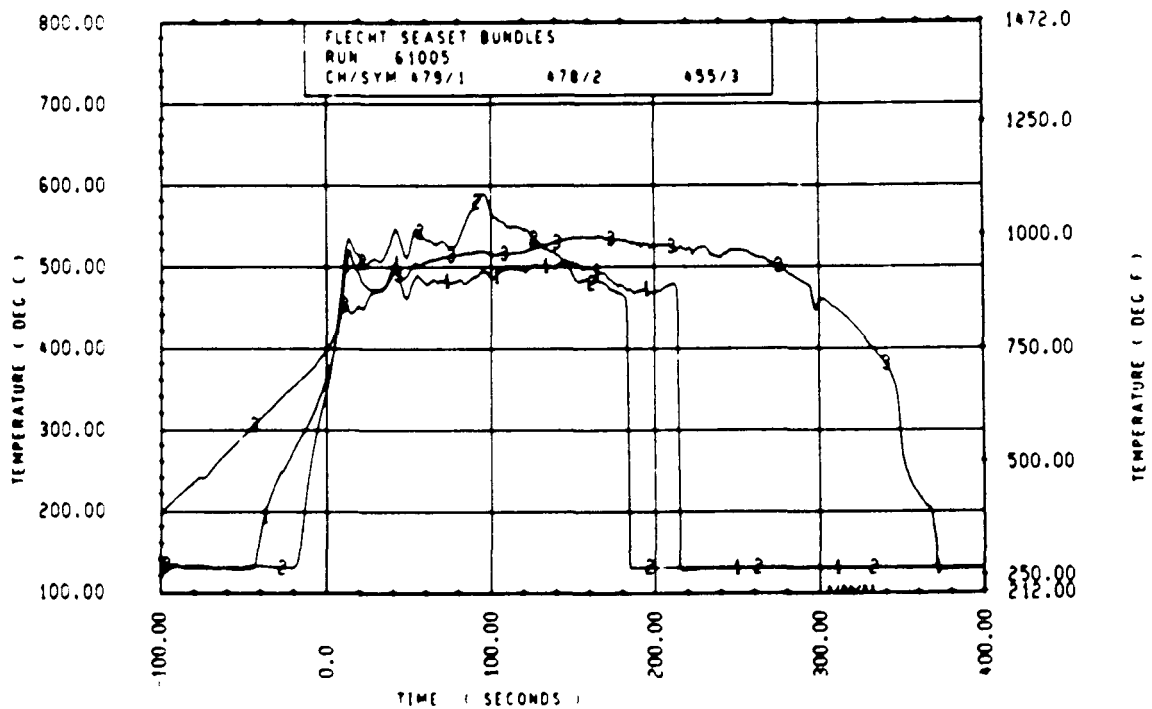


Figure E-17. Comparison of Radial Vapor Temperature Distribution Measurements, Run 61005, 3.05 m (120 in.) Elevation, Rod 13I

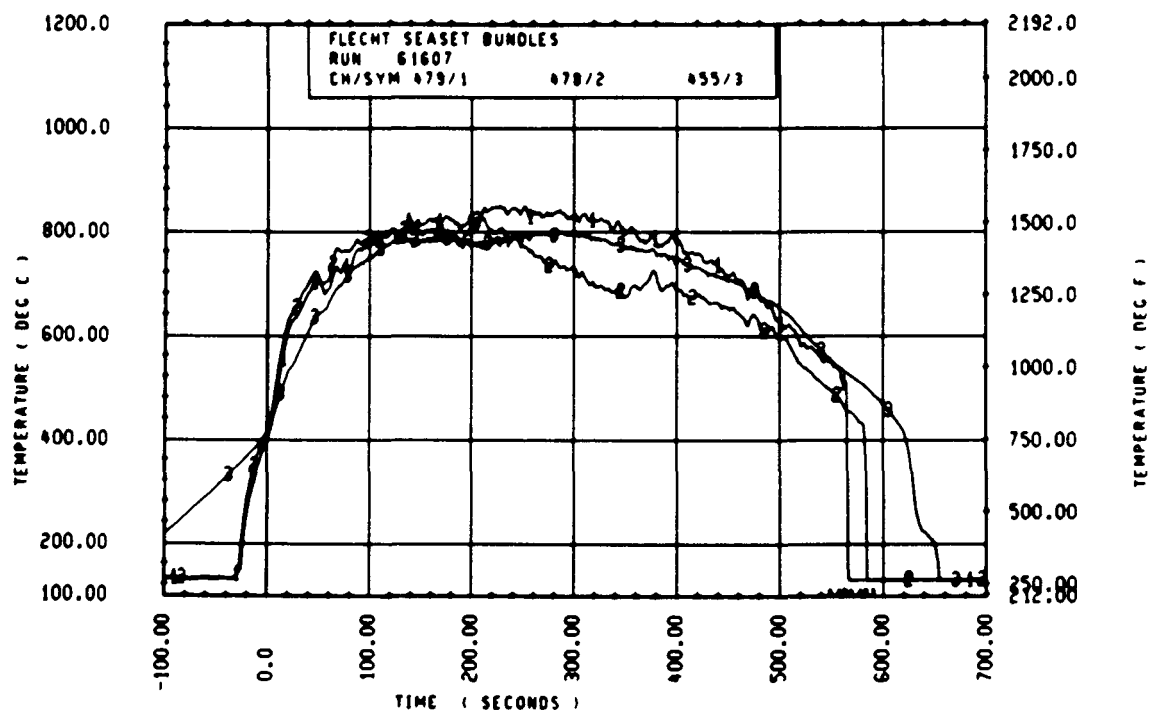


Figure E-18. Comparison of Radial Vapor Temperature Distribution Measurements, Run 61607, 3.05 m (120 in.) Elevation, Rod 13I

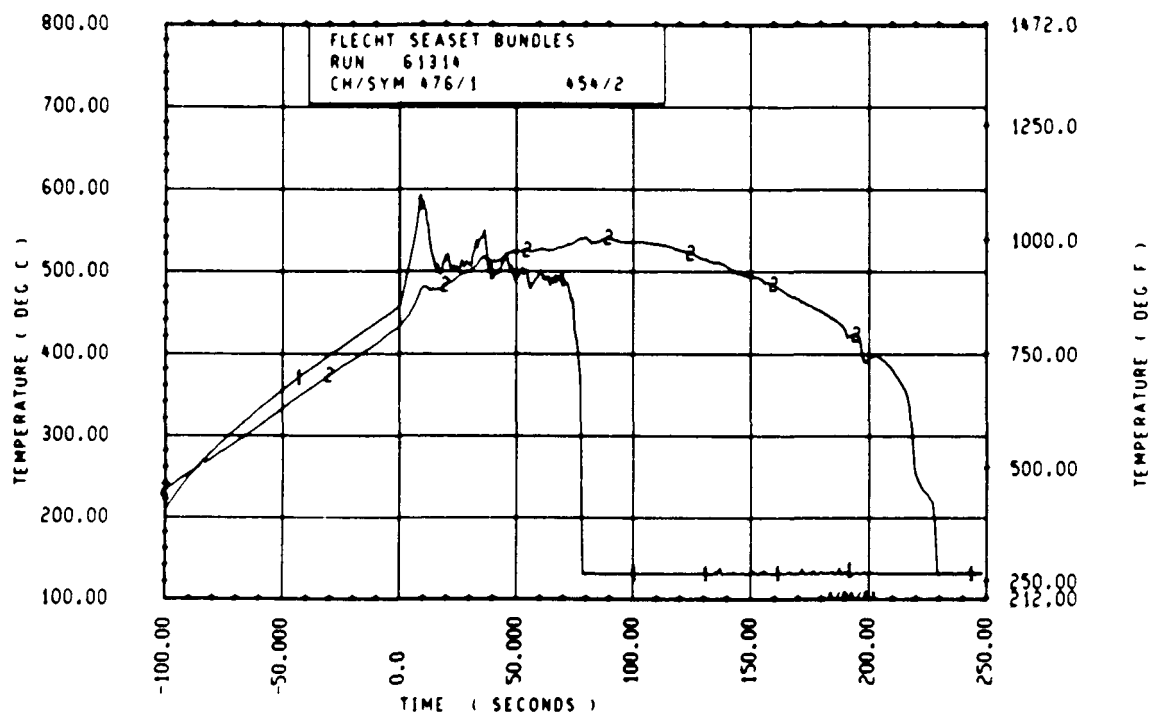


Figure E-19. Comparison of Radial Vapor Temperature Distribution Measurements, Run 61314, 3.05 m (120 in.) Elevation, Rod 7C

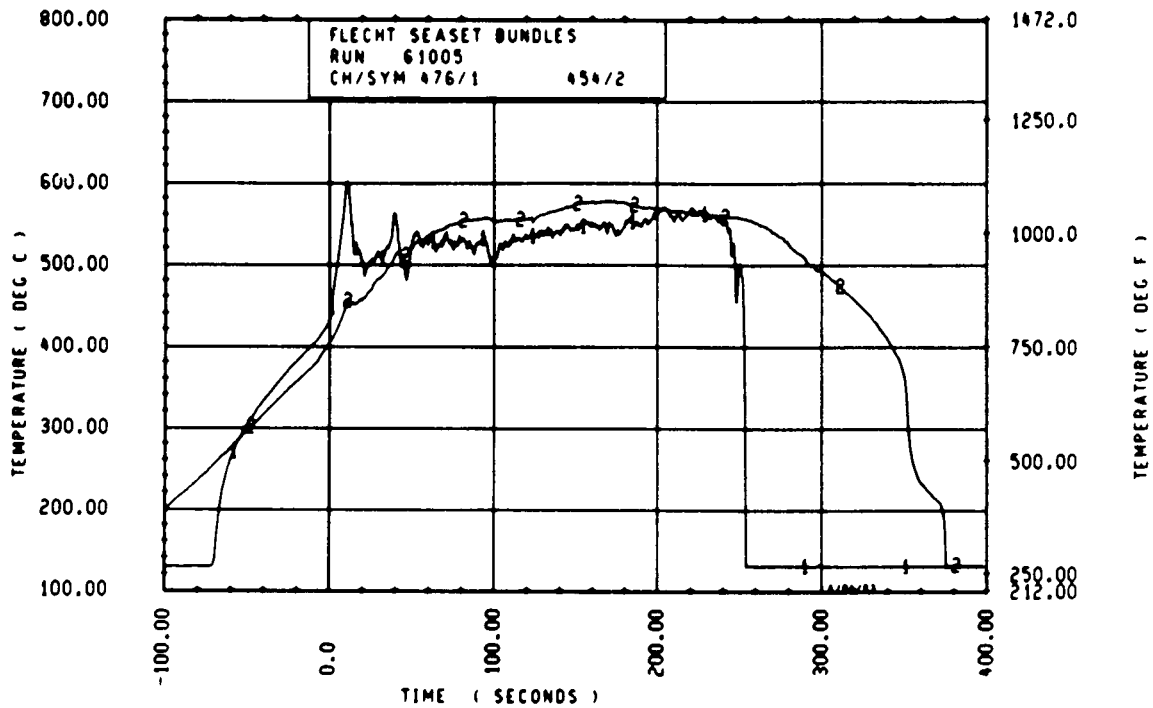


Figure E-20. Comparison of Radial Vapor Temperature Distribution Measurements, Run 61005, 3.05 m (120 in.) Elevation, Rod 7C

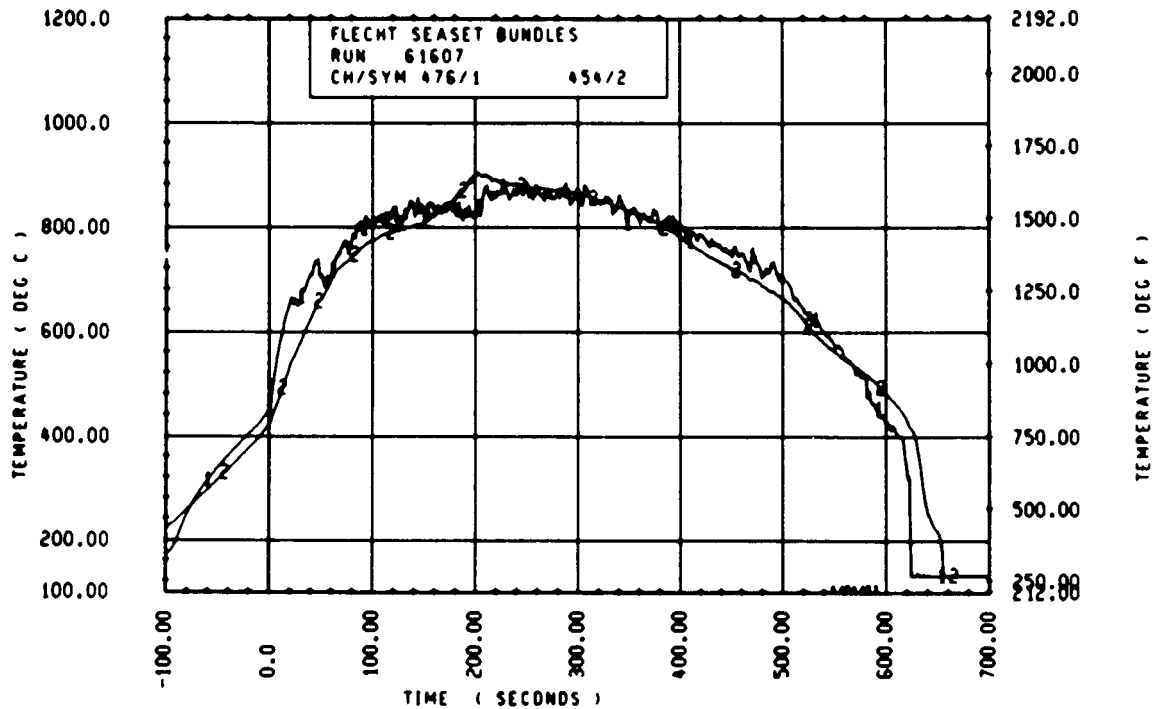


Figure E-21. Comparison of Radial Vapor Temperature Distribution Measurements, Run 61607, 3.05 m (120 in.) Elevation, Rod 7C

E-10,11,12	2.44 (96)	Channel 473 ^(a)	Channel 451, 10L
E-13,14,15	2.44 (96)	Channel 472 ^(a)	Channel 450, 4F
E-16,17,18	3.05 (120)	Channels 479, ^(a) 478 ^(a)	Channel 455, 13I
E-19,20,21	3.05 (120)	Channel 476	Channel 454, 7C

a. Self-aspirating steam probe

These figures generally show good comparisons between the thimble tube probes and subchannel instruments. During the bundle heatup period prior to flood, the subchannel instruments consistently measured a temperature greater than the thimble probe because of the radiation effects, which are shielded in the thimble probe, and the high thermal inertia of the thimble tubes. The heatup of the self-aspirating steam probes at the higher elevations was affected by water trapped within the probe, thereby keeping the temperature at saturation. Once this water was evaporated, the temperature quickly reached the level of the other probes. The low heatup power [1.3 kw/m (0.4 kw/ft)] allowed the probe to dry out and reach the correct flood initiation temperature. A better comparison between the subchannel instruments and the thimble probes was achieved in tests with higher power-to-flow ratios.

Comparisons between the subchannel vapor temperature instruments in symmetrical locations are shown in figures E-22 through E-25 for the following elevations for the highest power-to-flow ratio test:

Figure	Elevation [m (in.)]	Self-Aspirating Probe	Unshielded Thermocouple	Heater Rod Thermocouples
E-22 (sheet 1)	1.98 (78)	--	Channels 465, 467	--
E-22 (sheet 2)	1.98 (78)	--	Channels 463, 464	--
E-22 (sheet 3)	1.98 (78)	--	Channels 469, 462	--
E-23	2.44 (96)	Channels 472, 473	--	Channels 336, 346
E-24 (sheet 1)	2.44 (96)	Channel 471	Channel 470	--

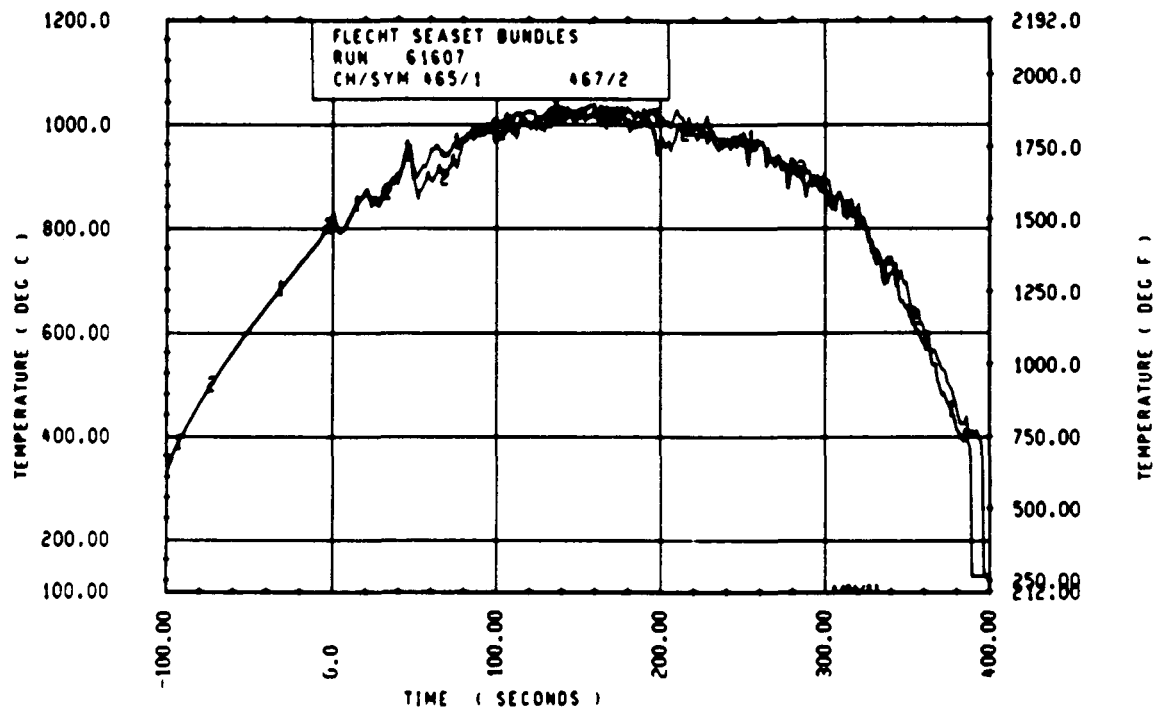


Figure E-22. Comparison of Subchannel Vapor Temperature Distribution Measurements, Run 61607, 1.98 m (78 in.) Elevation, Unshielded Thermocouples (sheet 1 of 3)

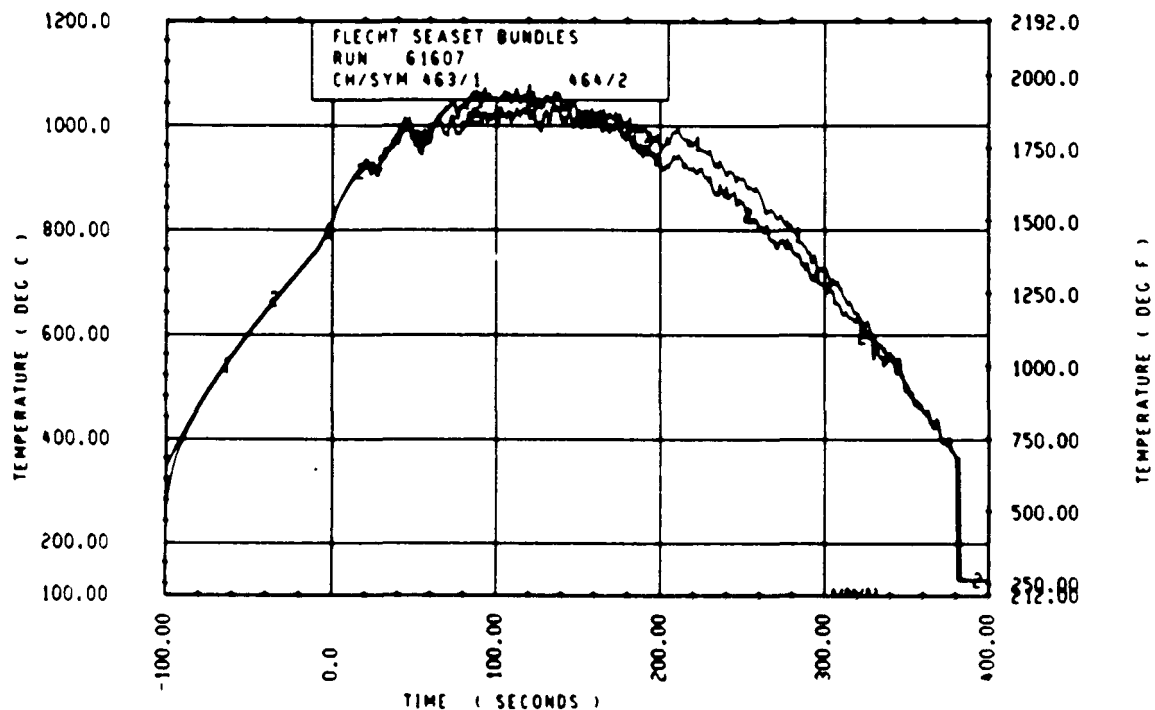


Figure E-22. Comparison of Subchannel Vapor Temperature Distribution Measurements, Run 61607, 1.98 m (78 in.) Elevation, Unshielded Thermocouples (sheet 2 of 3)

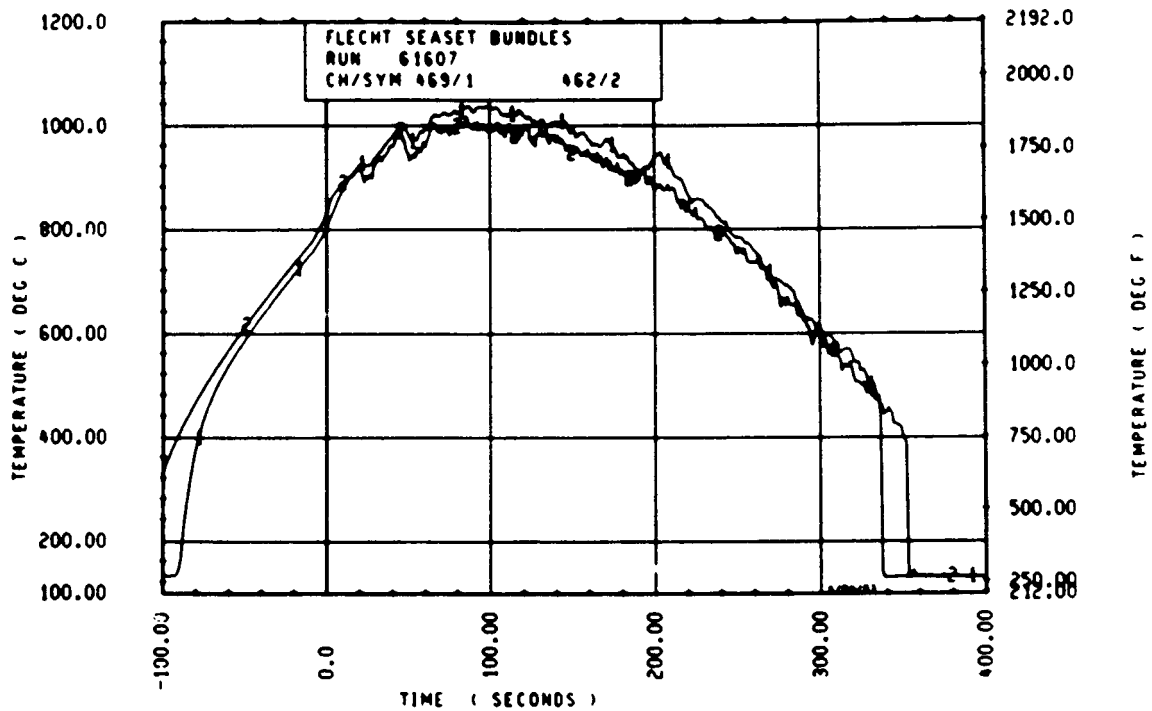


Figure E-22. Comparison of Subchannel Vapor Temperature Distribution Measurements, Run 61607, 1.98 m (78 in.) Elevation, Unshielded Thermocouples (sheet 3 of 3)

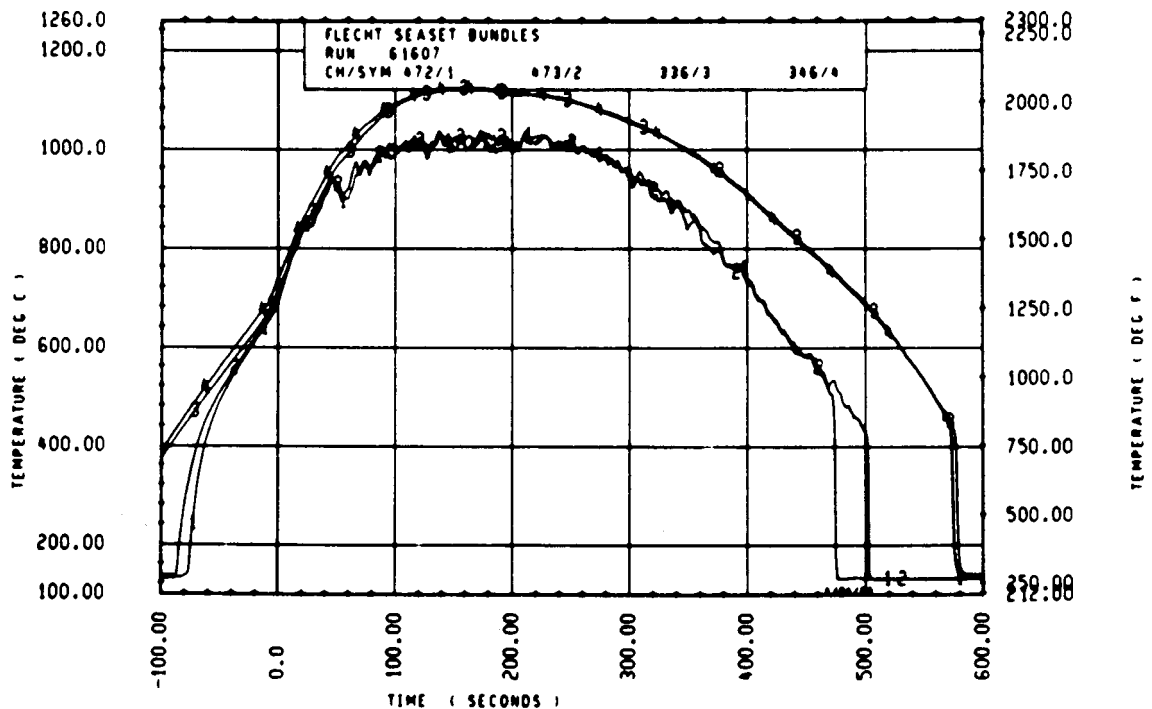


Figure E-23. Comparison of Subchannel Vapor Temperature Distribution Measurements, Run 61607, 2.44 m (96 in.) Elevation, Self-Aspirating Steam Probes and Heater Rod Thermocouples

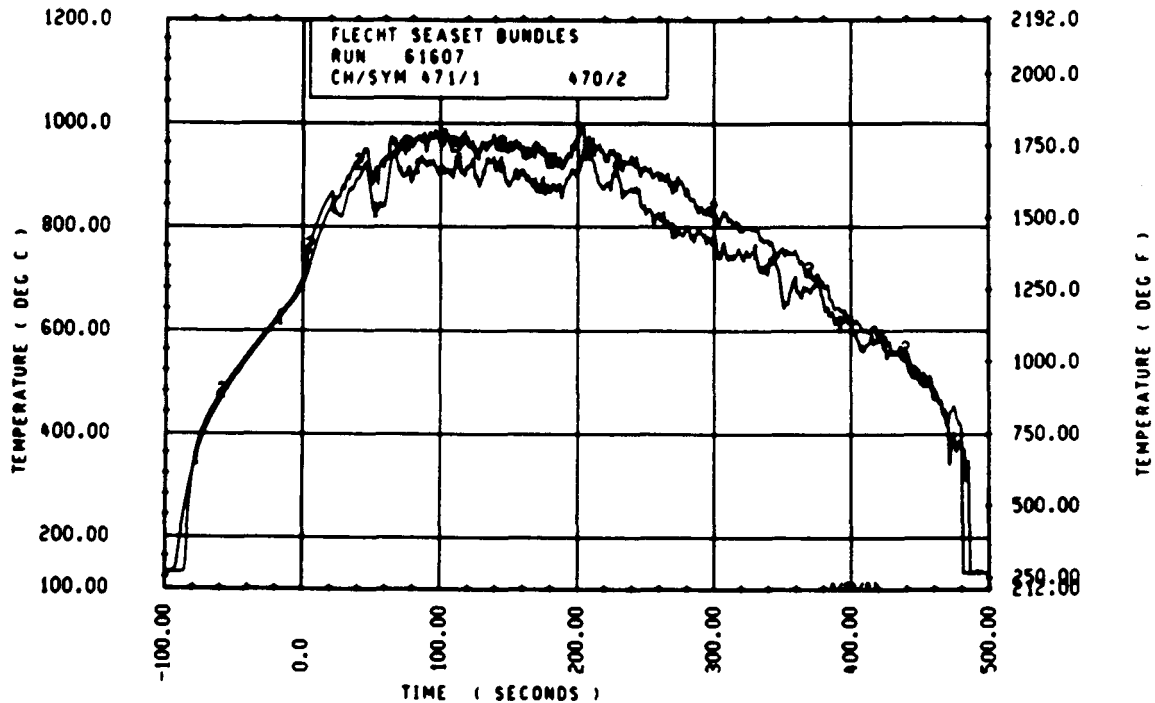


Figure E-24. Comparison of Subchannel Vapor Temperature Distribution Measurements, Run 61607, 2.44 m (96 in.) Elevation, Self-Aspirating Steam Probe and Unshielded Thermocouple (sheet 1 of 2)

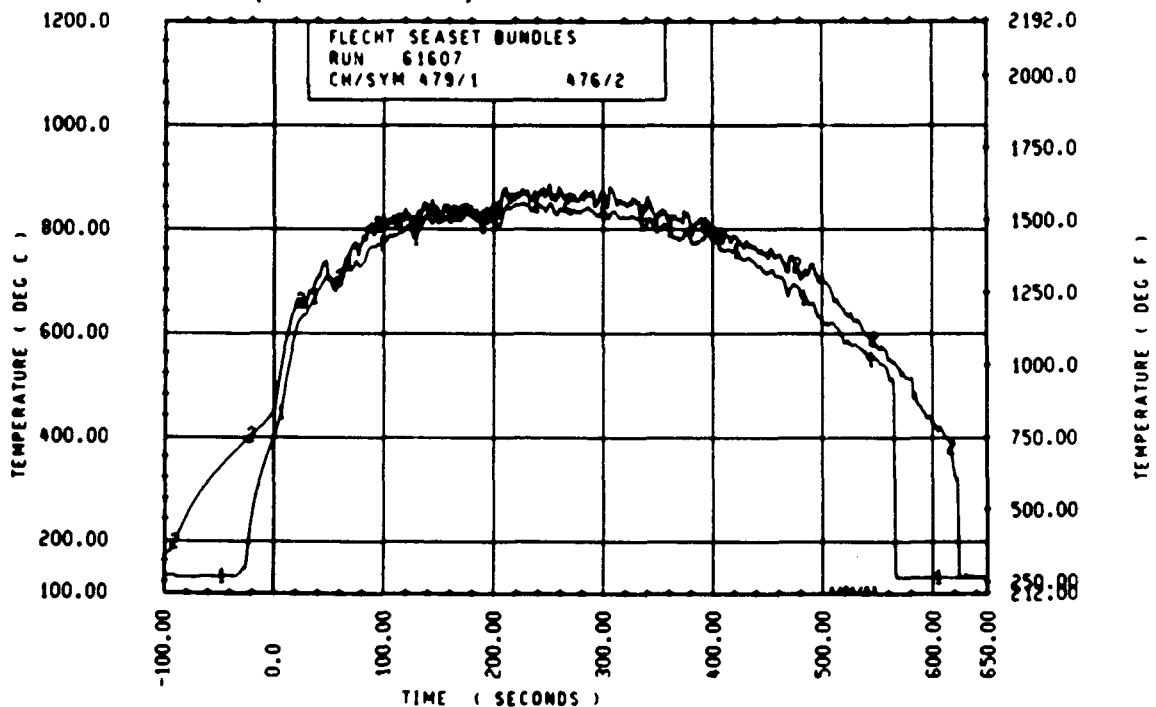


Figure E-24. Comparison of Subchannel Vapor Temperature Distribution Measurements, Run 61607, 3.05 m (120 in.) Elevation, Self-Aspirating Steam Probe and Unshielded Thermocouple (sheet 2 of 2)

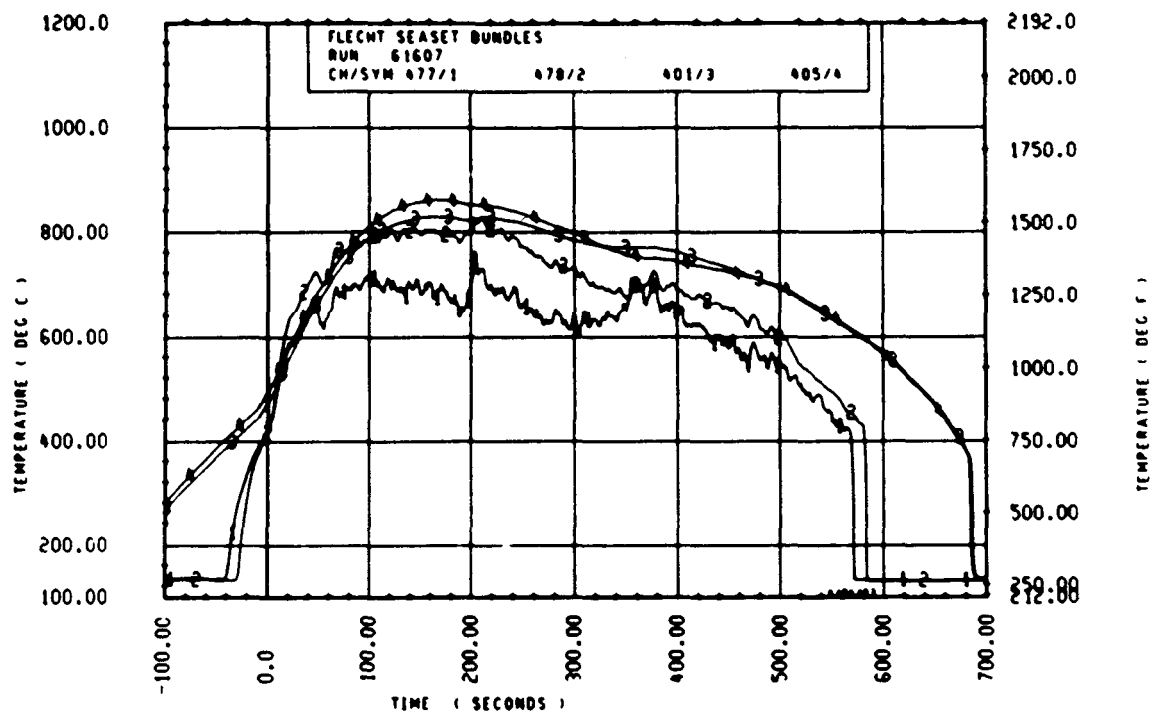


Figure E-25. Comparison of Subchannel Vapor Temperature Distribution Measurements, Run 61607, 3.05 m (120 in.) Elevation, Self-Aspirating Steam Probes and Heater Rod Thermocouples

E-24				
(sheet 2)	3.05 (120)	Channel 479	Channel 476	--
E-25	3.05 (120)	Channels 477, 478	--	Channels 401, 405

Also shown in figures E-23 and E-25 are corresponding symmetrical heater rod temperature measurements.

Generally, the vapor temperature measurements are symmetrical for all test conditions at the 1.98 and 2.44 m (78 and 96 in.) elevations. There were differences, however, between the self-aspirating steam probes and the unshielded thermocouples for the tests at the lower power-to-flow ratios, as shown in figures E-26 through E-29.

E-4. CONCLUSION

The thimble tube steam probe which aspirates through the top of the bundle, the self-aspirating steam probe, and the unshielded thermocouples provided comparable vapor temperature measurements. However, the temperature comparisons were much better at higher power-to-flow ratios. The low void fraction flows affect the thermal response of the self-aspirating steam probe first, then the unshielded thermocouple, and last the-thimble-tube steam probe.

The thimble tube steam probe which aspirates through the bottom of the rod bundle did not provide valid vapor temperature data.

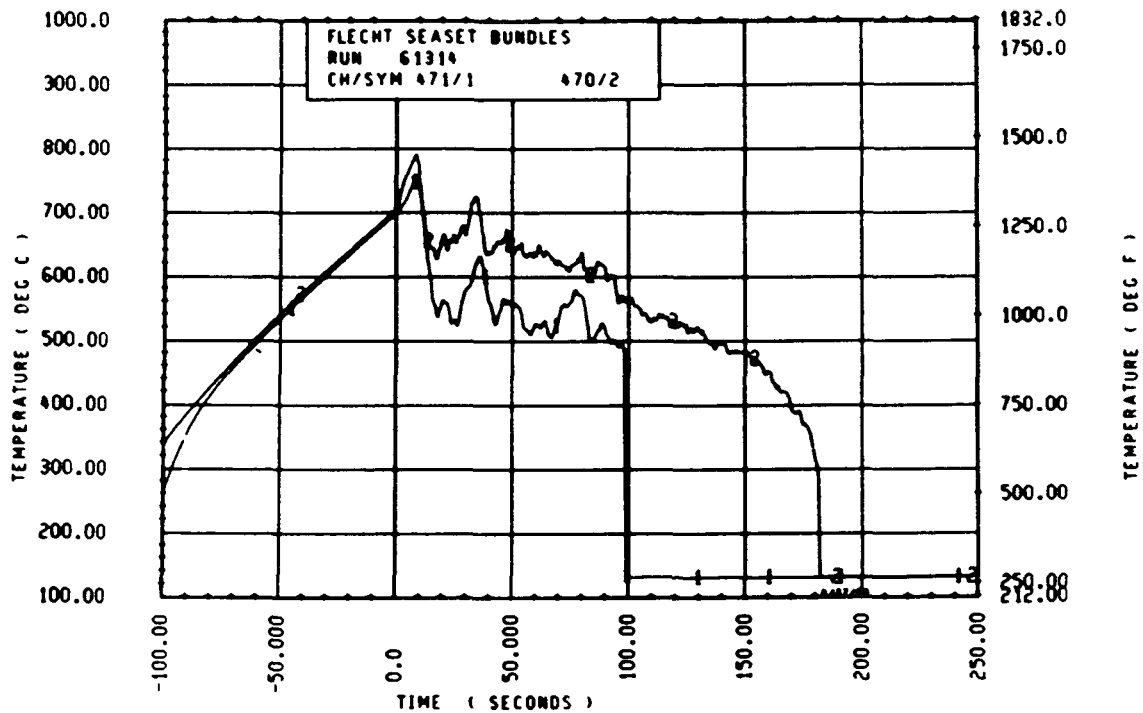


Figure E-26. Comparison of Subchannel Vapor Temperature Distribution Measurements, Run 61314, 2.44 m (96 in.) Elevation, Self-Aspirating Steam Probe and Unshielded Thermocouple

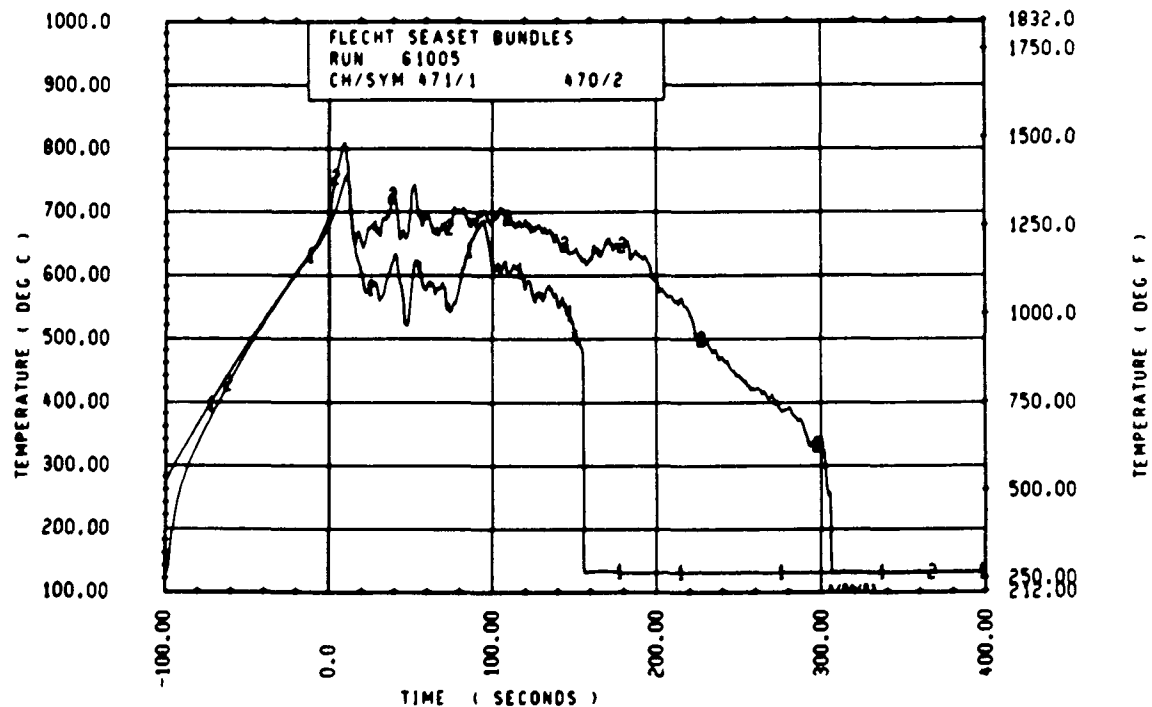


Figure E-27. Comparison of Subchannel Vapor Temperature Distribution Measurements, Run 61005, 2.44 m (96 in.) Elevation, Self-Aspirating Steam Probe and Unshielded Thermocouple

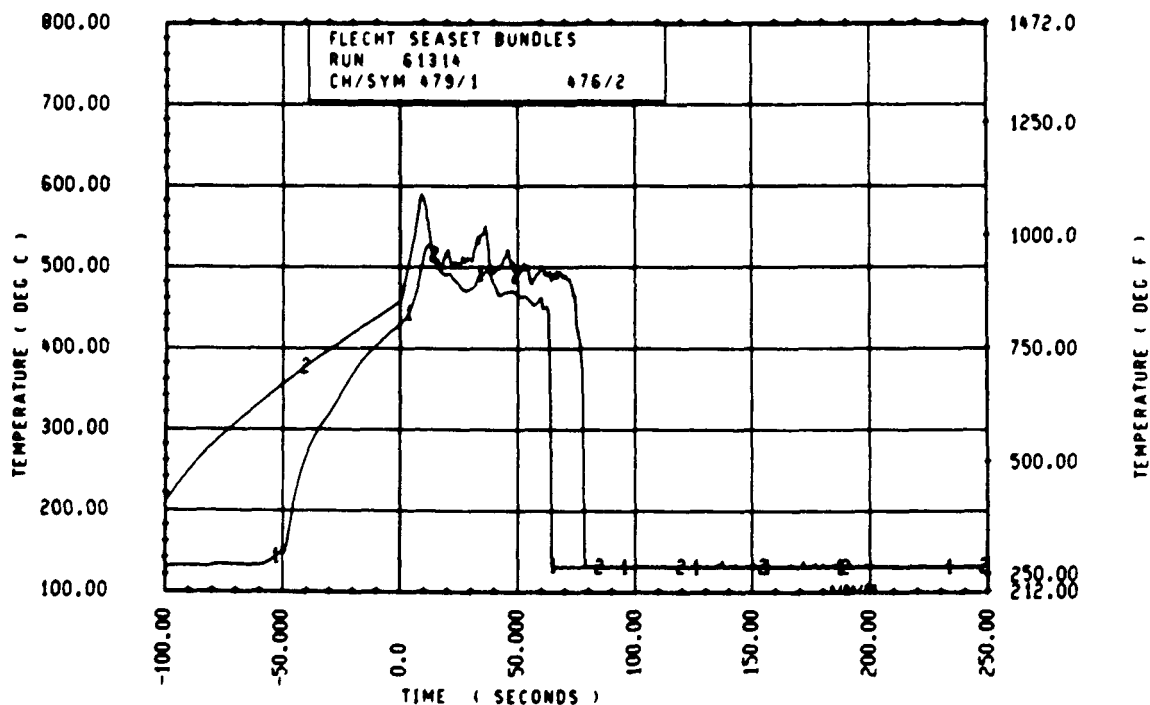


Figure E-28. Comparison of Subchannel Vapor Temperature Distribution Measurements, Run 61314, 3.05 m (120 in.) Elevation, Self-Aspirating Steam Probe and Unshielded Thermocouple

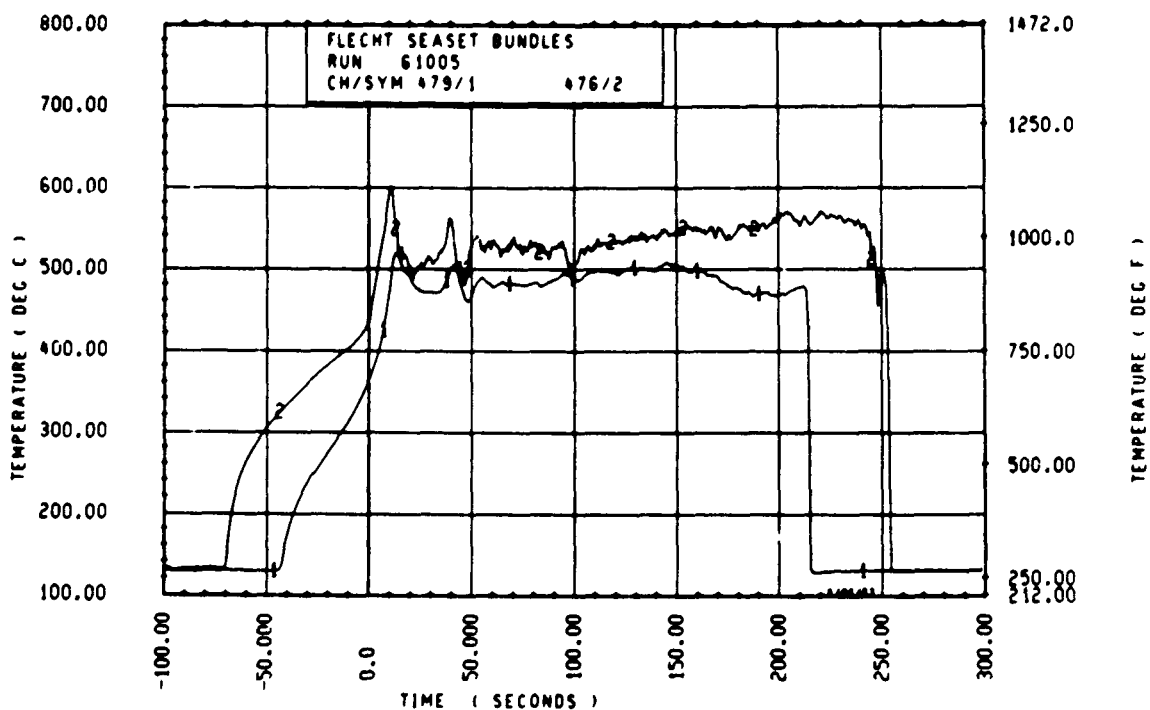


Figure E-29. Comparison of Subchannel Vapor Temperature Distribution Measurements, Run 61005, 3.05 m (120 in.) Elevation, Self-Aspirating Steam Probe and Unshielded Thermocouple

APPENDIX F

BUNDLE INSTRUMENTATION

The instrumentation for the 163-rod blocked bundle was based in part on the instrumentation in both the 161-rod unblocked bundle and the 21-rod bundle, to provide direct comparisons between the three bundles. However, the large number of thermocouples which failed during testing in the 161-rod bundle limited the number of comparisons between the two large bundles. Also, the utilization and placement of the two islands of noncoplanar, nonconcentric blockage in a bundle with only one line of symmetry provided for not only axial but also radial effects and, potentially, circumferential effects. Thus, there was a significant need to maximize the number of instrumented heater rods in the 163-rod blocked bundle.

Through the heater rod manufacturing quality assurance process, a total of 62 instrumented heater rods were selected as suitable for use in the 163-rod bundle, including three spare 21-rod bundle instrumented rods. These 62 rods were distributed across the bundle as shown in figure F-1. Of the 40 heater rods in the two blockage islands, 31 rods were instrumented; 28 of the 64 rods in the flow bypass region were instrumented, and 3 of the 59 peripheral rods were instrumented. These 62 instrumented heater rods had a total of 462 functional thermocouples at the start of bundle build. A total of 440 thermocouples could be hooked up to the computer; therefore, 22 thermocouples at the top and bottom 0.91 m (36 in.) of the bundle were utilized as spares.

The radial distribution of heater rod thermocouples as a function of elevation is shown in figures F-2 through F-29. The thermocouples are designated by computer channel numbers. Also shown in these figures are the location of the thimble wall thermocouples as initially connected and the vapor temperature instrumentation. All the vapor temperature instrumentation was connected to the computer. However, because only 21 computer channels were allocated to measuring thimble wall temperatures, there were 14 spare thimble thermocouples.

As in the last two 21-rod bundles with the 1.0 mm (0.040 in.) diameter thermocouples, there were an insignificant number of heater rod thermocouple failures (3.4 percent) in the 163-rod bundle. The failed rod thermocouples as

well as failed thimble thermocouples and vapor temperature instrumentation are listed in table F-1 as a function of run numbers. The failed thimble thermocouples were reassigned with the spare thimble thermocouples, as shown in table F-2.

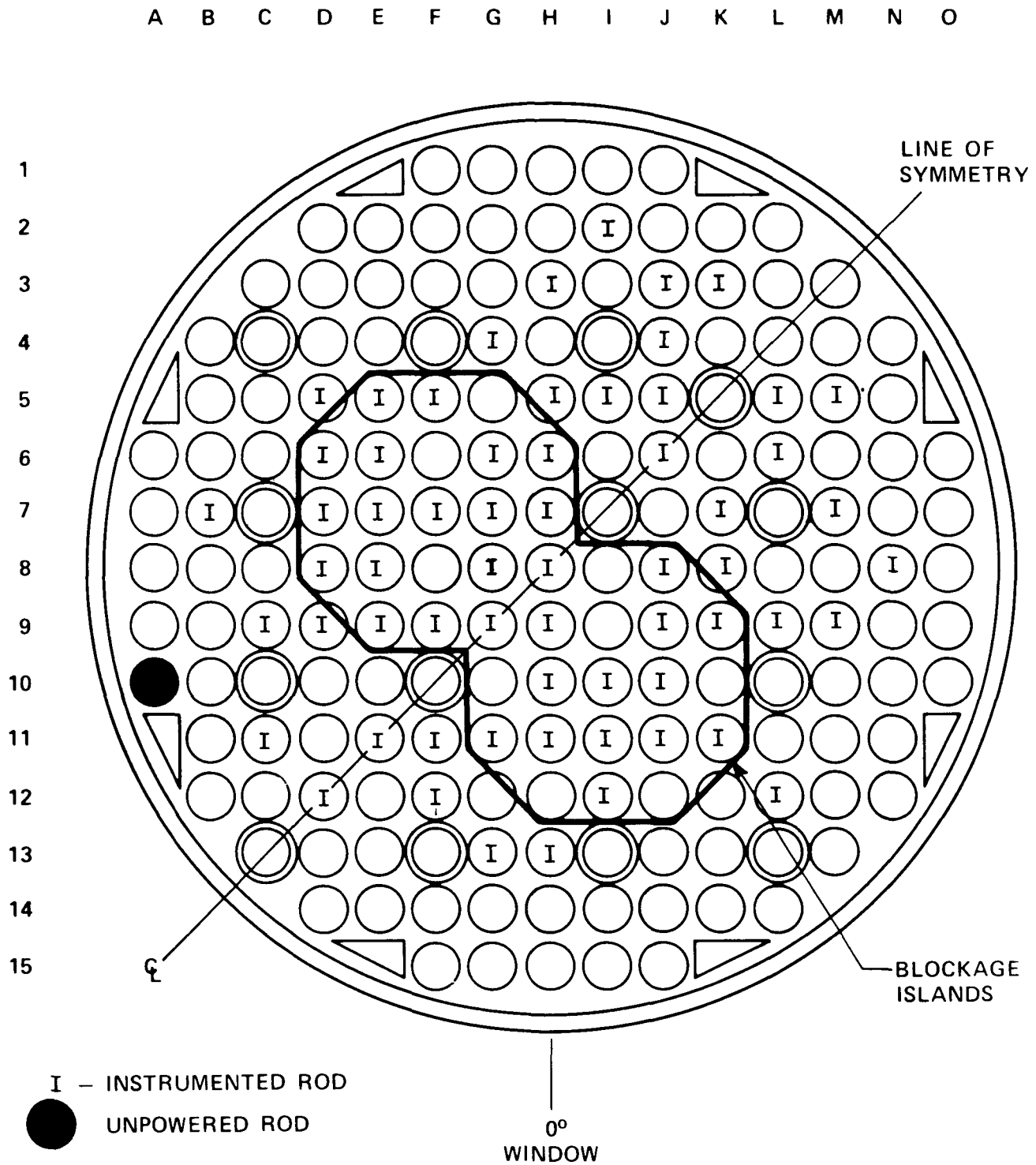


Figure F-1. Heater Rod Instrumentation Diagram

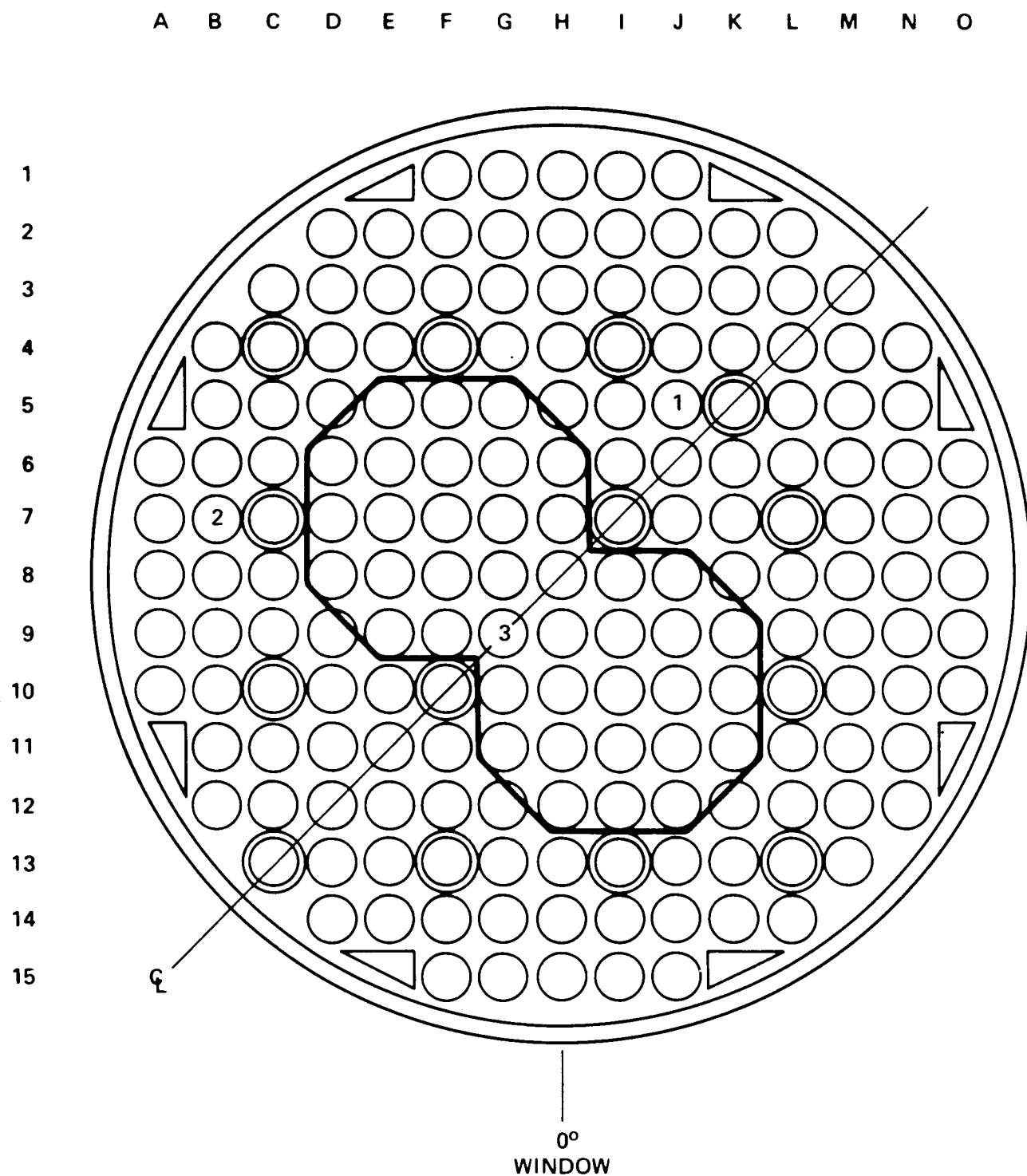


Figure F-2. Heater Rod Instrumentation, 0.30 m (12 in.) Elevation

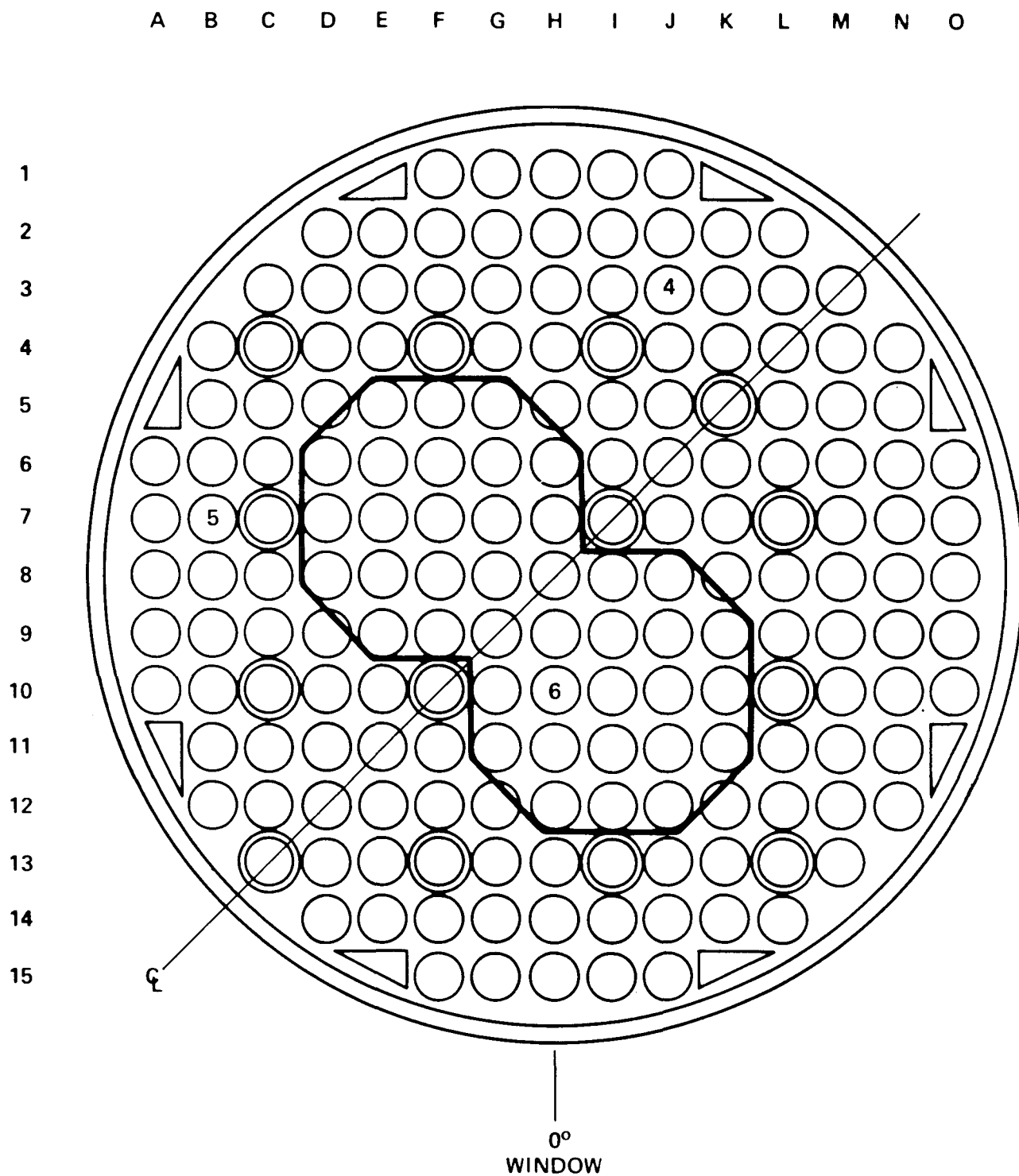


Figure F-3. Heater Rod Instrumentation, 0.61 m (24 in.) Elevation

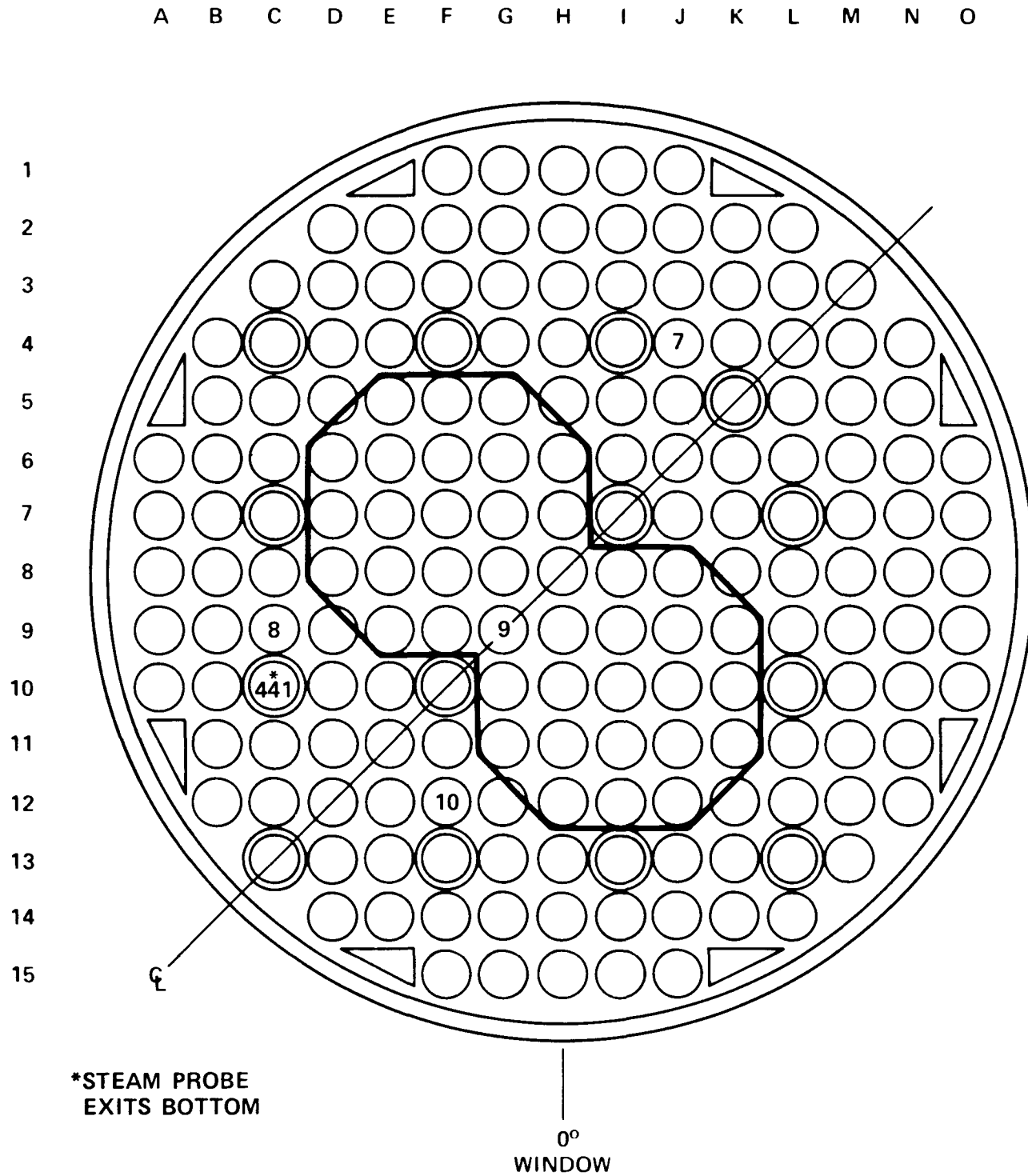


Figure F-4. Heater Rod Instrumentation, 0.99 m (39 in.) Elevation

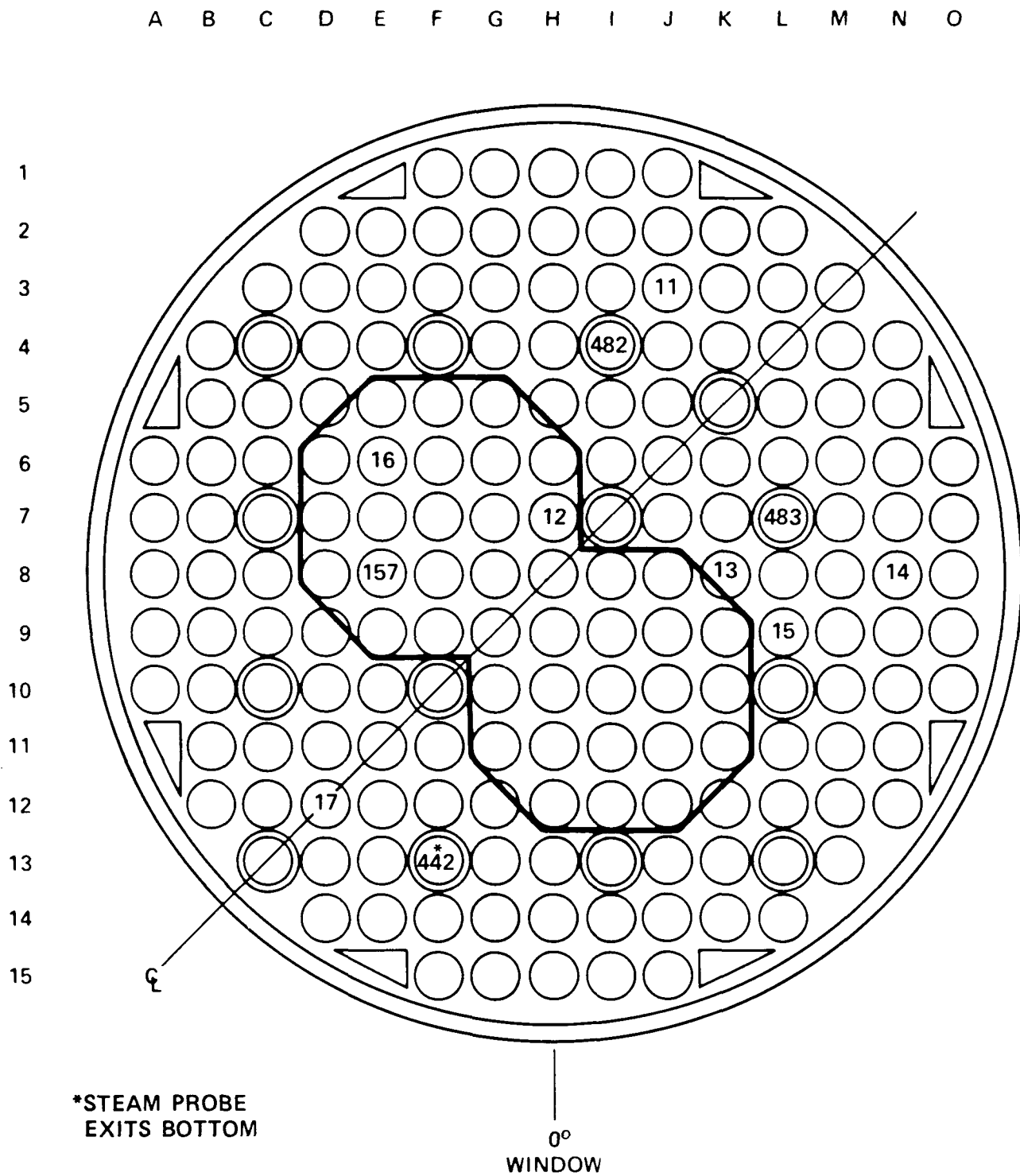


Figure F-5. Heater Rod Instrumentation, 1.22 m (48 in.) Elevation

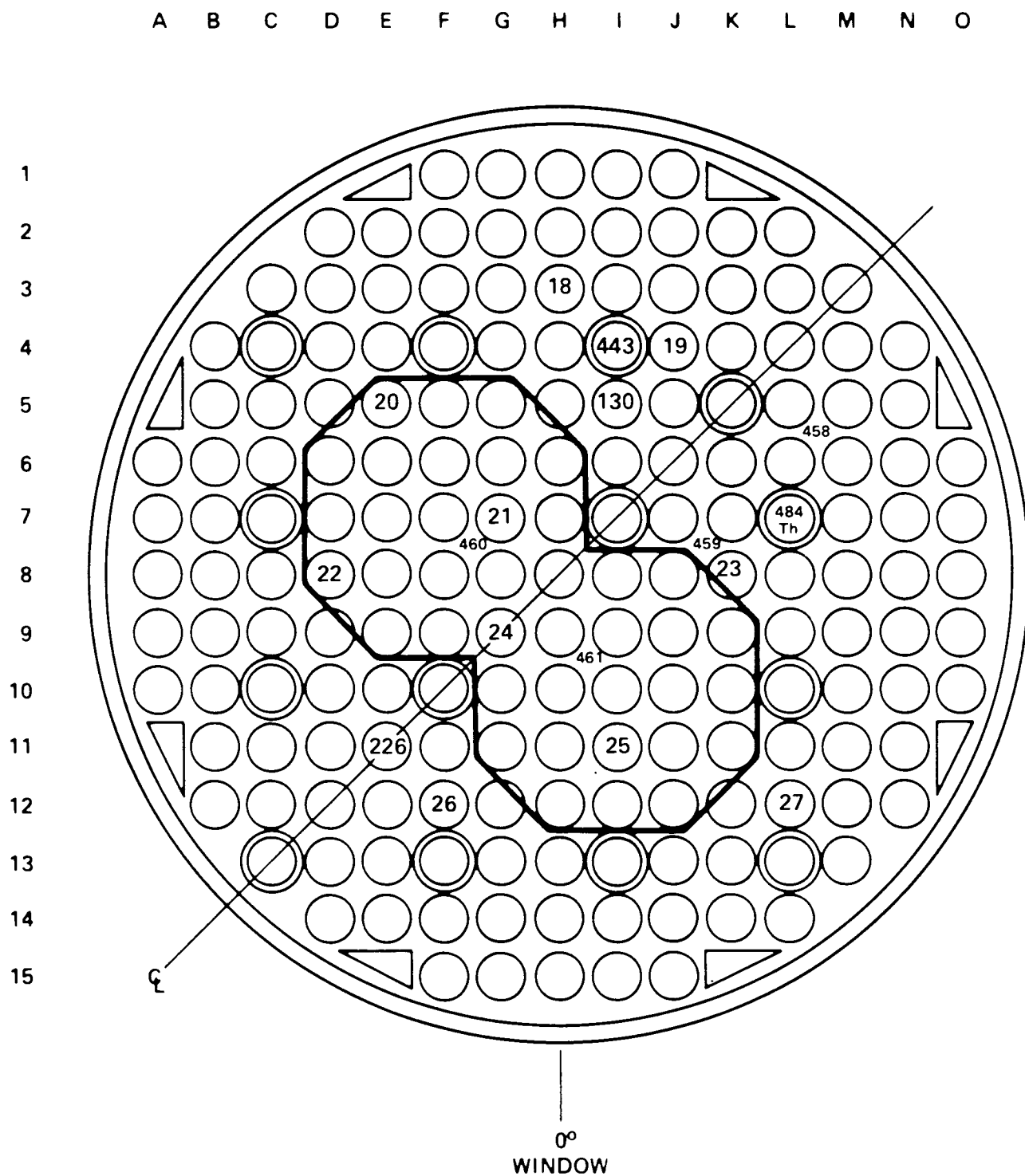


Figure F-6. Heater Rod Instrumentation, 1.52 m (60 in.) Elevation

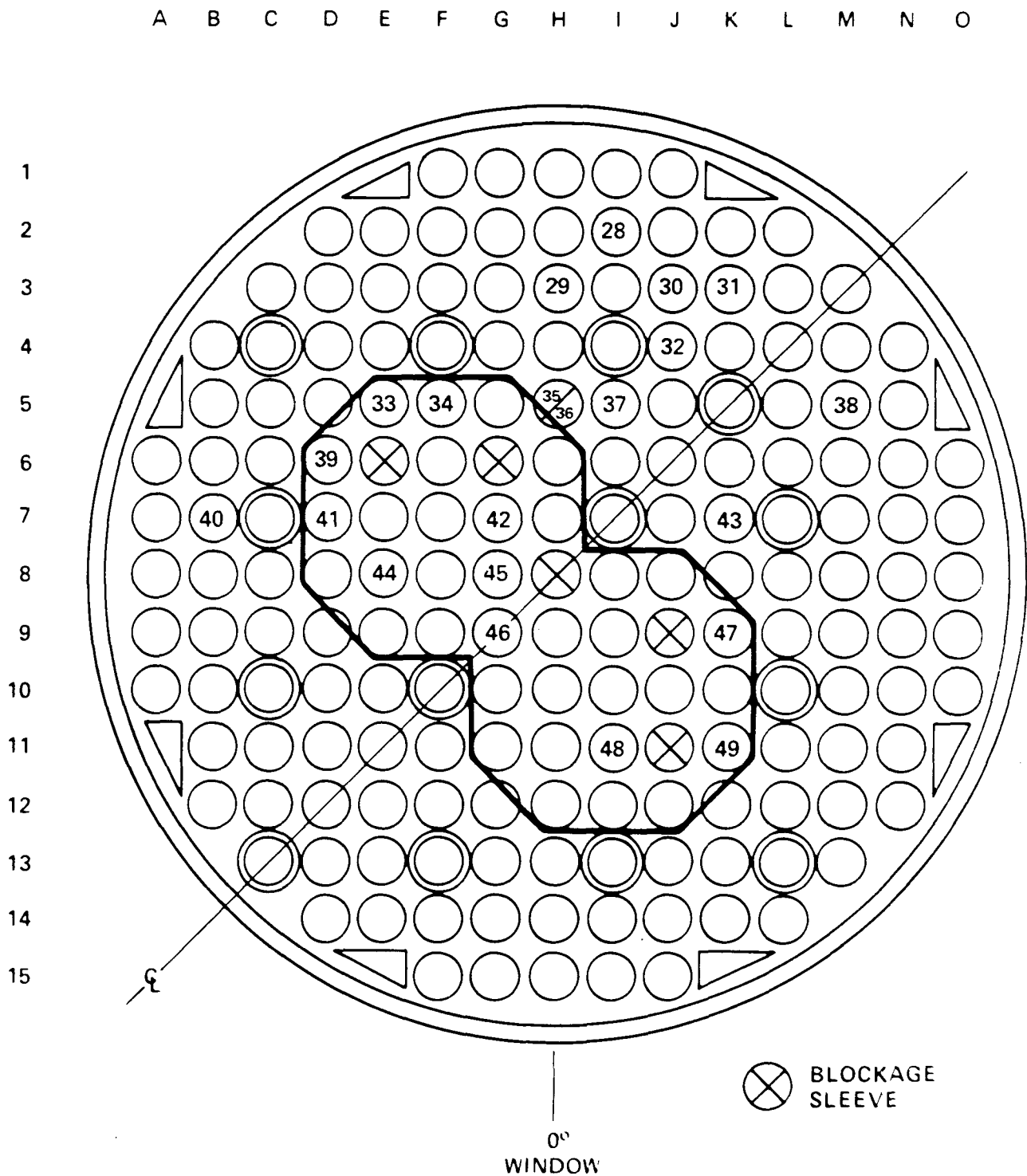


Figure F-7. Heater Rod Instrumentation, 1.70 m (67 in.) Elevation

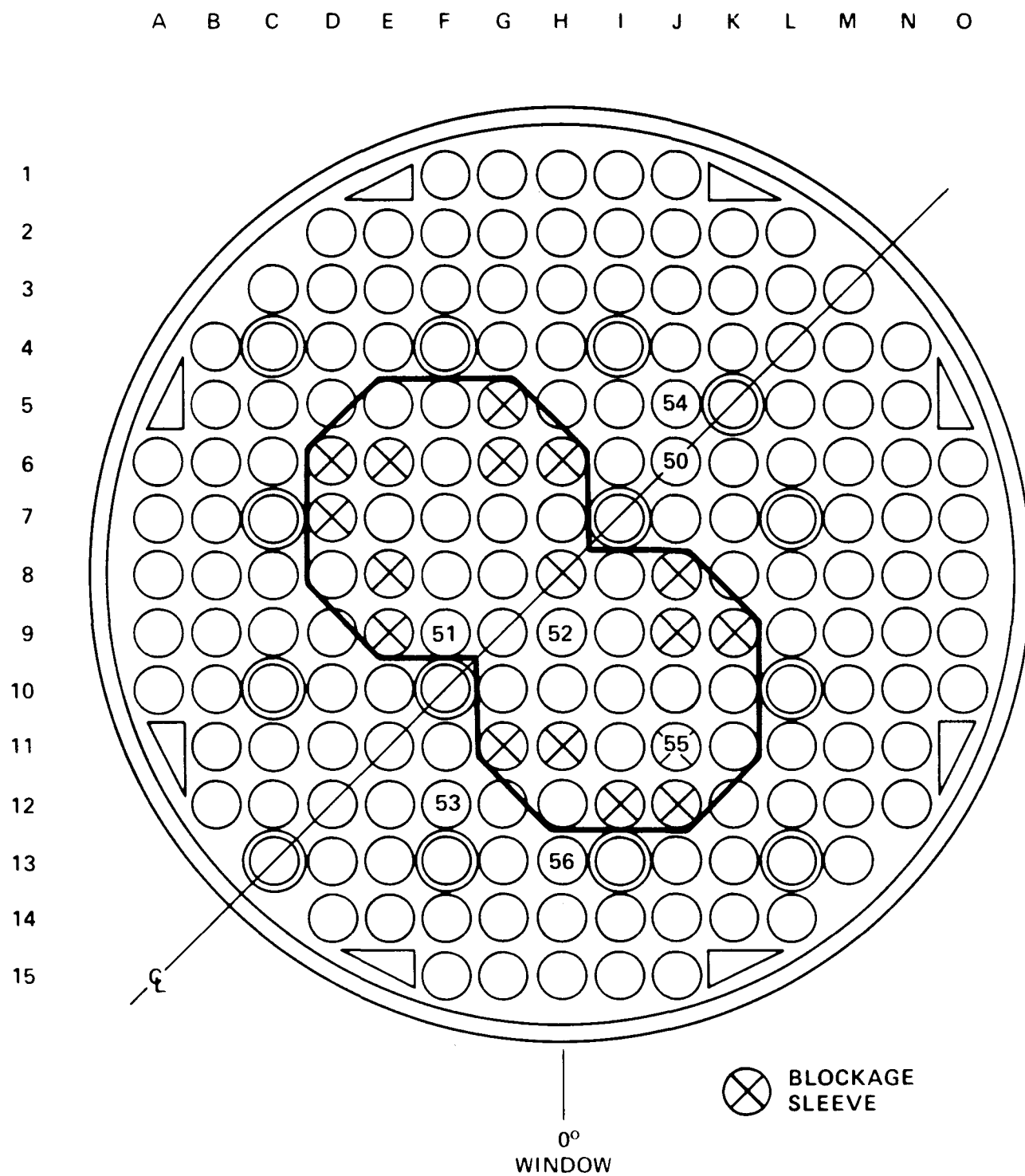


Figure F-8. Heater Rod Instrumentation, 1.75 m (69 in.) Elevation

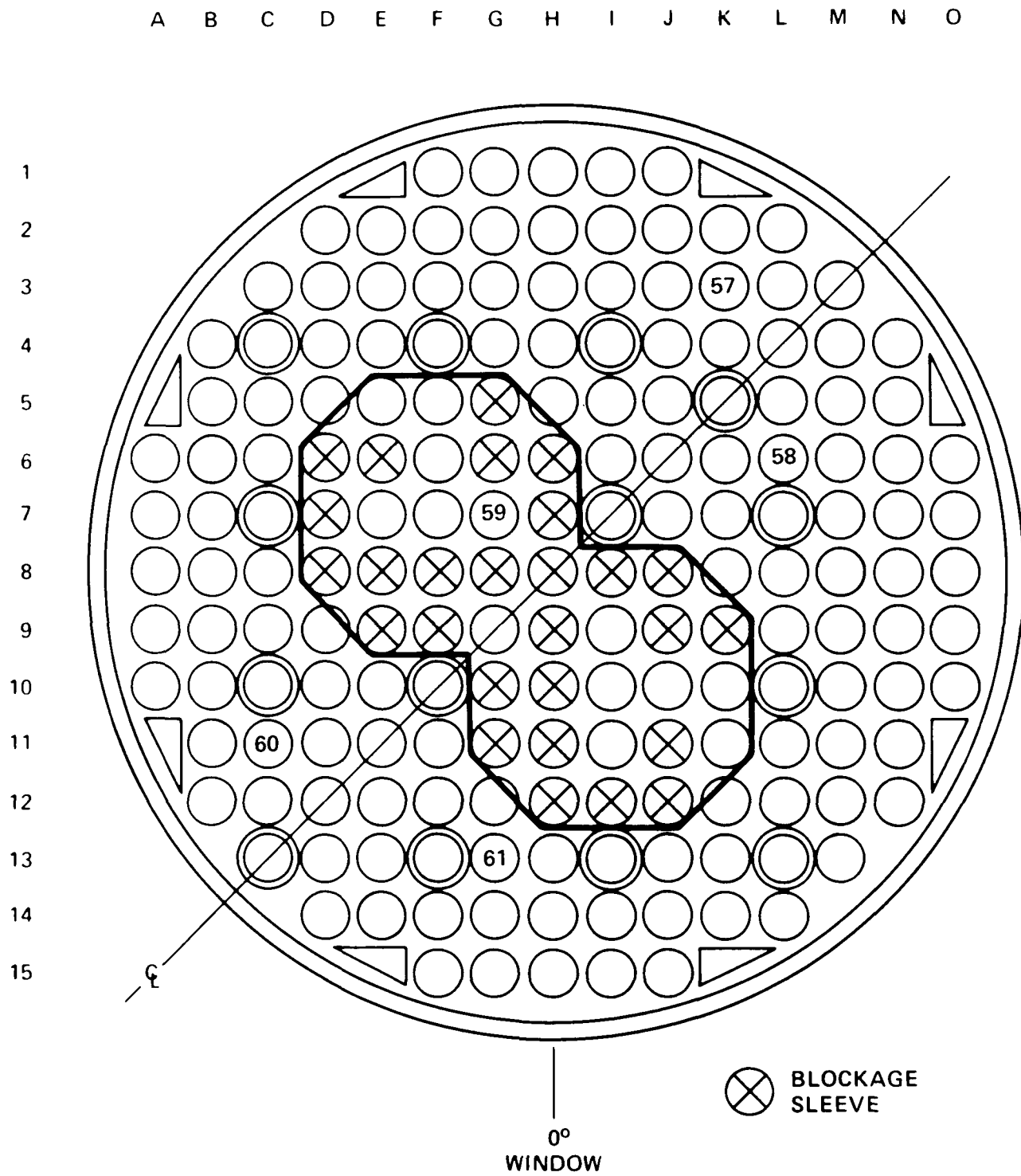


Figure F-9. Heater Rod Instrumentation, 1.78 m (70 in.) Elevation

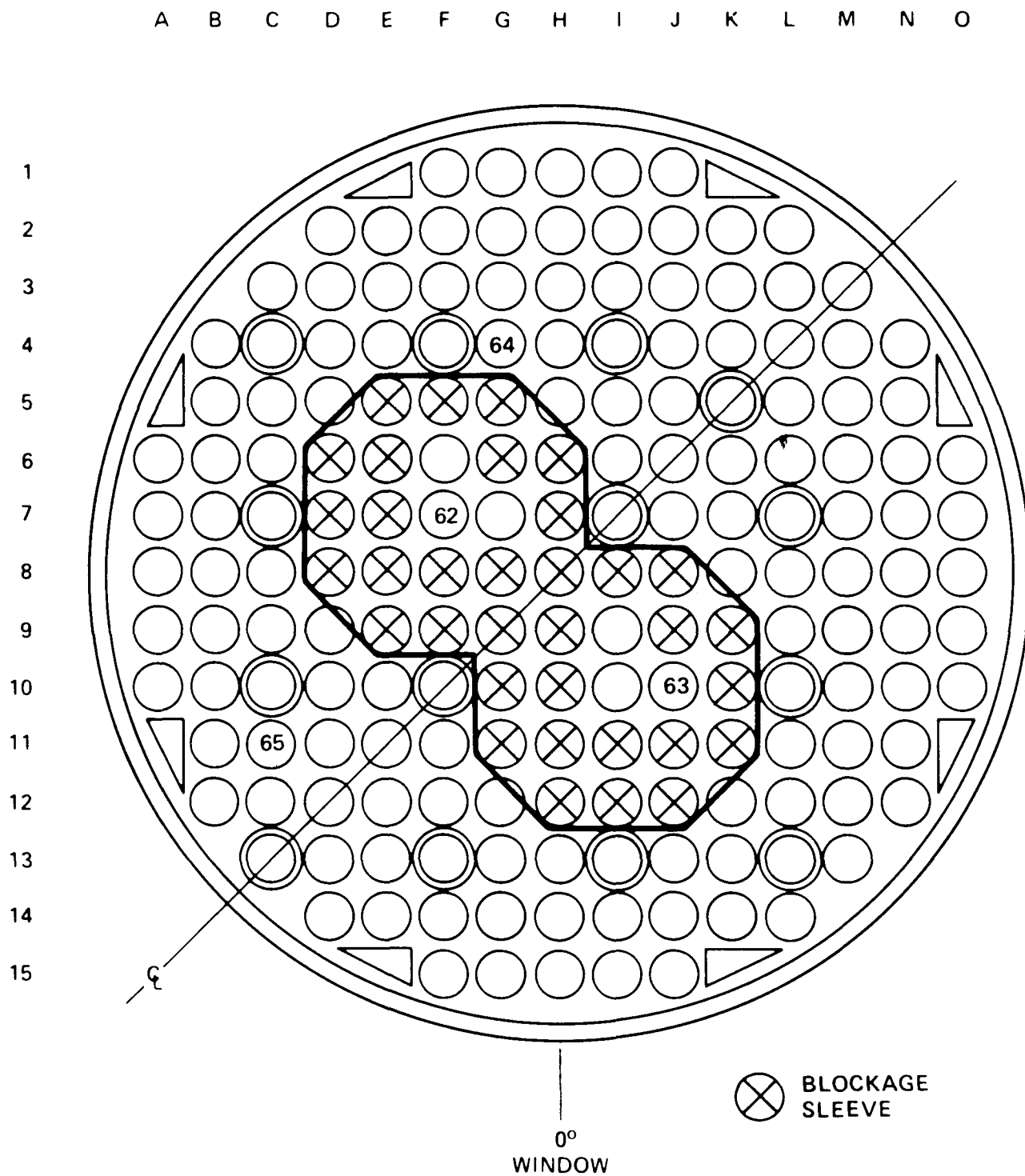


Figure F-10. Heater Rod Instrumentation, 1.80 m (71 in.) Elevation

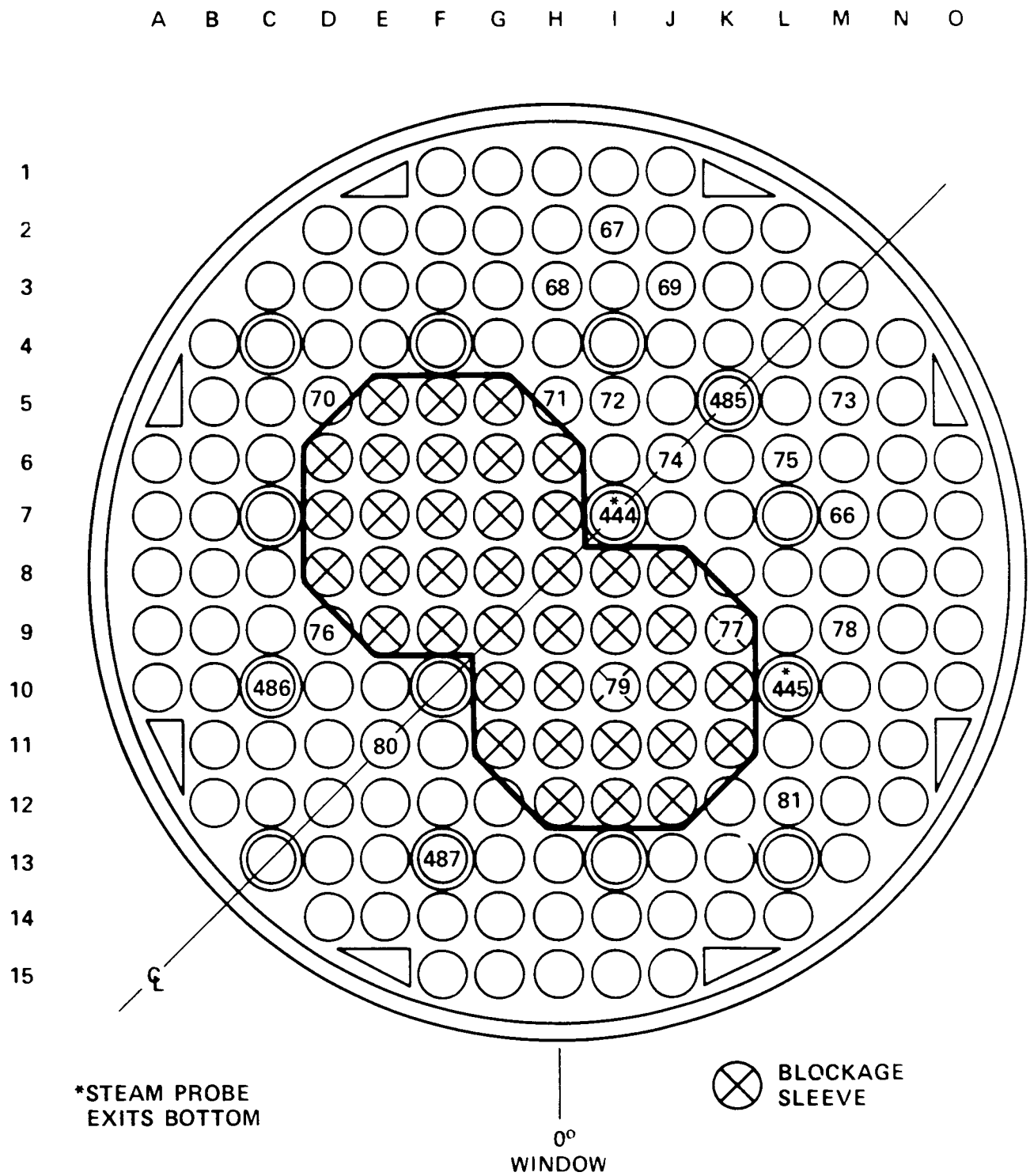


Figure F-11. Heater Rod Instrumentation, 1.83 m (72 in.) Elevation

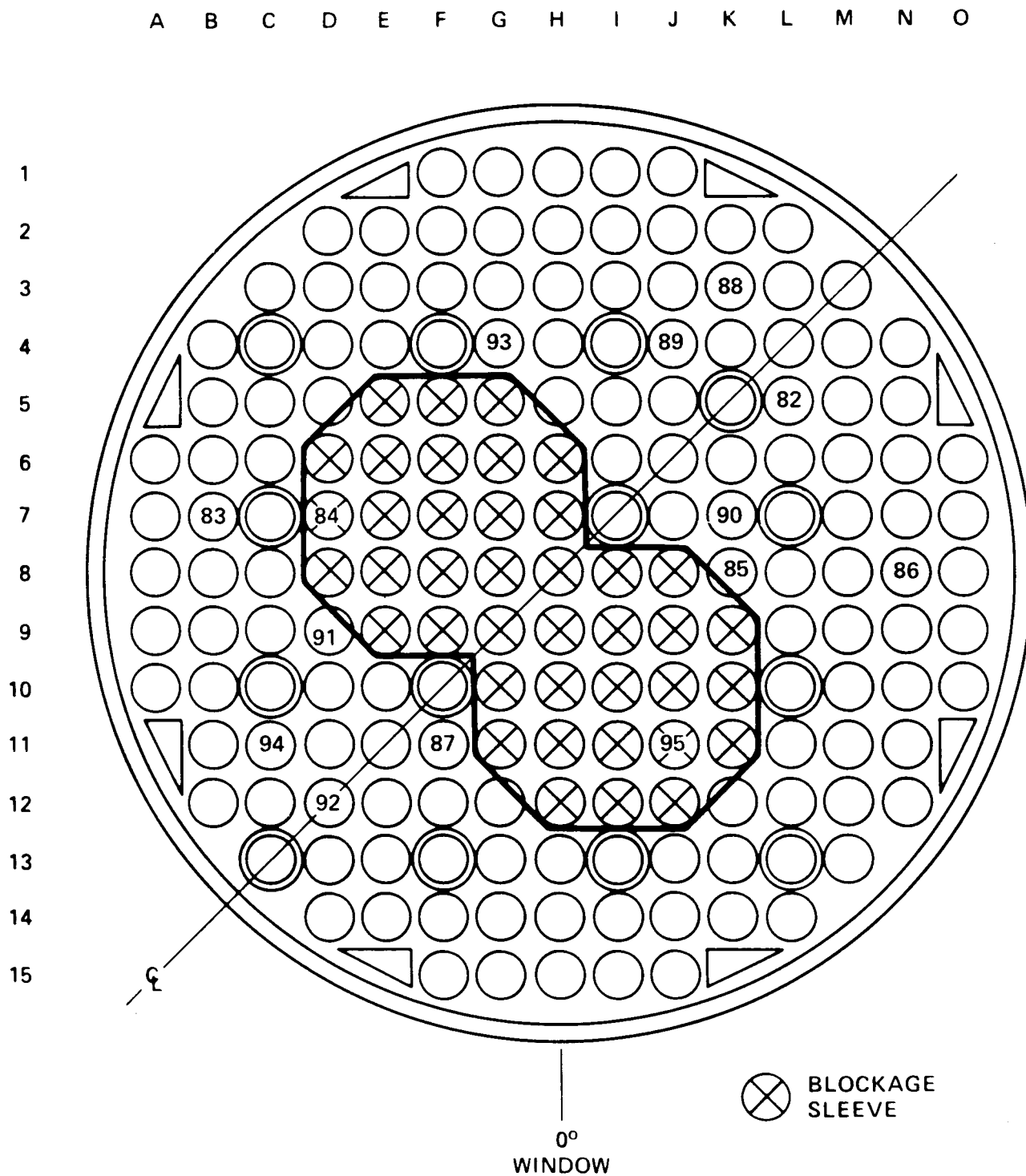


Figure F-12. Heater Rod Instrumentation, 1.85 m (73 in.) Elevation

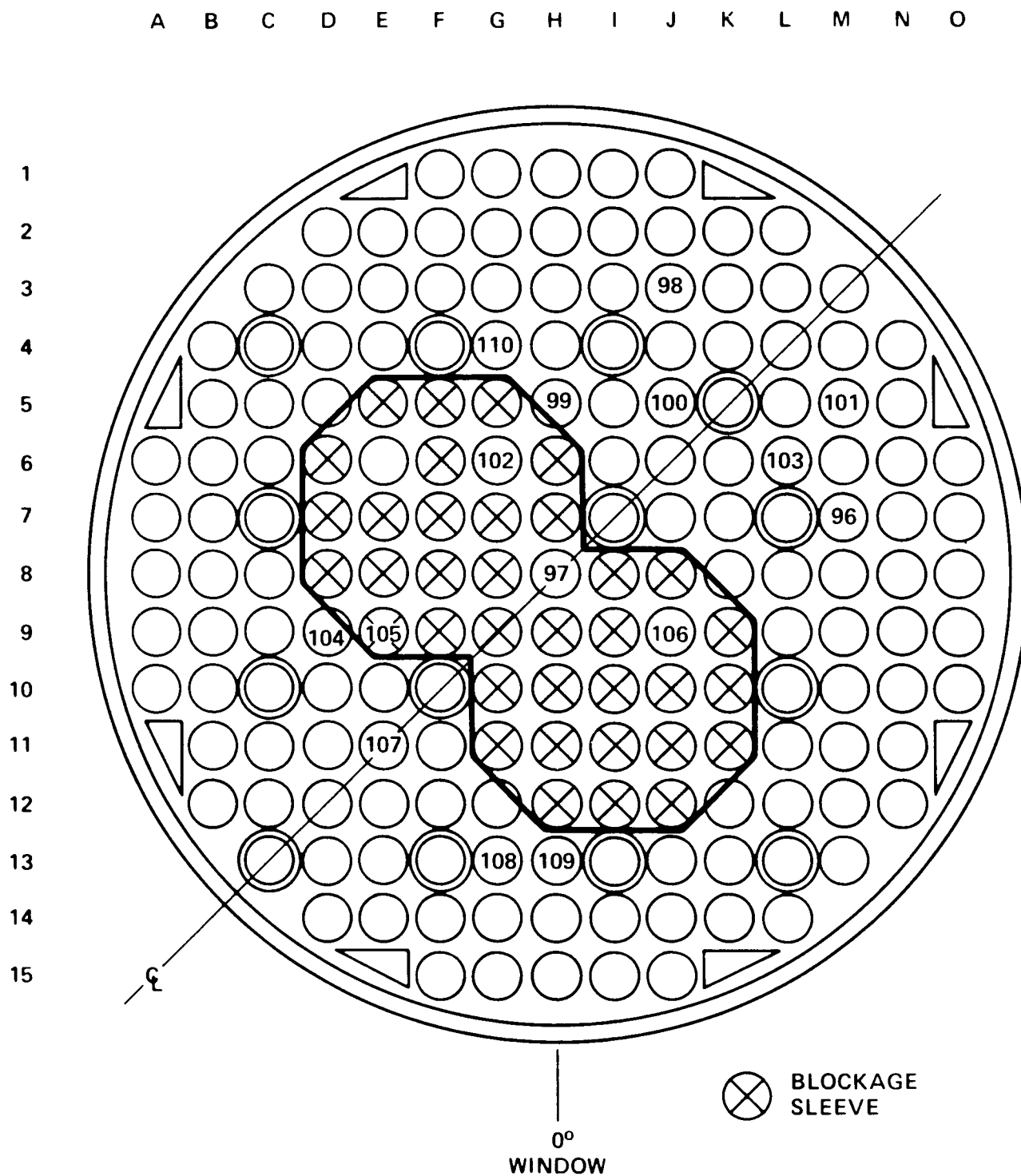


Figure F-13. Heater Rod Instrumentation, 1.88 m (74 in.) Elevation

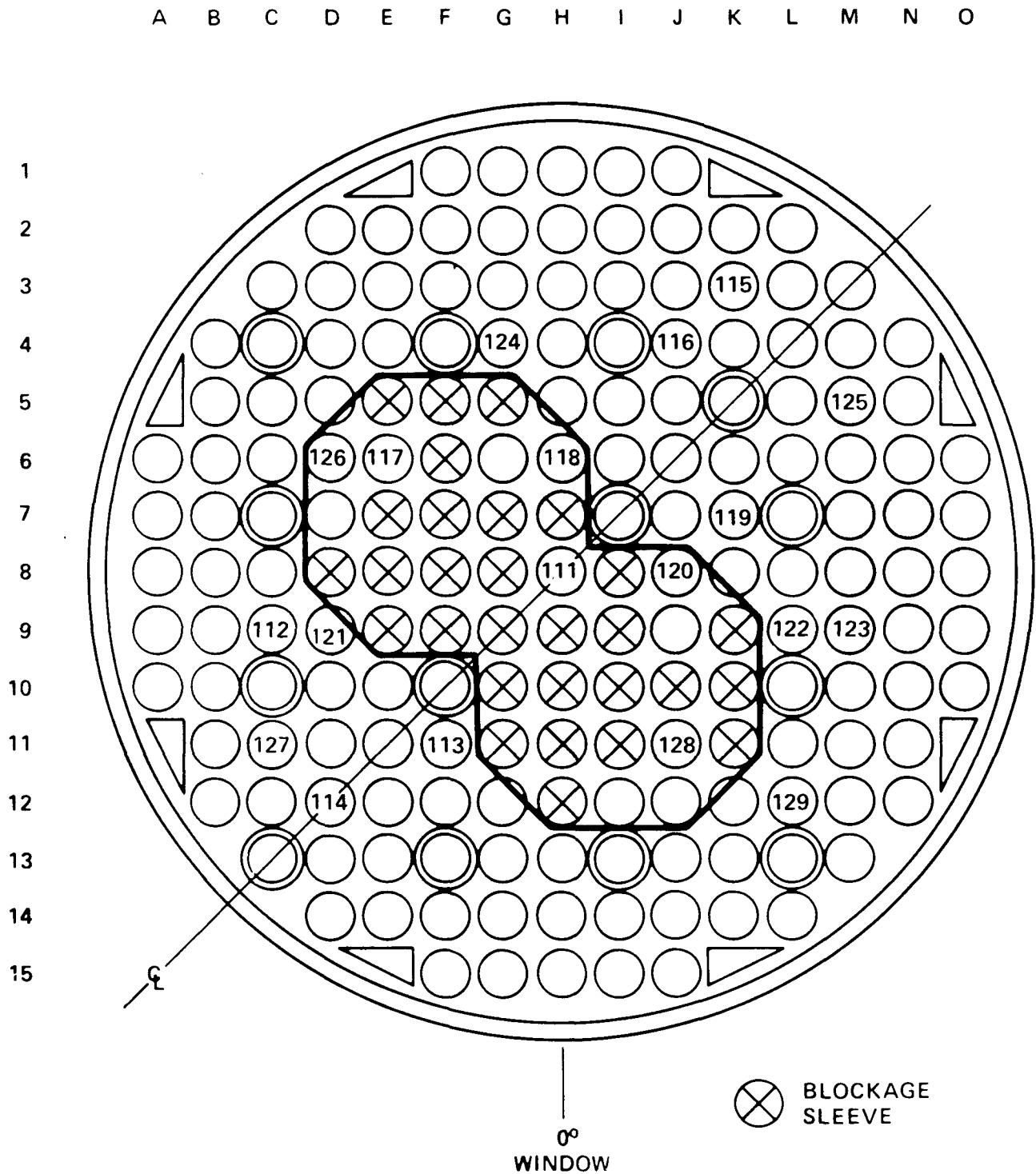


Figure F-14. Heater Rod Instrumentation, 1.91 m (75 in.) Elevation

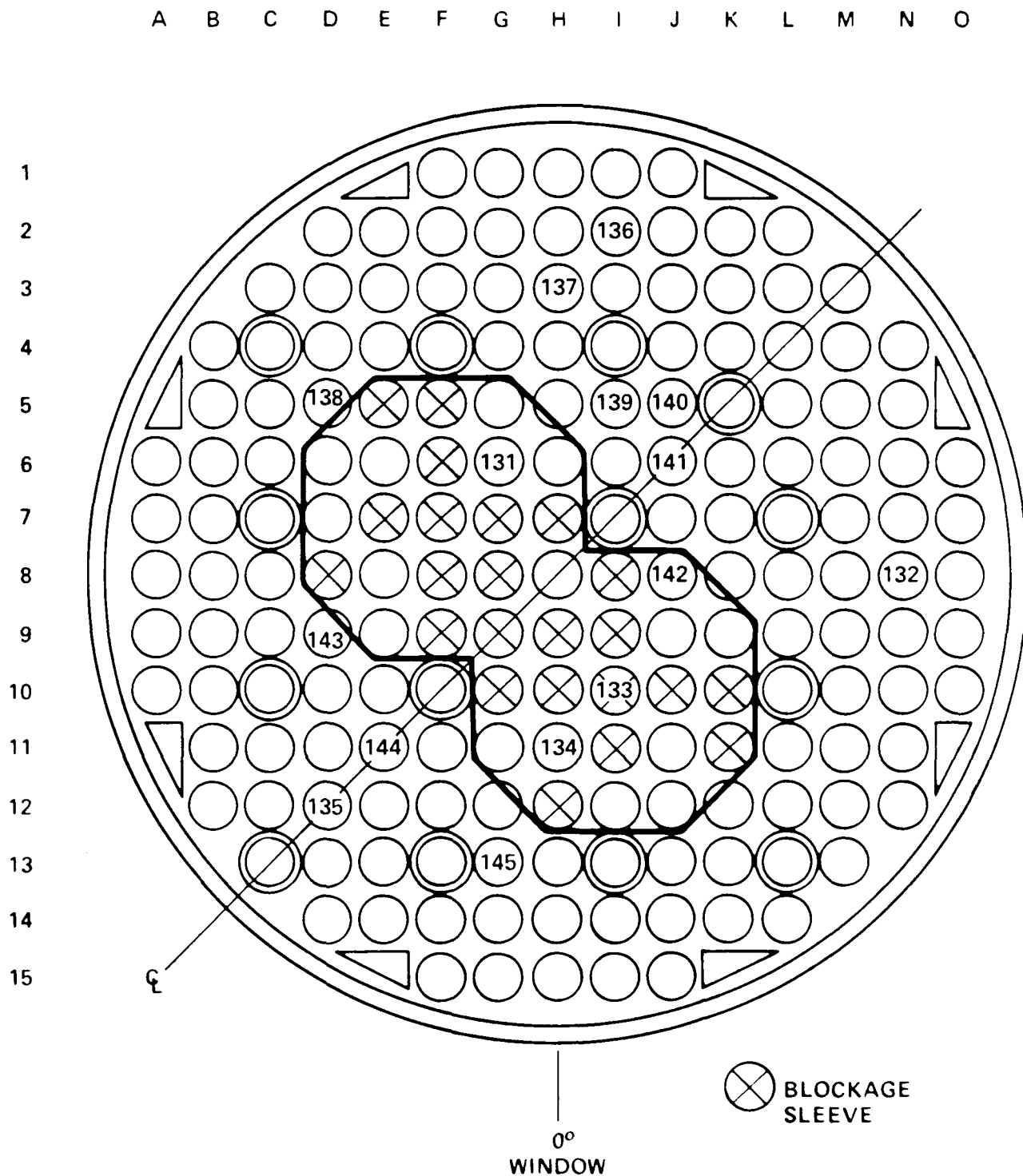


Figure F-15. Heater Rod Instrumentation, 1.93 m (76 in.) Elevation

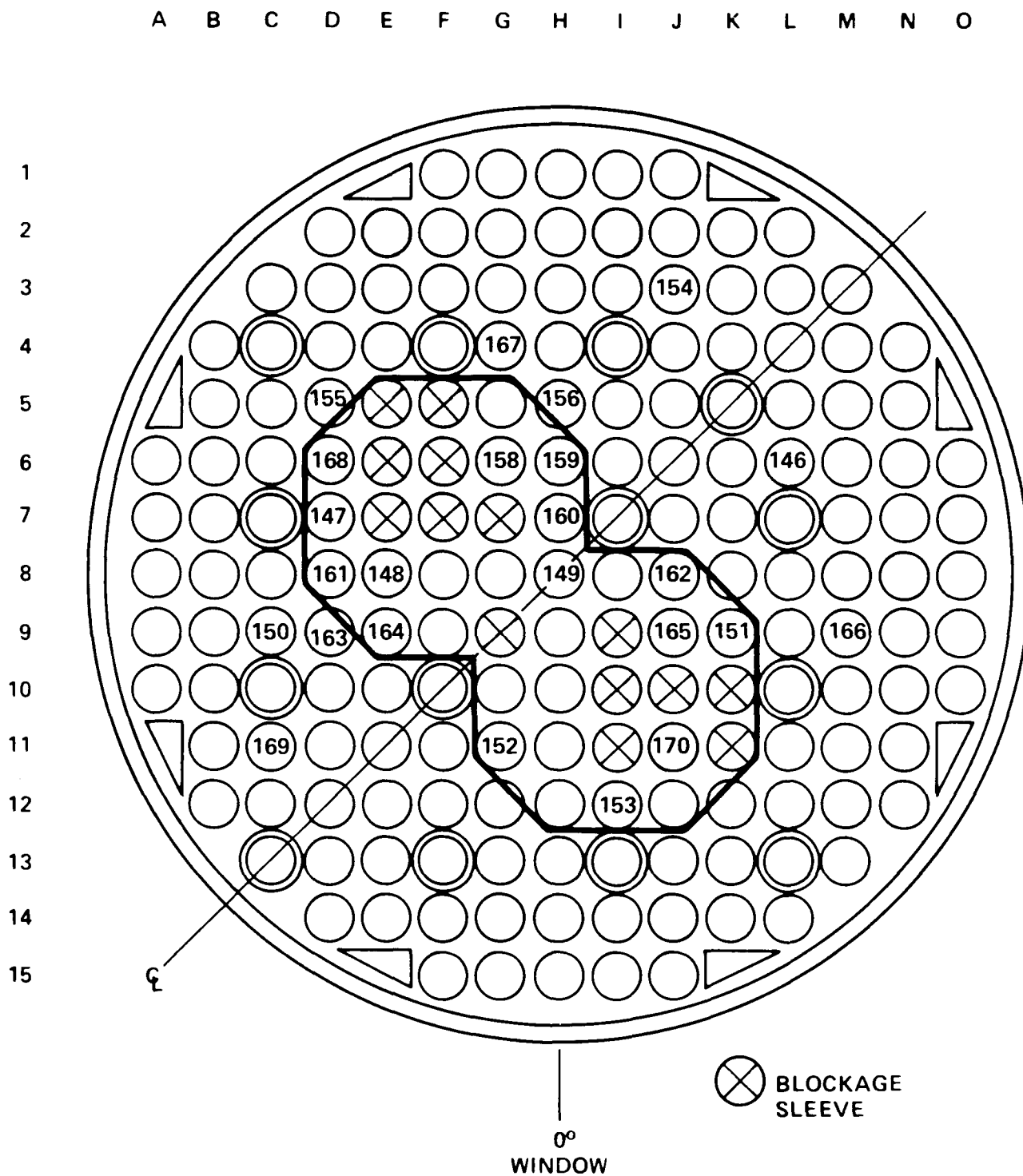


Figure F-16. Heater Rod Instrumentation, 1.96 m (77 in.) Elevation

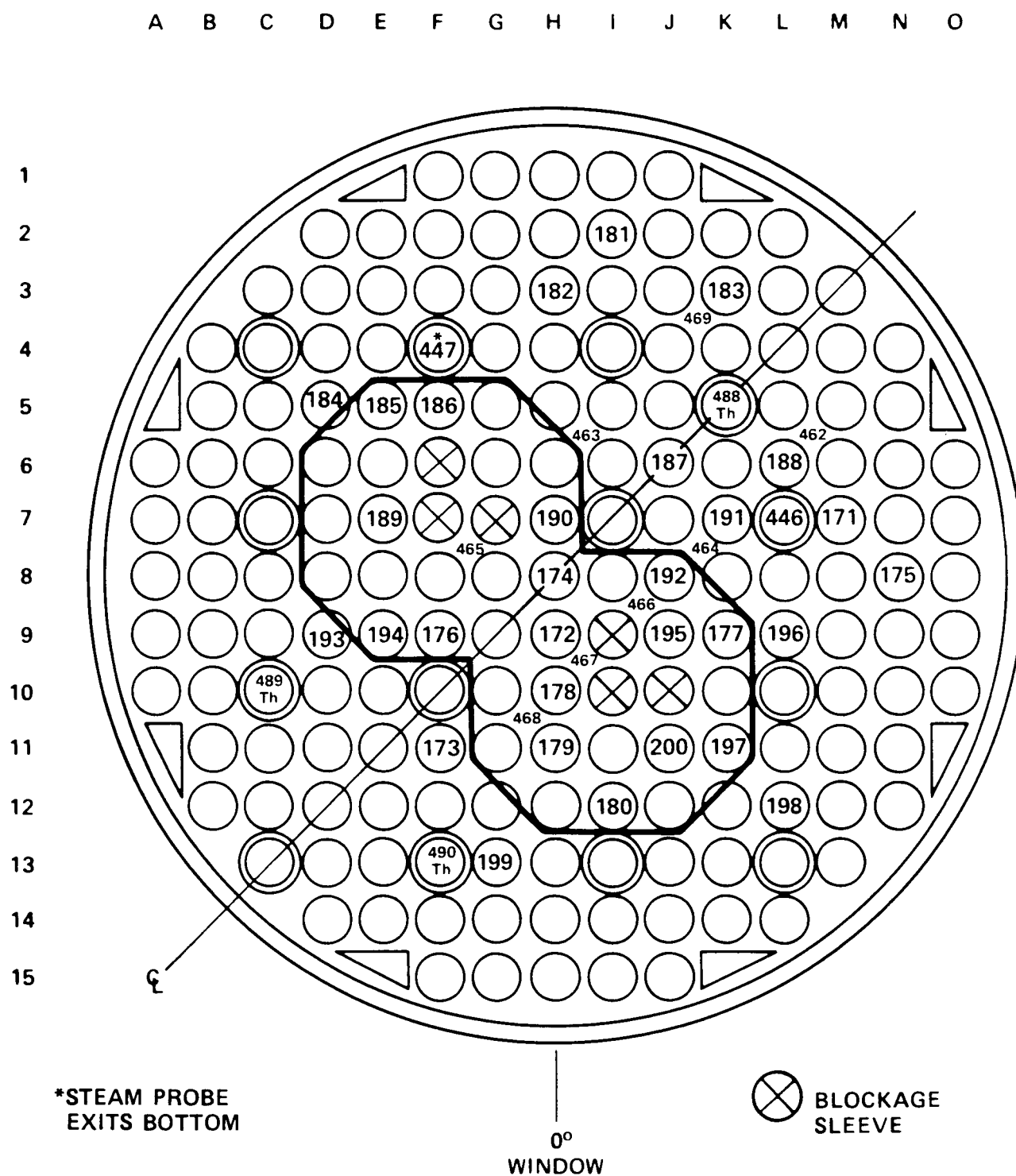


Figure F-17. Heater Rod Instrumentation, 1.98 m (78 in.) Elevation

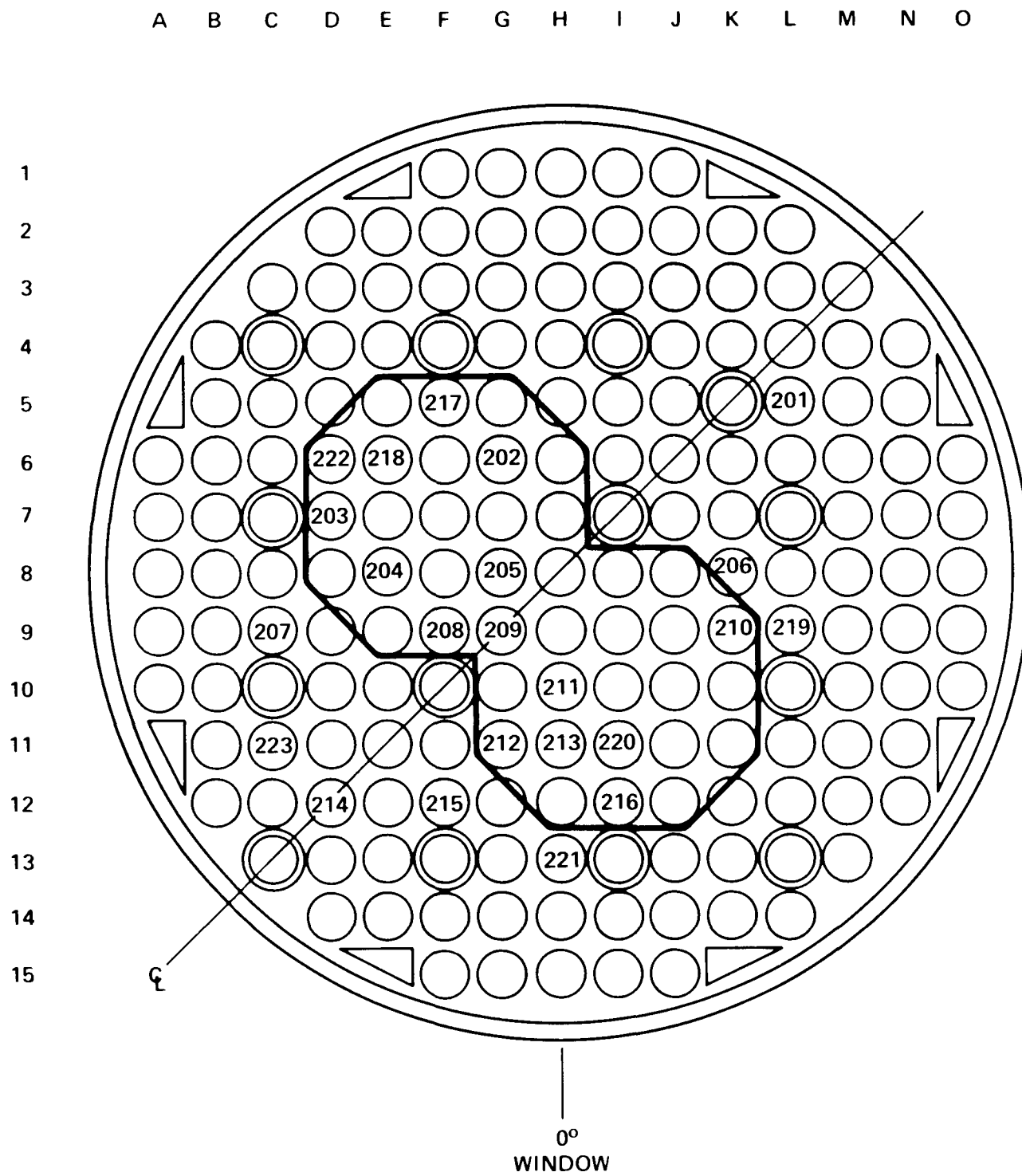


Figure F-18. Heater Rod Instrumentation, 2.01 m (79 in.) Elevation

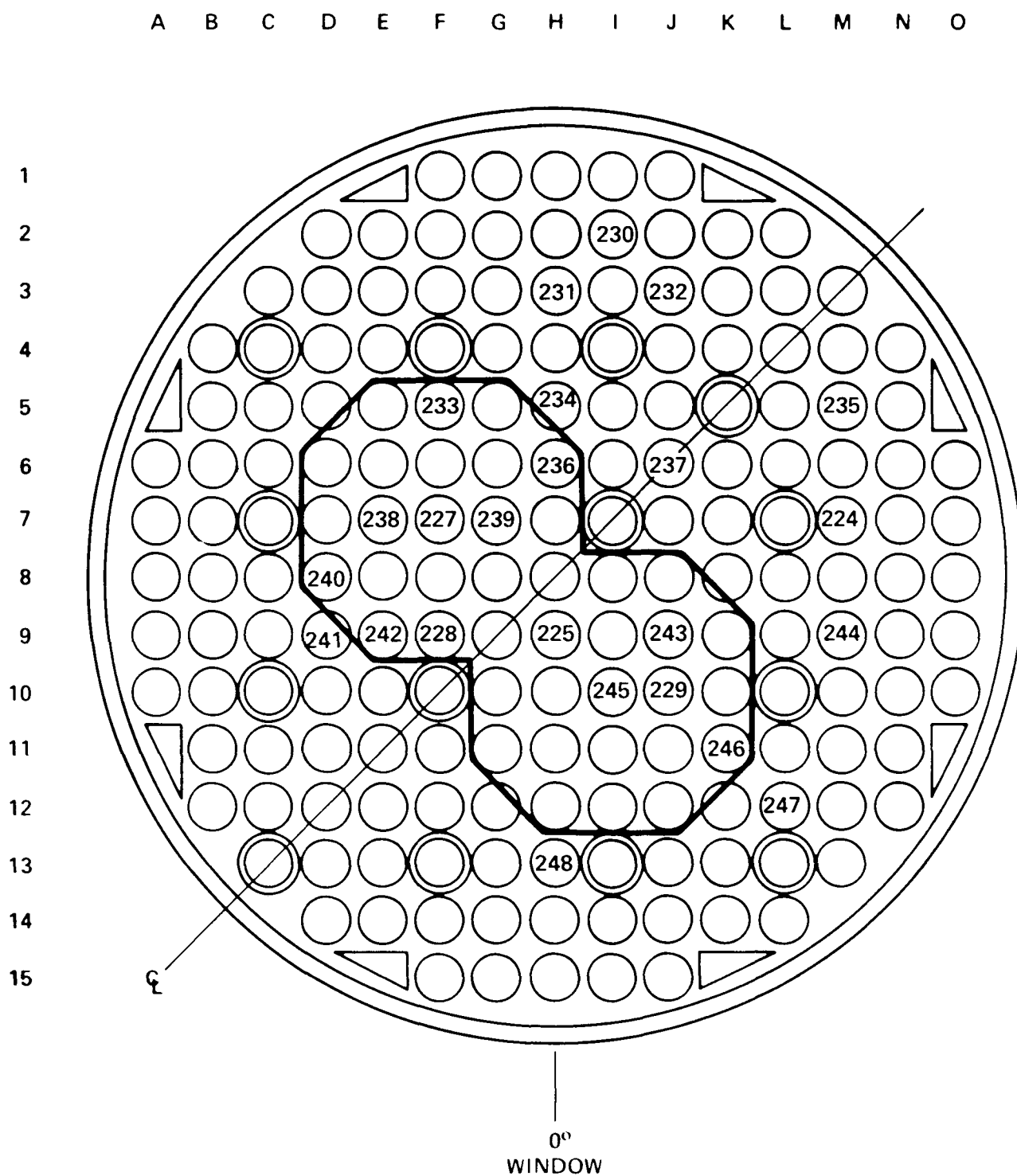


Figure F-19. Heater Rod Instrumentation, 2.03 m (80 in.) Elevation

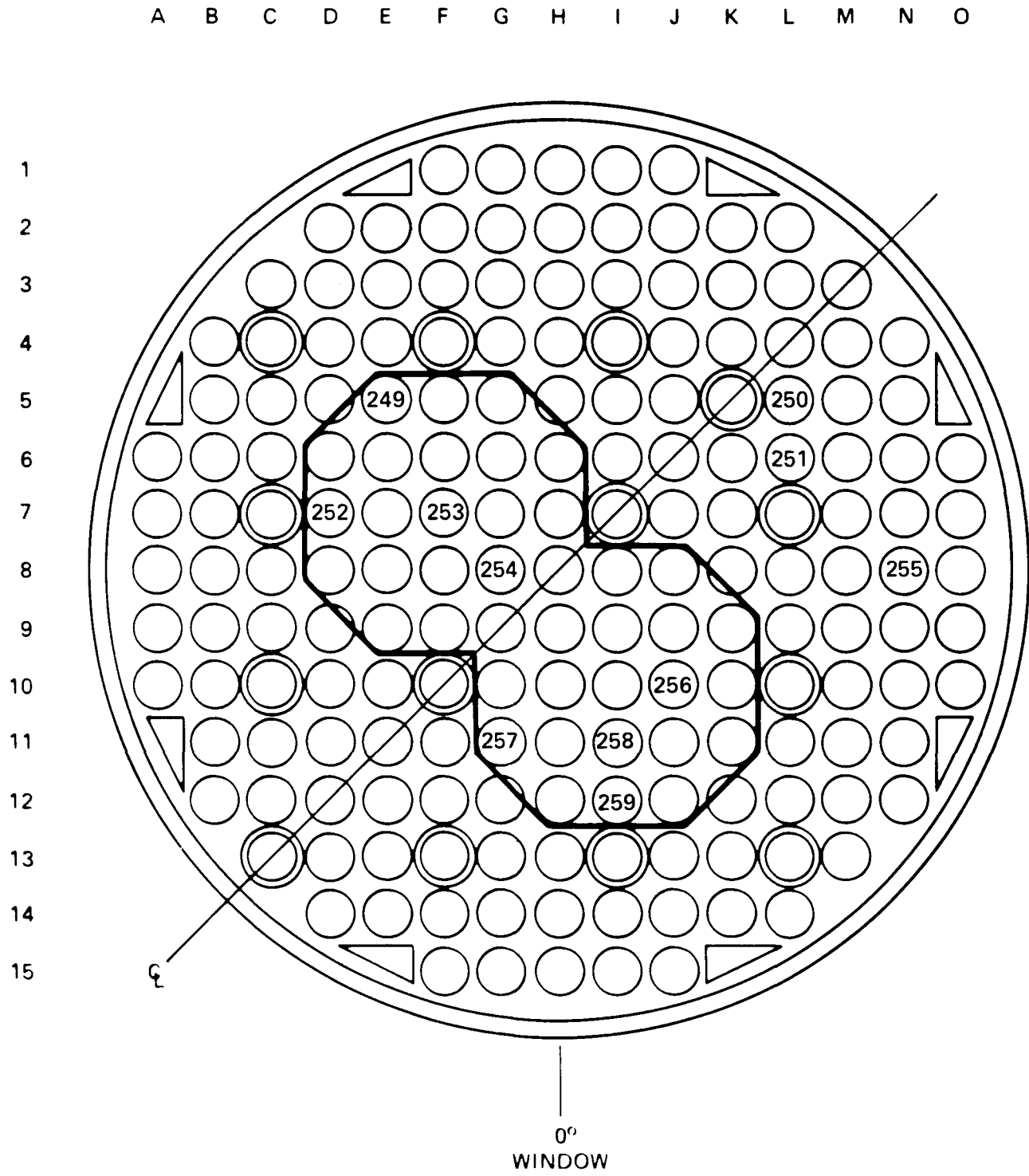


Figure F-20. Heater Rod Instrumentation, 2.06 m (81 in.) Elevation

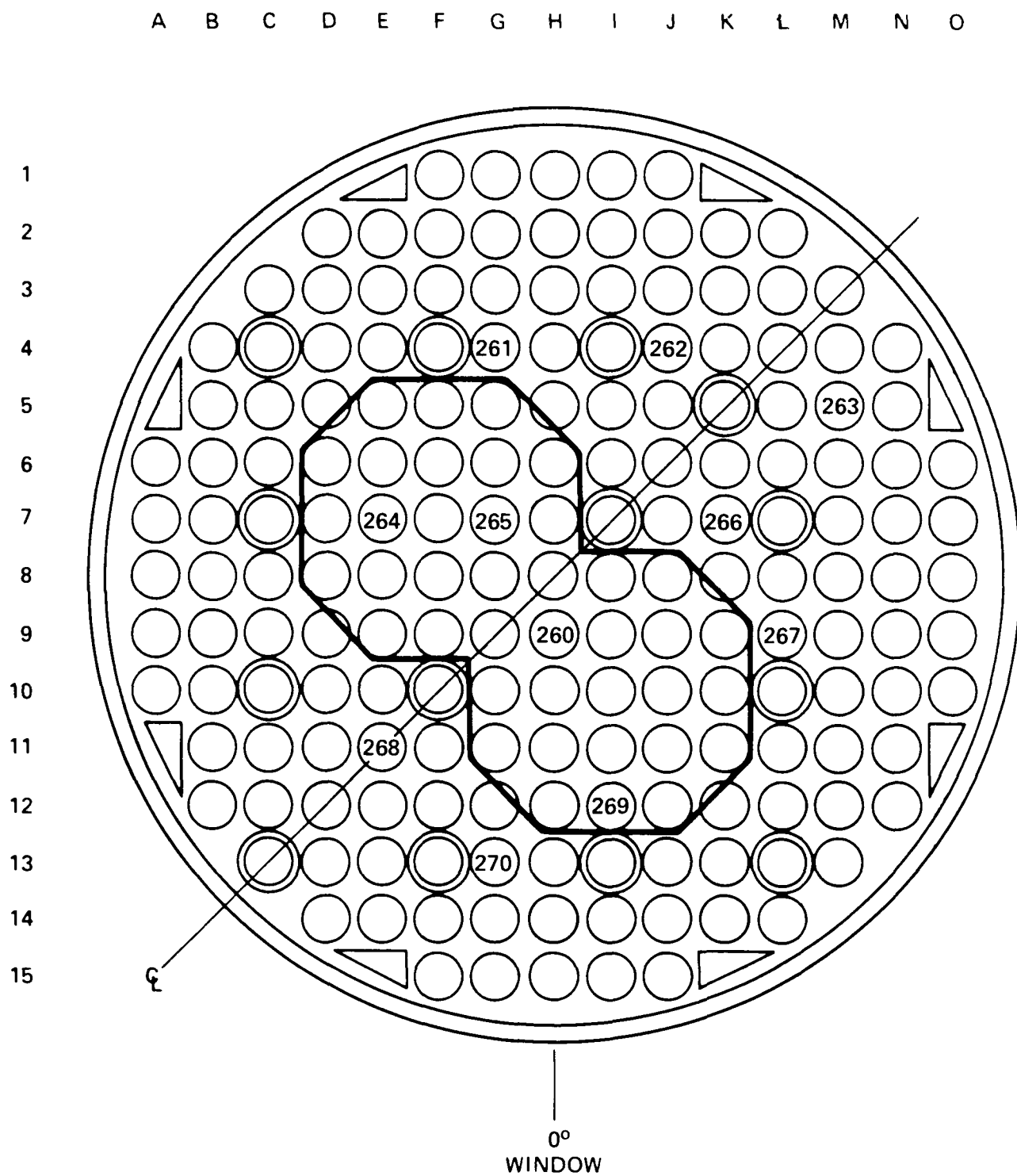


Figure F-21. Heater Rod Instrumentation, 2.13 m (84 in.) Elevation

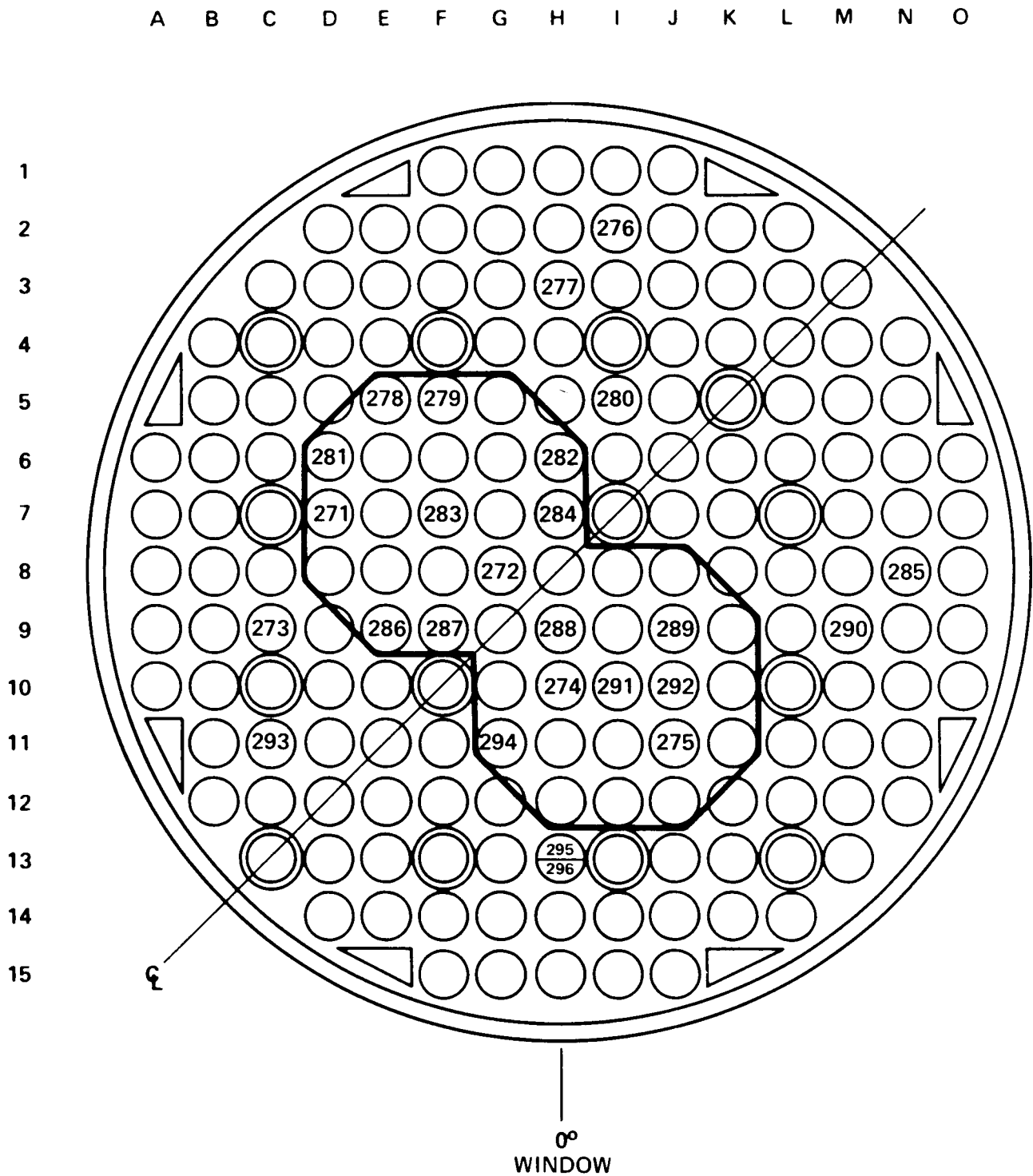


Figure F-22. Heater Rod Instrumentation, 2.18 m (86 in.) Elevation

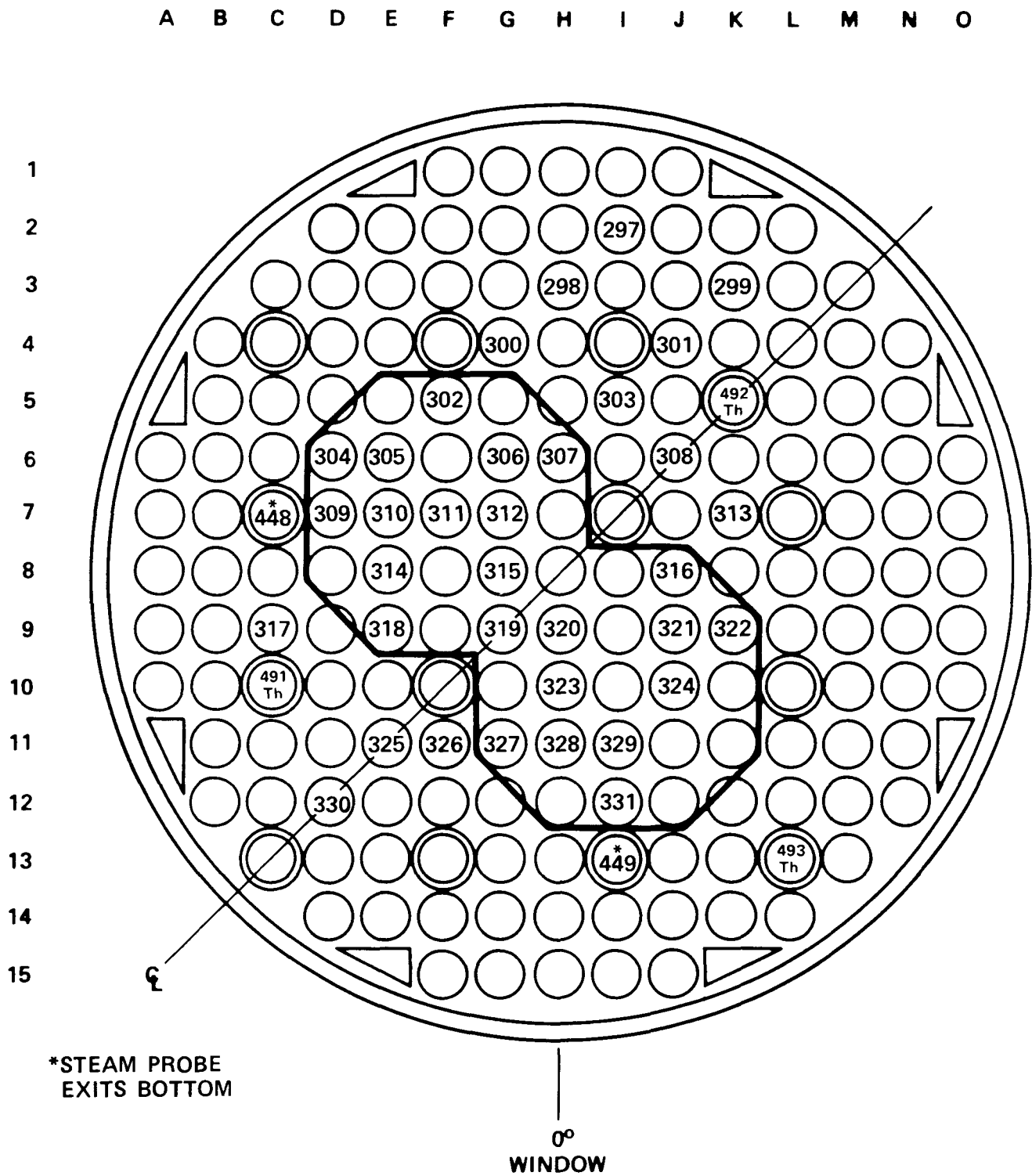


Figure F-23. Heater Rod Instrumentation, 2.29 m (90 in.) Elevation

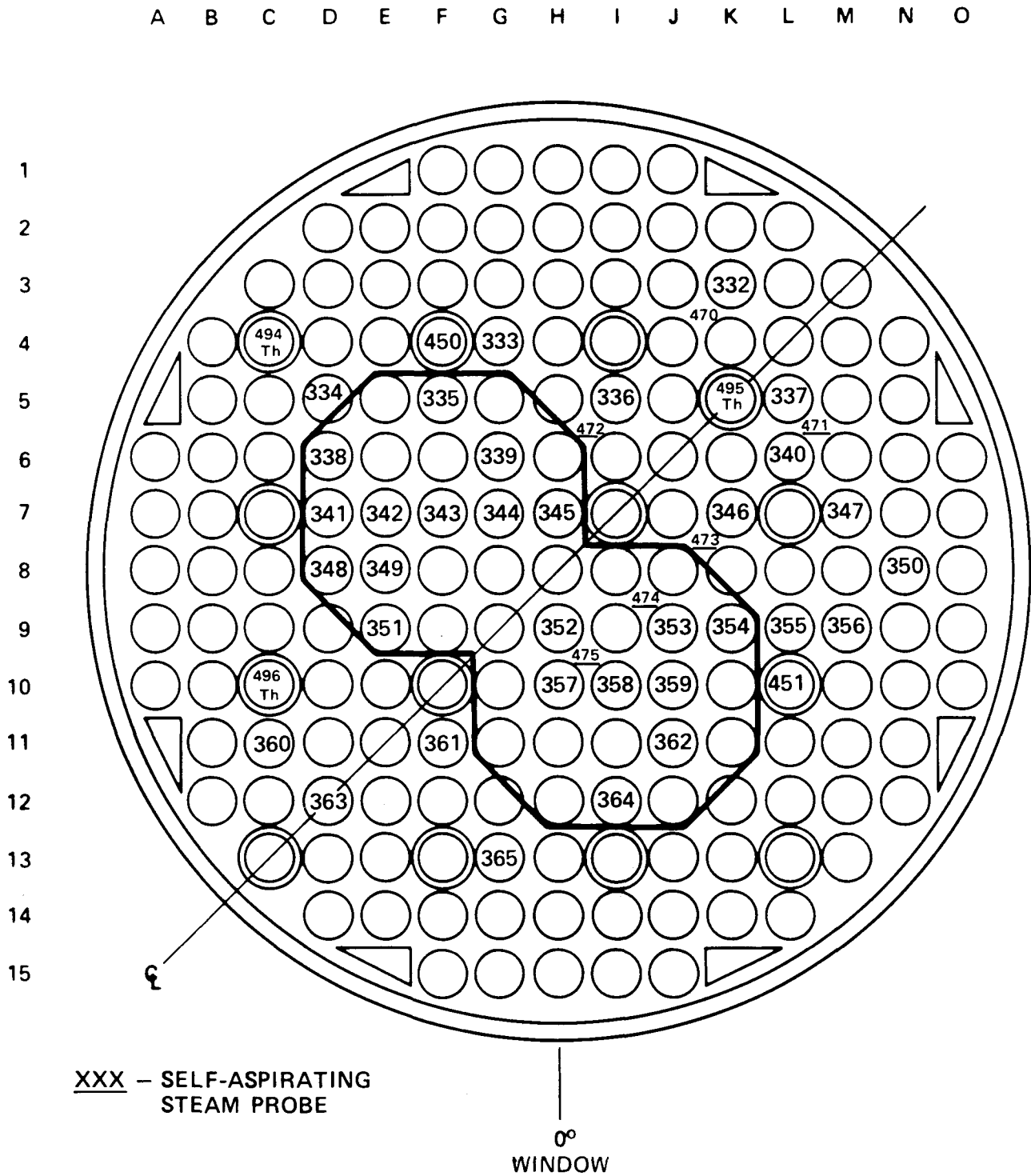


Figure F-24. Heater Rod Instrumentation, 2.44 m (96 in.) Elevation

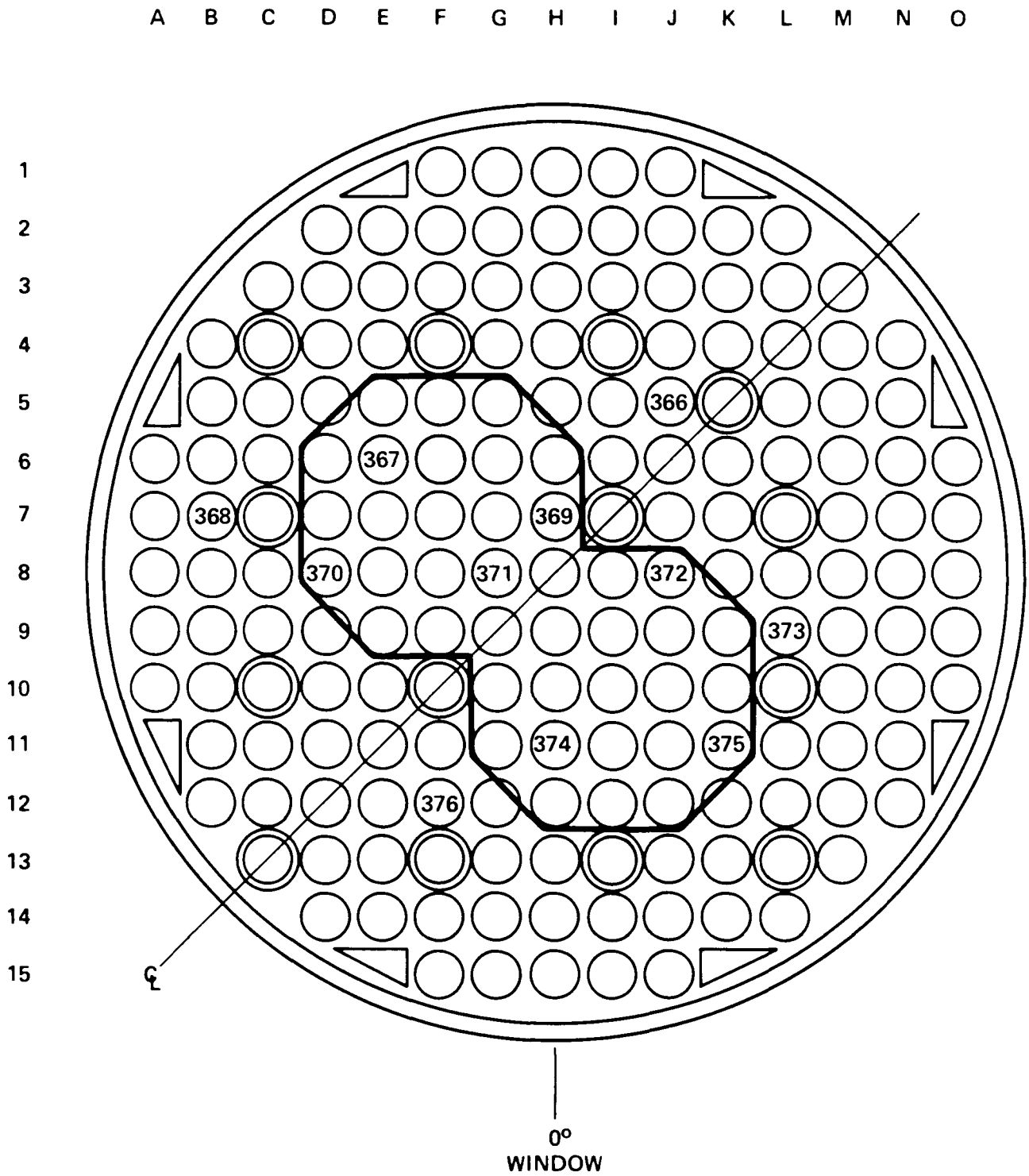


Figure F-25. Heater Rod Instrumentation, 2.59 m (102 in.) Elevation

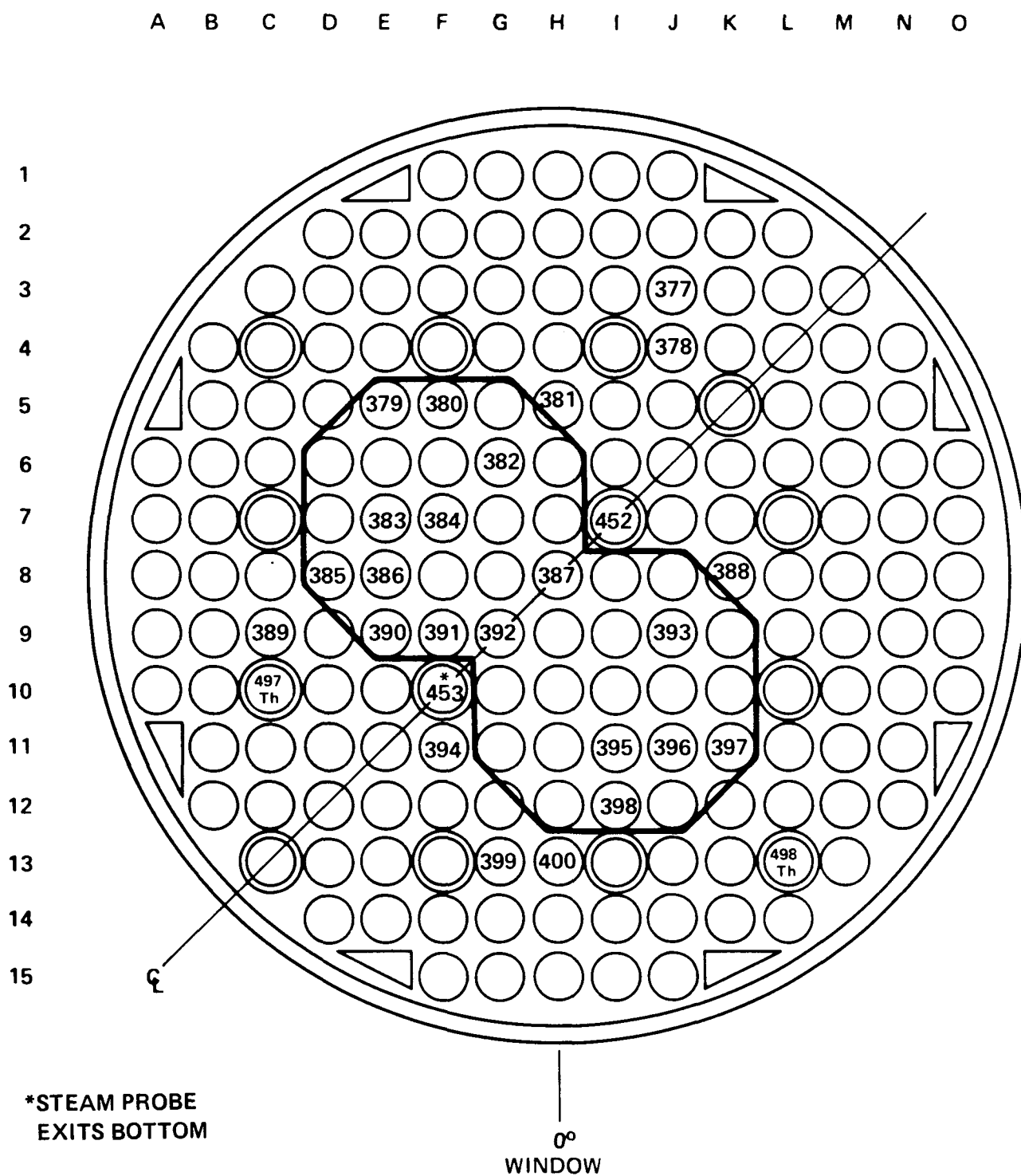


Figure F-26. Heater Rod Instrumentation, 2.82 m (111 in.) Elevation

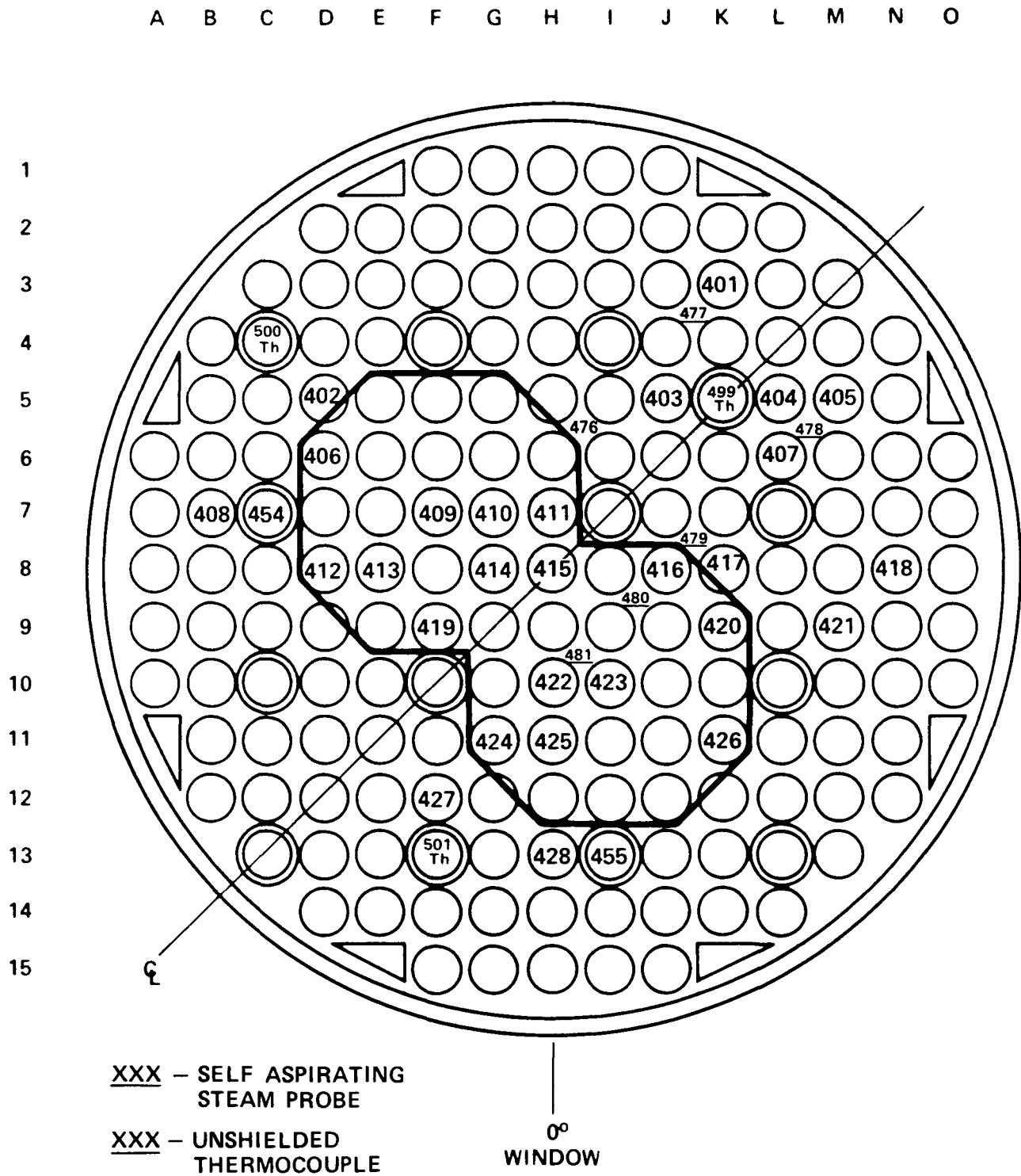


Figure F-27. Heater Rod Instrumentation, 3.05 m (120 in.) Elevation

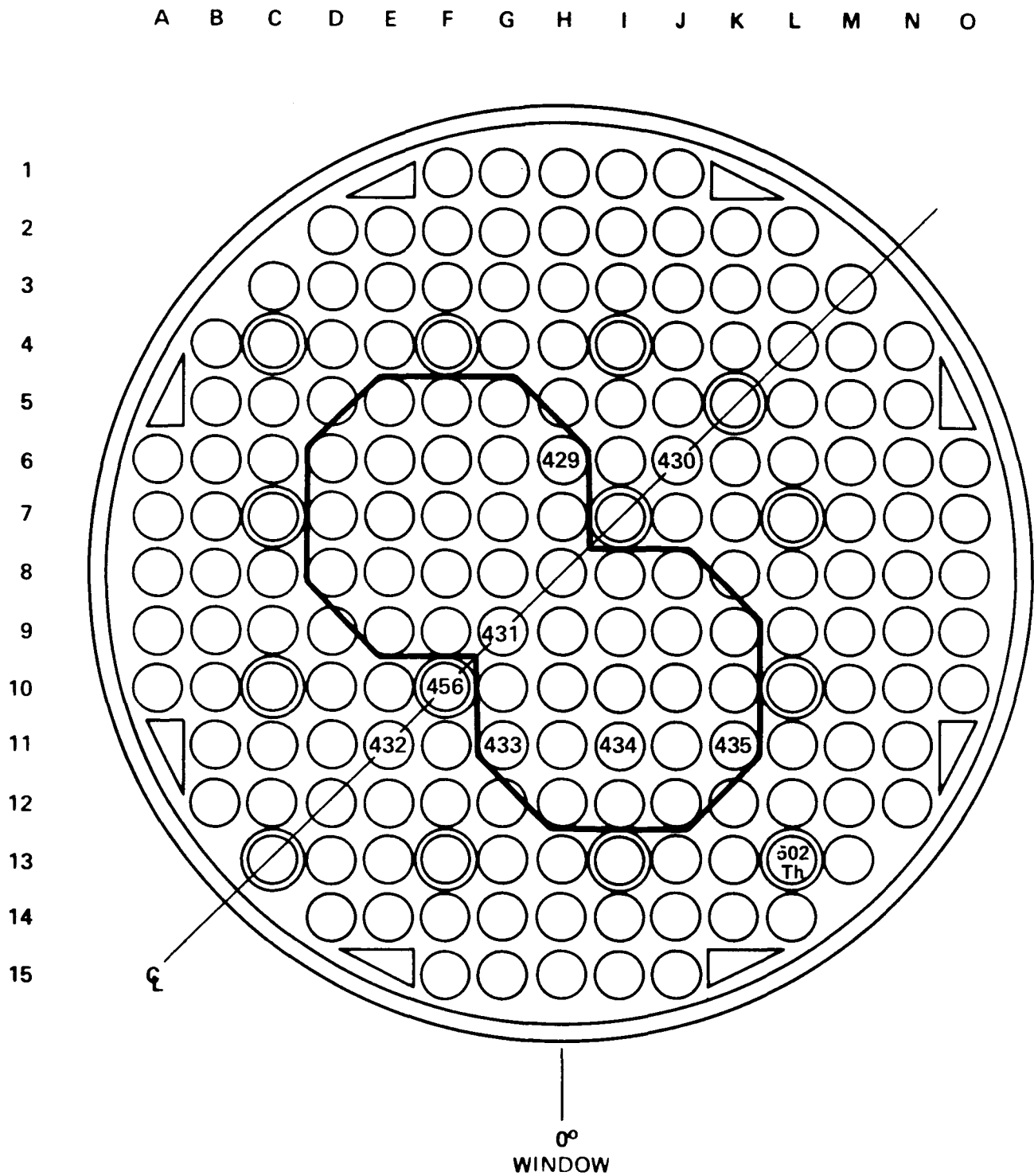


Figure F-28. Heater Rod Instrumentation, 3.35 m (132 in.) Elevation

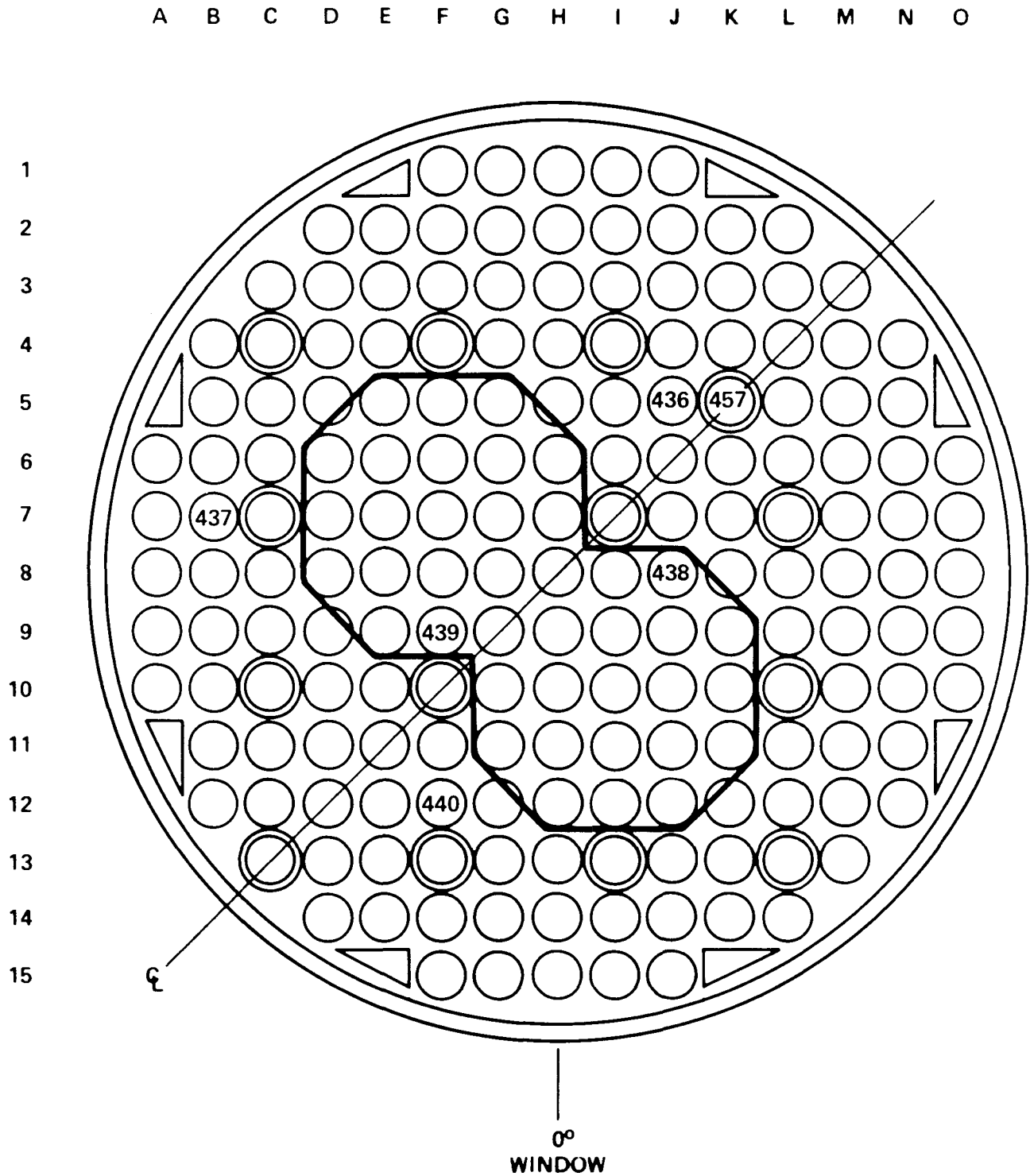


Figure F-29. Heater Rod Instrumentation, 3.50 m (138 in.) Elevation

TABLE F-1
BUNDLE FAILED THERMOCOUPLES

Run	Failed Thermocouples
60701	Channel 461 - bare fluid vapor temperature 1.47 m (58 in.)
61106	Channel 81 - heater rod temperature 12L 1.82 m (72 in.)
	Channel 351 - heater rod temperature 9E 2.44 m (96 in.)
61314	Channel 156 - heater rod temperature 5H 1.96 m (77 in.)
	Channel 181 - heater rod temperature 2I 1.98 m (78 in.)
	Channel 487 - thimble wall temperature 13F 1.82 m (72 in.)
	Channel 501 - thimble wall temperature 13F 3.05 m (120 in.)
61412	Channel 363 - heater rod temperature 12D 2.44 m (96 in.)
	Channel 490 - thimble wall temperature 13F 1.98 m (78 in.)
61509	Channel 222 - heater rod temperature 6D 2.01 m (79 in.)
	Channel 48 - heater rod temperature 11I 1.70 m (67 in.)
61607	Channel 148 - heater rod temperature 8E 1.96 m (77 in.)
	Channel 212 - heater rod temperature 11G 2.01 m (79 in.)
	Channel 338 - heater rod temperature 6D 2.44 m (96 in.)
	Channel 492 - thimble wall temperature 5K 2.29 m (90 in.)
61705	Channel 163 - heater rod temperature 9D 1.96 m (77 in.)
	Channel 488 - thimble wall temperature 5K 1.98 m (78 in.)
61916	Channel 116 - heater rod temperature 4J 1.91 m (75 in.)
62117	Channel 197 - heater rod temperature 11K 1.98 m (78 in.)
	Channel 330 - heater rod temperature 12D 2.24 m (90 in.)
62211	Channel 459 - bare fluid vapor temperature 1.47 m (58 in.)
62304	Channel 495 - thimble wall temperature 5K 2.44 m (96 in.)
62413	Channel 485 - thimble wall temperature 5K 1.82 m (72 in.)
62503	Channel 460 - bare fluid vapor temperature 1.47 m (58 in.)
62819	Channel 304 - heater rod temperature 6D 2.24 m (90 in.)

TABLE F-2
THIMBLE THERMOCOUPLE REASSIGNMENTS

Run	Reassigned Thermocouples
61412	Channel 487 - thimble 13L 1.83 m (72 in.) Channel 501 - thimble 10C 3.05 m (120 in.)
61509	Channel 490 - thimble 4C 1.98 m (78 in.)
61705	Channel 492 - thimble 13F 2.44 m (96 in.)
61810	Channel 488 - thimble 4C 2.82 m (111 in.)

APPENDIX G

HIGH-SPEED DROPLET MOVIE RESULTS

G-1. INTRODUCTION

In the 163-rod blocked bundle task, high-speed black and white motion pictures were taken through the housing windows at the 0.91 m (36 in.) and 2.73 m (108 in.) elevations for selected test runs. These motion pictures were utilized to determine the density and size distribution of droplets contained in the flow, as well as the droplet velocity, to provide a calculation of the heat transfer in the dispersed flow regime preceding the quench front during bundle reflood. The techniques previously developed and utilized for measuring droplet size and velocity in the 161-rod unblocked bundle were also used for the 163-rod blocked bundle. No movies were taken at the 1.83 m (36 in.) elevation window because the blockage sleeves prevented the use of backlighting.

A summary of the high-speed droplet movies is provided in table G-1 as a function of the test run number. The time of the movie after flow initiation is tabulated as well as an assessment of the film quality. In the early tests (runs 61005, 61106, and 61412), the movies at the 0.91 m (36 in.) window were taken at a time in the reflood transient when excessive amounts of water droplets were present and these drops were indistinguishable. At the 2.73 m (108 in.) window, the movie film broke after the camera was turned on for several tests (runs 61106, 61705, 61810, and 62304), because of the large acceleration forces imposed on the film during startup. For several other tests (runs 61412, 61509, and 61607), the film broke after the camera was stopped for the first recording increment, because of the large deceleration forces.

G-2. DROPLET MEASUREMENTS

A movie film was taken of a pair of perpendicular scales at the same focal distance as the droplets in the rod bundle (between the third and seventh rod rows). The film of the scales was then projected onto a wall such that the dimensions of the scales were larger by a factor of four than the actual size.

TABLE G-1
SUMMARY OF HIGH-SPEED DROPLET PHOTOGRAPHY

Run	Initial Test Conditions	Window Elevation [m (in.)]	Film Speed (frames/sec)	Time of Movie (sec)	Lighting	Focus	Remarks
61005	38 mm/sec (1.5 in./sec)	0.91 (36)	2000	14-26 34-40	-- --	-- --	Too much water Too much water
		2.74 (108)	2000	--	--	--	Film damaged
61106	25 mm/sec (0.98 in./sec)	0.91 (36)	2000	8-14 20-26 40-46	Good -- --	Good -- --	Too much water Too much water Film broke
		2.74 (108)	--	--	--	--	
61412	0.41 MPa (60 psia)	0.91 (36)	2000	6-12 18-24 30-36	Good -- --	Good -- --	Too much water Too much water Film broke after first stop and speed too slow
		2.74 (108)	2000	18-24	Good	Good	First 7.5 seconds only
61509	0.14 MPa (20 psia)	0.91 (36)	2000	10-32.5	Good	Good	Film broke after first stop and speed too slow
		2.74 (108)	2000	20-26	Good	Good	First 15 seconds only
61607	20 mm/sec (0.8 in./sec)	0.91 (36)	2000	4-26.5	Poor	Good	Film broke after first stop and speed too slow
		2.74 (108)	2000	20-26	Good	Poor	First 7.5 seconds only
61705	Repeat test at 38.6 mm/sec (1.52 in./sec)	0.91 (36)	2000	0-22.5	Poor	Fair	Film broke
		2.74 (108)	2500	--	--	--	

TABLE G-1 (cont)
SUMMARY OF HIGH-SPEED DROPLET PHOTOGRAPHY

Run	Initial Test Conditions	Window Elevation [m (in.)]	Film Speed (frames/sec)	Time of Movie (sec)	Lighting	Focus	Remarks
61810	17 mm/sec (0.65 in./sec) at 0.134MPa (19.5 psia)	2.74 (108)	2500	--	--	--	Film broke
61916	Stepped flow	0.91 (36)	2000	0-22.5	Good	Good	First 3 seconds only
		2.74 (108)	2500	10-28	Good	Good	
62015	Subcooling	0.91 (36)	2000	10-32.5	Good	Good	First 7.5 seconds only
		2.74 (108)	2500	18-36	Good	Fair	
62117	Hot/cold channels at 20 mm/sec (0.8 in./sec)	0.91 (36)	2000	4-26	Good	Good	
		2.74 (108)	2500	10-28	Poor	Poor	
62304	157 mm/sec (6.2 in./sec)	0.91 (36)	2000	0-22.5	Good	Good	First 3 seconds only
		2.74 (108)	2500	--	--	--	Film broke
62413	3.3 kw/m (1 kw/m)	0.91 (36)	2000	0-22.5	Good	Good	First 7.5 seconds only
		2.74 (108)	2500	6-24.5	Poor	Poor	Speed too slow
62605	Repeat test at 38 mm/sec (1.5 in./sec)	0.91 (36)	2000	0-22.5	Good	Good	First 7.5 seconds only
		2.74 (108)	2500	4-22	Poor	Fair	Speed too slow

The droplet films were subsequently projected onto the wall at exactly the same distance from the wall as the film of the scales. This procedure eliminated the uncertainty associated with using either the heater rod or the window as the reference dimension. In most tests, the diameter of the rod was found to be approximately 10.07 mm (0.3966 in.), which was only 6 percent larger than the rod actual size. The difference may be attributed to a slight rod misalignment or optical illusion.

The droplet movies were projected onto a fine-scale graph paper (readable to ± 0.5 mm) attached to the wall. A Lafayette Analyst model D projector which has frame-by-frame stop control was utilized. The clear and distinct droplets were traced directly on the graph paper and those which could be seen to travel some distance within the gap between the rods were considered for calculating droplet velocity. The droplets were identified with numbers and their initial and final positions were traced onto the graph paper. The number of movie frames between the initial and final positions was also recorded.

G-3. DATA REDUCTION

The droplet diameter and distance travelled were measured directly from the graph paper and tabulated. The actual or real drop diameter and velocity were obtained from the following simple relationships:

$$D_r = \frac{D_m}{S}$$

$$X_r = \frac{X_m}{S}$$

$$V_D = \frac{X_r}{N} \times \frac{FS}{1000}$$

where

D_r	= real drop diameter (mm)
D_m	= measured drop diameter (mm)
S	= scale factor = 4
X_r	= real distance travelled (mm)
X_m	= measured distance travelled (mm)

V_D = droplet velocity (m/sec)
N = number of movie frames for droplet to travel X_m
FS = film speed (frames/sec)

In the final stage of the data reduction process, it was found that the film speed at the 2.74 m (108 in.) elevation (2500 frames per second) was too slow for accurate deduction of the droplet diameter. (A preliminary review of the high-speed movies after run 61607 had led to the conclusion that the film speed should be increased from 2000 frames per second.) There was only one test (run 61916) in which the data at the 2.74 m (108 in.) elevation were accurately reduced.

G-4. DATA RESULTS

The frequency distributions for droplet diameters were obtained and are shown graphically in figures G-1 through G-12. The droplet velocity versus droplet diameter plots are shown in figures G-13 through G-24.

These droplet data results were generally very similar to the results from the 161-rod unblocked bundle. Therefore, the log-normal distribution⁽¹⁾ was utilized to represent the droplet diameter distribution, as previously used in the 161-rod bundle. To evaluate the appropriateness of the log-normal distribution for representing the droplet diameter data, the natural log of the actual drop diameter was plotted against the cumulative probability distribution. If the assumed distribution model is correct, the plotted data points would tend to lie in a straight line. As shown in figures G-25 through G-36, the cumulative probability distribution is quite linear; this indicates that the log-normal distribution is the appropriate representation for the droplet diameter distribution.

1. Loftus, M. J., et al., "PWR FLECHT SEASET Unblocked Bundle, Forced and Gravity Reflood Task Data Report," NRC/EPRI/Westinghouse-7, June 1980.

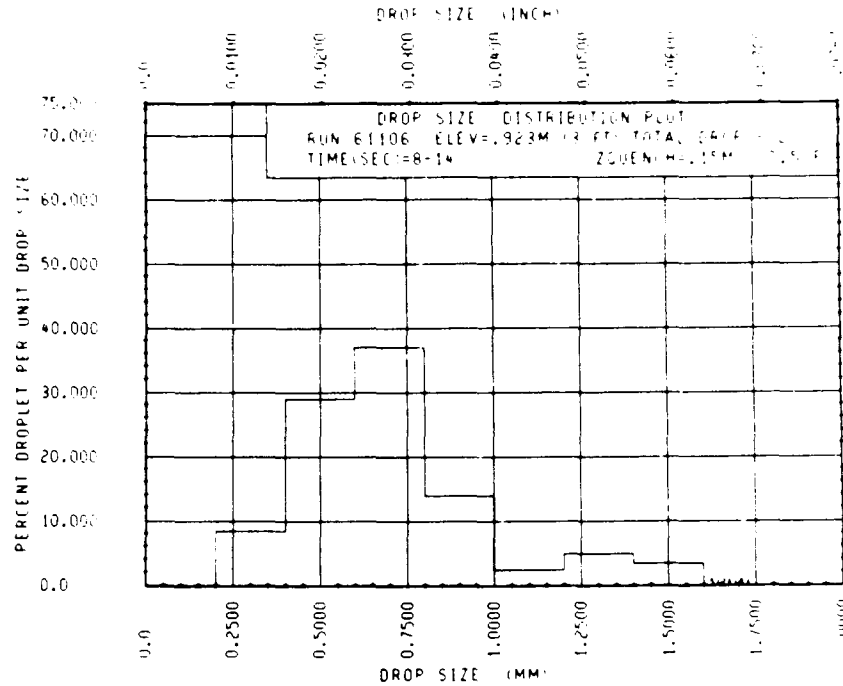


Figure G-1. Droplet Size Frequency Distribution, Run 61106, 0.91 m (36 in.) Elevation

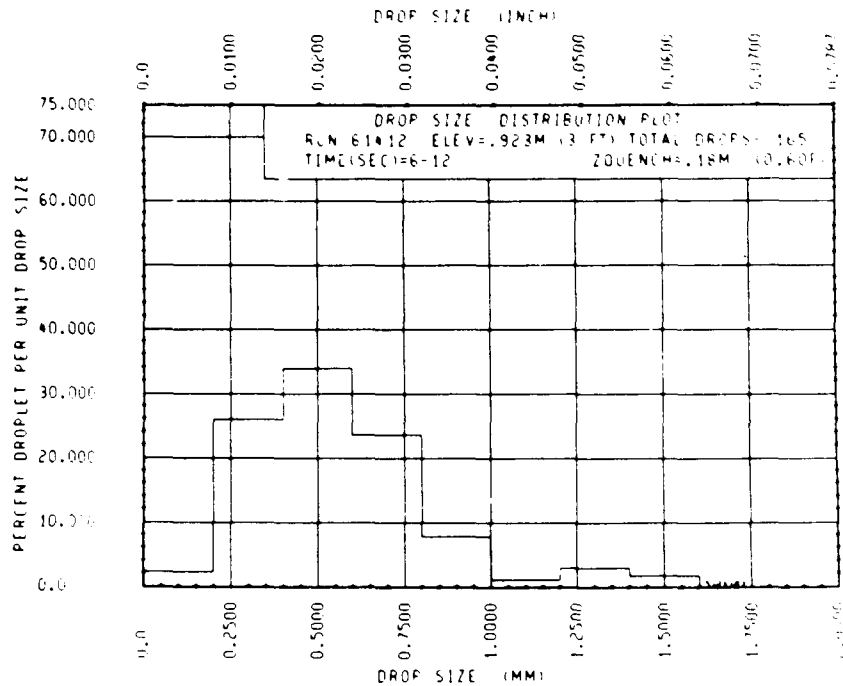


Figure G-2. Droplet Size Frequency Distribution, Run 61412, 0.91 m (36 in.) Elevation

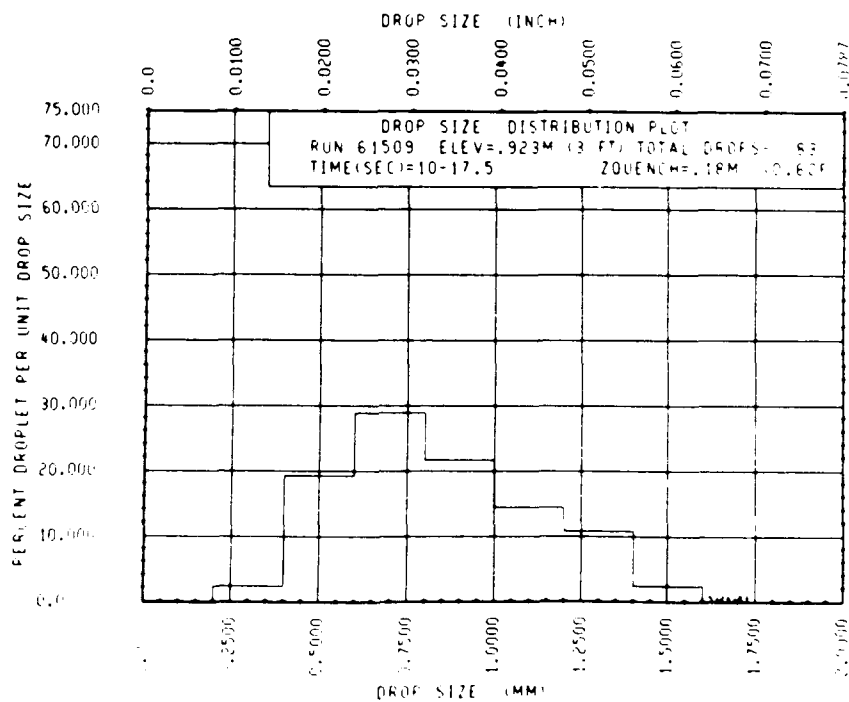


Figure G-3. Droplet Size Frequency Distribution, Run 61509, 0.91 m (36 in.) Elevation

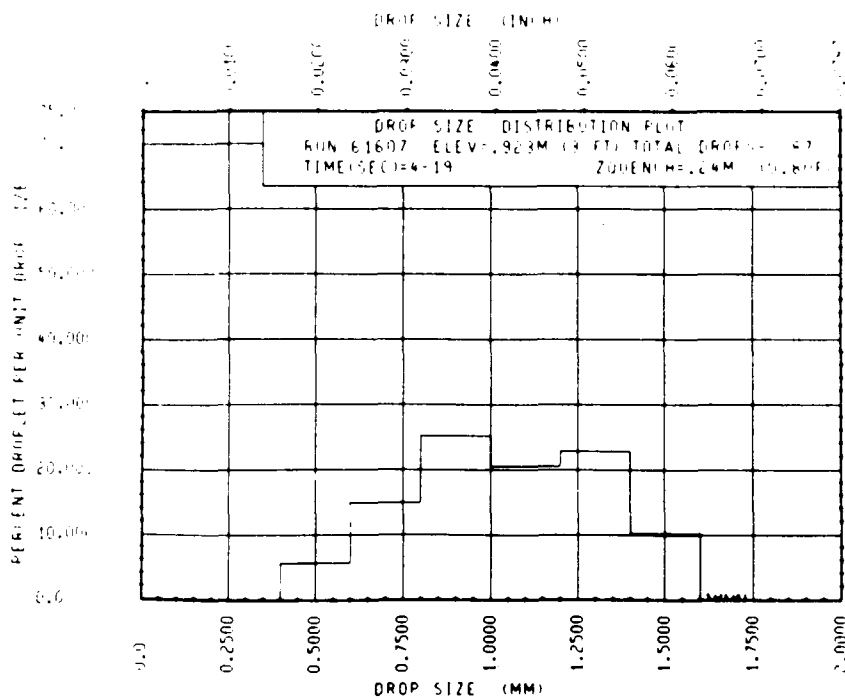


Figure G-4. Droplet Size Frequency Distribution, Run 61607, 0.91 m (36 in.) Elevation

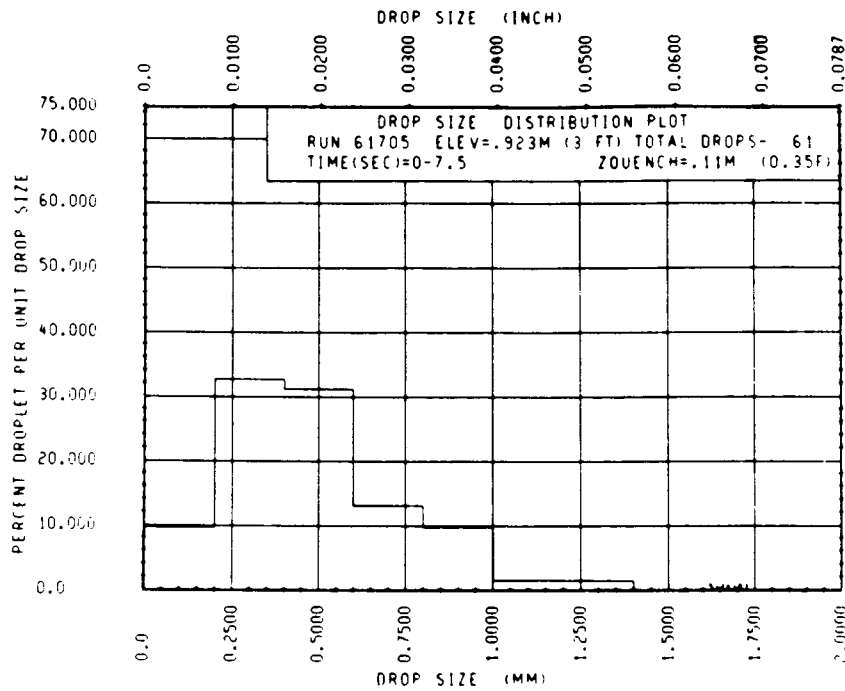


Figure G-5. Droplet Size Frequency Distribution, Run 61705, 0.91 m (36 in.) Elevation

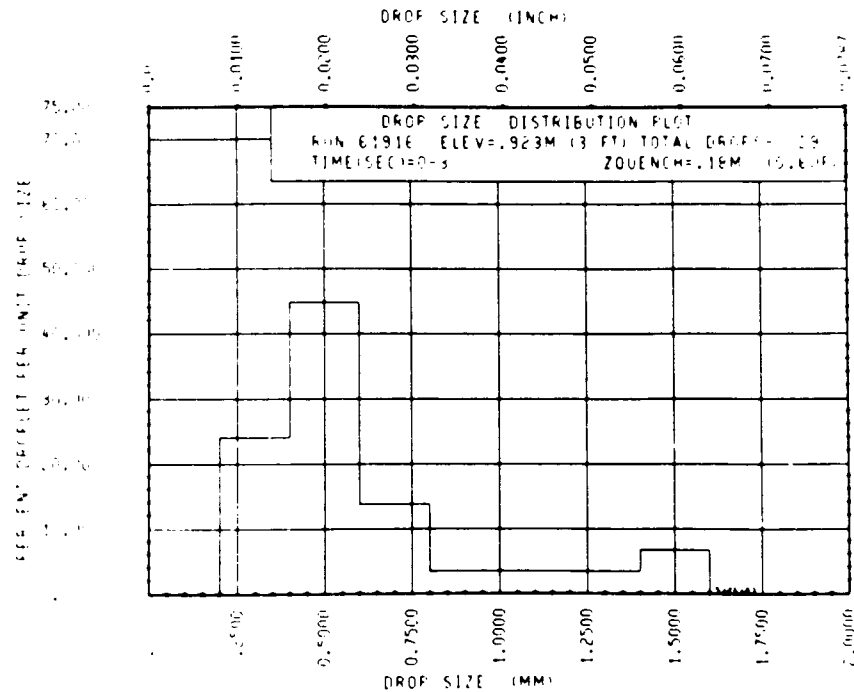


Figure G-6. Droplet Size Frequency Distribution, Run 61916, 0.91 m (36 in.) Elevation

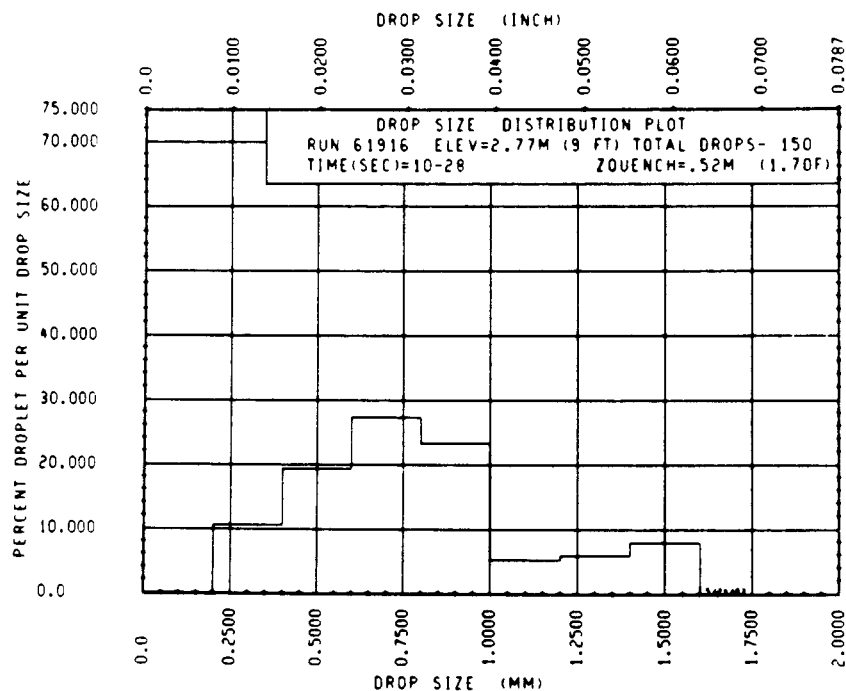


Figure G-7. Droplet Size Frequency Distribution, Run 61916, 2.74 m (108 in.) Elevation

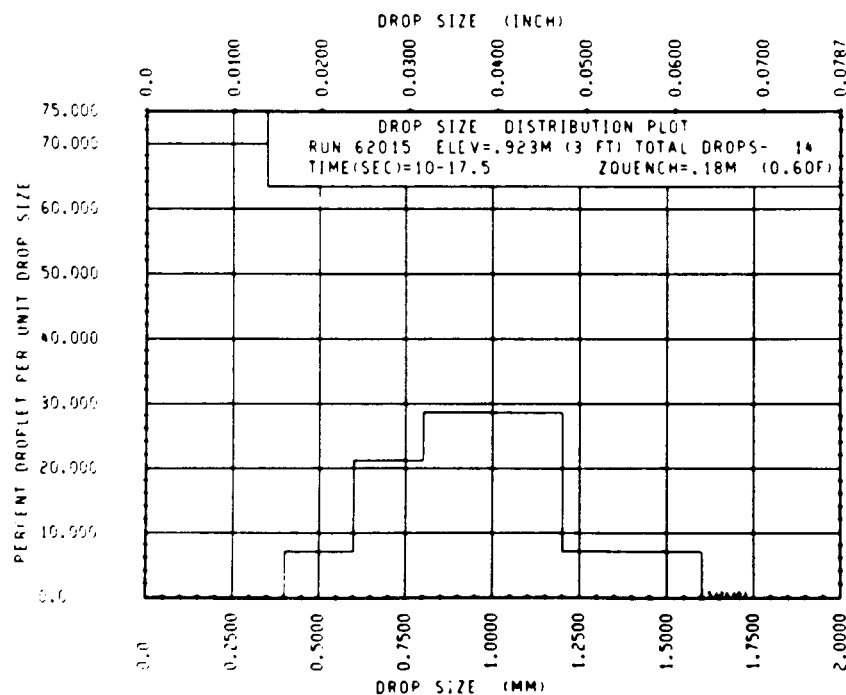


Figure G-8. Droplet Size Frequency Distribution, Run 62015, 0.91 m (36 in.) Elevation

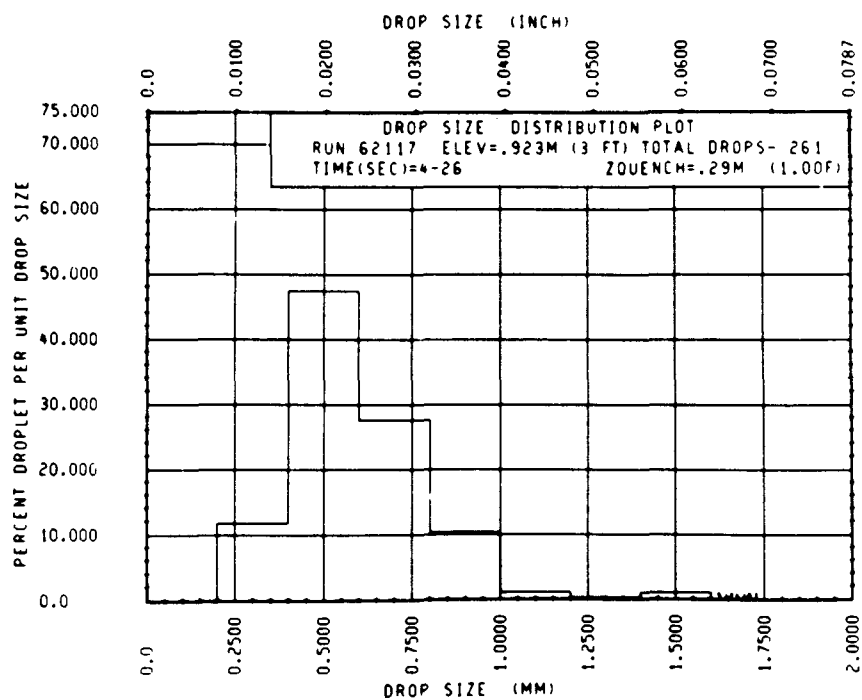


Figure G-9. Droplet Size Frequency Distribution, Run 62117, 0.91 m (36 in.) Elevation

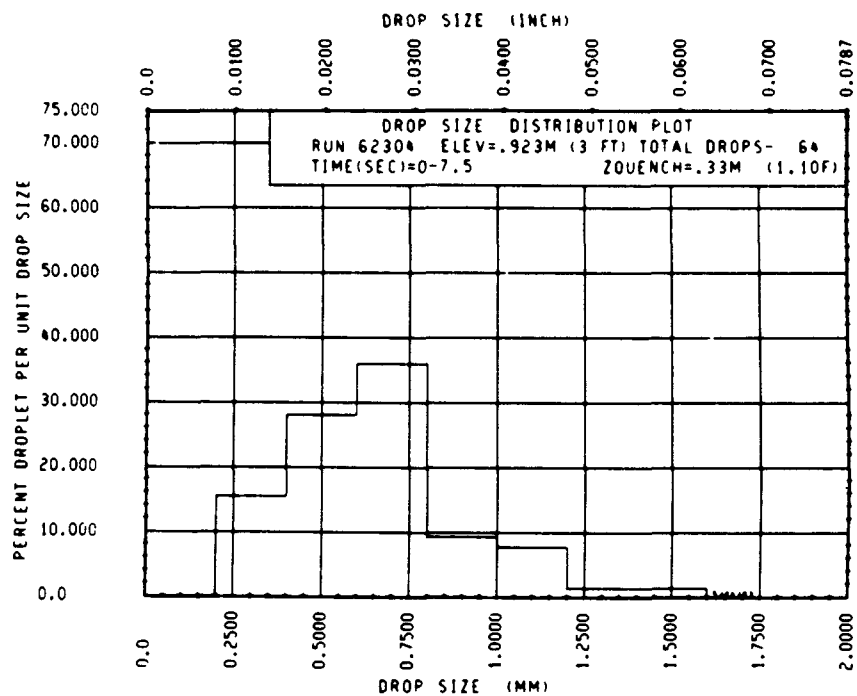


Figure G-10. Droplet Size Frequency Distribution, Run 62304, 0.91 m (36 in.) Elevation

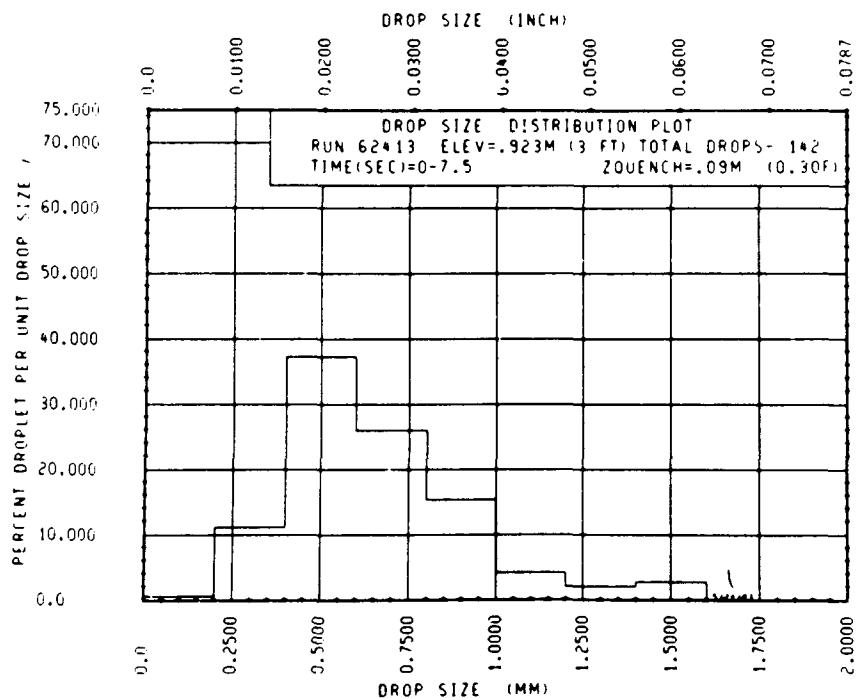


Figure G-11. Droplet Size Frequency Distribution, Run 62413, 0.91 m (36 in.) Elevation

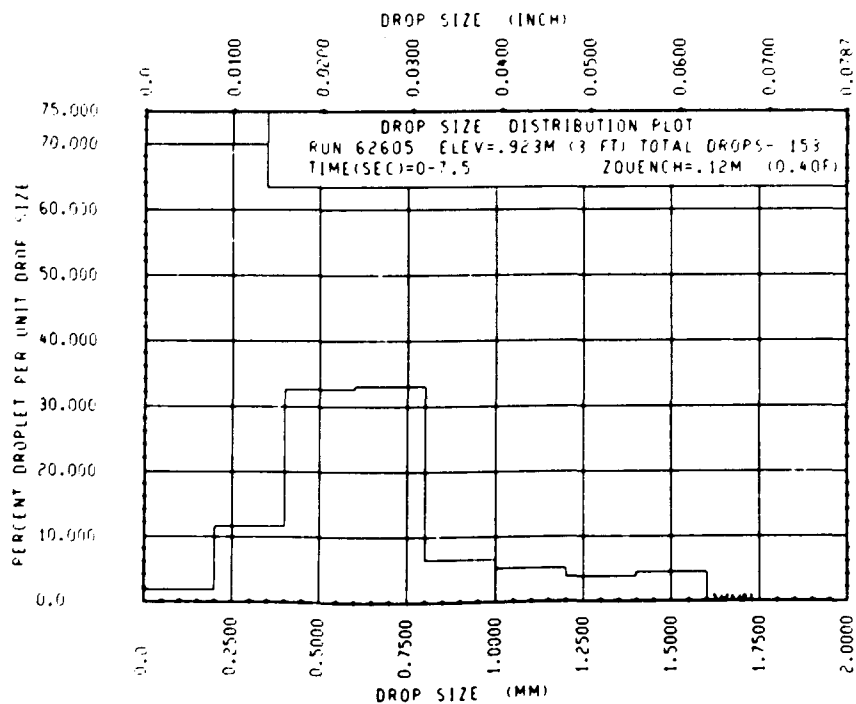


Figure G-12. Droplet Size Frequency Distribution, Run 62605, 0.91 m (36 in.) Elevation

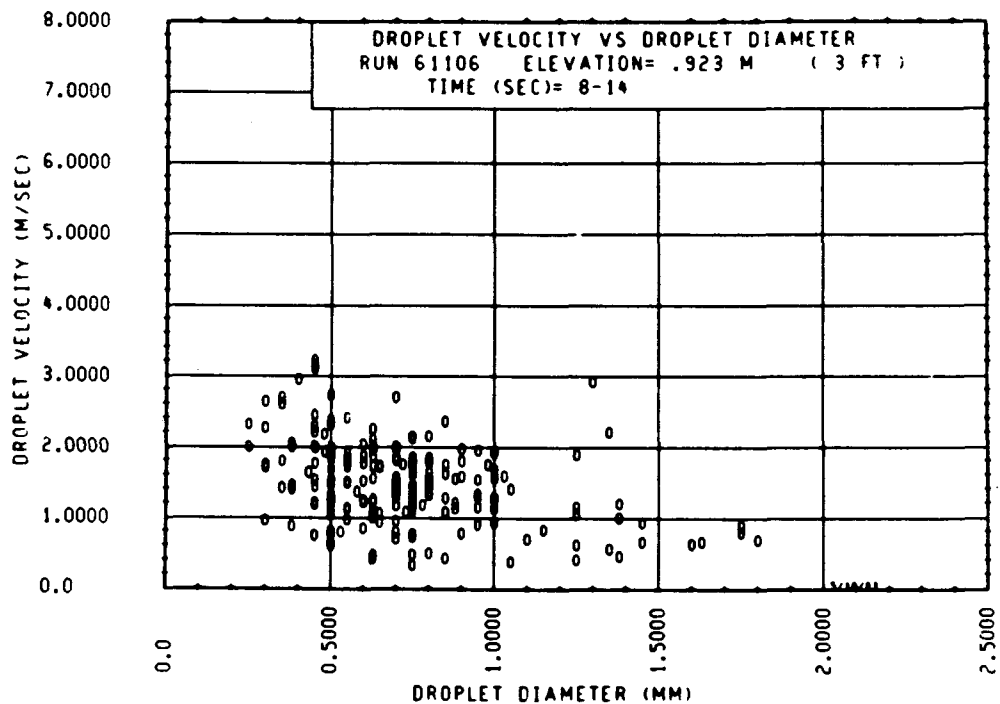


Figure G-13. Droplet Velocity Versus Droplet Diameter, Run 61106, 0.91 m (36 in.) Elevation

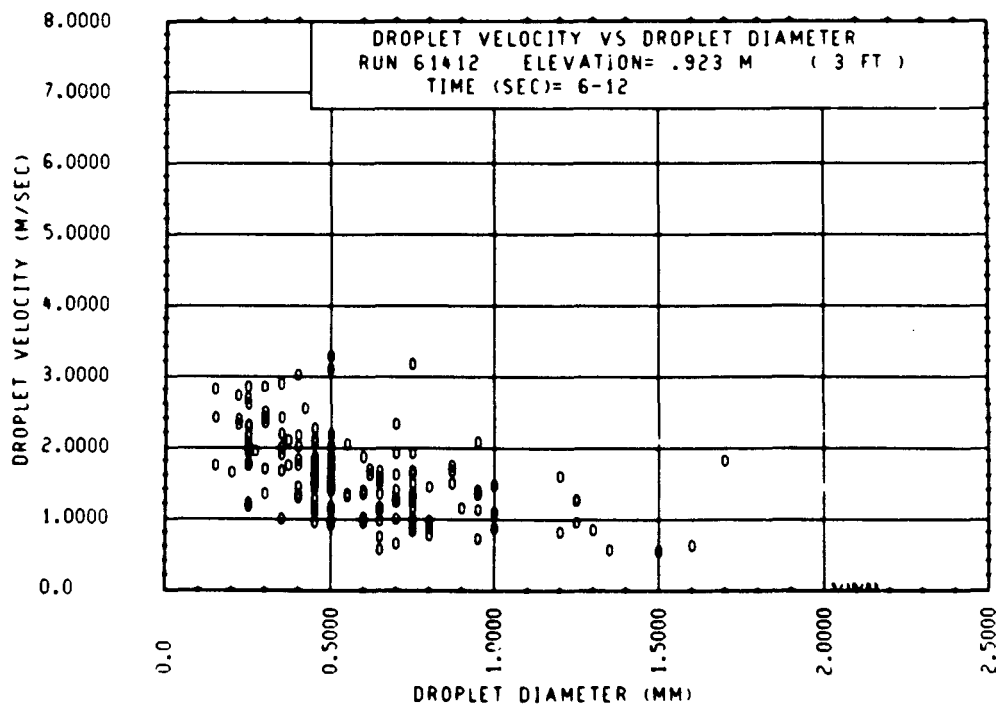


Figure G-14. Droplet Velocity Versus Droplet Diameter, Run 61412, 0.91 m (36 in.) Elevation

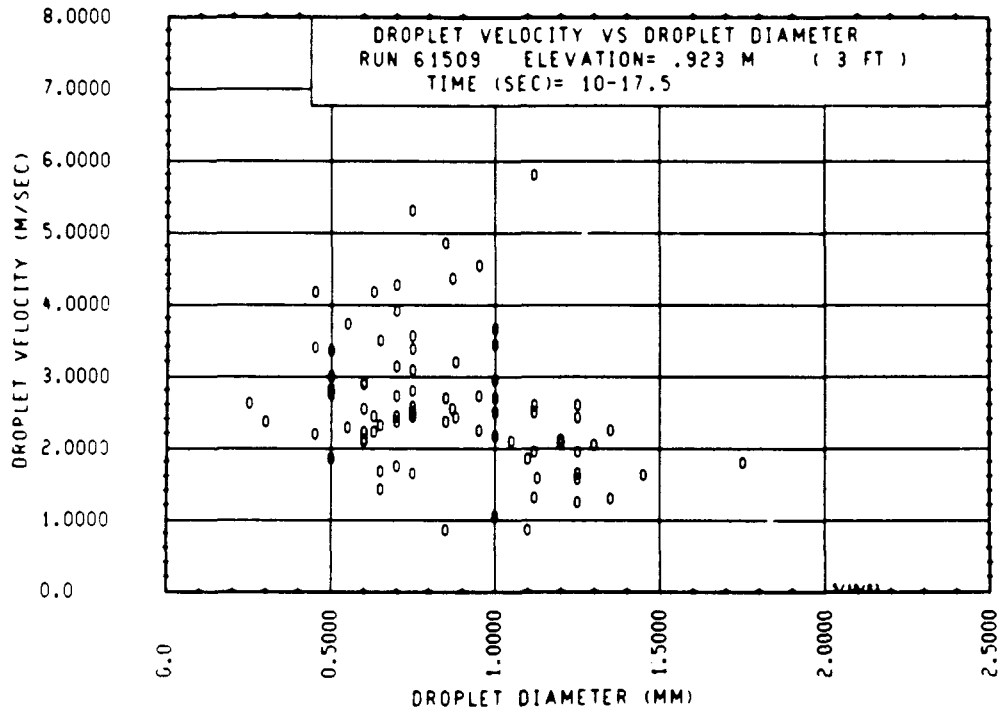


Figure G-15. Droplet Velocity Versus Droplet Diameter, Run 61509, 0.91 m (36 in.) Elevation

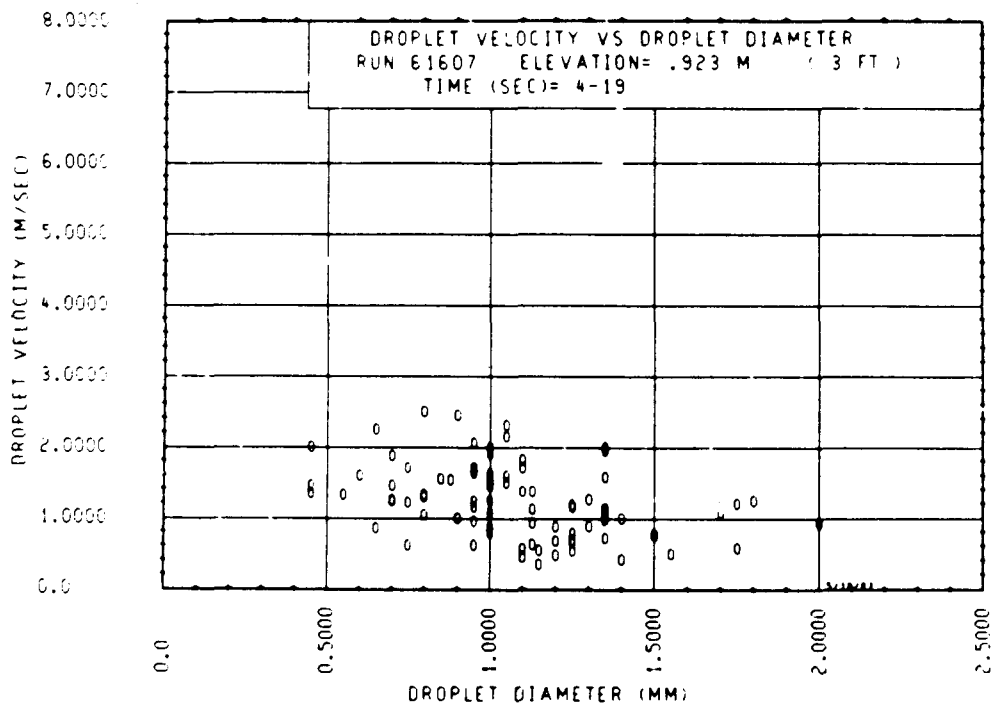


Figure G-16. Droplet Velocity Versus Droplet Diameter, Run 61607, 0.91 m (36 in.) Elevation

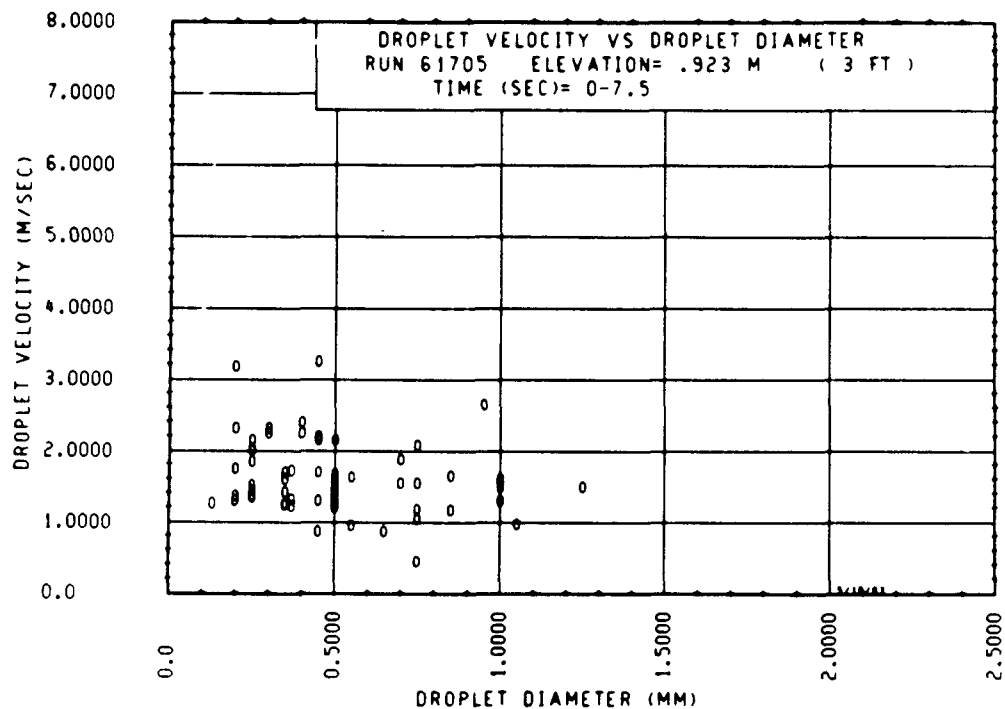


Figure G-17. Droplet Velocity Versus Droplet Diameter, Run 61705, 0.91 m (36 in.) Elevation

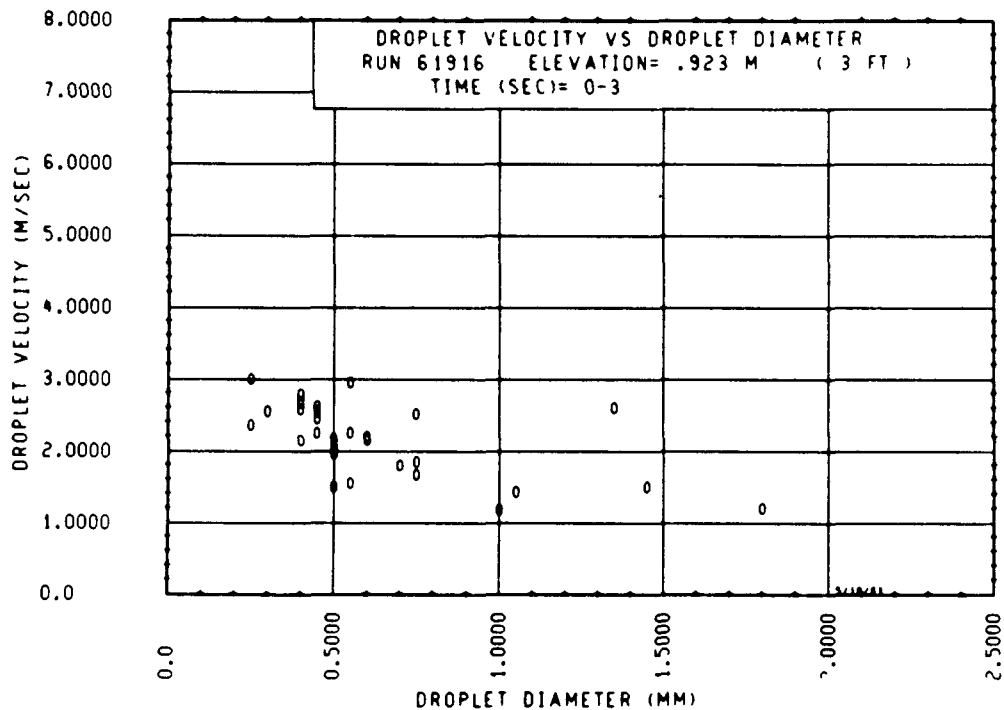


Figure G-18. Droplet Velocity Versus Droplet Diameter, Run 61916, 0.91 m (36 in.) Elevation

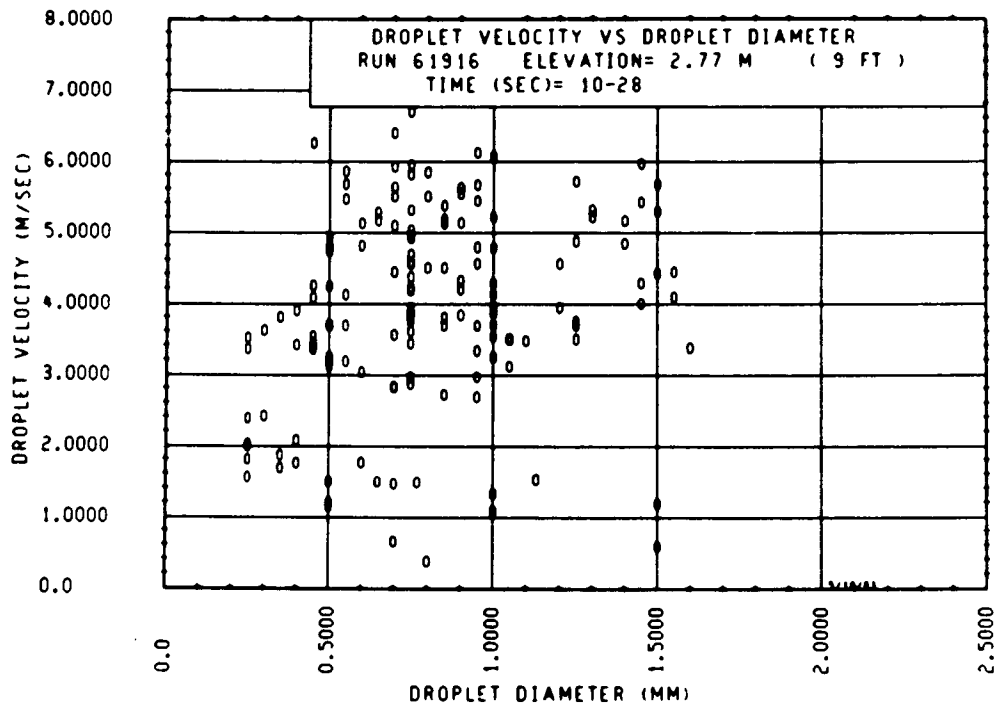


Figure G-19. Droplet Velocity Versus Droplet Diameter, Run 61916, 2.74 m (108 in.) Elevation

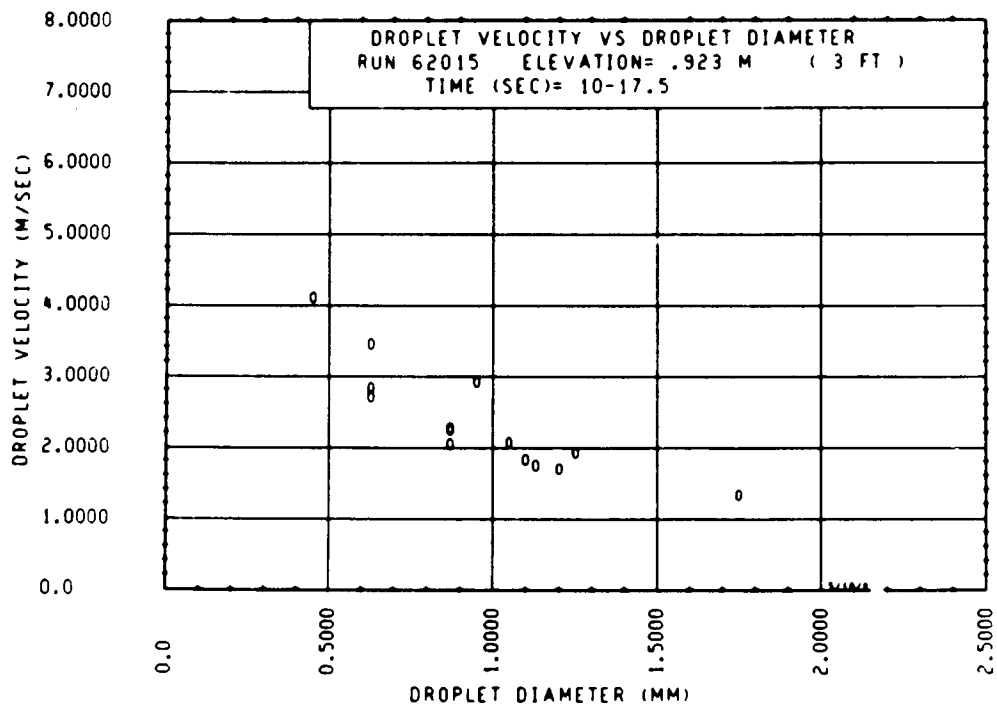


Figure G-20. Droplet Velocity Versus Droplet Diameter, Run 62015, 0.91 m (36 in.) Elevation

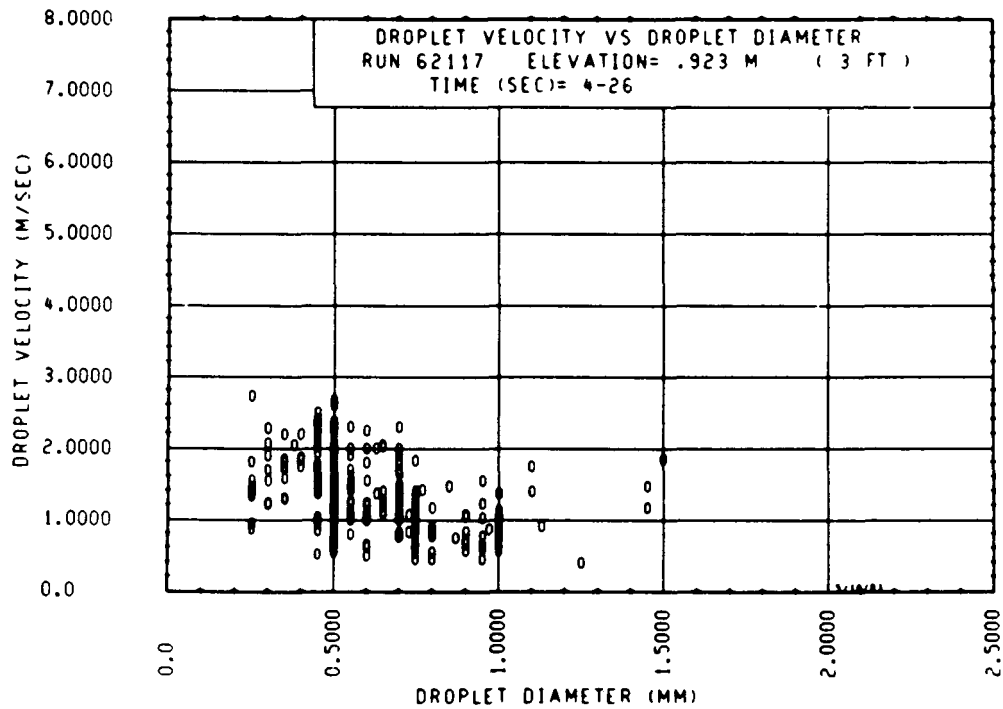


Figure G-21. Droplet Velocity Versus Droplet Diameter, Run 62117, 0.91 m (36 in.) Elevation

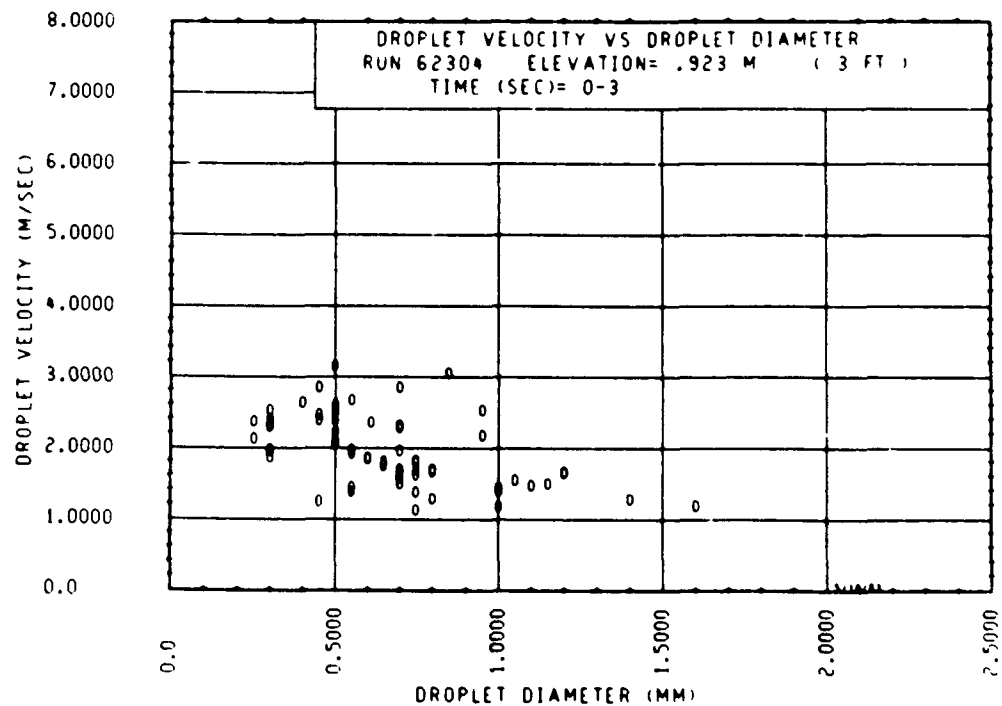


Figure G-22. Droplet Velocity Versus Droplet Diameter, Run 62304, 0.91 m (36 in.) Elevation

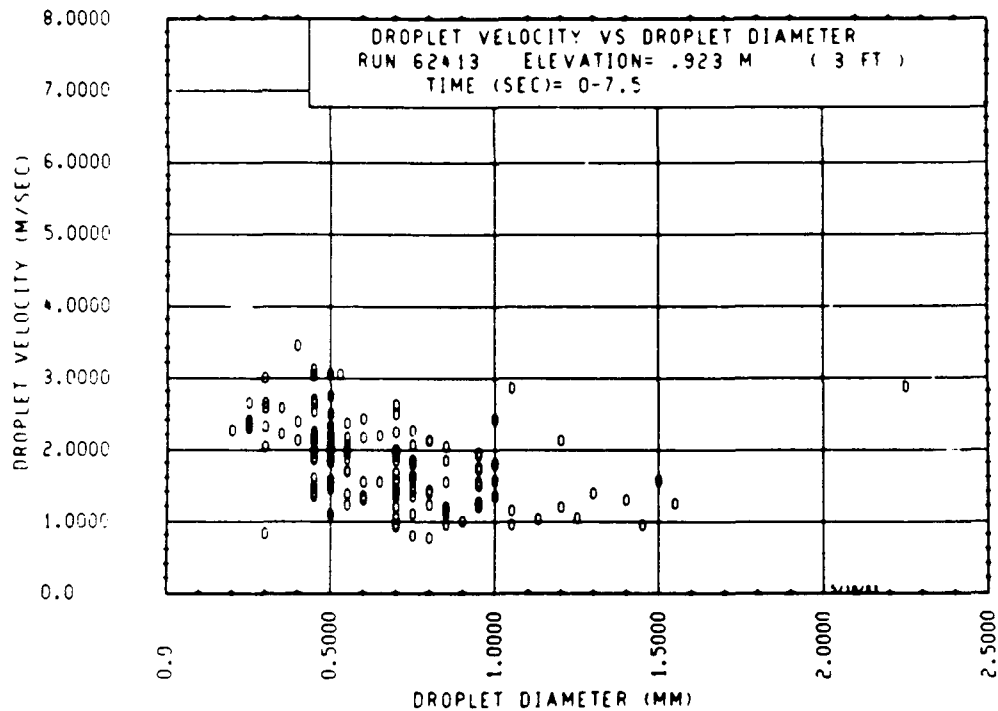


Figure G-23. Droplet Velocity Versus Droplet Diameter, Run 62413, 0.91 m (36 in.) Elevation

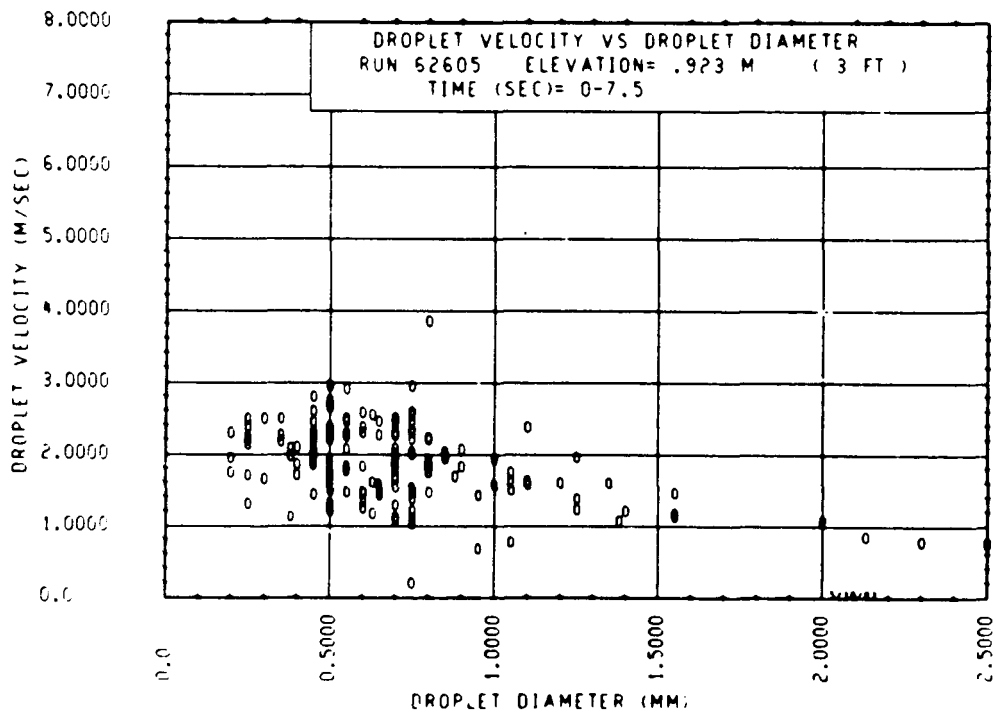


Figure G-24. Droplet Velocity Versus Droplet Diameter, Run 62605, 0.91 m (36 in.) Elevation

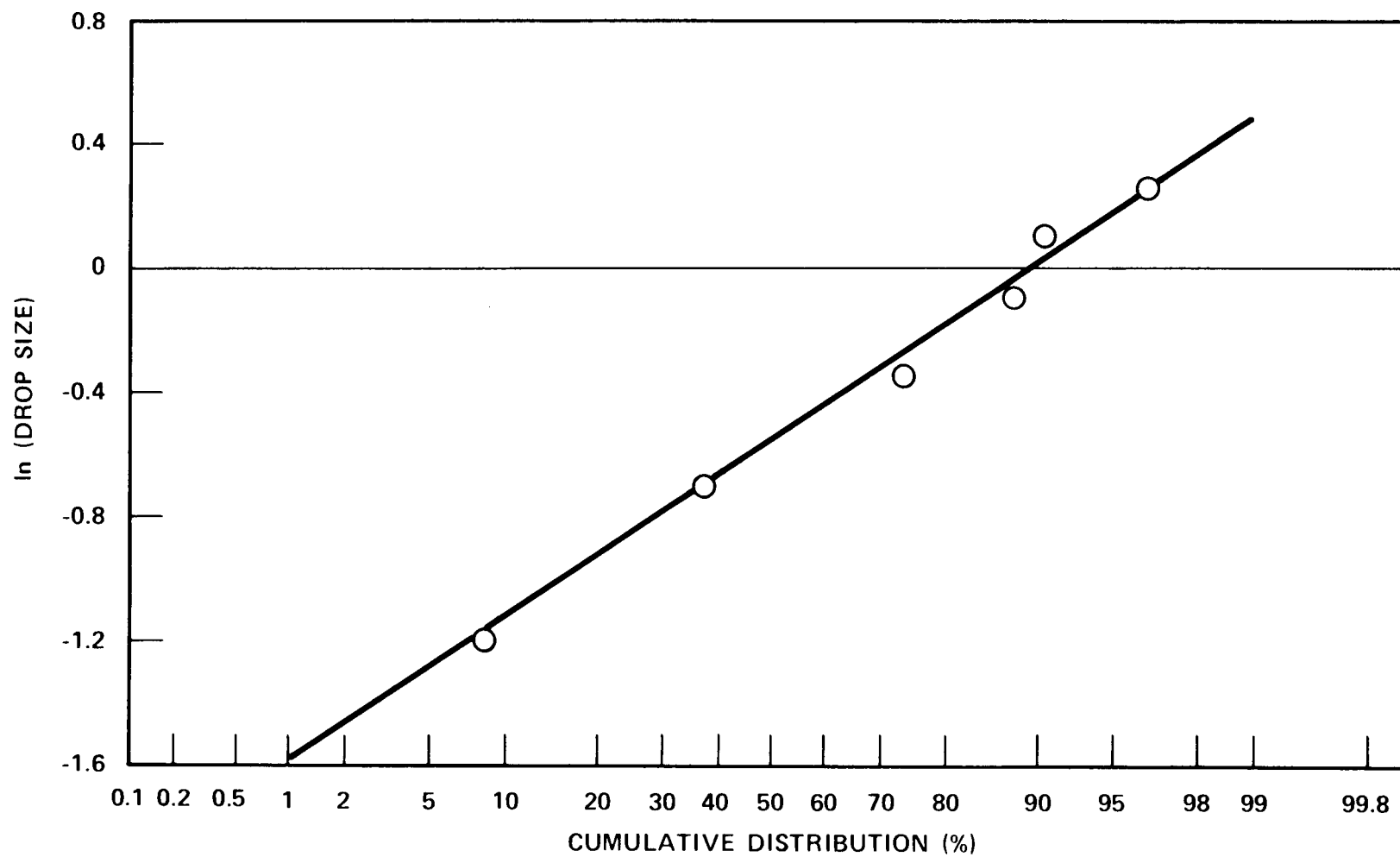


Figure G-25. Log Normal Distribution Probability Plot, Run 61106,
0.91 m (36 in.) Elevation

G-19

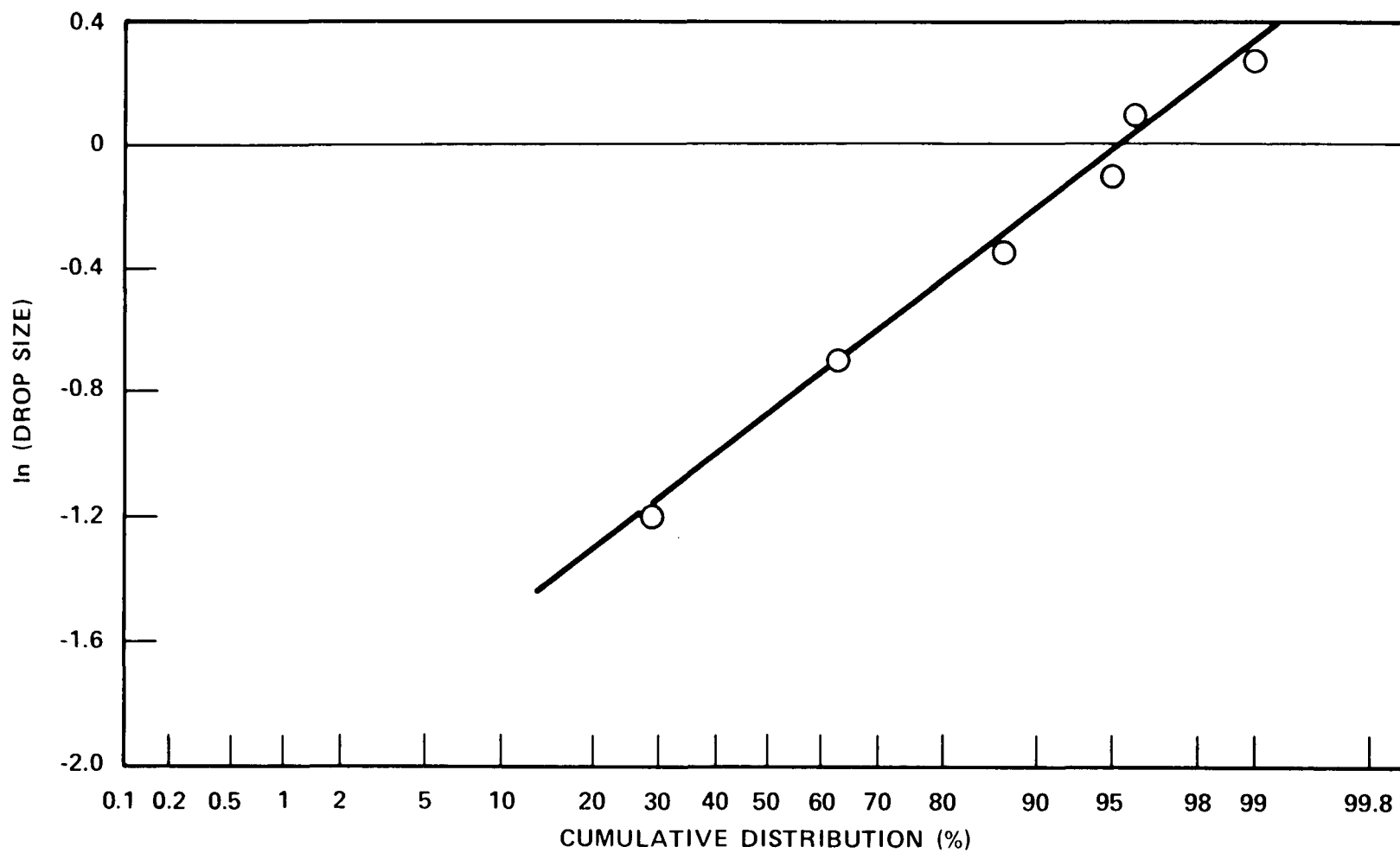


Figure G-26. Log Normal Distribution Probability Plot, Run 61412,
0.91 m (36 in.) Elevation

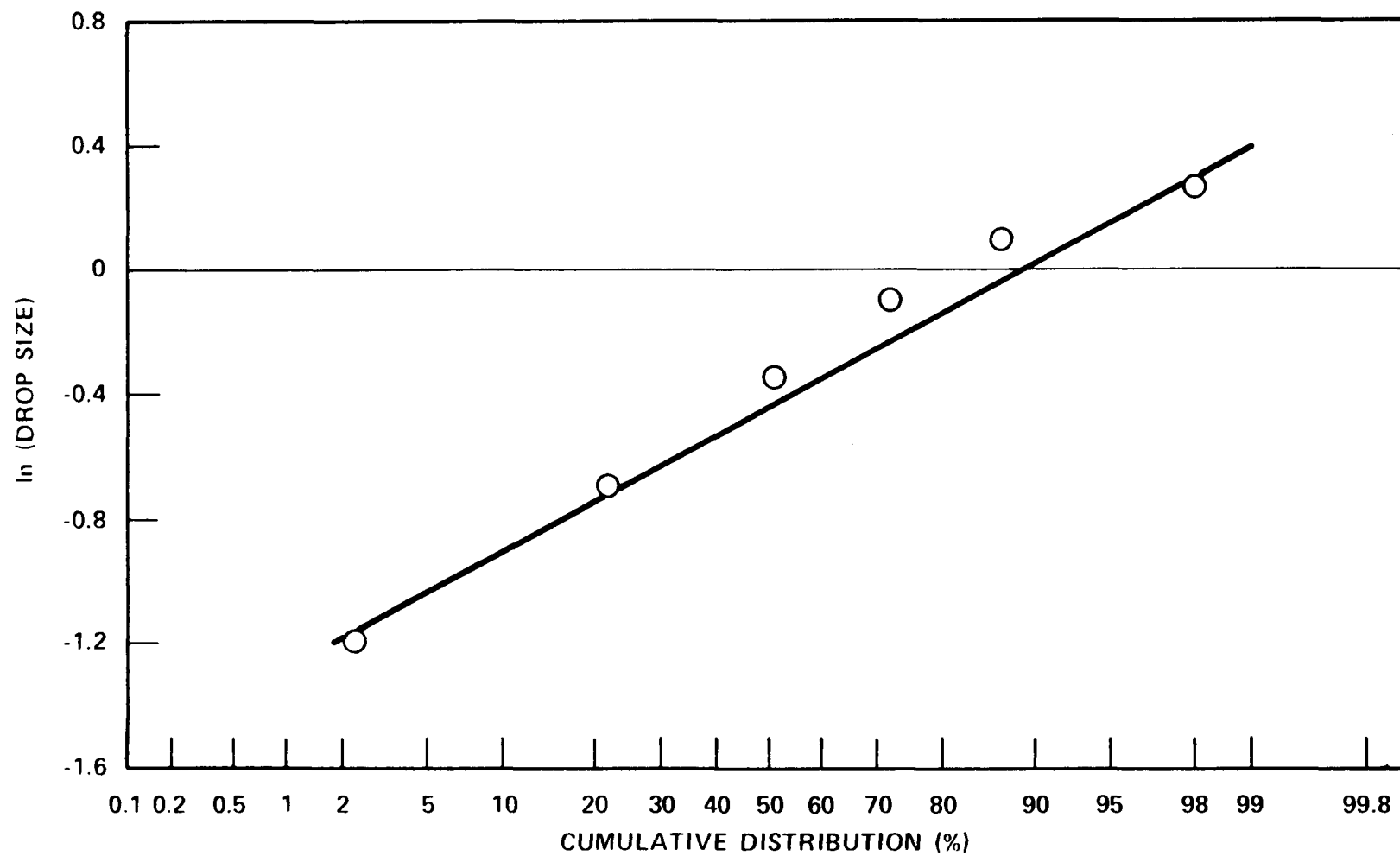


Figure G-27. Log Normal Distribution Probability Plot, Run 61509,
0.91 m (36 in.) Elevation

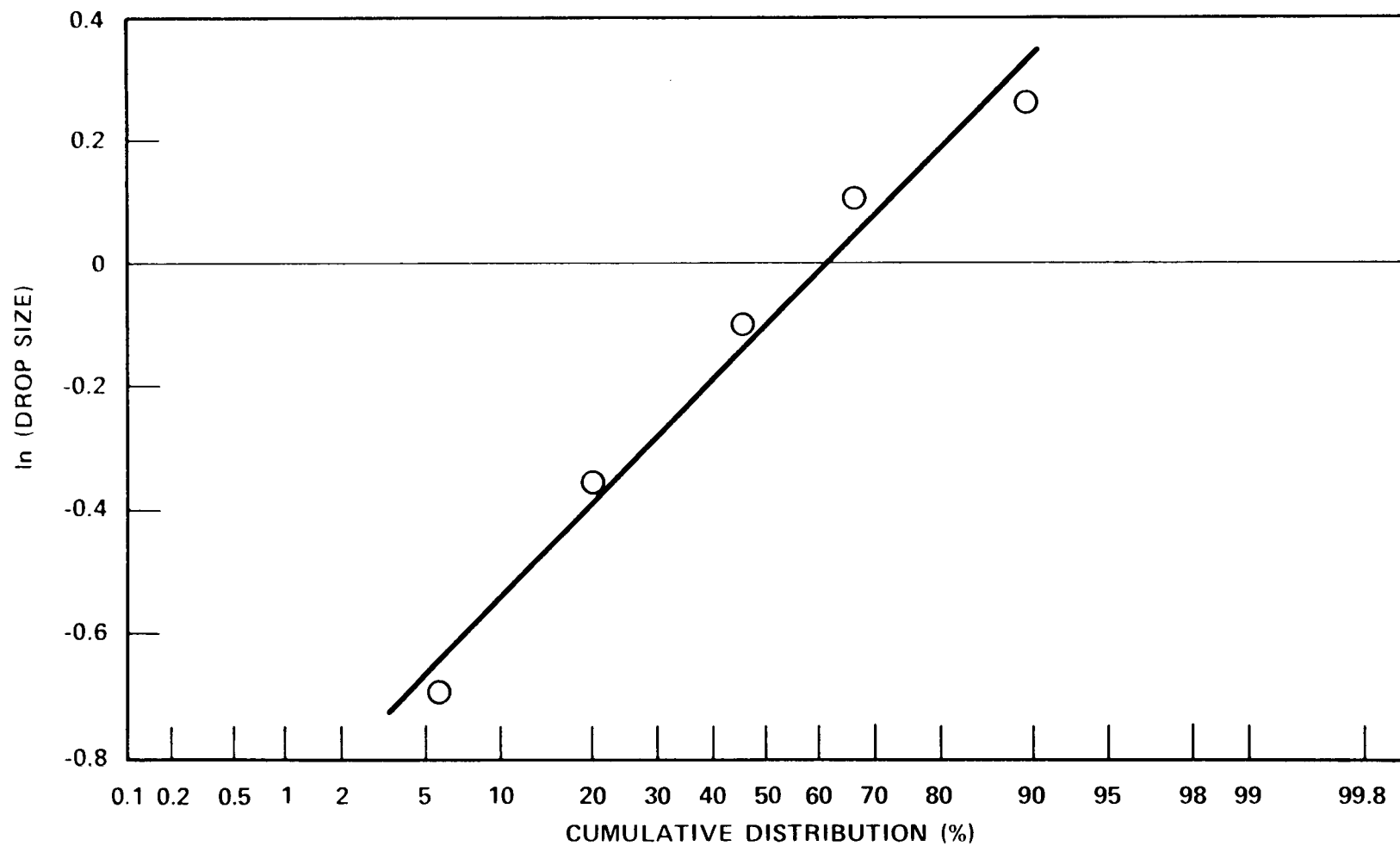


Figure G-28. Log Normal Distribution Probability Plot, Run 61607,
0.91 m (36 in.) Elevation

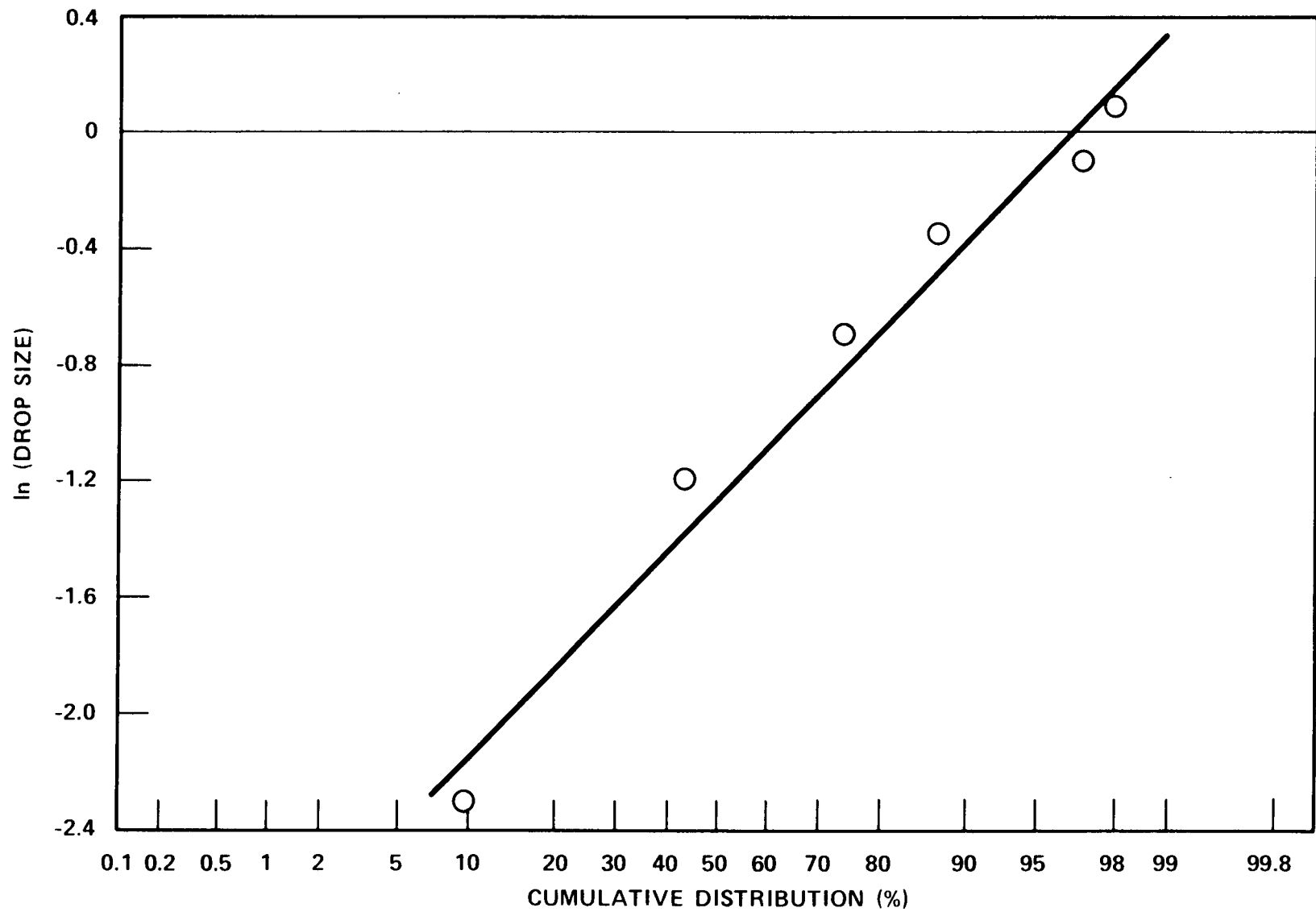


Figure G-29. Log Normal Distribution Probability Plot, Run 61705,
0.91 m (36 in.) Elevation

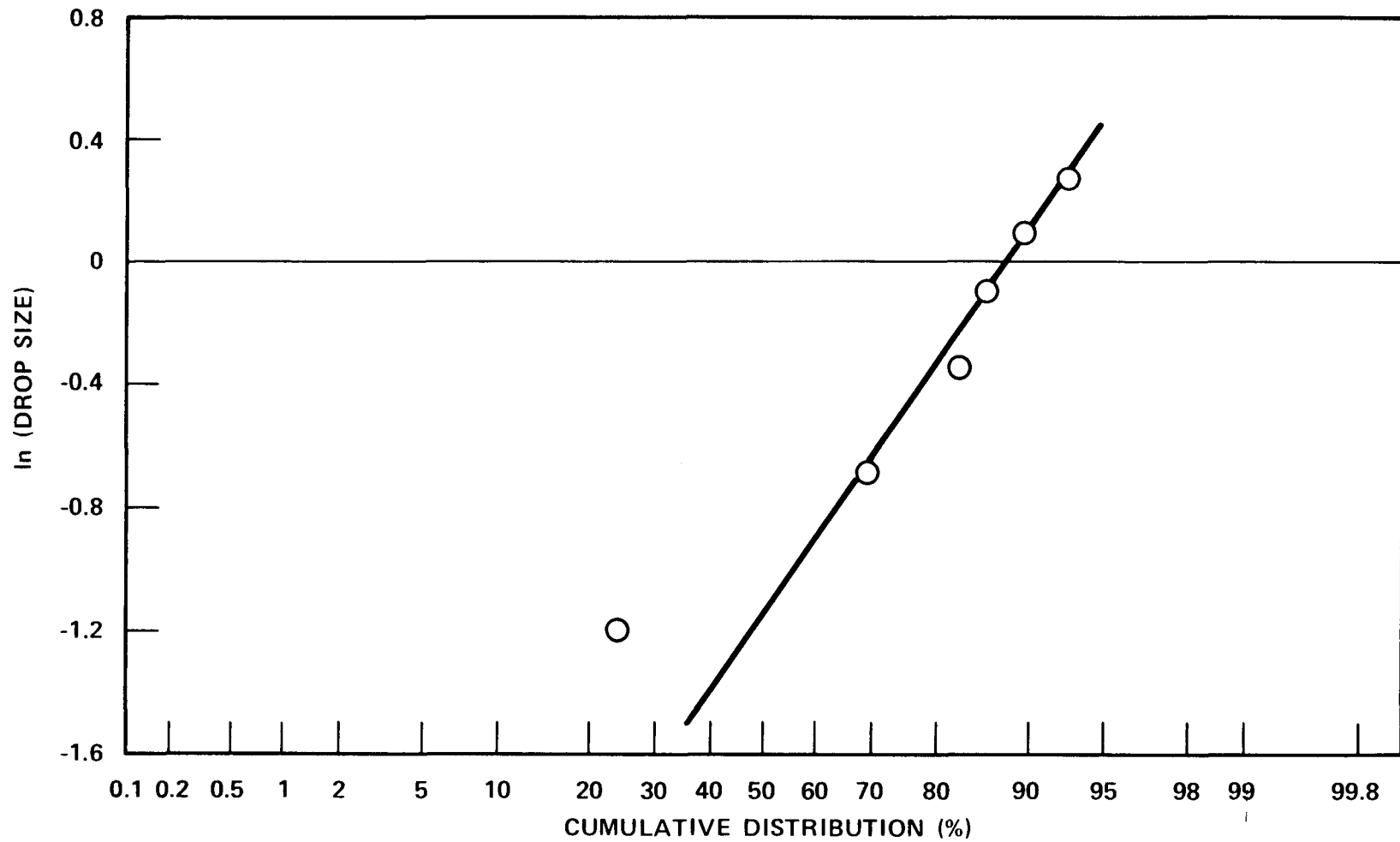


Figure G-30. Log Normal Distribution Probability Plot, Run 61916,
0.91 m (36 in.) Elevation

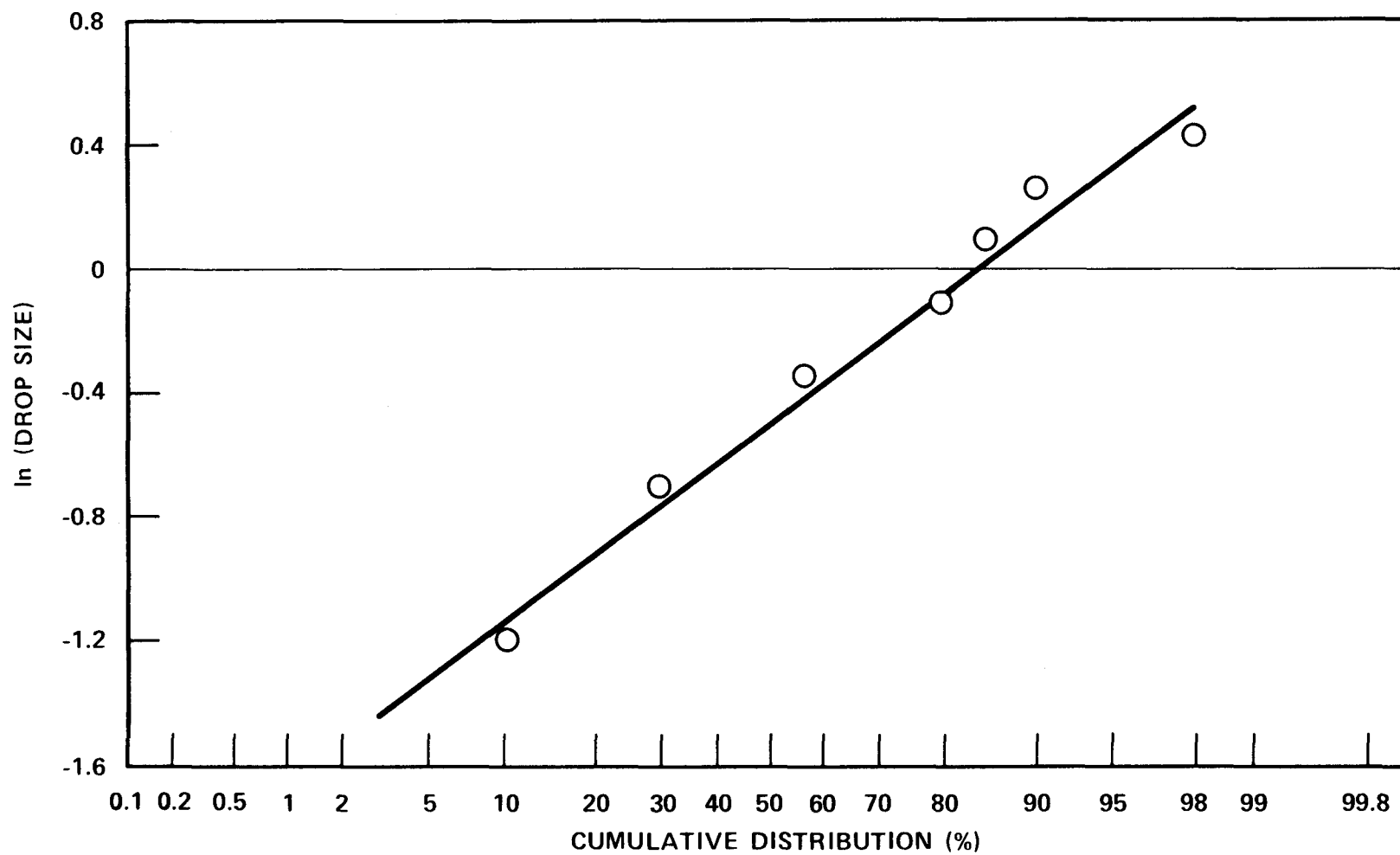


Figure G-31. Log Normal Distribution Probability Plot, Run 61916,
2.74 m (108 in.) Elevation

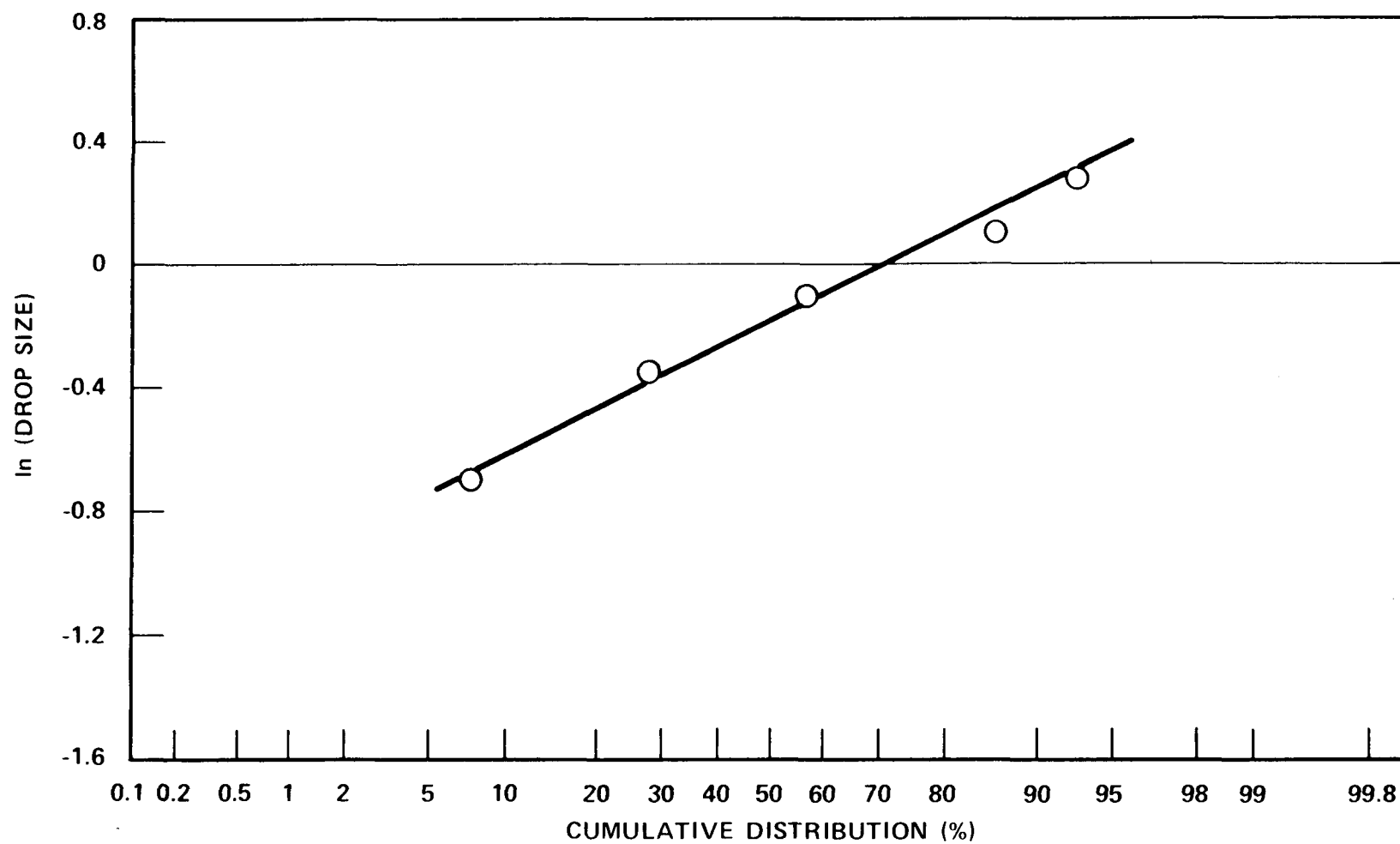


Figure G-32. Log Normal Distribution Probability Plot, Run 62015,
0.91 m (36 in.) Elevation

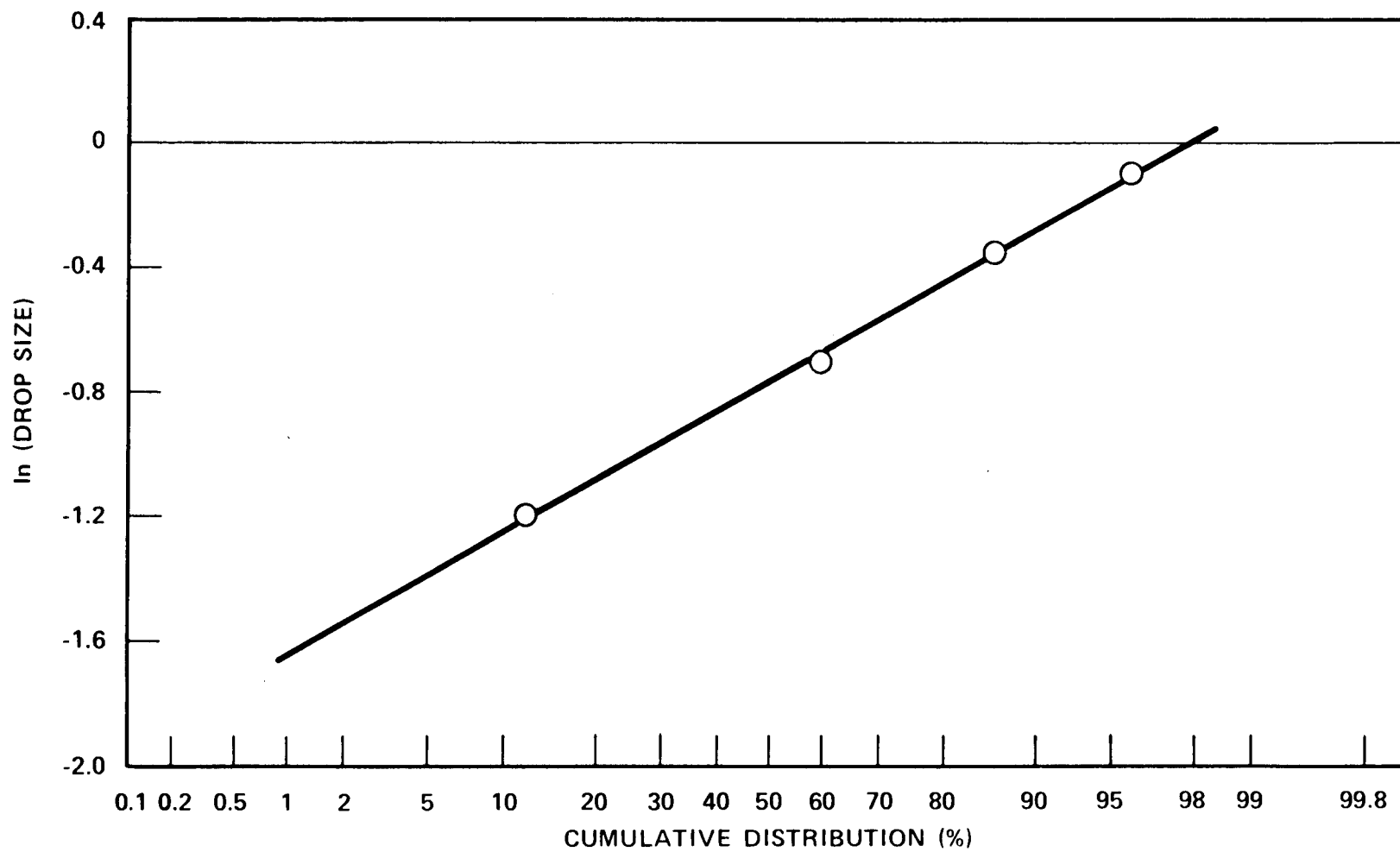


Figure G-33. Log Normal Distribution Probability Plot, Run 62117,
0.91 m (36 in.) Elevation

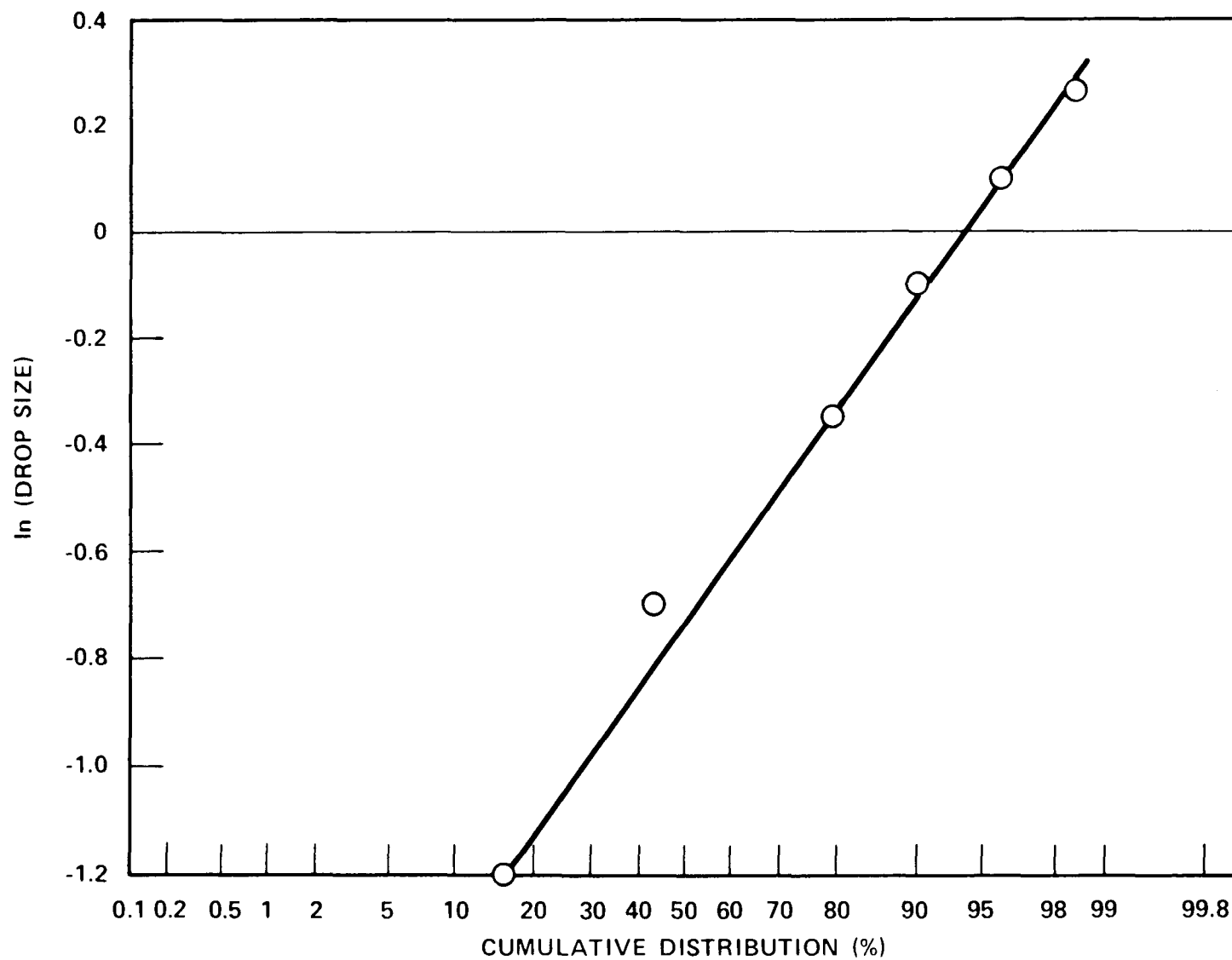


Figure G-34. Log Normal Distribution Probability Plot, Run 62304,
0.91 m (36 in.) Elevation

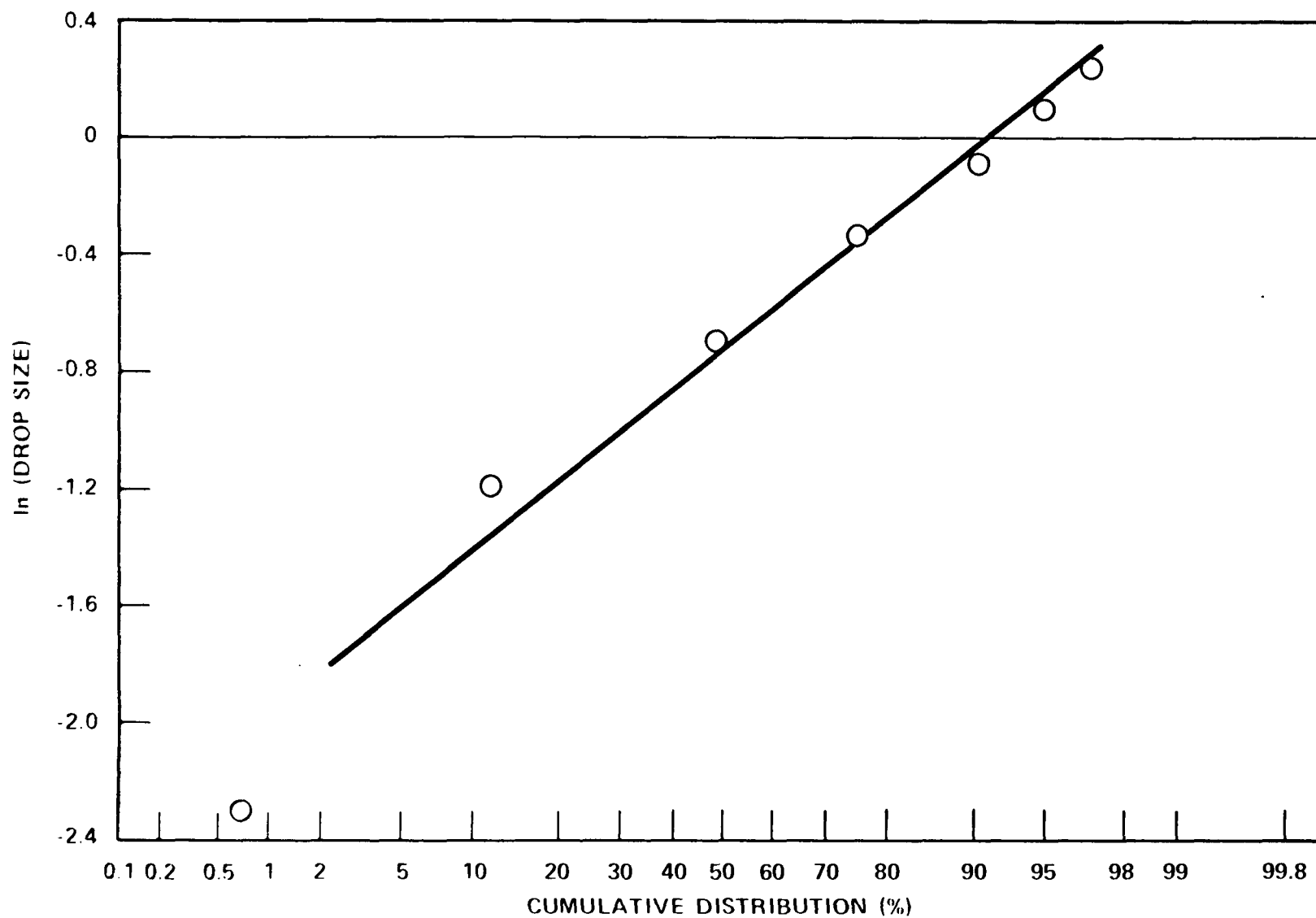


Figure G-35. Log Normal Distribution Probability Plot, Run 62413,
0.91 m (36 in.) Elevation

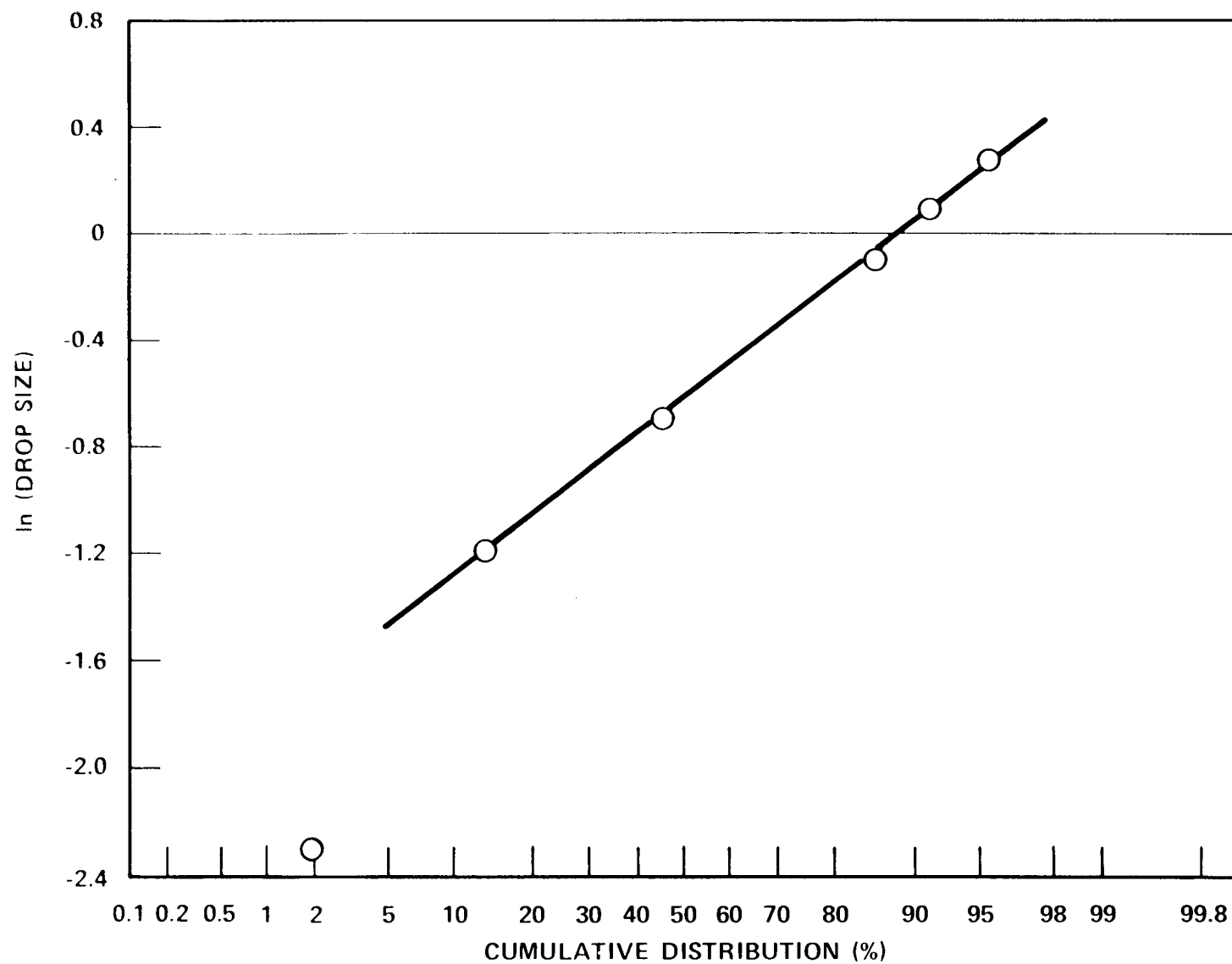


Figure G-36. Log Normal Distribution Probability Plot, Run 62605,
0.91 m (36 in.) Elevation

APPENDIX H

DATA TABLES AND PLOTS

This appendix contains a sampling of data collected for each of the 23 163-rod blocked bundle reflood tests. All the valid measured and reduced data are available from the NRC Data Bank. The data have not been analyzed or evaluated in great detail, and caution should be observed that erroneous data may exist despite efforts to ensure correct and accurate data. A data evaluation report, to be published at a later date, will present the results of the data evaluation in greater detail.

The following tables are provided for each test:

- o Summary and Comment Sheet -- lists the as-run test conditions, and comments on the as-run test conditions relative to the respective 161-rod unblocked bundle
- o Heater Rod Temperature Data -- lists the characteristics of the temperature-time history for heater rod thermocouples at the same locations for all reflood tests
- o Heater Rod Temperature-Time Statistical Data -- lists the maximum, minimum, and average of the temperature-time characteristics of all heater rod thermocouples as a function of elevation

The following plots are included for each test:

- o Heater rod temperatures and heat transfer coefficients as calculated by DATAR for comparable thermocouple locations in the 163-rod blocked bundle and the 161-rod unblocked bundle (except for runs 62117, 62503, and 62819, none of which had a comparable test in the unblocked bundle). Because of the large number of failed thermocouples in the 161-rod bundle tests, the same data comparisons could not be made from test to test. The specific rod thermocouple locations are listed for each test.
- o Bundle vapor temperatures for the following thermocouple locations:

¹ Except as noted on Summary and Comment Sheets

Location	Elevation [m (in.)]	Computer Channel Number
4I	1.52 (60)	443
7L	1.98 (78)	446
10L	2.44 (96)	451
7I	2.82 (111)	452
7C	3.05 (120)	454

- o Thimble wall temperatures for the following thermocouple locations:

Thimble	Elevation [m (in.)]	Computer Channel Number
10C	1.83 (72)	486
10C	2.29 (90)	491
10C	2.44 (96)	496
10C	2.82 (111)	497
5K	3.05 (120)	499

- o Housing wall temperatures for the following thermocouple locations:

Elevation [m (in.)]	Computer Channel Number
1.22 (48)	504
1.52 (60)	505
1.83 (72)	506
2.44 (96)	508
3.05 (120)	510

- o Fluid and exit vapor temperatures for the following thermocouple locations:

Location	Computer Channel Number
Injection line fluid	536
Upper plenum fluid	515
Upper plenum steam probe	517
Steam probe upstream of separator	528
Steam probe downstream of separator	530

- o Overall bundle, steam separator, and carryover tank levels:

Location	Computer Channel Number
Bundle housing	562
Upper plenum	561
Carryover tank	563
Steam separator	565
Downcomer (gravity reflood)	564

- o Exhaust steam flow rate (channel 306), injection mass flow rate (channel 203), bundle storage rate (channel 205), and carryover tank storage rate (channel 302)
- o Overall mass balance
- o All heater rod quench times as a function of elevation
- o Heater rod bundle axial differential pressures and void fractions

FLECHT SEASET 163-ROD BUNDLE FLOW BLOCKAGE TASK
SUMMARY AND COMMENT SHEET

Run: 60701
Test date: 8/16/82
Test type: Forced reflood (facility shakedown)
Parameter: Initial clad temperature effect

AS-RUN TEST CONDITIONS:

Upper plenum pressure	0.277 MPa (40.2 psia)
Initial peak clad temperature and location	264.6°C (508.2°F), 2I-1.93 m (76 in.)
Initial peak rod power:	
Peripheral rods	2.31 kW/m (0.704 kw/ft)
Bypass rods	2.28 kW/m (0.696 kw/ft)
Blockage island rods	2.30 kW/m (0.702 kw/ft)
Flooding rate	38.6 mm/sec (1.52 in./sec)
Coolant temperature	52.2°C (126°F)
Initial bundle water level	0 mm (0 in.)

COMMENTS:

Inlet mass flow:⁽¹⁾ -1% constant

No heat transfer plots are included.

1. Relative to run 30518

FLECHT SEASET 163 RUJ BUNDLE TEST SERIES

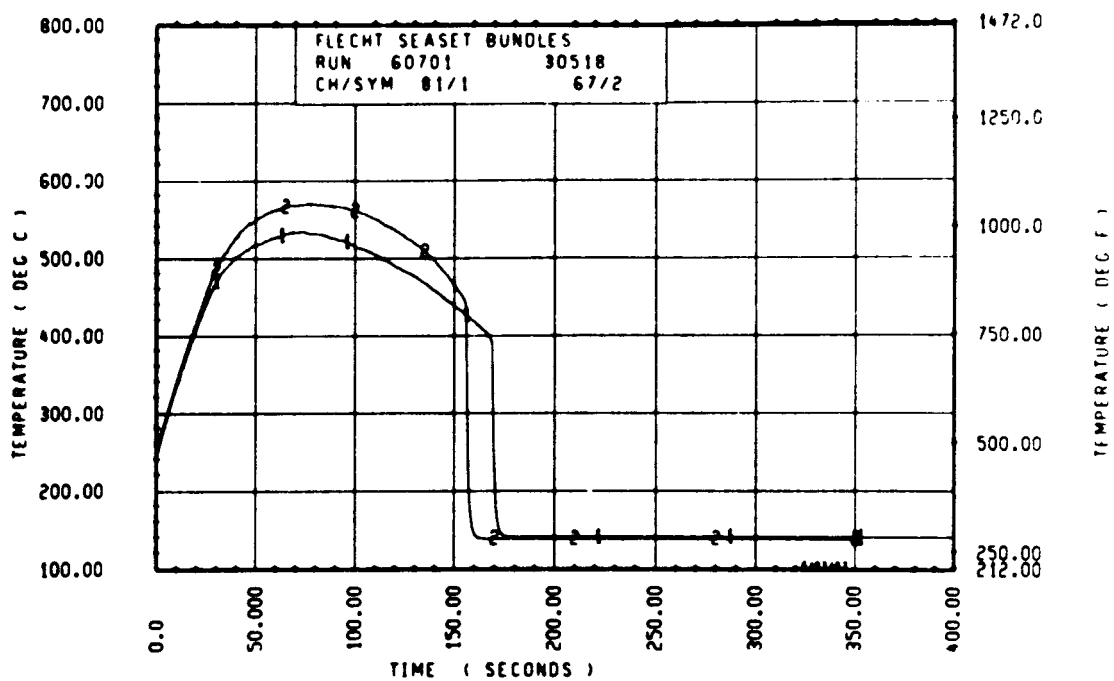
ROD/ELEV	CHAN.	NO	INITIAL AT FLOOD (DEG F)	MAXIMUM TEMPERATURE (DEG F)	TEMPERATURE RISE (DEG F)	TURNAROUND TIME (SECONDS)	QUENCH TEMPERATURE (DEG F)	QUENCH TIME (SECONDS)
96 1- 0		3	333.	364.	32.	7.0	265.	10.7
10H 2- 0		6	369.	475.	106.	16.1	474.	10.3
96 3- 3		9	420.	643.	223.	27.9	627.	42.1
3J 4- 0		11	444.	740.	296.	30.5	635.	67.4
7H 4- 0		12	443.	724.	281.	34.9	634.	64.3
8K 4- 0		13	441.	740.	299.	35.5	671.	73.9
8N 4- 0		14	445.	745.	300.	40.3	747.	59.0
12D 4- 0		17	440.	733.	293.	42.5	710.	55.7
5E 5- 0		20	472.	919.	447.	51.3	600.	40.0
76 5- 0		21	460.	937.	457.	47.4	750.	110.8
9G 5- 0		24	483.	943.	460.	52.6	772.	112.4
5E 5- 7		33	479.	930.	451.	54.3	760.	127.5
86 5- 7		45	481.	950.	469.	55.0	785.	140.5
9H 5- 9		52	470.	860.	418.	41.4	711.	140.5
76 5-10		59	464.	943.	500.	36.5	700.	154.2
7F 5-11		62	476.	927.	451.	66.1	769.	100.3
46 5-11		64	491.	966.	535.	65.0	747.	105.5
21 6- 0		67	503.	1134.	531.	53.0	717.	104.4
5D 6- 0		70	483.	945.	462.	54.5	740.	150.9
6J 6- 0		74	481.	1000.	519.	74.7	742.	170.9
7M 6- 0		86	477.	961.	484.	58.8	738.	164.3
11E 6- 0		89	481.	986.	505.	52.9	720.	165.6
8H 6- 2		97	475.	855.	420.	45.7	677.	143.0
5H 6- 2		99	495.	978.	483.	57.0	720.	169.0
9E 6- 2		155	440.	963.	523.	57.2	264.	465.1
8M 6- 3		111	482.	920.	443.	48.9	736.	148.1
46 6- 3		124	494.	1011.	517.	78.9	730.	181.0
11H 6- 4		134	478.	934.	456.	58.0	623.	133.2
9D 6- 4		143	480.	967.	507.	60.2	724.	170.0
9J 6- 5		165	483.	1013.	530.	56.1	640.	93.3
9M 6- 5		166	487.	1070.	583.	82.2	737.	161.7
8J 6- 6		192	492.	1030.	540.	67.2	935.	115.7
9D 6- 6		193	479.	1025.	546.	76.3	740.	182.7
11F 6- 6		173	486.	1044.	556.	75.8	720.	183.1
46 7- 0		261	487.	961.	474.	65.1	723.	213.0
7D 7- 6		309	468.	1091.	622.	99.4	754.	240.7
76 7- 6		312	479.	1125.	630.	96.7	570.	377.4
11E 7- 6		325	475.	1091.	616.	89.2	774.	235.1
5L 8- 0		337	434.	1001.	566.	126.9	713.	255.8
7H 8- 0		345	438.	1083.	646.	131.1	654.	217.0
7K 8- 0		346	454.	1054.	600.	122.5	757.	244.2
5J 8- 6		366	410.	947.	524.	112.4	757.	232.0
78 8- 6		368	417.	953.	536.	131.1	645.	291.9
7E 9- 3		383	395.	973.	576.	147.3	267.	574.5
8H 9- 3		397	391.	910.	514.	136.5	631.	291.1
9C 9- 3		389	393.	902.	509.	153.7	525.	311.2
11F 9- 3		394	395.	825.	431.	95.6	705.	197.2
7810- 0		408	363.	840.	483.	149.4	501.	327.1
8H10- 0		415	358.	849.	491.	146.2	274.	350.1
8K10- 0		417	364.	820.	462.	134.4	556.	310.0
8N10- 0		418	366.	840.	480.	136.5	605.	305.1
6H11- 0		429	332.	815.	284.	135.4	499.	203.0
9G11- 0		431	334.	563.	230.	69.8	544.	71.2
11E11- 0		432	329.	596.	267.	131.1	470.	261.0
5J11- 6		436	332.	555.	218.	54.5	534.	65.7
7811- 6		437	329.	630.	301.	143.1	567.	255.4
8J11- 6		438	334.	626.	292.	135.4	532.	203.0

RUN 60701 HEATEX ROD STATISTICAL DATA

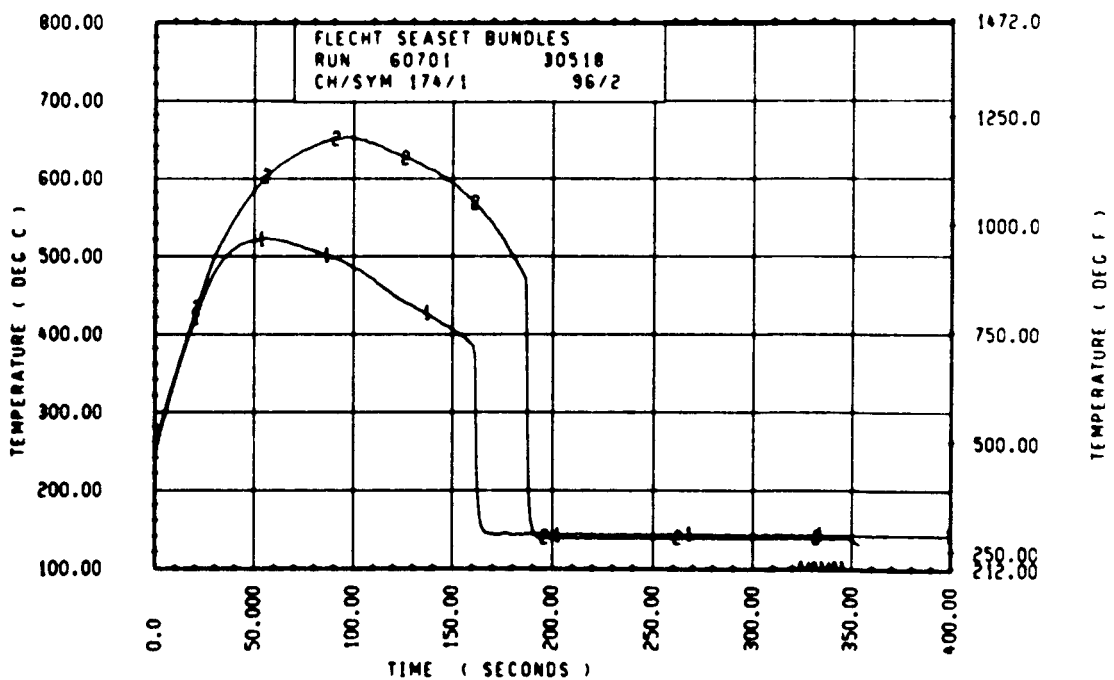
ELEV	INITIAL TEMP (DEG F)			MAX TEMP (DEG F)			TURNAROUND TIME (SEC)		
	MAX	MIN	MEAN	MAX	MIN	MEAN	MAX	MIN	MEAN
12	332.6	326.7	331.0	368.4	362.3	365.2	7.5	7.0	7.3
24	358.9	362.3	365.2	474.6	464.8	469.6	16.1	15.6	15.9
39	420.3	366.3	407.2	642.8	525.9	633.6	31.7	25.8	28.6
48	448.6	432.3	442.5	746.3	724.5	737.0	42.5	34.4	38.0
63	489.9	450.8	475.8	775.1	877.0	930.0	73.4	49.4	59.7
67	475.4	462.7	485.0	991.6	902.9	950.4	76.8	44.4	59.7
69	436.6	470.3	479.2	942.6	880.4	954.6	71.5	41.4	61.3
70	502.9	481.2	488.1	1033.8	965.8	996.2	85.0	64.5	70.6
71	491.0	474.7	481.7	1007.0	920.0	966.3	79.4	60.0	67.3
72	512.9	474.7	488.3	1035.0	945.2	987.7	74.7	55.4	66.4
73	445.3	472.5	466.4	1030.0	935.4	991.2	75.3	46.9	66.9
74	495.3	469.2	485.2	1039.7	885.6	960.4	69.8	33.8	55.4
75	447.5	464.2	485.3	1040.3	895.6	978.5	73.5	43.0	61.2
76	508.2	477.9	488.4	1069.9	922.5	997.4	81.1	44.4	62.7
77	493.1	464.4	484.1	1069.4	914.4	992.4	92.2	43.4	63.2
78	445.3	452.1	474.6	1101.4	910.4	990.1	93.3	44.0	68.6
79	514.7	474.7	486.1	1065.4	892.5	1031.8	82.7	36.1	72.6
80	484.9	462.8	478.9	1120.8	885.5	1002.1	95.8	58.6	80.0
81	491.0	464.9	476.6	1113.3	1010.1	1050.5	95.8	73.4	83.2
84	491.0	475.8	484.4	993.6	917.3	966.5	82.7	55.0	70.0
86	488.8	472.5	480.4	1105.0	978.2	1027.1	98.3	65.6	80.0
94	479.6	458.4	477.3	1140.5	1012.2	1077.3	112.0	81.1	96.7
96	454.0	434.5	442.4	1181.7	1000.8	1100.4	143.8	108.8	125.7
102	423.6	414.9	416.4	1039.0	891.5	978.6	145.1	112.0	128.1
111	399.6	380.5	394.0	975.0	820.1	966.2	153.7	95.6	132.5
120	375.5	343.0	363.0	904.4	715.1	824.6	166.6	74.7	139.6
132	333.7	320.2	331.0	663.8	563.5	607.7	166.6	64.6	123.8
138	333.7	320.6	331.0	633.1	512.4	579.1	161.2	46.2	110.1

RUN 60701 HEATEX ROD STATISTICAL DATA

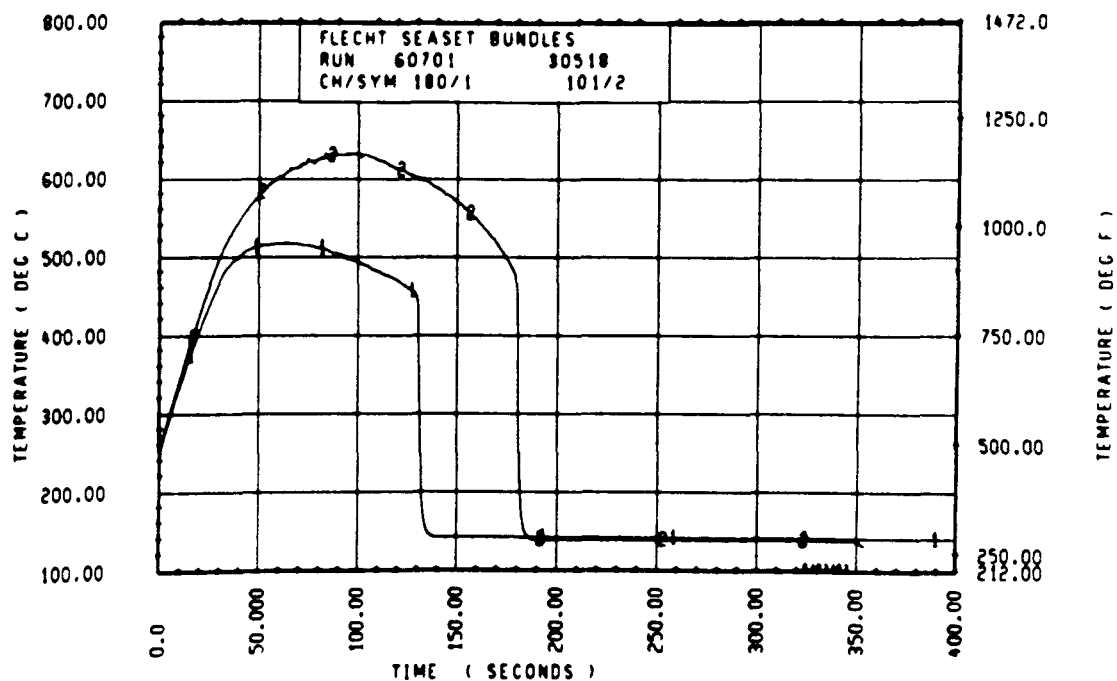
ELEV	TEMP RISE (DEG F)			QUENCH TEMP (DEG F)			QUENCH TIME (SEC)		
	MAX	MIN	MEAN	MAX	MIN	MEAN	MAX	MIN	MEAN
12	37.3	31.4	35.1	363.2	284.6	311.2	10.7	7.6	9.5
24	175.8	102.6	104.3	473.5	464.7	468.6	14.3	16.1	17.1
39	239.5	220.6	226.3	629.1	515.8	624.4	43.2	34.6	39.3
48	300.0	285.5	294.5	710.1	604.6	691.7	73.9	47.3	61.7
63	485.2	455.5	466.2	821.5	700.7	793.2	121.2	44.0	108.8
67	495.1	440.2	471.4	815.4	733.8	771.7	151.6	114.5	136.5
69	511.4	418.1	475.4	762.2	700.0	750.4	153.8	138.1	146.0
70	530.9	484.6	508.3	801.1	766.5	783.4	154.8	147.9	152.2
71	521.5	450.8	484.5	777.2	741.2	765.0	165.5	108.3	144.9
72	533.4	461.8	501.0	776.8	710.2	752.5	172.5	159.4	164.4
73	550.2	446.0	504.9	841.4	720.1	770.1	174.1	140.7	162.7
74	543.0	393.1	475.2	767.6	672.5	732.6	177.2	69.3	157.4
75	556.5	420.4	491.2	840.5	462.2	736.1	181.6	92.0	155.5
76	566.5	441.3	509.5	847.2	623.2	755.3	188.5	104.0	164.9
77	593.3	449.9	508.3	823.8	591.2	784.0	247.2	77.4	147.8
79	612.0	64.3	515.5	835.4	211.6	722.7	415.7	36.5	162.3
79	599.8	410.3	545.3	850.0	515.6	774.6	417.8	109.5	171.4
80	636.9	516.5	583.2	844.0	474.7	745.6	421.0	47.7	217.3
81	634.3	545.2	573.9	841.4	566.2	777.3	311.5	125.3	189.8
94	506.1	436.3	482.2	793.3	571.4	707.1	344.9	134.4	232.1
86	616.5	501.3	546.2	821.4	460.8	754.4	423.1	155.4	222.0
90	681.5	544.3	617.0	822.5	470.3	764.2	424.2	178.5	240.4
96	741.8	566.4	655.5	967.6	394.1	742.4	547.6	193.3	271.8
102	523.3	476.6	558.2	863.8	544.2	765.1	233.5	228.4	266.4
111	532.4	427.1	512.2	830.1	207.4	628.2	574.5	131.6	301.9
120	537.2	371.5	460.6	742.2	274.2	543.7	404.1	76.8	248.9
132	335.5	229.8	276.6	546.6	464.5	500.4	327.5	71.2	222.5
138	330.8	183.1	249.1	566.7	470.4	527.6	289.6	45.7	167.4



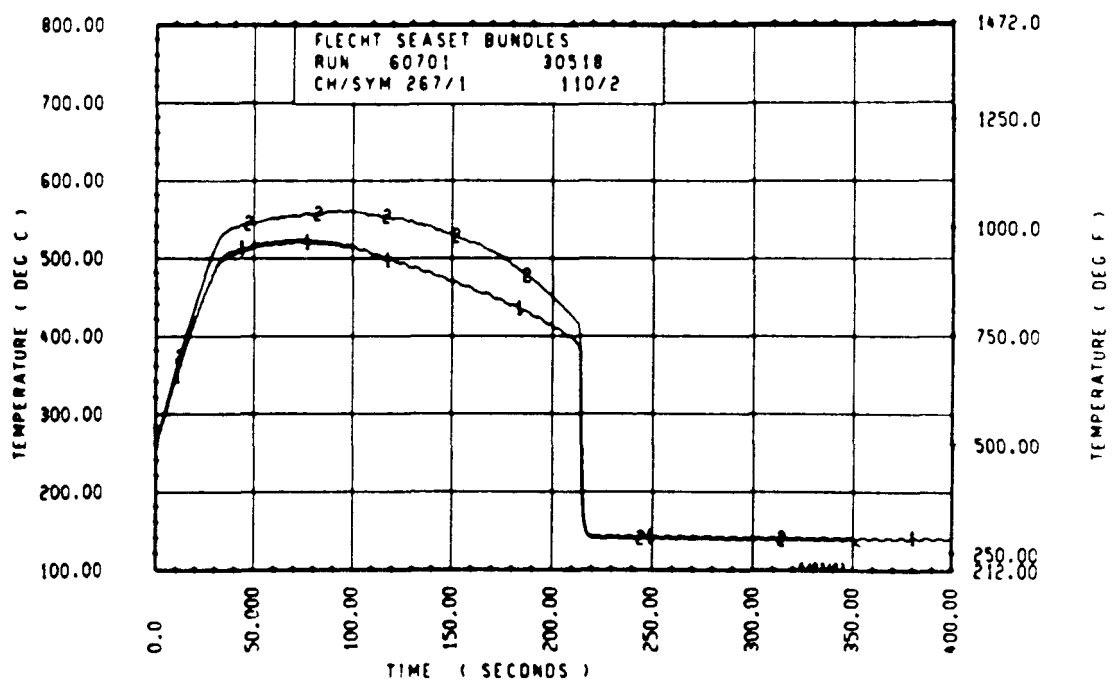
Rod 12L, 1.83 m (72 in.)



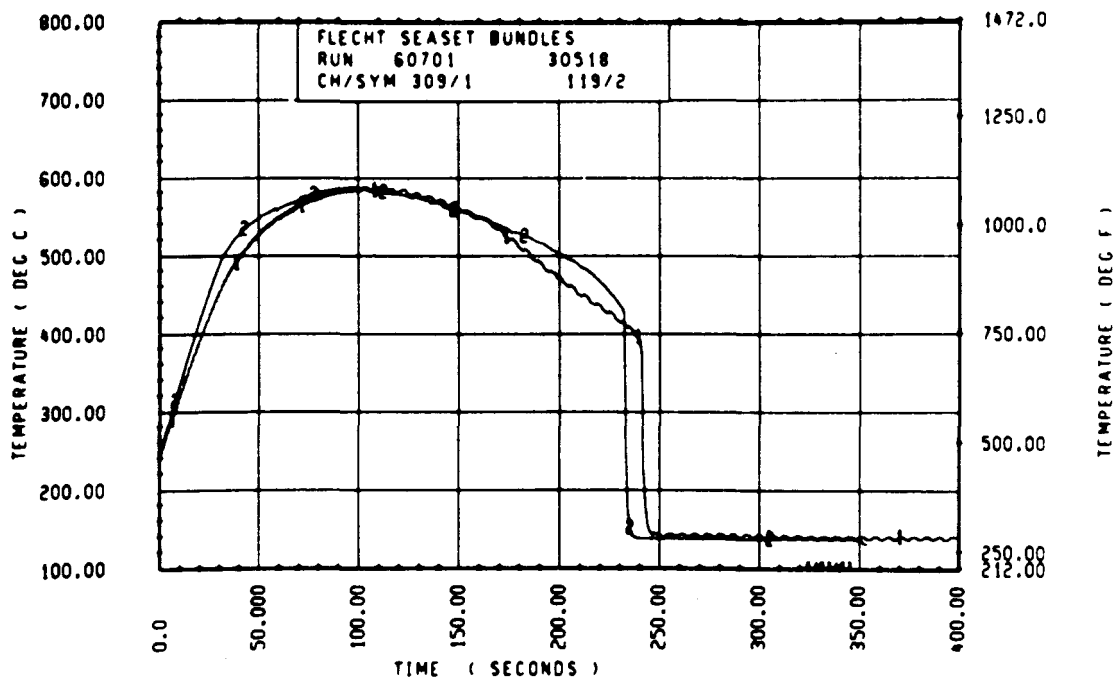
Rod 8H, 1.98 m (78 in.)



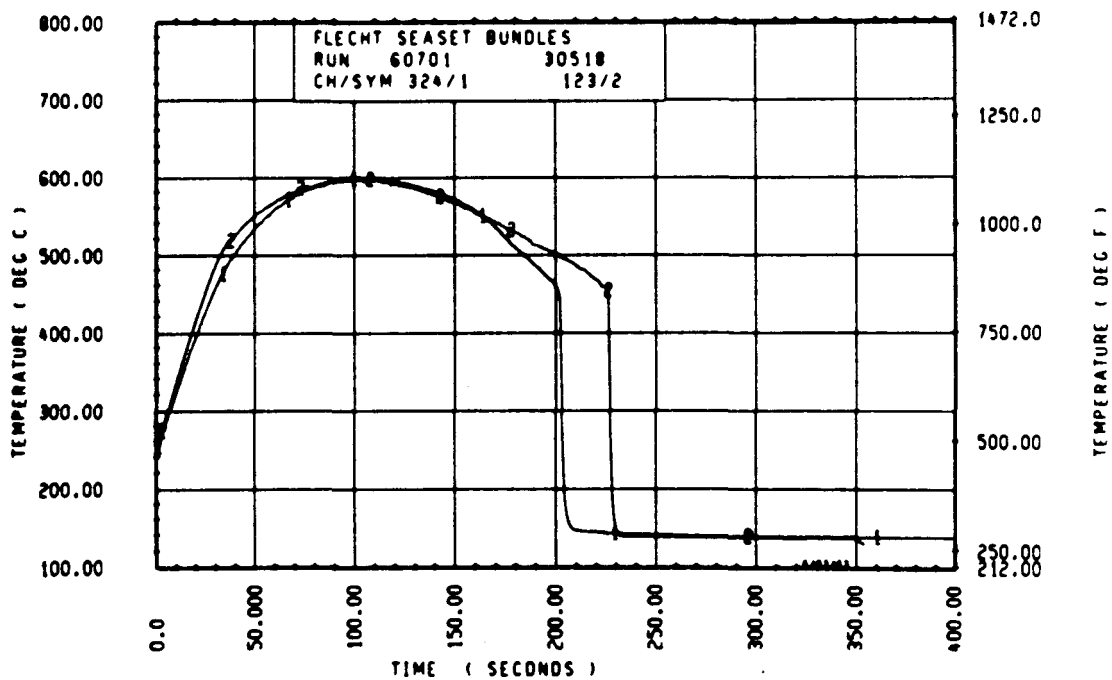
Rod 12I, 1.98 m (78 in.)



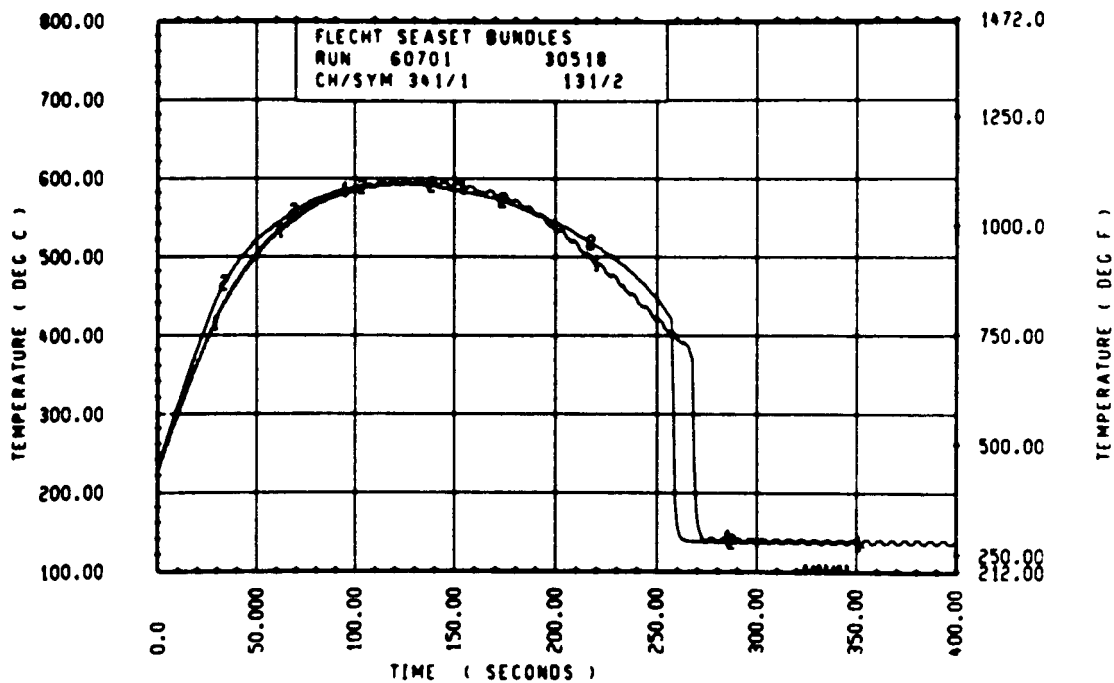
Rod 9L, 2.13 m (84 in.)



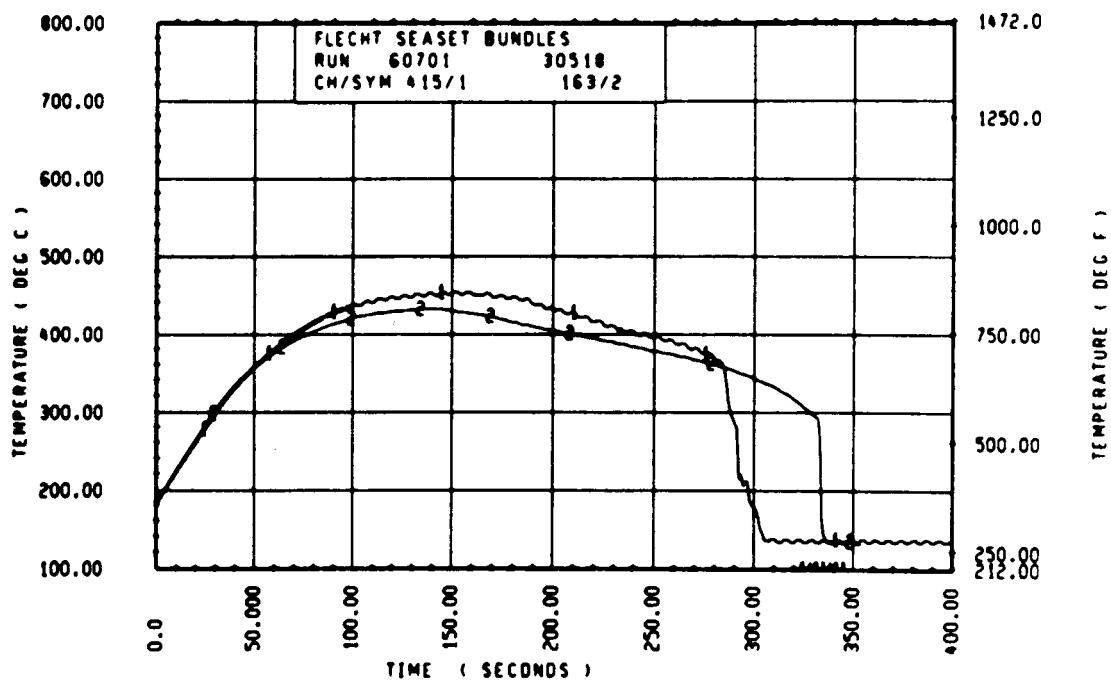
Rod 7D, 2.29 m (90 in.)



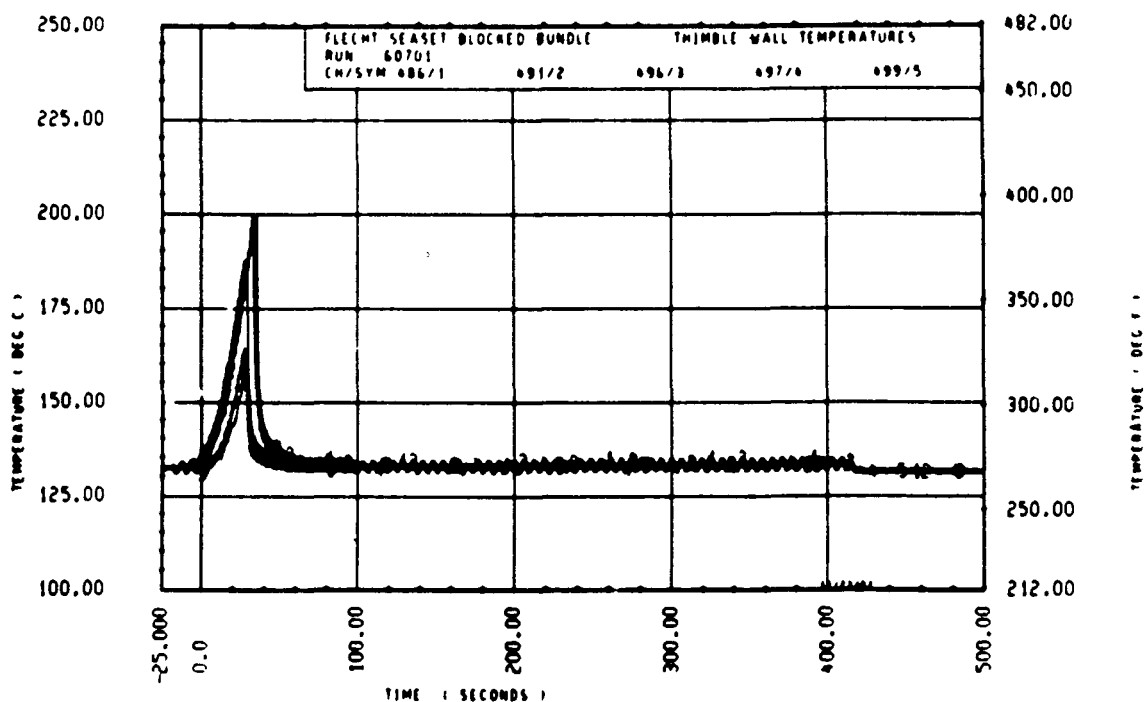
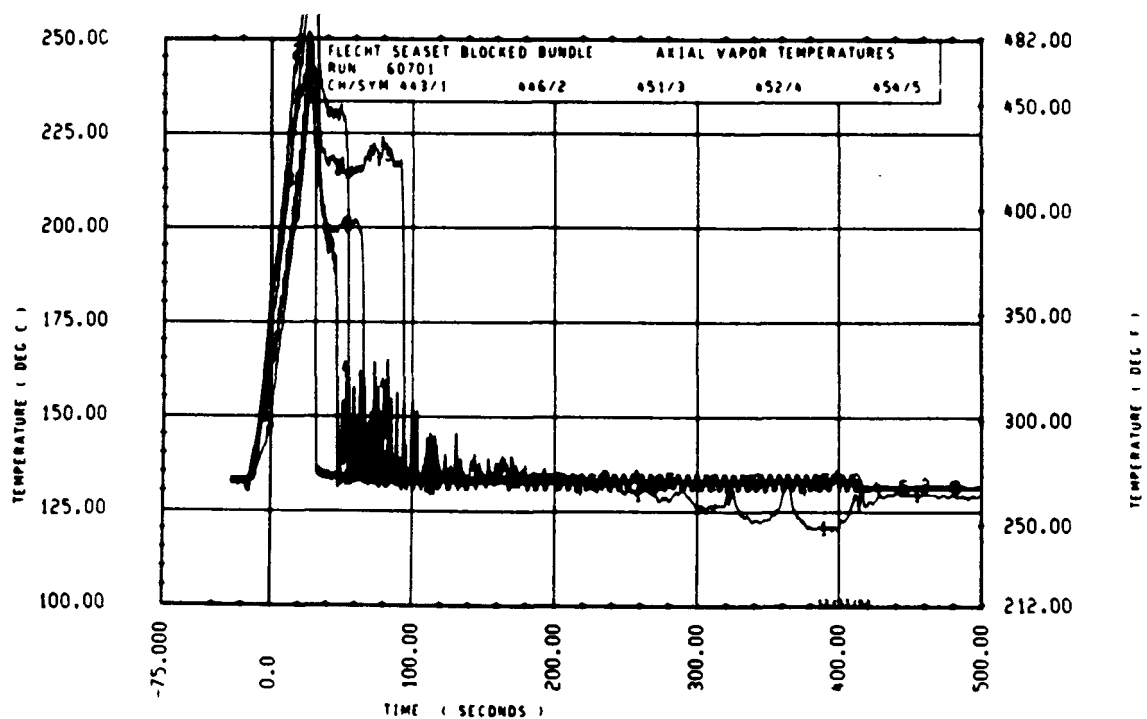
Rod 10J, 2.29 m (90 in.)

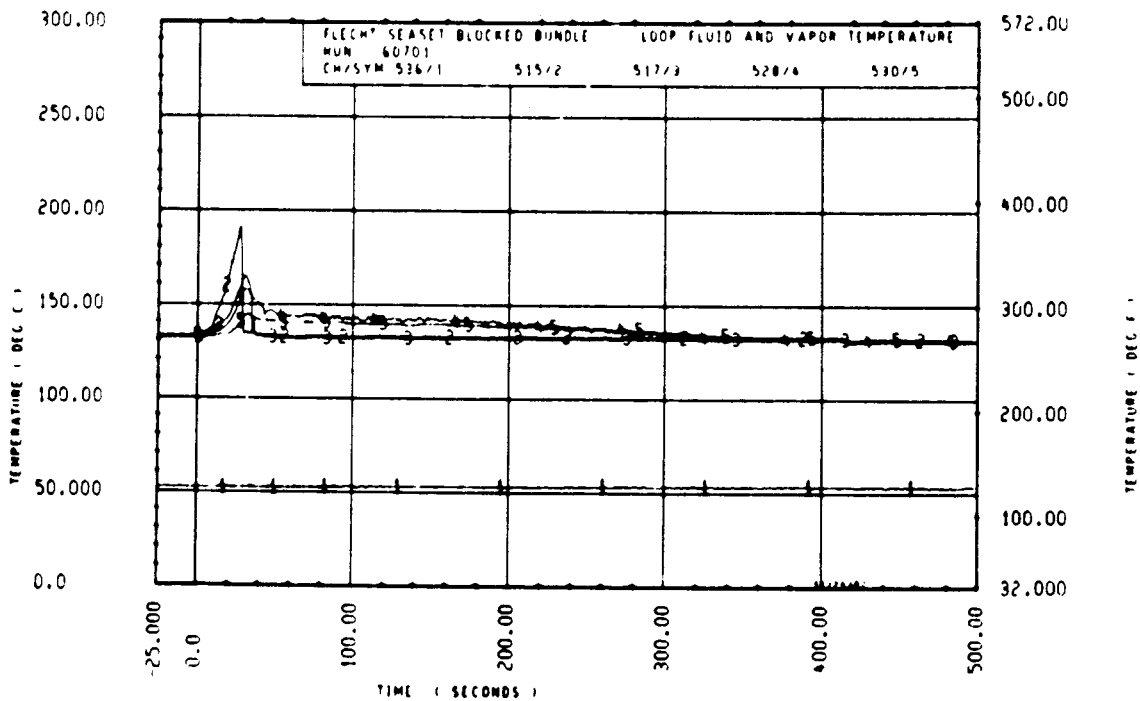
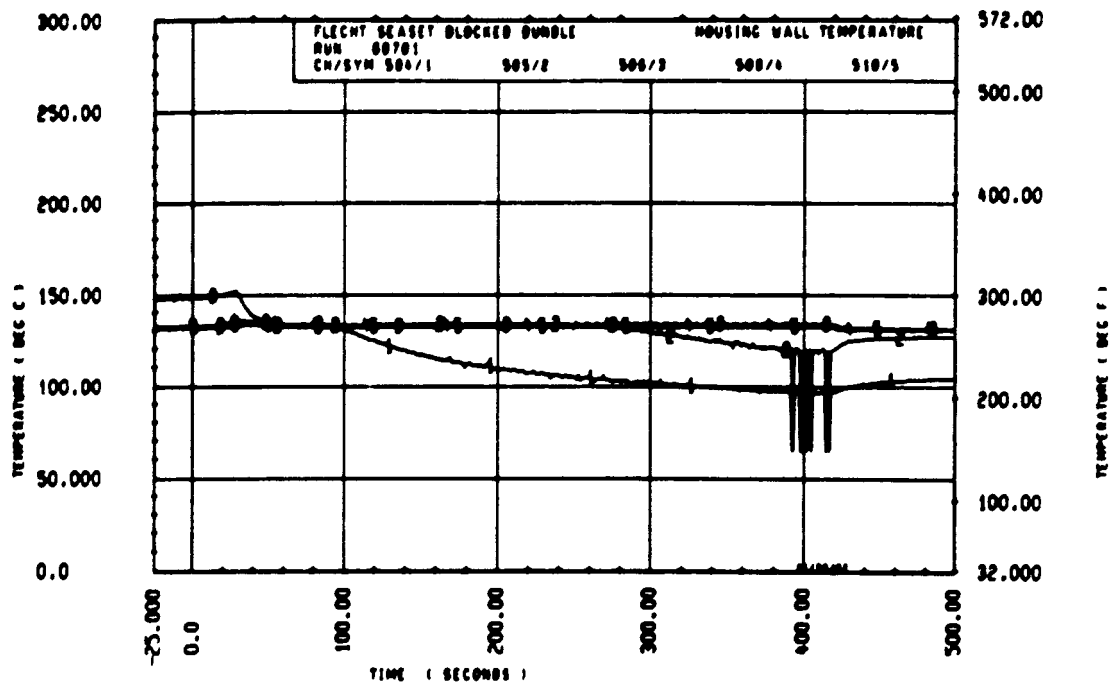


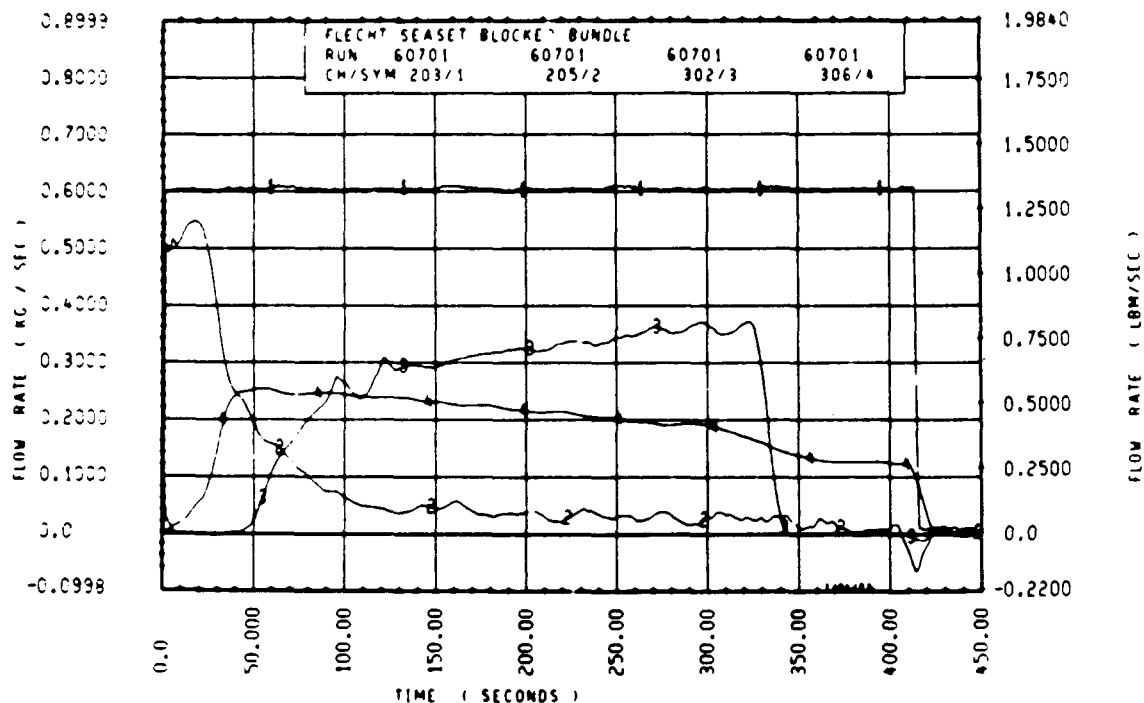
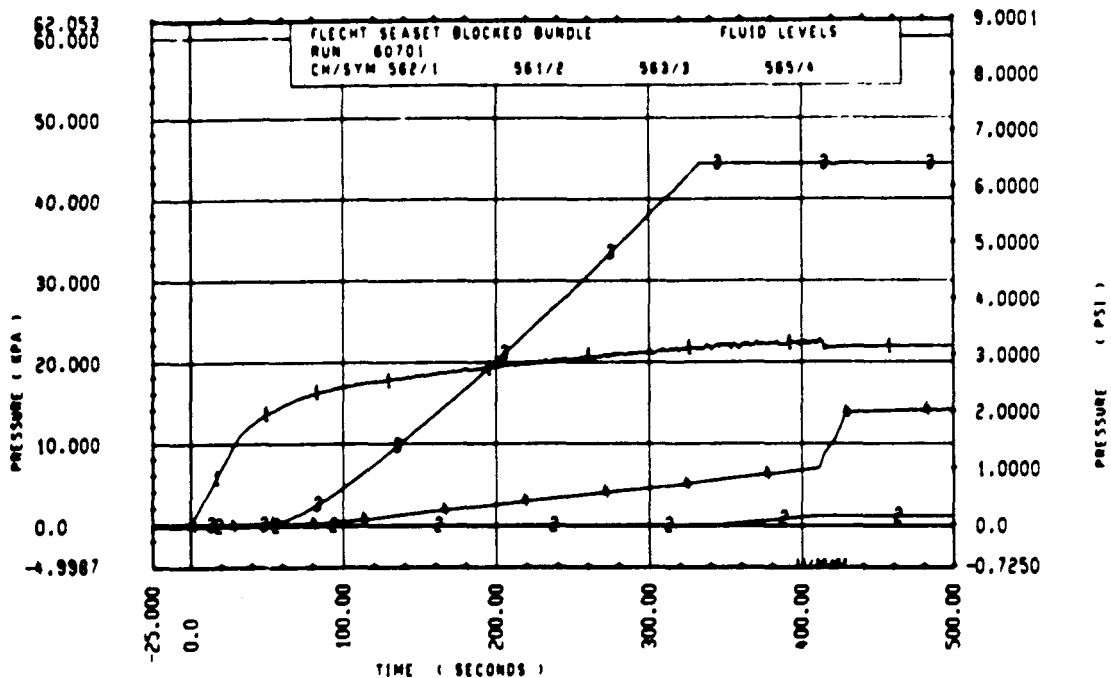
Rod 7D, 2.44 m (96 in.)

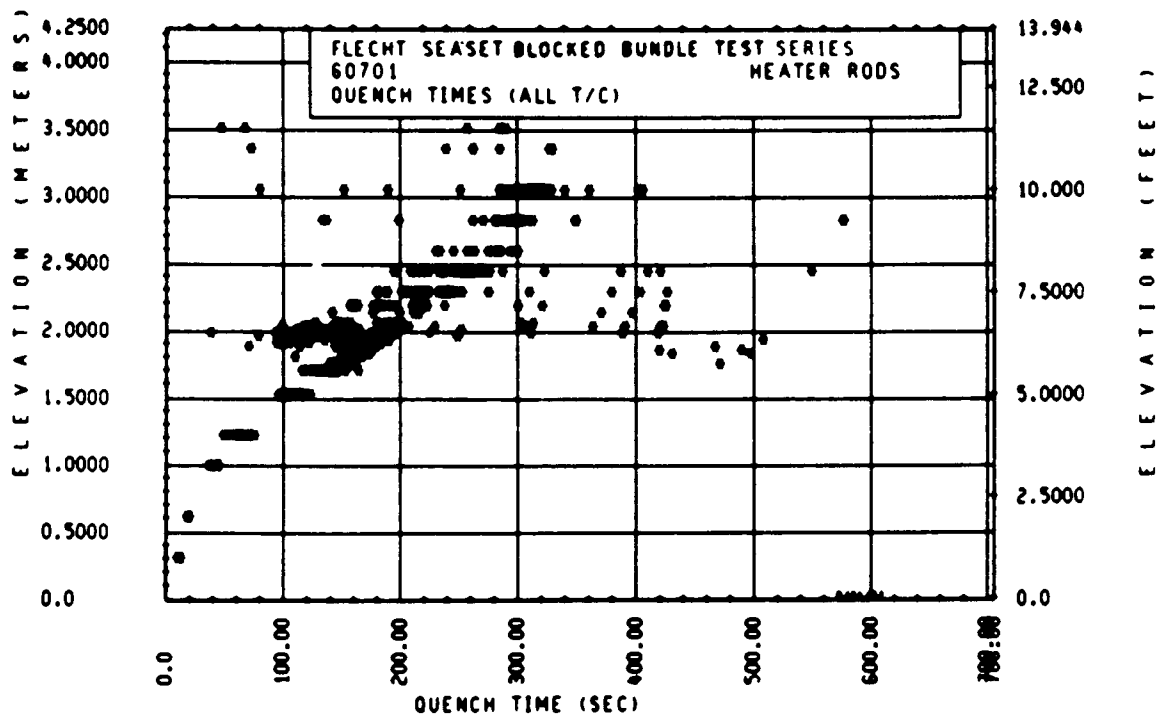
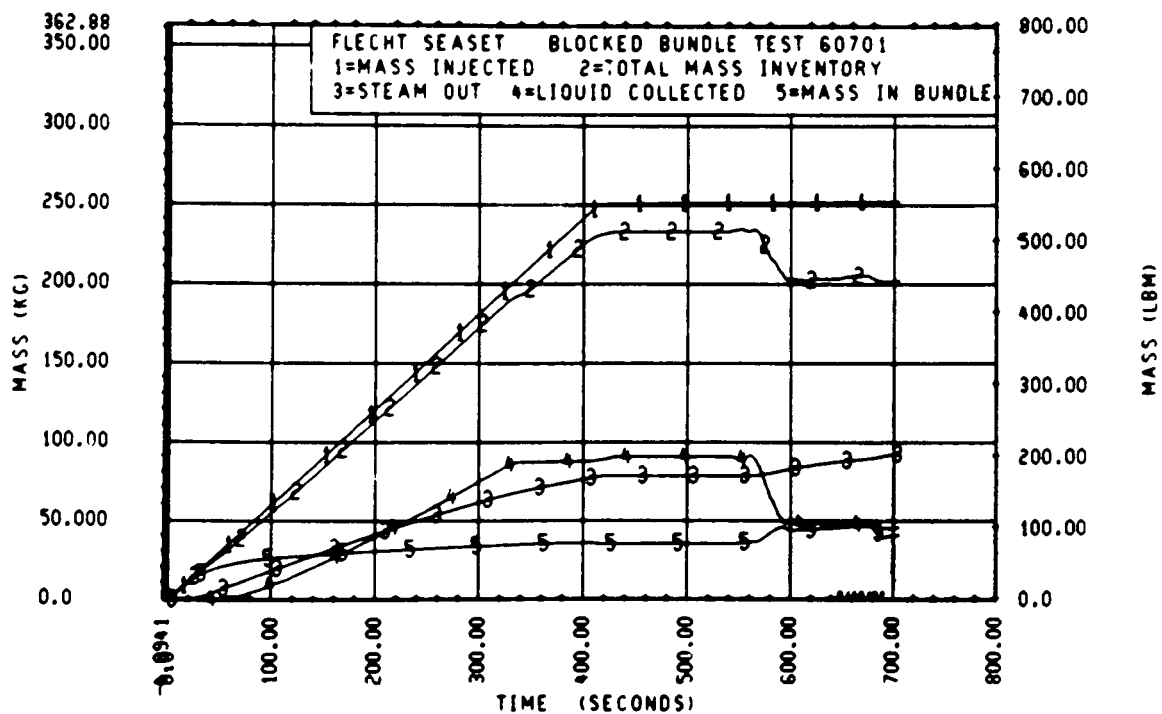


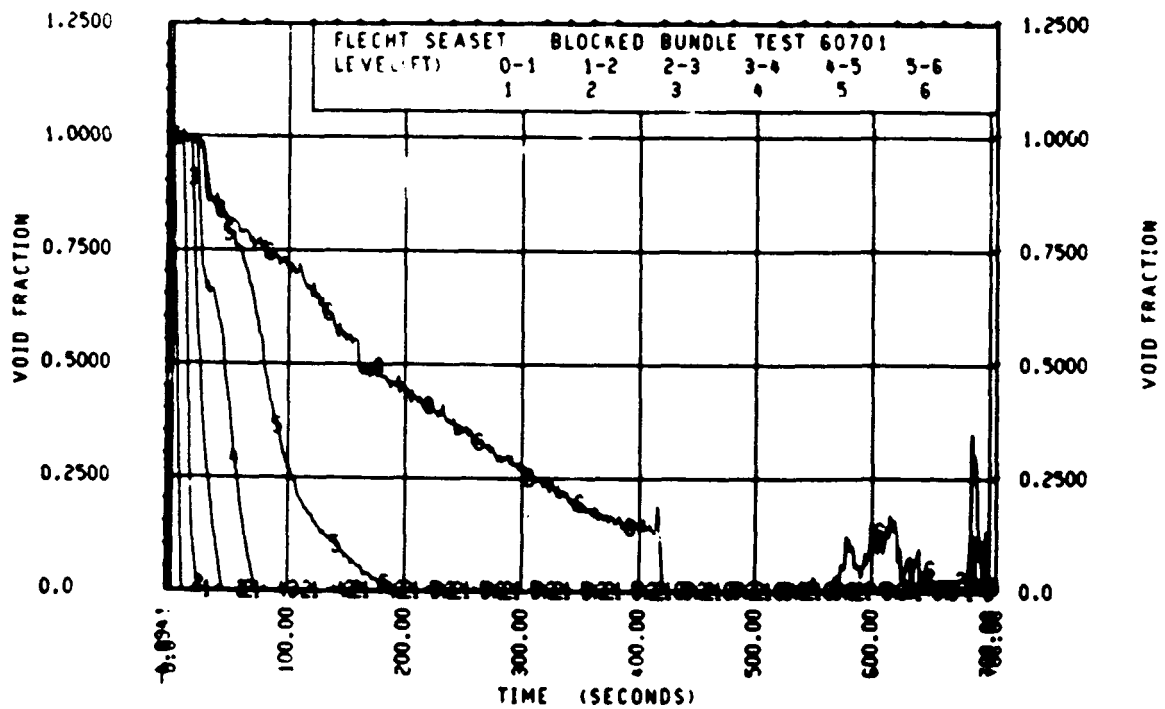
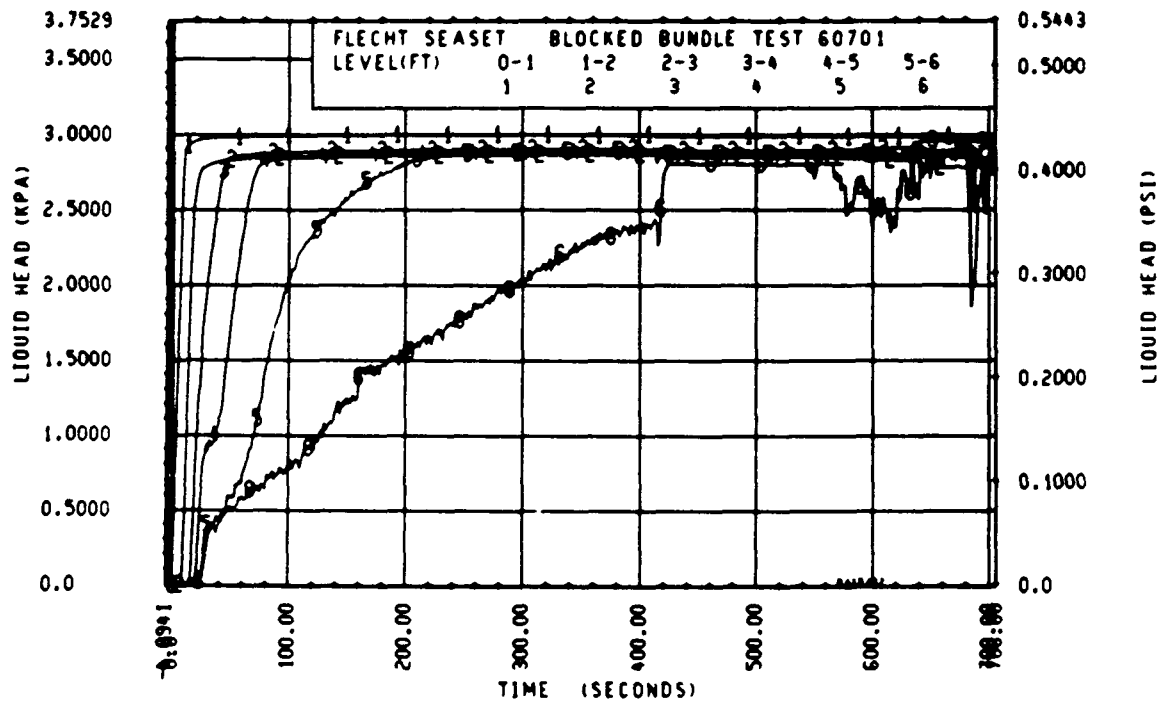
Rod 8H, 3.05 m (120 in.)

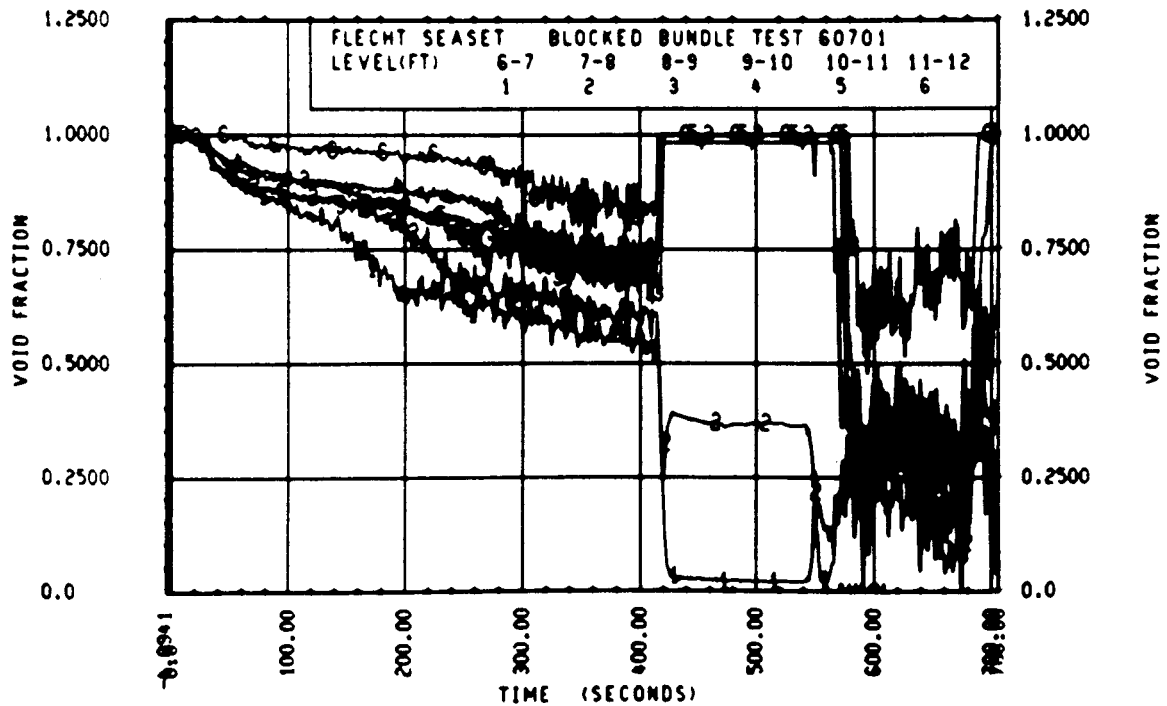
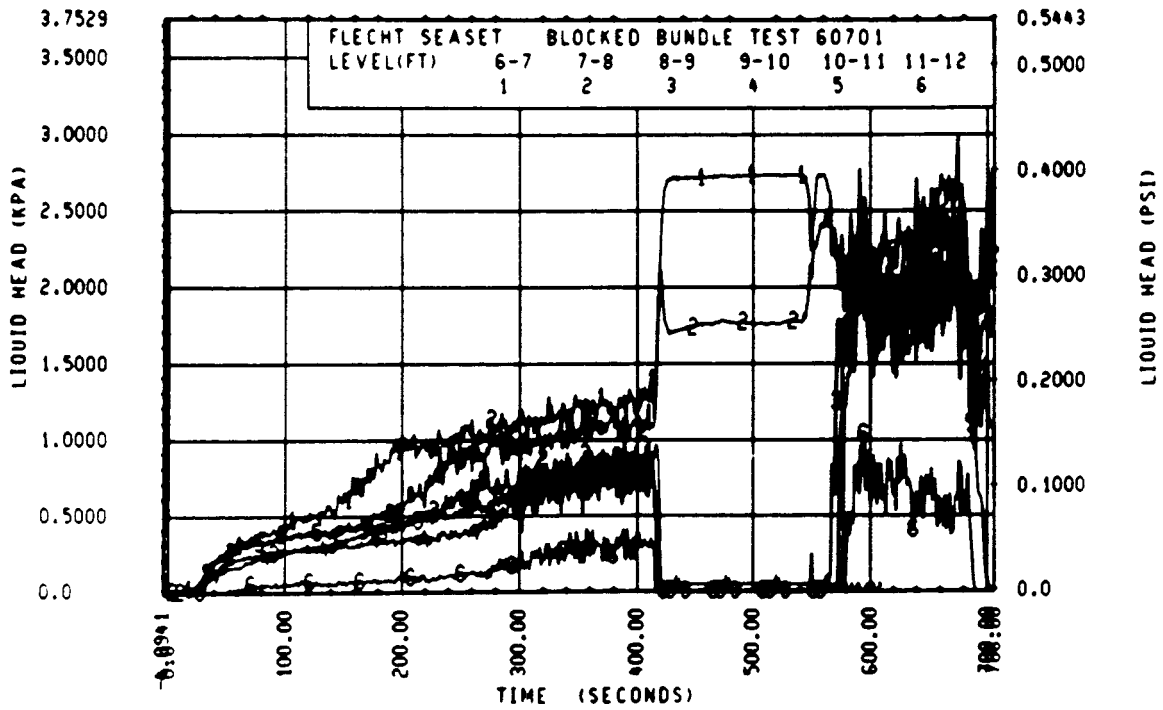












FLECHT SEASET 163-ROD BUNDLE FLOW BLOCKAGE TASK
SUMMARY AND COMMENT SHEET

Run: 60802
Test date: 8/18/82
Test type: Forced reflood
Parameter: Initial clad temperature effect

AS-RUN TEST CONDITIONS:

Upper plenum pressure	0.2710 MPa (39.30 psia)
Initial peak clad temperature and location	538.8°C (1001.9°F), 2I-1.93 m (76 in.)
Initial peak rod power:	
Peripheral rods	2.29 kW/m (0.698 kW/ft)
Bypass rods	2.30 kW/m (0.701 kW/ft)
Blockage island rods	2.30 kW/m (0.700 kW/ft)
Flooding rate	38.6 mm/sec (1.52 in./sec)
Coolant temperature	53.9°C (129°F)
Initial bundle water level	+4.6 mm (+0.18 in.)

COMMENTS:

Inlet mass flow: ⁽¹⁾ -0.6% exponentially increasing to +0.9% by 300 seconds

No heat transfer plots are included.

1. Relative to run 30817

FLECHT SEASET 163 ROJ BUNDLE TEST SERIES

RUN NUMBER 60802

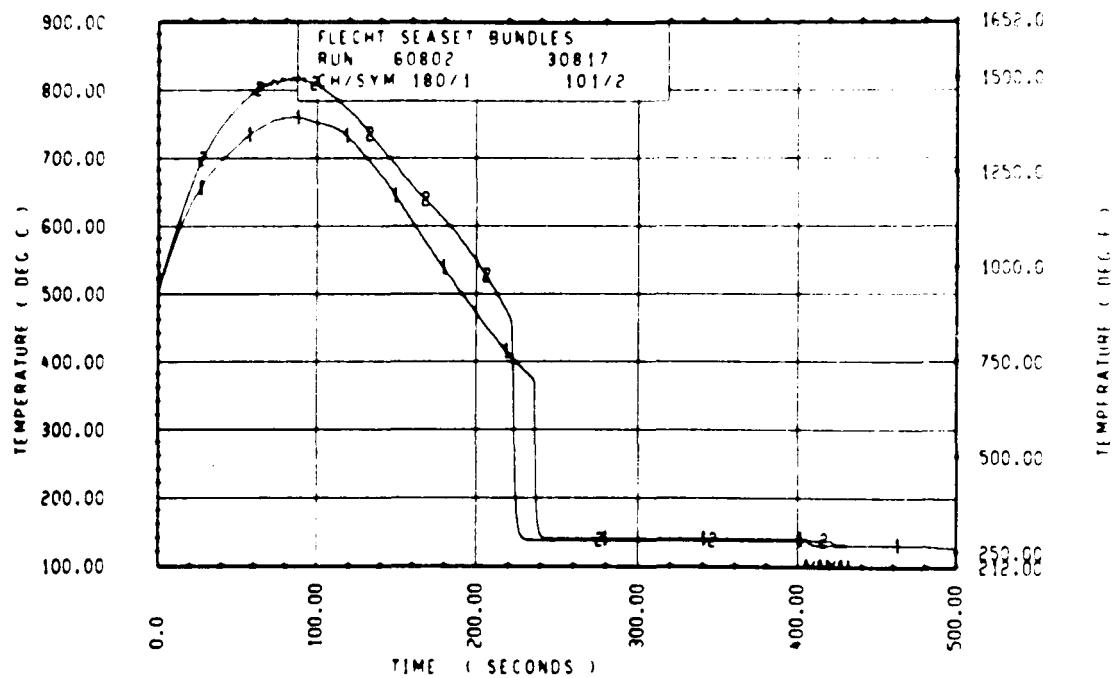
ROD/ELEV	CHAN. NO	INITIAL AT FLOOD (DEG F)	MAXIMUM TEMPERATURE (DEG F)	TEMPERATURE RISE (DEG F)	TURNAROUND TIME (SECONDS)	QUENCH TEMPERATURE (DEG F)	QUENCH TIME (SECONDS)
96 1- 0	3	476.	497.	22.	5.5	443.	14.0
10M 2- 0	6	594.	656.	62.	11.0	559.	33.9
96 3- 3	9	756.	882.	126.	17.0	703.	61.9
3J 4- 0	11	844.	1026.	182.	27.0	722.	95.7
7H 4- 0	12	819.	1013.	194.	29.5	705.	94.0
8K 4- 0	13	832.	1030.	198.	28.0	699.	98.0
8M 4- 0	14	826.	1012.	186.	25.0	749.	96.0
12D 4- 0	17	826.	1011.	185.	27.0	743.	90.6
5E 5- 0	20	909.	1207.	297.	40.0	744.	135.3
76 5- 0	21	945.	1273.	328.	45.0	788.	143.9
96 5- 0	24	943.	1271.	328.	46.5	794.	144.4
5E 5- 7	33	938.	1282.	344.	59.5	808.	166.9
8G 5- 7	45	938.	1322.	384.	64.0	785.	170.4
9M 5- 9	52	892.	1304.	412.	69.0	754.	183.3
76 5-10	59	949.	1335.	386.	65.0	951.	139.3
7F 5-11	62	904.	1293.	389.	63.0	894.	186.4
4G 5-11	64	958.	1353.	396.	65.0	754.	149.7
2I 6- 0	67	991.	1365.	374.	56.0	778.	190.8
5D 6- 0	70	935.	1323.	388.	75.0	735.	198.9
6J 6- 0	74	939.	1303.	364.	46.0	762.	205.1
7M 6- 0	66	930.	1310.	380.	60.5	734.	200.6
11E 6- 0	80	961.	1346.	385.	66.0	754.	197.5
8M 6- 2	97	896.	1233.	337.	55.0	665.	233.0
5M 6- 2	99	974.	1384.	410.	71.5	729.	216.1
5E 6- 2	105	800.	1303.	559.	98.5	279.	463.1
8M 6- 3	111	922.	1255.	332.	72.0	705.	236.6
4G 6- 3	124	970.	1398.	428.	73.5	765.	217.0
11M 6- 4	134	903.	1346.	443.	87.0	608.	219.5
9D 6- 4	143	955.	1410.	455.	87.5	779.	213.6
9J 6- 5	165	952.	1388.	436.	85.5	1087.	153.3
9M 6- 5	166	968.	1425.	457.	74.0	799.	220.1
8J 6- 6	192	964.	1393.	430.	76.0	884.	204.0
9D 6- 6	193	939.	1439.	500.	87.5	797.	221.9
11F 6- 6	173	962.	1433.	471.	87.0	765.	227.0
4G 7- 0	261	946.	1368.	420.	72.0	720.	257.7
7D 7- 6	309	902.	1503.	602.	124.0	755.	294.7
76 7- 6	312	924.	1445.	521.	112.0	563.	402.9
11E 7- 6	325	928.	1420.	492.	91.0	774.	278.4
5L 8- 0	337	807.	1346.	539.	96.5	755.	307.0
7H 8- 0	345	818.	1328.	510.	115.5	806.	298.0
7K 8- 0	346	849.	1414.	564.	118.0	766.	303.6
5J 8- 6	366	744.	1171.	427.	137.0	646.	341.0
78 8- 6	368	757.	1139.	382.	122.0	660.	336.1
7E 9- 3	383	687.	1239.	552.	133.5	566.	387.1
8H 9- 3	387	667.	1153.	486.	125.0	597.	351.1
9C 9- 3	389	677.	1164.	487.	149.5	611.	362.1
11F 9- 3	394	673.	1045.	372.	79.0	452.	142.3
7810- 0	408	579.	957.	377.	149.0	581.	376.7
8H10- 0	415	570.	1037.	467.	141.0	609.	335.0
8K10- 0	417	581.	1077.	497.	155.0	559.	364.7
8N10- 0	418	578.	1070.	492.	141.5	690.	363.1
6H11- 0	429	476.	745.	270.	139.0	512.	338.1
9G11- 0	431	472.	624.	151.	59.5	609.	62.8
11E11- 0	432	470.	646.	169.	109.0	485.	342.0
5J11- 6	436	477.	653.	176.	81.0	577.	125.9
7811- 6	437	462.	692.	231.	120.5	598.	301.8
8J11- 6	438	482.	745.	263.	134.5	545.	332.1

RUN 60802 HEATER ROD STATISTICAL DATA

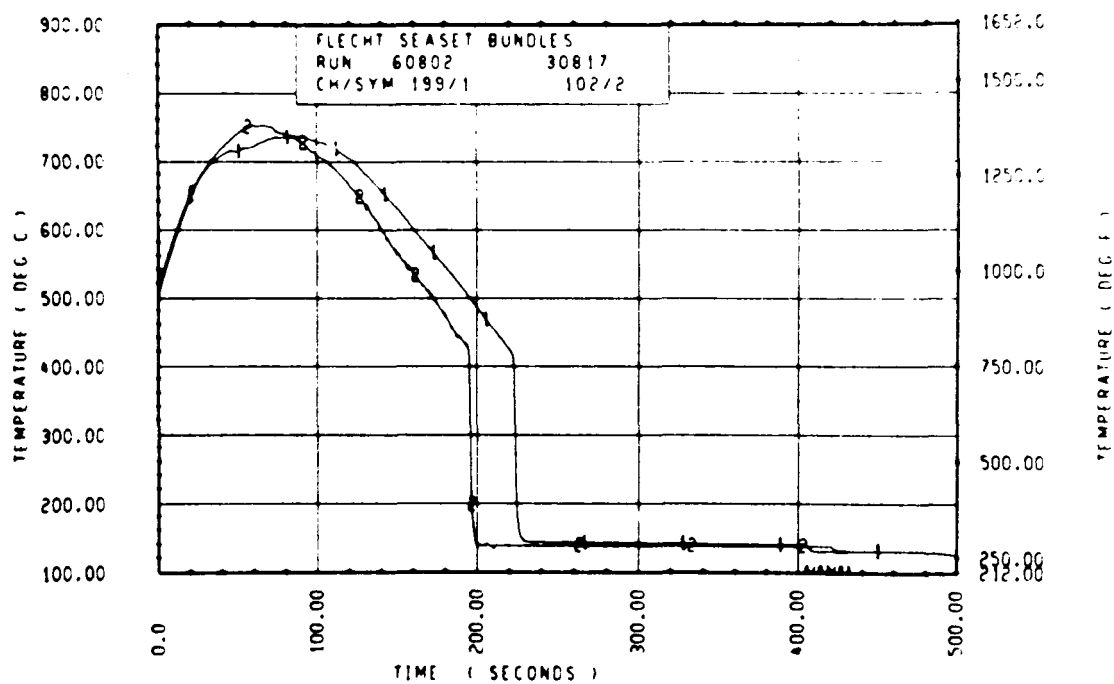
ELEV	INITIAL TEMP (DEG F)			MAX TEMP (DEG F)			TURNAROUND TIME (SEC)		
	MAX	MIN	MEAN	MAX	MIN	MEAN	MAX	MIN	MEAN
12	479.0	475.7	477.2	503.9	497.5	500.7	6.0	5.5	5.7
24	594.4	583.7	588.7	656.4	640.6	647.7	11.0	10.0	10.5
39	755.7	735.9	743.2	882.2	859.4	868.0	20.5	17.0	18.9
48	843.9	816.0	828.9	1029.7	1011.2	1017.9	23.5	25.0	27.1
60	969.9	883.2	927.7	1273.3	1165.1	1230.6	55.5	40.0	48.6
67	980.2	895.7	954.1	1335.3	1251.4	1302.2	64.0	44.0	55.0
69	952.4	891.5	929.5	1317.4	1204.8	1305.4	69.0	55.5	61.6
70	995.7	936.9	956.5	1350.1	1304.7	1330.6	65.0	59.0	62.0
71	957.6	903.9	933.6	1353.2	1293.2	1326.9	69.5	63.0	66.6
72	990.6	919.4	952.8	1379.6	1302.6	1343.0	75.0	46.0	63.0
73	979.2	918.4	952.0	1373.3	1319.5	1355.1	75.0	53.0	67.0
74	985.4	889.5	944.9	1401.8	1232.7	1338.1	75.5	53.0	66.4
75	988.5	892.6	947.8	1411.4	1254.6	1364.4	90.5	46.0	72.8
76	1001.9	902.9	958.4	1418.9	1302.6	1362.9	87.5	63.5	74.6
77	978.2	914.2	950.4	1442.4	1299.4	1391.7	97.0	66.5	80.8
78	978.2	914.2	951.1	1446.7	1315.3	1406.7	96.5	71.0	84.0
79	979.2	923.5	952.2	1458.4	1357.5	1427.9	103.5	73.0	87.3
80	964.8	908.1	937.9	1471.3	1377.5	1438.2	113.5	83.0	91.3
81	952.4	892.6	923.6	1458.4	1374.3	1427.0	109.0	74.5	91.0
84	967.9	898.8	941.3	1407.1	1230.6	1330.1	90.0	50.5	70.7
86	962.7	917.3	939.9	1461.6	1319.5	1390.8	199.5	65.5	87.4
90	927.6	884.3	905.4	1503.4	1360.6	1437.1	124.0	81.5	104.6
96	349.1	806.7	829.6	1488.4	1318.4	1418.6	133.0	75.0	117.2
102	758.8	735.9	748.0	1313.1	1091.6	1224.0	137.0	118.5	125.8
111	886.9	661.7	673.2	1238.9	993.6	1137.0	150.0	79.0	123.9
120	608.1	556.2	578.4	1123.7	785.9	998.5	172.5	72.5	139.9
132	477.9	469.2	473.1	745.3	623.8	691.9	147.0	59.5	114.9
138	482.2	457.2	467.7	745.3	582.6	659.0	134.5	36.0	91.3

RUN 60802 HEATER ROD STATISTICAL DATA

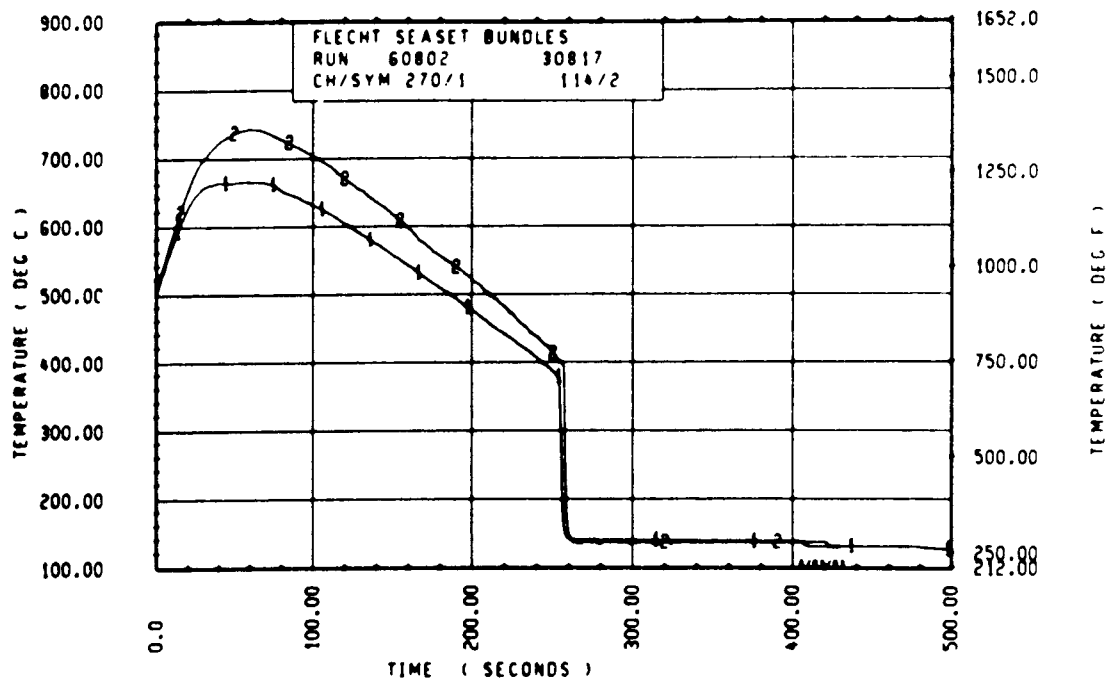
ELEV	TEMP RISE (DEG F)			QUENCH TEMP (DEG F)			QUENCH TIME (SEC)		
	MAX	MIN	MEAN	MAX	MIN	MEAN	MAX	MIN	MEAN
12	24.9	21.7	23.5	468.1	443.3	458.0	17.8	12.3	14.7
24	62.0	56.9	59.0	581.8	545.5	562.0	33.9	24.6	30.5
39	127.6	121.4	124.7	703.0	689.7	697.0	67.8	61.5	63.8
48	198.2	181.6	188.9	771.0	699.0	726.7	95.0	80.9	92.3
60	336.4	272.5	310.9	839.0	788.4	803.2	151.9	134.2	141.8
67	383.6	321.2	348.1	833.9	718.2	774.4	183.8	162.7	173.6
69	412.1	363.6	375.9	780.7	753.0	766.6	192.4	174.5	182.9
70	389.2	354.4	374.1	951.0	761.6	813.7	189.9	139.3	177.8
71	401.8	386.4	393.3	792.7	694.4	750.8	199.7	186.8	191.8
72	422.3	363.6	390.1	780.3	733.6	763.5	275.1	193.5	200.0
73	416.6	386.9	403.1	819.7	742.1	775.4	298.8	193.4	200.9
74	425.3	337.0	393.3	792.9	665.0	749.8	233.0	122.8	201.6
75	441.7	332.1	416.5	833.8	517.7	735.0	236.8	191.7	212.0
76	459.2	339.9	424.5	830.8	607.6	763.0	222.8	192.9	211.9
77	510.0	354.2	441.3	1086.7	581.6	757.1	285.1	153.3	222.7
78	509.0	383.3	455.6	1053.4	520.9	747.4	197.1	165.3	241.2
79	513.9	410.2	475.8	872.9	282.5	741.9	406.1	213.5	246.9
80	539.7	442.6	500.3	1057.4	493.7	746.1	411.1	185.8	265.9
81	538.8	450.8	503.4	889.2	379.7	767.1	325.8	229.0	254.4
84	448.9	297.8	388.8	786.1	580.9	701.2	394.1	247.8	275.5
86	526.7	356.8	463.0	895.4	285.7	711.2	413.1	231.0	279.3
90	601.5	454.6	531.7	921.0	521.4	757.6	412.3	254.0	294.7
96	659.9	486.9	589.0	888.8	418.1	746.4	478.1	279.7	319.9
102	566.8	355.6	476.0	769.3	589.4	676.8	392.1	311.9	333.0
111	565.7	327.8	463.8	924.2	452.7	651.6	493.5	152.3	342.1
120	545.3	221.3	420.1	831.0	266.3	606.4	504.1	79.4	354.3
132	269.6	151.4	218.9	624.7	457.3	520.2	388.1	62.8	273.0
138	263.1	122.1	191.3	598.2	489.9	557.9	356.1	37.8	230.8



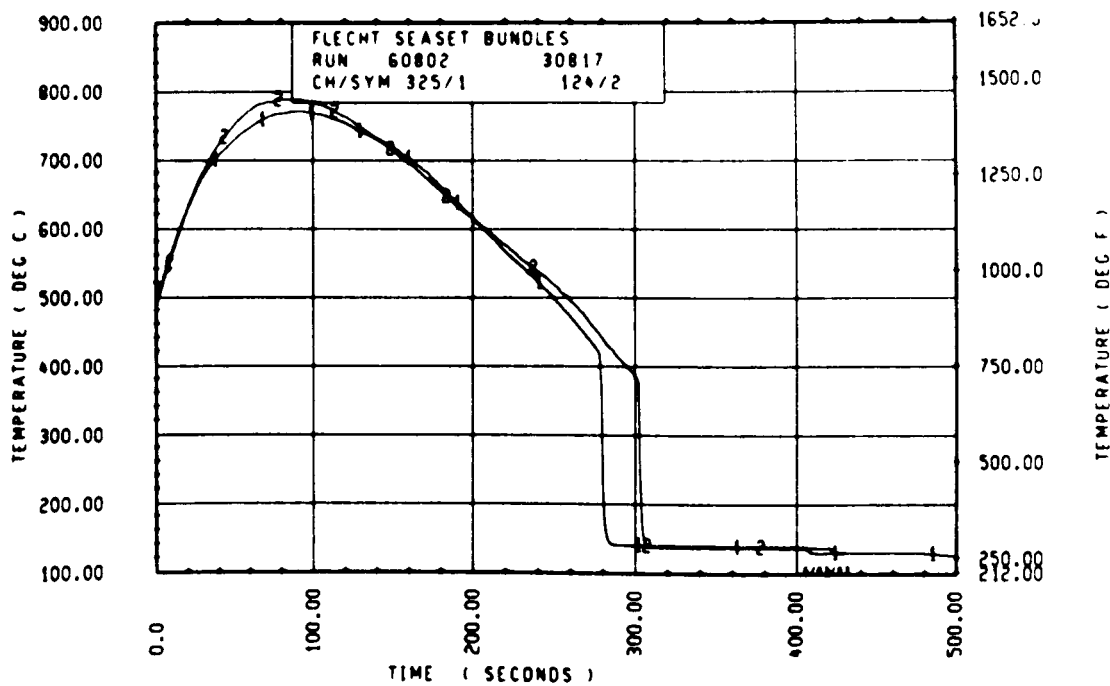
Rod 12I, 1.98 m (78 in.)



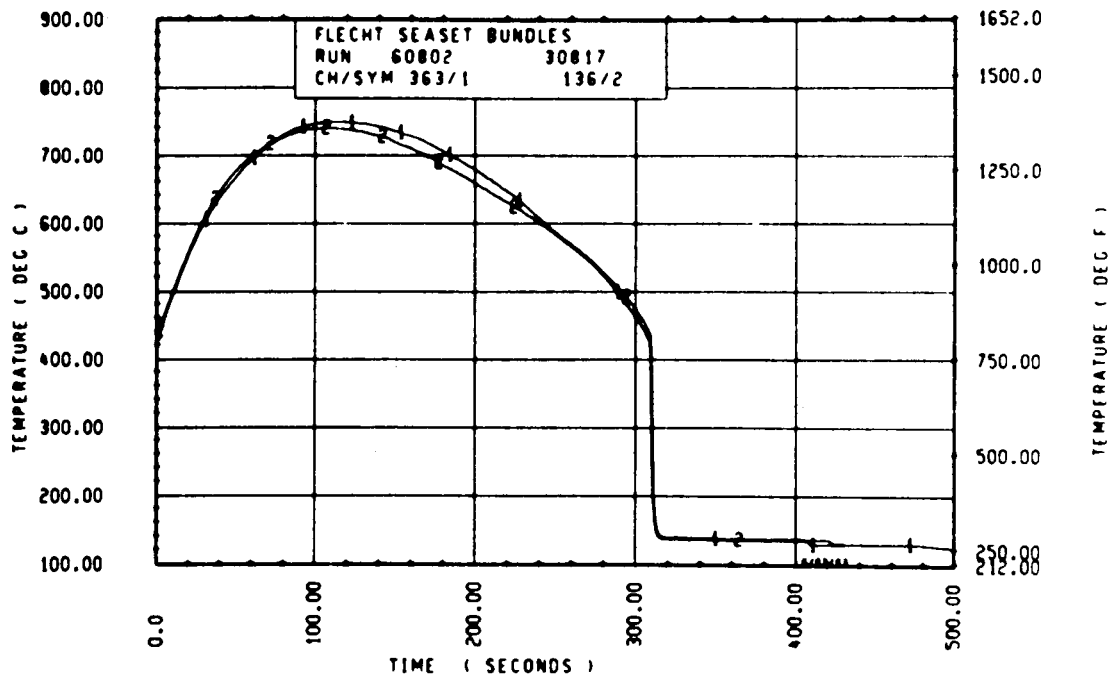
Rod 13G, 1.98 m (78 in.)



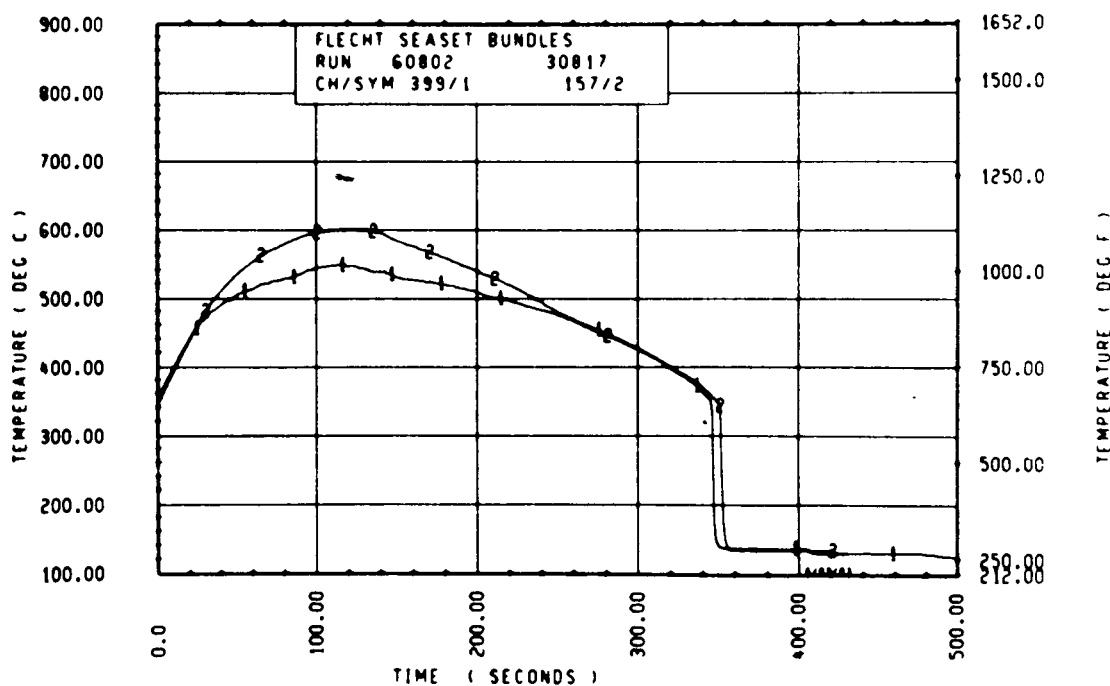
Rod 13G, 2.13 m (84 in.)



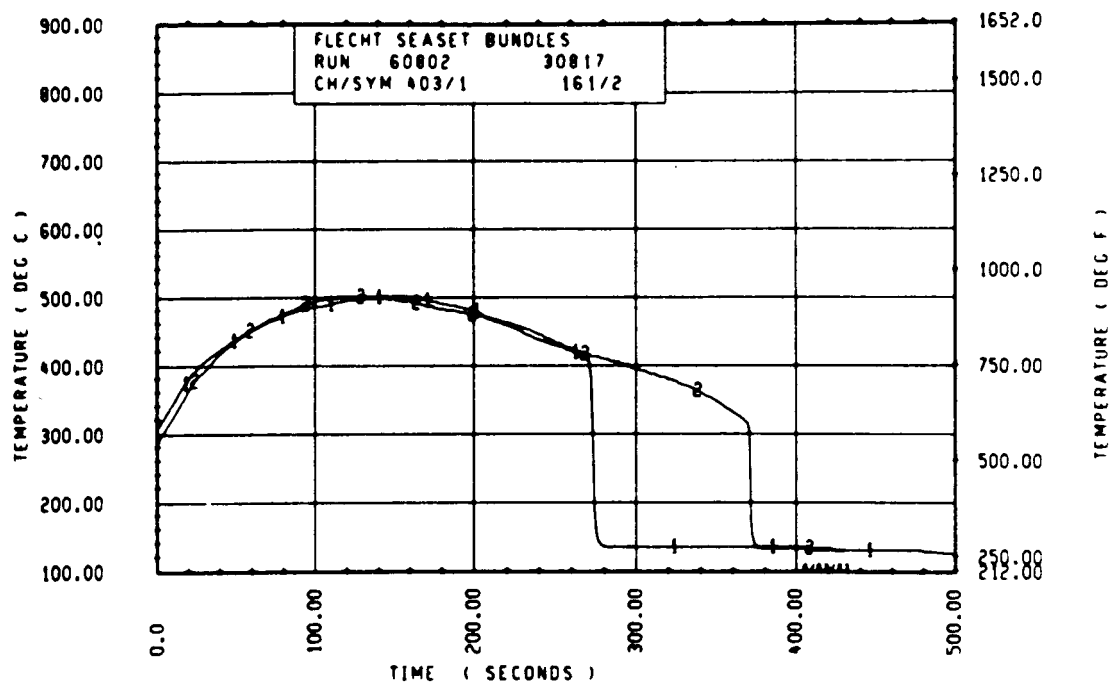
Rod 11E, 2.29 m (90 in.)



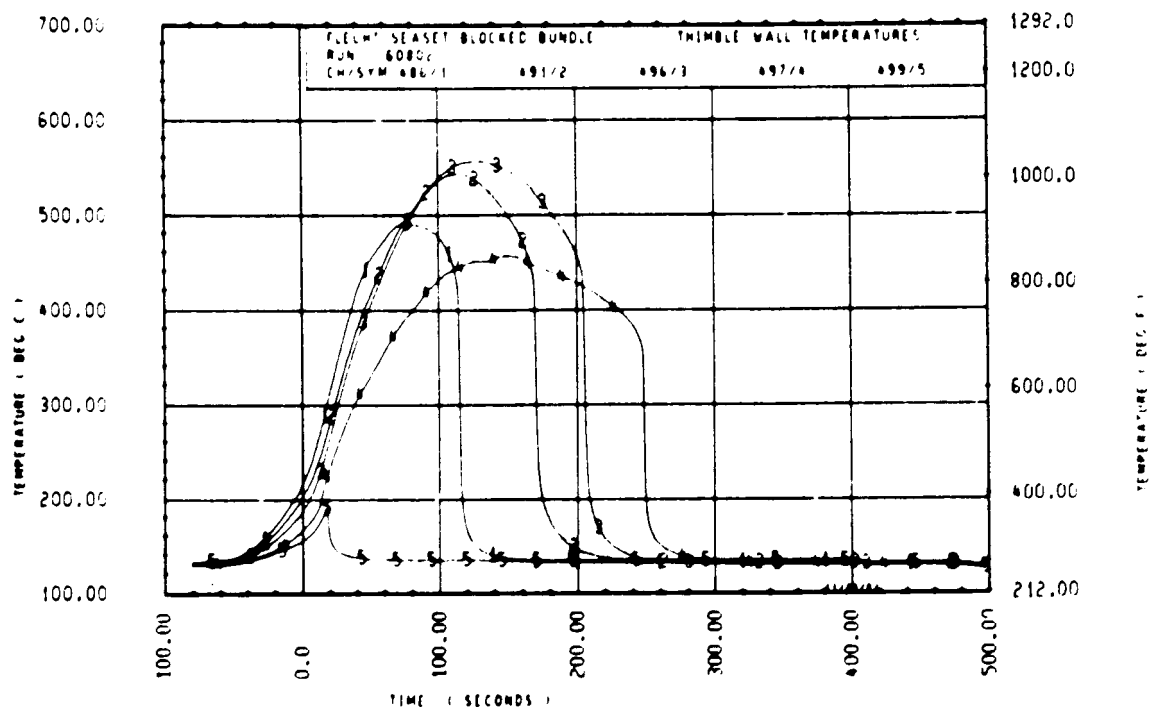
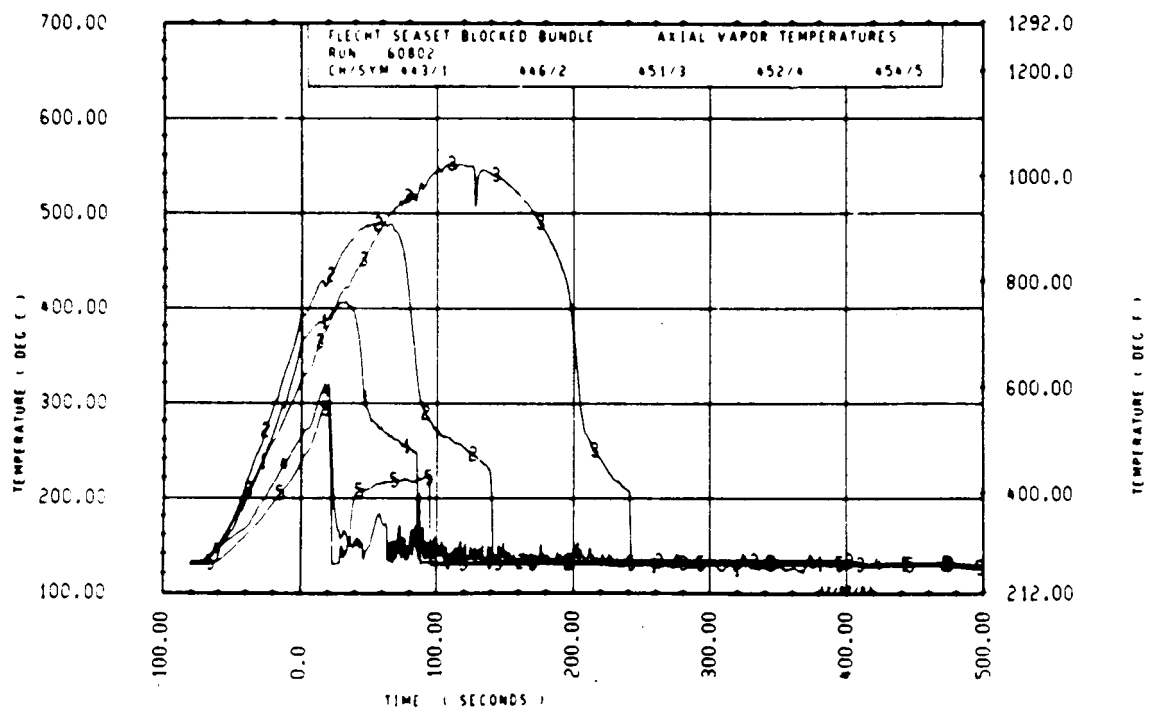
Rod 12D, 2.44 m (96 in.)

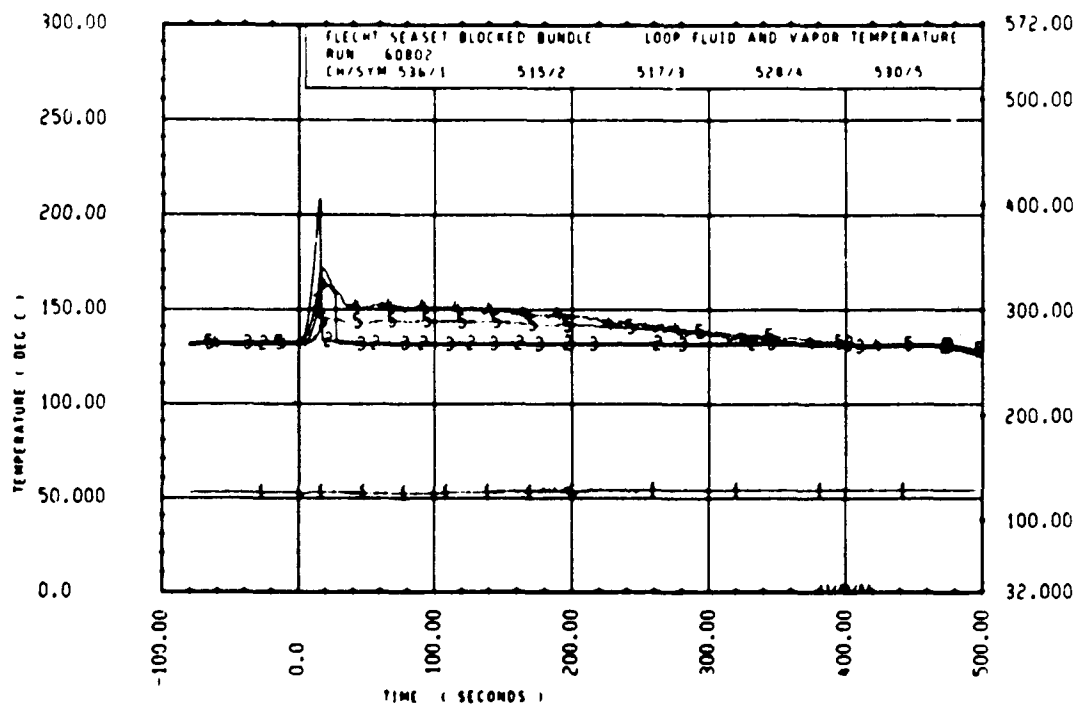
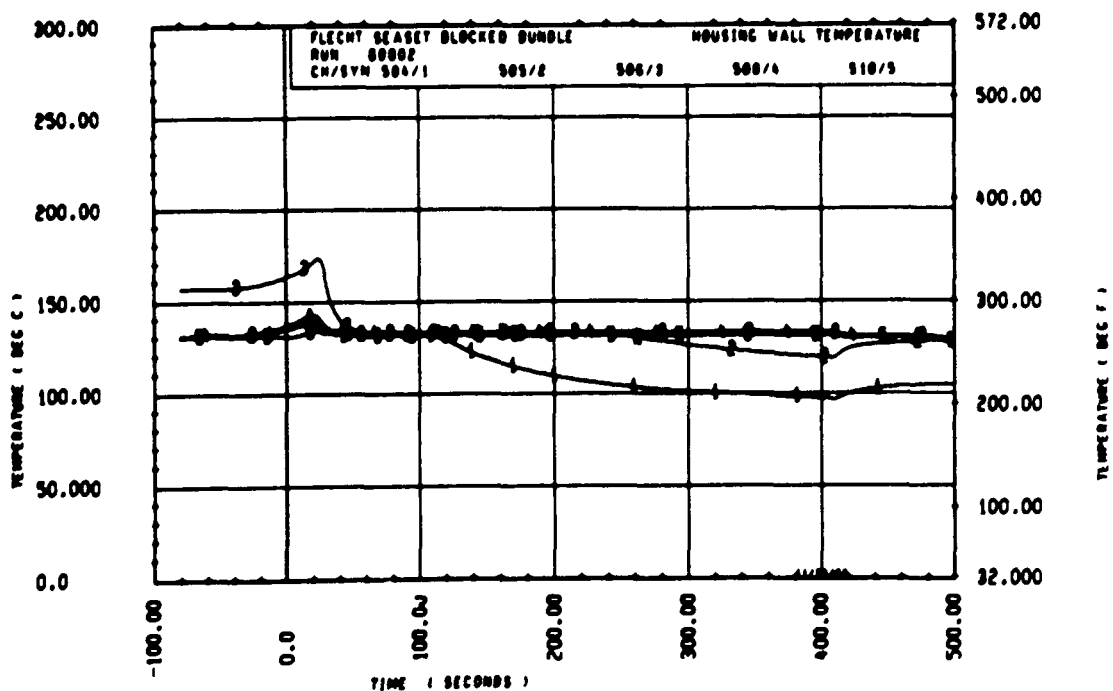


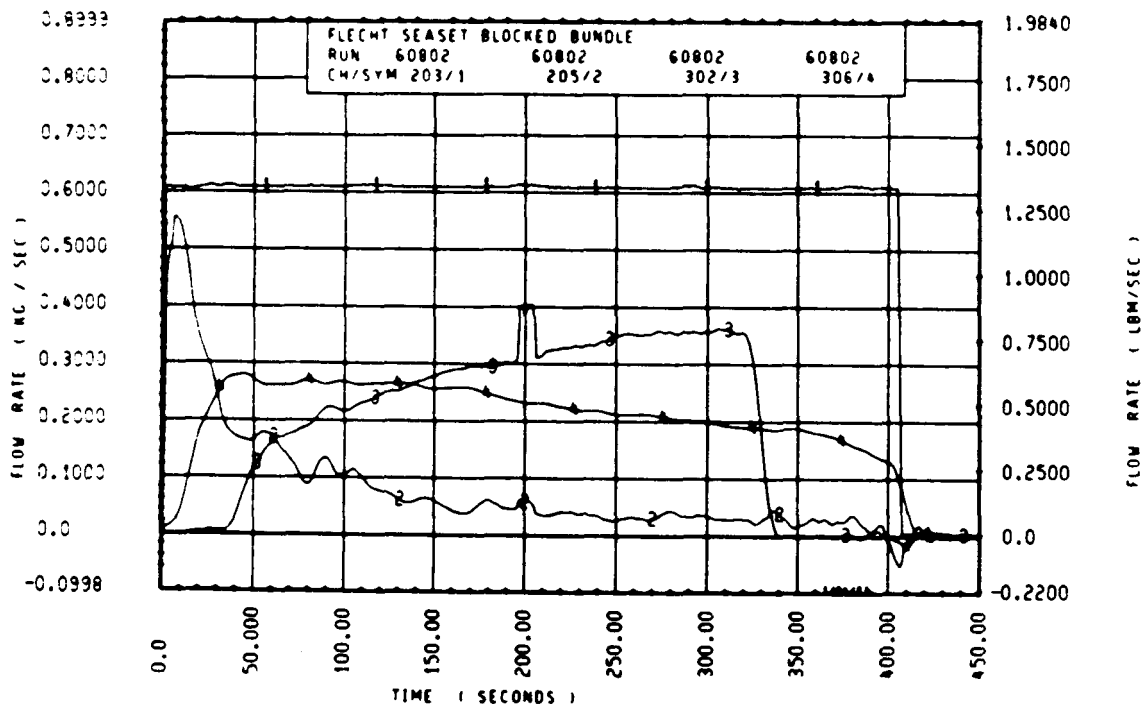
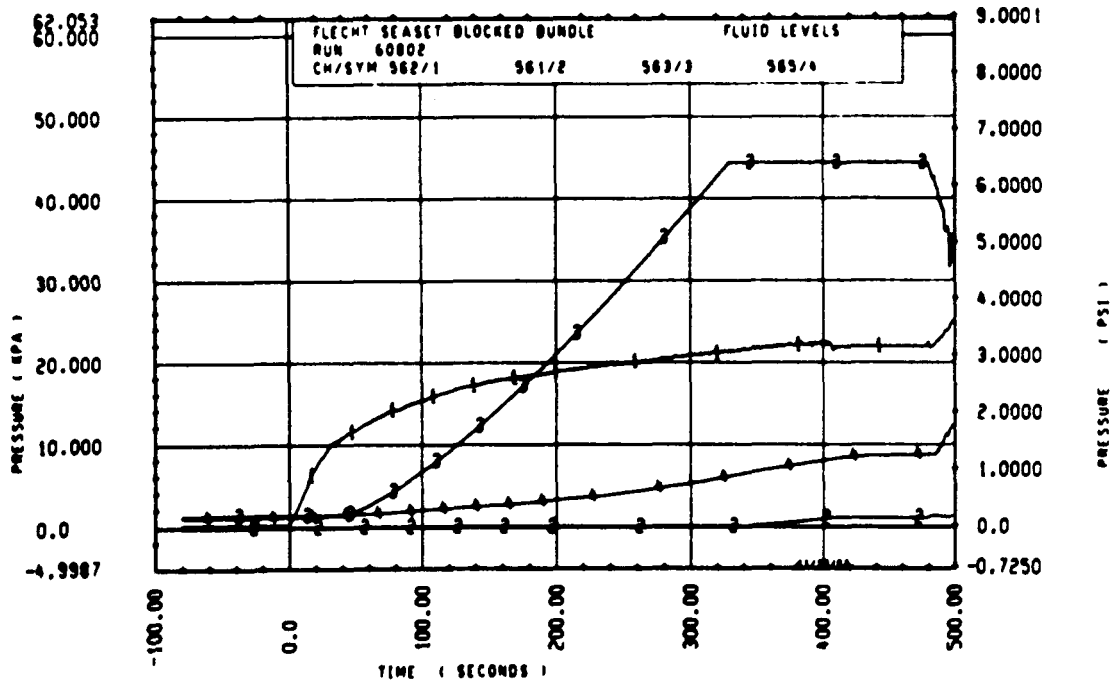
Rod 13G, 2.82 m (111 in.)

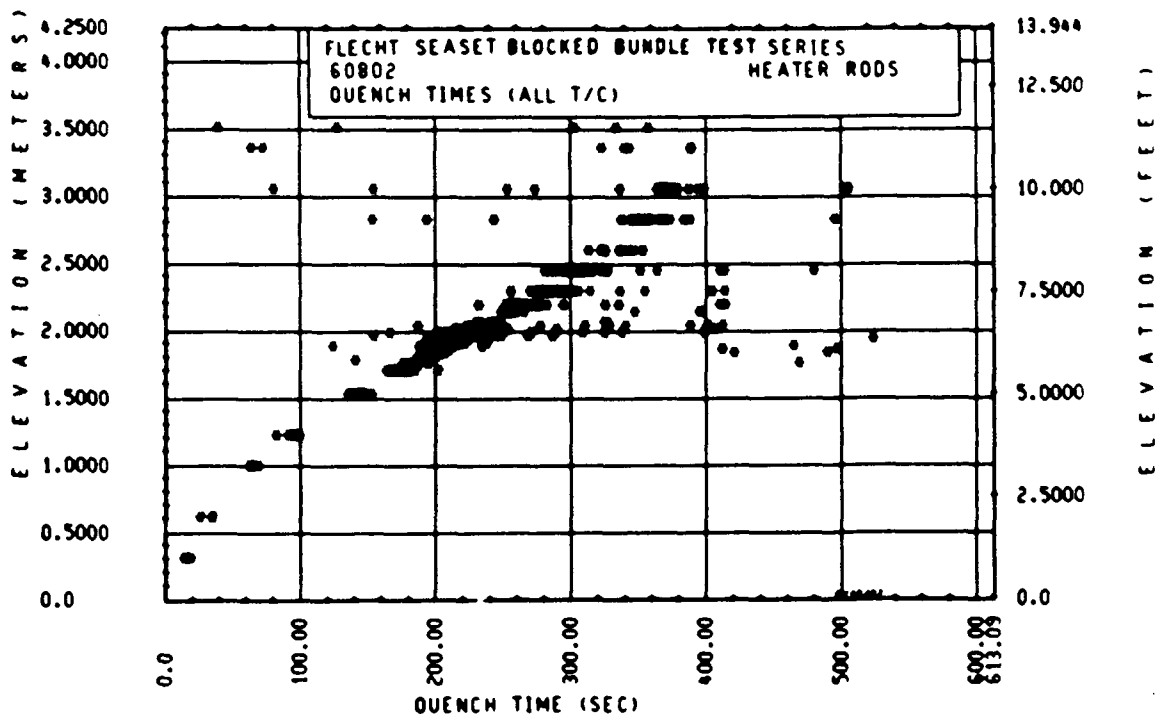
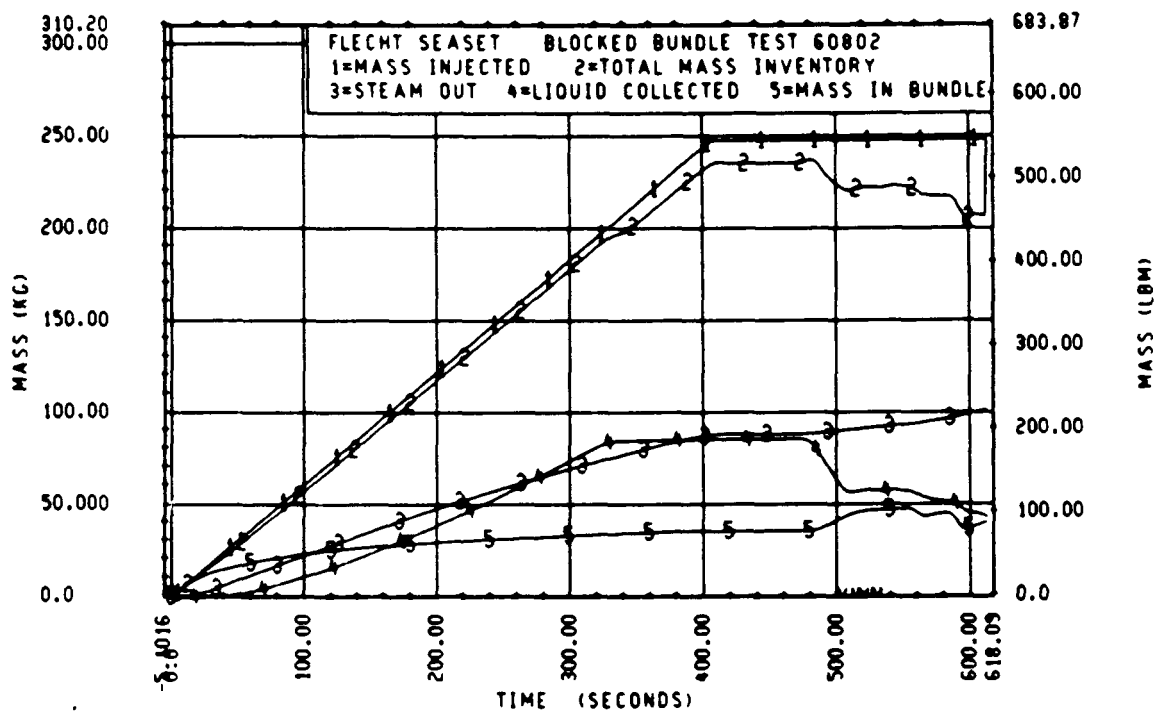


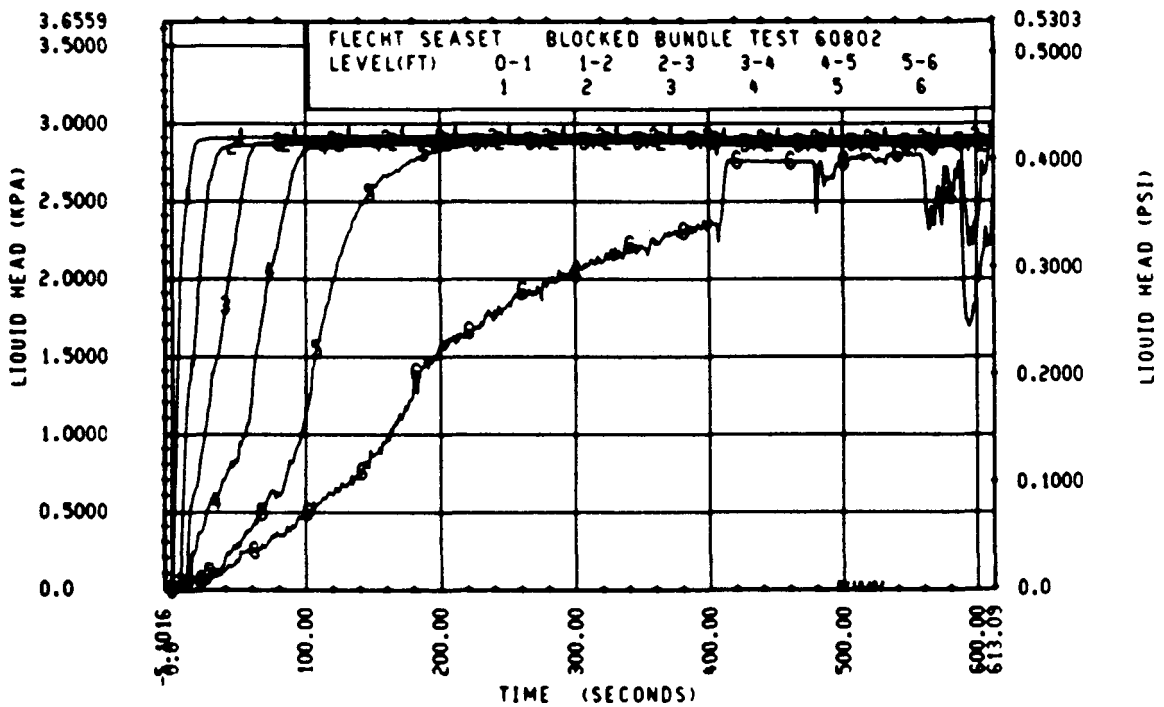
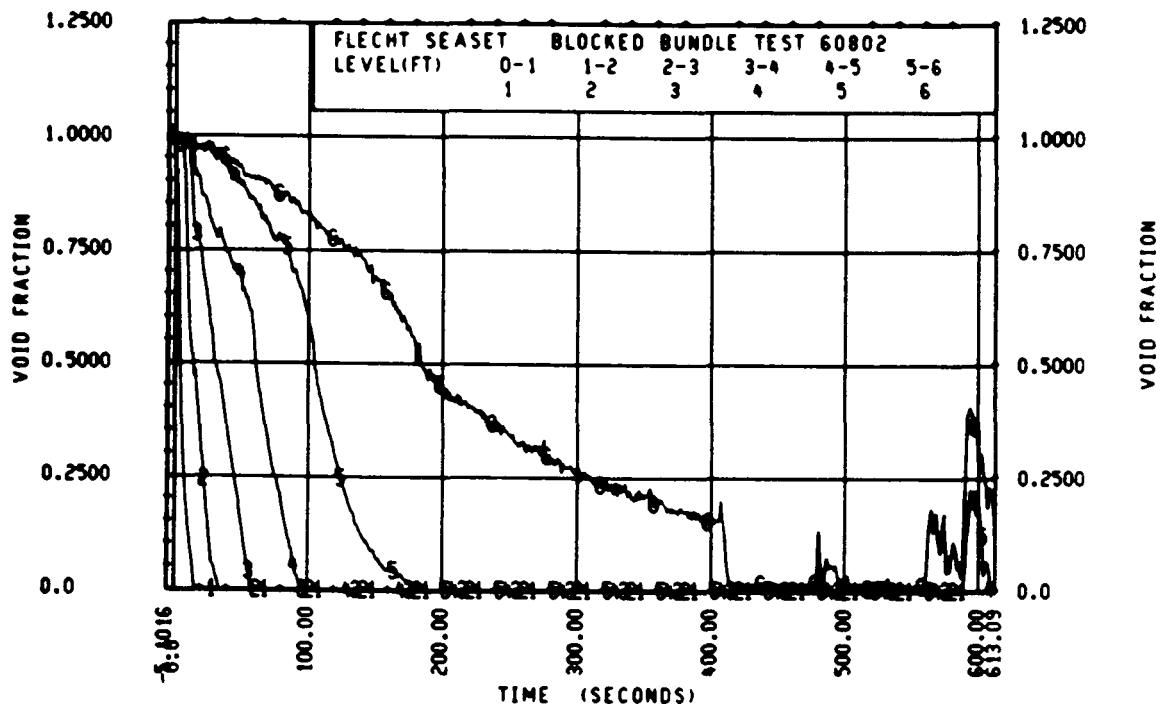
Rod 5J, 3.05 m (120 in.)

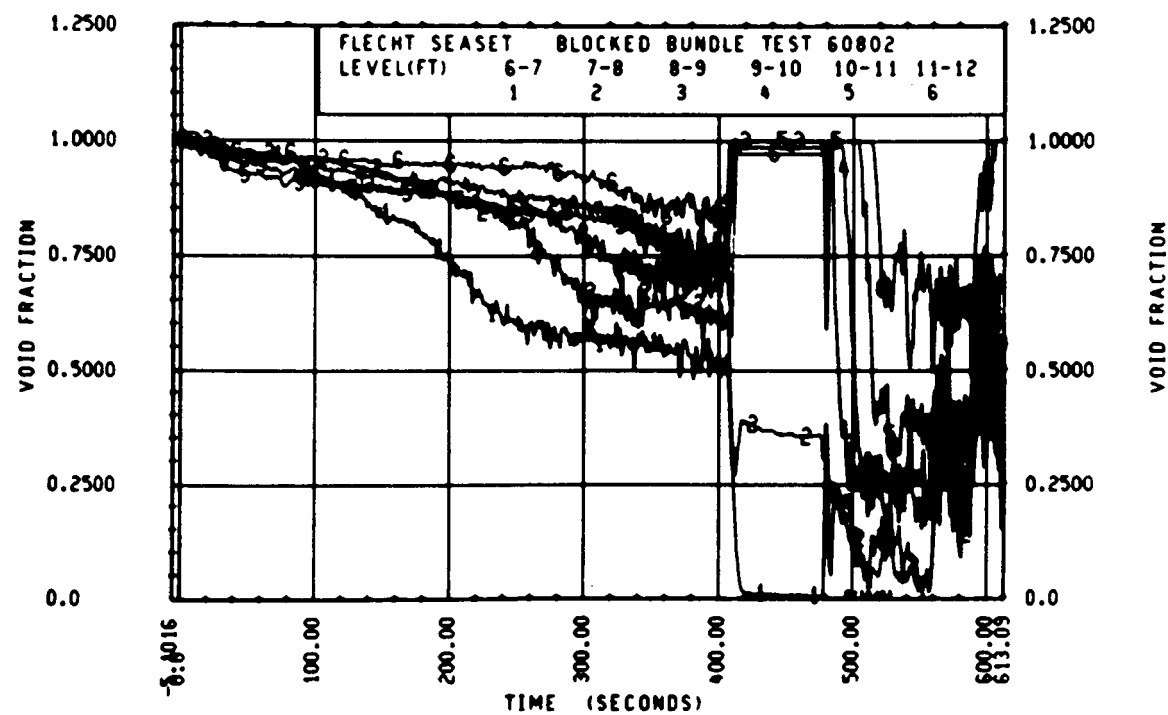
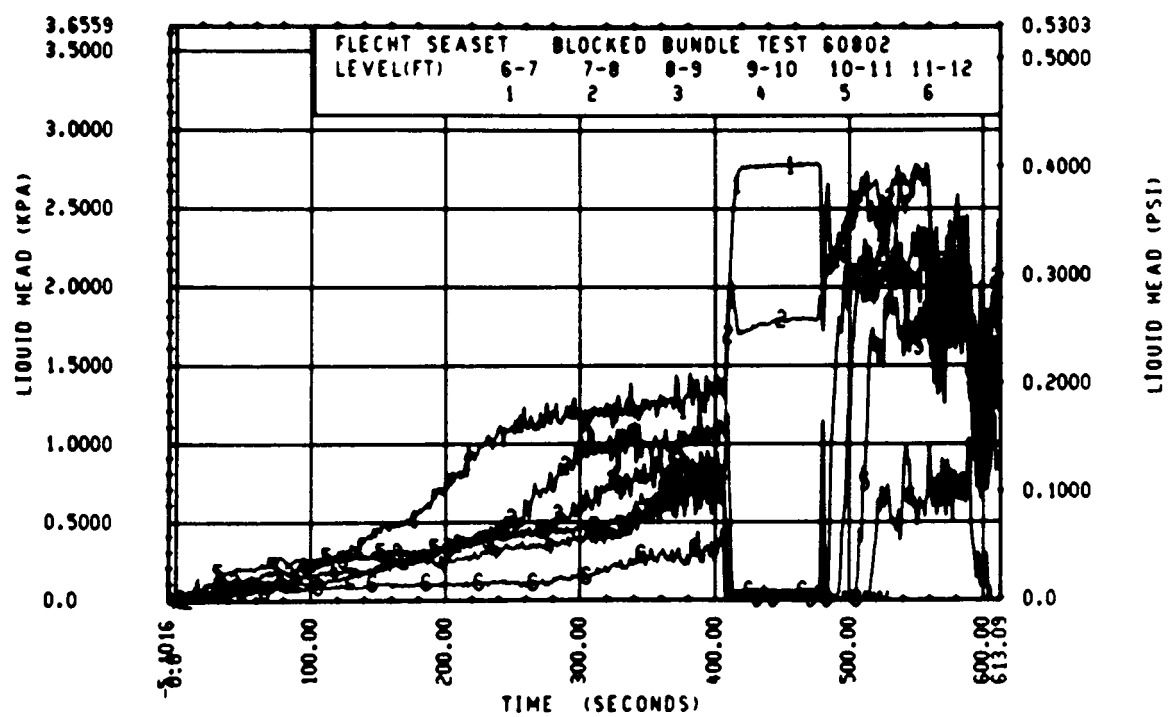












FLECHT SEASET 163-ROD BUNDLE FLOW BLOCKAGE TASK
SUMMARY AND COMMENT SHEET

Run: 60902
Test date: 8/23/82
Test type: Forced reflood
Parameter: Initial clad temperature effect

AS-RUN TEST CONDITIONS:

Upper plenum pressure	0.2703 MPa (39.20 psia)
Initial peak clad temperature and location	538.8°C (1001.9°F), 3K-1.78 m (70 in.)
Initial peak rod power:	
Peripheral rods	2.31 kw/m (0.703 kw/ft)
Bypass rods	2.29 kw/m (0.697 kw/ft)
Blockage island rods	2.30 kw/m (0.701 kw/ft)
Flooding rate	38.6 mm/sec (1.52 in./sec)
Coolant temperature	53.3°C (128°F)
Initial bundle water level	+4.6 mm (+0.18 in.)

COMMENTS:

This test was a repeat of run 60802 with an increase in the steam flow through the aspirating steam probes.

Inlet mass flow:⁽¹⁾ -2.6% exponentially decreasing to 0% by 300 seconds

Power decay:⁽¹⁾ peripheral rods, +0.5% constant
bypass rods, -0.5% linearly changing to +0.5% by 350 seconds
blockage rods, 0% constant

1. Relative to run 30817

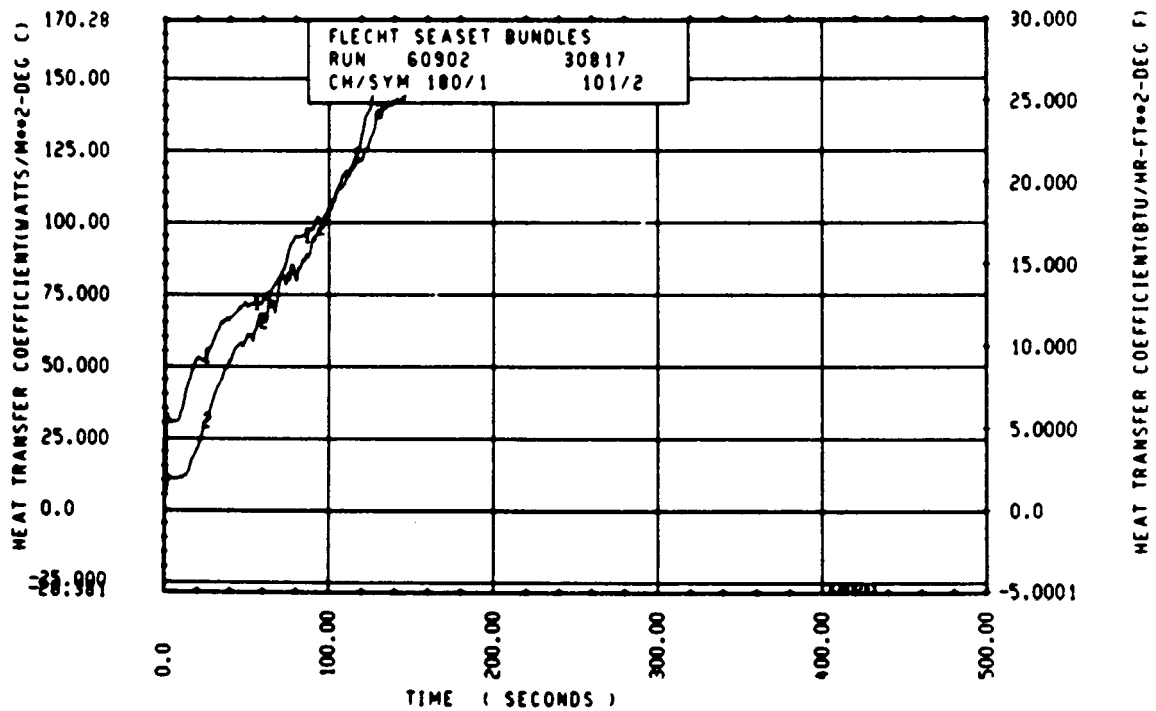
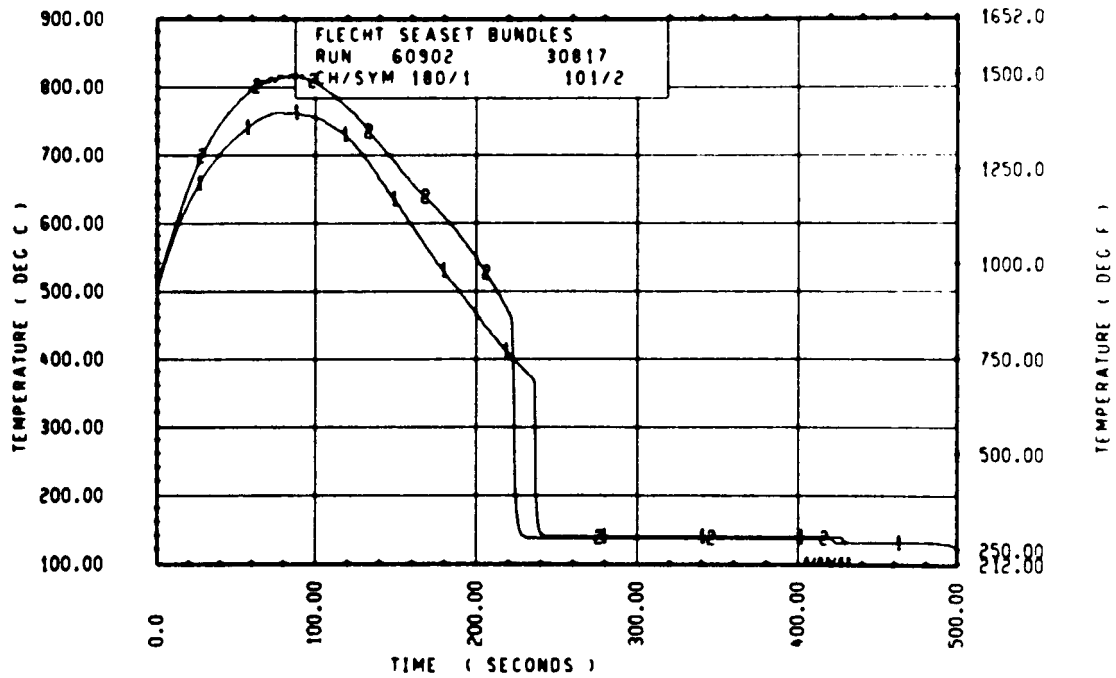
FLECHT SEASET 103 ROD BUNDLE TEST SERIES							
ROD/ELEV	CHAN. NO	INITIAL AT FLOOD (DEG F)	RUN NUMBER 69.2 MAXIMUM TEMPERATURE (DEG F)		TURNAROUND TIME (SECONDS)	QUENCH TEMPERATURE (DEG F)	QUENCH TIME (SECONDS)
			TEMPERATURE (DEG F)	TEMPERATURE RISE (DEG F)			
96 1- 3	3	478.	469.	2.	5.5	737.	13.9
10H 2- 6	6	599.	656.	59.	10.5	706.	32.5
96 3- 3	9	762.	860.	110.	19.5	707.	61.3
3J 4- 0	11	651.	1027.	175.	28.5	720.	95.0
7H 4- 0	12	627.	1015.	166.	29.5	711.	93.7
8K 4- 0	13	839.	1030.	191.	29.5	701.	97.9
6N 4- 7	14	836.	1017.	186.	25.5	704.	84.7
12D 4- 0	17	833.	1011.	178.	27.5	704.	89.4
5E 5- 0	20	918.	1224.	306.	43.5	793.	134.7
76 5- 2	21	952.	1270.	324.	45.5	793.	142.9
96 5- 0	24	940.	1272.	324.	45.5	751.	143.0
5E 5- 7	33	943.	1267.	344.	51.5	809.	160.4
8G 5- 7	45	948.	1330.	380.	67.5	790.	177.4
9H 5- 9	52	911.	1317.	413.	67.5	753.	160.4
76 5-10	59	955.	1342.	386.	57.5	704.	139.4
7F 5-11	62	916.	1274.	362.	55.5	700.	174.7
46 5-11	64	970.	1347.	377.	59.5	702.	149.2
2I 6- 0	67	999.	1375.	377.	58.5	745.	140.4
5D 6- 0	70	943.	1320.	376.	63.5	702.	140.7
6J 6- 0	74	947.	1317.	370.	53.0	700.	113.0
7M 6- 0	86	941.	1310.	374.	61.5	707.	144.4
11E 6- 0	80	969.	1344.	375.	57.0	774.	145.4
8M 6- 2	97	890.	1241.	343.	74.5	602.	242.1
5H 6- 2	99	980.	1363.	403.	55.0	763.	110.7
9E 6- 2	105	814.	1267.	353.	95.5	274.	479.1
8M 6- 3	111	928.	1207.	339.	55.5	641.	245.1
46 6- 3	124	980.	1369.	410.	66.5	757.	210.5
11H 6- 4	134	920.	1347.	420.	104.5	624.	217.1
9D 6- 4	143	965.	1414.	449.	89.0	742.	212.1
9J 6- 5	165	955.	1407.	452.	77.0	1025.	100.3
9M 6- 5	166	976.	1431.	455.	73.5	740.	214.4
8J 6- 6	192	908.	1460.	430.	74.0	600.	208.0
9B 6- 6	193	940.	1432.	480.	67.0	739.	220.9
11F 6- 6	173	971.	1424.	453.	82.0	707.	224.1
46 7- 0	261	964.	1300.	414.	73.0	722.	207.0
7D 7- 6	309	907.	1490.	589.	114.0	702.	244.0
76 7- 6	312	920.	1440.	514.	137.0	550.	404.1
11E 7- 6	325	937.	1430.	493.	87.5	810.	274.4
5L 8- 0	337	816.	1343.	532.	100.0	740.	300.4
7M 8- 0	345	835.	1332.	497.	126.5	970.	245.7
7K 8- 0	346	856.	1467.	553.	122.0	700.	305.0
5J 8- 6	366	706.	1161.	415.	134.0	600.	340.1
78 8- 6	368	705.	1130.	370.	107.5	600.	336.1
7E 9- 3	383	691.	1260.	569.	134.5	511.	424.1
8H 9- 3	387	670.	1038.	368.	121.0	502.	350.1
9C 9- 3	389	678.	1190.	511.	159.0	602.	302.0
11F 9- 3	394	676.	1147.	519.	149.0	770.	204.0
7810- 0	408	587.	957.	370.	151.1	600.	374.1
8M10- 0	415	585.	953.	368.	123.5	607.	300.5
8K10- 0	417	591.	945.	403.	151.0	600.	300.5
8M10- 0	418	587.	1009.	460.	134.0	603.	374.1
6M11- 0	429	480.	654.	176.	114.5	444.	344.7
9G11- 0	431	479.	757.	276.	143.5	440.	349.1
11E11- 0	432	472.	737.	264.	152.5	600.	242.0
5J11- 6	436	483.	640.	165.	100.0	542.	344.1
7811- 6	437	469.	710.	240.	124.5	500.	330.1
8J11- 6	438	483.	600.	140.	122.5	400.	200.1

RUN 60902 HEATER ROD STATISTICAL DATA

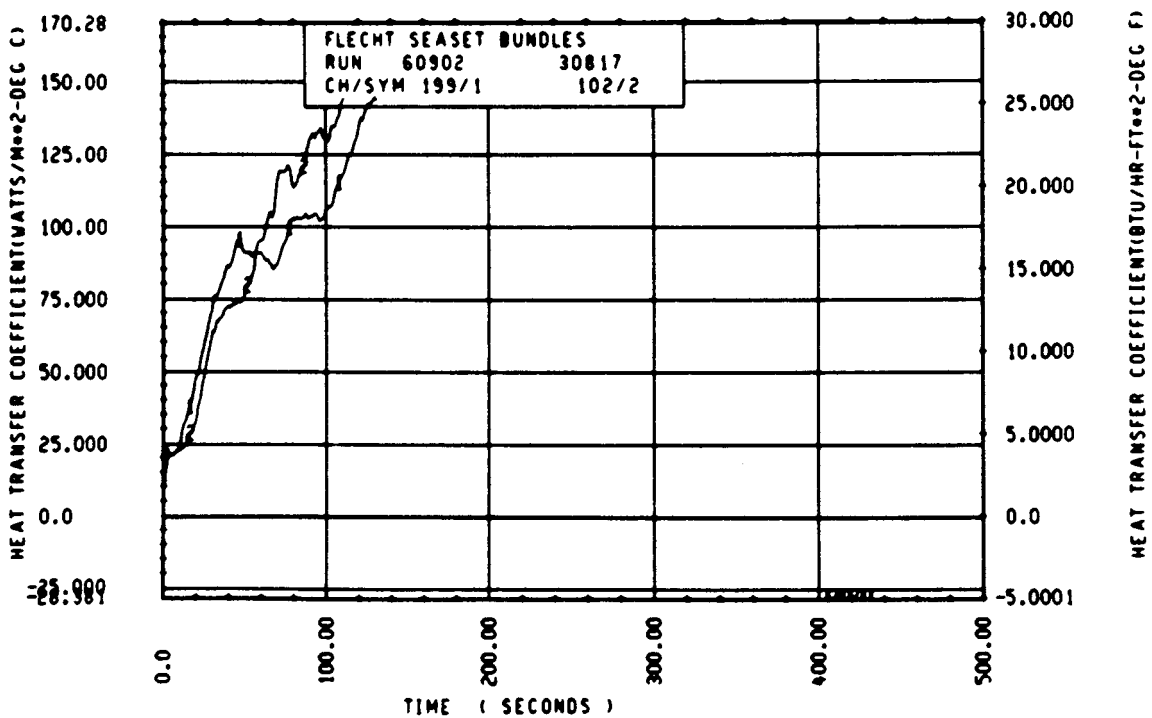
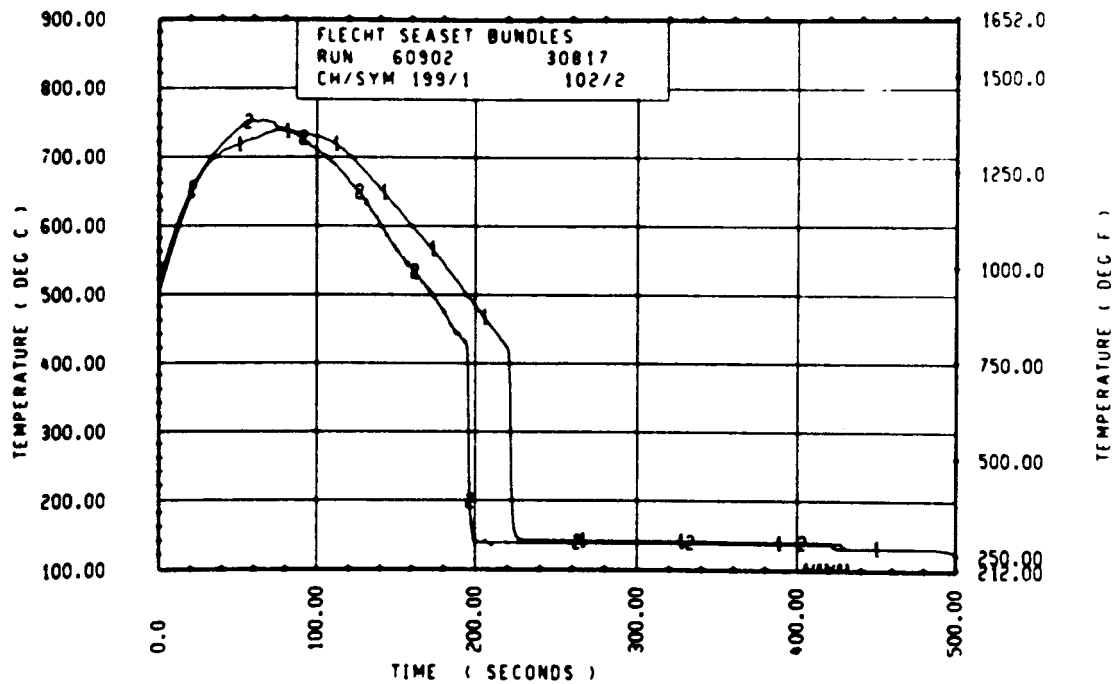
TEMP	INITIAL TEMP (DEG F)			MAX TEMP (DEG F)			TURNAROUND TIME (SEC)		
	MAX	MIN	MEAN	MAX	MIN	MEAN	MAX	MIN	MEAN
12	435.5	477.9	462.2	507.1	440.5	503.5	5.5	5.0	5.3
24	597.5	54.1	552.0	650.4	644.9	649.4	10.5	10.0	10.2
36	762.0	731.0	746.2	860.4	850.5	860.4	21.5	18.0	20.0
48	551.2	827.4	636.3	1024.7	1011.2	1020.0	25.1	25.0	27.1
60	475.2	665.2	435.5	1204.8	1153.7	1242.7	55.5	45.0	47.0
67	447.5	910.4	562.4	1330.5	1250.7	1300.8	61.0	36.0	52.6
69	454.6	910.5	546.2	1320.5	1294.2	1312.3	67.0	56.0	61.3
70	1001.9	945.2	963.7	1352.2	1310.0	1332.5	67.5	57.0	61.3
71	404.9	910.3	542.5	1340.4	1270.6	1322.2	67.0	55.0	61.6
72	446.6	936.7	567.0	1363.0	1315.3	1347.4	73.0	53.0	62.1
73	131.3	931.3	560.5	1374.6	1317.4	1357.1	67.5	53.0	64.0
74	447.6	891.5	532.1	1400.2	1241.6	1343.0	70.0	54.0	65.4
75	444.7	845.4	545.0	1410.9	1267.1	1367.4	79.0	50.0	70.6
76	1001.9	919.4	965.4	1420.5	1241.1	1384.5	104.5	63.0	74.4
77	404.4	927.0	550.2	1432.0	1312.0	1394.0	99.5	67.0	77.2
78	436.4	924.7	550.5	1444.4	1314.0	1413.4	106.5	70.0	80.2
79	485.5	931.3	561.4	1450.4	1305.0	1430.4	102.0	73.0	83.7
80	464.9	931.5	547.9	1464.1	1390.5	1442.7	119.5	82.0	89.0
81	450.9	903.9	534.5	1470.2	1364.9	1431.6	111.0	82.0	89.6
84	476.1	911.1	552.6	1488.2	1244.3	1342.3	99.0	61.0	71.0
90	474.1	927.7	546.6	1465.4	1324.0	1406.5	109.0	63.5	88.0
91	436.4	855.4	515.3	1504.4	1305.9	1440.2	118.0	81.0	102.2
96	456.4	810.0	541.1	1560.4	1321.6	1420.1	124.0	100.0	118.0
102	772.4	373.3	723.3	1527.9	500.7	1140.9	171.5	167.0	129.3
111	592.1	674.1	681.2	1259.0	981.3	1154.0	169.0	162.0	135.3
121	519.7	563.5	566.7	1143.5	440.1	1010.5	174.5	71.0	146.4
132	432.2	472.5	477.4	770.5	647.0	723.0	152.5	111.0	135.5
133	463.3	454.4	471.6	745.4	645.6	677.0	124.0	103.0	116.5

RUN 60902 HEATER ROD STATISTICAL DATA

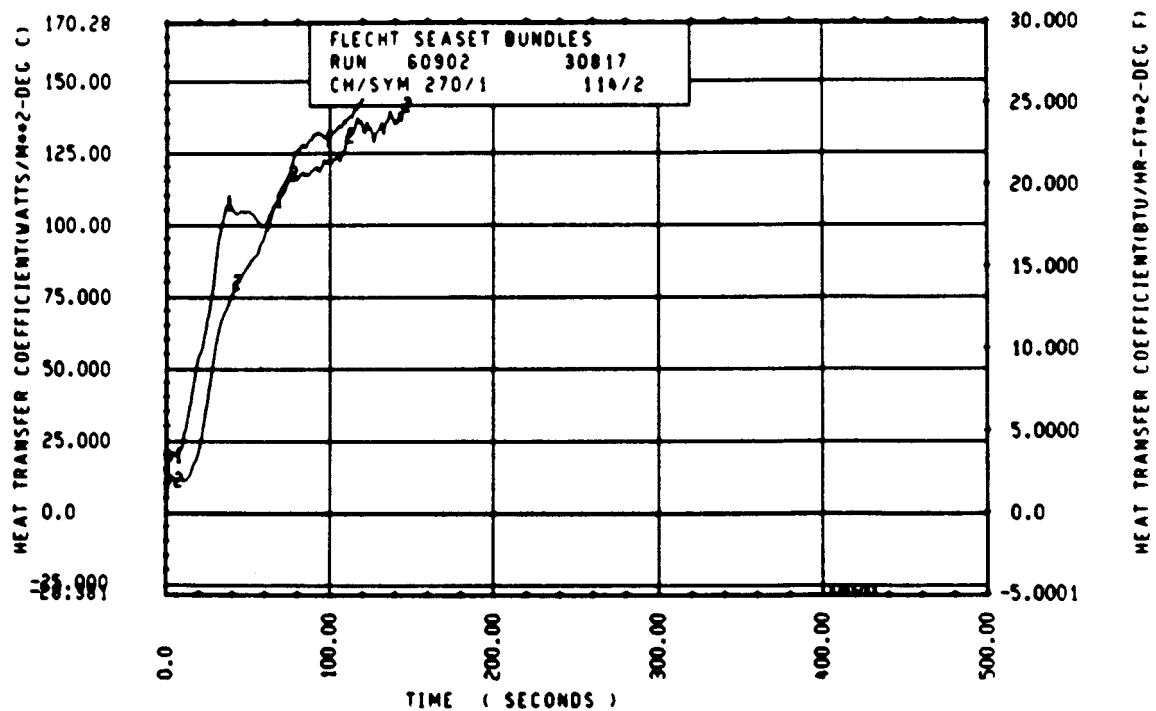
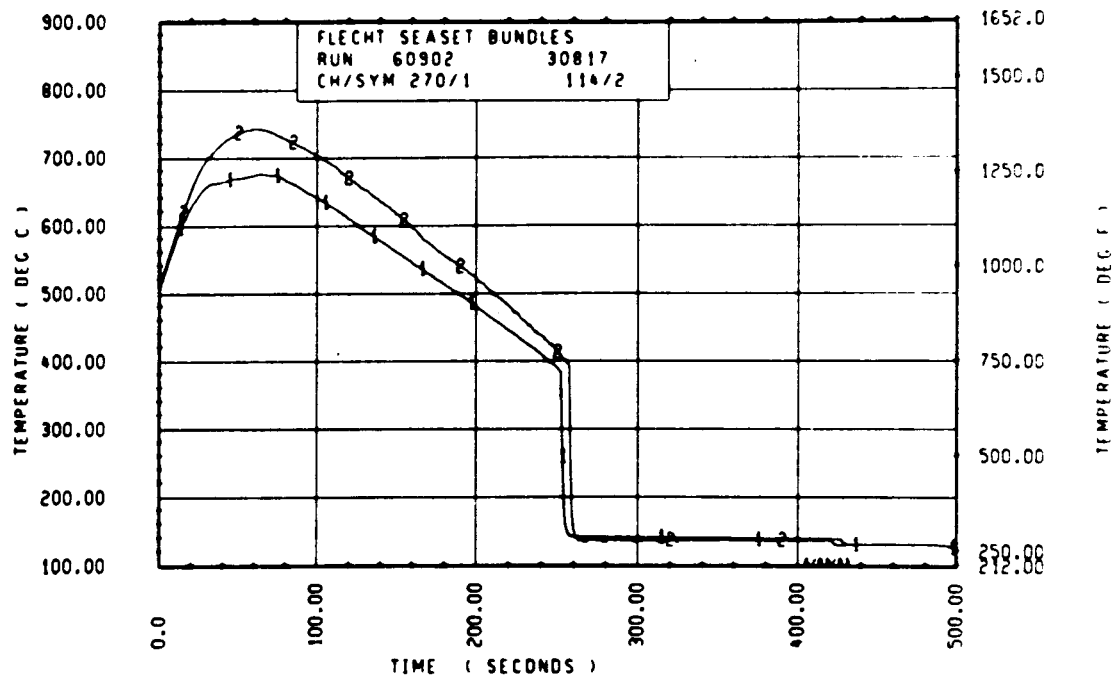
TEMP	TEMPERATURE (DEG F)			QUENCH TEMP (DEG F)			QUENCH TIME (SEC)		
	MAX	MIN	MEAN	MAX	MIN	MEAN	MAX	MIN	MEAN
12	21.5	21.5	21.5	470.4	435.1	450.4	13.7	13.5	13.5
24	50.5	54.7	55.0	561.7	440.5	504.9	33.0	20.0	31.7
36	122.5	115.1	118.2	710.3	597.6	708.4	65.9	60.4	62.4
48	192.0	175.4	183.7	777.0	701.3	736.4	97.9	74.0	91.0
60	335.5	271.4	307.1	820.5	773.4	800.5	151.8	134.3	141.1
67	344.1	315.1	344.4	814.0	745.5	779.0	181.9	163.2	172.2
69	413.4	352.2	372.1	754.2	705.0	770.0	193.9	173.4	181.9
71	386.1	350.3	366.8	404.2	701.2	810.4	188.9	134.4	176.8
72	390.7	362.3	379.6	763.2	700.3	743.0	149.2	174.7	168.1
73	411.1	371.1	396.5	744.5	737.4	760.7	203.8	143.4	198.7
74	410.7	385.1	396.5	821.0	745.3	774.0	217.4	140.9	199.4
75	425.6	337.8	351.0	767.3	652.2	759.4	242.1	139.4	201.6
76	533.6	334.4	417.5	831.0	507.1	737.4	245.1	144.4	210.8
77	455.4	320.1	419.1	820.1	624.1	765.2	222.0	183.4	210.6
78	492.4	361.7	436.4	1025.5	543.3	750.0	360.1	160.5	224.1
79	455.5	341.7	452.0	1023.5	515.0	744.2	370.0	170.0	247.3
80	444.5	413.4	465.5	850.0	540.4	700.4	386.1	214.0	239.1
81	524.6	457.5	495.0	1007.5	440.0	743.4	431.8	144.5	272.5
84	524.3	452.1	447.3	668.6	574.5	702.1	335.9	224.8	250.7
90	450.3	303.1	389.7	803.4	560.6	761.4	347.1	241.0	279.5
96	522.0	353.4	454.9	883.0	470.0	724.0	433.2	235.1	261.9
102	506.6	444.4	524.9	844.5	500.6	751.0	404.1	250.0	299.7
111	555.2	402.0	564.1	477.1	497.1	743.4	432.1	245.7	323.5
121	564.1	127.4	425.1	434.0	434.2	675.0	595.5	190.4	345.5
132	573.0	305.0	472.9	621.4	471.4	633.4	427.1	252.6	350.1
133	551.1	253.3	431.5	644.1	412.2	612.9	435.0	73.4	354.4
134	297.5	171.2	245.6	660.4	434.3	497.5	341.8	242.6	339.3
135	245.4	164.7	206.0	544.0	204.6	507.4	310.1	164.4	285.5



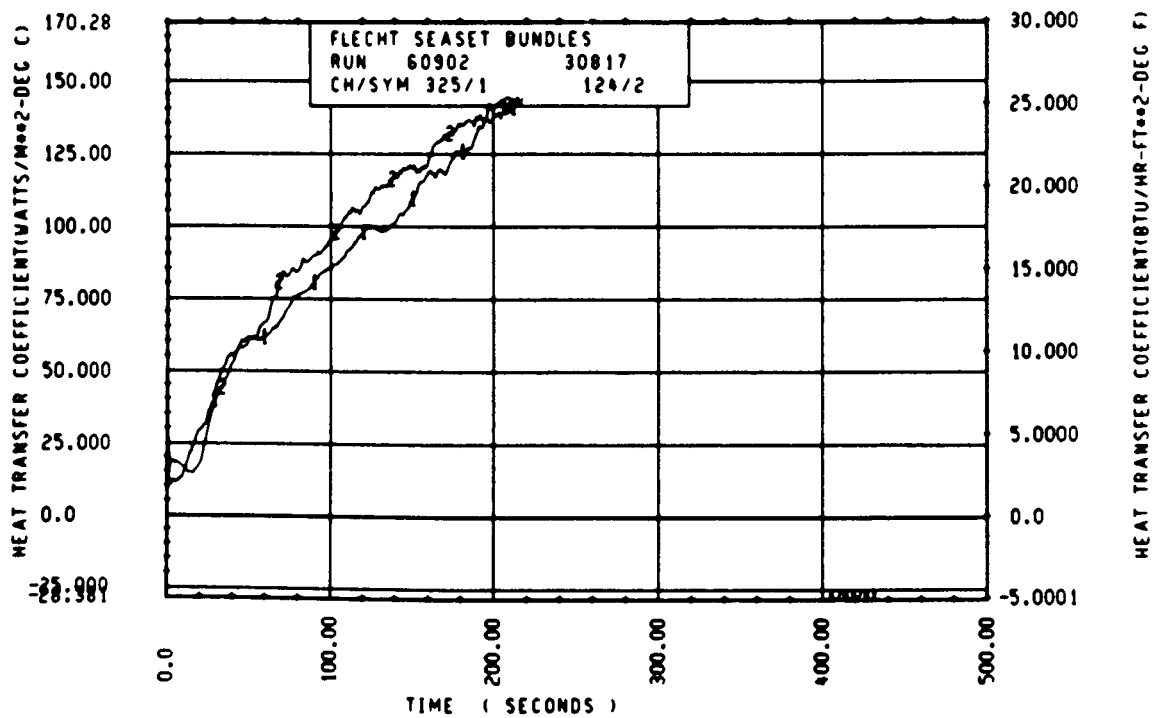
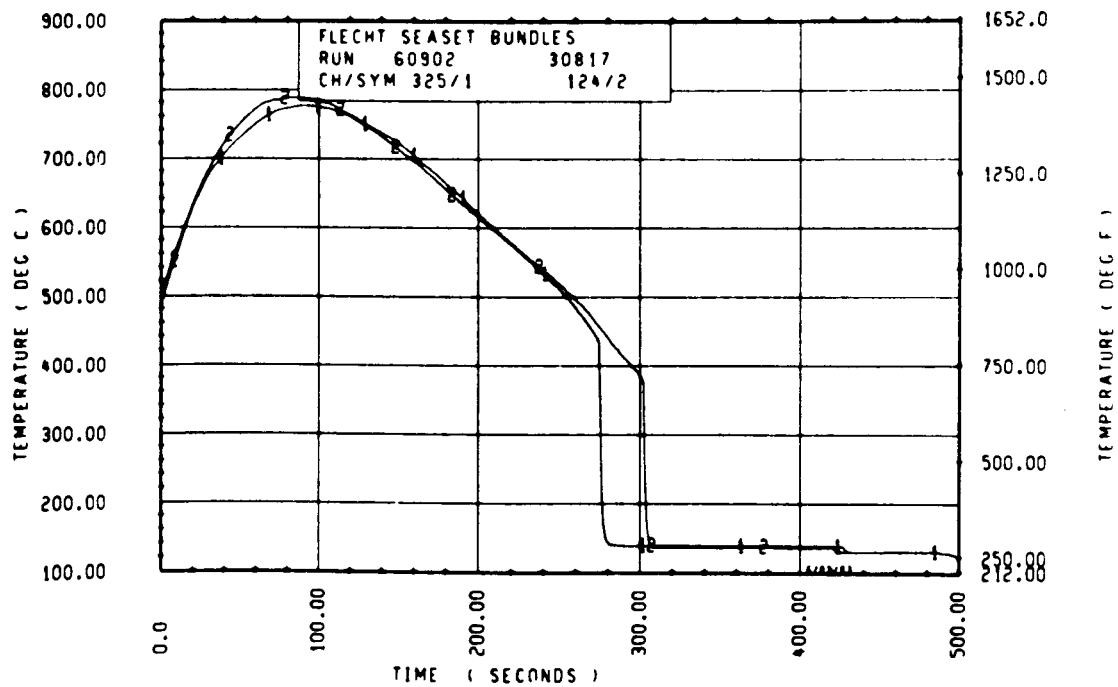
Rod 12I, 1.98 m (78 in.)



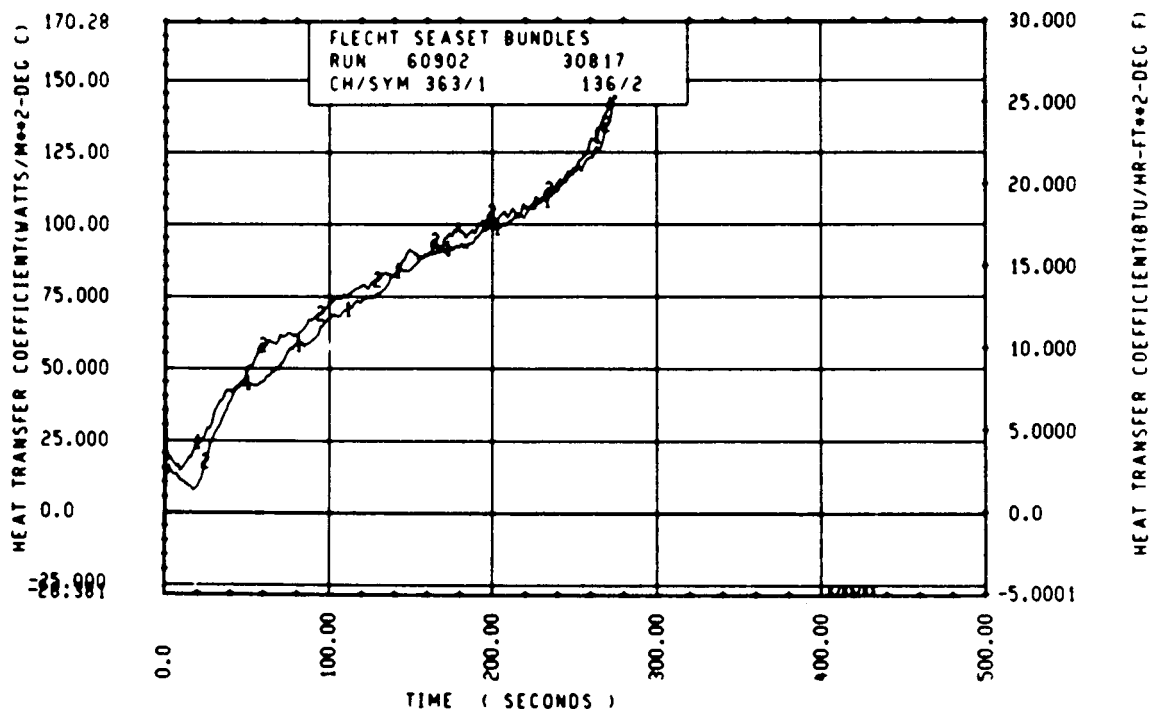
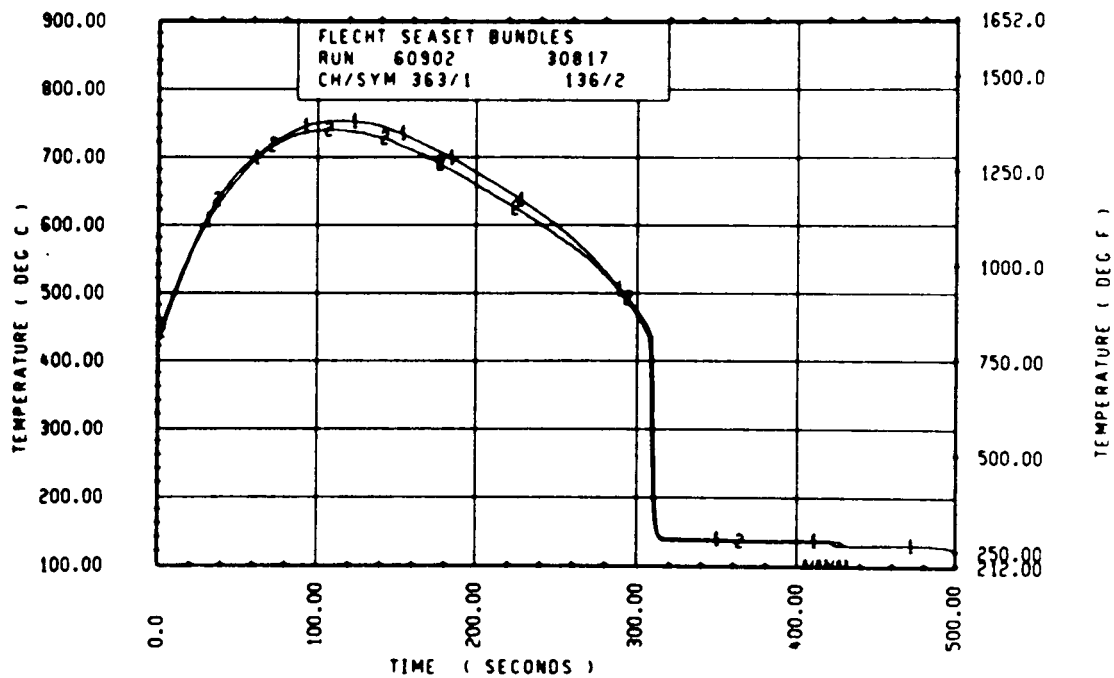
Rod 13G, 1.98 m (78 in.)



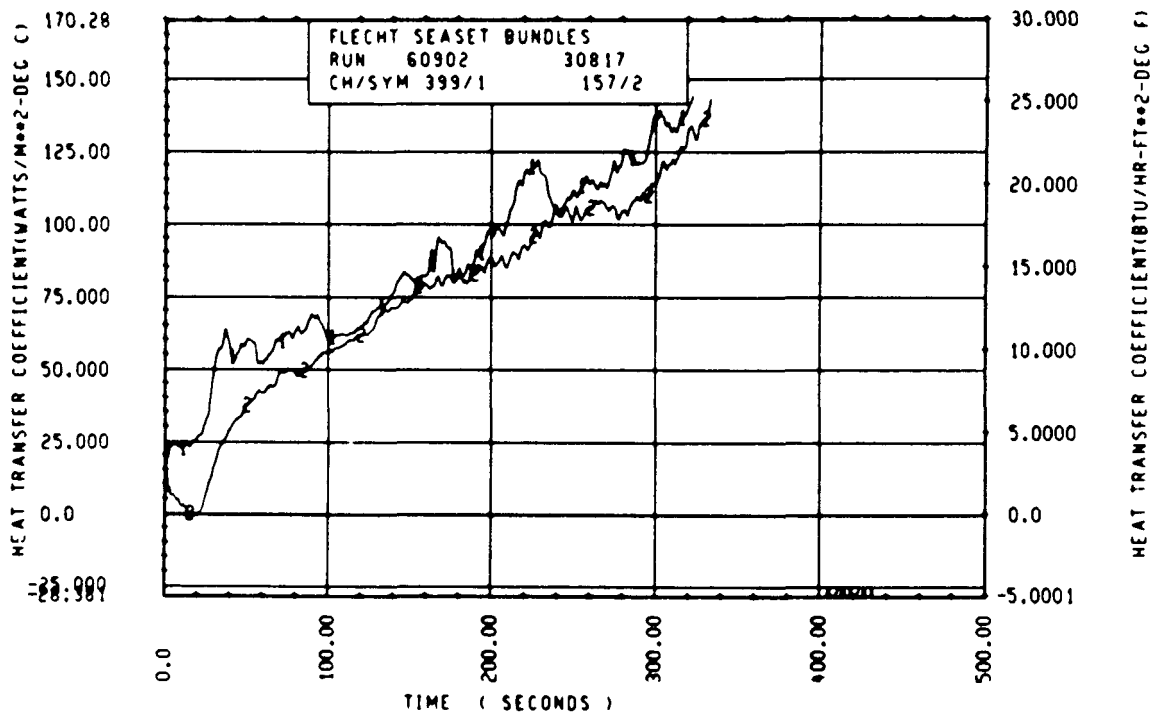
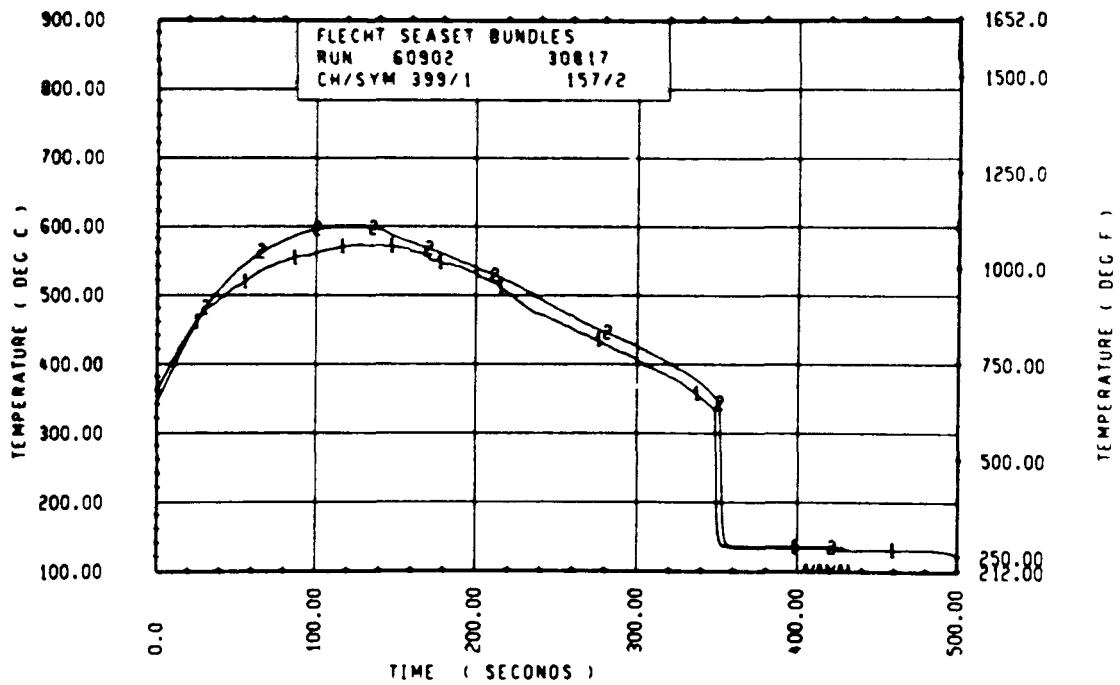
Rod 13G, 2.13 m (84 in.)



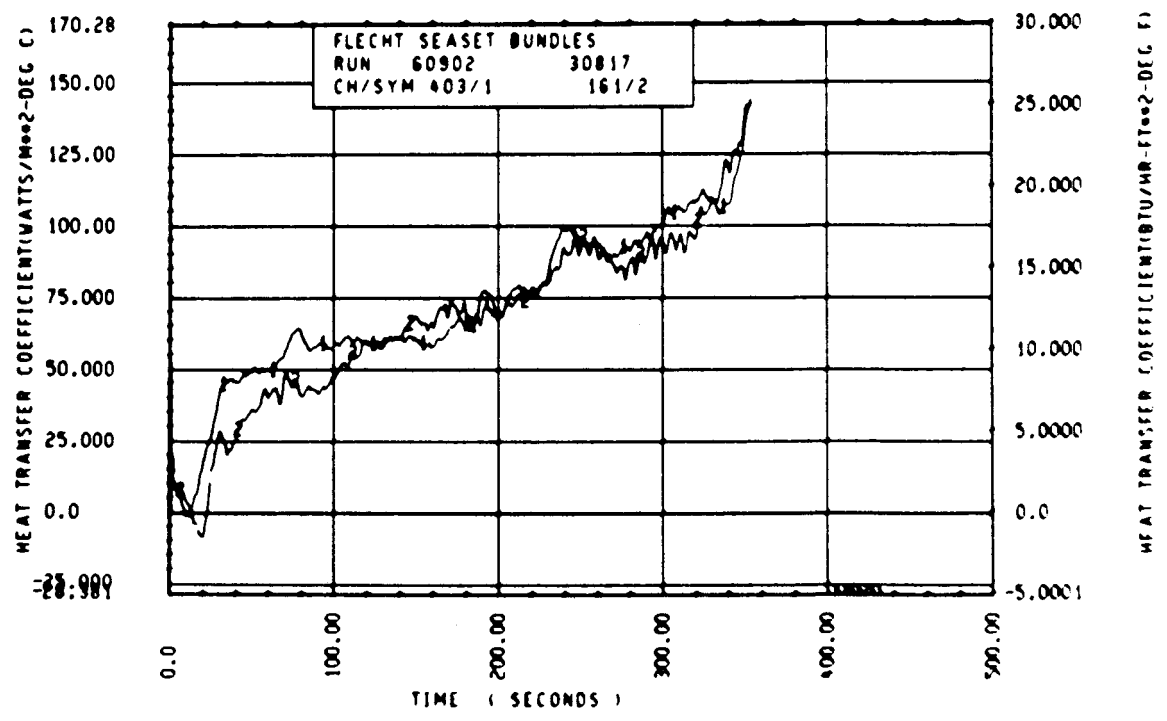
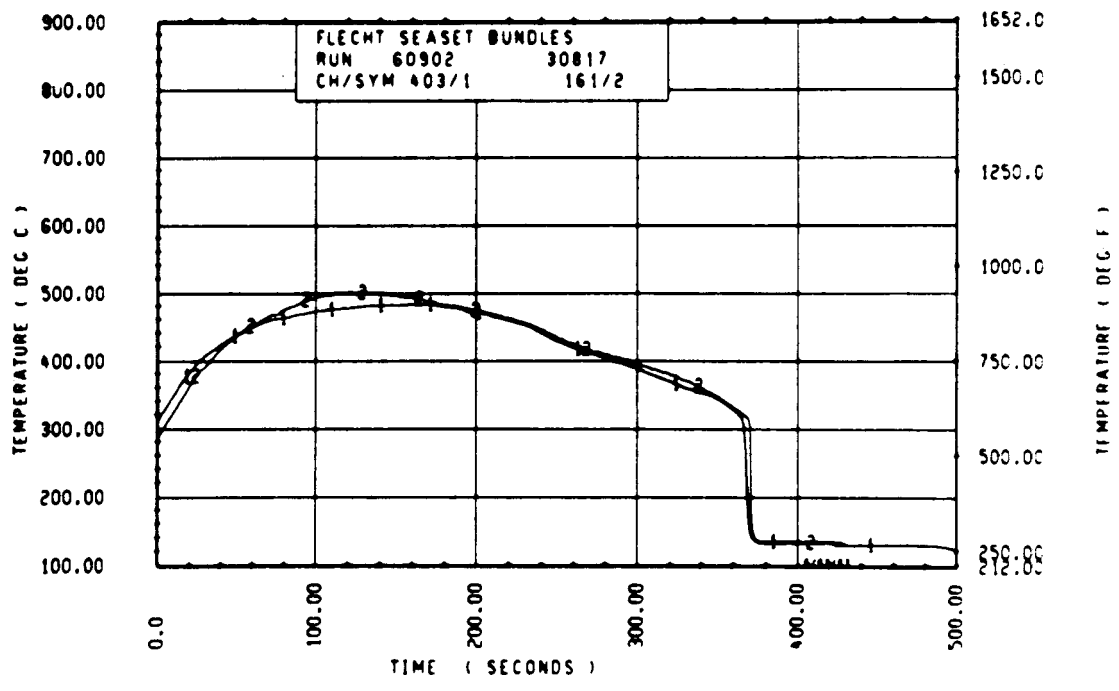
Rod 11E, 2.29 m (90 in.)



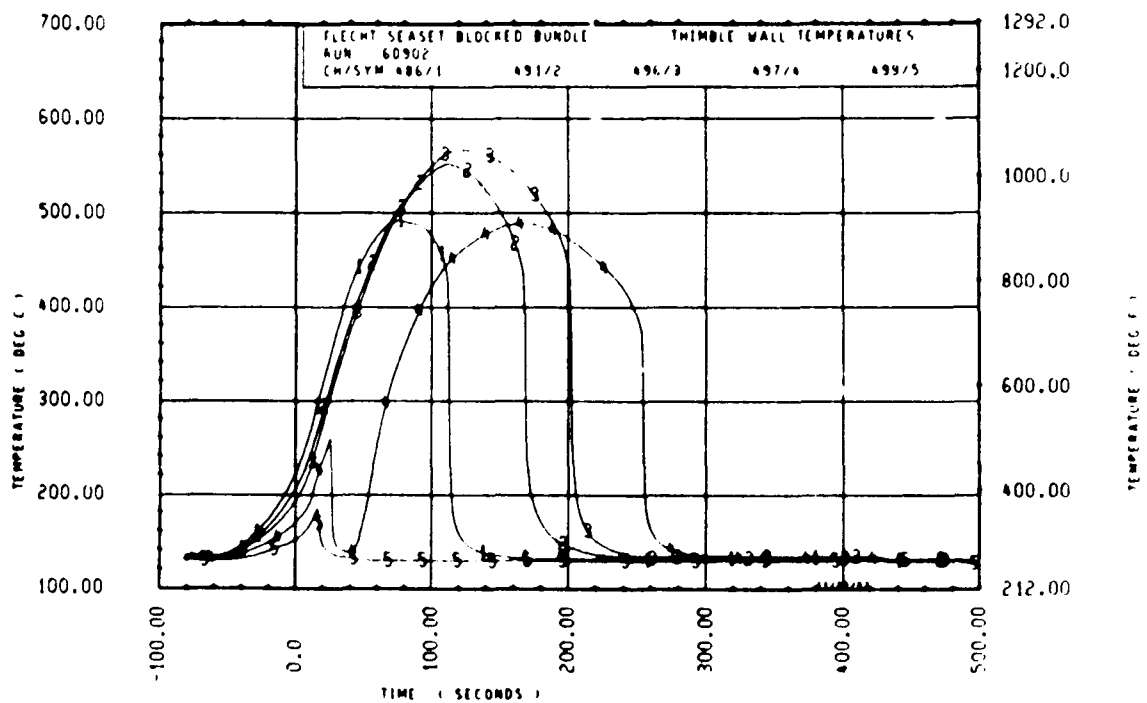
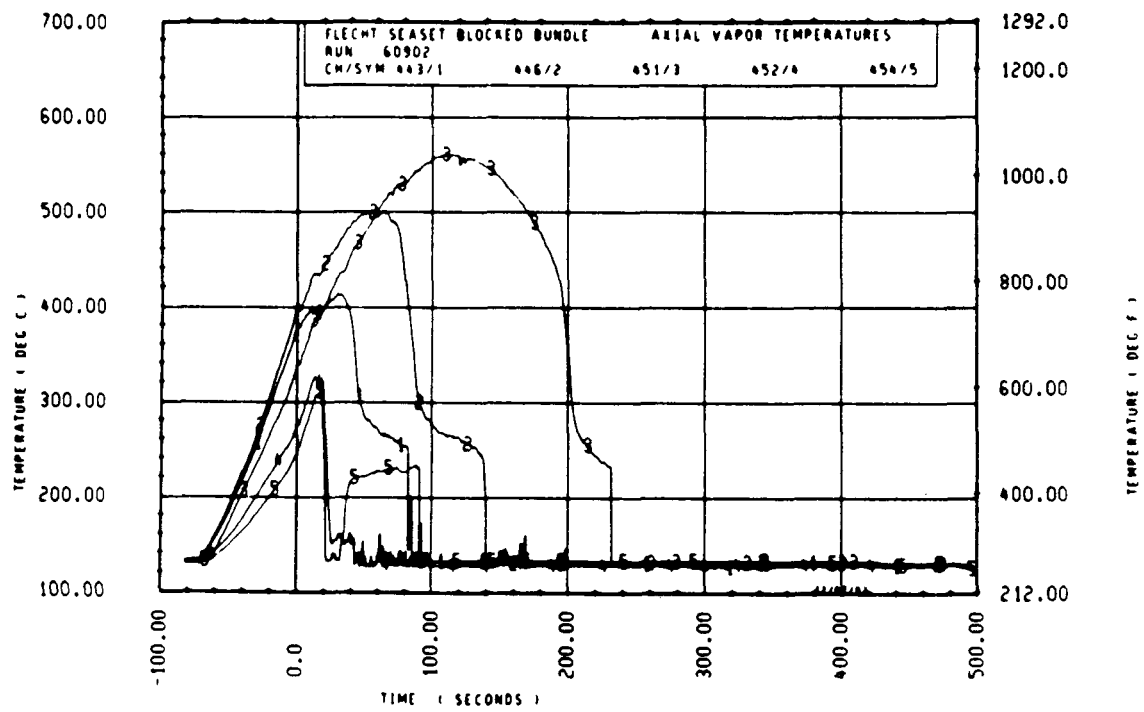
Rod 12D, 2.44 m (96 in.)

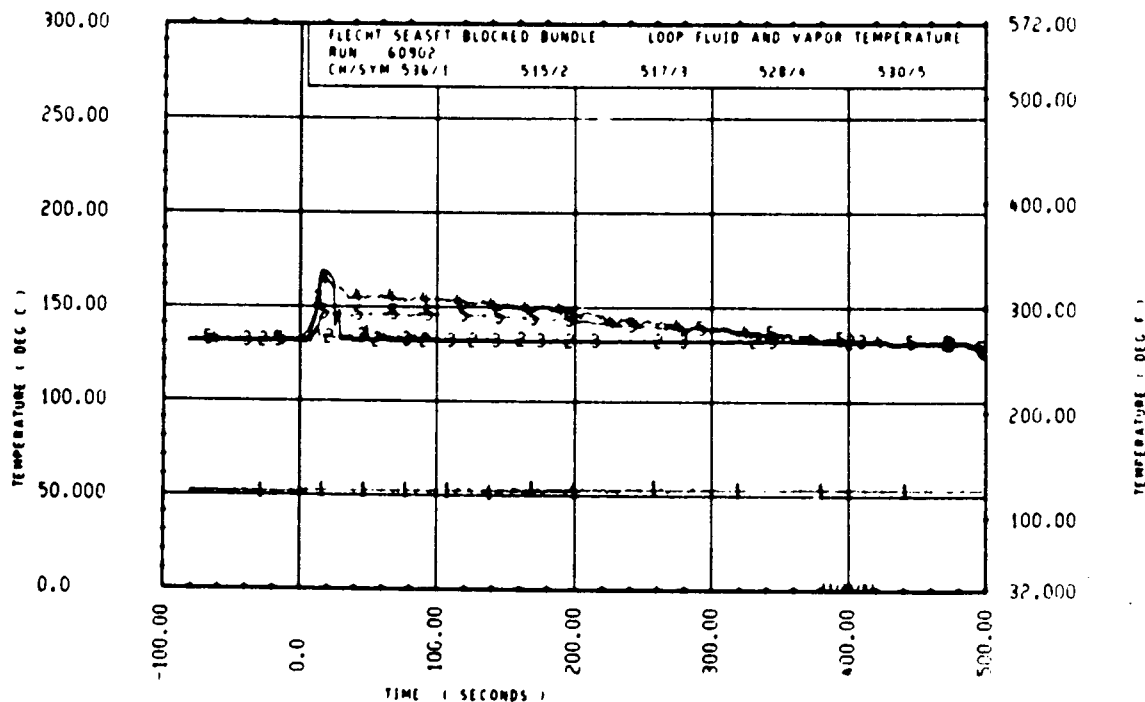
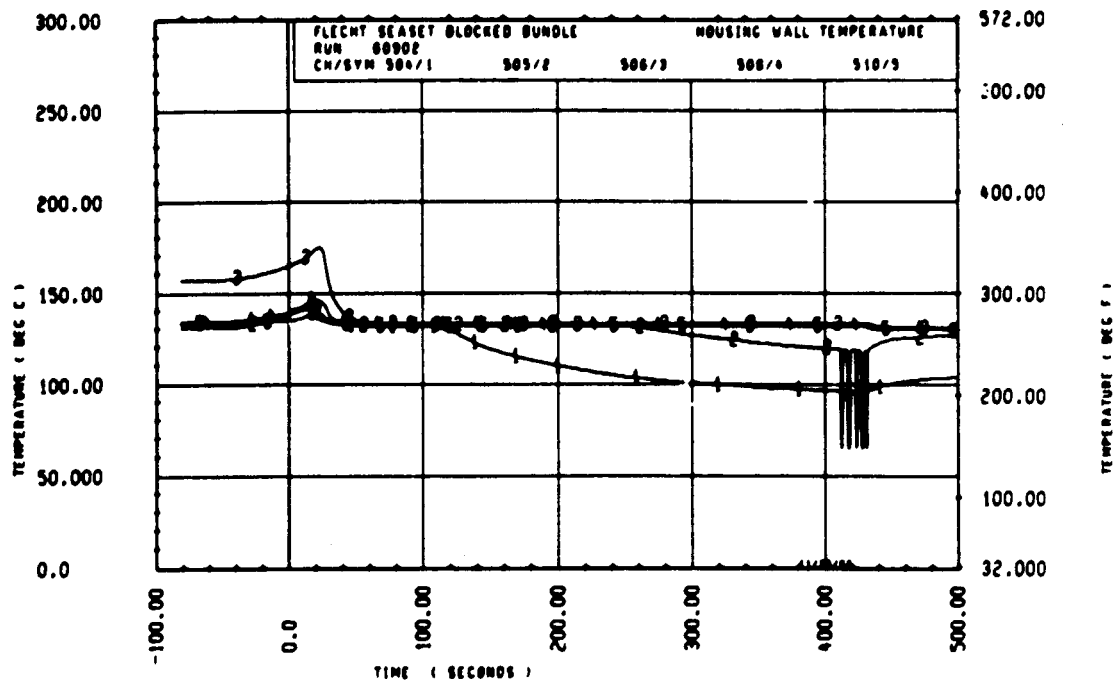


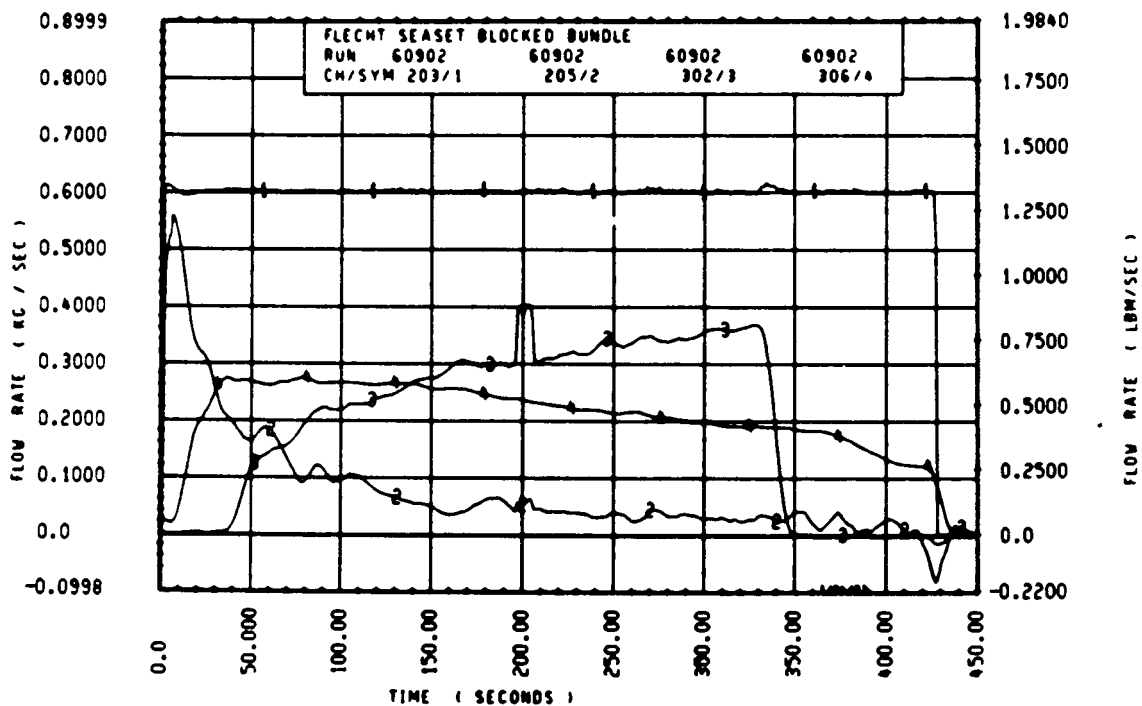
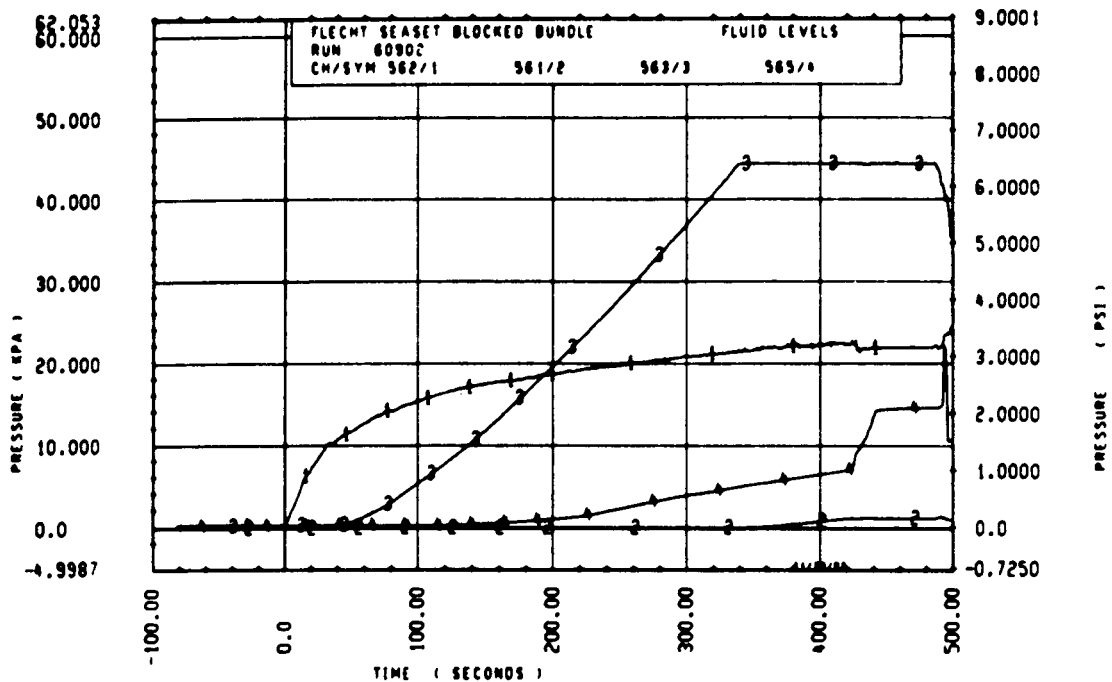
Rod 13G, 2.82 m (111 in.)

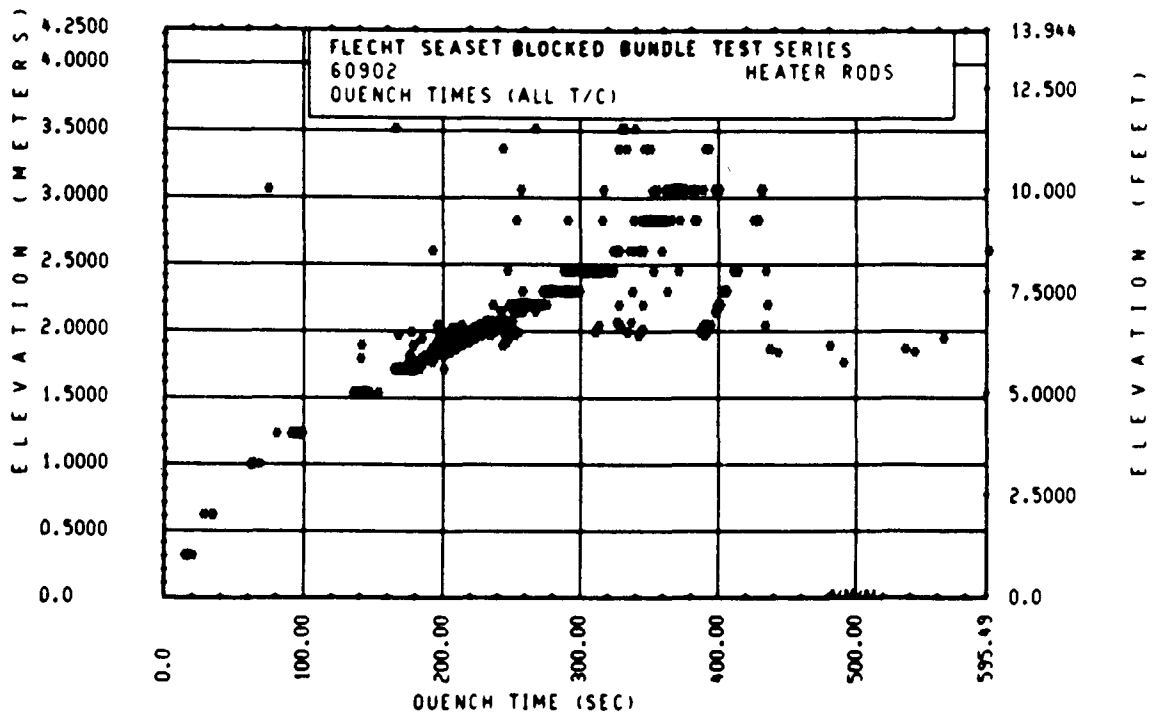
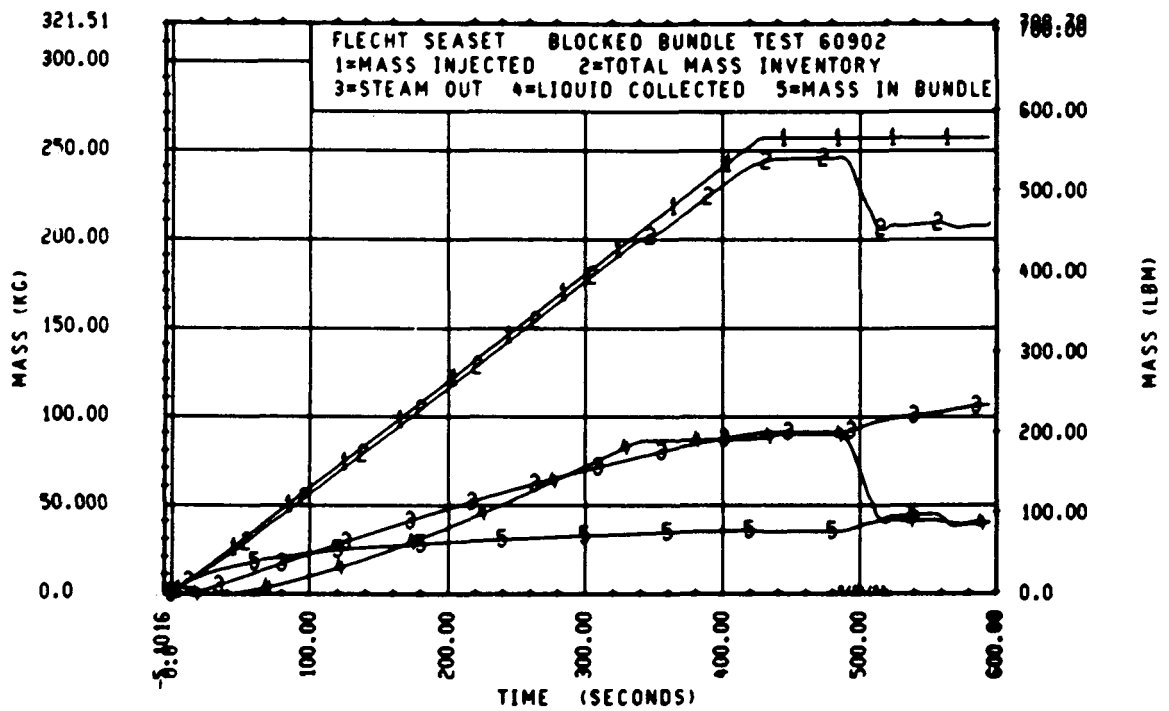


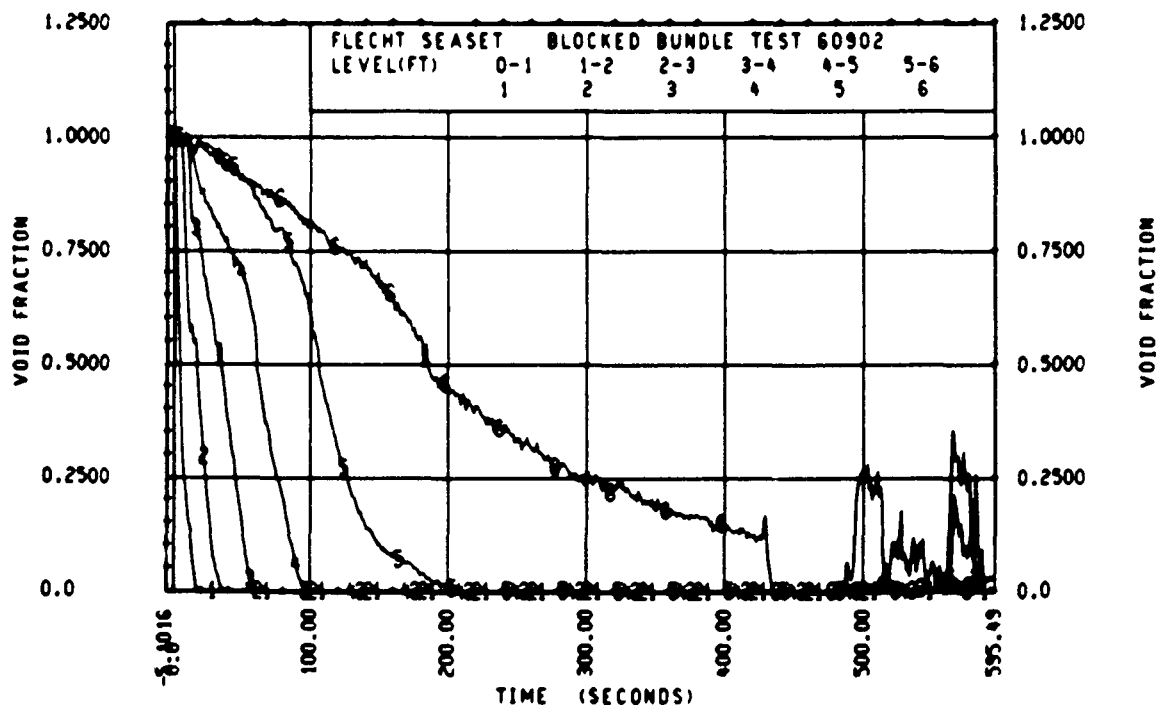
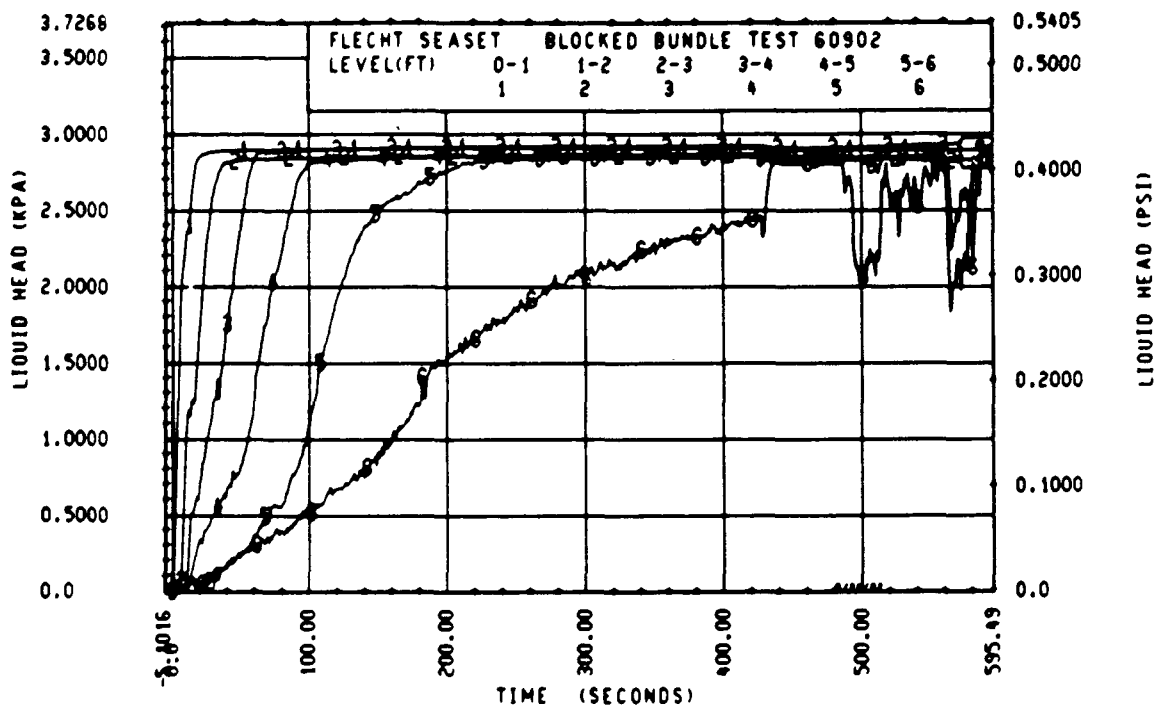
Rod 5J, 3.05 m (120 in.)

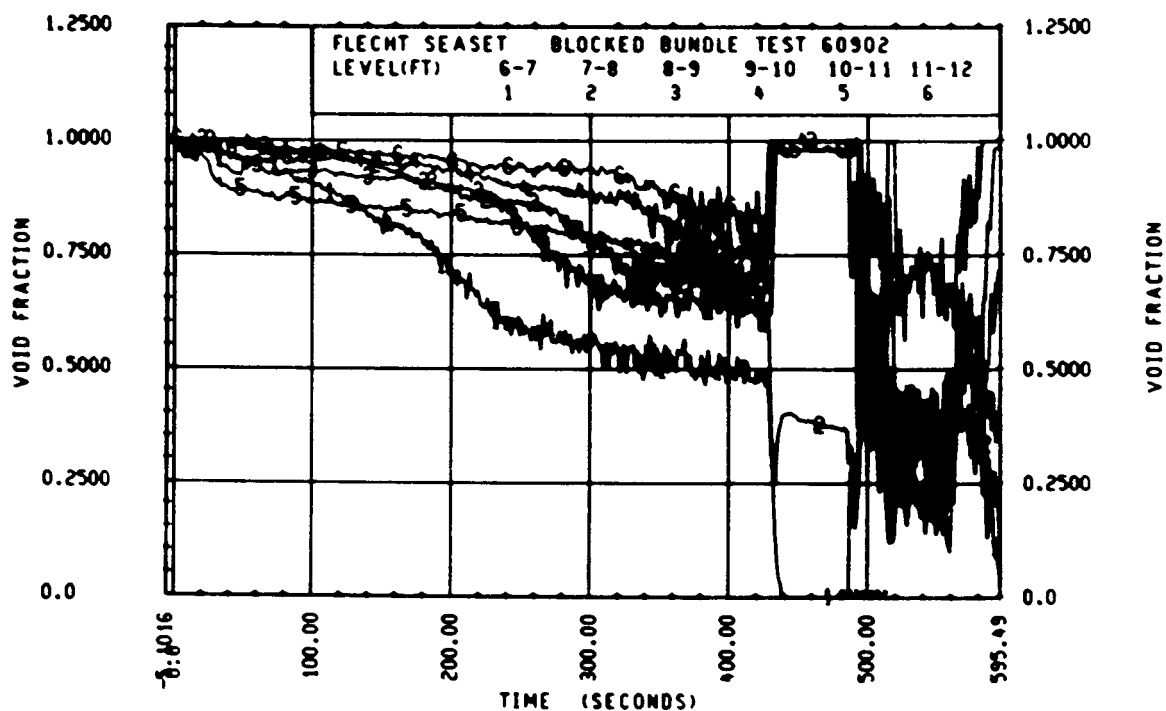
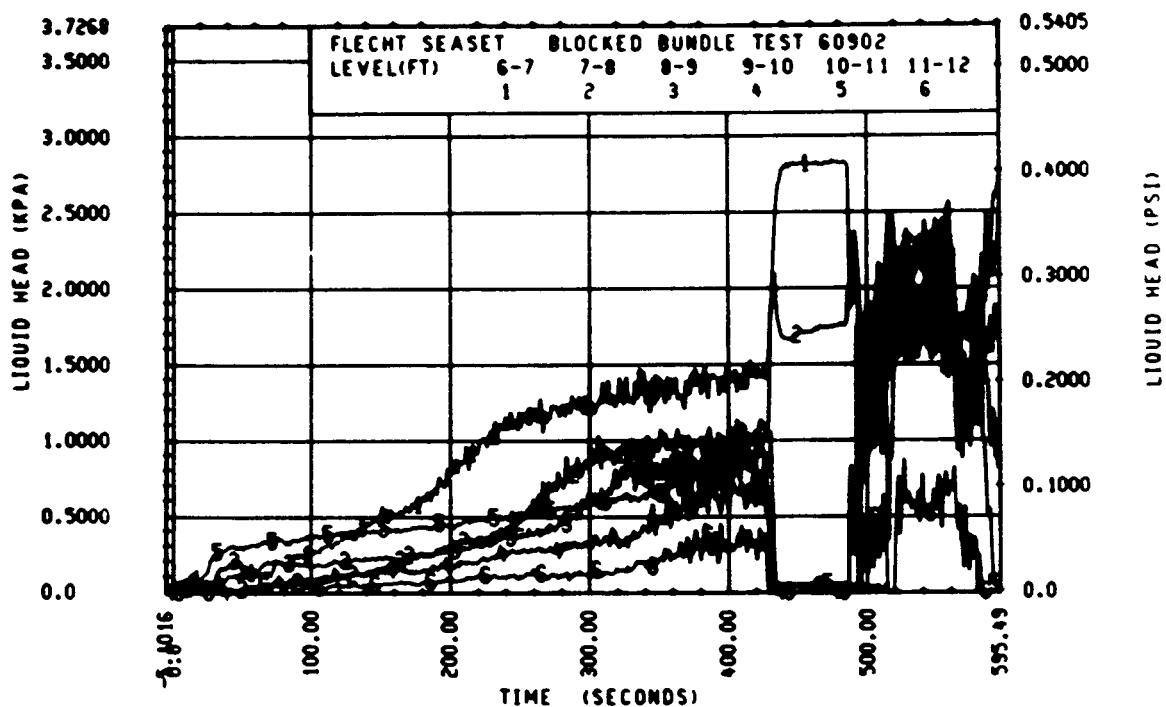












FLECHT SEASET 163-ROD BUNDLE FLOW BLOCKAGE TASK
SUMMARY AND COMMENT SHEET

Run: 61005
Test date: 8/24/82
Test type: Forced reflood
Parameter: Flooding rate effect

AS-RUN TEST CONDITIONS:

Upper plenum pressure	0.271 MPa (39.3 psia)
Initial peak clad temperature and location	871.6°C (1600.9°F), 2I-1.93 m (76 in.)
Initial peak rod power:	
Peripheral rods	2.30 kW/m (0.702 kW/ft)
Bypass rods	2.28 kW/m (0.696 kW/ft)
Blockage island rods	2.29 kW/m (0.698 kW/ft)
Flooding rate	38.6 mm/sec (1.52 in./sec)
Coolant temperature	51.7°C (125°F)
Initial bundle water level	+4.5 mm (+0.18 in.)

COMMENTS:

Inlet mass flow: ⁽¹⁾ -0.4% linearly increasing to +1.3% by 400 seconds

Power decay: ⁽¹⁾ peripheral rods, +0.5% at 110 seconds and thereafter
bypass rods, -1.5% linearly decreasing to -0.5% by 400
seconds
blockage rods, -0.5% constant

1. Relative to run 31203

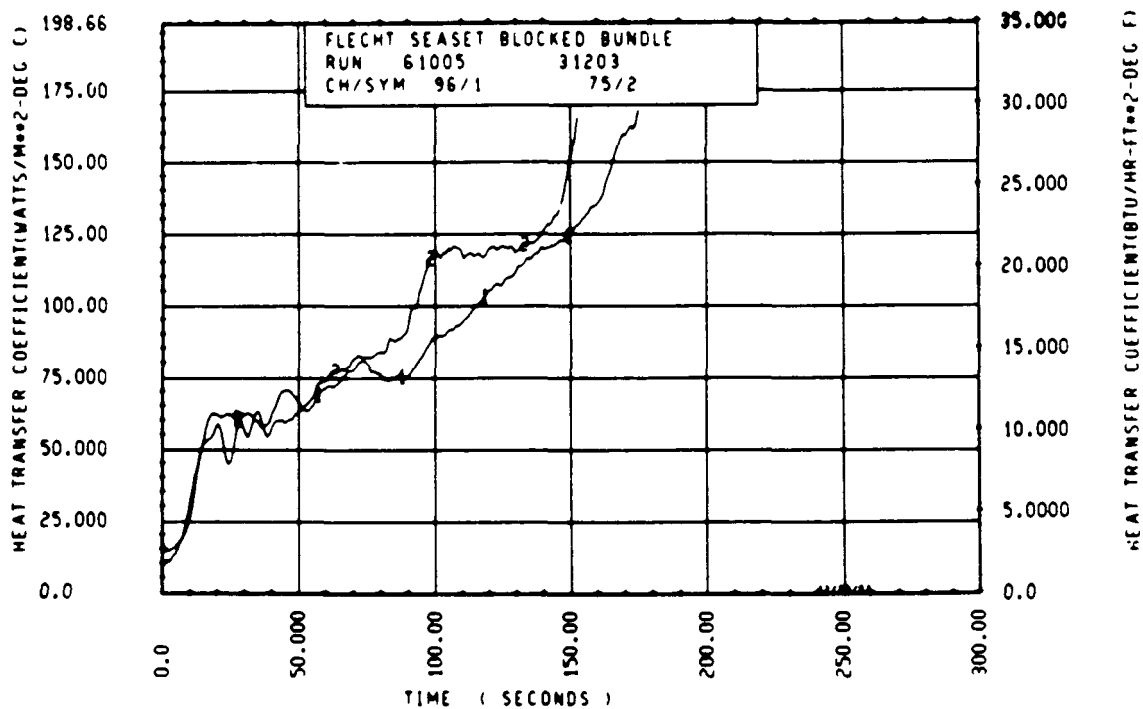
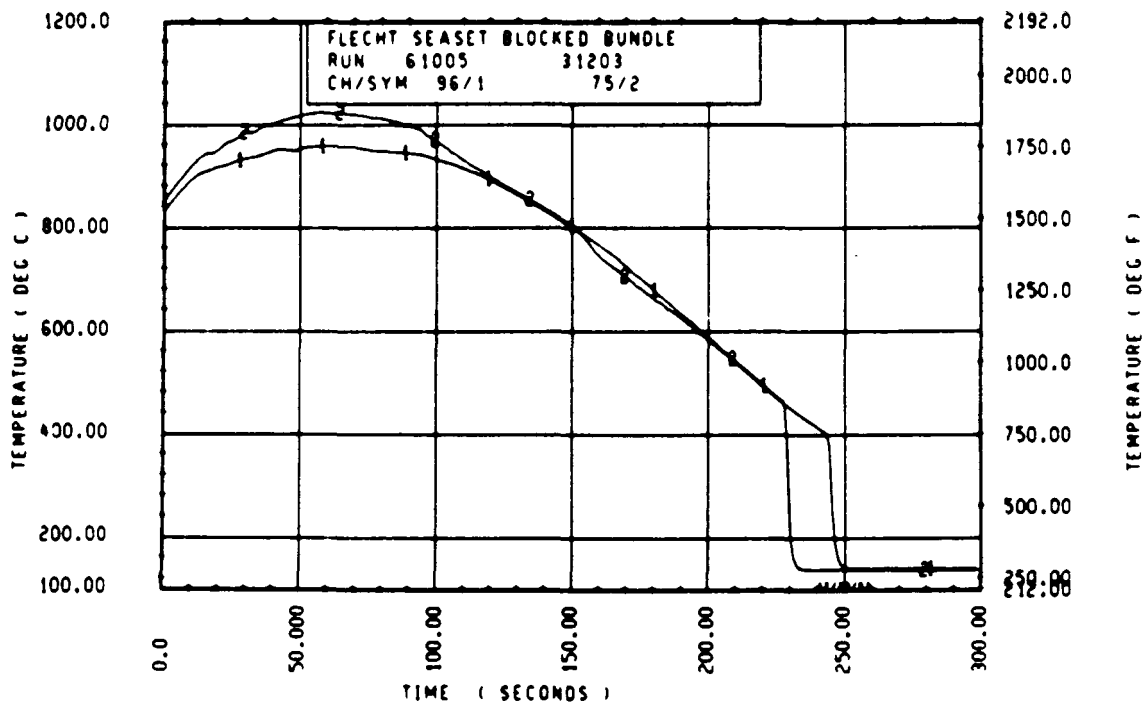
FLECHT SEASET 163 ROD BUNDLE TEST SERIES								
RUN NUMBER 61005								
ROD/ELEV	CHAM. NO	INITIAL AT FLOOD (DEG F)	MAXIMUM TEMPERATURE (DEG F)	TEMPERATURE RISE (DEG F)	TURNAROUND TIME (SECONDS)	QUENCH TEMPERATURE (DEG F)	QUENCH TIME (SECONDS)	
9G 1- 0	3	669.	686.	17.	5.0	552.	22.5	
10H 2- 0	6	877.	917.	40.	8.5	619.	46.0	
9G 3- 3	9	1184.	1260.	76.	14.0	747.	84.7	
3J 4- 0	11	1348.	1449.	101.	19.0	767.	116.6	
7H 4- 0	12	1313.	1424.	111.	18.0	733.	119.5	
8K 4- 0	13	1346.	1460.	120.	23.0	756.	121.0	
8H 4- 0	14	1335.	1436.	121.	17.5	654.	113.5	
12D 4- 0	17	1323.	1419.	96.	19.5	773.	116.9	
5E 5- 0	20	1474.	1666.	191.	52.5	835.	168.3	
7G 5- 0	21	1533.	1762.	169.	41.0	793.	171.9	
9G 5- 0	24	1509.	1677.	168.	40.5	825.	168.9	
3E 5- 7	33	1524.	1722.	198.	60.5	827.	203.1	
8G 5- 7	45	1525.	1746.	223.	66.5	834.	214.1	
9H 5- 9	52	1456.	1695.	239.	75.0	838.	216.6	
7G 5-10	59	1496.	1717.	221.	72.0	723.	226.1	
7F 5-11	62	1446.	1669.	223.	72.0	780.	225.1	
4G 5-11	64	1533.	1714.	182.	51.0	799.	233.1	
2I 6- 0	67	1586.	1799.	213.	53.0	791.	234.9	
5D 6- 0	70	1488.	1710.	222.	61.5	760.	232.5	
6J 6- 0	74	1521.	1695.	173.	52.0	779.	236.7	
7H 6- 0	66	1526.	1739.	213.	60.0	740.	233.3	
11E 6- 0	80	1553.	1764.	151.	56.0	801.	230.1	
8H 6- 2	97	1365.	1626.	261.	81.5	711.	264.2	
5H 6- 2	99	1539.	1739.	200.	62.5	773.	249.8	
9E 6- 2	105	1307.	1723.	416.	94.0	284.	511.2	
8H 6- 3	111	1408.	1648.	240.	84.0	755.	268.0	
4G 6- 3	124	1552.	1759.	207.	70.5	797.	255.0	
11H 6- 4	134	1467.	1731.	264.	92.5	610.	282.2	
9D 6- 4	143	1532.	1776.	244.	73.5	807.	261.0	
9J 6- 5	165	1521.	1748.	227.	86.0	939.	250.9	
9H 6- 5	166	1573.	1798.	225.	65.0	819.	262.1	
8J 6- 6	192	1548.	1766.	218.	77.0	790.	272.9	
9D 6- 6	193	1527.	1791.	264.	75.0	806.	272.0	
11F 6- 6	173	1553.	1779.	226.	57.0	840.	262.1	
4G 7- 0	261	1514.	1661.	147.	41.0	721.	302.0	
7D 7- 6	309	1461.	1734.	274.	78.5	729.	348.6	
7G 7- 6	312	1487.	1746.	258.	81.5	752.	337.5	
11E 7- 6	325	1484.	1713.	226.	69.5	799.	328.0	
5L 8- 0	337	1296.	1647.	351.	103.0	744.	366.8	
7H 8- 0	345	1328.	1678.	350.	160.5	785.	356.1	
7K 8- 0	346	1345.	1657.	312.	122.5	740.	362.2	
5J 8- 6	366	1145.	1396.	251.	137.0	603.	397.0	
7B 8- 6	368	1143.	1410.	267.	77.5	672.	387.1	
7E 9- 3	383	1077.	1435.	358.	172.5	672.	409.2	
8H 9- 3	387	1034.	1378.	344.	169.5	564.	411.7	
9C 9- 3	389	1032.	1335.	304.	150.5	635.	414.2	
11F 9- 3	394	1029.	1314.	286.	173.5	834.	331.7	
7B10- 0	408	846.	1232.	386.	161.0	629.	430.2	
8H10- 0	415	849.	1279.	429.	178.5	678.	396.1	
8K10- 0	417	855.	1238.	383.	165.5	372.	433.2	
8N10- 0	418	865.	1283.	418.	124.5	642.	431.4	
6H11- 0	429	674.	838.	163.	113.5	539.	403.1	
9G11- 0	431	674.	914.	236.	173.5	760.	224.1	
11E11- 0	432	673.	670.	197.	169.0	714.	246.9	
5J11- 6	436	661.	825.	165.	117.0	699.	310.0	
7B11- 6	437	638.	939.	301.	215.2	603.	406.0	
8J11- 6	438	674.	826.	152.	117.0	523.	425.0	

RUN 61005 HEATER ROD STATISTICAL DATA

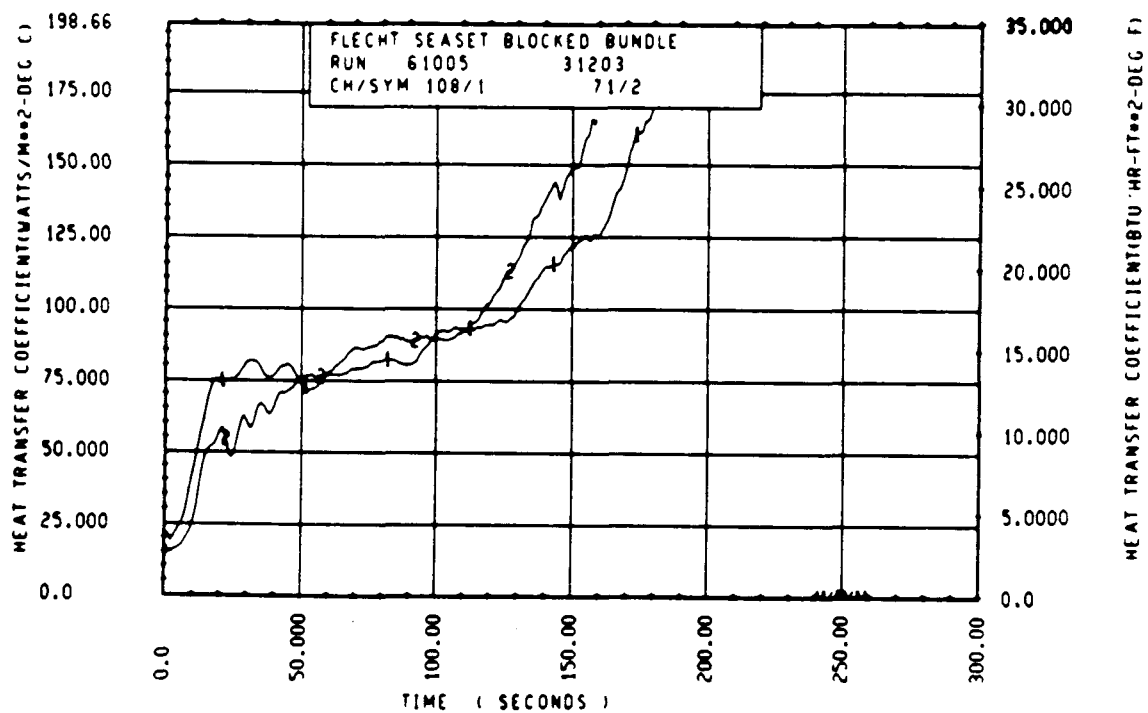
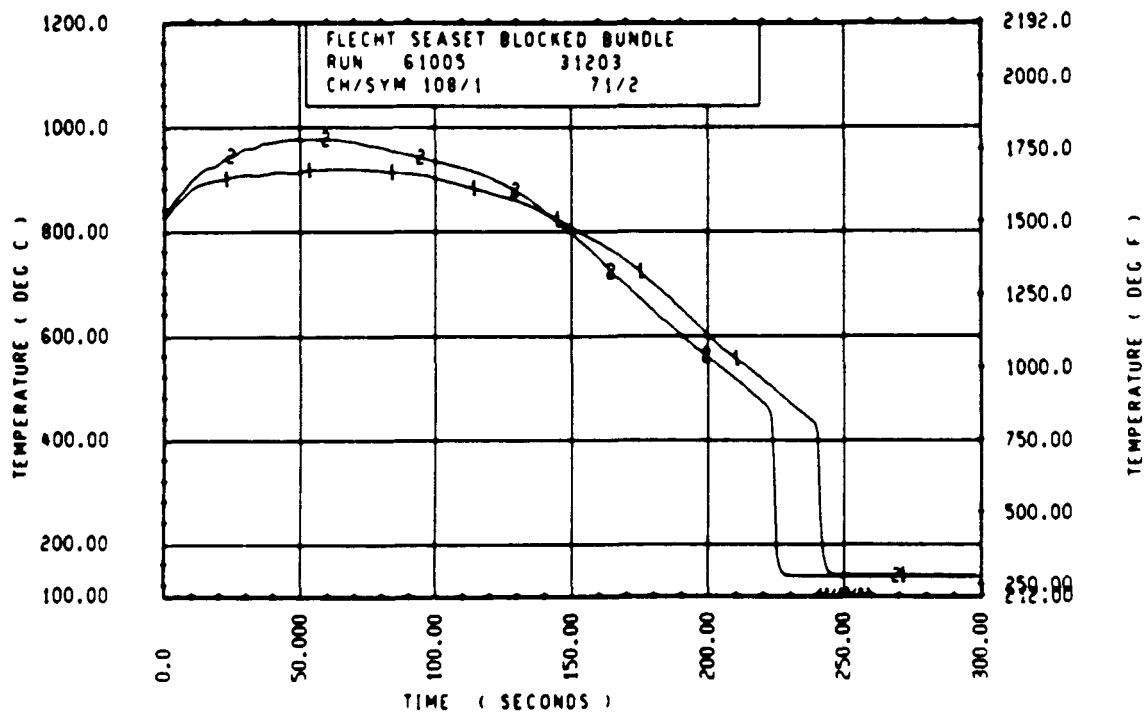
ELEV	INITIAL TEMP (DEG F)			MAX TEMP (DEG F)			TURNAROUND TIME (SEC)		
	MAX	MIN	MEAN	MAX	MIN	MEAN	MAX	MIN	MEAN
12	675.3	669.0	672.5	692.1	685.8	689.7	5.0	5.0	5.0
24	377.0	856.3	863.9	917.3	894.6	902.5	8.5	8.5	8.5
39	1183.7	1135.1	1154.0	1259.8	1208.7	1227.4	14.0	12.5	13.2
48	1346.0	1313.1	1327.7	1454.5	1410.9	1440.5	26.9	17.5	21.3
60	1532.6	1399.7	1491.6	1709.9	1539.1	1659.7	52.5	36.0	41.0
67	1586.8	1483.0	1543.8	1770.1	1659.2	1722.3	65.5	40.0	46.7
69	1527.2	1456.3	1503.0	1769.9	1693.3	1701.0	75.0	43.5	55.3
70	1596.8	1495.9	1528.1	1773.5	1683.4	1721.1	72.0	41.0	55.0
71	1532.6	1445.6	1486.8	1715.5	1601.4	1649.1	72.0	53.5	64.2
72	1590.1	1469.1	1535.3	1799.2	1695.5	1737.3	75.5	41.5	56.6
73	1587.9	1473.4	1529.7	1781.3	1683.4	1729.0	79.0	41.0	54.3
74	1589.0	1364.8	1505.9	1765.8	1620.2	1723.0	81.5	53.0	64.2
75	1596.6	1408.2	1514.9	1801.4	1648.2	1738.0	91.0	43.0	66.4
76	1606.9	1443.5	1540.1	1826.6	1704.3	1764.2	92.5	52.5	64.0
77	1578.2	1476.6	1526.8	1816.1	1682.3	1761.4	87.5	55.0	72.8
78	1587.9	1334.2	1533.5	1835.4	1534.8	1771.8	95.5	55.0	74.0
79	1574.9	1492.7	1539.7	1816.1	1762.3	1788.0	94.0	55.5	75.7
80	1548.9	1495.9	1523.8	1834.2	1772.4	1805.1	93.0	60.5	76.7
81	1544.6	1433.4	1497.5	1811.6	1726.6	1780.6	95.5	62.5	83.8
84	1551.1	1456.3	1506.4	1896.5	1595.5	1653.0	75.5	40.5	54.2
86	1567.3	1460.6	1516.7	1755.0	1643.8	1706.9	78.0	40.5	65.4
90	1494.8	1411.4	1465.7	1772.4	1672.4	1723.3	96.5	60.5	77.3
96	1369.1	1236.9	1331.8	1727.7	1598.7	1678.0	166.0	78.5	110.9
102	1186.6	1038.5	1147.9	1507.7	1366.9	1447.2	169.5	77.5	139.5
111	1777.1	1924.6	1845.9	1442.4	1274.4	1366.2	181.5	80.5	160.3
120	910.1	803.6	854.1	1337.4	1093.6	1251.5	215.2	110.5	165.7
132	675.3	666.9	672.2	945.2	833.5	886.0	181.5	113.5	155.3
138	674.3	637.5	653.0	939.0	825.3	856.5	215.2	110.0	147.2

RUN 61005 HEATER ROD STATISTICAL DATA

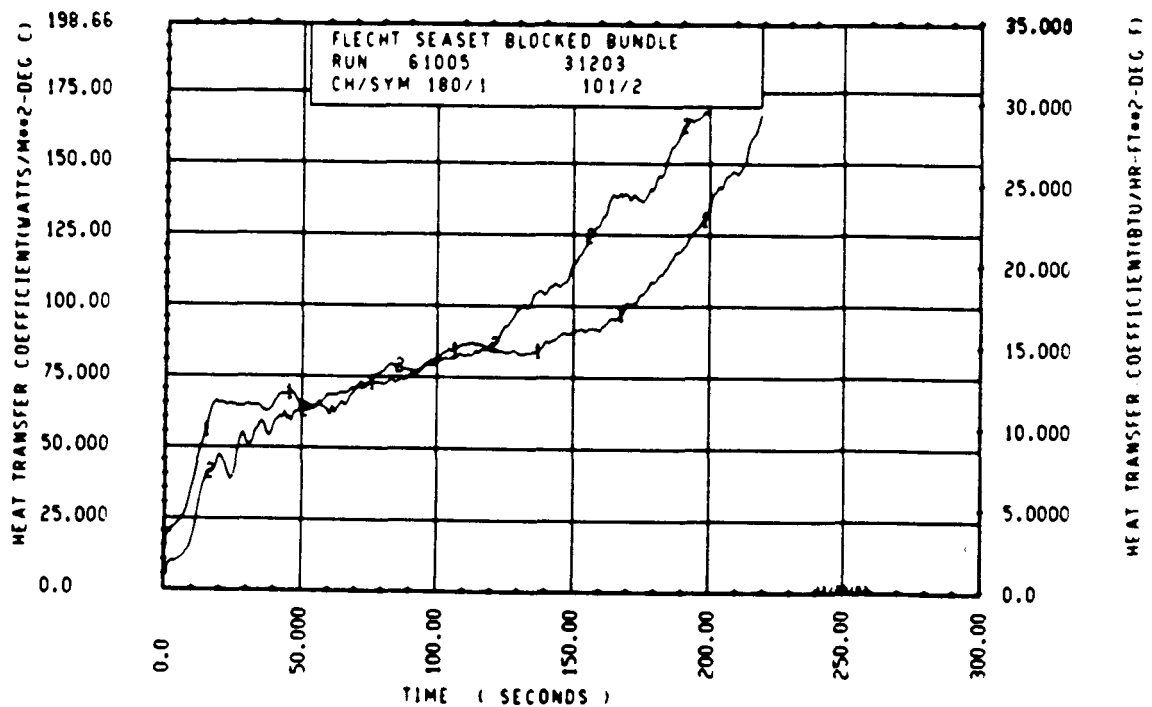
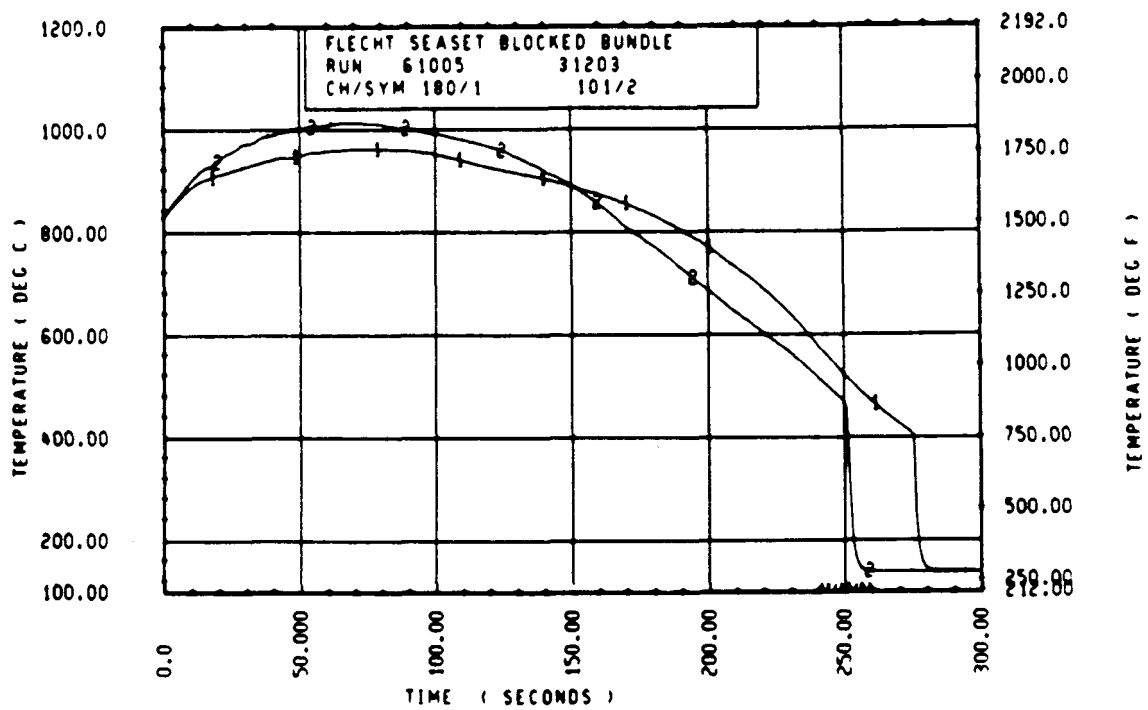
ELEV	TEMP (ISE) (DEG F)			QUENCH TEMP (DEG F)			QUENCH TIME (SEC)		
	MAX	MIN	MEAN	MAX	MIN	MEAN	MAX	MIN	MEAN
12	17.9	16.3	17.2	551.9	544.7	549.0	24.7	22.5	23.8
24	46.3	37.2	38.6	620.3	612.2	614.0	46.0	44.3	45.0
39	76.0	65.6	73.5	766.4	744.4	749.0	87.3	81.9	84.4
48	120.0	96.3	107.9	804.0	732.8	771.3	121.0	112.5	116.4
60	191.3	139.5	169.1	917.0	744.0	832.7	179.4	157.4	169.2
67	222.8	161.6	178.6	912.4	757.5	867.9	214.1	194.3	205.5
69	239.1	174.9	198.7	837.9	782.0	869.2	222.0	207.7	214.9
70	220.7	173.7	193.0	826.3	722.6	800.9	226.1	215.2	219.7
71	223.4	181.7	201.3	815.2	774.6	799.2	233.1	223.2	227.1
72	240.8	151.1	202.0	831.0	743.0	788.3	241.8	226.9	234.4
73	213.2	169.6	195.3	843.7	780.3	866.7	243.1	228.0	236.2
74	273.6	171.4	217.1	846.8	682.7	770.7	264.2	230.2	245.2
75	282.0	182.2	223.1	873.0	543.9	768.5	269.1	239.1	253.4
76	254.1	180.1	224.1	869.1	613.5	791.1	282.2	245.1	256.9
77	291.3	197.7	232.6	938.6	652.2	778.0	293.2	253.5	268.4
79	281.6	200.6	238.3	894.3	541.9	770.4	307.7	257.1	273.7
79	287.8	210.2	248.4	887.7	633.3	782.4	310.2	260.5	279.4
80	321.8	246.2	281.2	892.1	659.6	786.6	313.1	272.0	286.3
81	316.9	238.3	289.1	861.4	690.0	788.0	312.2	277.9	291.3
84	163.6	135.2	146.6	815.1	694.6	736.3	316.2	291.0	302.4
86	223.0	130.3	190.2	835.2	685.4	756.2	334.1	302.2	313.9
90	290.4	225.8	257.5	847.7	686.5	782.7	360.1	322.0	334.9
96	330.7	311.1	346.2	822.3	696.4	770.9	377.3	351.1	361.2
102	336.3	251.1	299.3	734.0	581.0	672.2	412.6	365.2	388.2
111	400.3	224.2	324.4	833.7	564.4	660.1	423.2	331.7	402.4
120	464.8	290.1	397.4	1054.9	527.5	647.3	452.4	248.7	411.6
132	269.8	163.4	213.8	754.6	467.0	606.0	446.2	223.1	342.7
138	301.5	152.1	203.5	825.7	495.3	629.3	425.2	172.9	347.7



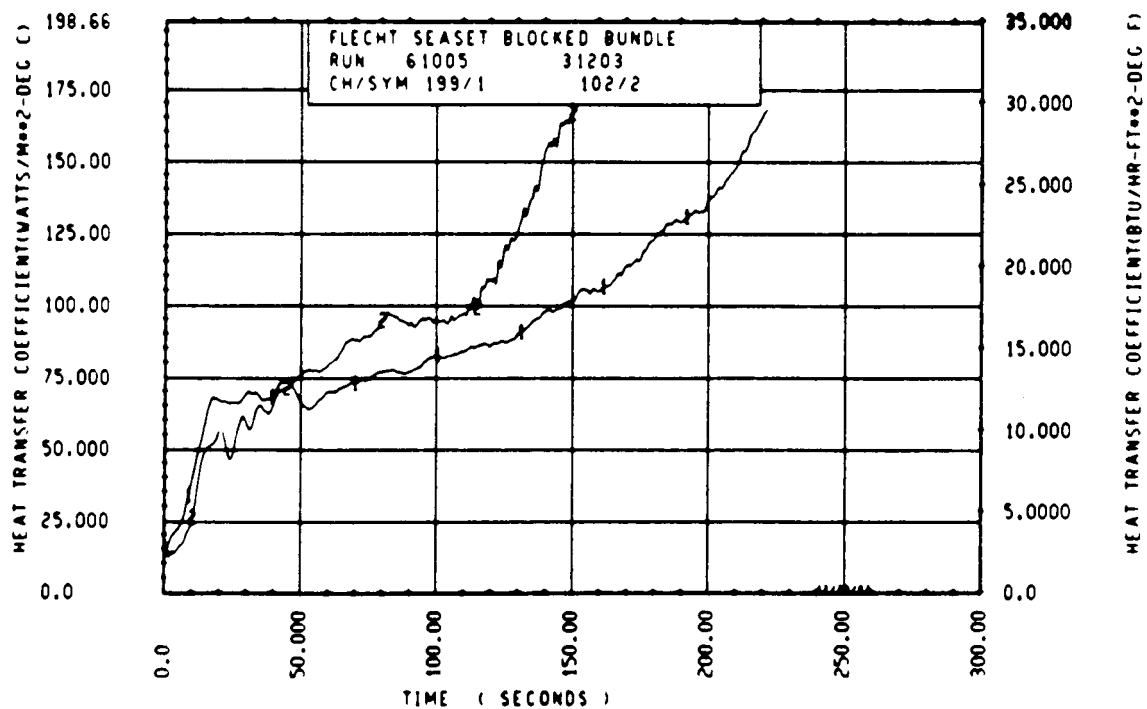
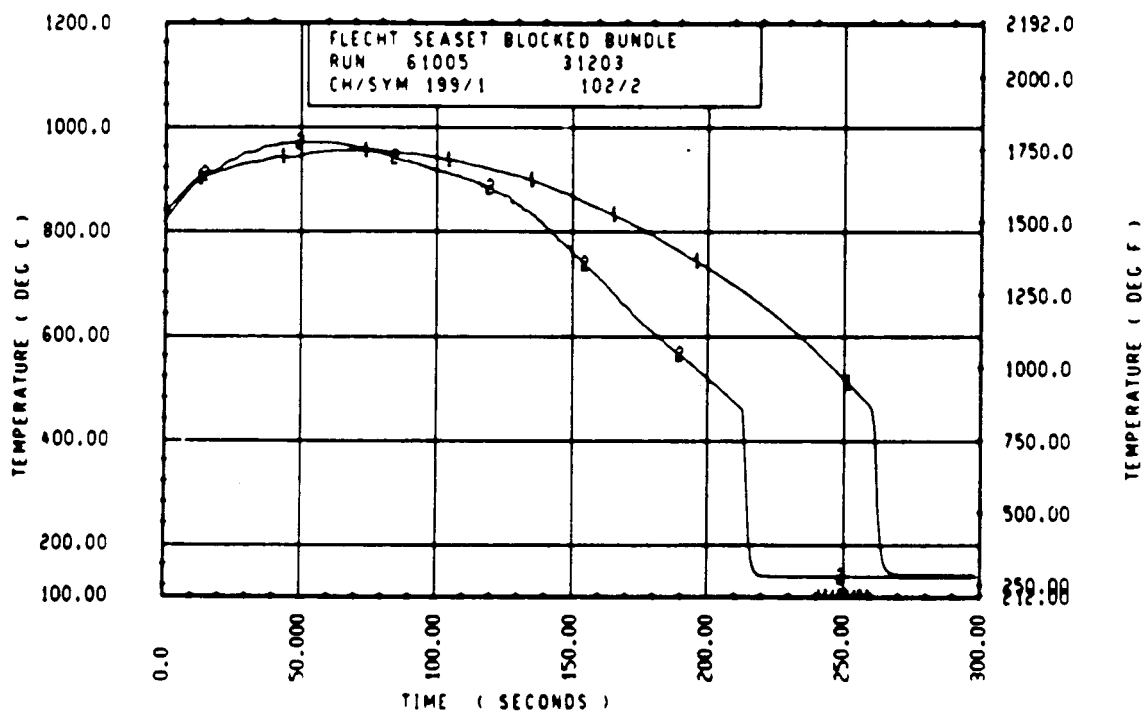
Rod 7M, 1.88 m (74 in.)



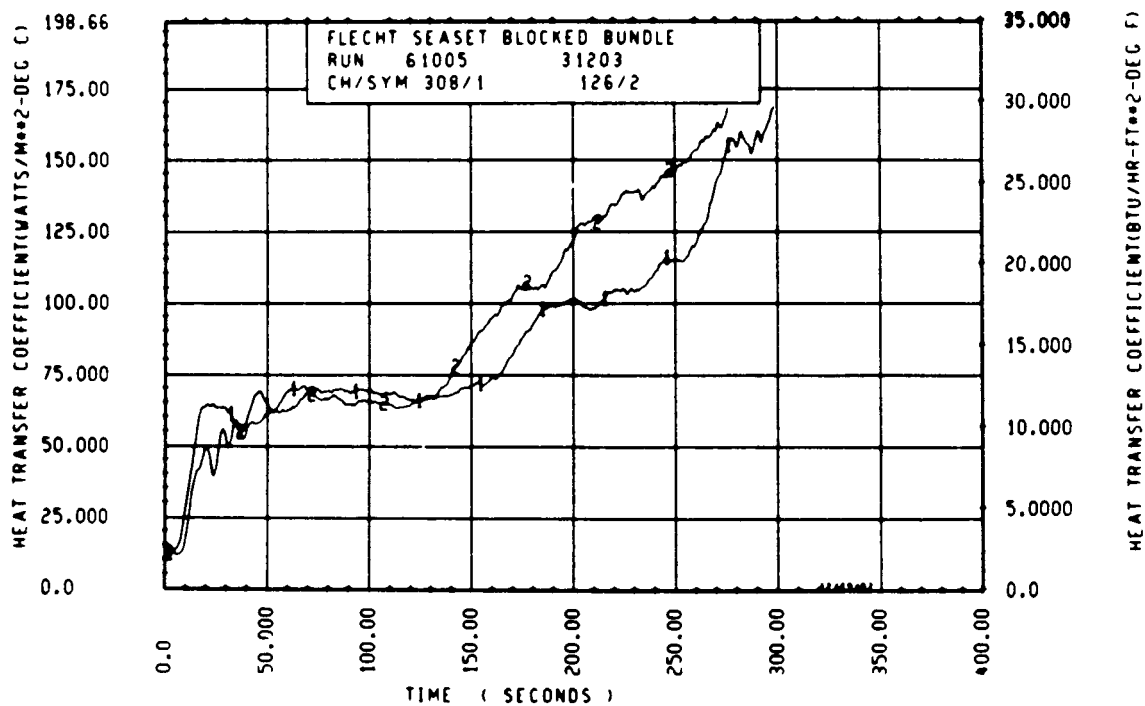
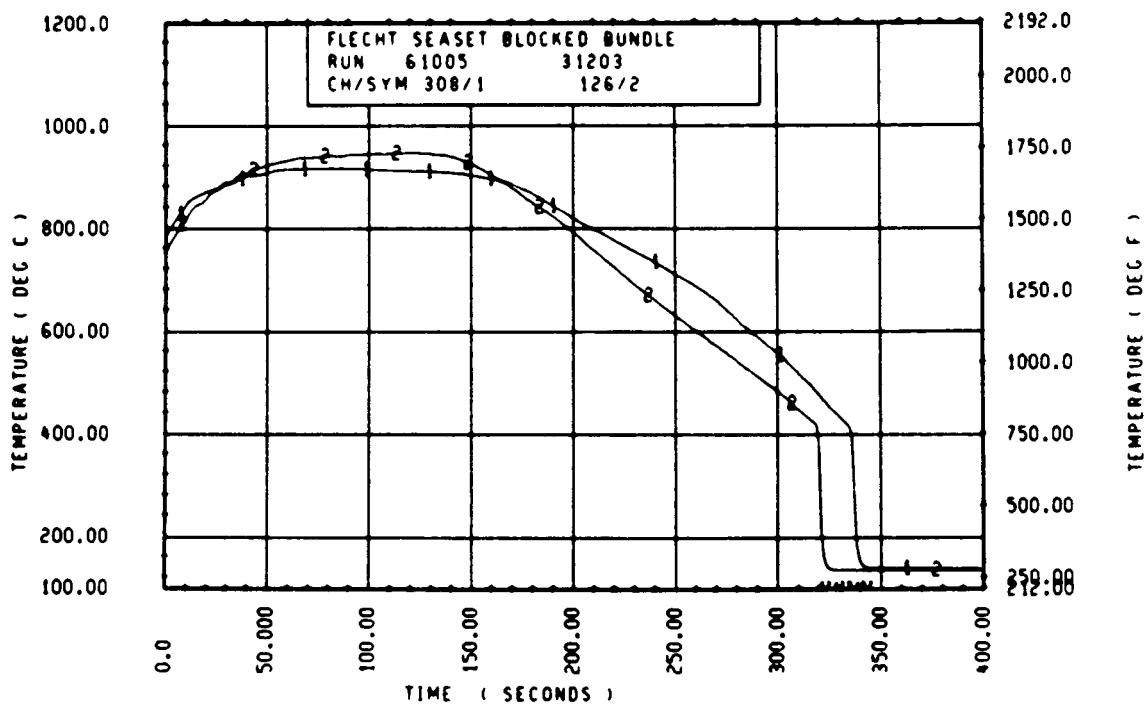
Rod 13G, 1.88 m (74 in.)



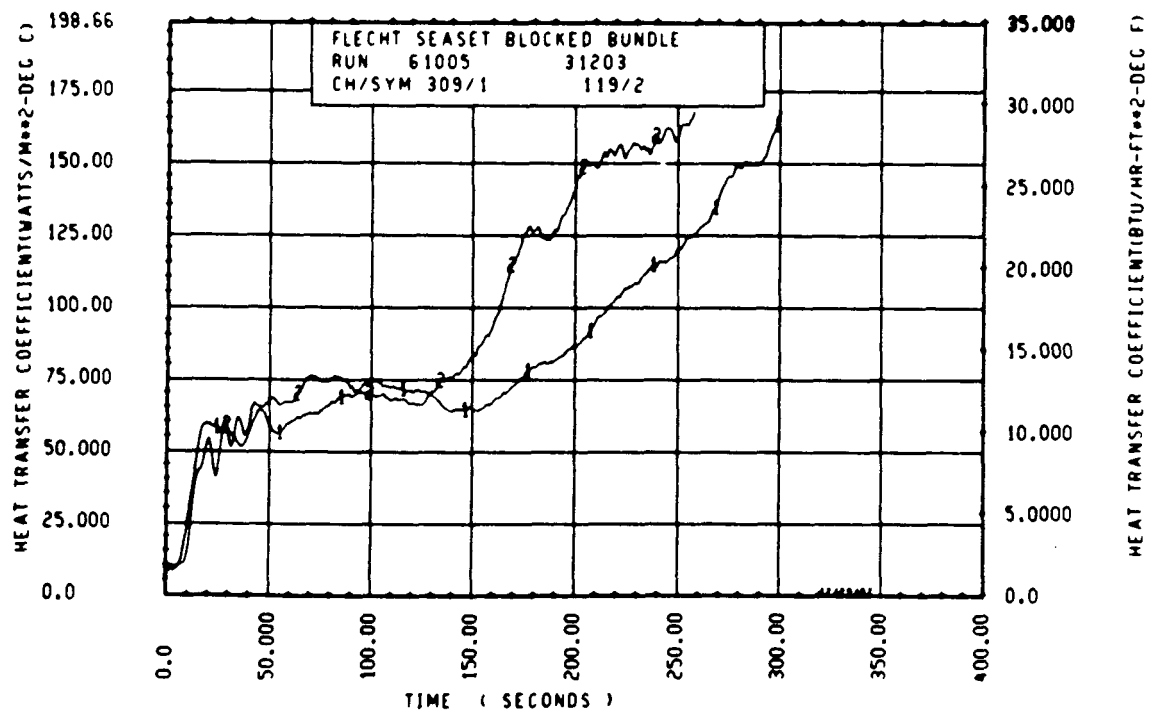
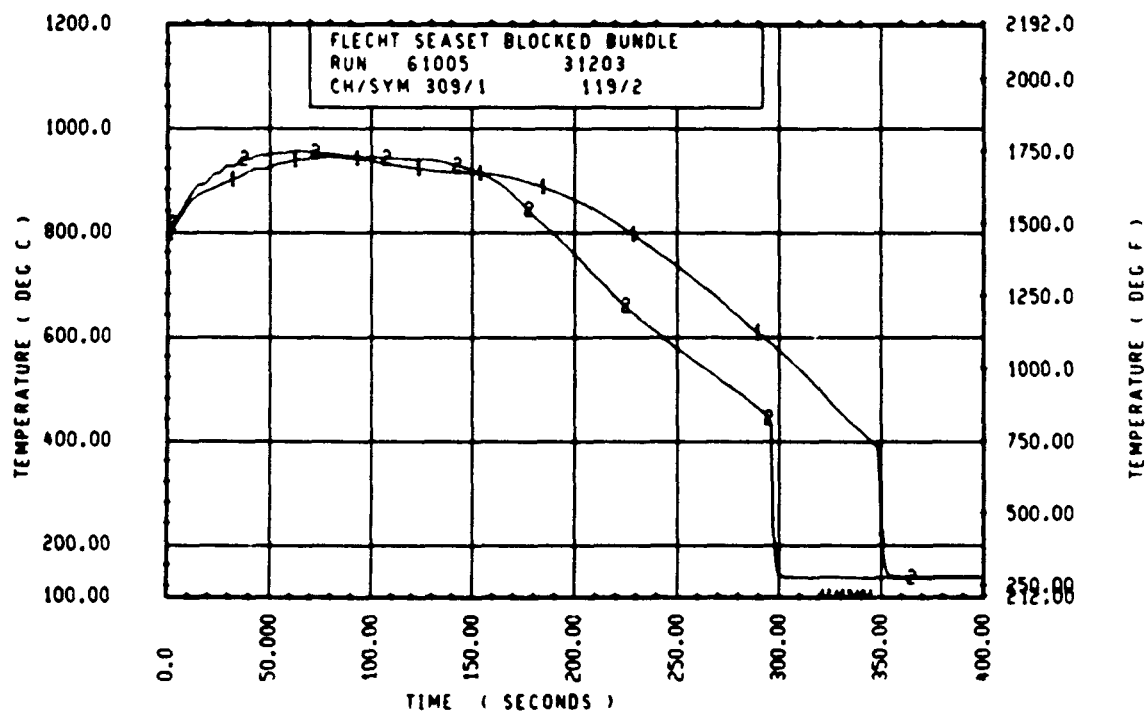
Rod 121, 1.98 m (78 in.)



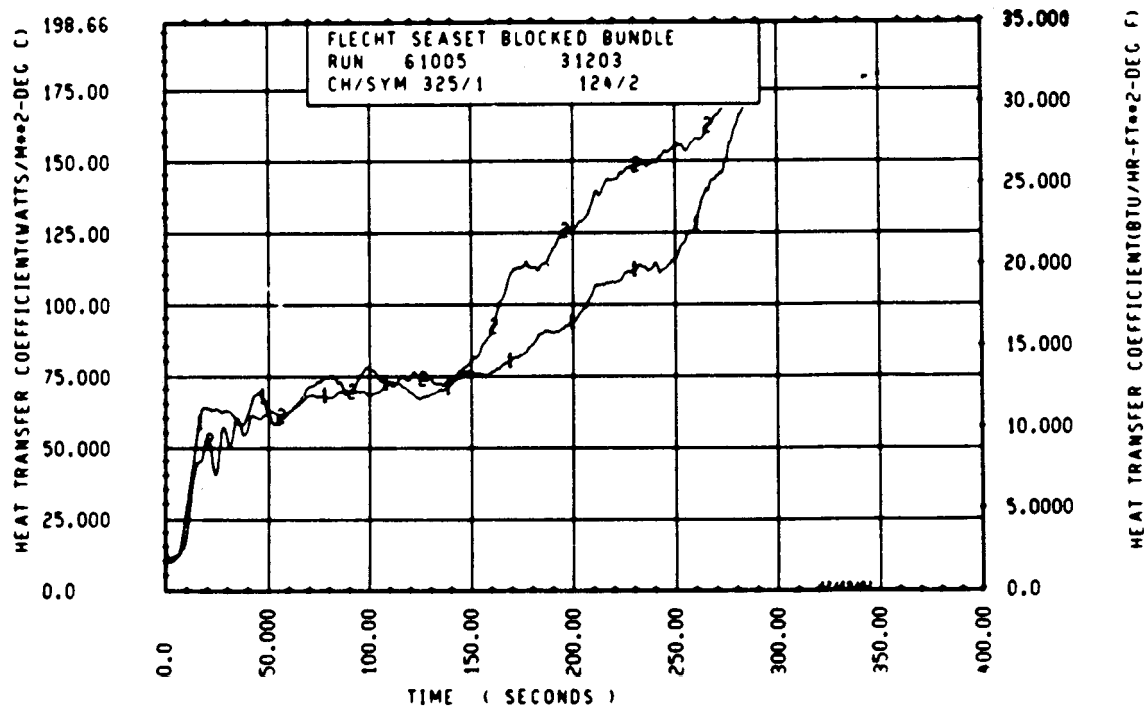
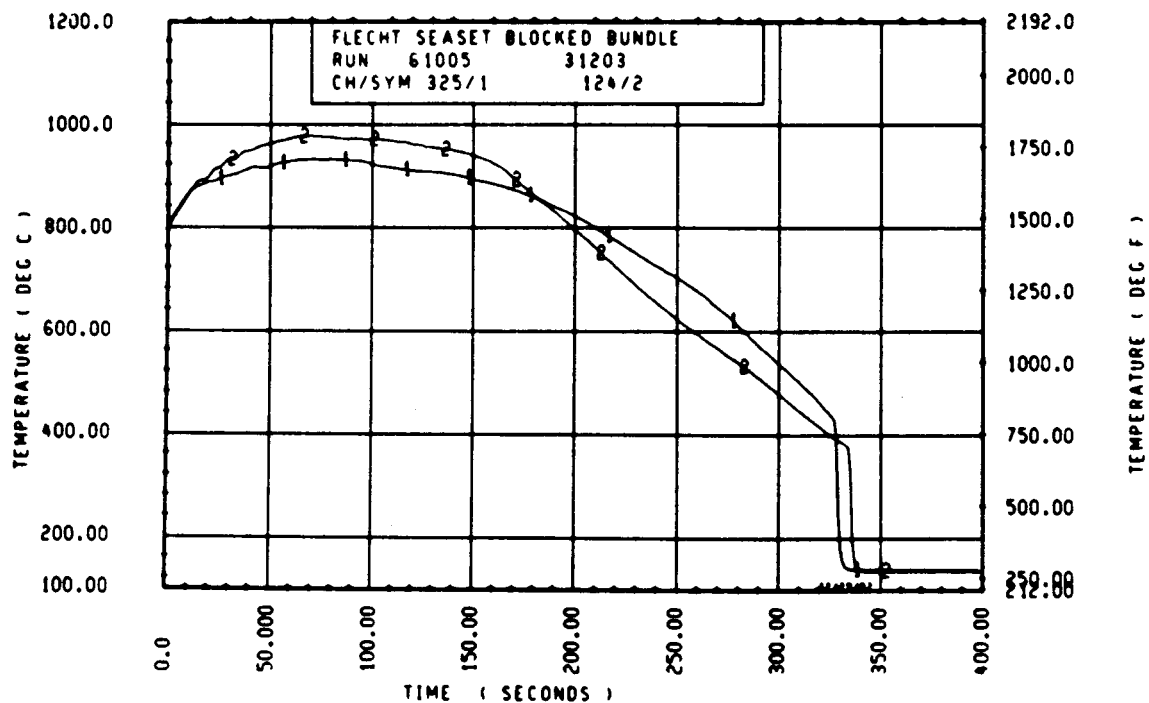
Rod 13G, 1.98 m (78 in.)



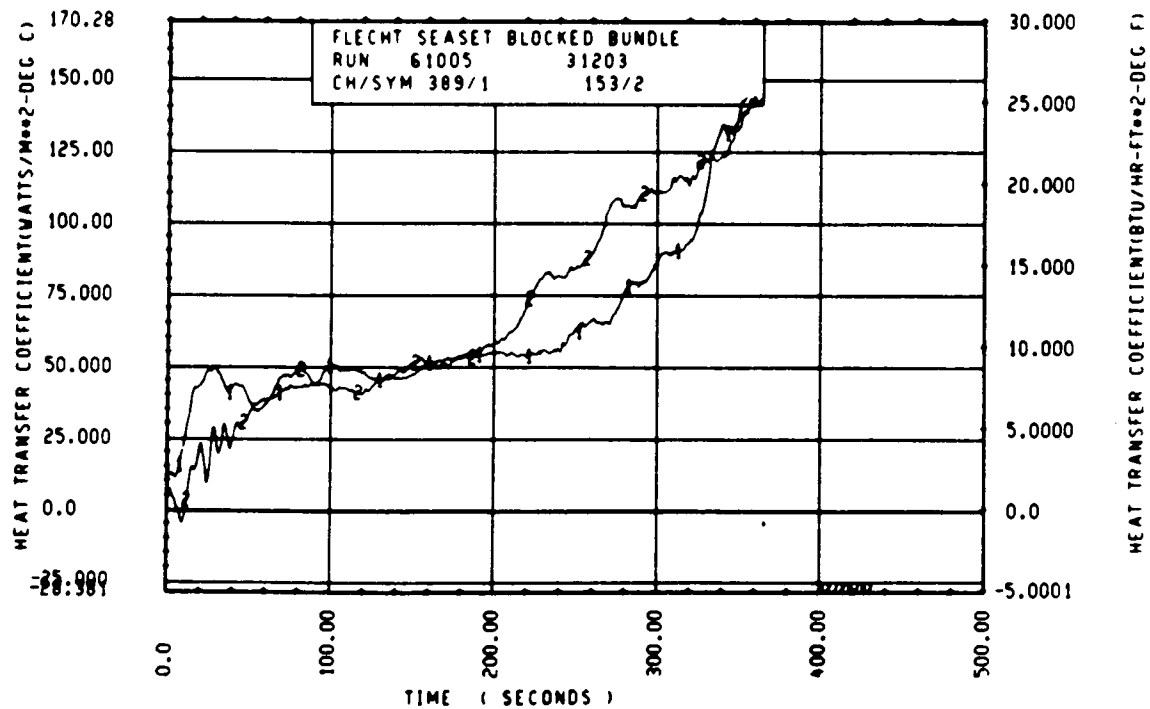
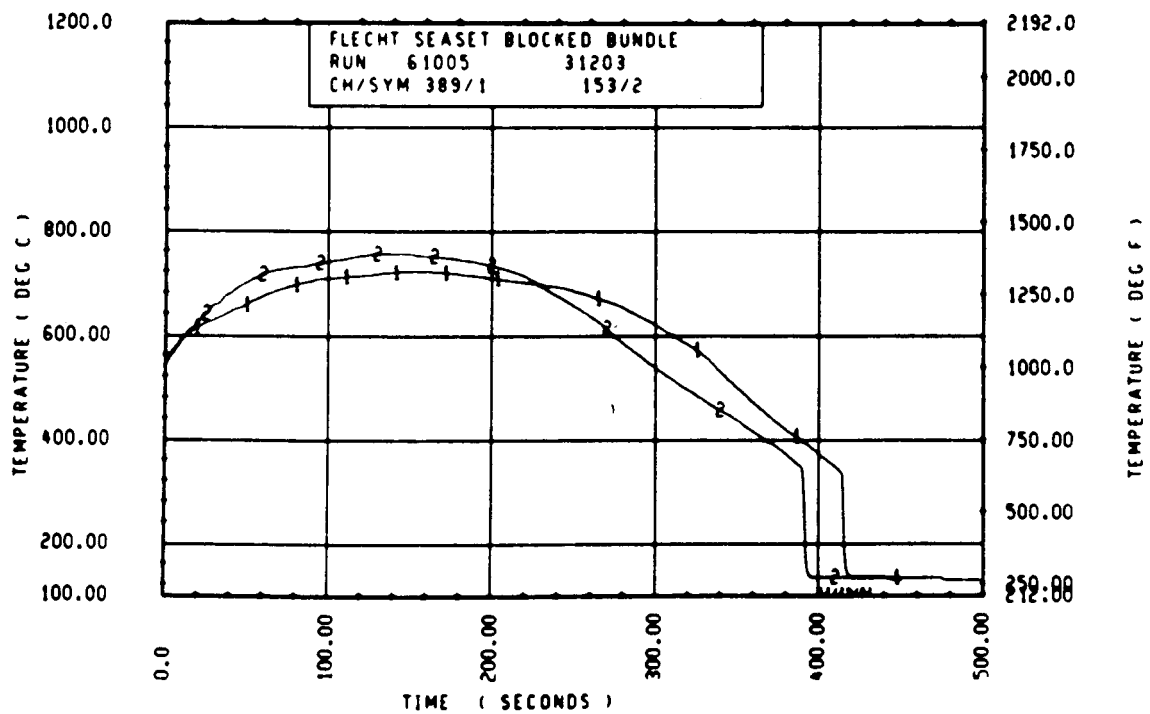
Rod 6J, 2.29 m (90 in.)



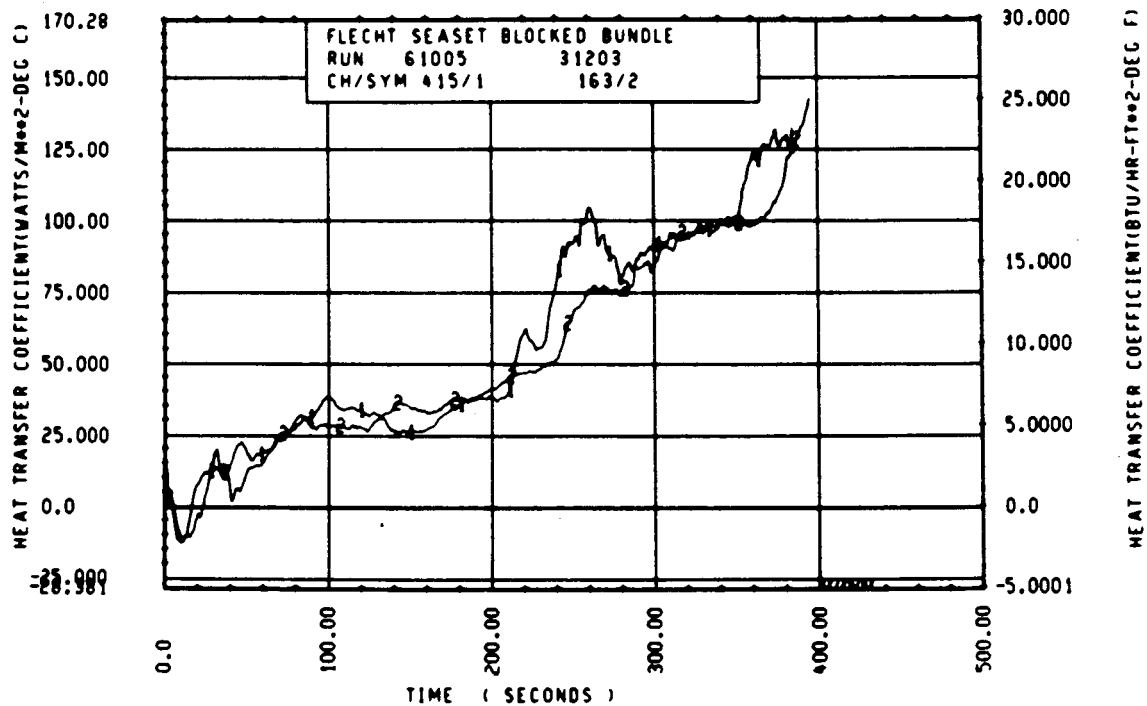
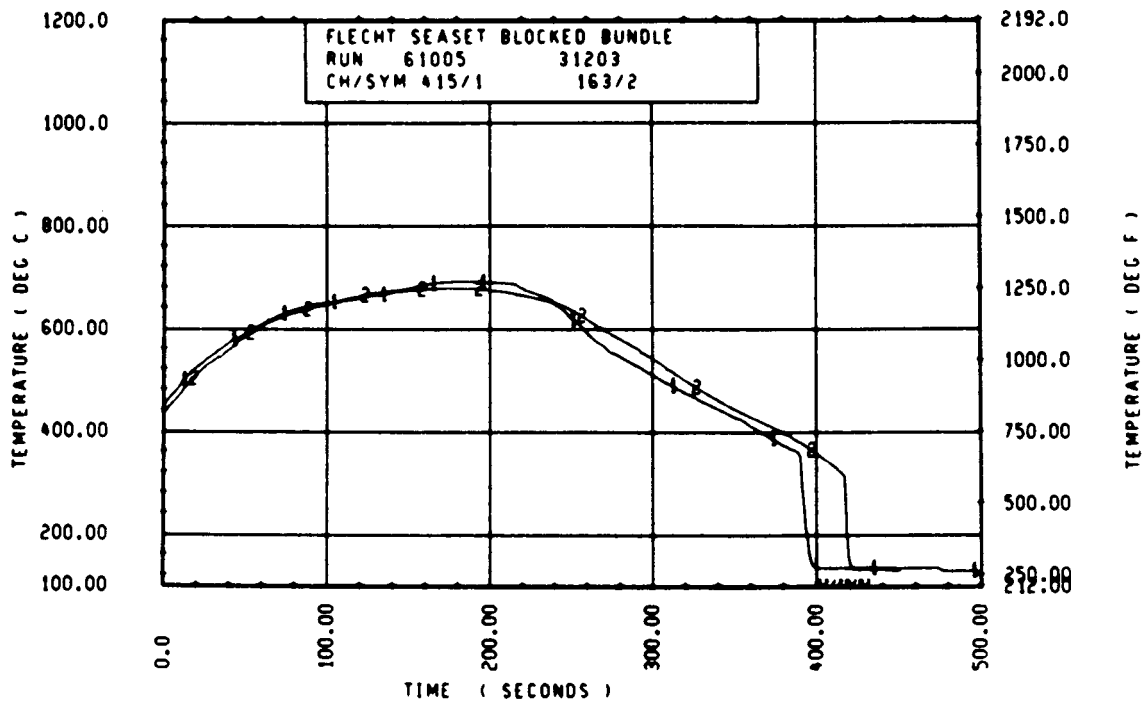
Rod 7D, 2.29 m (90 in.)



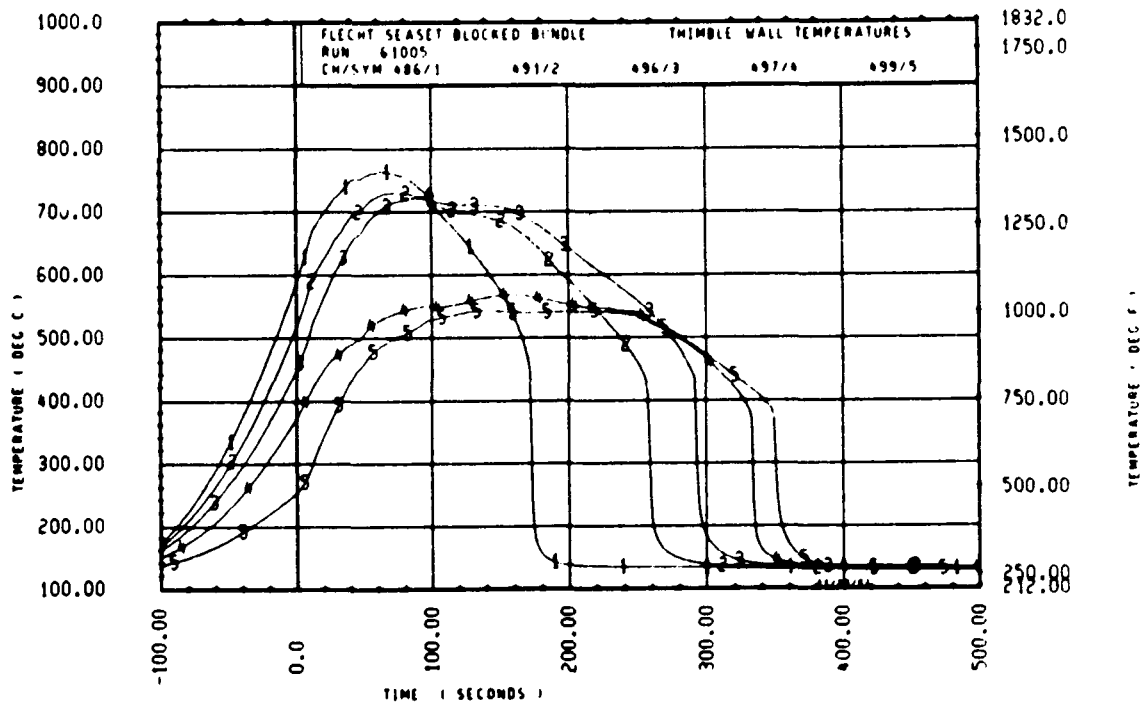
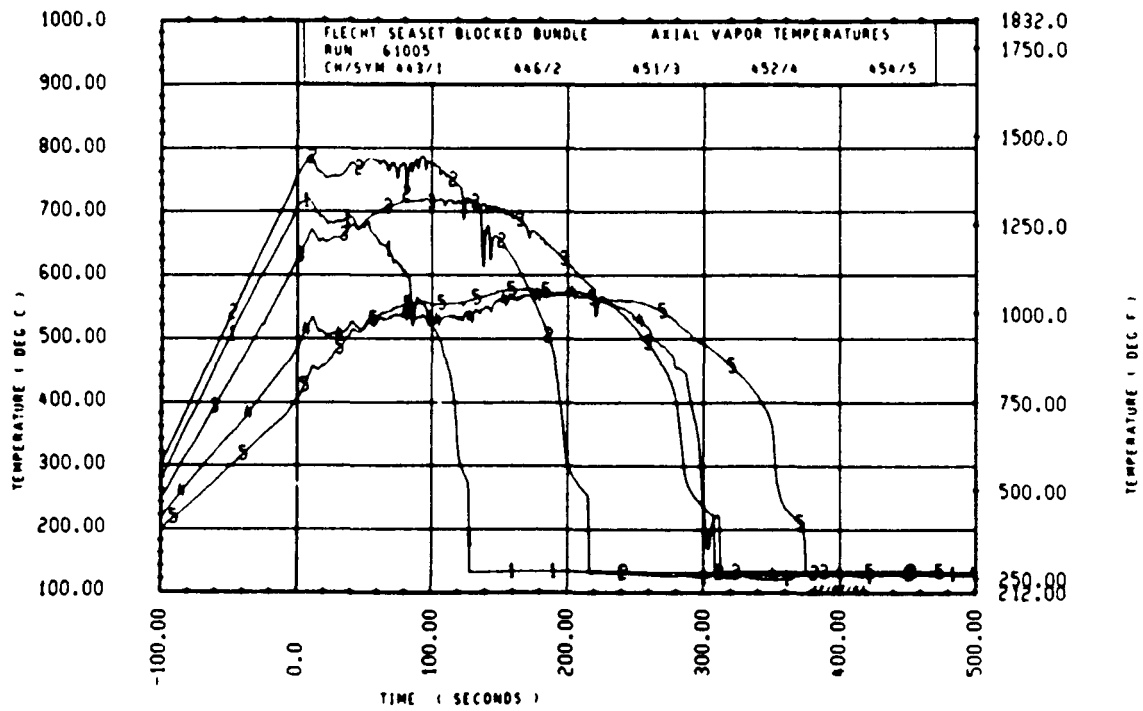
Rod 11E, 2.29 m (90 in.)

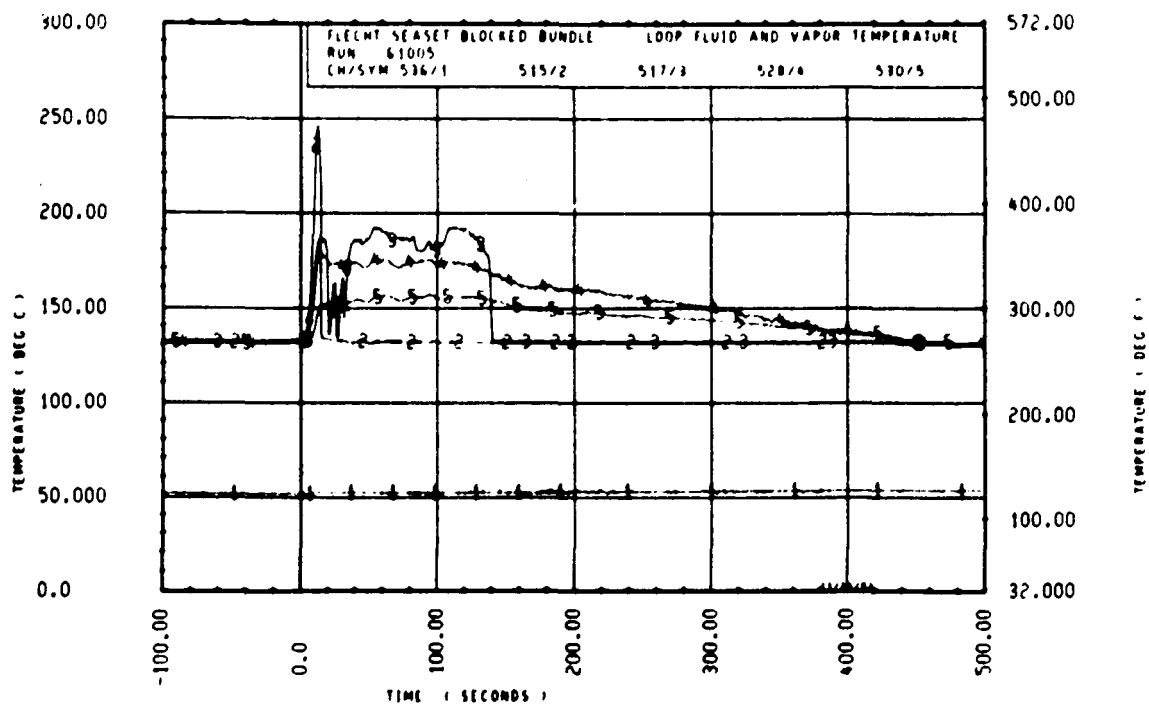
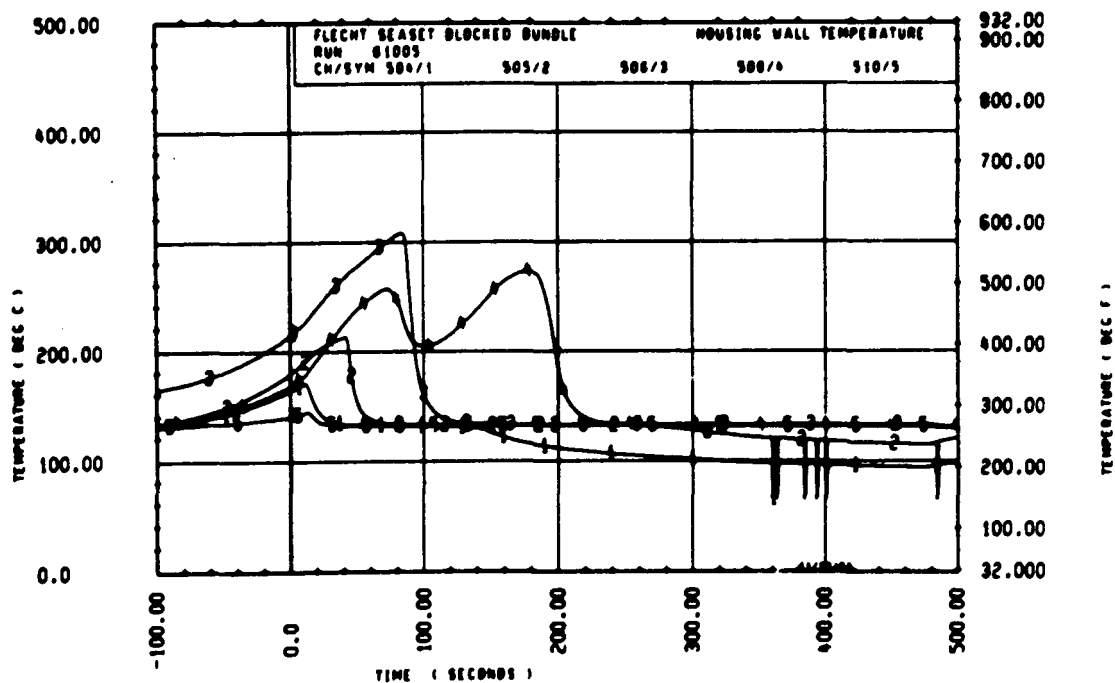


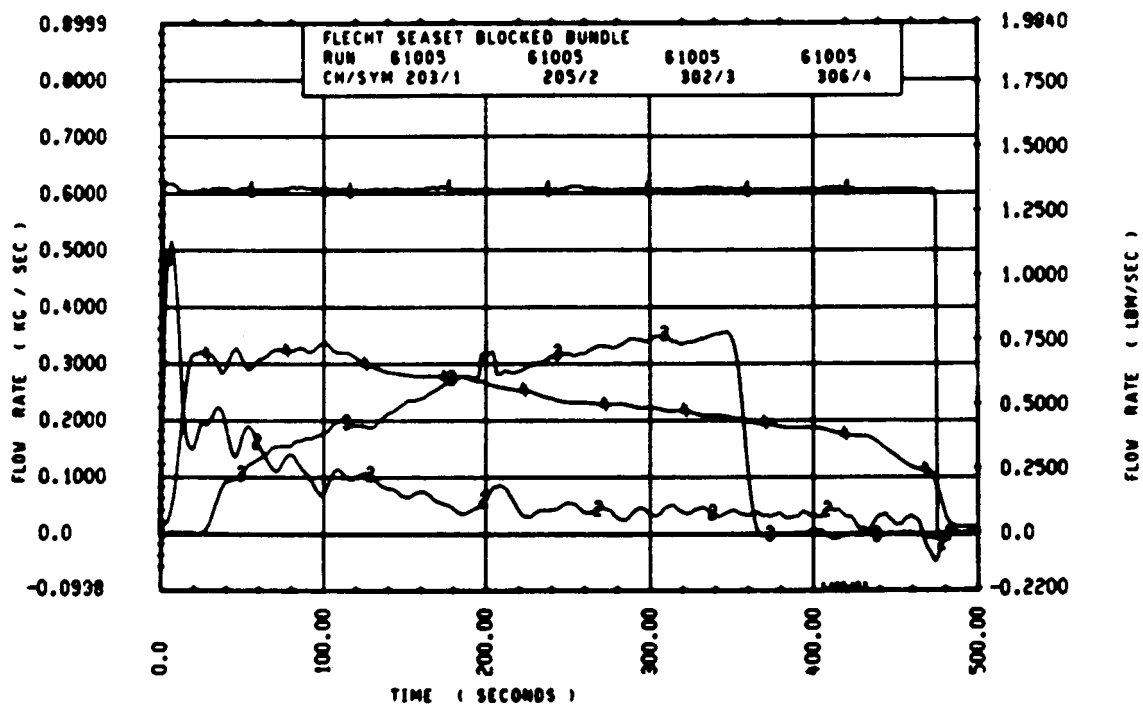
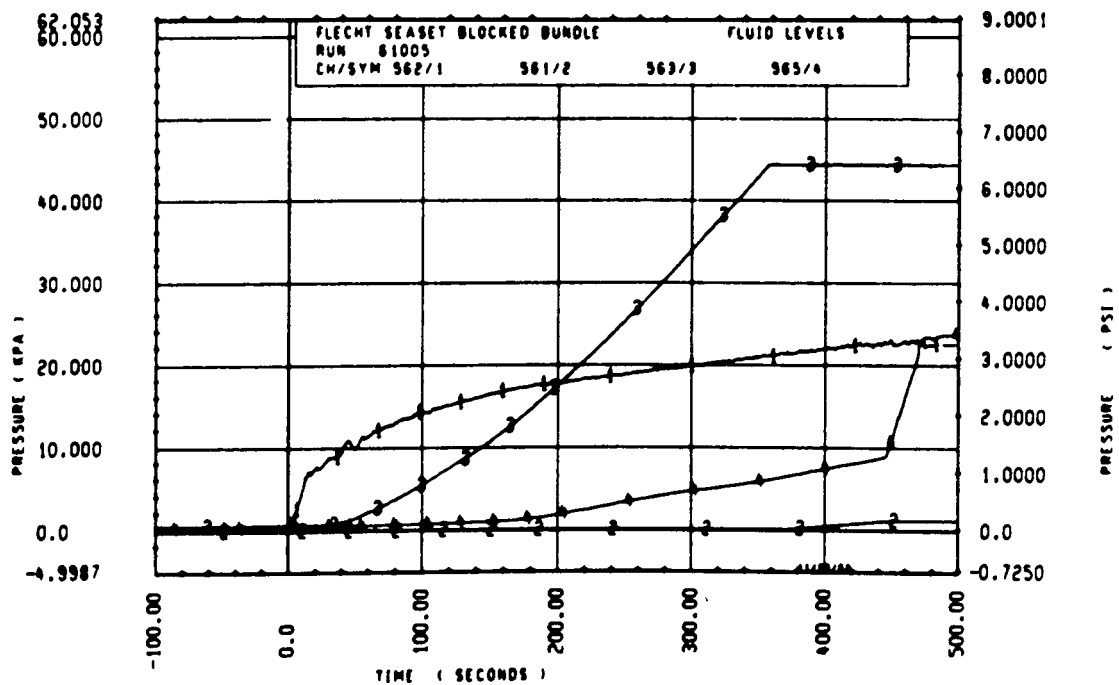
Rod 9C, 2.82 m (111 in.)

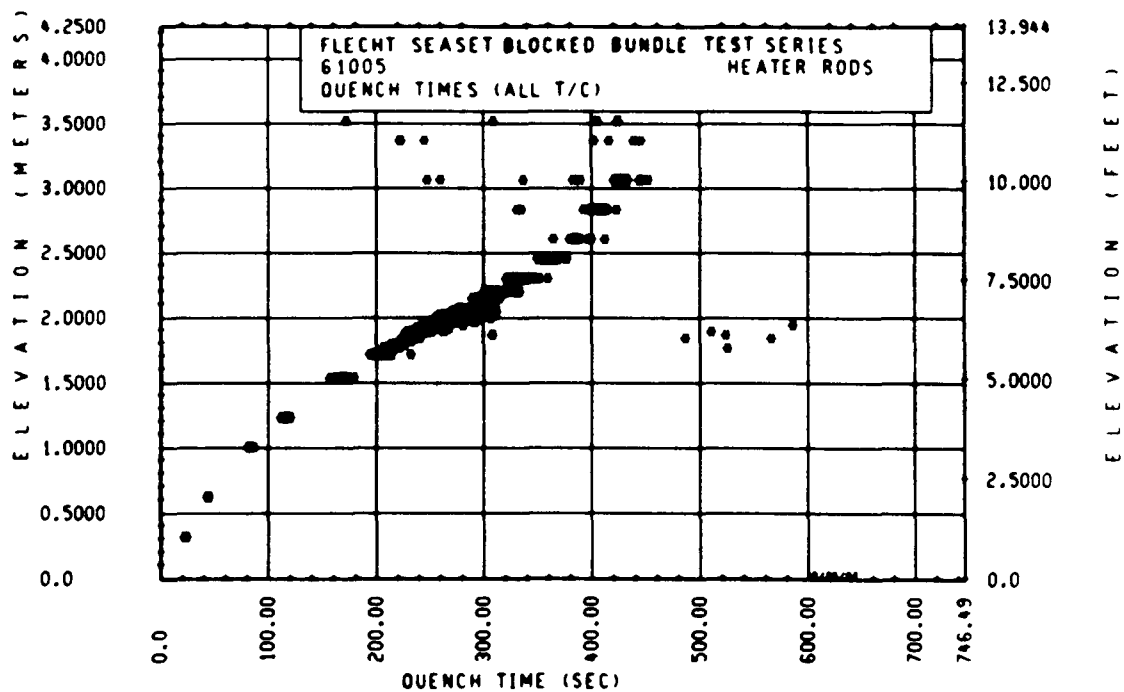
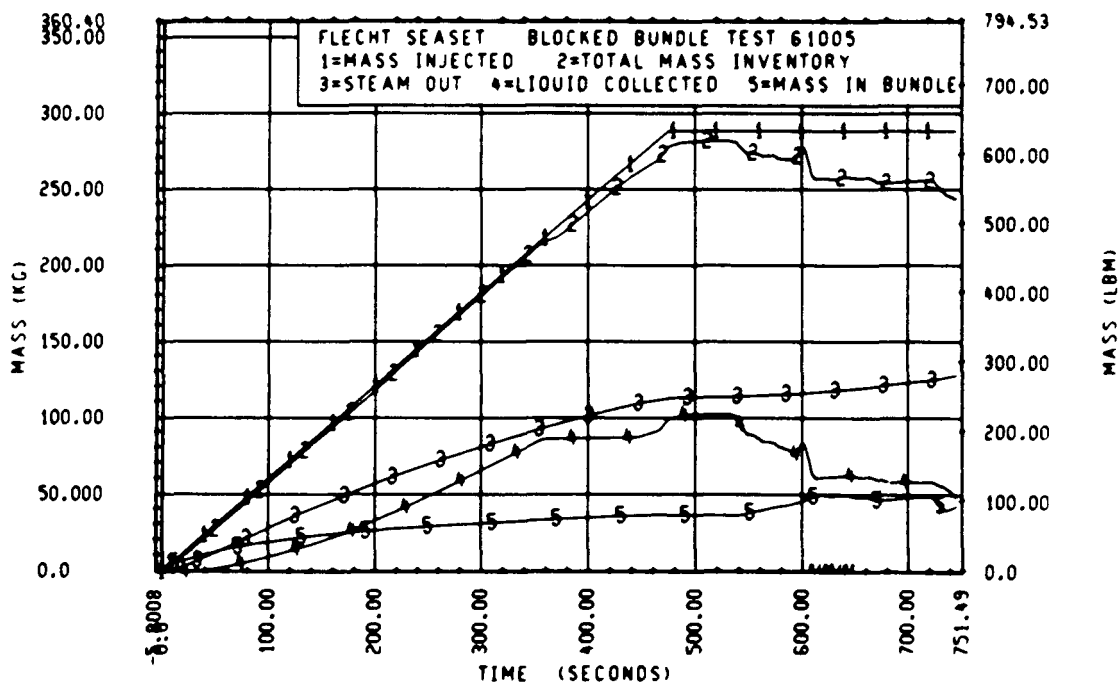


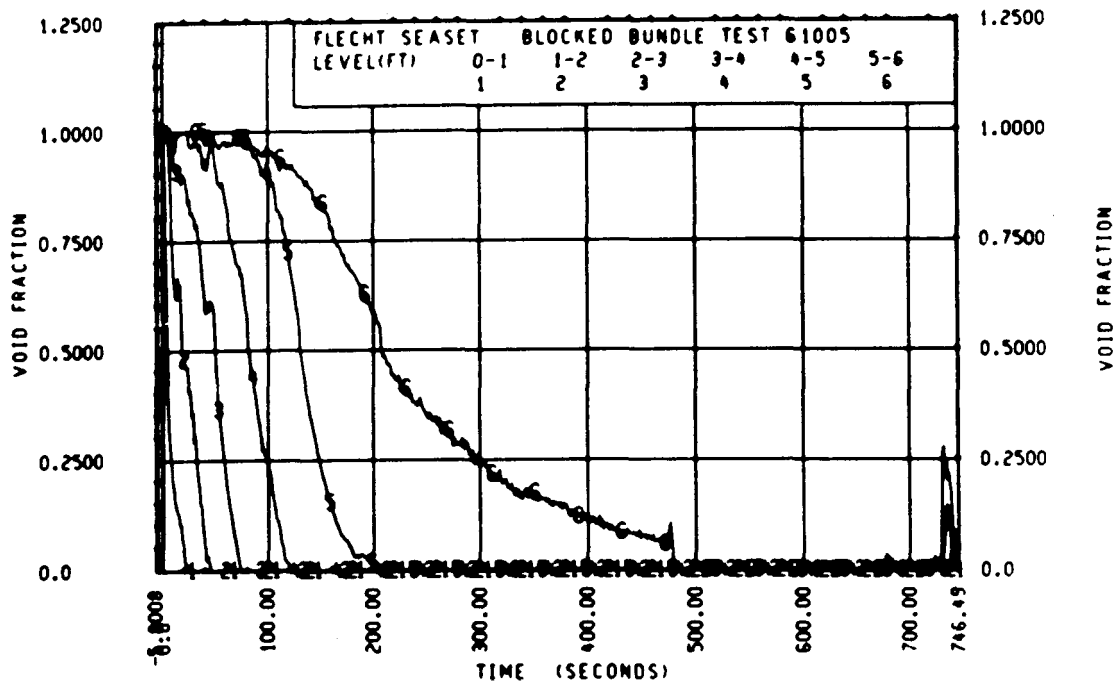
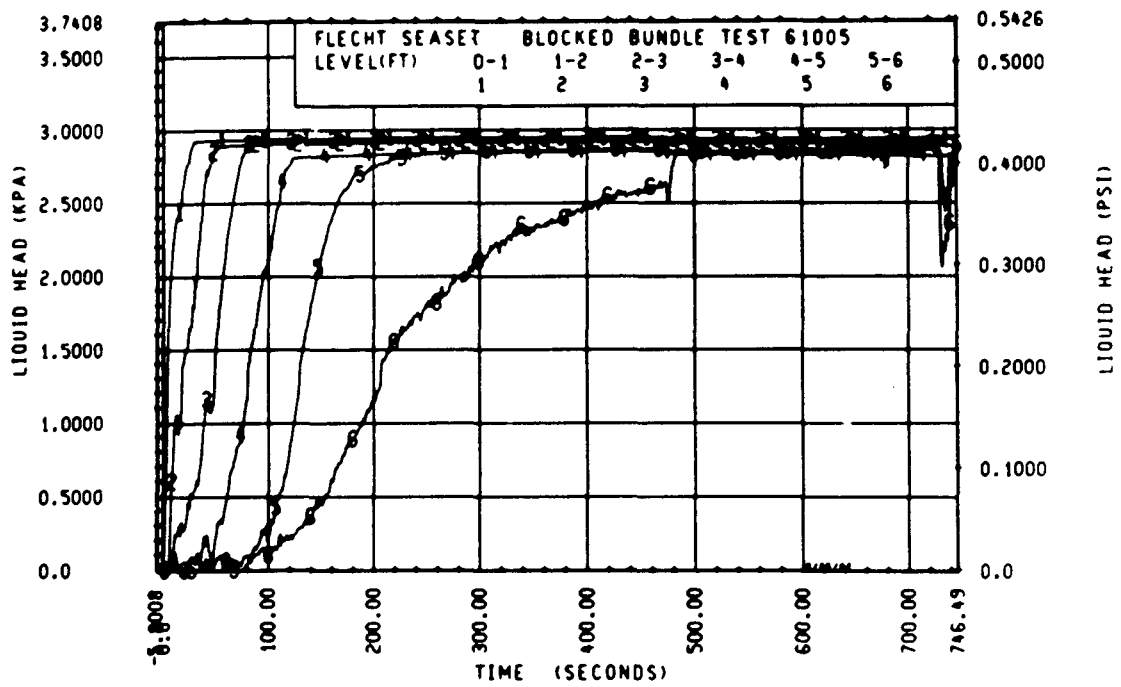
Rod 8H, 3.05 m (120 in.)

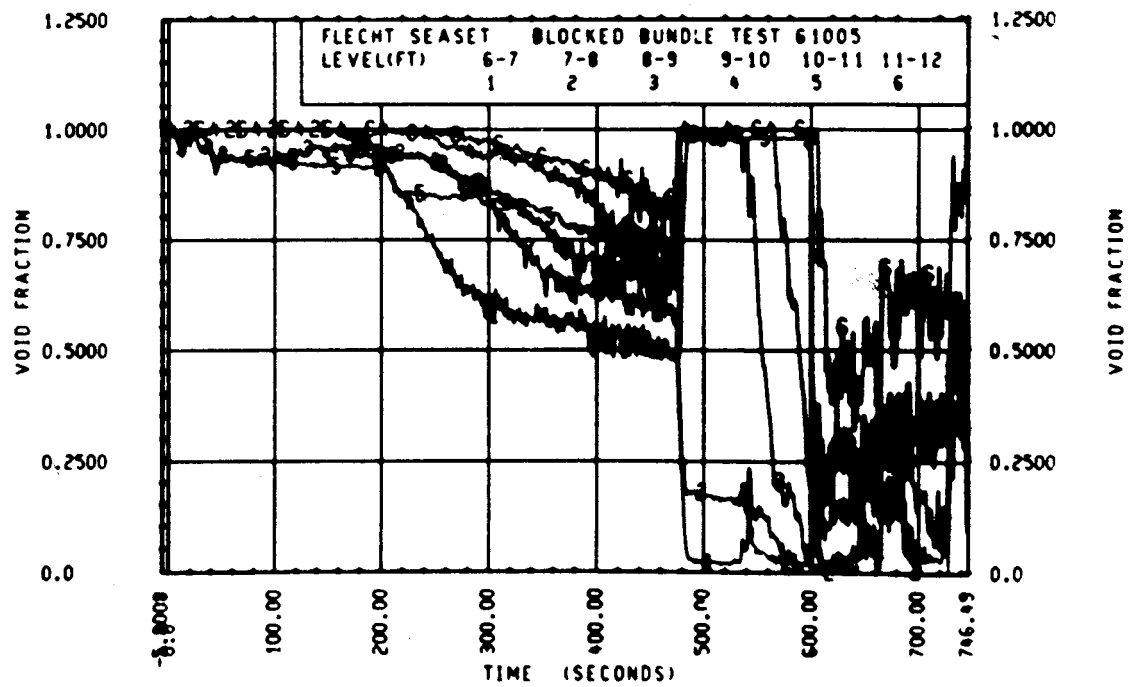
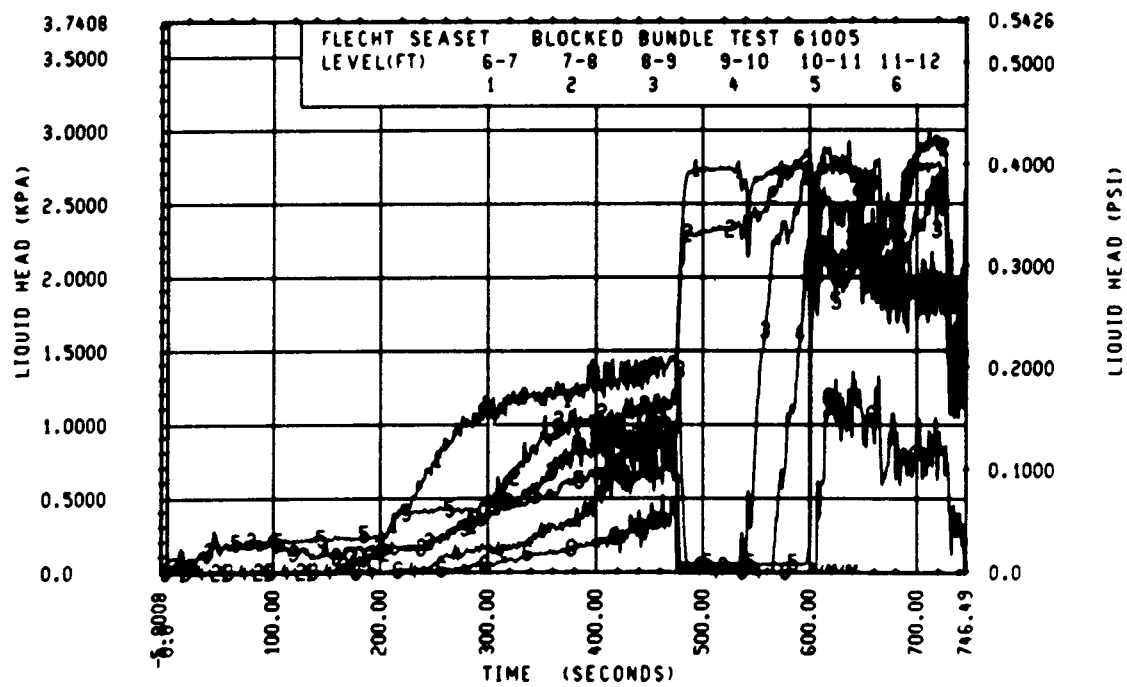












FLECHT SEASET 163-ROD BUNDLE FLOW BLOCKAGE TASK
SUMMARY AND COMMENT SHEET

Run: 61106
Test date: 8/26/82
Test type: Forced reflood
Parameter: Flooding rate effect

AS-RUN TEST CONDITIONS:

Upper plenum pressure	0.277 MPa (40.2 psia)
Initial peak clad temperature and location	885.7°C (1626.2°F), 2I-1.93 m (76 in.)
Initial peak rod power:	
Peripheral rods	2.30 kW/m (0.702 kw/ft)
Bypass rods	2.28 kW/m (0.695 kw/ft)
Blockage island rods	2.30 kW/m (0.701 kw/ft)
Flooding rate	24.9 mm/sec (0.981 in./sec)
Coolant temperature	52.8°C (127°F)
Initial bundle water level	+1.5 mm (+0.06 in.)

COMMENTS:

The mass flow through the steam probes which aspirated through the bottom of the bundle was reduced.

Inlet mass flow:⁽¹⁾ +0.6% constant

Power decay:⁽¹⁾ peripheral rods, 0% linearly increasing to +0.5% by 120 seconds
bypass rods, -1.3% constant
blockage rods, 0% constant

1. Relative to run 31504

FLECHT SEASET 163 ROJ BUNDLE TEST SERIES

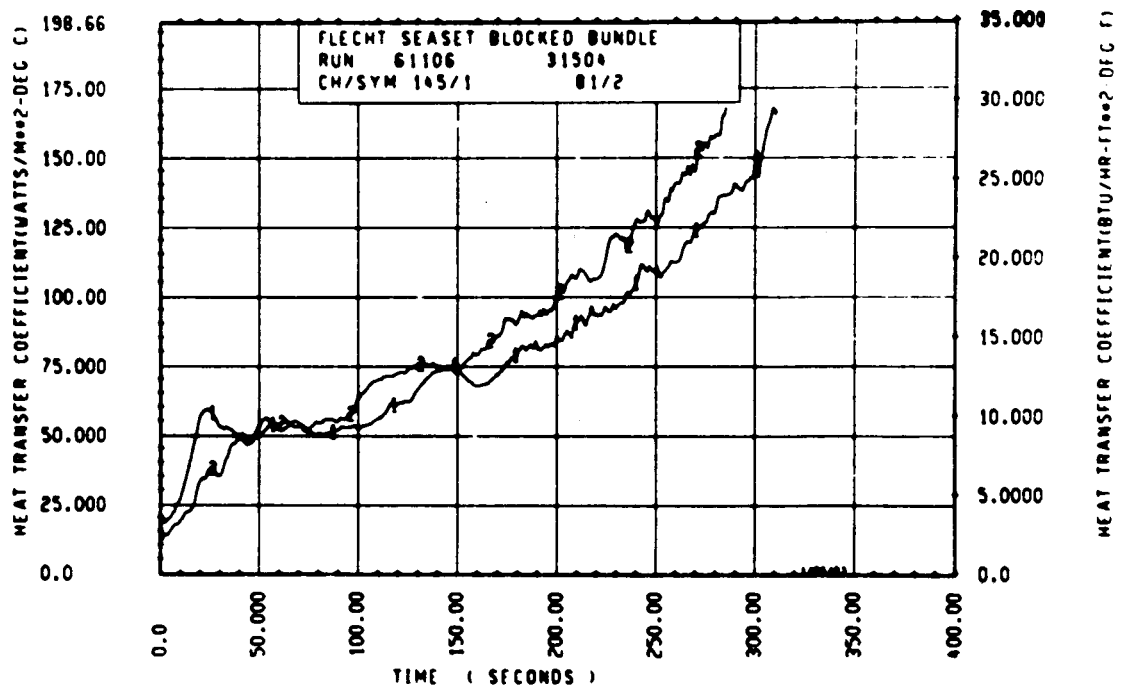
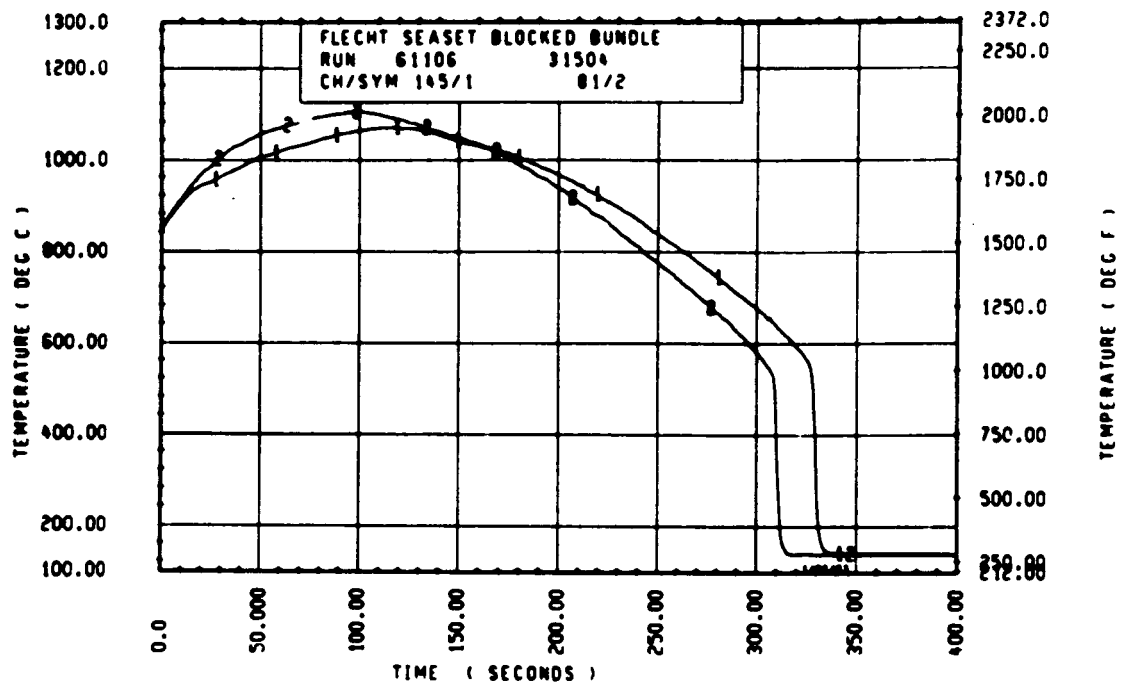
RJD/ELEV	CHAN. NO	INITIAL AT FLOOD (DEG F)	MAXIMUM TEMPERATURE (DEG F)	TEMPERATURE RISE (DEG F)	TURNAROUND TIME (SECONDS)	QUENCH TEMPERATURE (DEG F)	QUENCH TIME (SECONDS)
96 1- C	3	691.	744.	23.	7.0	570.	23.4
10M 2- C	6	903.	950.	23.	11.5	603.	24.6
96 3- 3	9	1236.	1337.	102.	19.5	742.	100.7
3J 4- C	11	1372.	1547.	177.	47.0	744.	141.4
7M 4- C	12	1354.	1540.	167.	45.5	790.	142.4
6K 4- C	13	1373.	1570.	205.	45.5	784.	150.4
8M 4- C	14	1372.	1561.	189.	47.0	820.	137.4
120 4- 0	17	1351.	1542.	171.	44.0	843.	130.4
5E 5- C	20	1516.	1627.	312.	69.5	947.	217.6
76 5- C	21	1576.	1863.	287.	73.0	921.	213.4
96 5- 2	24	1552.	1840.	293.	30.5	925.	215.0
5E 5- 7	33	1563.	1911.	348.	35.0	890.	208.5
86 5- 7	45	1566.	1904.	380.	117.5	972.	269.0
9M 5- 9	52	1551.	1939.	438.	111.0	1043.	273.0
76 5-10	59	1527.	1937.	409.	170.0	922.	265.4
7F 5-11	62	1471.	1968.	437.	112.5	1034.	200.4
46 5-11	64	1548.	1924.	376.	39.0	907.	244.0
21 6- C	67	1605.	1933.	347.	91.5	950.	300.0
50 6- 0	70	1510.	1967.	397.	126.0	927.	312.8
6J 6- 0	74	1547.	1970.	329.	94.5	892.	310.4
7M 6- 0	86	1554.	1948.	394.	94.5	942.	273.0
11E 6- 0	87	1574.	1960.	324.	32.0	910.	305.0
8M 6- 2	97	1394.	1941.	507.	149.5	740.	342.0
5M 6- 2	99	1556.	1960.	402.	139.0	884.	320.0
9E 6- 2	105	1354.	1954.	604.	134.5	1243.	310.5
8M 6- 3	111	1429.	1933.	505.	153.0	858.	346.7
46 6- 3	124	1573.	1943.	420.	126.5	927.	334.0
11M 6- 4	134	1495.	1942.	497.	136.0	785.	333.0
90 6- 4	143	1563.	1969.	430.	156.0	923.	343.0
9J 6- 5	165	1547.	2020.	461.	143.5	967.	357.0
9M 6- 5	166	1601.	2017.	416.	98.5	931.	346.7
8J 6- 6	192	1566.	2015.	427.	129.0	900.	353.0
90 6- 6	193	1574.	2014.	445.	154.0	968.	358.0
11F 6- 6	173	1580.	1905.	465.	134.0	975.	343.7
46 7- 0	201	1525.	1922.	397.	134.0	758.	394.3
70 7- 6	309	1512.	2013.	501.	152.0	847.	440.7
76 7- 6	312	1541.	2031.	490.	147.0	820.	440.7
11E 7- 6	325	1510.	1942.	435.	125.5	933.	434.0
5L 8- C	337	1325.	1805.	501.	126.0	772.	491.0
7M 8- 0	345	1359.	1979.	621.	132.0	811.	485.4
7K 8- 0	346	1373.	1927.	554.	132.0	797.	479.4
5J 8- 6	366	1159.	1892.	533.	175.0	800.	525.1
78 8- 6	368	1172.	1720.	548.	137.5	651.	524.5
7E 9- 3	383	1121.	1783.	643.	177.0	709.	544.1
8M 9- 3	387	1066.	1724.	663.	255.2	647.	550.0
9C 9- 3	389	1061.	1850.	595.	155.5	700.	520.5
11F 9- 3	394	1060.	1800.	547.	227.2	900.	475.4
7810- 0	400	869.	1440.	624.	176.0	844.	500.5
8M10- 0	415	876.	1848.	770.	203.2	644.	531.4
8M10- C	417	679.	1544.	670.	214.2	820.	567.7
8M10- 0	418	899.	1543.	605.	145.5	657.	582.1
6M11- 0	429	695.	1461.	506.	276.2	540.	604.2
9611- 0	431	691.	1533.	642.	263.2	540.	592.2
11E11- 0	432	687.	1433.	551.	226.2	551.	547.3
5J11- 6	436	673.	1154.	481.	377.2	705.	541.4
7611- 6	437	651.	1144.	539.	255.2	602.	504.1
8J11- 6	438	697.	1149.	502.	239.2	497.	678.0

RUN 61106 HEATER KUD STATISTICAL DATA

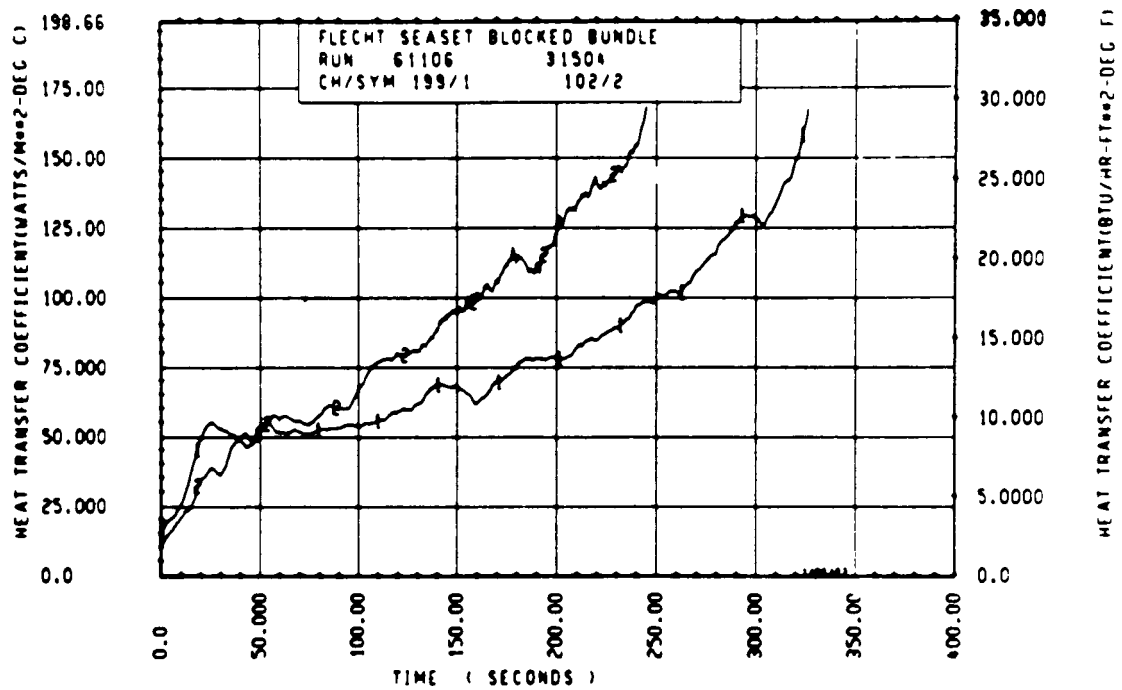
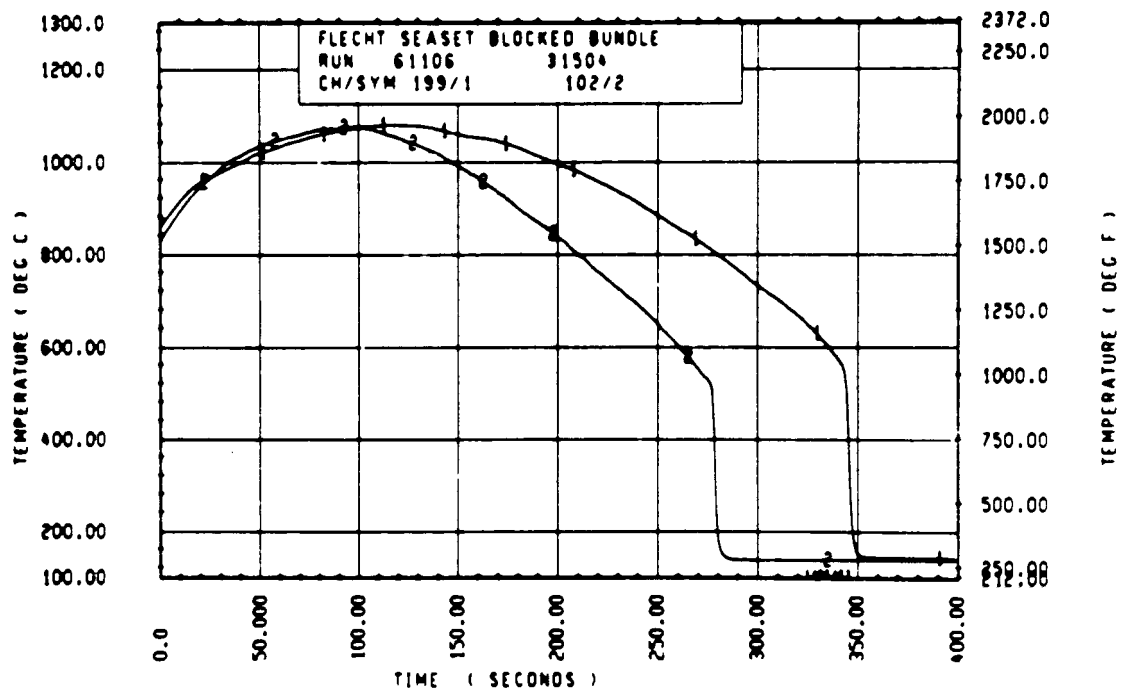
ELEV	TEMP KISC (DEG F)			QUENCH TEMP (DEG F)			QUENCH TIME (SEC)		
	MAX	MIN	MEAN	MAX	MIN	MEAN	MAX	MIN	MEAN
12	23.0	22.0	22.6	570.0	500.7	570.3	27.6	25.4	26.8
24	52.6	49.0	50.9	653.3	631.6	642.1	54.0	49.9	51.8
37	112.5	97.0	105.4	861.9	783.7	792.9	172.9	97.8	99.9
48	211.1	170.7	189.9	883.1	783.8	819.1	150.4	135.9	141.3
60	316.8	248.5	293.4	987.5	887.5	910.1	224.0	200.0	216.0
67	387.7	290.3	319.4	988.1	887.9	914.1	273.9	259.1	265.4
69	437.8	312.5	352.5	1047.8	874.6	925.4	289.0	273.6	279.4
70	409.4	312.3	354.1	967.0	824.1	900.3	299.5	281.1	287.6
71	436.7	343.6	390.3	933.0	842.6	854.8	301.0	285.9	293.5
72	744.7	323.8	461.7	962.8	882.9	924.8	314.9	293.0	303.8
73	422.2	327.1	373.6	1007.7	845.9	933.6	322.9	294.0	310.5
74	511.4	355.3	421.2	968.0	745.9	899.9	342.0	309.0	324.0
75	513.2	346.4	417.4	936.2	751.8	852.8	345.7	307.9	330.1
76	578.2	350.3	413.3	1047.0	784.9	941.1	353.0	315.9	335.2
77	486.4	371.3	435.6	969.6	832.7	925.2	357.9	339.9	349.9
78	498.2	394.2	436.9	1008.3	734.6	825.5	371.1	337.9	355.3
79	498.5	372.3	440.8	958.0	730.0	849.4	373.6	337.0	363.6
80	516.3	412.5	475.8	971.6	840.2	917.9	394.3	357.9	371.2
81	516.6	420.5	480.0	941.7	844.8	901.0	388.7	370.0	380.2
84	440.8	342.2	383.7	888.0	734.9	784.2	413.6	380.7	398.5
86	451.2	337.1	404.2	1044.9	790.7	890.9	427.2	381.9	404.5
91	536.2	431.0	463.1	1088.9	780.0	890.3	454.9	467.3	438.0
96	714.0	269.3	505.5	998.0	732.4	849.9	494.0	440.3	476.6
102	666.2	533.3	585.8	777.3	614.5	642.4	530.2	504.7	516.4
111	680.6	484.4	594.3	960.2	800.0	734.0	560.2	475.9	545.5
120	779.1	541.4	676.3	807.1	500.3	657.4	673.2	430.0	580.2
132	642.1	509.4	556.5	582.7	430.8	541.5	678.0	547.3	601.2
138	536.8	477.4	495.2	474.0	440.9	472.9	578.0	189.7	534.3

RUN 61106 HEATER KUD STATISTICAL DATA

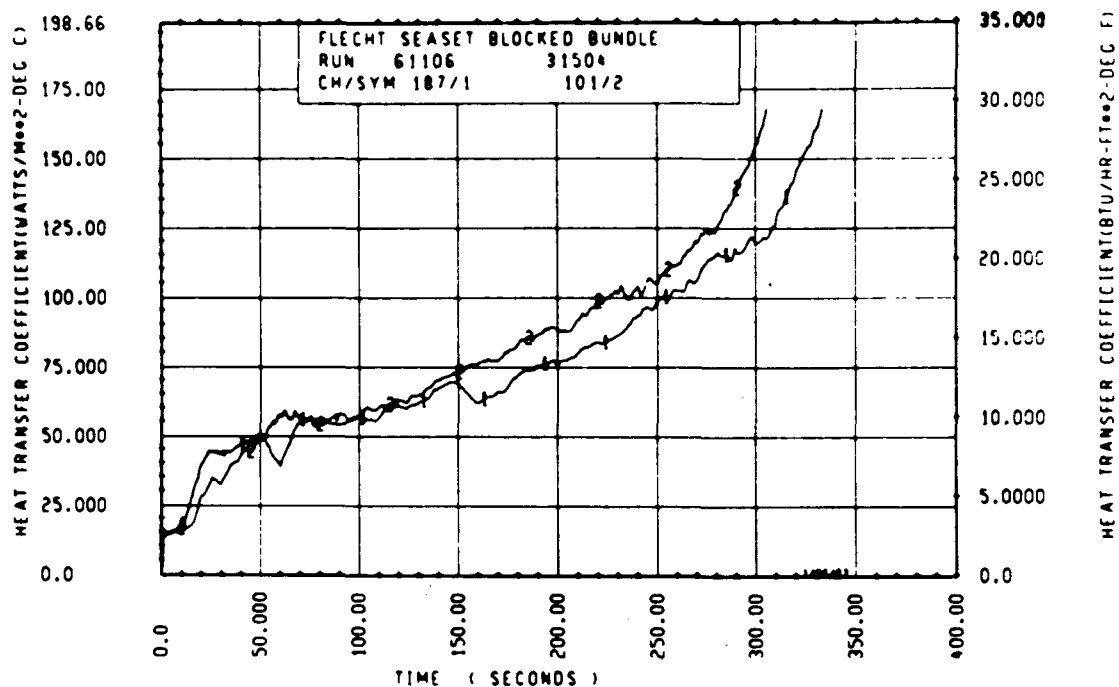
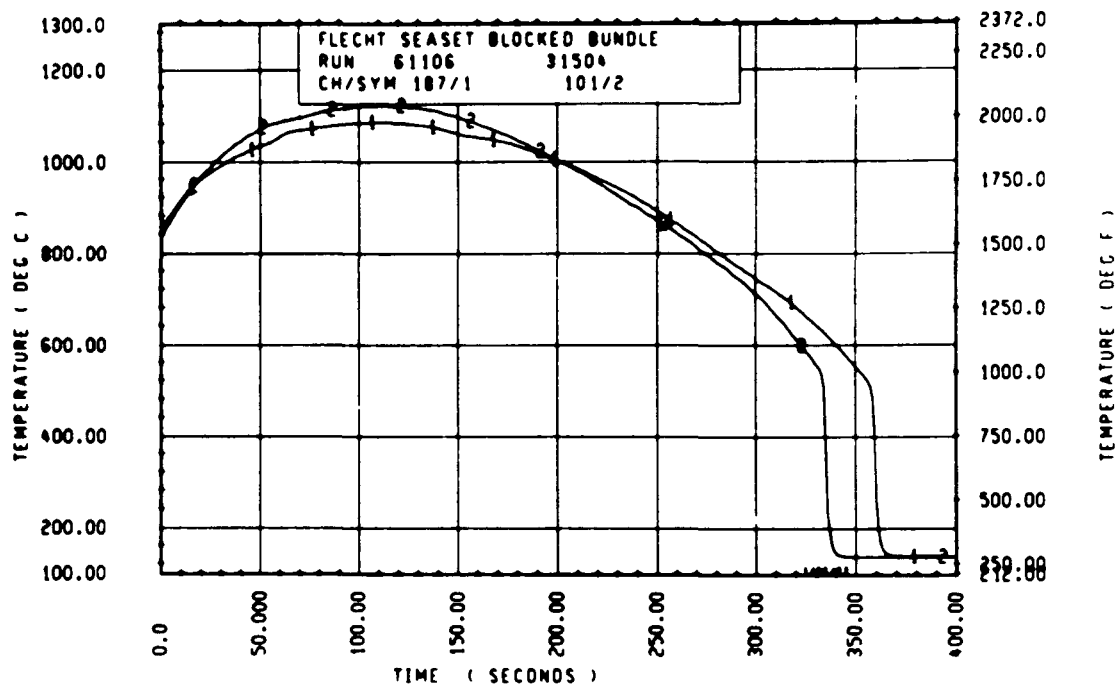
ELEV	INITIAL TEMP (DEG F)			MAX TEMP (DEG F)			TURNAROUND TIME (SEC)		
	MAX	MIN	MEAN	MAX	MIN	MEAN	MAX	MIN	MEAN
12	541.1	600.0	664.7	714.0	700.4	712.0	7.0	7.0	7.0
24	92.9	97.0	804.9	955.0	925.0	930.9	12.0	11.0	11.5
37	1235.8	1171.0	1198.5	1337.4	1232.7	1301.9	27.5	19.5	23.3
48	1344.1	1351.1	1309.2	1570.1	1522.0	1559.0	47.5	44.0	45.7
60	1576.0	1431.5	1514.7	1880.3	1703.2	1813.2	80.5	59.0	69.5
67	1510.9	1526.1	1574.9	1953.4	1838.8	1894.4	119.5	83.0	85.1
69	1552.1	1501.2	1536.6	1934.0	1802.5	1869.1	111.0	85.5	88.2
70	1516.3	1527.2	1553.9	1930.7	1873.8	1900.0	105.0	74.0	92.4
71	1547.8	1471.3	1514.9	1944.0	1844.6	1904.8	112.5	80.5	98.8
72	1517.4	1389.5	1527.3	1980.5	1834.2	1924.6	153.0	89.0	102.9
73	1604.2	1484.4	1549.7	1964.2	1872.7	1922.6	113.0	85.5	90.5
74	1611.9	1394.4	1530.0	1982.0	1901.0	1951.2	144.5	93.0	112.1
75	1511.9	1428.5	1537.7	1993.0	1944.8	1955.2	152.5	83.5	112.4
76	1526.2	1474.5	1566.1	2017.4	1920.3	1979.1	156.0	93.5	112.8
77	1500.9	1502.3	1560.0	2037.3	1932.1	1995.0	163.0	88.5	120.4
78	1614.1	1534.4	1571.5	2052.5	1935.5	2008.4	167.5	97.0	121.4
79	1513.0	1520.7	1576.0	2072.3	1930.9	2010.9	156.5	87.0	124.9
80	1592.2	1520.7	1559.1	2069.9	1957.3	2038.9	155.0	102.0	128.3
81	1586.8	1480.1	1537.3	2074.7	1924.0	2025.3	154.0	98.5	129.7
84	1582.5	1462.7	1527.2	1981.5	1894.4	1910.9	163.0	92.5	112.7
86	1507.5	1492.0	1555.2	2032.0	1824.7	1954.5	163.5	78.0	122.4
90	1546.7	1434.9	1505.4	2060.7	1865.9	1960.4	153.5	90.0	133.3
96	1412.5	1112.3	1359.0	2040.0	1843.5	1945.1	228.2	30.5	140.3
102	1298.7	1356.8	1175.0	1847.8	1802.3	1764.8	253.2	134.5	175.1
111	1120.5	1344.3	1181.1	1763.5	1574.4	1674.9	255.2	124.0	195.7
120	934.9	828.4	883.4	1682.2	1391.2	1559.7	268.2	124.5	215.6
132	598.4	880.0	690.9	1333.2	1190.0	1247.5	276.2	220.2	253.9
138	597.4	651.2	669.4	1199.5	1134.0	1164.7	377.2	103.5	249.7



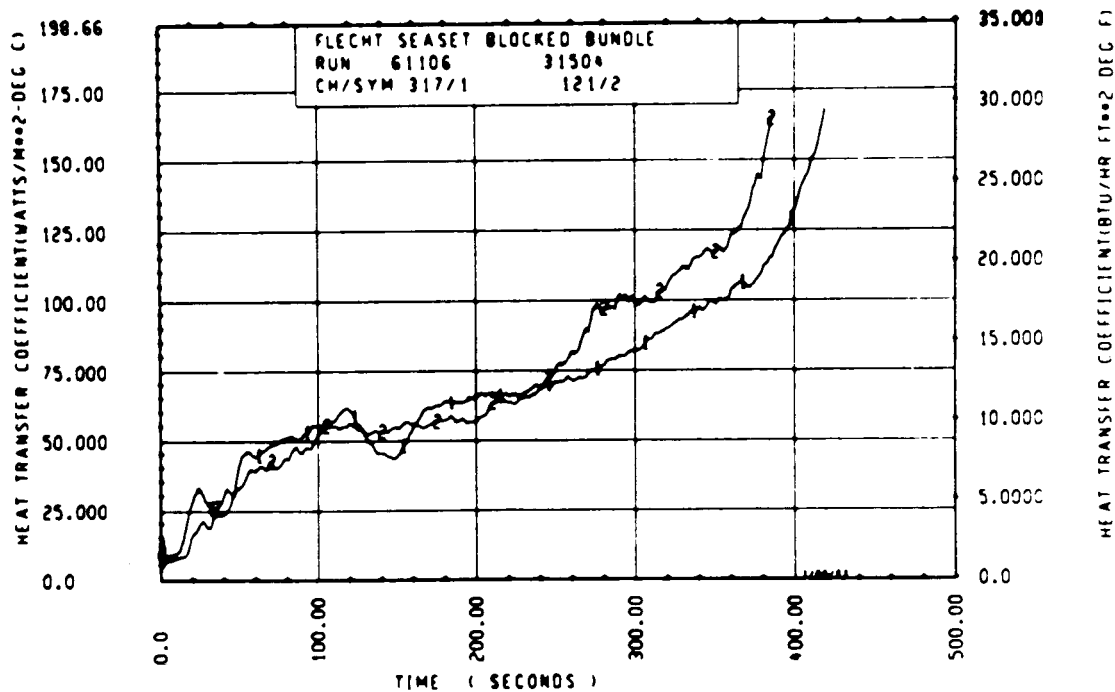
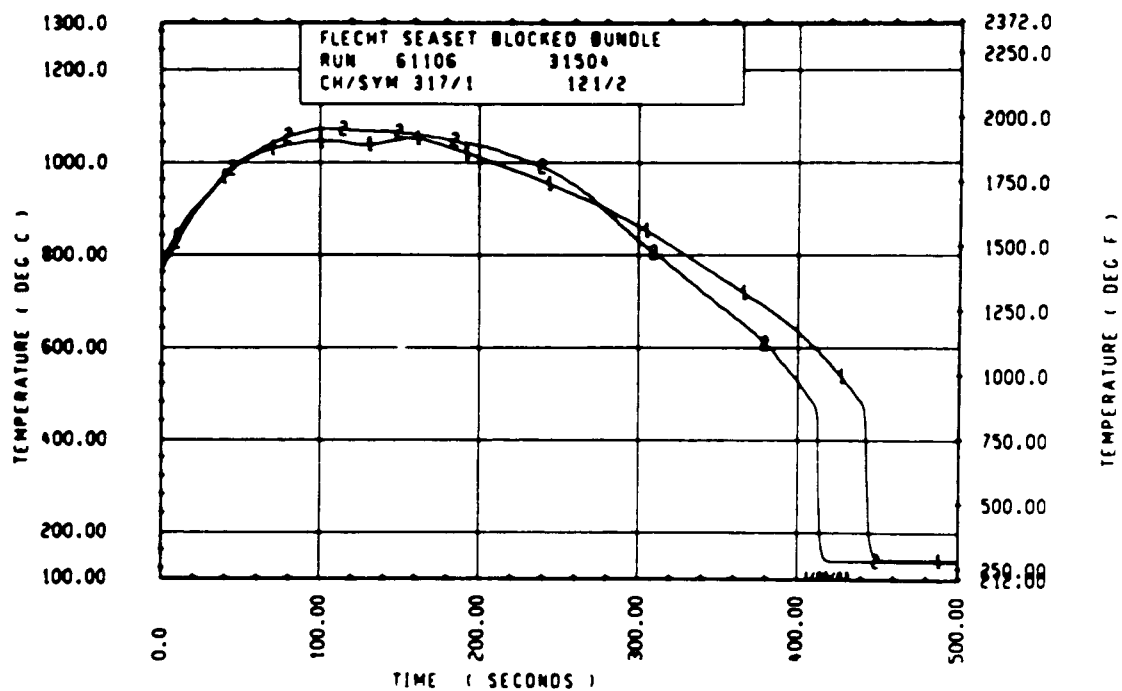
Rod 13G, 1.93 m (76 in.)



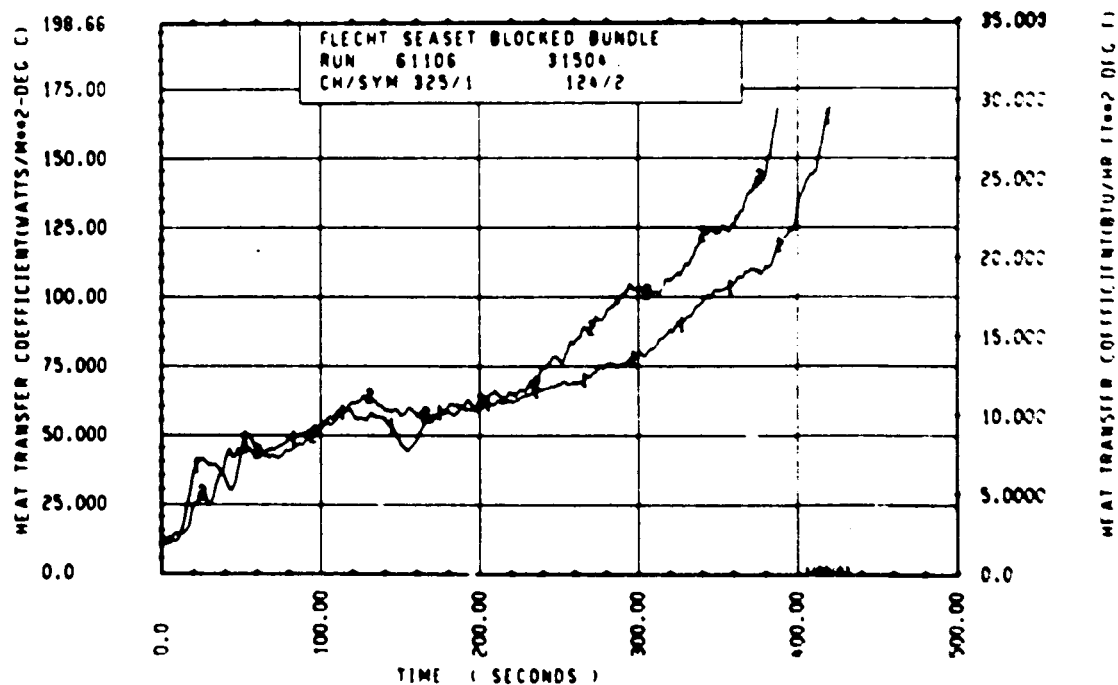
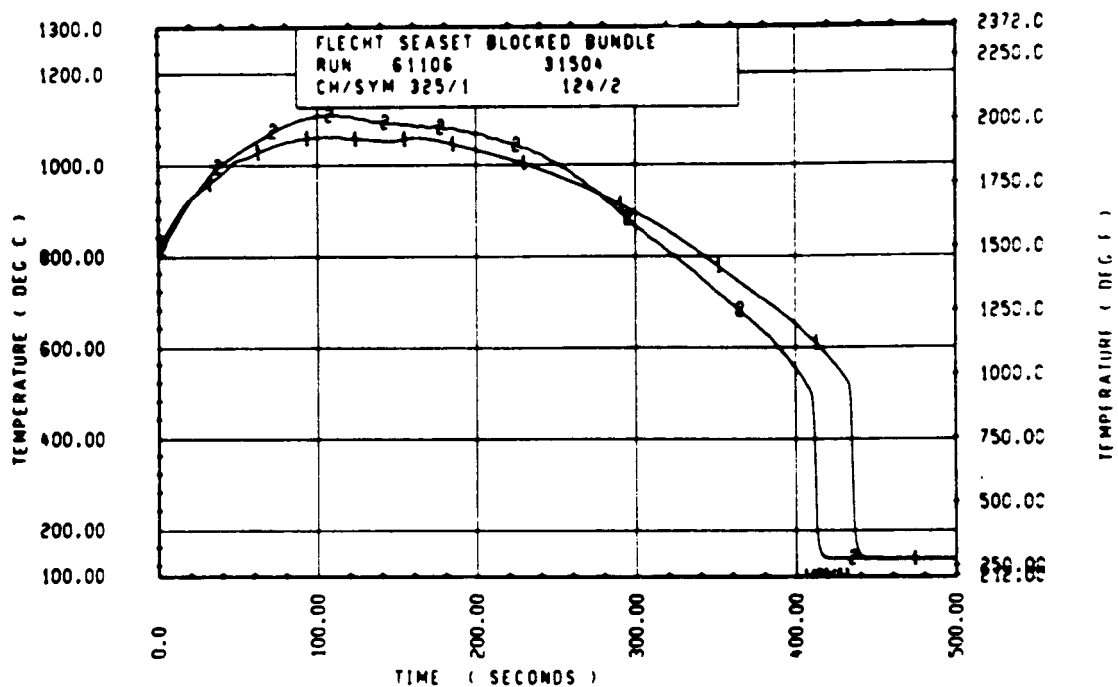
Rod 13G, 1.98 m (78 in.)



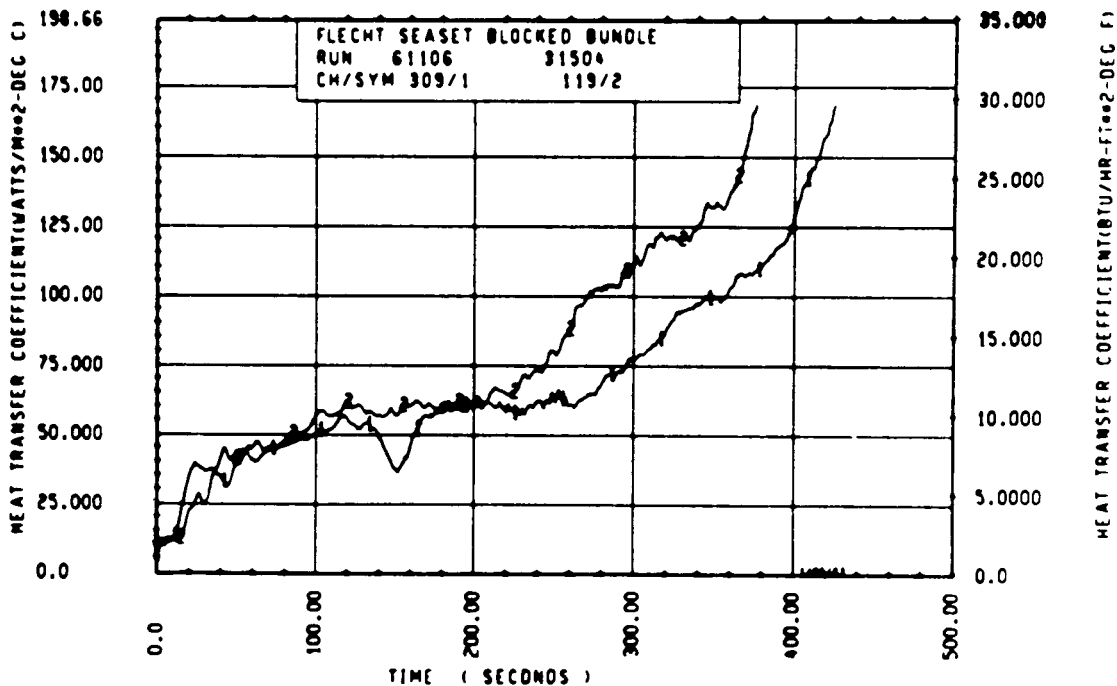
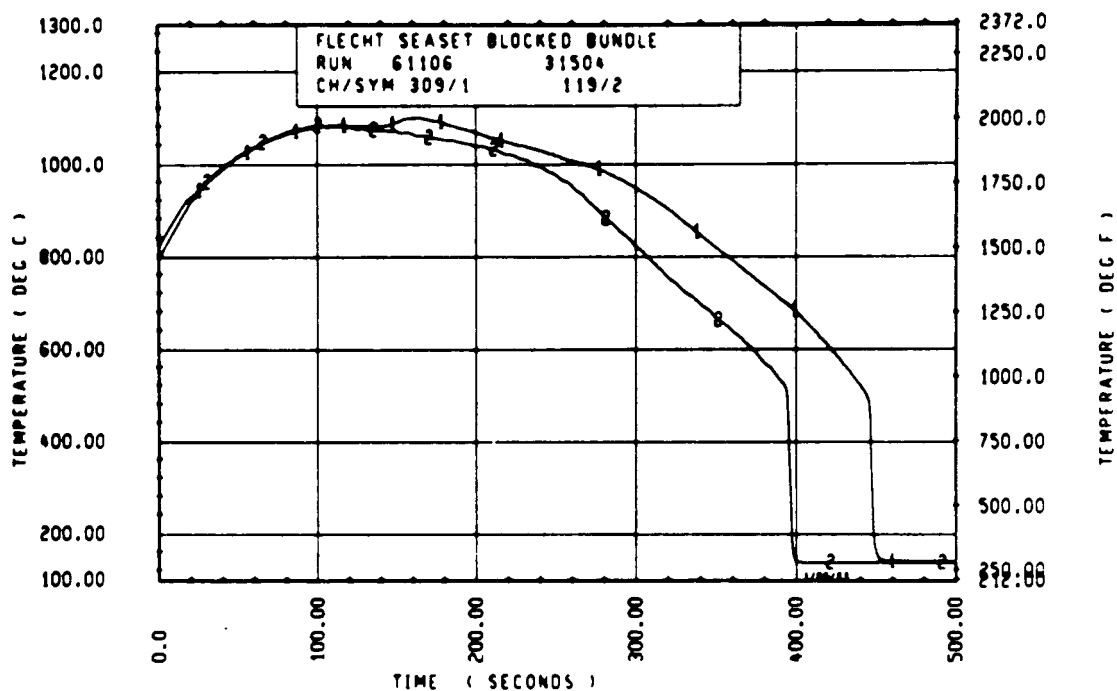
Rod 6J, 1.98 m (78 in.)



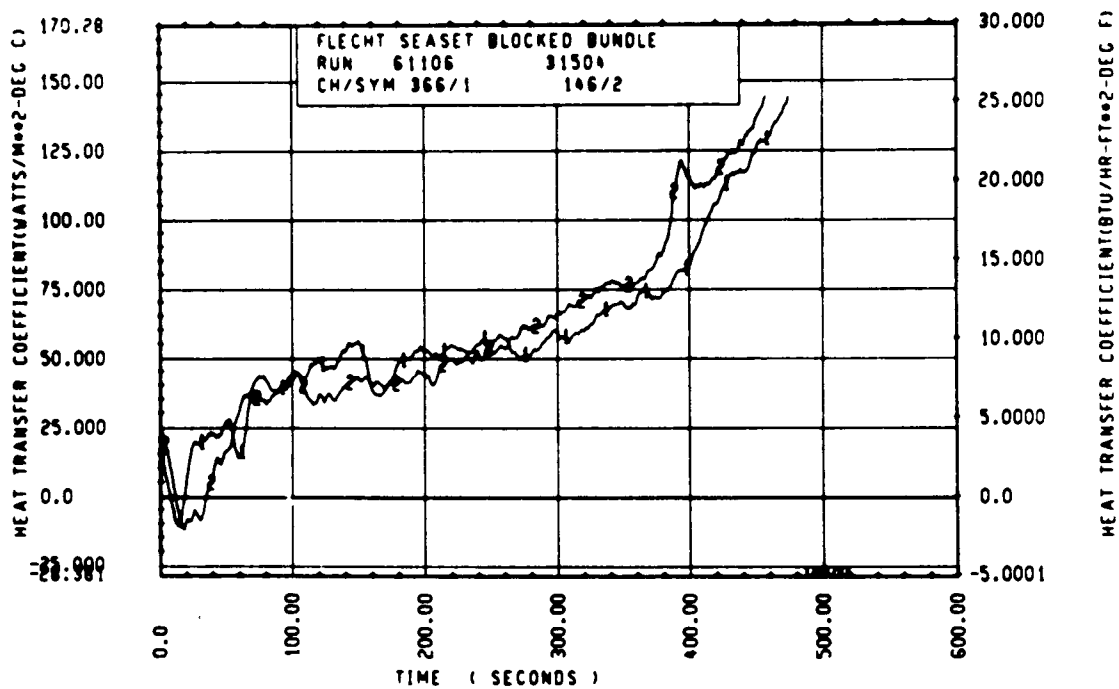
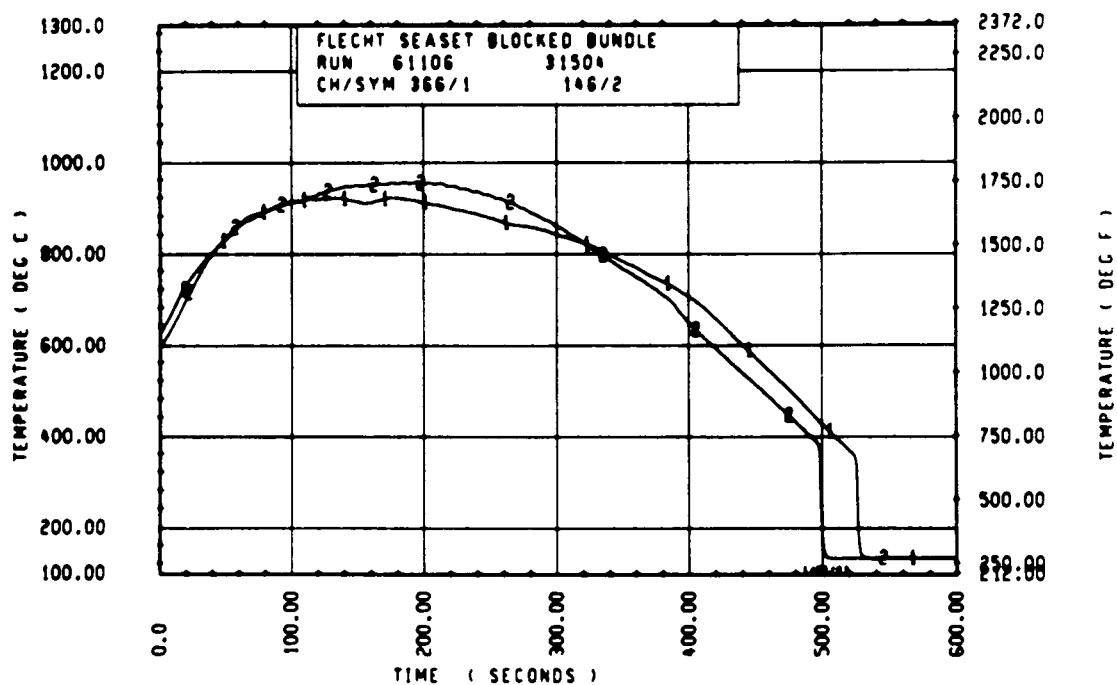
Rod 9C 2.29 m (90 in.)



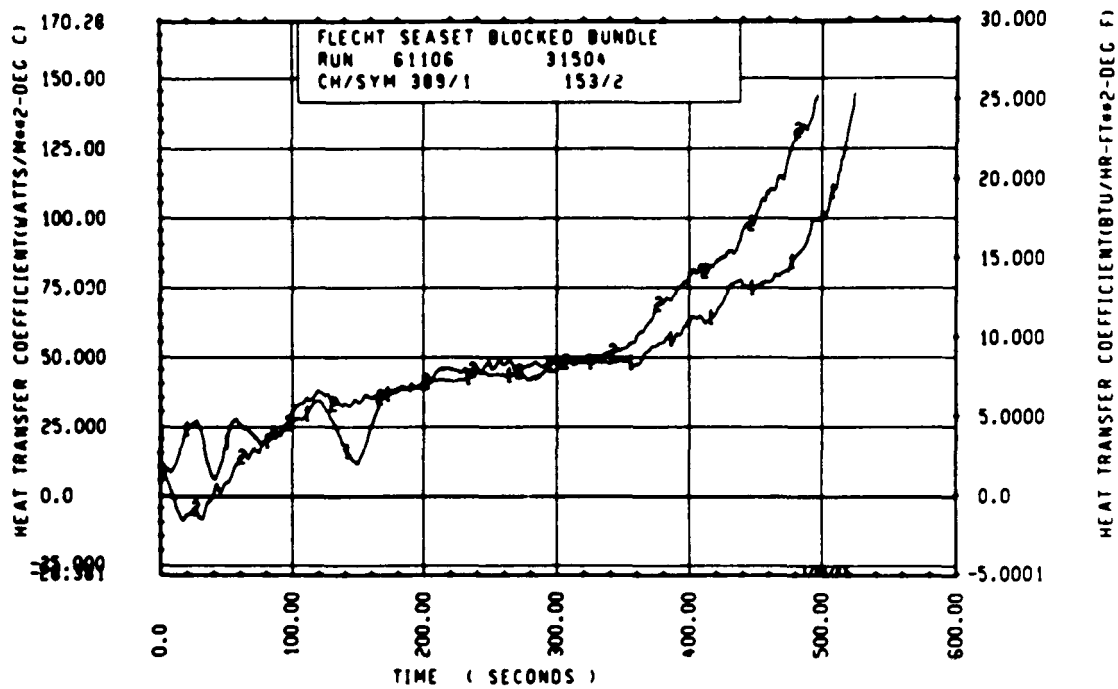
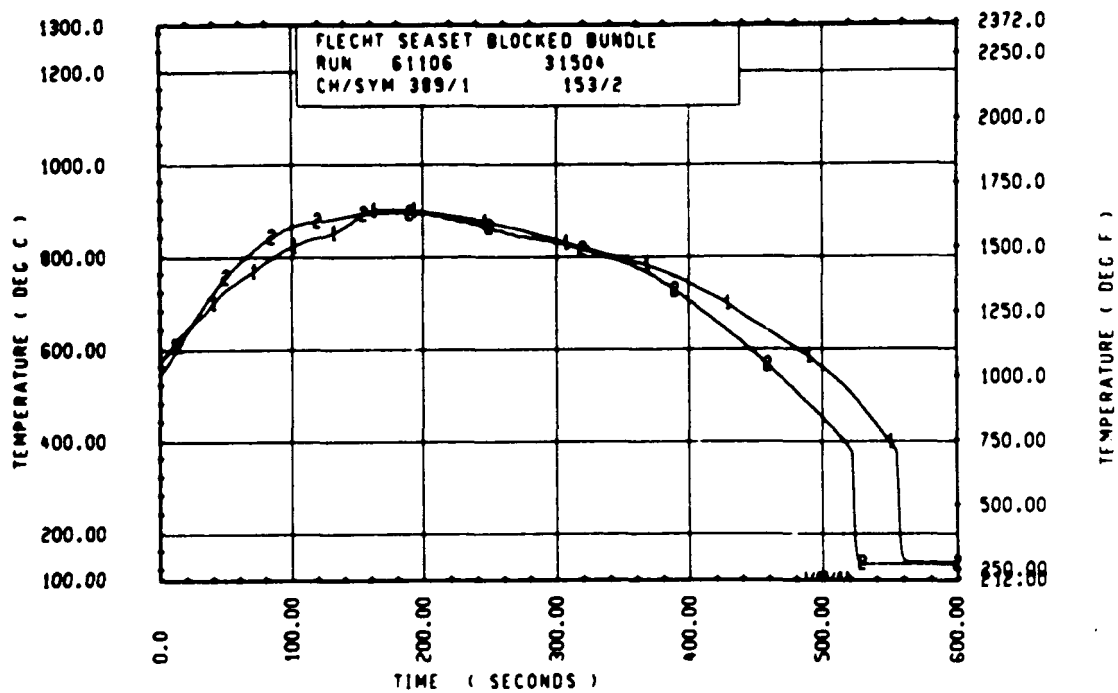
Rod 11E, 2.29 m (90 in.)



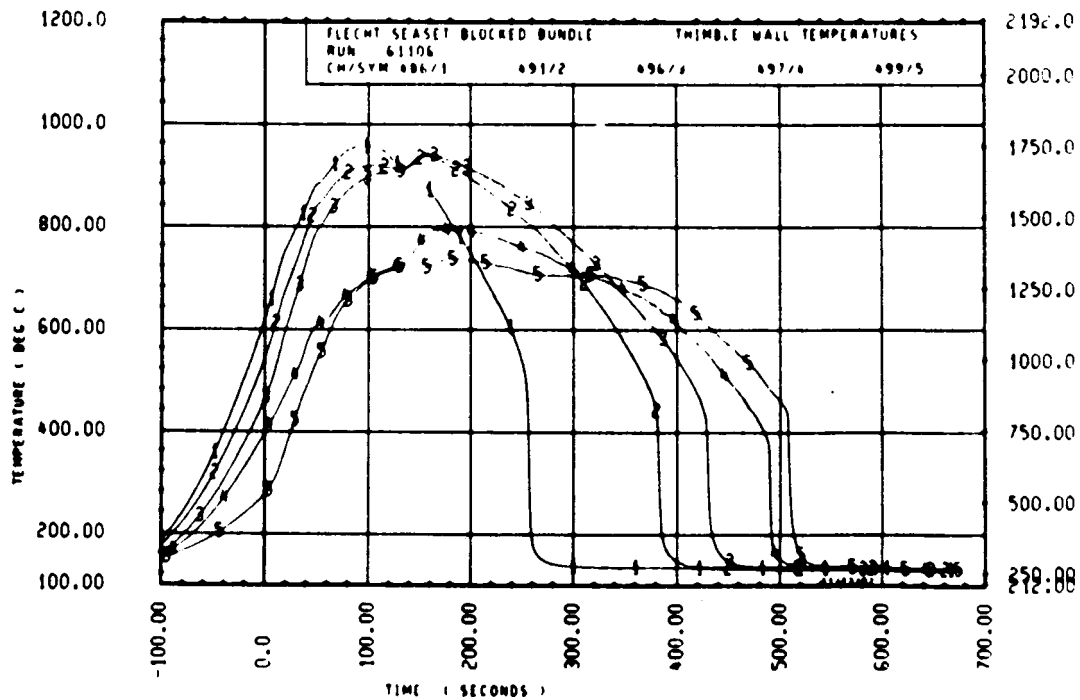
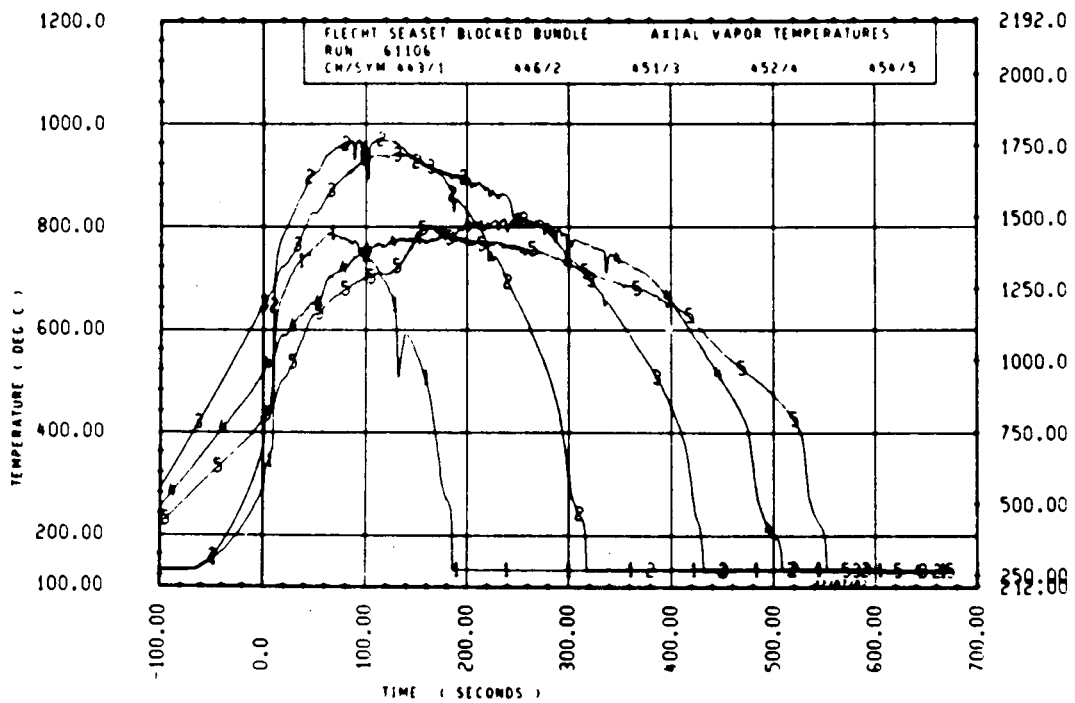
Rod 7D, 2.29 m (90 in.)

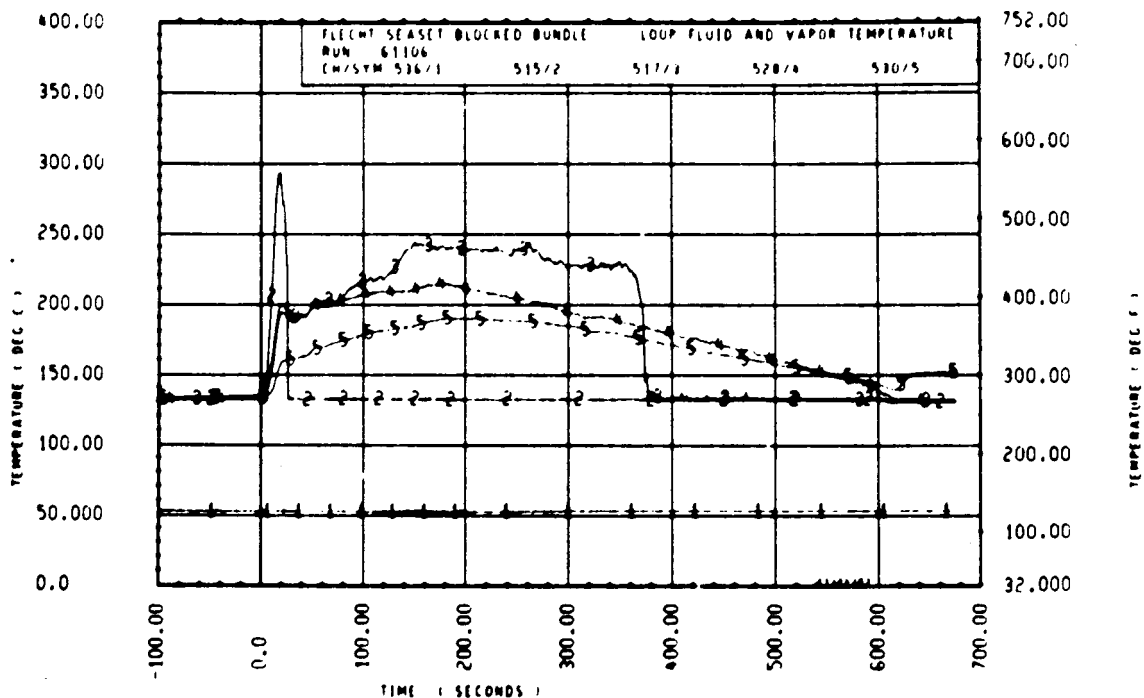
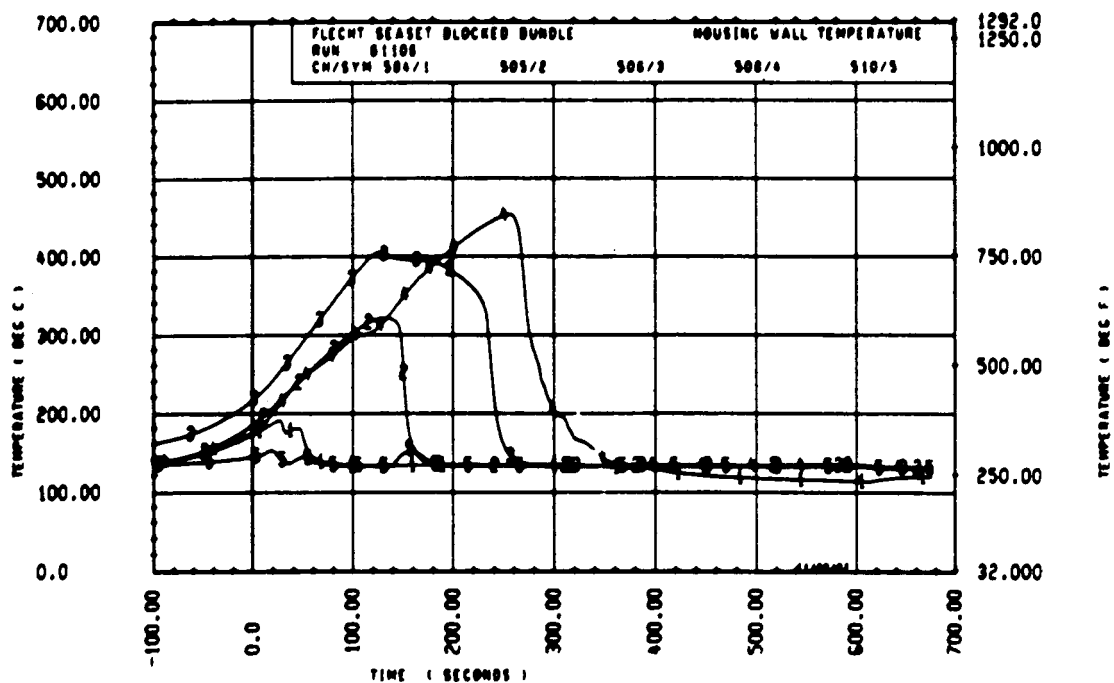


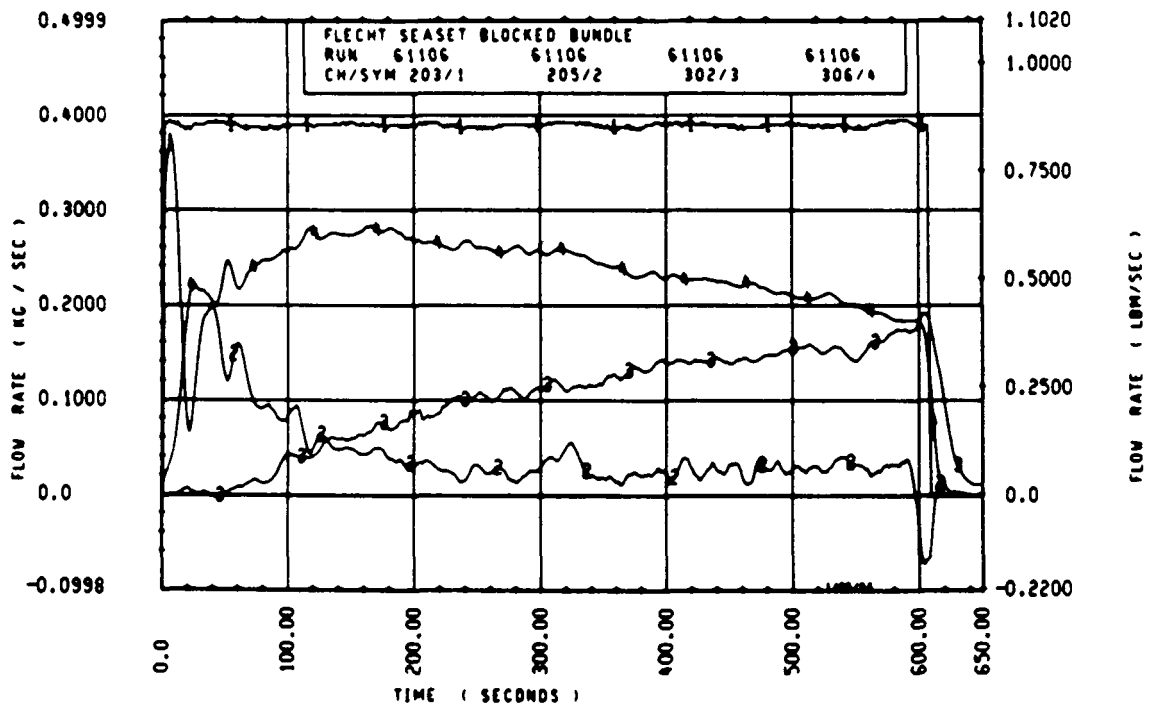
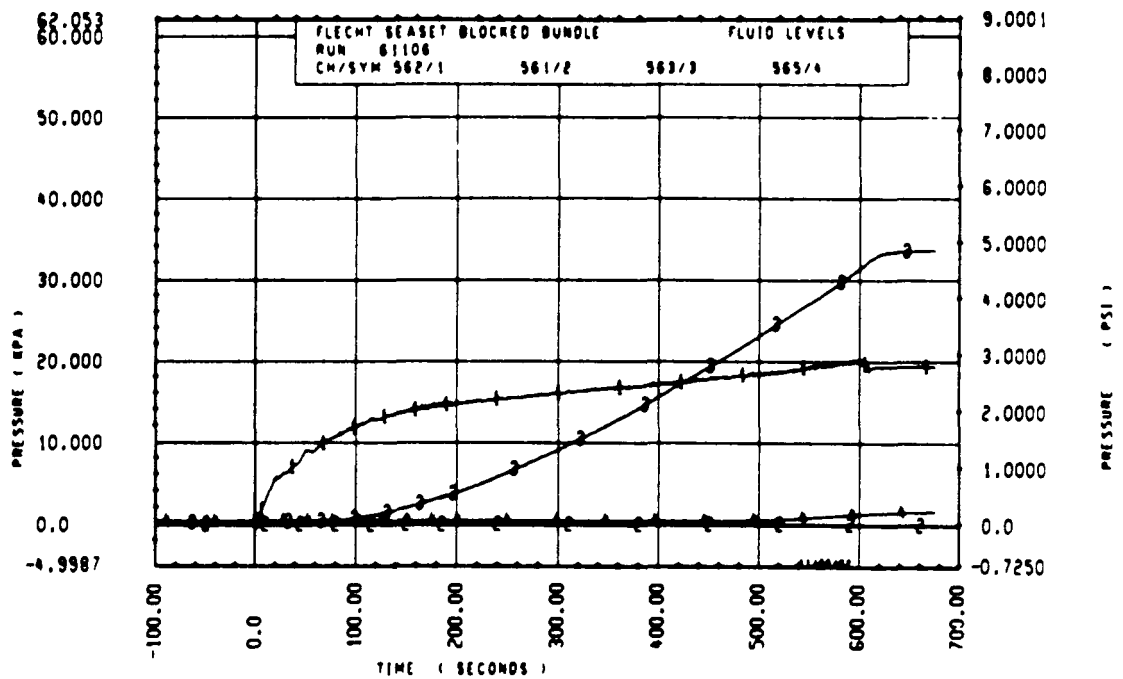
Rod 5J 2.59 m (102 in.)

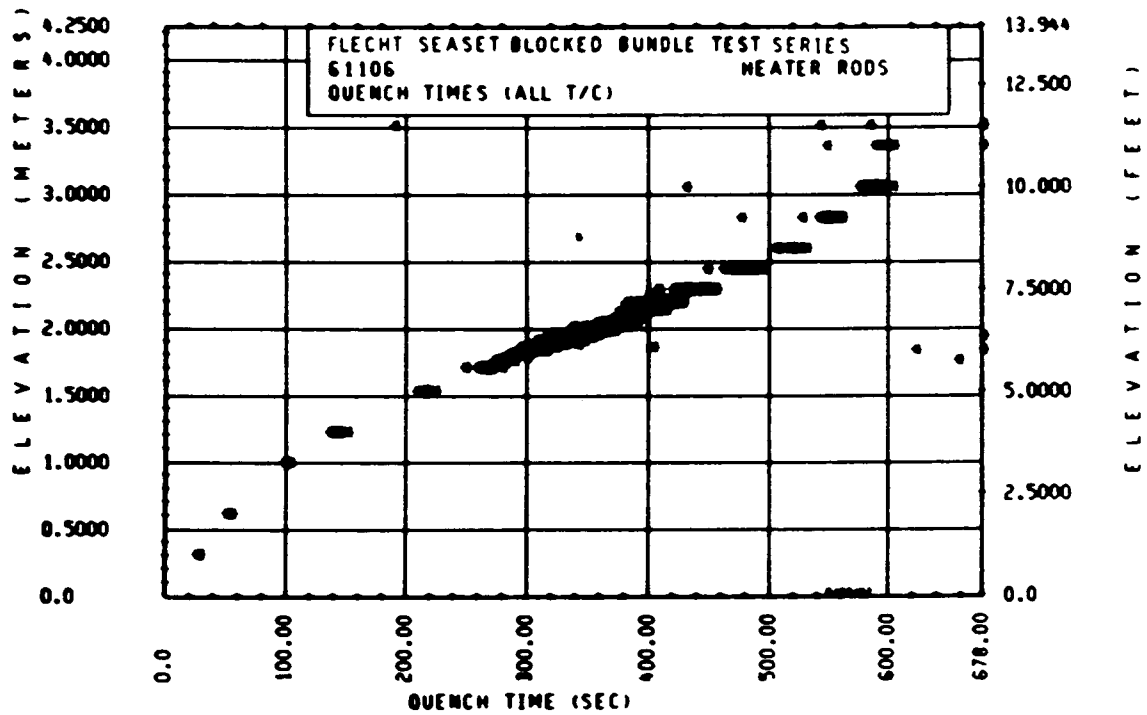
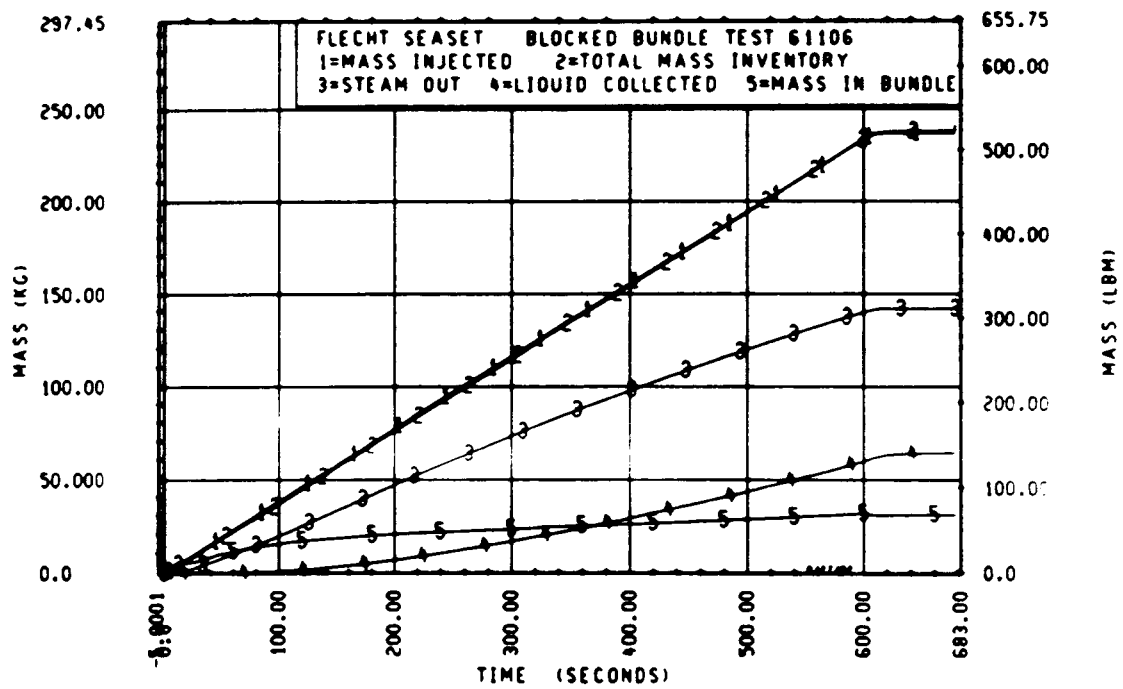


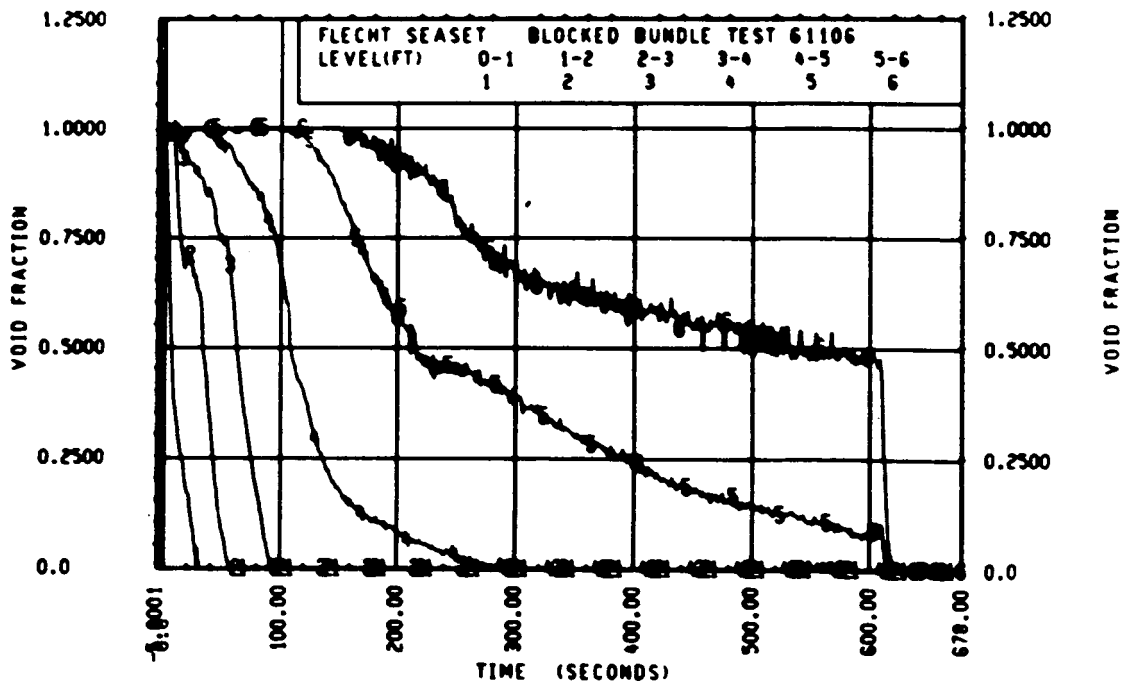
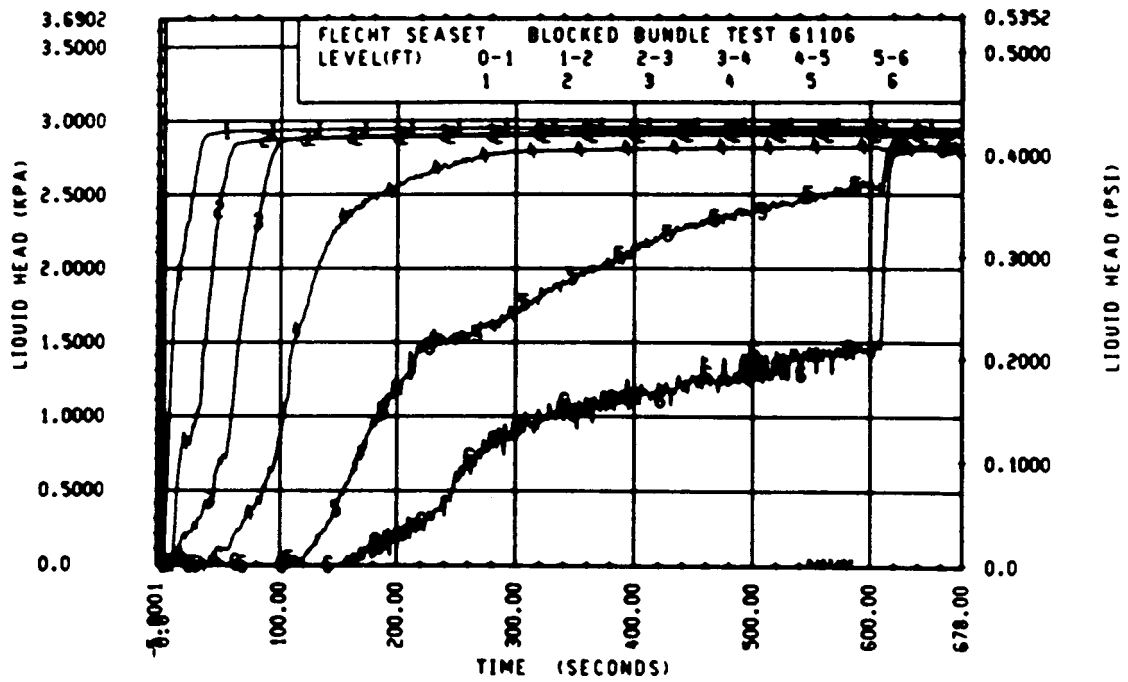
Rod 9C, 2.82 m (111 in.)

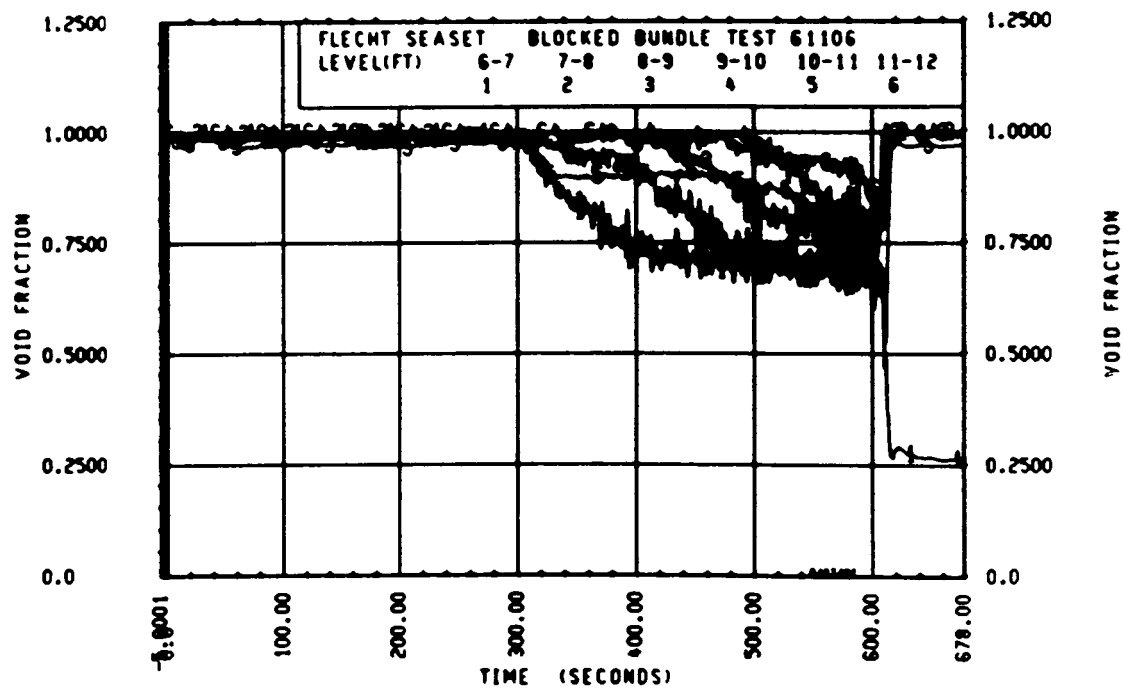
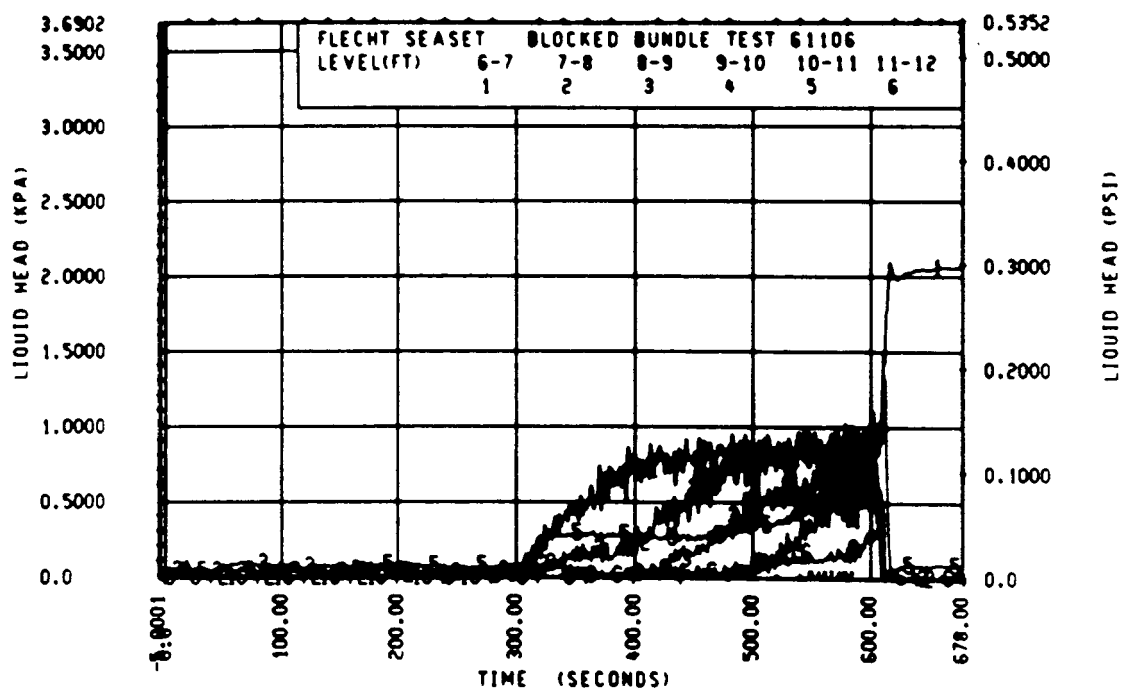












FLECHT SEASET 163-ROD BUNDLE FLOW BLOCKAGE TASK
SUMMARY AND COMMENT SHEET

Run: 61208
Test date: 8/31/82
Test type: Forced reflood
Parameter: Flooding rate effect

AS-RUN TEST CONDITIONS:

Upper plenum pressure	0.269 MPa (39.0 psia)
Initial peak clad temperature and location	871°C (1599.8°F), 3H-1.70 m (67 in.)
Initial peak rod power:	
Peripheral rods	1.31 kw/m (0.400 kw/ft)
Bypass rods	1.32 kw/m (0.403 kw/ft)
Blockage island rods	1.31 kw/m (0.400 kw/ft)
Flooding rate	15 mm/sec (0.60 in./sec)
Coolant temperature	51.1°C (124°F)
Initial bundle water level	-1.5 mm (-0.06 in.)

COMMENTS:

Inlet mass flow:⁽¹⁾ +1.3% constant

Power decay:⁽¹⁾ peripheral rods, -0.5% linearly increasing to -2.5% by 400 seconds
bypass rods, +1% exponentially increasing to -3% by 400 seconds
blockage rods, -1.5% exponentially increasing to +3.5% by 400 seconds

1. Relative to run 34006

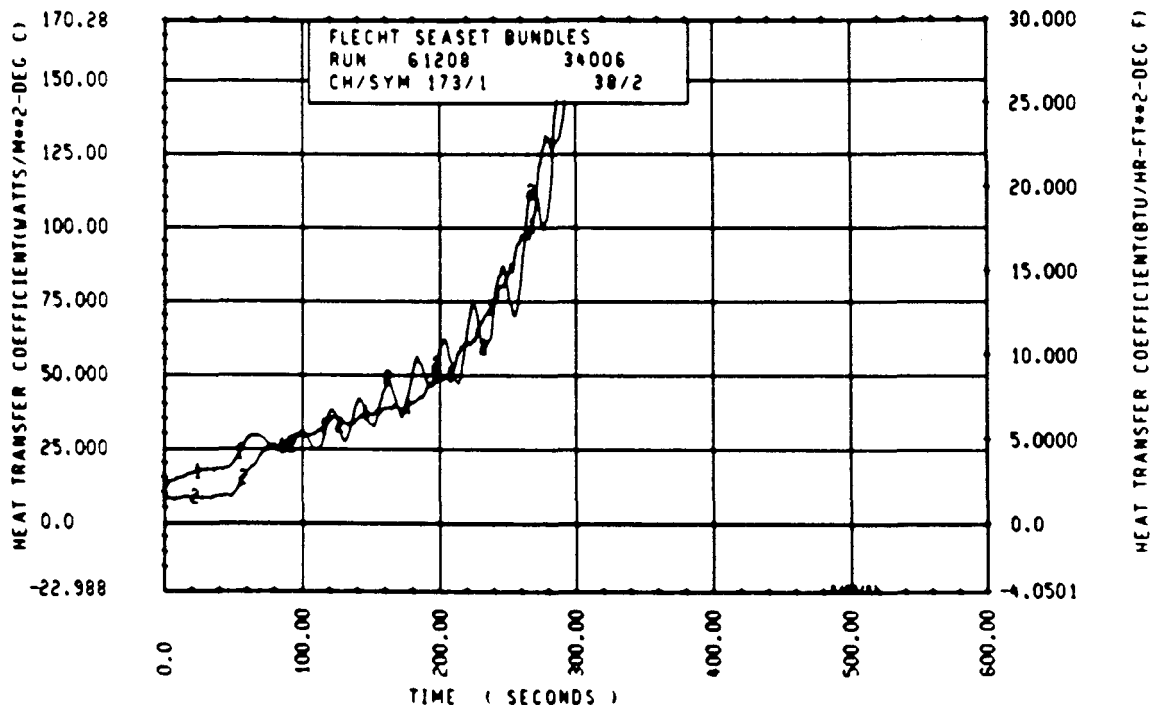
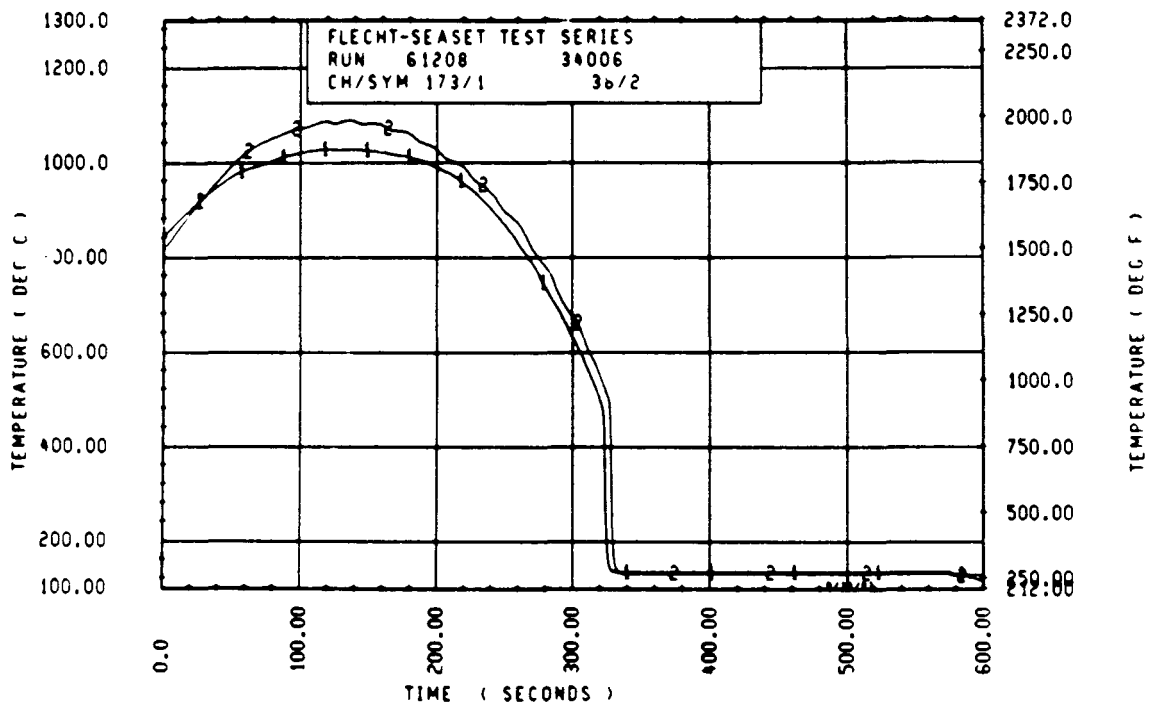
FLECHT SEASET 103 KUJ BUNDLE TEST SERIES							
RUN NUMBER 61208							
RJD/ELEV	CHAN. NO	INITIAL AT FLOOD (DEG F)	MAXIMUM TEMPERATURE (DEG F)	TEMPERATURE RISE (DEG F)	TIJNARQJN TIME (SECONDS)	QUENCH TEMPERATURE (DEG F)	QUENCH TIME (SECONDS)
96 1- 0	3	682.	690.	17.	9.5	542.	24.5
10H 2- 0	6	694.	734.	40.	21.5	600.	57.0
96 3- 3	9	1214.	1309.	96.	47.5	774.	140.0
3J 4- 0	11	1361.	1441.	180.	51.5	758.	147.4
7H 4- 0	12	1340.	1487.	148.	52.8	720.	144.4
8K 4- 0	13	1368.	1517.	149.	53.0	730.	153.4
8N 4- 0	14	1351.	1485.	134.	53.8	775.	140.4
12L 4- 0	17	1344.	1460.	117.	50.0	742.	140.4
5E 5- 0	20	1504.	1717.	212.	51.5	744.	212.0
76 5- 0	21	1554.	1760.	207.	62.0	800.	208.0
96 5- 0	24	1533.	1740.	210.	58.5	807.	209.2
5E 5- 7	33	1543.	1803.	254.	73.0	802.	254.4
86 5- 7	45	1538.	1837.	314.	113.5	877.	259.4
9H 5- 9	52	1476.	1840.	370.	116.8	904.	264.5
76 5-10	59	1498.	1851.	353.	116.5	904.	266.4
7F 5-11	62	1439.	1826.	387.	122.0	932.	277.5
46 5-11	64	1532.	1843.	312.	126.5	944.	281.5
21 6- 0	67	1562.	1813.	250.	144.0	935.	274.4
5D 6- 0	70	1494.	1805.	307.	113.0	950.	282.4
6J 6- 0	74	1533.	1847.	314.	117.5	894.	284.5
7H 6- 0	86	1547.	1838.	291.	95.8	884.	274.0
11E 6- 0	89	1552.	1803.	250.	97.5	841.	280.0
8H 6- 2	97	1355.	1817.	462.	150.0	772.	310.0
9H 6- 2	99	1536.	1880.	344.	121.8	900.	306.2
9E 6- 2	105	1341.	1835.	495.	146.5	1170.	294.6
8H 6- 3	111	1395.	1844.	449.	156.5	840.	319.8
46 6- 3	124	1550.	1893.	343.	120.0	800.	311.4
11H 6- 4	134	1469.	1854.	384.	148.5	738.	326.0
9D 6- 4	143	1546.	1889.	343.	121.5	843.	316.4
9J 6- 5	165	1514.	1914.	399.	147.5	830.	324.2
9H 6- 5	166	1582.	1844.	310.	116.0	883.	317.2
8J 6- 6	192	1556.	1930.	373.	139.0	885.	326.5
9D 6- 6	193	1549.	1896.	348.	122.5	913.	328.6
11F 6- 6	173	1549.	1863.	314.	116.5	800.	322.4
46 7- 0	261	1504.	1960.	401.	117.0	752.	300.5
70 7- 6	309	1473.	1924.	447.	185.0	847.	400.4
76 7- 6	312	1518.	1980.	473.	180.0	834.	401.5
11E 7- 6	325	1491.	1941.	421.	194.8	856.	400.4
5L 8- 0	337	1311.	1846.	535.	158.5	743.	443.0
7H 8- 0	345	1336.	1985.	649.	211.0	810.	441.6
7K 8- 0	346	1354.	1953.	598.	135.8	754.	435.1
5J 8- 6	366	1150.	1816.	667.	162.8	623.	474.7
78 8- 6	368	1132.	1867.	735.	181.8	612.	484.8
7E 9- 3	383	1097.	1814.	717.	231.1	703.	484.4
8H 9- 3	387	1042.	1824.	782.	251.0	600.	501.0
9C 9- 3	389	1041.	1830.	789.	234.1	648.	493.4
11F 9- 3	394	1042.	1722.	680.	226.1	632.	444.0
7810- 0	408	853.	1484.	631.	205.1	601.	521.2
8H10- 0	415	866.	1744.	879.	254.6	622.	523.
8K10- 0	417	870.	1658.	788.	243.1	590.	523.0
8H10- 0	418	880.	1482.	582.	196.8	638.	515.1
6H11- 0	429	692.	1322.	629.	255.1	540.	510.1
9G11- 0	431	685.	1470.	785.	255.3	602.	444.4
11E11- 0	432	692.	1390.	700.	303.1	543.	523.1
5J11- 6	436	677.	1110.	439.	158.0	632.	492.0
7811- 6	437	636.	1173.	537.	328.1	540.	540.4
8J11- 6	439	684.	1222.	538.	194.5	552.	535.1

RUN 61208 HEATER ROD STATISTICAL DATA

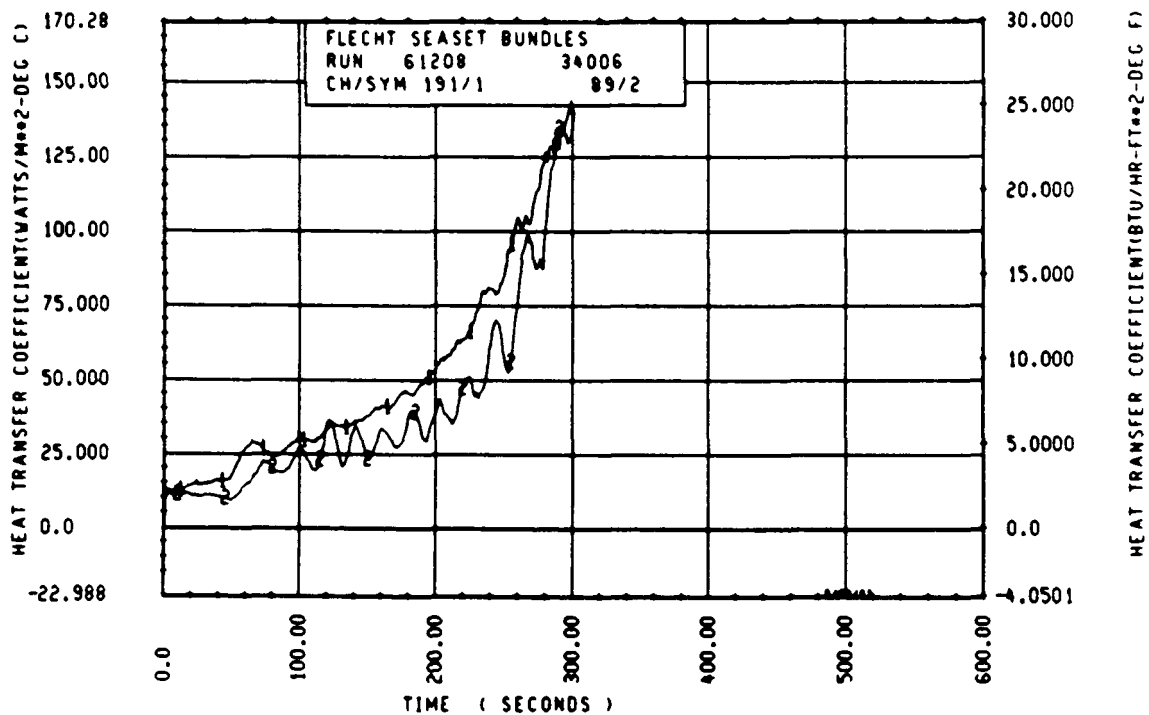
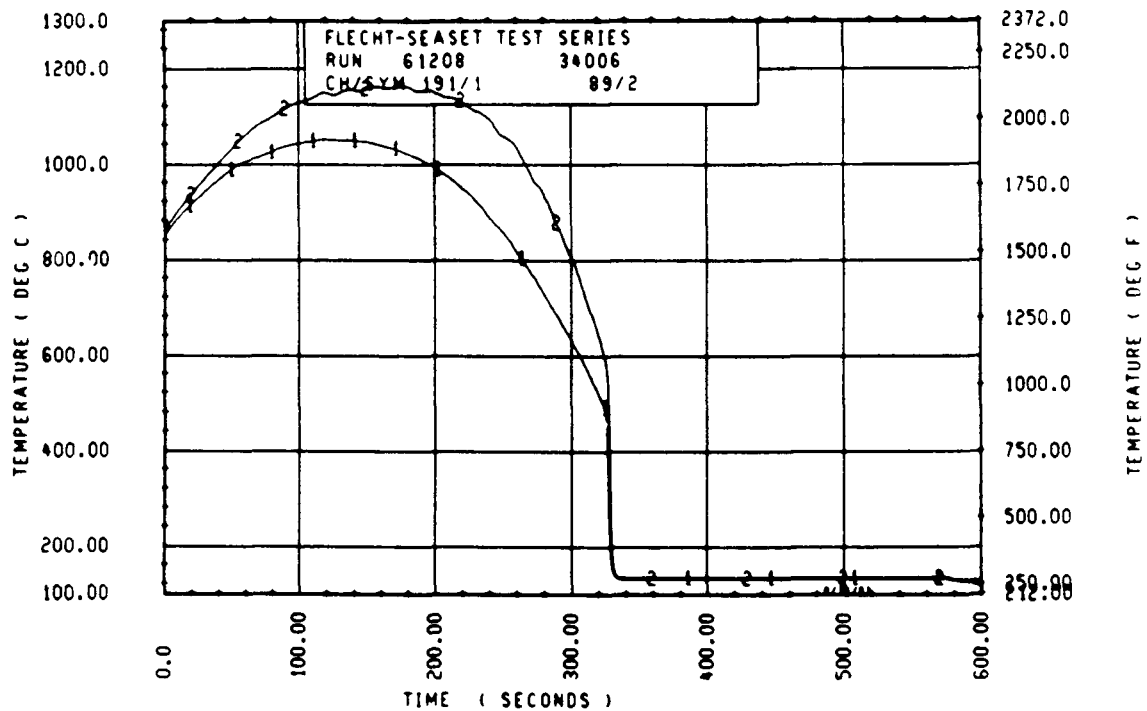
ELEV	INITIAL TEMP (DEG F)			MAX TEMP (DEG F)			TURNAROUND TIME (SEC)		
	MAX	MIN	MEAN	MAX	MIN	MEAN	MAX	MIN	MEAN
12	584.8	578.5	681.6	700.5	590.5	648.4	11.0	9.5	10.6
24	173.6	860.5	875.3	433.8	540.7	915.2	22.5	21.5	21.0
39	1219.1	1174.4	1193.4	1308.4	1274.4	1285.1	50.5	45.5	47.7
49	1371.2	1334.5	1357.2	1517.5	1465.4	1445.8	53.0	50.0	51.9
67	1558.7	1424.6	1516.9	1770.1	1641.6	1718.3	69.5	53.5	59.8
67	1594.8	1505.5	1555.3	1656.4	1723.3	1747.9	113.5	55.5	86.6
64	1534.8	1475.5	1515.0	1645.5	1764.6	1815.9	116.5	94.5	108.2
73	1549.8	1444.8	1536.1	1851.2	1764.6	1806.1	115.5	82.5	98.3
71	1531.6	1439.2	1490.2	1843.3	1772.4	1817.8	122.0	83.5	106.9
72	1594.4	1463.3	1543.9	1872.7	1835.5	1850.2	124.5	84.5	103.5
73	1586.8	1464.1	1527.9	1870.5	1757.4	1822.3	134.5	83.5	103.2
74	1594.4	1355.4	1506.9	1847.6	1804.3	1851.7	151.5	92.5	129.4
75	1598.7	1345.4	1517.0	1901.0	1785.8	1850.5	156.5	83.5	118.7
76	1594.4	1447.8	1543.6	1918.5	1815.5	1872.8	152.5	85.0	117.2
77	1582.5	1473.4	1534.7	1927.5	1742.5	1881.5	231.1	85.5	133.5
78	1590.1	1465.2	1546.6	1932.1	1746.7	1867.7	154.5	107.0	129.7
79	1595.7	1504.5	1551.3	1928.6	1795.8	1844.6	157.0	93.5	129.8
87	1570.6	1501.2	1534.8	1948.2	1827.4	1910.3	156.5	100.5	131.1
81	1556.4	1464.9	1521.9	1934.4	1832.0	1901.3	153.5	115.0	135.4
84	1547.8	1445.6	1503.8	1914.0	1811.8	1885.3	143.5	107.5	128.7
86	1574.2	1475.5	1527.9	1984.5	1782.4	1918.7	173.5	103.0	141.6
97	1514.2	1425.3	1476.0	2043.4	1804.6	1946.5	212.1	117.5	155.4
96	1388.1	1268.1	1345.0	1948.7	1785.5	1913.9	224.1	103.5	167.6
102	1191.6	1075.1	1156.5	1866.5	1688.7	1834.6	228.1	102.0	194.1
111	1099.8	1041.1	1062.9	1848.9	1573.6	1744.2	251.1	155.5	224.3
120	925.6	821.2	888.9	1757.4	1414.6	1628.0	257.1	140.5	237.5
132	925.1	881.6	887.6	1475.2	1204.6	1388.9	317.1	197.5	258.9
138	533.7	638.5	661.7	1277.5	1110.4	1208.4	323.1	158.0	244.0

RUN 61208 HEATER ROD STATISTICAL DATA

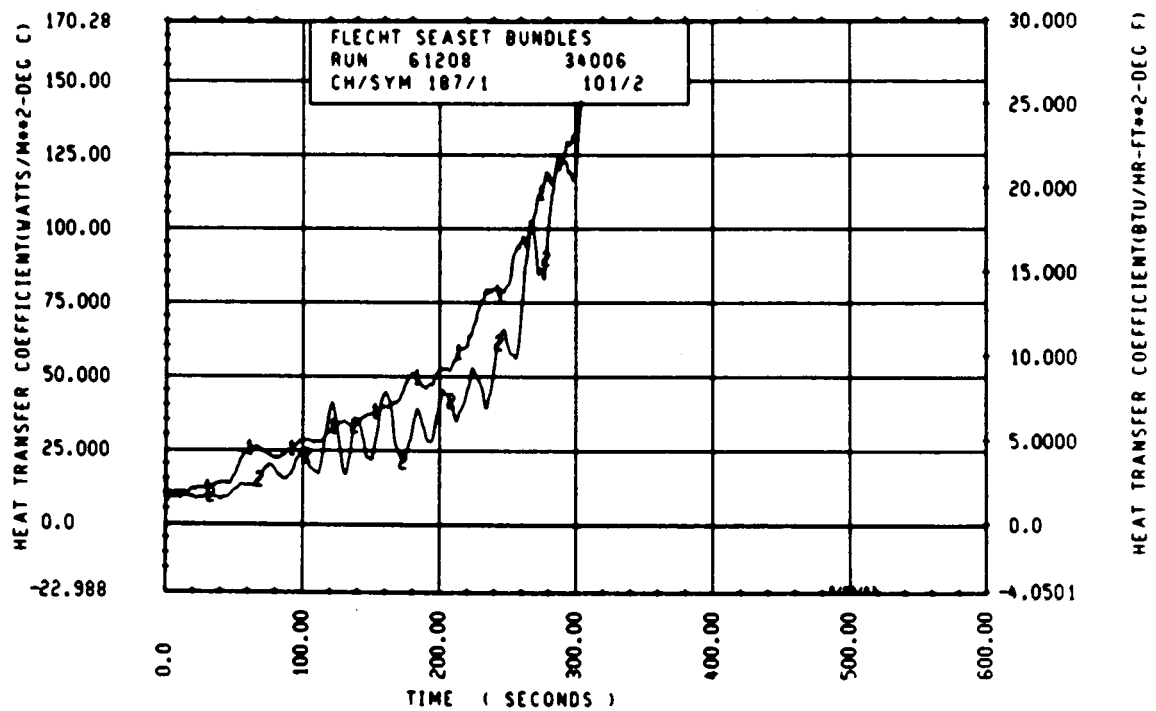
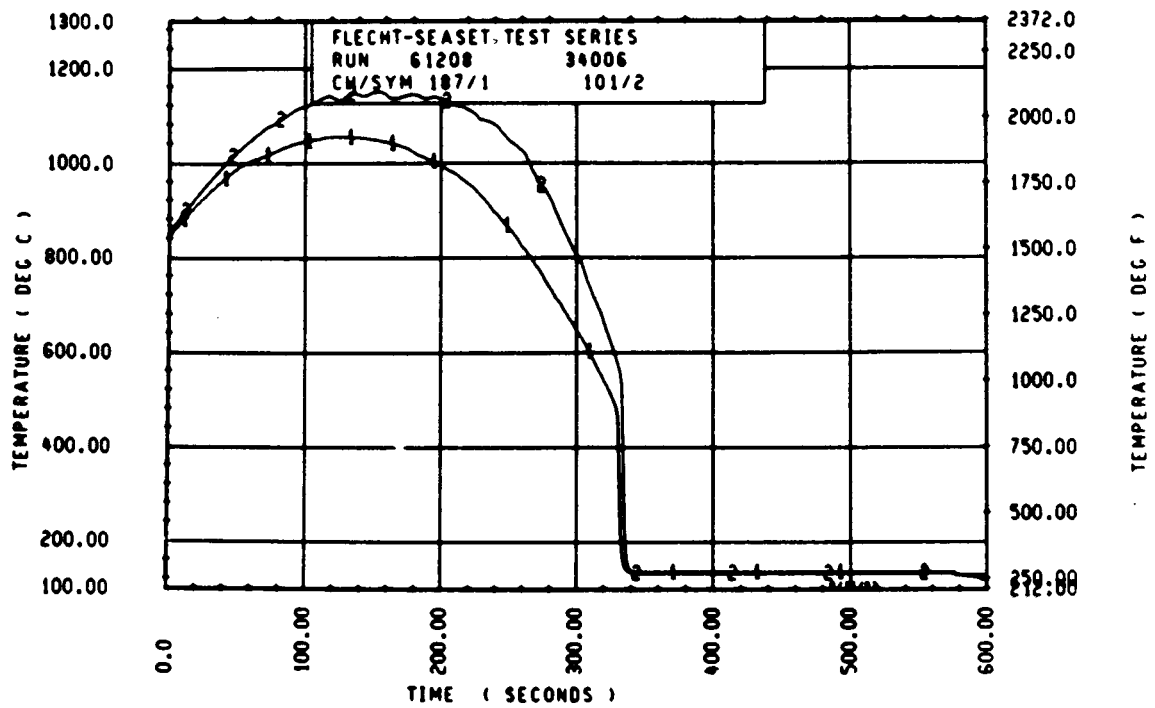
ELEV	TEMP RISE (DEG F)			WUENCH TEMP (DEG F)			WUENCH TIME (SEC)		
	MAX	MIN	MEAN	MAX	MIN	MEAN	MAX	MIN	MEAN
12	17.0	15.7	16.8	542.2	573.5	560.2	27.4	24.5	25.4
24	42.2	36.2	37.9	654.5	643.4	652.5	57.5	53.7	55.0
39	100.0	78.2	91.7	767.0	764.6	761.4	144.4	114.4	105.3
49	149.5	118.4	138.4	812.1	748.1	754.4	153.9	144.4	148.1
67	228.5	160.4	201.4	910.6	832.2	868.6	218.5	200.0	211.5
67	318.8	174.6	242.6	943.6	822.6	864.9	254.9	245.5	250.4
69	370.0	247.4	290.9	954.1	824.5	873.6	271.4	260.0	265.2
70	355.3	191.5	276.5	984.2	844.0	903.5	279.5	268.4	274.9
71	387.1	247.3	327.5	984.2	817.8	907.1	282.2	271.8	275.5
72	377.2	220.3	292.4	1031.8	845.5	902.2	293.0	274.8	284.7
73	359.9	232.7	294.4	963.7	823.1	845.5	294.4	284.0	291.2
74	461.9	247.7	344.8	977.6	702.4	840.6	318.0	293.0	302.7
75	444.0	246.1	333.5	929.6	865.9	848.9	319.3	297.0	309.3
76	435.1	247.7	329.2	917.4	738.6	873.0	328.0	303.7	313.5
77	472.8	258.7	346.8	910.1	704.1	855.0	331.1	315.5	324.2
78	416.6	260.5	341.1	923.7	700.3	860.8	333.5	308.4	324.2
79	392.2	262.7	340.3	950.4	801.8	859.6	343.0	325.5	335.2
87	439.3	301.5	370.5	964.4	758.0	860.1	348.9	332.0	341.6
81	428.2	337.2	380.4	961.1	724.0	840.2	353.4	344.4	350.1
84	458.5	328.9	381.5	751.5	707.7	734.1	372.1	355.2	365.4
86	467.8	246.7	390.8	928.4	725.1	814.6	371.9	365.7	374.2
97	517.3	333.6	460.9	840.6	758.2	850.5	425.1	342.0	405.4
96	552.9	443.5	568.9	868.8	727.6	865.6	447.0	447.0	450.5
102	713.7	554.7	676.0	745.0	555.6	667.7	476.2	468.1	468.8
111	792.0	495.6	681.3	753.5	631.8	664.5	571.7	467.1	494.2
120	888.4	530.7	757.7	1041.0	558.2	654.6	531.5	411.5	474.4
132	785.4	578.1	693.3	861.8	522.6	545.7	535.1	444.4	511.5
139	612.7	439.1	546.7	1049.5	544.0	745.2	540.9	344.8	404.0



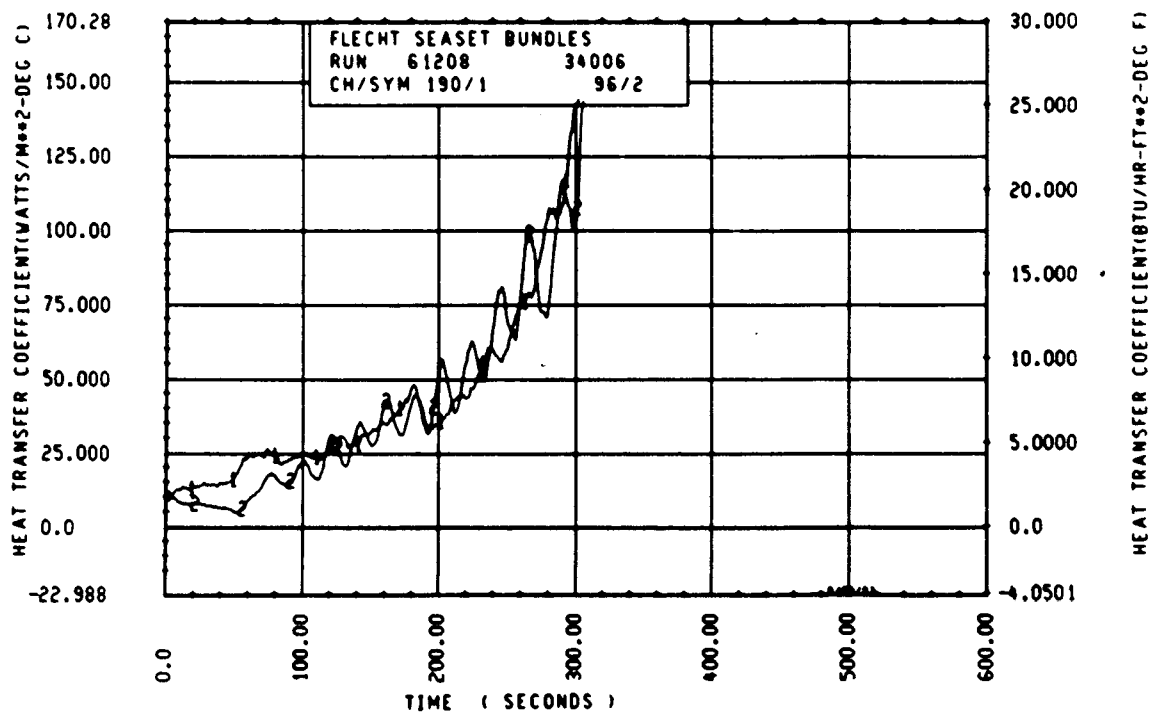
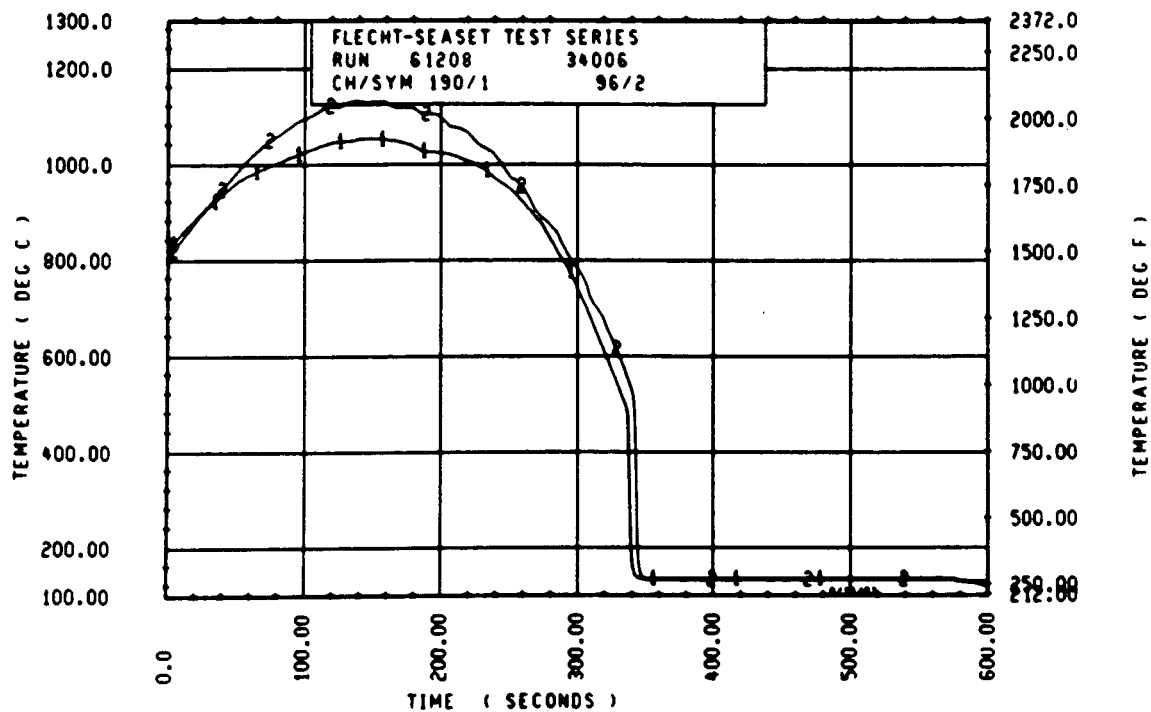
Rod 11F, 1.98 m (78 in.)



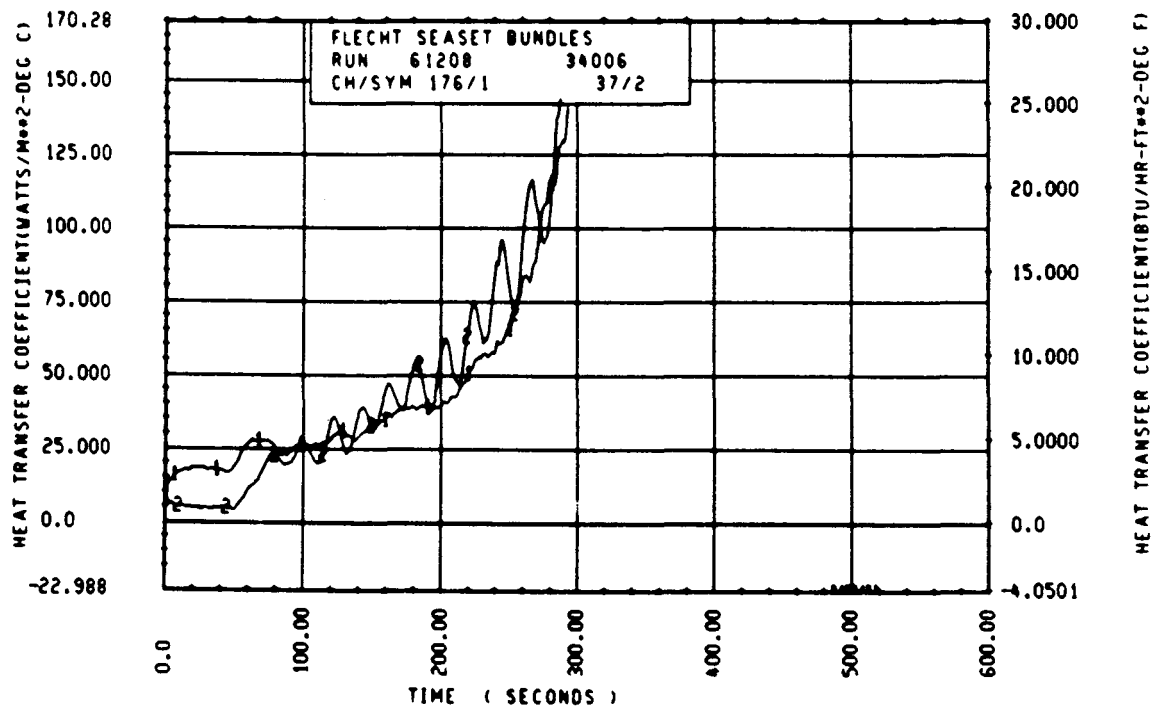
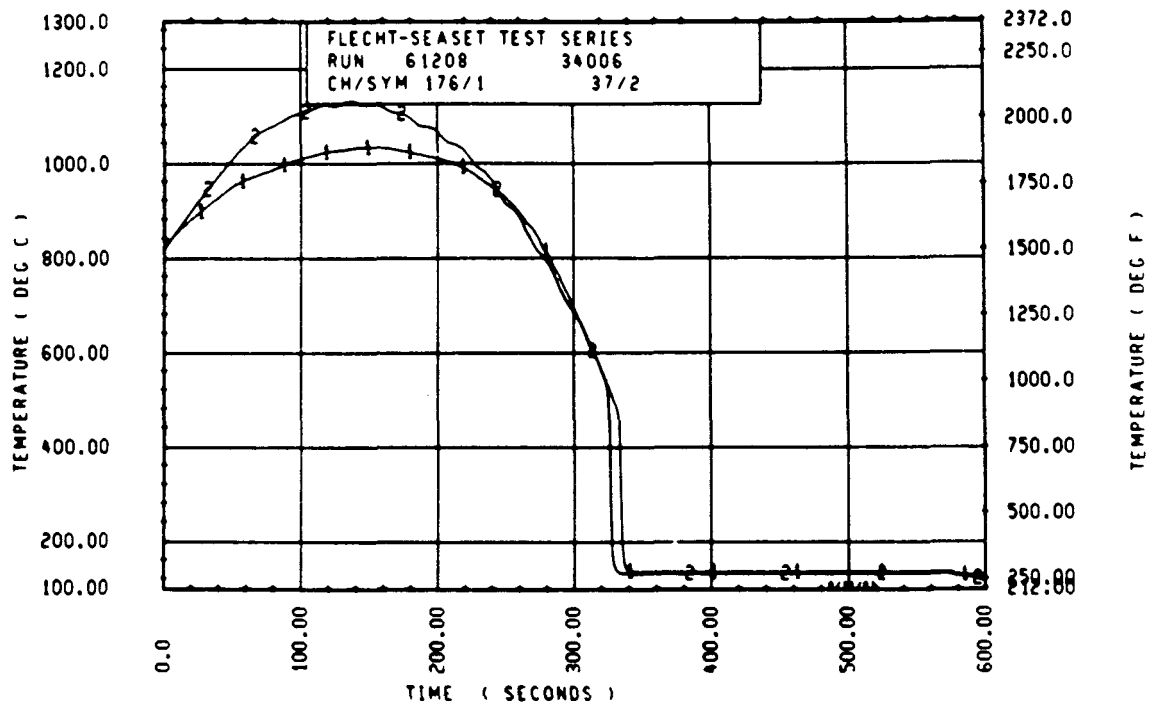
Rod 7K, 1.98 m (78 in.)



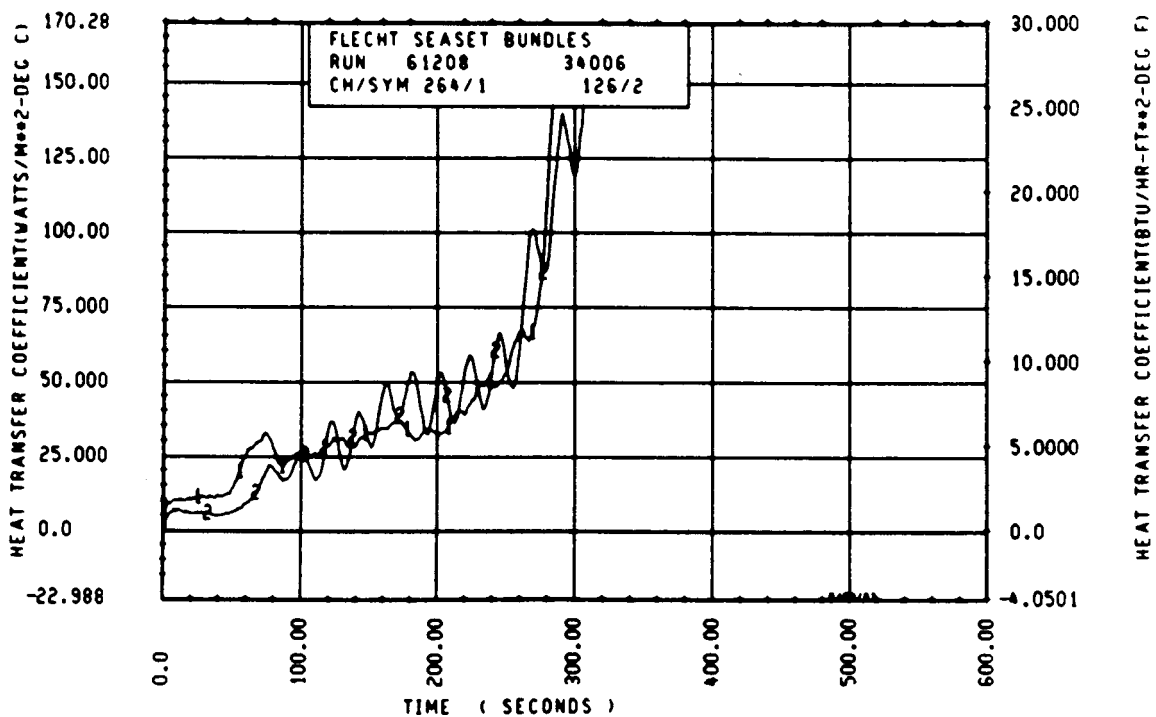
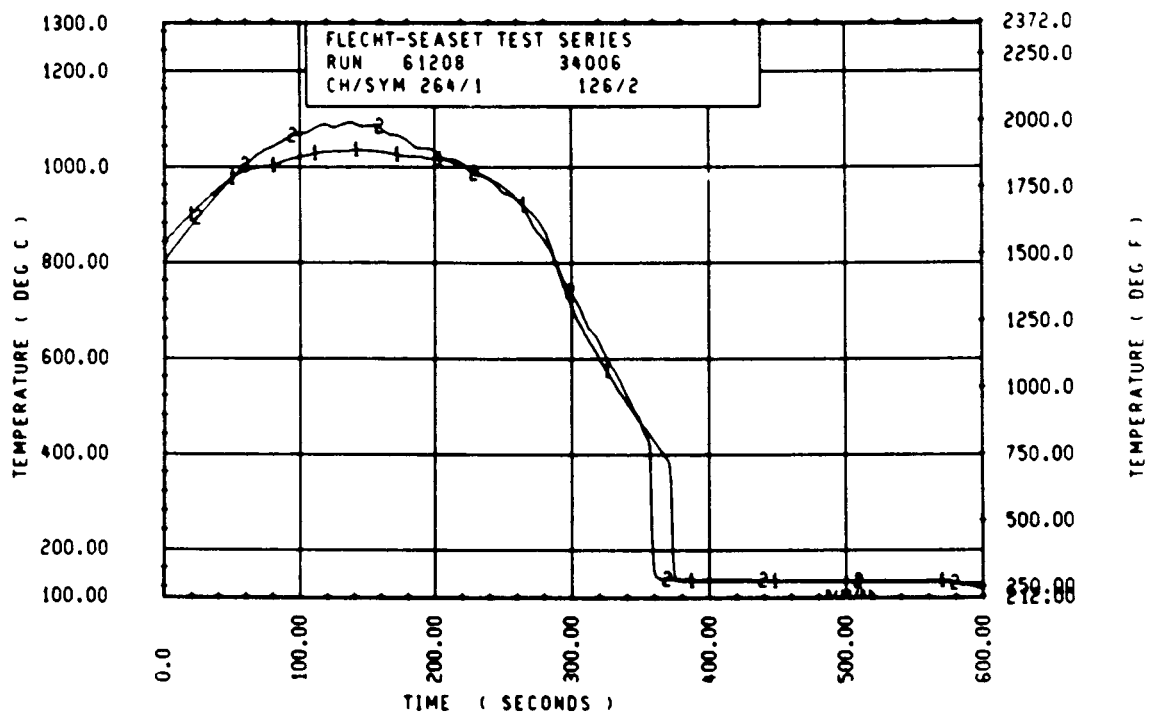
Rod 6J, 1.98 m (78 in.)



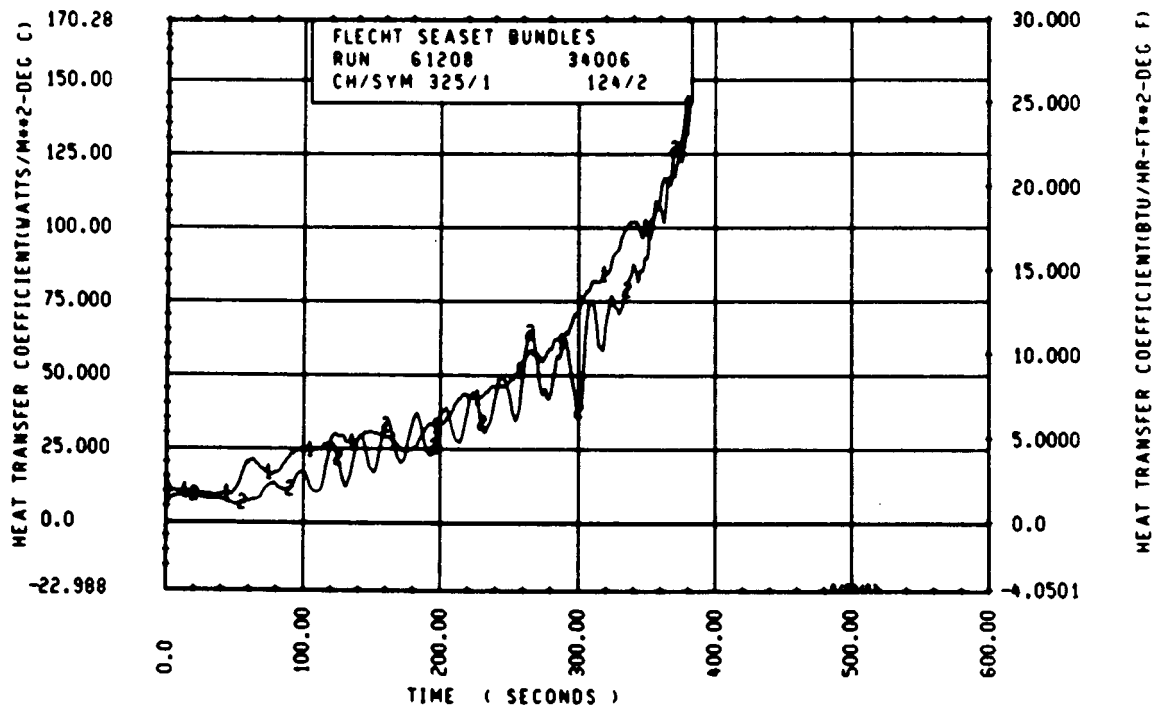
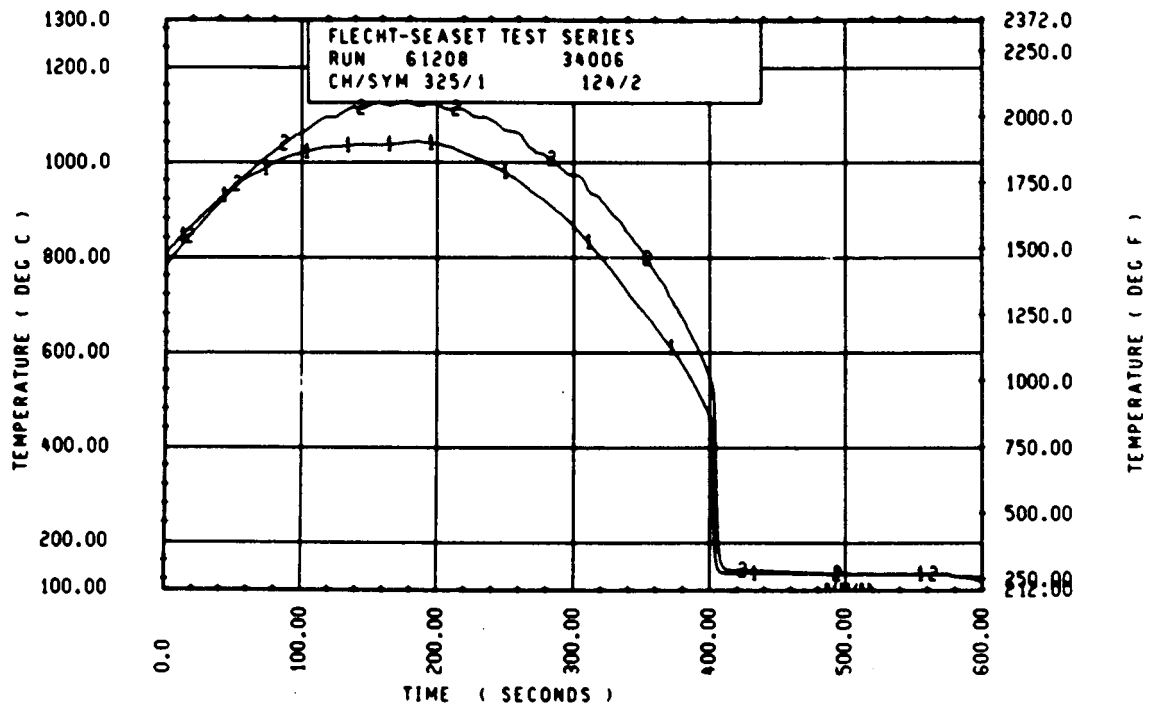
Rod 7H, 1.98 m (78 in.)



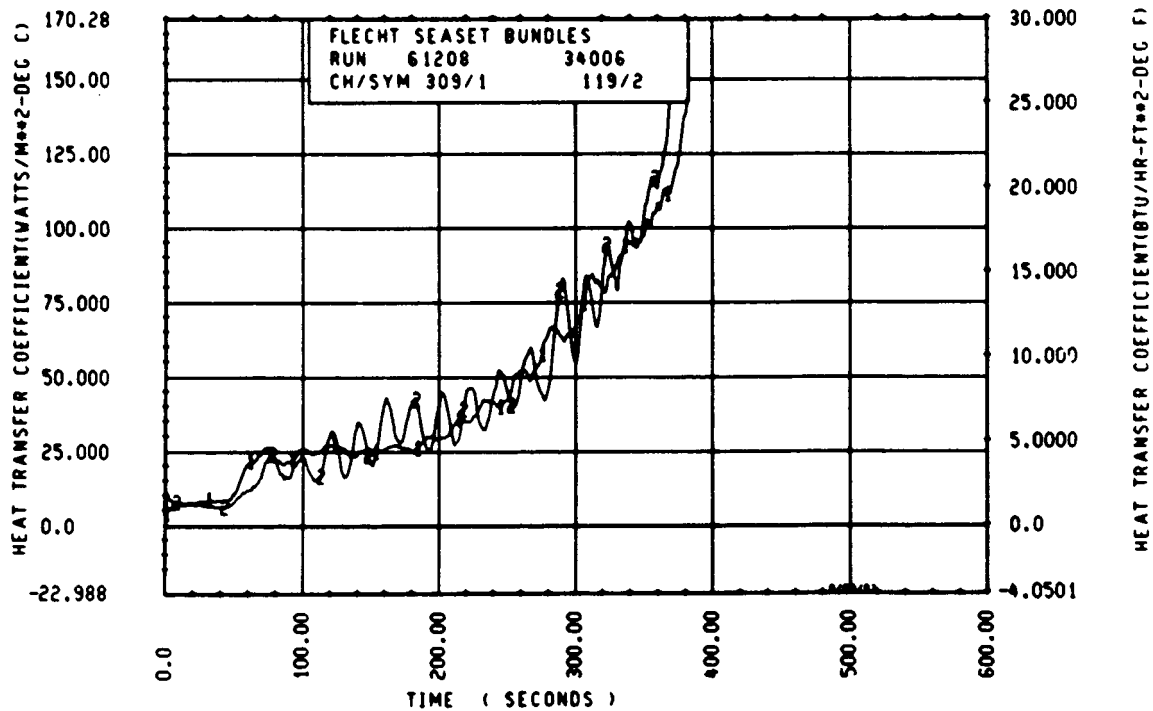
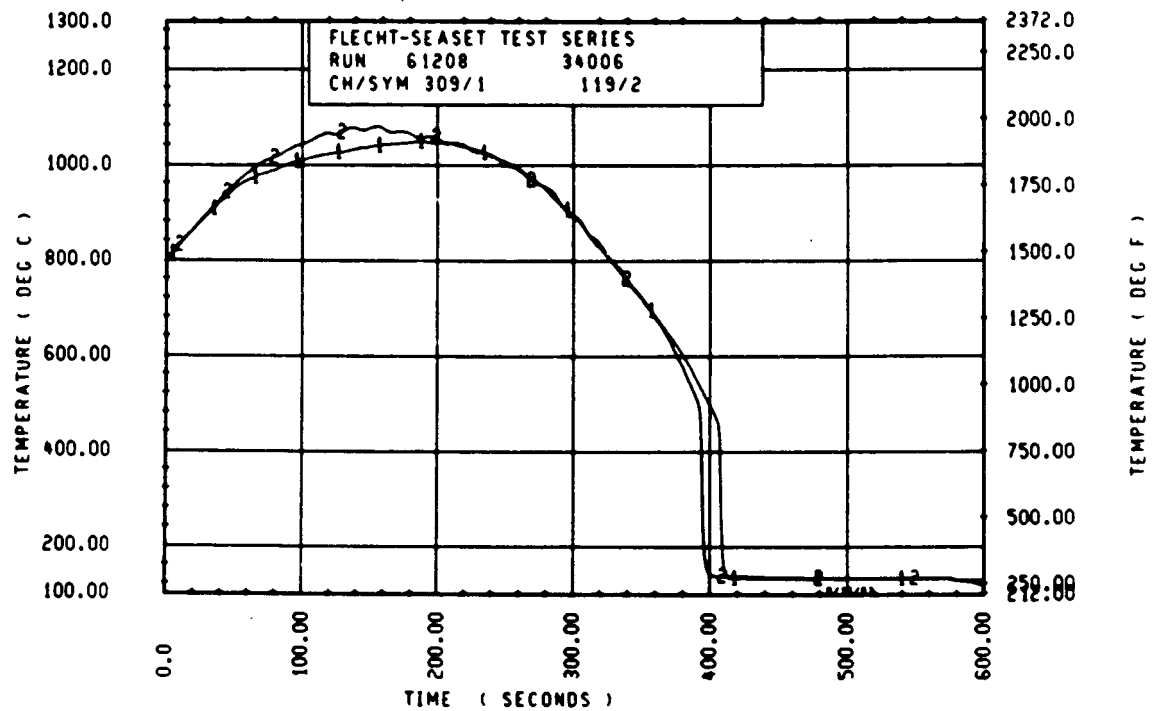
Rod 9F, 1.98 m (78 in.)



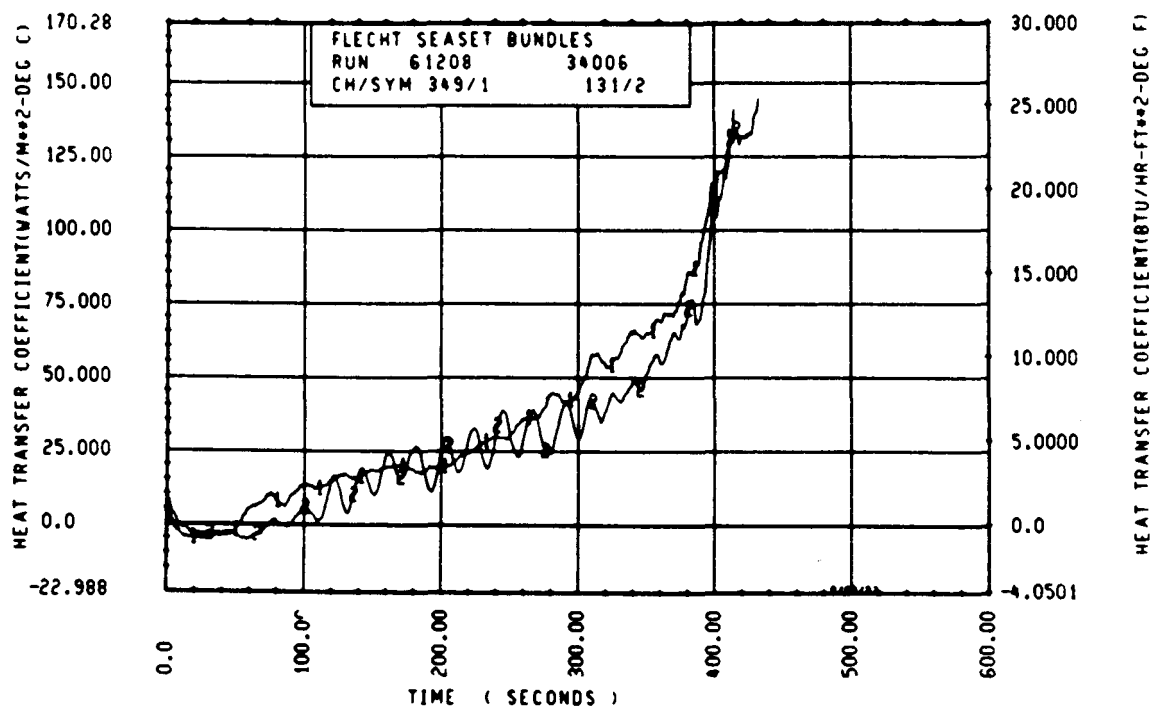
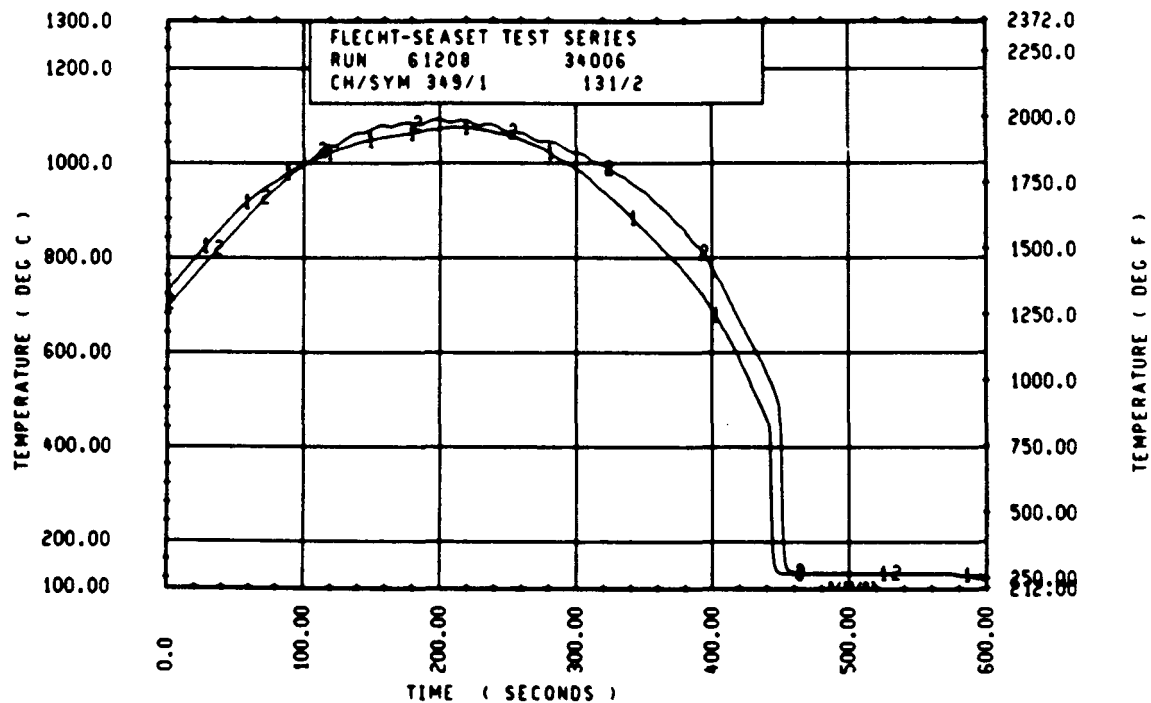
Rod 7E, 2.13 m (84 in.)



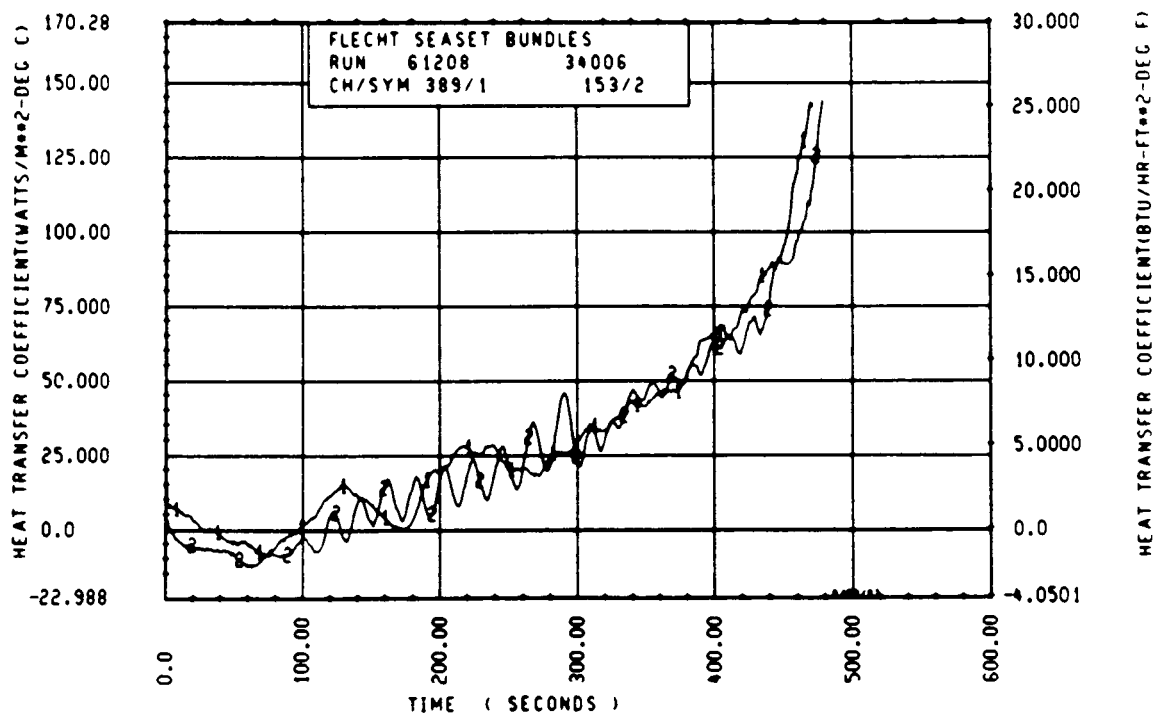
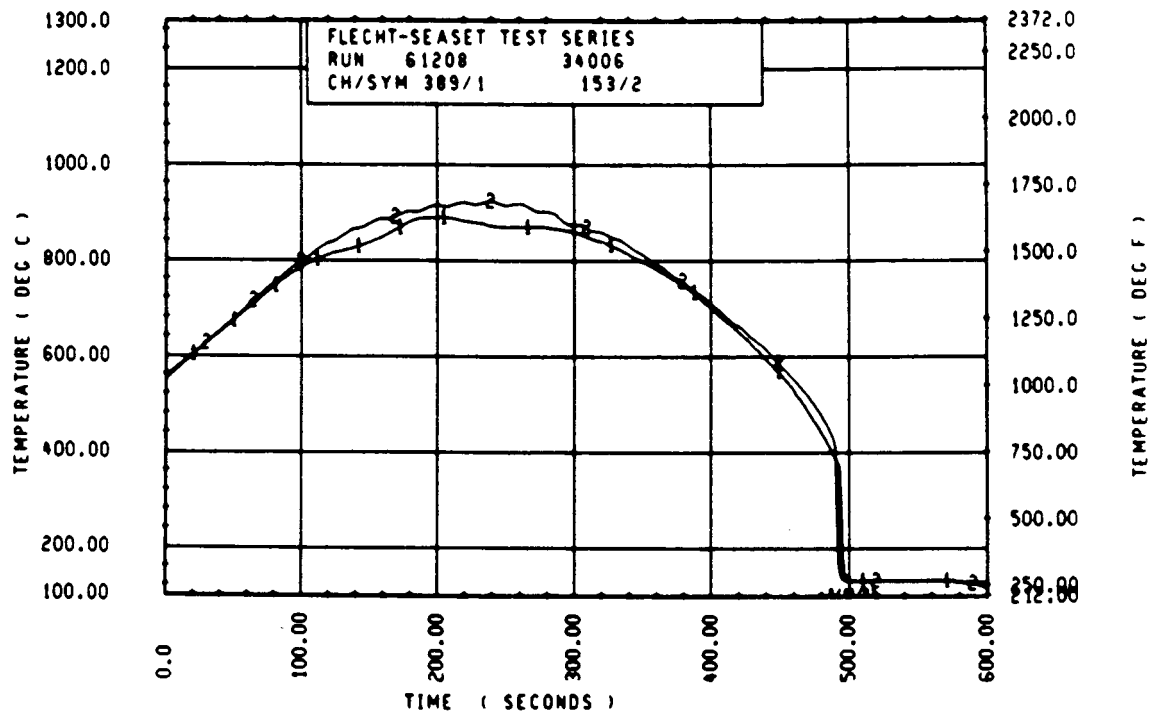
Rod 11E, 2.29 m (90 in.)



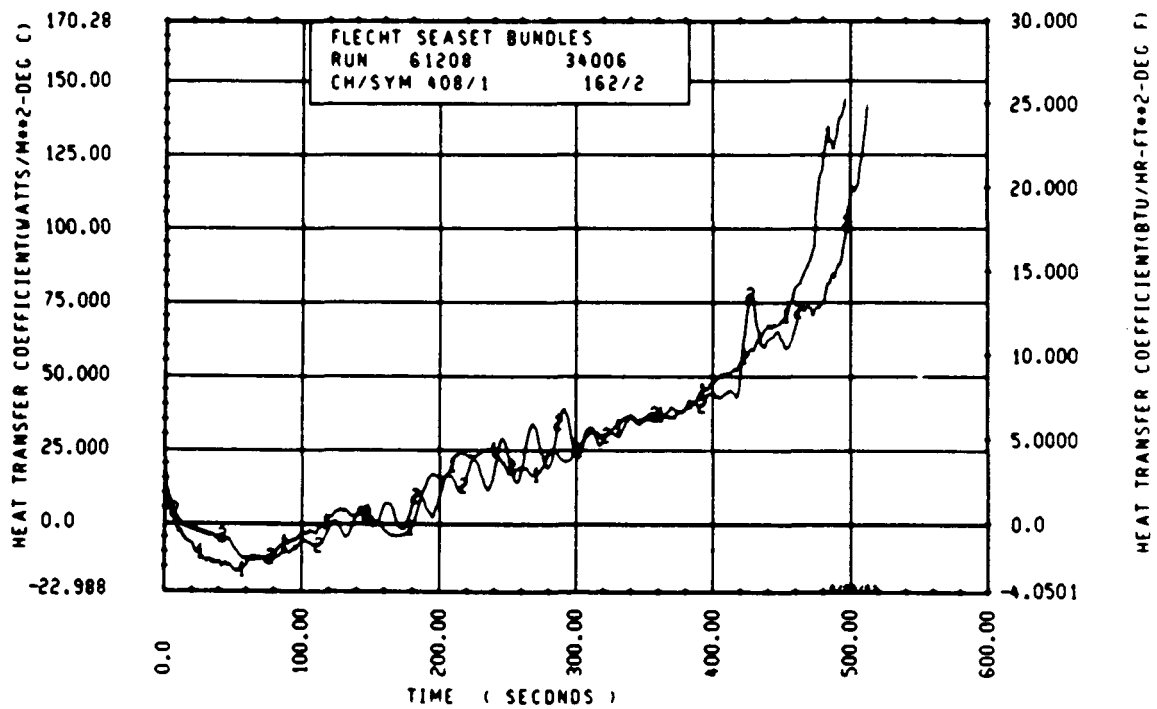
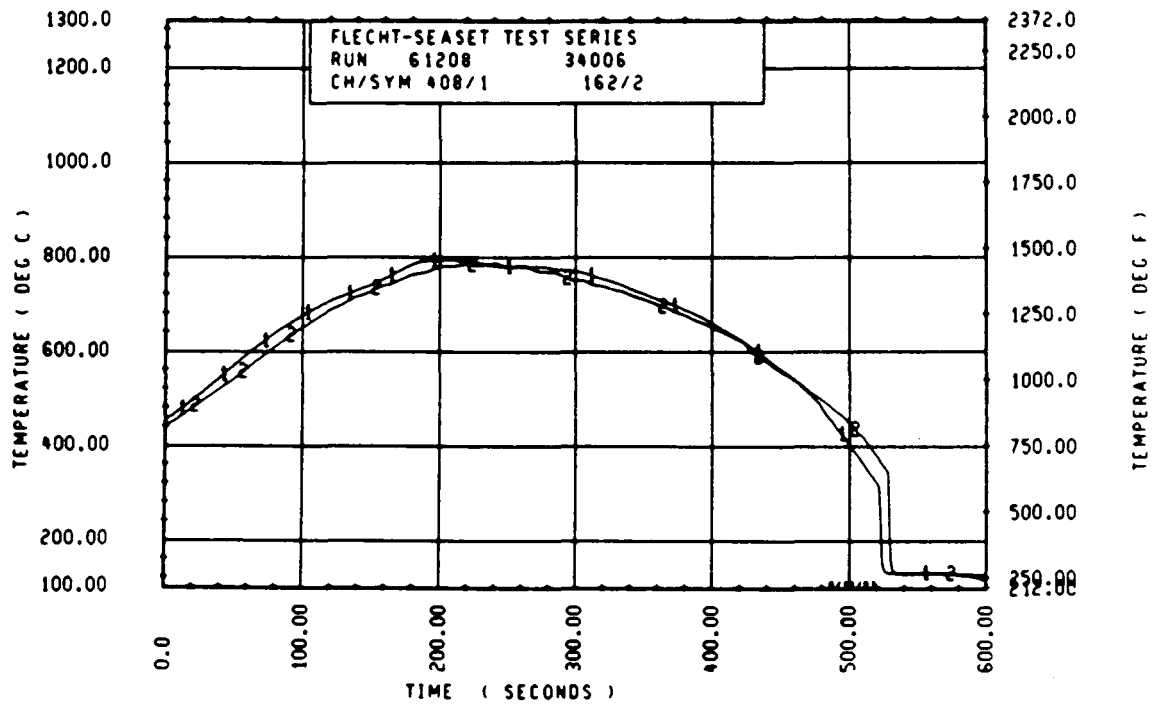
Rod 7D, 2.29 m (90 in.)



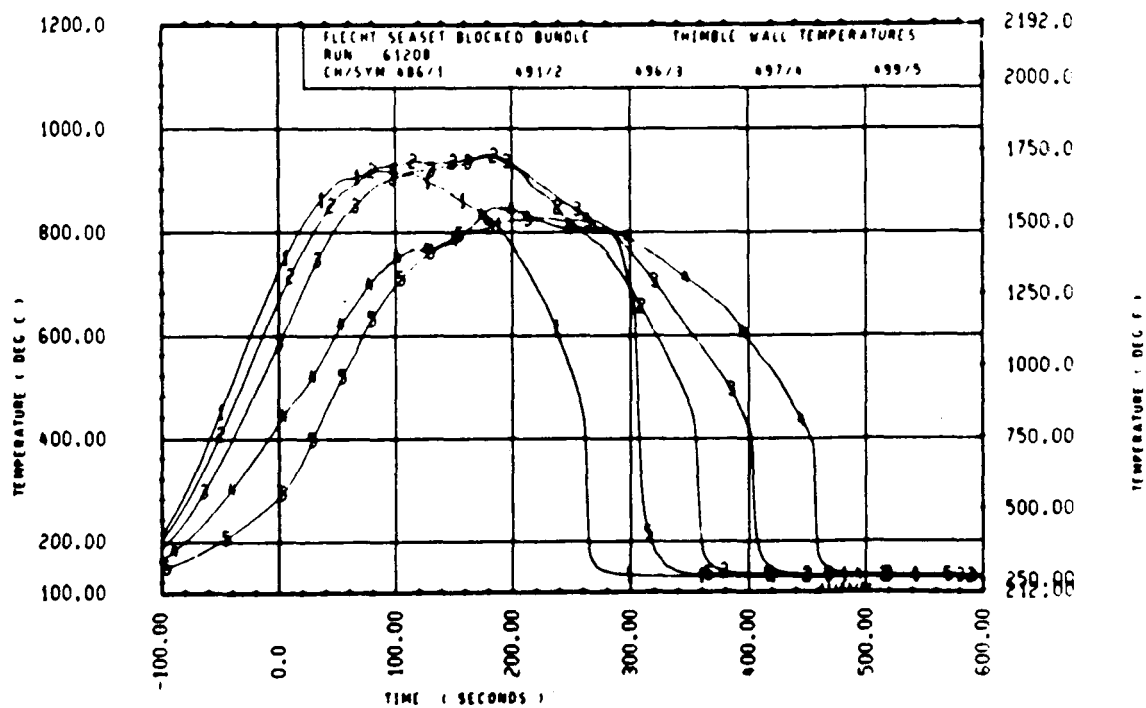
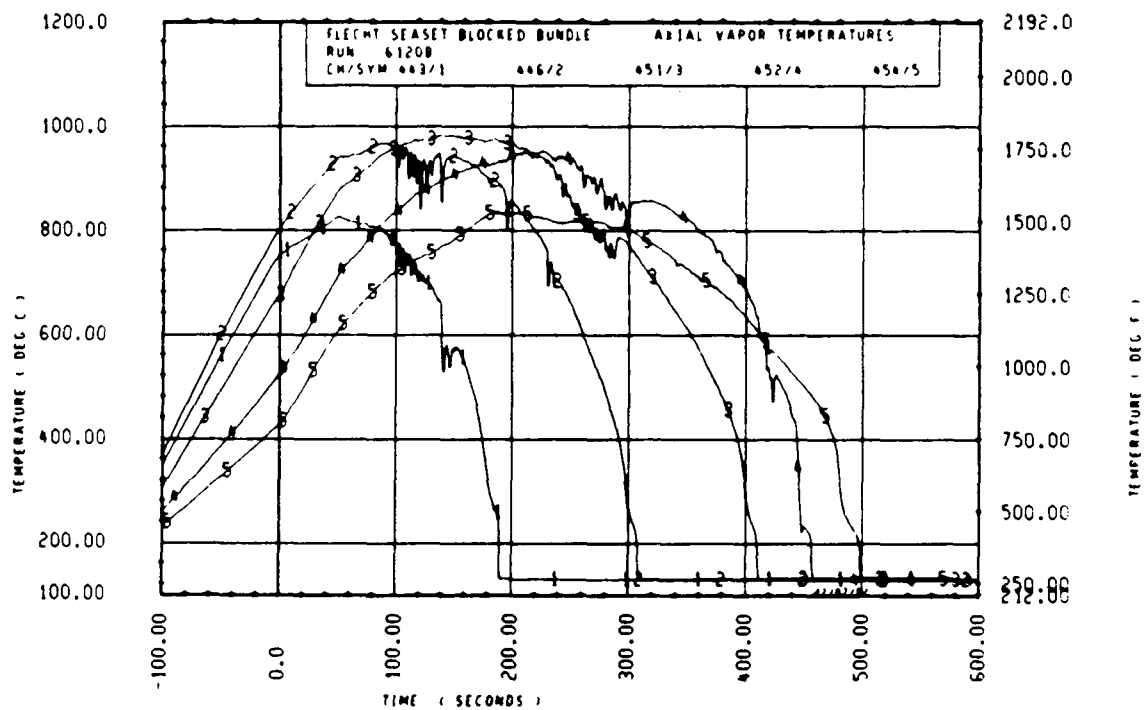
Rod 8E, 2.44 m (96 in.)

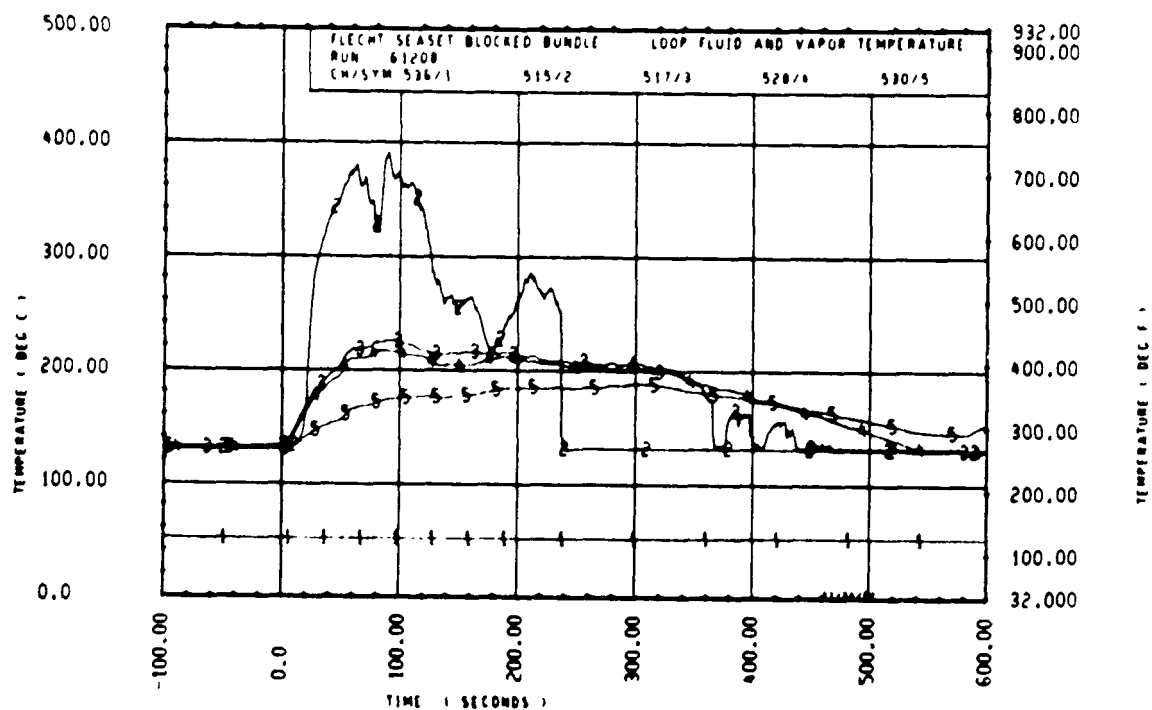
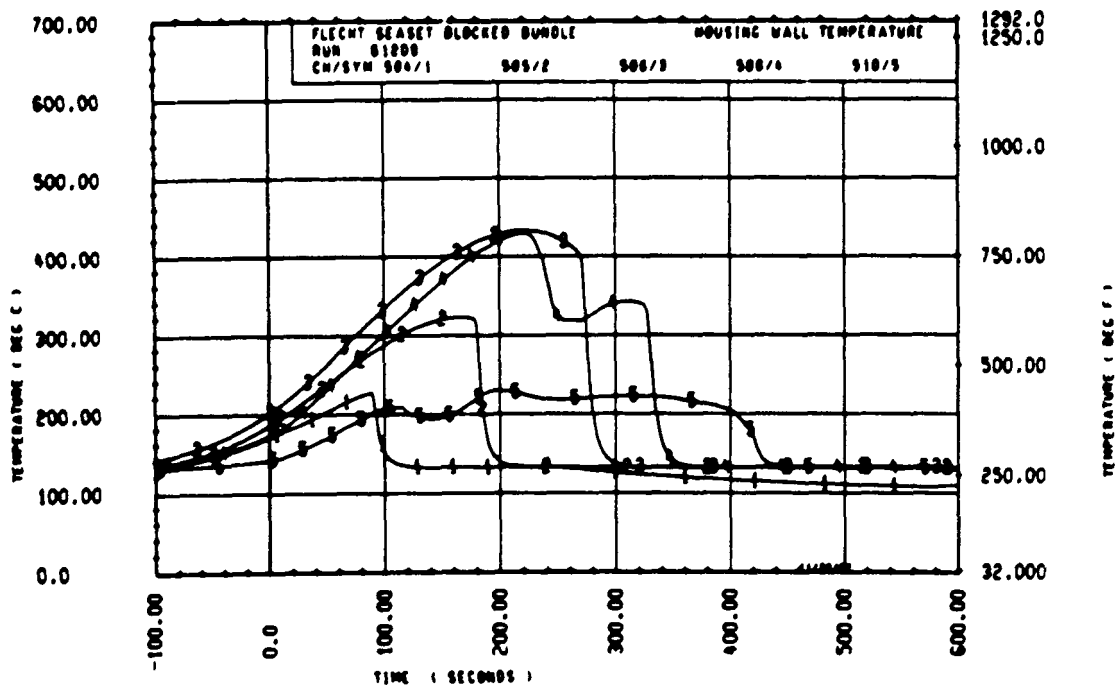


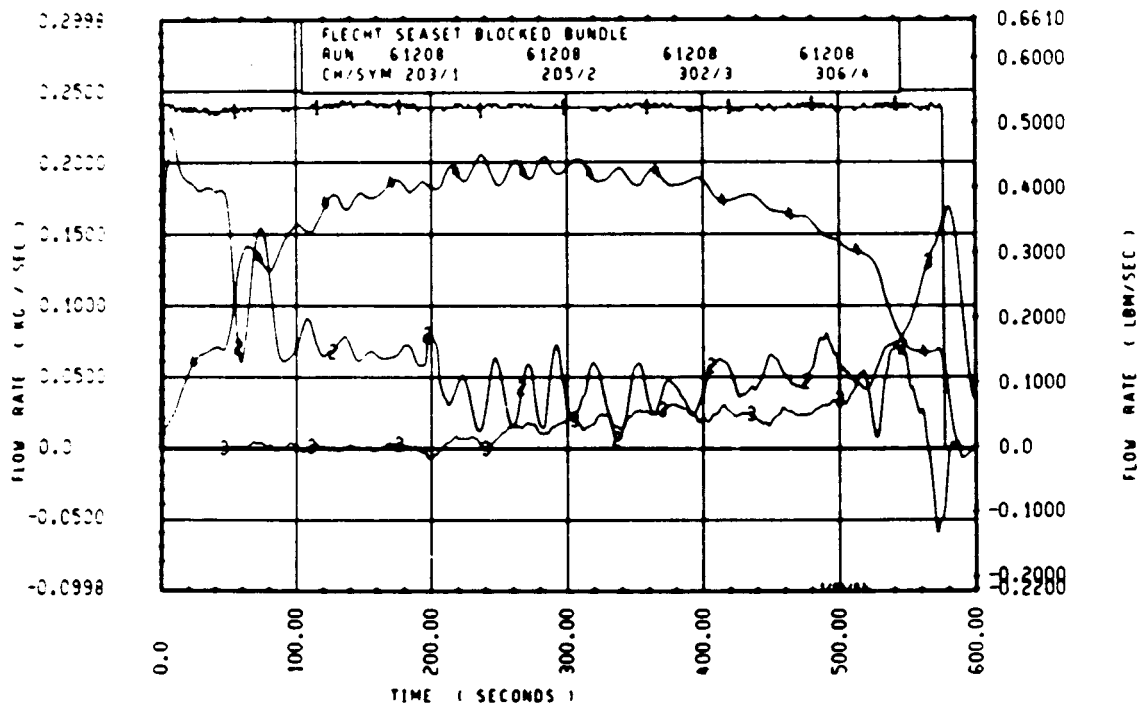
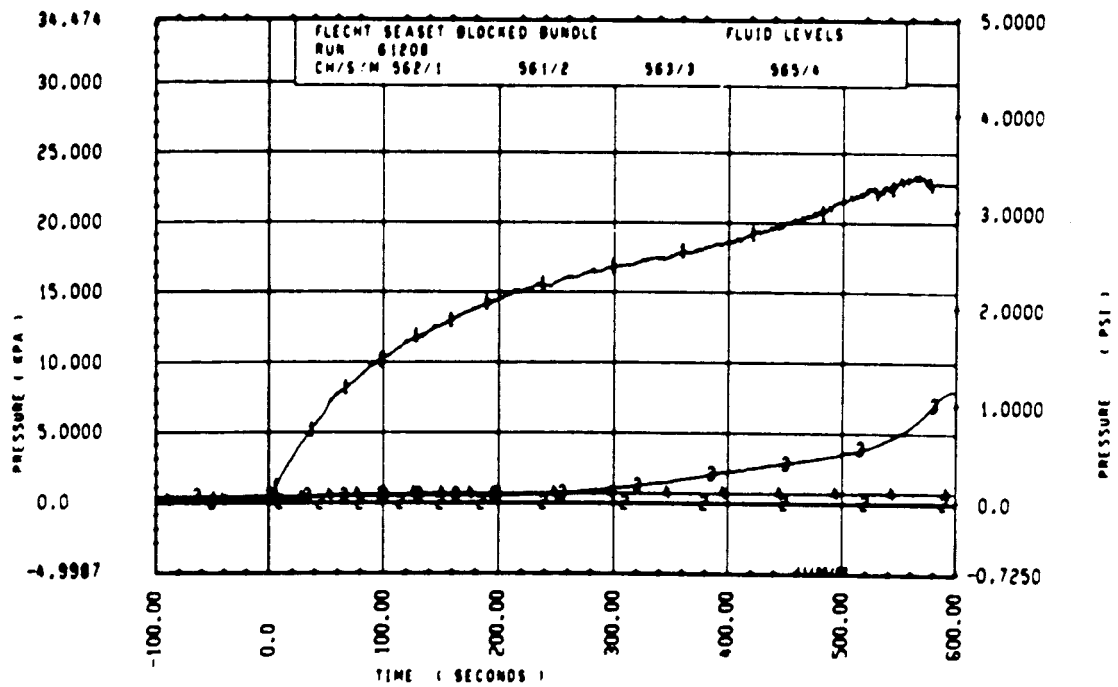
Rod 9C, 2.82 m (111 in.)

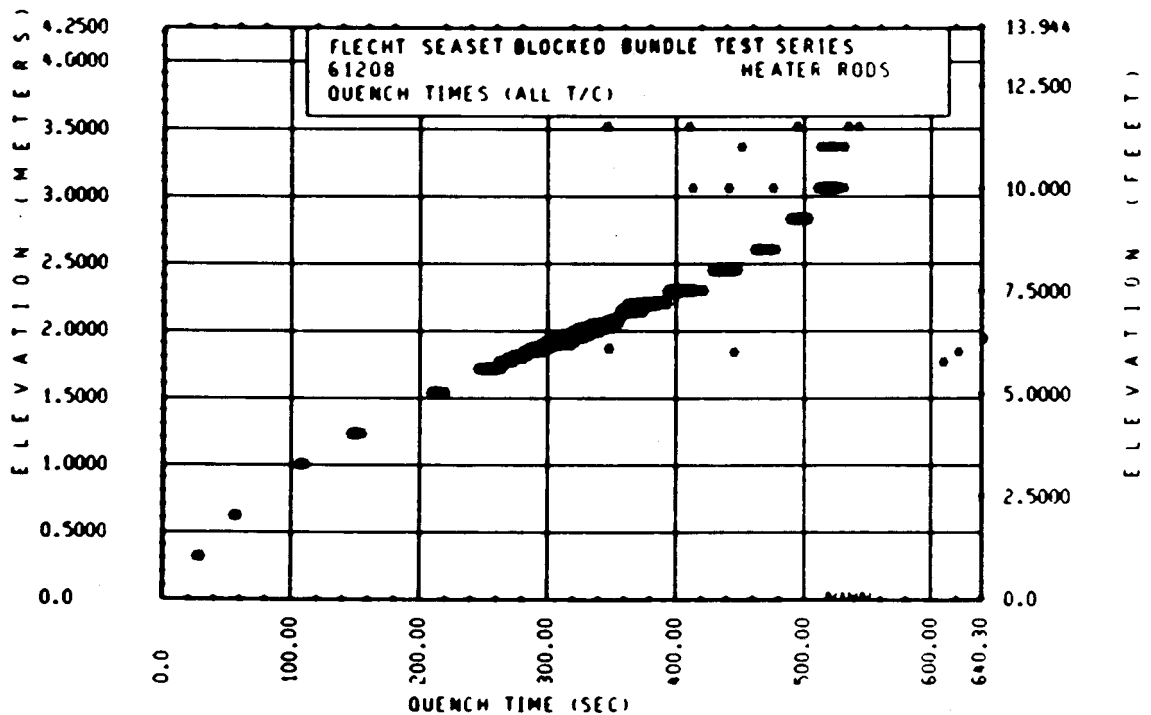
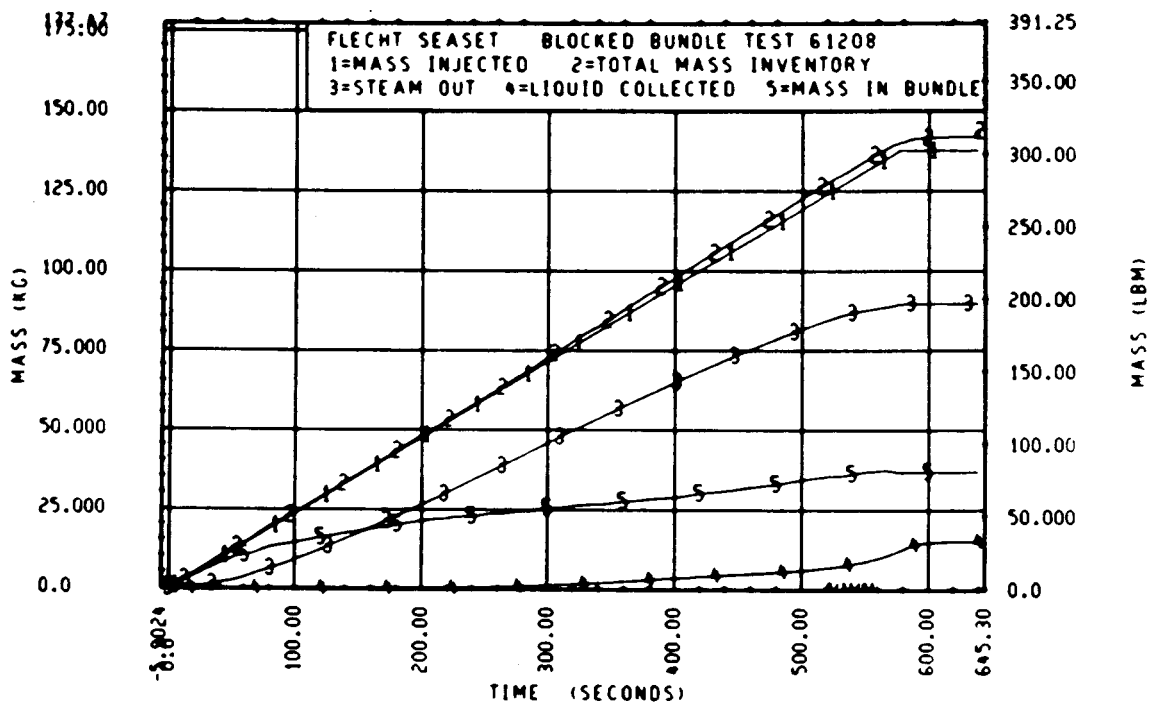


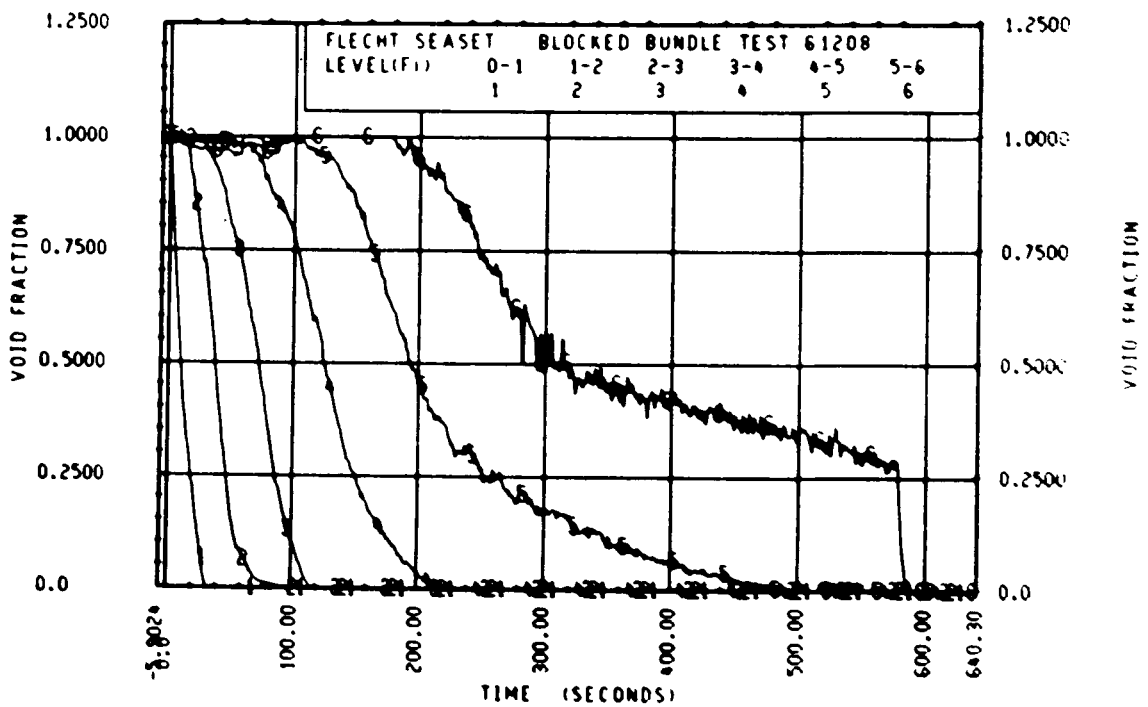
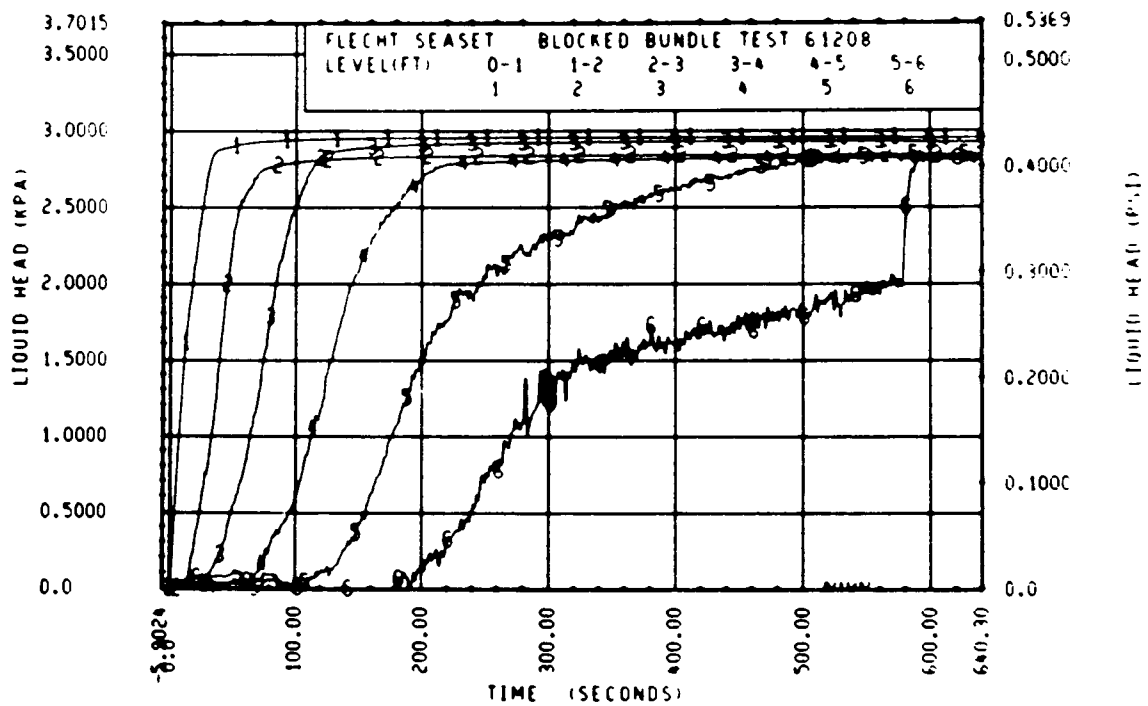
Rod 7B, 3.05 m (120 in.)

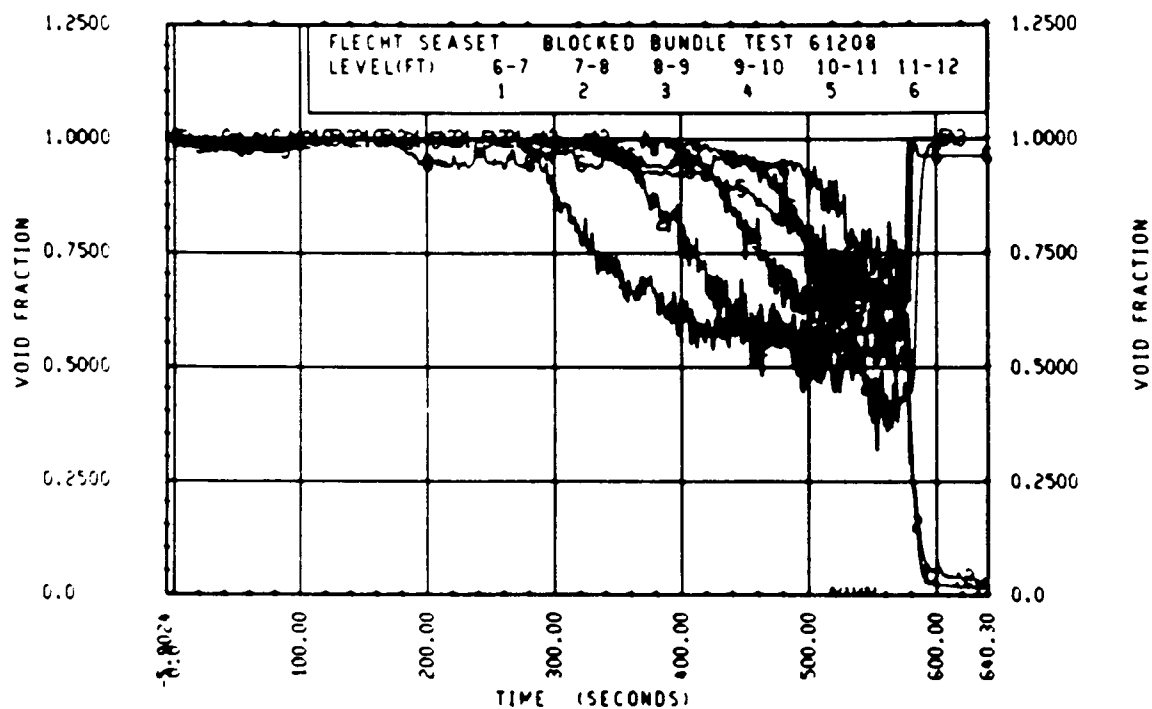
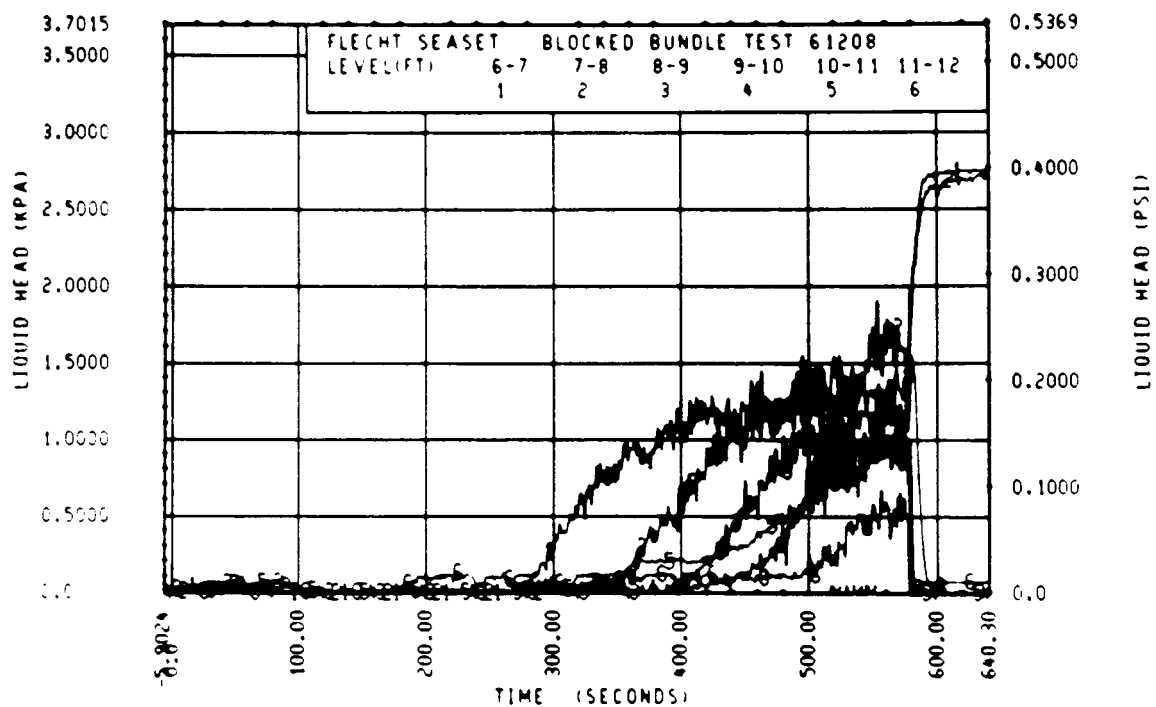












FLECHT SEASET 163-ROD BUNDLE FLOW BLOCKAGE TASK
SUMMARY AND COMMENT SHEET

Run: 61314
Test date: 9/2/82
Test type: Forced reflood
Parameter: Peak power effect

AS-RUN TEST CONDITIONS:

Upper plenum pressure	0.274 MPa (39.7 psia)
Initial peak clad temperature and location	876.5°C (1609.7°F), 8N-1.93 m (76 in.)
Initial peak rod power:	
Peripheral rods	1.31 kw/m (0.398 kw/ft)
Bypass rods	1.30 kw/m (0.395 kw/ft)
Blockage island rods	1.31 kw/m (0.398 kw/ft)
Flooding rate	38.6 mm/sec (1.52 in./sec)
Coolant temperature	51.7°C (125°F)
Initial bundle water level	-4.6 mm (-0.18 in.)

COMMENTS:

Inlet mass flow:⁽¹⁾ -0.6% linearly increasing to +2.9% by 240 seconds

Power decay:⁽¹⁾ peripheral rods, -1% linearly decreasing to 0% by 120 seconds
bypass rods, -1.5% constant for 150 seconds and -2% thereafter
blockage rods, -0.5% constant

1. Relative to run 31021

FLECHT SEASEI 103 RDD BUNDLE TEST SERIES

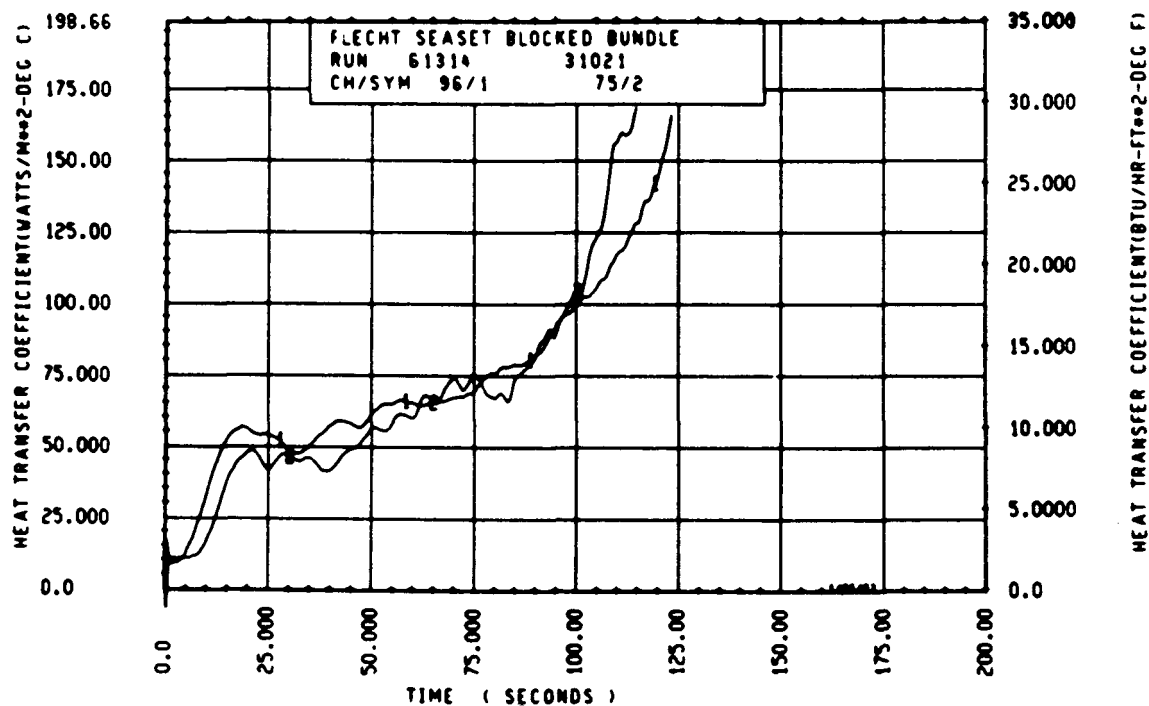
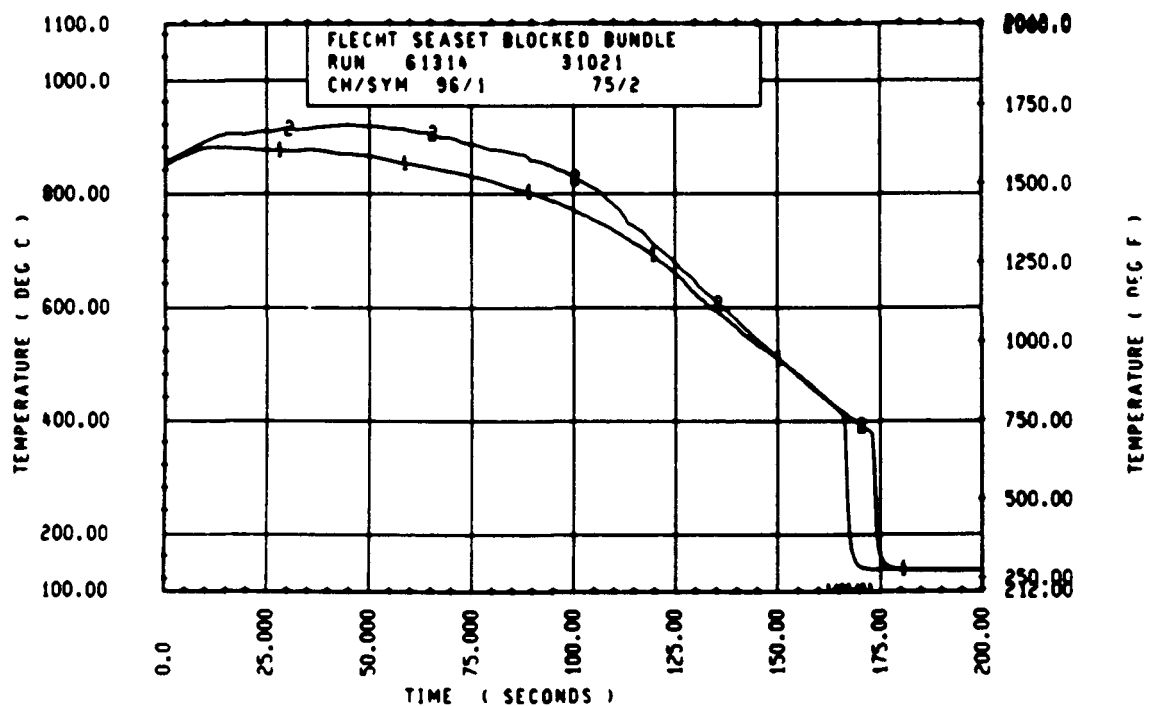
ROD/ELEV	CHAN.	NO	INITIAL AT FLOOD (DEG F)	MAXIMUM TEMPERATURE (DEG F)	TEMPERATURE RISE (DEG F)	TURNAROUND TIME (SECONDS)	QUENCH TEMPERATURE (DEG F)	QUENCH TIME (SECONDS)
96 1- 0		3	686.	694.	8.	4.5	657.	19.9
10M 2- 0		6	985.	921.	16.	7.1	615.	40.0
96 3- 3		9	1226.	1265.	27.	8.5	700.	71.4
3J 4- 0		11	1366.	1404.	36.	9.5	677.	94.9
7M 4- 0		12	1366.	1462.	42.	11.0	675.	97.8
8K 4- 0		13	1376.	1419.	44.	11.5	697.	97.1
8M 4- 0		14	1368.	1404.	36.	10.5	675.	95.4
12D 4- 0		17	1356.	1396.	34.	9.5	701.	95.2
5E 5- 0		20	1523.	1570.	53.	14.0	740.	133.0
76 5- 0		21	1579.	1630.	50.	11.0	734.	131.0
96 5- 0		24	1552.	1601.	49.	11.0	742.	131.9
5E 5- 7		33	1556.	1612.	55.	10.5	730.	132.0
86 5- 7		45	1555.	1614.	59.	11.5	630.	152.0
9M 5- 9		52	1494.	1504.	70.	14.0	721.	150.3
76 5-10		59	1512.	1577.	65.	13.0	653.	154.5
7F 5-11		62	1452.	1522.	70.	14.0	747.	160.9
46 5-11		64	1543.	1603.	60.	11.0	776.	162.0
2I 6- 0		67	1596.	1640.	50.	11.5	791.	162.4
5D 6- 0		70	1500.	1555.	55.	10.5	707.	162.8
6J 6- 0		74	1534.	1588.	54.	12.0	706.	166.7
7M 6- 0		66	1556.	1612.	54.	11.0	770.	166.4
11E 6- 0		80	1546.	1595.	48.	10.5	754.	164.0
8M 6- 2		97	1571.	1647.	76.	36.5	700.	170.9
9M 6- 2		99	1542.	1597.	54.	11.5	740.	171.0
9E 6- 2		105	1554.	1500.	146.	62.0	1106.	159.6
84 6- 3		111	1412.	1469.	57.	36.5	642.	179.0
46 6- 3		124	1560.	1619.	59.	12.0	753.	174.7
11M 6- 4		134	1467.	1535.	47.	11.0	750.	179.4
9D 6- 4		143	1556.	1612.	54.	11.0	613.	177.5
9J 6- 5		165	1533.	1580.	53.	11.0	752.	184.1
9M 6- 5		166	1562.	1650.	58.	11.0	707.	175.8
8J 6- 6		192	1577.	1636.	52.	12.5	815.	178.7
9D 6- 6		193	1560.	1626.	60.	35.5	743.	183.8
11F 6- 6		173	1559.	1614.	55.	11.0	736.	179.9
46 7- 0		261	1507.	1565.	58.	11.0	655.	200.1
7D 7- 6		309	1494.	1566.	66.	35.5	753.	214.1
76 7- 6		312	1529.	1594.	65.	12.0	712.	215.1
11E 7- 6		325	1492.	1551.	59.	36.5	690.	211.1
5L 8- 0		337	1313.	1434.	121.	51.5	735.	229.1
7M 8- 0		345	1354.	1476.	121.	61.0	750.	210.1
7K 8- 0		346	1363.	1463.	100.	37.0	689.	226.1
5J 8- 6		366	1150.	1272.	123.	48.0	652.	245.4
7B 8- 6		368	1141.	1262.	121.	77.0	633.	245.2
7E 9- 3		383	1112.	1243.	136.	70.0	642.	250.1
8M 9- 3		387	1056.	1182.	124.	66.0	622.	235.9
9C 9- 3		399	1045.	1163.	118.	79.0	595.	254.1
11F 9- 3		394	1051.	1171.	120.	62.5	724.	210.0
78L0- 0		408	860.	1065.	204.	94.0	557.	202.2
8M10- 0		415	873.	1035.	162.	58.0	659.	194.3
8K10- 0		417	869.	1021.	153.	71.0	590.	250.1
8N10- 0		418	869.	1105.	216.	94.0	591.	270.1
6M11- 0		429	713.	757.	54.	29.0	621.	116.7
9611- 0		431	695.	777.	81.	50.0	624.	159.4
11E11- 0		432	696.	809.	112.	72.5	494.	236.0
5J11- 6		436	676.	727.	50.	34.0	526.	216.1
7811- 6		437	650.	768.	138.	98.5	641.	194.5
8J11- 6		438	652.	737.	45.	23.0	510.	220.0

RUN 61314 HEATER KJQ STATISTICAL DATA

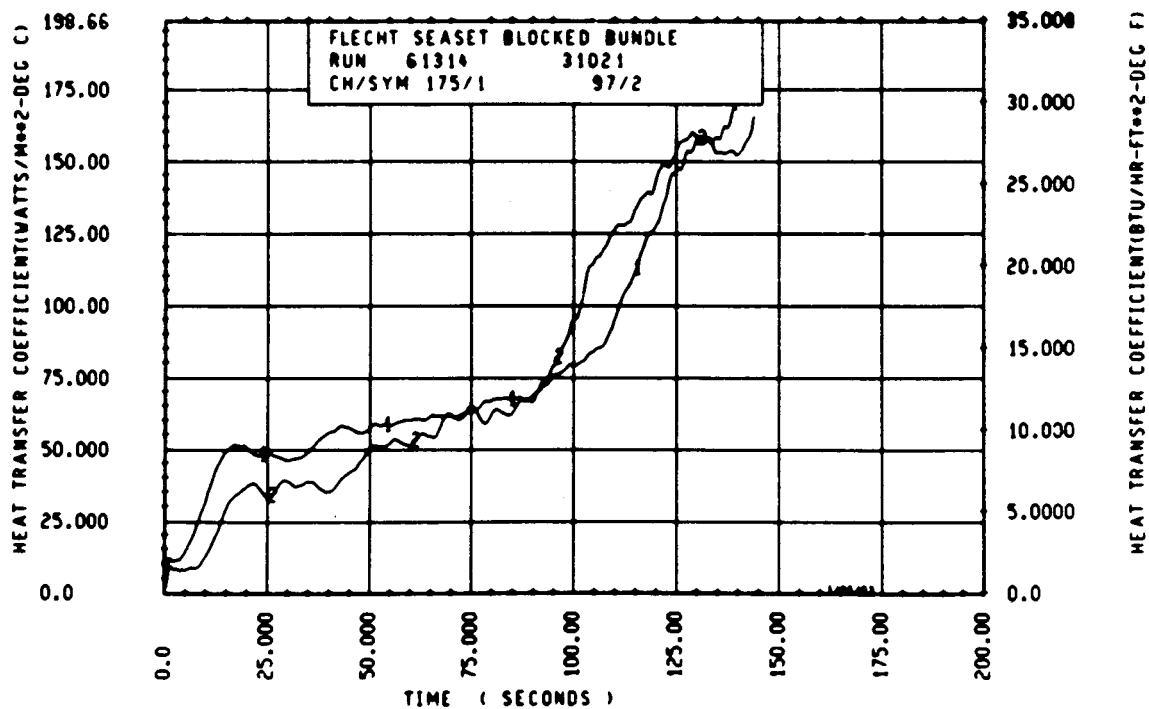
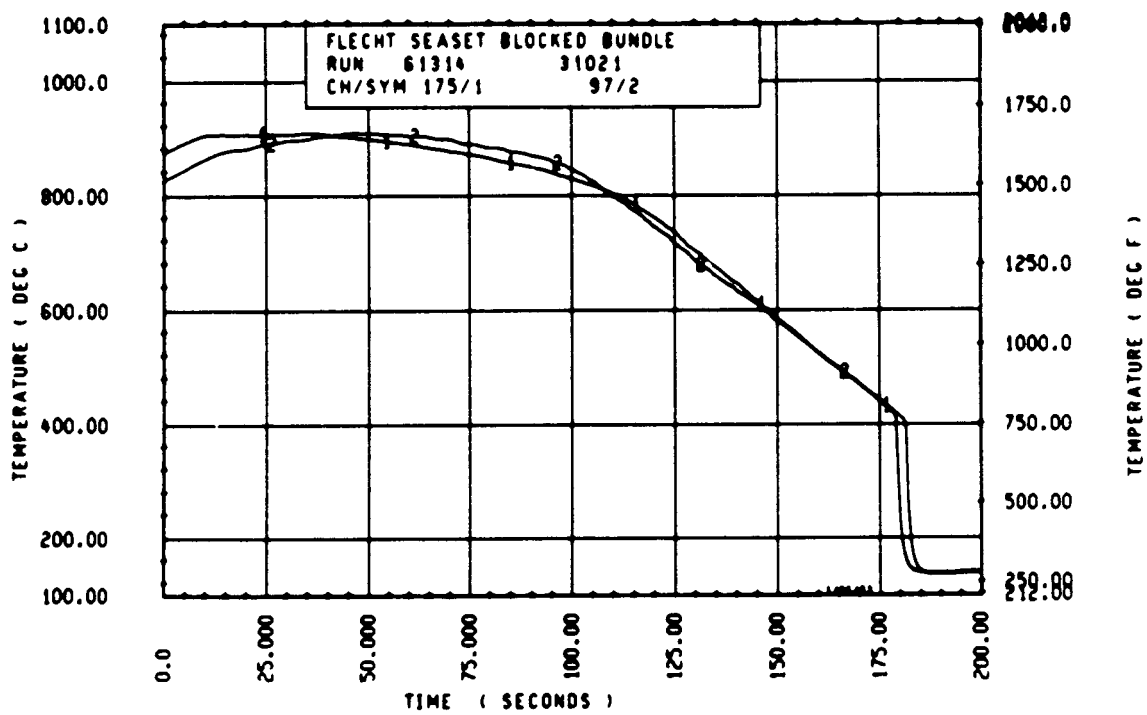
ELEV	INITIAL TEMP (DEG F)			MAX TEMP (DEG F)			TURNAROUND TIME (SEC)		
	MAX	MIN	MEAN	MAX	MIN	MEAN	MAX	MIN	MEAN
12	577.9	684.3	680.2	646.3	692.1	694.2	4.5	4.6	4.3
24	444.9	873.4	685.3	921.4	388.4	900.4	7.0	8.5	6.8
34	1235.8	1103.0	1204.3	1262.4	1200.7	1230.6	8.5	8.5	8.5
48	1390.2	1356.4	1370.8	1427.4	1390.2	1408.4	11.5	9.5	10.3
60	1579.3	1444.5	1531.0	1624.3	1498.6	1579.2	14.0	9.5	11.2
67	1607.5	1520.7	1565.2	1655.9	1570.6	1610.8	13.0	9.5	11.1
69	1537.0	1493.7	1520.2	1593.3	1564.6	1578.5	14.0	10.5	11.8
70	1672.0	1483.3	1534.3	1648.2	1543.5	1589.1	35.0	10.5	16.3
71	1543.5	1452.0	1500.6	1663.4	1521.6	1582.7	14.0	11.0	12.0
72	1599.8	1473.4	1545.8	1654.0	1539.1	1604.8	35.5	10.5	12.9
73	1591.2	1477.7	1532.9	1641.0	1530.0	1588.2	12.0	10.5	11.5
74	1596.8	1371.2	1515.2	1640.2	1440.7	1574.0	36.5	10.5	20.3
75	1573.1	1412.5	1526.3	1653.7	1464.1	1583.5	38.5	10.0	19.2
76	1539.7	1466.1	1552.8	1663.6	1531.5	1608.9	36.5	10.5	16.6
77	1592.3	1491.6	1549.5	1602.2	1539.1	1614.0	40.5	10.5	17.0
78	1578.0	1550.1	1529.6	1670.2	1566.7	1583.4	36.5	8.5	17.8
79	1605.3	1506.6	1555.9	1654.8	1570.6	1622.2	36.5	10.5	16.8
80	1590.1	1506.8	1553.1	1640.2	1566.8	1622.4	46.0	10.5	28.3
81	1566.8	1472.3	1537.6	1634.4	1579.2	1614.1	37.5	11.0	29.9
84	1566.4	1453.1	1515.0	1622.4	1515.3	1570.3	12.0	10.5	10.9
85	1538.8	1477.7	1543.8	1651.5	1520.4	1600.0	13.5	10.0	11.1
90	1537.0	1430.3	1494.2	1599.8	1558.2	1561.9	37.0	11.0	25.4
96	1407.1	1202.7	1357.2	1532.6	1418.9	1474.7	59.0	37.0	54.7
102	1203.5	1080.5	1168.9	1332.1	1263.8	1298.5	79.0	56.5	53.5
111	1112.3	1044.2	1072.8	1240.3	1153.7	1190.6	112.0	47.0	70.2
121	927.6	825.3	873.8	1124.7	953.4	1058.6	114.0	52.5	81.5
132	702.6	690.3	696.2	810.8	747.4	784.7	79.5	29.0	56.9
138	692.1	650.1	666.8	780.0	720.6	753.8	98.5	23.0	59.5

RUN 61314 HEATER KJQ STATISTICAL DATA

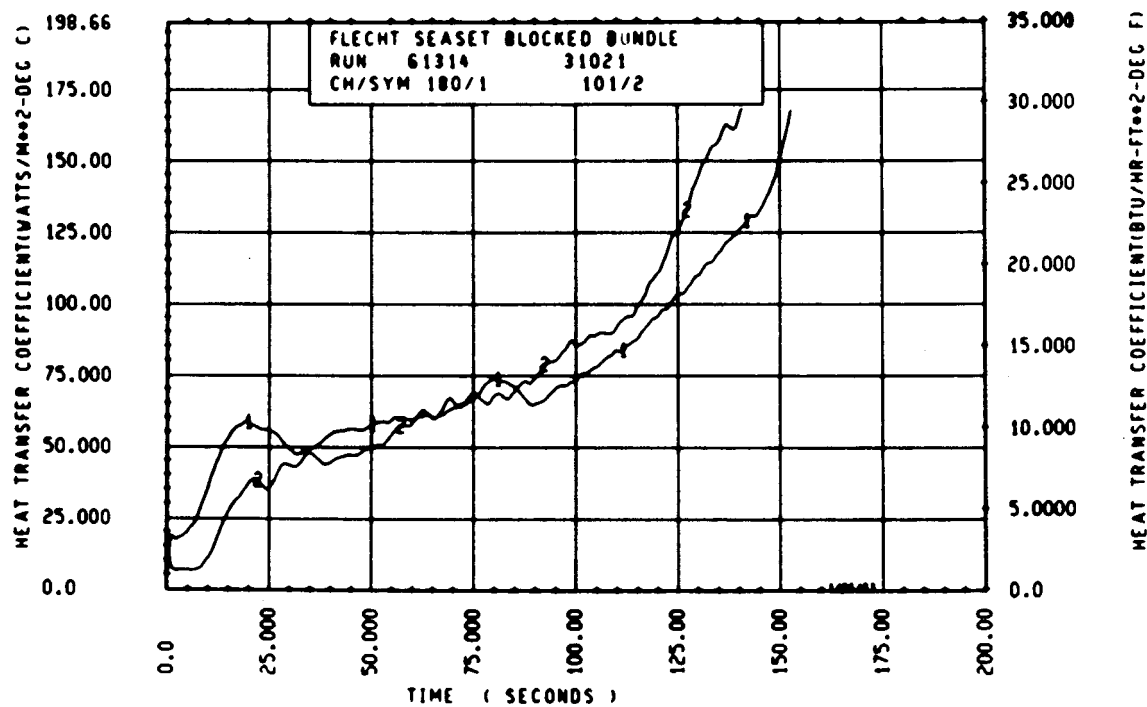
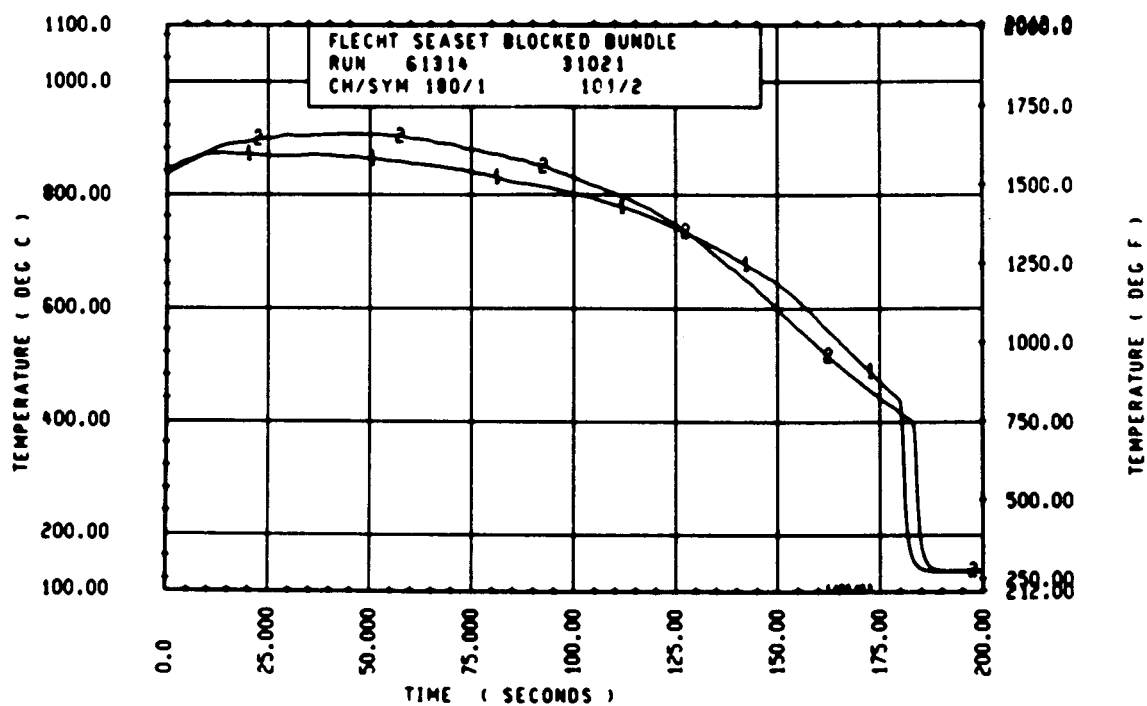
ELEV	TEMP KJQ (DEG F)			QUENCH TEMP (DEG F)			QUENCH TIME (SEC)		
	MAX	MIN	MEAN	MAX	MIN	MEAN	MAX	MIN	MEAN
12	8.4	7.3	8.0	500.0	500.0	500.3	21.1	19.9	20.6
24	16.5	14.0	15.1	614.0	599.7	604.0	40.0	37.5	38.5
34	26.1	22.4	26.5	764.1	599.7	763.4	73.9	69.5	71.1
48	42.2	33.7	38.1	713.0	574.9	697.4	97.5	94.0	95.7
60	56.3	41.2	49.3	706.3	599.0	744.9	134.9	129.4	131.0
67	59.6	42.5	51.6	794.1	636.1	728.1	153.0	143.7	149.9
69	78.3	48.7	56.3	750.1	627.9	722.0	159.0	152.0	155.5
70	55.0	46.2	55.1	817.2	743.4	777.1	151.7	154.5	156.8
71	69.8	52.0	62.1	784.3	740.5	763.3	152.0	158.0	160.6
72	65.7	47.7	55.0	813.2	754.1	776.3	150.7	160.4	163.6
73	60.7	50.4	55.3	770.5	703.2	760.3	169.9	163.2	166.1
74	78.0	48.9	54.4	815.0	695.3	761.2	177.5	162.5	170.4
75	74.3	48.7	57.3	815.2	646.0	750.4	179.0	163.0	172.4
76	70.7	47.5	56.0	830.4	751.3	770.2	174.4	167.4	174.7
77	325.1	41.2	65.1	883.1	745.6	764.0	184.1	167.2	177.9
78	66.7	10.5	53.3	960.1	249.5	781.4	197.2	171.6	179.9
79	75.2	45.7	56.3	883.4	682.0	744.7	189.7	170.4	183.5
80	94.1	51.1	64.8	839.0	751.0	744.0	192.4	182.0	186.2
81	110.1	52.0	76.4	845.1	681.4	780.9	192.6	185.5	186.6
84	65.0	49.4	55.3	794.7	640.5	693.6	203.0	190.9	199.4
86	63.9	47.7	56.2	892.4	624.8	767.2	277.1	189.4	200.0
90	86.9	50.1	67.7	870.6	622.6	740.0	217.1	203.7	211.2
96	167.1	107.0	122.5	777.2	574.2	720.1	232.1	210.1	227.2
102	172.3	86.5	121.6	711.7	535.8	645.3	246.1	195.0	237.3
111	157.3	97.3	123.8	779.4	575.1	623.0	257.1	210.0	247.5
120	225.0	120.1	184.7	834.3	493.7	611.4	274.1	83.4	246.7
132	112.4	54.1	88.5	624.0	401.5	522.9	254.0	110.7	210.0
138	137.9	44.3	85.0	660.0	509.9	577.1	231.3	128.9	198.1



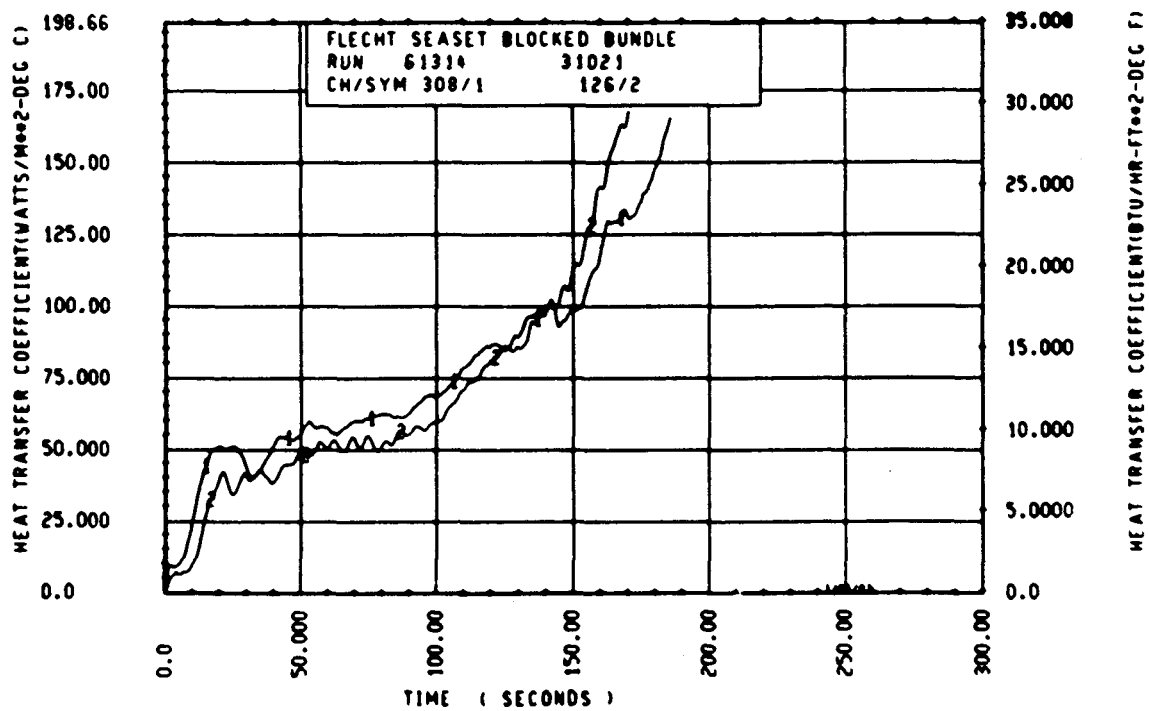
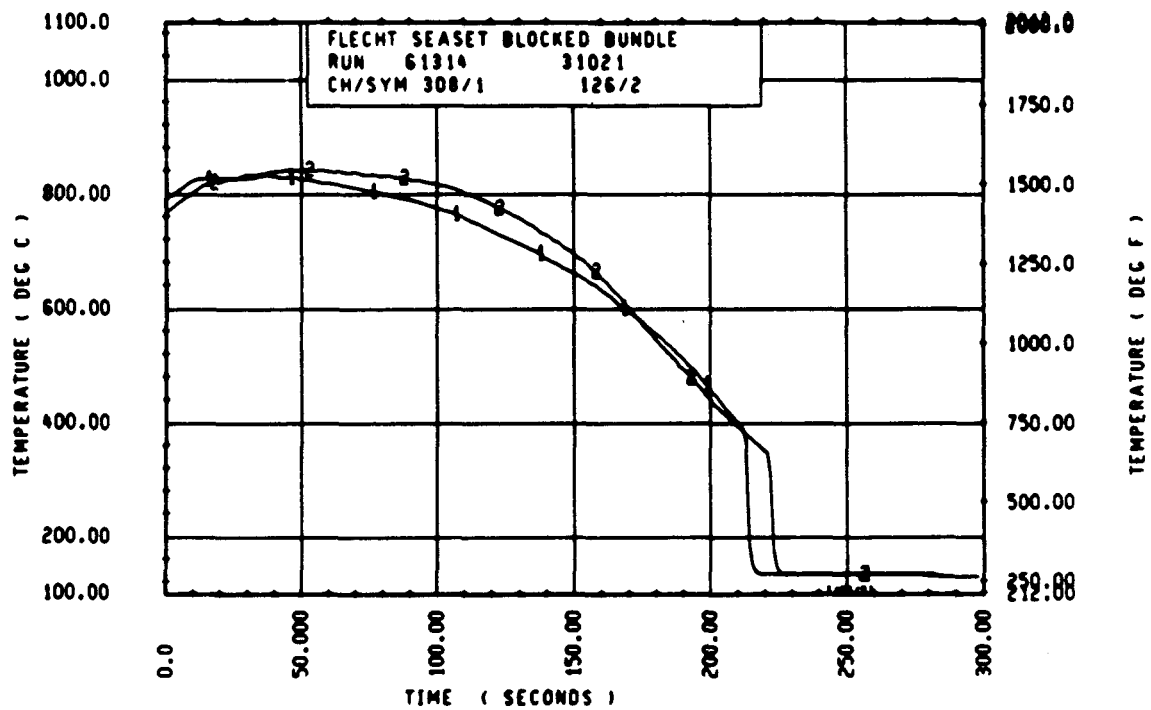
Rod 7M, 1.88 m (74 in.)



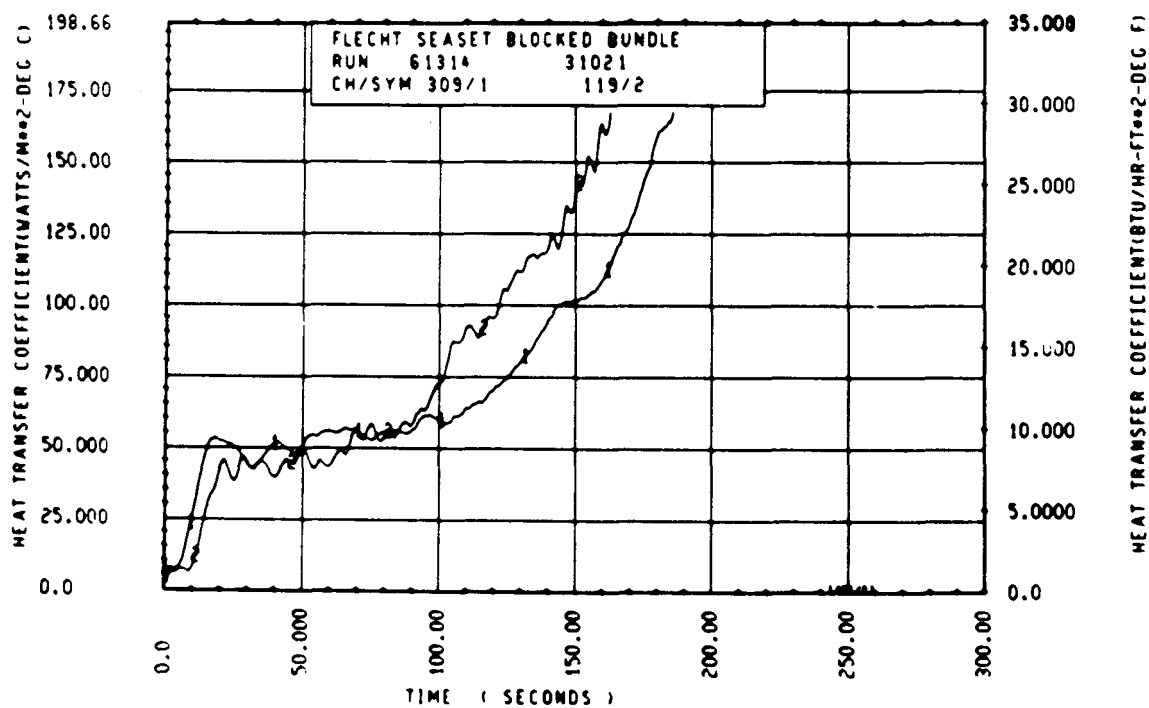
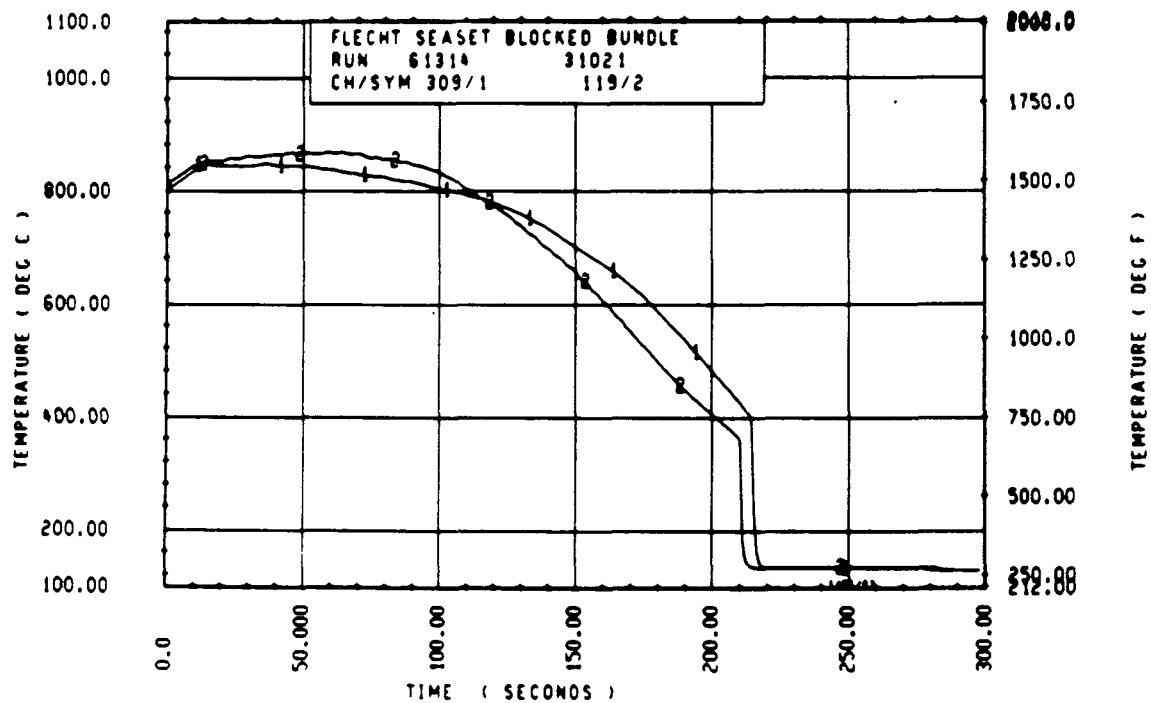
Rod 8N, 1.98 m (78 in.)



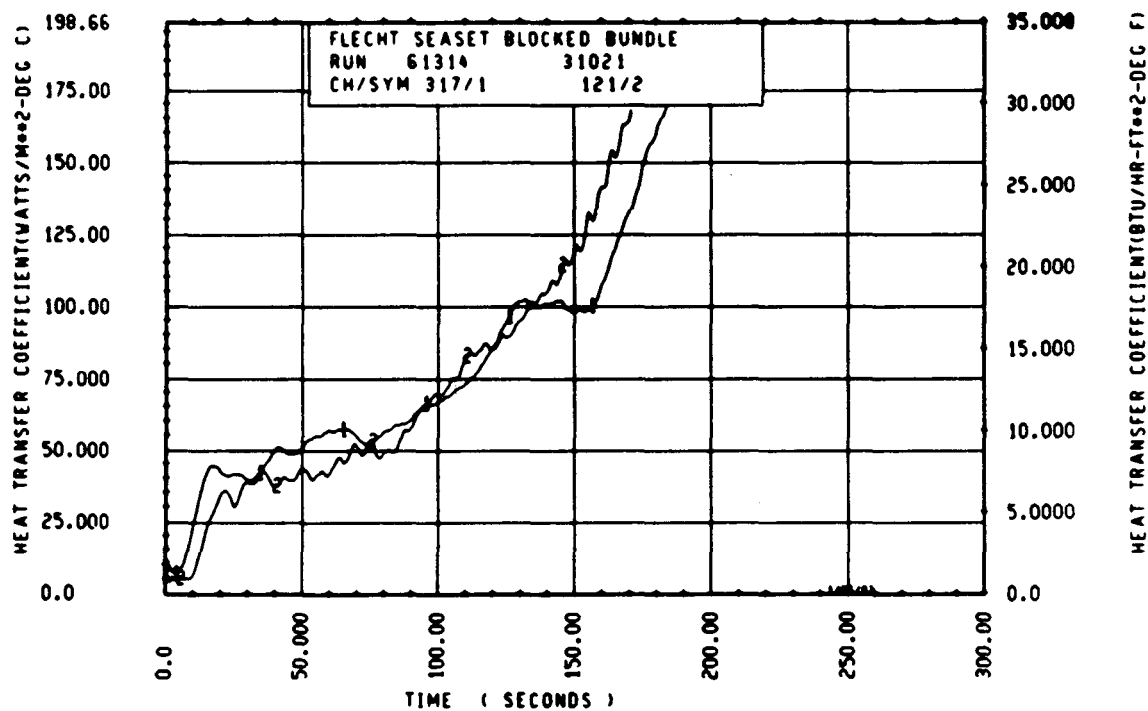
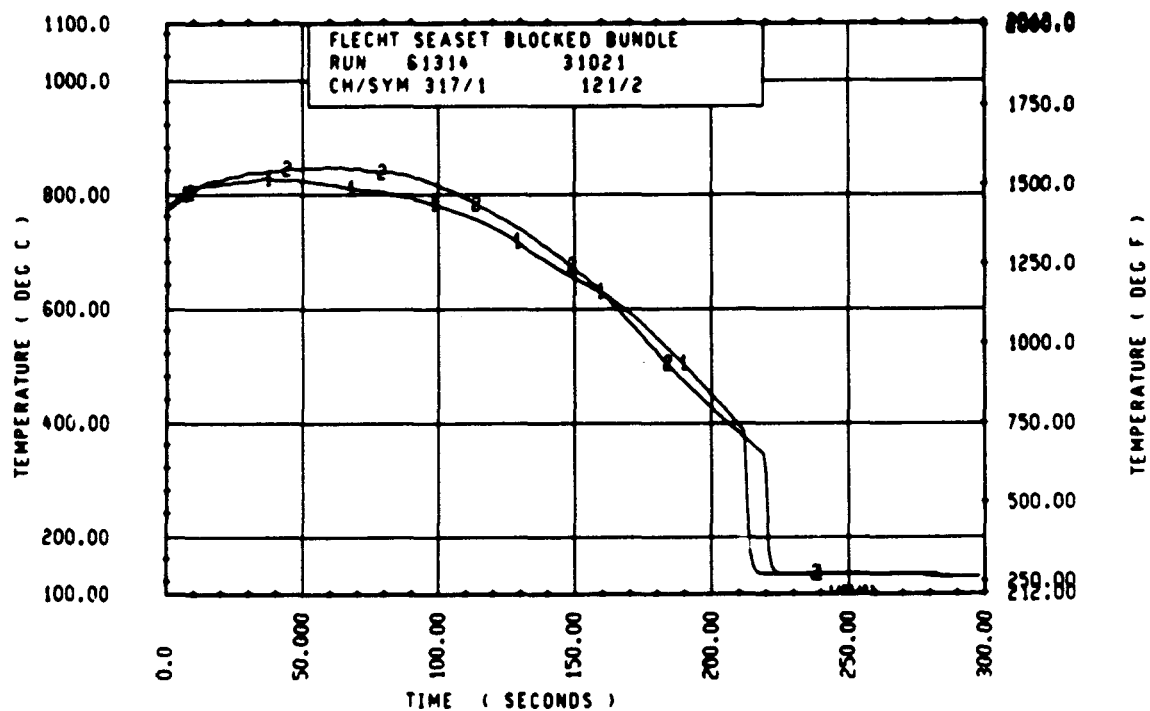
Rod 12I, 1.98 m (78 in.)



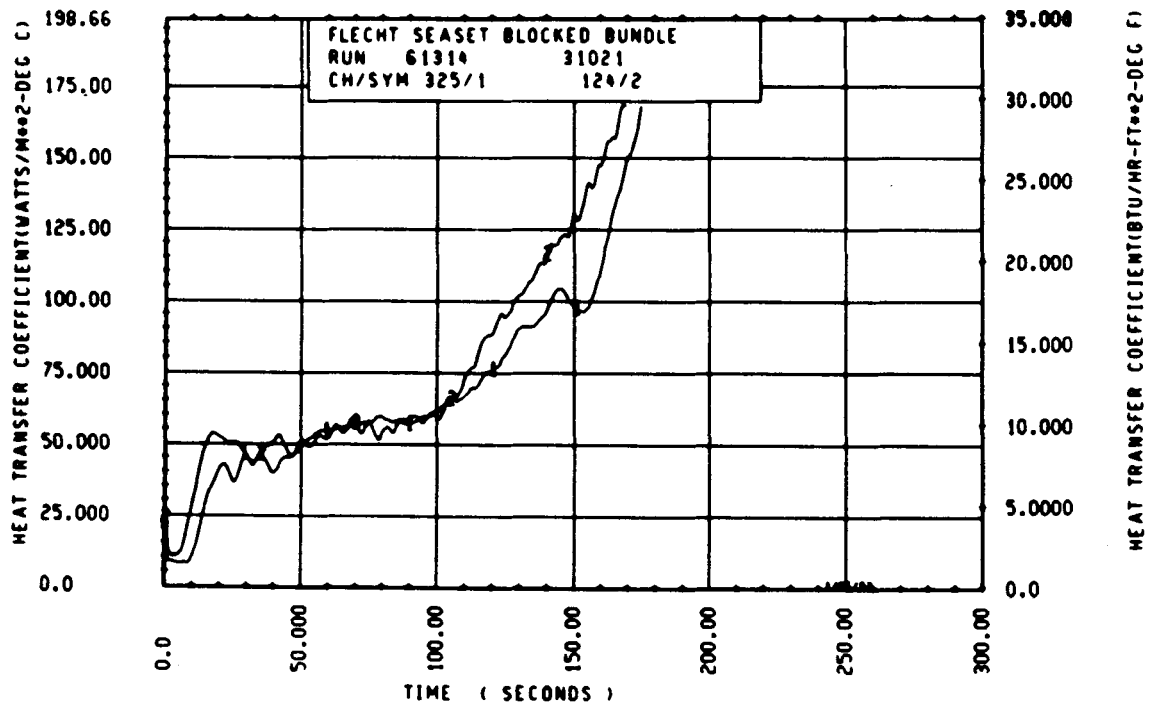
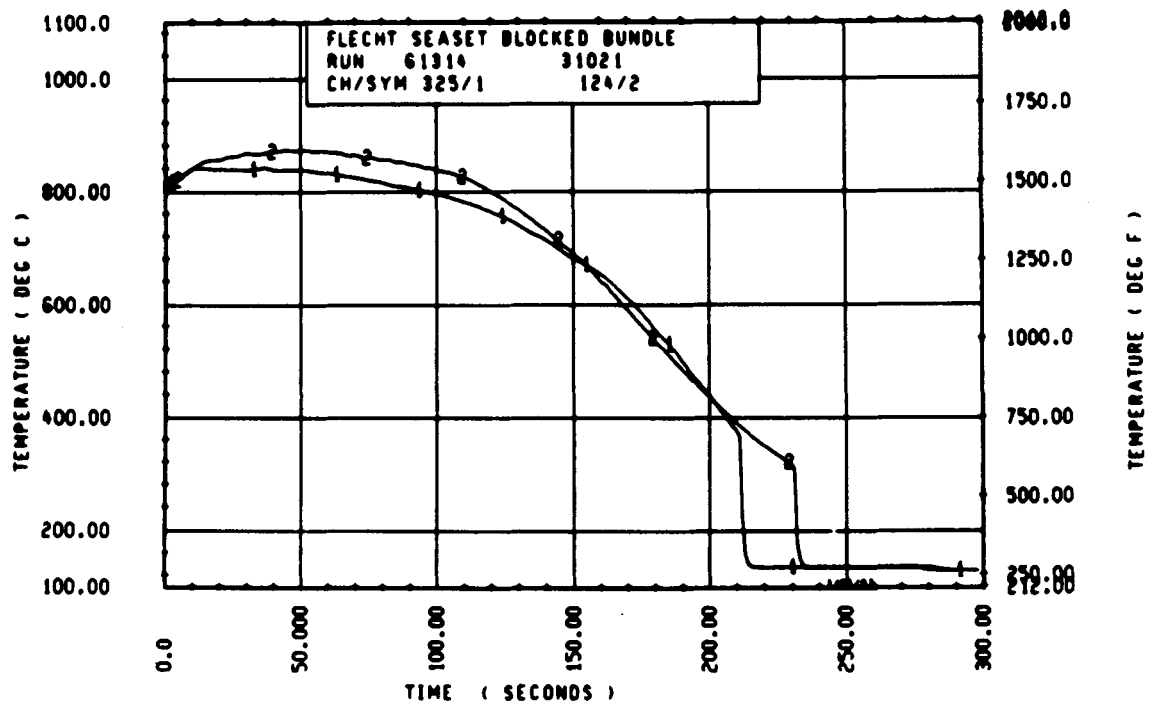
Rod 6J, 2.29 m (90 in.)



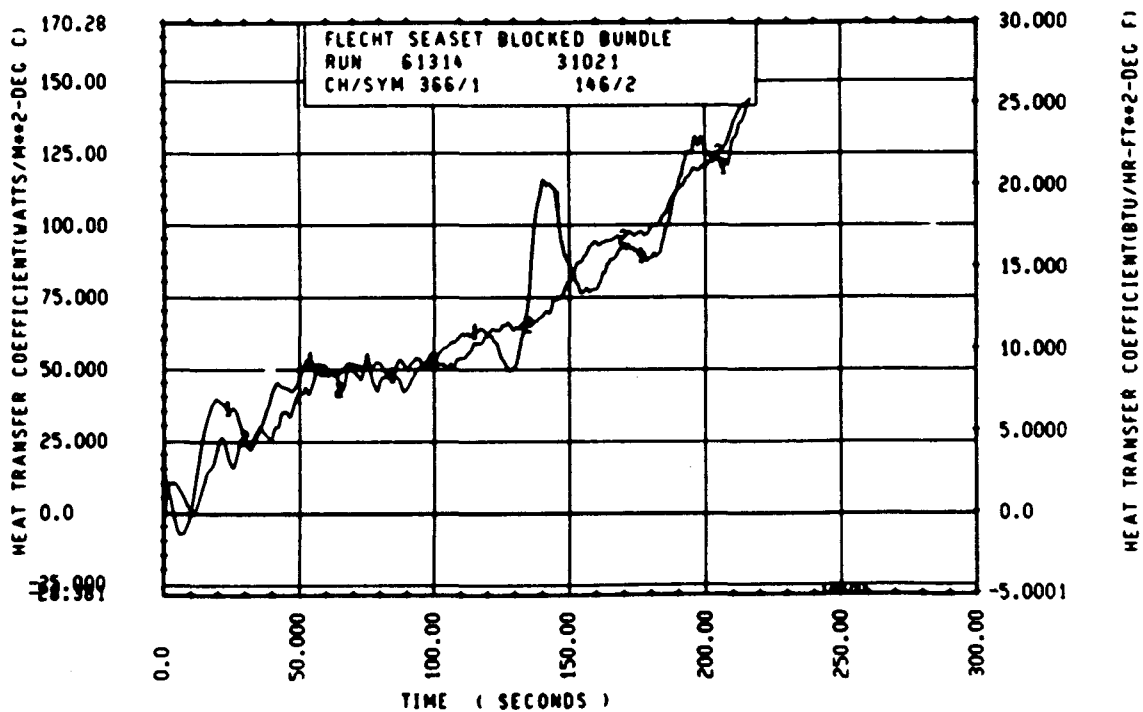
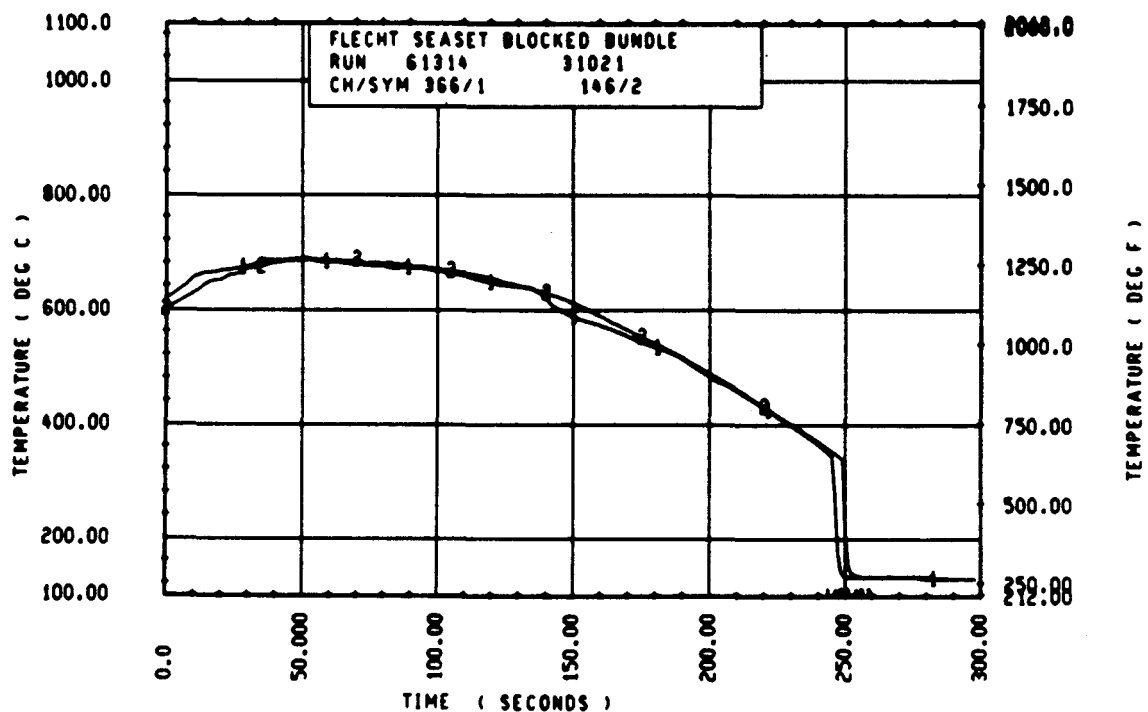
Rod 7D, 2.29 m (90 in.)



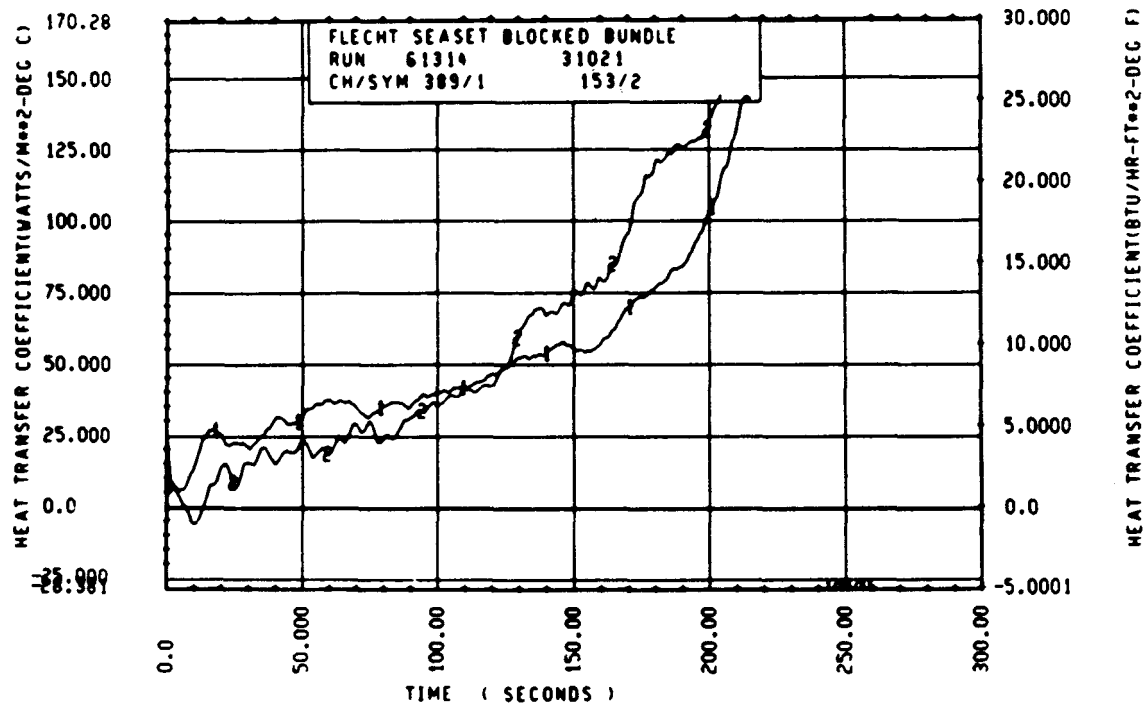
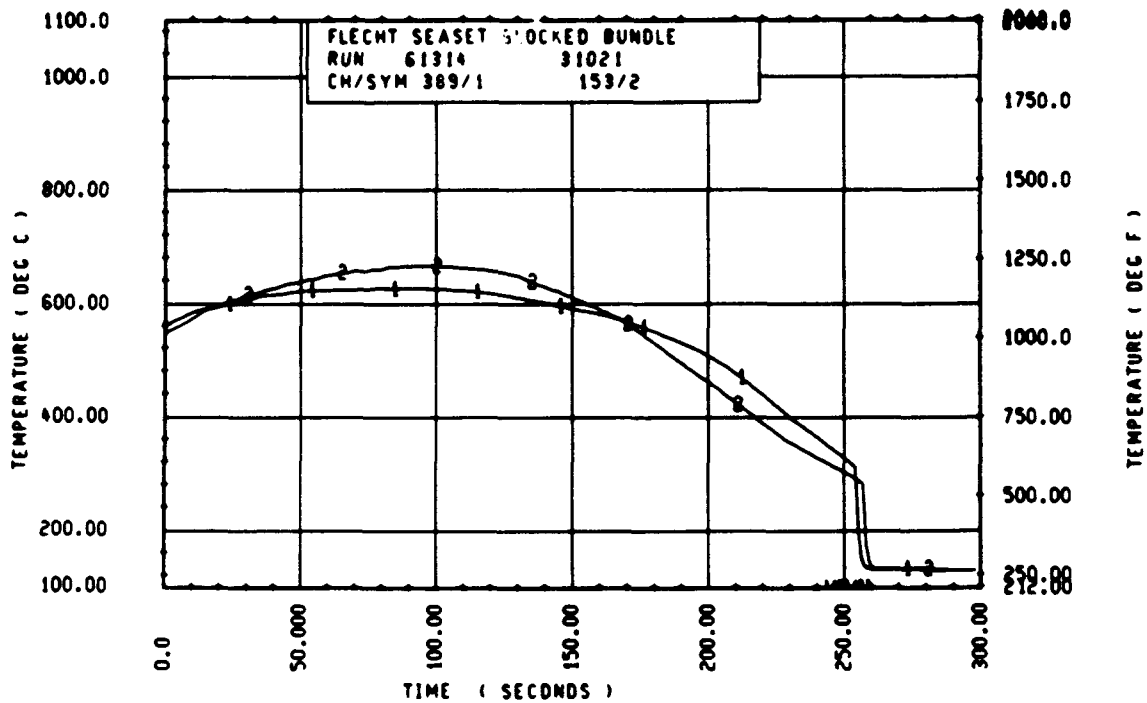
Rod 9C, 2.29 m (90 in.)



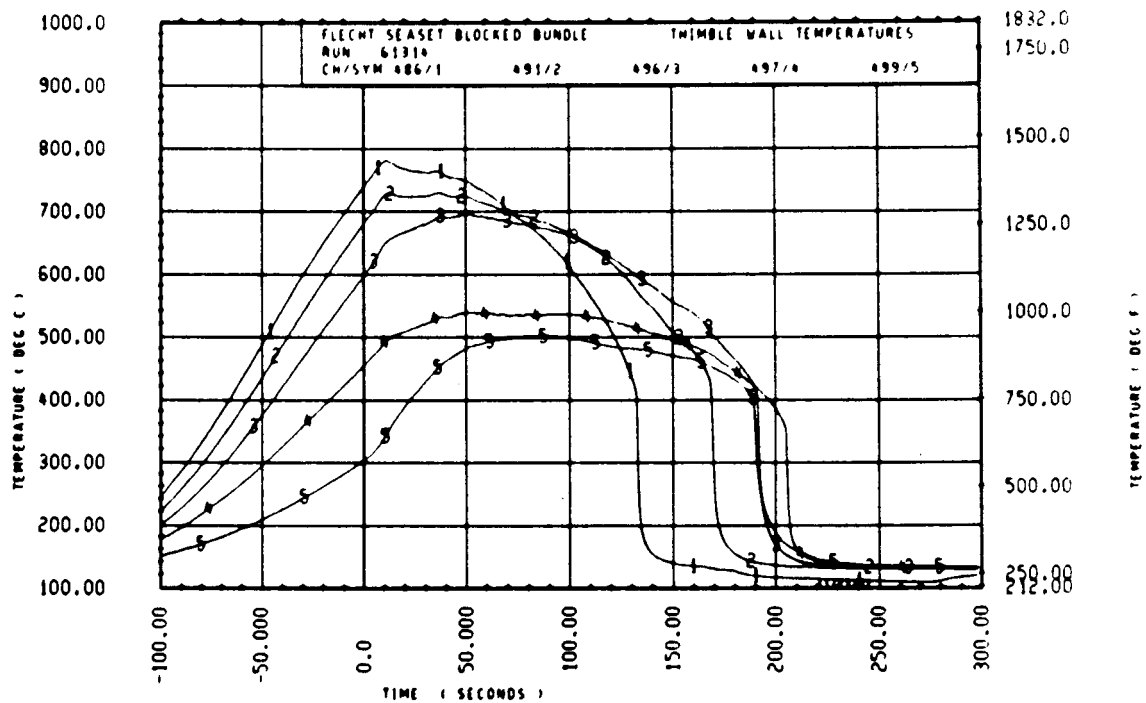
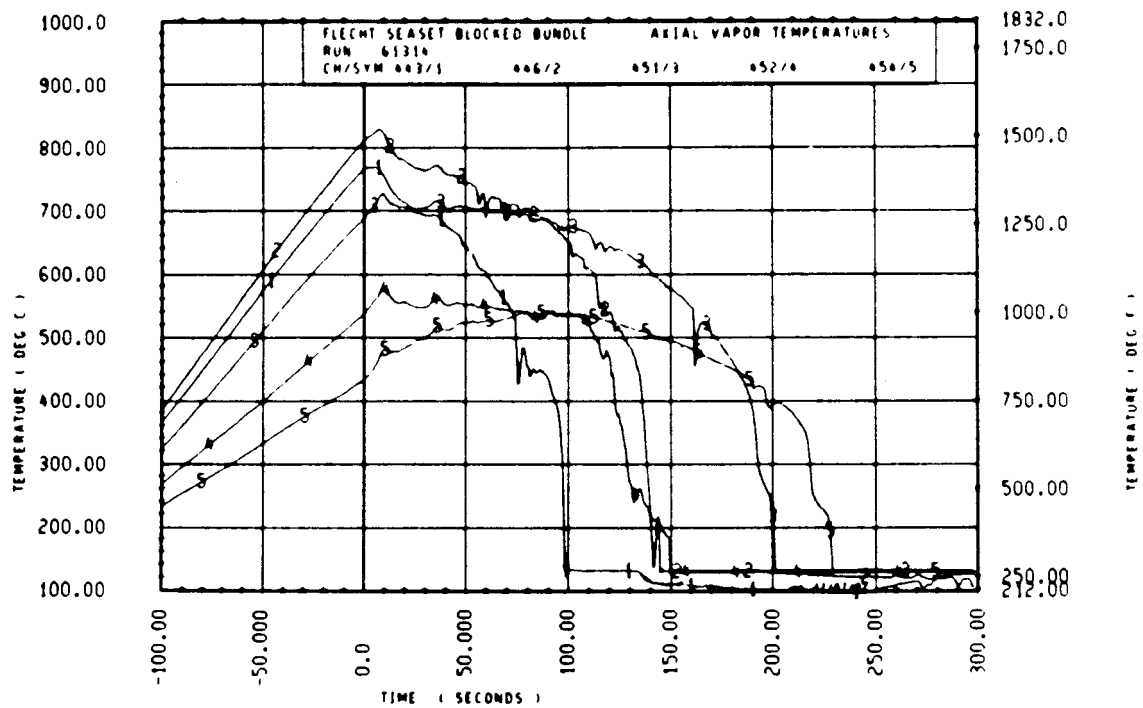
Rod 11E, 2.29 m (90 in.)

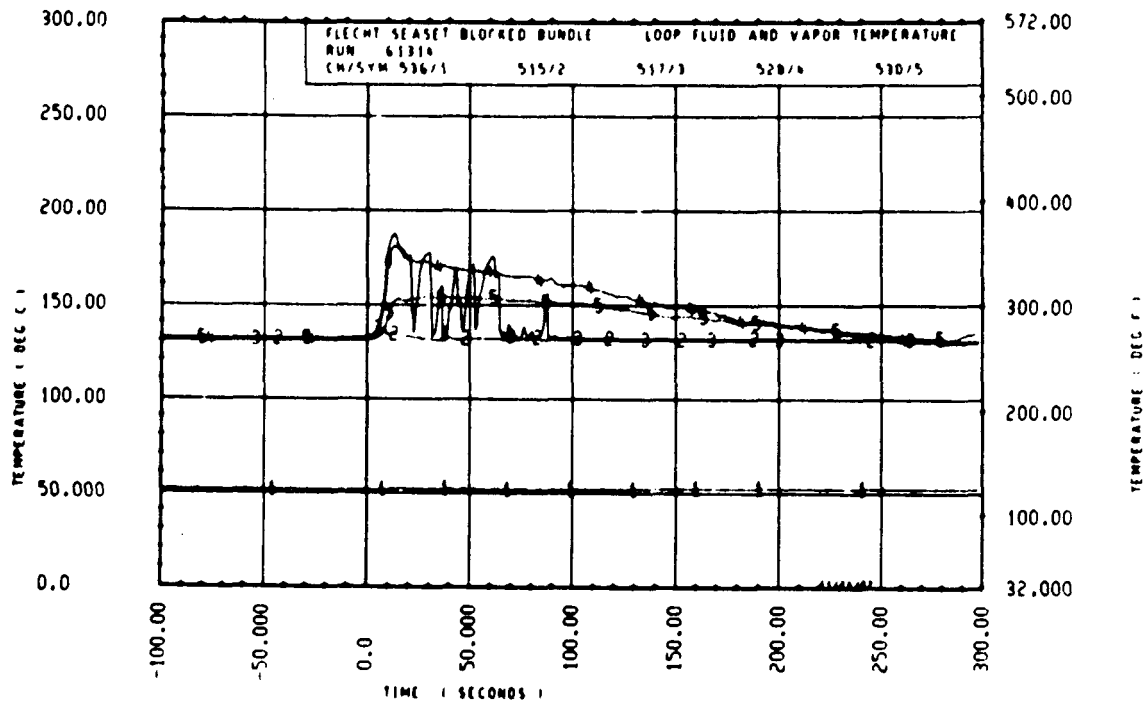
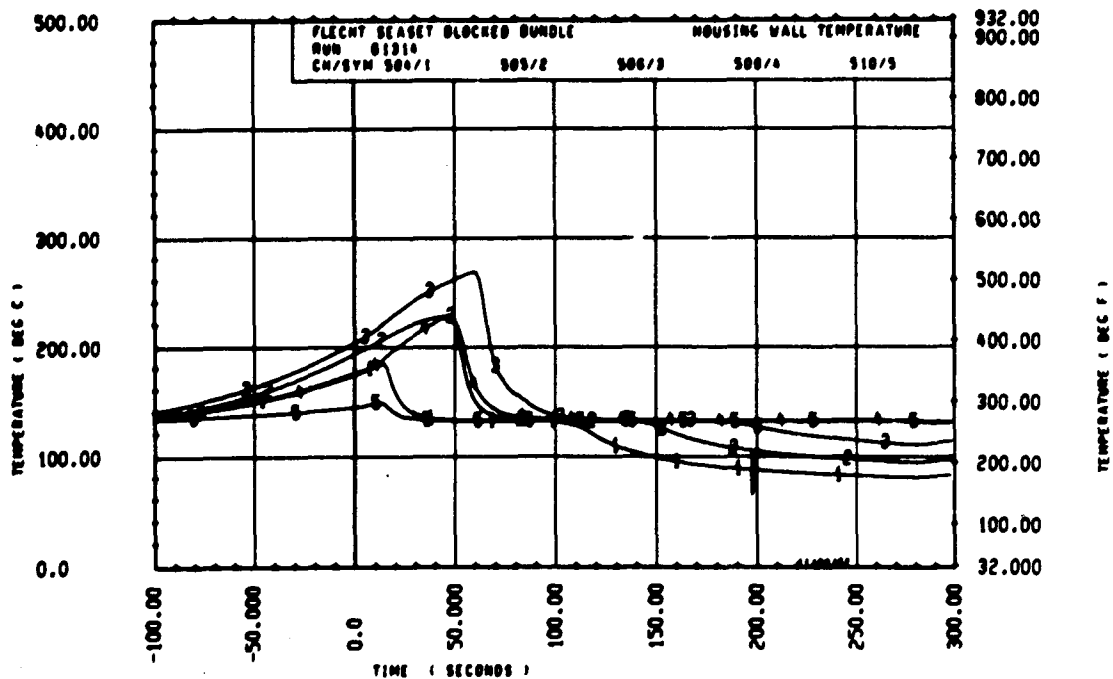


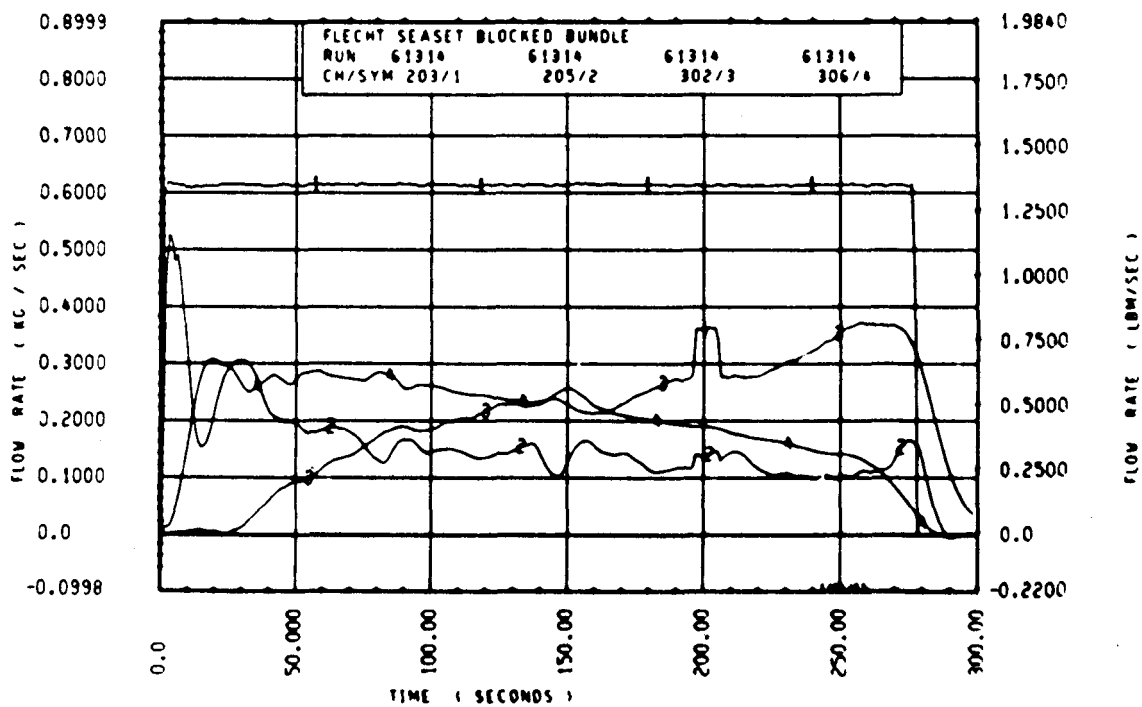
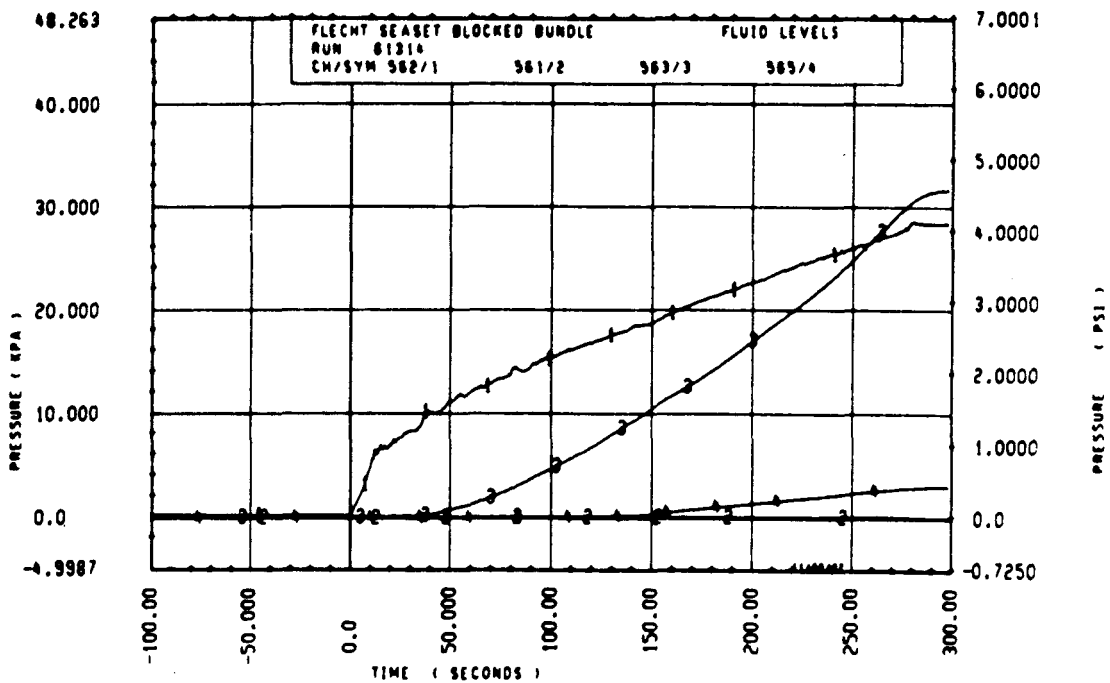
Rod 5J, 2.59 m (102 in.)

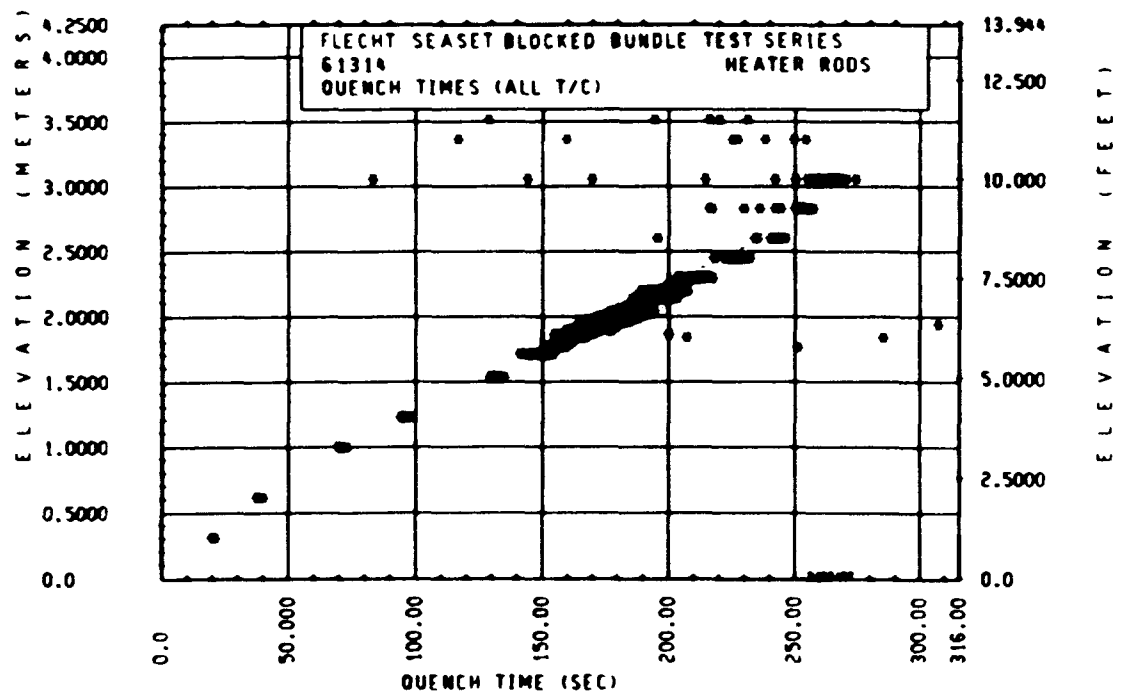
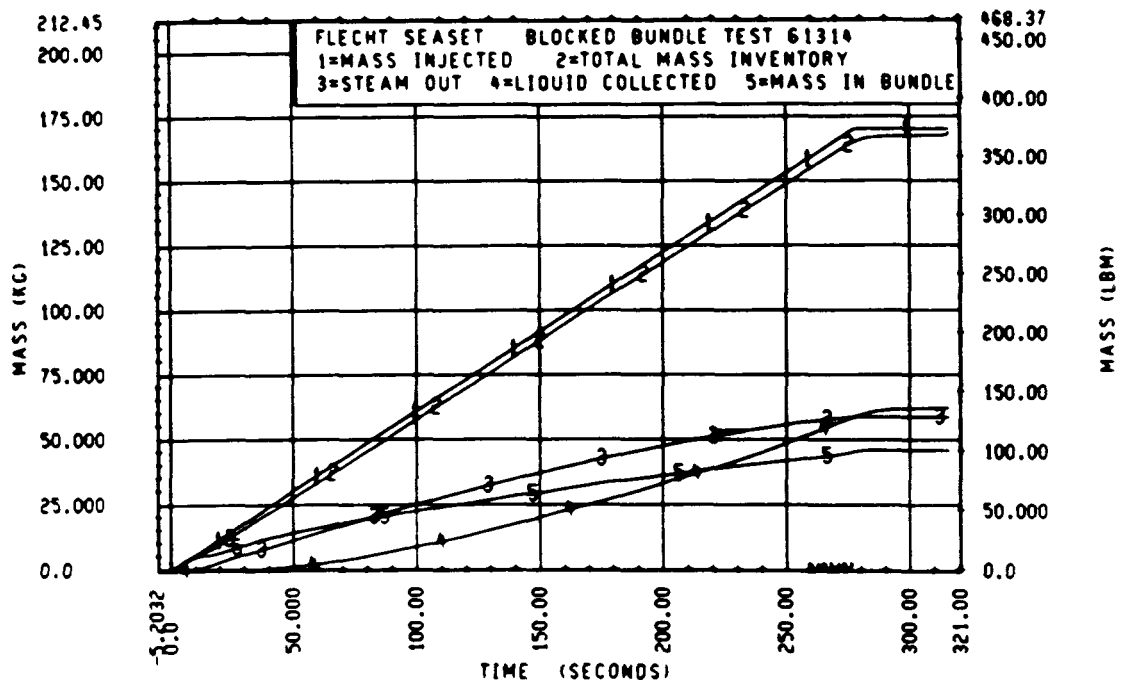


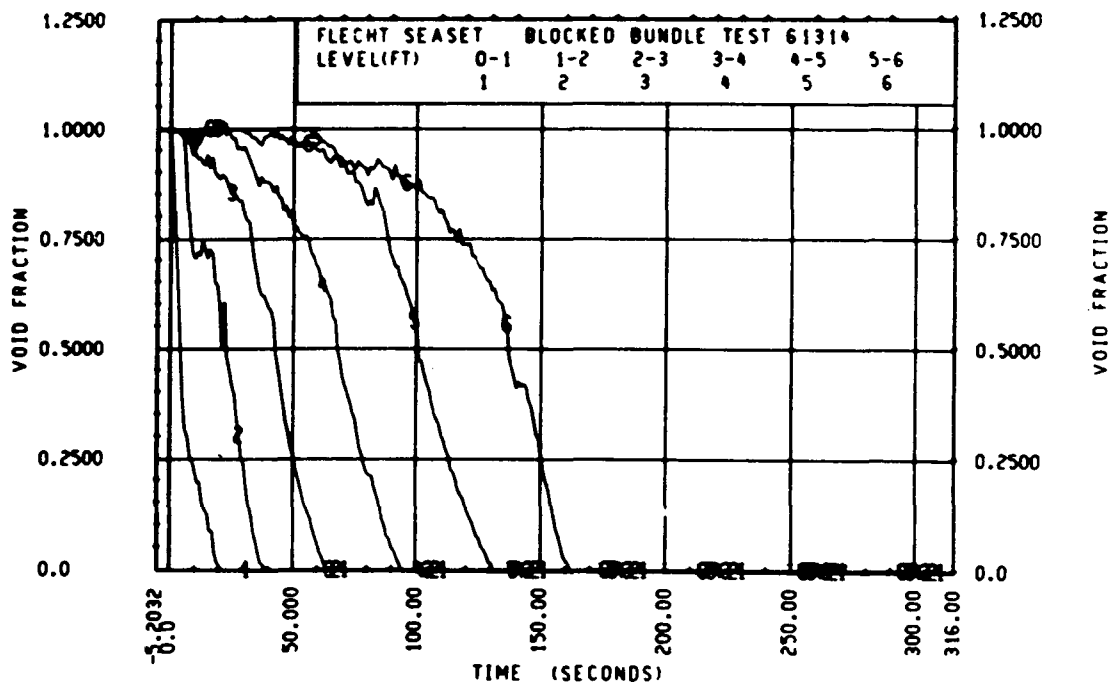
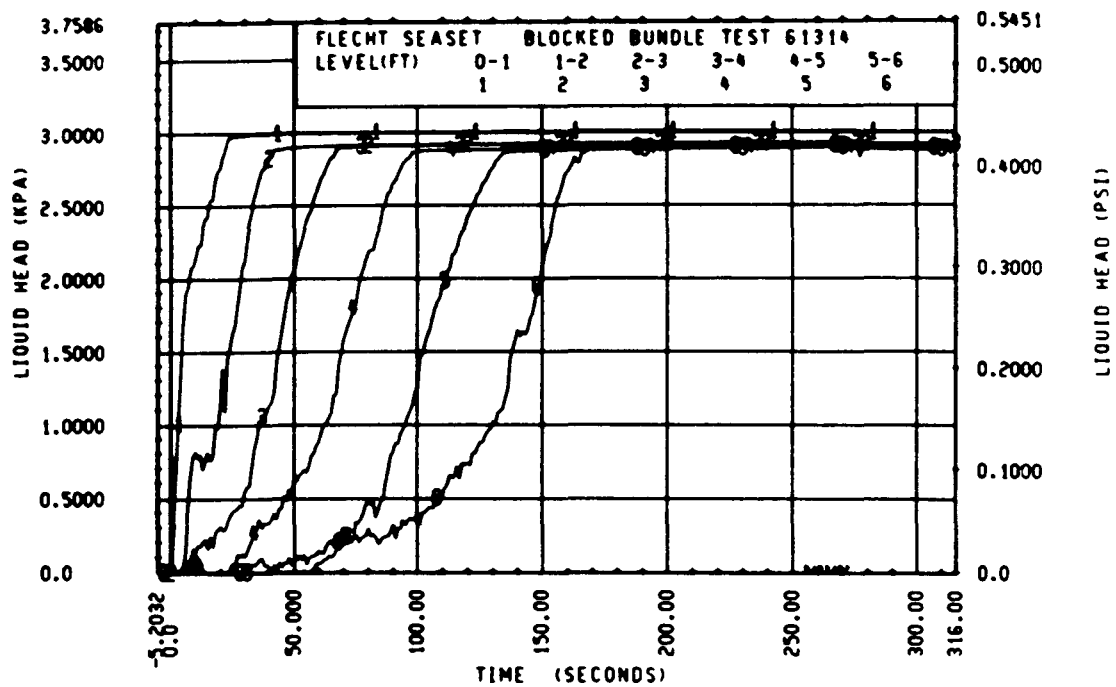
Rod 9C, 2.82 m (111 in.)

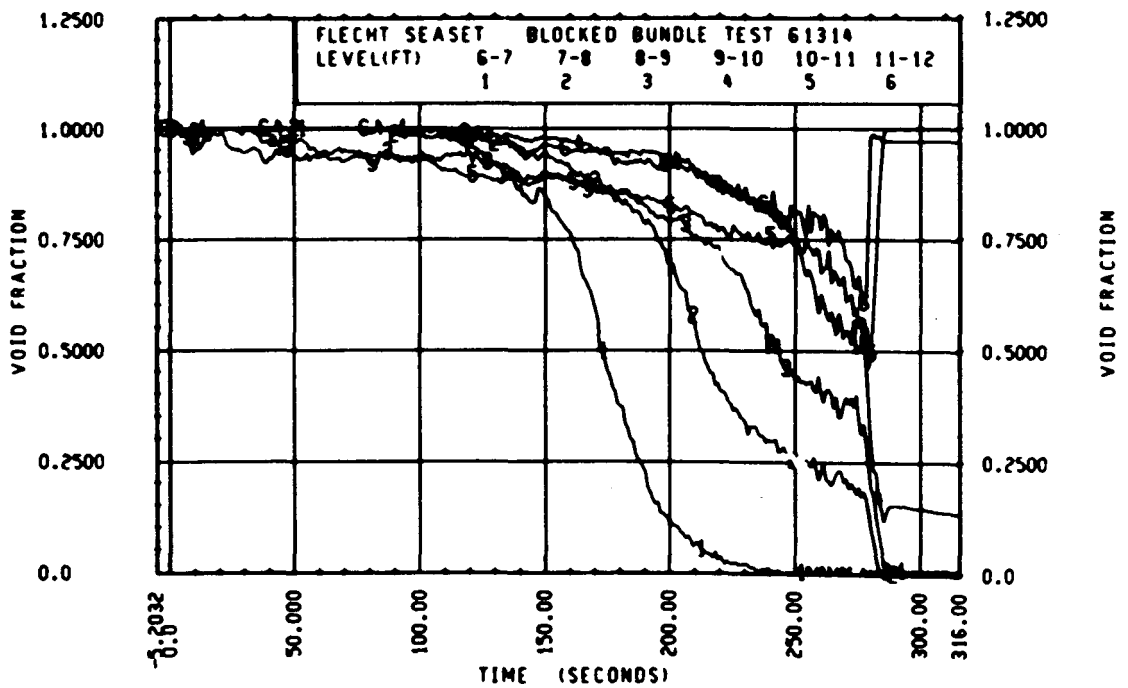
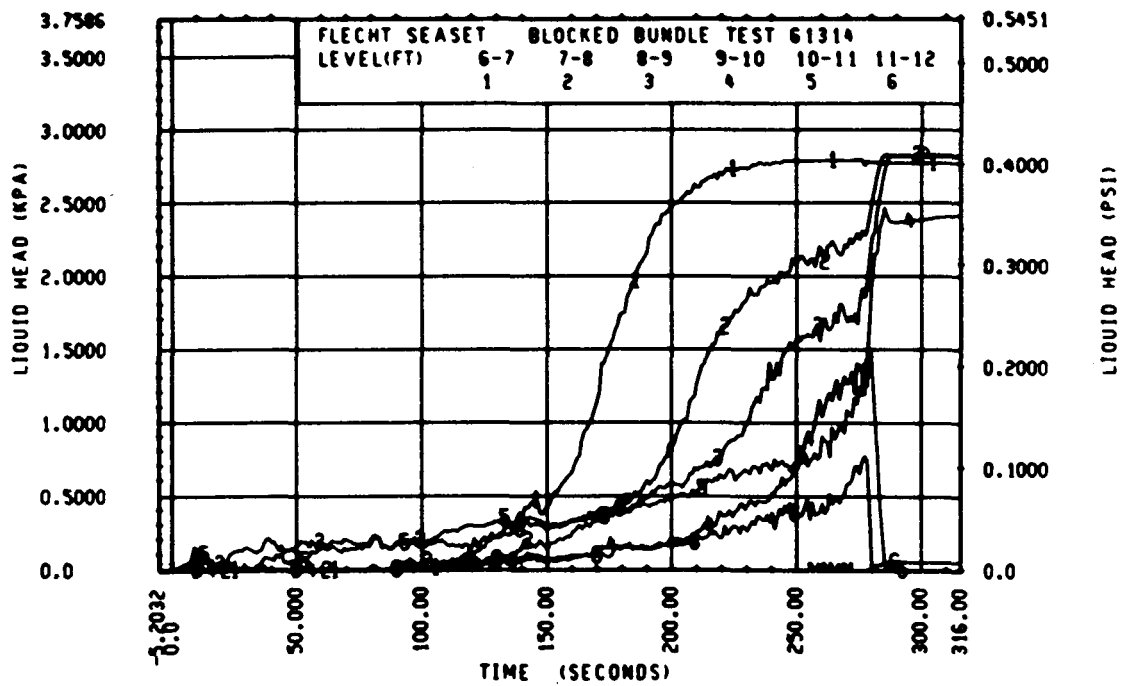












FLECHT SEASET 163-ROD BUNDLE FLOW BLOCKAGE TASK
SUMMARY AND COMMENT SHEET

Run: 61412
Test date: 9/8/82
Test type: Forced reflood
Parameter: Pressure effect

AS-RUN TEST CONDITIONS:

Upper plenum pressure	0.404 MPa (58.6 psia)
Initial peak clad temperature and location	874.7°C (1606.4°F), 8N-1.93 m (76 in.)
Initial peak rod power:	
Peripheral rods	2.26 kw/m (0.690 kw/ft)
Bypass rods	2.27 kw/m (0.691 kw/ft)
Blockage island rods	2.27 kw/m (0.691 kw/ft)
Flooding rate	24 mm/sec (0.97 in./sec) for 120 sec 26 mm/sec (1.03 in./sec) onward
Coolant temperature	63.9°C (147°F)
Initial bundle water level	-6.1 mm (-0.24 in.)

COMMENTS:

Inlet mass flow: ⁽¹⁾ -3% for 80 seconds, 0% for 40 seconds, -6.6% for
20 seconds, and -1% average thereafter
Power decay: ⁽¹⁾ peripheral rods, -1.6% constant
bypass rods, -2% constant
blockage rods, -1% constant

1. Relative to run 32013

FLECHT SEASET 163 ROD BUNDLE TEST SERIES

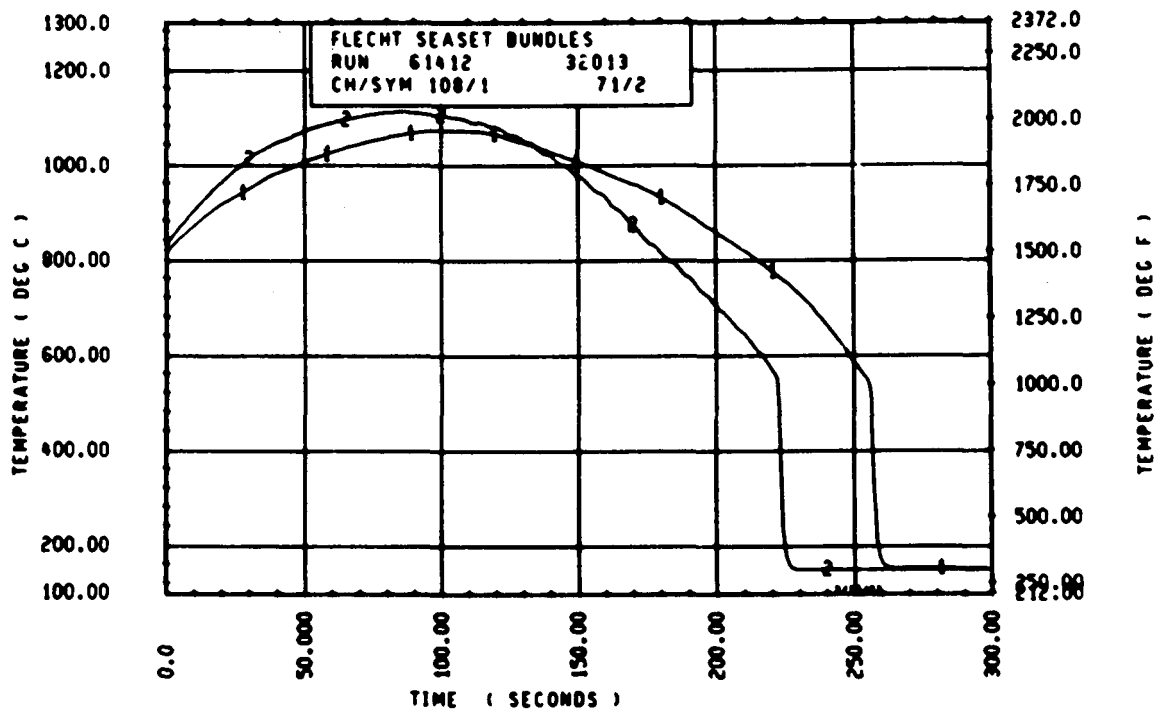
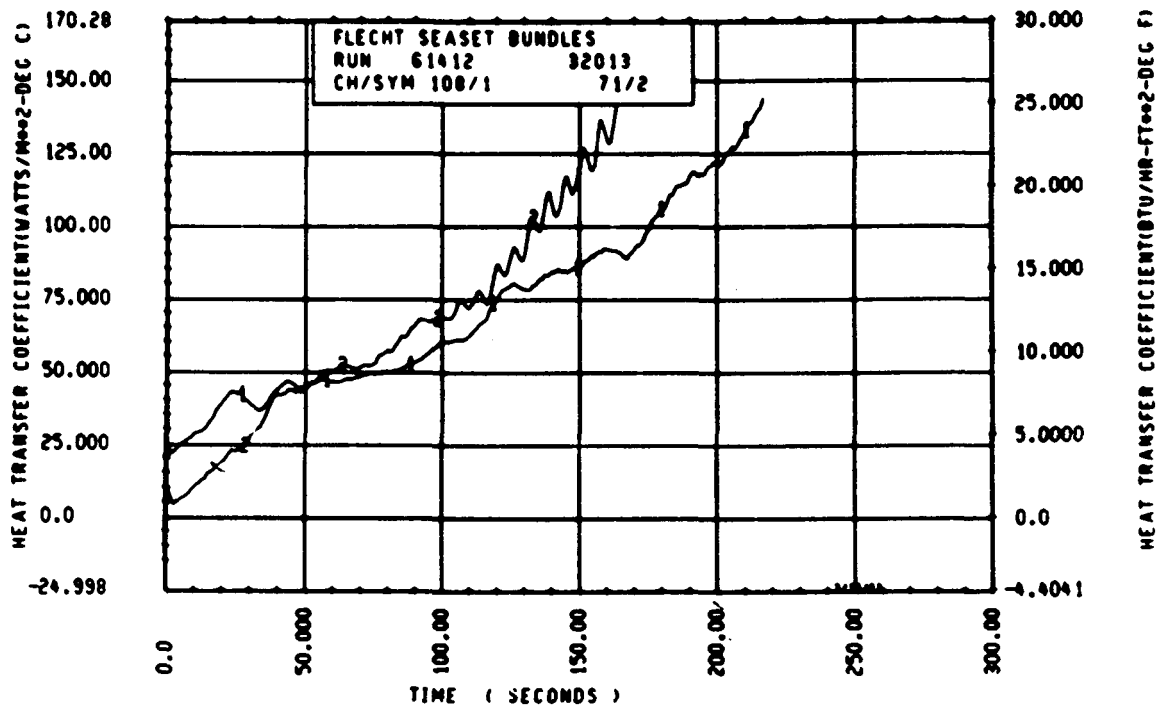
ROD/ELEV	CHAN.	NO	INITIAL AT FLOOD (DEG F)	MAXIMUM TEMPERATURE (DEG F)	TEMPERATURE RISE (DEG F)	TURNAROUND TIME (SECONDS)	QUENCH TEMPERATURE (DEG F)	QUENCH TIME (SECONDS)
96 1- C	3		697.	747.	21.	6.5	627.	19.5
10M 2- 0	6		697.	747.	52.	12.5	627.	43.4
96 3- 3	9		1230.	1333.	104.	21.5	631.	63.6
3J 4- 0	11		1300.	1347.	174.	34.5	620.	119.7
7H 4- 3	12		1351.	1394.	166.	36.5	620.	120.9
8K 4- 0	13		1373.	1371.	197.	38.5	622.	125.1
8N 4- 0	14		1363.	1350.	193.	39.0	600.	117.8
12D 4- 0	17		1356.	1320.	169.	43.0	607.	116.3
5E 5- 0	20		1320.	1307.	207.	61.0	1021.	176.4
76 5- 0	21		1369.	1327.	208.	53.0	1032.	170.4
96 5- 6	24		1348.	1321.	273.	71.5	1031.	172.4
5E 5- 7	33		1341.	1344.	340.	74.0	972.	212.4
86 5- 7	40		1347.	1343.	380.	92.0	977.	220.1
9M 5- 9	52		1407.	1341.	424.	94.5	1022.	224.4
76 5-10	55		1313.	1321.	417.	93.7	1047.	225.1
7F 5-11	62		1452.	1390.	444.	96.5	1021.	230.0
46 5-11	64		1535.	1310.	381.	78.5	937.	241.1
21 6- 0	67		1500.	1349.	301.	84.5	1004.	234.1
3D 6- 0	70		1444.	1361.	341.	83.5	1012.	238.6
0J 6- 0	74		1532.	1390.	365.	85.5	943.	245.6
7M 6- 0	66		1552.	1330.	380.	83.0	945.	230.0
11E 6- 0	67		1562.	1390.	330.	79.0	940.	240.1
8M 6- 2	97		1375.	1364.	444.	119.0	80.	267.4
3H 6- 2	99		1545.	1340.	404.	93.0	944.	250.0
9E 6- 2	105		1313.	1337.	363.	122.5	1039.	249.0
8H 6- 3	111		1417.	1385.	468.	111.0	932.	272.1
46 6- 3	124		1556.	1369.	410.	91.0	903.	266.1
11H 6- 4	134		1461.	1343.	414.	109.5	833.	276.4
9D 6- 4	143		1500.	1383.	447.	96.5	944.	272.1
9J 6- 5	165		1529.	1370.	440.	110.0	940.	286.0
9M 6- 5	166		1509.	2000.	441.	83.0	1030.	269.1
8J 6- 6	192		1573.	2000.	427.	97.0	930.	286.1
3D 6- 6	193		1564.	2023.	459.	90.5	1012.	284.1
11F 6- 6	173		1502.	1380.	420.	97.7	977.	274.0
46 7- 0	201		1511.	1317.	410.	97.5	620.	310.1
7D 7- 6	309		1495.	2006.	513.	134.5	922.	356.1
76 7- 6	312		1532.	2000.	505.	119.5	920.	351.2
11E 7- 6	325		1464.	1344.	510.	135.5	920.	351.1
3L 8- 0	337		1314.	1313.	600.	109.0	830.	364.7
7H 8- 0	345		1343.	1372.	631.	122.5	623.	364.3
7K 8- 0	346		1373.	1367.	543.	110.0	821.	361.4
5J 8- 6	366		1150.	1748.	642.	96.0	733.	412.1
78 8- 6	368		1137.	1763.	626.	130.0	720.	408.0
7E 9- 3	383		1116.	1616.	701.	185.5	700.	431.2
8H 9- 3	387		1060.	1737.	677.	197.5	700.	430.2
9C 9- 3	389		1055.	1649.	643.	146.0	700.	435.2
11F 9- 3	394		1059.	1673.	610.	171.5	600.	422.2
7810- 0	408		868.	1021.	603.	154.0	700.	460.2
8H10- 0	415		869.	1003.	712.	206.2	674.	454.2
5K10- 0	417		870.	1000.	704.	172.0	600.	407.2
8N10- 0	418		697.	1037.	640.	147.0	717.	407.2
6H11- 0	429		709.	1100.	471.	106.5	500.	467.2
9611- 0	431		703.	1342.	639.	213.2	920.	336.0
11E11- 0	432		704.	1020.	616.	107.5	571.	463.2
5J11- 6	436		687.	1121.	434.	159.5	644.	454.4
7811- 6	437		661.	1040.	504.	194.5	603.	420.4
8J11- 6	438		702.	1073.	376.	157.5	540.	466.2

RUN 61412 HEATER ROD STATISTICAL DATA

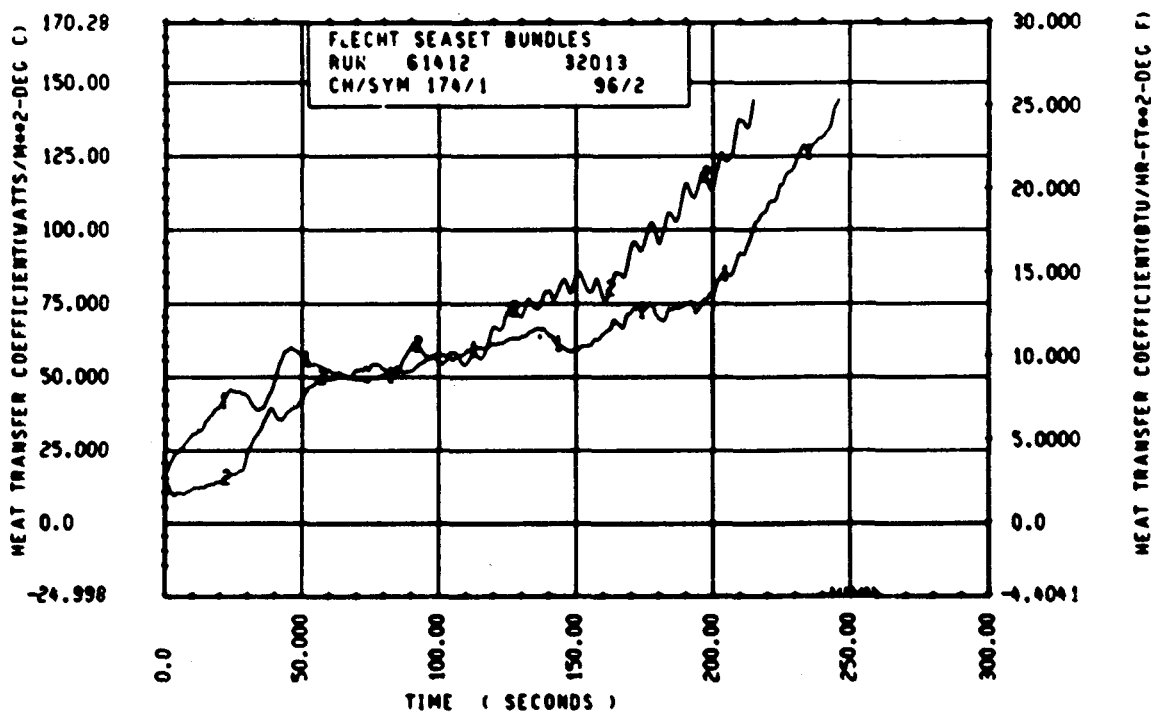
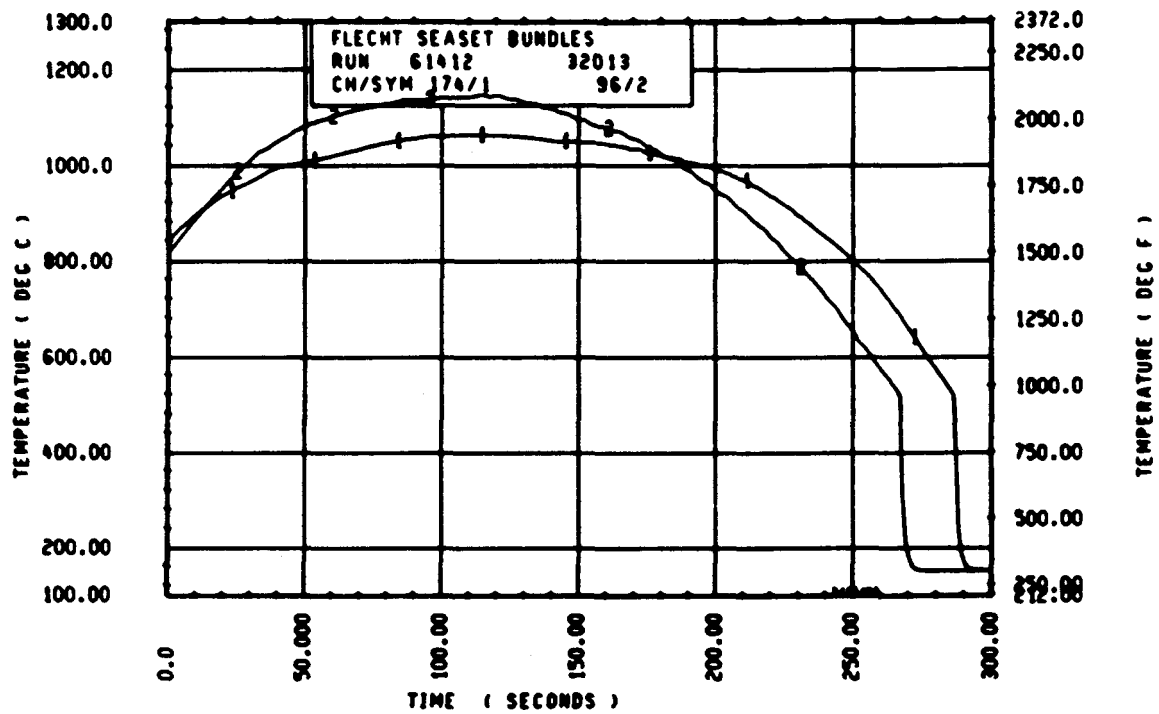
ELEV	INITIAL TEMP (DEG F)			MAX TEMP (DEG F)			TURNAROUND TIME (SEC)		
	MAX	MIN	MEAN	MAX	MIN	MEAN	MAX	MIN	MEAN
12	697.4	695.2	696.3	717.2	713.6	715.4	6.5	6.5	6.5
24	896.7	871.4	884.1	947.2	910.5	928.3	12.5	12.0	12.3
36	1229.5	1182.7	1206.1	1333.2	1247.3	1290.0	35.0	21.0	26.5
48	1382.8	1351.1	1366.0	1576.0	1529.0	1552.1	43.5	36.5	38.7
60	1569.5	1531.0	1550.3	1854.6	1714.4	1784.0	71.5	51.5	57.6
67	1500.9	1515.1	1508.1	1526.6	1547.5	1537.1	92.0	84.0	73.9
69	1535.9	1487.3	1511.6	1411.4	1552.7	1484.2	94.5	73.0	83.3
70	1630.9	1491.5	1554.6	1420.0	1665.9	1493.0	94.5	76.0	84.3
71	1534.8	1452.0	1497.9	1410.0	1673.8	1540.0	96.5	78.5	84.3
72	1651.9	1475.4	1563.8	1465.1	1690.5	1531.4	100.0	73.0	83.4
73	1589.0	1477.7	1533.7	1465.1	1670.1	1491.0	95.5	69.0	82.3
74	1598.7	1375.4	1514.3	1475.7	1664.3	1441.6	119.0	80.0	94.5
75	1500.9	1416.8	1458.1	1974.2	1600.2	1930.4	111.0	73.0	90.1
76	1506.4	1467.0	1536.7	2005.7	1433.2	1972.7	117.5	83.0	93.5
77	1589.0	1484.4	1536.4	2020.4	1403.3	1973.1	136.5	81.0	102.1
78	1505.3	1515.5	1510.4	2024.1	1424.1	1990.5	135.5	81.5	99.7
79	1503.1	1508.8	1506.2	2053.7	1414.4	1997.2	134.5	82.5	102.0
80	1542.5	1505.5	1524.0	2057.2	1431.6	2018.4	135.0	82.0	104.0
81	1577.1	1464.9	1521.4	2030.5	1435.5	2012.8	126.0	93.0	107.1
84	1555.0	1449.9	1502.9	1466.8	1634.4	1441.3	130.5	80.0	98.3
86	1569.0	1477.7	1523.1	2023.5	1467.0	1967.2	135.5	78.5	102.4
90	1534.8	1406.1	1469.0	2054.6	1439.9	2014.2	130.5	93.0	112.0
96	1434.9	1153.7	1347.4	2042.0	1674.5	1900.5	172.0	108.0	132.7
102	1200.3	1030.7	1115.3	1694.2	1703.5	1698.0	185.5	96.0	132.1
111	1116.4	1055.5	1087.2	1810.1	1630.1	1718.2	214.2	108.0	165.6
120	939.1	831.5	879.6	1767.7	1473.2	1600.4	216.2	144.0	184.2
132	710.9	694.5	702.0	1350.1	1175.5	1261.6	223.2	160.0	181.0
138	702.6	554.5	679.3	1311.0	1073.0	1190.2	215.2	159.0	189.0

RUN 61412 HEATER ROD STATISTICAL DATA

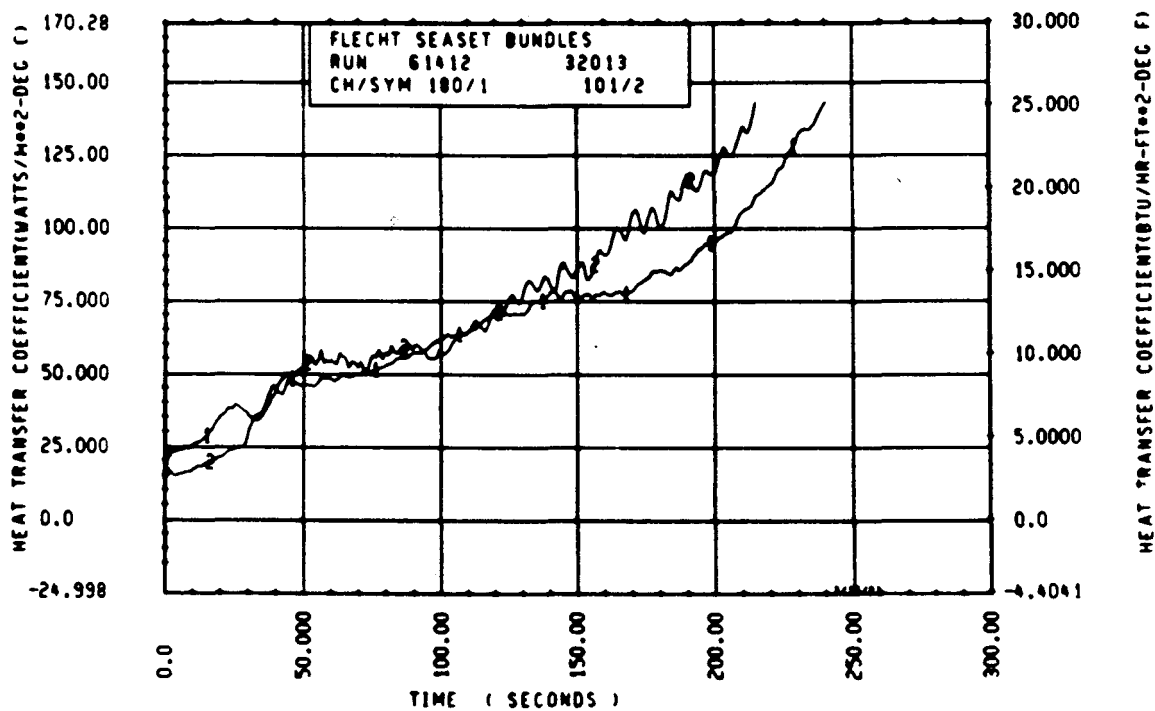
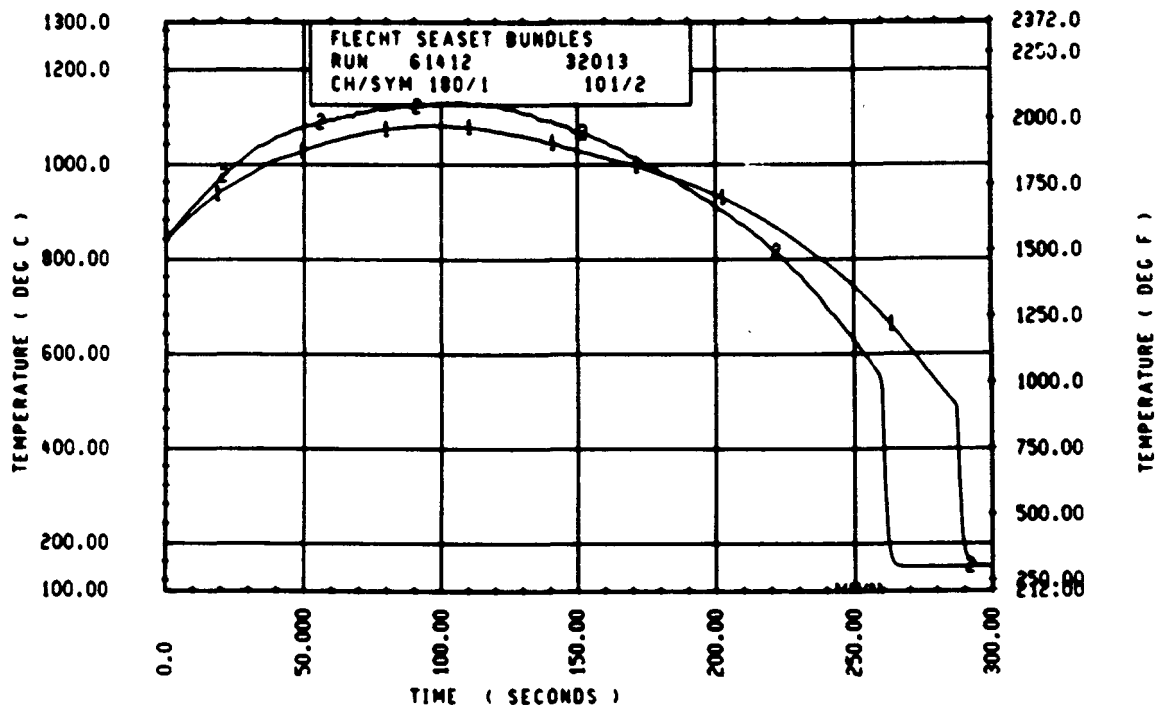
ELEV	TEMP K152 (DEG F)			QUENCH TEMP (DEG F)			QUENCH TIME (SEC)		
	MAX	MIN	MEAN	MAX	MIN	MEAN	MAX	MIN	MEAN
12	19.0	14.3	16.8	616.5	600.5	608.0	21.0	19.0	20.4
24	50.5	45.5	46.2	690.1	607.0	608.0	43.4	43.7	42.0
36	120.0	92.9	107.0	637.4	622.5	630.0	85.2	82.0	84.0
48	149.3	105.7	167.1	660.7	611.0	641.4	125.1	117.8	120.1
60	239.2	237.1	270.1	1034.0	932.4	993.5	182.4	170.9	175.6
67	381.9	284.0	320.0	1022.0	925.2	984.5	220.1	204.1	211.0
69	424.1	341.5	364.9	1022.0	951.0	976.2	229.0	214.8	223.0
70	426.7	316.2	368.4	1048.6	921.0	997.2	237.0	223.0	228.1
71	444.5	345.5	392.7	1025.4	903.4	996.7	243.1	224.4	235.0
72	465.0	335.7	363.1	1009.1	911.4	987.4	249.1	230.0	241.8
73	431.4	351.3	384.3	1034.0	933.1	992.1	255.1	238.0	246.3
74	496.7	364.9	427.3	1020.1	776.6	953.5	273.1	250.4	257.4
75	458.4	357.5	413.3	1010.4	758.6	967.0	275.9	244.8	263.4
76	481.0	367.0	422.1	1034.0	838.4	941.0	277.7	250.0	268.0
77	480.7	371.5	427.7	1020.2	820.1	947.1	288.3	264.1	274.8
78	470.5	397.2	430.0	1011.0	770.5	944.1	295.1	272.5	284.8
79	436.8	380.1	434.6	1030.1	722.1	944.4	293.7	270.1	290.0
80	528.9	414.4	471.2	1062.0	821.4	934.5	303.1	280.7	296.9
81	552.6	432.1	463.4	984.3	883.2	935.0	311.0	295.1	303.4
84	476.2	384.4	415.4	960.7	762.0	814.4	326.7	310.5	318.0
86	476.3	371.8	426.1	940.7	813.0	880.0	339.6	314.2	328.0
90	557.4	443.9	515.2	957.0	804.9	911.0	364.1	340.4	352.3
95	732.6	544.2	619.1	930.7	810.1	869.7	391.1	370.3	380.9
102	739.4	590.6	646.3	866.0	637.8	737.3	419.5	343.1	406.7
111	716.3	544.5	639.0	910.1	711.2	773.7	440.2	411.2	430.5
120	518.4	540.4	723.3	1240.0	504.0	730.4	466.2	241.0	442.6
132	639.1	470.7	575.8	919.7	554.9	633.8	471.5	336.0	447.3
138	643.1	376.4	510.9	1027.0	545.5	602.4	466.2	275.0	395.7



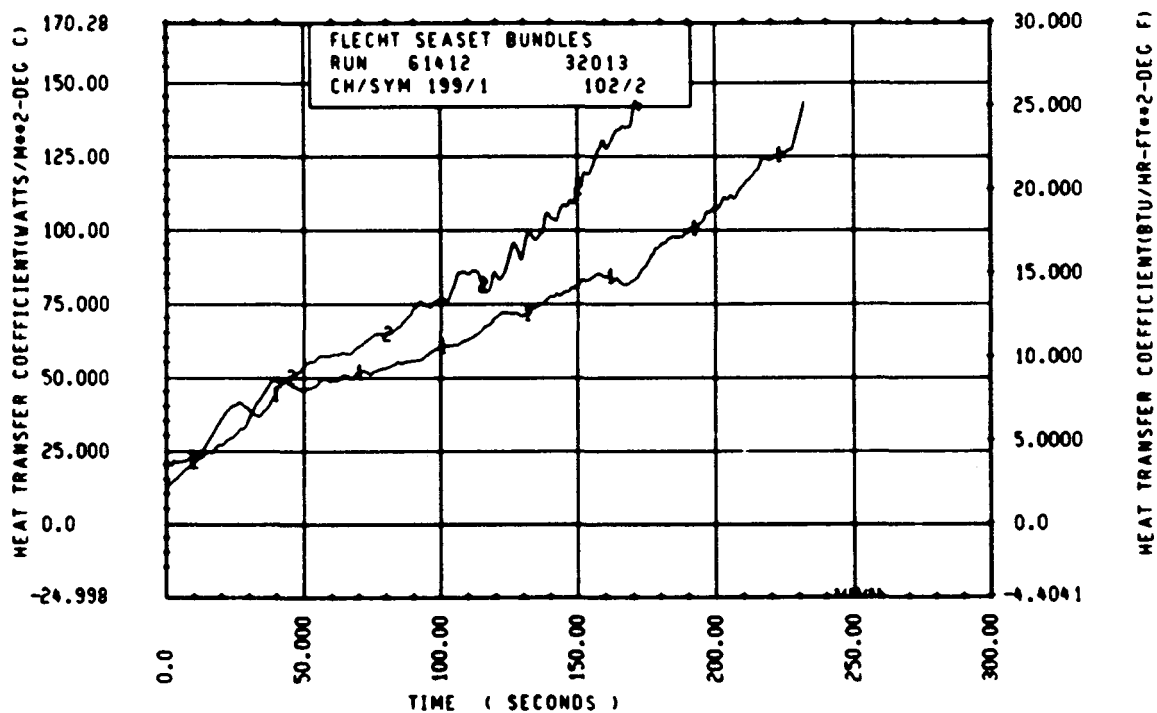
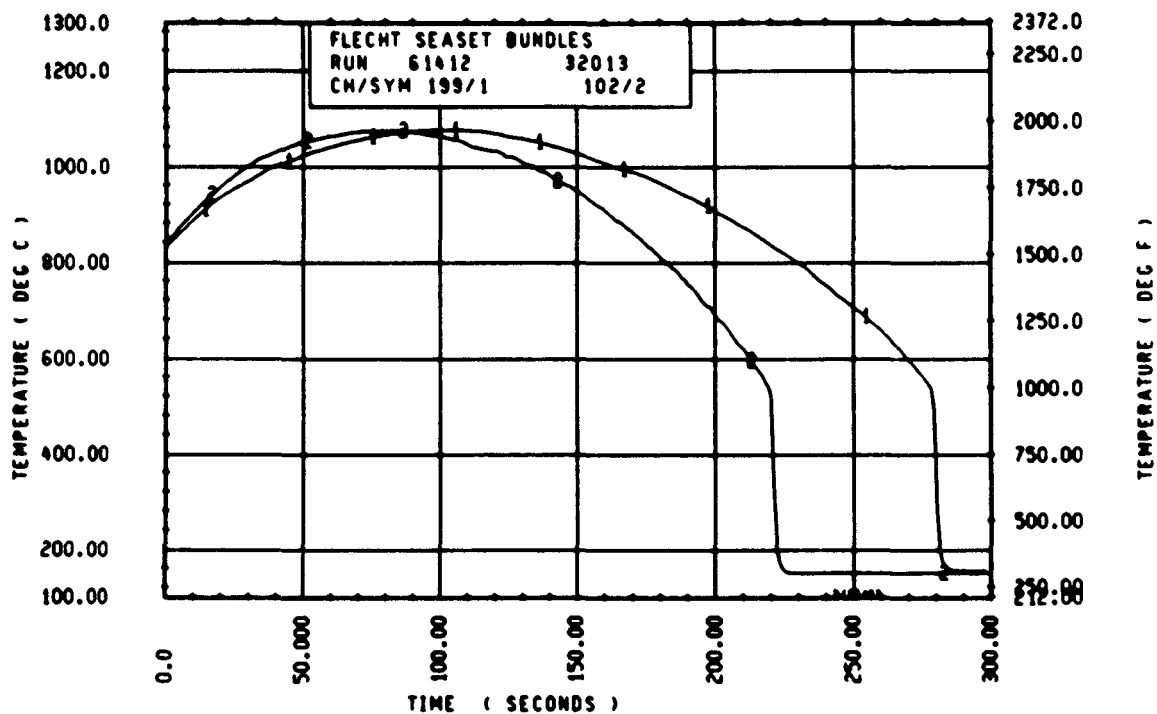
Rod 13G, 1.88 m (74 in.)



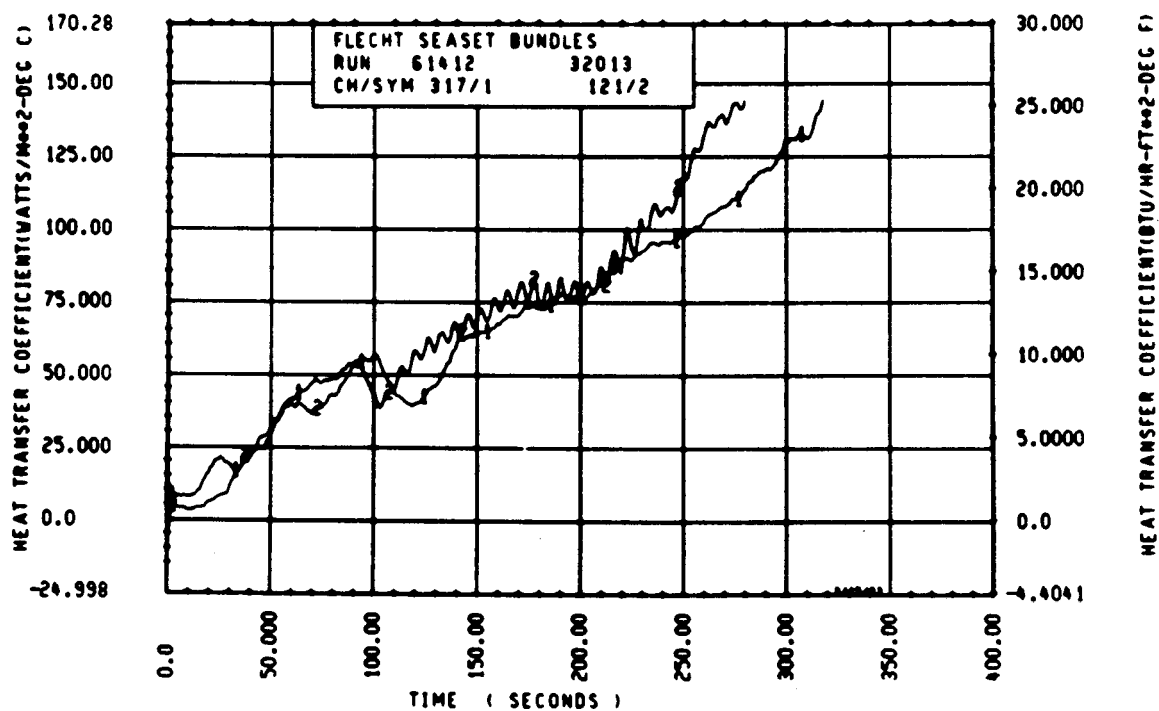
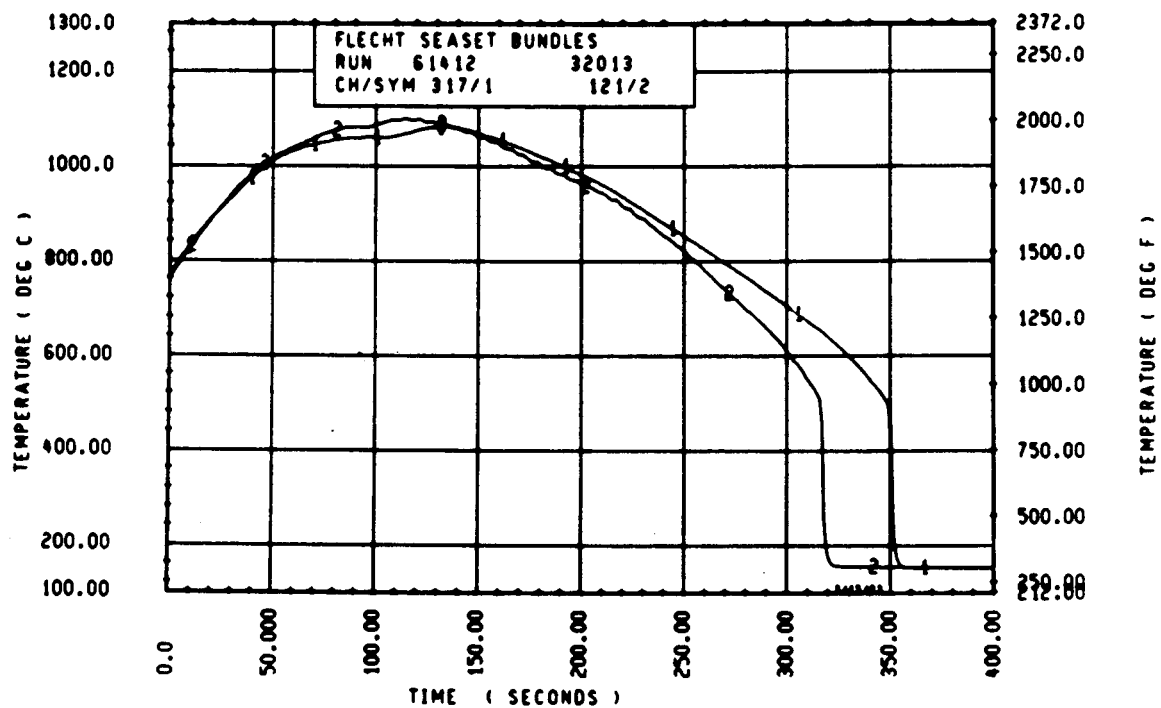
Rod 8H, 1.98 m (78 in.)



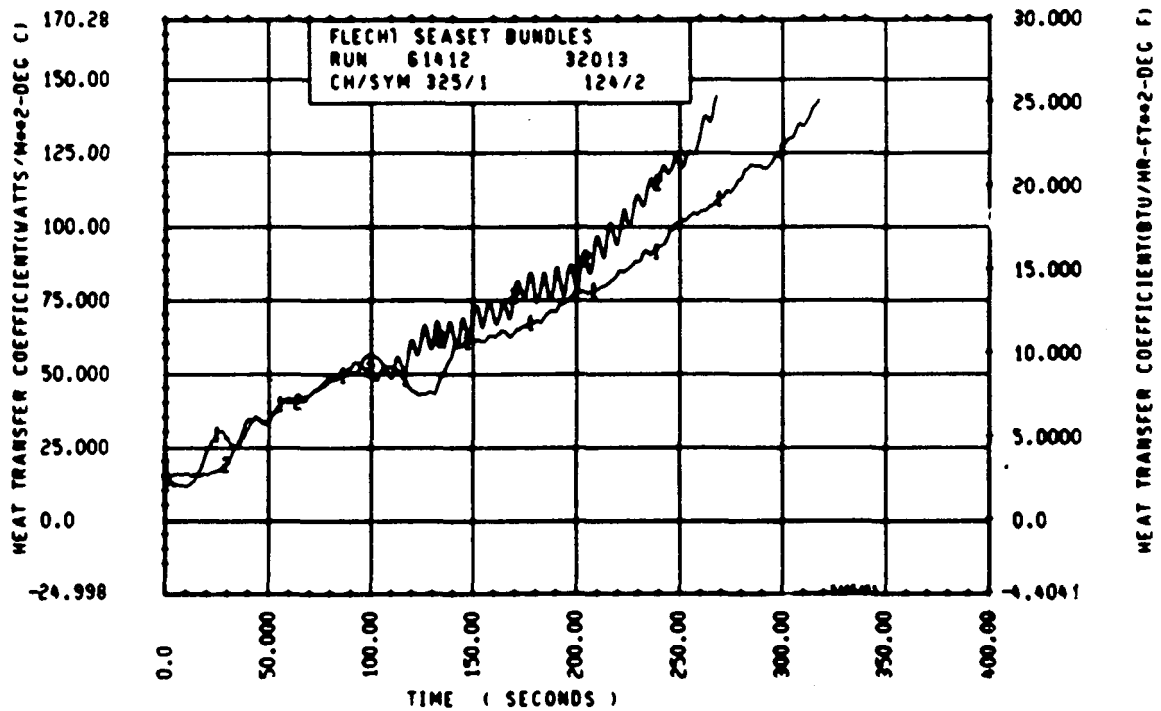
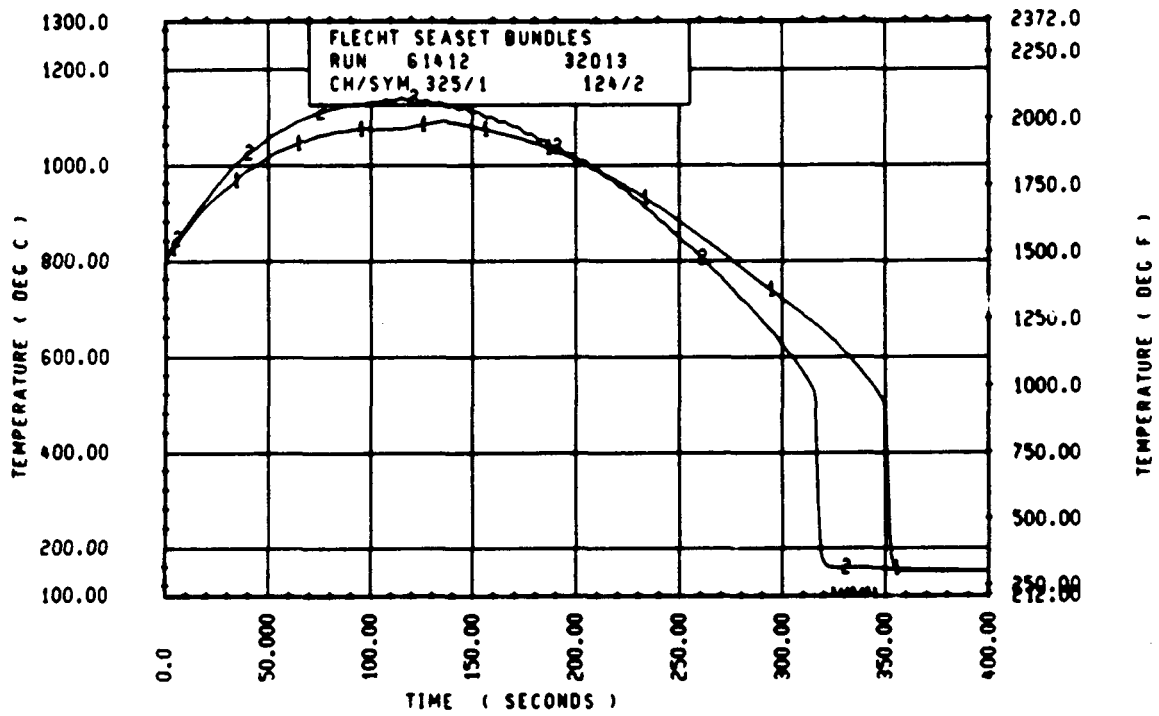
Rod 121, 1.98 m (78 in.)



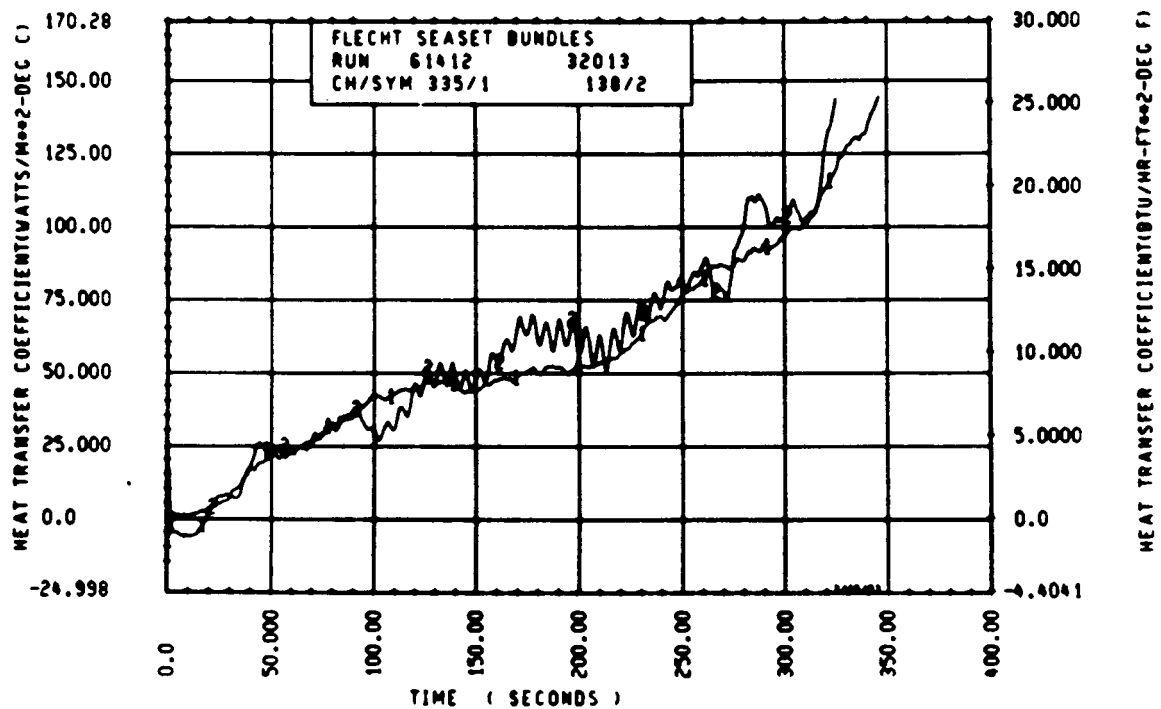
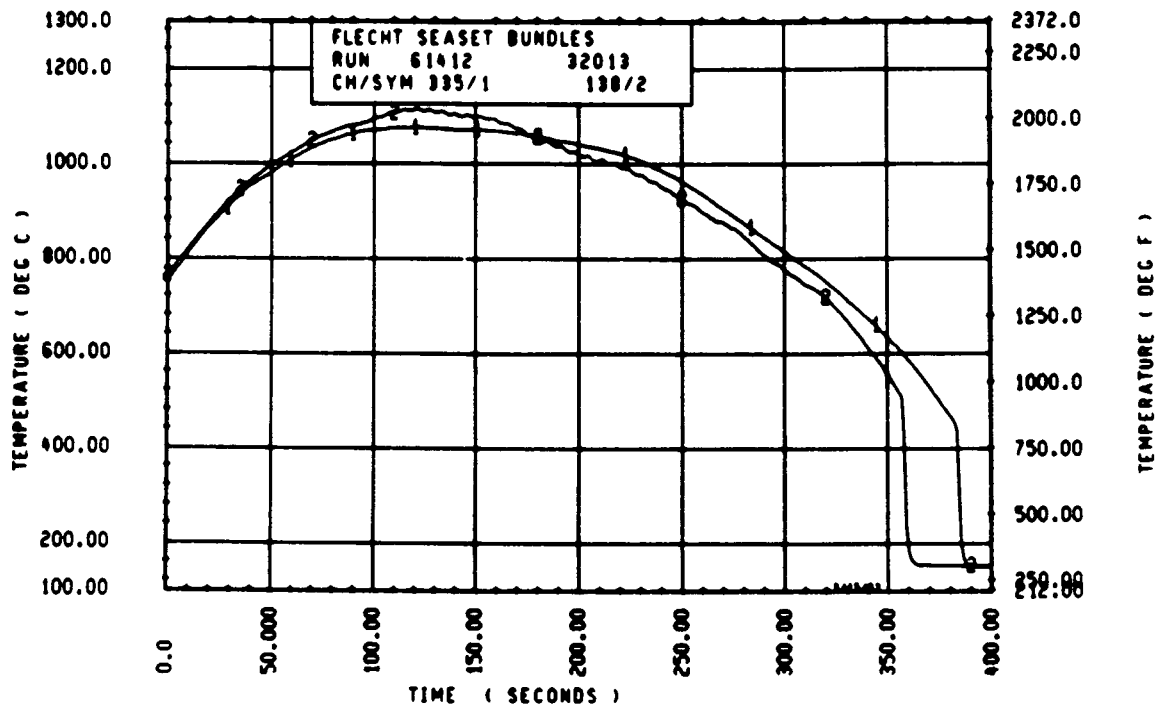
Rod 13G, 1.98 m (78 in.)



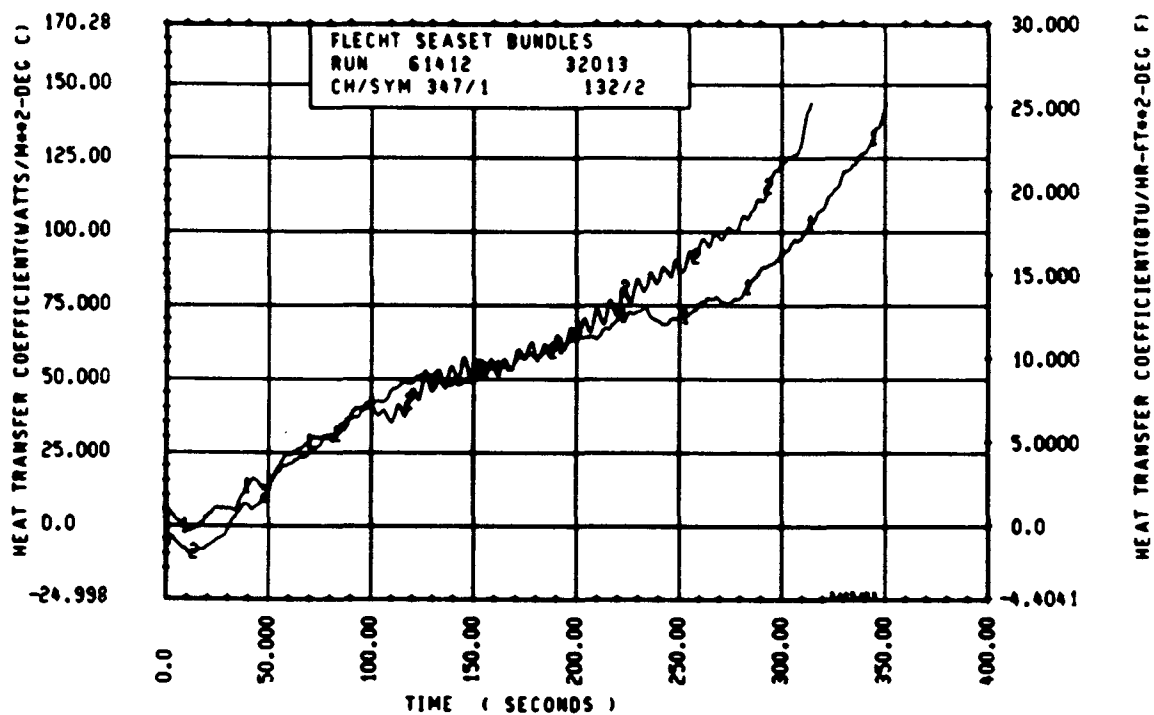
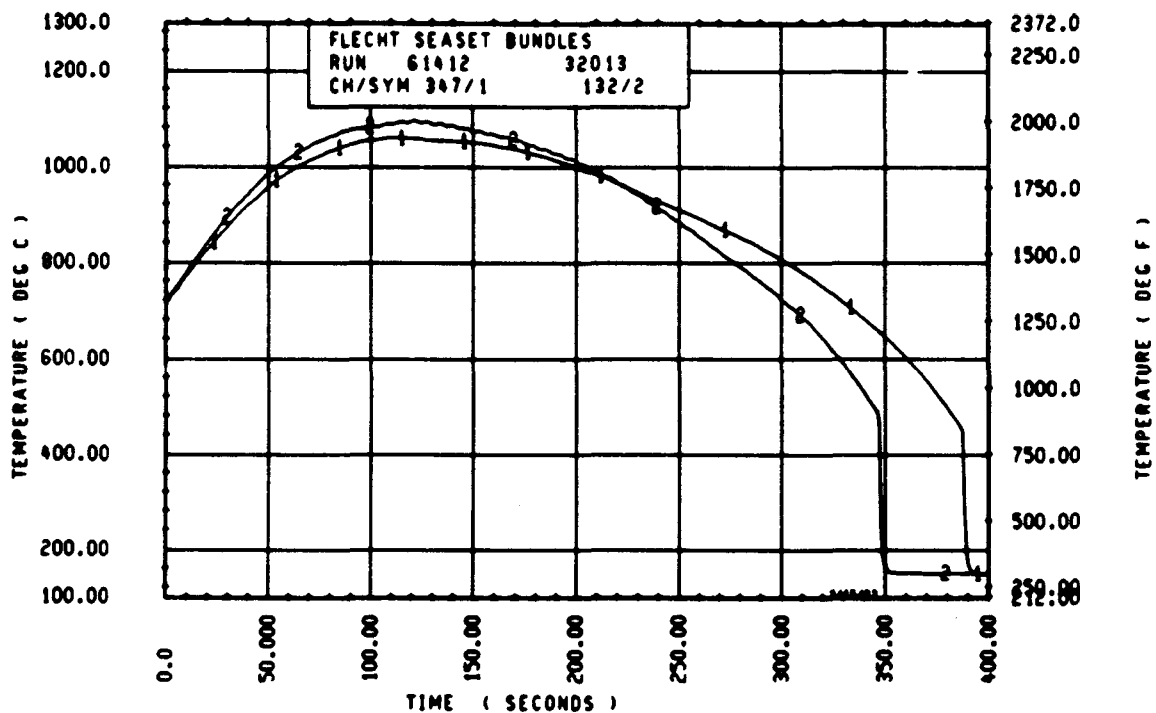
Rod 9C, 2.29 m (90 in.)



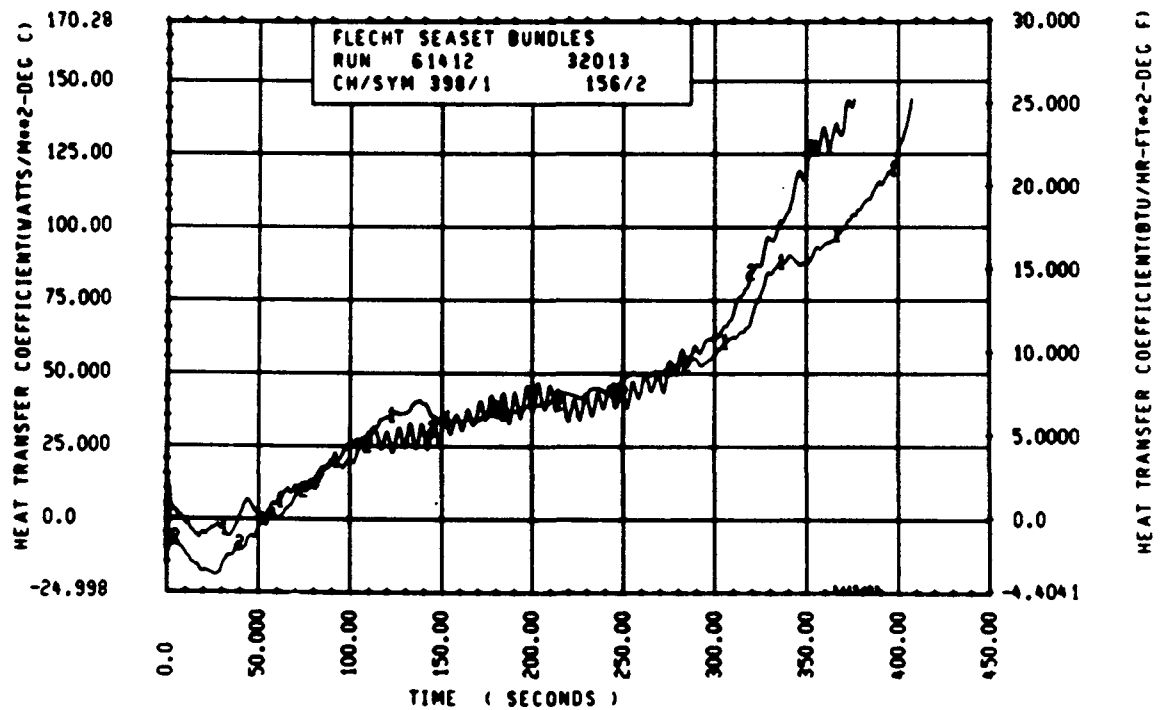
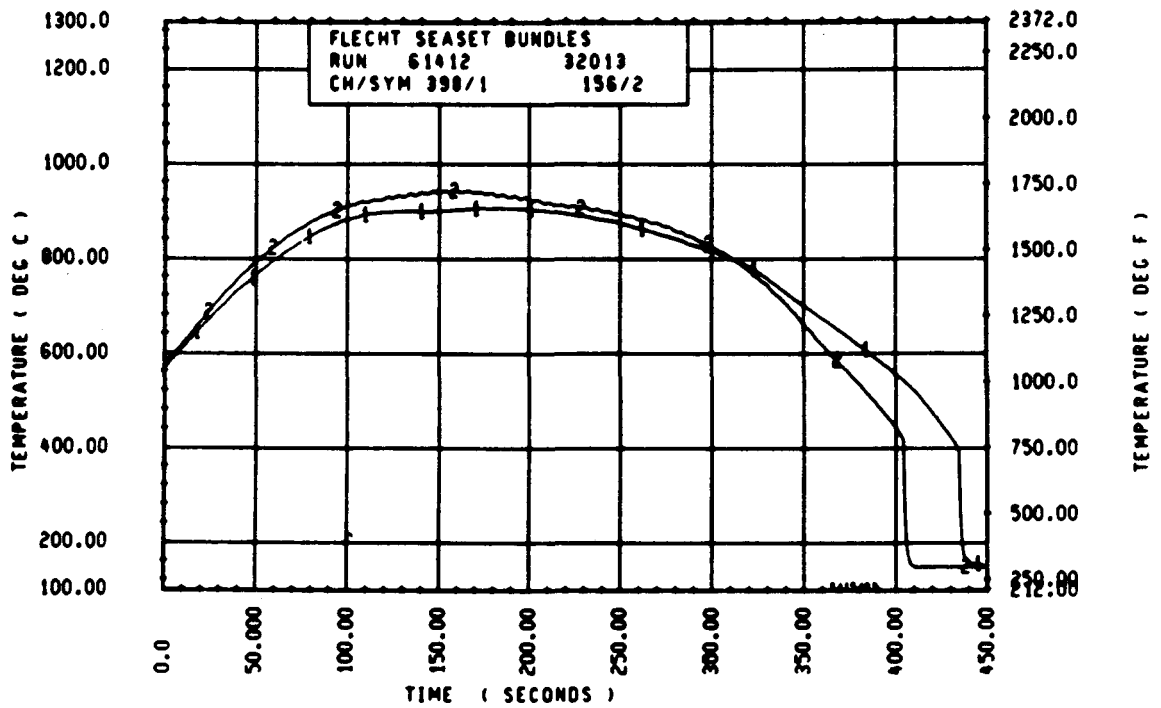
Rod 11E, 2.29 m (90 in.)



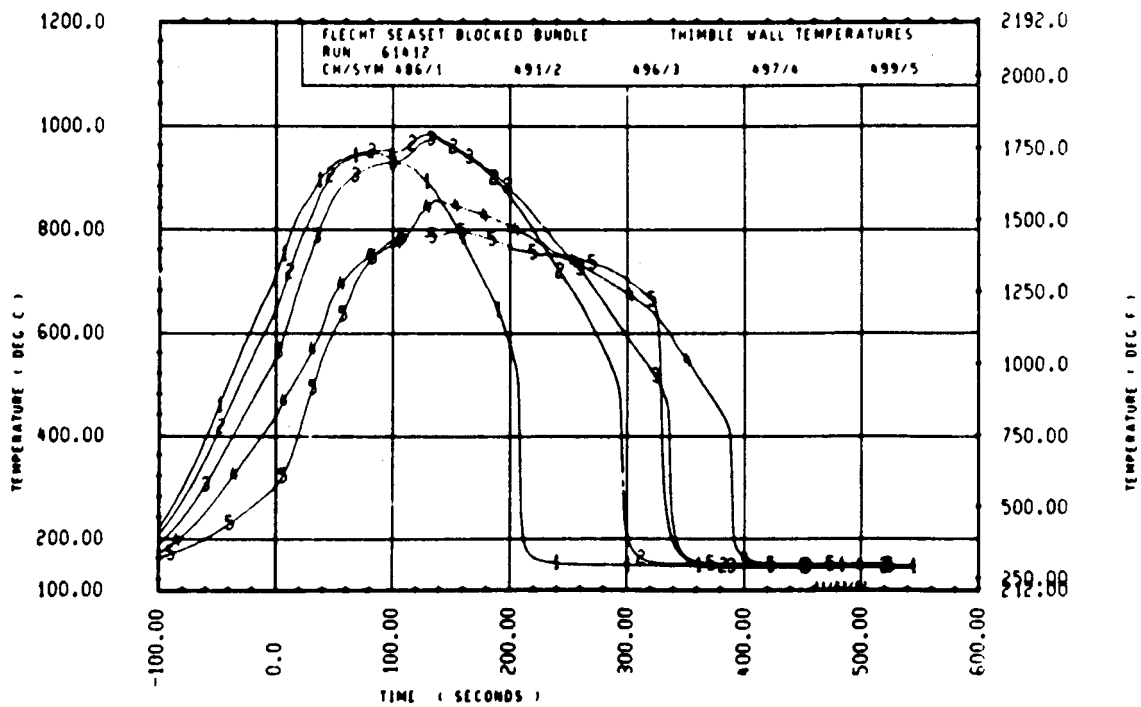
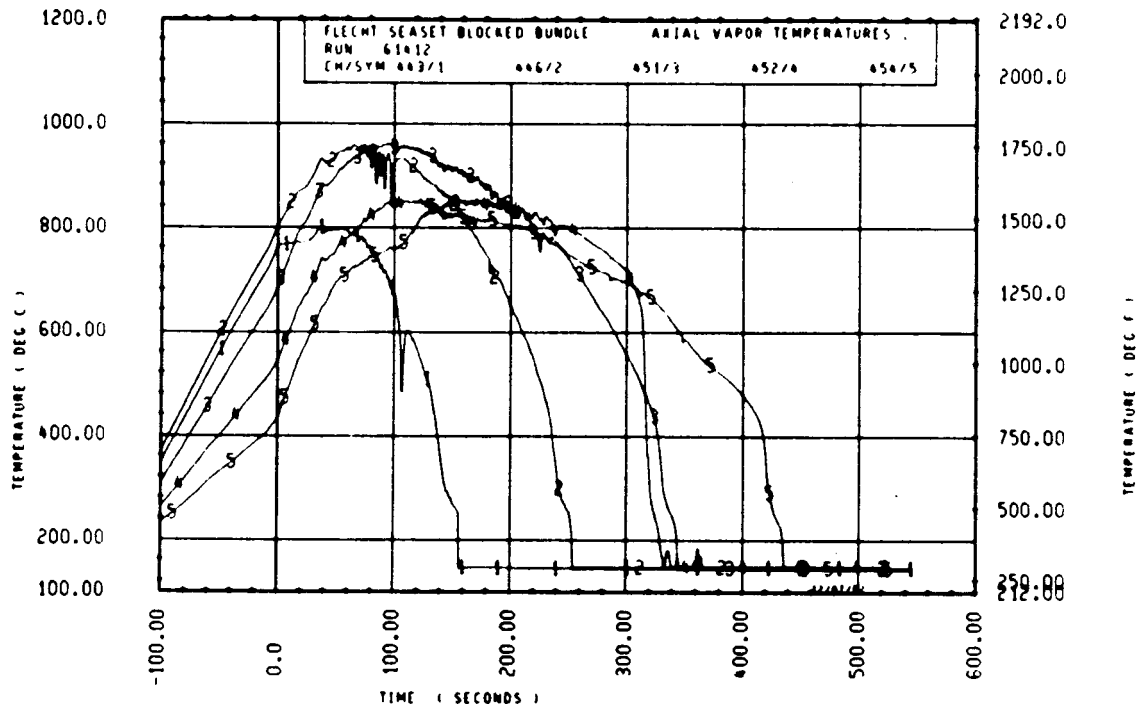
Rod 5F, 2.44 m (96 in.)

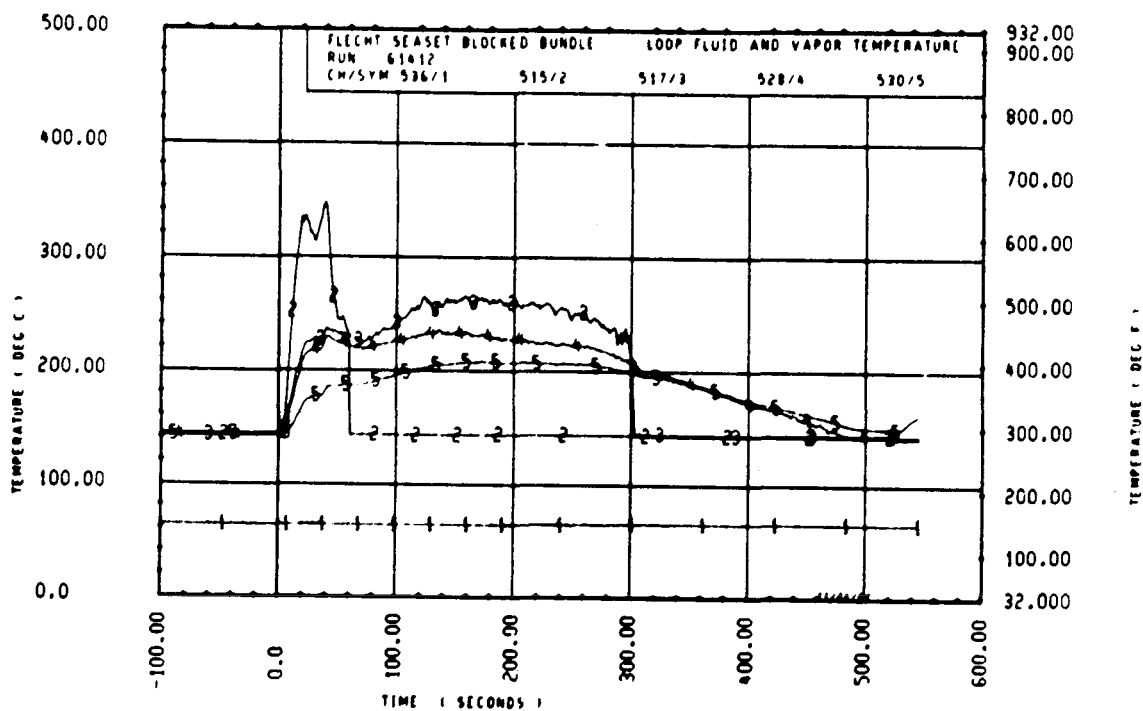
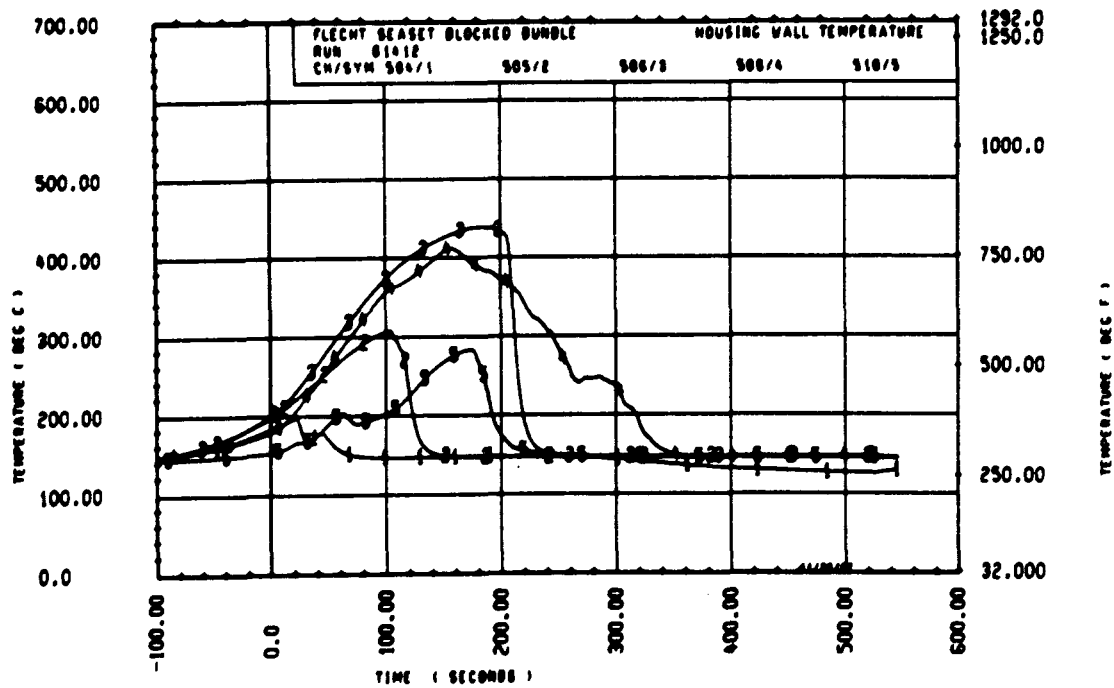


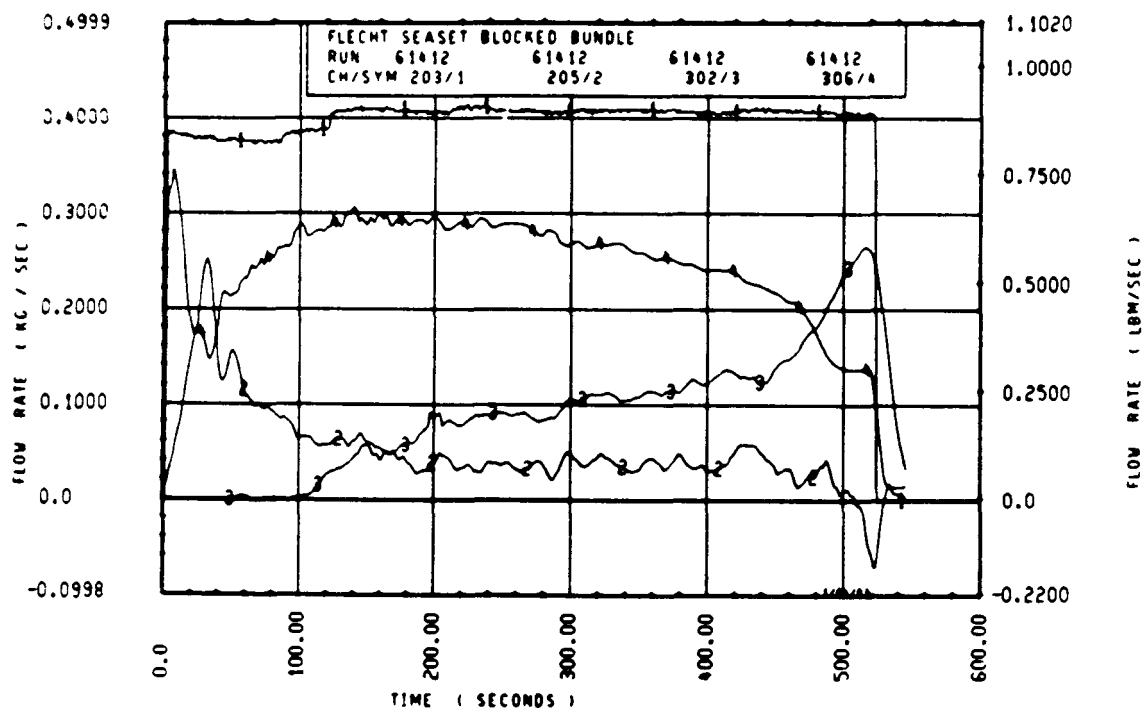
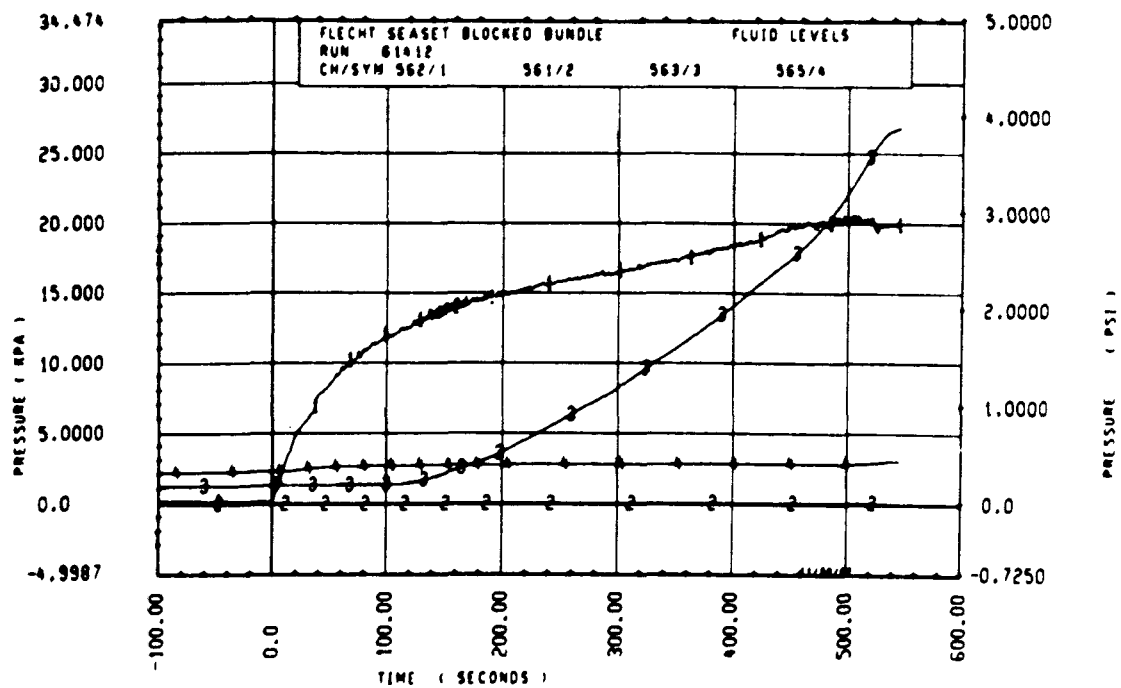
Rod 7M, 2.44 m (96 in.)

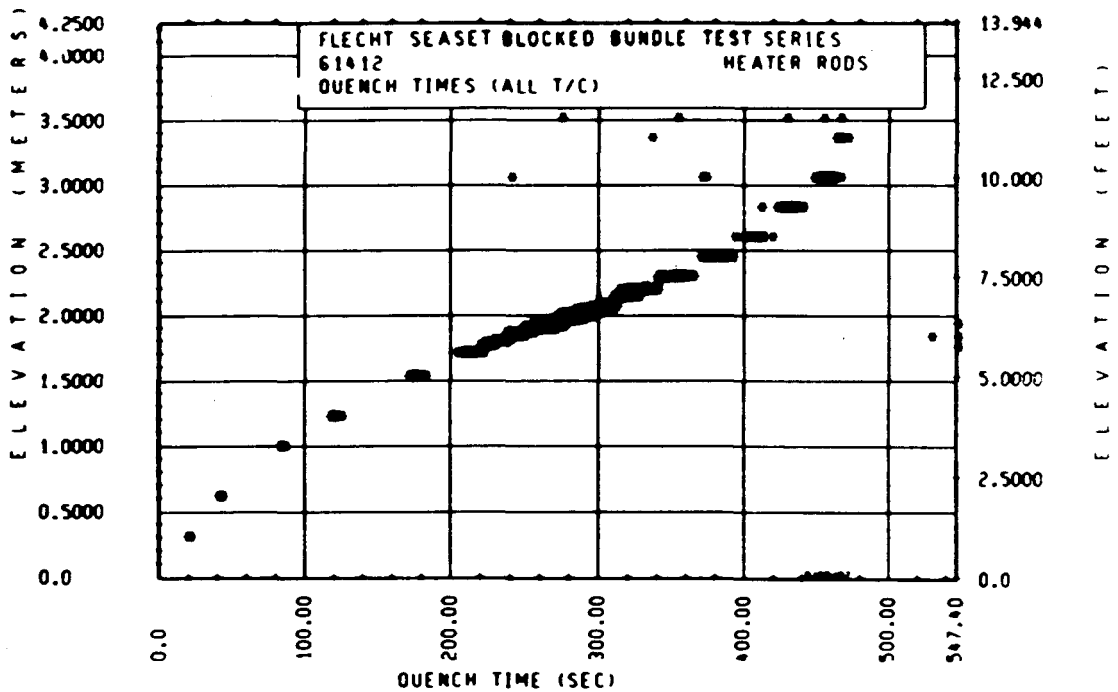
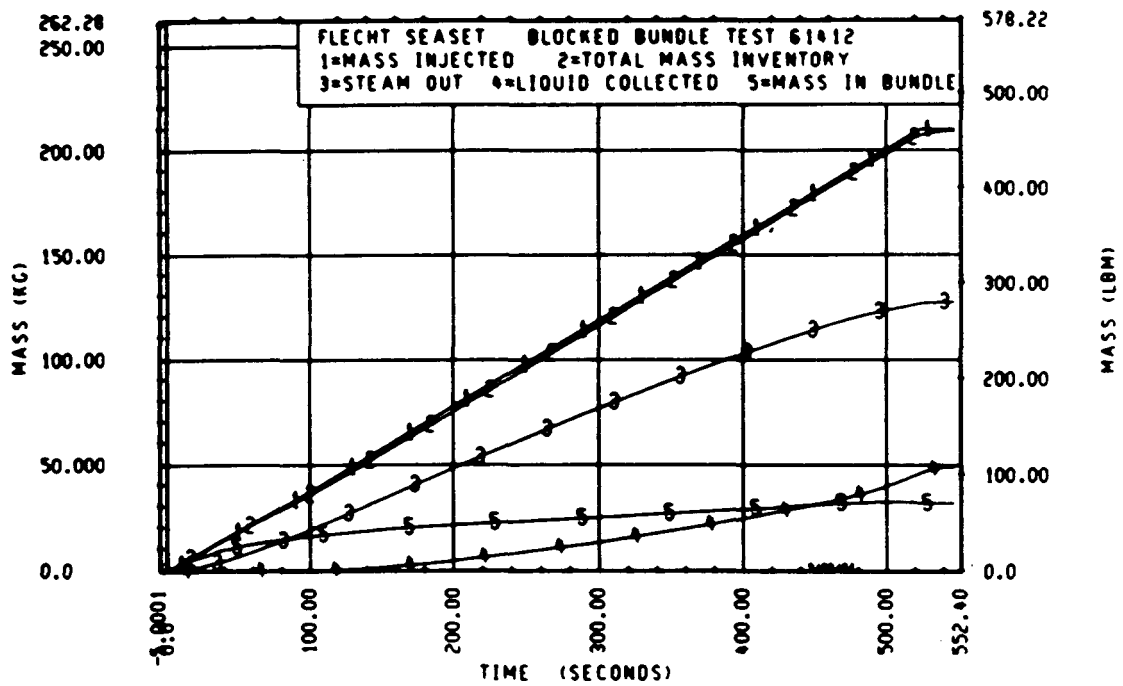


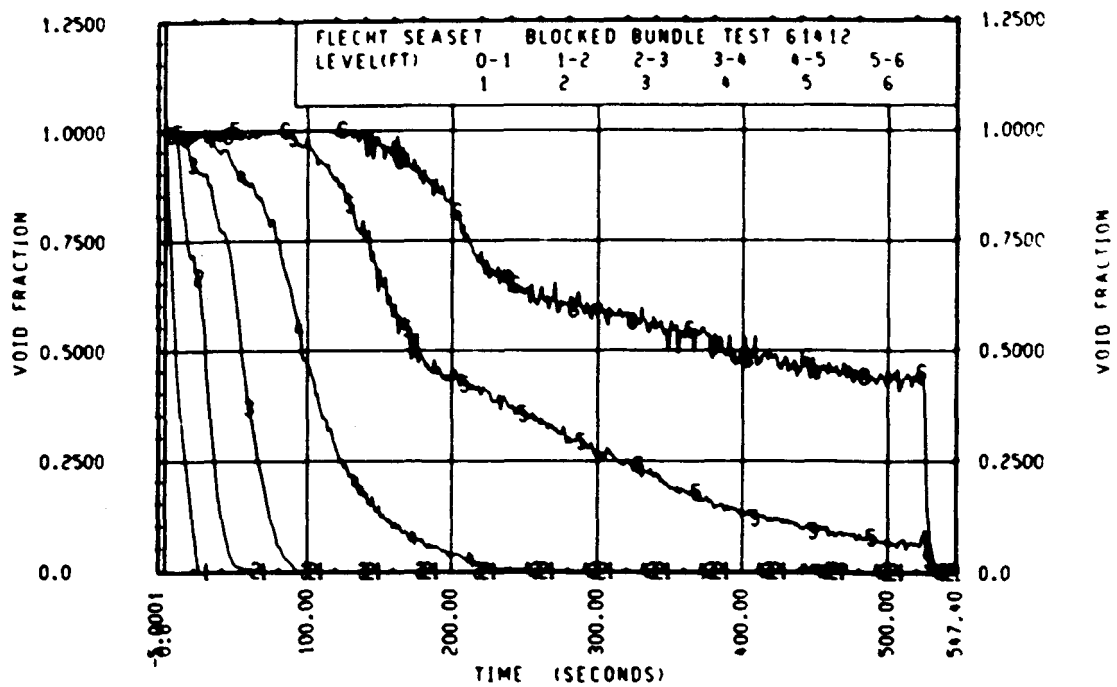
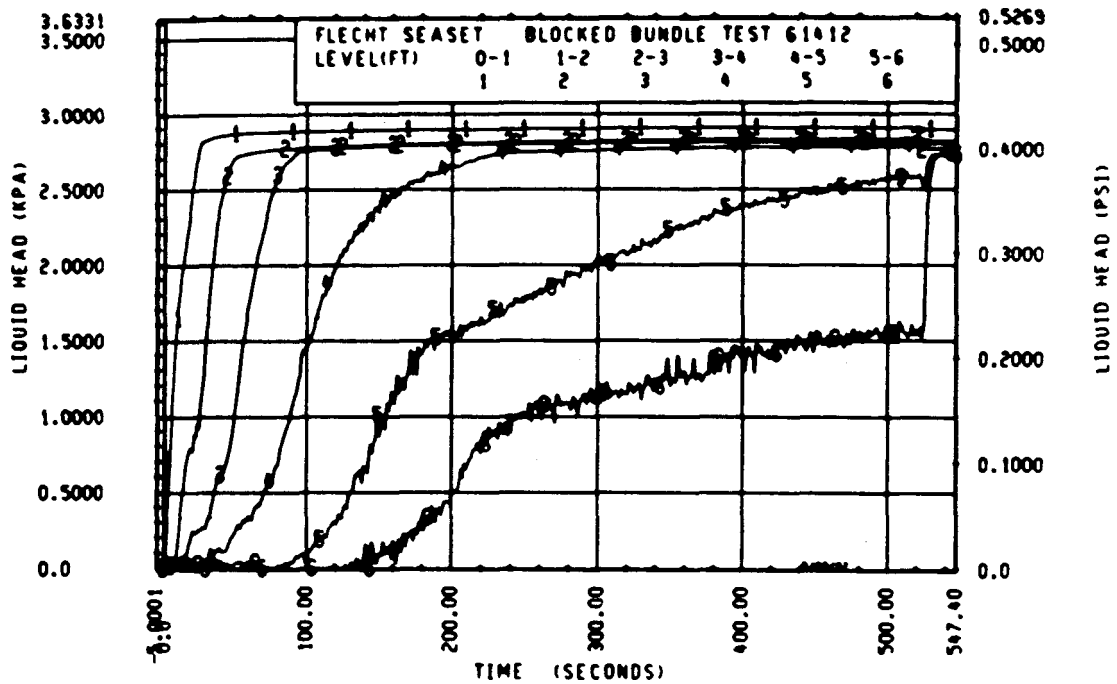
Rod 121, 2.82 m (111 in.)

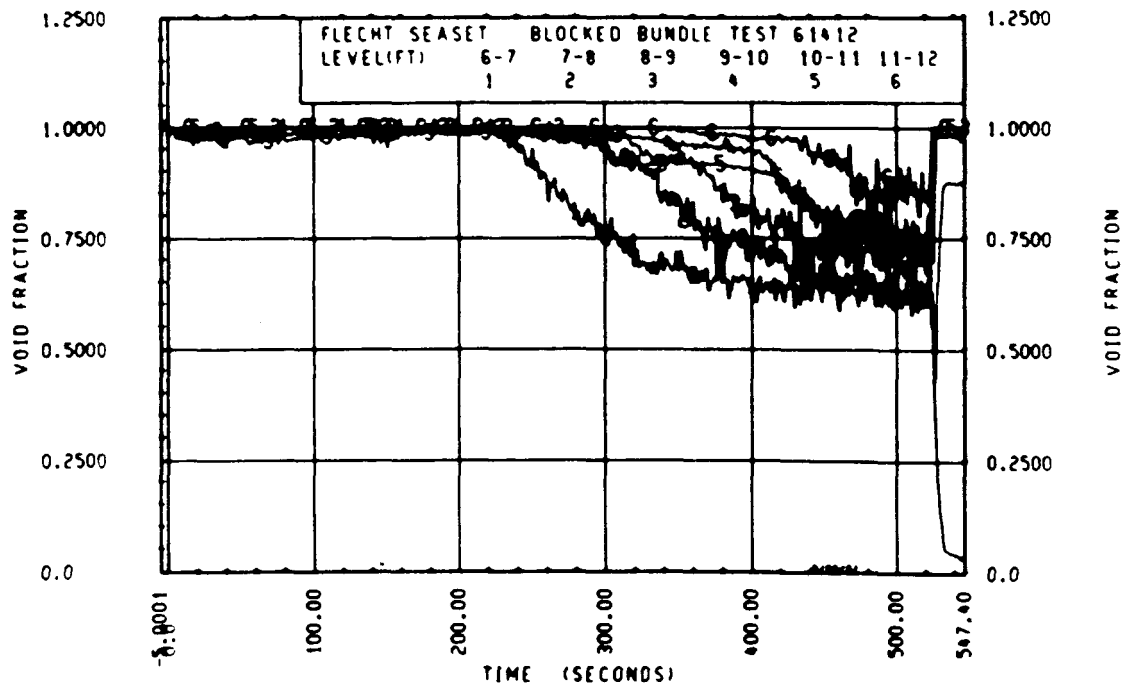
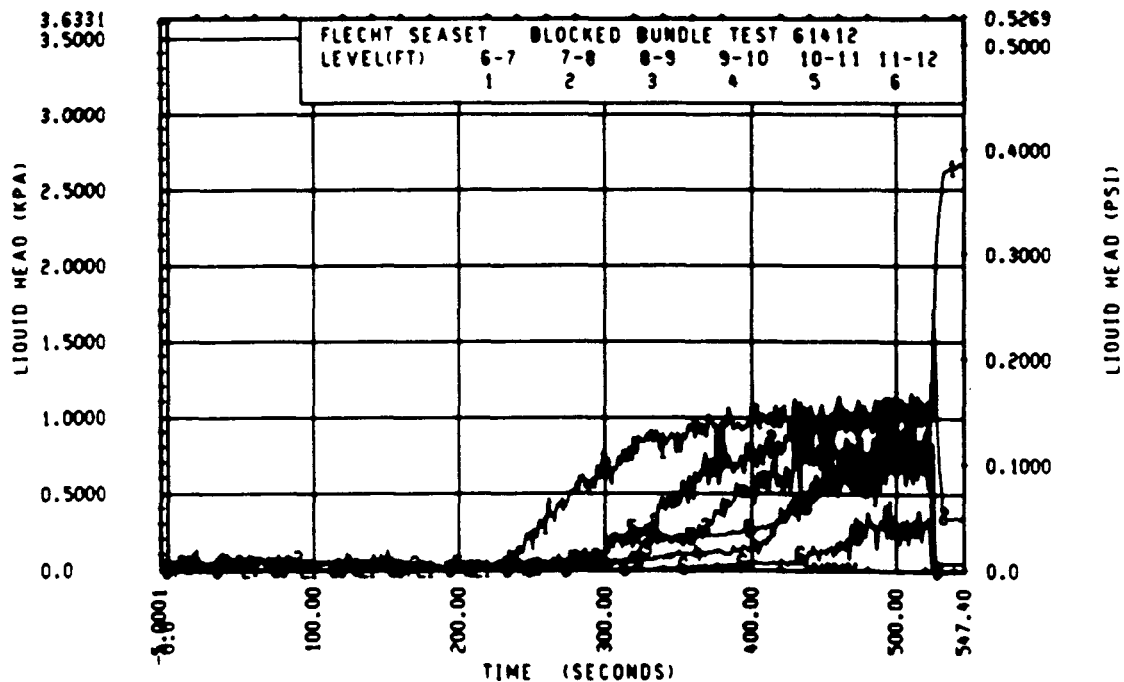












FLECHT SEASET 163-ROD BUNDLE FLOW BLOCKAGE TASK
SUMMARY AND COMMENT SHEET

Run: 61509
Test date: 9/10/82
Test type: Forced reflood
Parameter: Pressure effect

AS-RUN TEST CONDITIONS:

Upper plenum pressure	0.139 MPa (20.1 psia)
Initial peak clad temperature and location	876.5°C (1609.7°F), 8N-1.93 m (76 in.)
Initial peak rod power:	
Peripheral rods	2.37 kw/m (0.723 kw/ft)
Bypass rods	2.36 kw/m (0.719 kw/ft)
Blockage island rods	2.37 kw/m (0.721 kw/ft)
Flooding rate	26.9 mm/sec (1.06 in./sec)
Coolant temperature	35°C (95°F)
Initial bundle water level	+9.4 mm (+0.37 in.)

COMMENTS:

Carryover tank filled up at approximately 590 seconds.

Inlet mass flow: ⁽¹⁾ -1.3% for first 60 seconds and +2.5% thereafter

Power decay: ⁽¹⁾ peripheral rods, -2.5% linearly increasing to -4% by 400 seconds
bypass rods, -4% linearly increasing to -6.5% by 400 seconds
blockage rods, +2% linearly increasing to +4% by 400 seconds

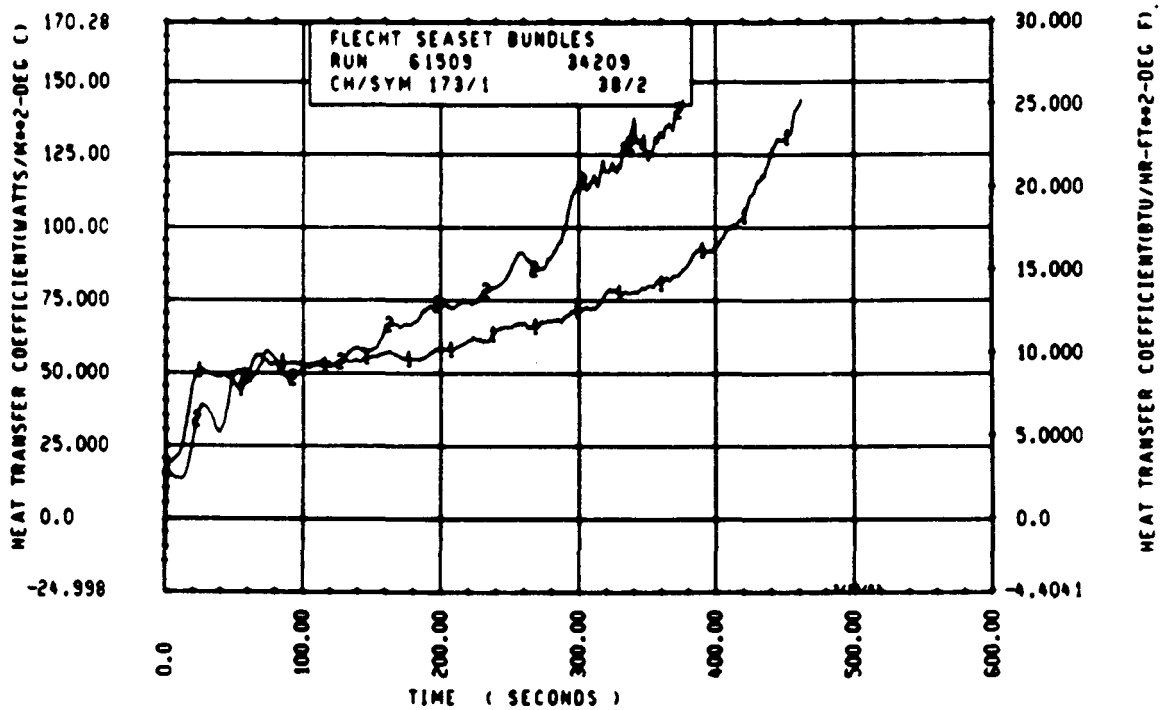
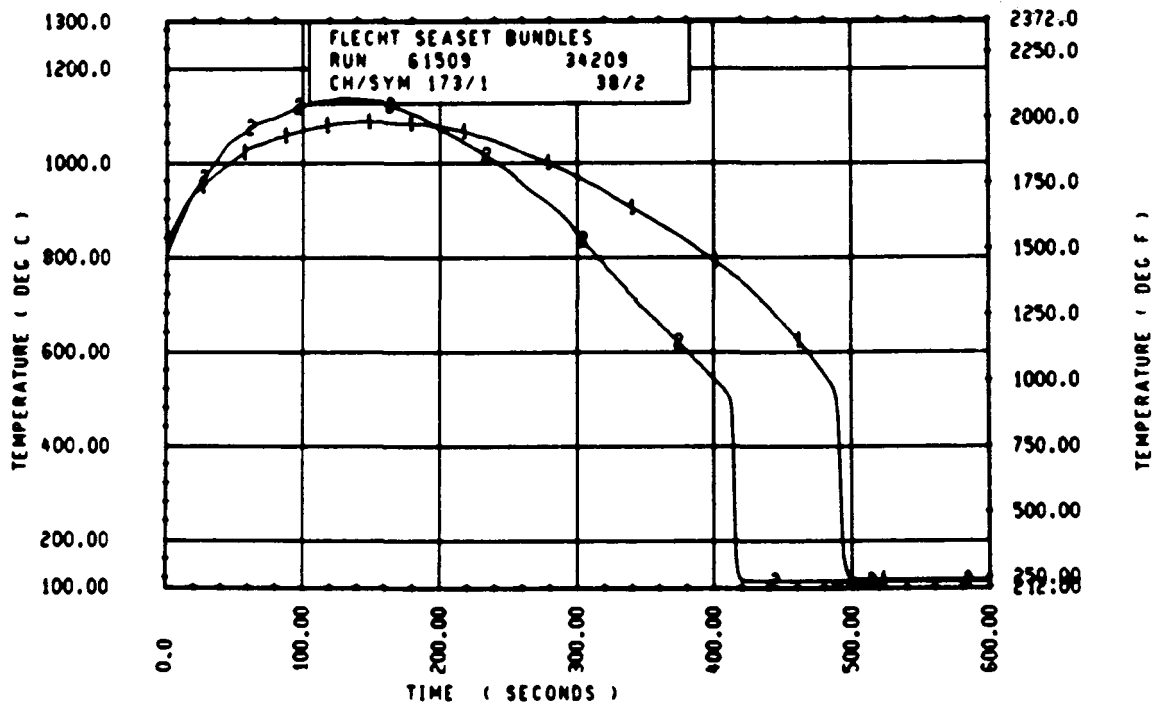
FLECHT SEASET 163 ROD BUNDLE TEST SERIES							
ROD/ELEV	CHAN. NO	RUN NUMBER 61509		TURNAROUND TIME (SECONDS)	QUENCH TEMPERATURE (DEG F)	QUENCH TIME (SECONDS)	
		INITIAL AT FLOOD (DEG F)	MAXIMUM TEMPERATURE (DEG F)				
96 1- 3	3	654.	676.	22.	6.5	540.	28.8
10H 2- 0	6	870.	925.	55.	12.0	593.	66.4
96 3- 3	9	1273.	1326.	124.	39.5	644.	134.4
3J 4- 0	11	1347.	1543.	197.	56.5	600.	201.3
7H 4- 0	12	1329.	1561.	232.	56.0	665.	202.5
8K 4- 0	13	1349.	1578.	229.	57.0	696.	203.1
8M 4- 0	14	1357.	1564.	207.	57.0	697.	196.0
12D 4- 0	17	1332.	1519.	186.	54.5	695.	195.4
5E 5- 0	20	1498.	1859.	301.	82.5	852.	298.8
76 5- 2	21	1552.	1896.	344.	83.0	839.	294.9
96 5- 0	24	1528.	1891.	363.	96.0	823.	299.7
5E 5- 7	33	1526.	1874.	348.	112.0	881.	306.9
86 5- 7	45	1527.	1926.	394.	127.0	921.	371.8
9H 5- 9	52	1468.	1885.	417.	134.0	951.	384.7
76 5-10	59	1493.	1896.	464.	132.5	900.	391.8
7F 5-11	62	1434.	1867.	433.	155.5	902.	399.7
46 5-11	64	1520.	1874.	354.	124.0	869.	416.8
21 6- 0	67	1594.	1947.	303.	84.5	925.	418.6
5D 6- 0	70	1481.	1874.	343.	144.0	894.	418.8
6J 6- 0	74	1510.	1816.	306.	94.0	833.	427.0
7H 6- 0	66	1533.	1925.	392.	100.0	807.	415.9
11E 6- 0	80	1537.	1863.	440.	125.0	838.	422.8
8H 6- 2	97	1353.	1864.	510.	192.5	739.	470.6
5H 6- 2	99	1517.	1902.	385.	152.5	919.	445.6
9E 6- 2	105	1317.	1944.	626.	136.0	1160.	442.1
8H 6- 3	111	1393.	1694.	501.	188.0	776.	484.7
46 6- 3	124	1534.	1931.	397.	125.0	880.	461.7
11H 6- 4	134	1451.	1965.	514.	186.5	885.	494.7
9D 6- 4	143	1534.	1998.	404.	136.0	879.	477.8
9J 6- 5	165	1511.	1965.	454.	188.5	886.	507.9
9H 6- 5	166	1575.	1991.	416.	178.0	922.	472.7
8J 6- 6	192	1555.	1964.	409.	156.5	849.	512.8
9D 6- 6	193	1543.	2022.	479.	133.0	910.	499.7
11F 6- 6	173	1528.	1991.	482.	145.0	918.	489.7
46 7- 0	261	1453.	1740.	207.	153.5	762.	547.8
7D 7- 6	309	1473.	1867.	394.	219.1	806.	626.9
76 7- 6	312	1511.	1873.	362.	194.0	867.	606.6
11E 7- 6	325	1477.	1642.	366.	132.5	885.	603.9
5L 8- 0	337	1288.	1720.	432.	142.0	748.	673.4
7H 8- 0	345	1318.	1814.	495.	333.1	797.	680.0
7K 8- 0	346	1343.	1763.	421.	155.0	784.	663.7
5J 8- 6	366	1116.	1450.	333.	313.1	630.	720.6
78 8- 6	368	1139.	1550.	417.	215.1	850.	724.9
7E 9- 3	383	1090.	1548.	458.	344.1	695.	764.5
8H 9- 3	387	1037.	1450.	421.	355.1	641.	768.2
9C 9- 3	389	1034.	1433.	399.	230.1	613.	772.6
11F 9- 3	394	1024.	1414.	390.	356.1	761.	693.7
7810- 0	408	856.	1337.	481.	233.1	591.	816.3
8H10- 0	415	844.	1360.	516.	374.1	674.	758.8
8K10- 0	417	851.	1457.	405.	352.1	580.	816.0
8N10- 0	418	877.	1343.	466.	152.5	623.	811.9
6H11- 0	429	673.	855.	184.	127.0	512.	816.1
9611- 0	431	663.	961.	296.	368.1	672.	456.8
11E11- 0	432	666.	963.	297.	222.1	501.	588.0
5J11- 6	436	655.	821.	166.	92.5	477.	732.9
7811- 6	437	643.	991.	348.	259.1	433.	854.1
8J11- 6	438	664.	843.	179.	135.5	490.	835.1

RUN 61509 HEATER RJD STATISTICAL DATA

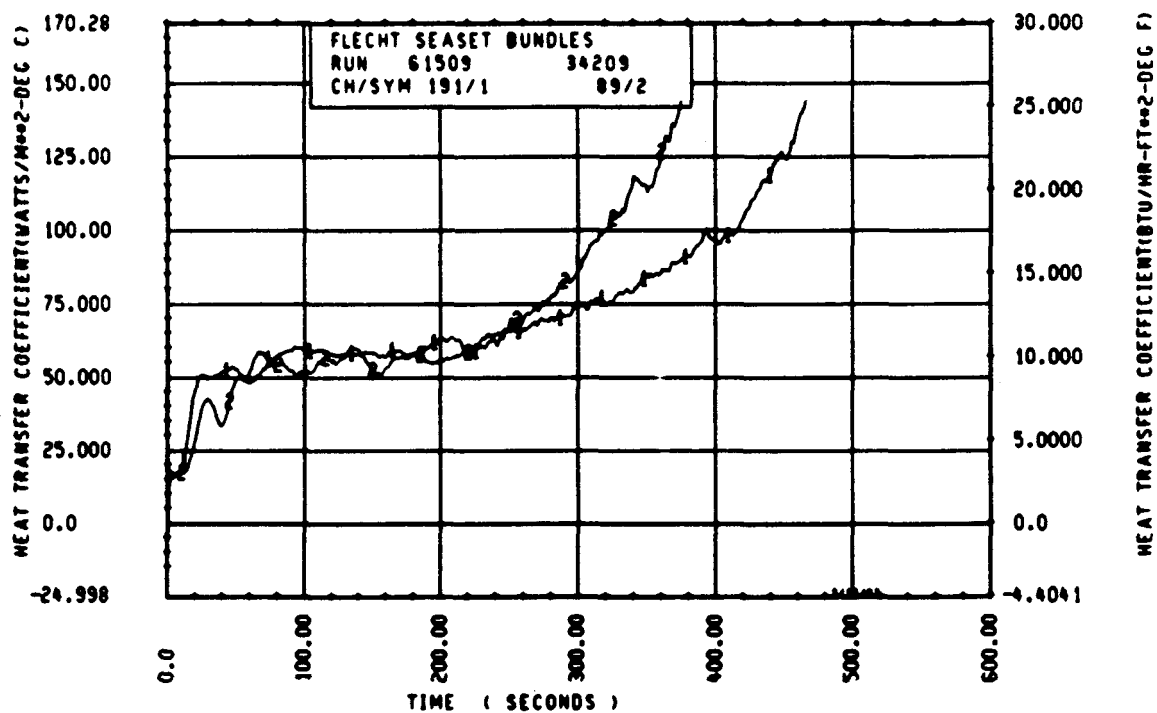
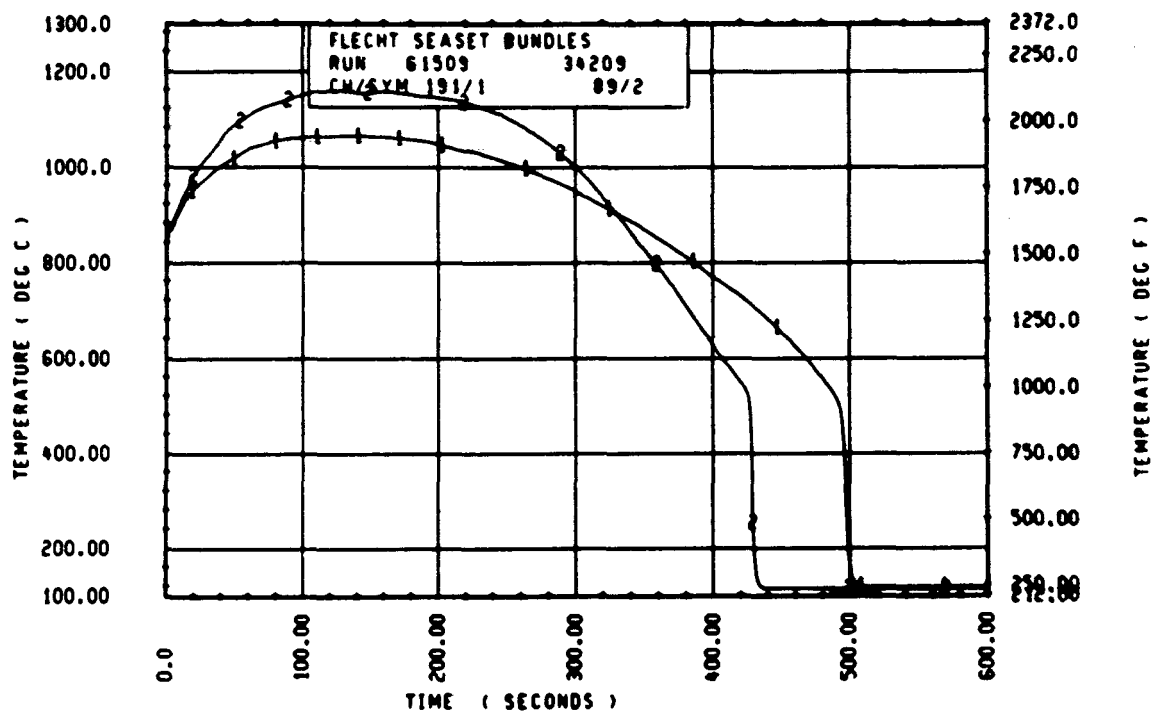
ELEV	INITIAL TEMP (DEG F)			MAX TEMP (DEG F)			TURNAROUND TIME (SEC)		
	MAX	MIN	MEAN	MAX	MIN	MEAN	MAX	MIN	MEAN
12	564.8	651.2	656.8	686.9	573.2	678.8	5.5	6.0	6.3
24	869.8	843.9	856.0	924.5	894.6	908.7	12.0	11.7	11.5
39	1203.5	1149.6	1172.4	1327.4	1275.4	1297.4	39.5	29.5	33.7
48	1360.6	1329.0	1345.1	1580.8	1518.5	1563.4	58.5	53.0	56.2
60	1552.2	1430.5	1506.0	1714.8	1754.2	1844.5	98.0	59.5	81.2
67	1599.8	1491.6	1541.4	1926.3	1799.2	1866.4	127.0	75.0	98.6
69	1516.4	1468.1	1498.6	1886.3	1857.1	1852.7	134.0	82.0	107.3
70	1590.1	1483.5	1518.9	1910.2	1853.5	1886.1	132.5	75.0	103.4
71	1519.7	1433.9	1480.7	1877.2	1335.1	1862.8	155.5	100.0	129.0
72	1594.4	1444.9	1531.2	1947.0	1816.1	1906.5	158.5	84.0	111.3
73	1583.6	1456.3	1514.4	1967.7	1855.1	1892.5	144.5	81.5	106.5
74	1586.8	1353.3	1493.5	1971.1	1848.9	1915.7	192.5	86.5	132.1
75	1587.9	1393.3	1501.5	1972.3	1842.2	1917.6	188.0	84.5	127.4
76	1699.7	1443.5	1532.9	2006.9	1904.5	1951.6	186.5	64.5	133.3
77	1574.9	1464.9	1523.9	2024.4	1918.3	1964.5	224.1	93.0	160.1
78	1609.7	1463.8	1537.7	2036.1	1843.3	1977.7	214.1	91.5	155.6
79	1582.5	1493.7	1543.6	2040.8	1942.4	1993.3	218.1	103.0	165.5
80	1567.3	1454.2	1529.5	2057.2	1871.6	2004.3	217.1	95.5	157.4
81	1556.5	1452.5	1514.8	2037.3	1945.5	2002.4	217.1	107.5	171.4
84	1512.1	1392.3	1467.6	1950.2	1688.9	1776.8	225.1	61.0	133.4
86	1561.9	1457.4	1518.3	1895.3	1746.7	1820.8	333.1	61.5	188.5
90	1515.3	1418.9	1472.5	1965.6	1769.0	1841.8	343.1	84.0	167.4
96	1382.8	1280.7	1335.6	1867.4	1719.9	1815.2	342.1	95.0	211.8
102	1170.3	1315.3	1344.8	1842.7	1444.9	1569.4	352.1	152.0	283.4
111	1089.5	1019.4	1048.0	1547.8	1333.2	1444.8	372.1	86.5	298.5
120	909.1	756.4	852.8	1424.2	1122.6	1318.1	462.1	89.5	295.8
132	673.2	657.5	665.4	688.9	827.4	918.1	376.1	86.0	240.7
138	663.8	642.8	650.7	990.5	821.2	884.6	360.1	92.5	211.9

RUN 61509 HEATER RJD STATISTICAL DATA

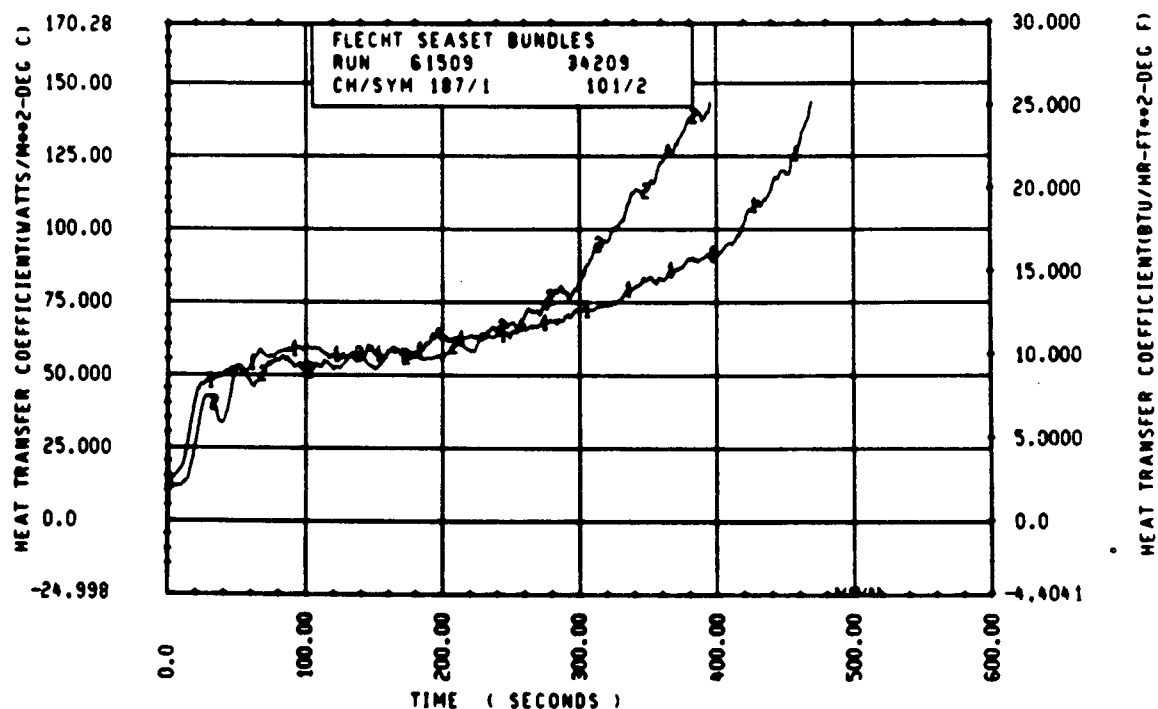
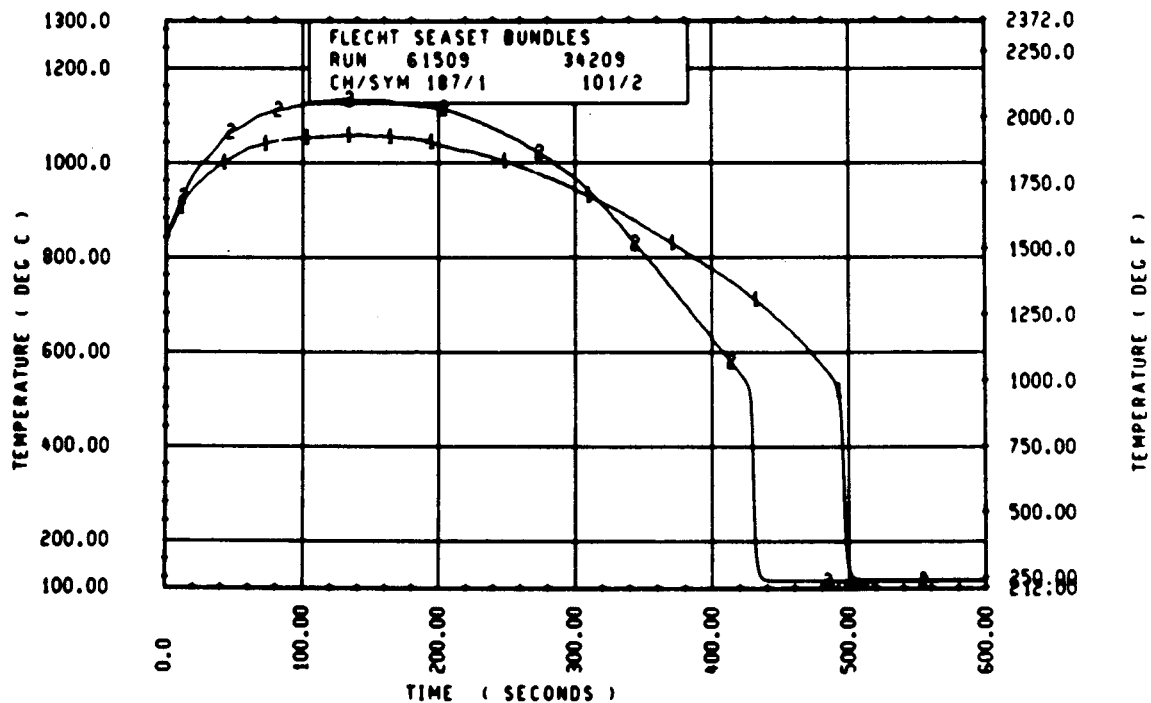
ELEV	TEMP RISE (DEG F)			QUENCH TEMP (DEG F)			QUENCH TIME (SEC)		
	MAX	MIN	MEAN	MAX	MIN	MEAN	MAX	MIN	MEAN
12	22.1	22.1	22.1	555.2	532.7	542.5	39.5	28.0	29.9
24	54.7	50.7	52.7	596.5	559.6	583.1	66.9	63.4	64.8
39	134.2	115.7	125.0	716.4	668.3	694.1	138.3	133.3	133.5
48	245.2	186.4	218.3	743.8	664.9	697.4	203.1	168.4	197.5
60	367.0	282.4	338.4	881.8	764.1	816.5	315.7	293.8	301.1
67	399.1	286.8	318.9	920.7	775.8	848.7	384.9	359.7	368.7
69	417.1	299.3	354.1	951.4	784.9	835.5	399.8	383.7	391.1
70	427.2	306.4	367.2	933.0	771.3	850.6	417.7	384.8	400.2
71	433.2	354.2	382.1	980.5	798.4	962.6	417.7	392.0	406.7
72	475.2	306.2	369.1	940.1	772.9	873.1	438.5	415.9	423.0
73	443.7	343.4	378.1	985.8	808.1	867.2	443.8	416.5	432.0
74	510.4	363.6	422.2	919.3	640.2	845.2	483.0	435.8	452.5
75	500.9	361.5	416.1	947.3	462.6	822.4	493.0	435.8	464.8
76	514.4	365.3	418.2	965.0	685.1	883.2	475.3	445.8	469.8
77	510.2	388.5	446.6	945.0	697.6	848.4	525.9	472.7	494.9
78	511.7	374.5	440.0	961.8	667.1	863.9	534.8	475.7	502.0
79	529.1	393.6	449.7	982.2	645.9	870.0	527.4	476.7	511.9
80	539.2	417.4	474.8	942.9	791.7	870.4	539.5	501.7	520.4
81	528.6	456.2	487.6	949.4	825.5	877.7	546.8	514.5	532.3
84	473.2	250.0	309.2	795.5	722.6	755.6	578.6	543.1	556.7
86	359.7	263.5	302.4	900.4	753.7	867.8	552.8	553.5	576.7
90	418.0	319.3	369.3	913.9	763.6	835.2	551.8	581.6	617.8
96	535.5	402.9	474.6	875.6	705.8	797.8	711.4	637.6	670.9
102	503.2	333.5	434.5	731.3	541.2	680.7	753.1	708.0	722.4
111	478.8	307.0	396.8	806.9	602.9	674.8	783.7	643.6	754.9
120	548.1	324.2	465.3	775.3	242.7	593.4	829.0	514.7	740.4
132	299.9	169.9	252.7	671.8	434.8	544.4	834.1	456.8	696.1
138	347.8	165.8	233.3	691.0	477.1	528.3	854.1	397.7	721.1



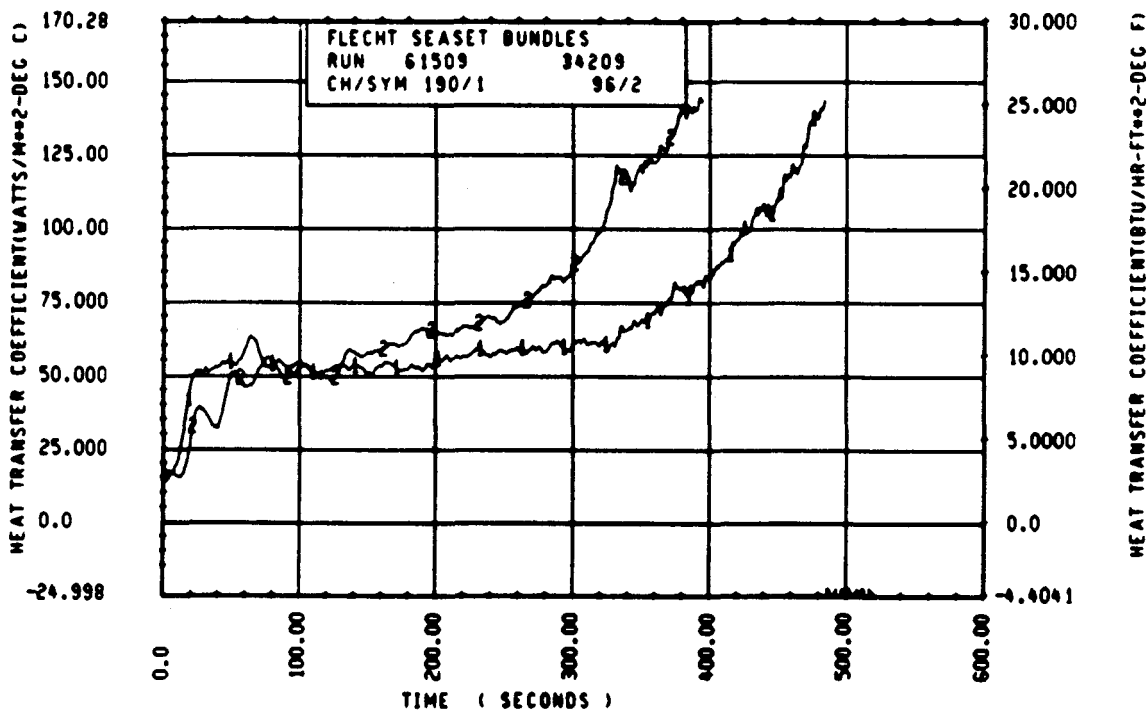
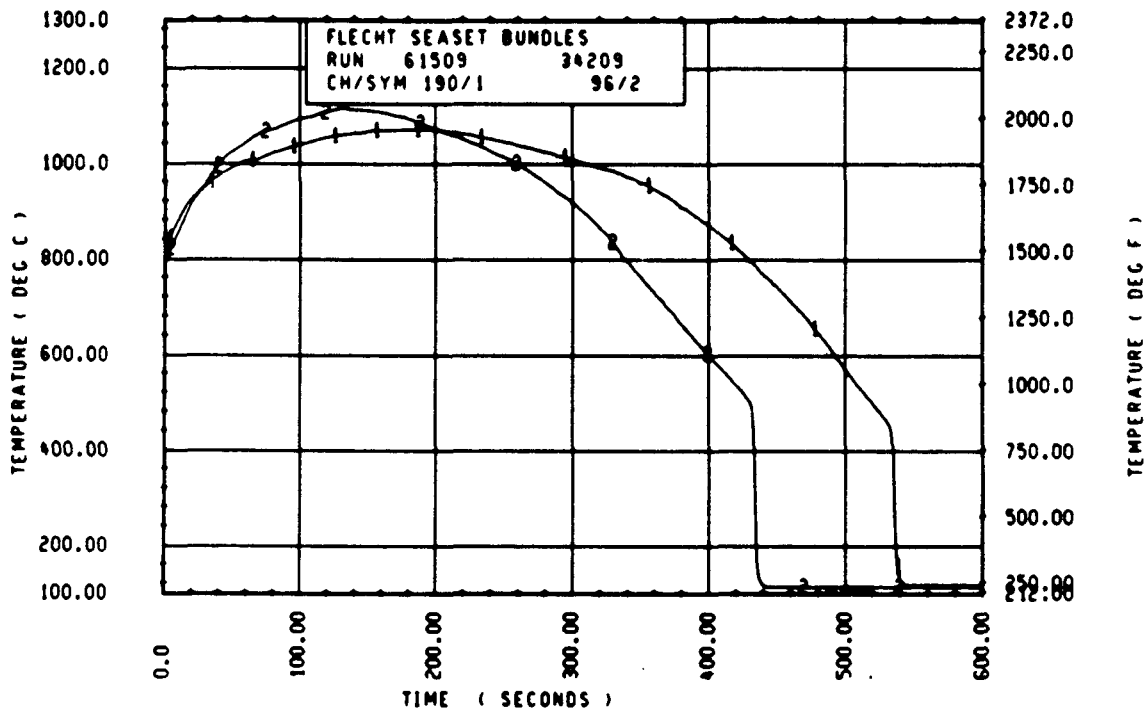
Rod 11F, 1.98 m (78 in.)



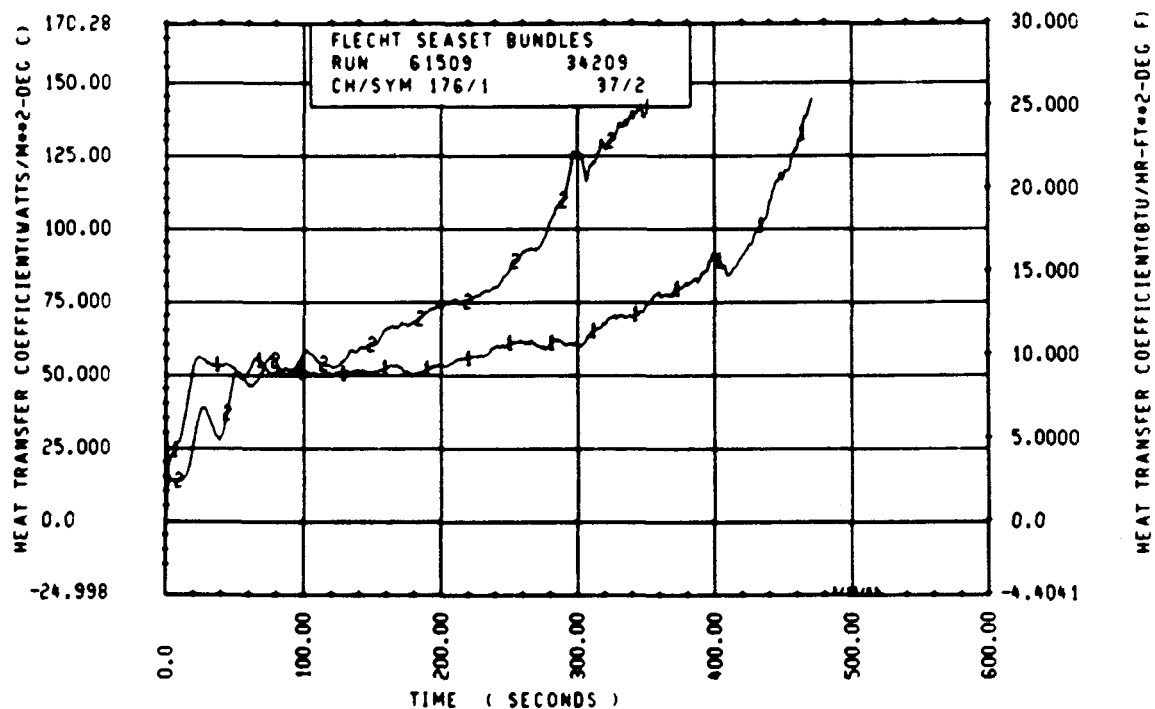
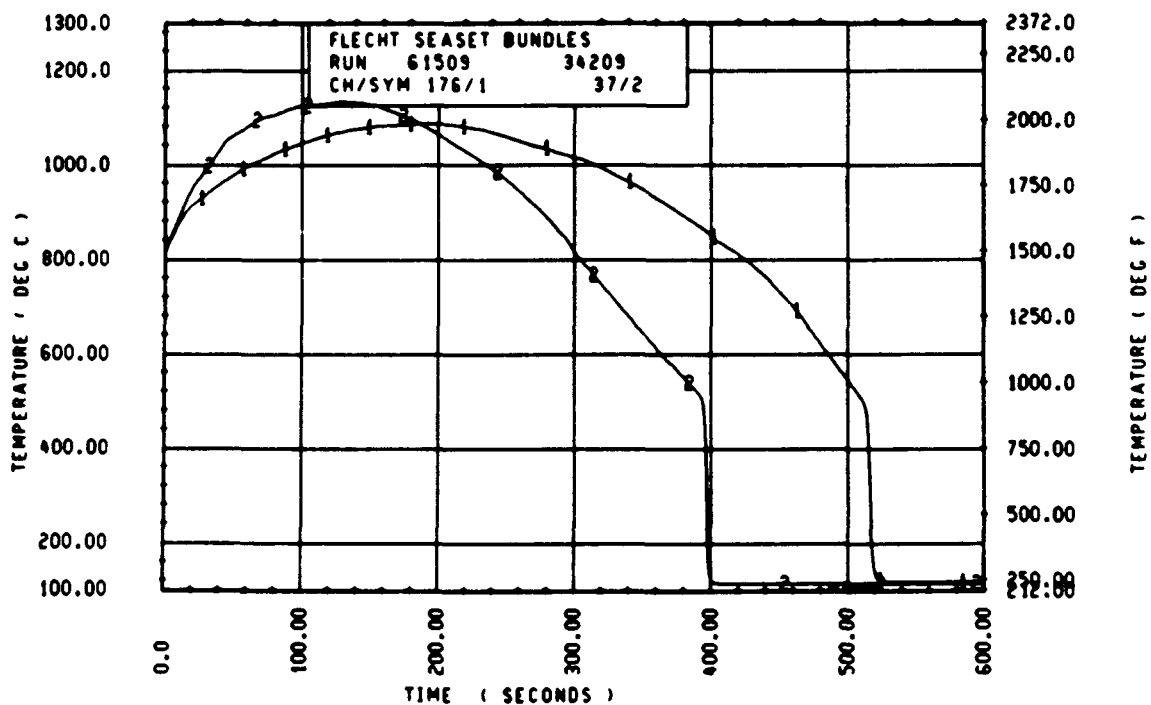
Rod 7K, 1.98 m (78 in.)



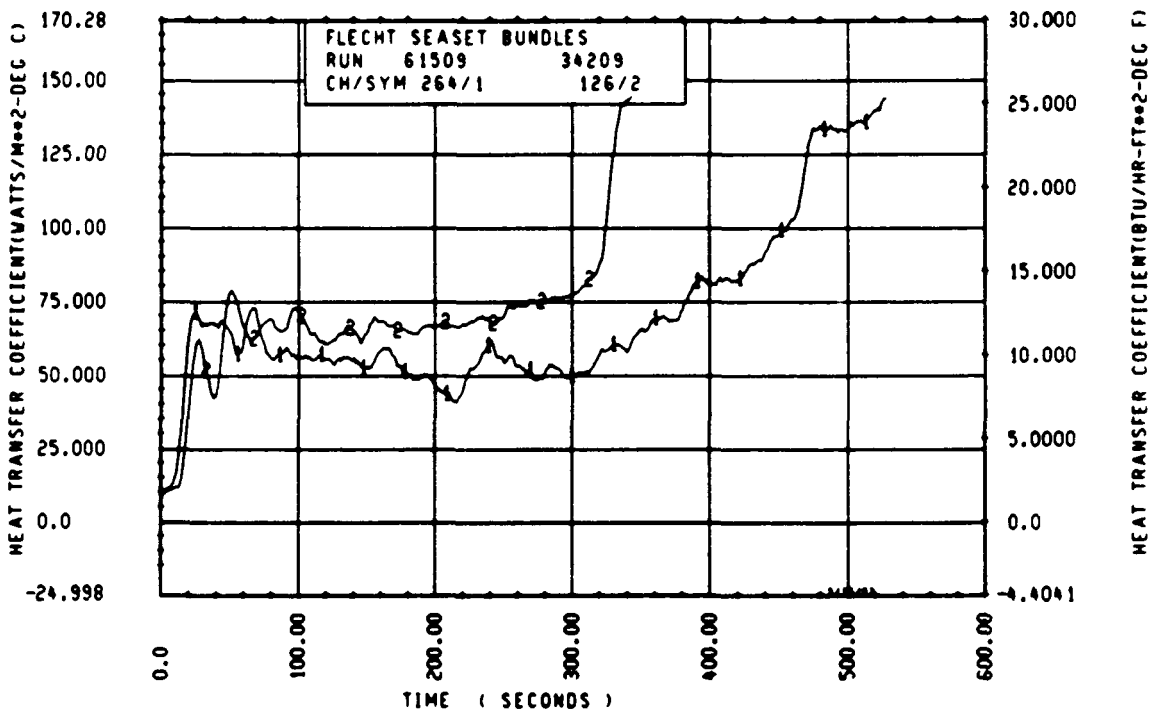
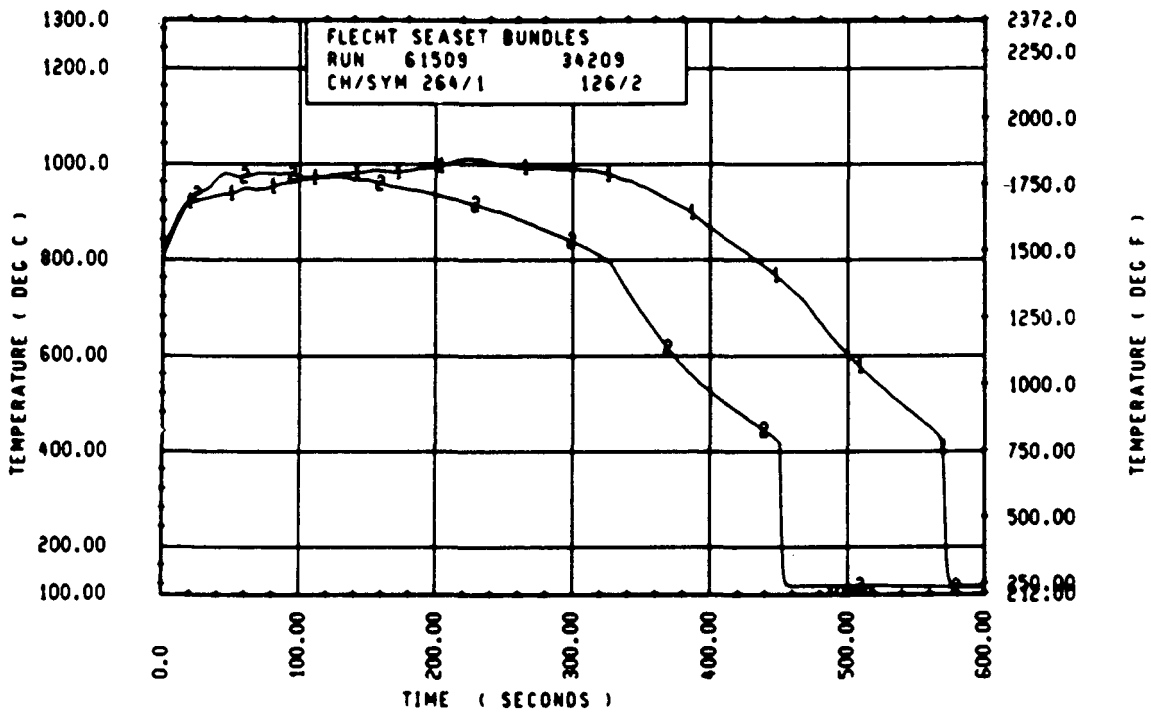
Rod 6J, 1.98 m (78 in.)



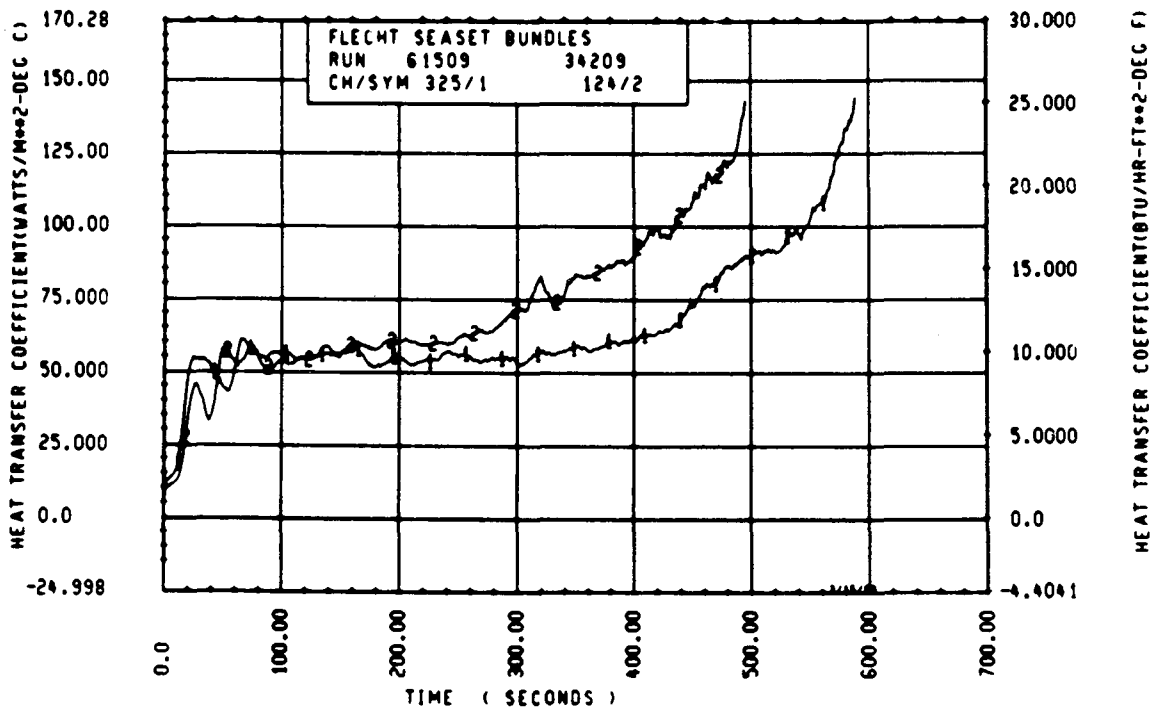
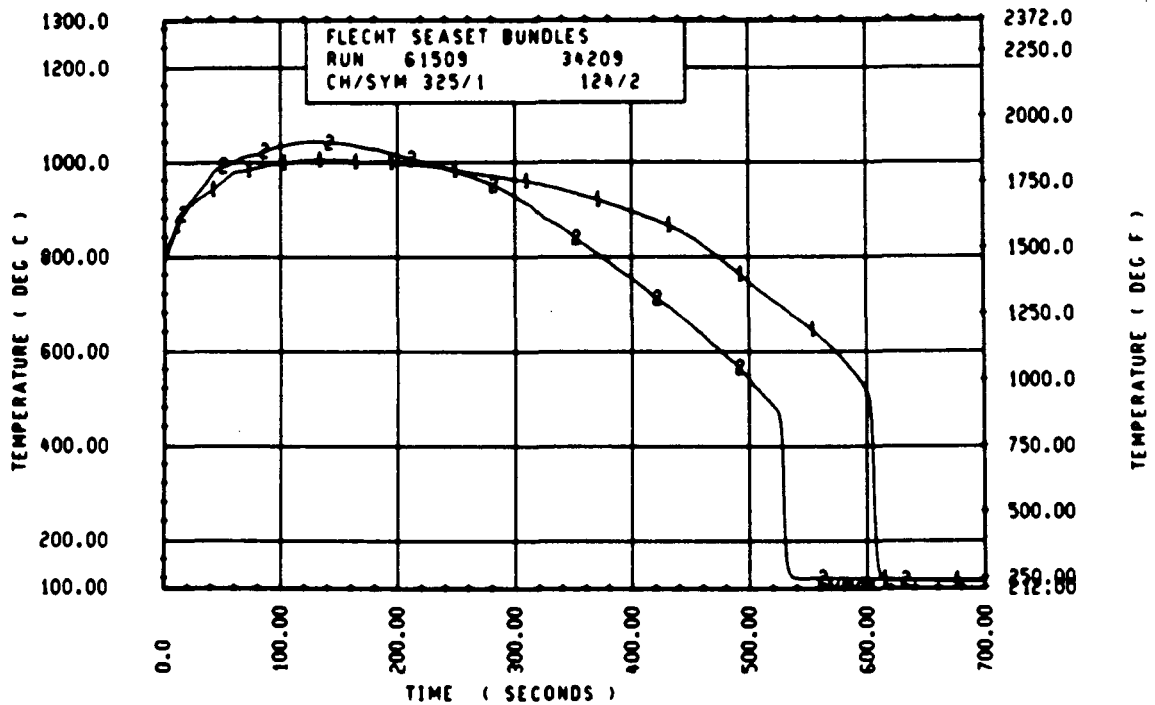
Rod 7H, 1.98 m (78 in.)



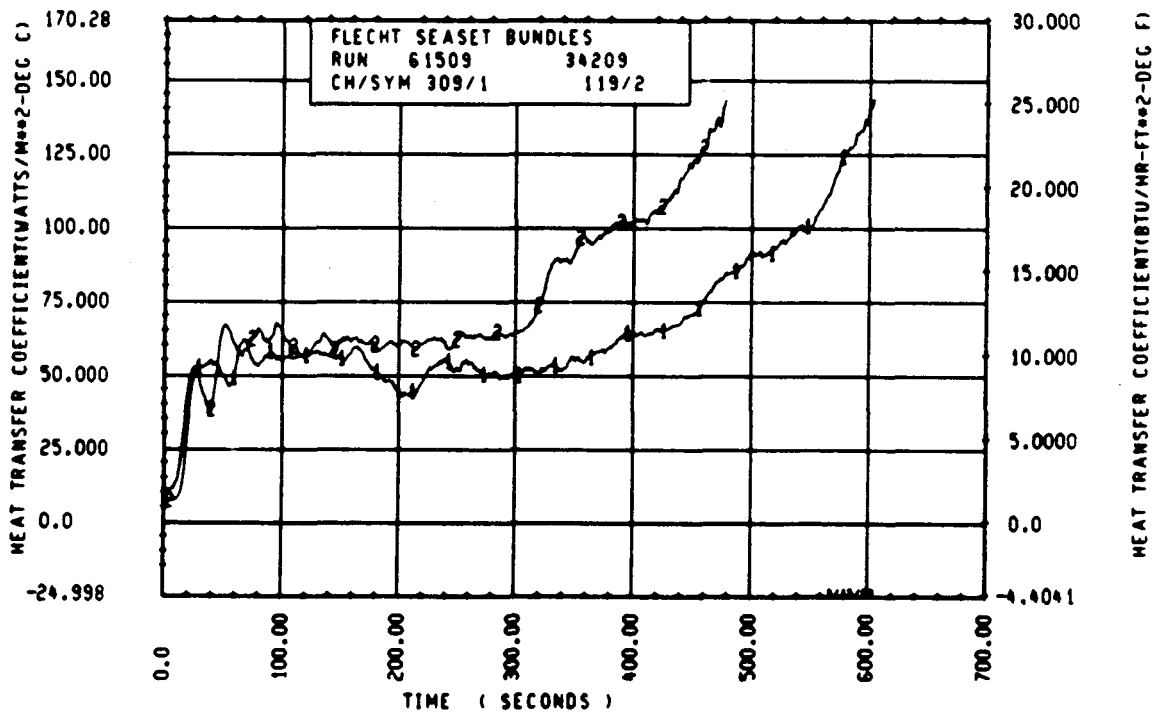
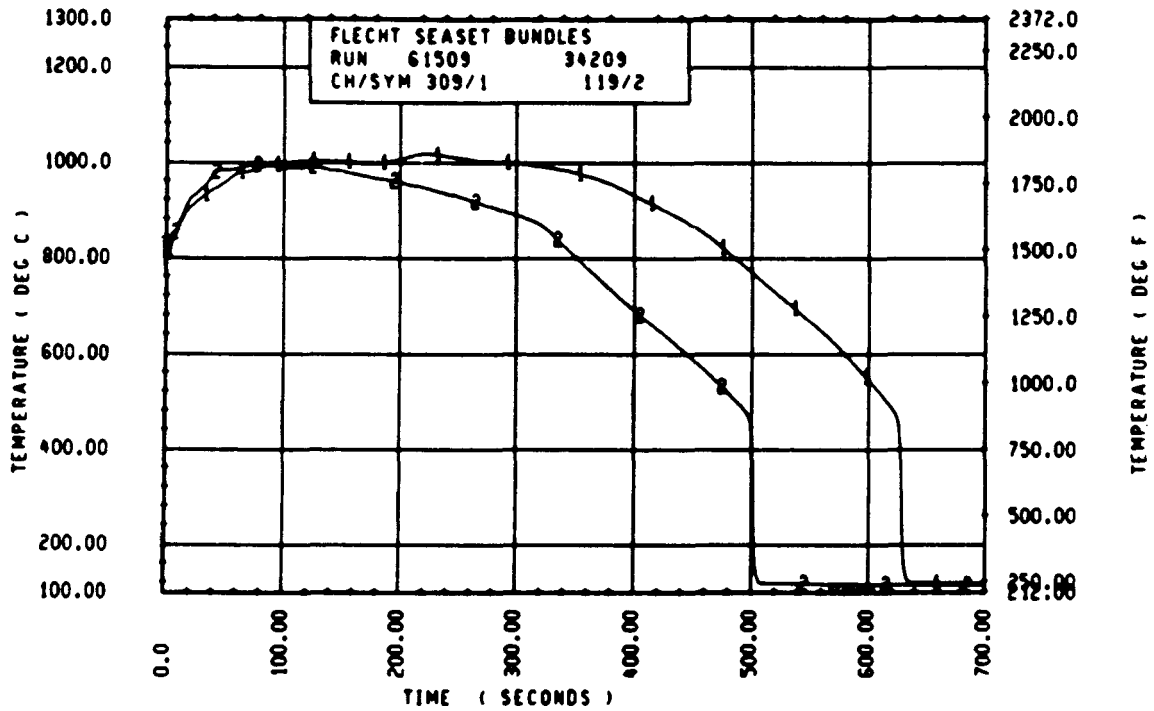
Rod 9F, 1.98 m (78 in.)



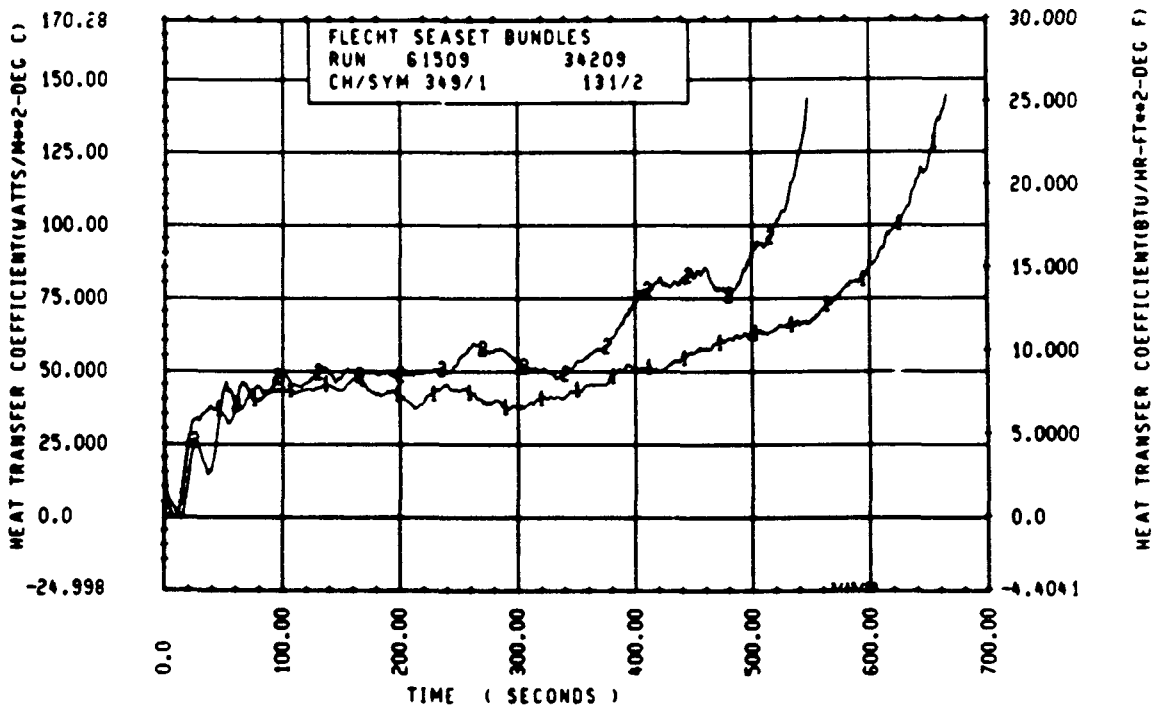
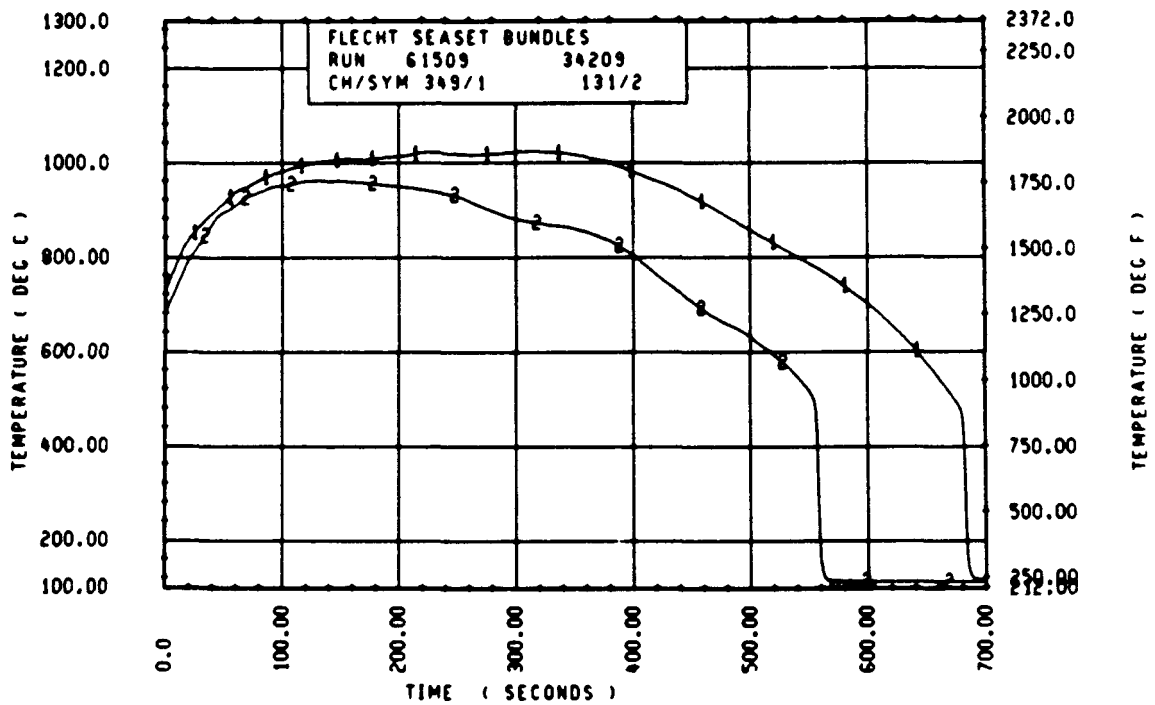
Rod 7E, 2.13 m (84 in.)



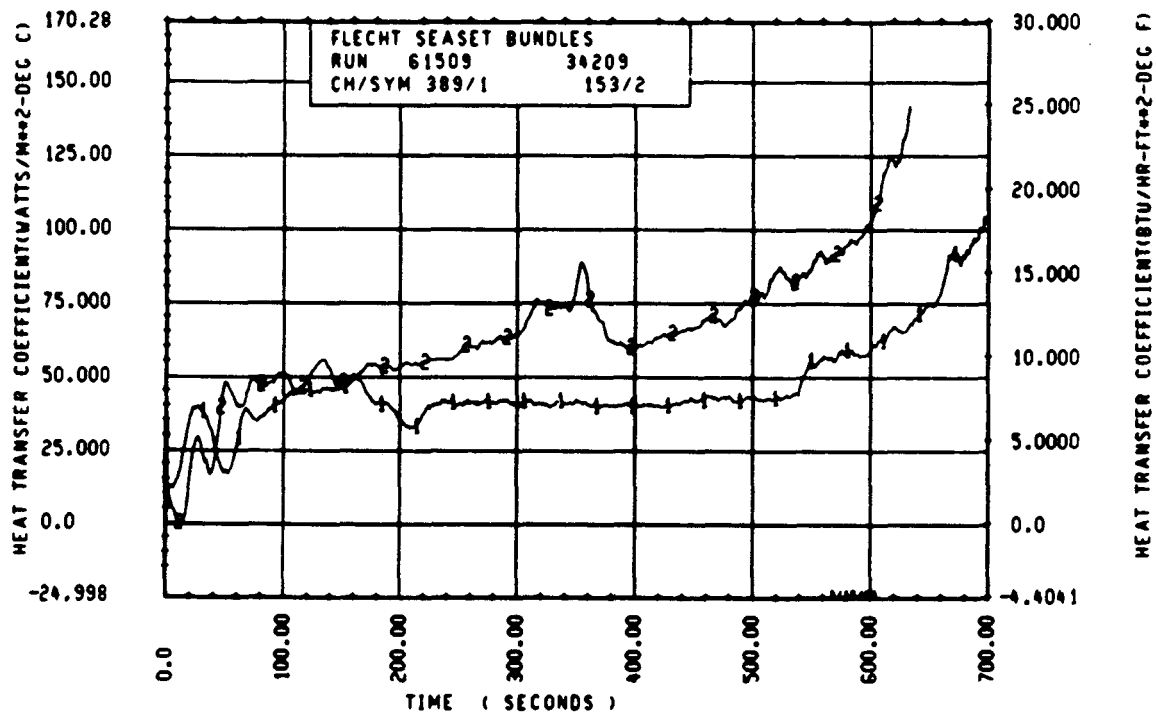
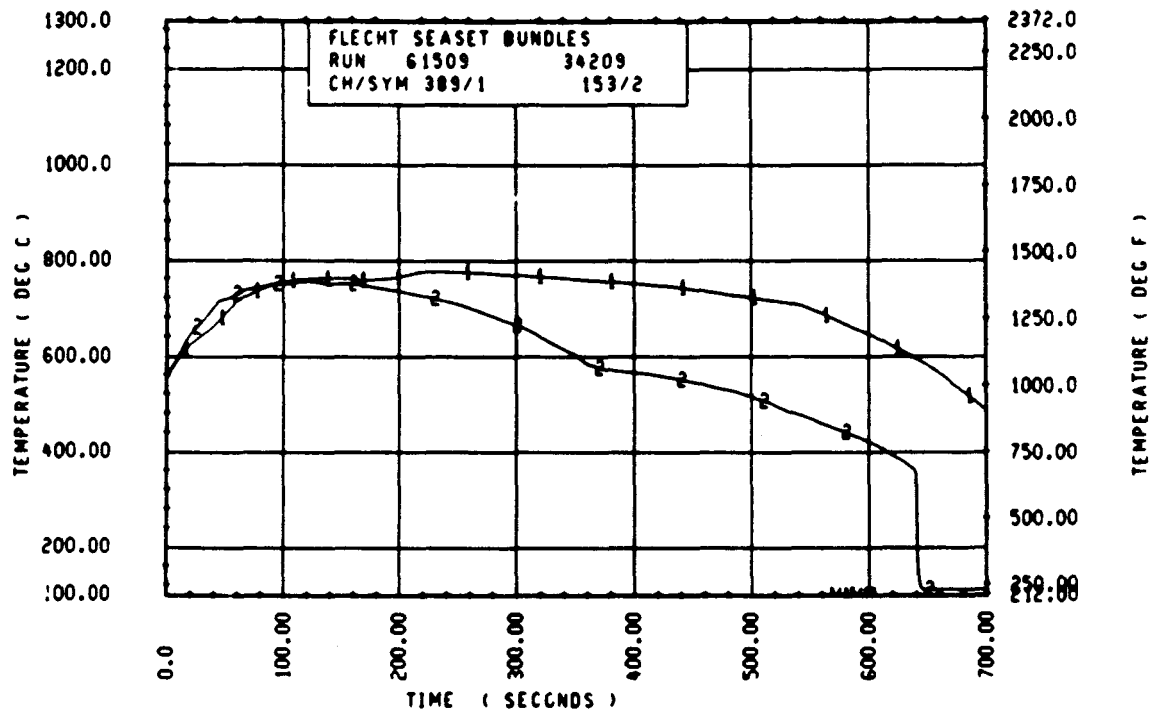
Rod 11E, 2.29 m (90 in.)



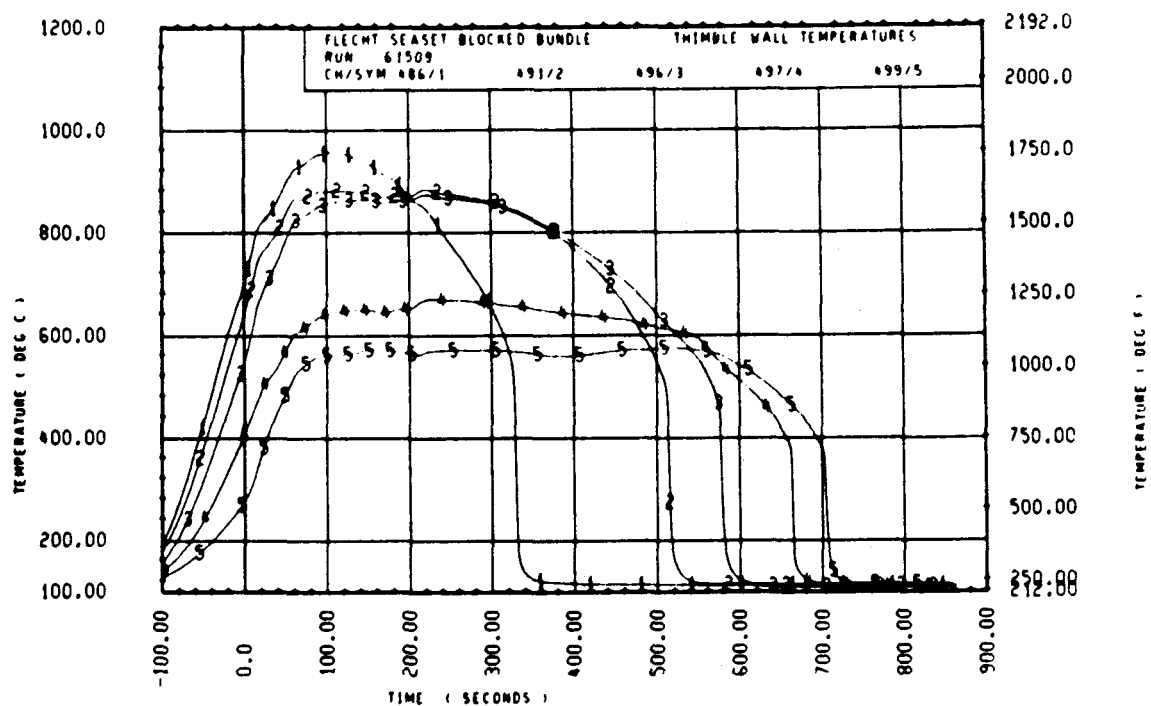
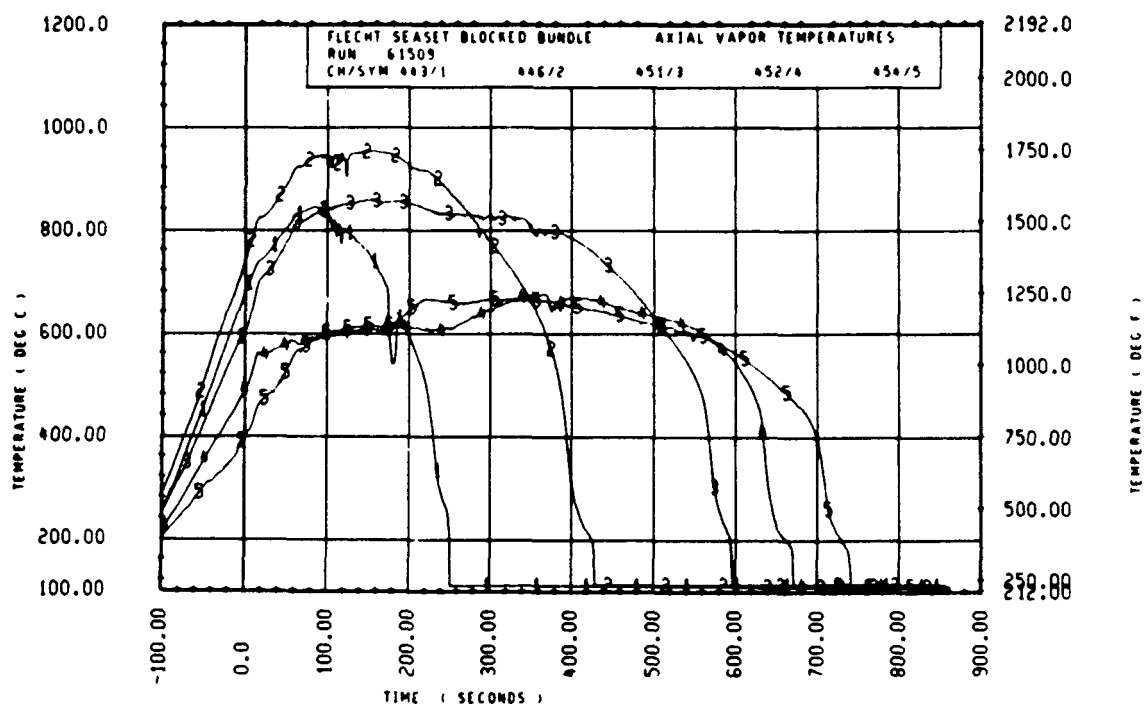
Rod 7D, 2.29 m (90 in.)

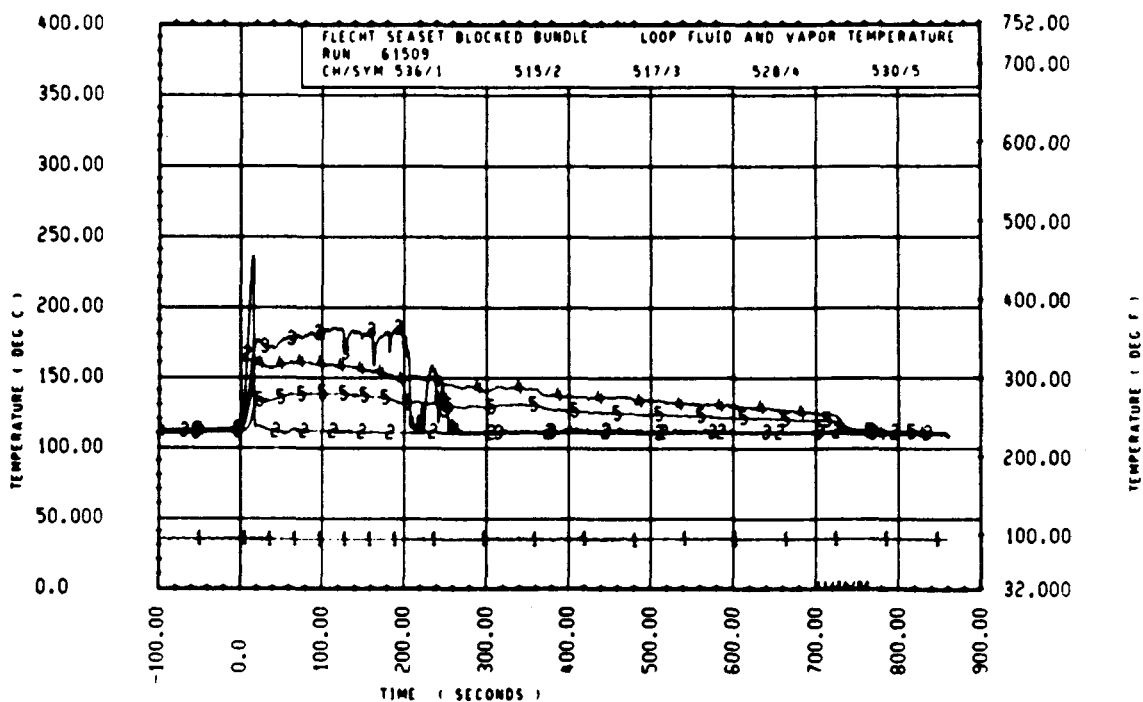
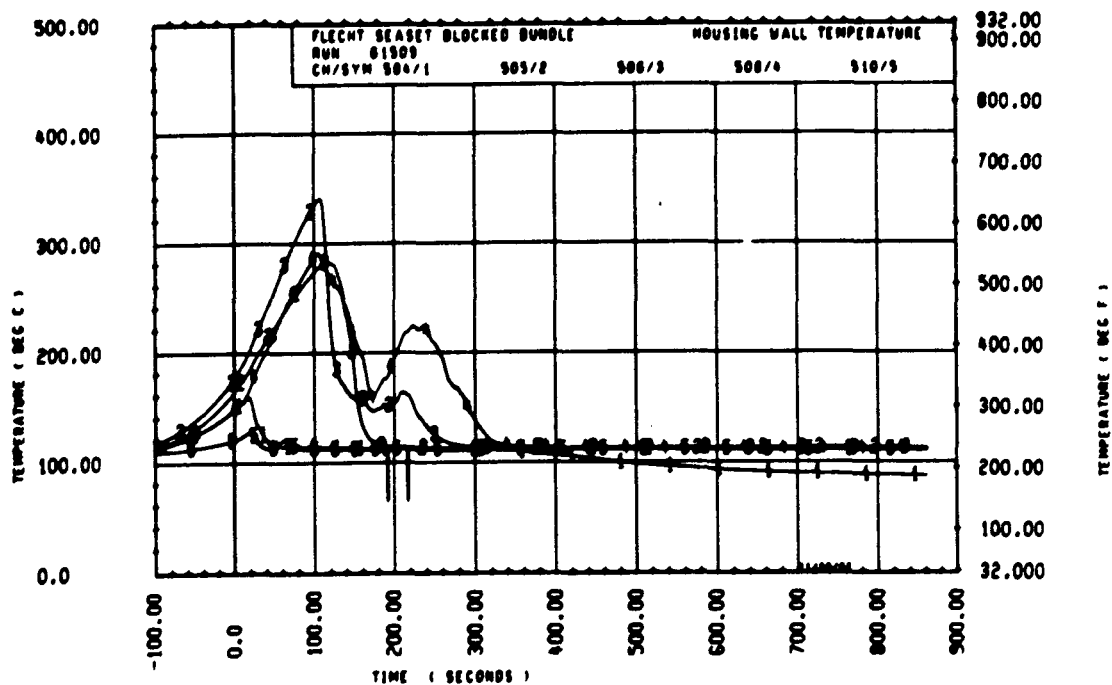


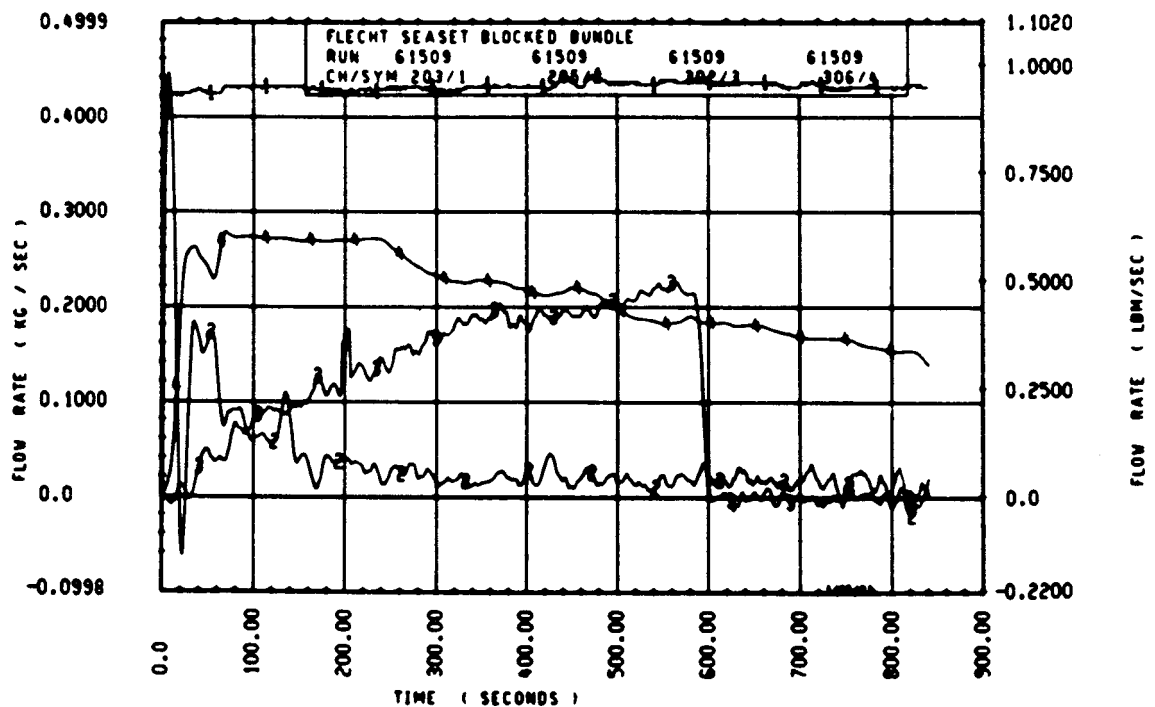
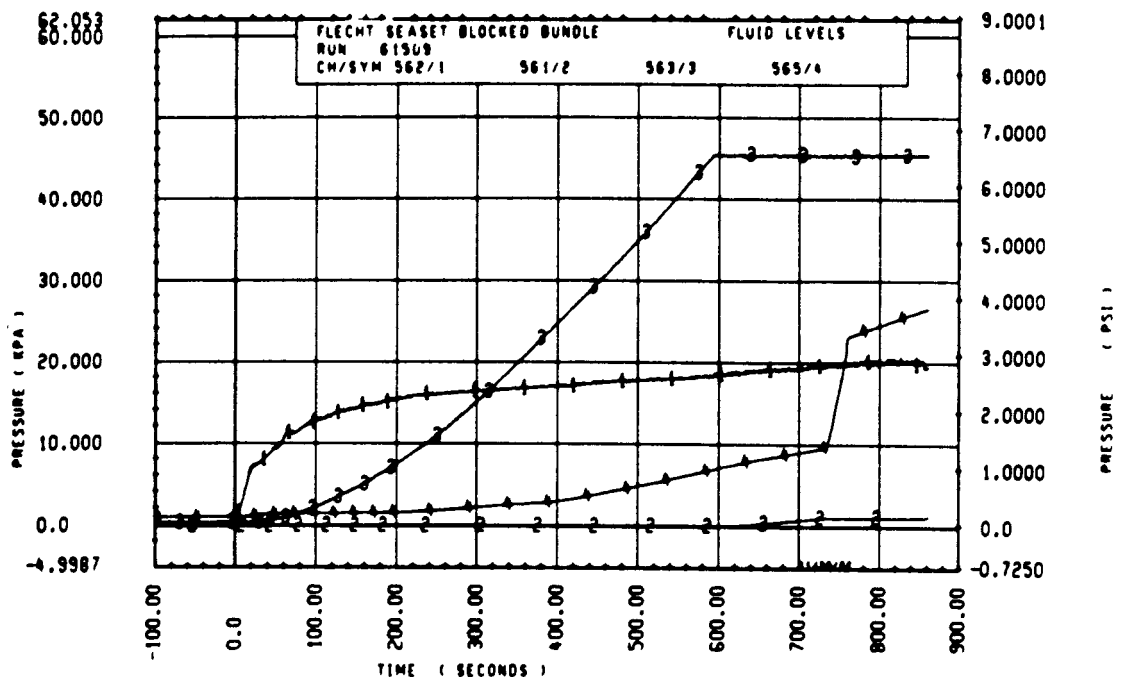
Rod 8F, 2.44 m (96 in.)

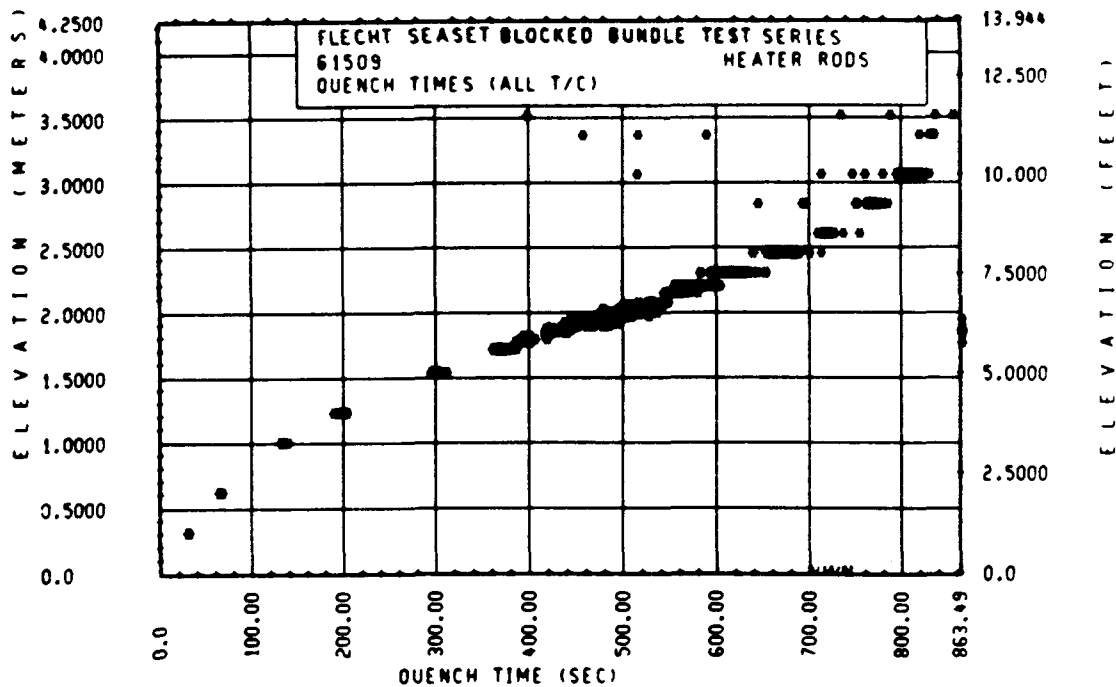
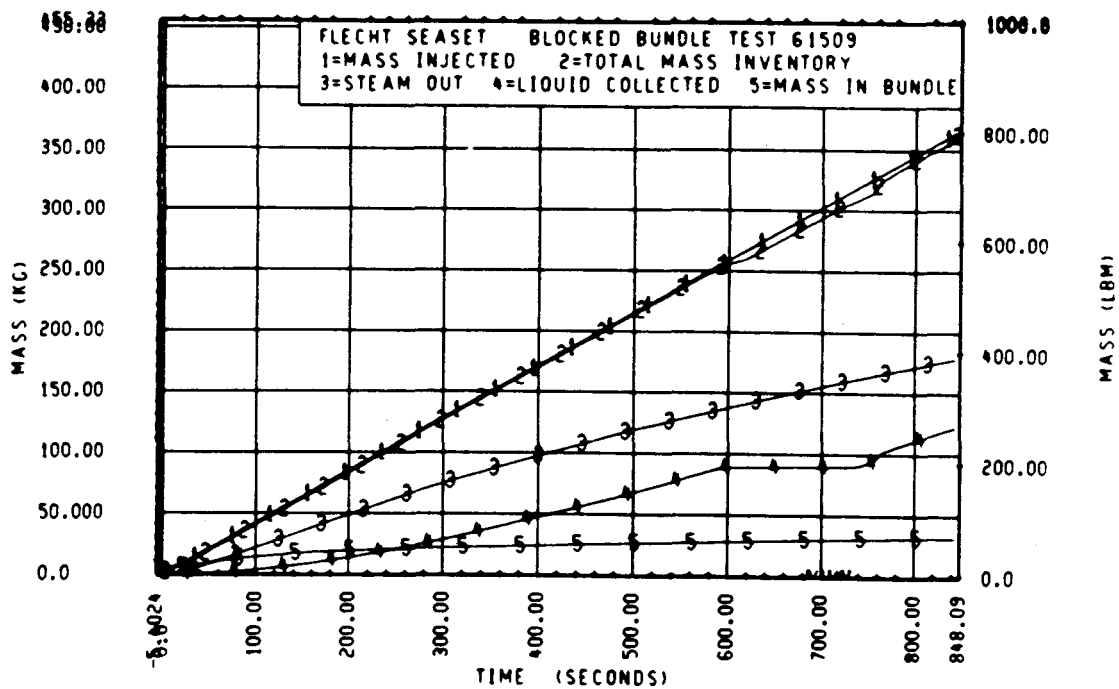


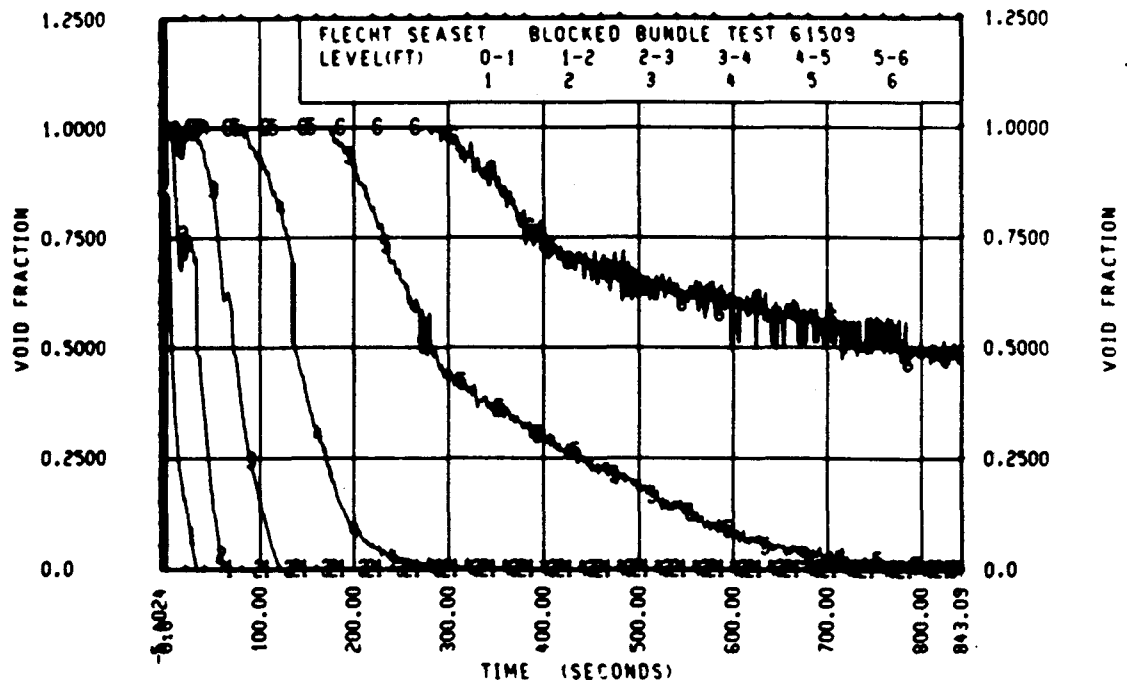
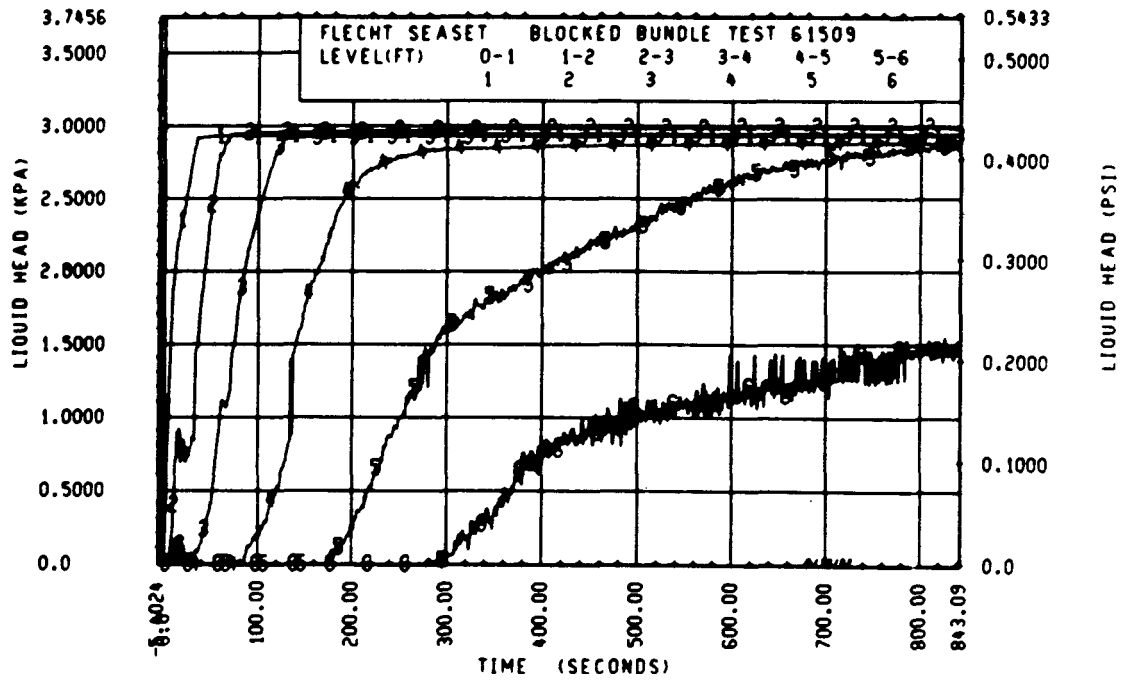
Rod 9C, 2.82 m (111 in.)

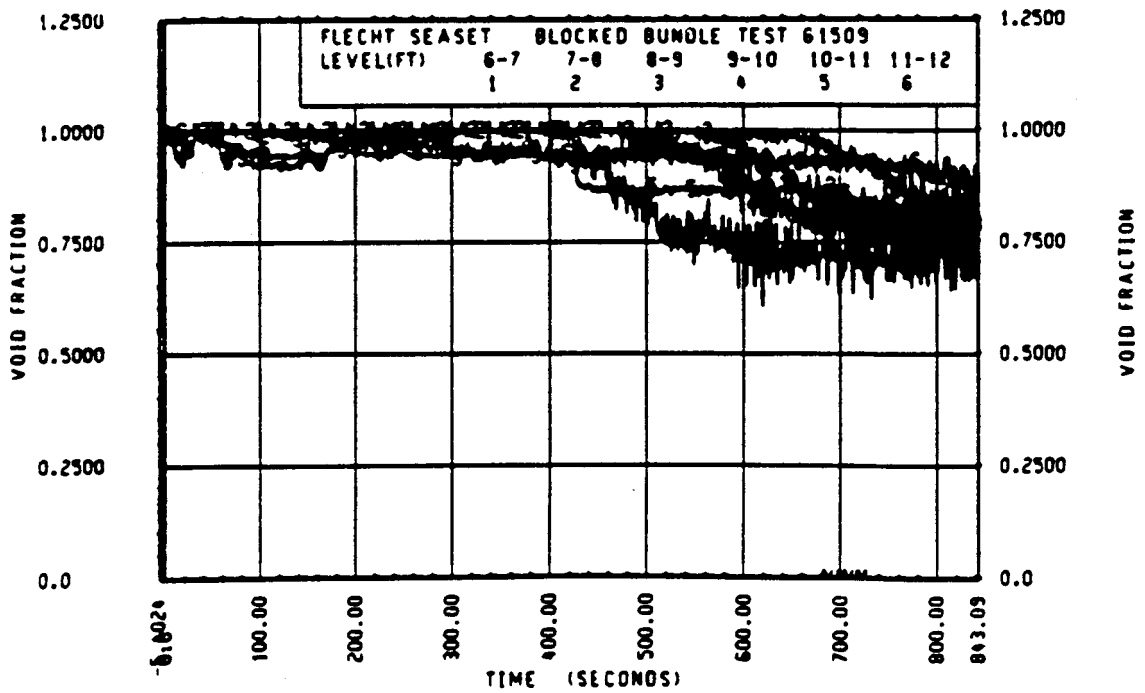
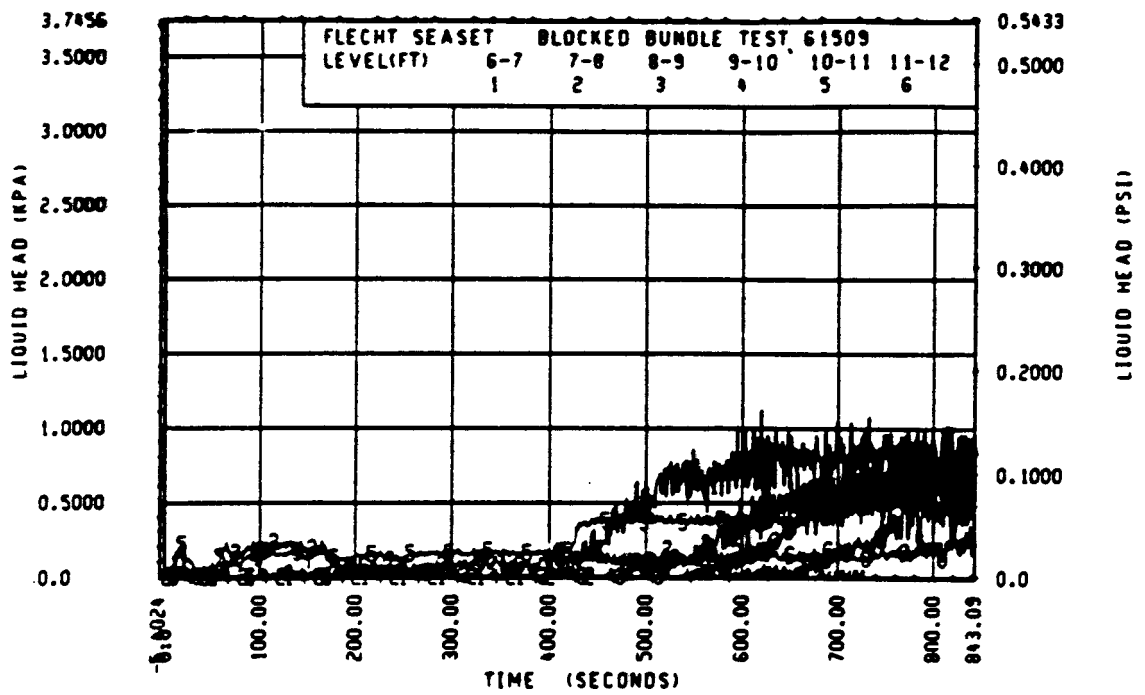












FLECHT SEASET 163-ROD BUNDLE FLOW BLOCKAGE TASK
SUMMARY AND COMMENT SHEET

Run: 61607
Test date: 9/13/82
Test type: Forced reflood
Parameter: Flooding rate effect

AS-RUN TEST CONDITIONS:

Upper plenum pressure	0.276 MPa (40.1 psia)
Initial peak clad temperature and location	877.7°C (1611.9°F), 8N-1.93 m (76 in.)
Initial peak rod power:	
Peripheral rods	2.30 kw/m (0.702 kw/ft)
Bypass rods	2.29 kw/m (0.697 kw/ft)
Blockage island rods	2.30 kw/m (0.702 kw/ft)
Flooding rate	21 mm/sec (0.81 in./sec)
Coolant temperature	52.8°C (127°F)
Initial bundle water level	-0.51 mm (-0.02 in.)

COMMENTS:

Inlet mass flow: ⁽¹⁾ -1.5% average for first 60 seconds, linearly increasing to +2.5% by 220 seconds, and averaging -1.5% thereafter

Power decay: ⁽¹⁾ peripheral rods, 0% constant
bypass rods, -1% constant
blockage rods, 0% constant

1. Relative to run 31805

FLECHT SEASET 103 RDD BUNDLE TEST SERIES

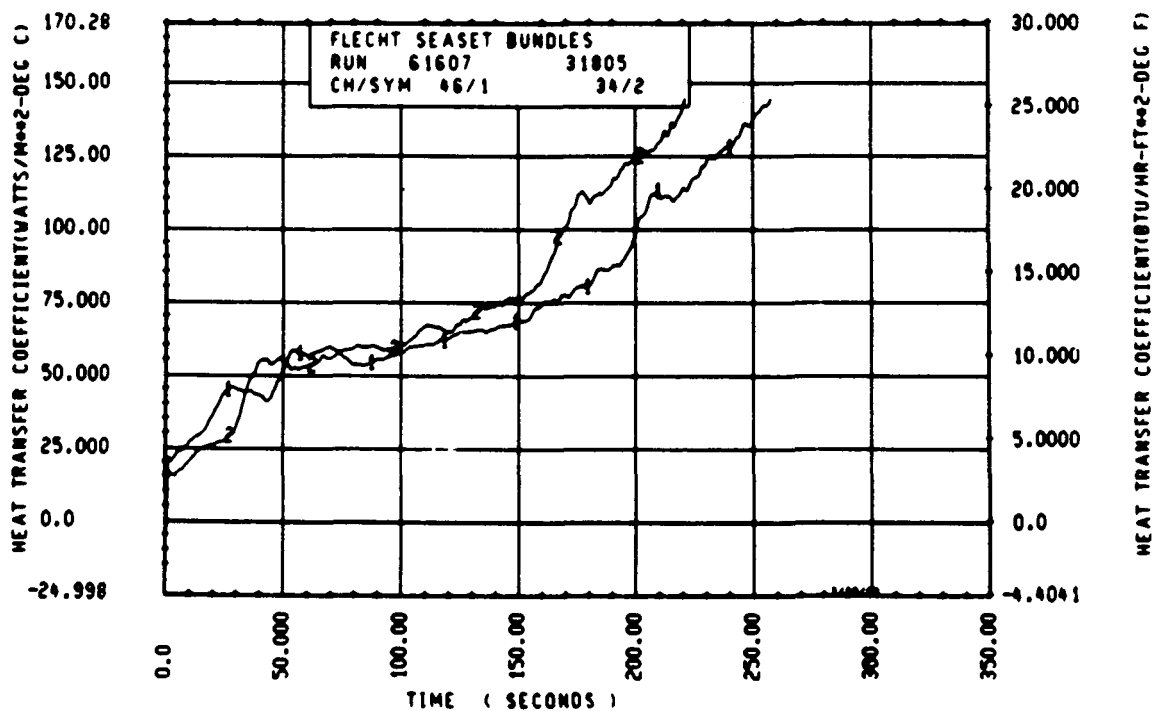
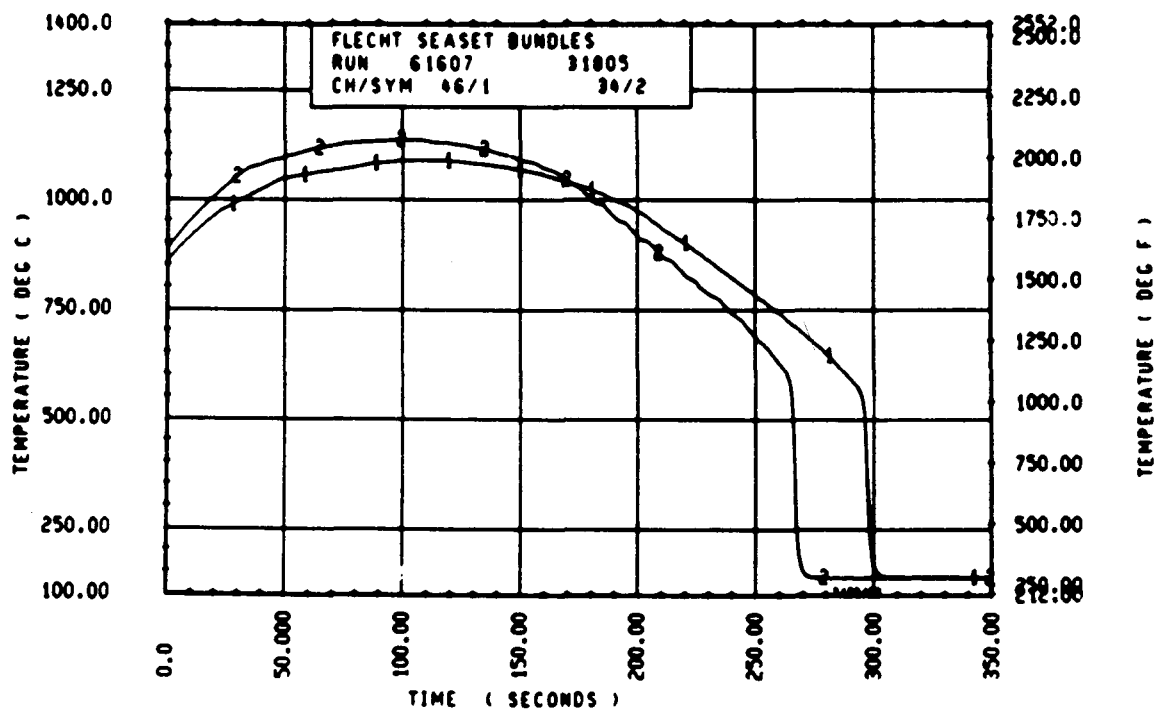
ROD/ELEV	CHAN. NO	T INITIAL AT FLOOD (DEG F)	RUN NUMBER MAXIMUM TEMPERATURE (DEG F)	TEMPERATURE RISE (DEG F)	TURNAROUND TIME (SECONDS)	QUENCH TEMPERATURE (DEG F)	QUENCH TIME (SECONDS)
96 1- 0	3	684.	708.	24.	7.5	597.	23.5
10M 2- 0	6	694.	754.	61.	14.5	606.	24.2
96 3- 3	9	1231.	1308.	137.	39.5	831.	103.4
3J 4- 0	11	1367.	1544.	232.	48.0	811.	152.4
7H 4- 0	12	1352.	1562.	230.	47.0	802.	155.4
8K 4- 0	13	1371.	1615.	244.	47.5	783.	161.4
8N 4- 0	14	1366.	1603.	237.	48.0	848.	150.4
120 4- 0	17	1353.	1570.	223.	51.0	861.	150.4
5E 5- 0	20	1524.	1865.	361.	68.0	975.	240.7
76 5- 0	21	1575.	1924.	354.	68.5	1017.	231.0
96 5- 0	24	1550.	1911.	361.	65.0	1012.	234.0
5E 5- 7	33	1547.	1970.	424.	113.0	983.	301.8
86 5- 7	45	1550.	2030.	480.	117.5	964.	320.7
9M 5- 9	52	1494.	2000.	514.	118.0	1035.	319.4
76 5-10	59	1513.	2031.	518.	118.0	1024.	322.0
7F 5-11	62	1454.	2009.	505.	123.0	983.	336.8
46 5-11	64	1537.	2012.	475.	116.0	910.	345.9
21 6- 0	67	1597.	2023.	427.	106.5	952.	349.0
50 6- 0	70	1497.	1985.	488.	117.0	945.	343.8
6J 6- 0	74	1531.	1940.	459.	104.5	926.	354.0
7K 6- 0	66	1555.	2027.	462.	97.0	937.	344.8
11E 6- 0	80	1557.	1990.	433.	100.5	941.	347.0
8M 6- 2	97	1373.	2014.	641.	167.5	840.	384.7
5H 6- 2	99	1541.	2060.	518.	121.5	941.	377.8
9E 6- 2	105	1344.	2041.	697.	156.5	1274.	364.5
8M 6- 3	111	1416.	2144.	626.	157.0	934.	392.7
46 6- 3	124	1557.	2064.	512.	122.0	940.	380.0
11M 6- 4	134	1460.	2079.	600.	156.0	806.	402.2
9D 6- 4	143	1551.	2165.	554.	199.0	940.	400.4
9J 6- 5	165	1528.	2100.	579.	166.5	944.	416.9
9M 6- 5	166	1542.	2091.	496.	124.0	979.	398.9
8J 6- 6	192	1572.	2120.	548.	145.0	945.	426.0
9D 6- 6	193	1560.	2009.	549.	120.0	980.	419.8
11F 6- 0	173	1554.	2089.	530.	122.5	950.	411.7
46 7- 0	261	1451.	1983.	442.	122.0	733.	470.5
7D 7- 6	309	1467.	2074.	542.	210.1	881.	530.7
76 7- 6	312	1525.	2128.	603.	158.0	938.	517.3
11E 7- 6	325	1494.	2067.	573.	204.1	861.	523.0
5L 8- 0	337	1312.	1993.	681.	145.5	793.	579.0
7H 8- 0	345	1351.	2109.	758.	178.0	830.	580.0
7K 8- 0	346	1364.	2057.	693.	159.0	811.	572.4
5J 8- 6	366	1134.	1849.	710.	148.0	649.	615.9
7a 8- 6	368	1143.	1861.	718.	202.1	675.	615.0
7E 9- 3	393	1104.	1841.	737.	235.1	758.	651.4
8M 9- 3	387	1052.	1643.	791.	301.1	726.	659.0
9C 9- 3	389	1047.	1800.	753.	209.1	692.	661.1
11F 9- 3	394	1043.	1714.	676.	251.1	744.	648.0
7810- 0	408	865.	1645.	781.	212.1	672.	692.1
8H10- 0	415	669.	1778.	459.	325.1	638.	696.1
8K10- 0	417	669.	1681.	612.	252.1	601.	690.7
8N10- 0	418	887.	1544.	711.	177.0	672.	684.5
6H11- 0	429	696.	1368.	672.	355.1	584.	710.7
9G11- 0	431	692.	1462.	776.	321.1	650.	544.6
11E11- 0	432	694.	1592.	698.	266.1	558.	698.1
5J11- 6	436	677.	1243.	566.	408.1	447.	660.2
7B11- 6	437	642.	1314.	672.	243.1	611.	702.0
8J11- 6	438	664.	1307.	616.	333.1	545.	725.3

RUN 61607 HEATEK RJD STATISTICAL DATA

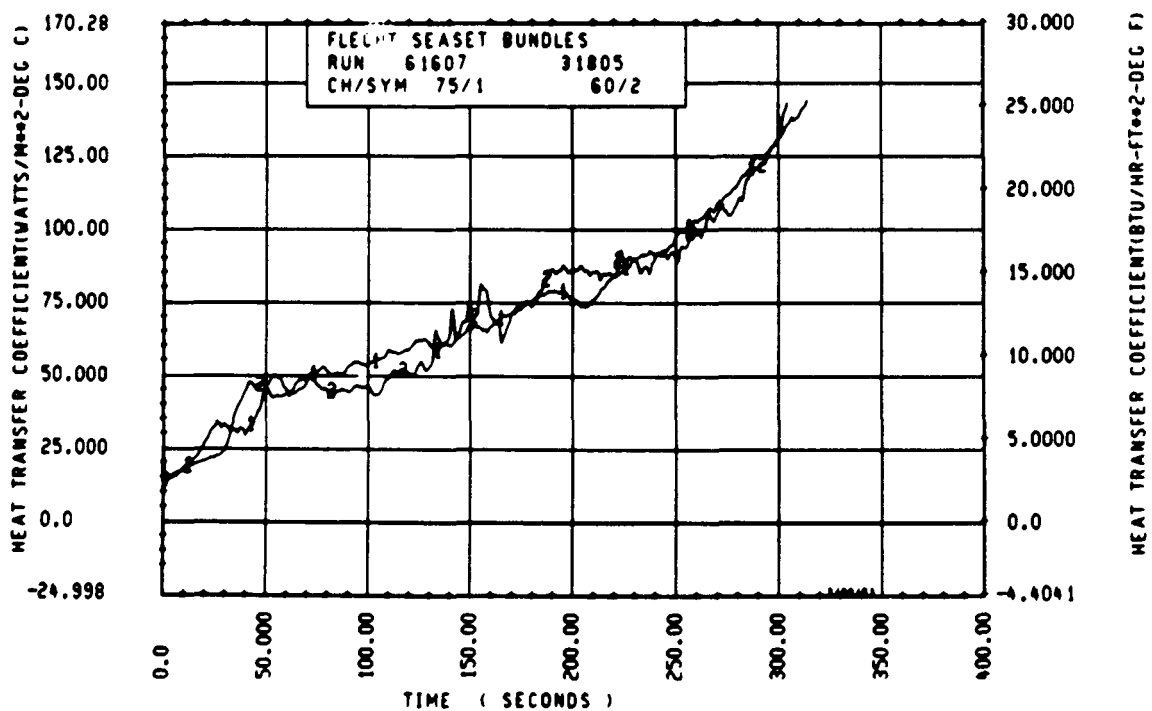
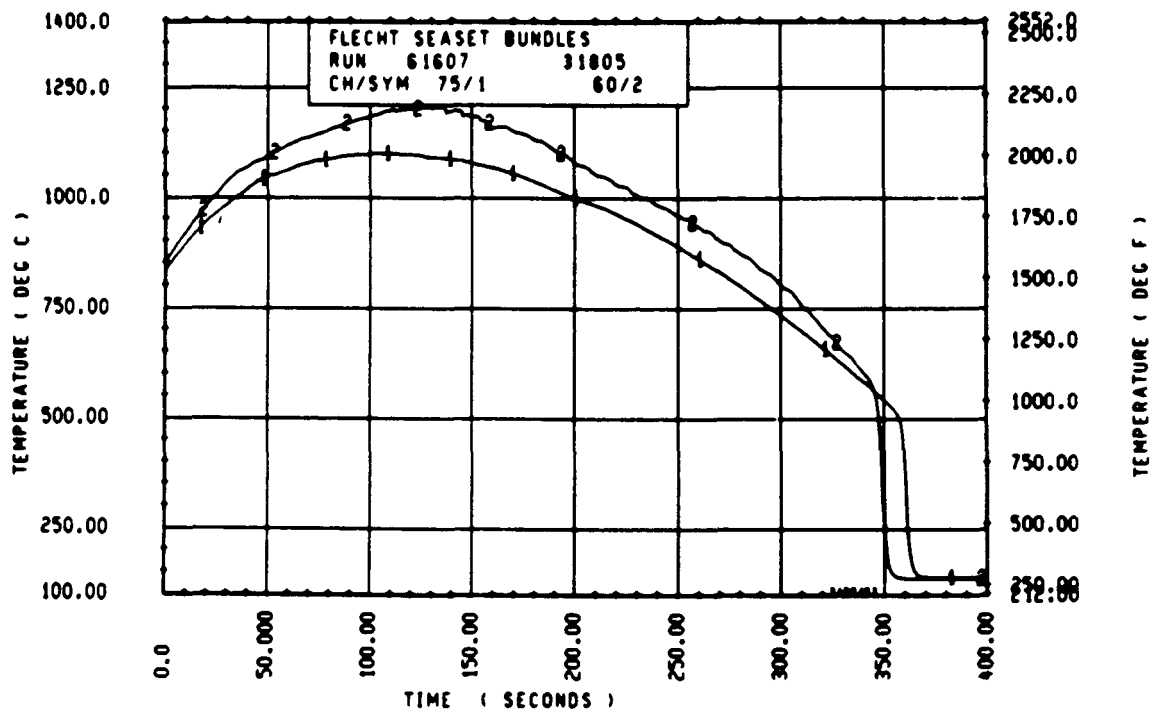
ELEV	INITIAL TEMP (DEG F)			MAX TEMP (DEG F)			TURNAROUND TIME (SEC)		
	MAX	MIN	MEAN	MAX	MIN	MEAN	MAX	MIN	MEAN
12	585.8	683.7	684.4	709.4	767.6	768.5	8.0	7.5	7.7
24	893.6	863.6	874.0	954.4	925.4	933.5	15.5	14.5	14.8
39	1230.6	1178.6	1204.7	1308.0	1334.2	1345.1	44.0	38.5	40.9
48	1343.9	1352.2	1361.5	1615.2	1570.0	1601.5	64.5	47.0	51.7
60	1576.0	1457.4	1533.6	1448.2	1740.0	1804.5	88.5	70.5	81.9
67	1554.3	1514.3	1561.2	2036.1	1916.0	1963.5	117.5	88.0	100.5
69	1533.8	1493.7	1514.0	2008.1	1954.6	1975.0	118.0	101.0	107.4
70	1606.4	1498.0	1537.7	2031.4	1942.4	1990.8	118.0	95.0	105.9
71	1537.0	1454.2	1499.3	2011.0	1944.3	1986.2	123.0	95.5	112.7
72	1576.6	1469.2	1547.8	2050.2	1984.9	2016.3	134.5	92.5	107.0
73	1576.1	1476.6	1533.9	2045.5	1951.6	2004.2	122.5	80.5	106.9
74	1599.8	1373.3	1513.5	2070.0	1948.7	2042.0	167.5	101.5	121.2
75	1604.3	1417.8	1525.2	2071.2	1984.6	2045.9	167.0	96.0	124.4
76	1611.9	1462.8	1550.3	2105.2	2013.6	2074.1	199.0	94.5	126.5
77	1592.3	1480.4	1546.1	2124.3	1998.7	2065.6	195.9	96.5	136.2
78	1611.9	1518.6	1564.8	2142.2	1997.6	2111.9	200.1	109.5	140.4
79	1606.4	1504.9	1565.1	2188.7	2012.7	2112.3	204.1	100.5	144.5
80	1586.8	1504.9	1552.2	2173.2	2044.4	2128.4	202.1	113.0	148.3
81	1581.3	1473.4	1534.5	2168.4	2050.3	2123.5	177.0	118.5	144.8
84	1545.7	1433.9	1499.4	2126.7	1980.5	2063.4	204.1	99.0	129.1
86	1587.9	1476.6	1536.8	2112.4	1951.6	2051.5	213.1	97.5	148.6
90	1531.6	1430.7	1496.7	2152.4	1947.6	2084.5	219.1	117.0	162.2
96	1401.8	1271.3	1334.0	2145.0	1960.5	2063.0	224.1	138.5	174.5
102	1193.1	1040.3	1115.3	2012.7	1817.3	1900.2	239.1	148.0	170.0
111	1104.0	1040.3	1067.0	1890.8	1670.2	1784.8	331.1	141.0	240.9
120	924.6	822.2	871.8	1865.9	1525.0	1685.3	320.1	160.5	259.2
132	696.3	686.9	692.6	1461.6	1327.9	1367.6	396.1	260.1	325.5
138	689.0	641.7	665.9	1375.4	1243.1	1307.8	438.1	243.1	312.7

RUN 61607 HEATEK RJD STATISTICAL DATA

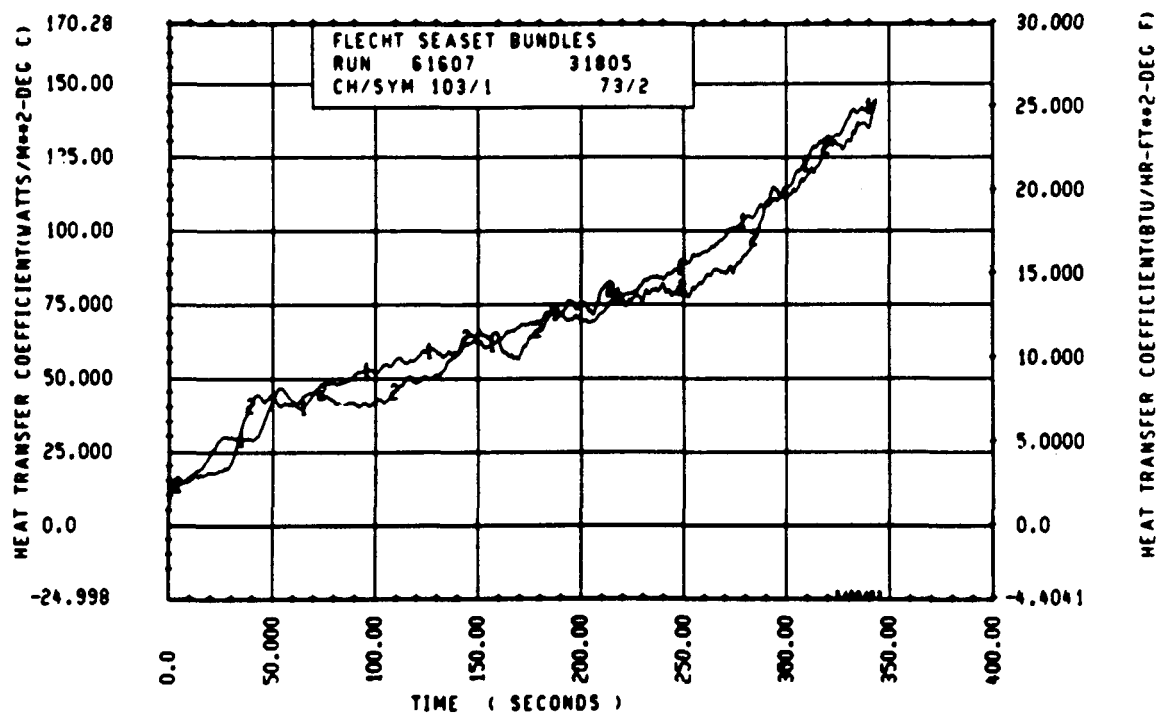
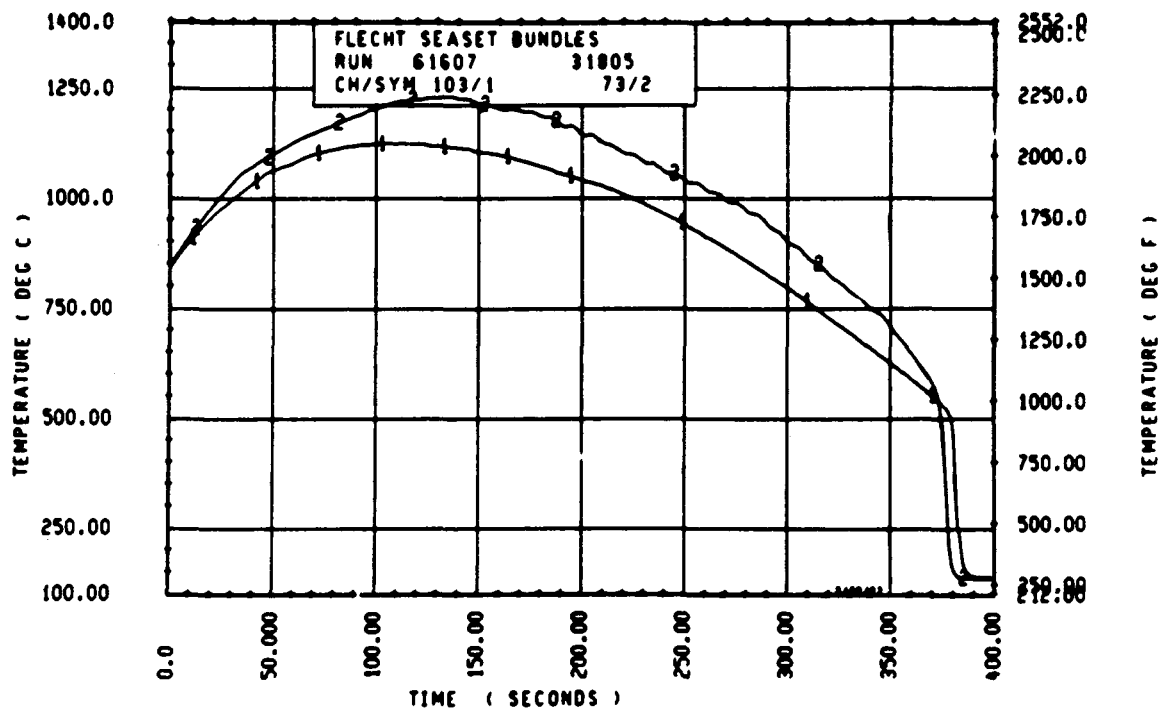
ELEV	TEMP RISE (DEG F)			QUENCH TEMP (DEG F)			QUENCH TIME (SEC)		
	MAX	MIN	MEAN	MAX	MIN	MEAN	MAX	MIN	MEAN
12	24.1	24.1	24.1	597.2	588.4	592.3	25.6	23.5	24.9
24	60.8	56.9	58.8	666.4	652.1	661.5	54.2	51.0	52.5
39	155.8	128.7	144.4	831.3	804.6	820.9	136.9	103.3	104.4
48	251.4	222.7	236.0	872.5	763.5	824.3	161.4	150.3	153.7
60	379.1	305.0	351.0	1044.3	877.9	971.8	251.8	231.0	239.3
67	486.1	353.9	402.3	1029.1	914.1	973.6	310.7	288.9	299.7
69	514.3	430.2	456.6	1035.1	929.8	963.0	325.9	311.8	318.8
70	518.3	385.4	453.2	1044.2	867.3	960.8	337.7	319.7	326.6
71	555.0	421.0	486.9	1025.3	897.5	953.8	345.9	329.0	338.3
72	565.0	411.1	476.5	1018.6	892.1	944.5	361.8	343.8	350.2
73	519.8	432.6	476.3	1010.4	861.9	939.2	369.8	345.9	358.7
74	645.6	444.4	529.0	959.2	727.4	915.9	390.5	365.5	375.7
75	626.5	444.7	515.7	961.2	747.1	967.7	373.6	365.8	369.9
76	626.0	452.3	523.8	986.5	805.6	931.9	473.5	370.4	394.1
77	593.8	458.5	539.4	983.7	810.8	937.4	428.7	398.4	409.2
78	604.5	471.4	541.1	1062.2	810.4	934.3	437.7	404.8	418.0
79	616.0	471.2	547.3	1217.0	877.7	945.6	438.3	404.8	424.8
80	634.1	512.8	576.2	976.7	803.9	925.1	448.8	425.7	435.4
81	637.7	544.5	584.3	1005.8	821.2	907.6	455.9	437.8	444.9
84	624.4	445.5	503.5	863.5	733.1	780.4	483.0	461.7	470.3
86	564.4	452.6	512.7	972.5	747.9	865.4	537.8	488.6	486.7
90	645.2	506.0	543.9	958.8	743.1	884.3	545.9	511.9	526.3
95	784.7	615.1	709.9	917.2	776.8	845.0	589.9	565.4	573.5
102	844.5	655.2	745.3	763.0	630.6	764.1	624.1	606.9	613.9
111	804.0	612.6	722.8	740.2	667.2	738.5	663.0	647.4	653.7
120	915.9	638.7	813.6	947.8	572.1	674.3	693.1	578.6	684.8
132	769.5	641.0	695.0	855.0	534.7	667.0	723.1	594.8	692.3
138	722.1	565.6	641.9	820.5	446.9	618.7	725.3	403.3	618.2



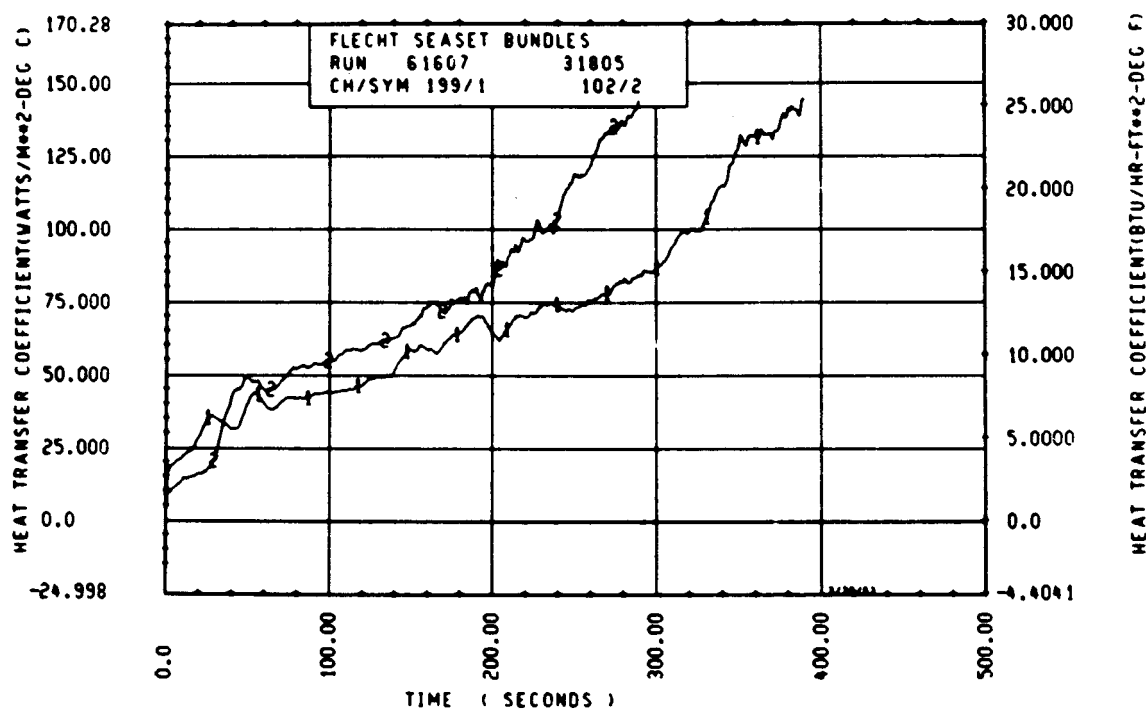
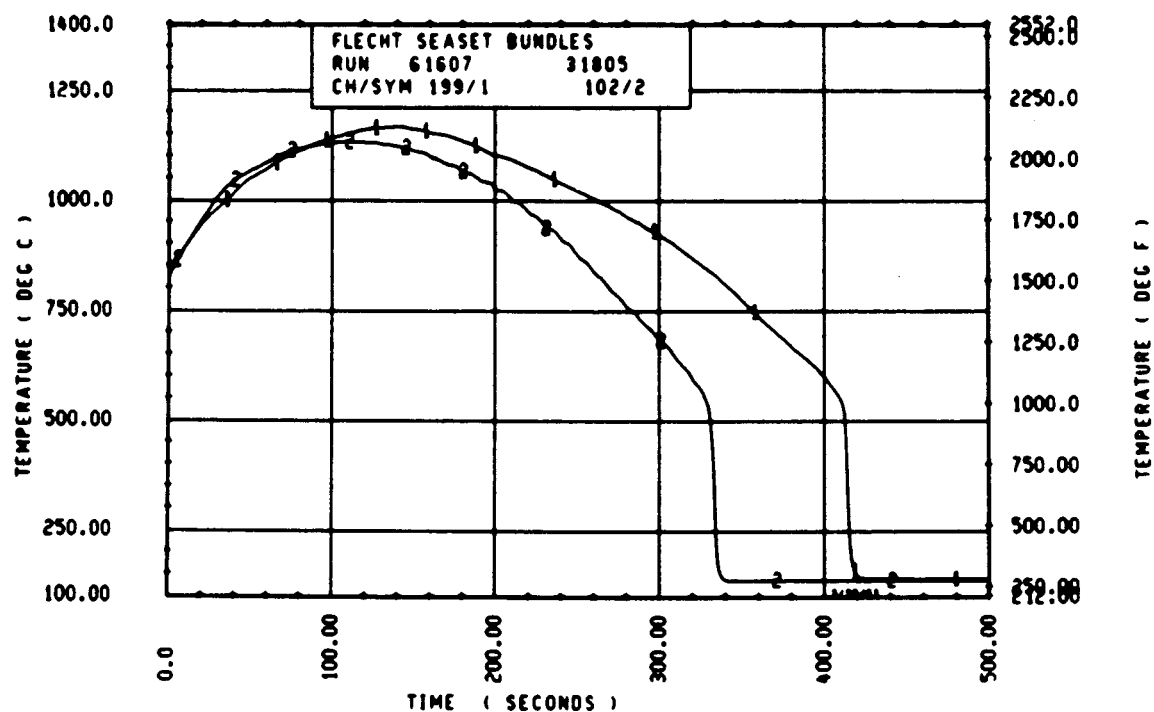
Rod 9G, 1.70 m (67 in.)



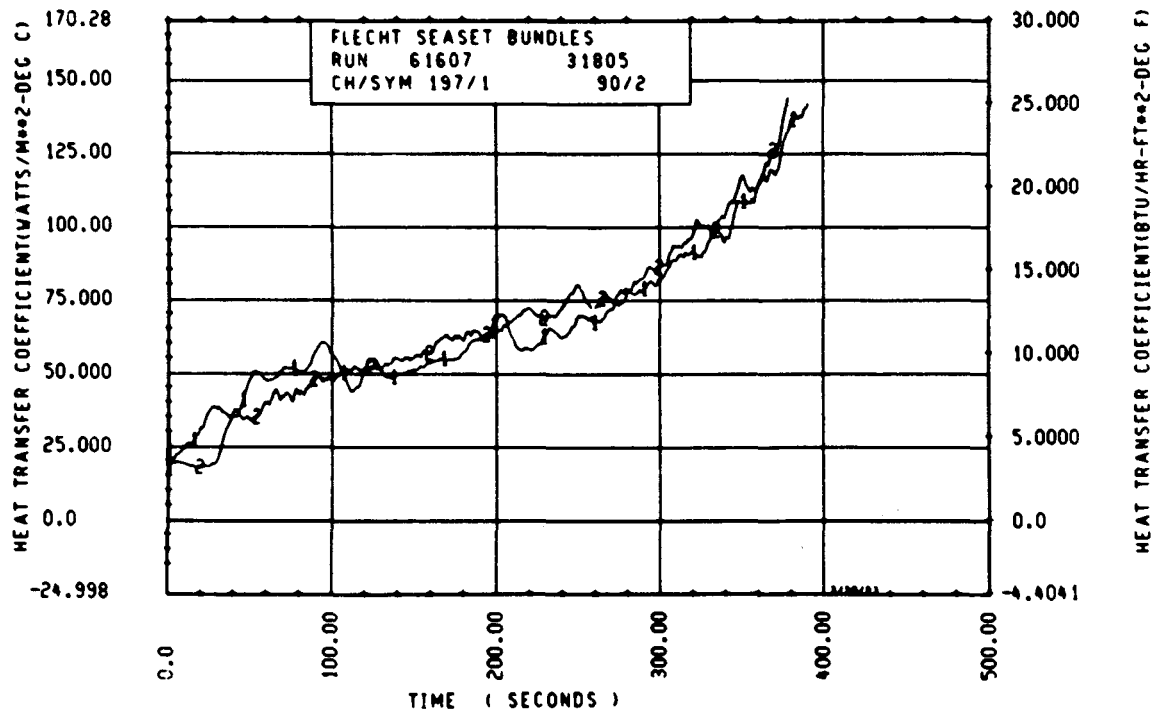
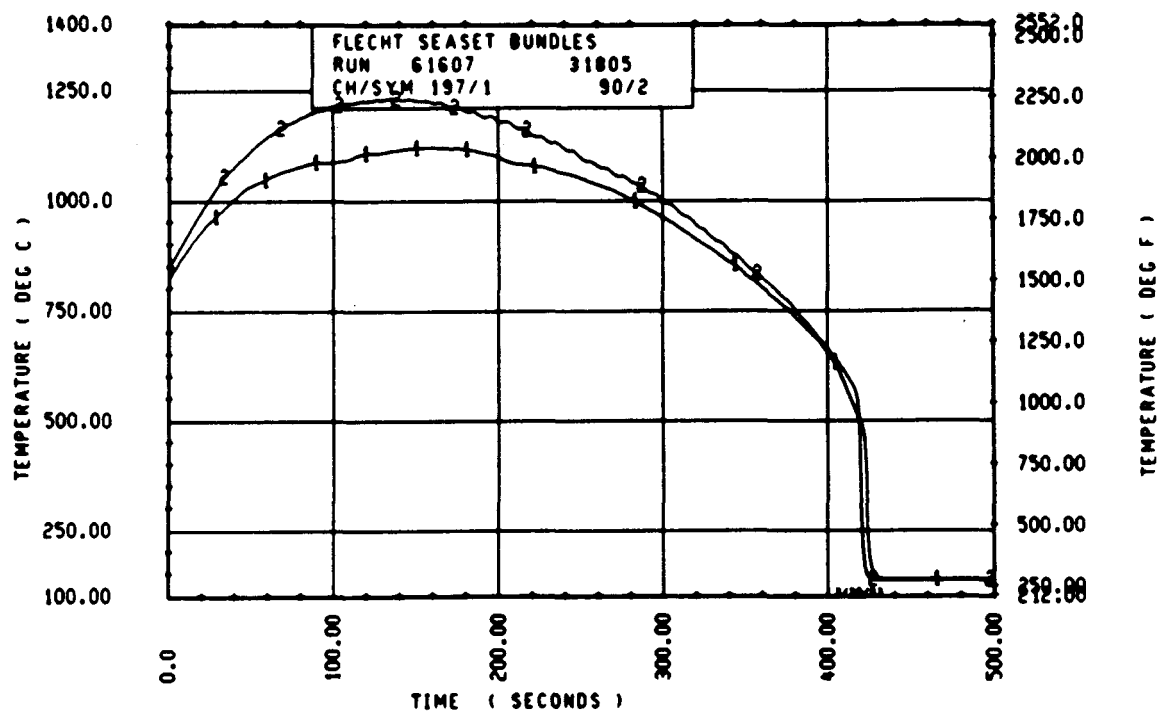
Rod 6L, 1.83 m (72 in.)



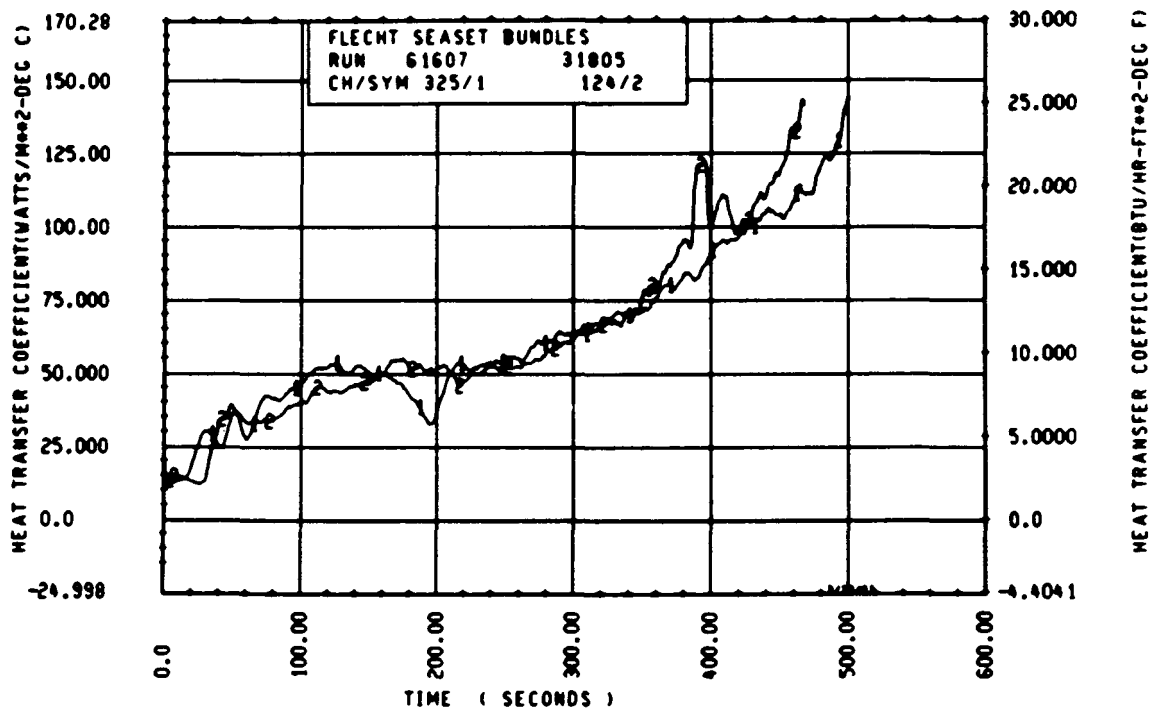
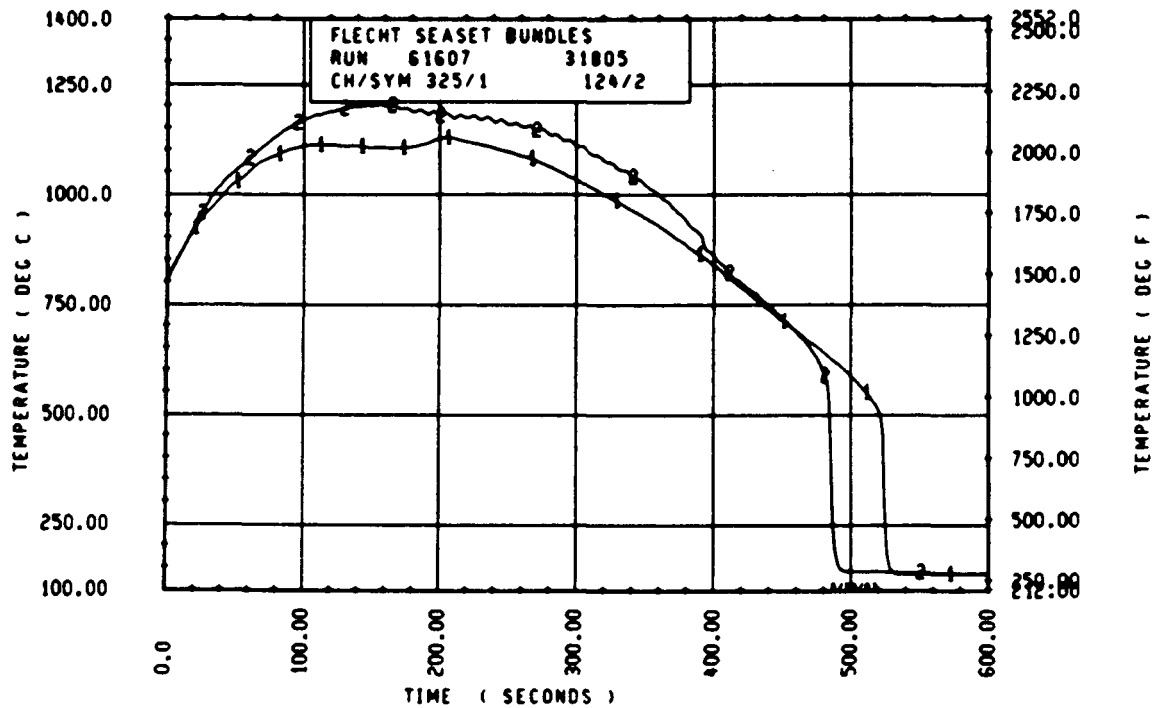
Rod 6L, 1.88 m (74 in.)



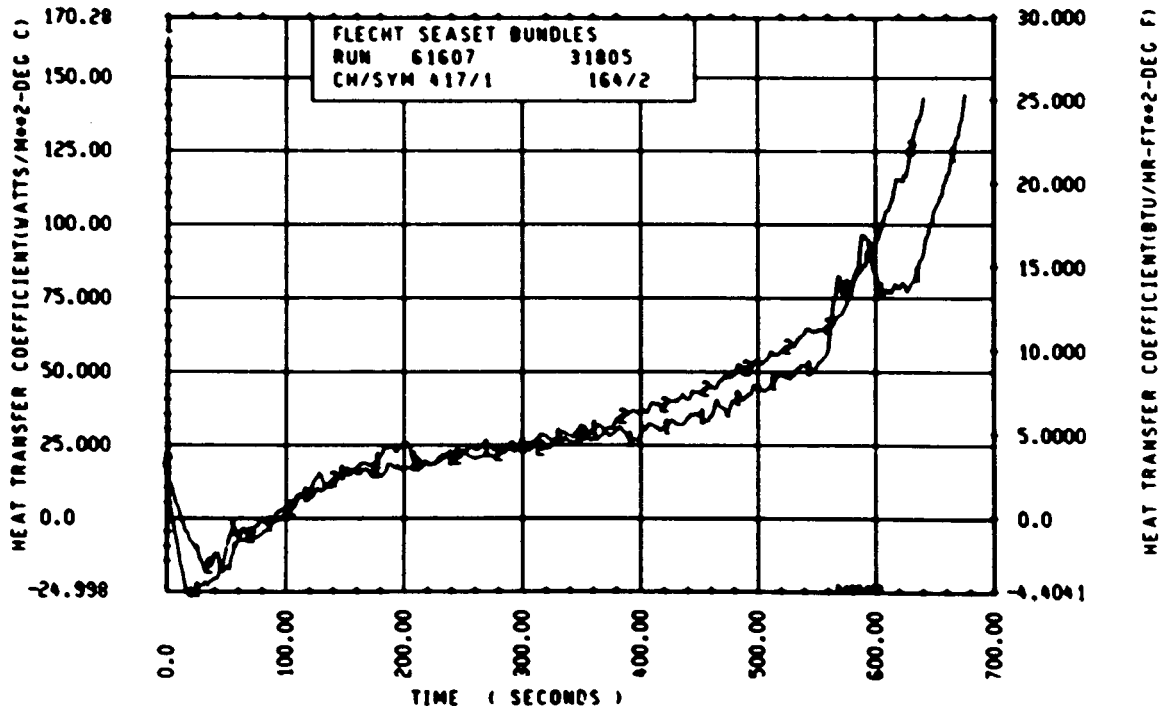
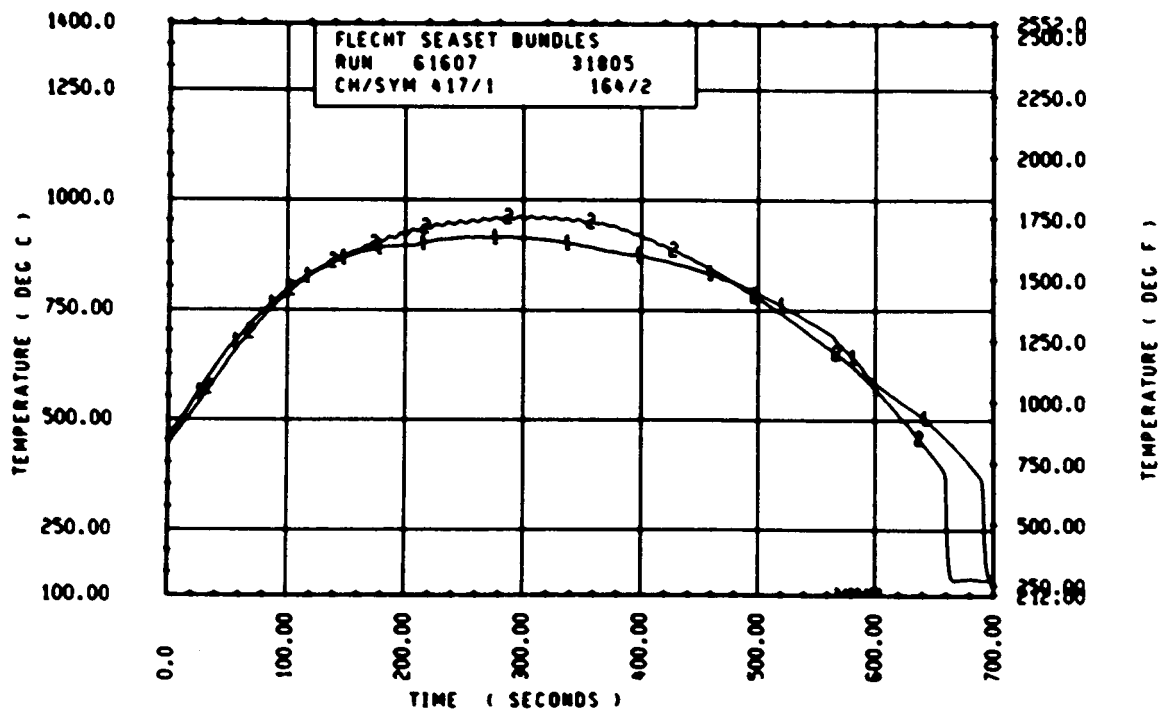
Rod 13G, 1.98 m (78 in.)



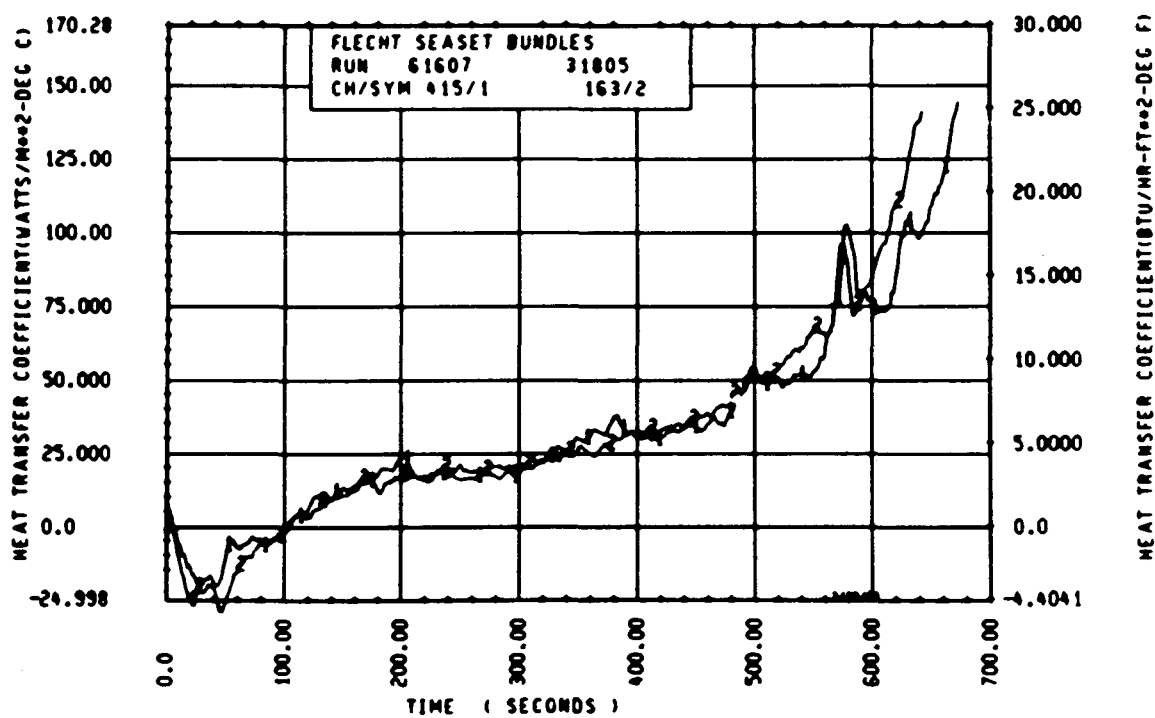
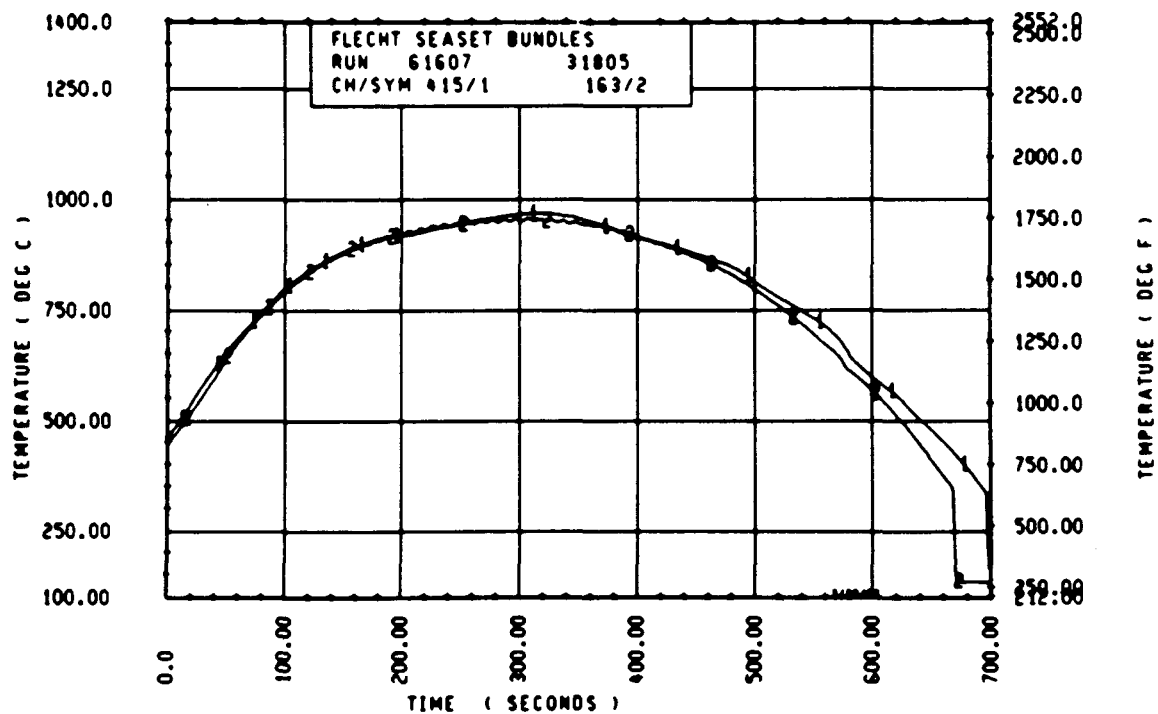
Rod 11K, 1.98 m (78 in.)



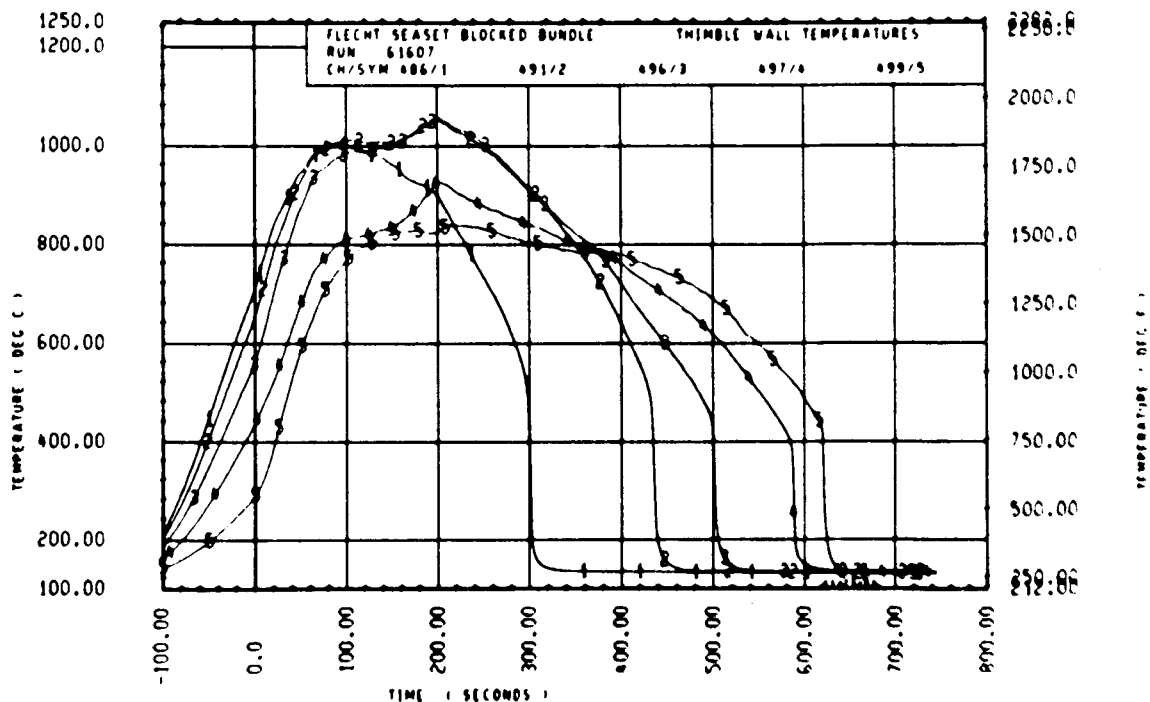
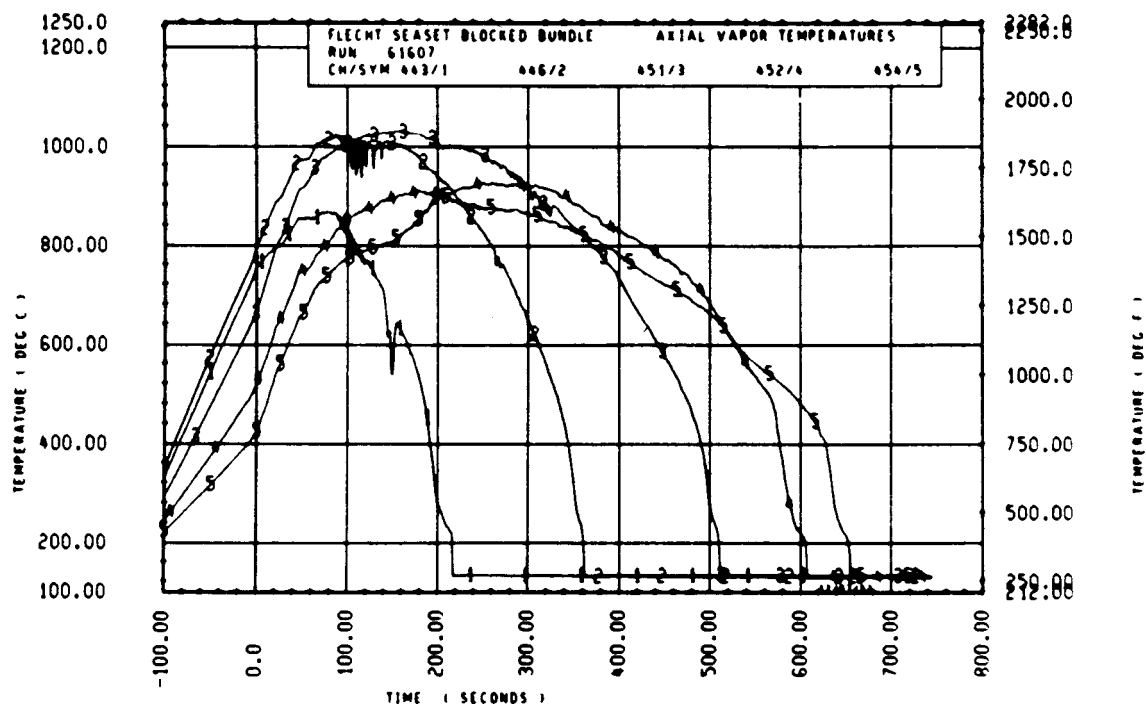
Rod 11E, 2.29 m (90 in.)

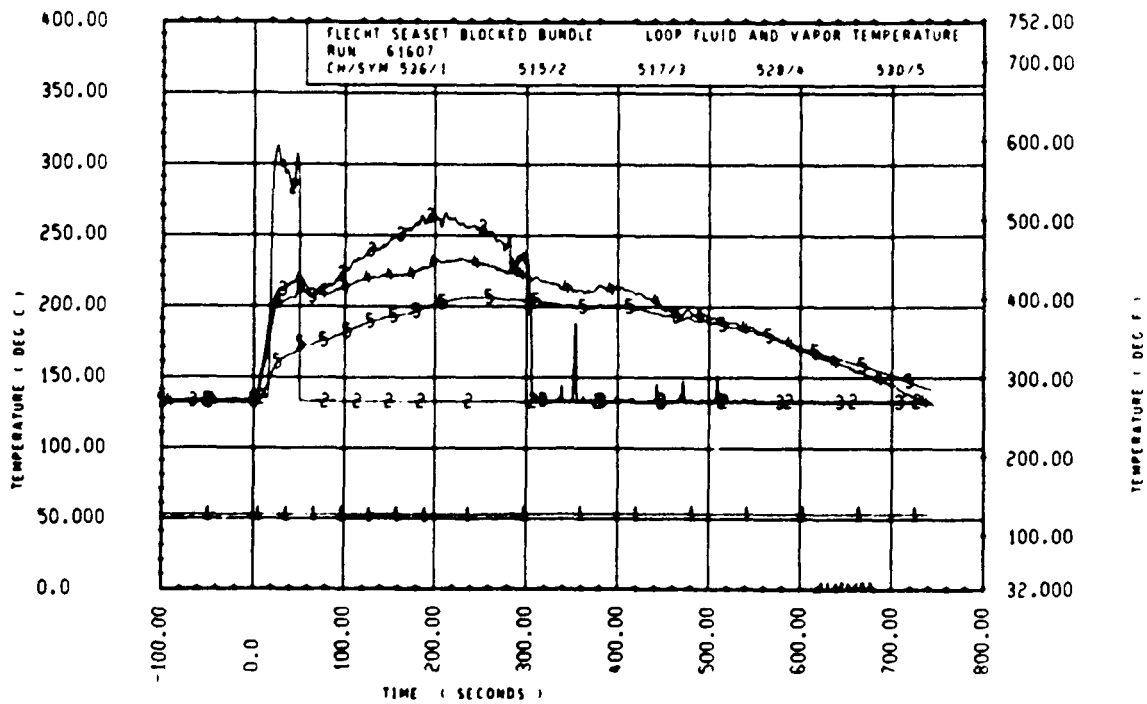
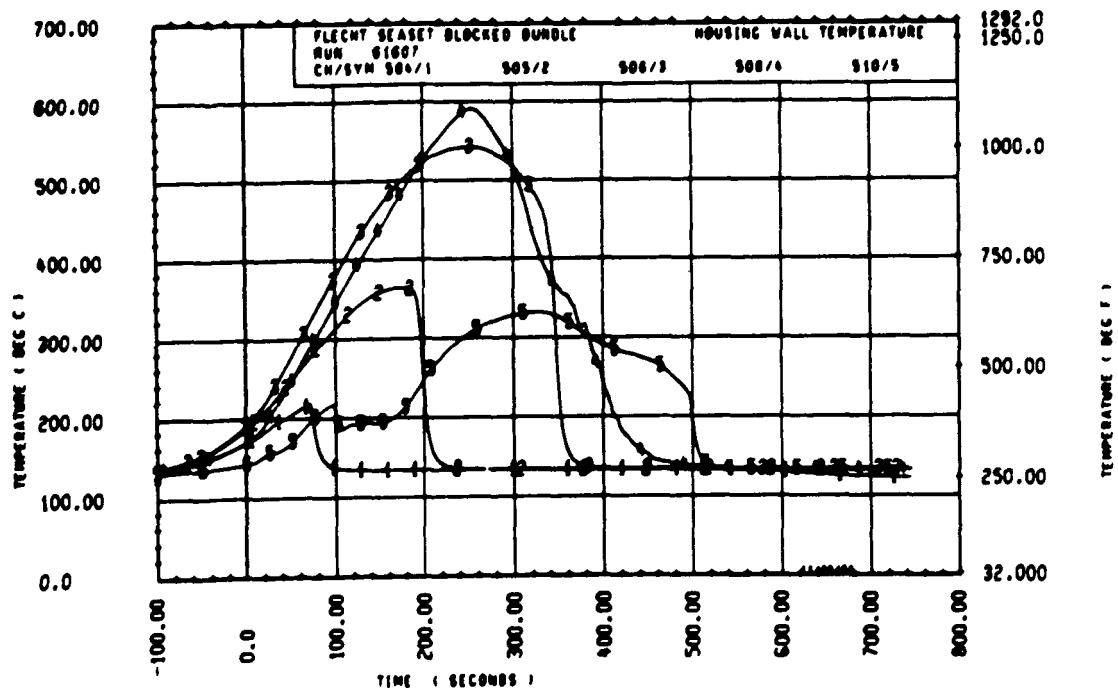


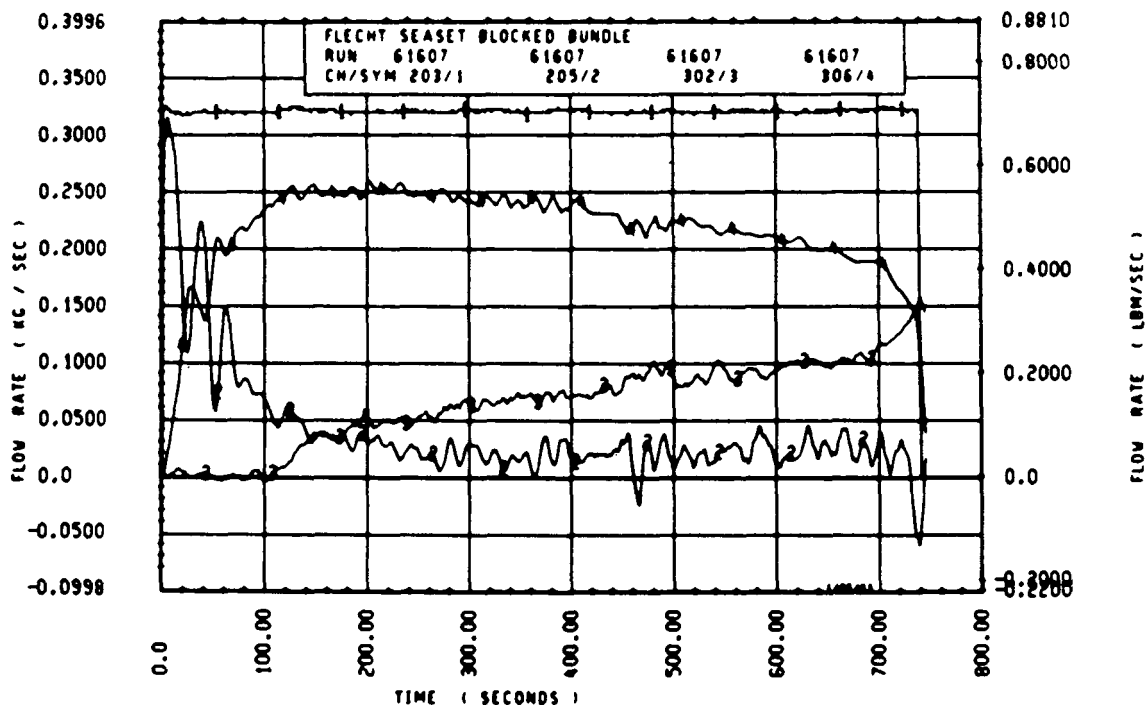
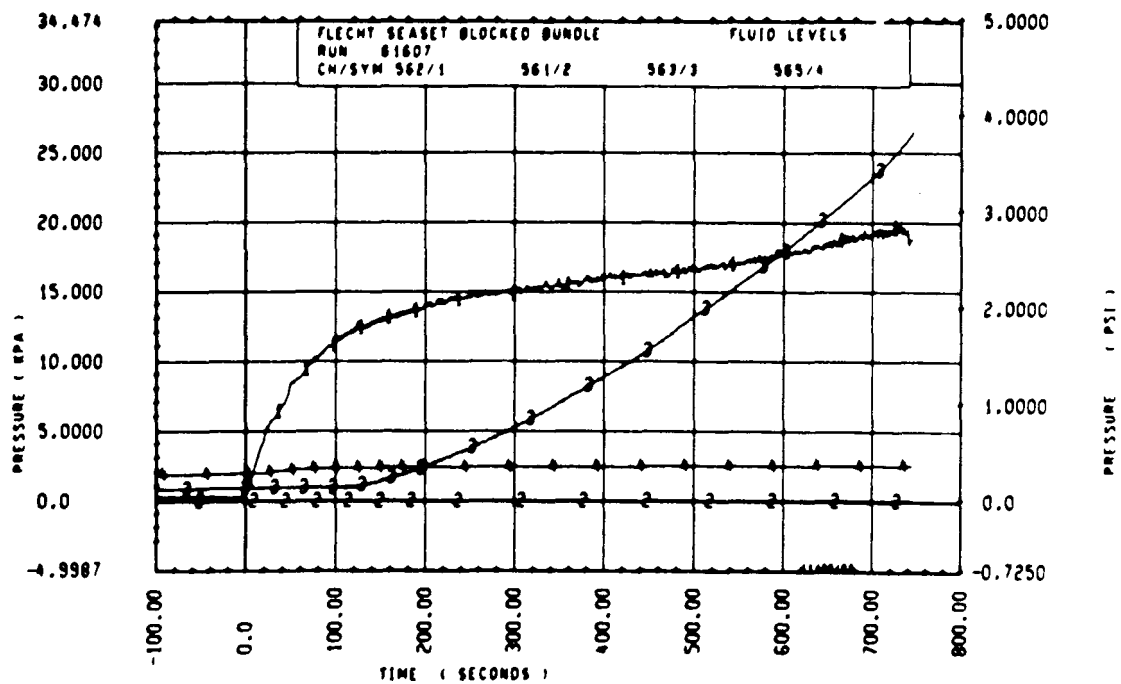
Rod 8K, 2.59 m (102 in.)

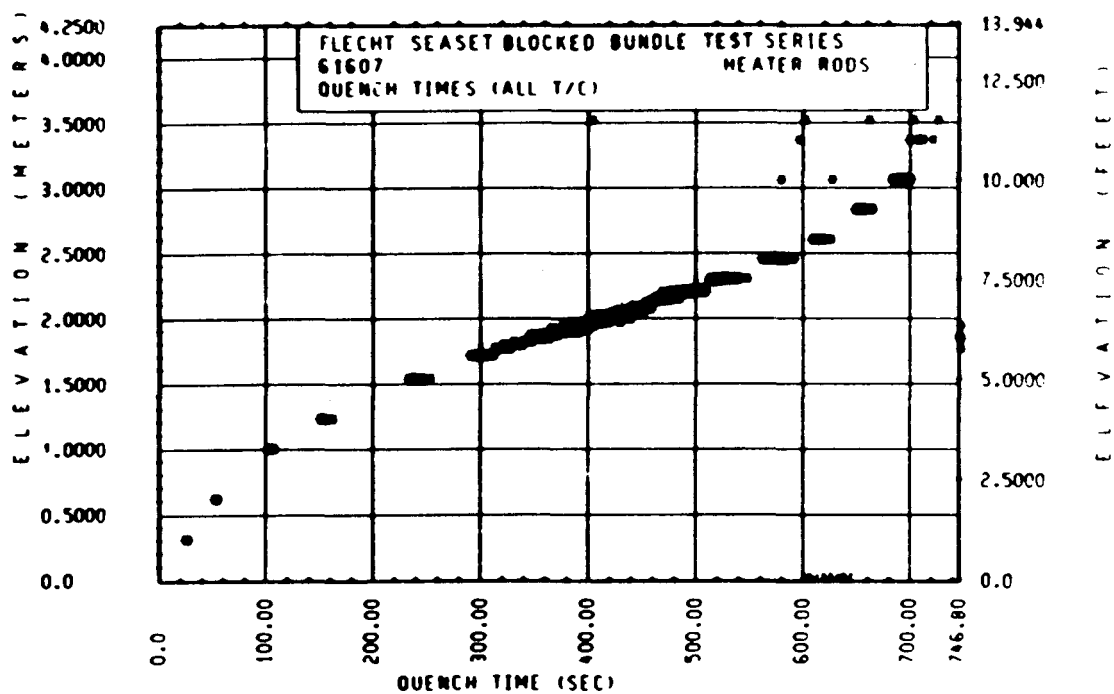
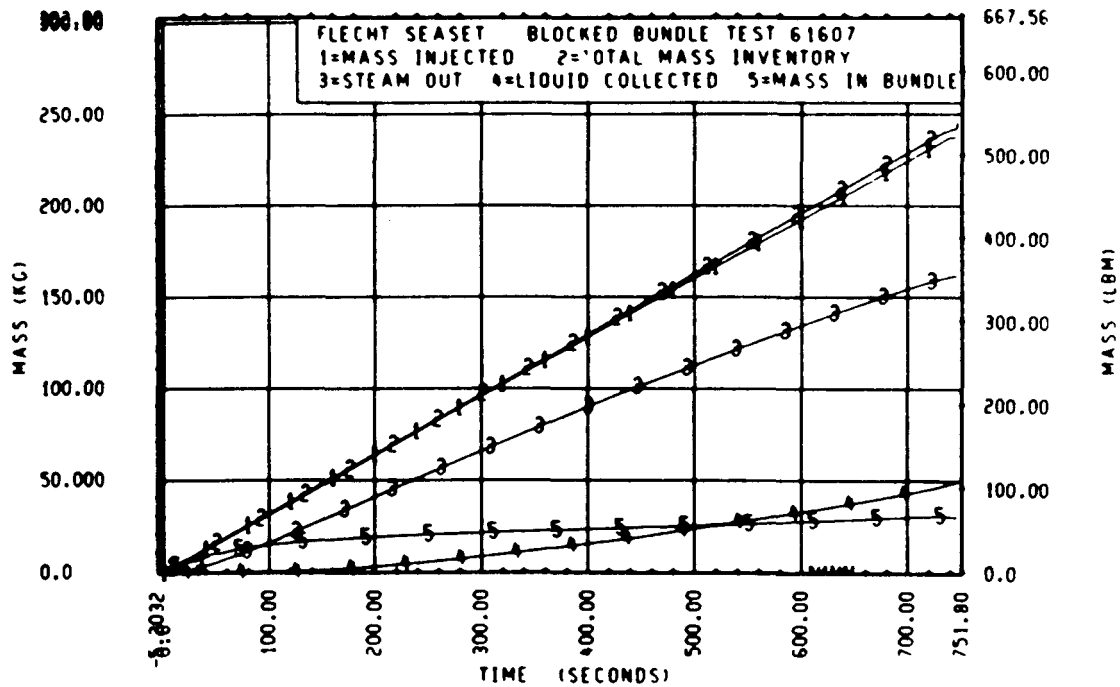


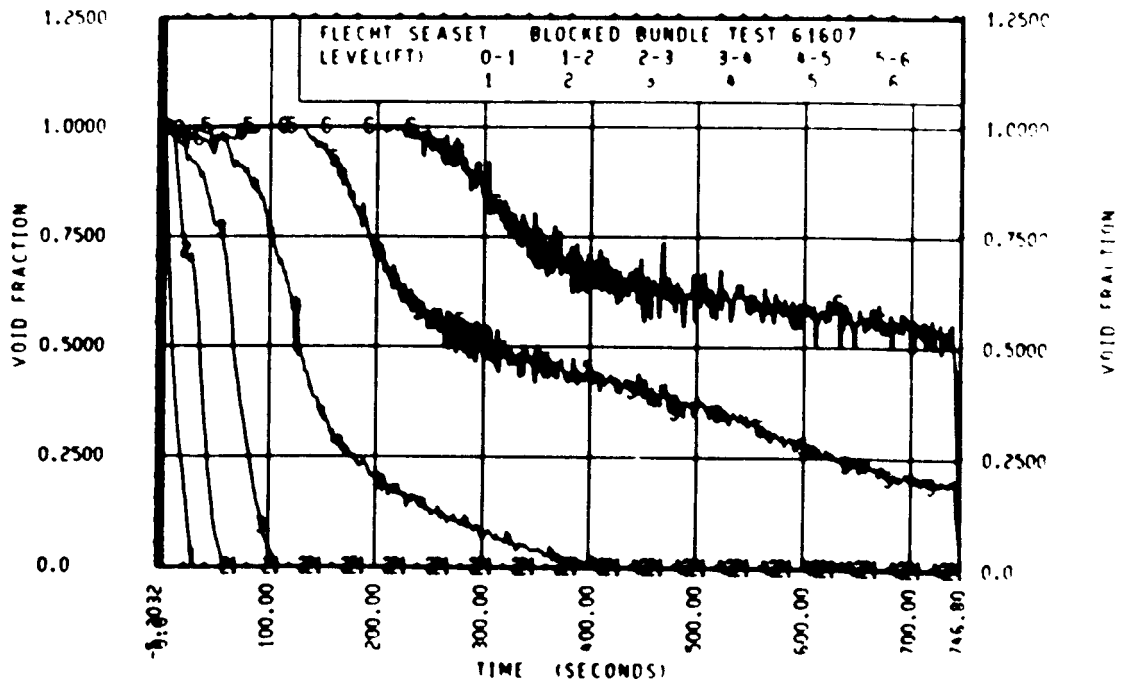
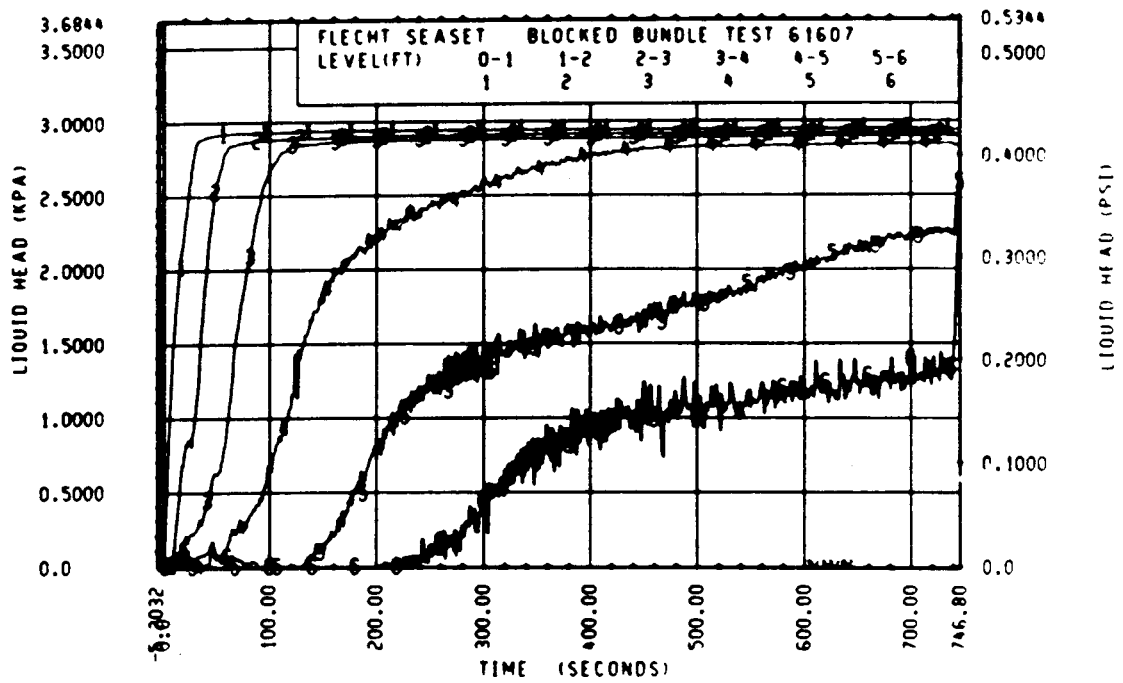
Rod 8H, 3.05 m (120 in.)

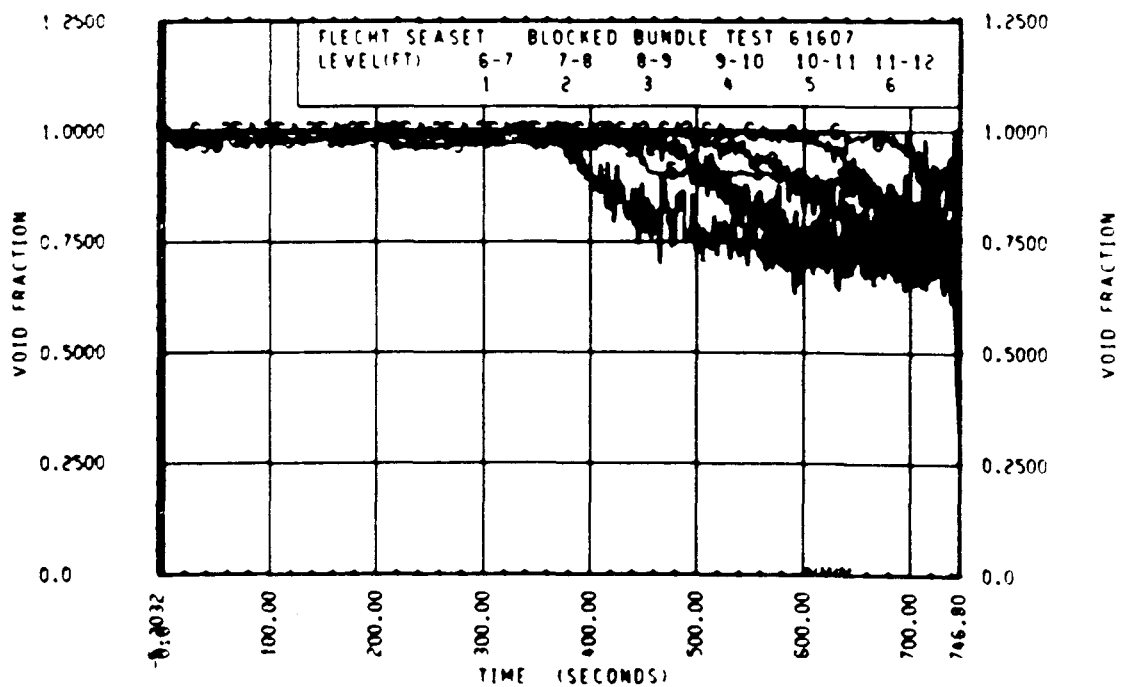
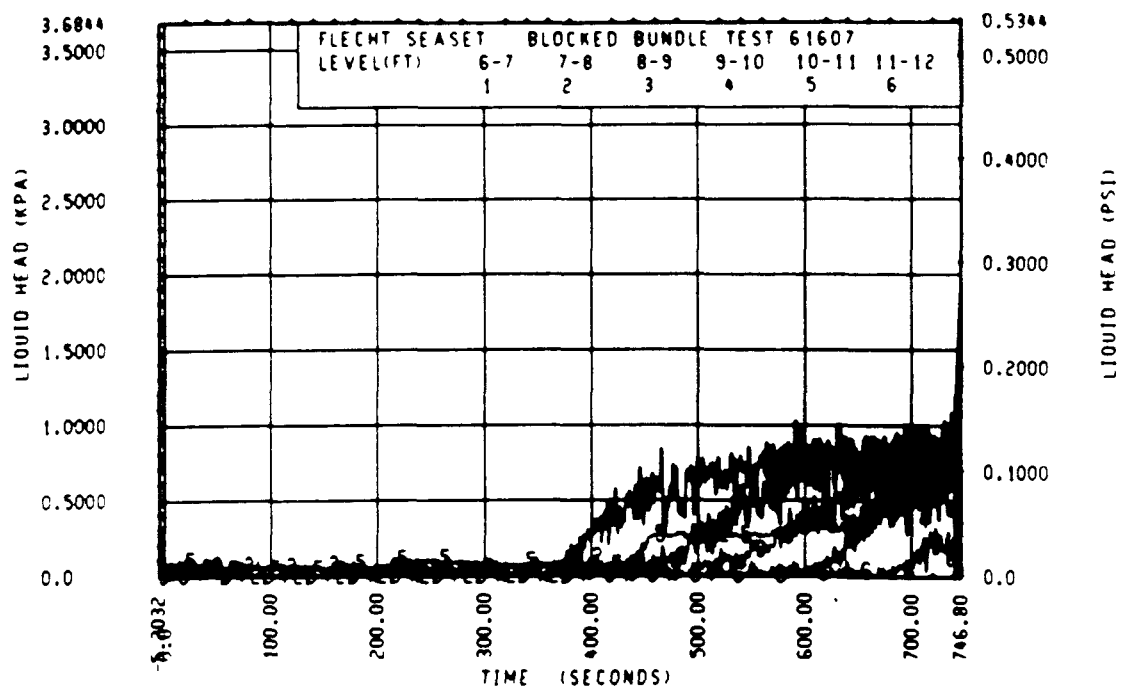












FLECHT SEASET 163-ROD BUNDLE FLOW BLOCKAGE TASK
SUMMARY AND COMMENT SHEET

Run: 61705
Test date: 9/14/82
Test type: Forced reflood
Parameter: Data repeatability (first)

AS-RUN TEST CONDITIONS:

Upper plenum pressure	0.273 MPa (39.6 psia)
Initial peak clad temperature and location	873.5°C (1604.3°F), 6E-2.01 m (79 in.)
Initial peak rod power:	
Peripheral rods	2.29 kw/m (0.698 kw/ft)
Bypass rods	2.29 kw/m (0.699 kw/ft)
Blockage island rods	2.29 kw/m (0.699 kw/ft)
Flooding rate	38.1 mm/sec (1.50 in./sec)
Coolant temperature	52.2°C (126°F)
Initial bundle water level	+1.0 mm (+0.04 in.)

COMMENTS:

Carryover tank filled up at approximately 370 seconds.

Inlet mass flow: ⁽¹⁾ -0.8% to 340 seconds and step decrease to +0.6%

Power decay: ⁽¹⁾ peripheral rods, -0.5% linearly increasing to -1% by 400 seconds
bypass rods, +0.25% linearly increasing to -0.5% by 400 seconds
blockage rods, 0% linearly increasing to -0.25% by 400 seconds

1. Relative to run 61005

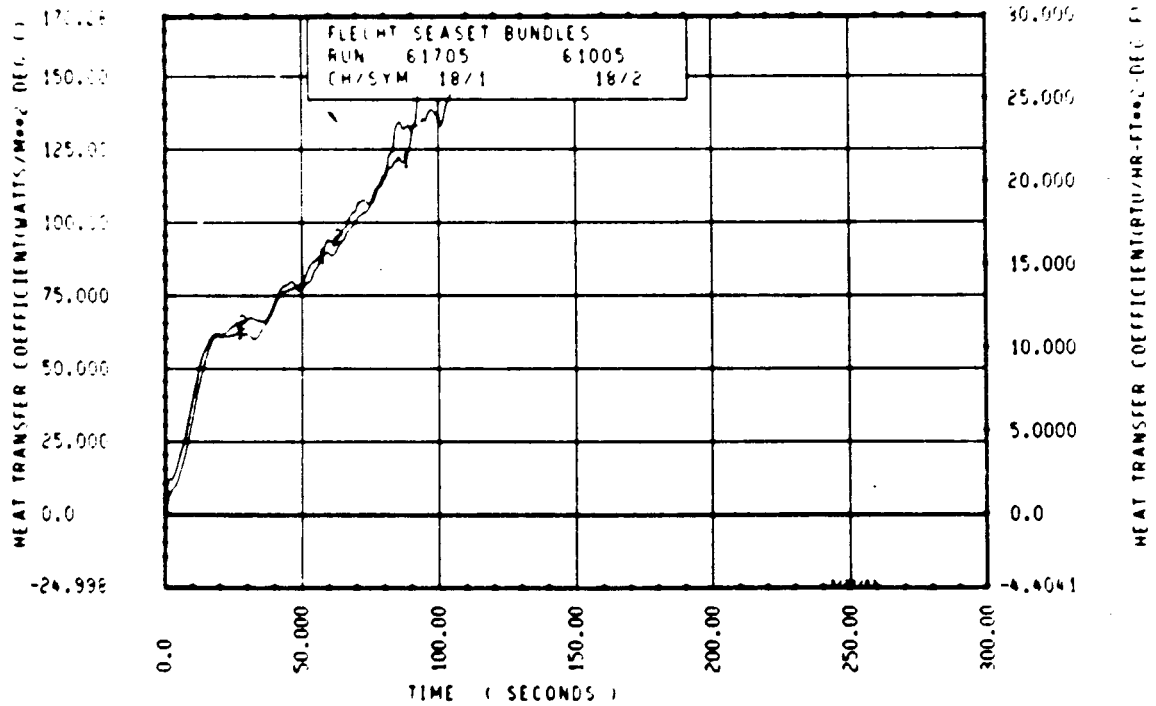
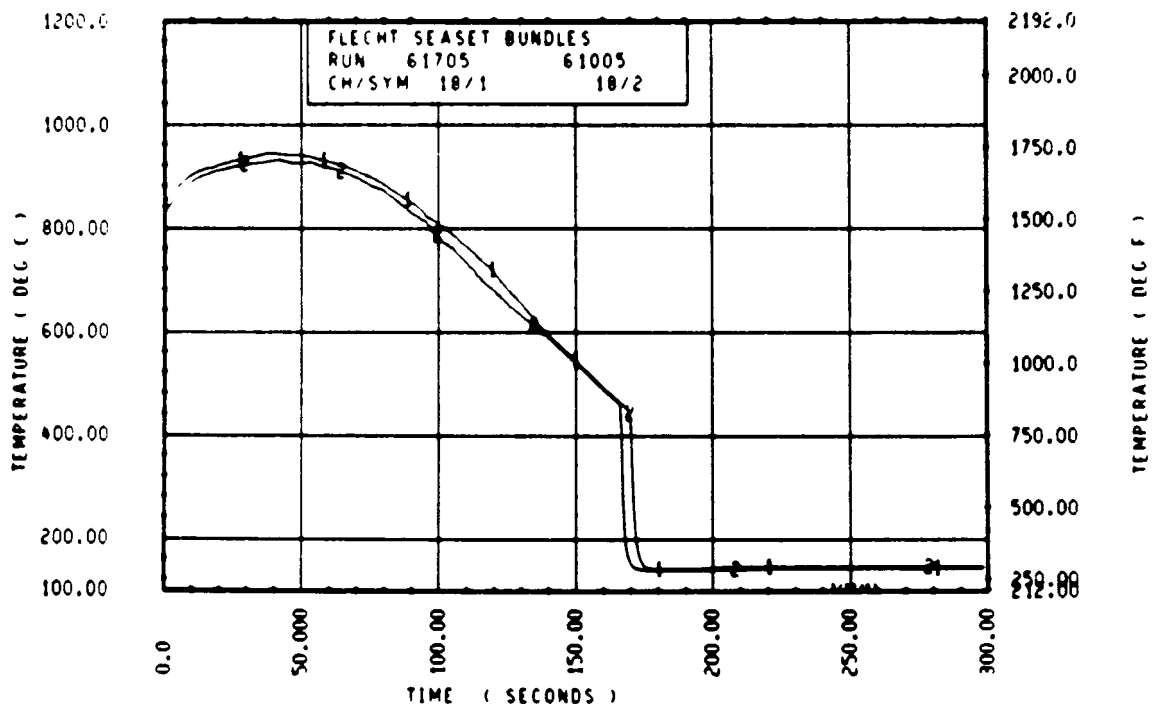
FLECHT SEASET 163 ROD BUNDLE TEST SERIES							
RUN NUMBER 61705							
ROD/ELEV	CHAN. NO	INITIAL AT FLOOD (DEG F)	MAXIMUM TEMPERATURE (DEG F)	TEMPERATURE RISE (DEG F)	TIME AROUND TIME (SECONDS)	QUENCH TEMPERATURE (DEG F)	QUENCH TIME (SECONDS)
9G 1- C	3	664.	684.	15.	4.5	574.	19.0
10H 2- C	6	900.	935.	35.	7.5	656.	42.5
9G 3- 3	9	1234.	1296.	63.	12.5	767.	61.8
3J 4- C	11	1362.	1469.	107.	25.5	756.	115.1
7H 4- C	12	1356.	1465.	108.	24.5	746.	116.6
8K 4- C	13	1373.	1484.	111.	25.5	746.	119.4
8M 4- 0	14	1353.	1446.	94.	19.5	767.	114.4
12D 4- 0	17	1345.	1434.	89.	20.0	773.	114.4
5E 5- C	20	1526.	1705.	179.	38.0	665.	167.8
7G 5- C	21	1580.	1743.	163.	37.5	647.	166.1
9G 5- C	24	1552.	1719.	167.	38.0	655.	167.3
5E 5- 7	33	1546.	1721.	175.	56.0	644.	199.4
6G 5- 7	45	1553.	1746.	192.	65.5	665.	202.1
9H 5- 9	52	1454.	1701.	202.	68.5	623.	204.3
7G 5-10	59	1524.	1732.	211.	77.5	663.	210.6
7F 5-11	62	1465.	1690.	225.	77.5	644.	213.0
4G 5-11	64	1551.	1737.	186.	65.5	683.	221.7
2I 6- C	67	1593.	1812.	218.	50.0	932.	221.0
5D 6- C	70	1501.	1714.	213.	68.5	680.	220.3
6J 6- C	74	1537.	1699.	162.	38.0	662.	225.1
7M 6- 0	66	1551.	1751.	200.	55.5	865.	220.0
11E 6- 0	80	1546.	1724.	179.	56.0	844.	220.1
6H 6- 2	97	1351.	1646.	255.	92.5	604.	227.0
5H 6- 2	99	1547.	1748.	201.	66.5	645.	235.1
9E 6- 2	105	1352.	1713.	361.	91.5	1287.	207.2
8H 6- 3	111	1433.	1675.	242.	91.0	952.	232.1
4G 6- 3	124	1563.	1770.	207.	67.0	695.	241.6
11H 6- 4	134	1486.	1746.	257.	92.0	637.	239.0
9D 6- 4	143	1545.	1805.	260.	80.5	927.	243.5
9J 6- 5	165	1536.	1758.	222.	92.5	996.	244.5
9M 6- 5	166	1566.	1809.	221.	56.0	932.	245.2
8J 6- 6	192	1574.	1762.	203.	76.0	1024.	243.7
9U 6- 6	193	1550.	1818.	268.	80.0	951.	254.0
11F 6- 6	173	1545.	1801.	257.	80.0	904.	250.7
4G 7- 0	261	1485.	1640.	155.	38.0	813.	285.7
7D 7- 6	309	1483.	1712.	229.	82.5	887.	314.5
7G 7- 6	312	1525.	1744.	219.	77.5	884.	310.1
11E 7- 6	325	1455.	1732.	237.	72.0	890.	311.4
5L 8- 0	337	1244.	1630.	330.	116.0	802.	345.0
7H 8- 0	345	1352.	1662.	310.	91.0	620.	336.0
7K 8- C	346	1353.	1642.	288.	114.0	799.	339.0
5J 8- 6	366	1148.	1394.	250.	127.5	704.	371.1
7B 8- 6	368	1115.	1425.	310.	111.0	727.	365.0
7E 9- 3	383	1093.	1419.	326.	175.0	725.	384.1
8H 9- 3	387	1051.	1328.	277.	177.0	619.	388.1
9C 9- 3	389	1016.	1326.	309.	130.5	665.	393.0
11F 9- 3	394	1037.	1334.	297.	105.0	771.	349.4
7B10- 0	408	825.	1221.	396.	136.0	625.	410.0
8M10- C	415	862.	1202.	341.	105.0	646.	343.7
8K10- C	417	870.	1183.	313.	129.5	641.	406.1
6M10- C	416	867.	1261.	394.	139.0	654.	414.1
6M11- 0	429	671.	791.	120.	41.0	534.	172.4
9U11- 0	431	665.	851.	186.	92.0	671.	251.1
11E11- 0	432	664.	917.	248.	104.5	566.	360.0
5J11- 6	436	655.	770.	115.	40.5	534.	365.1
7B11- 6	437	624.	911.	282.	161.5	551.	359.5
6J11- 6	438	665.	763.	98.	37.5	535.	359.5

RUN 61705 HEATER ROD STATISTICAL DATA

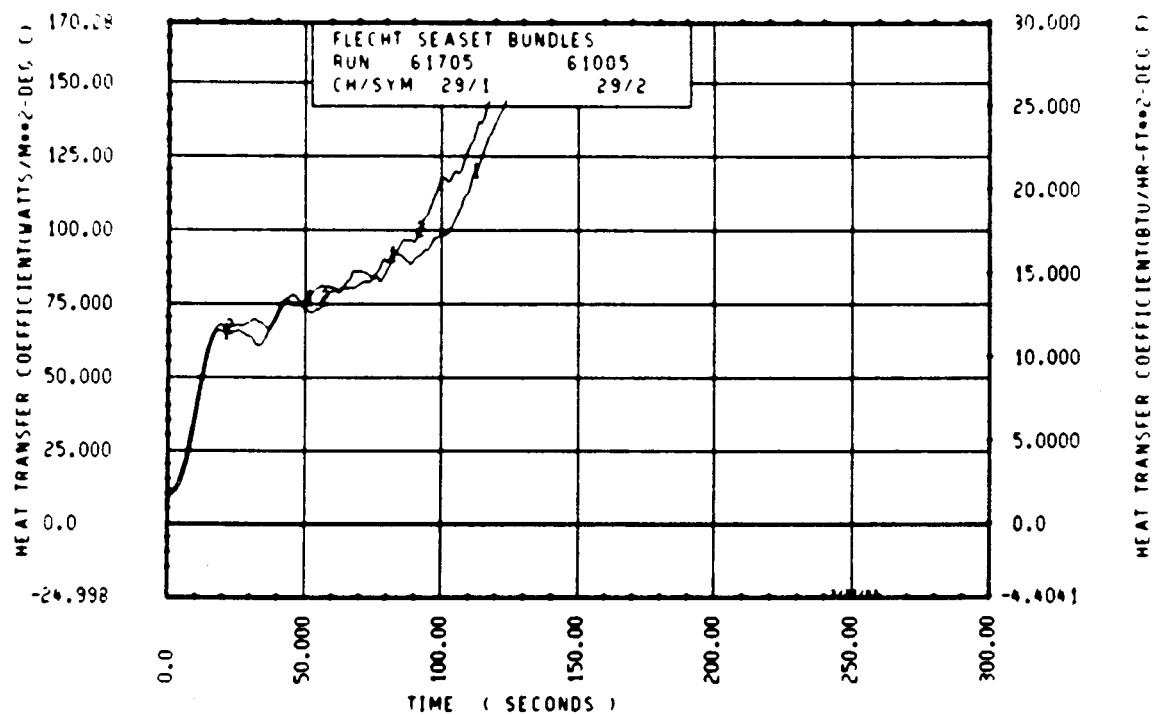
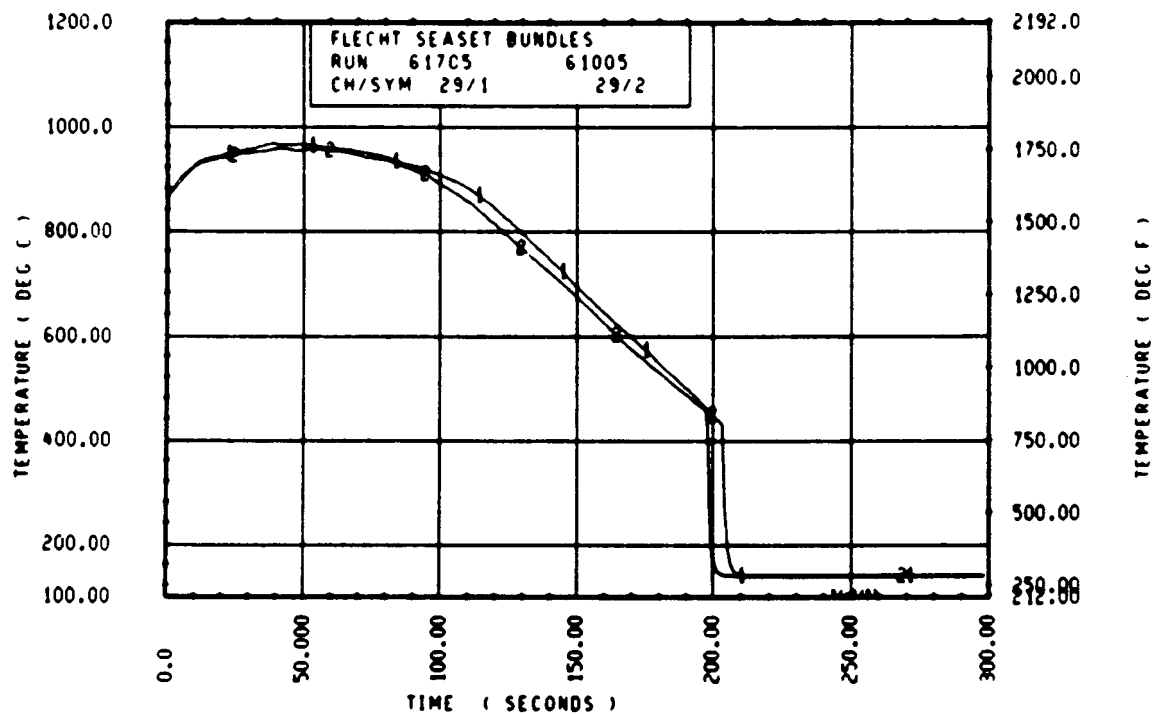
ELEV	INITIAL TEMP (DEG F)			MAX TEMP (DEG F)			TURNAROUND TIME (SEC)		
	MAX	MIN	MEAN	MAX	MIN	MEAN	MAX	MIN	MEAN
12	673.2	664.0	671.5	687.9	683.7	686.2	4.5	4.0	4.3
24	699.8	664.6	674.1	934.8	897.7	912.8	7.5	7.5	7.5
39	1233.7	1168.4	1206.4	1296.3	1257.7	1270.7	13.5	11.5	12.4
48	1381.6	1344.6	1362.4	1487.3	1433.8	1467.0	27.0	19.5	24.1
60	1580.3	1457.4	1536.0	1764.6	1613.0	1702.9	39.5	37.0	36.1
67	1603.1	1488.4	1554.4	1775.7	1684.5	1728.4	65.5	37.0	42.5
69	1536.1	1499.1	1516.2	1713.2	1676.8	1700.8	66.5	36.5	46.1
70	1603.2	1464.1	1532.3	1768.0	1702.1	1729.3	77.5	39.5	55.5
71	1551.1	1464.4	1501.4	1736.7	1670.2	1700.6	77.5	55.5	65.9
72	1598.8	1464.4	1547.6	1811.6	1698.8	1749.2	82.5	37.5	51.5
73	1584.0	1441.4	1523.8	1794.7	1666.9	1729.4	83.0	40.0	56.0
74	1592.3	1391.2	1510.2	1802.5	1646.0	1742.7	92.5	46.0	65.7
75	1596.6	1432.6	1523.8	1815.0	1674.6	1748.4	91.0	48.0	66.3
76	1598.8	1477.7	1550.1	1822.9	1737.8	1777.3	92.0	49.0	64.3
77	1587.9	1497.0	1545.6	1825.2	1699.8	1771.5	94.0	49.5	77.5
78	1597.7	1521.6	1560.9	1846.7	1753.4	1793.9	94.5	48.5	73.6
79	1604.3	1491.6	1563.5	1837.6	1765.7	1801.3	105.0	55.5	76.8
80	1586.9	1507.7	1554.5	1856.9	1773.5	1818.4	94.0	60.0	74.1
81	1584.7	1491.6	1543.2	1846.7	1747.8	1811.9	114.5	62.0	63.0
84	1537.0	1438.2	1498.8	1772.4	1585.7	1655.6	86.0	37.0	50.1
86	1582.5	1463.6	1530.3	1744.5	1639.4	1692.0	78.0	14.0	46.1
90	1533.5	1427.5	1486.6	1765.7	1668.0	1718.2	94.0	52.0	73.7
96	1406.1	1299.5	1333.4	1732.2	1621.8	1673.4	156.0	69.5	98.6
102	1202.4	1115.4	1172.3	1496.9	1397.5	1447.3	173.5	88.5	132.3
111	1099.4	1016.3	1055.3	1416.9	1278.6	1350.9	198.0	61.0	146.5
120	905.0	804.6	860.1	1292.1	1102.9	1222.2	180.0	95.5	143.6
132	673.2	664.6	668.4	921.4	788.0	866.6	177.5	41.0	105.1
138	664.8	624.1	645.7	911.1	763.0	832.9	161.5	37.5	90.1

RUN 61705 HEATER ROD STATISTICAL DATA

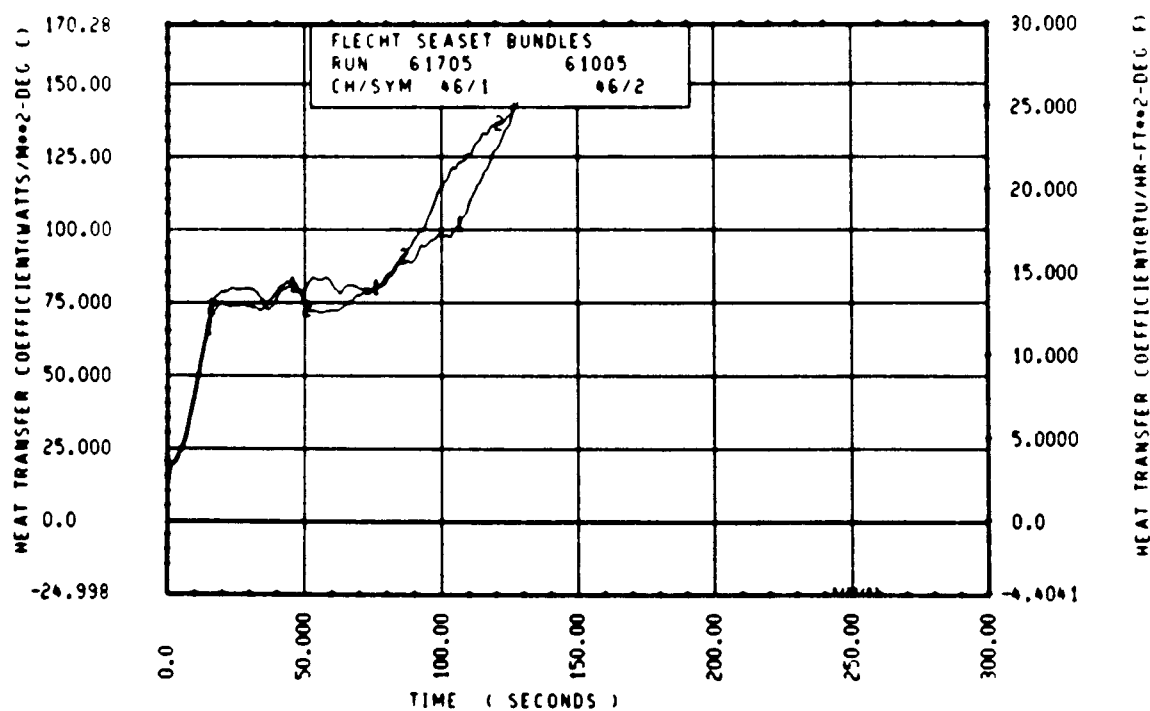
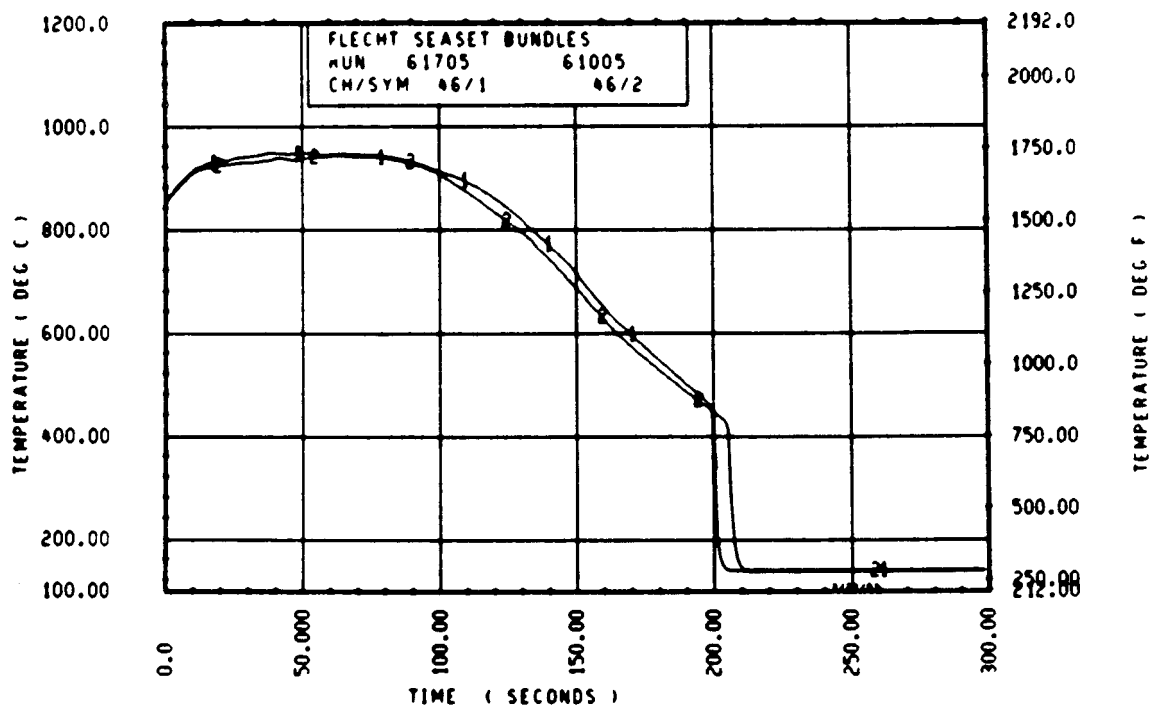
ELEV	TEMP RISE (DEG F)			QUENCH TEMP (DEG F)			QUENCH TIME (SEC)		
	MAX	MIN	MEAN	MAX	MIN	MEAN	MAX	MIN	MEAN
12	14.7	14.7	14.7	577.3	571.7	574.4	20.4	19.0	19.5
24	35.0	33.1	33.7	657.6	632.2	646.6	42.5	40.4	41.1
39	68.6	61.5	64.4	767.3	761.1	763.1	83.5	81.0	81.9
48	111.6	89.0	104.1	773.0	747.6	760.2	119.4	114.4	116.1
60	185.3	155.6	168.9	866.5	831.7	850.1	172.9	164.6	168.1
67	214.6	153.4	169.0	885.1	789.7	847.1	203.1	164.9	199.4
69	201.9	167.3	162.6	887.4	823.0	851.5	212.9	201.1	207.3
70	218.0	179.5	197.0	936.8	862.7	891.2	215.7	207.5	210.9
71	225.1	183.4	199.1	943.5	871.6	894.4	221.7	212.0	216.6
72	250.6	161.7	201.6	932.2	860.7	893.5	227.0	220.0	222.4
73	225.5	187.7	205.6	939.8	863.8	891.3	231.0	216.9	225.5
74	274.1	200.2	226.5	928.0	862.2	895.1	236.0	225.0	231.1
75	256.3	182.4	224.7	1238.1	678.6	926.6	241.9	216.7	234.2
76	264.5	194.4	227.2	1025.0	837.4	925.6	246.0	232.0	239.8
77	273.4	144.4	225.4	1028.2	833.8	946.0	252.0	236.9	245.2
78	268.4	193.7	232.9	1024.4	828.9	943.6	258.0	243.4	250.7
79	274.4	204.5	237.7	1084.1	721.9	955.6	261.0	247.1	254.0
80	318.6	216.4	263.4	1016.3	869.9	947.5	267.0	250.0	261.5
81	306.7	230.3	266.7	1046.2	883.2	942.4	271.9	254.4	266.5
84	239.7	125.1	156.6	953.7	762.9	826.1	289.1	266.0	262.5
86	209.7	112.9	161.7	941.8	792.3	838.4	298.1	262.1	251.1
90	274.4	192.0	231.0	982.6	814.0	887.6	322.9	302.1	311.5
96	357.7	268.3	320.0	938.2	773.3	843.8	350.5	324.9	339.6
102	317.4	215.9	275.0	915.0	659.3	740.3	371.1	304.9	356.4
111	335.5	251.1	295.0	843.4	618.6	696.6	393.0	329.1	361.1
120	421.8	286.9	362.2	1013.5	582.8	659.7	415.1	142.4	391.3
132	240.3	120.0	150.2	671.2	483.3	536.4	421.3	172.4	340.6
138	282.0	96.2	187.2	705.6	530.0	572.3	399.5	219.9	342.2



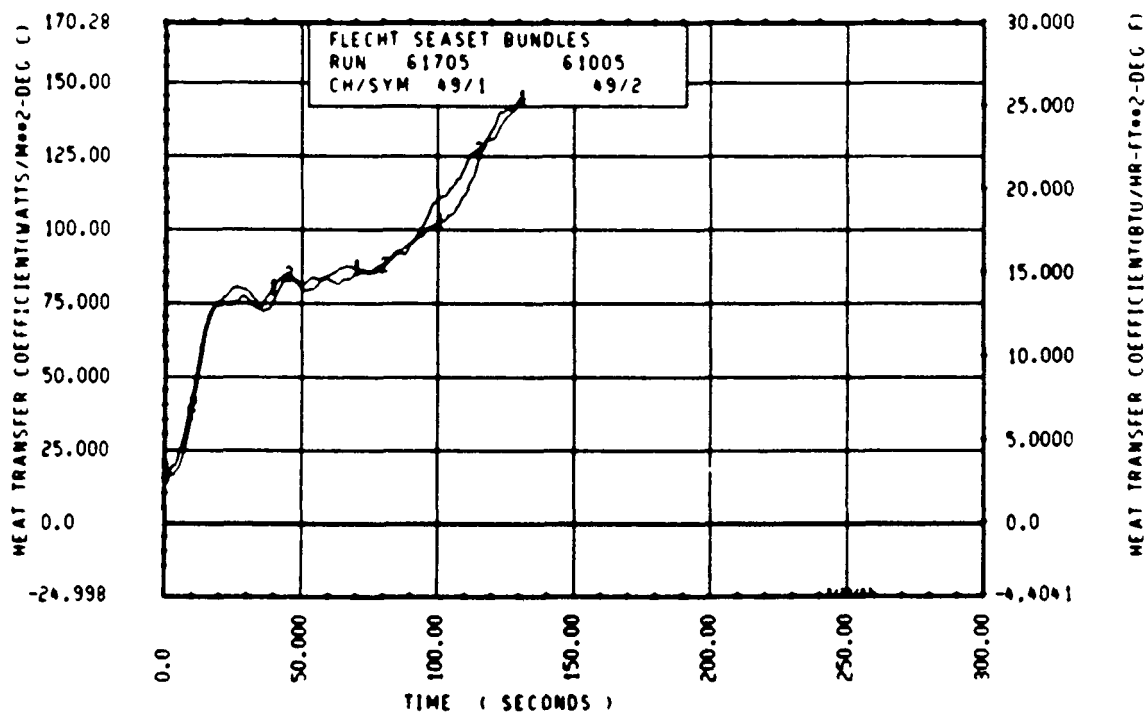
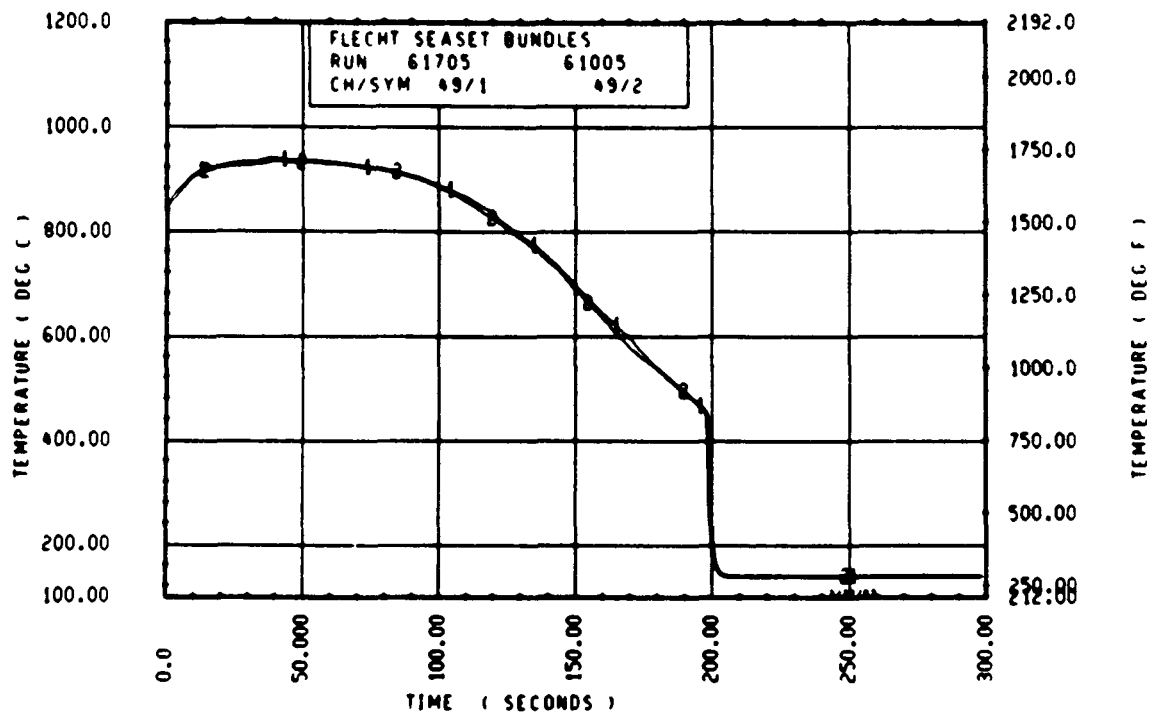
Rod 3H, 1.52 m (60 in.)



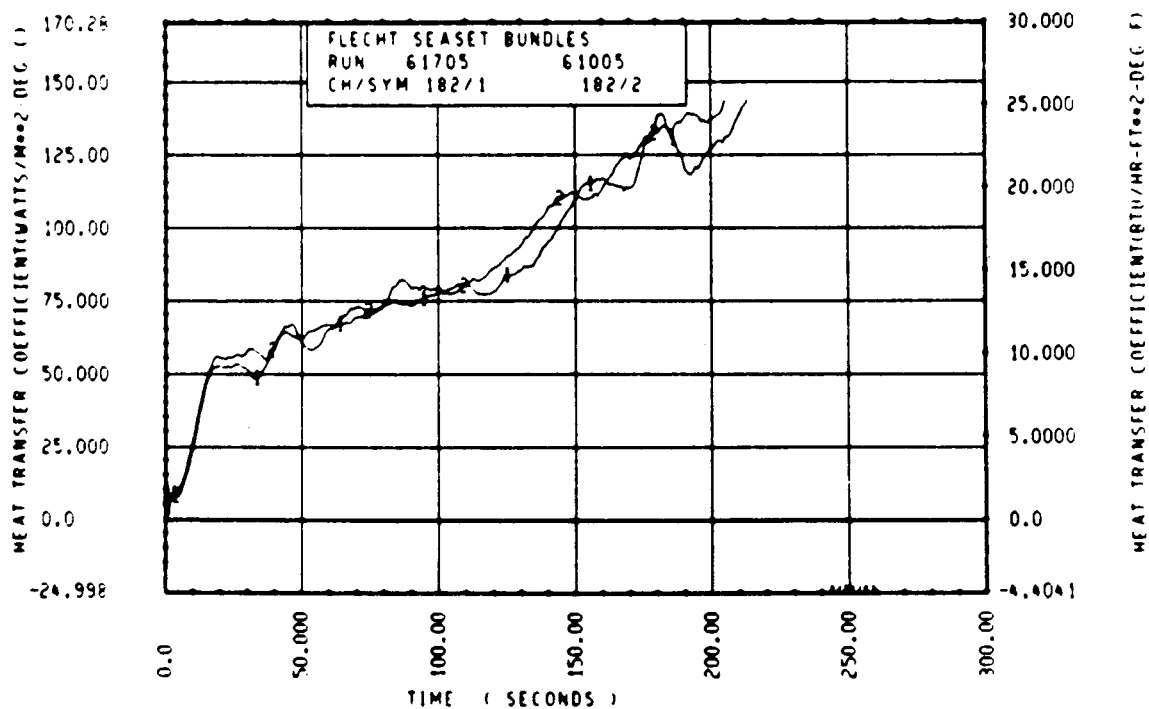
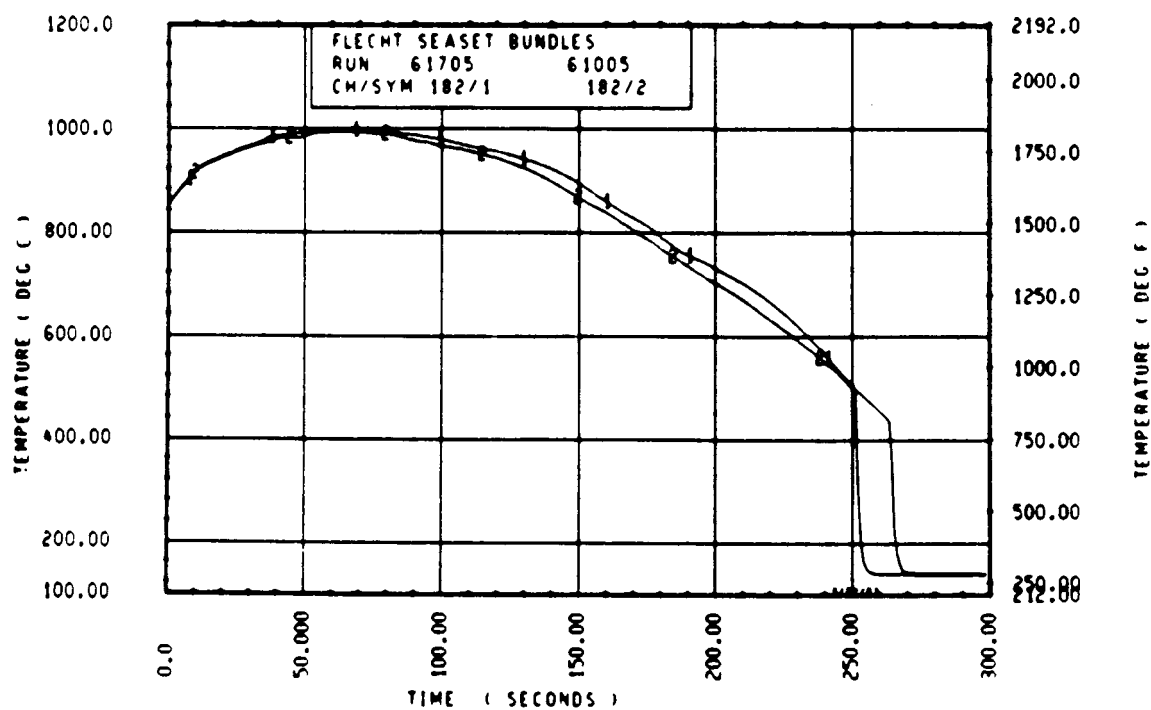
Rod 3H, 1.70 m (67 in.)



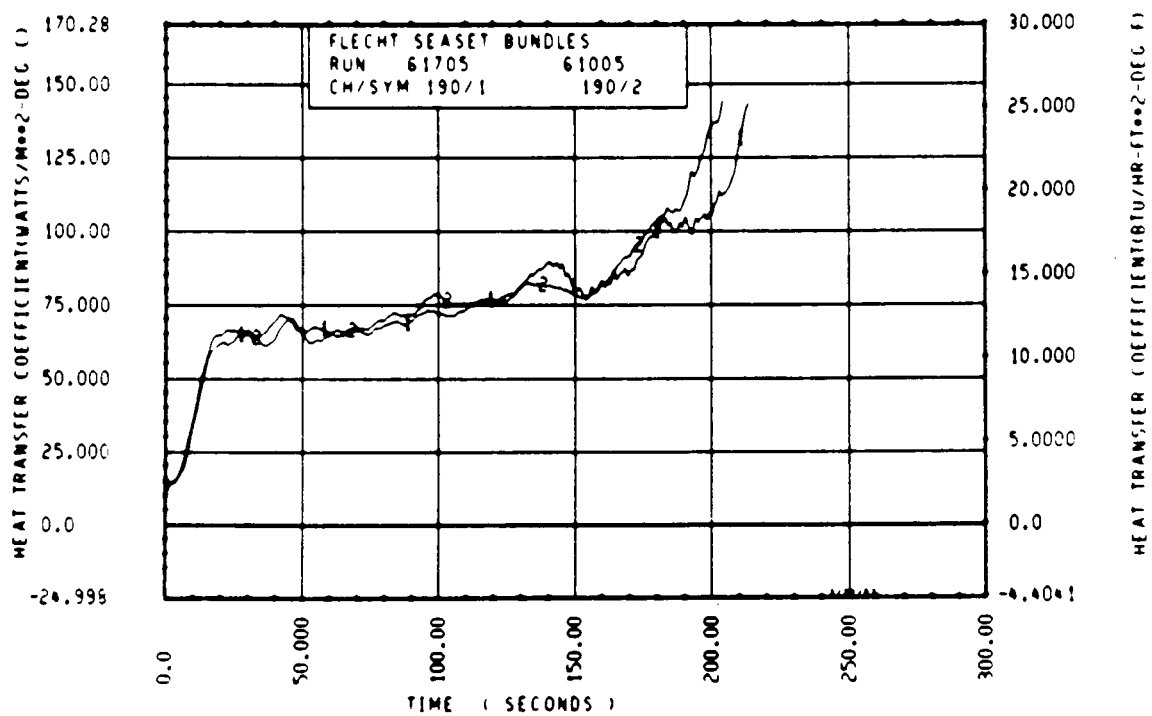
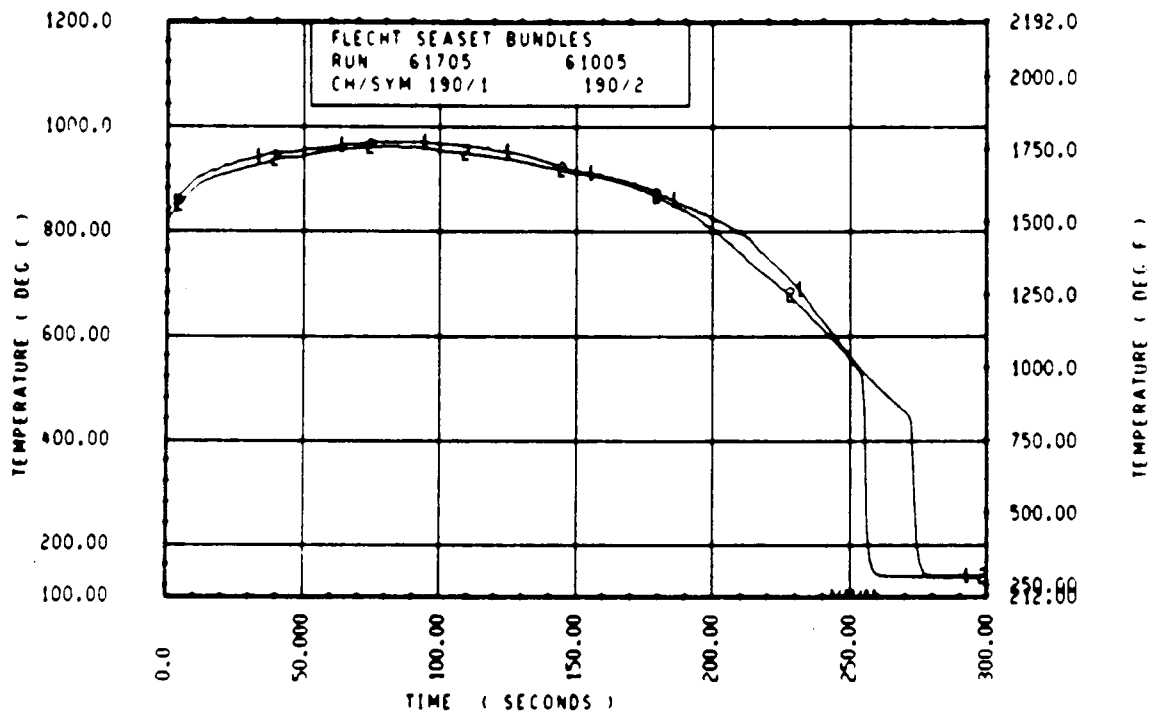
Rod 9G, 1.70 m (67 in.)



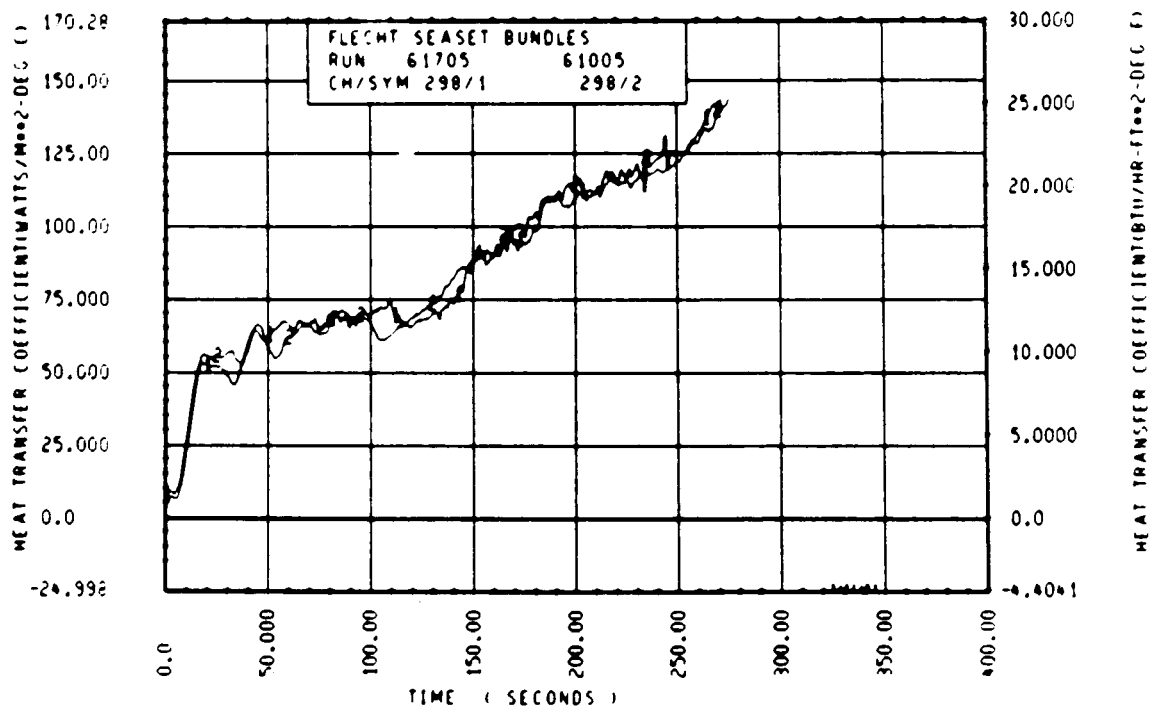
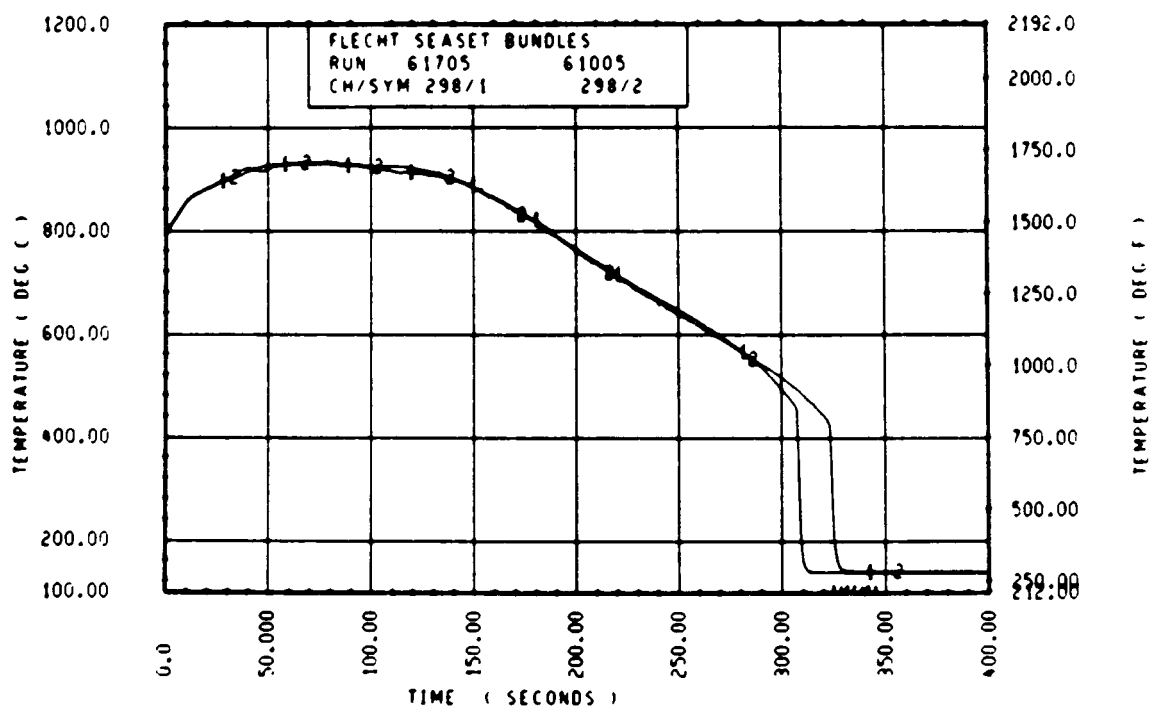
Rod 11K, 1.70 m (67 in.)



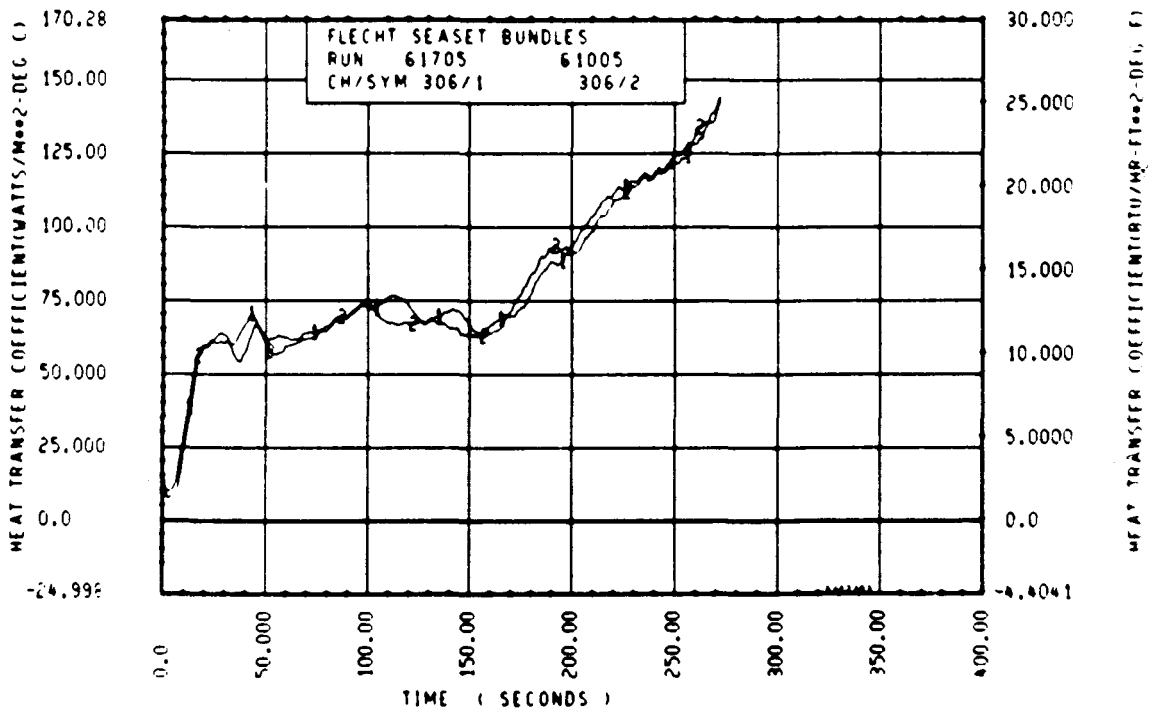
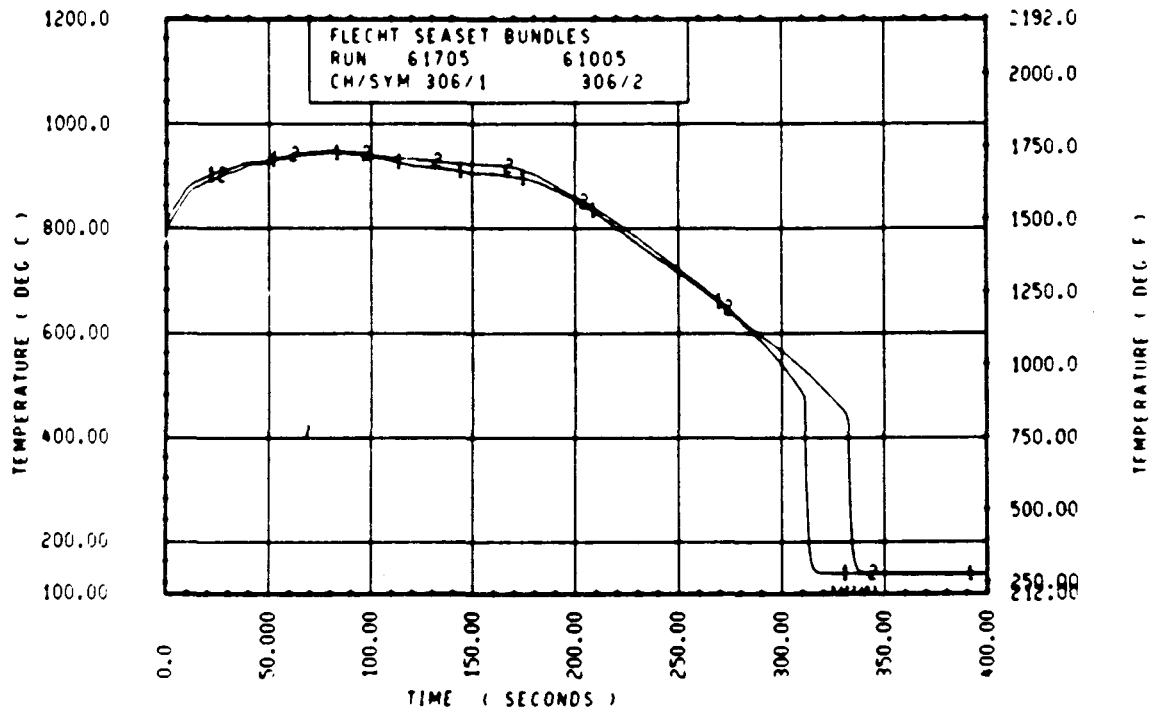
Rod 3H, 1.98 m (78 in.)



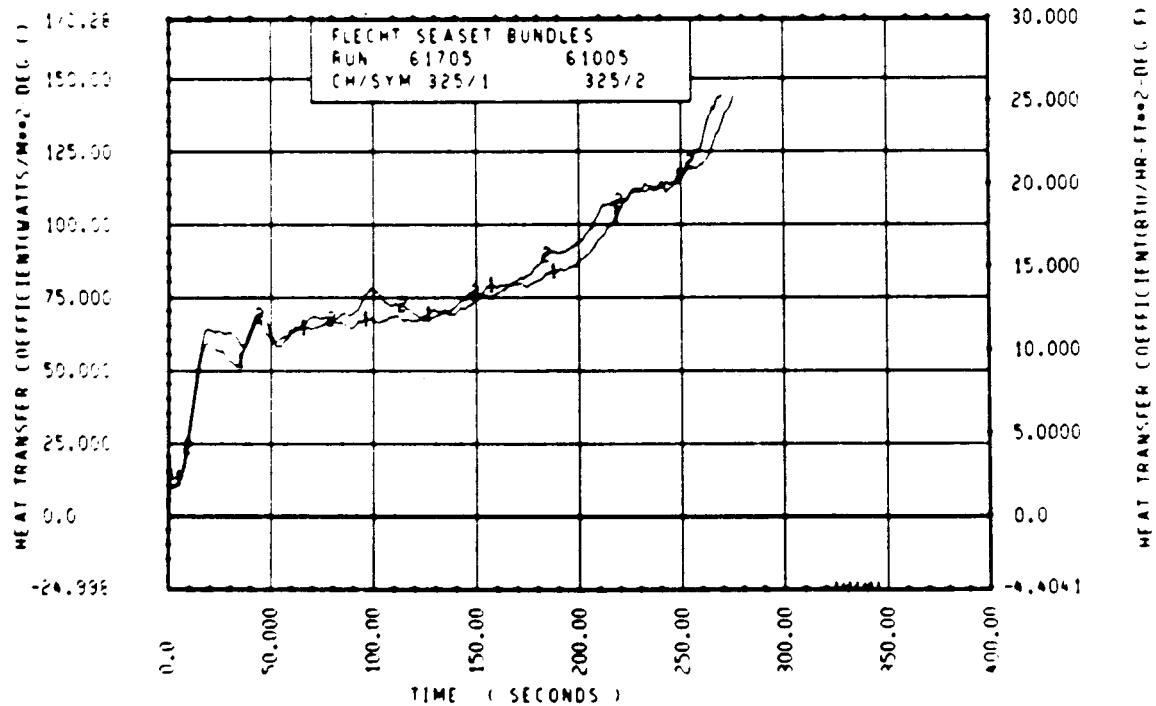
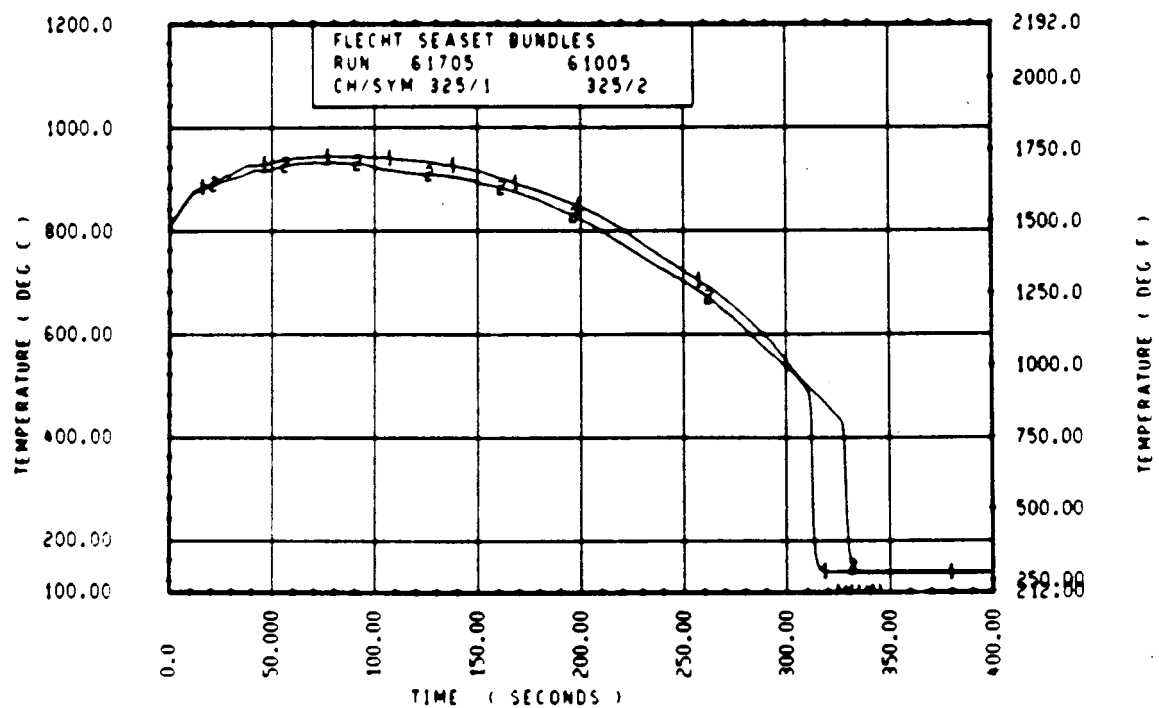
Rod 7H, 1.98 m (78 in.)



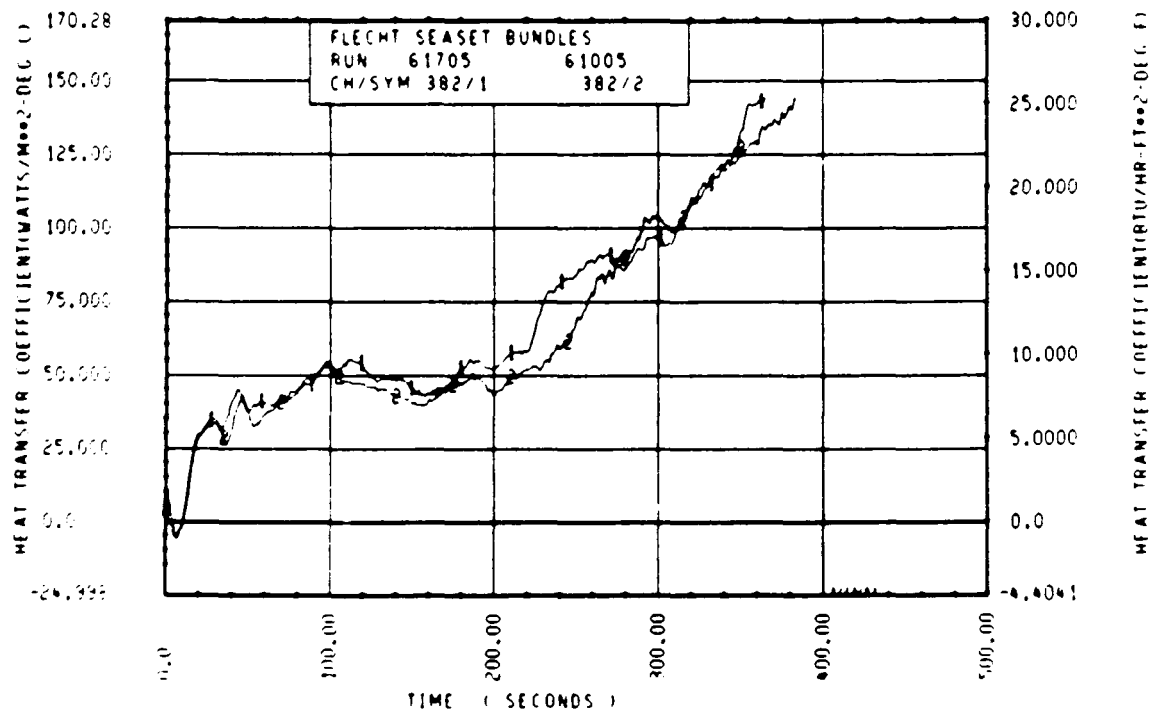
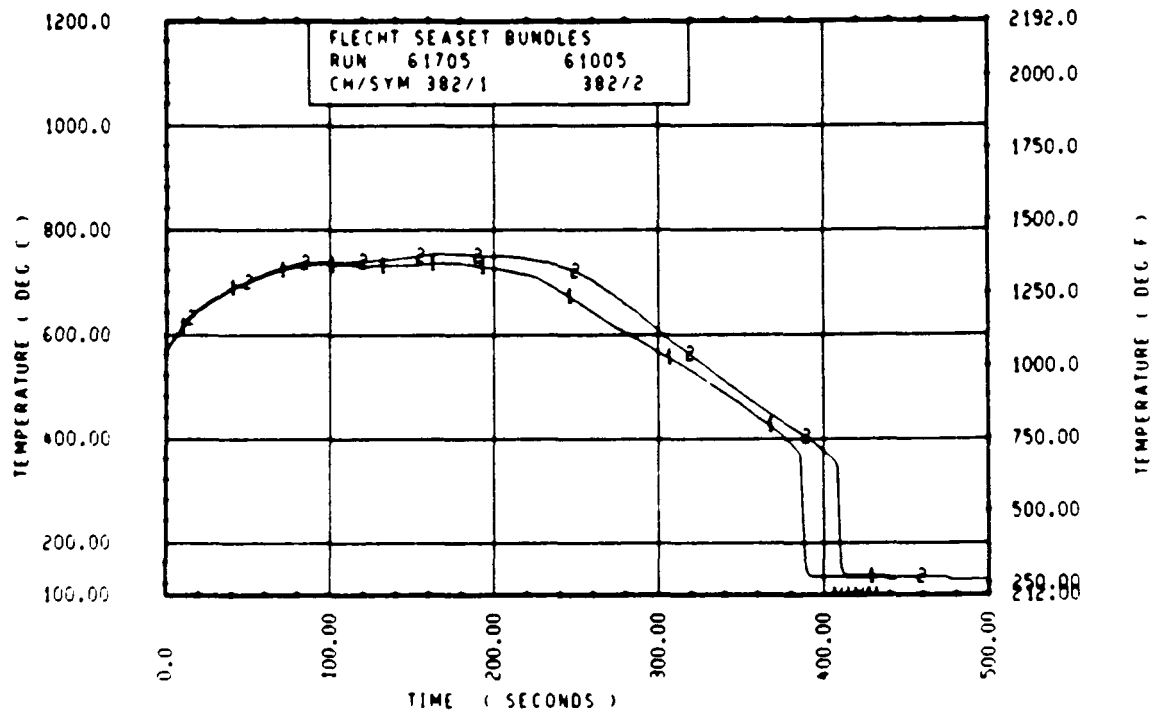
Rod 3H, 2.29 m (90 in.)



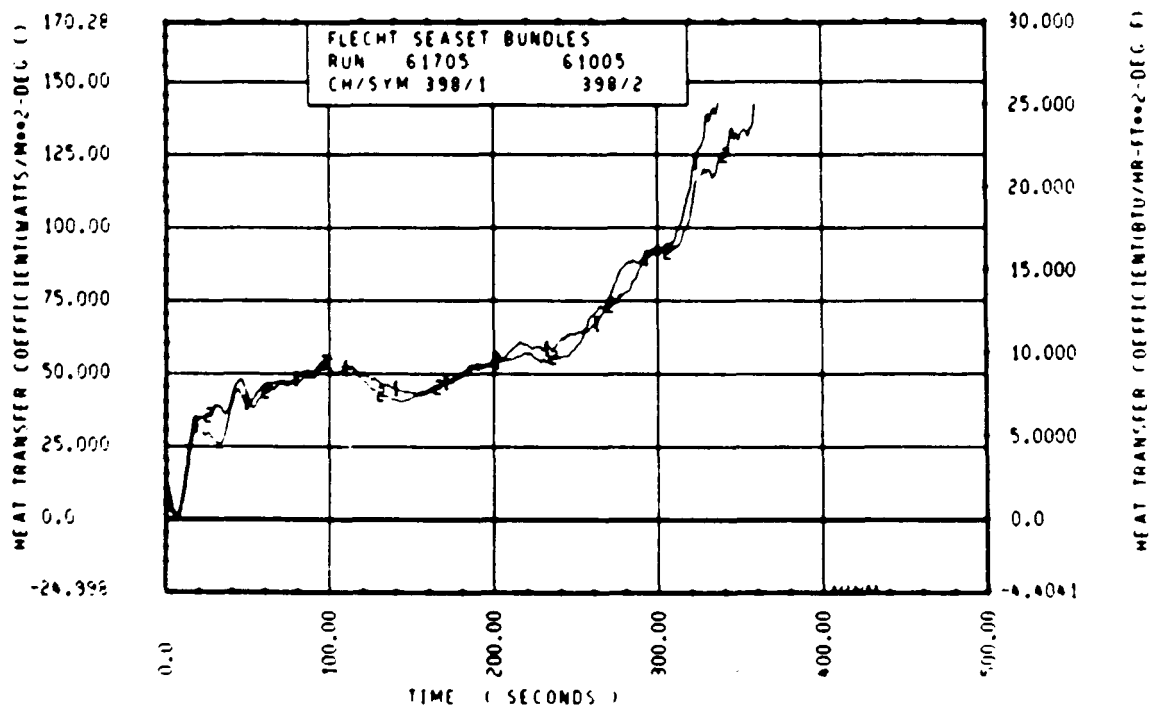
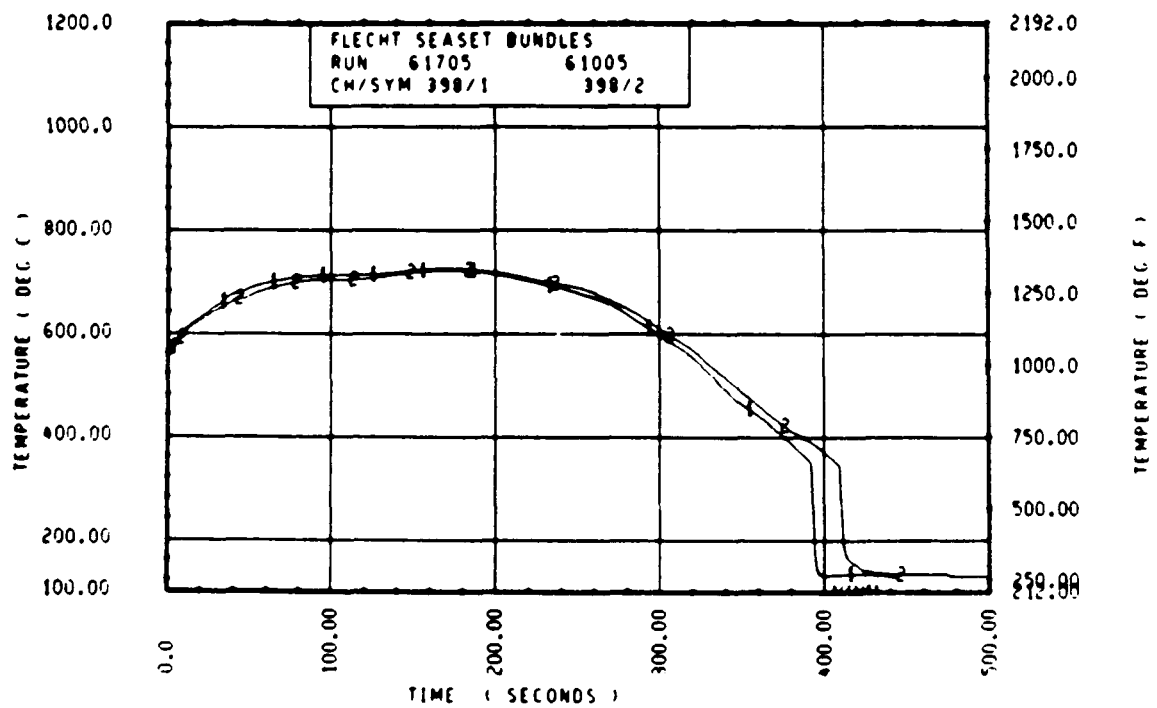
Rod 6G, 2.29 m (90 in.)



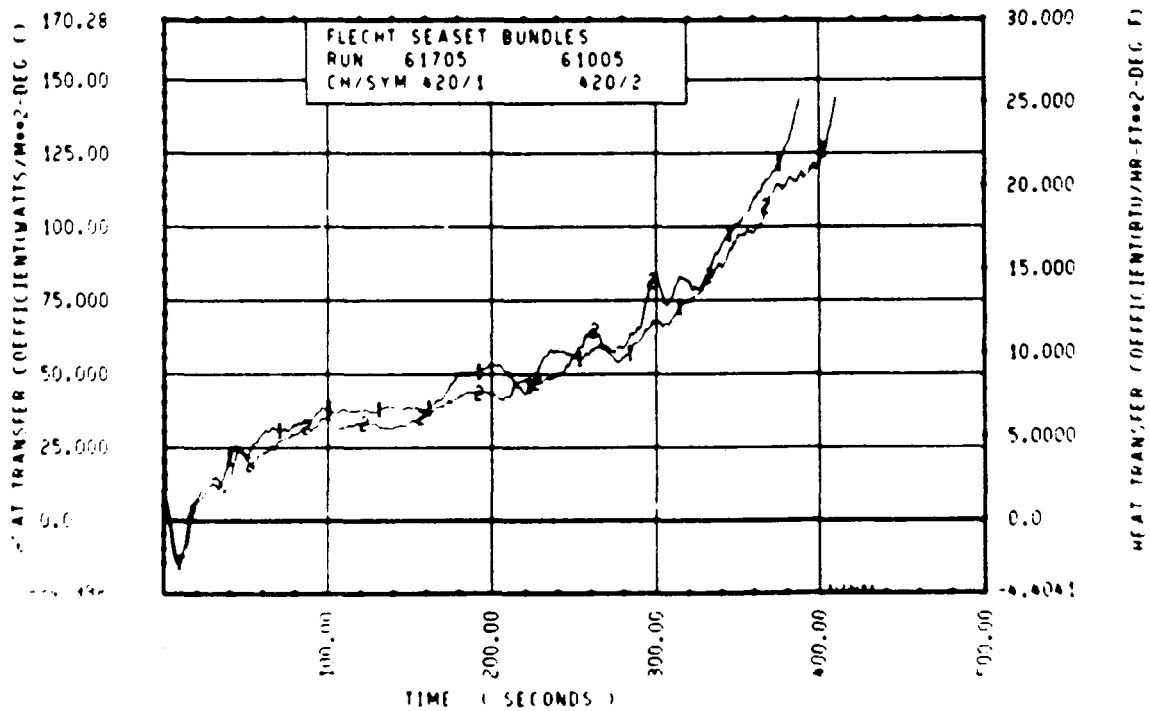
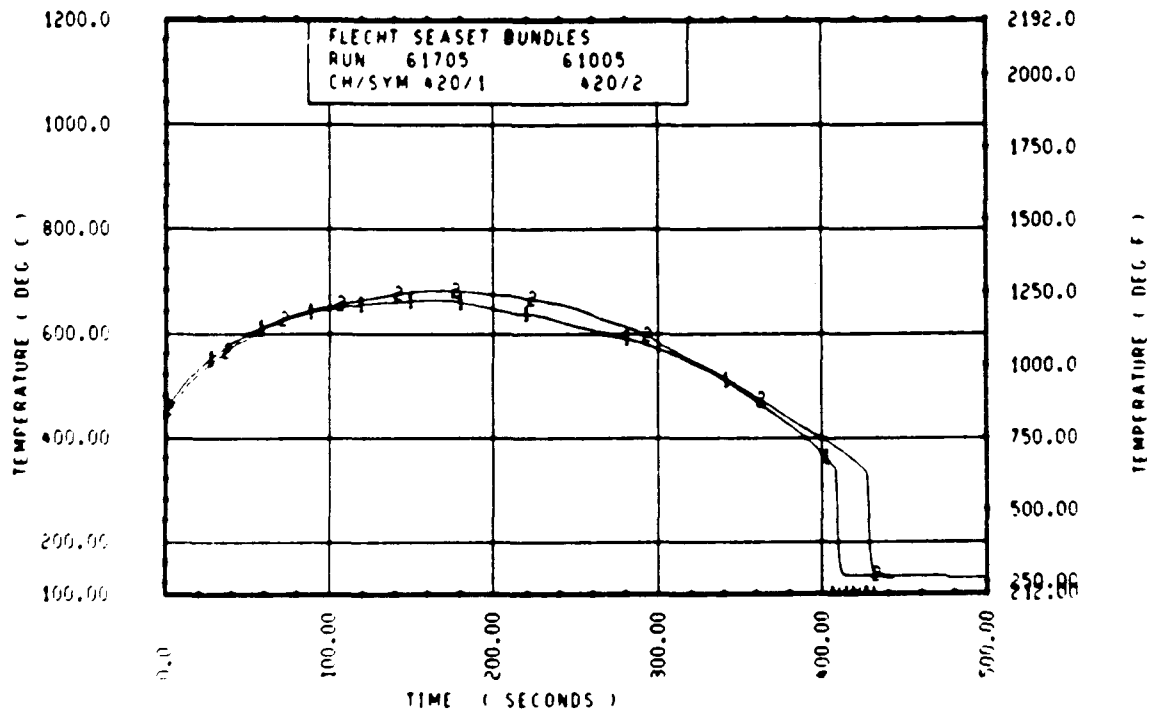
Rod 11E, 2.29 m (90 in.)



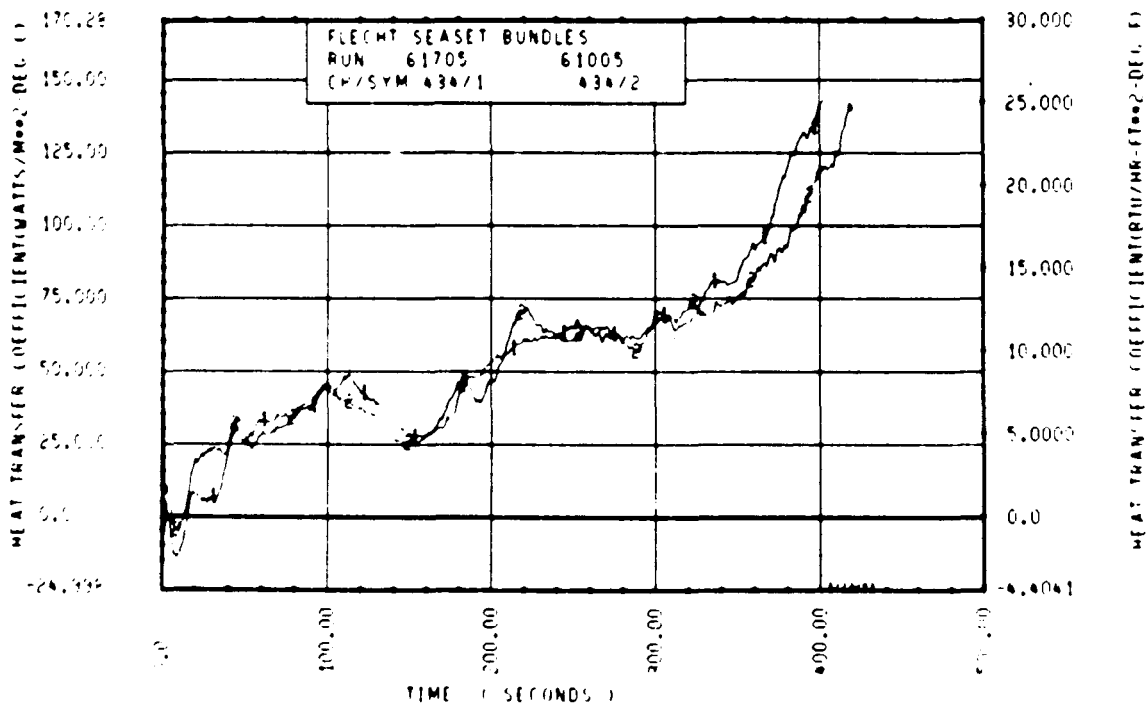
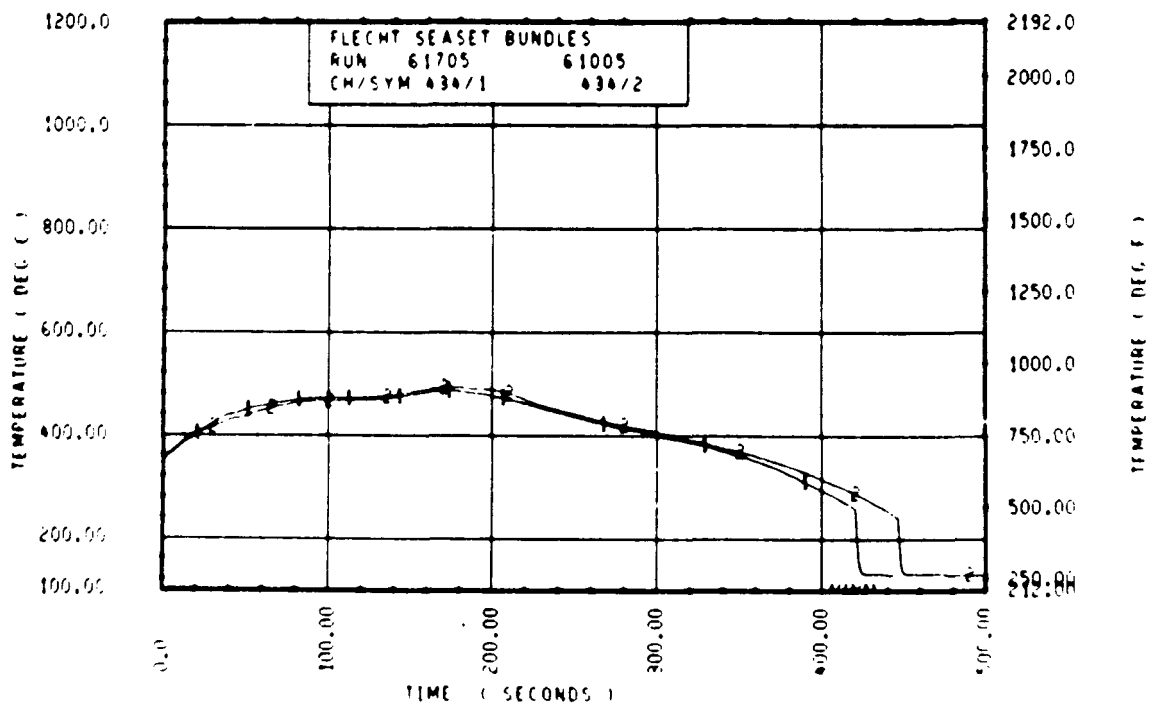
Rod 6G, 2.82 m (111 in.)



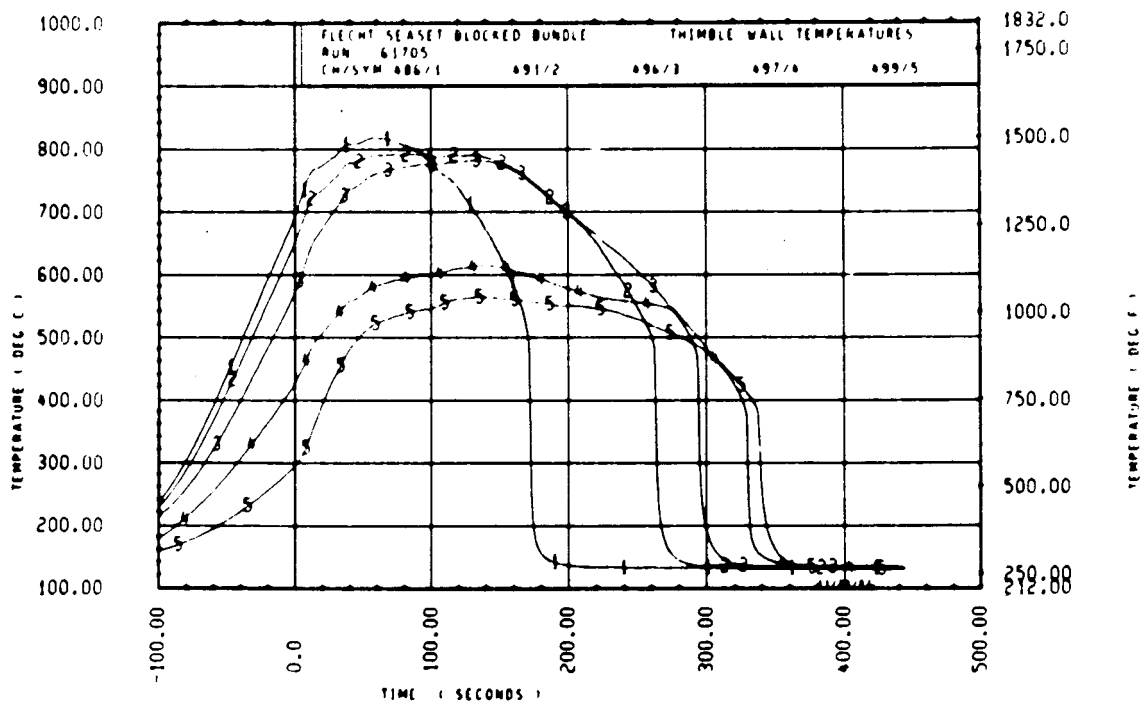
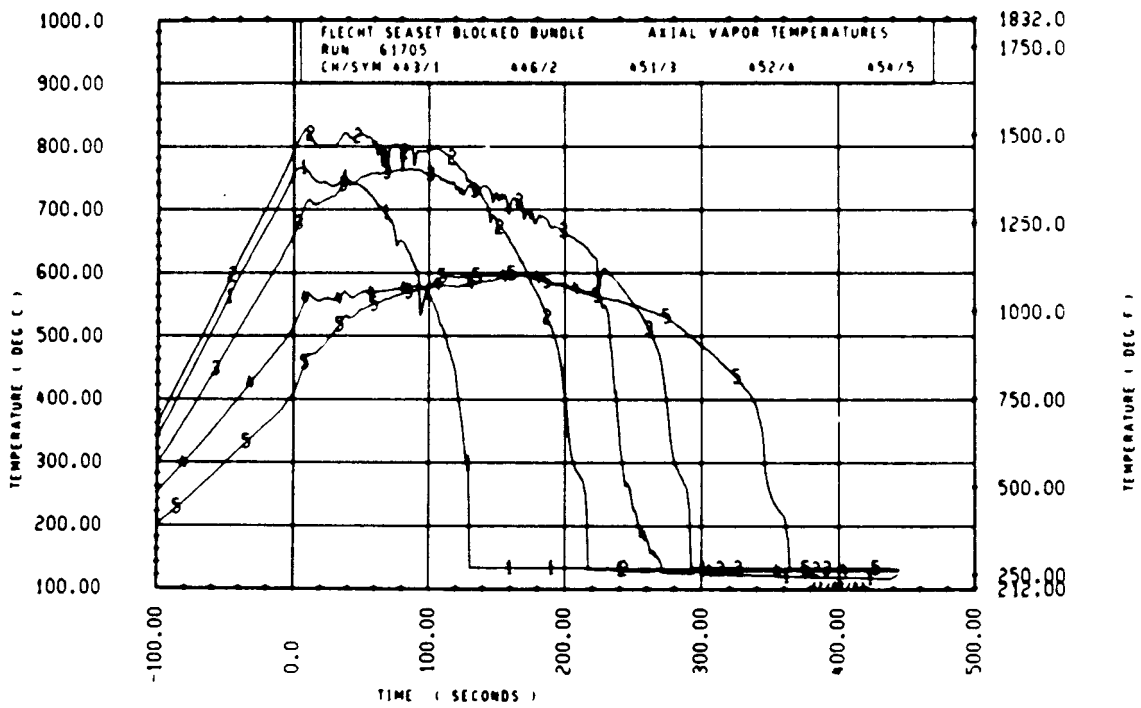
Rod 12I, 2.82 m (111 in.)

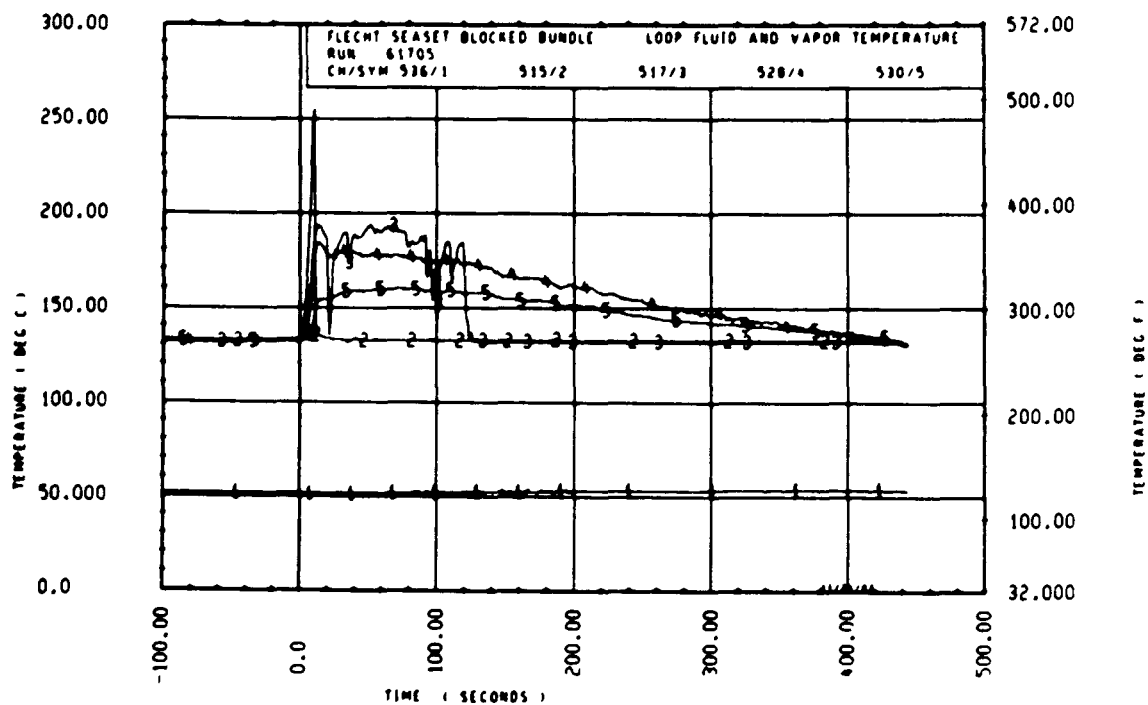
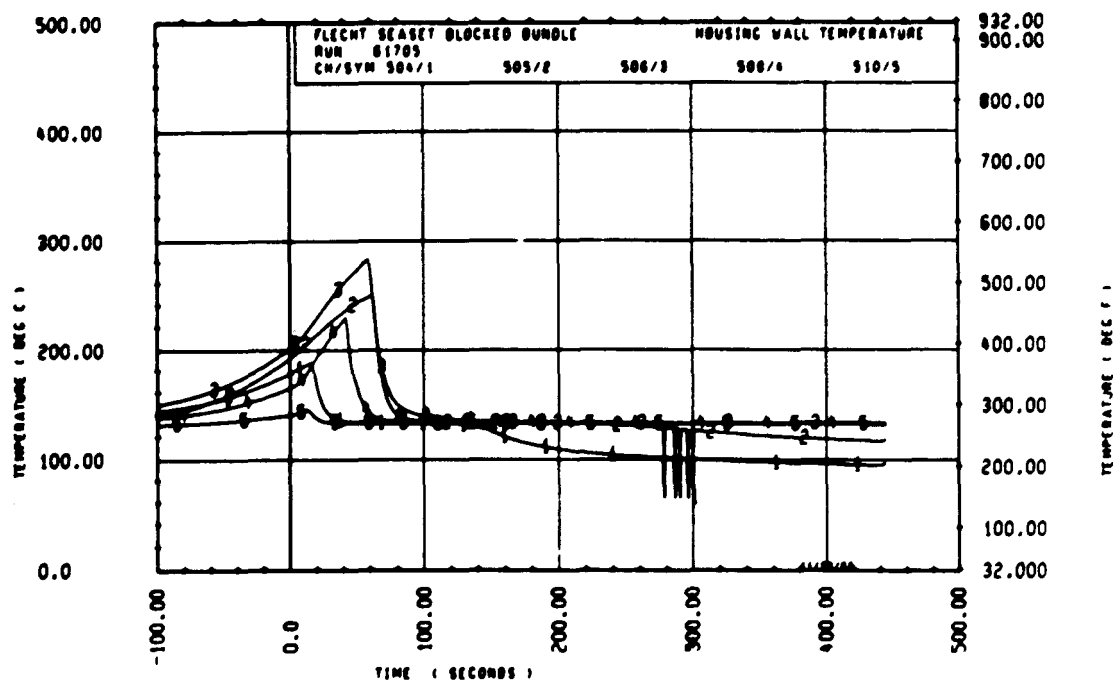


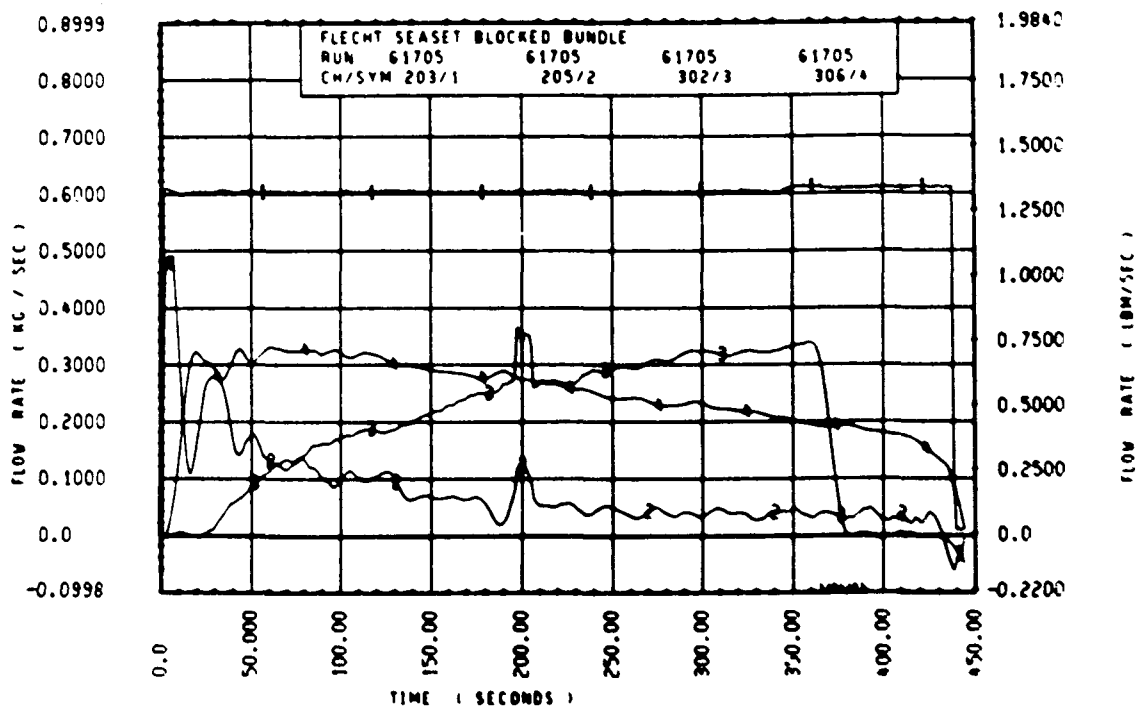
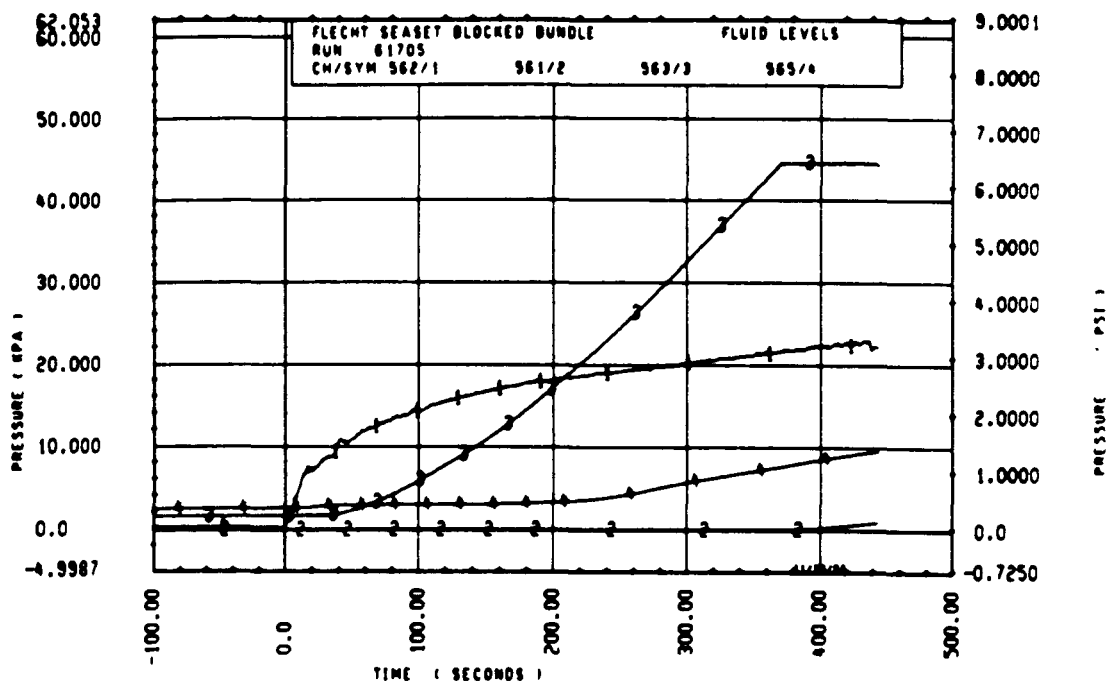
Rod 9K, 3.05 m (120 in.)

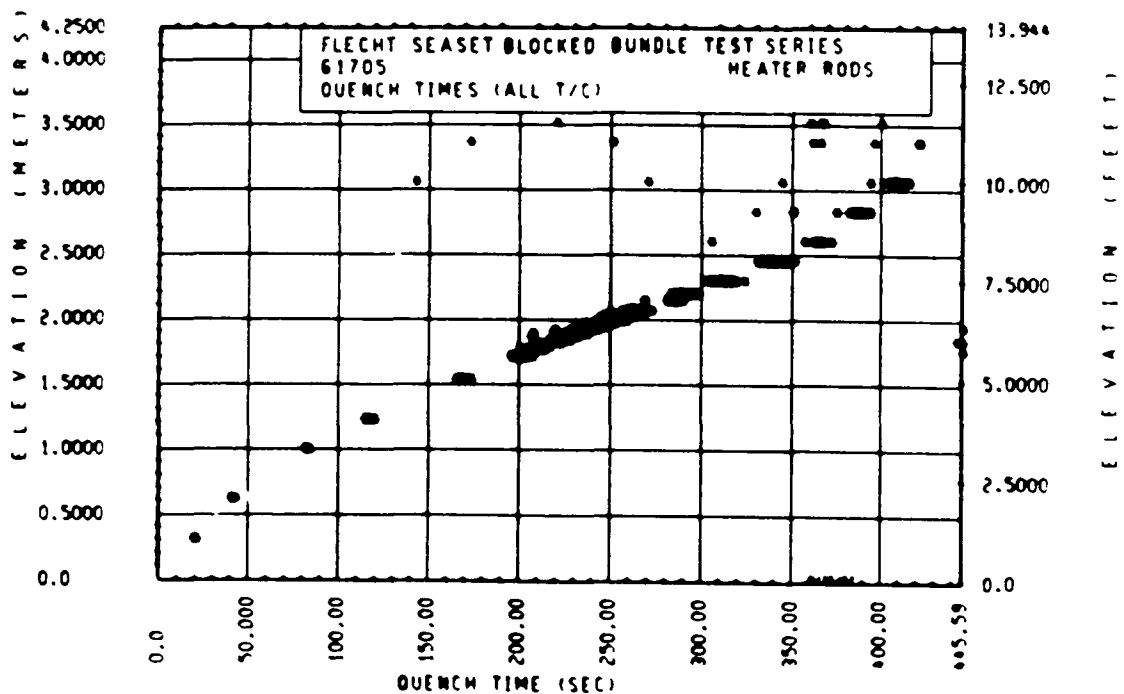
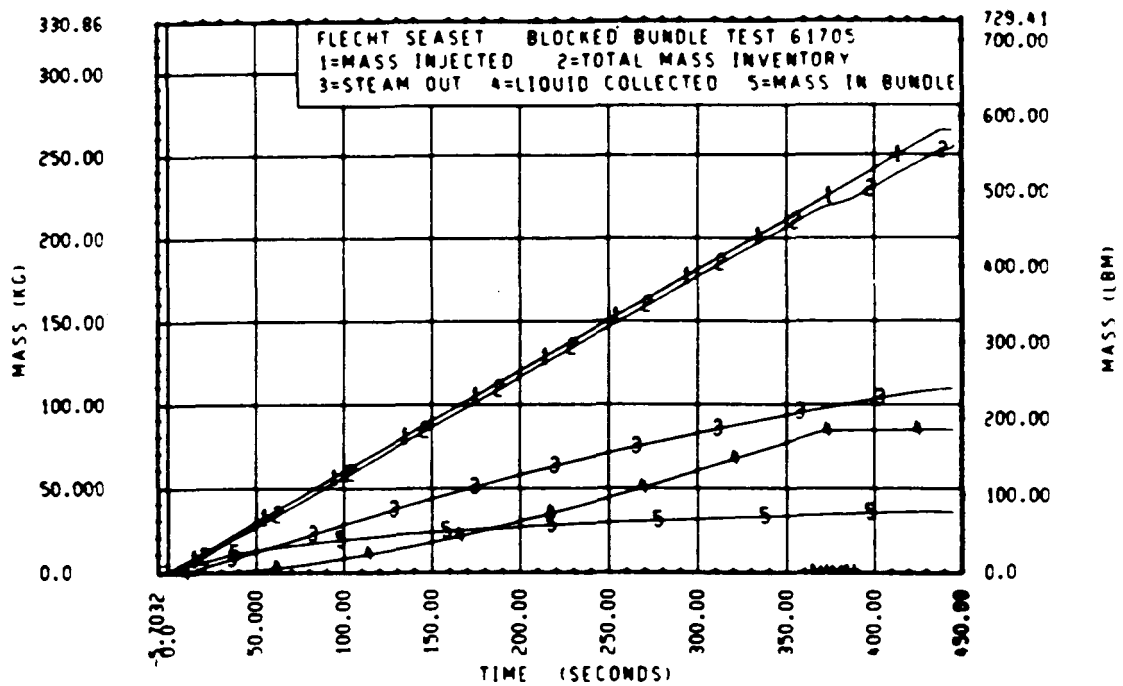


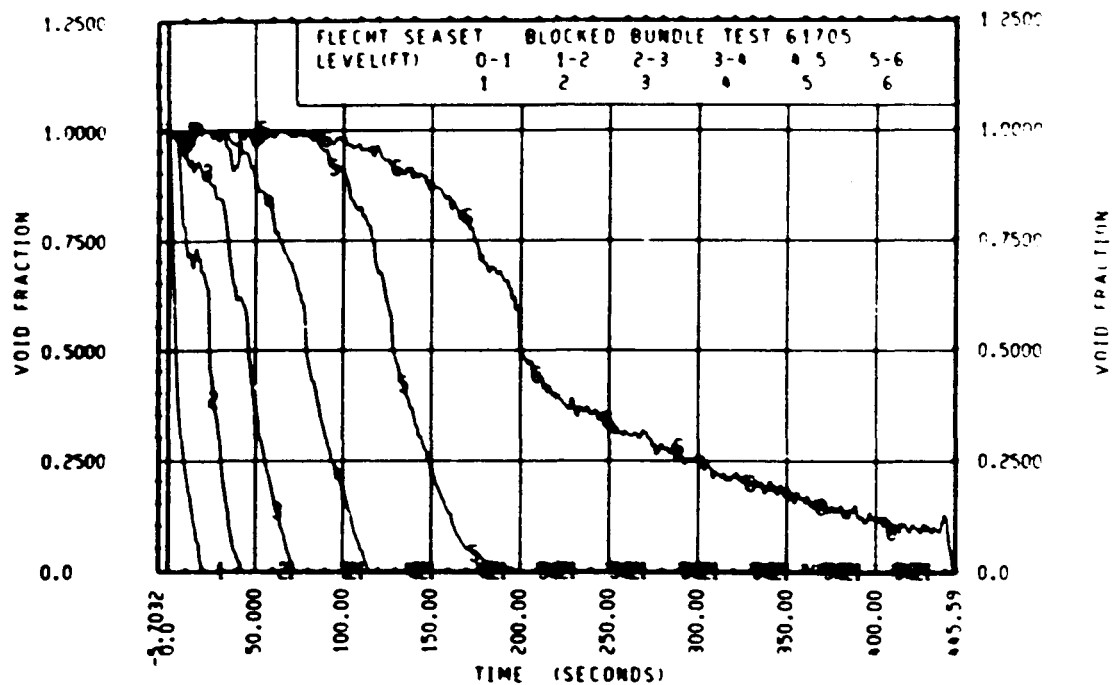
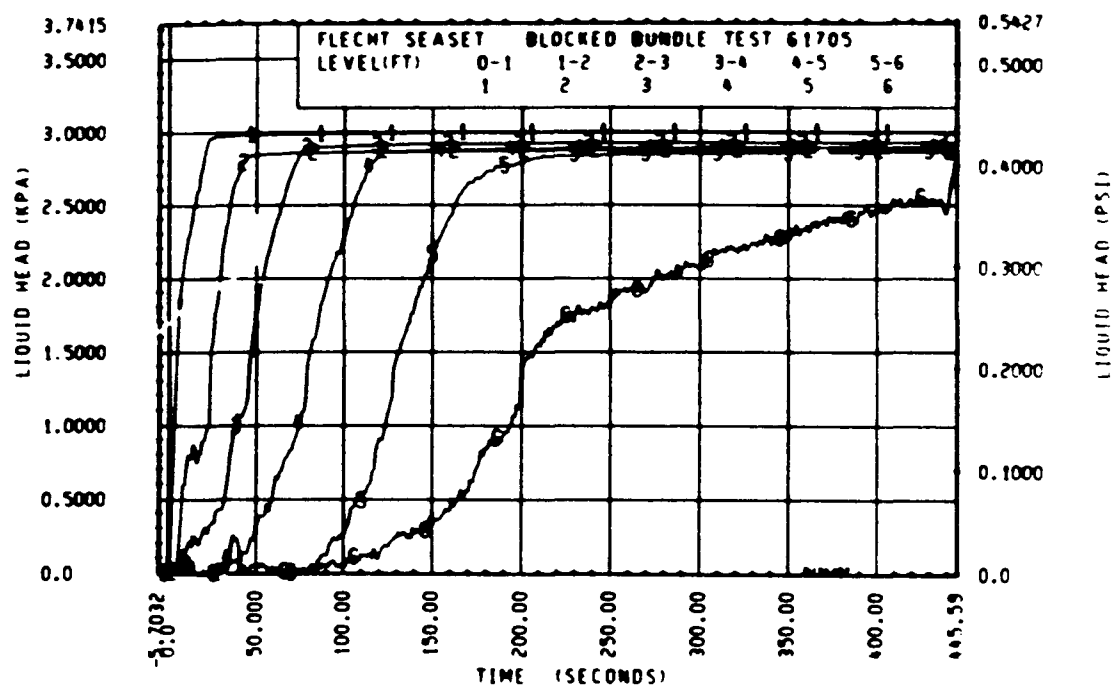
Rod 111, 3.35 m (132 in.)

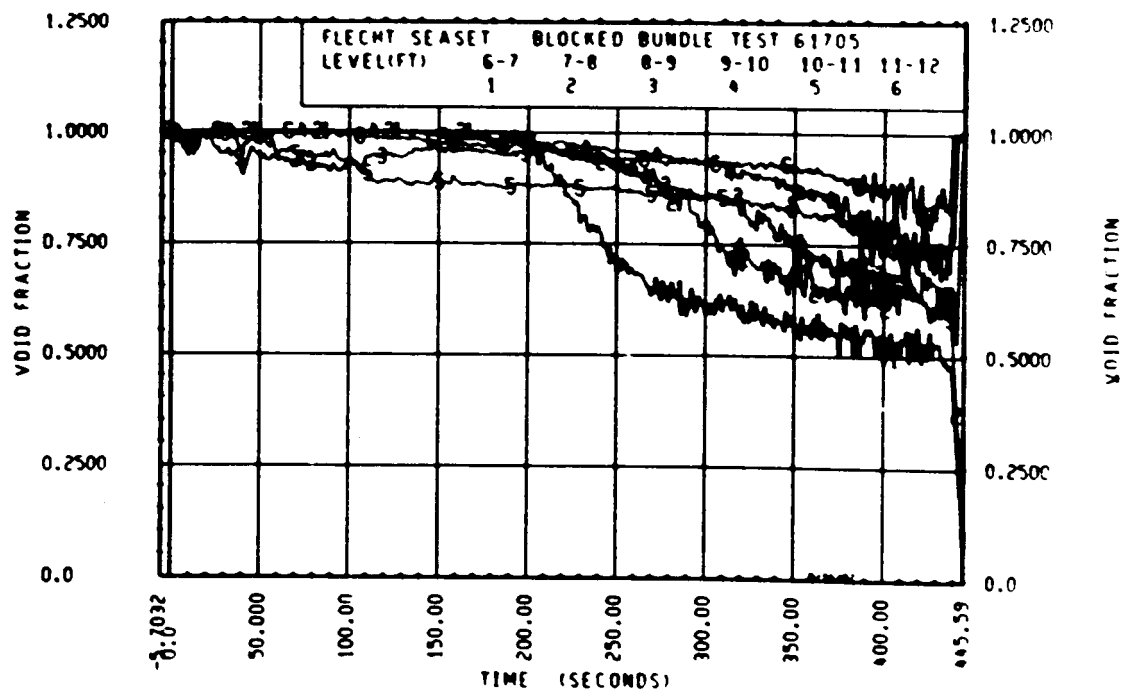
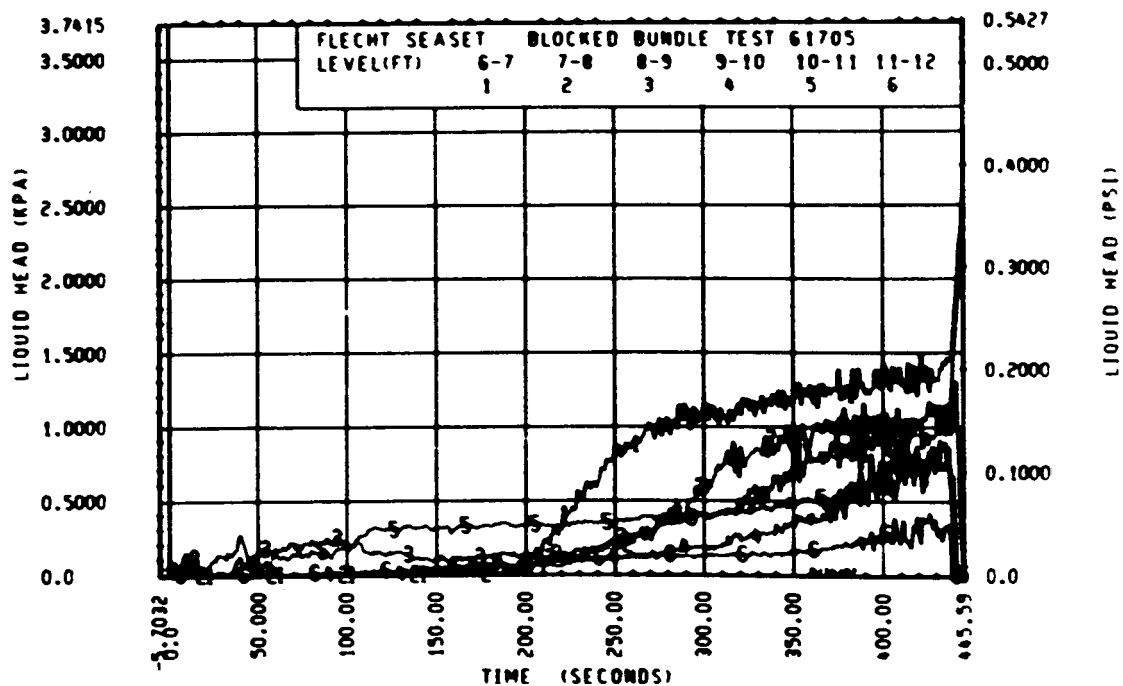












FLECHT SEASET 163-ROD BUNDLE FLOW BLOCKAGE TASK
SUMMARY AND COMMENT SHEET

Run: 61810
Test date: 9/16/82
Test type: Forced reflood
Parameter: Pressure effect

AS-RUN TEST CONDITIONS:

Upper plenum pressure	0.1358 MPa (19.70 psia)
Initial peak clad temperature and location	871.6°C (1600.9°F), 6E-2.01 m (79 in.)
Initial peak rod power:	
Peripheral rods	1.38 kw/m (0.422 kw/ft)
Bypass rods	1.38 kw/m (0.422 kw/ft)
Blockage island rods	1.39 kw/m (0.424 kw/ft)
Flooding rate	17 mm/sec (0.65 in./sec)
Coolant temperature	33.9°C (93°F)
Initial bundle water level	-6.1 mm (-0.24 in.)

COMMENTS:

Inlet mass flow:⁽¹⁾ -2.6% linearly increasing to -5% by 50 seconds and
linearly decreasing to +1% by 160 seconds

Power decay:⁽¹⁾ peripheral rods, 0% linearly increasing to -3% by 400
seconds
bypass rods, 0% linearly increasing to -5% by 400 seconds
blockage islands rods, 0% linearly increasing to +4.6% by
400 seconds

1. Relative to run 34711

FLECHT SEASET 163 ROD BUNDLE TEST SERIES

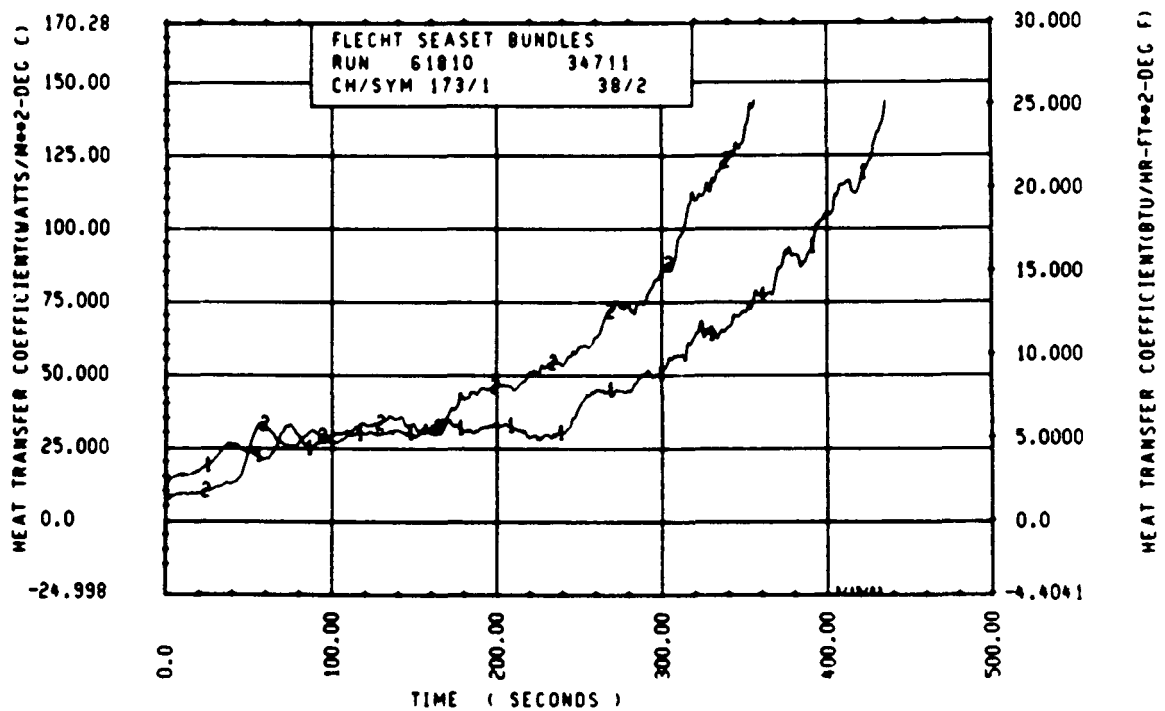
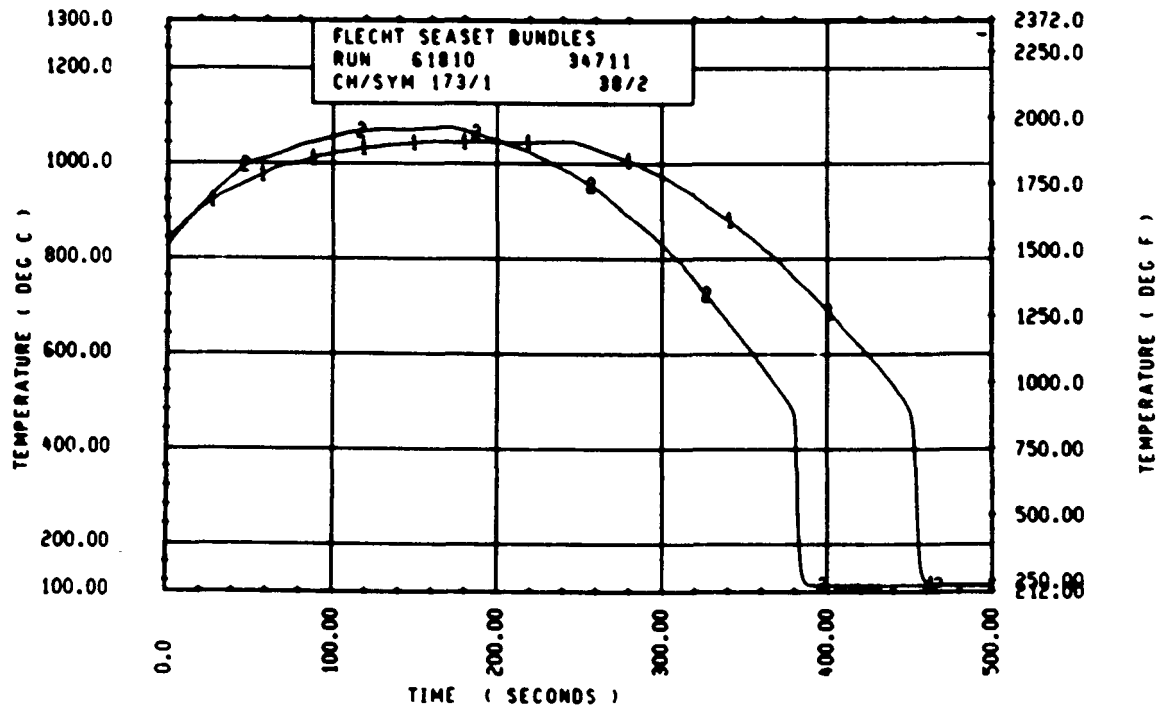
ROD/ELEV	CHAN. NO	RUN NUMBER 61810					
		INITIAL AT FLUCL (DEG F)	MAXIMUM TEMPERATURE (DEG F)	TEMPERATURE RISE (DEG F)	TURNAROUND TIME (SECONDS)	QUENCH TEMPERATURE (DEG F)	QUENCH TIME (SECONDS)
9G 1- 0	3	655.	676.	18.	9.5	543.	33.4
10H 2- C	6	875.	920.	45.	20.0	552.	75.5
9G 3- 3	9	1217.	1302.	85.	30.5	644.	139.3
3J 4- C	11	1352.	1496.	144.	61.5	623.	158.5
7H 4- C	12	1342.	1500.	158.	63.5	645.	198.4
8K 4- C	13	1363.	1533.	170.	65.0	657.	203.0
8M 4- C	14	1347.	1493.	146.	63.0	645.	194.5
12D 4- C	17	1344.	1463.	119.	64.0	666.	191.5
5E 5- C	20	1513.	1743.	230.	69.5	806.	282.8
7G 5- 0	21	1566.	1792.	224.	68.5	761.	277.7
9G 5- C	24	1540.	1763.	223.	70.0	603.	280.0
5E 5- 7	33	1537.	1822.	285.	118.5	696.	340.8
6G 5- 7	45	1540.	1872.	331.	146.0	623.	347.5
9H 5- 9	52	1478.	1643.	366.	150.0	651.	356.0
7G 5-10	59	1494.	1867.	368.	159.0	665.	363.8
7F 5-11	62	1442.	1843.	401.	157.5	697.	375.5
4G 5-11	64	1527.	1858.	331.	139.5	643.	385.4
2I 6- 0	67	1587.	1827.	241.	103.5	651.	388.4
5D 6- C	70	1467.	1814.	327.	140.0	667.	385.8
6J 6- C	74	1520.	1853.	334.	140.5	786.	396.8
7H 6- 0	66	1545.	1848.	303.	117.5	775.	385.5
11E 6- 0	80	1537.	1825.	288.	117.0	834.	391.4
8H 6- 2	97	1350.	1839.	482.	206.2	756.	424.5
5H 6- 2	99	1522.	1900.	378.	160.0	867.	416.5
9E 6- 2	105	1330.	1875.	545.	191.0	1162.	467.7
8H 6- 3	111	1396.	1870.	473.	202.2	831.	432.7
4G 6- 3	124	1542.	1902.	360.	157.0	827.	429.7
11H 6- 4	134	1465.	1896.	432.	200.0	676.	445.5
9D 6- 4	143	1545.	1933.	389.	235.2	855.	442.5
9J 6- 5	165	1520.	1939.	419.	200.0	681.	456.5
9H 6- 5	166	1582.	1913.	330.	156.5	677.	438.5
8J 6- 6	192	1567.	1950.	383.	184.5	646.	458.8
9D 6- 6	193	1555.	1945.	389.	237.2	845.	462.8
11F 6- 6	173	1547.	1917.	370.	161.0	605.	453.0
4G 7- C	261	1450.	1846.	392.	145.0	690.	506.5
7D 7- 6	309	1474.	1934.	456.	246.2	785.	567.5
7G 7- 6	312	1521.	1940.	419.	206.2	774.	564.5
11E 7- 6	325	1463.	1909.	446.	245.2	754.	559.5
5L 8- C	337	1254.	1788.	489.	191.5	716.	613.0
7H 8- 0	345	1343.	1923.	580.	300.2	725.	621.5
7K 8- C	346	1349.	1886.	537.	199.0	711.	610.5
5J 8- 6	366	1122.	1711.	589.	196.0	585.	655.7
7B 8- 6	368	1125.	1722.	600.	245.2	597.	648.8
7E 9- 3	383	1090.	1705.	610.	306.2	662.	667.2
8H 9- 3	387	1640.	1656.	616.	324.2	619.	686.2
9C 9- 3	389	1630.	1608.	572.	247.2	627.	666.2
11F 9- 3	394	1626.	1581.	556.	255.2	567.	689.8
7B10- 0	408	847.	1423.	576.	253.2	550.	713.2
6H10- 0	415	855.	1541.	686.	290.2	562.	720.8
6K10- C	417	857.	1462.	604.	291.2	543.	721.0
6N10- C	418	872.	1353.	481.	197.5	565.	715.2
6H11- 0	429	681.	981.	301.	195.0	527.	694.1
9G11- C	431	664.	1103.	434.	299.2	699.2	699.2
11E11- C	432	661.	1120.	459.	282.2	475.	704.5
5J11- 6	436	675.	874.	199.	138.0	556.	326.8
7B11- 6	437	645.	1060.	435.	287.2	493.	724.5
8J11- 6	438	674.	906.	234.	196.5	507.	718.7

RUN 61810 HEATER ROD STATISTICAL DATA

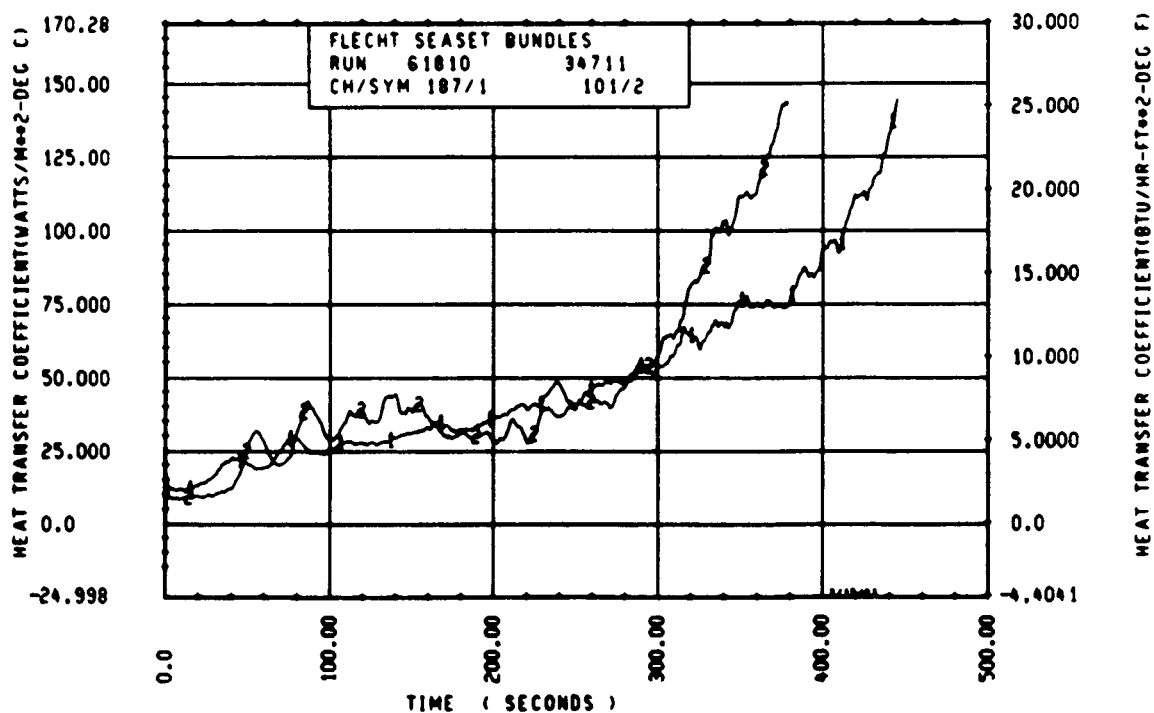
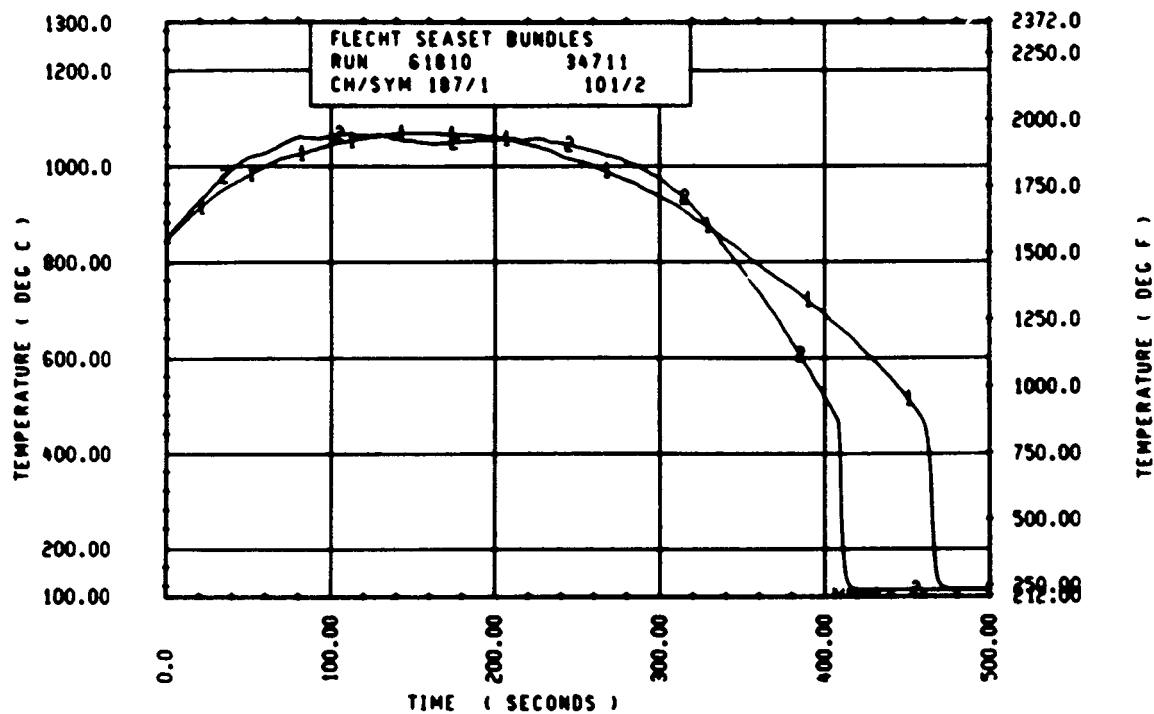
ELEV	INITIAL TEMP (DEG F)			MAX TEMP (DEG F)			TURNAROUND TIME (SEC)		
	MAX	MIN	MEAN	MAX	MIN	MEAN	MAX	MIN	MEAN
12	659.6	656.5	656.4	676.4	675.3	676.0	10.0	9.0	9.5
24	875.0	842.9	854.3	920.4	881.2	895.3	20.0	16.5	19.2
39	1217.0	1166.1	1167.4	1301.5	1256.7	1274.1	47.5	30.5	36.0
48	1373.3	1341.6	1354.2	1532.6	1462.7	1506.7	65.5	61.5	63.6
60	1569.5	1452.0	1522.4	1804.8	1679.0	1746.7	104.0	64.5	76.2
67	1591.2	1506.6	1548.5	1871.6	1748.9	1809.1	146.0	68.5	110.7
69	1518.6	1477.7	1506.9	1843.3	1793.6	1818.6	150.0	122.5	135.1
70	1594.4	1474.6	1524.4	1867.0	1773.5	1817.6	159.0	69.5	114.7
71	1527.2	1442.4	1485.8	1858.0	1776.8	1824.4	157.5	87.5	134.5
72	1589.0	1453.1	1535.7	1894.2	1813.9	1849.5	158.0	97.0	129.4
73	1581.4	1444.6	1514.4	1877.2	1778.0	1834.2	163.0	91.5	126.6
74	1587.9	1356.4	1444.0	1906.8	1633.1	1870.5	206.2	112.5	155.8
75	1592.2	1397.6	1511.3	1905.6	1800.3	1868.4	231.2	94.0	156.9
76	1598.7	1445.6	1534.9	1933.2	1821.8	1892.8	235.2	93.0	167.2
77	1582.5	1471.3	1535.0	1949.3	1808.2	1909.9	243.2	99.5	174.7
78	1597.7	1508.8	1552.0	1959.6	1829.7	1922.6	243.2	132.5	176.9
79	1600.9	1500.1	1554.2	1975.7	1821.8	1927.8	239.2	99.5	160.2
80	1589.0	1503.4	1546.4	1984.9	1844.4	1942.4	244.2	132.0	181.5
81	1581.4	1477.7	1536.2	1978.0	1894.2	1939.8	245.2	140.0	165.2
84	1516.4	1347.6	1473.4	1953.9	1714.3	1845.2	247.2	104.0	173.0
86	1571.6	1457.4	1515.3	1939.0	1757.9	1880.8	259.2	134.0	190.1
90	1528.3	1278.6	1477.1	1959.6	1757.9	1901.8	293.2	138.0	206.5
96	1398.6	1270.2	1345.5	1952.8	1753.4	1876.8	301.2	160.5	225.1
102	1185.8	1042.1	1144.1	1858.0	1657.0	1756.1	319.2	196.0	251.6
111	1095.7	1022.5	1055.4	1705.4	1448.8	1602.9	324.2	150.0	268.8
120	913.2	809.6	859.6	1603.1	1292.1	1465.9	384.2	171.5	279.1
132	680.6	660.6	667.6	1169.2	981.3	1075.6	337.2	172.5	270.4
138	675.3	604.4	642.3	1080.2	873.9	956.3	306.2	136.0	244.2

RUN 61810 HEATER ROD STATISTICAL DATA

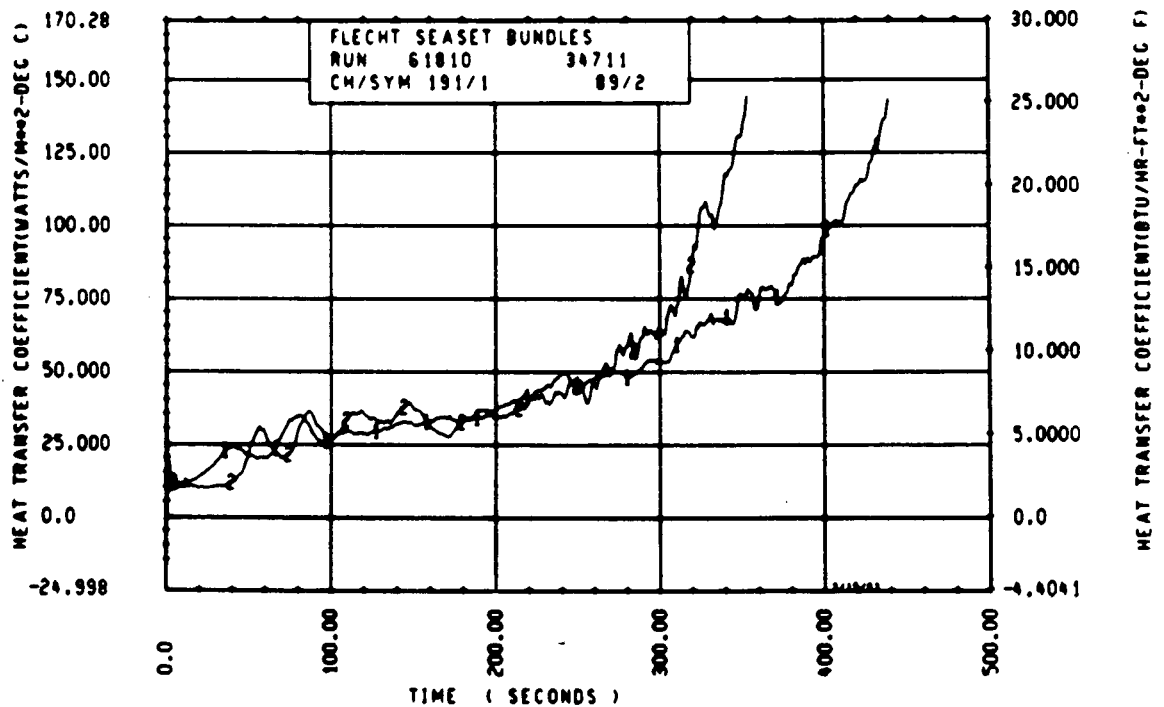
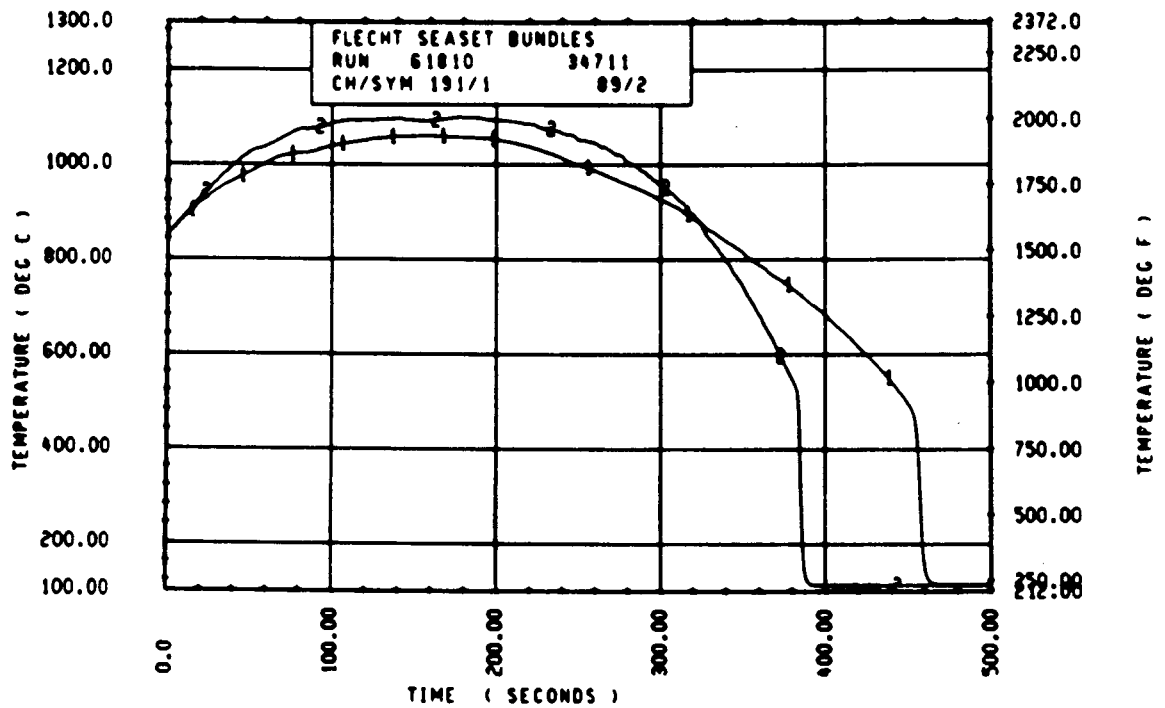
ELEV	TEMP RISE (DEG F)			QUENCH TEMP (DEG F)			QUENCH TIME (SEC)		
	MAX	MIN	MEAN	MAX	MIN	MEAN	MAX	MIN	MEAN
12	17.9	16.8	17.2	533.0	510.9	522.4	35.9	33.4	34.4
24	45.4	36.3	41.0	554.9	533.7	546.9	75.5	70.9	73.2
39	96.8	75.1	86.7	689.8	644.4	658.9	143.3	135.4	138.6
48	169.9	119.0	152.6	720.2	623.2	661.3	203.0	189.9	195.7
60	250.0	174.3	224.4	864.5	744.5	786.4	293.9	277.7	283.4
67	331.4	197.3	261.6	922.6	769.4	839.8	353.9	332.9	341.6
69	365.6	277.2	311.7	950.6	791.6	846.9	367.9	353.6	359.7
70	368.0	207.0	242.7	885.3	790.6	841.4	379.9	362.6	369.1
71	400.9	260.5	338.6	911.4	808.4	864.9	385.9	369.9	379.1
72	409.4	237.0	313.6	932.5	775.1	846.3	404.9	384.0	391.4
73	381.6	246.0	314.3	908.0	792.5	852.6	412.9	389.0	400.4
74	464.5	267.6	371.0	942.9	696.6	828.8	432.3	403.4	416.7
75	472.6	257.3	357.1	897.5	441.7	794.8	445.2	407.8	427.6
76	470.4	244.4	352.9	894.6	670.4	840.0	445.9	417.8	435.2
77	429.7	284.2	374.4	861.6	693.6	830.9	476.6	438.9	452.2
78	430.2	297.2	376.7	902.0	668.0	818.4	484.9	442.0	461.3
79	453.7	274.0	366.6	897.4	611.4	831.4	481.9	446.0	467.6
80	465.9	244.0	353.4	874.1	707.4	807.7	498.3	462.6	460.2
81	446.3	367.4	403.6	849.7	746.0	792.7	500.9	460.0	490.0
84	453.7	244.4	371.0	736.3	643.2	695.9	524.0	500.0	511.6
86	416.4	241.5	355.4	811.3	695.7	746.0	550.9	509.3	527.0
90	534.1	287.7	424.6	839.6	713.3	790.3	586.7	546.7	564.7
96	600.4	403.3	531.3	818.9	698.9	762.9	627.7	592.0	610.8
102	698.1	554.9	612.0	714.7	584.5	641.1	662.2	634.1	647.4
111	633.5	366.2	547.5	797.8	567.3	649.3	694.1	607.9	661.2
120	711.4	412.6	606.7	1053.5	464.8	595.7	727.9	350.6	696.7
132	500.2	300.7	407.6	527.5	239.5	445.5	729.2	694.1	706.7
138	435.4	196.6	313.4	701.6	492.8	575.7	724.9	326.8	532.6



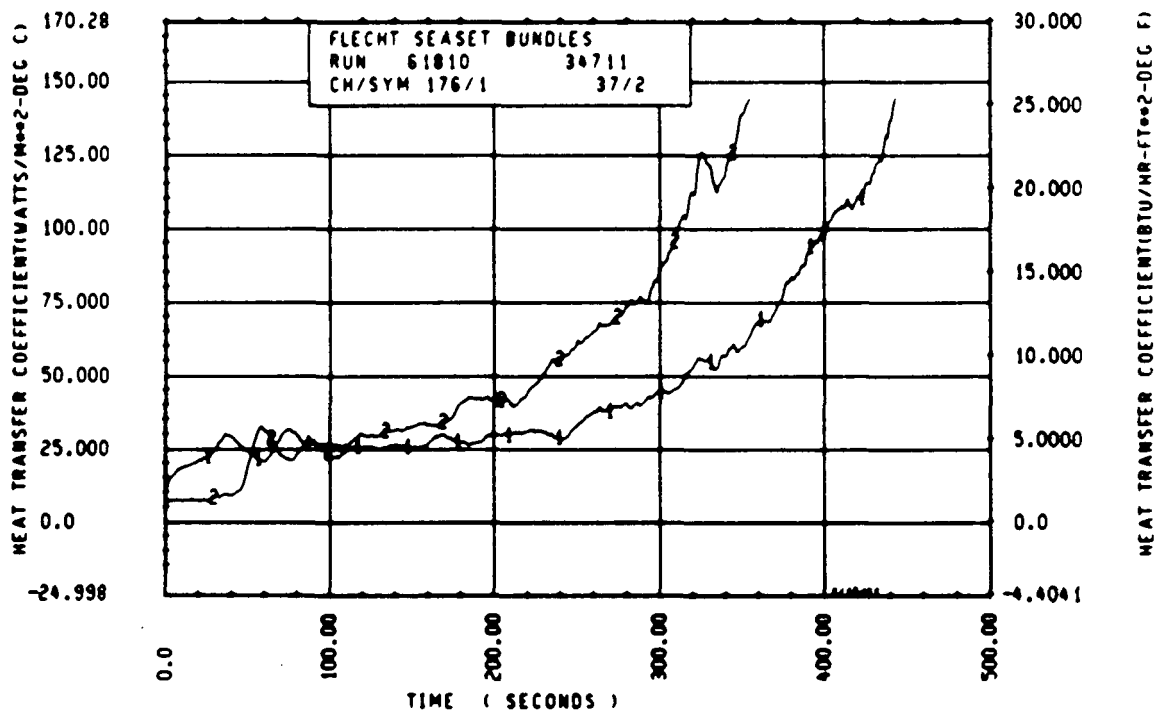
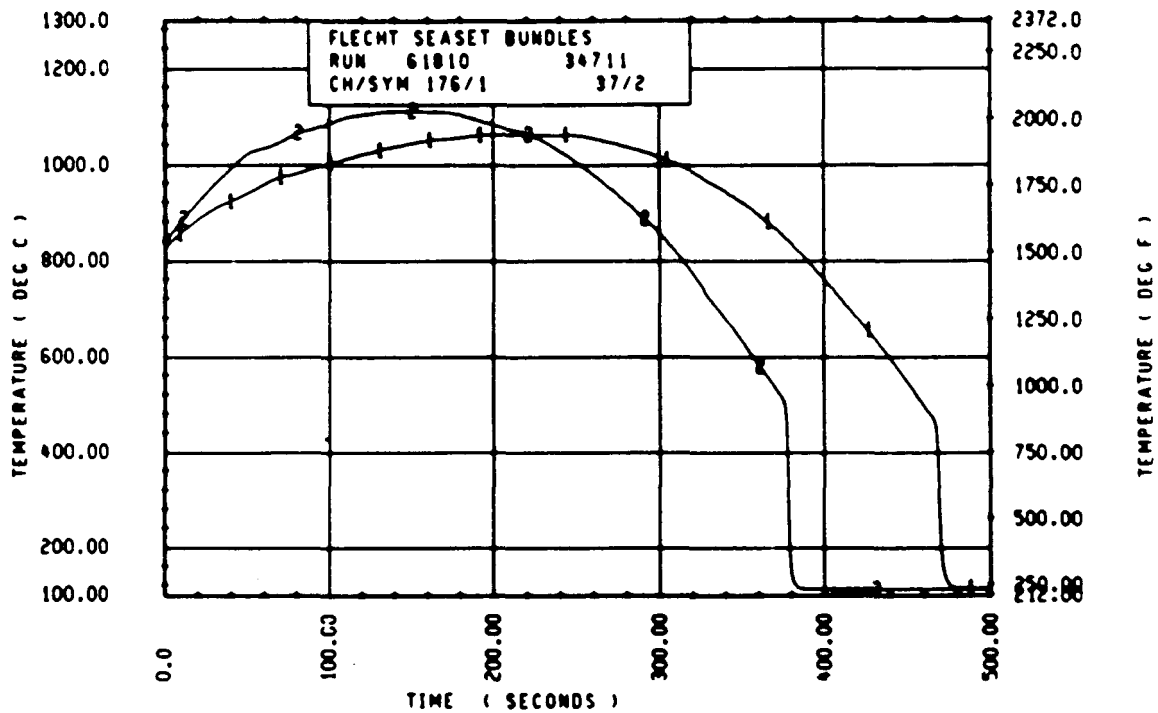
Rod 11F, 1.98 m (78 in.)



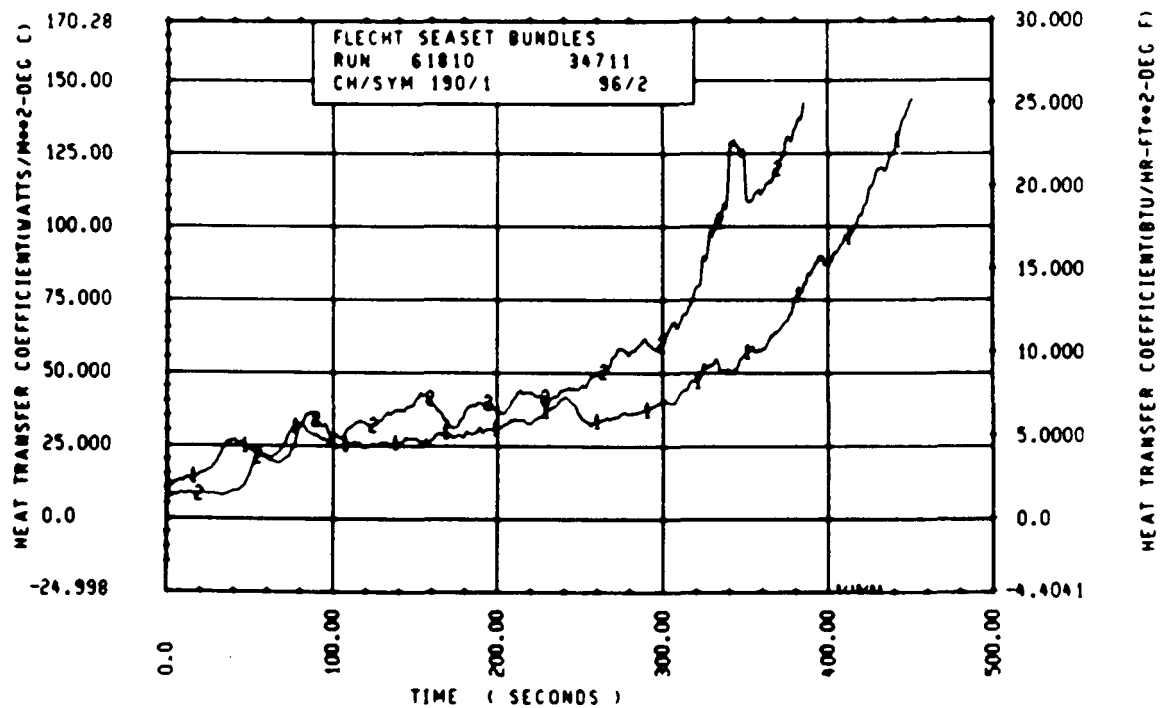
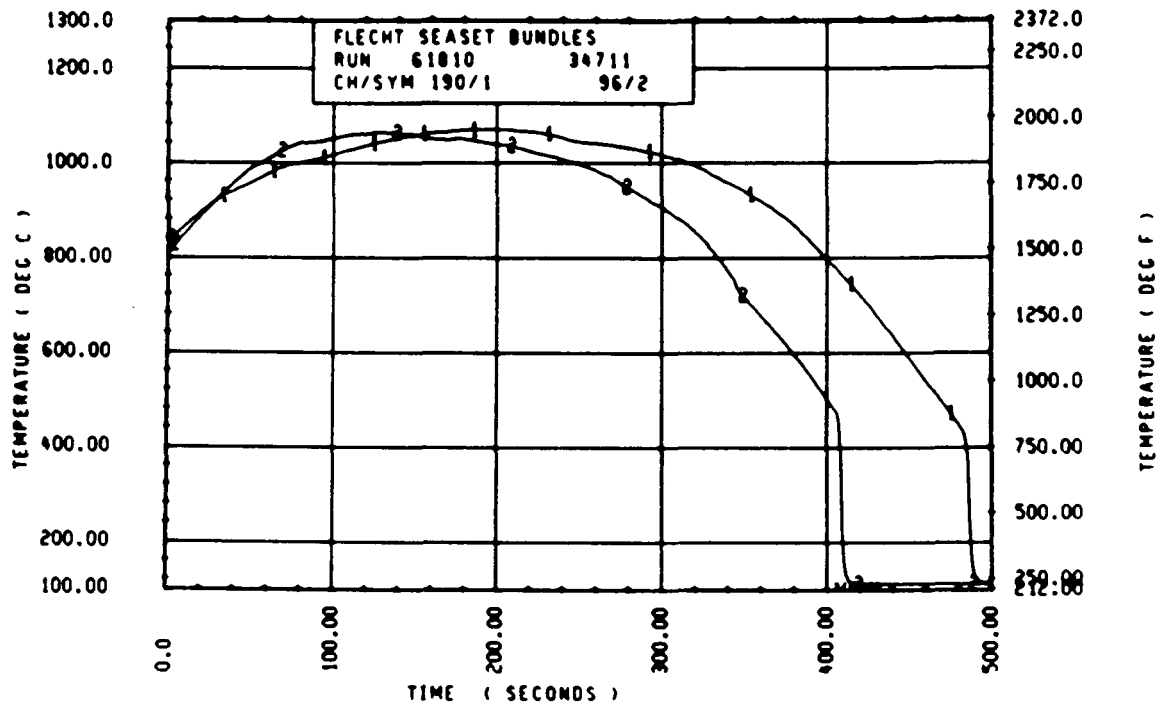
Rod 6J, 1.98 m (78 in.)



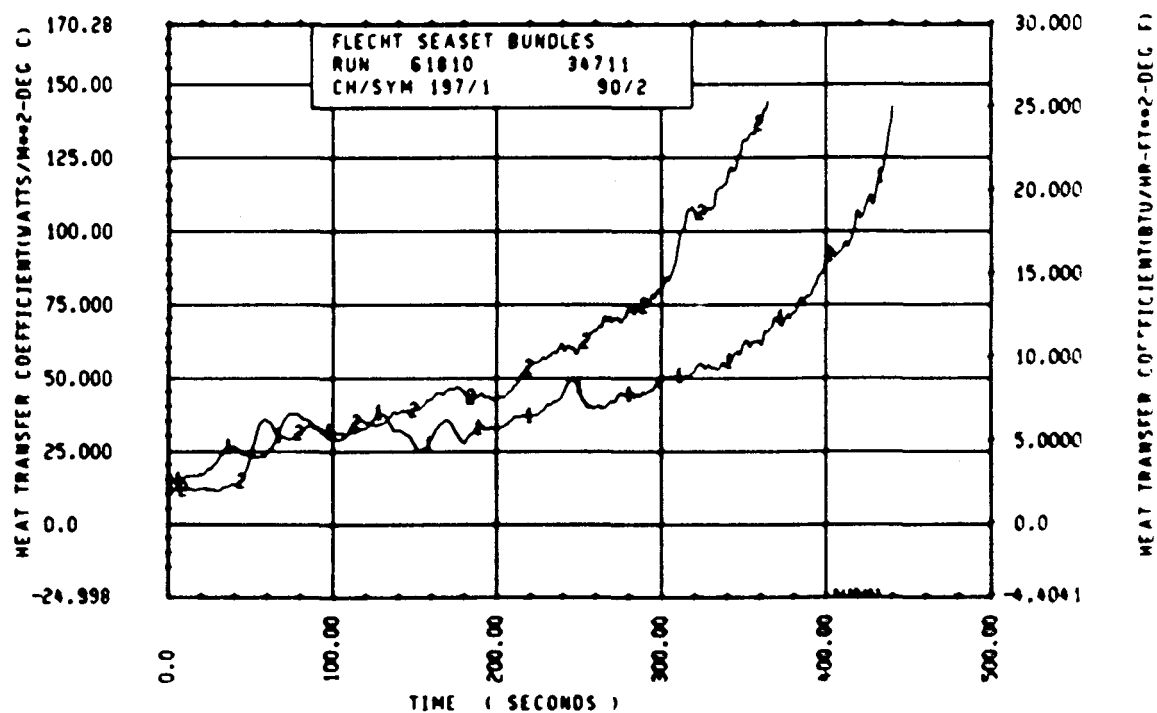
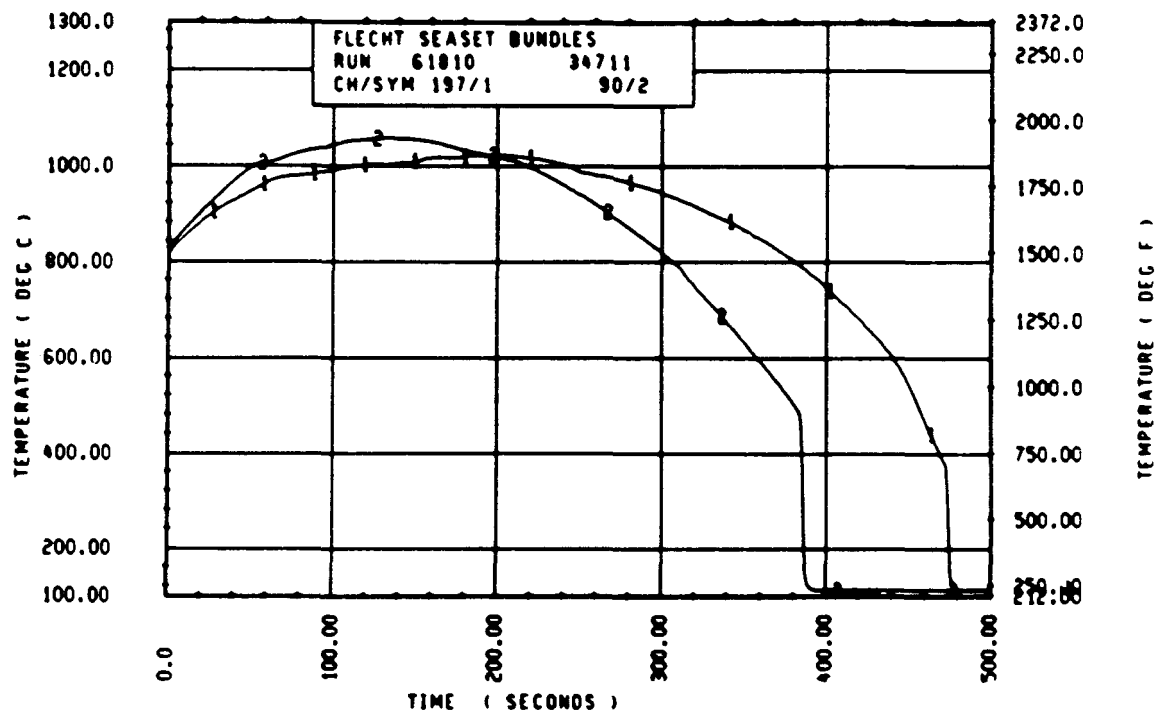
Rod 7K, 1.98 m (78 in.)



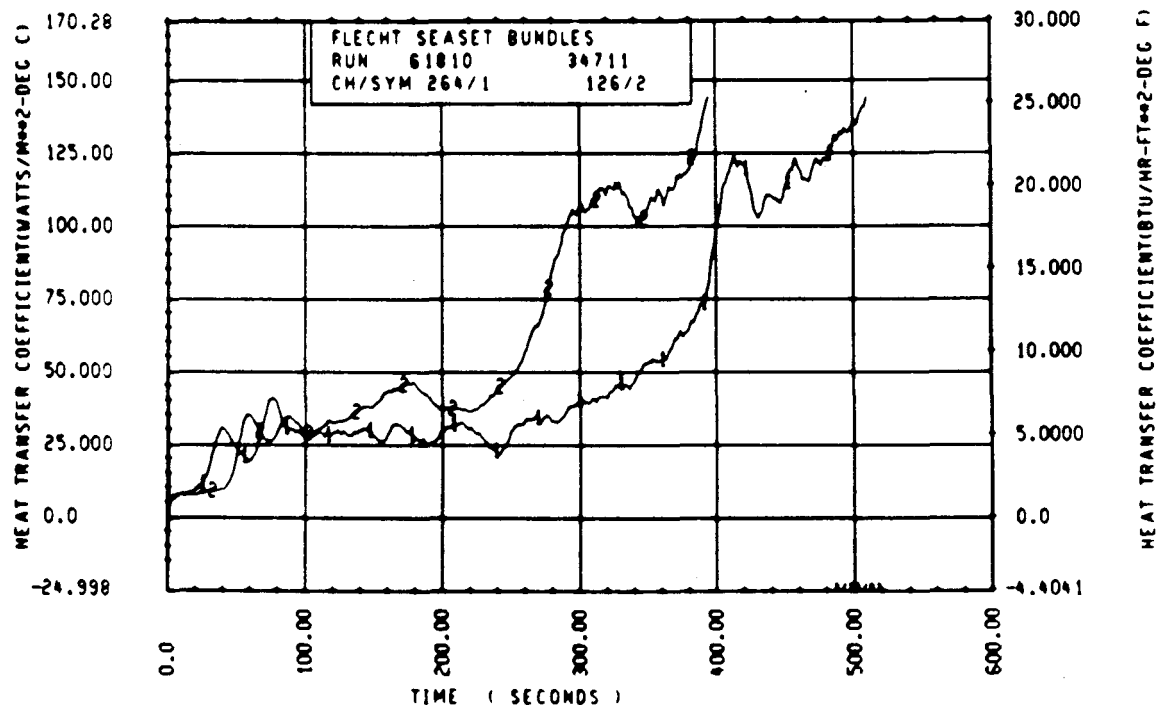
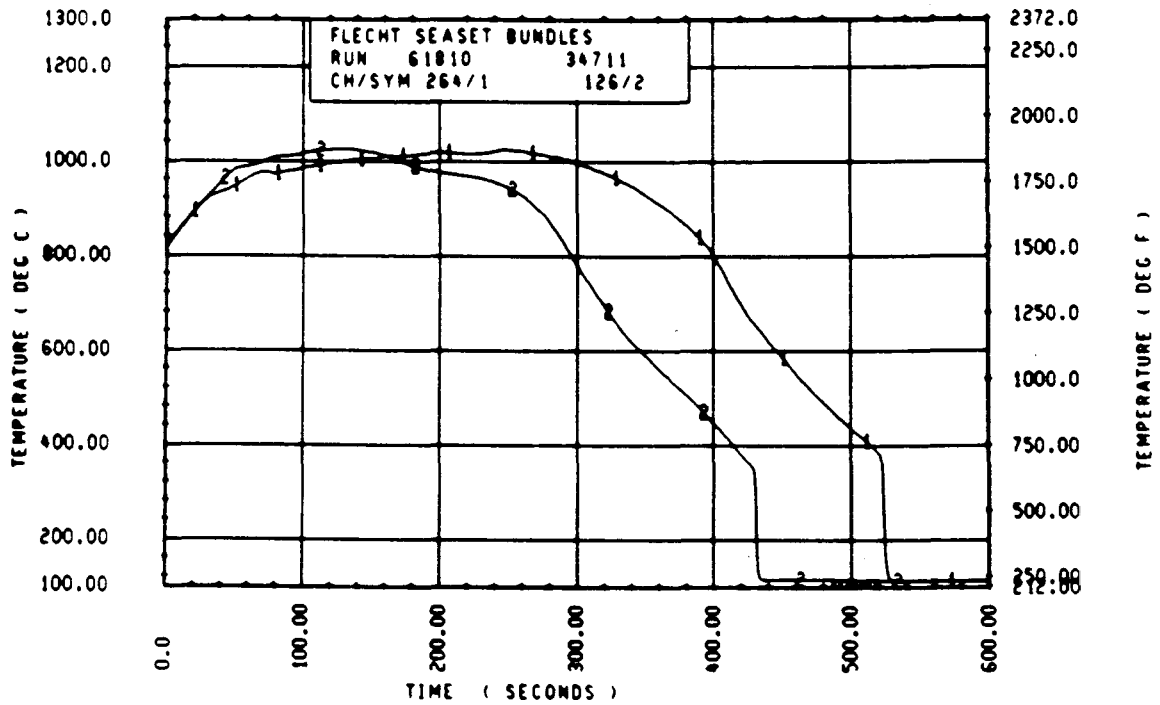
Rod 9F, 1.98 m (78 in.)



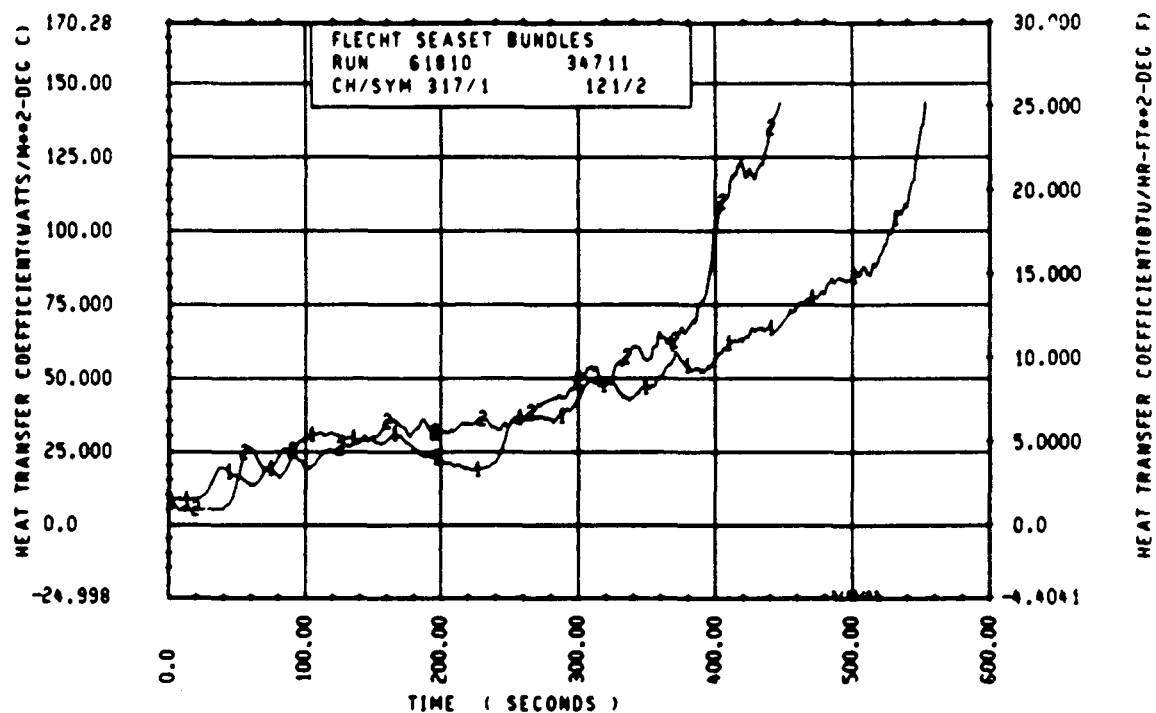
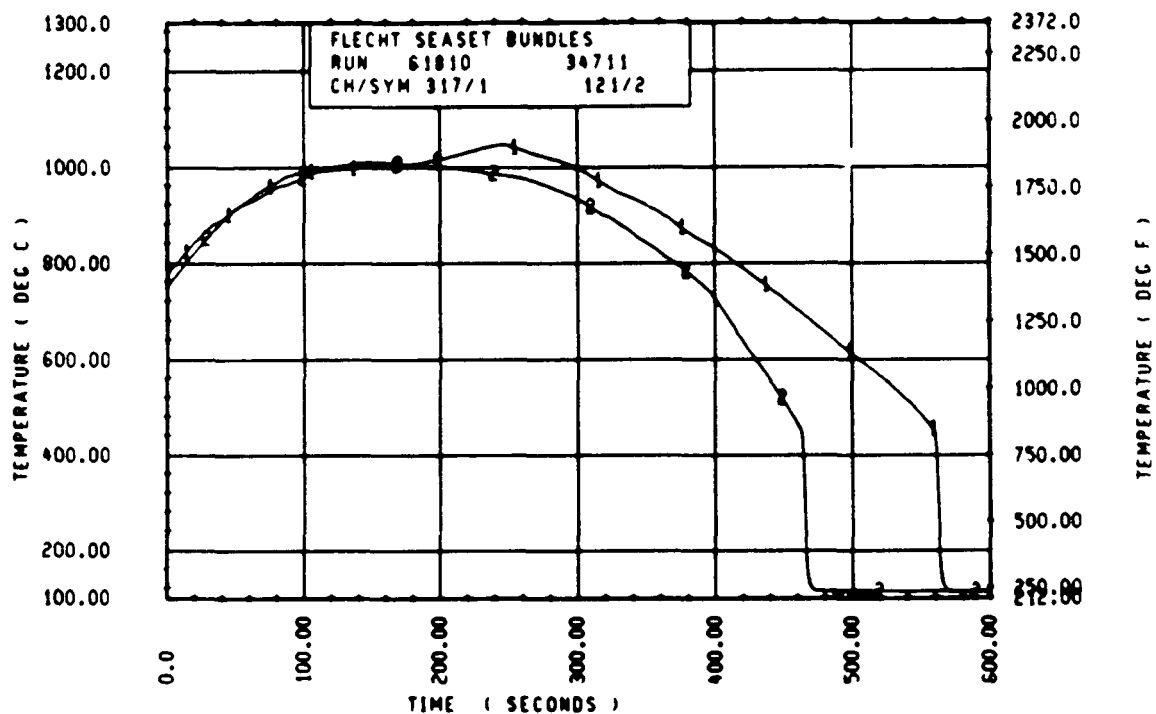
Rod 7F, 1.98 m (78 in.)



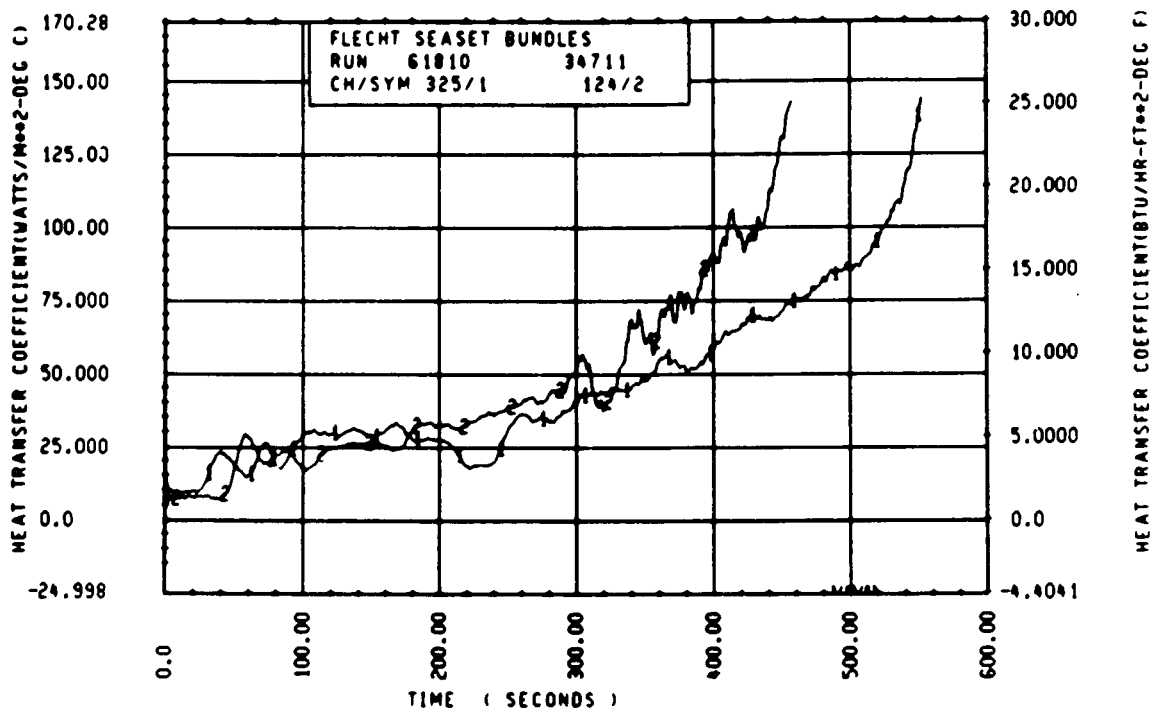
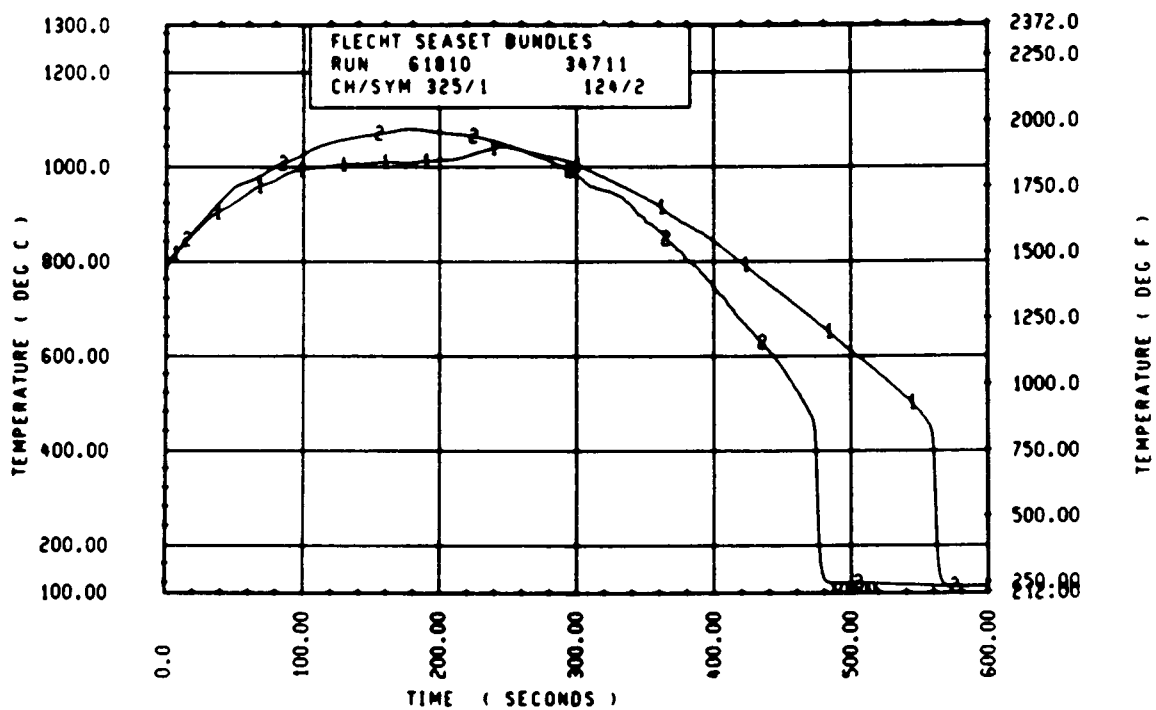
Rod 11K, 1.98 m (78 in.)



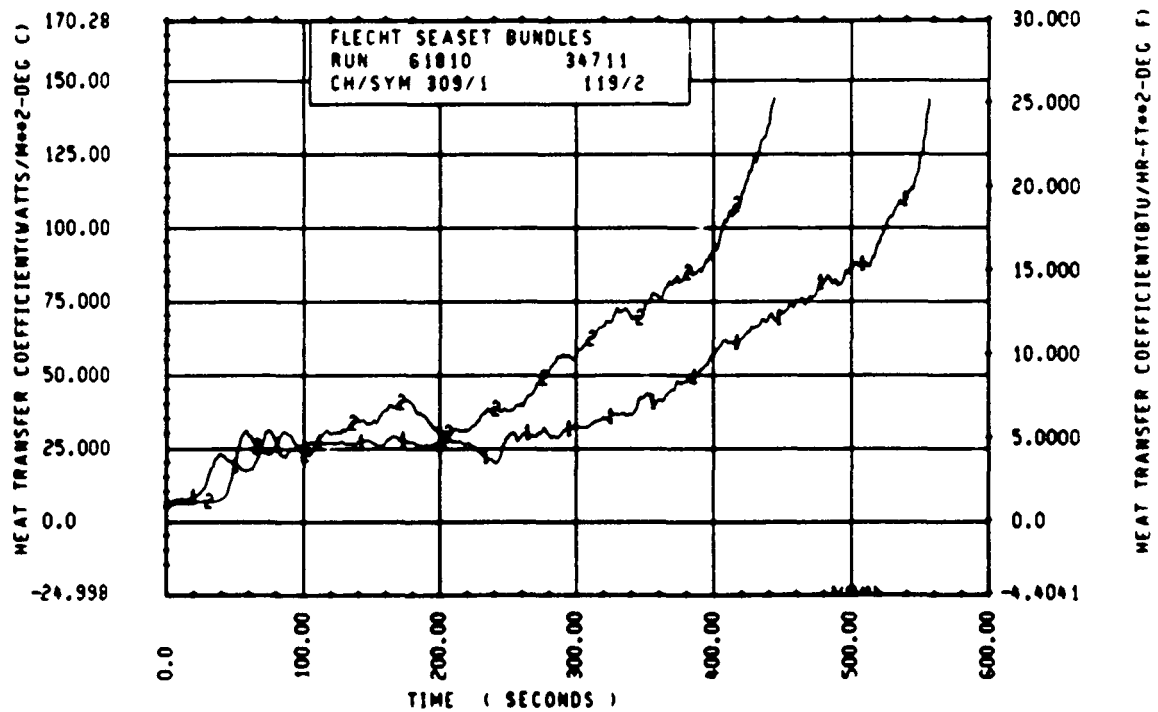
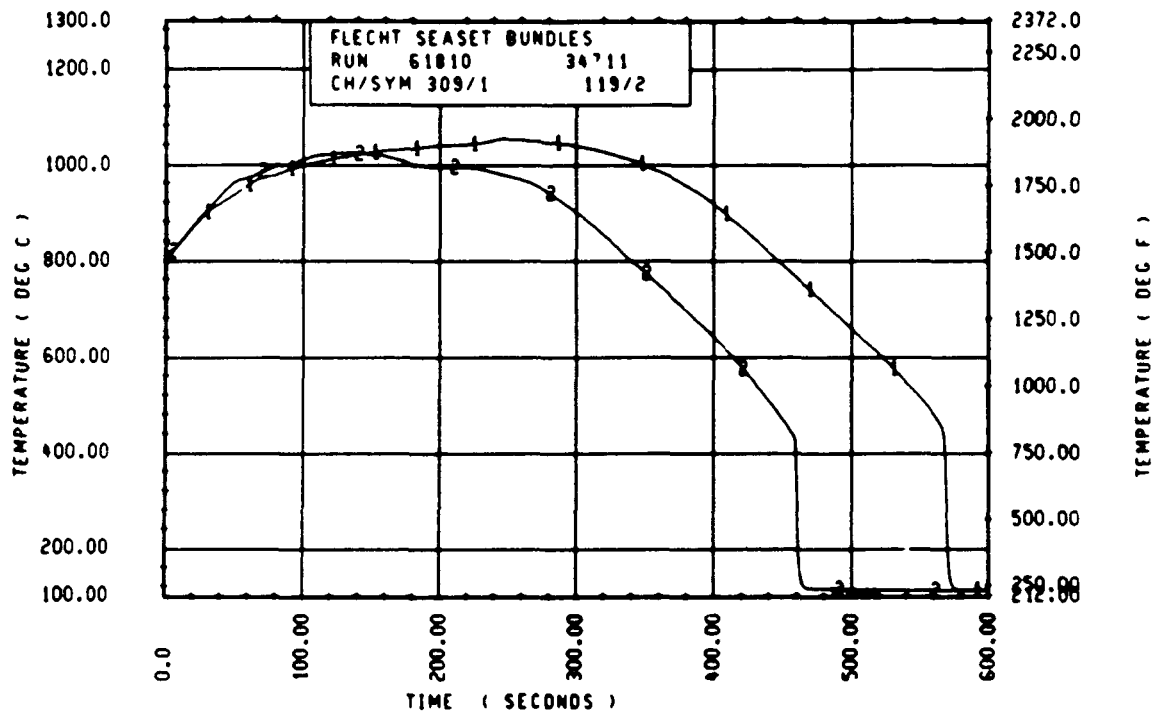
Rod 7E, 2.13 m (84 in.)



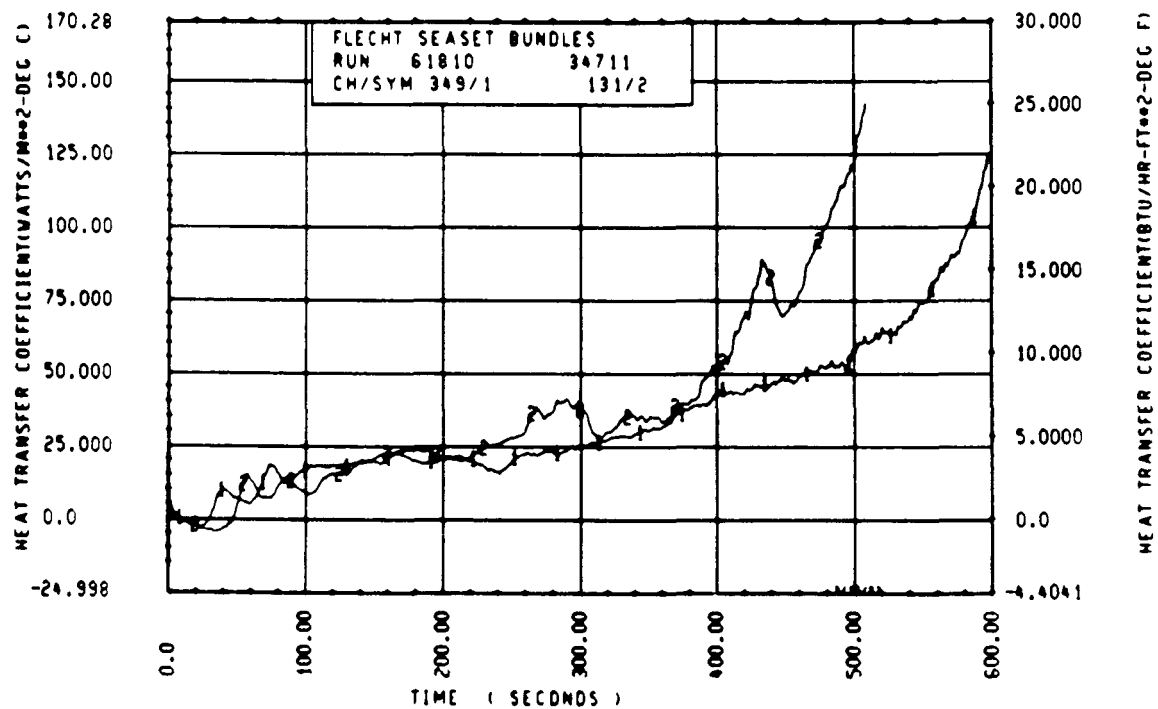
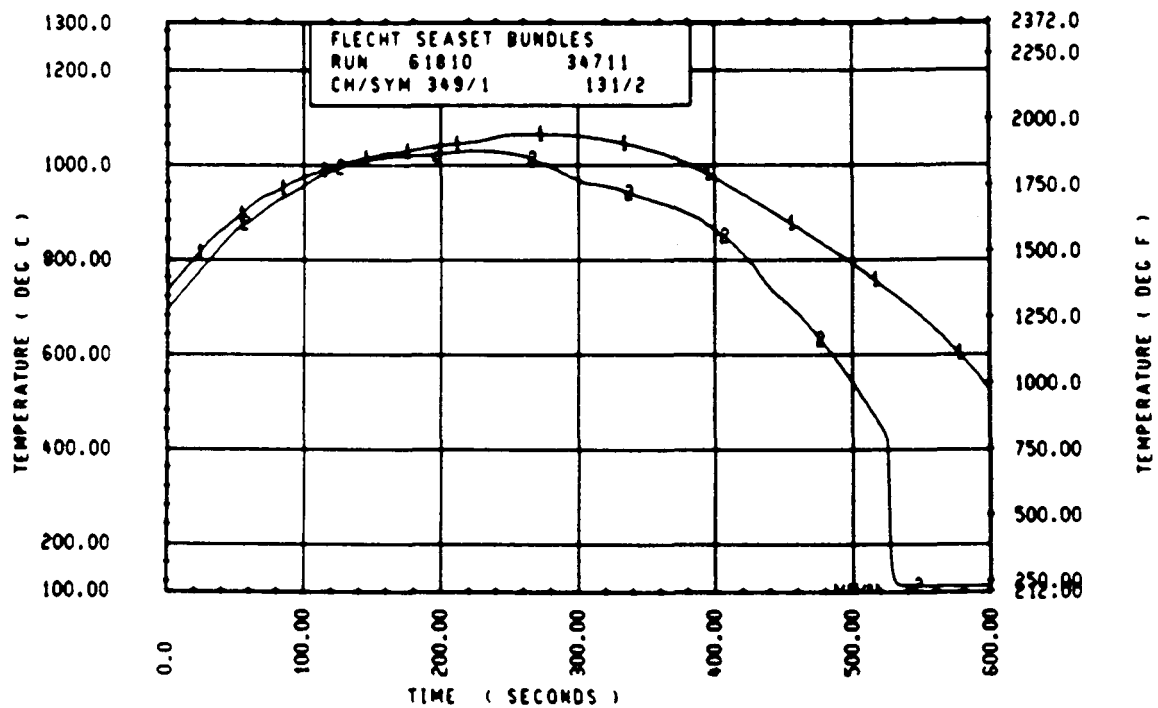
Rod 9C, 2.29 m (90 in.)



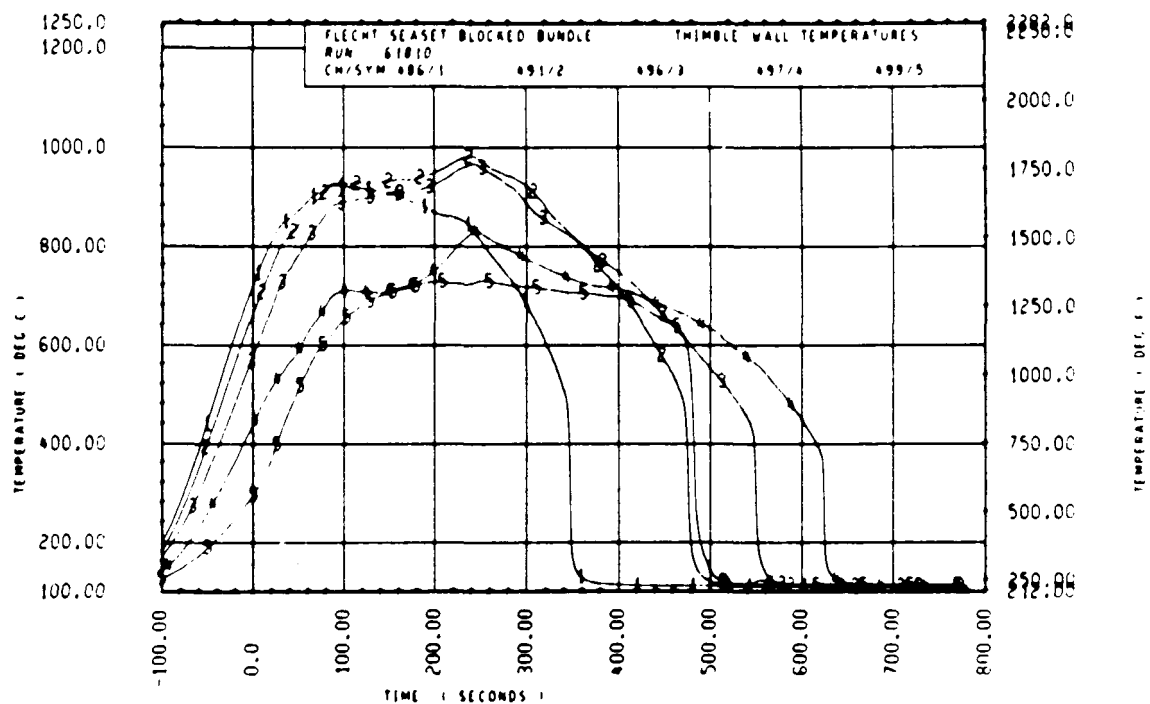
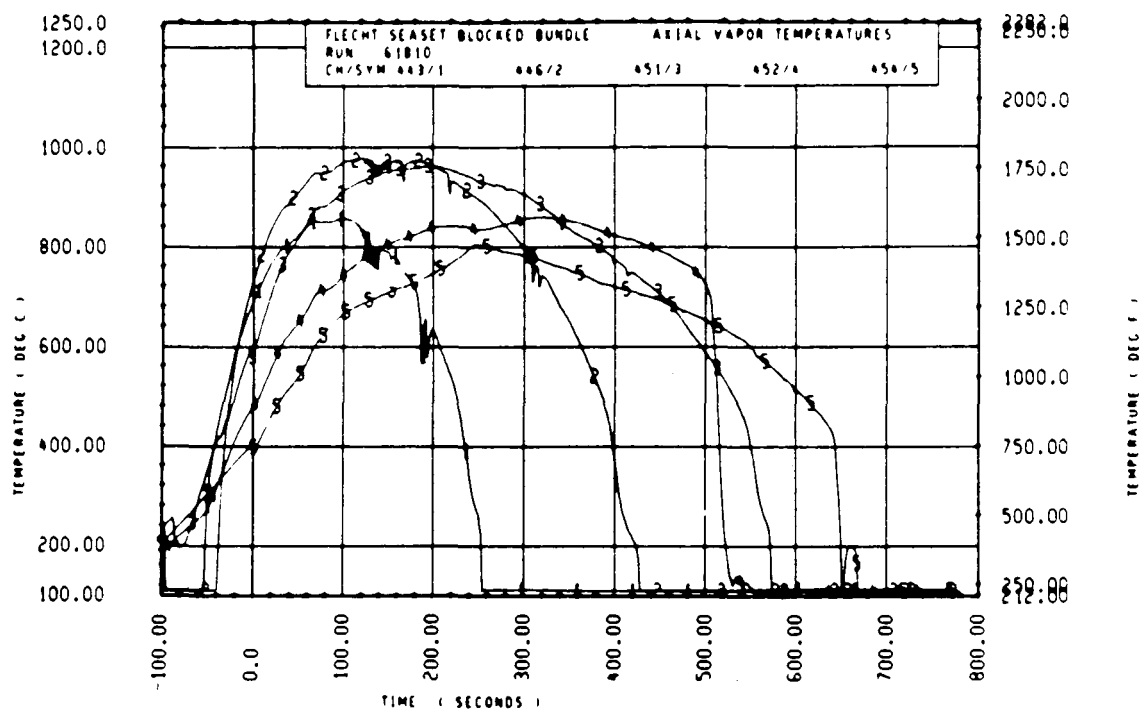
Rod 11E, 2.29 m (90 in.)

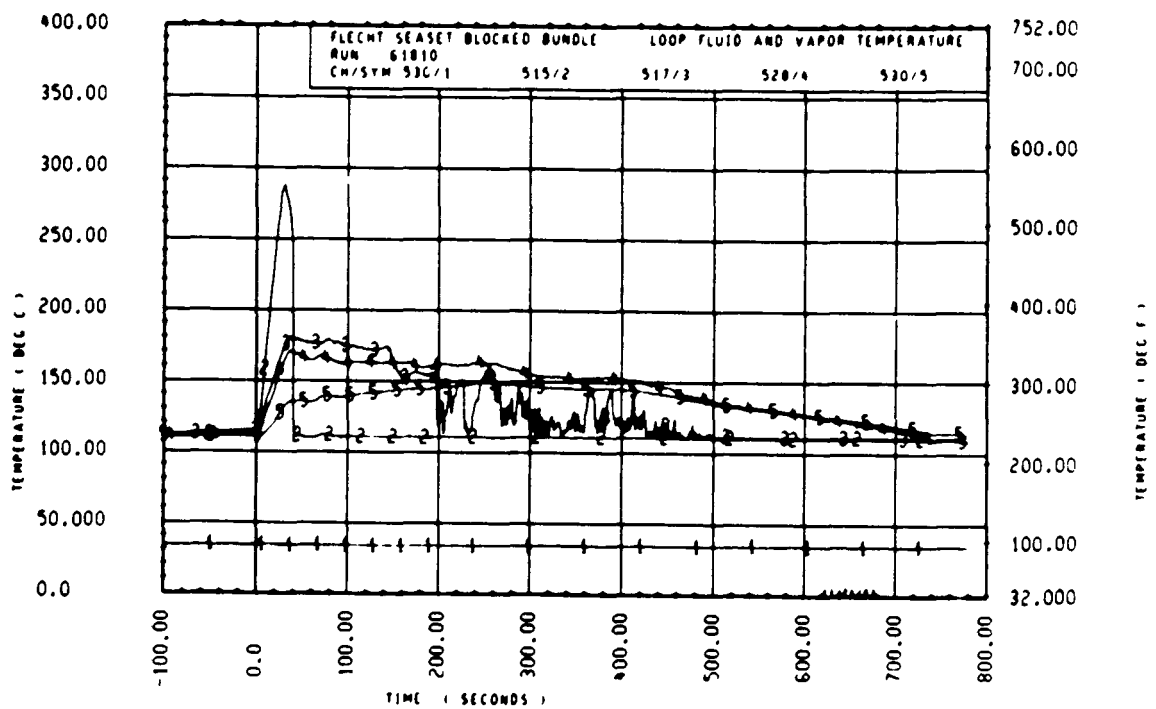
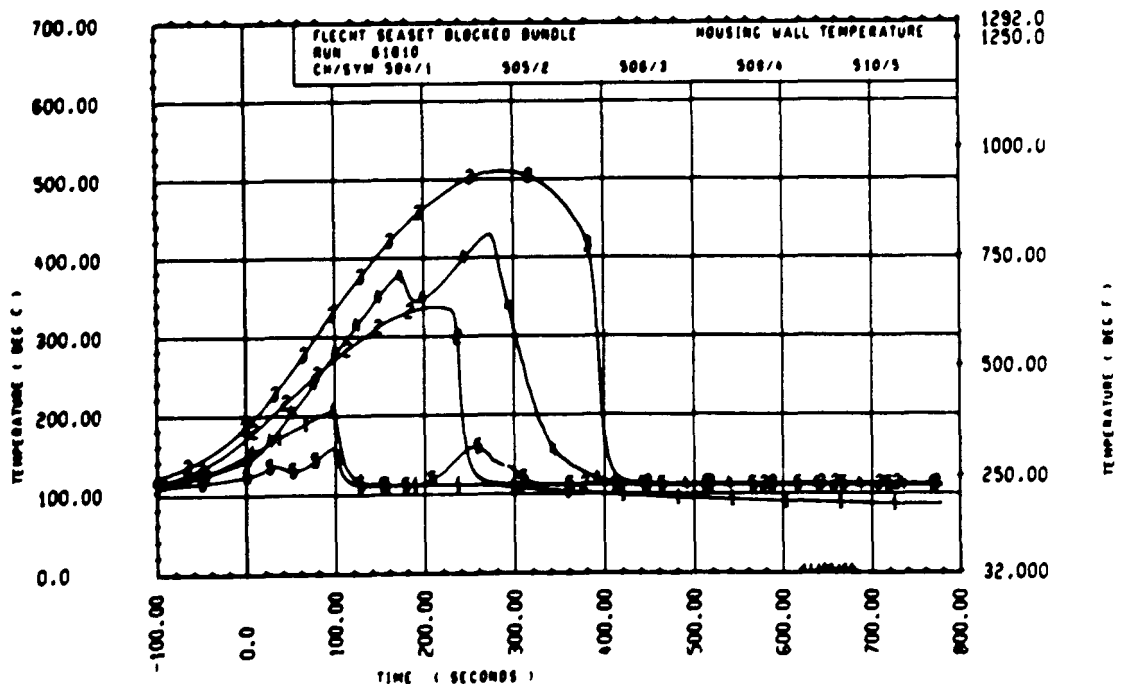


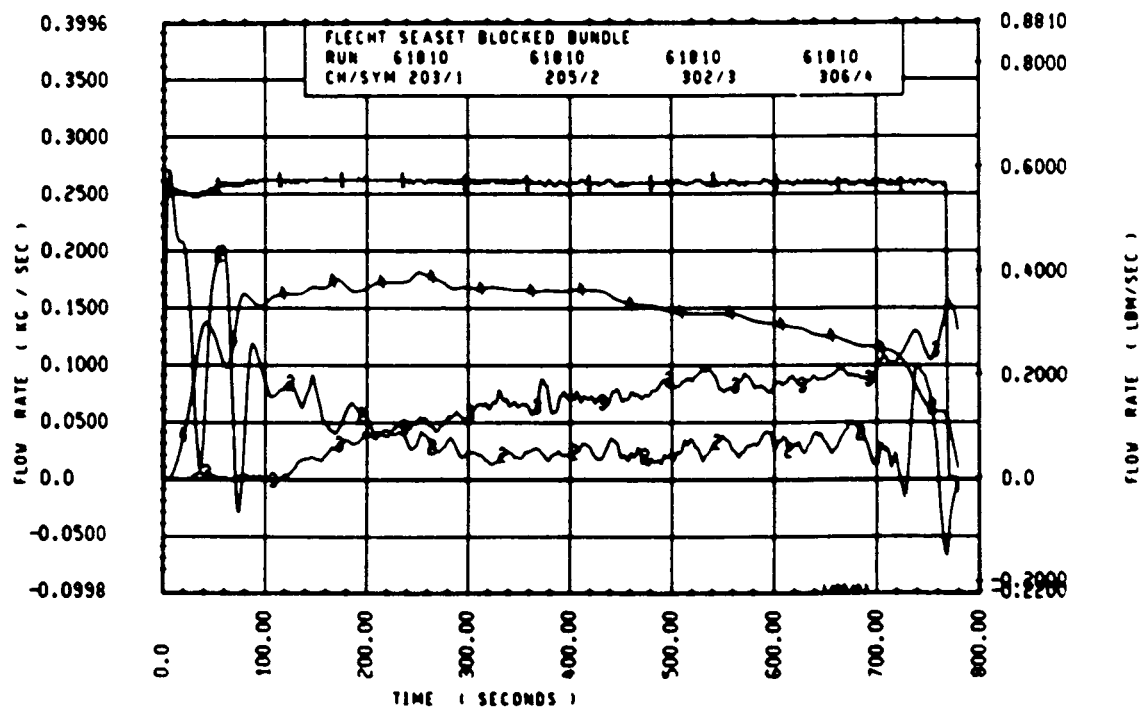
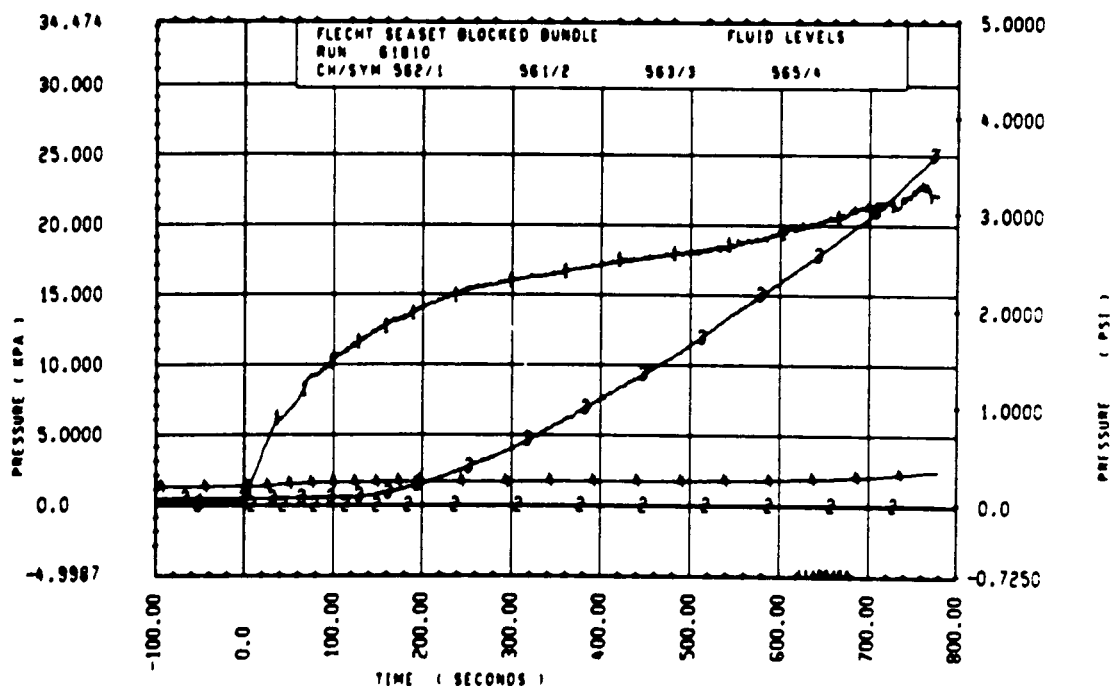
Rod 7D, 2.29 m (90 in.)

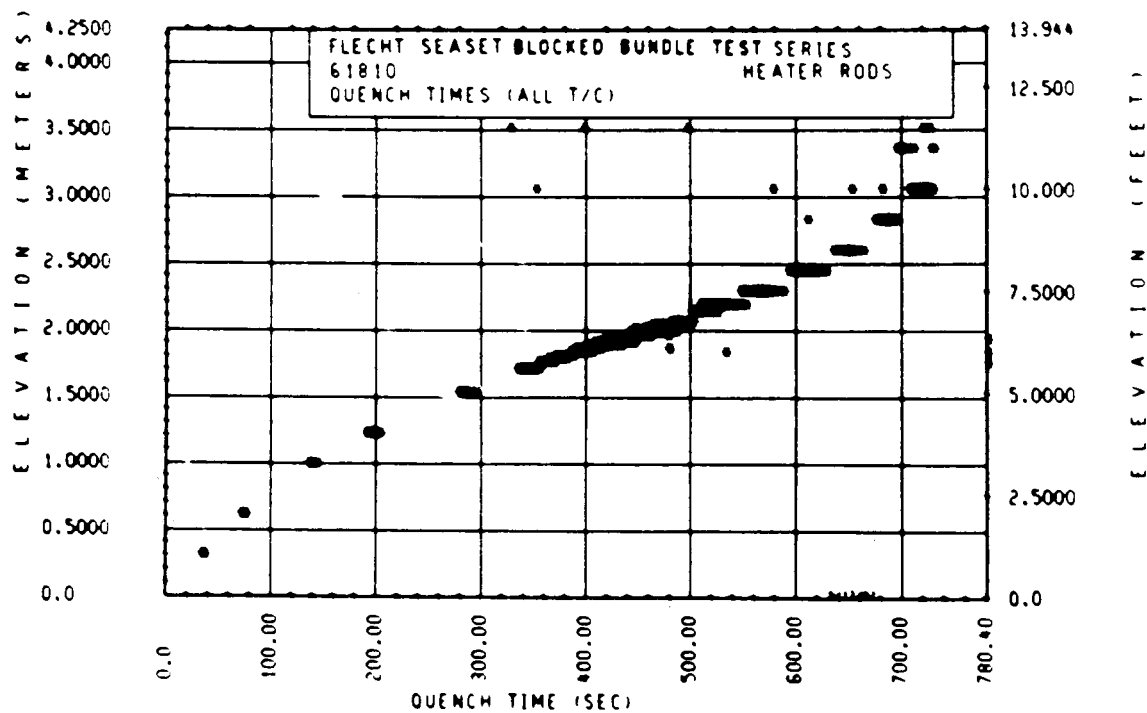
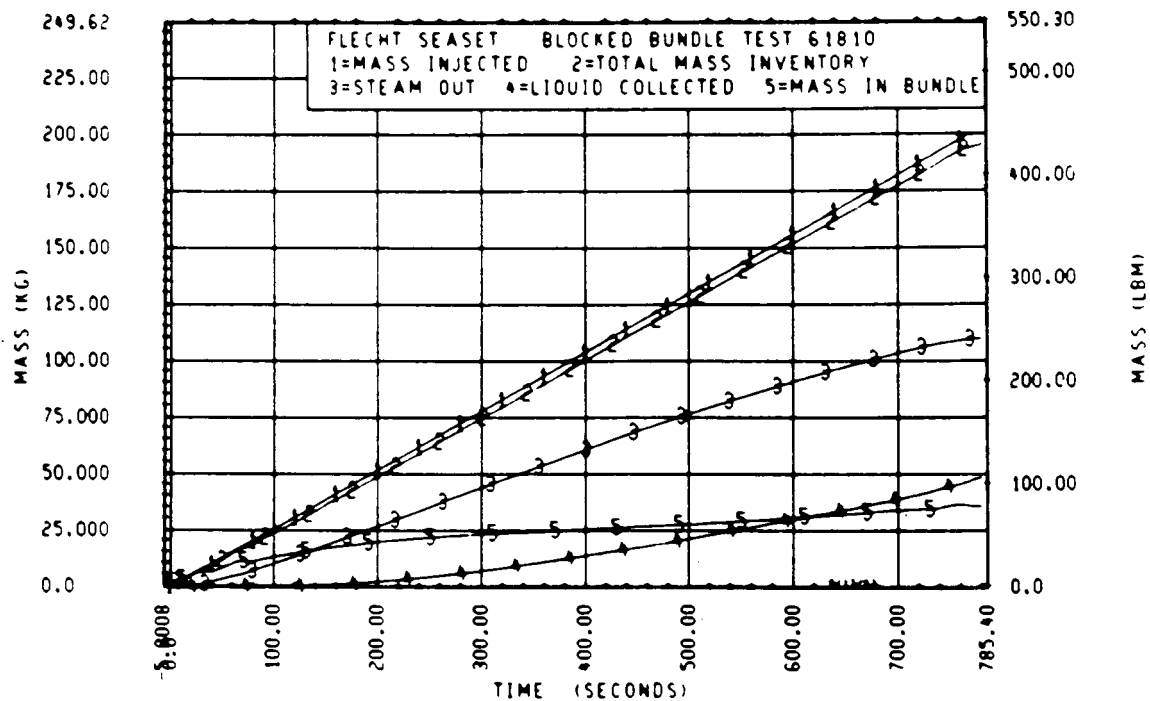


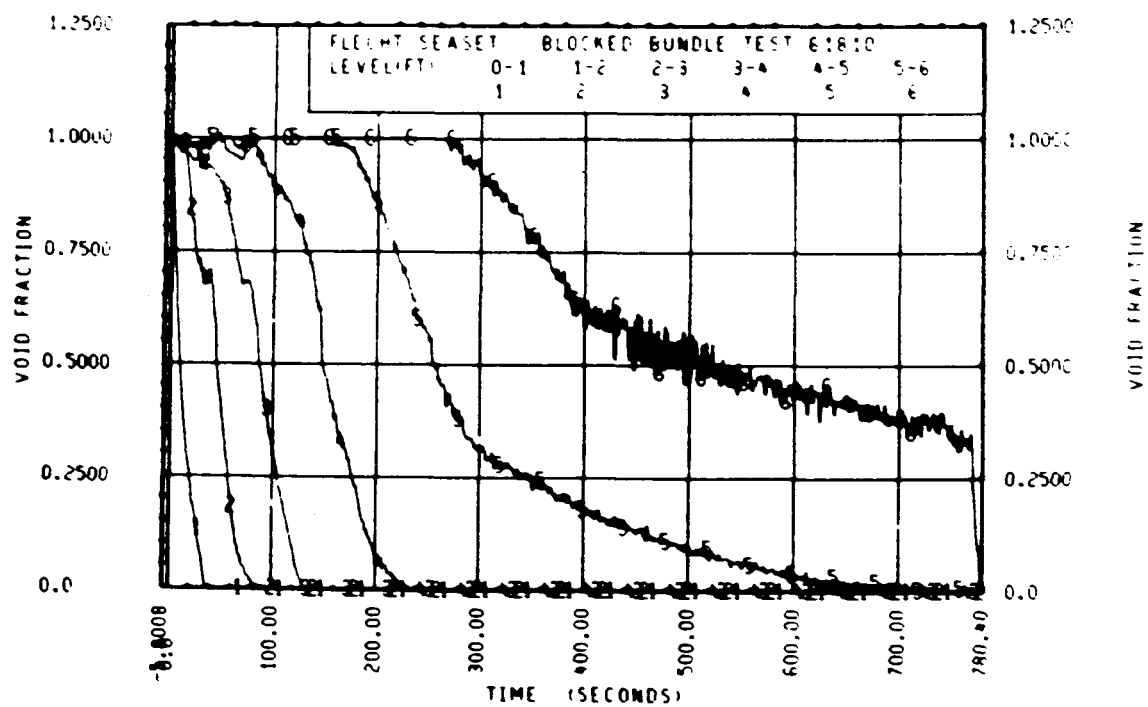
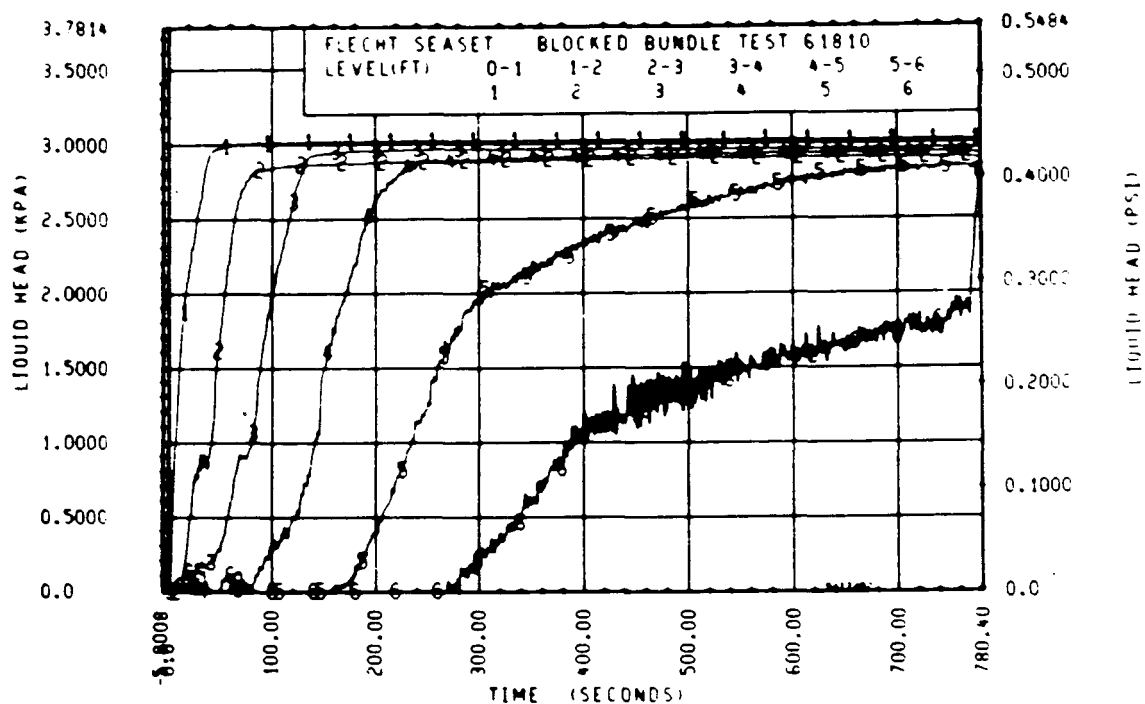
Rod 8E, 2.44 m (96 in.)

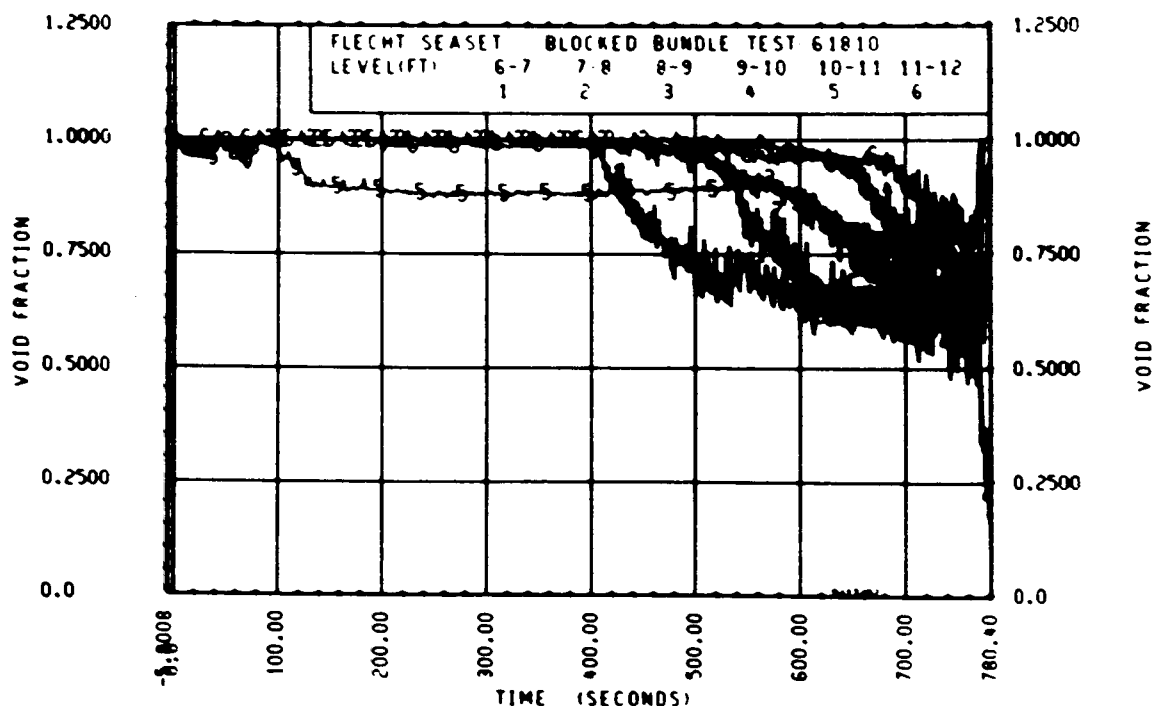
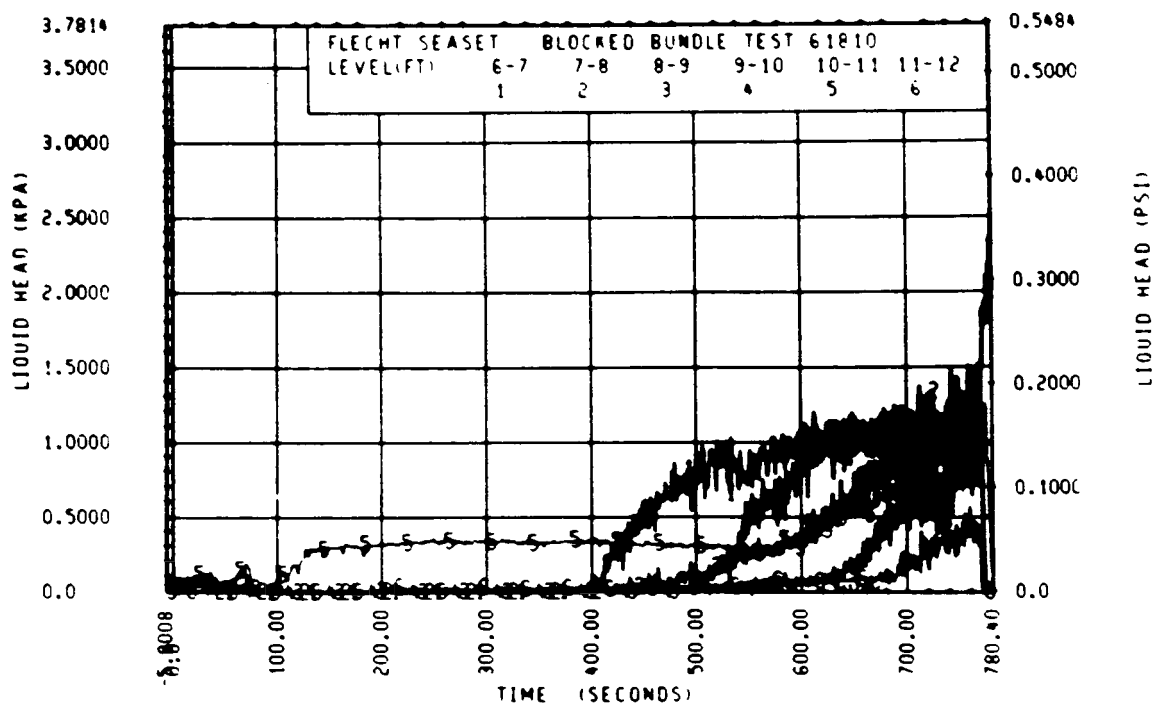












FLECHT SEASET 163-ROD BUNDLE FLOW BLOCKAGE TASK
SUMMARY AND COMMENT SHEET

Run: 61916
Test date: 9/17/82
Test type: Forced reflood
Parameter: Stepped flow effect

AS-RUN TEST CONDITIONS:

Upper plenum pressure	0.277 MPa (40.2 psia)
Initial peak clad temperature and location	877.1°C (1610.8°F), 8N-1.93 m (76 in.)
Initial peak rod power:	
Peripheral rods	2.29 kw/m (0.699 kw/ft)
Bypass rods	2.29 kw/m (0.699 kw/ft)
Blockage island rods	2.30 kw/m (0.701 kw/ft)
Flooding rate	154 mm/sec (6.07 in./sec) for 7 sec 21 mm/sec (0.81 in./sec) onward
Coolant temperature	52.2°C (126°F)
Initial bundle water level	-2 mm (-0.1 in.)

COMMENTS:

Inlet mass flow:⁽¹⁾ -0.8% for entire test

Power decay:⁽¹⁾ peripheral rods, 0% constant
bypass rods, -0.5% constant
blockage rods, 0% constant

1. Relative to run 32333

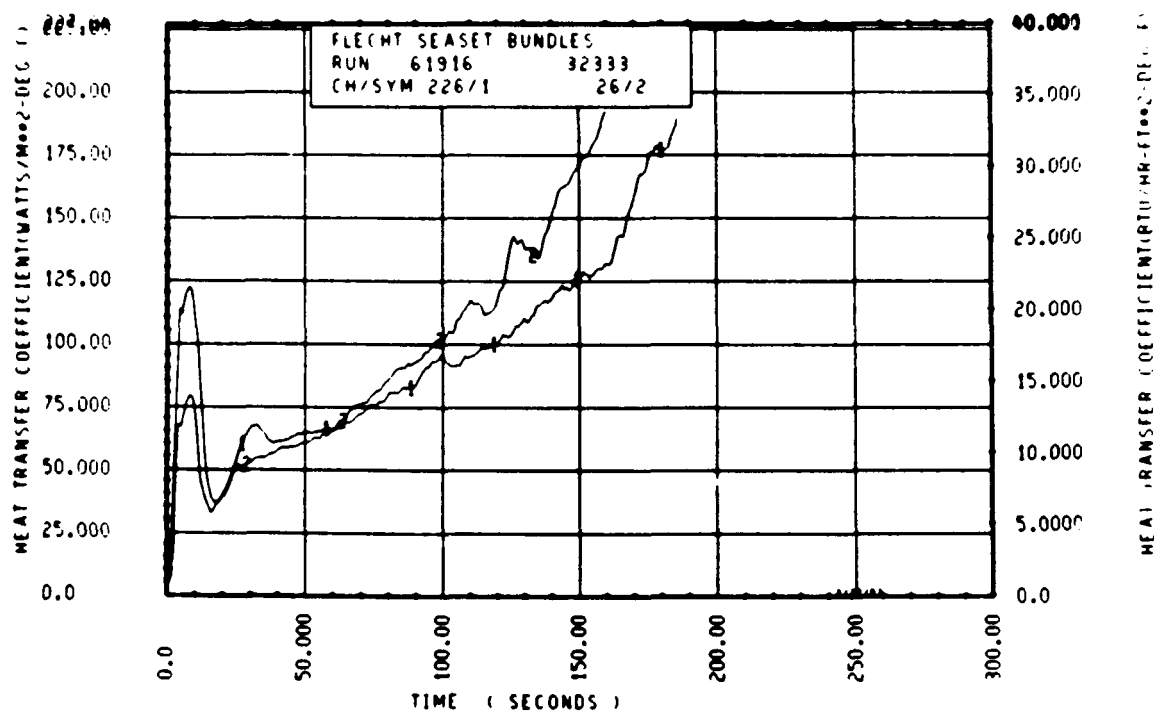
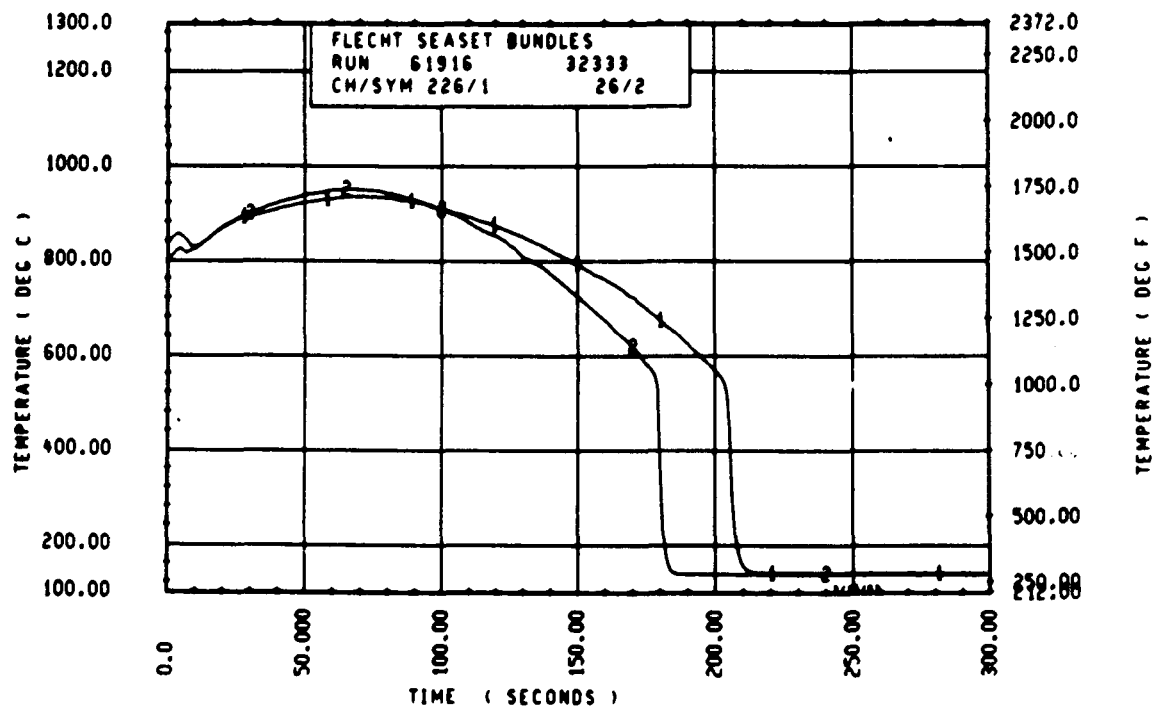
FLECHT SEASET 163 RDD BUNDLE TEST SERIES								
RUN NUMBER 51016								
RDD/ELEV	CHAN. NO	INITIAL AT FLOOD (DEG F)	MAXIMUM TEMPERATURE (DEG F)	TEMPERATURE RISE (DEG F)	TURNAROUND TIME (SECONDS)	QUENCH TEMPERATURE (DEG F)	QUENCH TIME (SECONDS)	
90 1- C	3	607.	692.	5.	1.5	630.	6.2	
10M 2- C	6	644.	907.	13.	2.5	665.	32.4	
96 3- 3	4	1232.	1254.	22.	3.0	607.	77.7	
3J 4- C	11	1305.	1419.	54.	27.0	764.	124.3	
7H 4- C	12	1352.	1411.	59.	26.0	764.	125.6	
6K 4- C	13	1372.	1436.	66.	38.5	773.	132.3	
6A 4- C	14	1365.	1414.	51.	40.0	610.	121.4	
120 4- C	17	1353.	1395.	42.	26.0	655.	120.4	
5E 5- C	20	1524.	1737.	213.	68.5	970.	205.4	
76 5- C	21	1577.	1790.	213.	70.0	1011.	199.6	
90 5- C	24	1550.	1707.	217.	87.0	1010.	202.5	
5E 5- 7	33	1540.	1625.	280.	91.5	962.	204.8	
60 5- 7	45	1550.	1603.	353.	111.5	944.	271.8	
4M 5- 9	52	1480.	1876.	392.	116.5	1010.	276.8	
76 5-10	54	1513.	1896.	384.	112.0	972.	283.7	
7F 5-11	62	1452.	1869.	417.	119.0	970.	298.4	
40 5-11	64	1530.	1860.	341.	108.5	864.	300.4	
21 6- C	67	1561.	1917.	326.	94.5	941.	306.8	
50 6- C	70	1500.	1839.	339.	113.0	967.	305.1	
6J 6- C	74	1524.	1798.	269.	95.5	860.	317.7	
7M 6- C	80	1553.	1869.	316.	95.0	920.	302.7	
110 6- C	80	1552.	1834.	282.	93.5	844.	307.7	
6M 6- 2	97	1380.	1643.	464.	133.5	850.	342.0	
5M 6- 2	94	1530.	1929.	391.	120.0	953.	340.4	
4E 6- 2	105	1347.	1848.	551.	137.0	1274.	314.8	
6M 6- 3	111	1421.	1876.	455.	134.5	920.	350.4	
40 6- 3	124	1550.	1930.	372.	111.0	913.	350.8	
11M 6- 4	134	1483.	1938.	455.	134.0	742.	364.0	
90 6- 4	143	1555.	1972.	417.	139.5	954.	361.8	
9J 6- 5	165	1534.	1971.	437.	163.5	922.	374.8	
9M 6- 5	166	1592.	1947.	355.	114.5	950.	356.8	
6J 6- 6	192	1585.	1970.	387.	130.0	944.	376.8	
90 6- 6	193	1587.	1999.	431.	132.0	897.	384.4	
11F 6- 6	173	1500.	1952.	392.	131.0	916.	370.8	
46 7- C	261	1464.	1851.	382.	111.0	756.	430.3	
70 7- 6	309	1490.	1891.	395.	181.5	661.	492.4	
76 7- 6	312	1537.	2014.	477.	221.1	603.	480.8	
11E 7- 6	325	1493.	1922.	429.	172.0	691.	483.7	
5L 8- C	337	1312.	1904.	592.	167.0	785.	537.8	
7H 8- C	345	1340.	1999.	653.	229.1	920.	523.8	
7K 8- 0	346	1364.	1949.	585.	193.0	606.	532.8	
5J 8- 6	366	1141.	1765.	623.	191.5	606.	576.4	
78 8- 6	368	1140.	1627.	487.	210.1	667.	574.8	
7E 4- 3	383	1109.	1790.	681.	267.1	761.	606.1	
6M 4- 3	367	1057.	1525.	469.	296.1	700.	611.4	
9C 9- 3	389	1051.	1591.	540.	265.1	711.	612.0	
11F 9- 3	394	1051.	1704.	653.	265.1	667.	613.0	
7810- 0	408	650.	1451.	595.	313.1	612.	646.1	
6M10- C	415	600.	1354.	494.	325.1	623.	647.0	
6K10- C	417	607.	1374.	508.	197.0	655.	636.1	
6M10- C	410	681.	1522.	641.	193.5	660.	642.8	
6M11- C	424	640.	895.	198.	208.1	575.	643.1	
4611- C	431	604.	1164.	495.	275.1	602.	470.2	
11E11- C	432	644.	1199.	505.	272.1	530.	646.4	
5J11- 6	430	675.	816.	141.	147.0	615.	629.5	
7811- 6	437	640.	1188.	548.	402.1	700.	593.0	
8J11- 6	438	640.	925.	235.	339.1	574.	654.7	

KUN 61916 HEATER ROD STATISTICAL DATA

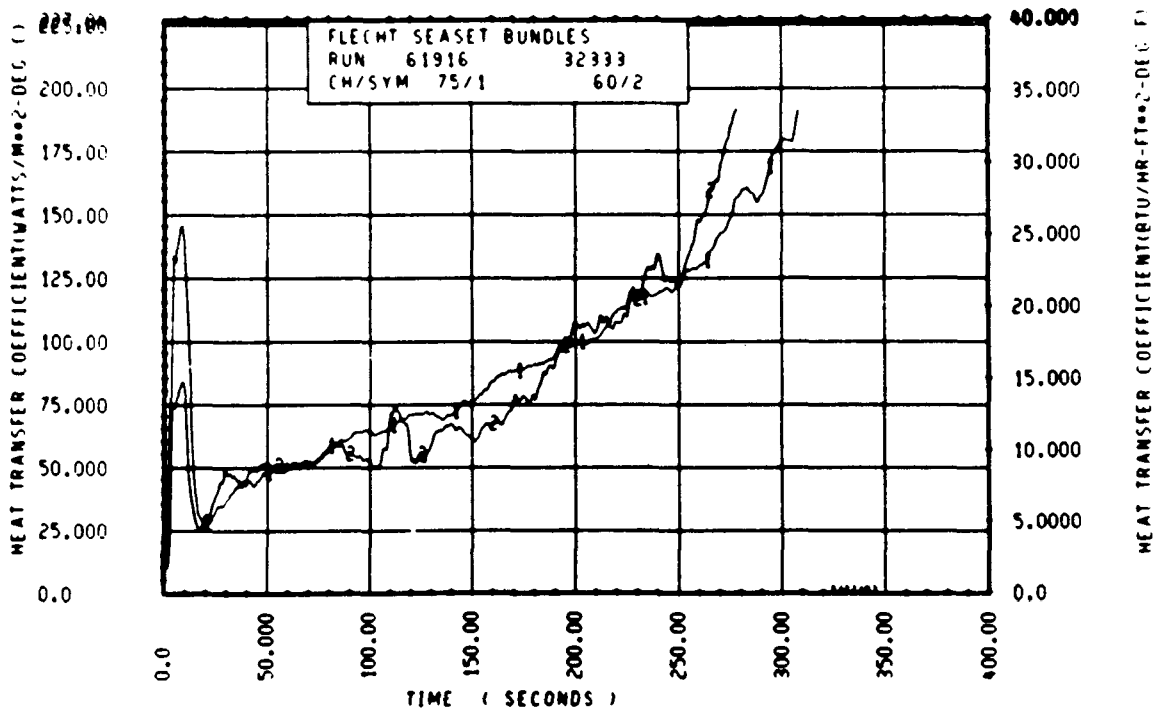
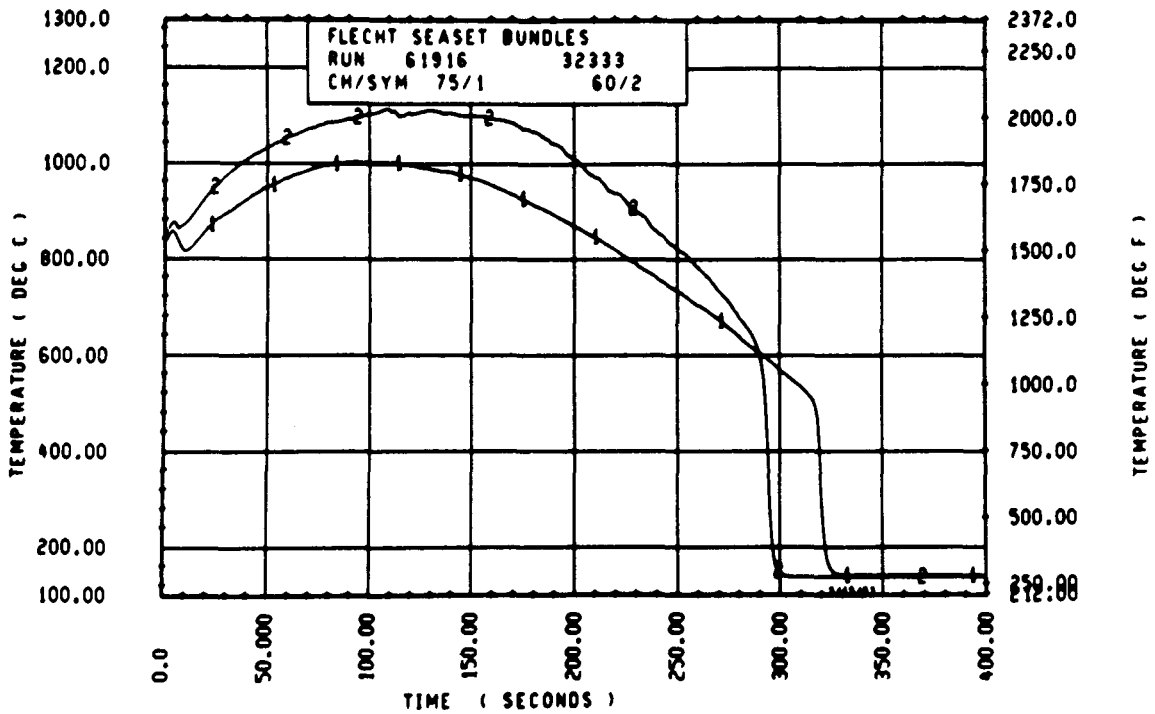
ELEV	INITIAL TEMP (DEG F)			MAX TEMP (DEG F)			TURNAROUND TIME (SEC)		
	MAX	MIN	MEAN	MAX	MIN	MEAN	MAX	MIN	MEAN
12	666.4	664.8	665.5	692.1	690.0	691.1	1.5	1.5	1.5
24	893.6	862.5	874.6	907.0	873.9	887.0	2.5	2.5	2.5
36	1231.6	1164.6	1204.0	1253.5	1208.7	1226.7	25.0	3.0	13.0
48	1383.6	1352.2	1365.2	1436.1	1395.4	1420.8	40.0	25.0	31.0
60	1577.1	1465.4	1535.2	1808.2	1616.3	1724.0	87.0	61.0	69.5
67	1603.1	1513.1	1551.2	1903.3	1751.2	1816.2	111.5	66.5	91.4
69	1532.7	1466.3	1517.5	1878.4	1721.0	1801.1	116.5	91.5	99.7
70	1604.2	1479.6	1552.7	1897.6	1772.4	1825.0	117.0	76.5	97.3
71	1536.1	1452.6	1494.2	1679.5	1785.8	1844.8	120.0	67.0	106.6
72	1602.6	1467.6	1540.4	1924.0	1798.0	1871.1	123.5	92.0	100.1
73	1591.2	1456.5	1526.5	1906.8	1785.8	1849.9	137.0	91.0	101.1
74	1544.4	1374.6	1513.0	1928.6	1843.3	1890.3	133.5	92.0	114.9
75	1599.8	1421.6	1524.2	2154.1	1830.8	1903.8	134.5	91.5	116.6
76	1610.6	1464.4	1552.5	1972.3	1851.2	1921.7	140.0	166.0	122.4
77	1592.3	1490.5	1546.0	1980.3	1863.7	1941.1	163.5	107.5	126.7
78	1604.7	1516.8	1565.2	1996.7	1870.5	1960.8	192.5	110.0	134.6
79	1607.5	1506.6	1560.2	2010.4	1872.7	1965.7	140.5	116.5	130.4
80	1590.1	1504.4	1555.5	2032.6	1890.8	1987.8	164.0	110.0	134.1
81	1585.6	1467.3	1542.2	2027.9	1937.8	1989.8	163.5	123.0	138.4
84	1531.6	1422.1	1486.7	1993.0	1732.2	1856.7	153.5	111.0	133.6
86	1582.5	1472.3	1530.5	2004.5	1818.4	1909.0	221.1	114.5	170.4
90	1534.2	1405.6	1494.7	2046.6	1877.2	1958.0	234.1	134.0	192.6
96	1406.2	1270.2	1354.4	2044.3	1832.0	1961.8	248.1	156.0	205.1
102	1145.1	1074.1	1101.0	1856.9	1627.3	1792.7	267.1	174.5	214.2
111	1109.2	1042.1	1070.2	1790.2	1525.0	1689.8	296.1	176.5	246.6
120	920.4	822.2	866.6	1649.3	1159.9	1506.6	325.1	151.6	253.4
132	697.4	666.4	692.4	1336.3	655.3	1136.8	311.1	193.0	256.7
136	640.0	634.6	664.6	1167.9	816.0	979.8	402.1	139.5	260.6

KUN 61916 HEATER ROD STATISTICAL DATA

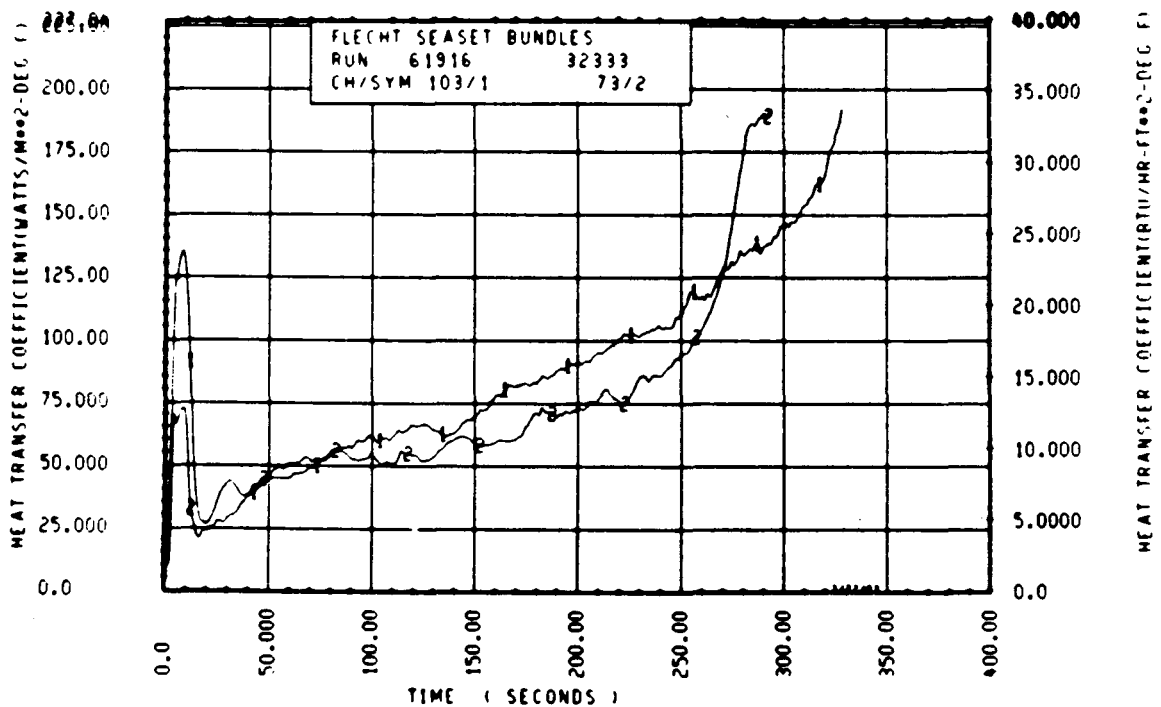
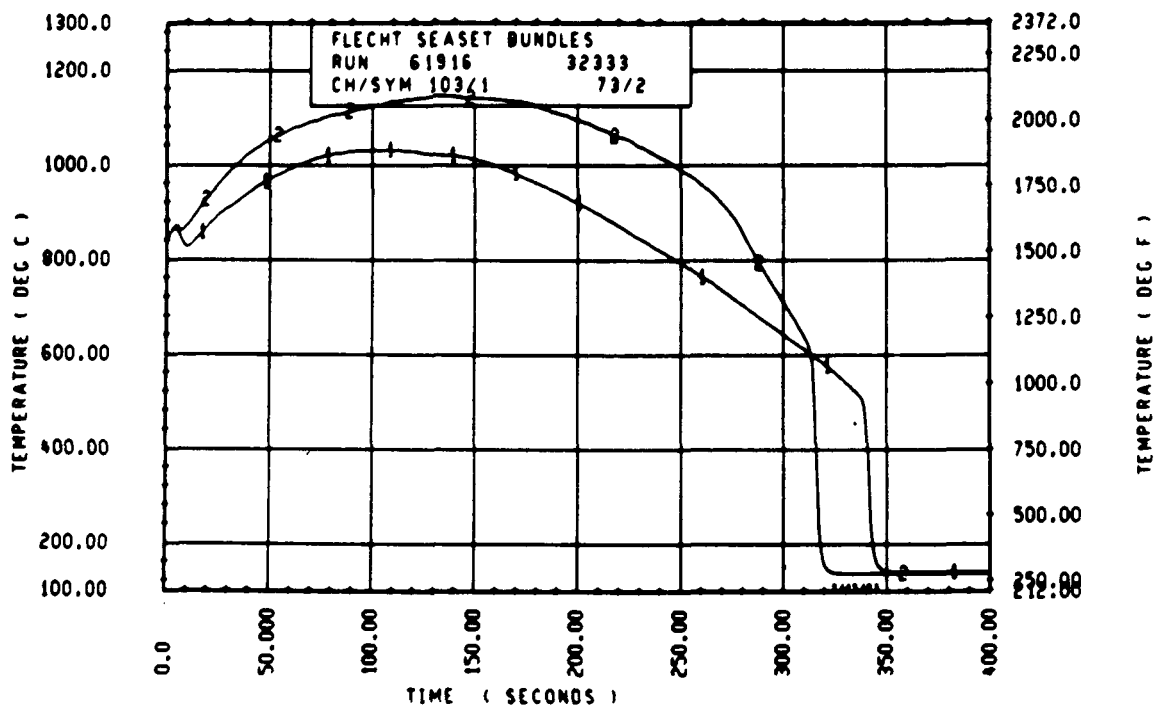
ELEV	TEMP RISE (DEG F)			QUENCH TEMP (DEG F)			QUENCH TIME (SEC)		
	MAX	MIN	MEAN	MAX	MIN	MEAN	MAX	MIN	MEAN
12	6.3	5.2	5.6	637.6	626.2	632.5	6.5	6.2	6.4
24	13.4	11.4	12.4	665.3	658.1	662.8	32.4	29.0	30.4
36	27.6	17.7	22.6	839.6	774.9	804.8	81.4	76.4	78.7
48	70.1	42.2	50.5	853.0	773.2	806.8	132.3	120.6	124.5
60	233.3	134.0	186.6	1020.1	891.2	963.2	213.9	196.9	205.6
67	353.3	213.4	285.1	1007.9	878.1	946.0	271.8	250.0	254.6
69	342.1	206.6	283.6	1017.8	877.4	932.0	298.5	264.7	278.6
70	384.5	237.6	294.5	986.9	899.3	951.2	297.8	277.6	285.5
71	417.3	264.4	350.6	970.3	884.4	923.9	306.9	289.6	298.5
72	423.6	266.6	324.7	1009.1	862.5	928.0	322.6	302.7	310.3
73	368.7	284.1	323.4	982.4	886.5	937.7	332.3	301.9	316.5
74	406.1	244.6	377.2	984.7	797.4	914.1	348.8	323.6	335.1
75	602.0	286.7	374.6	989.2	526.7	882.4	363.0	321.9	346.4
76	469.5	286.2	364.2	1009.1	741.5	917.3	364.0	331.9	354.3
77	441.2	324.5	342.6	977.4	779.5	911.1	400.3	356.6	370.6
78	439.3	343.2	345.7	983.5	736.9	901.5	409.8	363.6	386.4
79	468.4	320.5	347.4	978.4	662.2	897.4	401.8	361.9	387.8
80	484.4	364.6	432.3	979.7	792.5	896.3	413.8	384.9	400.7
81	445.3	414.5	447.5	947.8	851.6	882.1	424.5	344.4	410.9
84	471.2	301.5	386.0	821.2	708.2	765.9	444.5	422.6	435.2
86	436.1	317.3	372.6	923.0	770.2	844.4	472.9	431.3	449.6
90	541.1	345.6	466.3	935.3	786.7	871.5	508.6	469.0	486.9
96	677.7	516.4	606.4	926.5	747.2	833.2	550.0	516.9	533.3
102	686.5	467.1	631.7	938.8	626.0	726.1	587.1	460.7	562.3
111	704.7	461.5	614.6	999.9	666.5	746.8	617.1	534.6	662.5
120	786.7	244.4	637.6	1068.7	559.4	674.2	652.4	154.6	616.1
132	639.6	167.4	444.4	802.3	518.4	596.5	658.1	470.2	624.6
136	546.3	146.7	315.2	776.7	579.2	679.5	654.7	151.4	511.5



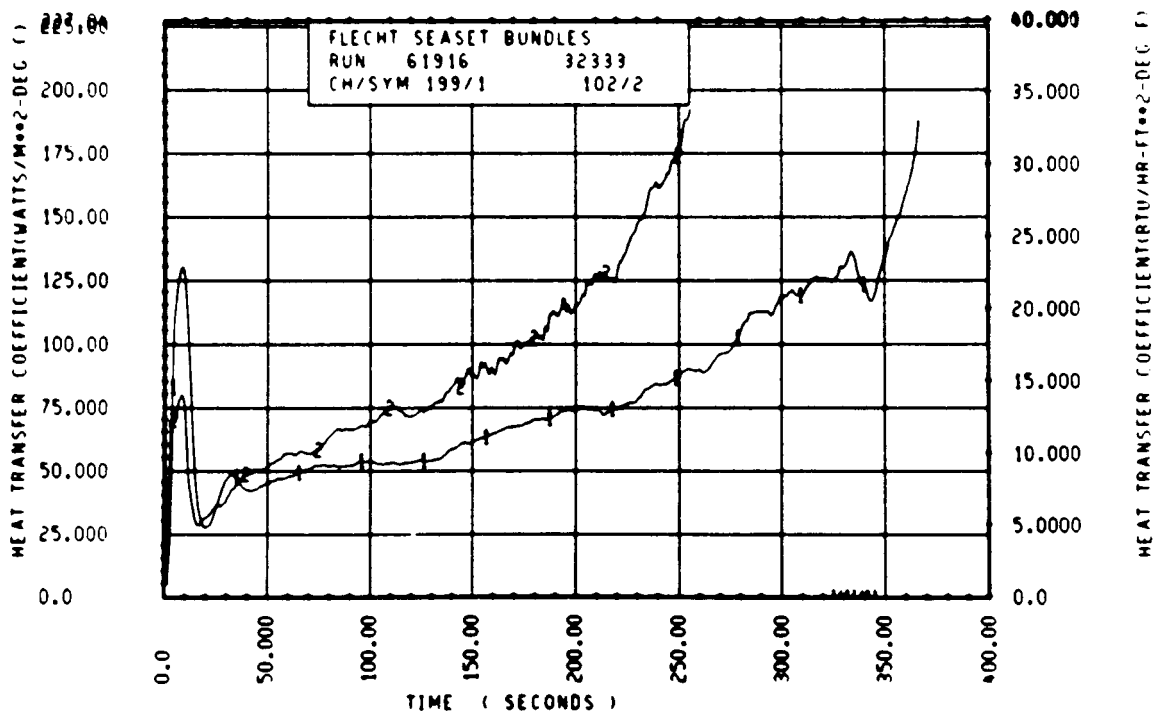
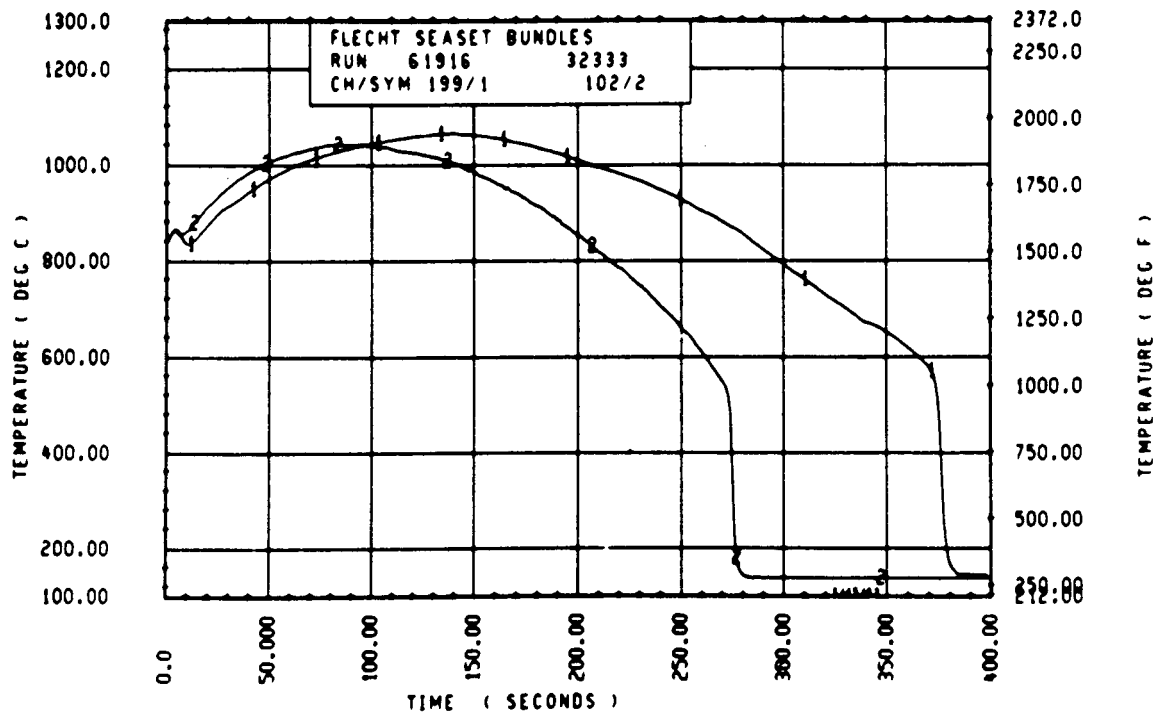
Rod 11E, 1.52 m (60 in.)



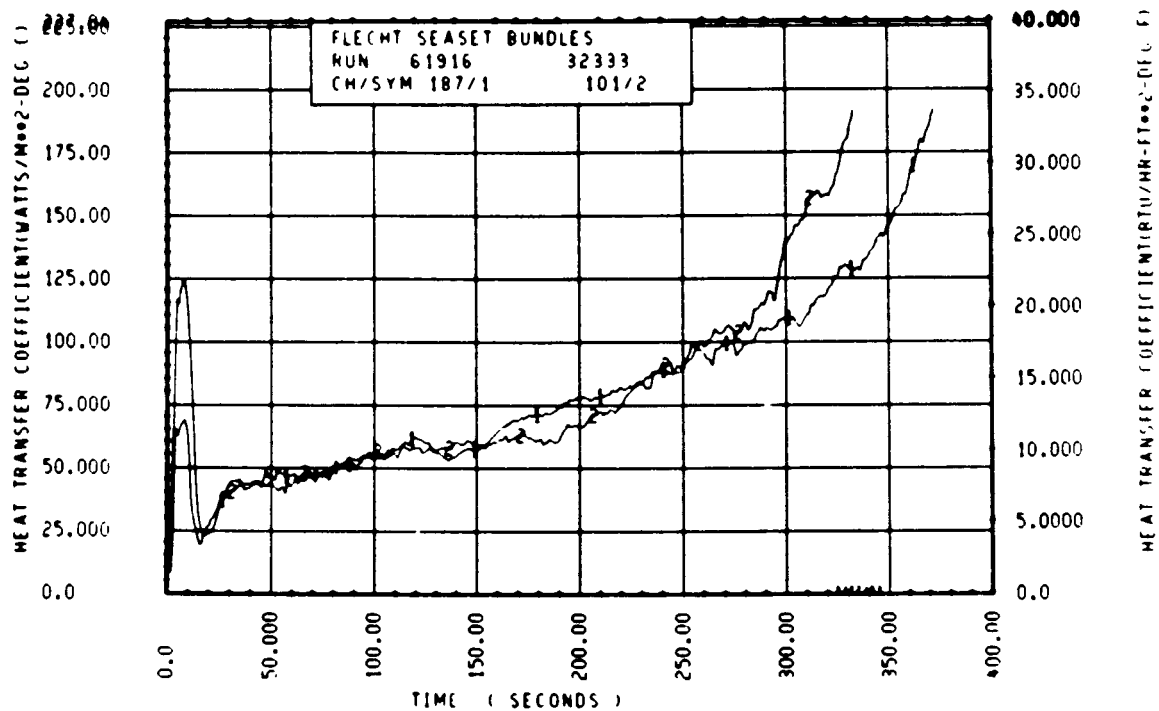
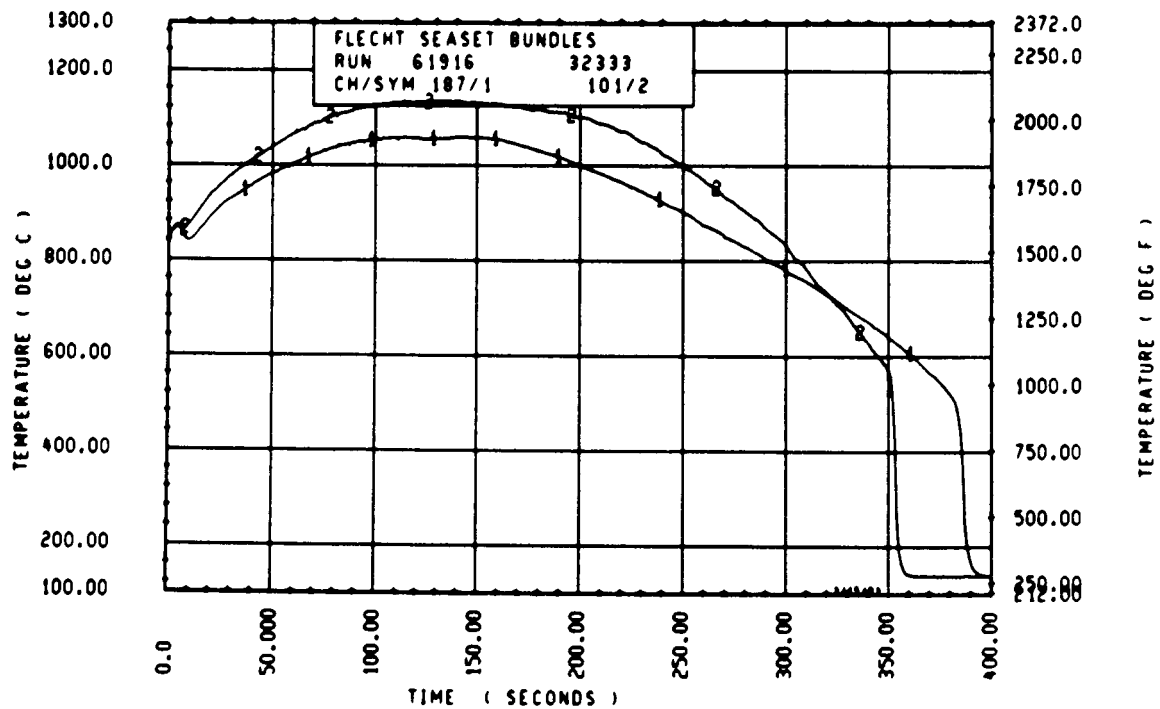
Rod 6L, 1.83 m (72 in.)



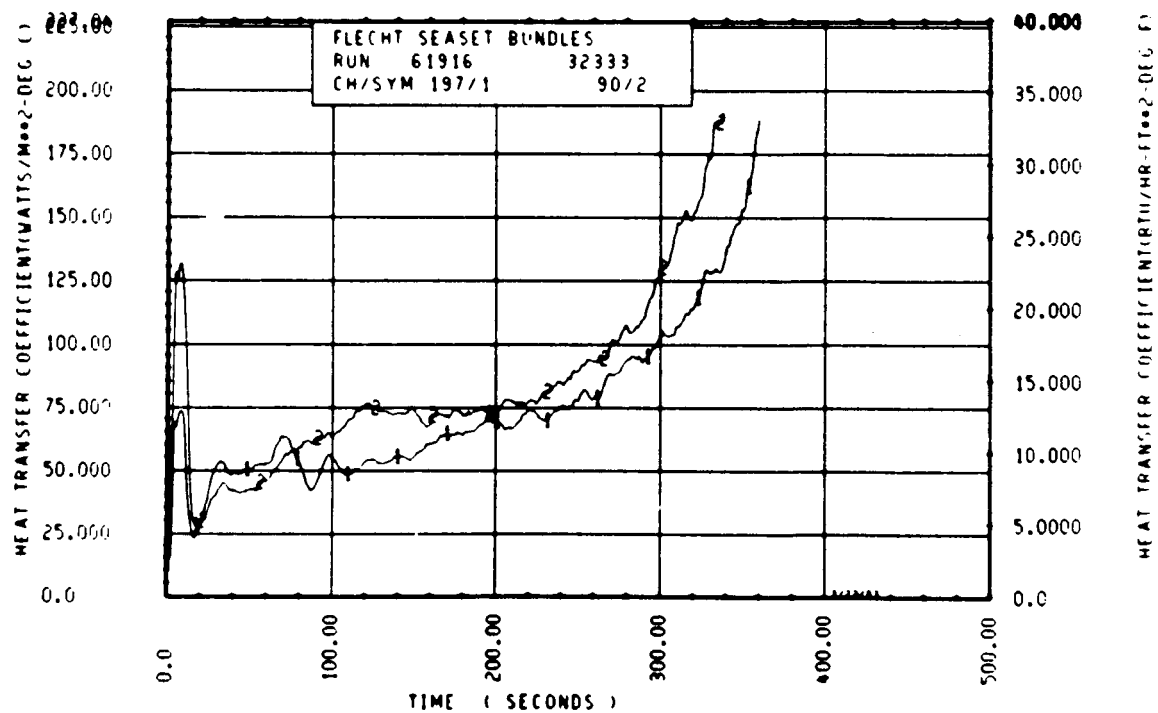
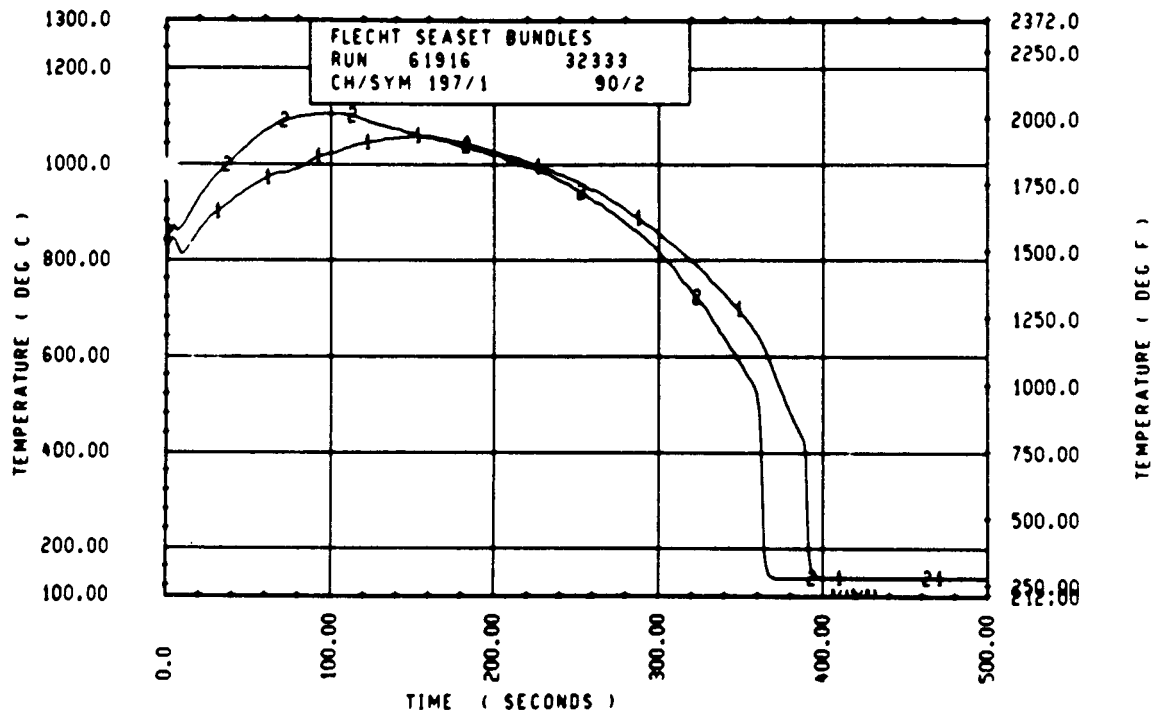
Rod 6L, 1.88 m (74 in.)



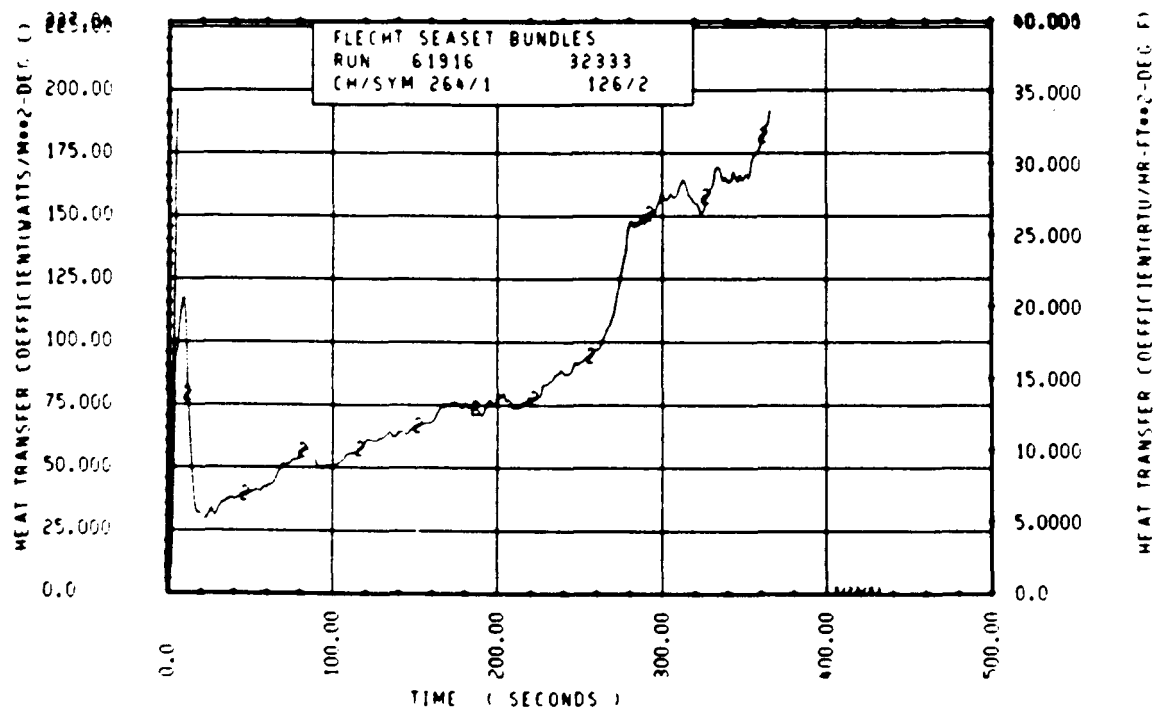
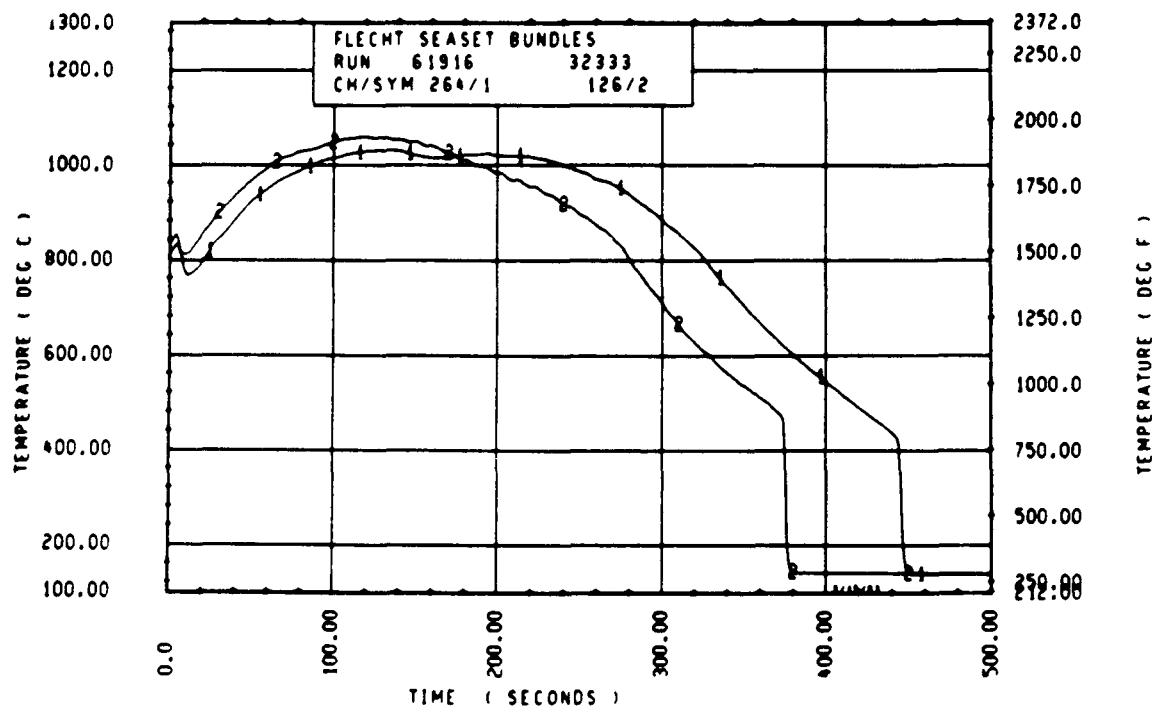
Rod 13G, 1.98 m (78 in.)



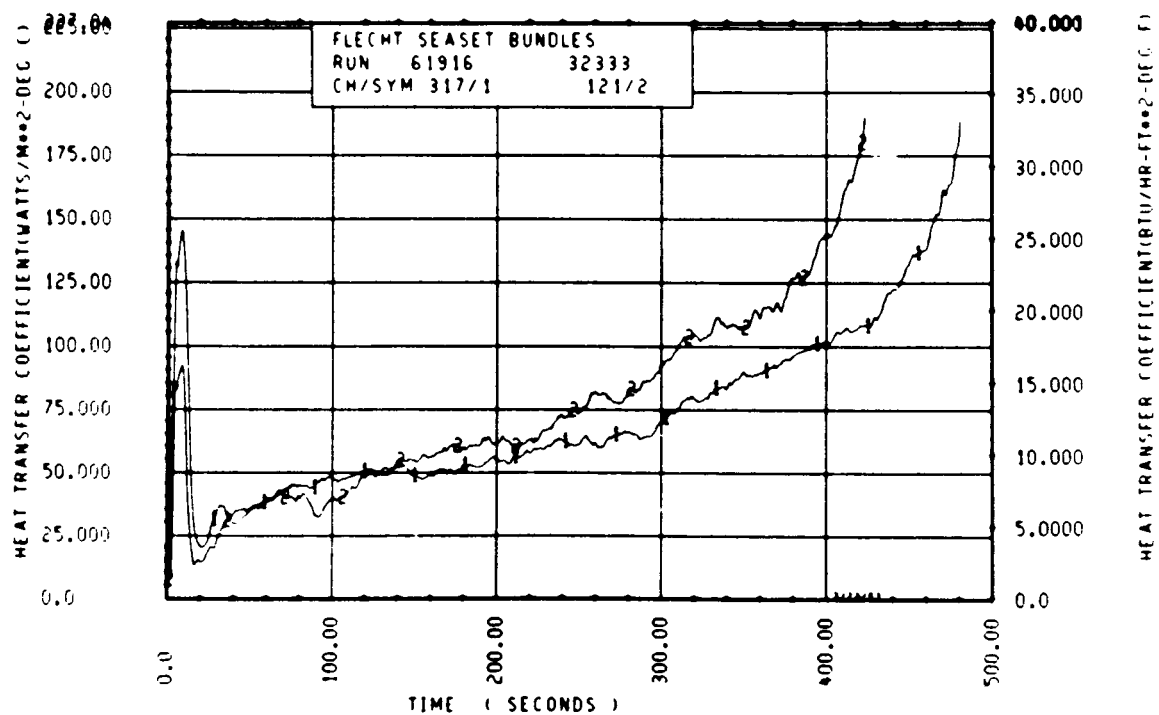
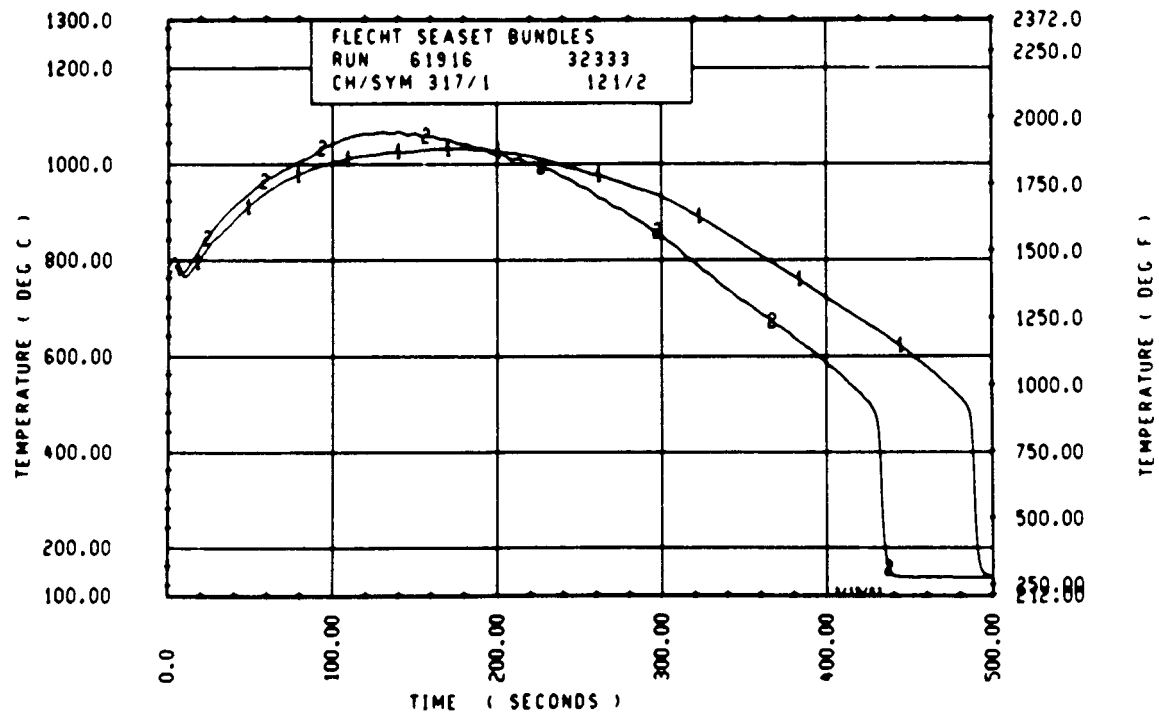
Rod 6J, 1.98 m (78 in.)



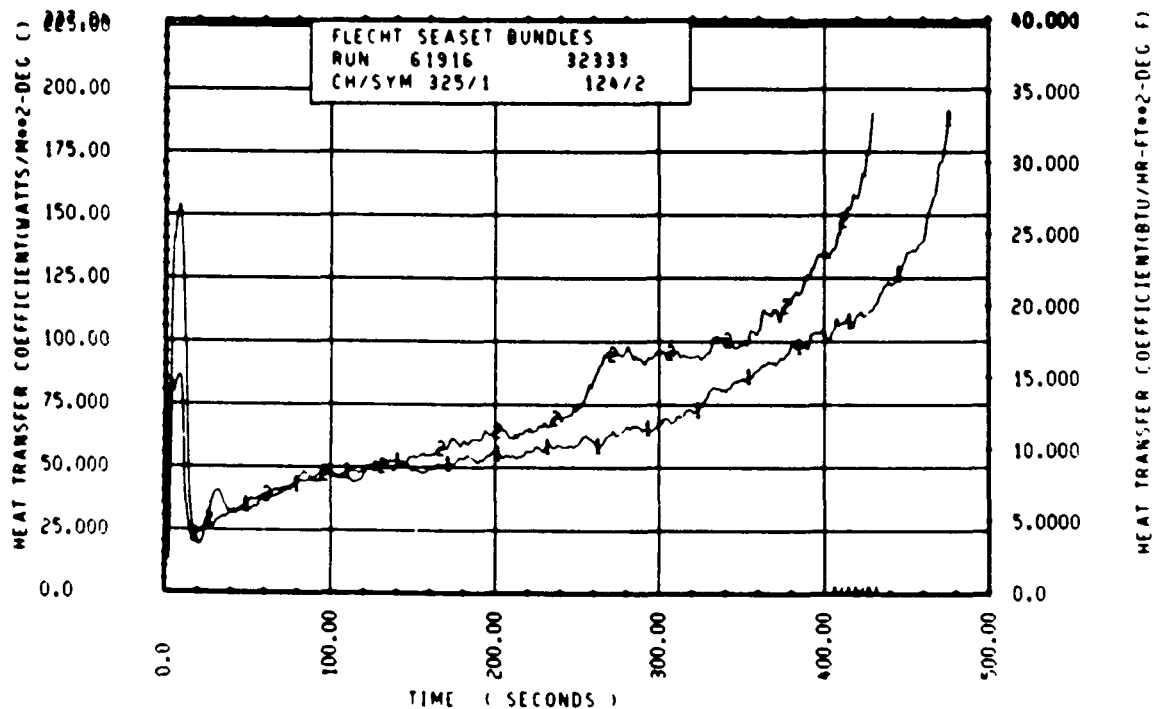
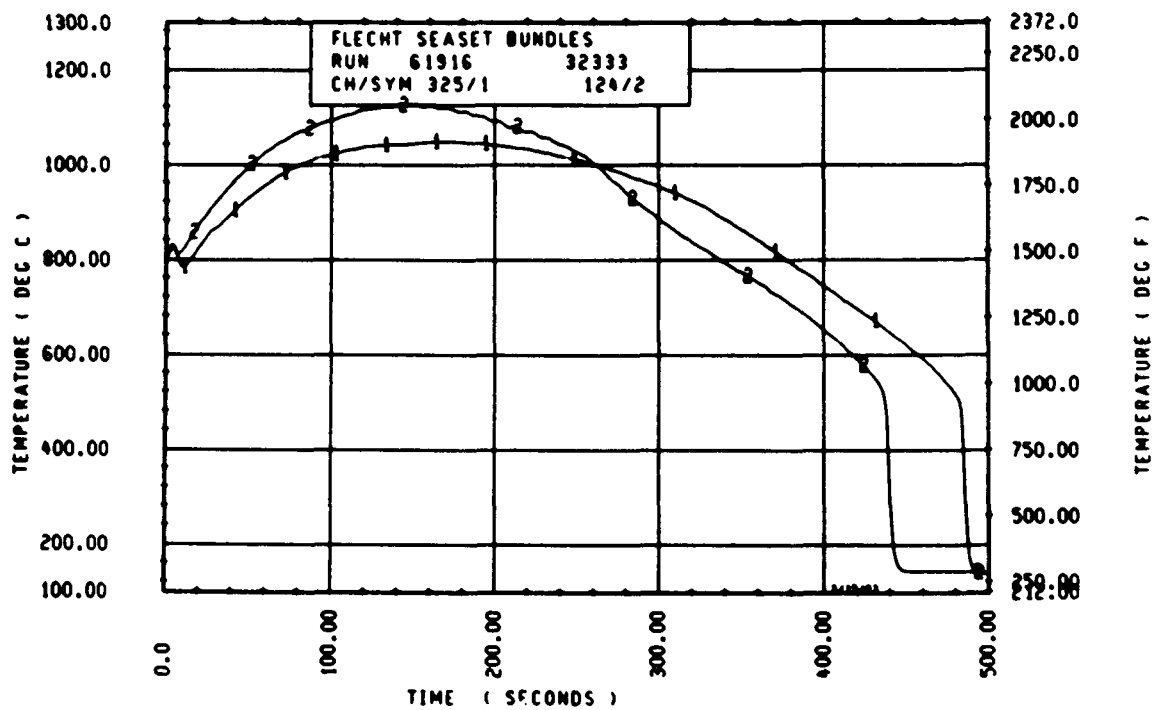
Rod 11K, 1.98 m (78 in.)



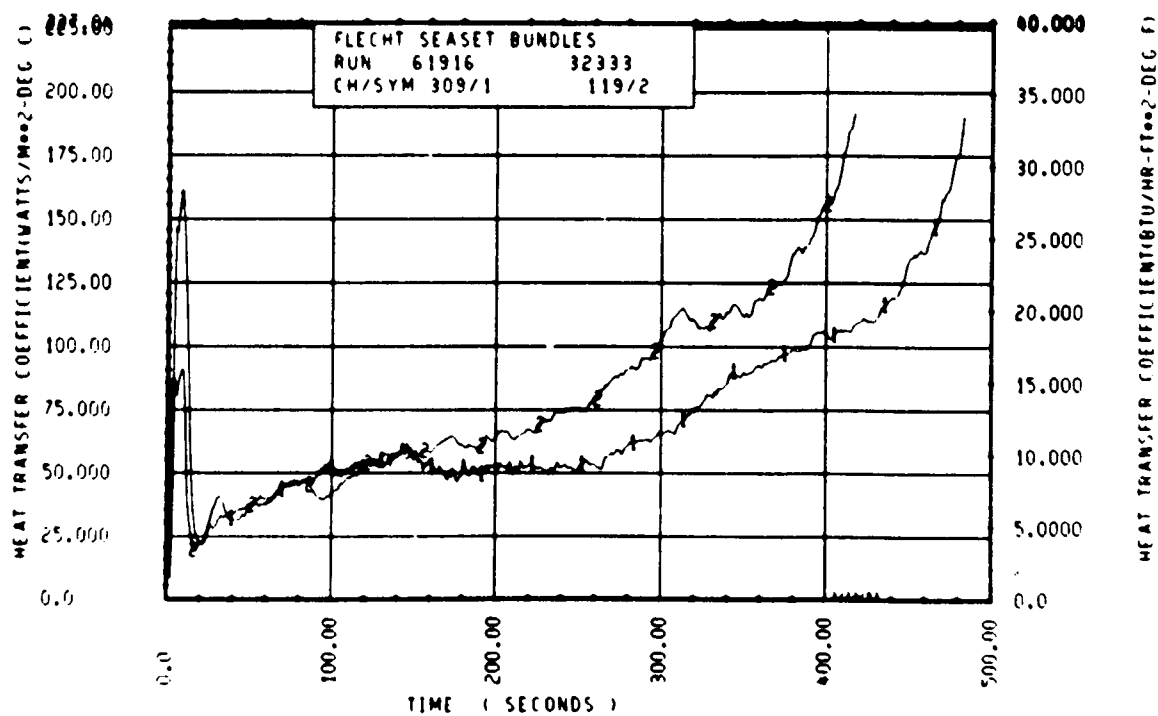
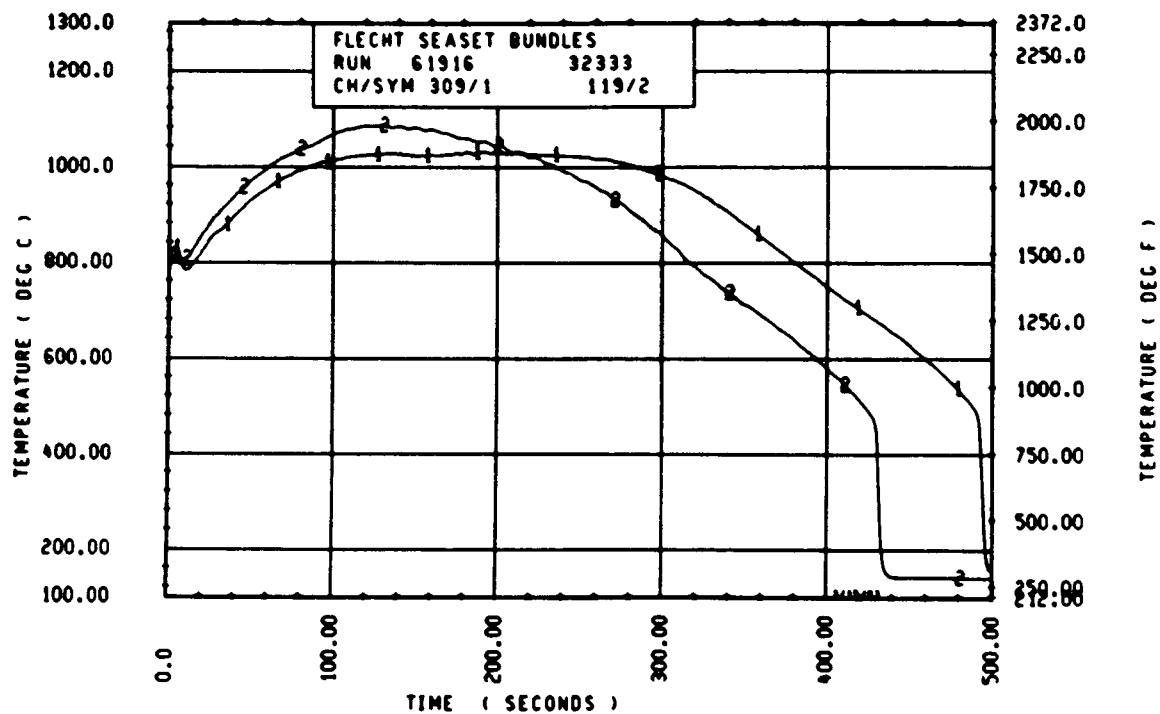
Rod 7E, 2.13 m (84 in.)



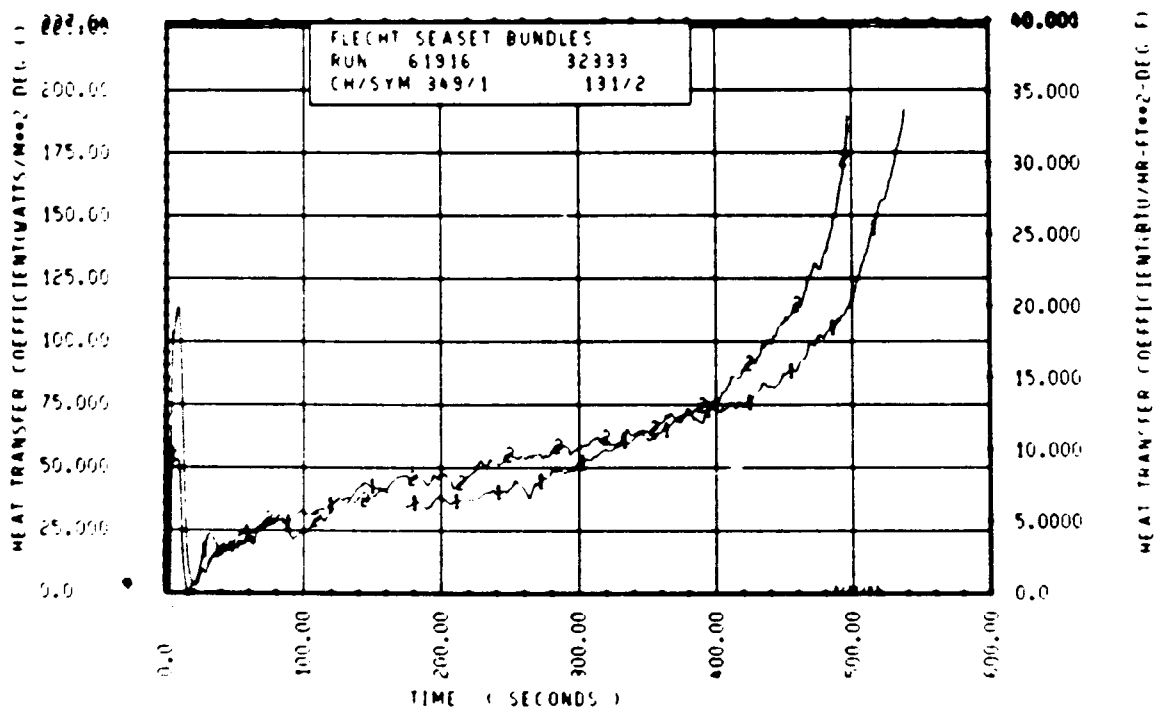
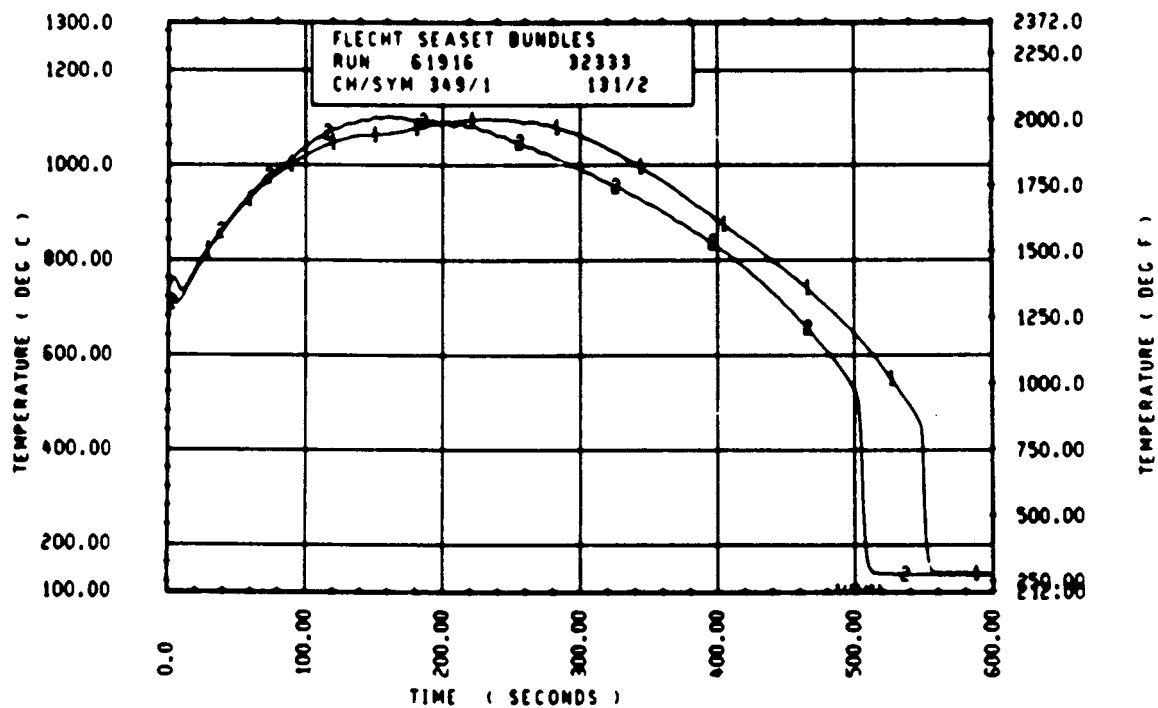
Rod 9C, 2.29 m (90 in.)



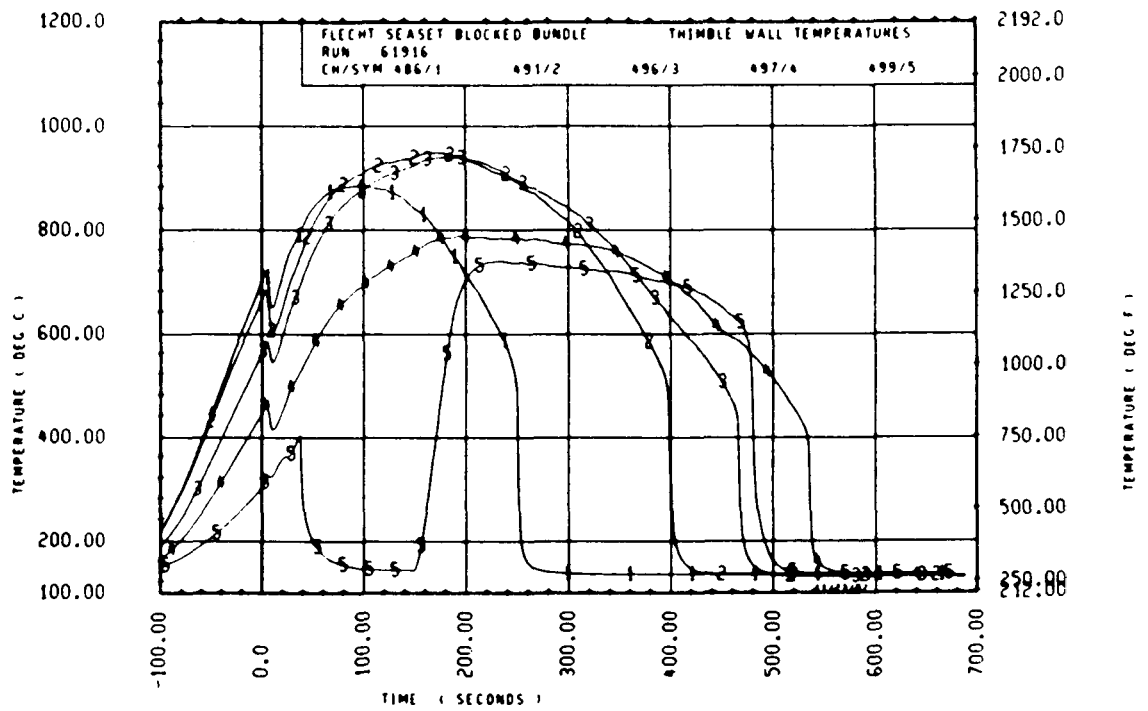
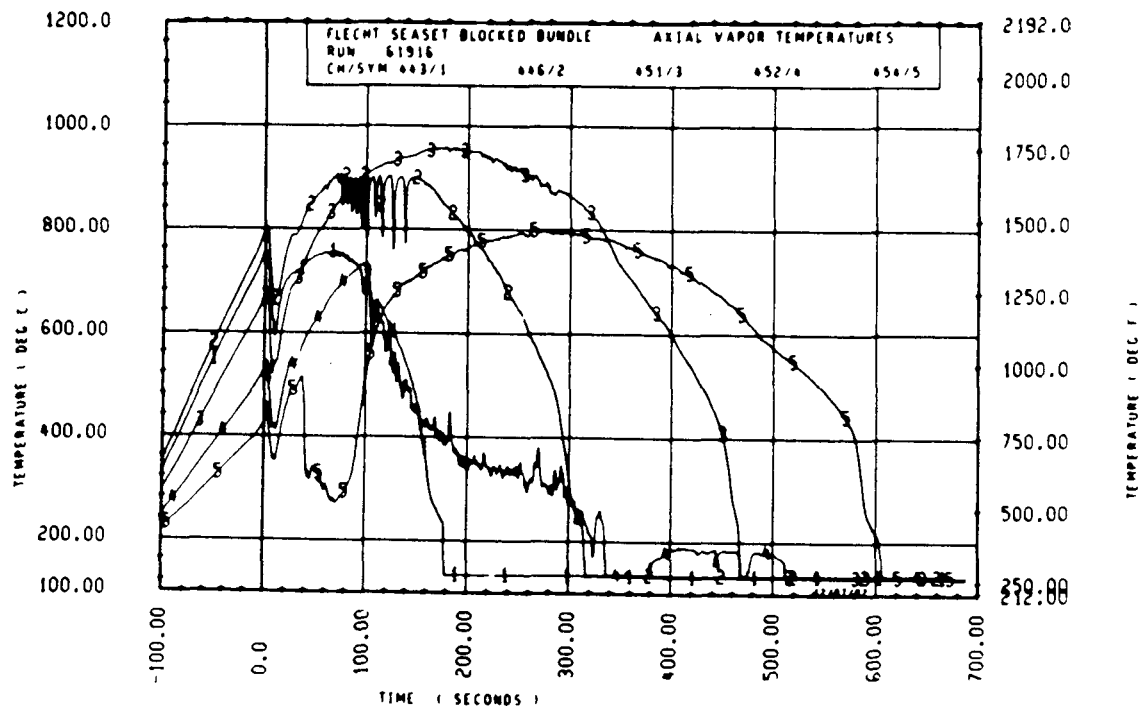
Rod 11E, 2.29 m (90 in.)

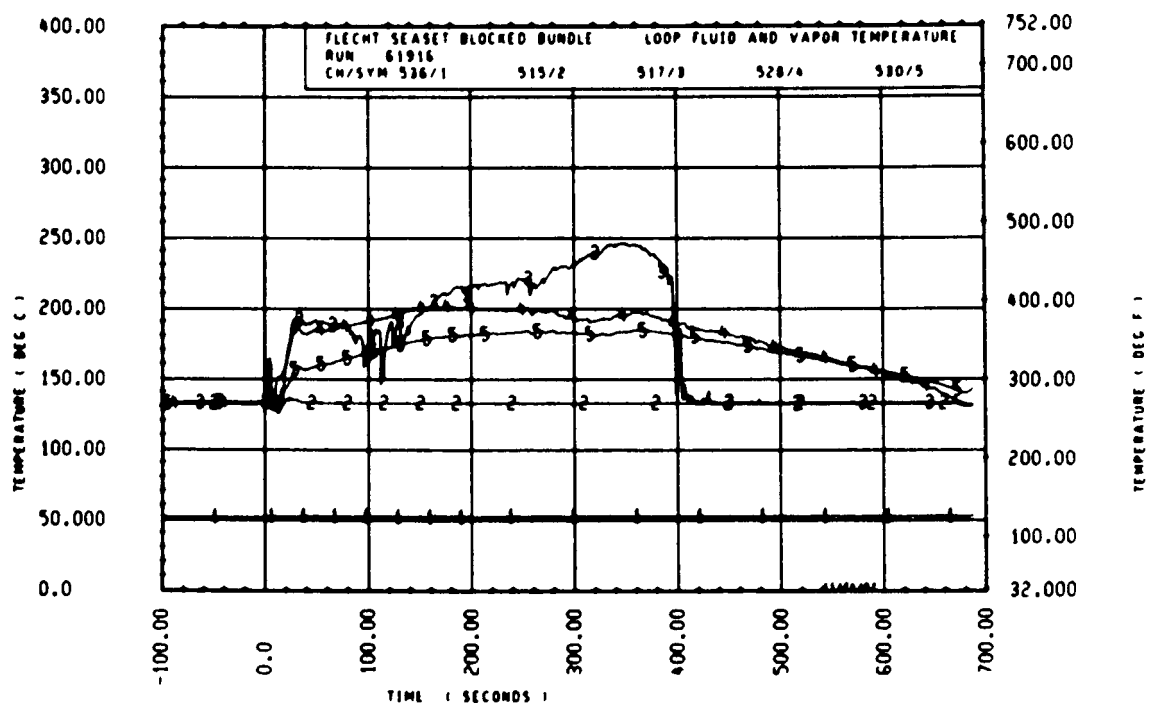
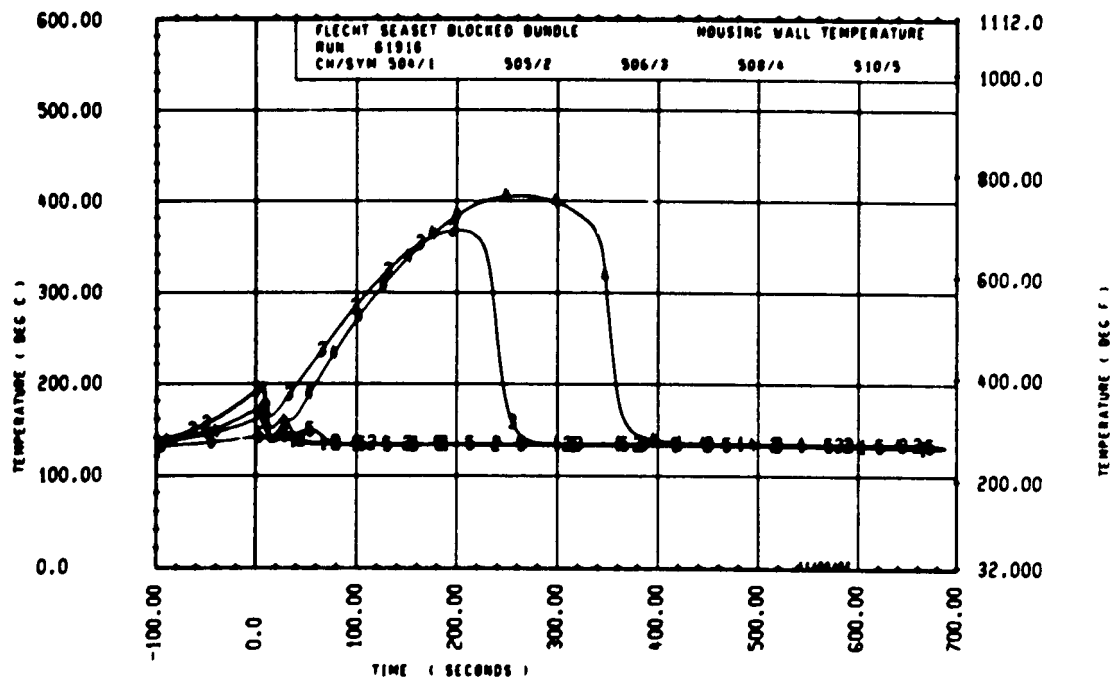


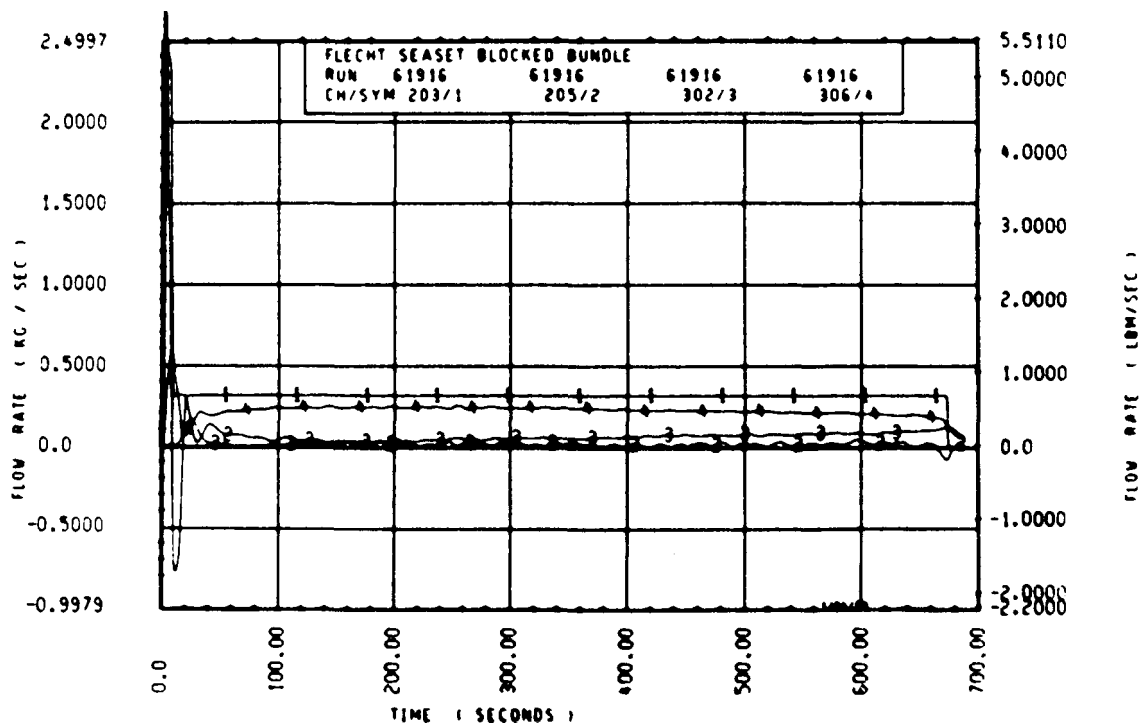
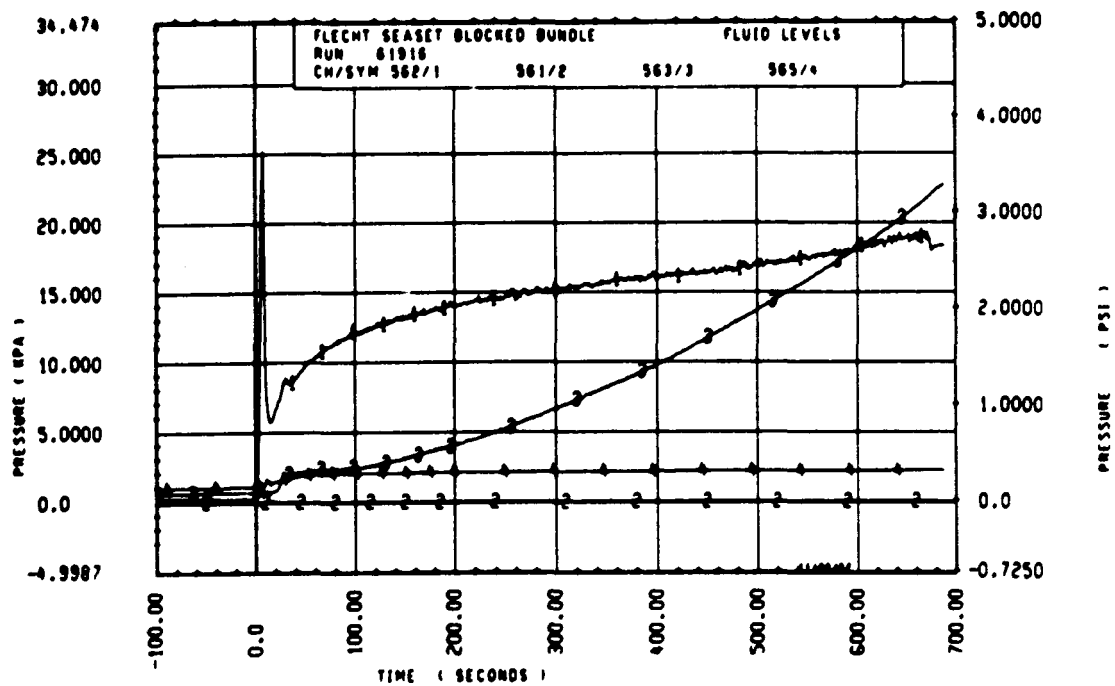
Rod 7D, 2.29 m (90 in.)

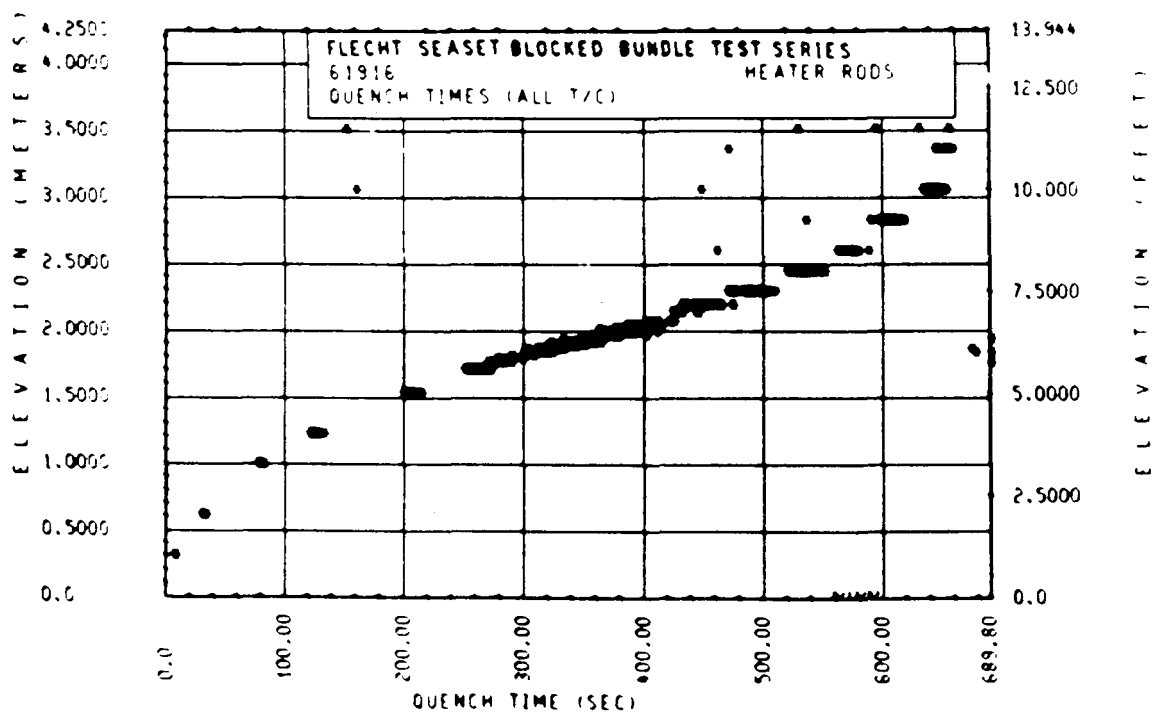
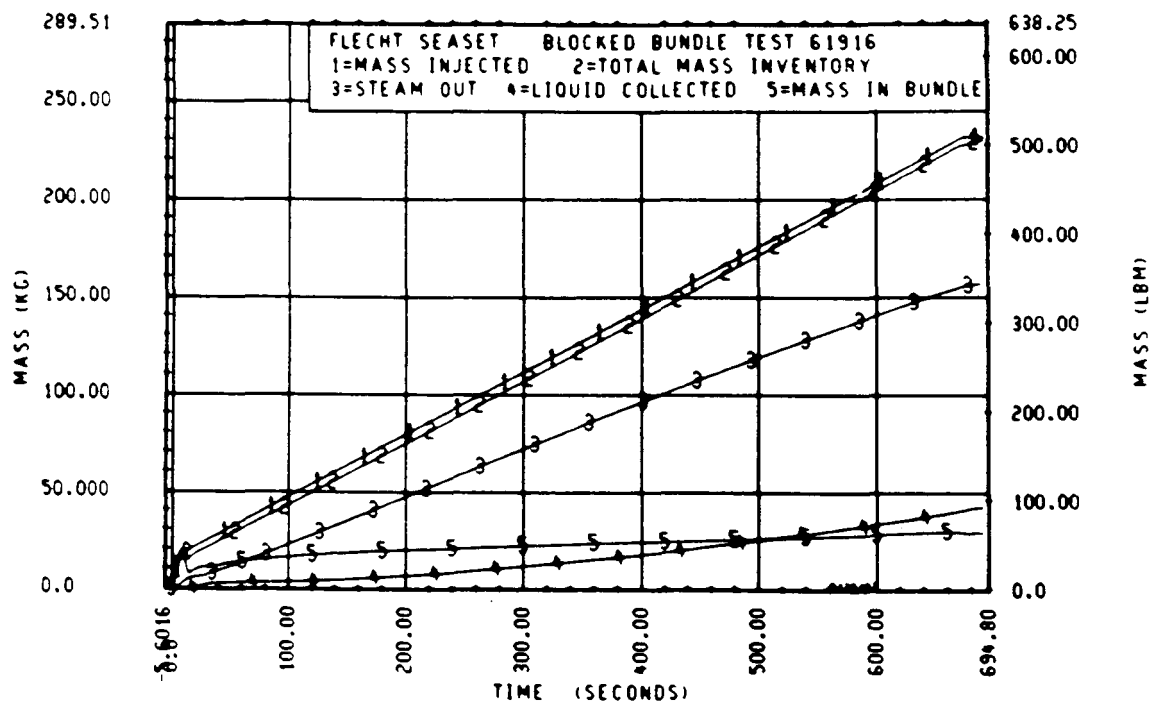


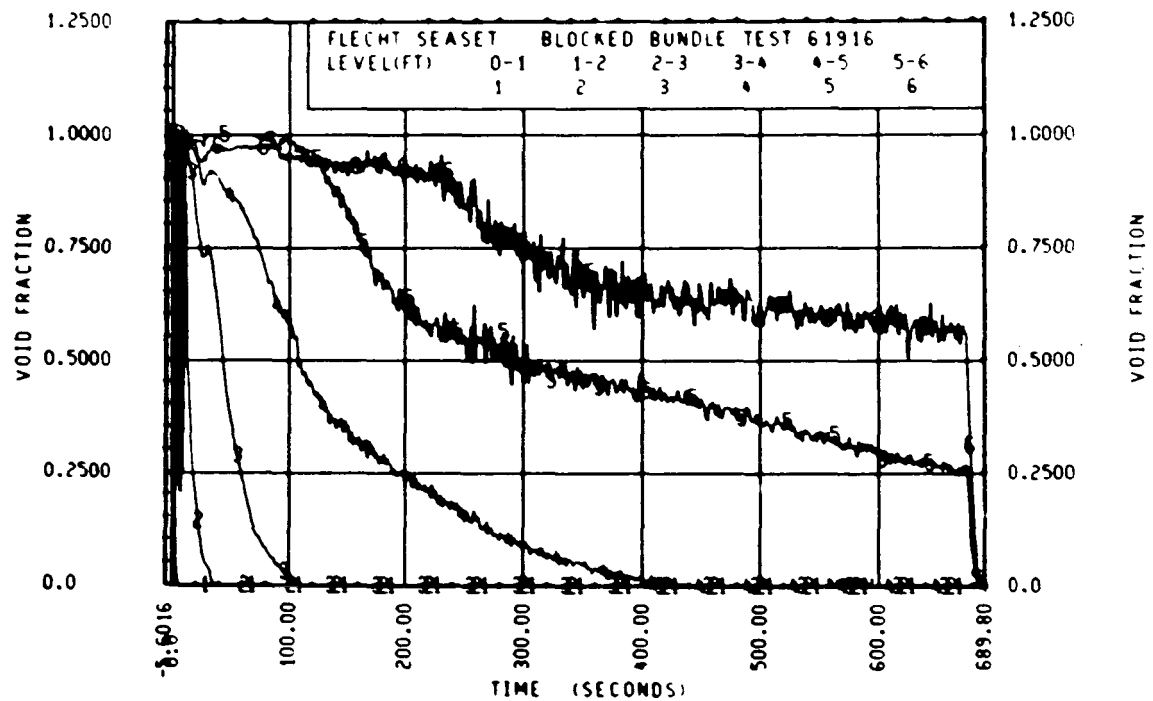
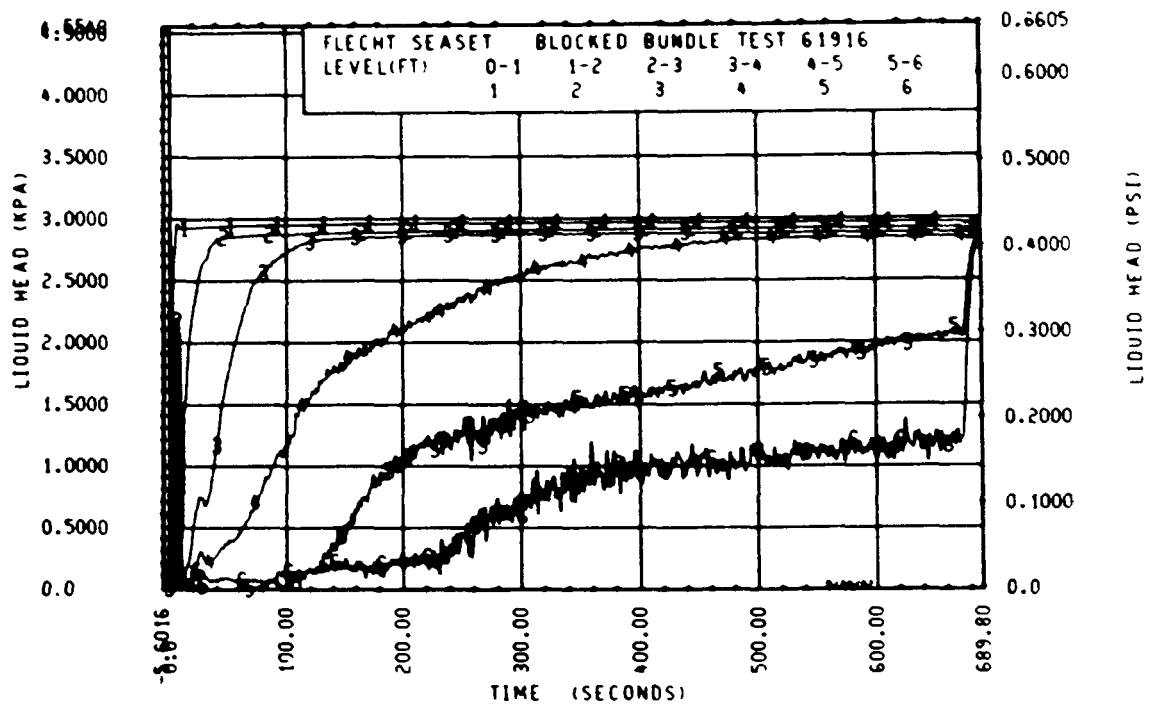
Rod 8E, 2.44 m (96 in.)

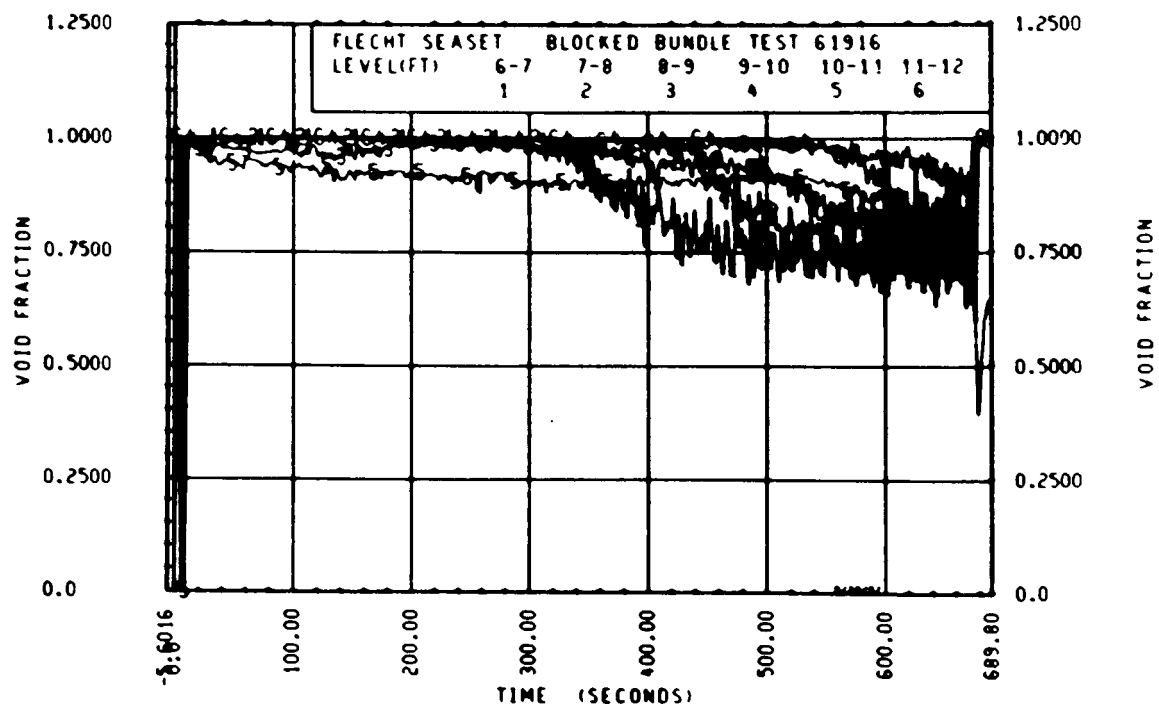
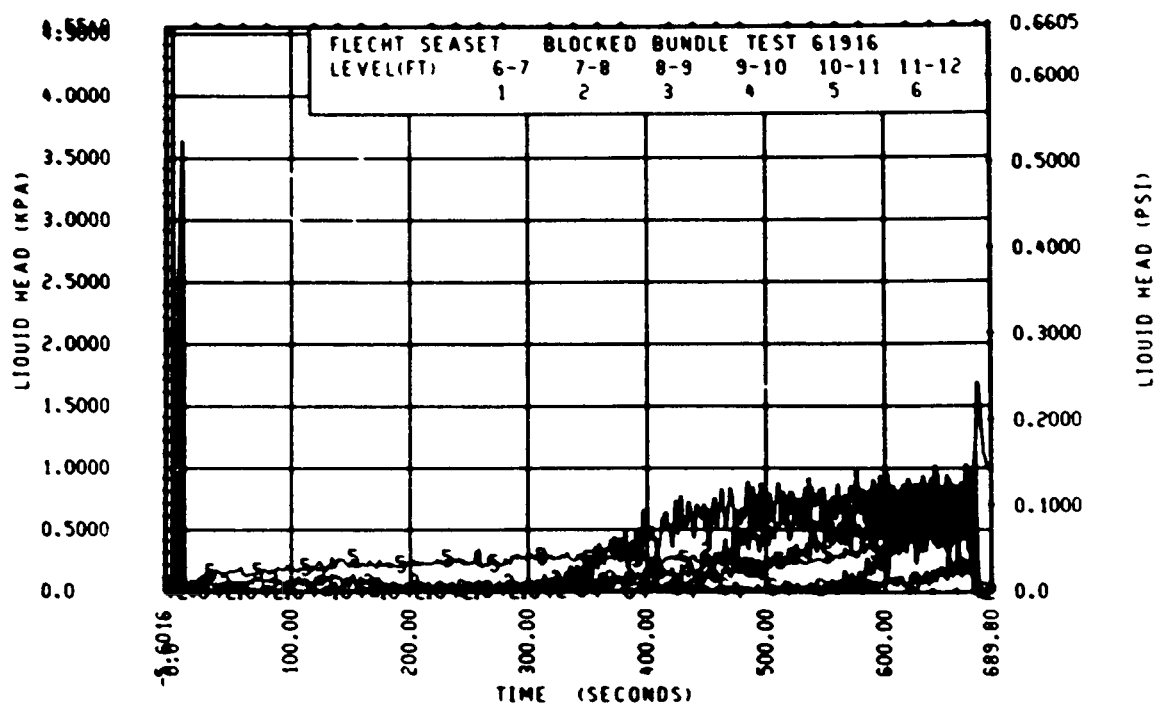












FLECHT SEASET 163-ROD BUNDLE FLOW BLOCKAGE TASK
SUMMARY AND COMMENT SHEET

Run: 62015
Test date: 9/20/82
Test type: Forced reflood
Parameter: Inlet subcooling effect

AS-RUN TEST CONDITIONS:

Upper plenum pressure	0.277 MPa (40.2 psia)
Initial peak clad temperature and location	877.1°C (1610.8°F), 8N-1.93 m (76 in.)
Initial peak rod power:	
Peripheral rods	2.32 kW/m (0.707 kW/ft)
Bypass rods	2.29 kW/m (0.699 kW/ft)
Blockage island rods	2.29 kW/m (0.697 kW/ft)
Flooding rate	25 mm/sec (0.98 in./sec) for 60 sec 27.7 mm/sec (1.09 in./sec) for 140 sec 29.7 mm/sec (1.17 in./sec) onward
Coolant temperature	119.4°C (247°F)
Initial bundle water level	-2.5 mm (-0.1 in.)

COMMENTS:

Inlet mass flow: ⁽¹⁾ -2.6% for first 60 seconds, -1.1% for next 140
seconds, -8.6% for next 100 seconds, and 0% thereafter

Power decay: ⁽¹⁾ peripheral rods, +1% constant
bypass rods, -0.5% constant
blockage rods, -0.7% constant

1. Relative to run 32114

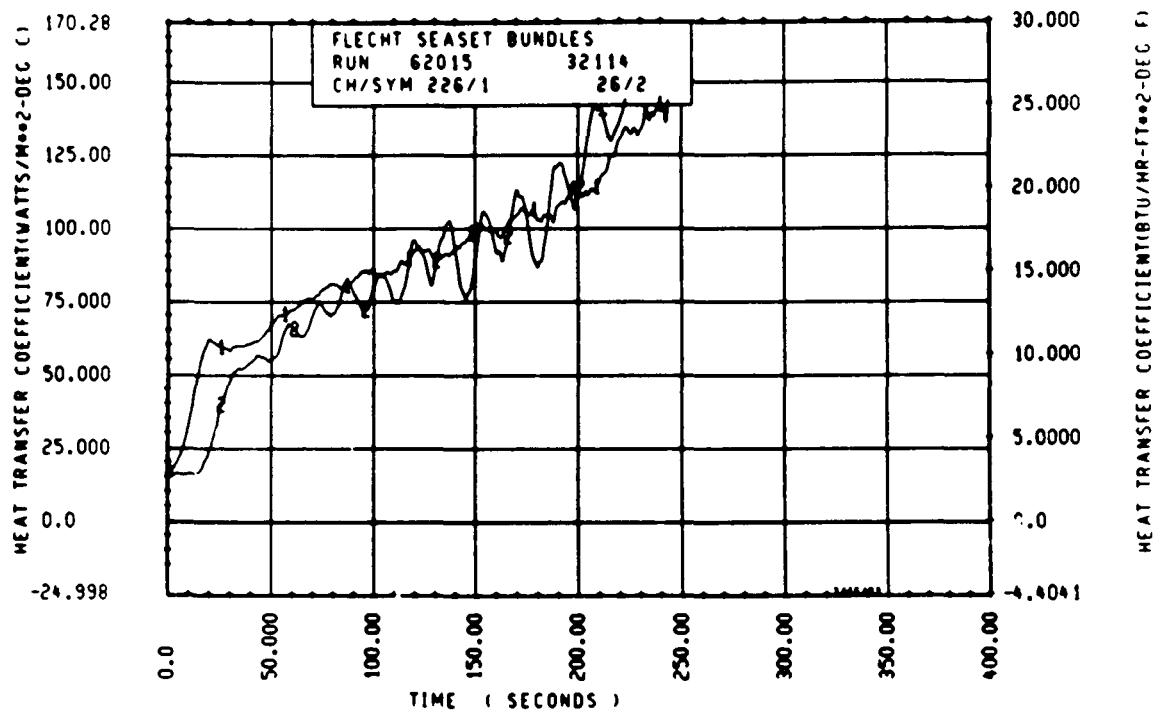
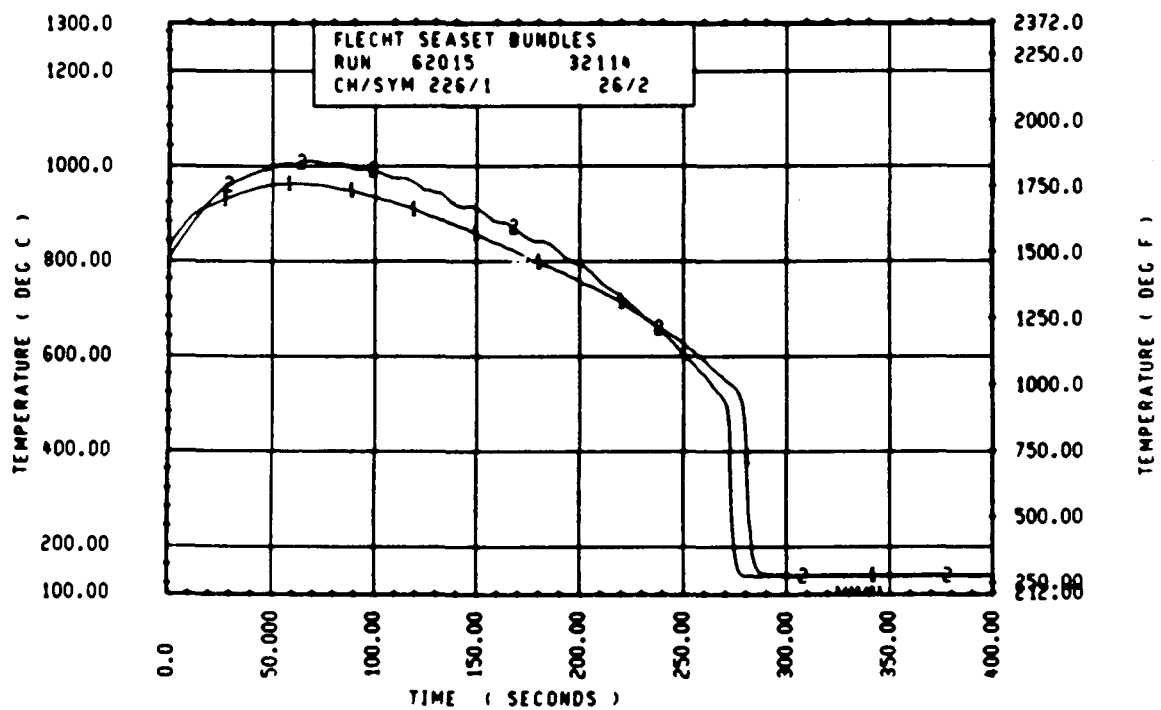
FLECHT SEASET 163 ROD BUNDLE TEST SERIES							
RUN NUMBER 62015							
ROD/ELEV	CHAN. NO	INITIAL AT FLOOD (DEG F)	MAXIMUM TEMPERATURE (DEG F)	TEMPERATURE RISE (DEG F)	TURNAROUND TIME (SECONDS)	QUENCH TEMPERATURE (DEG F)	QUENCH TIME (SECONDS)
96 1- C	3	677.	699.	22.	6.5	561.	27.4
10M 2- C	6	883.	934.	51.	11.0	657.	55.4
46 3- 3	9	1216.	1310.	92.	31.0	856.	111.4
3J 4- C	11	1357.	1512.	155.	38.5	835.	172.6
7H 4- C	12	1336.	1517.	179.	46.0	835.	174.6
8K 4- C	13	1361.	1545.	184.	46.0	823.	161.7
6M 4- C	14	1361.	1526.	166.	45.0	863.	169.3
12J 4- C	17	1347.	1489.	143.	36.5	863.	170.2
5E 5- C	20	1507.	1777.	270.	68.0	863.	262.6
76 5- C	21	1556.	1818.	260.	70.5	936.	276.7
96 5- C	24	1532.	1797.	265.	66.0	936.	279.6
5E 5- 7	33	1530.	1814.	283.	73.0	872.	339.7
66 5- 7	45	1536.	1853.	318.	101.5	870.	346.5
9M 5- 9	52	1479.	1814.	335.	88.5	914.	354.0
76 5-10	59	1499.	1841.	342.	109.0	856.	361.6
7F 5-11	62	1445.	1805.	360.	109.5	852.	370.6
46 5-11	64	1530.	1850.	320.	71.5	835.	382.6
21 6- C	67	1591.	1919.	328.	70.5	830.	386.6
5D 6- C	70	1469.	1803.	313.	90.5	843.	361.6
6J 6- C	74	1522.	1800.	278.	72.5	797.	395.6
7H 6- C	66	1543.	1867.	324.	74.0	850.	376.6
11E 6- C	80	1532.	1825.	294.	74.0	852.	376.6
8M 6- 2	97	1365.	1763.	399.	142.0	827.	401.2
5M 6- 2	98	1527.	1876.	349.	95.0	851.	409.6
9E 6- 2	105	1326.	1855.	527.	143.5	284.	665.2
6M 6- 3	111	1407.	1798.	391.	143.0	829.	410.0
46 6- 3	124	1547.	1884.	337.	108.0	826.	415.7
11M 6- 4	134	1465.	1875.	410.	144.5	730.	419.7
9D 6- 4	143	1534.	1936.	396.	108.5	846.	423.7
9J 6- 5	165	1512.	1895.	383.	144.0	916.	428.1
9M 6- 5	166	1587.	1923.	336.	72.5	914.	418.6
6J 6- 6	192	1554.	1909.	350.	116.5	873.	436.6
9U 6- 6	193	1551.	1948.	397.	112.5	845.	441.6
11F 6- 6	173	1546.	1916.	368.	106.5	850.	426.6
46 7- C	261	1469.	1773.	304.	71.5	727.	476.1
7D 7- 6	309	1470.	1826.	356.	115.0	751.	520.4
76 7- 6	312	1510.	1872.	362.	116.5	854.	510.6
11E 7- 6	325	1484.	1849.	365.	110.5	854.	502.1
5L 6- C	337	1307.	1756.	449.	119.0	756.	546.1
7H 8- C	345	1342.	1829.	487.	172.5	874.	521.6
7K 8- C	346	1359.	1791.	433.	140.0	745.	543.4
5J 8- 6	366	1239.	1572.	432.	212.2	647.	581.2
76 8- 6	368	1140.	1529.	389.	205.2	634.	561.1
7E 9- 3	383	1098.	1577.	479.	172.5	700.	604.2
8M 9- 3	387	1045.	1486.	441.	173.5	624.	608.0
9C 9- 3	389	1045.	1496.	451.	206.2	664.	595.2
11F 9- 3	394	1037.	1495.	458.	205.2	644.	595.2
7810- C	408	860.	1359.	498.	212.2	601.	630.2
8M10- C	415	862.	1409.	548.	207.2	528.	574.3
6K10- C	417	868.	1383.	515.	211.2	635.	622.5
8M10- C	418	860.	1381.	492.	143.0	640.	627.2
6M11- C	425	692.	948.	256.	123.0	717.	290.3
9M11- C	431	686.	1084.	396.	174.0	716.	501.7
11E11- C	432	691.	1145.	454.	212.2	526.	626.0
5J11- 6	436	676.	963.	286.	176.0	561.	616.2
7611- 6	437	647.	1074.	427.	218.2	414.	672.4
8J11- 6	438	685.	919.	235.	145.0	553.	623.2

RUN 62015 HEATER ROD STATISTICAL DATA

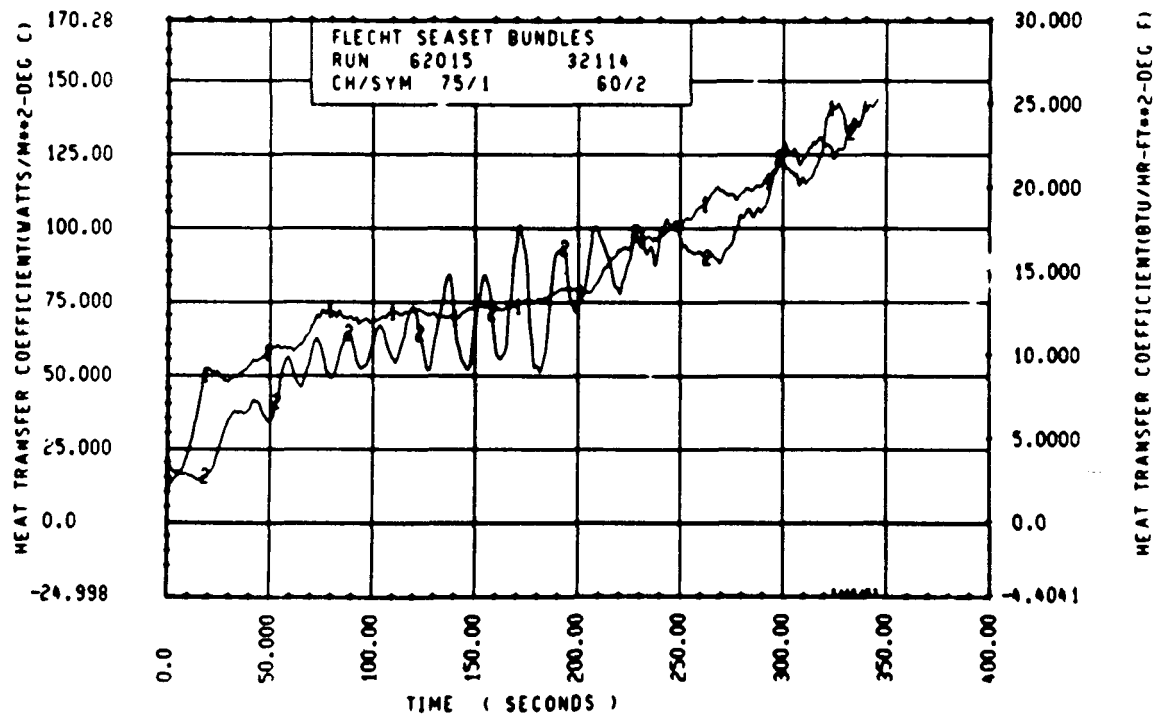
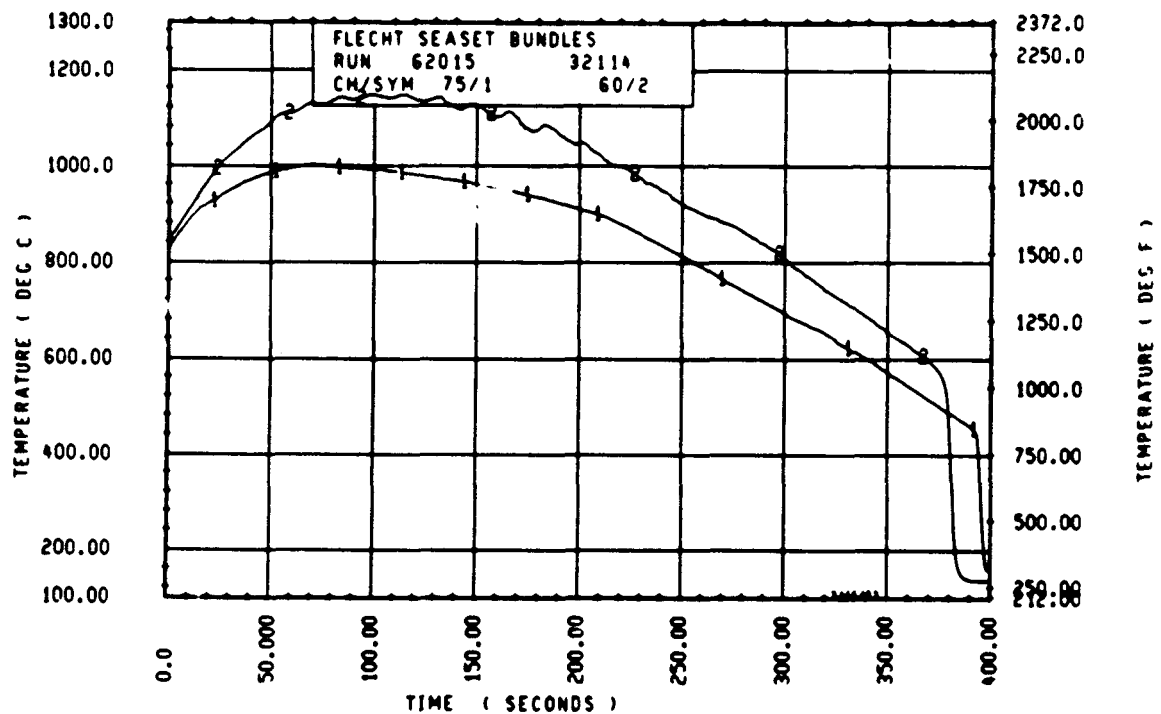
ELEV	INITIAL TEMP (DEG F)			MAX TEMP (DEG F)			TURNAROUND TIME (SEC)		
	MAX	MIN	MEAN	MAX	MIN	MEAN	MAX	MIN	MEAN
12	684.6	677.4	681.3	706.8	699.5	703.3	6.5	6.5	6.5
24	883.2	860.5	869.8	933.8	907.0	918.0	11.0	10.5	10.8
39	1218.1	1173.4	1192.8	1310.0	1276.5	1290.6	31.5	27.5	30.1
48	1368.0	1338.5	1354.7	1544.5	1489.4	1524.5	46.0	36.5	43.2
60	1560.8	1446.7	1520.8	1848.9	1668.0	1773.7	70.5	50.5	64.1
67	1596.6	1500.1	1544.1	1864.8	1775.7	1818.1	101.5	61.0	70.4
69	1524.0	1478.8	1507.9	1820.6	1760.1	1800.2	88.5	67.0	76.1
70	1598.7	1473.4	1524.9	1868.2	1808.2	1828.3	109.0	61.0	75.7
71	1530.5	1444.6	1484.0	1850.1	1799.2	1816.1	109.5	70.5	85.2
72	1591.2	1455.2	1537.1	1919.4	1800.3	1858.7	113.0	68.0	79.0
73	1585.7	1460.6	1518.1	1912.5	1798.0	1841.0	117.5	66.0	83.7
74	1585.7	1364.8	1502.1	1909.1	1763.5	1858.0	142.0	70.0	97.4
75	1592.2	1407.1	1511.7	1907.9	1798.0	1861.8	145.5	69.0	100.6
76	1610.8	1447.6	1541.3	1949.3	1854.6	1892.3	144.5	71.5	94.8
77	1586.8	1472.3	1533.3	1939.0	1829.7	1896.4	145.5	72.5	114.6
78	1610.8	1503.4	1550.5	1965.4	1865.9	1912.6	151.5	71.0	112.9
79	1592.2	1504.5	1554.6	1953.9	1870.5	1921.2	152.5	72.5	119.1
80	1573.8	1502.3	1545.3	1984.9	1880.6	1940.2	145.0	73.5	115.7
81	1568.4	1473.4	1529.2	1958.5	1855.7	1932.3	168.0	85.5	121.5
84	1516.4	1412.5	1474.8	1884.0	1676.8	1771.3	145.5	61.5	90.3
86	1566.2	1470.2	1522.4	1876.1	1762.3	1811.5	145.5	65.5	93.8
90	1517.5	1421.0	1476.6	1895.3	1798.0	1847.8	144.5	71.0	111.5
96	1389.1	1264.0	1343.3	1876.1	1755.6	1819.3	198.5	100.0	148.9
102	1190.0	1032.8	1148.4	1654.8	1529.4	1602.9	212.2	145.5	187.2
111	1097.8	1036.9	1060.3	1577.1	1430.6	1512.4	212.2	97.5	176.1
120	926.6	824.3	866.5	1461.6	1267.1	1396.5	214.2	128.5	193.3
132	692.1	681.6	687.9	1145.4	948.3	1066.7	213.2	123.0	168.6
138	684.6	647.0	665.4	1074.0	919.4	1015.3	218.2	145.0	191.5

RUN 62015 HEATER ROD STATISTICAL DATA

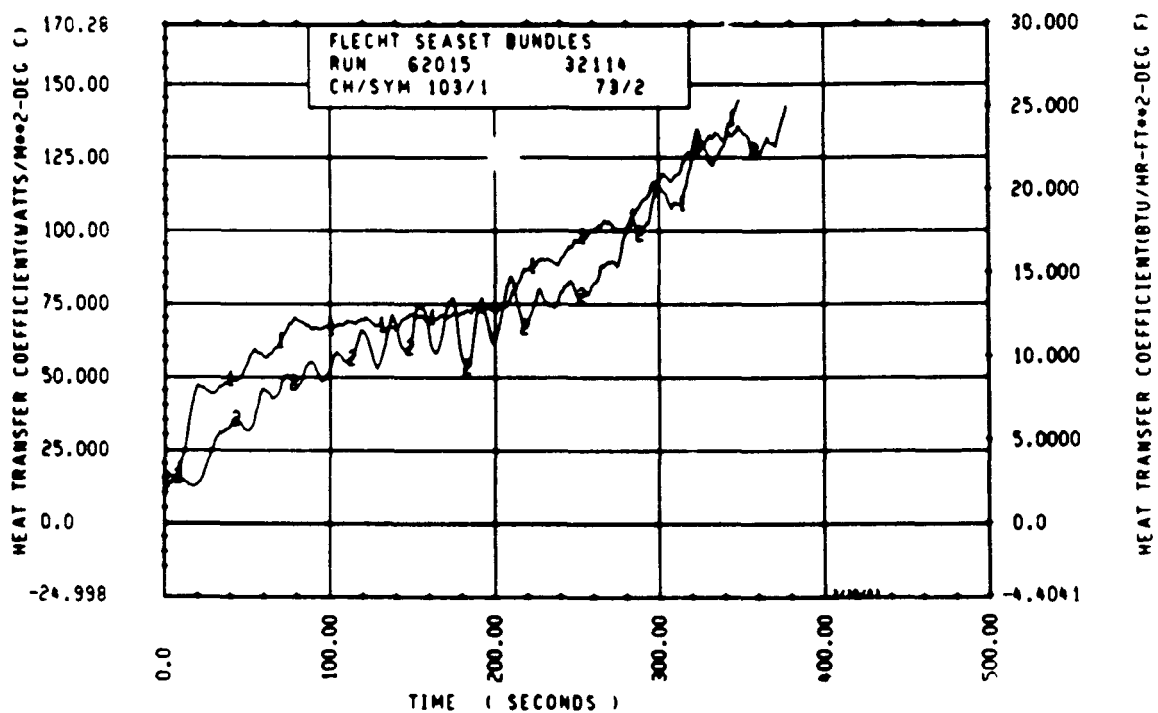
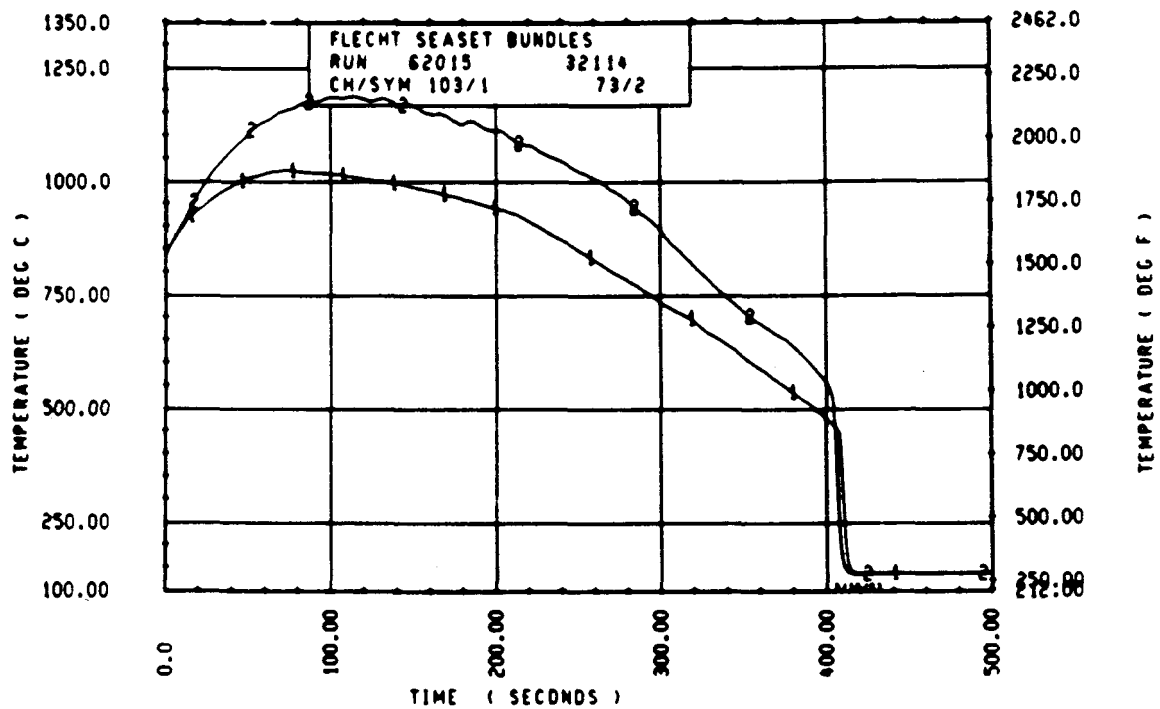
ELEV	TEMP RISE (DEG F)			QUENCH TEMP (DEG F)			QUENCH TIME (SEC)		
	MAX	MIN	MEAN	MAX	MIN	MEAN	MAX	MIN	MEAN
12	22.1	22.0	22.0	565.8	555.0	560.6	30.0	27.4	28.7
24	50.6	46.5	48.2	656.9	624.4	640.0	55.4	53.1	54.2
39	104.2	91.8	97.7	866.7	807.9	839.7	119.4	111.4	115.0
48	187.0	142.5	169.8	883.0	821.2	846.8	181.7	169.3	173.5
60	288.1	217.9	252.9	966.4	841.3	890.8	292.7	273.0	283.2
67	317.6	243.2	269.0	906.7	812.2	870.5	350.5	326.8	338.9
69	335.1	255.6	292.2	913.8	816.5	853.8	371.0	350.7	356.7
70	342.0	269.4	303.4	915.2	788.8	854.6	377.6	357.0	365.5
71	360.2	301.6	332.2	888.4	815.2	847.5	382.9	363.9	373.0
72	389.2	276.5	321.6	863.7	797.3	839.9	395.9	376.8	386.2
73	349.4	298.2	323.0	900.1	772.7	839.1	403.1	376.0	392.1
74	439.8	305.1	355.9	897.3	752.5	844.0	410.0	393.0	402.3
75	414.3	294.5	350.1	1089.9	626.8	854.7	417.1	361.8	407.6
76	421.6	298.1	350.9	926.4	730.3	857.2	426.9	398.1	417.4
77	417.1	323.8	363.2	918.1	756.6	866.3	448.1	416.8	427.4
78	398.1	332.2	362.0	932.7	733.7	856.0	457.6	424.9	435.6
79	427.0	323.7	366.6	944.0	651.8	859.2	451.0	419.9	440.8
80	449.0	355.1	394.9	899.9	788.4	853.3	466.9	440.1	452.4
81	449.4	352.4	403.1	907.5	789.1	840.7	469.8	451.9	458.6
84	383.9	242.9	291.4	783.2	670.7	726.7	486.1	468.2	477.6
86	329.4	225.1	269.1	841.4	718.2	780.6	511.5	471.1	489.6
90	415.6	338.6	371.0	869.1	751.2	818.6	536.0	451.9	515.4
96	547.6	407.0	476.0	874.1	721.2	789.5	566.0	521.9	546.3
102	587.9	389.2	454.6	965.6	594.5	684.4	595.2	472.0	567.5
111	513.2	365.0	452.1	748.5	609.2	673.5	614.2	582.2	600.4
120	605.4	422.6	527.9	1130.2	528.0	641.1	641.1	259.7	608.5
132	454.3	256.1	378.8	716.5	286.8	552.9	643.2	240.3	565.8
138	427.1	234.6	349.8	808.2	419.2	574.1	672.4	462.3	603.1



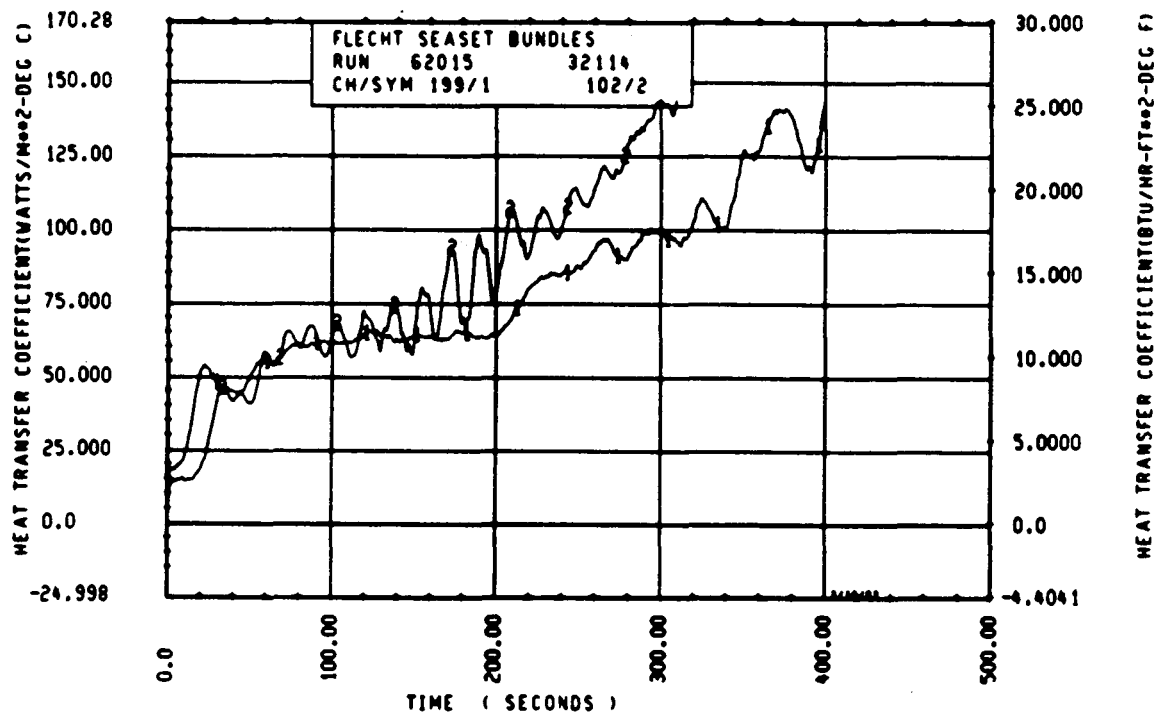
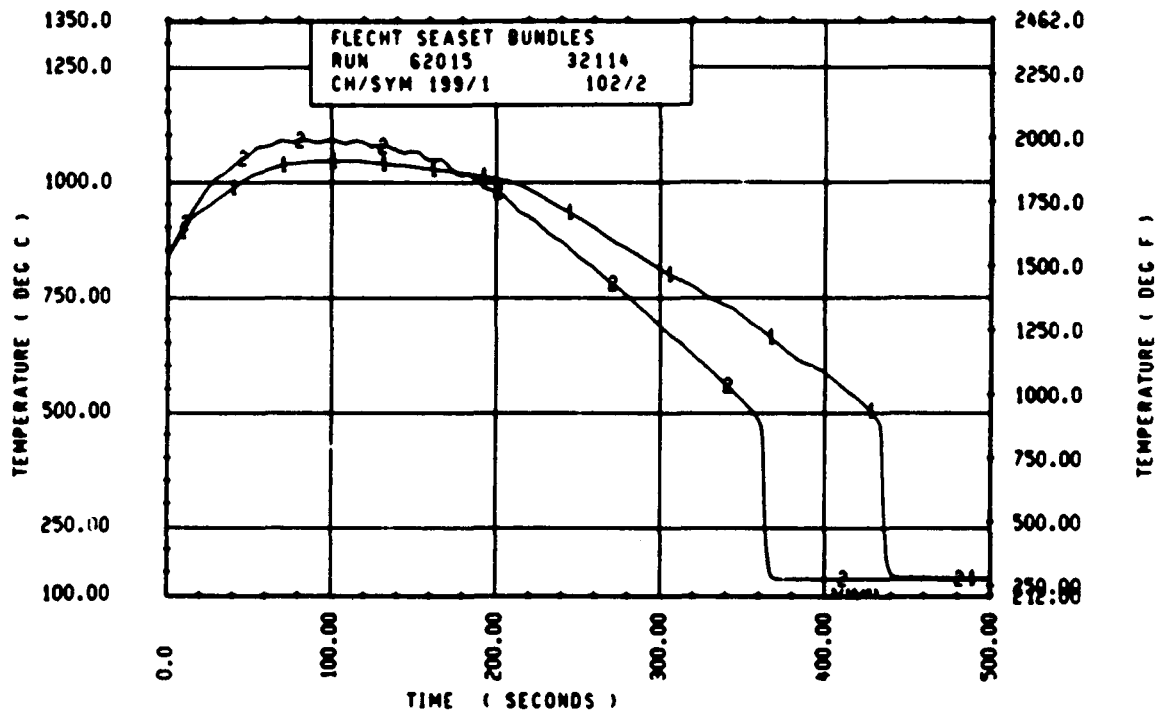
Rod 11E, 1.52 m (60 in.)



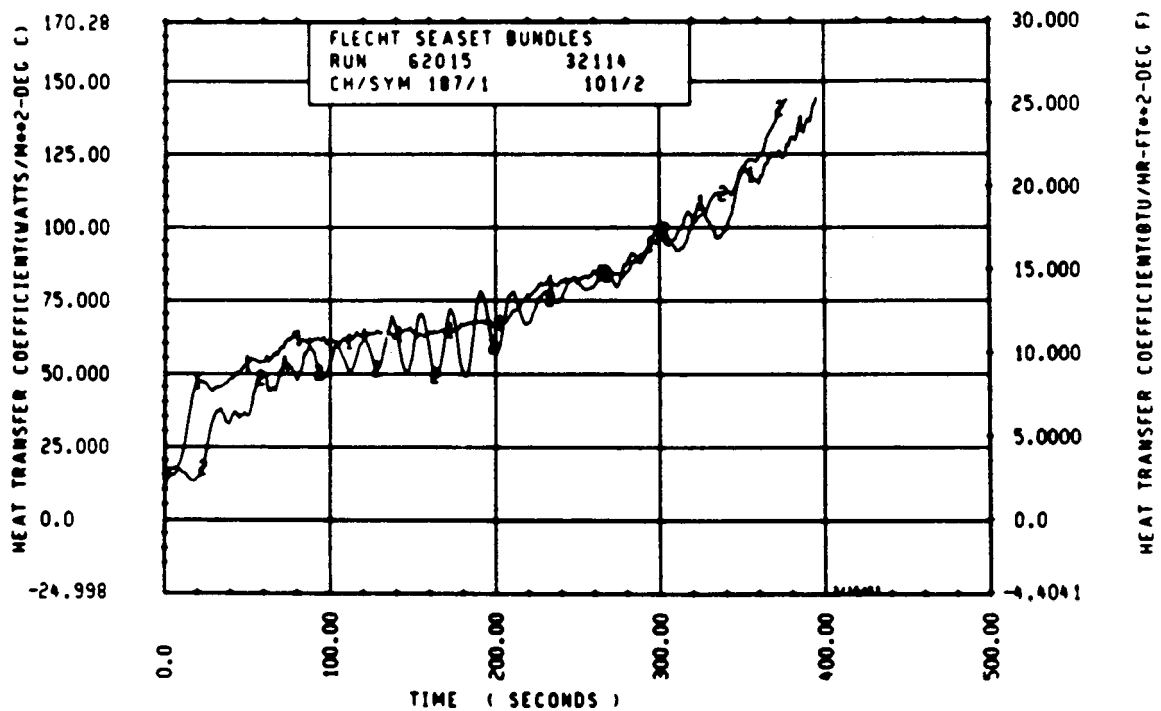
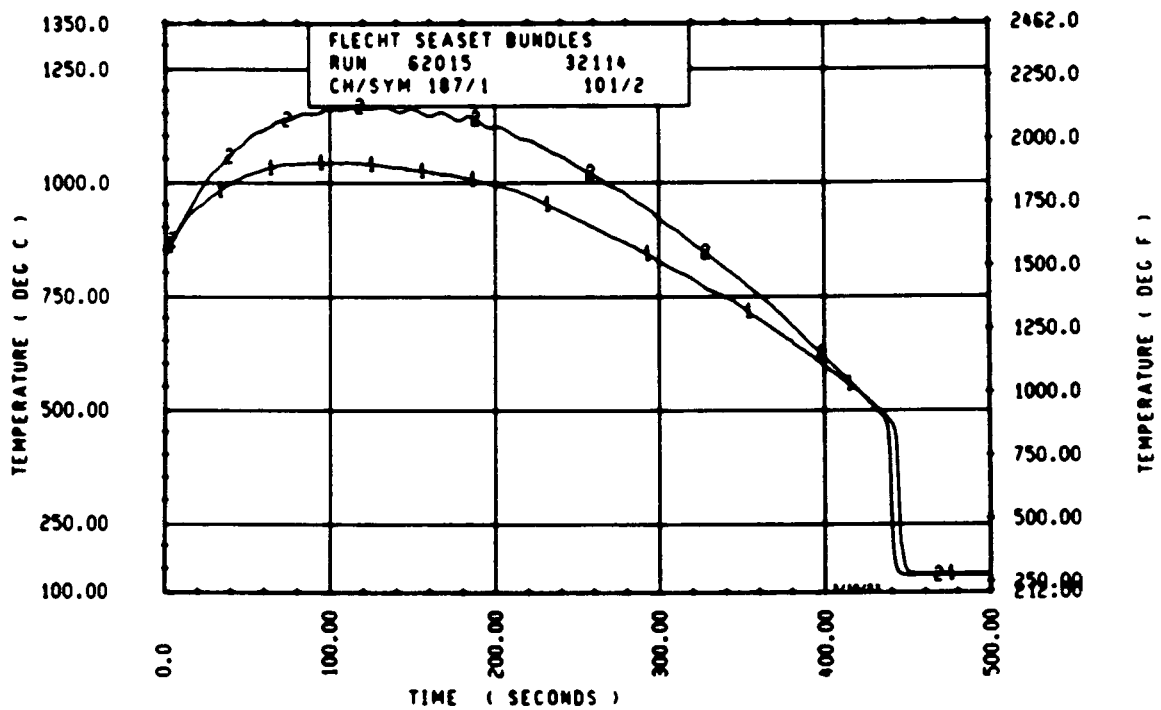
Rod 6L, 1.83 m (72 in.)



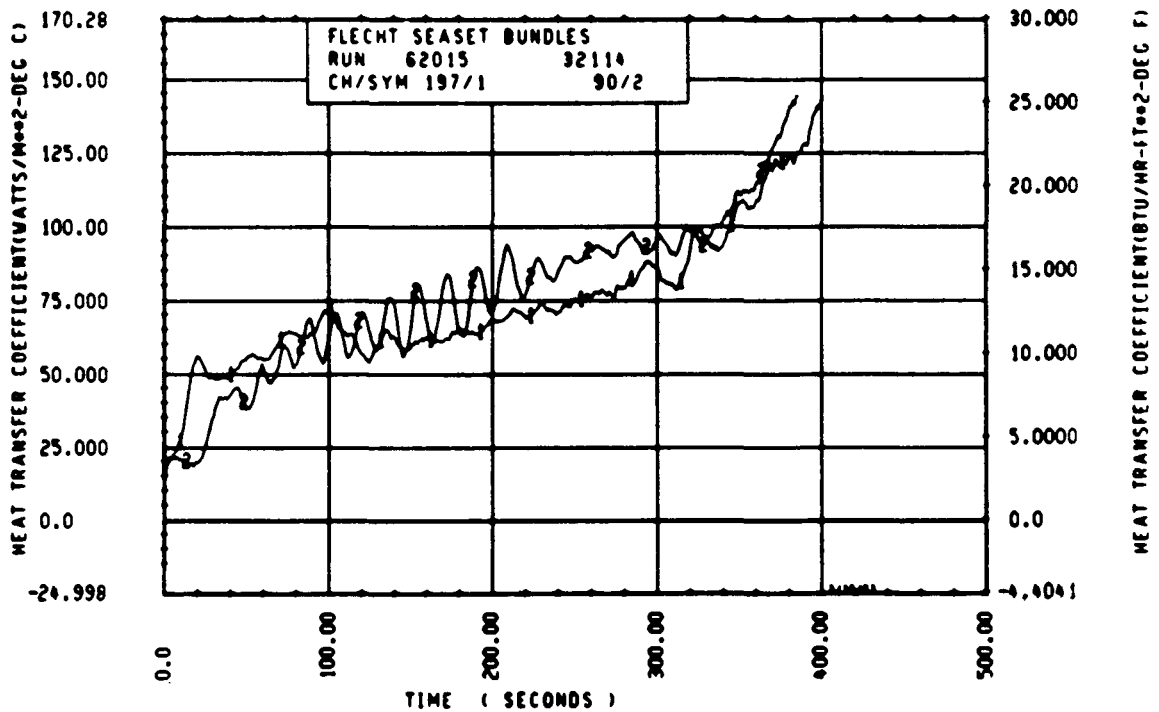
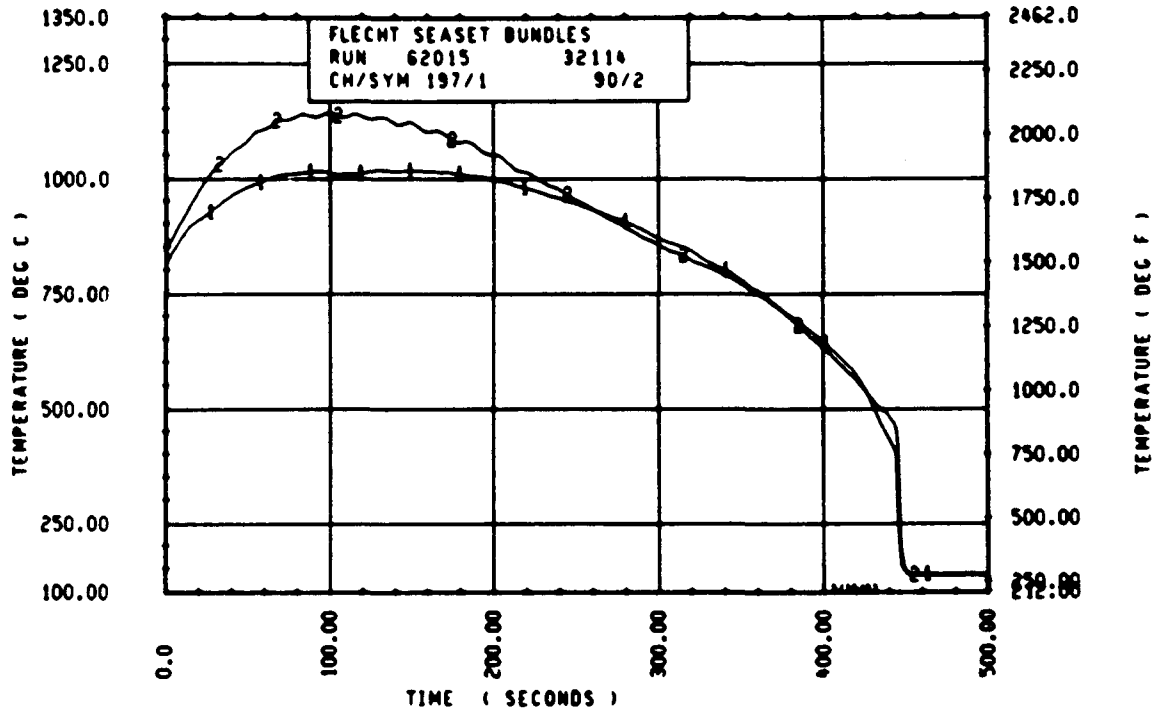
Rod 6L, 1.88 m (74 in.)



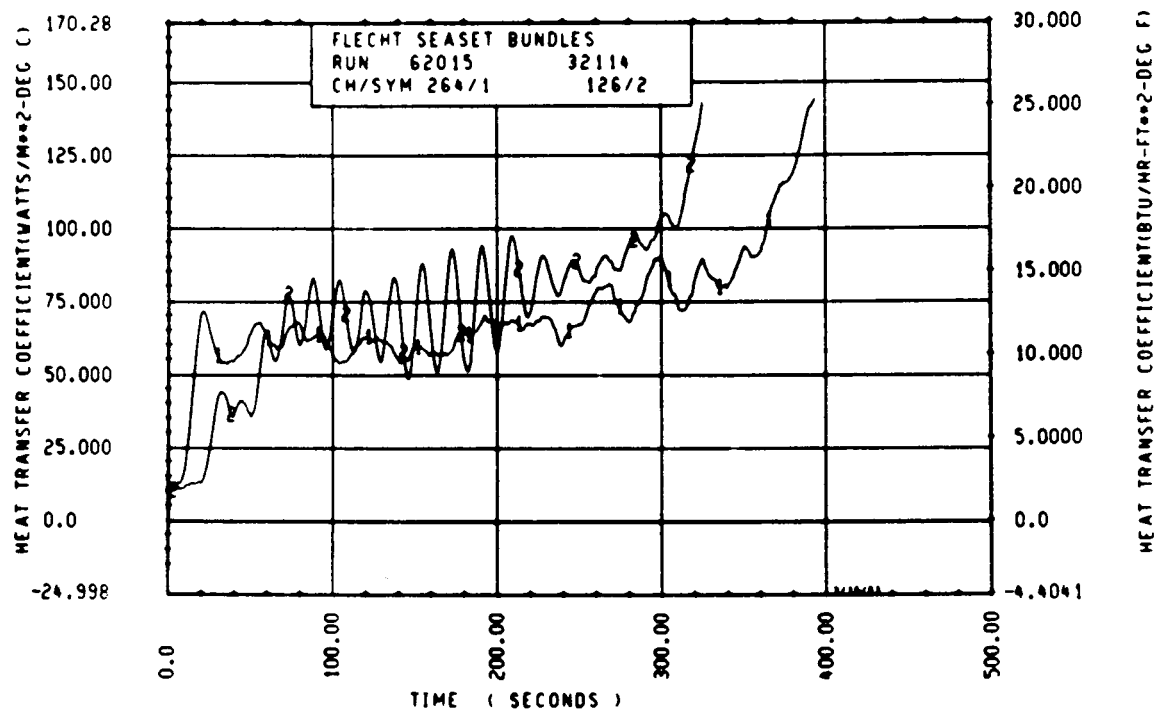
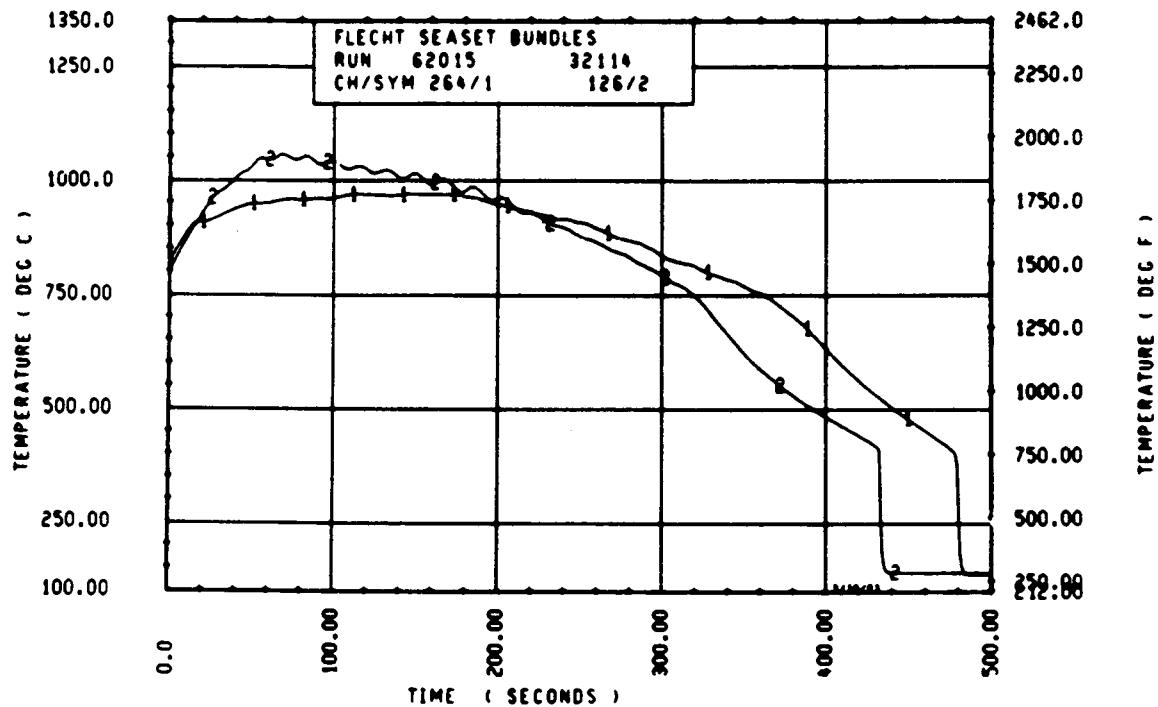
Rod 13G, 1.98 m (78 in.)



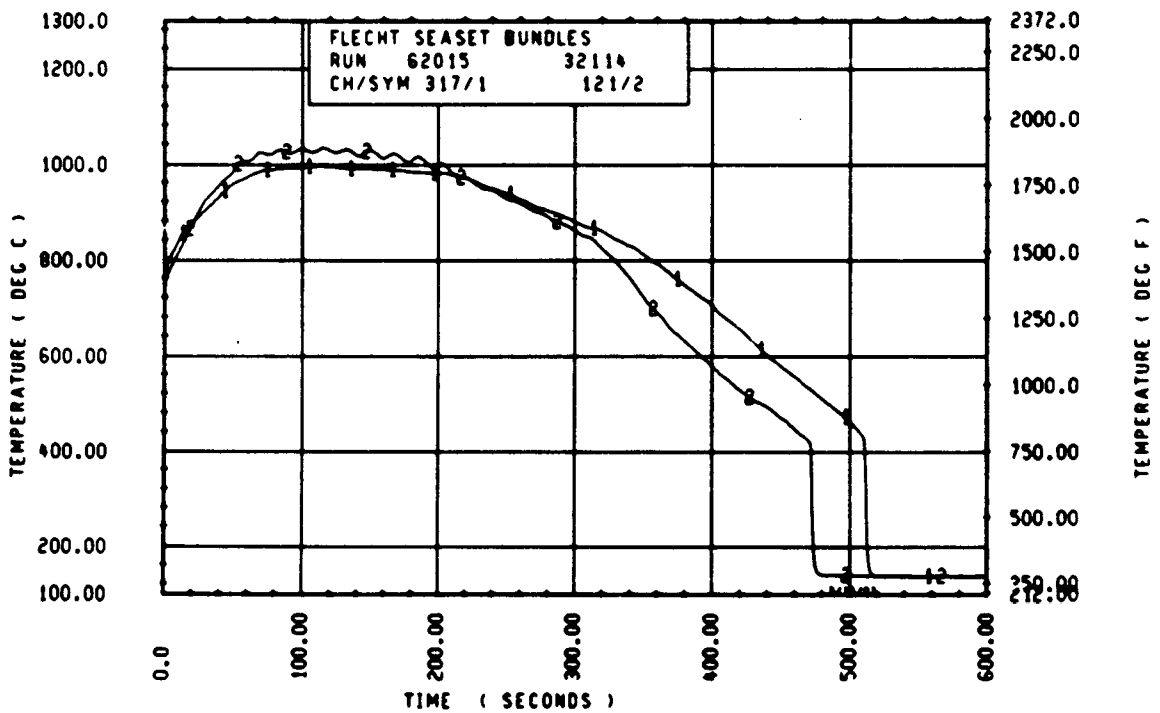
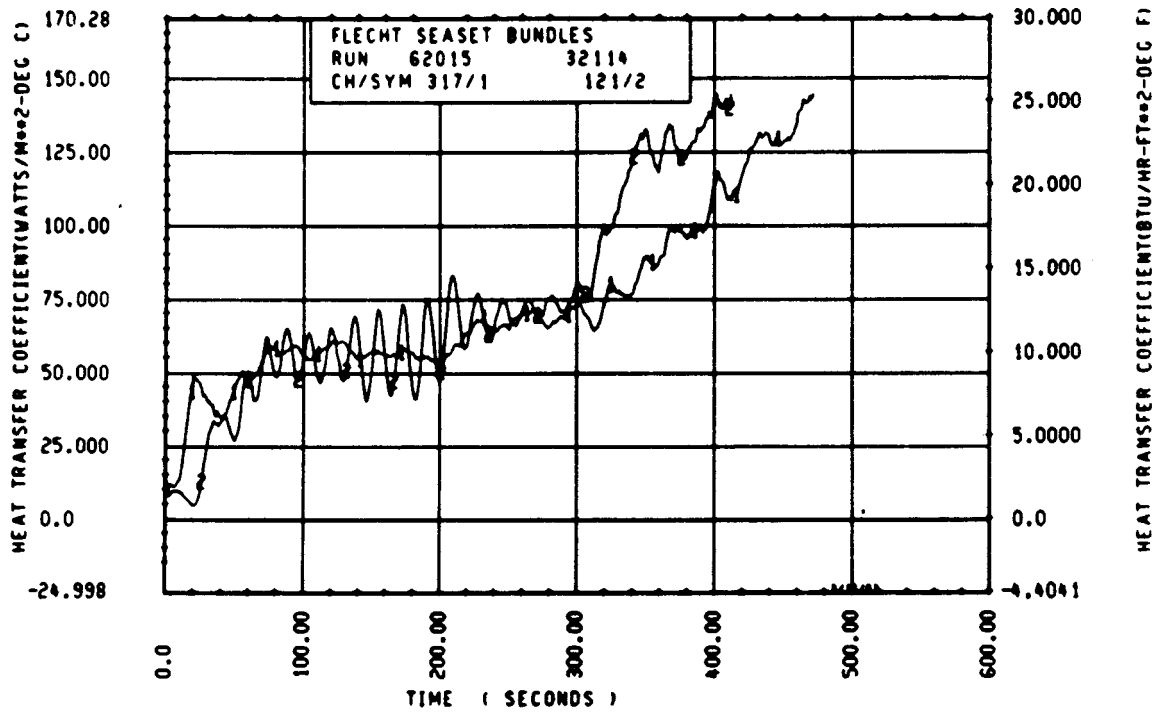
Rod 6J, 1.98 m (78 in.)



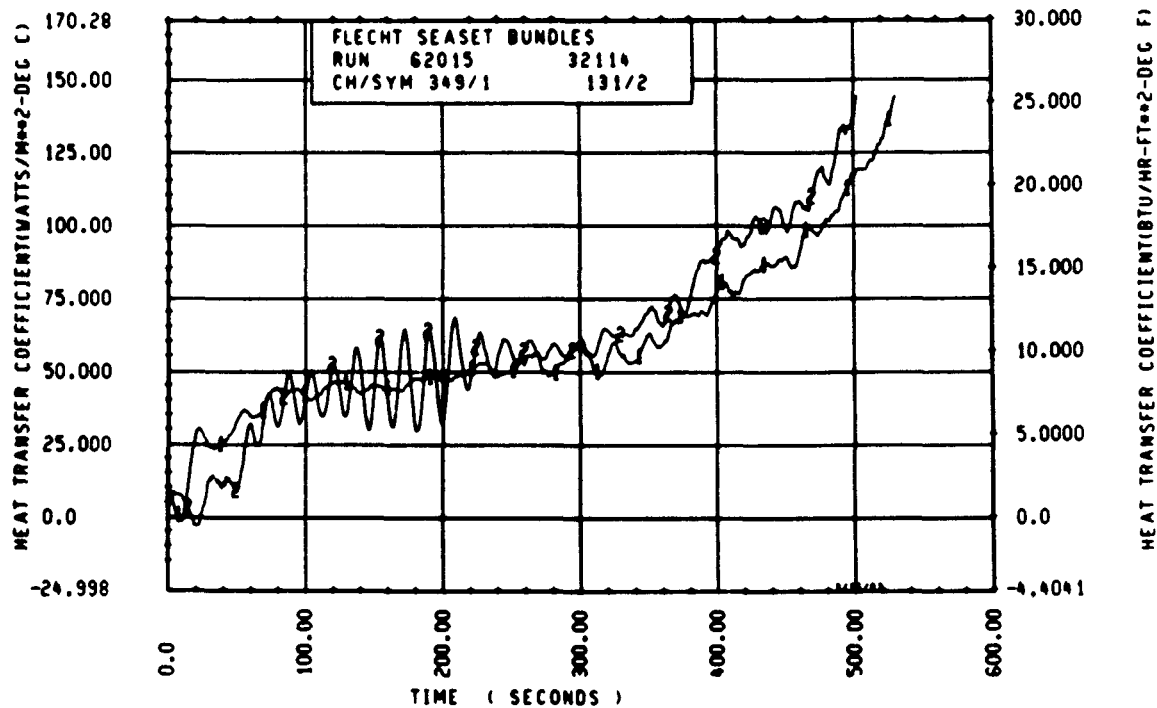
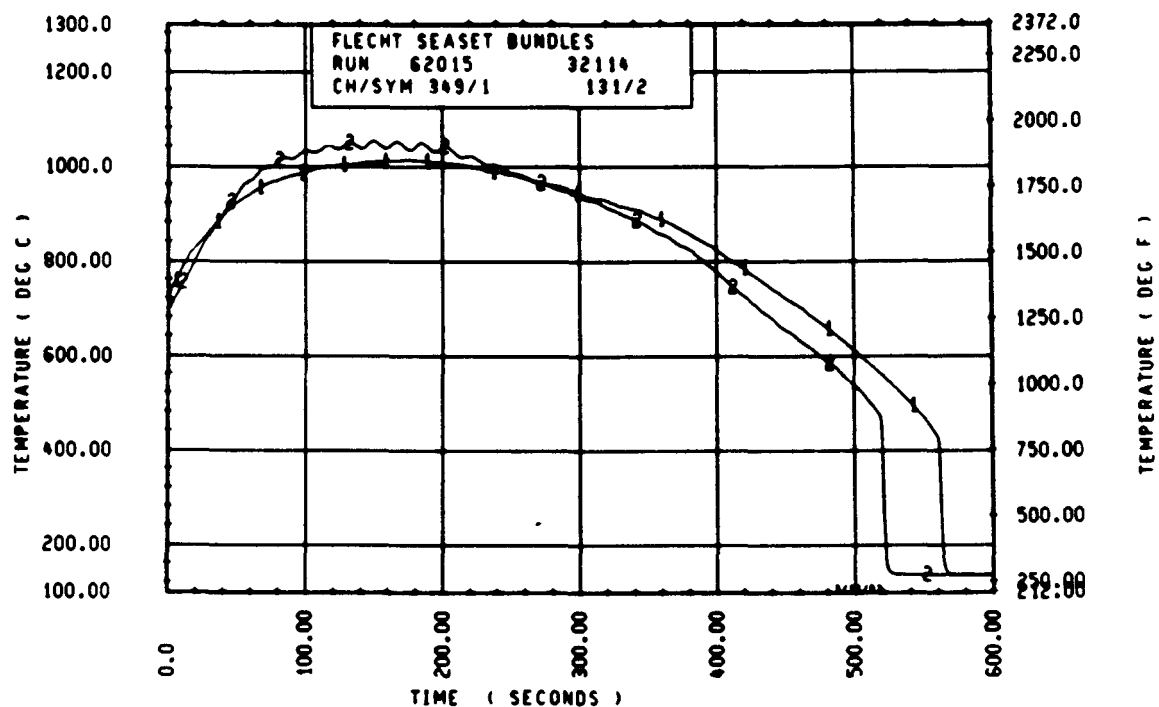
Rod 11K, 1.98 m (78 in.)



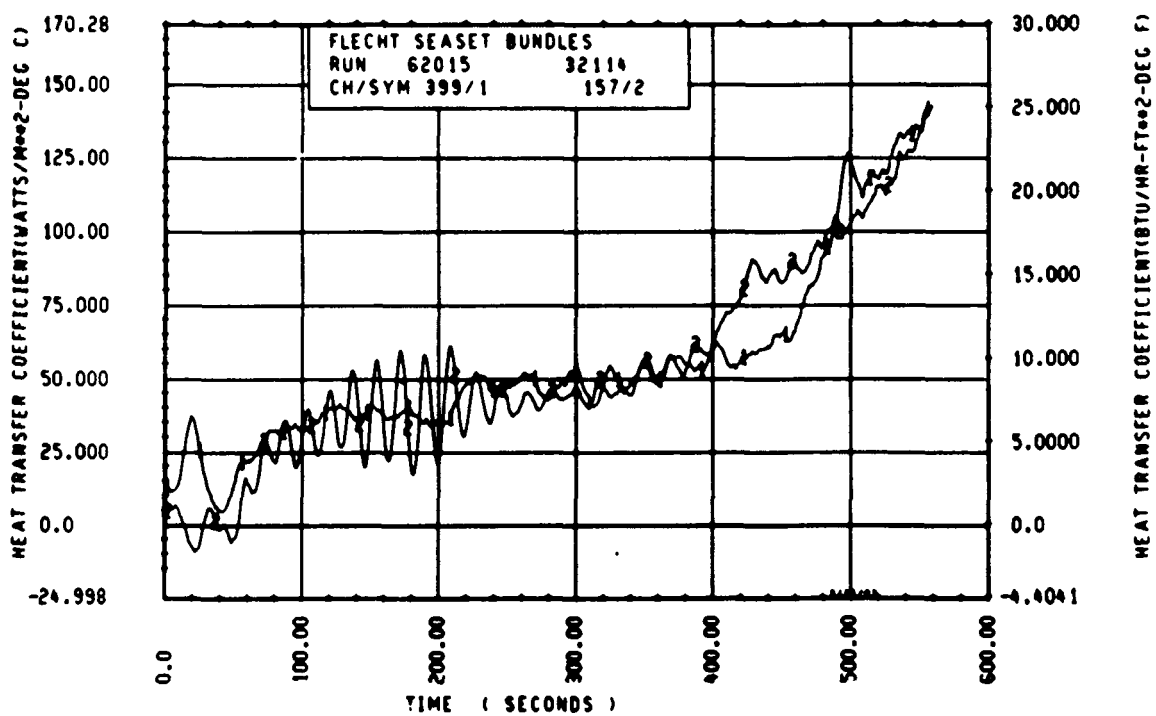
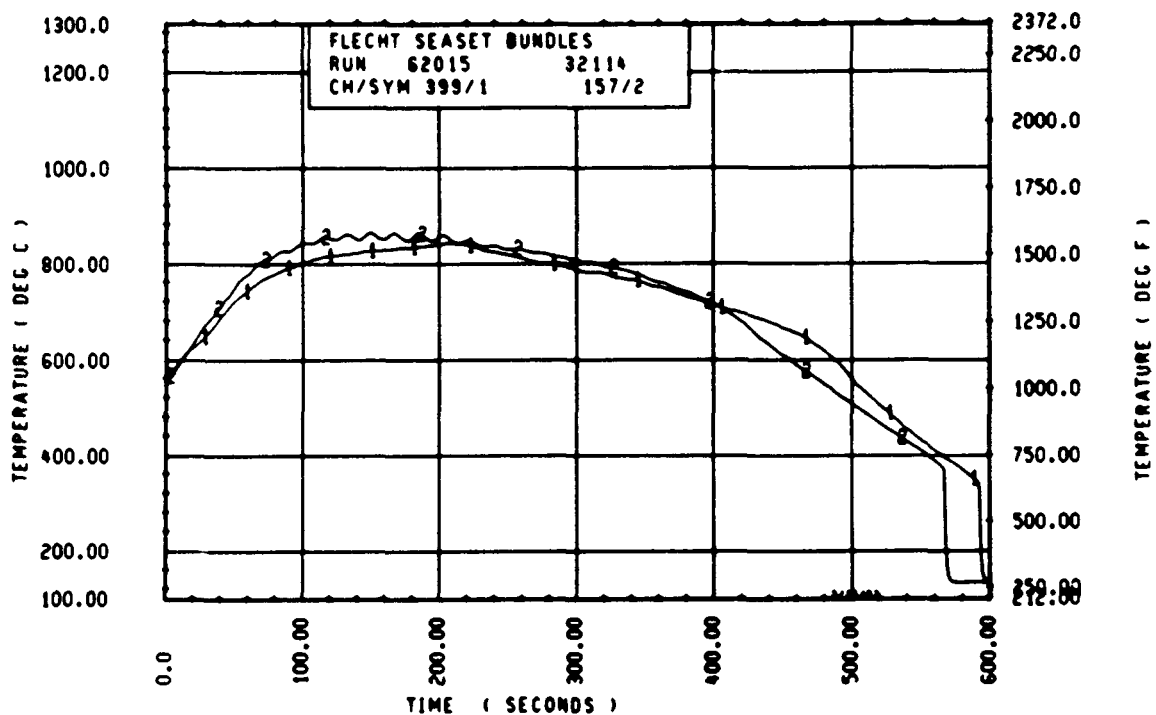
Rod 7E, 2.13 m (84 in.)



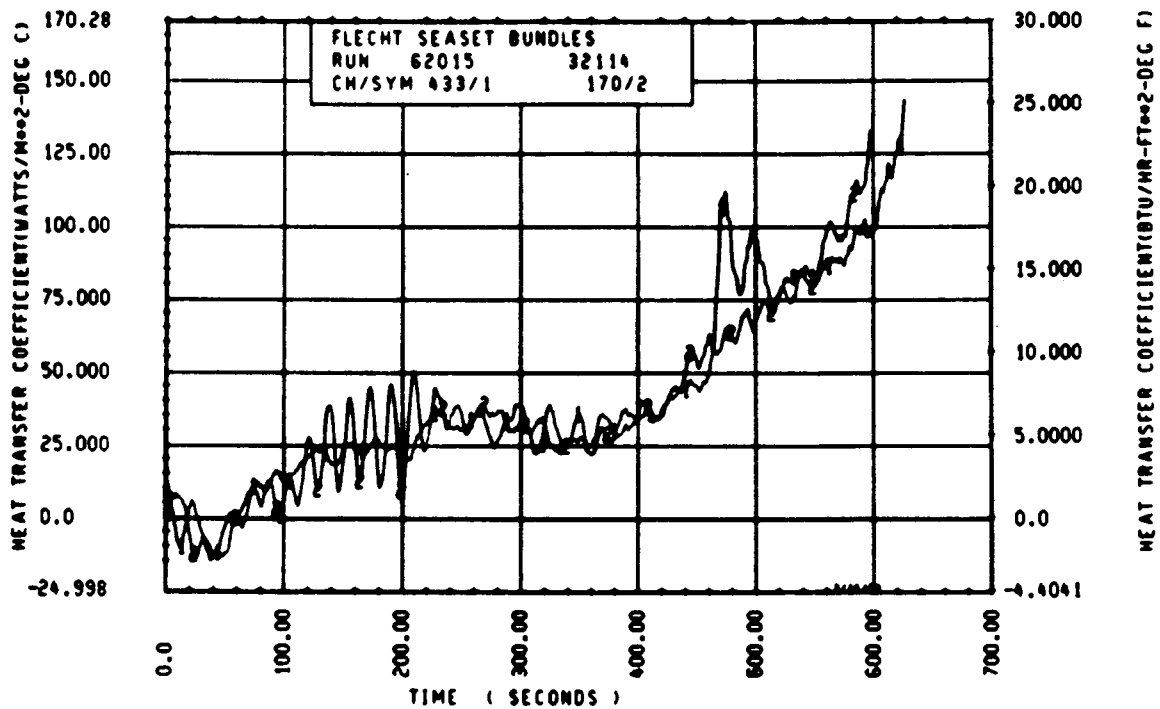
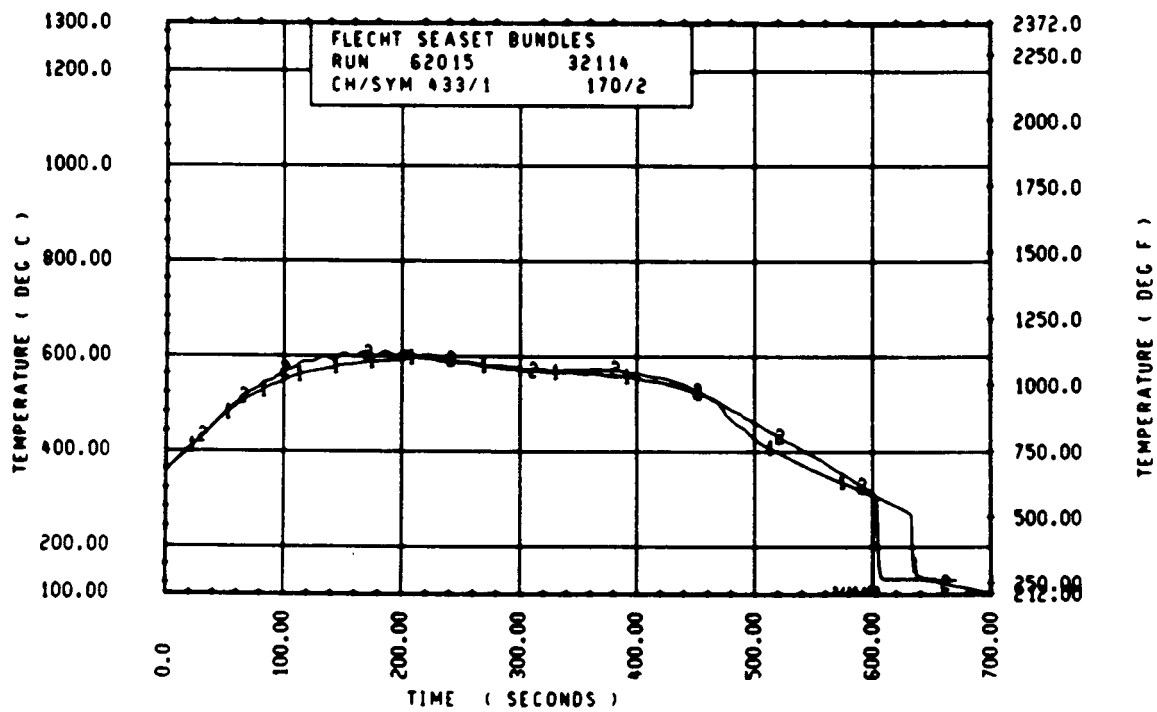
Rod 9C, 2.29 m (90 in.)



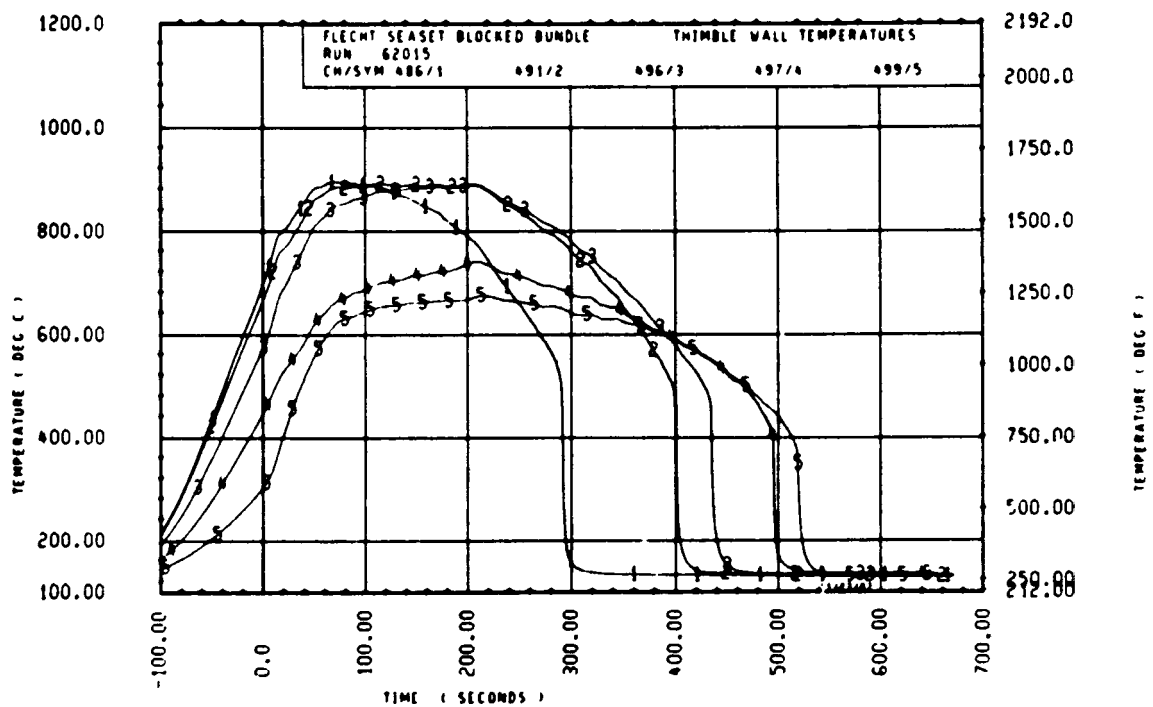
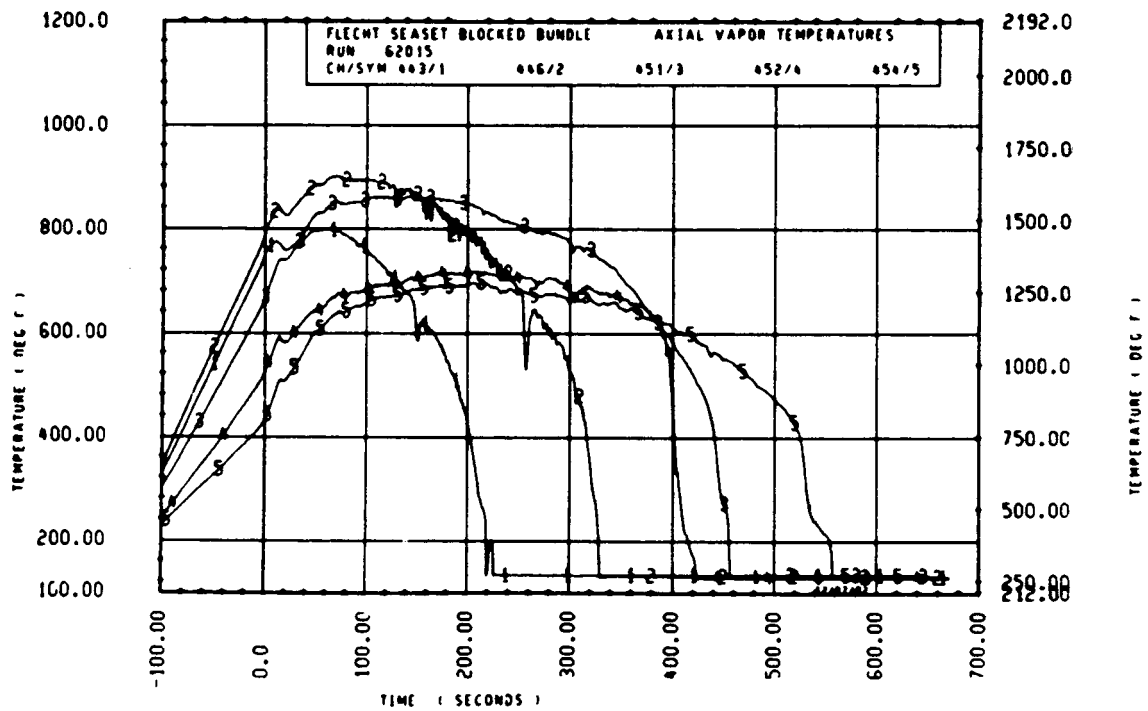
Rod 8E, 2.44 m (96 in.)

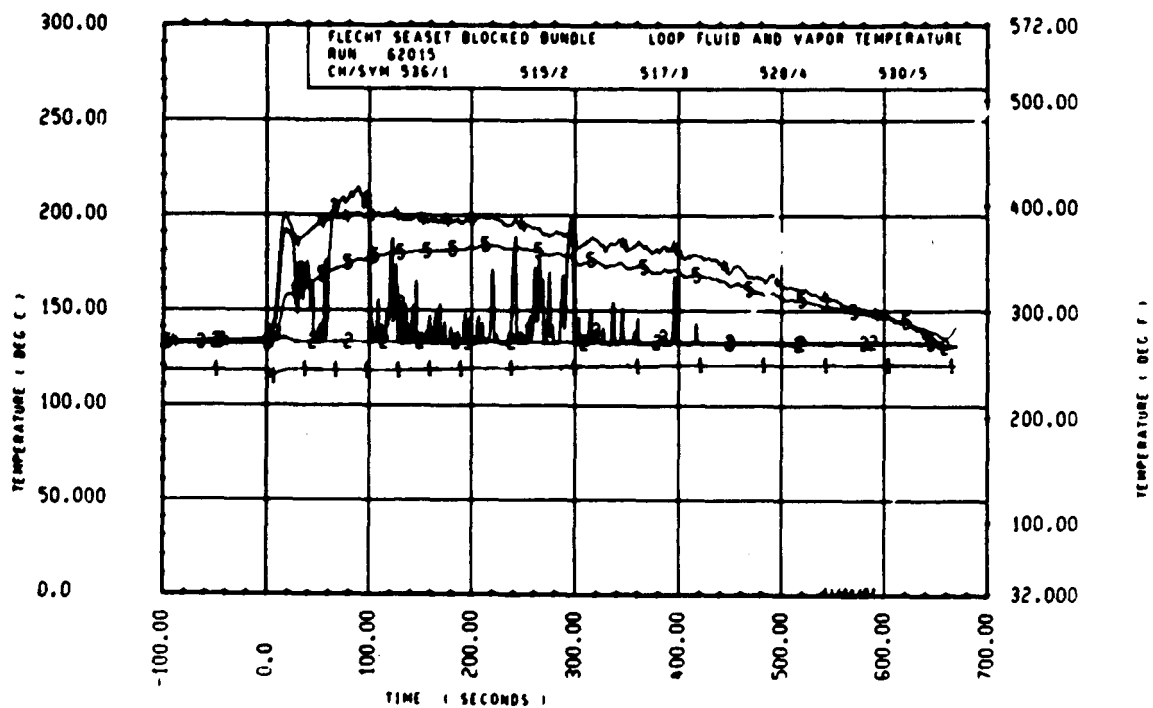
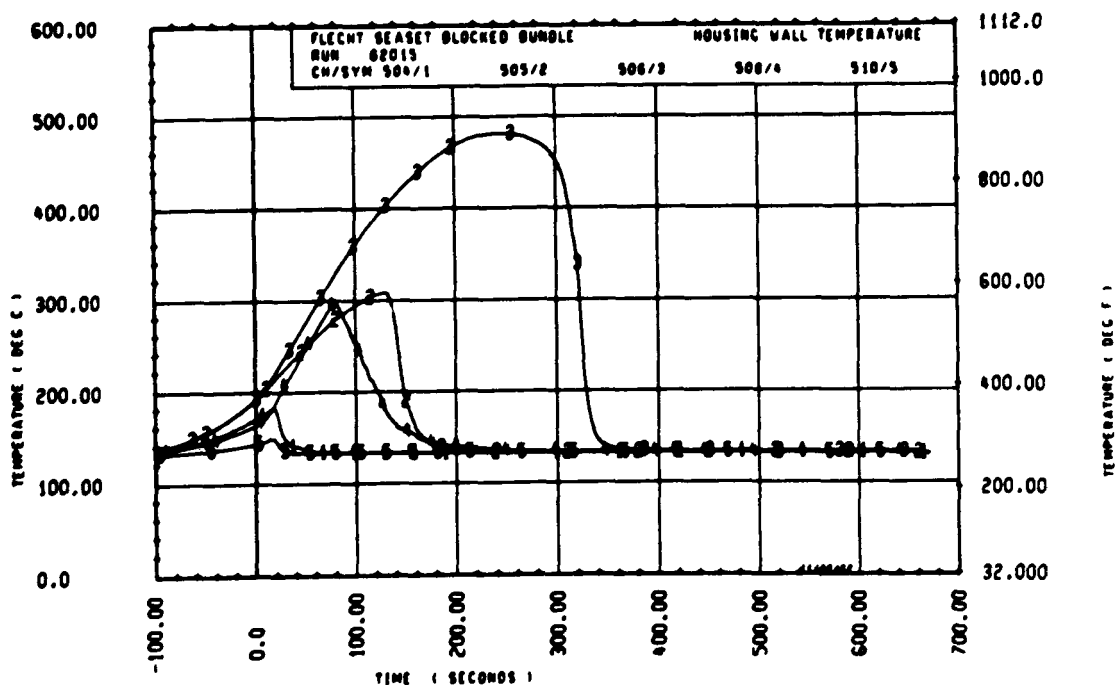


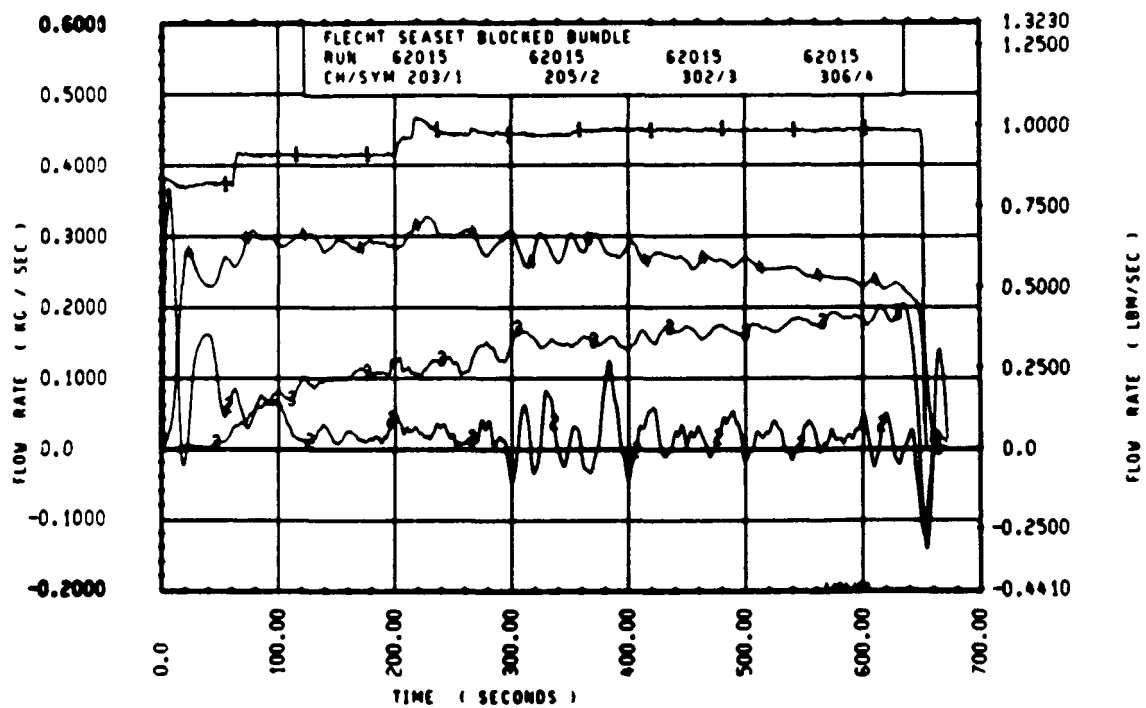
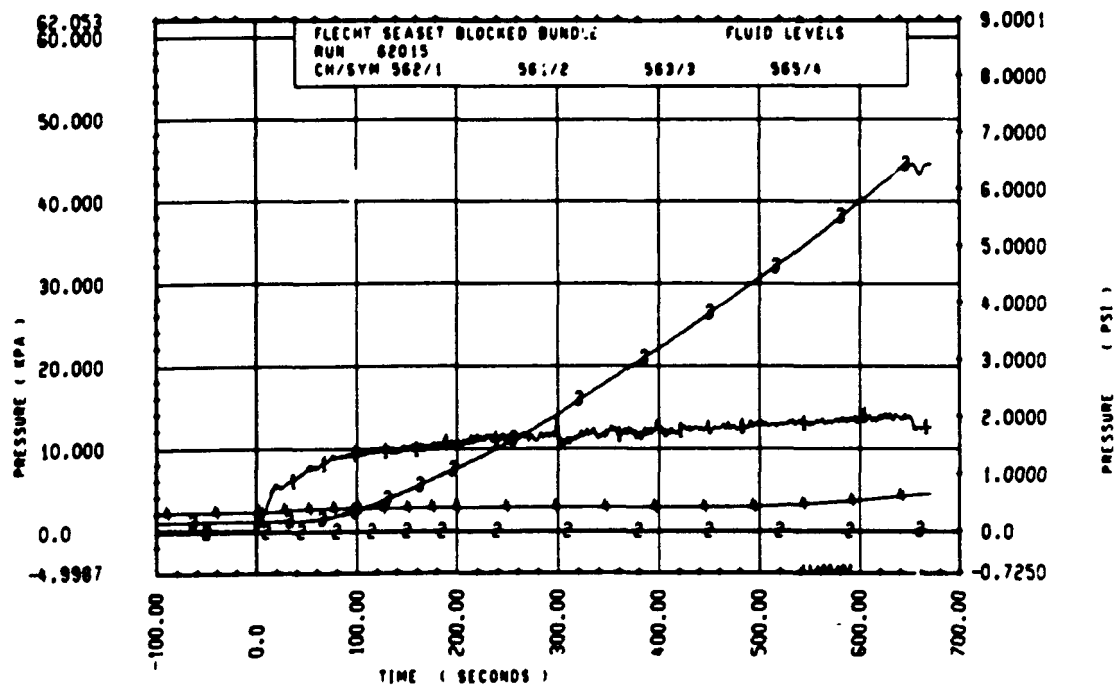
Rod 13G, 2.82 m (111 in.)

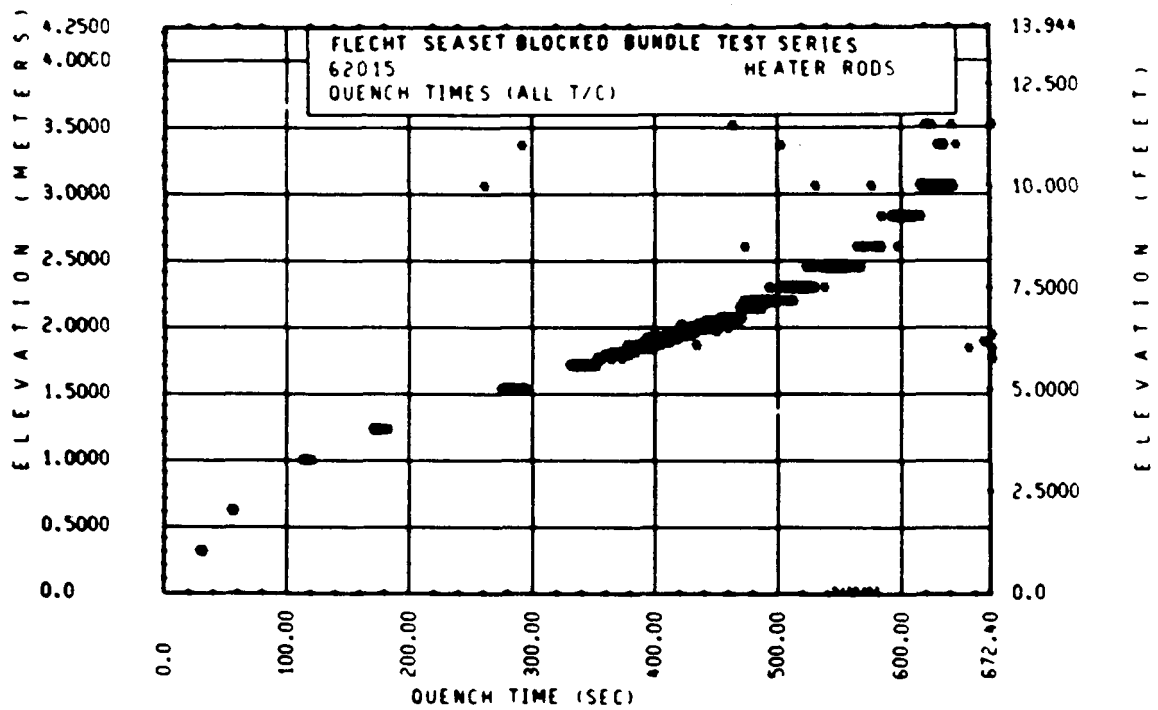
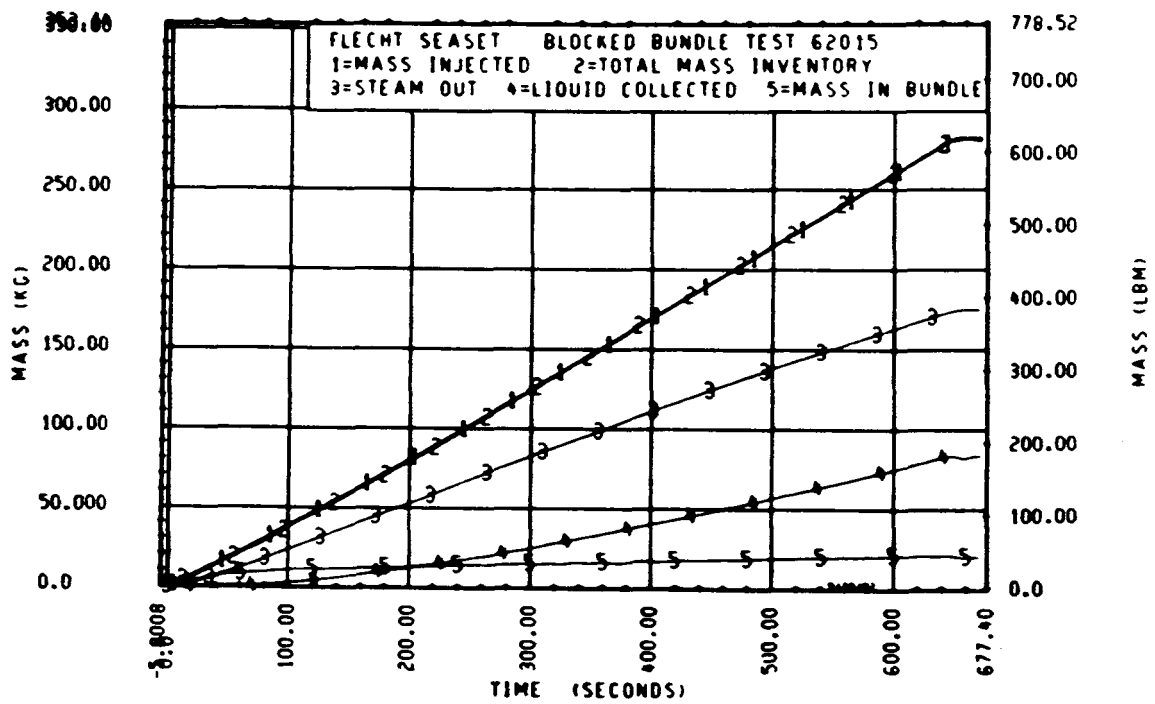


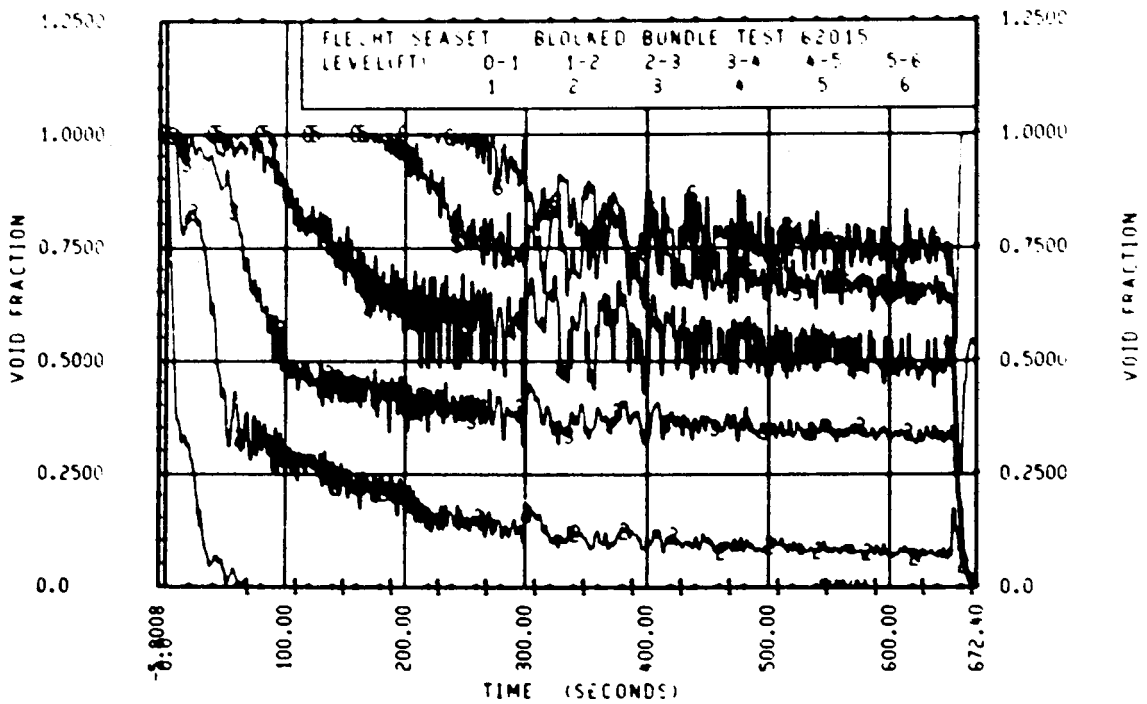
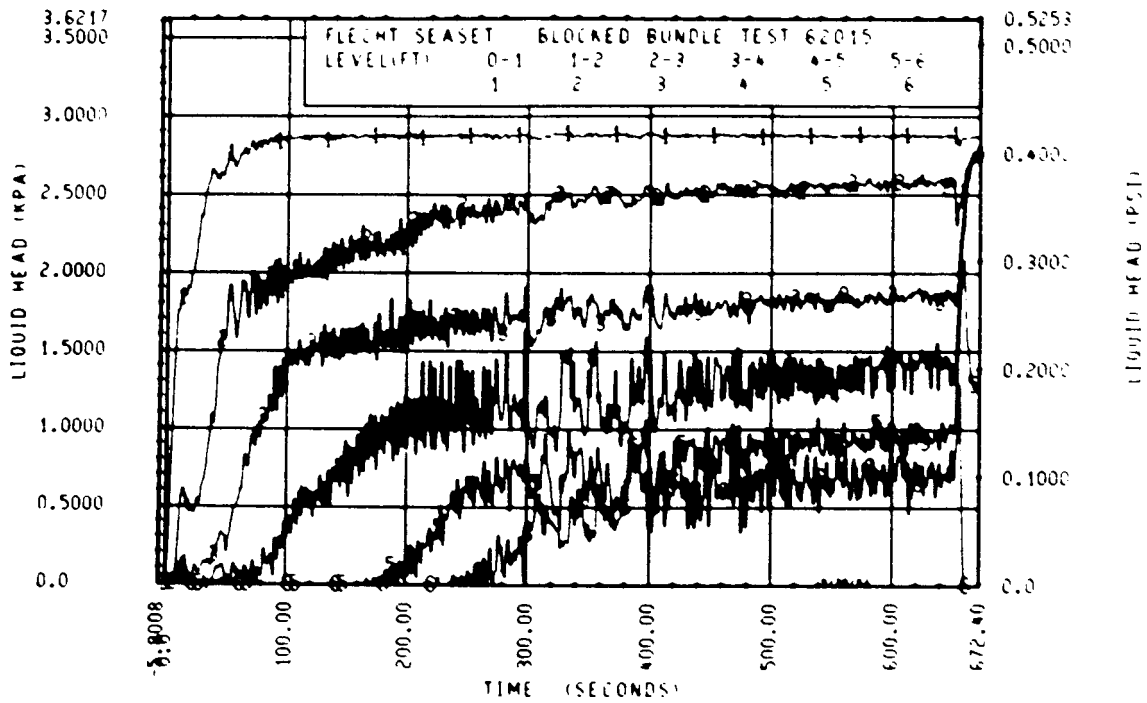
Rod 11G, 3.35 m (132 in.)

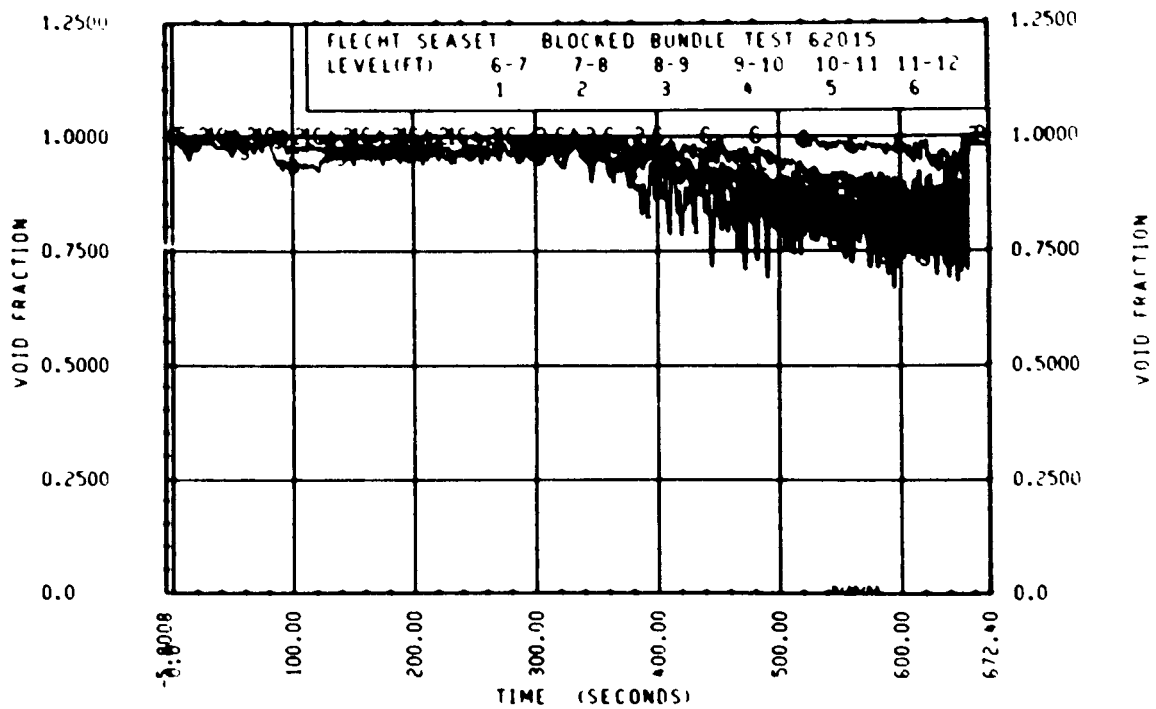
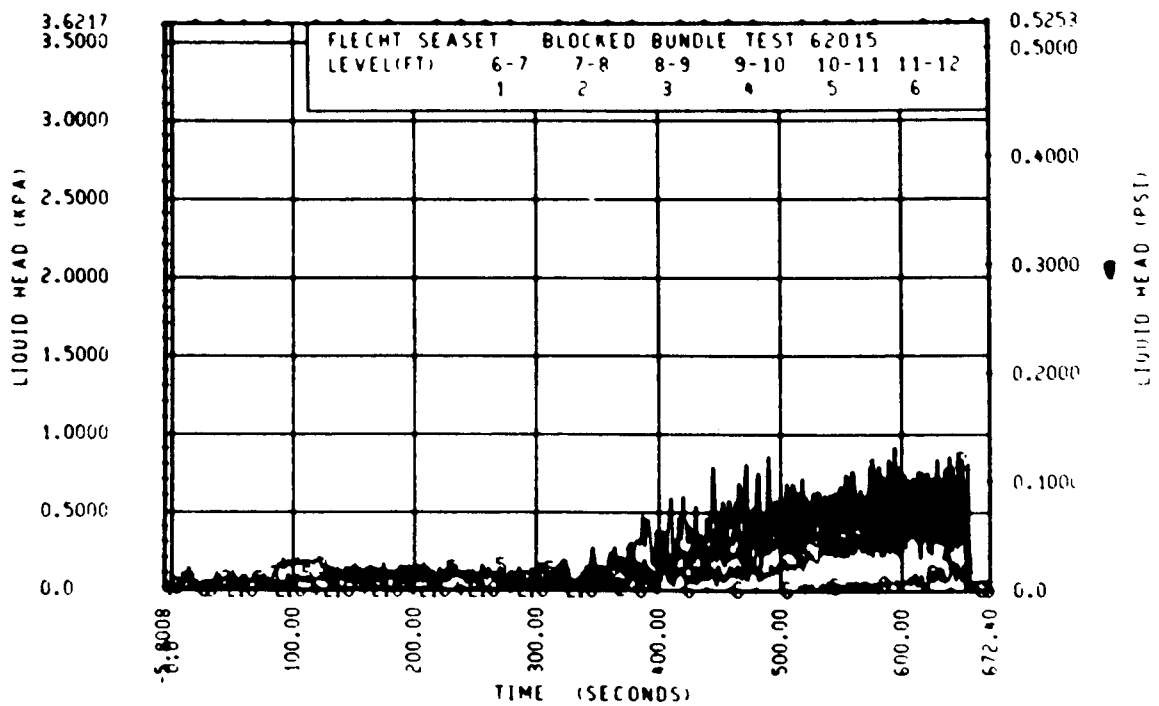












FLECHT SEASET 163-ROD BUNDLE FLOW BLOCKAGE TASK
SUMMARY AND COMMENT SHEET

Run: 62117
Test date: 9/21/82
Test type: Forced reflood
Parameter: Hot/cold channel effect

AS-RUN TEST CONDITIONS:

Upper plenum pressure	0.277 MPa (40.2 psia)
Initial peak clad temperature and location	871.6°C (1600.9°F), 7G-1.70 m (67 in.)
Initial peak rod power:	
Peripheral rods	1.31 kw/m (0.400 kw/ft)
Bypass rods	1.31 kw/m (0.400 kw/ft)
Blockage island rods	2.31 kw/m (0.705 kw/ft)
Flooding rate	20 mm/sec (0.79 in./sec)
Coolant temperature	53°C (127°F)
Initial bundle water level	-6.98 mm (-0.275 in.)

COMMENTS:

There was no corresponding test conducted in the 161-rod unblocked bundle; however, rod temperatures and heat transfer coefficients were compared to those of run 61607, which was run at the same conditions but with a uniform power profile.

FLECHT SEASET 163 ROD BUNDLE TEST SERIES
RUN NUMBER 62117

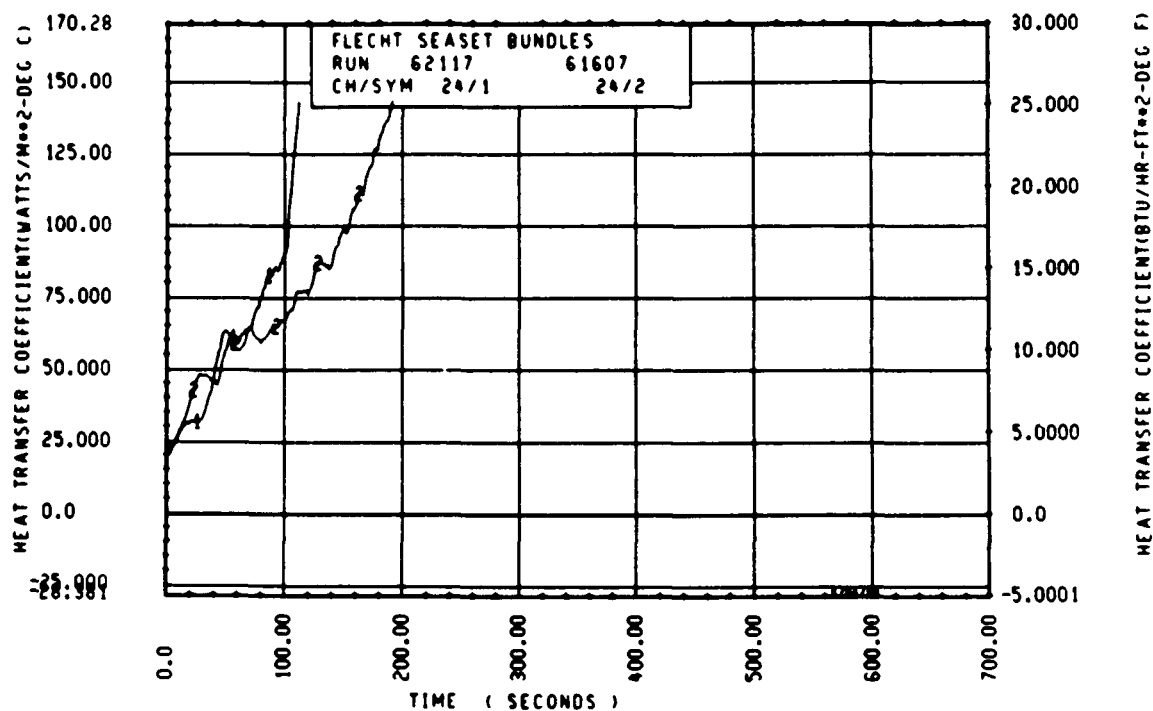
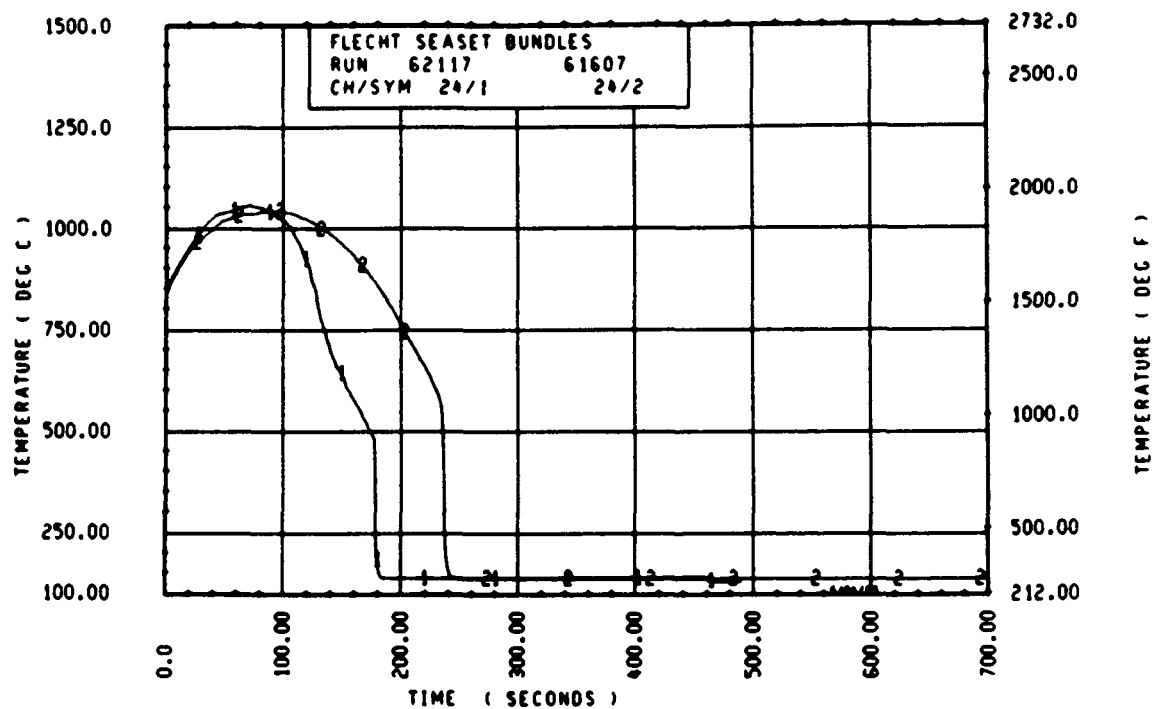
ROD/ELEV	CHAN. NO	TEMPERATURE AT FLECHT (DEG F)	MAXIMUM TEMPERATURE (DEG F)	TEMPERATURE RISE (DEG F)	TURNAROUND TIME (SECONDS)	QUENCH TEMPERATURE (DEG F)	QUENCH TIME (SECONDS)
96 1- 0	3	692.	721.	29.	9.0	586.	25.0
10M 2- 0	6	903.	981.	78.	19.0	683.	51.0
96 3- 3	9	1243.	1430.	186.	35.0	783.	92.0
3J 4- 0	11	960.	1118.	159.	50.5	704.	111.1
7H 4- 0	12	1330.	1584.	247.	45.5	766.	130.0
6A 4- 0	13	1053.	1292.	239.	53.0	766.	118.6
6M 4- 0	14	953.	1118.	165.	49.0	747.	108.3
12D 4- 0	17	956.	1112.	155.	49.5	742.	109.6
5E 5- 0	20	1446.	1761.	313.	67.5	899.	178.4
76 5- 0	21	1587.	1953.	366.	69.0	891.	176.6
46 5- 0	24	1500.	1936.	369.	71.0	886.	177.4
5E 5- 7	33	1464.	1867.	403.	92.5	906.	209.6
86 5- 7	45	1571.	2078.	508.	107.0	935.	217.0
4H 5- 9	52	1515.	2058.	543.	106.0	1014.	220.0
76 5-10	59	1520.	2061.	532.	107.5	943.	225.0
7F 5-11	62	1478.	2044.	567.	107.0	999.	231.6
46 5-11	64	1132.	1647.	515.	99.0	920.	220.0
21 6- 0	67	1114.	1445.	330.	93.5	836.	223.0
5D 6- 0	70	1134.	1495.	361.	109.0	964.	221.7
6J 6- 0	74	1072.	1553.	481.	107.0	867.	228.0
7H 6- 0	66	1073.	1434.	361.	99.0	803.	220.5
11E 6- 0	80	1096.	1560.	462.	109.0	871.	224.0
8H 6- 2	97	1388.	2052.	664.	161.5	902.	257.0
5H 6- 2	99	1166.	1718.	552.	110.0	937.	241.9
9E 6- 2	105	1246.	1869.	623.	128.0	1366.	227.2
8H 6- 3	111	1427.	2063.	636.	164.0	931.	263.2
46 6- 3	124	1148.	1653.	505.	106.0	877.	245.6
11M 6- 4	134	1446.	1976.	527.	146.5	794.	262.0
9D 6- 4	143	1180.	1773.	588.	128.0	923.	253.0
9J 6- 5	165	1511.	2050.	539.	149.5	936.	277.6
9M 6- 5	166	1114.	1563.	449.	112.0	889.	247.7
8J 6- 6	192	1503.	1930.	426.	133.5	926.	274.1
9J 6- 6	193	1189.	1772.	583.	126.5	921.	266.0
11F 6- 6	173	1161.	1704.	543.	121.0	891.	257.0
46 7- 0	261	1093.	1564.	471.	98.5	730.	289.1
7D 7- 6	309	1442.	1983.	540.	142.5	844.	340.6
76 7- 6	312	1536.	2158.	620.	153.5	1105.	303.6
11E 7- 6	325	1030.	1630.	600.	137.0	833.	320.0
5L 8- 0	337	914.	1396.	482.	139.0	727.	351.1
7H 8- 0	345	1354.	2092.	738.	178.0	799.	368.1
7K 8- 0	346	985.	1586.	600.	159.5	824.	341.7
5J 8- 6	366	810.	1399.	581.	202.1	636.	375.1
7K 8- 6	368	820.	1343.	554.	129.5	639.	374.5
7E 9- 3	383	1106.	1870.	764.	174.5	736.	410.7
8A 9- 3	387	1060.	1874.	808.	182.5	718.	409.1
9C 9- 3	389	771.	1341.	569.	187.0	664.	394.1
11F 9- 3	394	822.	1446.	623.	200.1	860.	365.2
7B 10- 0	408	626.	1170.	544.	169.0	809.	372.1
8M 10- 0	415	886.	1581.	695.	211.1	656.	433.2
8K 10- 0	417	601.	1261.	580.	231.1	681.	406.1
8M 10- 0	418	633.	1104.	471.	141.5	620.	407.5
6M 11- 0	429	690.	1006.	310.	228.1	350.	430.1
96 11- 0	431	703.	1342.	639.	183.5	873.	309.8
11E 11- 0	432	534.	1032.	498.	179.5	511.	394.4
5J 11- 6	436	520.	711.	191.	290.1	605.	375.1
7B 11- 6	437	490.	931.	441.	241.1	774.	367.4
8J 11- 6	438	693.	1037.	344.	221.1	567.	434.7

KUM 62117 HEATER ROD STATISTICAL DATA

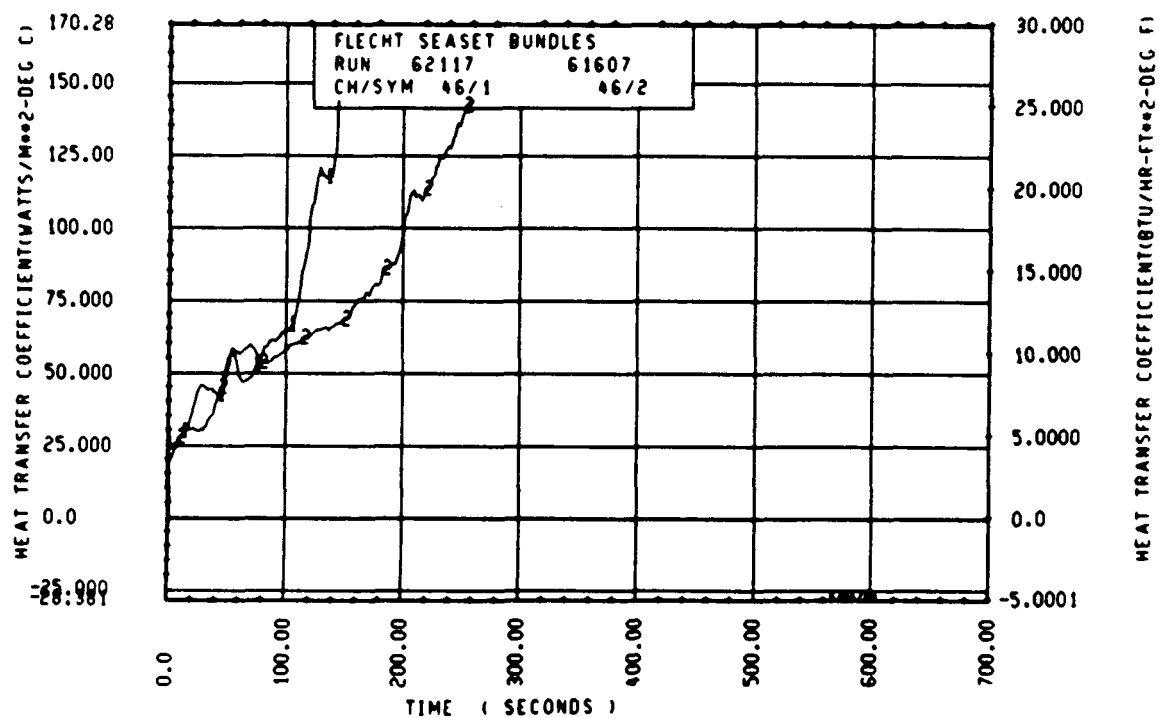
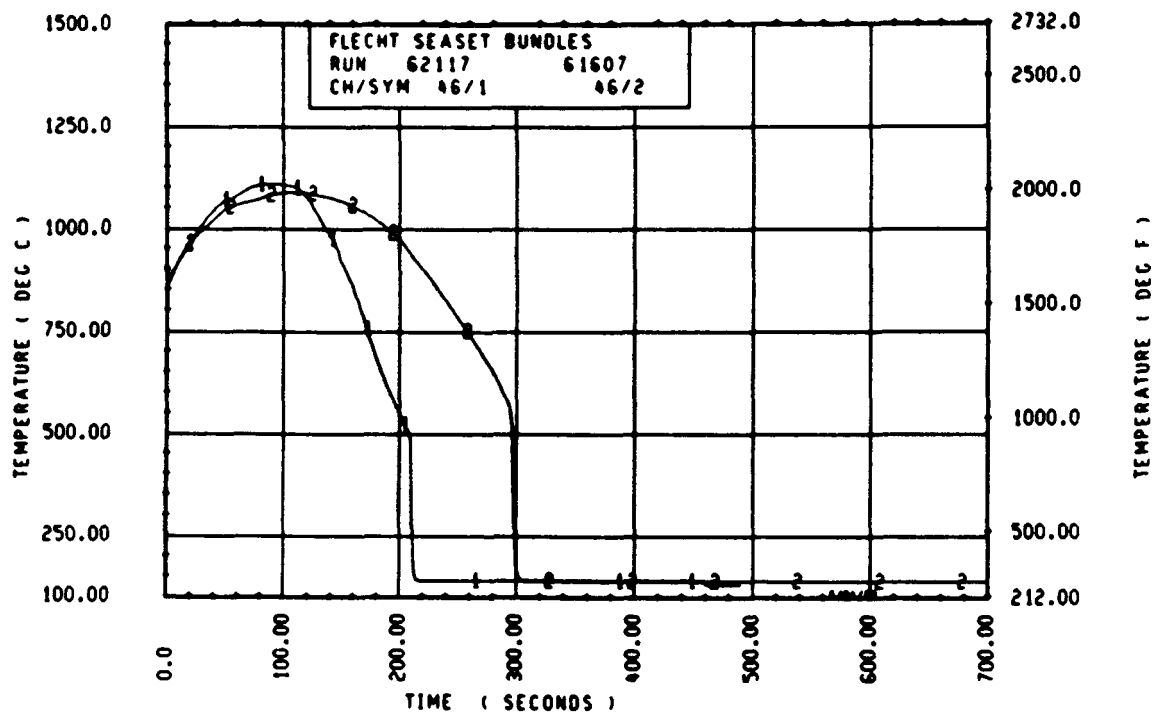
ELEV	INITIAL TEMP (DEG F)			MAX TEMP (DEG F)			TURNAROUND TIME (SEC)		
	MAX	MIN	MEAN	MAX	MIN	MEAN	MAX	MIN	MEAN
12	692.1	519.9	577.6	721.4	536.9	599.1	9.0	8.0	8.5
24	902.9	636.5	727.0	981.3	680.6	782.5	20.0	19.0	19.7
39	1243.1	835.7	965.7	1429.6	953.4	1101.3	36.0	35.0	35.7
48	1363.8	953.4	1124.7	1603.1	1112.3	1334.0	53.0	41.0	48.2
60	1586.8	1019.4	1277.0	1952.8	1243.1	1584.6	80.5	56.0	71.3
67	1600.9	1065.8	1295.2	2078.2	1341.6	1667.3	107.0	77.0	90.2
69	1515.3	1073.0	1230.7	2058.3	1433.8	1666.8	106.0	95.0	99.4
70	1528.3	1059.6	1166.4	2060.7	1370.1	1556.0	107.5	86.0	97.1
71	1477.7	1048.3	1282.0	2044.3	1392.3	1772.3	110.0	98.5	103.6
72	1147.5	1066.8	1100.8	1757.9	1403.9	1546.6	131.0	90.5	104.4
73	1130.9	1031.6	1086.3	1727.7	1405.0	1529.3	121.5	91.0	107.6
74	1390.2	1067.9	1165.6	2052.5	1427.4	1658.0	161.5	95.5	118.5
75	1443.5	1074.1	1212.7	2063.0	1428.5	1698.1	164.0	94.5	122.5
76	1448.8	1081.3	1187.9	2013.9	1436.0	1651.4	149.0	96.0	117.7
77	1520.7	1075.1	1354.7	2070.0	1456.3	1824.3	159.0	95.0	124.5
78	1568.4	1080.2	1340.3	2130.3	1451.0	1812.1	159.0	94.5	125.4
79	1595.5	1052.4	1385.9	2166.4	1447.8	1855.7	160.5	105.5	127.3
80	1594.4	1061.7	1339.7	2154.1	1439.2	1821.8	159.5	96.5	124.4
81	1579.3	1017.4	1395.4	2168.4	1455.2	1868.9	160.5	103.0	129.6
84	1546.7	1021.5	1225.4	2155.3	1414.6	1696.4	158.0	96.5	123.1
86	1589.0	1030.7	1362.8	2191.1	1393.3	1857.9	162.5	92.0	132.9
90	1538.1	713.0	1315.4	2210.4	1384.9	1881.1	163.5	90.5	141.4
96	1421.1	903.9	1183.5	2168.4	1348.0	1810.9	180.0	93.5	151.2
102	1196.2	751.5	1035.3	2046.6	1382.8	1741.6	202.1	124.5	156.7
111	1120.6	744.3	968.1	1903.3	1140.2	1643.4	224.1	139.5	178.7
120	935.9	608.1	777.7	1727.7	965.8	1408.5	244.1	93.0	180.4
132	702.6	532.6	647.6	1350.1	765.1	1127.6	228.1	64.0	177.2
138	693.2	489.5	575.2	1096.7	710.9	938.9	290.1	116.0	207.0

KUM 62117 HEATER ROD STATISTICAL DATA

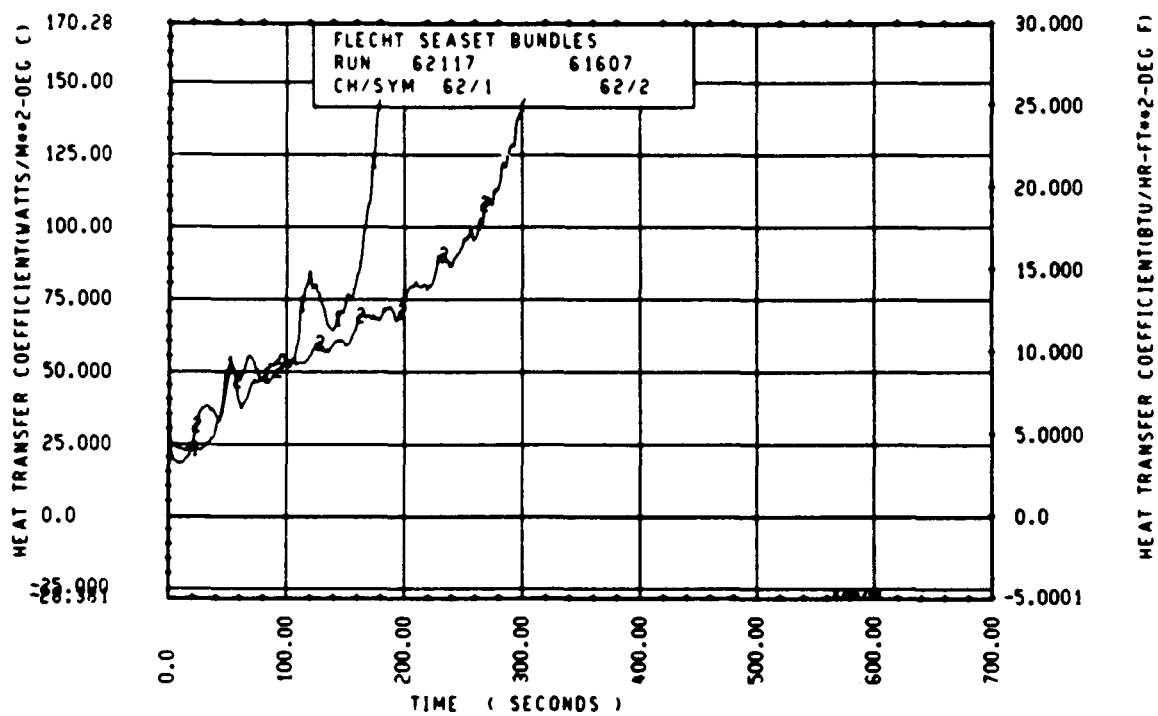
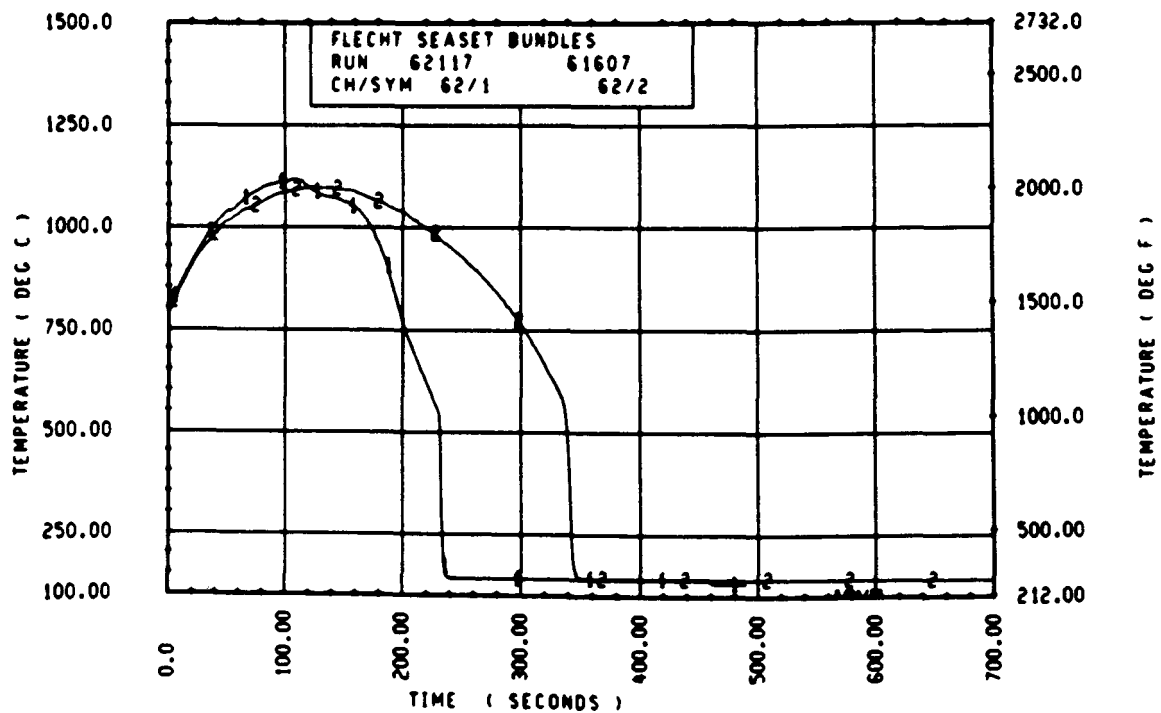
ELEV	TEMP RISE (DEG F)			QUENCH TEMP (DEG F)			QUENCH TIME (SEC)		
	MAX	MIN	MEAN	MAX	MIN	MEAN	MAX	MIN	MEAN
12	29.2	17.0	21.4	588.0	498.5	529.8	25.0	16.5	19.5
24	78.4	44.1	55.5	682.6	589.2	628.8	51.8	33.0	40.8
39	186.5	111.4	135.6	783.0	719.8	755.0	92.6	73.8	79.7
48	249.9	154.7	209.3	827.3	709.0	760.9	130.0	108.3	118.2
60	370.0	223.7	307.6	910.9	783.5	850.7	178.4	161.3	171.2
67	507.6	257.6	372.1	935.0	781.4	862.6	217.0	191.7	201.6
69	543.0	360.6	436.1	1013.7	831.9	904.2	220.0	199.4	210.1
70	532.3	284.4	389.6	1006.2	803.3	888.0	225.8	206.0	212.5
71	566.6	344.0	490.3	999.1	810.7	927.9	231.9	217.7	224.3
72	639.0	305.1	445.8	1018.1	792.8	880.5	231.1	219.9	224.0
73	608.5	309.7	441.1	995.4	809.7	881.9	233.1	216.9	227.0
74	664.4	316.2	492.4	962.2	795.0	872.7	260.1	230.7	240.5
75	635.5	318.5	485.5	1292.2	666.6	911.1	266.9	226.3	245.1
76	587.7	333.4	463.5	978.6	793.9	886.4	263.0	231.9	248.7
77	575.2	364.0	464.6	960.7	793.9	884.1	290.9	247.7	265.8
78	583.4	343.9	471.9	1162.0	711.3	908.5	295.8	249.3	268.1
79	620.3	360.3	469.8	1114.4	795.7	921.7	289.8	248.0	272.4
80	639.9	367.2	482.1	1039.0	810.2	905.7	294.8	261.7	277.9
81	597.8	347.3	473.5	1033.6	776.7	903.1	298.5	267.7	286.4
84	608.6	360.1	470.4	1003.6	679.5	773.3	312.6	282.6	293.5
86	606.5	331.6	495.2	1103.9	703.7	803.3	331.1	276.0	306.6
90	746.5	354.1	561.7	1144.5	746.2	874.5	343.1	303.9	327.0
96	781.3	396.6	627.4	1023.2	701.2	837.2	369.1	338.5	353.6
102	850.5	554.4	706.3	769.3	596.6	700.1	391.4	369.1	381.8
111	808.3	376.2	675.3	999.1	614.4	727.6	415.3	243.6	394.6
120	827.7	357.7	630.8	1173.7	590.1	699.7	435.9	239.0	397.2
132	648.5	232.4	480.0	873.2	479.0	563.4	440.1	309.8	406.8
138	440.9	191.1	363.8	974.2	567.4	747.8	439.7	160.7	296.0



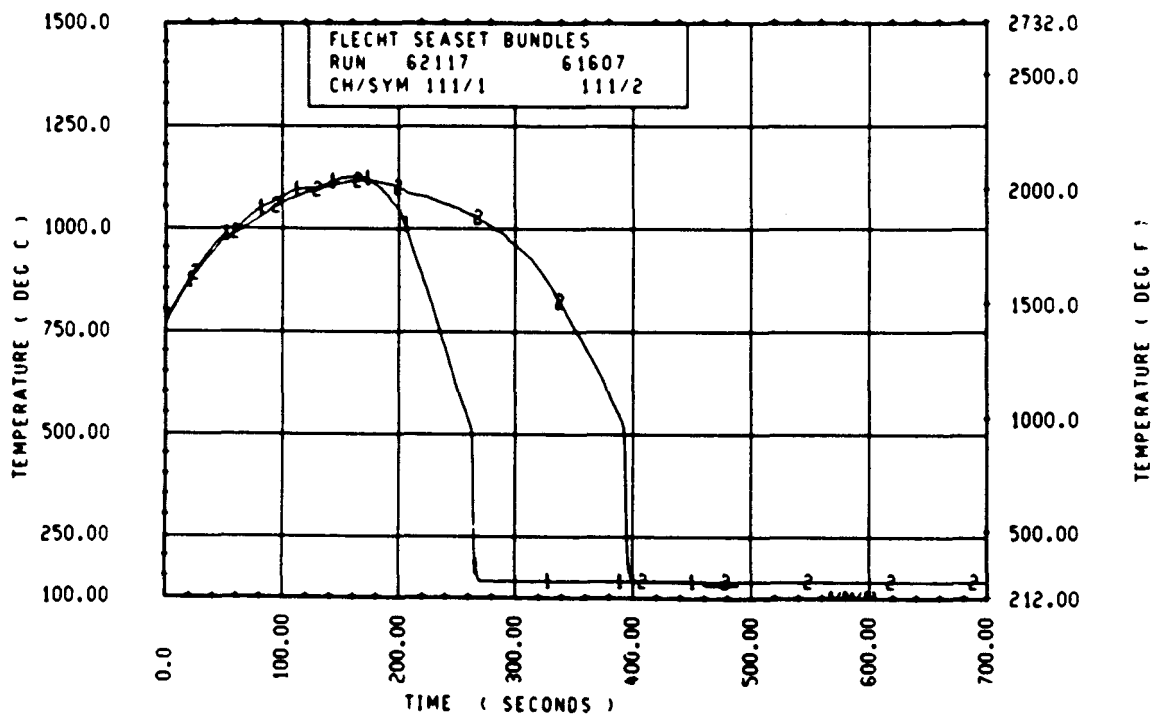
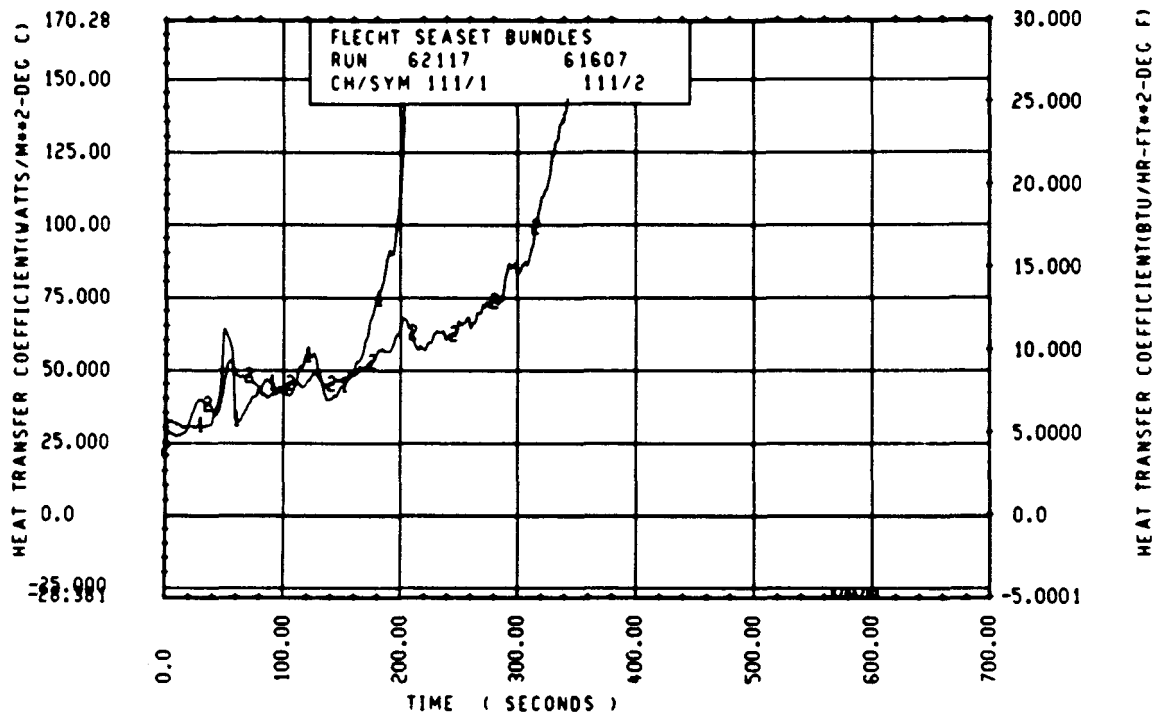
Rod 9G, 1.52 m (60 in.)



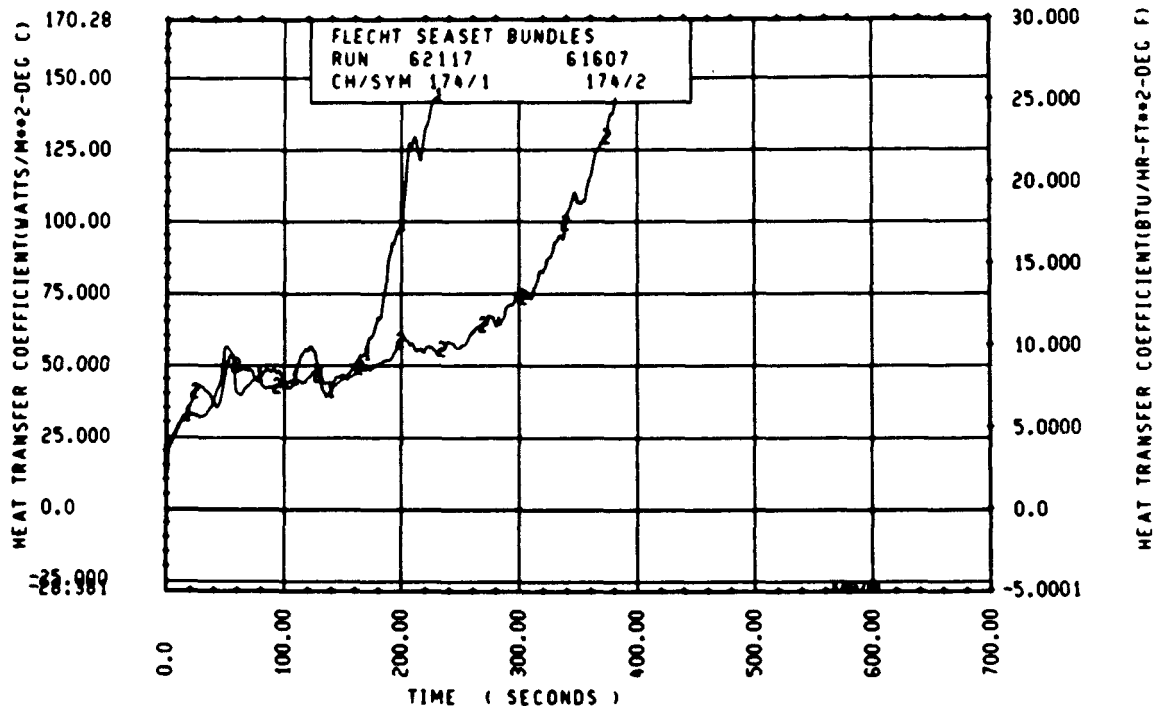
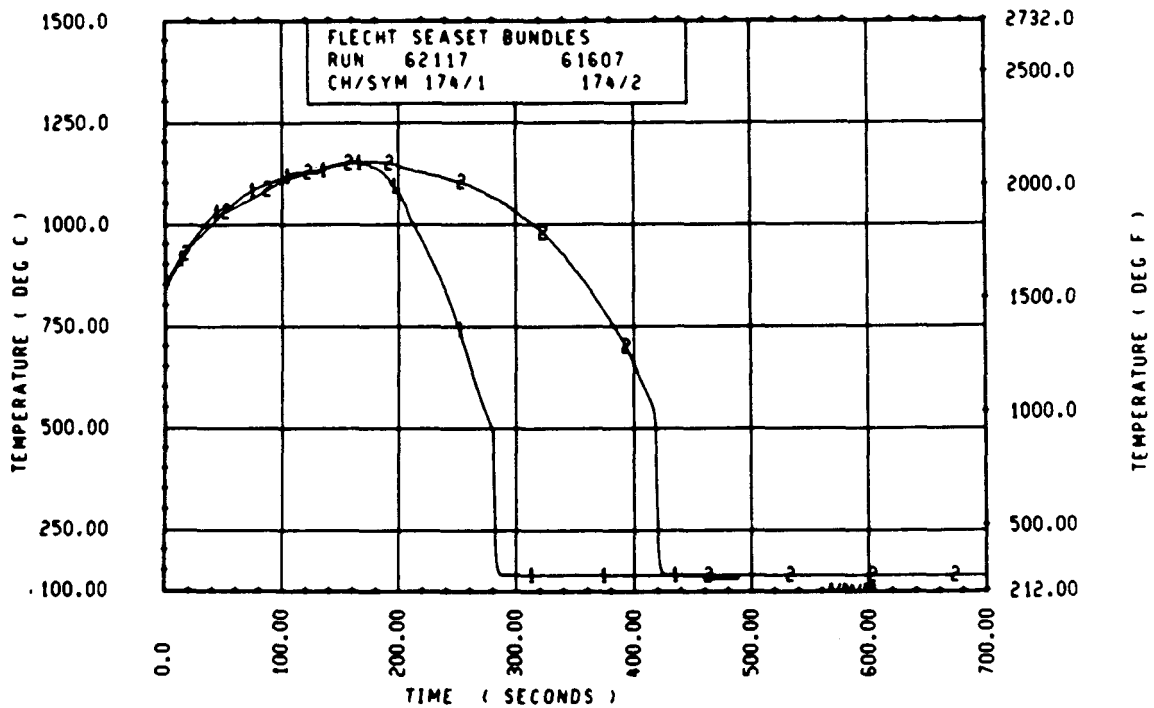
Rod 9G, 1.70 m (67 in.)



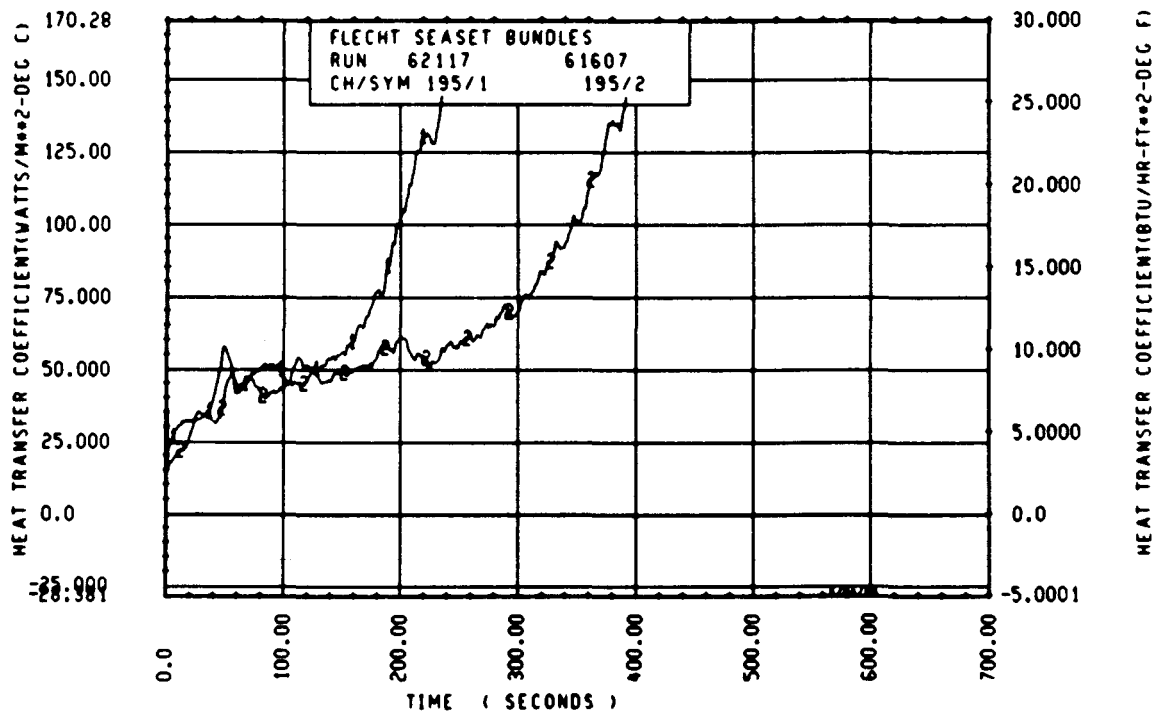
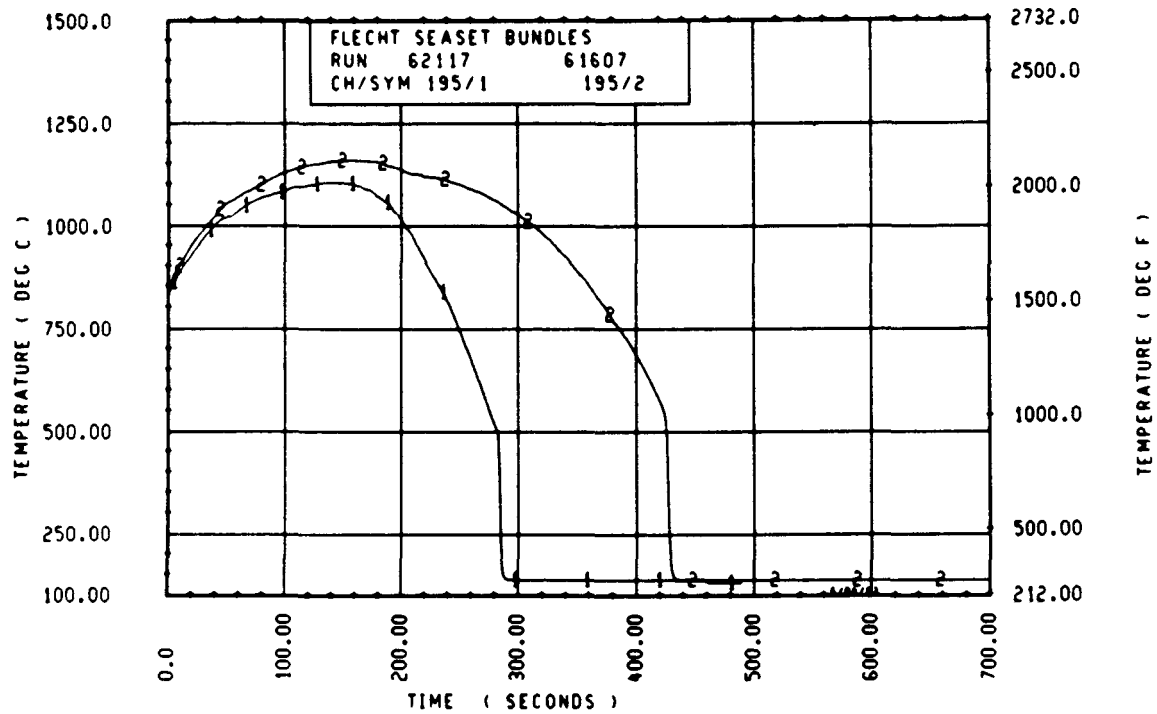
Rod 7F, 1.80 m (71 in.)



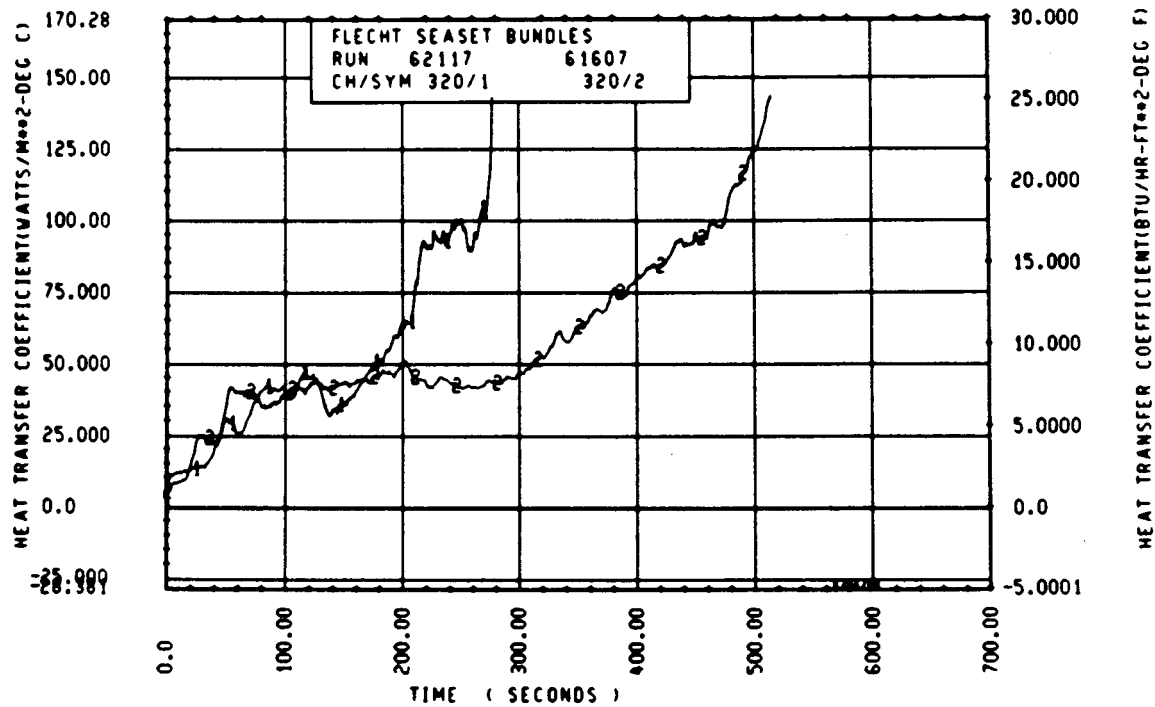
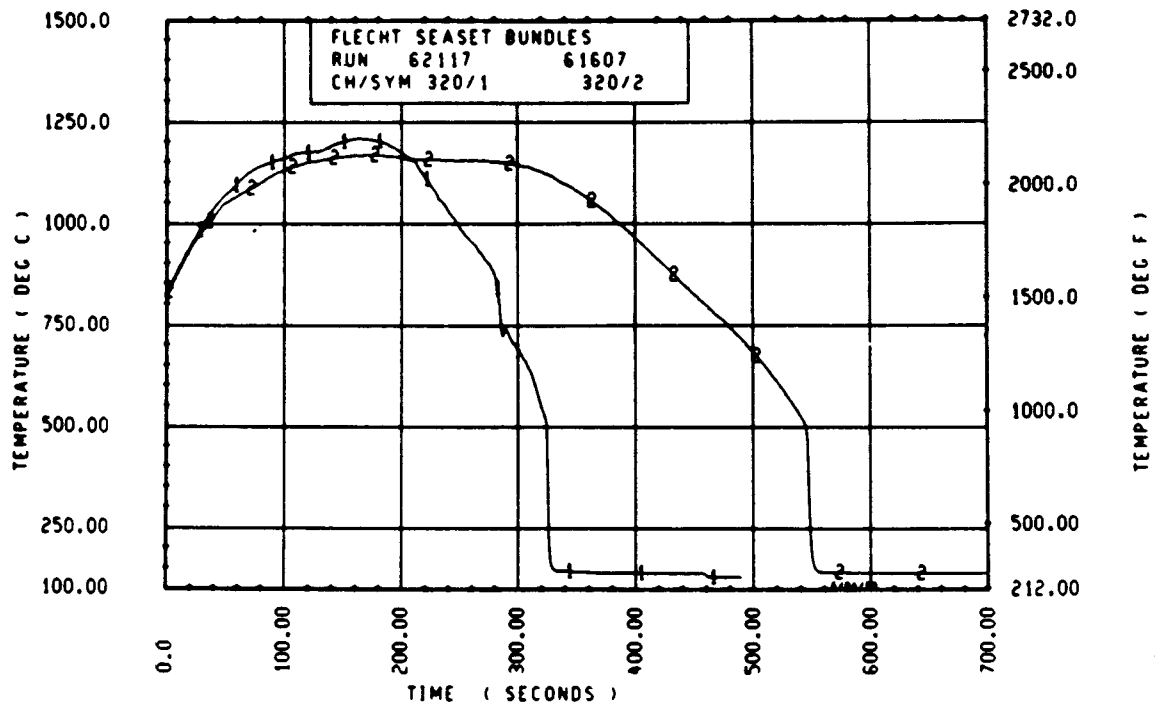
Rod 8H, 1.91 m (75 in.)



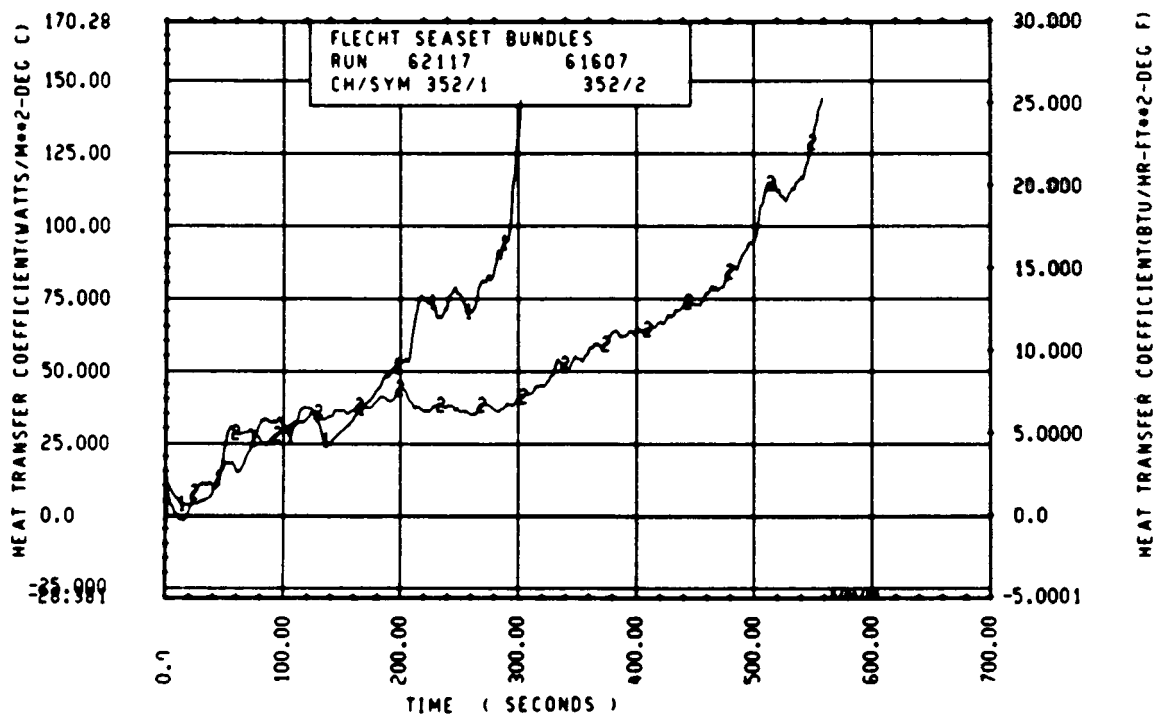
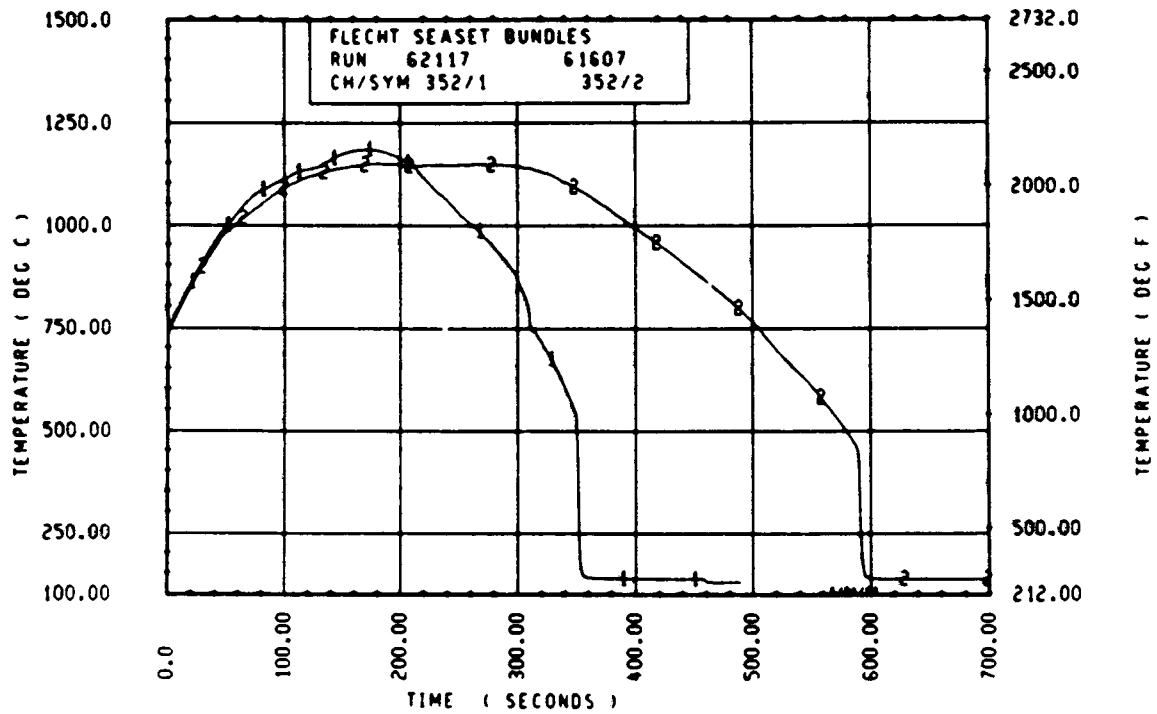
Rod 8H, 1.98 m (78 in.)



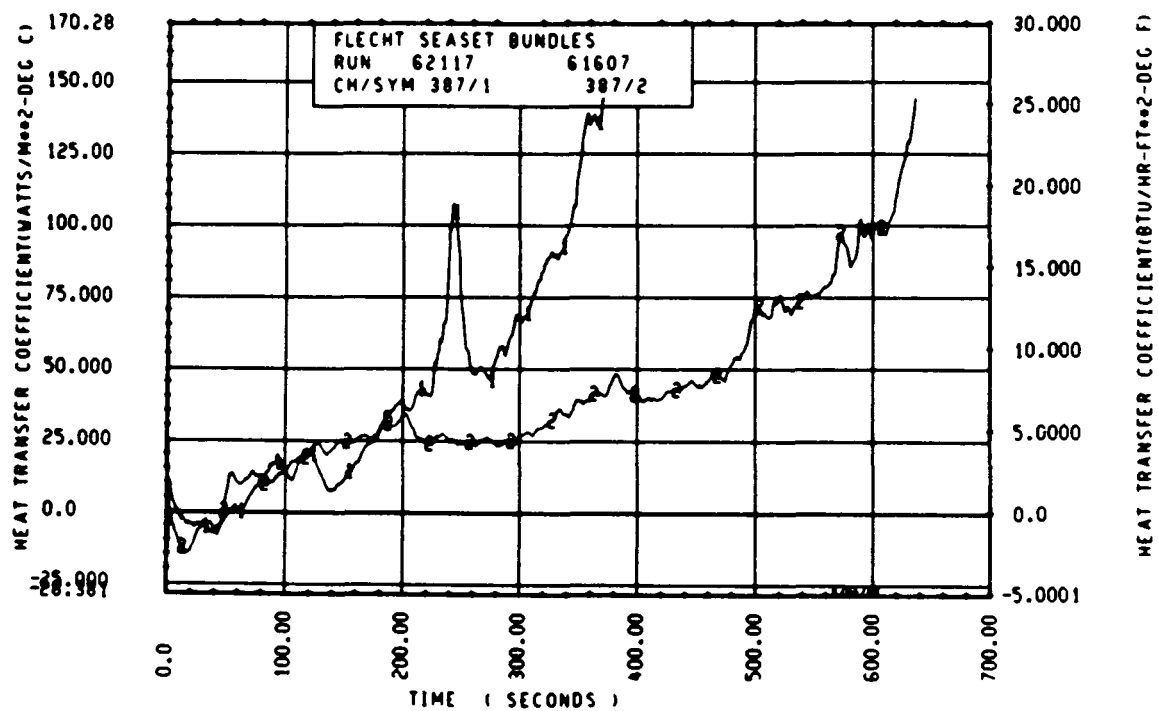
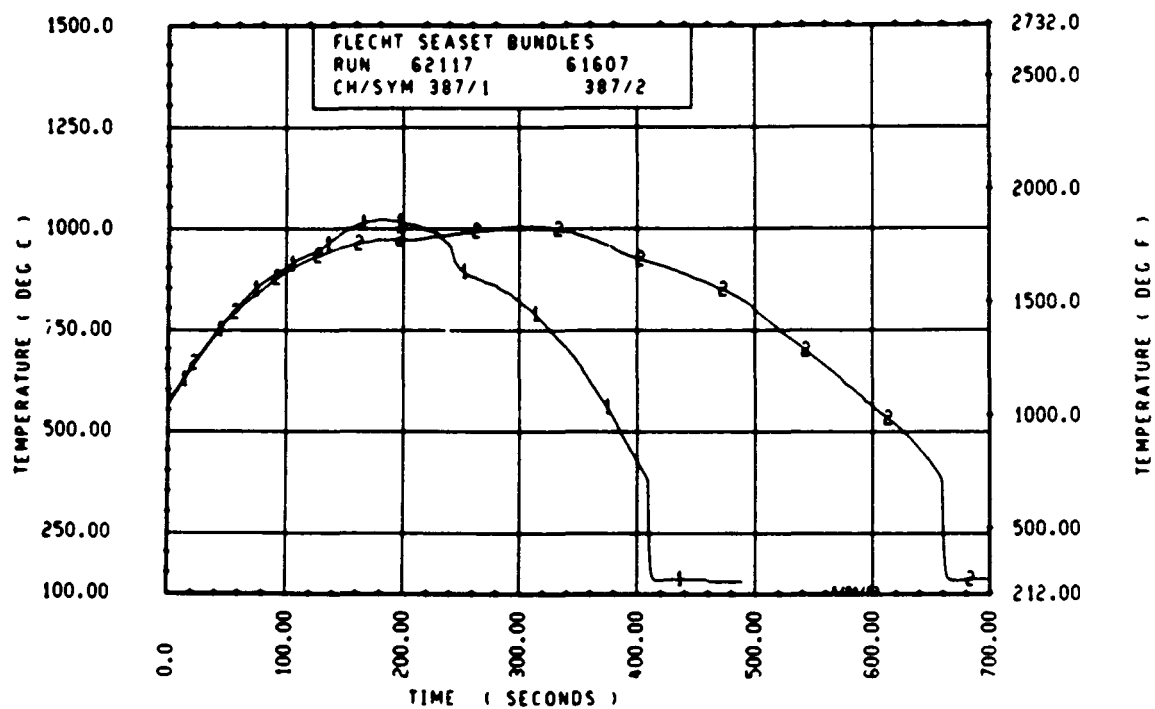
Rod 9J, 1.98 m (78 in.)



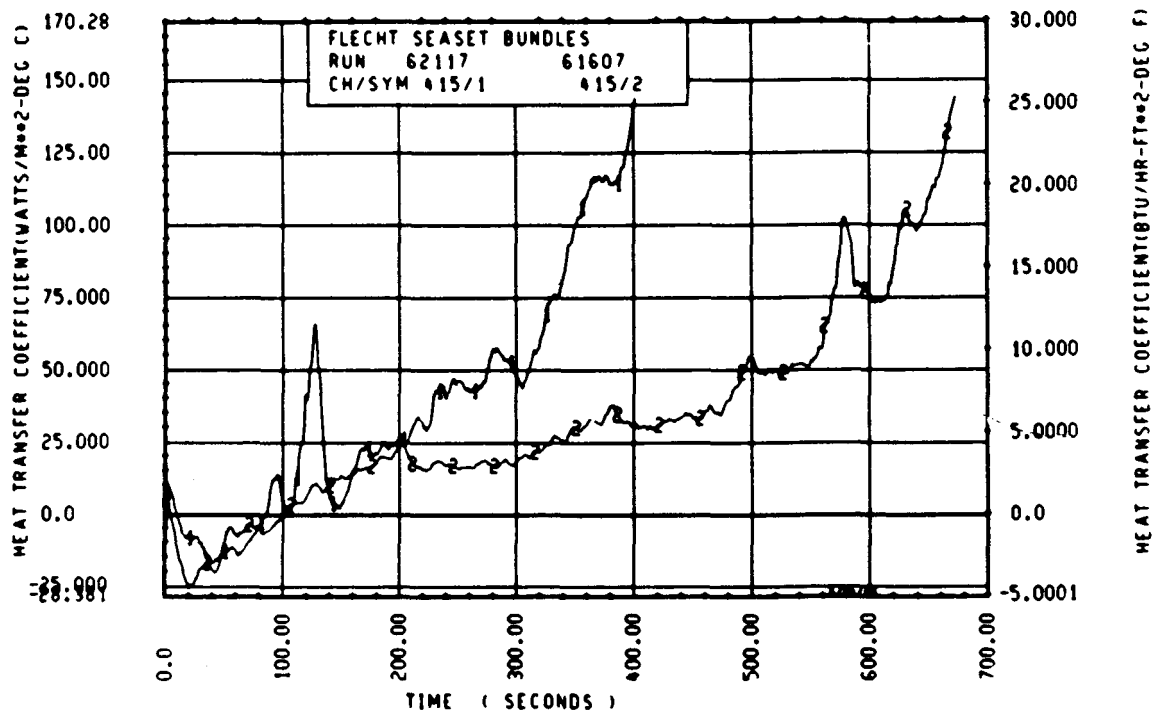
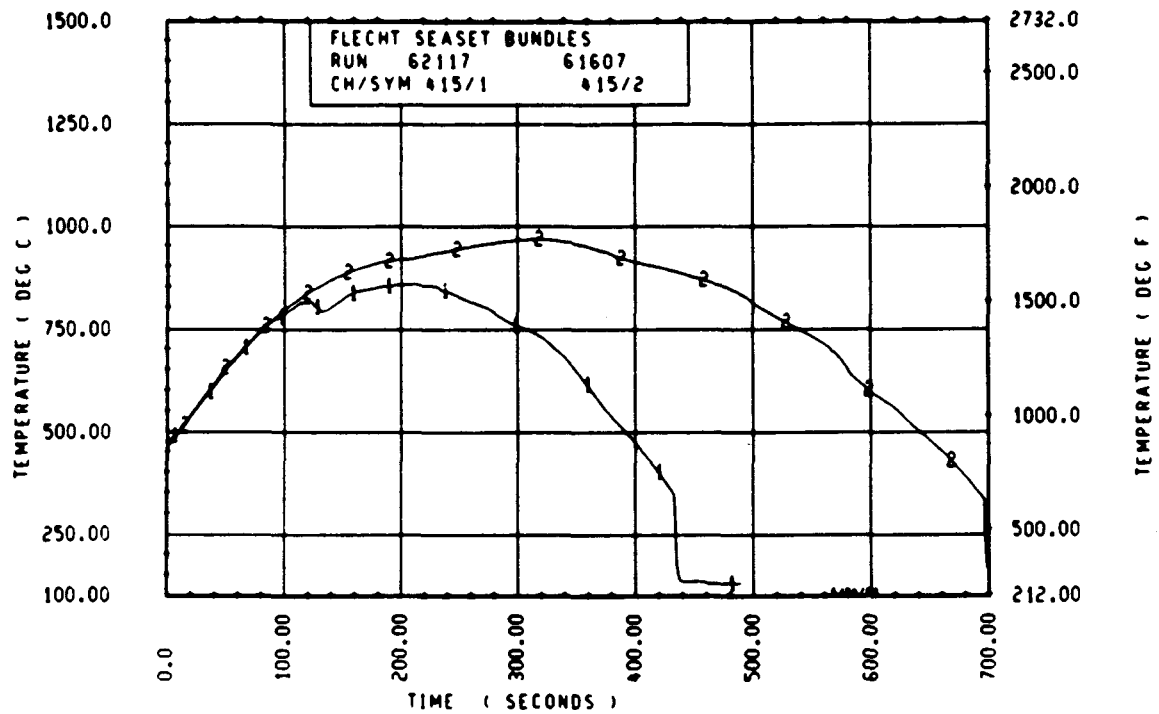
Rod 9H, 2.29 m (90 in.)



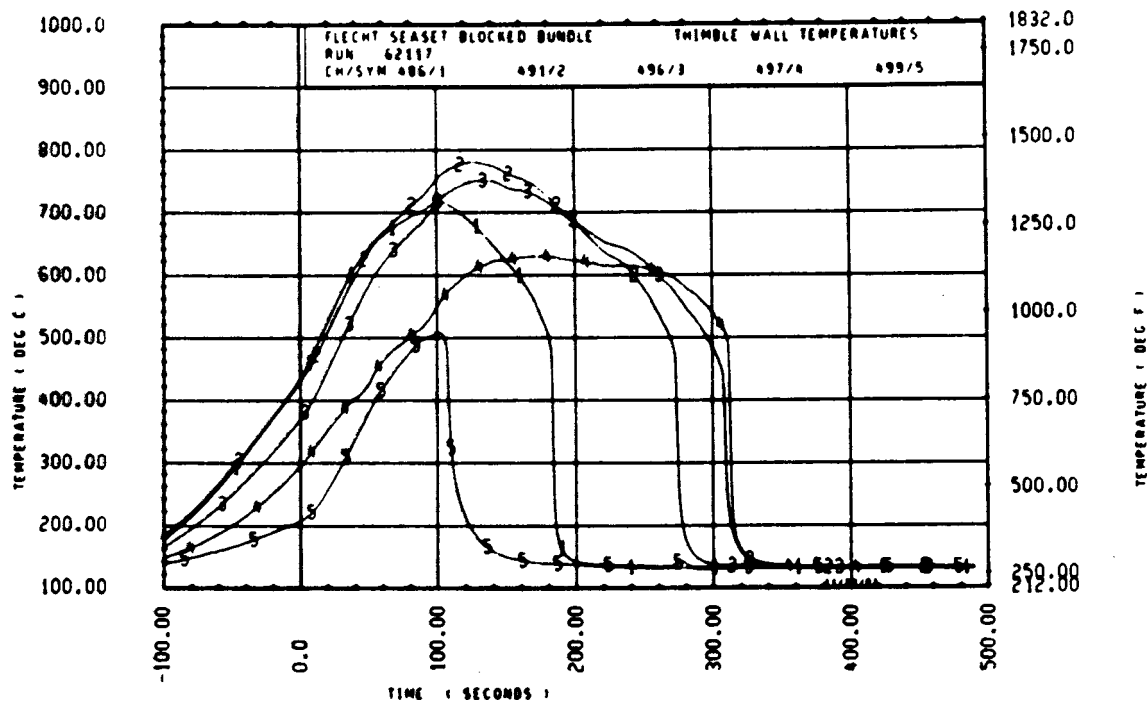
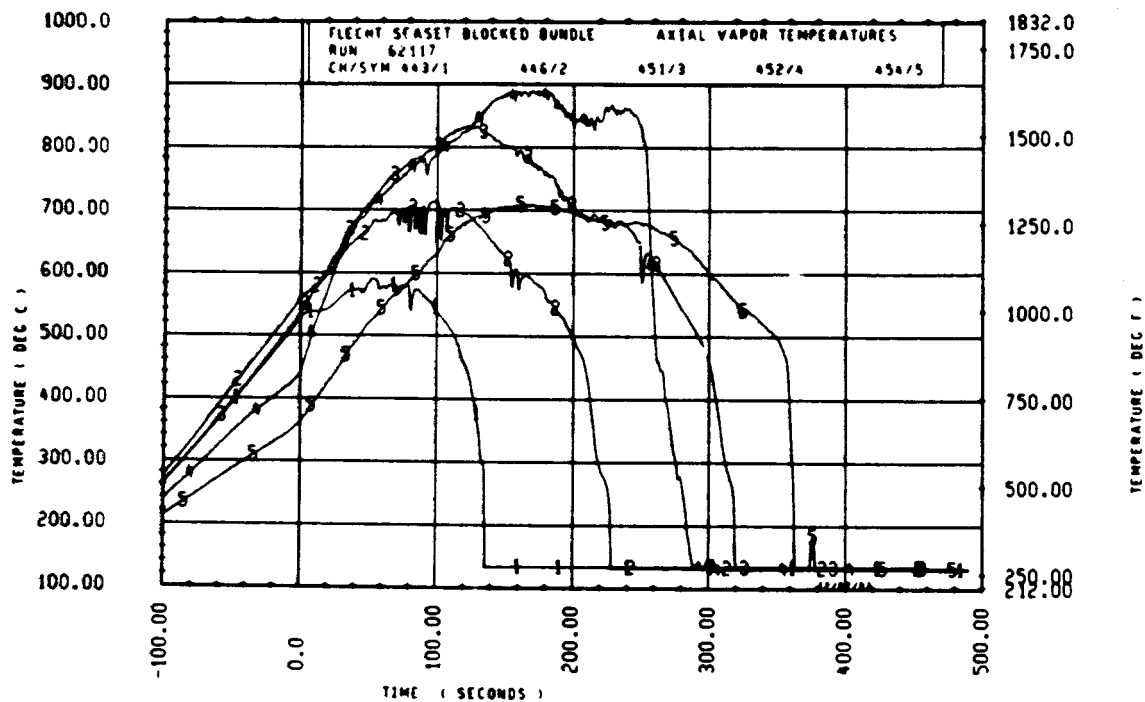
Rod 9H, 2.44 m (96 in.)

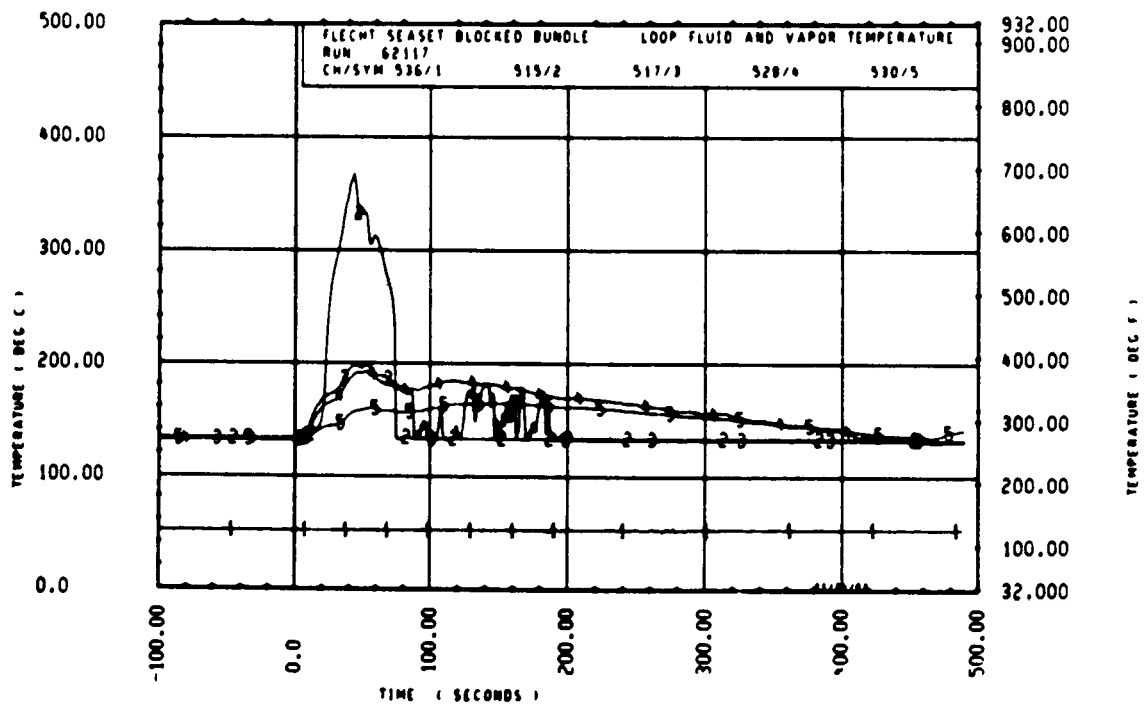
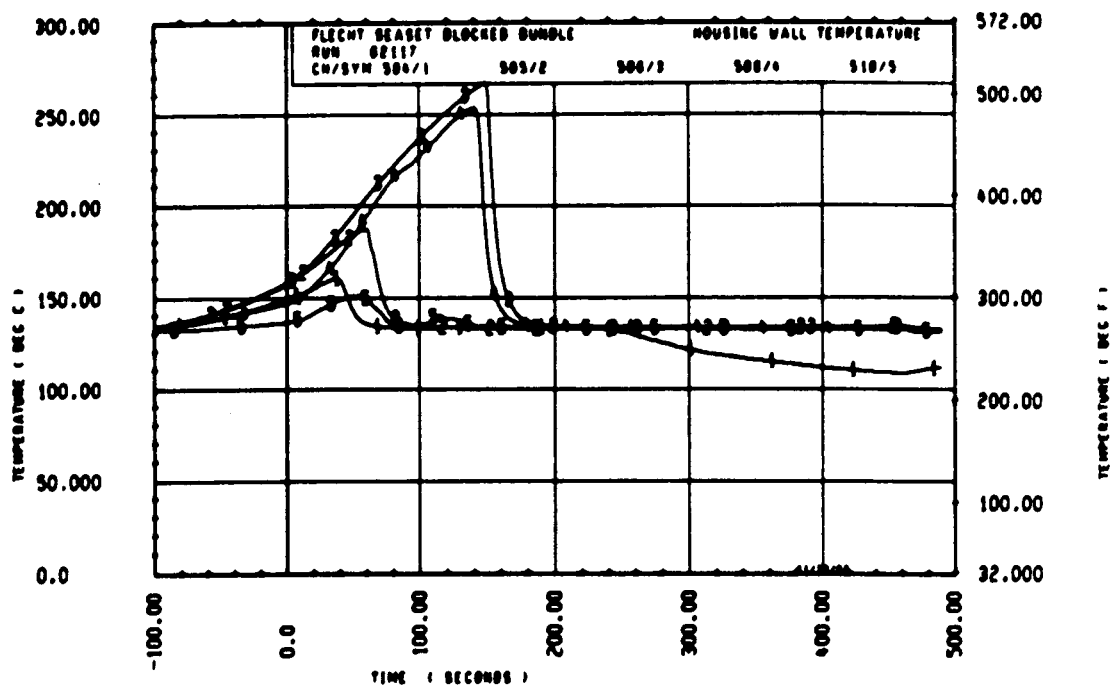


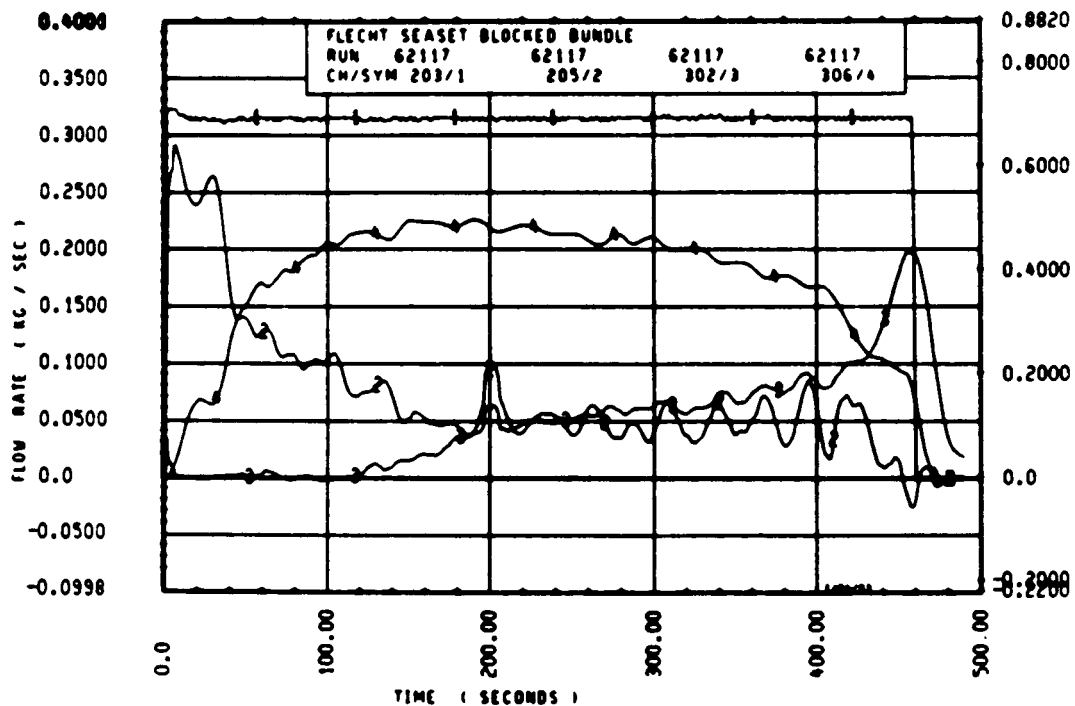
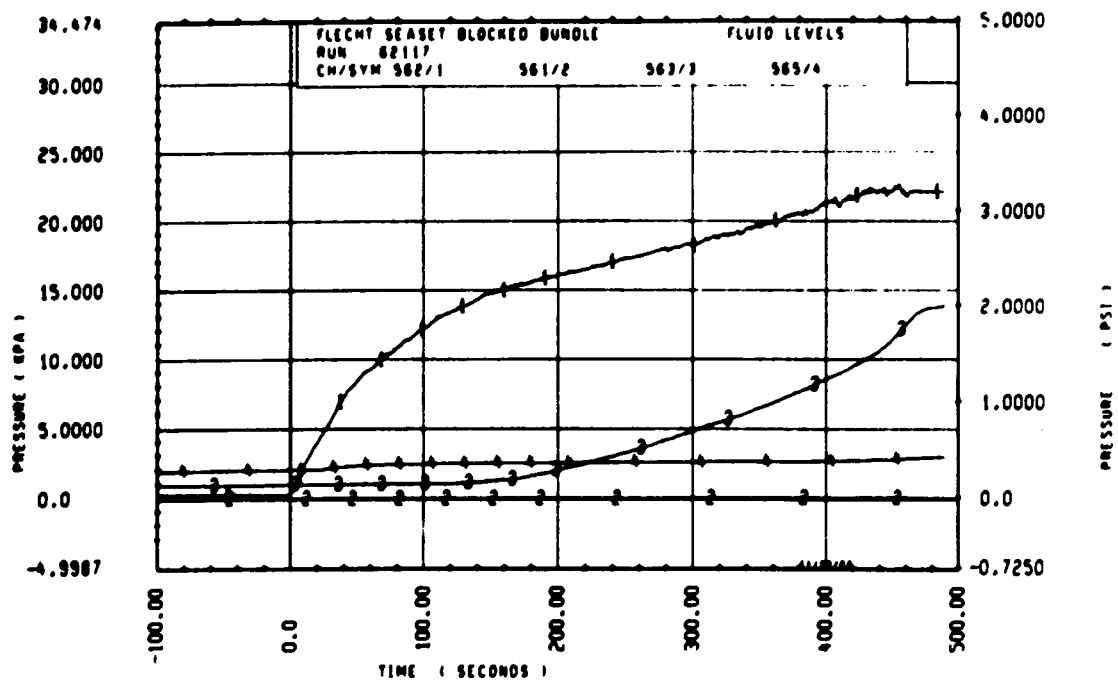
Rod 8H, 2.82 m (111 in.)

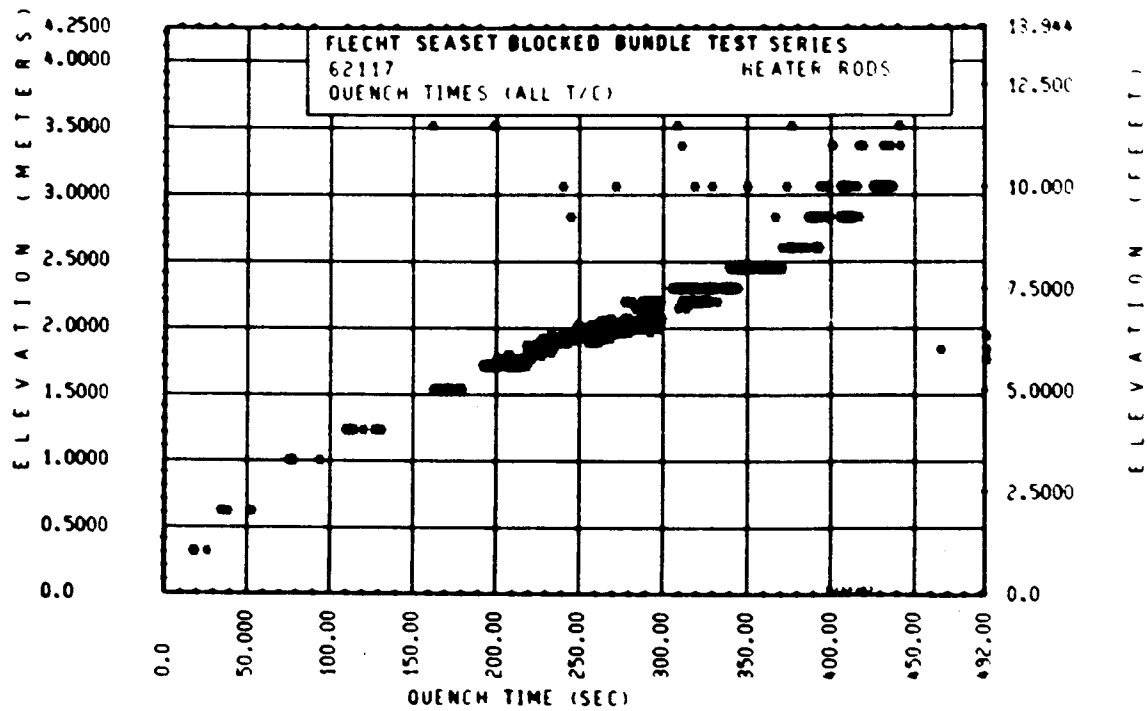
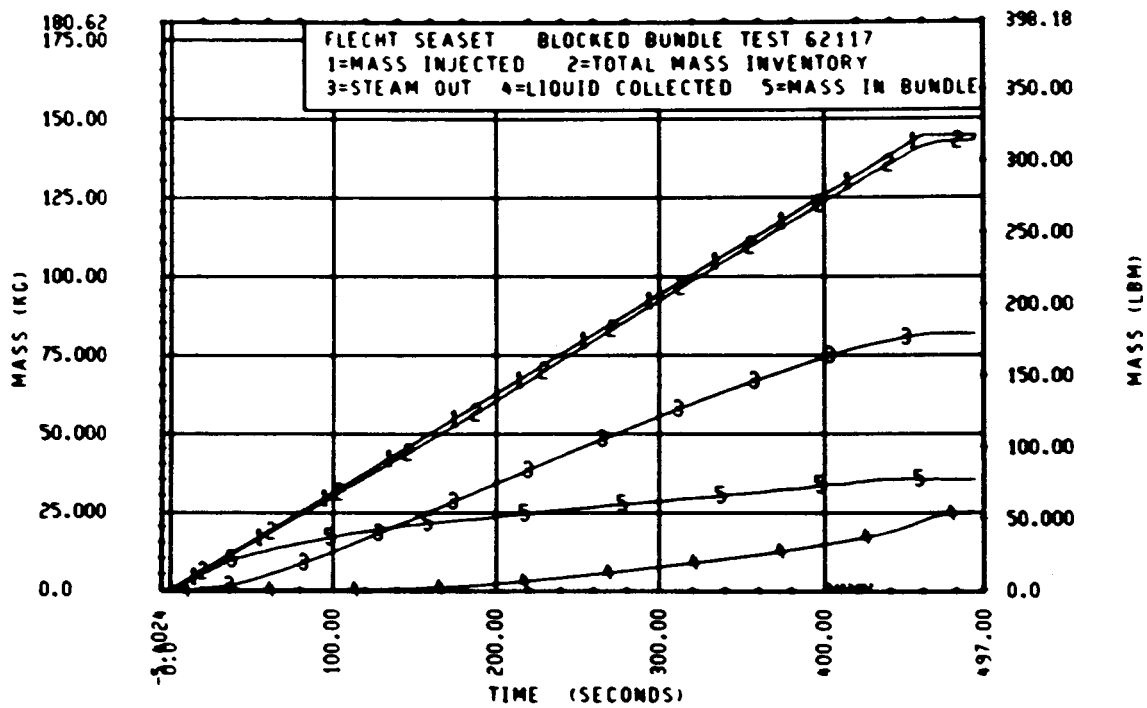


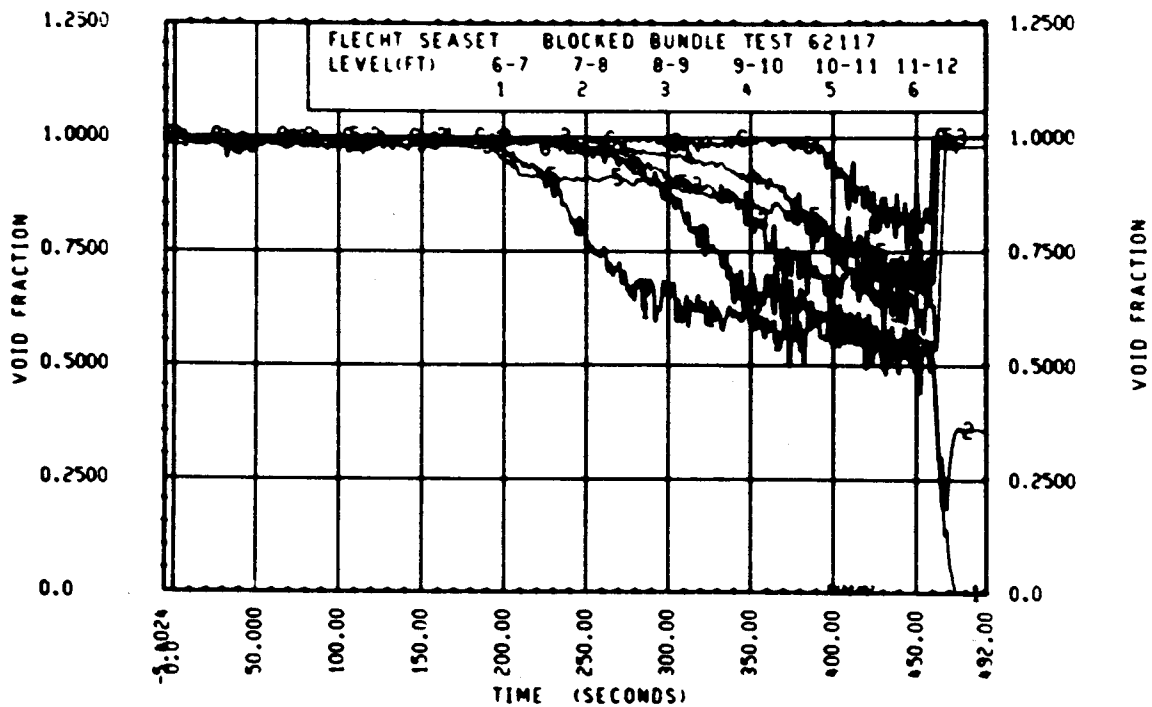
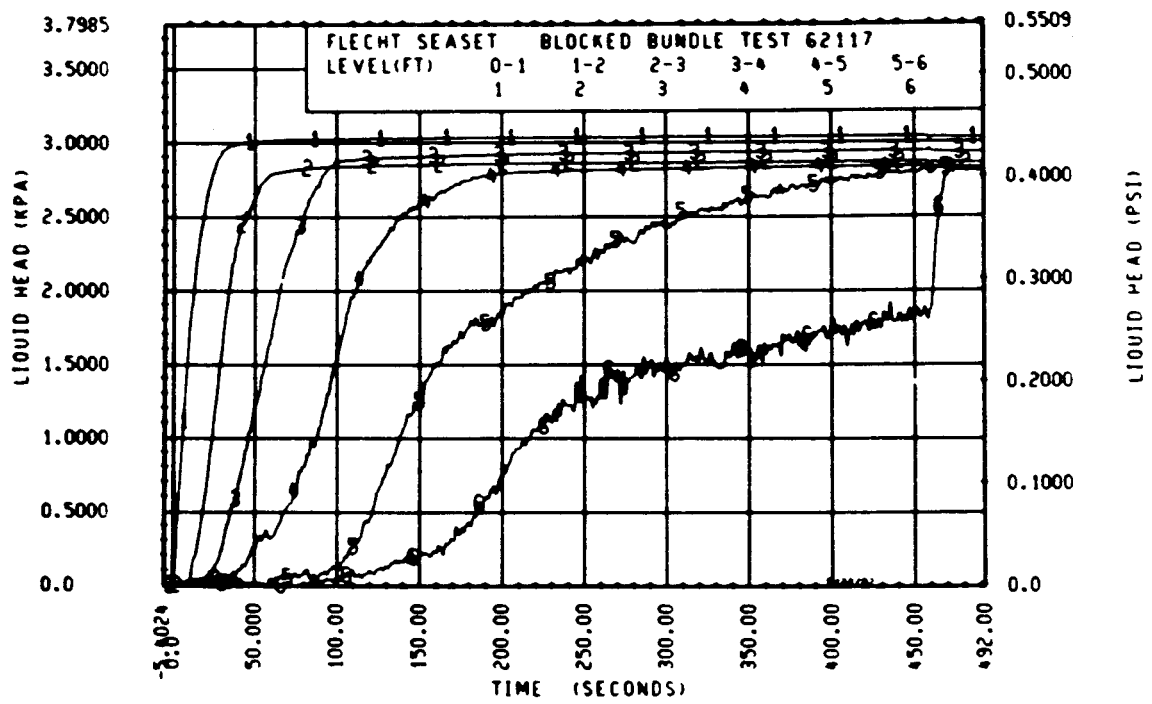
Rod 8H, 3.05 m (120 in.)

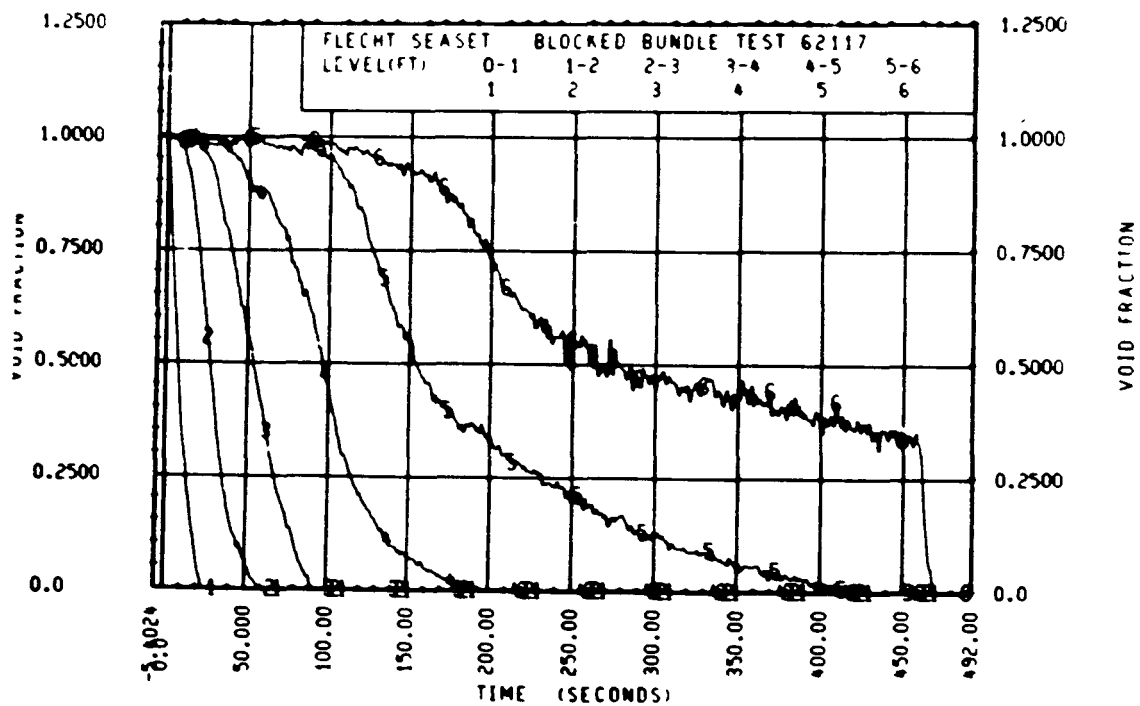
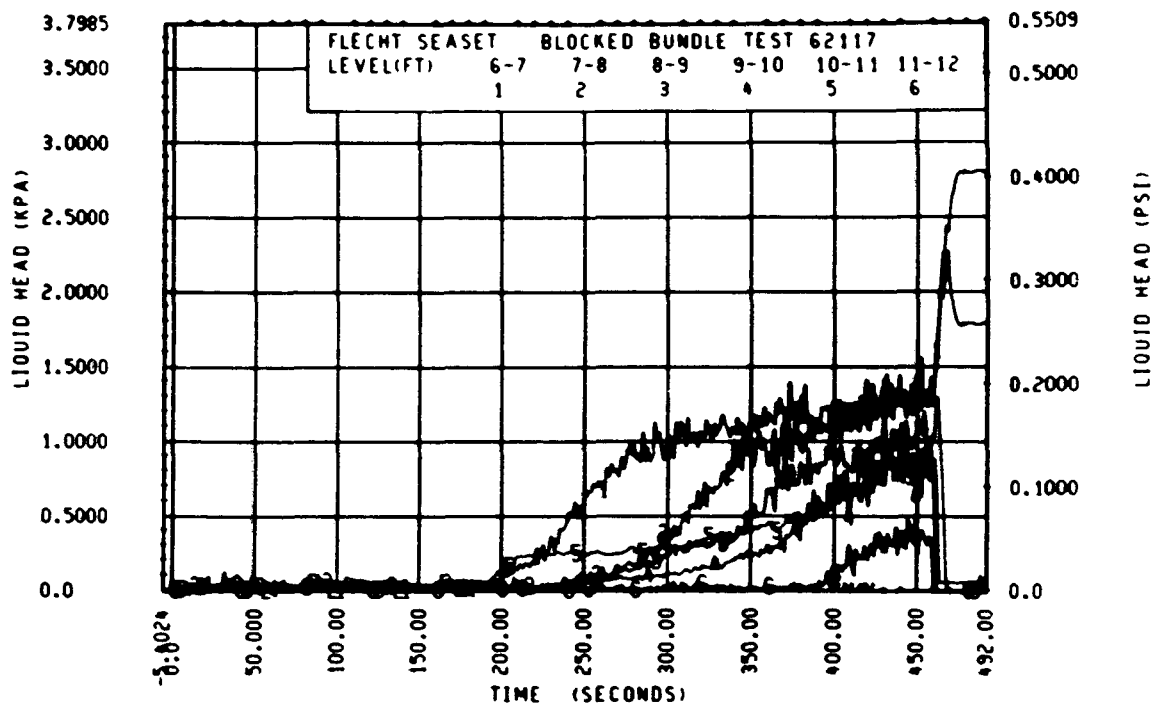












FLECHT SEASET 163-ROD BUNDLE FLOW BLOCKAGE TASK
SUMMARY AND COMMENT SHEET

Run: 62211
Test date: 9/22/82
Test type: Forced reflood
Parameter: Pressure effect

AS-RUN TEST CONDITIONS:

Upper plenum pressure	0.137 MPa (19.9 psia)
Initial peak clad temperature and location	871.0°C (1599.8°F), 8N-1.93 m (76 in.)
Initial peak rod power:	
Peripheral rods	1.31 kw/m (0.400 kw/ft)
Bypass rods	1.31 kw/m (0.398 kw/ft)
Blockage island rods	1.31 kw/m (0.400 kw/ft)
Flooding rate	28 mm/sec (1.1 in./sec) for 30 seconds 27 mm/sec (1.06 in./sec) onward
Coolant temperature	33.9°C (94°F)
Initial bundle water level	-2.5 mm (-0.10 in.)

COMMENTS:

Inlet mass flow: ⁽¹⁾ Linearly increasing to -2.6% by 30 seconds, step decrease to 0%, and 0% thereafter

Power decay: ⁽¹⁾ peripheral rods, -0.5% constant
bypass rods, -0.5% linearly increasing to -1% by 400 seconds
blockage rods, -0.5% constant

1. Relative to run 31922

FLECHT SEASET 163 ROD BUNDLE TEST SERIES

RUN NUMBER 62211

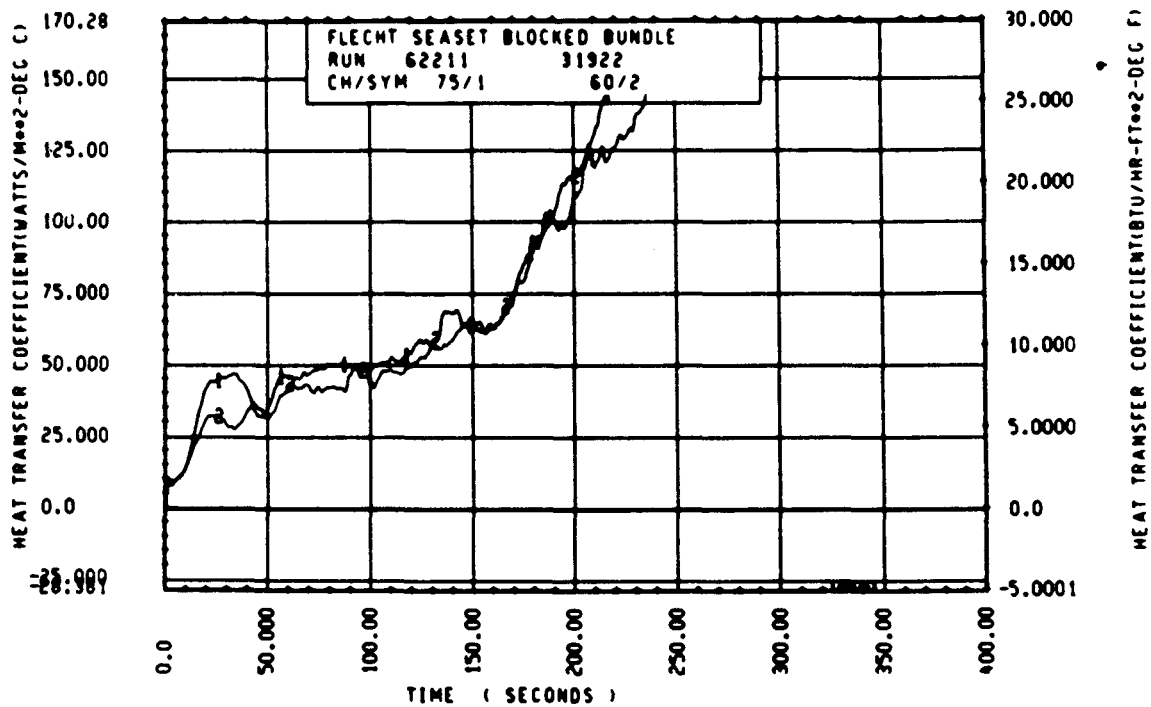
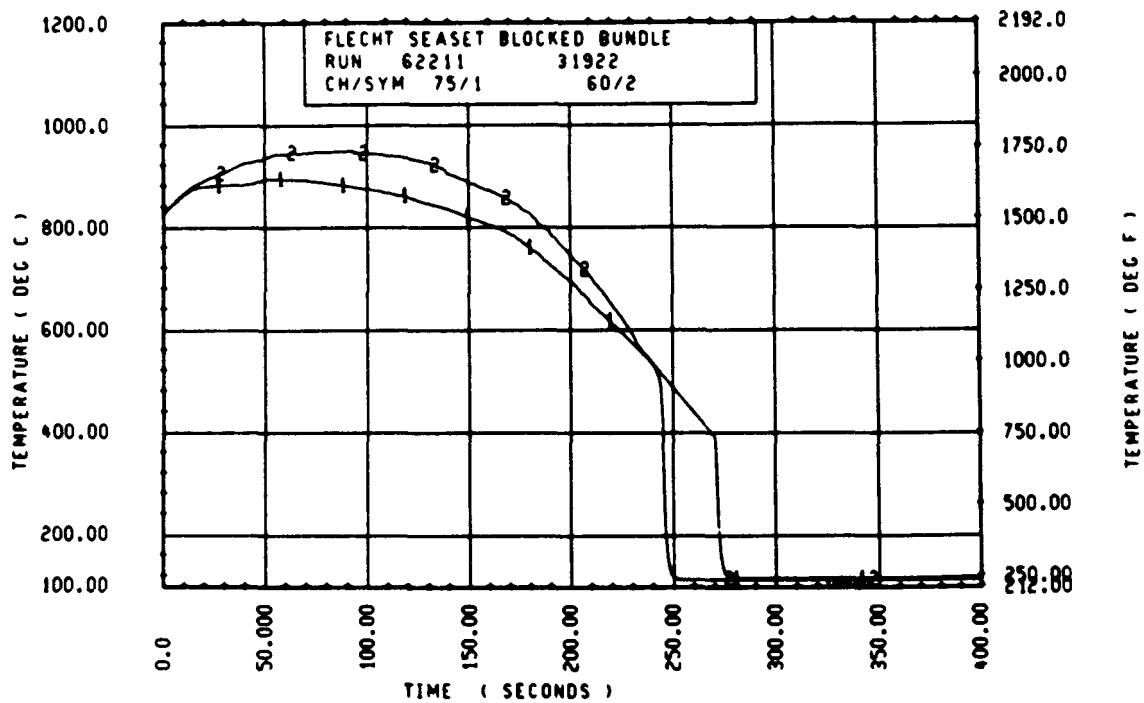
ROD/ELEV	CHAN. NO	INITIAL AT FLUO (DEG F)	MAXIMUM TEMPERATURE (DEG F)	TEMPERATURE RISE (DEG F)	TURNAROUND TIME (SECONDS)	QUENCH TEMPERATURE (DEG F)	QUENCH TIME (SECONDS)
9G 1- 0	3	654.	670.	12.	6.0	499.	27.0
10H 2- 0	6	875.	901.	26.	10.5	543.	57.2
9G 3- 3	9	1210.	1255.	45.	14.0	636.	106.4
3J 4- 0	11	1347.	1405.	58.	16.0	618.	144.6
7H 4- 0	12	1337.	1403.	65.	17.0	616.	147.6
6K 4- 0	13	1360.	1426.	67.	16.5	642.	147.4
8H 4- 0	14	1347.	1406.	59.	18.0	634.	144.4
12U 4- 0	17	1340.	1393.	54.	15.0	655.	144.4
5E 5- 0	20	1500.	1601.	101.	50.5	743.	204.9
76 5- 0	21	1559.	1644.	85.	49.0	697.	206.9
9G 5- 0	24	1526.	1617.	89.	49.5	701.	206.0
5E 5- 7	33	1524.	1624.	95.	51.0	724.	241.7
8U 5- 7	45	1541.	1637.	96.	48.5	786.	239.9
9H 5- 9	52	1482.	1586.	104.	22.5	765.	243.1
76 5-10	59	1492.	1604.	113.	75.0	773.	254.9
7F 5-11	62	1438.	1551.	113.	75.0	871.	252.1
4G 5-11	64	1522.	1642.	120.	52.5	760.	265.9
2I 6- 0	67	1574.	1694.	121.	51.5	787.	267.6
5D 6- 0	70	1480.	1588.	108.	51.5	753.	266.1
6J 6- 0	74	1516.	1619.	102.	53.0	742.	274.0
7H 6- 0	66	1542.	1662.	120.	53.0	745.	263.9
11E 6- 0	80	1528.	1617.	89.	51.0	762.	267.9
8H 6- 2	97	1352.	1512.	160.	105.5	787.	272.9
5H 6- 2	99	1517.	1648.	131.	79.0	799.	282.0
9E 6- 2	105	1334.	1597.	262.	112.0	1202.	255.6
6H 6- 3	111	1390.	1535.	145.	106.0	847.	278.0
4G 6- 3	124	1534.	1665.	126.	52.5	779.	289.0
11H 6- 4	134	1462.	1612.	150.	110.0	652.	292.0
9D 6- 4	143	1537.	1687.	150.	79.0	806.	292.9
9J 6- 5	165	1511.	1622.	111.	99.5	786.	298.6
9H 6- 5	166	1584.	1701.	117.	51.0	775.	294.1
6J 6- 6	192	1561.	1658.	97.	71.0	826.	296.9
9D 6- 6	193	1551.	1702.	151.	76.5	826.	304.0
11F 6- 6	173	1543.	1665.	121.	74.5	762.	301.0
4G 7- 0	261	1465.	1569.	105.	52.5	695.	333.8
7D 7- 6	309	1471.	1587.	116.	75.5	729.	367.5
7G 7- 6	312	1513.	1613.	100.	51.0	779.	352.6
11E 7- 6	325	1483.	1592.	109.	52.0	725.	364.6
5L 8- 0	337	1296.	1499.	201.	117.5	696.	399.1
7H 8- 0	345	1347.	1551.	204.	100.5	660.	393.5
7K 8- 0	346	1344.	1530.	187.	101.0	699.	391.0
5J 8- 6	366	1117.	1318.	201.	101.0	629.	422.0
7B 8- 6	368	1117.	1329.	212.	142.0	582.	424.1
7E 9- 3	383	1093.	1310.	217.	192.5	601.	433.2
6H 9- 3	387	1038.	1207.	169.	208.1	548.	428.2
9L 9- 3	389	1034.	1221.	187.	149.0	562.	437.1
11F 9- 3	394	1033.	1206.	173.	104.5	645.	381.2
7B10- 0	408	841.	1099.	258.	153.0	606.	428.0
8H10- 0	415	846.	1092.	244.	174.0	537.	450.9
6K10- 0	417	855.	1075.	220.	174.0	544.	442.3
6H10- 0	418	870.	1112.	242.	114.5	546.	461.0
6H11- 0	429	676.	757.	80.	76.0	475.	391.8
9G11- 0	431	668.	748.	80.	50.0	398.	212.6
11E11- 0	432	660.	752.	92.	54.5	391.	375.5
5J11- 6	436	670.	732.	62.	51.5	466.	346.6
7B11- 6	437	636.	797.	160.	154.5	436.	361.5
6J11- 6	438	672.	740.	68.	53.0	446.	400.6

RUN 62211 HEATER ROD STATISTICAL DATA

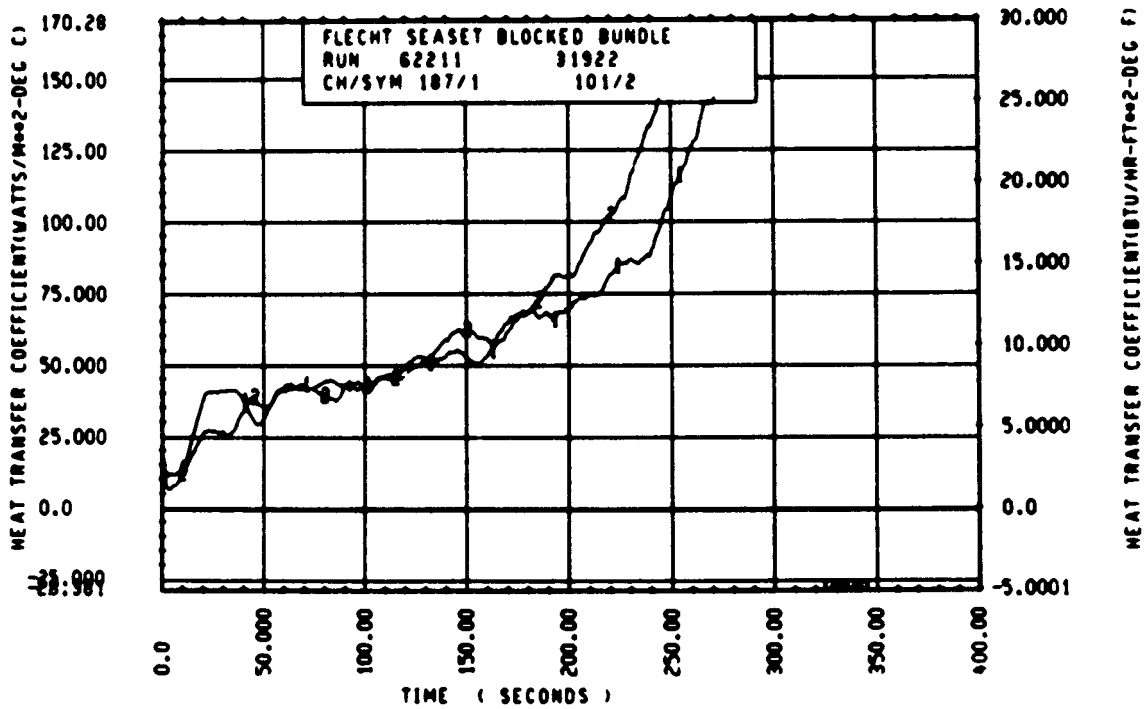
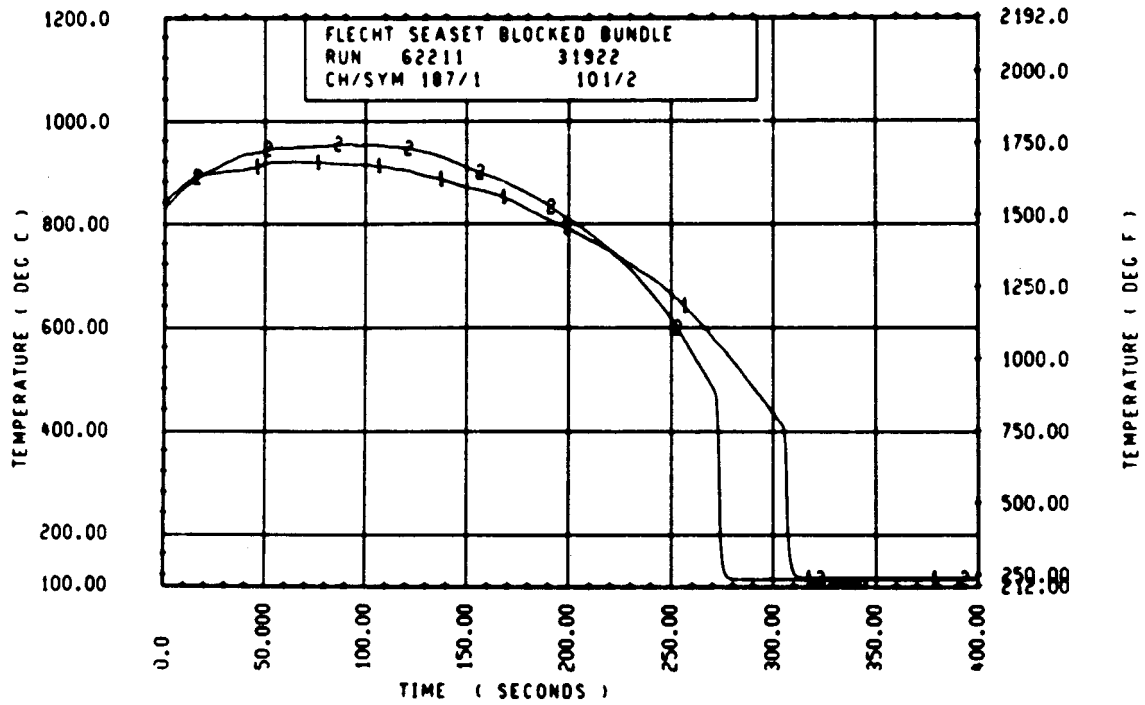
ELEV	INITIAL TEMP (DEG F)			MAX TEMP (DEG F)			TURNAROUND TIME (SEC)		
	MAX	MIN	MEAN	MAX	MIN	MEAN	MAX	MIN	MEAN
12	661.7	656.5	659.4	673.2	670.1	671.5	6.0	5.5	5.6
24	875.0	845.0	856.7	900.8	867.7	880.1	10.5	10.0	10.2
39	1209.7	1155.6	1177.8	1254.6	1201.4	1222.2	15.0	14.0	14.5
48	1366.9	1337.4	1350.2	1428.5	1393.3	1411.7	18.0	15.0	16.5
60	1558.7	1426.4	1510.9	1658.1	1502.3	1600.8	52.5	16.5	42.1
67	1586.8	1498.0	1544.6	1676.8	1594.4	1632.6	53.0	16.5	40.1
69	1519.6	1462.0	1504.7	1625.1	1573.8	1601.9	54.0	22.5	47.2
70	1587.9	1460.6	1516.3	1668.0	1594.4	1620.9	75.0	50.5	59.6
71	1521.8	1436.1	1477.5	1641.6	1551.1	1591.3	75.0	50.5	62.4
72	1580.3	1442.4	1530.1	1699.8	1587.9	1648.7	92.5	50.5	57.8
73	1573.8	1425.3	1508.8	1690.0	1565.1	1626.9	76.5	50.5	56.4
74	1574.2	1352.2	1493.7	1691.0	1512.0	1629.5	107.5	51.5	71.6
75	1586.8	1390.2	1505.2	1687.8	1534.8	1630.8	106.0	50.5	71.9
76	1599.6	1441.3	1535.8	1717.7	1611.9	1663.1	110.0	50.0	68.8
77	1583.6	1462.7	1530.3	1703.2	1571.6	1651.2	139.0	51.0	80.9
78	1599.8	701.6	1519.3	1728.9	1140.2	1647.7	164.0	52.0	80.6
79	1590.1	1495.9	1552.2	1703.2	1641.6	1667.6	114.5	17.0	77.7
80	1577.1	1496.9	1540.7	1717.7	1639.4	1680.7	106.0	17.5	83.1
81	1571.7	1469.1	1527.1	1702.1	1613.0	1670.4	96.0	50.0	76.0
84	1521.8	1398.6	1476.6	1606.4	1506.6	1568.0	53.0	15.5	30.0
86	1573.6	1459.5	1523.4	1651.5	1542.4	1610.2	53.0	15.5	27.1
90	1520.7	1418.9	1477.7	1635.0	1544.5	1596.6	138.5	22.0	65.6
96	1392.3	1285.4	1343.0	1592.2	1487.3	1547.3	147.5	74.5	112.4
102	1174.4	1089.5	1144.5	1406.2	1305.8	1346.0	198.0	97.5	154.2
111	1092.6	1019.4	1052.2	1310.0	1174.4	1236.3	208.1	74.0	160.4
120	907.0	804.6	853.7	1191.0	964.8	1097.6	197.0	77.5	162.1
132	676.4	659.6	666.8	793.2	723.4	755.9	117.0	40.0	72.0
138	672.2	607.0	639.0	797.4	664.8	720.0	154.5	26.0	67.2

RUN 62211 HEATER ROD STATISTICAL DATA

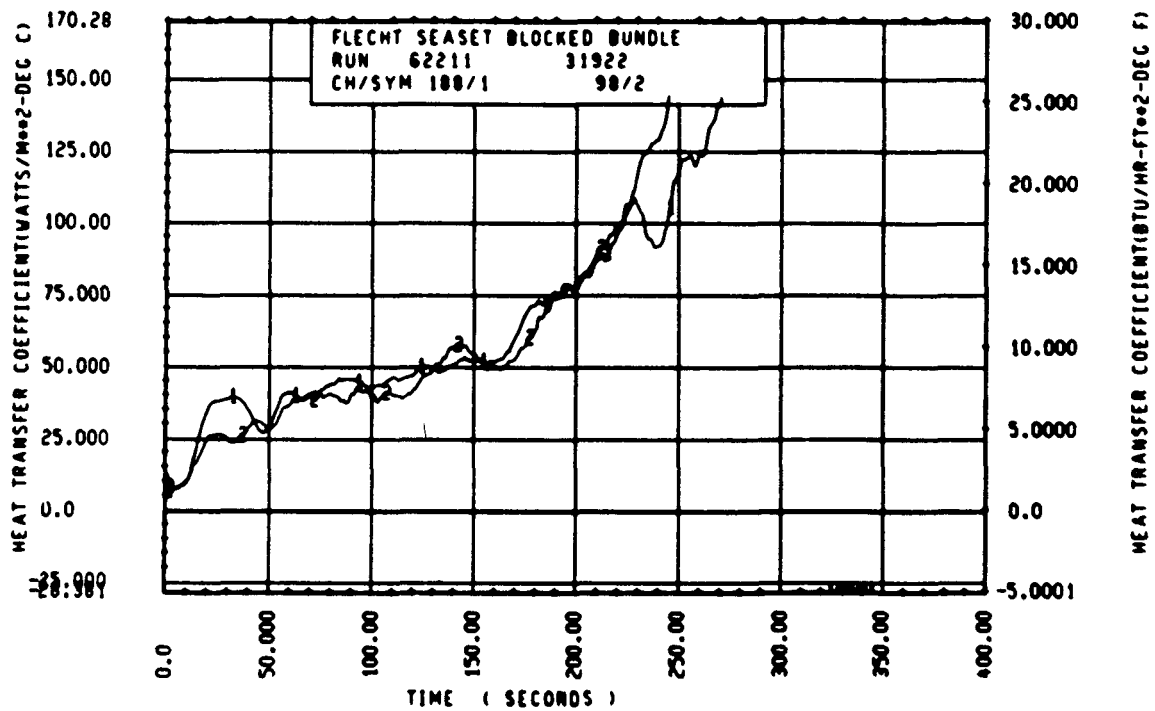
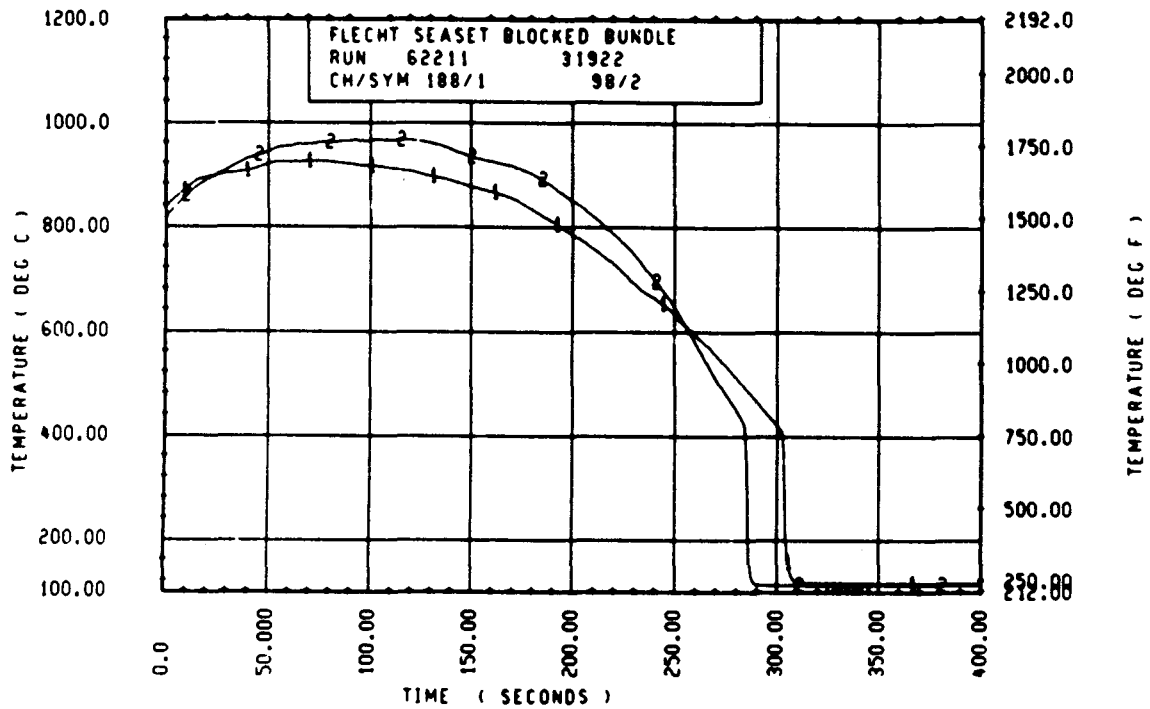
ELEV	TEMP RISE (DEG F)			QUENCH TEMP (DEG F)			QUENCH TIME (SEC)		
	MAX	MIN	MEAN	MAX	MIN	MEAN	MAX	MIN	MEAN
12	11.6	11.6	11.6	519.6	498.7	506.3	28.7	27.0	27.9
24	25.9	21.7	23.4	543.3	533.1	538.4	37.2	34.9	35.7
39	47.7	39.6	44.4	645.0	626.4	635.1	109.1	103.9	106.1
48	66.8	53.8	61.5	668.6	617.5	638.3	147.8	142.7	145.1
60	107.5	66.3	84.8	743.1	682.8	706.4	212.4	201.7	207.7
67	106.6	69.8	86.0	787.7	667.6	703.6	252.0	236.8	243.3
69	105.5	76.9	97.2	765.1	700.8	728.8	260.0	243.1	251.3
70	133.8	80.1	104.6	807.6	710.7	752.4	260.7	252.8	255.4
71	119.8	104.2	113.8	871.0	718.9	776.3	265.9	252.1	260.0
72	159.6	89.1	118.6	810.3	735.0	760.8	274.0	263.9	268.9
73	139.8	93.6	118.1	800.7	707.3	759.4	279.1	264.1	272.5
74	191.2	102.5	135.6	830.0	706.8	771.1	283.0	272.9	278.5
75	172.7	92.6	125.5	847.3	464.1	749.6	290.0	274.3	263.6
76	172.6	89.5	127.2	836.1	652.0	782.5	294.4	280.0	289.1
77	162.6	91.4	120.9	855.1	719.0	790.3	306.9	287.8	295.6
78	438.7	73.7	128.5	877.0	608.3	784.1	315.1	293.6	301.4
79	157.5	73.2	115.3	956.3	675.6	793.8	317.9	295.9	304.9
80	182.9	79.7	140.0	860.3	718.5	791.1	321.8	302.0	312.2
81	210.9	101.8	143.3	910.7	741.8	806.8	323.8	307.0	315.3
84	108.0	76.0	91.5	789.4	636.3	689.5	339.6	322.1	333.3
86	107.9	72.6	86.8	801.6	628.1	699.1	353.1	328.1	341.5
90	151.9	93.2	118.4	906.6	705.0	758.8	370.0	350.0	361.2
96	249.6	159.7	204.3	890.7	672.9	734.9	400.1	373.6	389.5
102	256.6	143.5	201.5	726.4	546.6	620.7	424.1	367.8	412.6
111	238.3	131.3	184.1	740.6	534.5	591.2	439.1	351.8	426.2
120	304.6	160.1	243.8	848.7	367.7	569.1	467.2	217.8	429.4
132	122.1	63.9	84.1	475.2	391.5	423.3	440.1	212.6	375.4
138	159.8	57.8	81.0	603.7	437.6	480.5	400.6	40.1	303.8



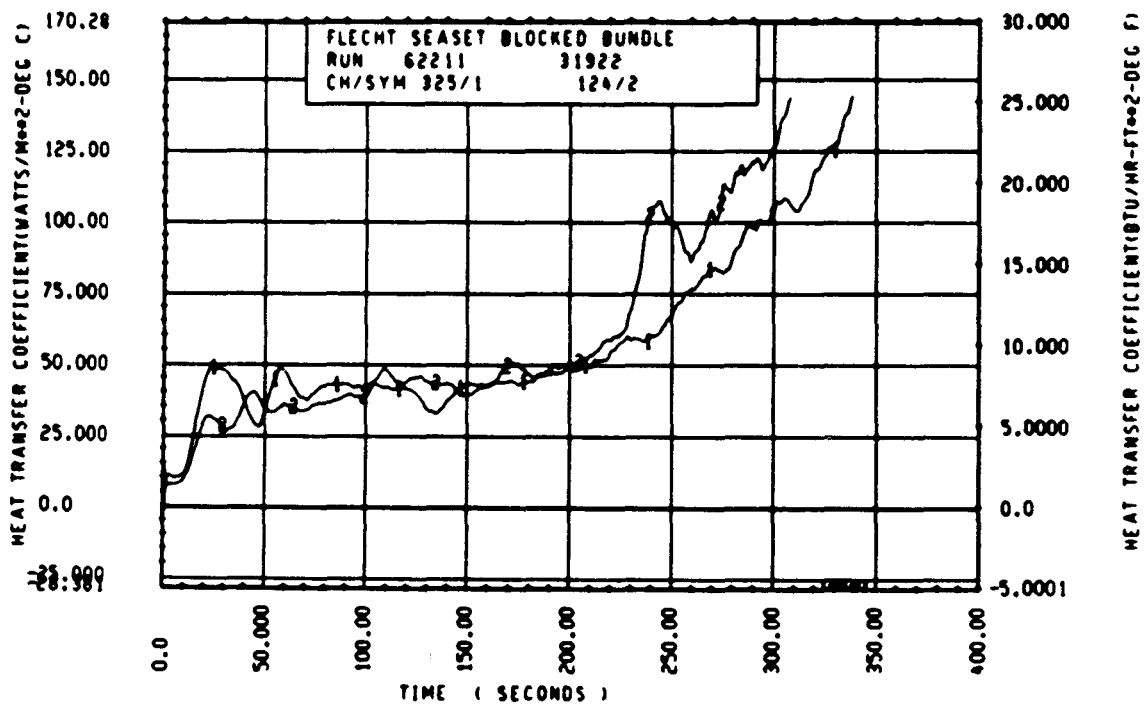
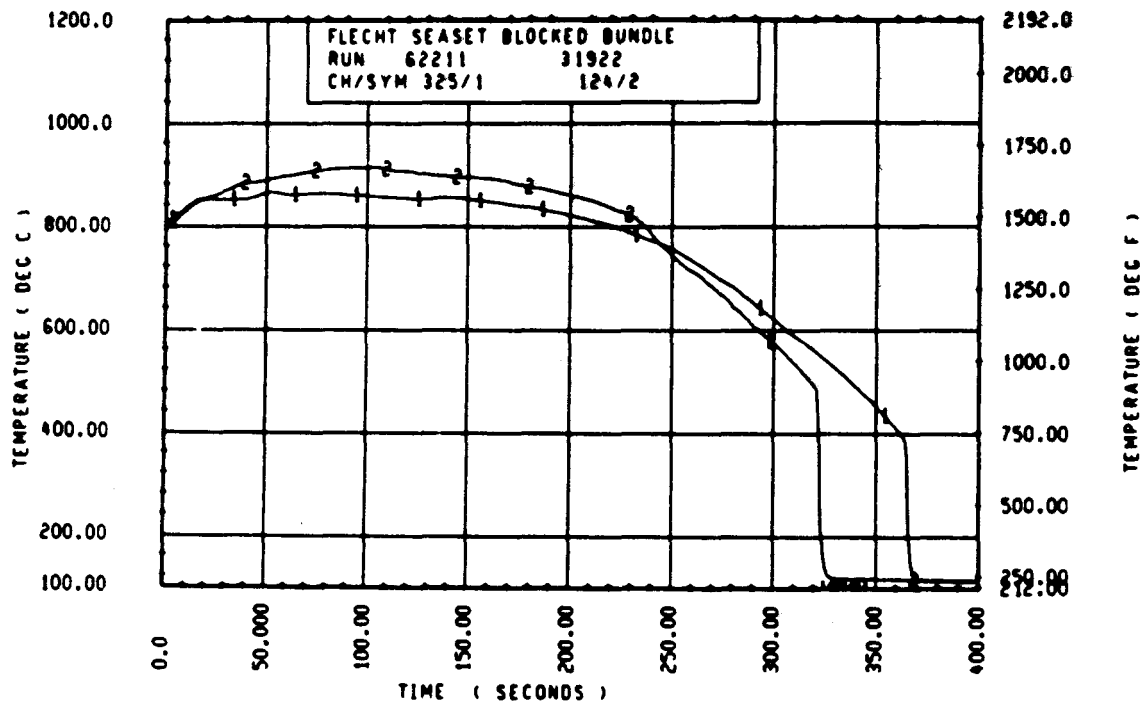
Rod 6L, 1.83 m (72 in.)



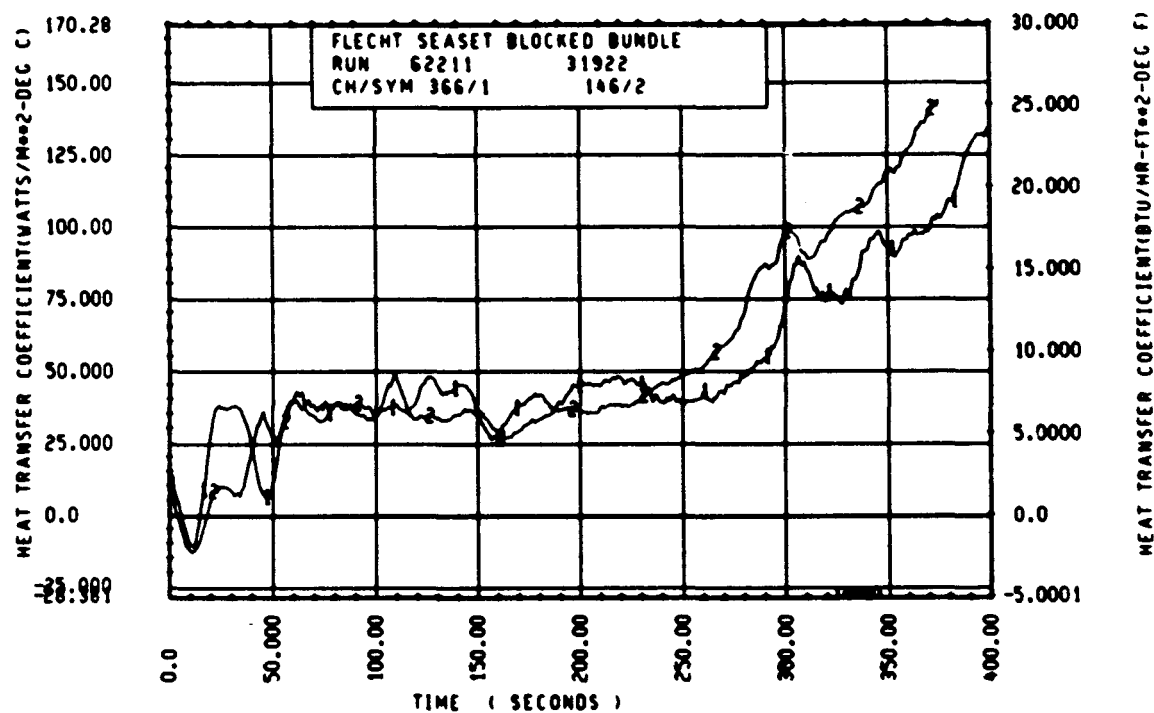
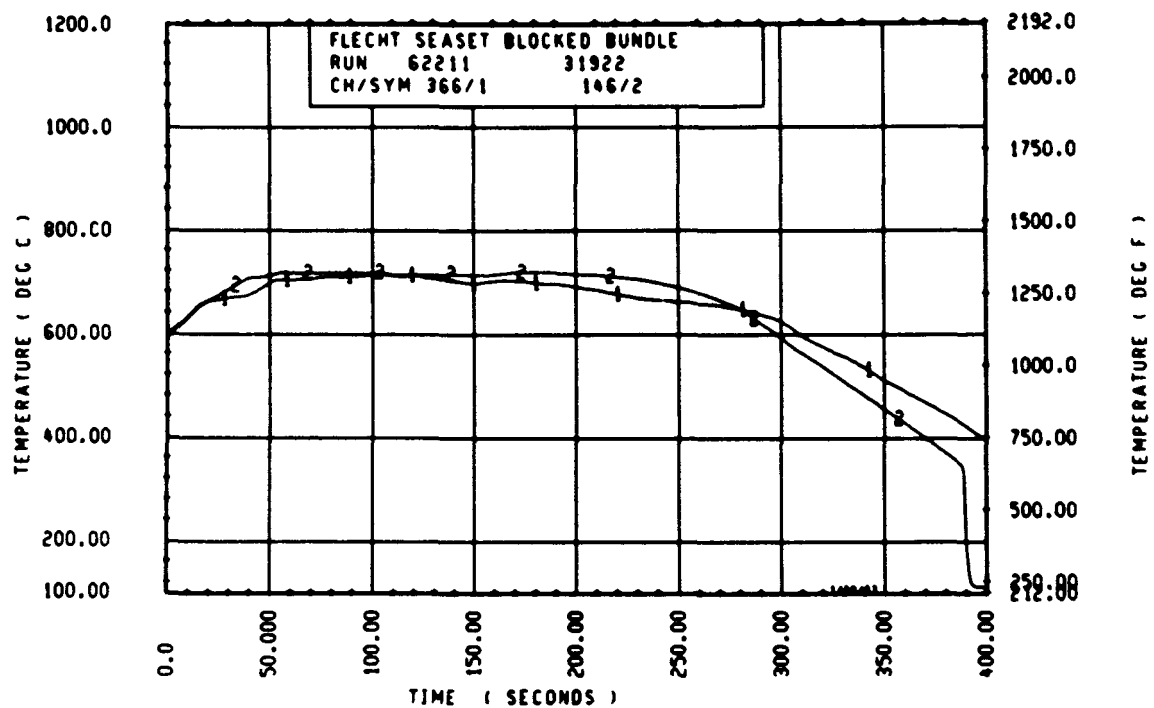
Rod 6J, 1.98 m (78 in.)



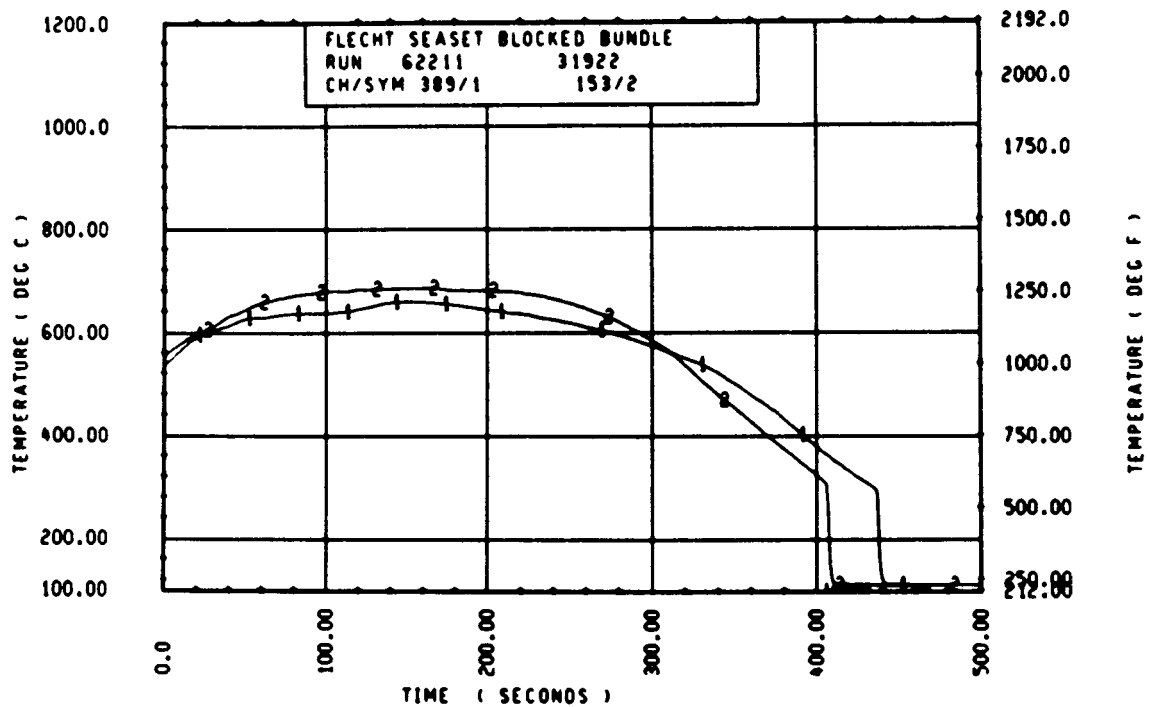
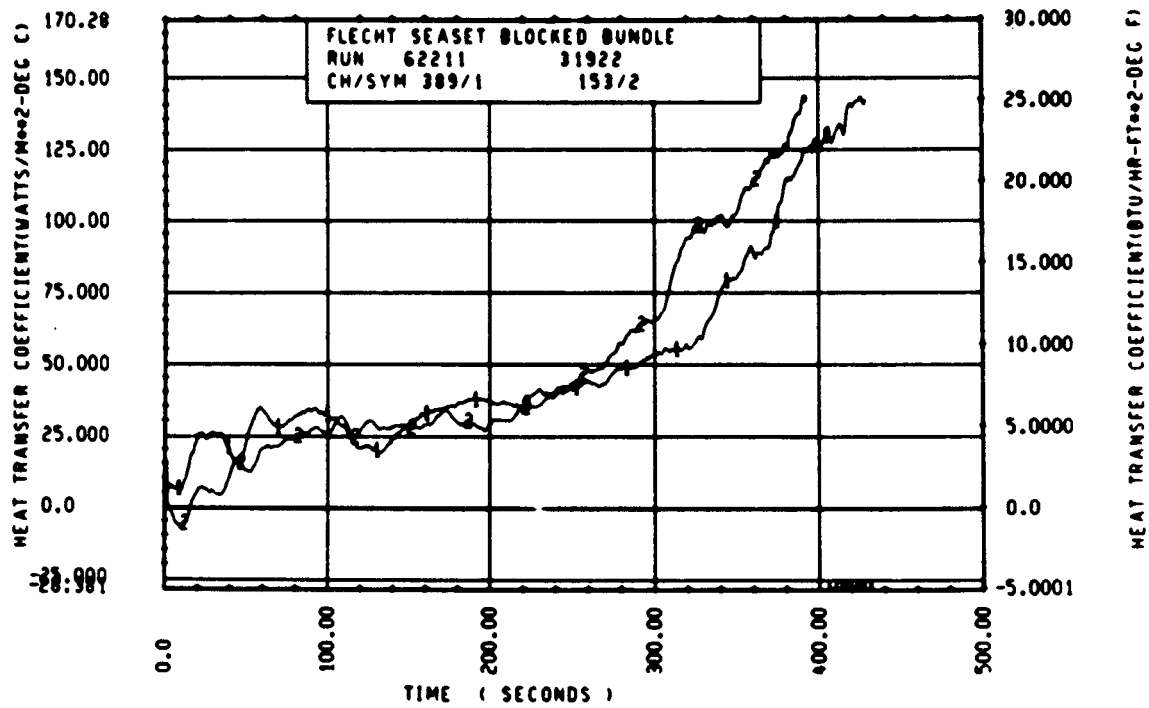
Rod 6L, 1.98 m (78 in.)



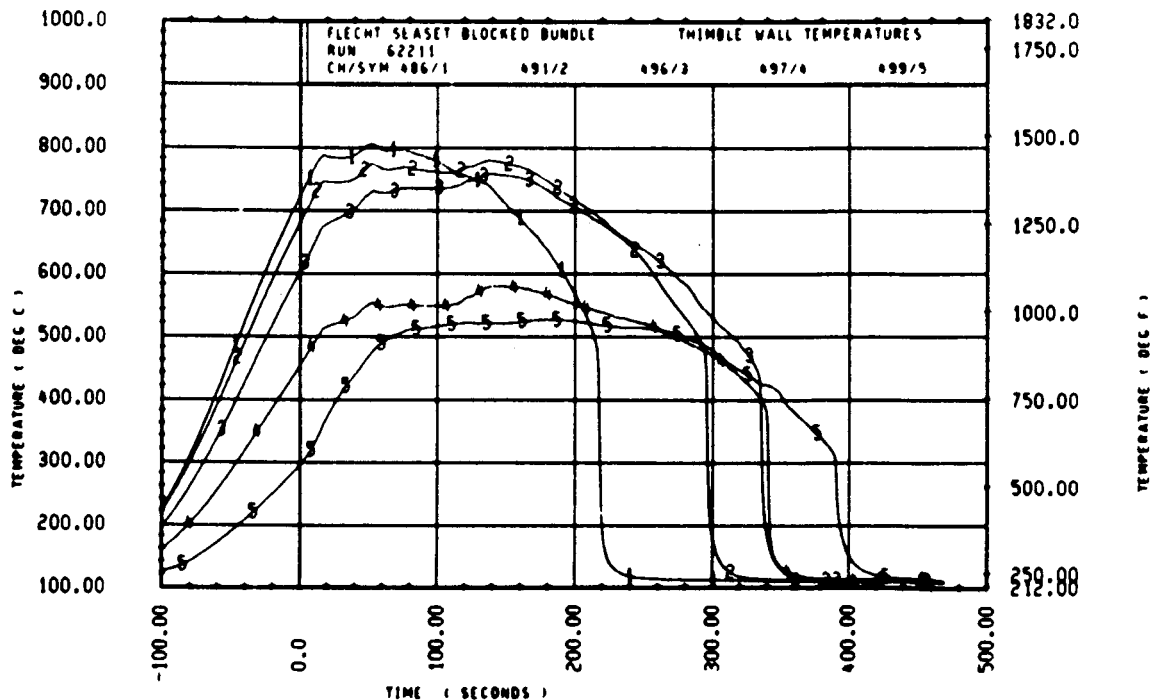
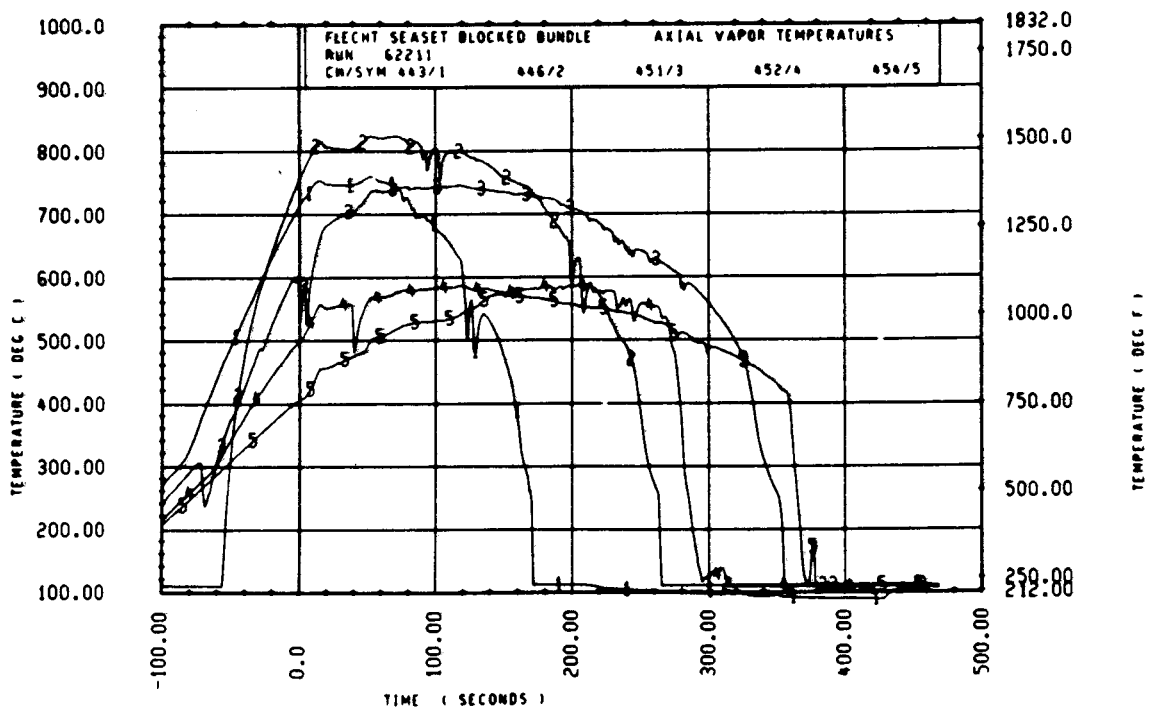
Rod 11E, 2.29 m (90 in.)

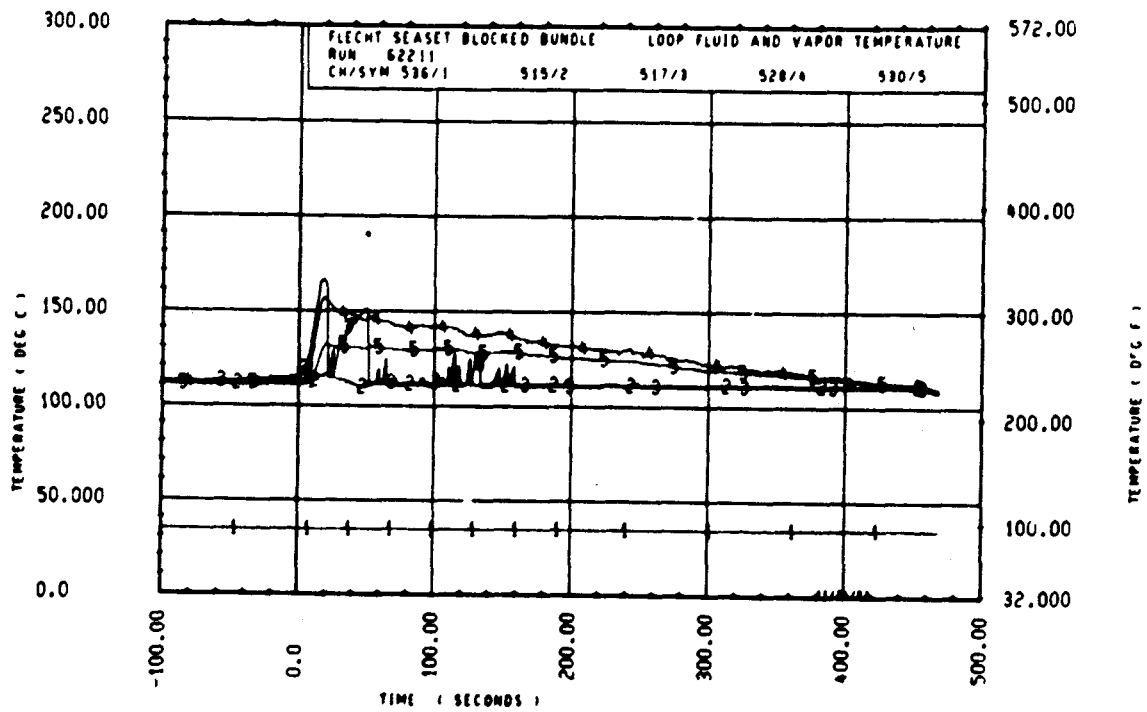
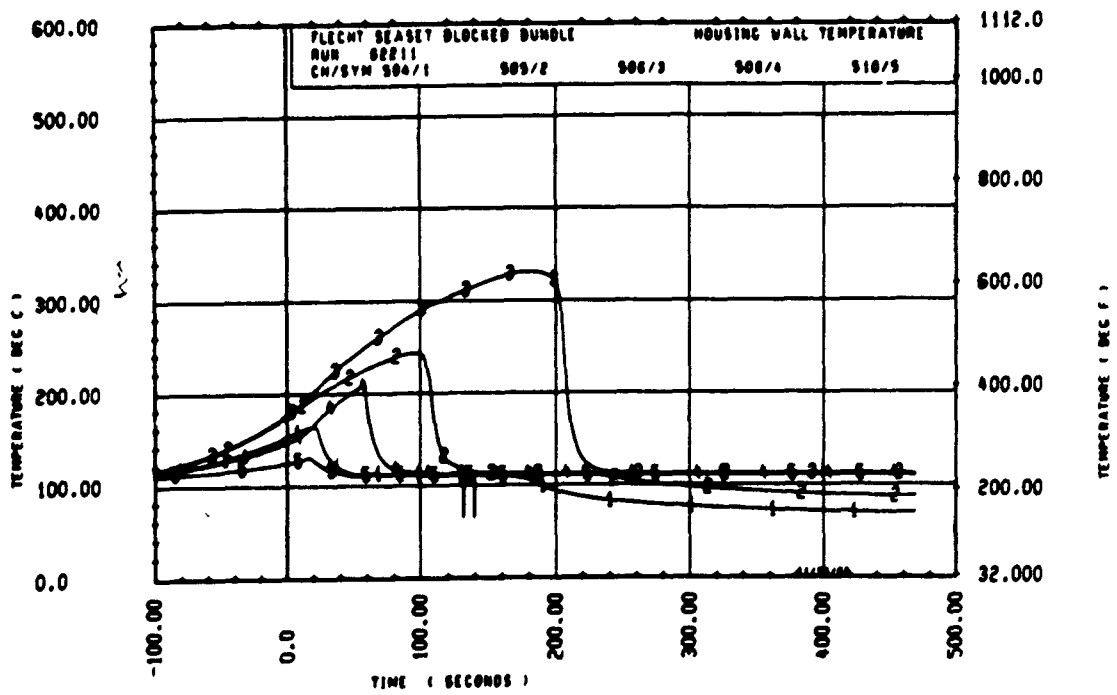


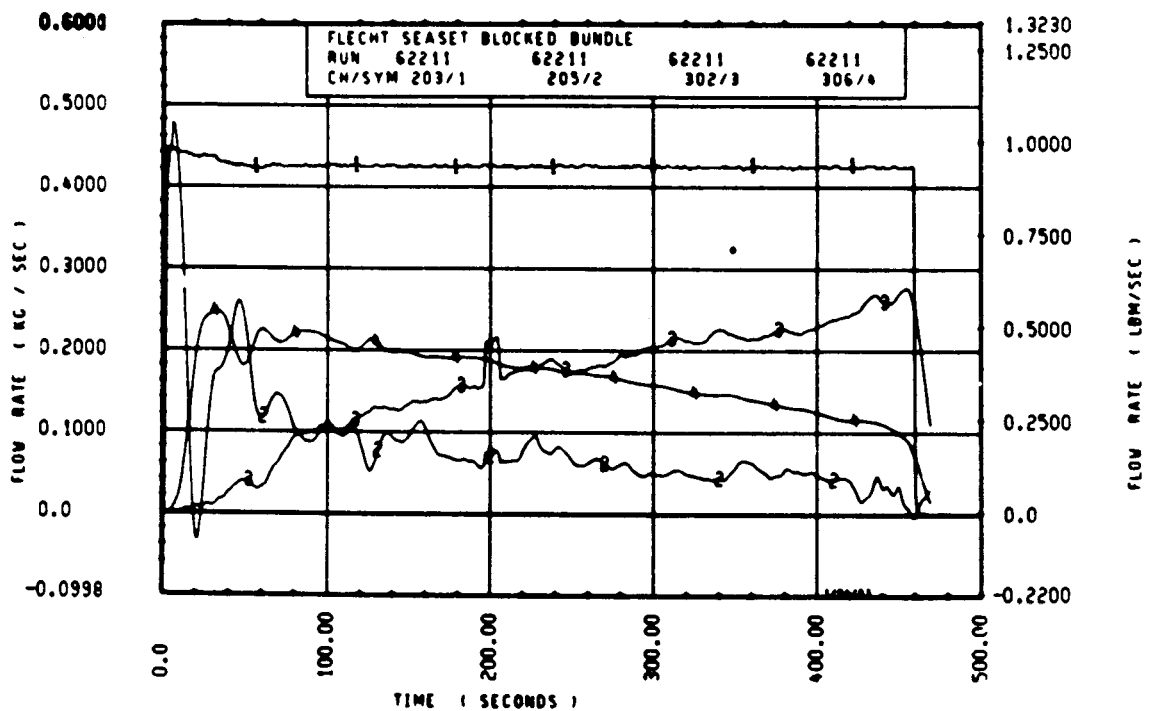
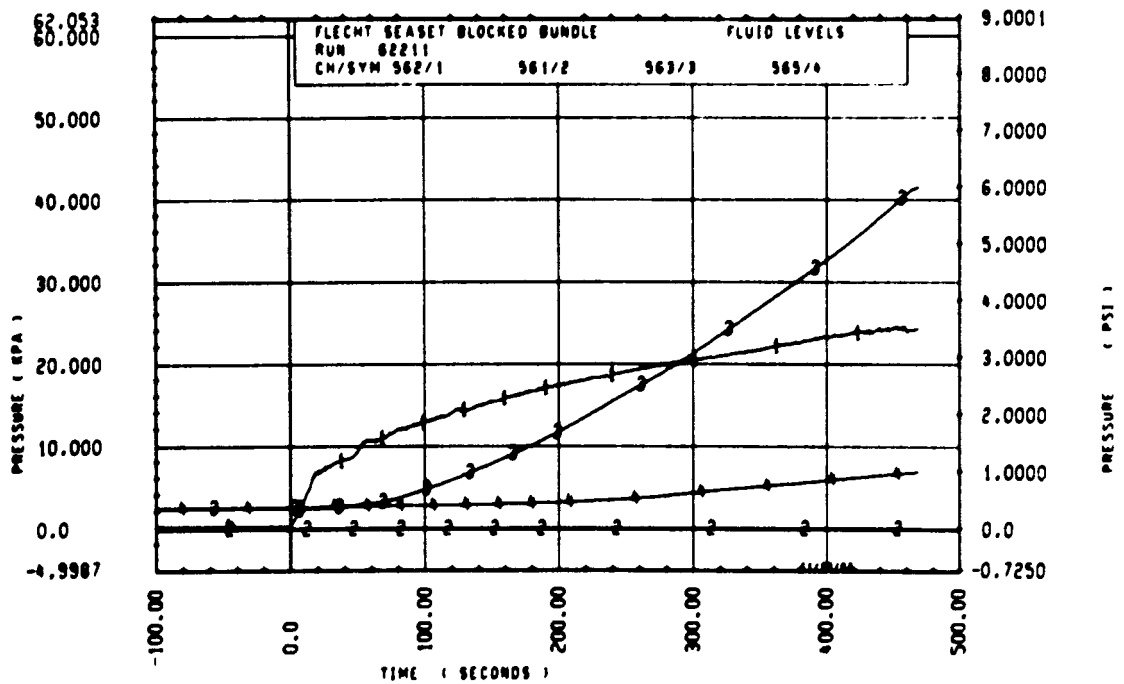
Rod 5J, 2.59 m (102 in.)

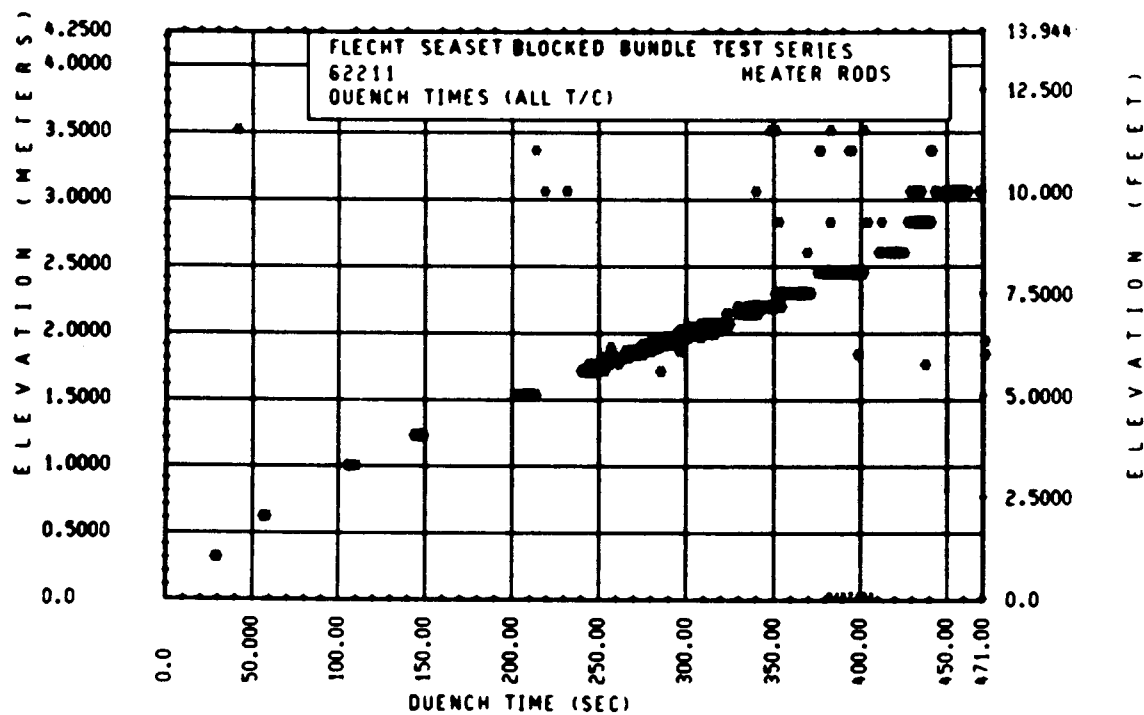
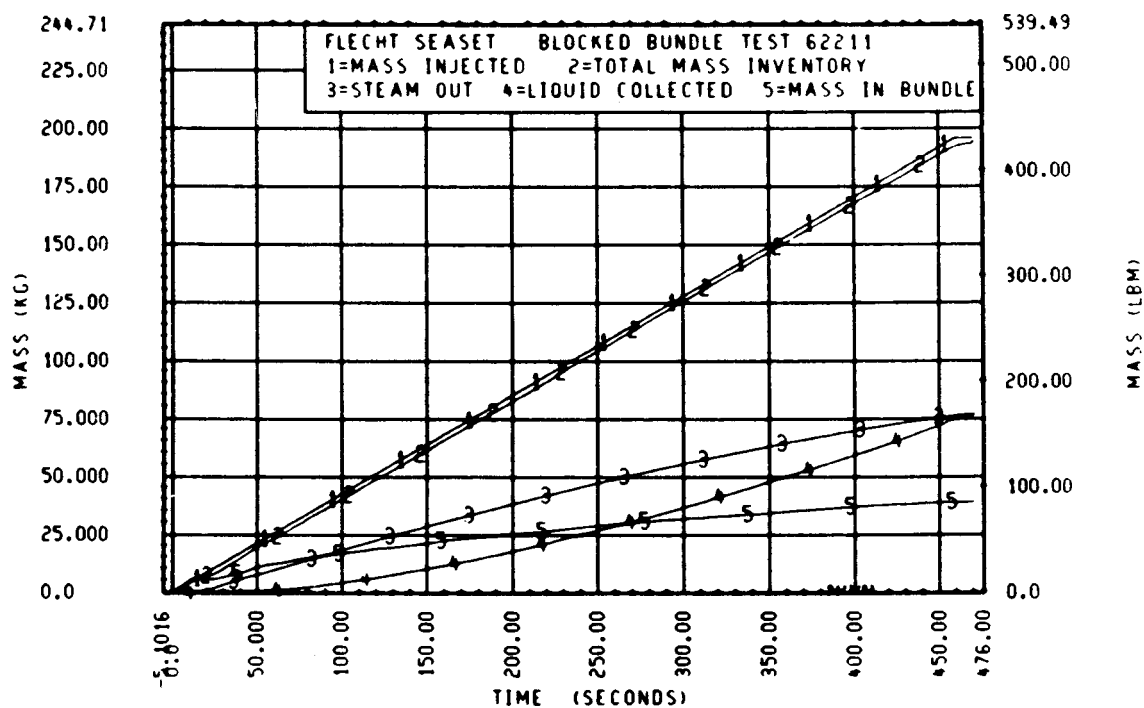


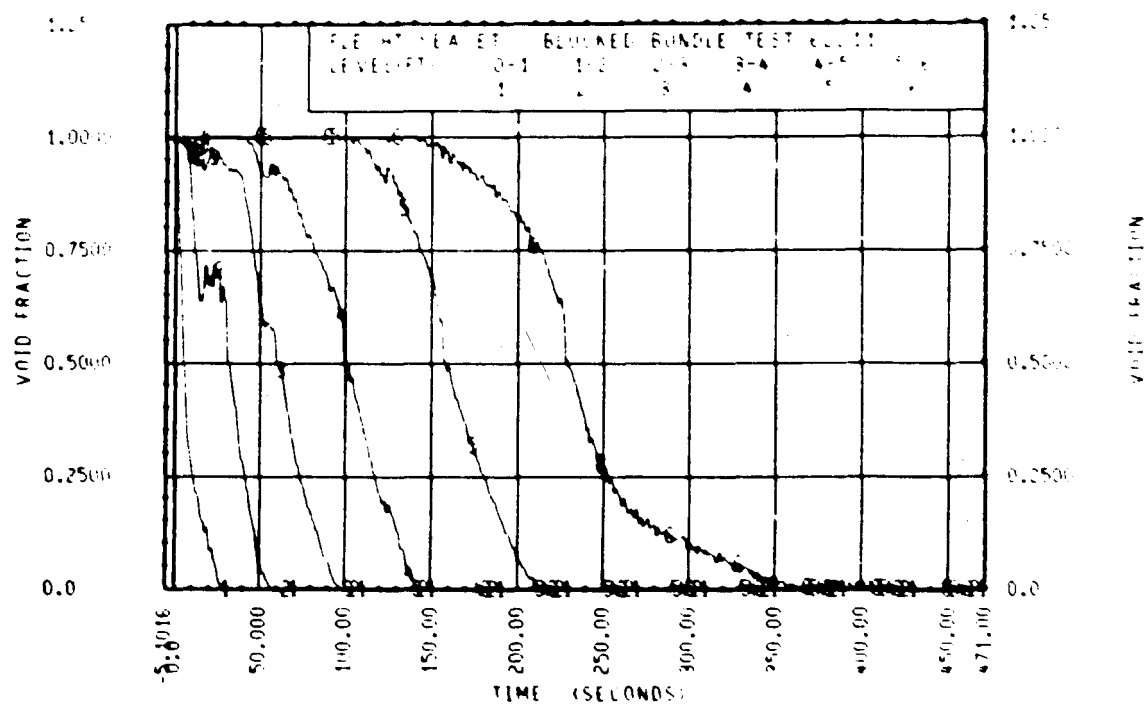
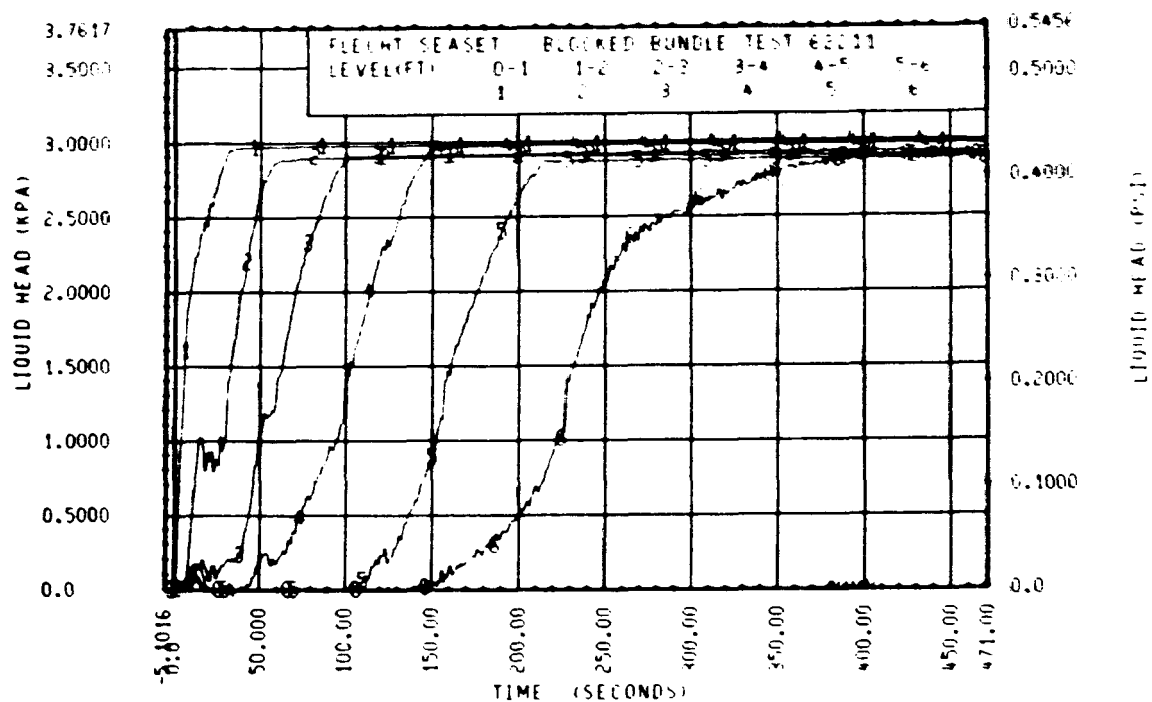
Rod 9C, 2.82 m (111 in.)

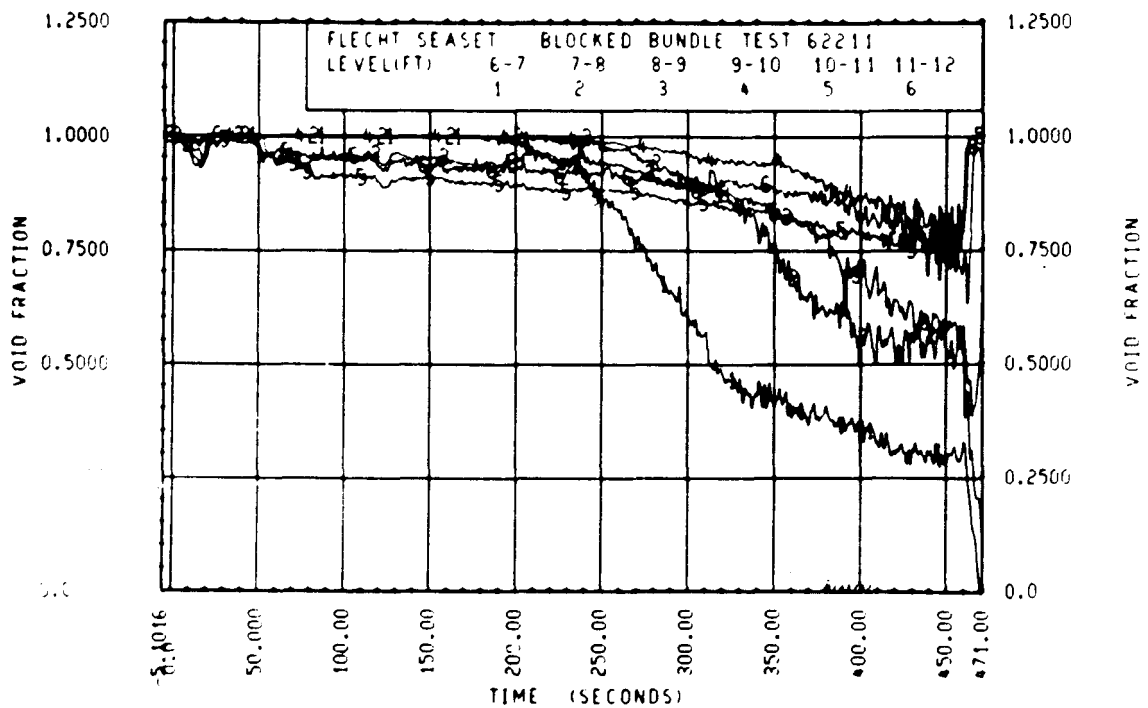
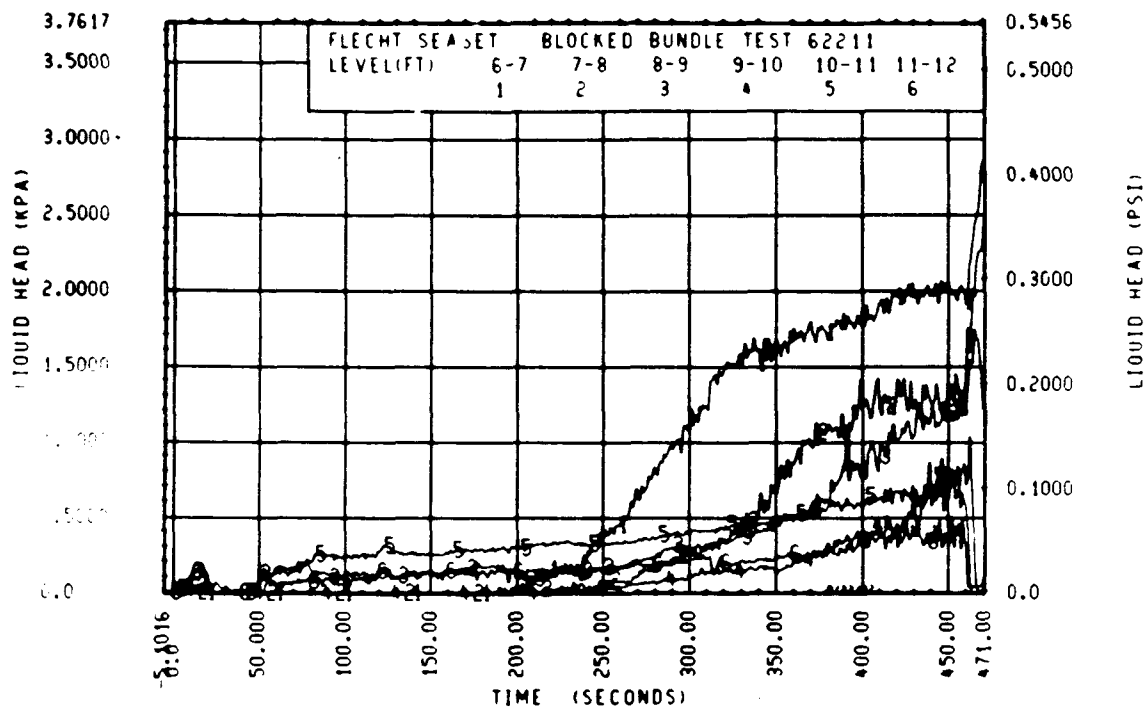












FLECHT SEASET 163-ROD BUNDLE FLOW BLOCKAGE TASK
SUMMARY AND COMMENT SHEET

Run: 62304
Test date: 9/23/82
Test type: Forced reflood
Parameter: Flooding rate effect

AS-RUN TEST CONDITIONS:

Upper plenum pressure	0.277 MPa (40.2 psia)
Initial peak clad temperature and location	877.1°C (1610.8°F), 8N-1.98 m (78 in.)
Initial peak rod power:	
Peripheral rods	2.30 kw/m (0.701 kw/ft)
Bypass rods	2.29 kw/m (0.699 kw/ft)
Blockage island rods	2.30 kw/m (0.700 kw/ft)
Flooding rate	155 mm/sec (6.1 in./sec)
Coolant temperature	53.3°C (128°F)
Initial bundle water level	+5.1 mm (+0.20 in.)

COMMENTS:

Carryover tank filled up at approximately 80 seconds.

Inlet mass flow: ⁽¹⁾ -3.6% linearly decreasing to 0% by 20 seconds and
+0.5% thereafter

Power decay: ⁽¹⁾ peripheral rods, 0% constant
bypass rods, -0.5% constant
blockage rods, - 0.5% linearly decreasing to 0% by 115
seconds

1. Relative to run 31701

5

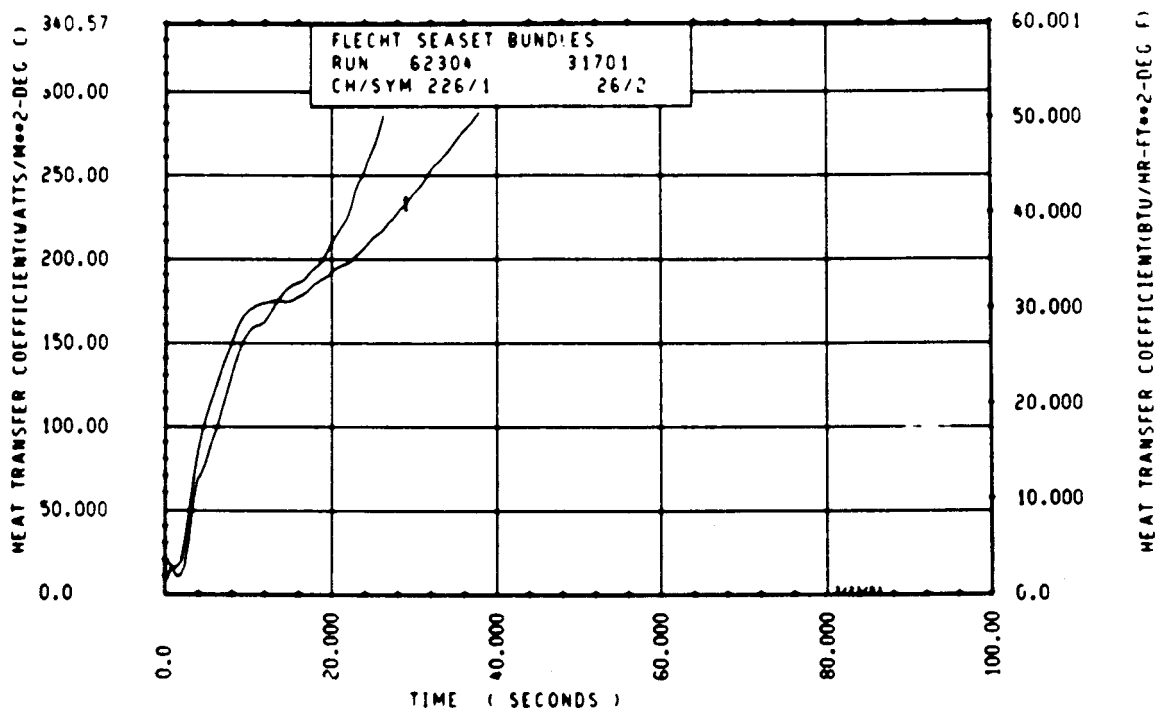
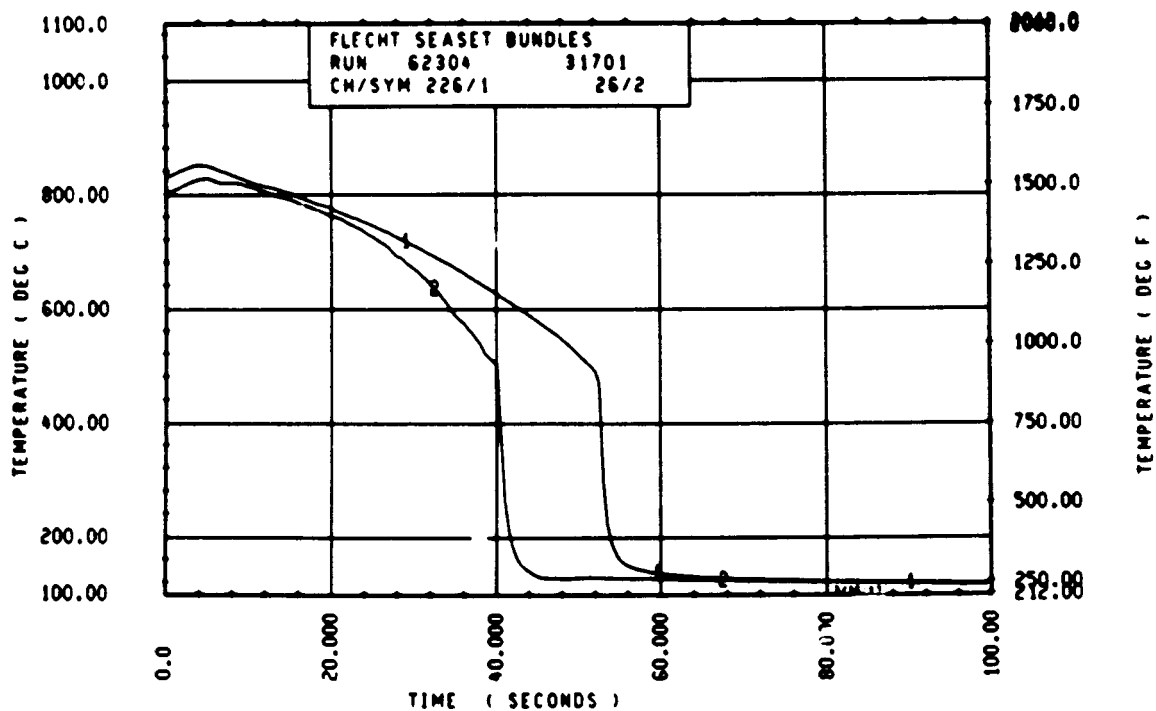
FLECHT SEASET 163 ROD BUNDLE TEST SERIES RUN NUMBER 62304							
ROD/ELEV	CHAN. NO	INITIAL AT FLUCC (DEG F)	MAXIMUM TEMPERATURE (DEG F)	TEMPERATURE RISE (DEG F)	TURNAROUND TIME (SECONDS)	QUENCH TEMPERATURE (DEG F)	QUENCH TIME (SECONDS)
96 1- C	3	683.	690.	7.	2.0	634.	6.6
10H 2- 0	6	695.	910.	15.	3.0	754.	13.9
96 3- 3	9	1224.	1249.	25.	3.5	876.	26.4
3J 4- C	11	1363.	1394.	32.	4.0	870.	36.5
7H 4- C	12	1348.	1381.	33.	4.0	840.	38.0
8K 4- C	13	1368.	1403.	35.	4.0	866.	36.0
8N 4- C	14	1361.	1391.	31.	3.5	886.	36.9
12D 4- C	17	1352.	1382.	30.	3.5	865.	37.9
5E 5- C	20	1511.	1551.	40.	4.0	906.	52.5
76 5- C	21	1567.	1606.	39.	4.0	944.	51.5
96 5- 10	24	1539.	1578.	39.	4.0	940.	51.0
5E 5- 7	33	1540.	1581.	41.	4.0	866.	60.5
66 5- 7	45	1555.	1595.	40.	4.0	815.	61.4
9M 5- 9	52	1492.	1536.	44.	4.0	745.	60.7
76 5- 10	59	1510.	1552.	42.	4.0	829.	63.4
7F 5- 11	62	1453.	1495.	42.	4.0	844.	58.2
46 5- 11	64	1534.	1581.	42.	4.0	601.	65.7
2I 6- C	67	1590.	1632.	42.	4.0	847.	66.6
5D 6- 0	70	1495.	1535.	40.	4.0	808.	66.0
6J 6- 10	74	1527.	1567.	40.	4.0	834.	66.4
7M 6- 0	66	1552.	1590.	38.	4.0	826.	65.7
11E 6- 0	80	1553.	1592.	39.	4.0	612.	65.4
8M 6- 2	97	1372.	1410.	38.	3.5	821.	58.5
5M 6- 2	96	1534.	1575.	41.	4.0	786.	67.4
4E 6- 2	105	1350.	1407.	57.	7.5	402.	89.2
8M 6- 3	111	1416.	1454.	38.	4.0	853.	61.4
46 6- 3	124	1555.	1598.	42.	4.0	632.	69.9
11M 6- 4	134	1481.	1517.	37.	4.0	769.	50.5
9D 6- 4	143	1546.	1586.	40.	4.0	790.	71.2
9J 6- 5	165	1524.	1564.	40.	4.0	886.	67.4
9M 6- 5	166	1590.	1633.	43.	4.0	831.	72.2
8J 6- 6	192	1572.	1610.	38.	4.0	939.	63.9
9D 6- 6	193	1558.	1599.	41.	4.0	786.	73.0
11F 6- 6	173	1556.	1598.	41.	4.0	792.	72.9
46 7- 0	261	1484.	1525.	41.	4.0	776.	80.9
7D 7- 6	309	1481.	1522.	41.	4.0	771.	88.1
76 7- 6	312	1522.	1565.	43.	4.0	887.	79.2
11E 7- 6	325	1487.	1528.	41.	4.0	750.	88.9
5L 8- C	337	1304.	1348.	39.	4.0	700.	98.0
7H 8- 0	345	1359.	1399.	40.	4.0	724.	95.7
7K 8- 10	346	1360.	1401.	41.	4.0	712.	94.6
5J 8- 6	366	1139.	1176.	37.	4.0	683.	104.6
78 8- 6	368	1124.	1159.	35.	4.0	632.	105.5
7E 9- 3	383	1100.	1134.	34.	4.0	594.	111.0
8H 9- 3	387	1054.	1086.	32.	4.0	584.	111.5
9C 9- 3	389	1042.	1070.	28.	4.0	589.	108.4
11F 9- 3	394	1040.	1070.	30.	4.0	562.	109.4
7810- 0	408	850.	878.	28.	4.5	286.	64.0
8M10- 0	415	863.	890.	28.	4.5	536.	68.4
8K10- 10	417	863.	890.	28.	4.5	465.	80.6
8N10- C	418	879.	909.	30.	4.5	427.	86.4
6M11- 0	429	695.	712.	17.	4.0	612.	17.1
9611- 0	431	691.	709.	18.	4.0	623.	15.1
11E11- 10	432	693.	710.	17.	4.0	614.	16.0
5J11- 6	436	674.	691.	17.	4.0	550.	27.0
7811- 6	437	643.	660.	17.	4.0	549.	27.0
8J11- 6	438	686.	703.	17.	4.0	591.	20.4

RUN 62304 HEATER ROD STATISTICAL DATA

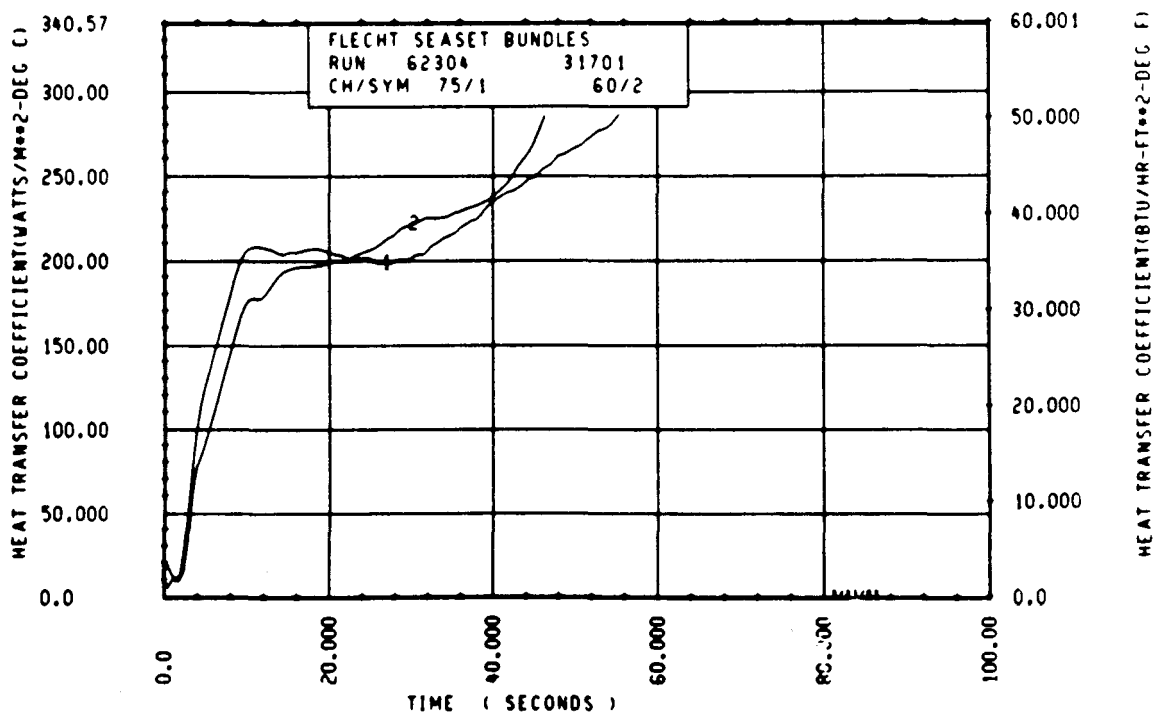
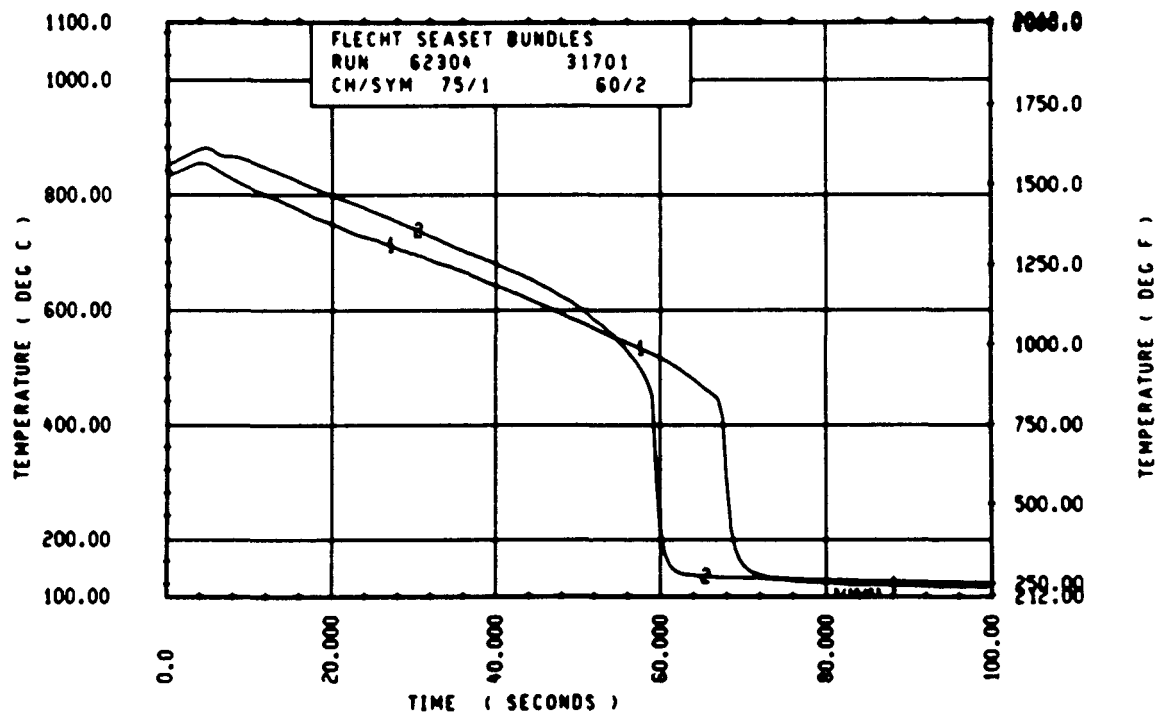
ELEV	INITIAL TEMP (DEG F)			MAX TEMP (DEG F)			TURNAROUND TIME (SEC)		
	MAX	MIN	MEAN	MAX	MIN	MEAN	MAX	MIN	MEAN
12	684.8	682.7	684.1	692.1	690.0	691.4	2.0	2.0	2.0
24	894.6	866.7	876.3	910.1	881.2	891.1	3.0	3.0	3.0
39	1224.3	1174.4	1193.9	1249.3	1199.3	1218.0	3.5	3.5	3.5
48	1378.6	1346.0	1361.7	1409.3	1380.7	1393.3	4.0	3.5	3.8
60	1567.3	1434.9	1522.6	1607.5	1474.5	1562.3	4.5	3.5	4.1
67	1602.0	1512.1	1557.7	1642.7	1553.2	1598.0	4.5	3.5	4.0
69	1532.7	1491.6	1517.0	1573.8	1535.9	1557.0	4.0	4.0	4.0
70	1603.1	1476.6	1529.9	1644.9	1519.6	1571.1	4.0	4.0	4.0
71	1539.2	1453.1	1489.6	1581.4	1494.8	1532.1	4.5	4.0	4.1
72	1593.3	1453.1	1541.6	1637.2	1493.7	1582.9	4.0	4.0	4.0
73	1587.9	1443.5	1523.1	1627.3	1484.1	1564.1	4.5	4.0	4.0
74	1585.8	1372.2	1507.2	1625.1	1410.3	1547.9	4.0	3.5	4.0
75	1595.5	1415.7	1518.9	1637.2	1454.2	1559.8	5.0	4.0	4.1
76	1609.7	1455.3	1547.6	1651.5	1494.8	1588.4	4.0	3.5	4.0
77	1590.1	1484.1	1543.6	1632.8	1520.7	1583.6	4.5	4.0	4.0
78	1610.8	1521.8	1560.8	1653.7	1563.0	1601.2	4.5	4.0	4.0
79	1603.1	1507.7	1562.2	1643.8	1548.9	1602.9	4.5	4.0	4.0
80	1582.5	1504.5	1550.0	1622.9	1546.7	1591.7	4.5	4.0	4.1
81	1577.1	1473.4	1533.5	1616.3	1518.5	1575.9	4.5	4.0	4.1
84	1542.4	1428.5	1494.7	1581.4	1467.0	1533.4	4.0	3.5	3.7
86	1586.8	1475.5	1535.5	1626.2	1513.1	1575.1	4.0	3.5	3.9
90	1529.4	1423.2	1488.6	1572.7	1463.8	1528.0	4.0	4.0	4.0
96	1400.7	1253.5	1349.1	1442.4	1291.1	1389.3	4.5	4.0	4.0
102	1193.1	1014.3	1149.1	1234.7	1047.2	1186.8	4.0	4.0	4.0
111	1099.8	1036.0	1064.5	1134.0	1066.8	1095.5	4.0	4.0	4.0
120	923.5	820.1	866.3	951.3	848.1	894.7	5.0	4.0	4.4
132	695.3	685.8	691.2	712.0	703.6	708.4	4.0	4.0	4.0
138	685.8	642.8	664.2	702.6	659.6	680.8	4.0	4.0	4.0

RUN 62304 HEATER ROD STATISTICAL DATA

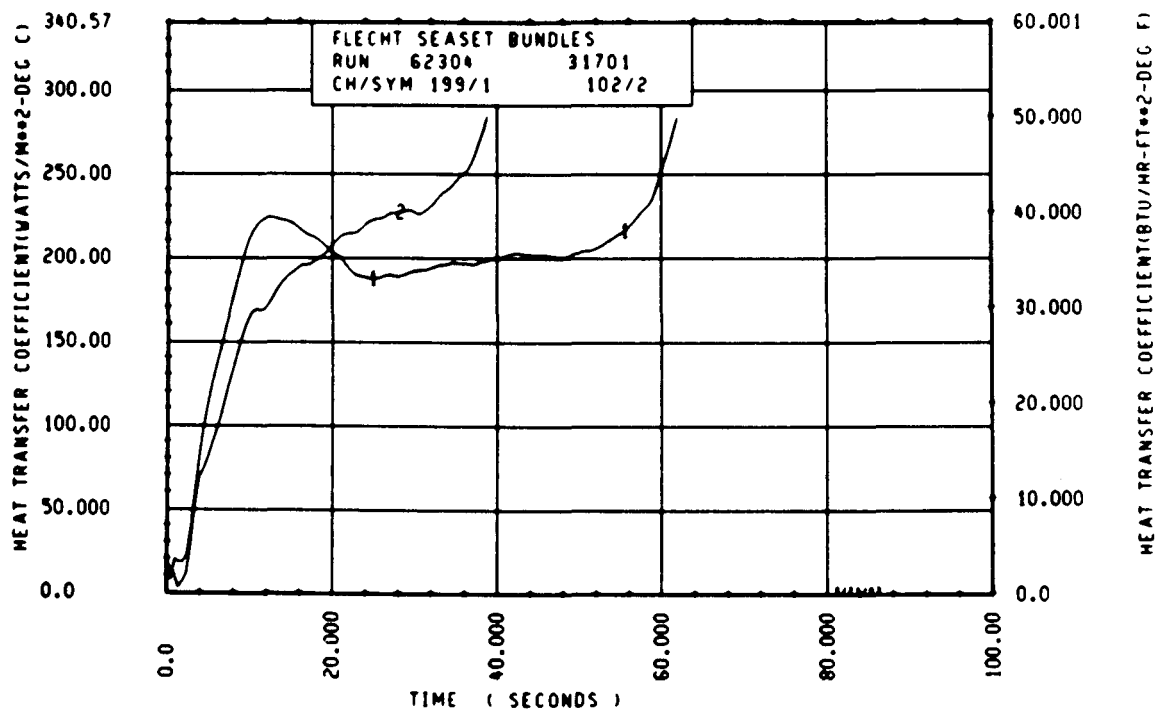
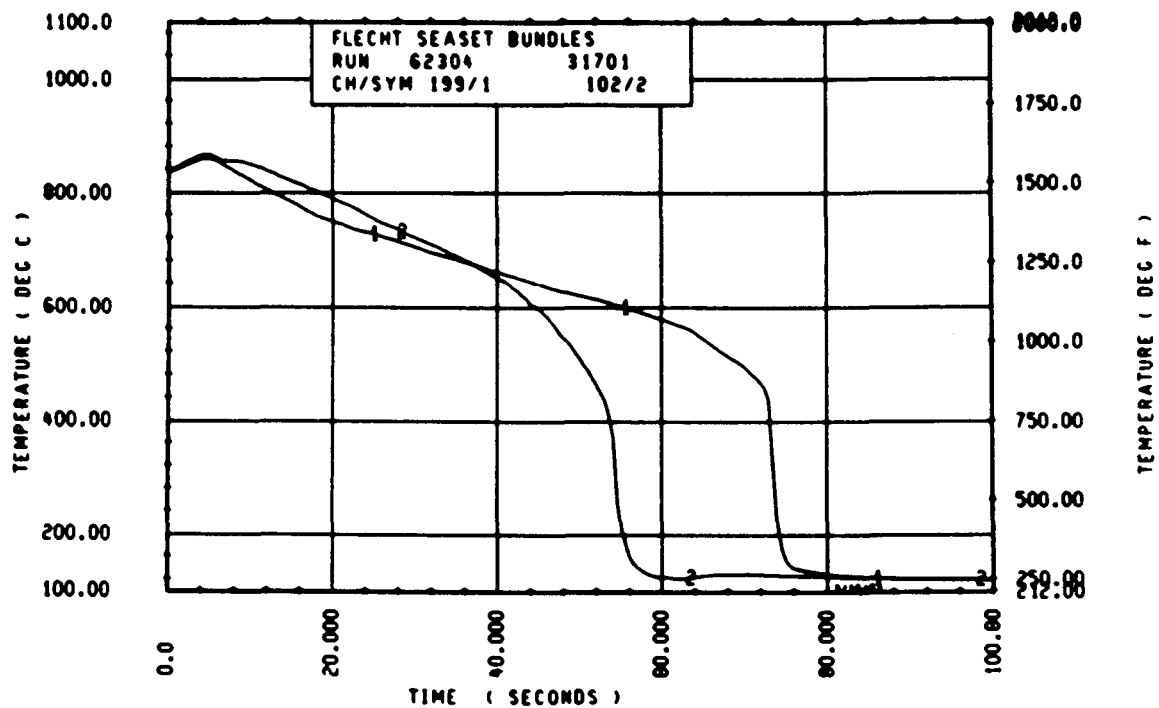
ELEV	TEMP RISE (DEG F)			QUENCH TEMP (DEG F)			QUENCH TIME (SEC)		
	MAX	MIN	MEAN	MAX	MIN	MEAN	MAX	MIN	MEAN
12	7.3	7.3	7.3	634.2	627.9	630.9	6.9	6.6	6.6
24	15.5	14.5	14.6	754.2	747.6	751.6	13.9	13.0	13.3
39	25.9	20.8	24.2	875.7	815.9	854.9	27.5	26.4	27.0
48	34.8	29.5	31.7	887.5	839.9	867.6	38.0	36.5	37.3
60	43.3	35.3	39.5	944.3	850.3	905.7	53.3	51.0	52.0
67	42.2	36.8	40.3	891.7	731.9	849.3	62.1	58.6	60.3
69	44.3	37.9	40.1	860.5	745.4	817.3	64.0	60.7	62.3
70	43.0	39.0	41.2	854.4	820.0	834.7	65.5	63.4	64.3
71	44.9	41.2	42.5	843.9	764.3	812.9	65.7	58.3	63.4
72	43.9	37.9	41.2	858.0	760.9	823.1	67.4	65.4	66.3
73	43.3	36.8	40.9	859.2	745.1	814.0	68.4	64.6	67.2
74	42.5	38.1	40.7	871.9	776.7	819.4	69.2	51.1	65.2
75	46.0	36.8	40.9	1133.0	718.7	848.9	70.9	32.9	63.9
76	43.8	36.6	40.9	937.1	769.1	836.4	71.5	50.5	66.7
77	43.5	36.6	40.0	930.1	785.0	872.8	73.0	53.3	65.2
78	45.5	36.0	40.5	964.7	741.4	855.4	73.9	43.1	67.0
79	44.6	36.6	40.7	1044.6	792.8	876.7	75.4	46.4	66.6
80	44.4	38.1	41.7	1043.1	799.6	873.6	76.4	42.9	68.2
81	45.5	39.0	42.4	998.6	806.1	886.3	77.5	49.6	69.0
84	43.3	35.8	38.7	934.0	722.7	791.3	81.7	62.5	77.4
86	42.4	36.6	39.6	924.8	703.3	774.5	83.9	67.2	80.4
90	43.3	37.6	41.1	940.8	715.9	777.5	90.2	79.2	87.4
96	42.5	37.5	40.2	833.5	673.3	734.8	98.0	91.2	95.8
102	41.7	33.0	37.6	722.1	602.0	671.4	105.5	102.5	104.0
111	34.2	26.6	31.0	661.7	561.9	584.6	112.5	94.0	109.7
120	31.0	24.6	28.4	673.1	284.6	489.8	106.4	14.2	74.7
132	17.6	16.7	17.2	623.0	583.8	606.0	20.5	15.1	17.5
138	17.9	14.7	16.6	591.2	283.5	499.4	53.0	20.4	31.4



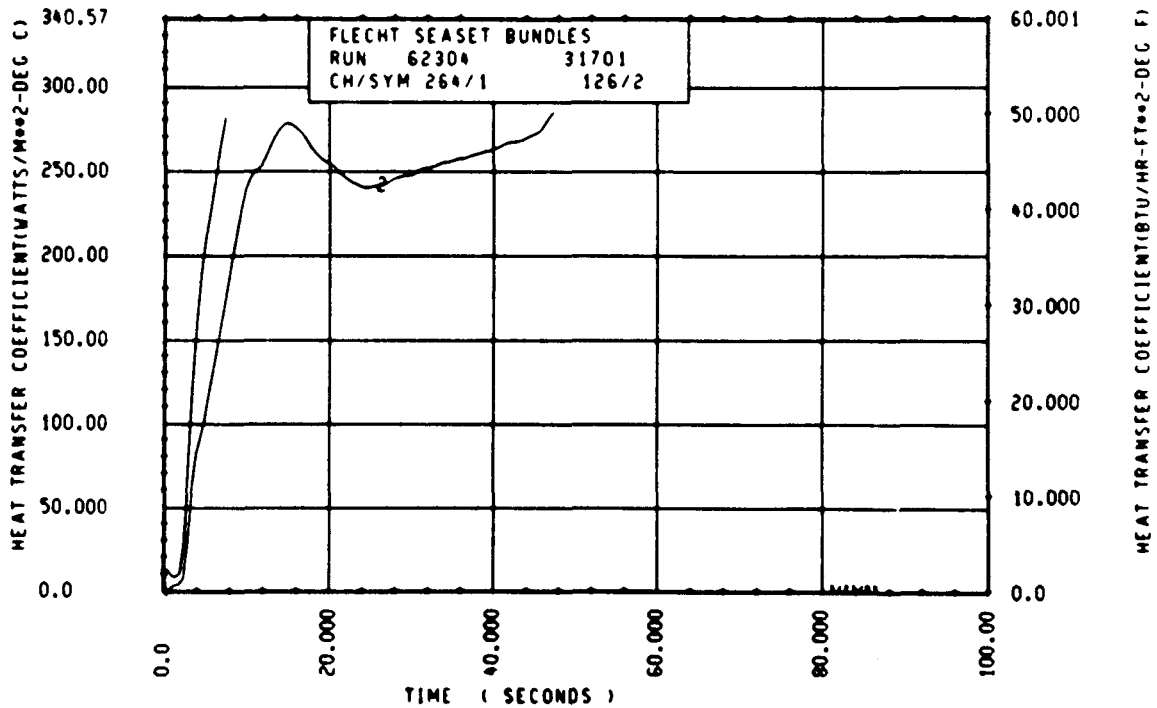
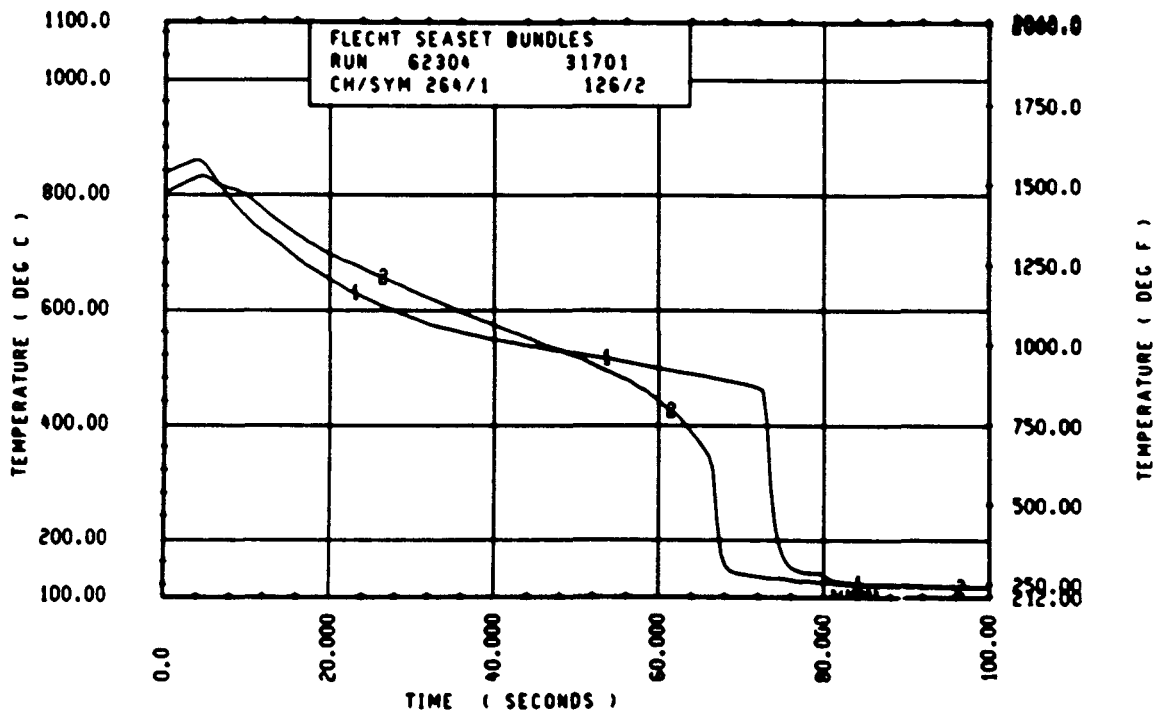
Rod 11E, 1.52 m (60 in.)



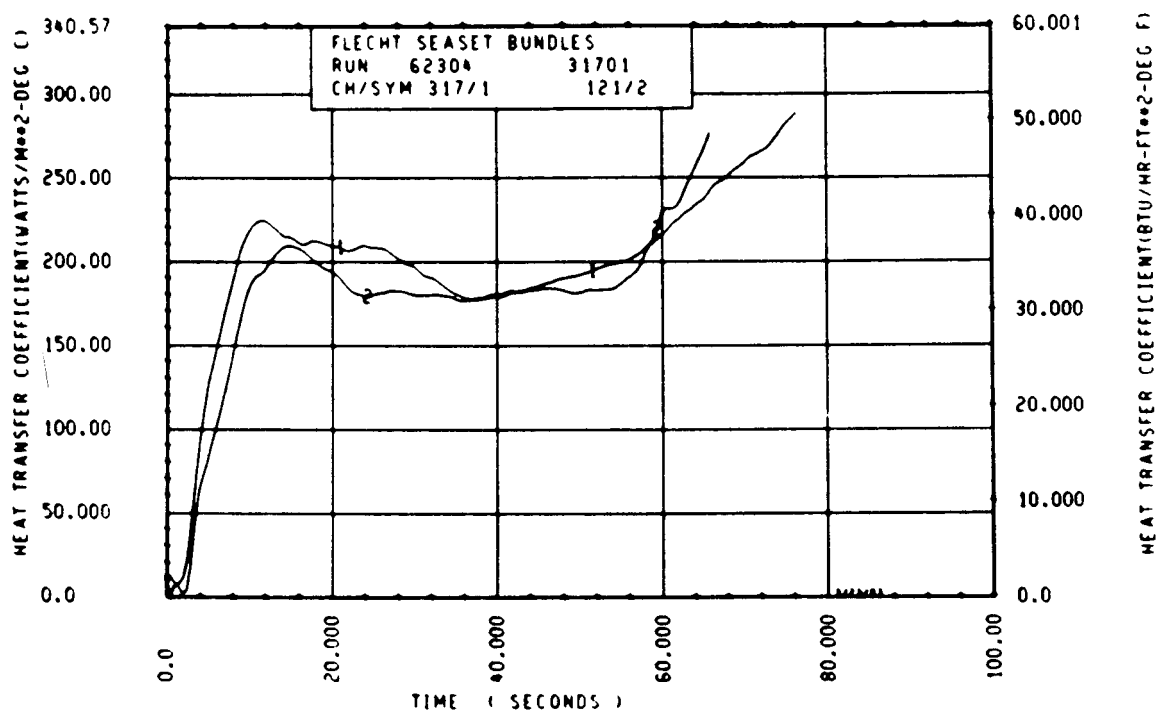
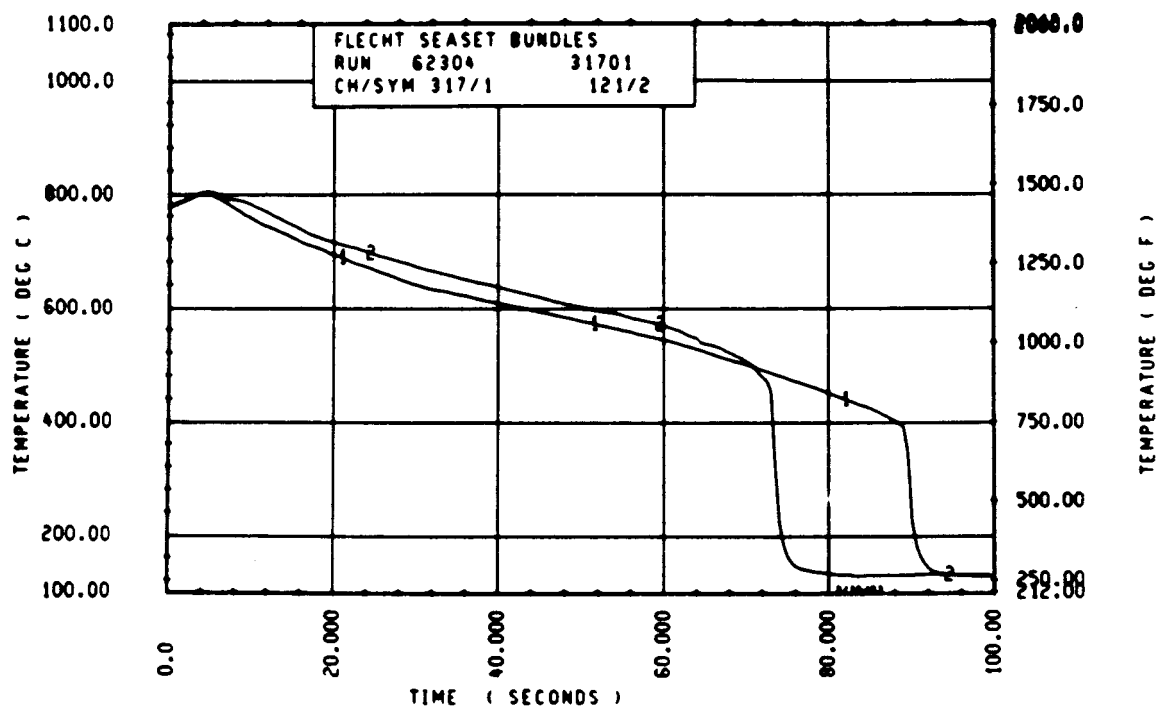
Rod 6L, 1.88 m (74 in.)



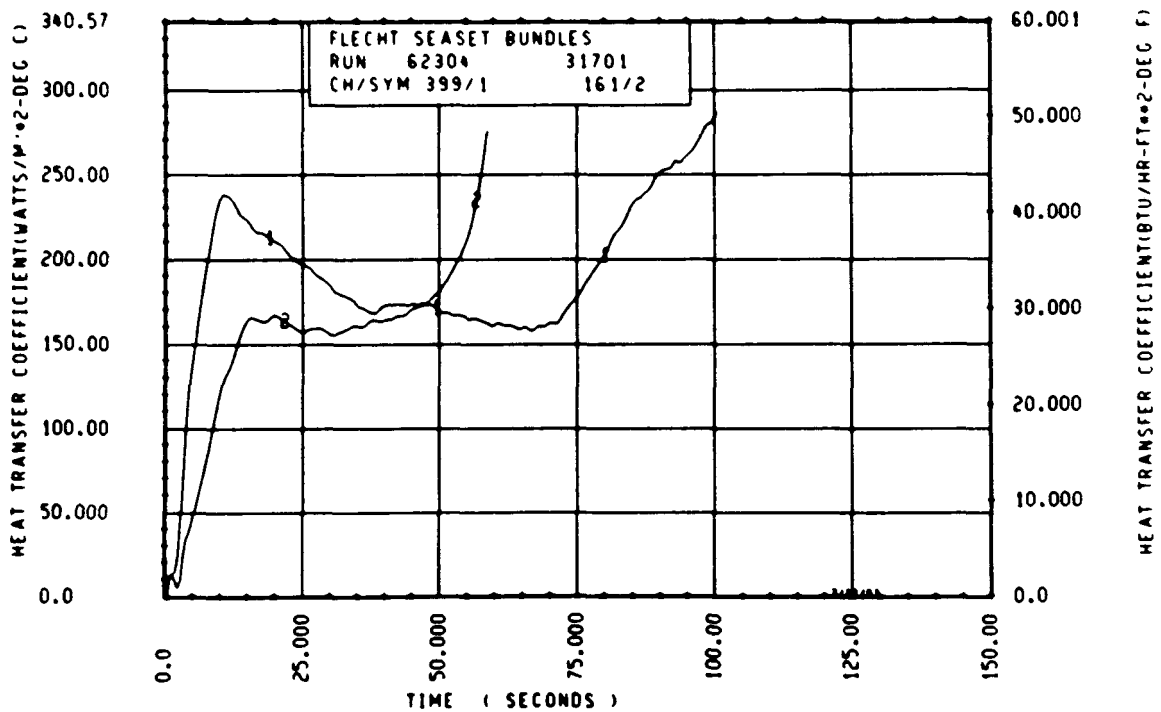
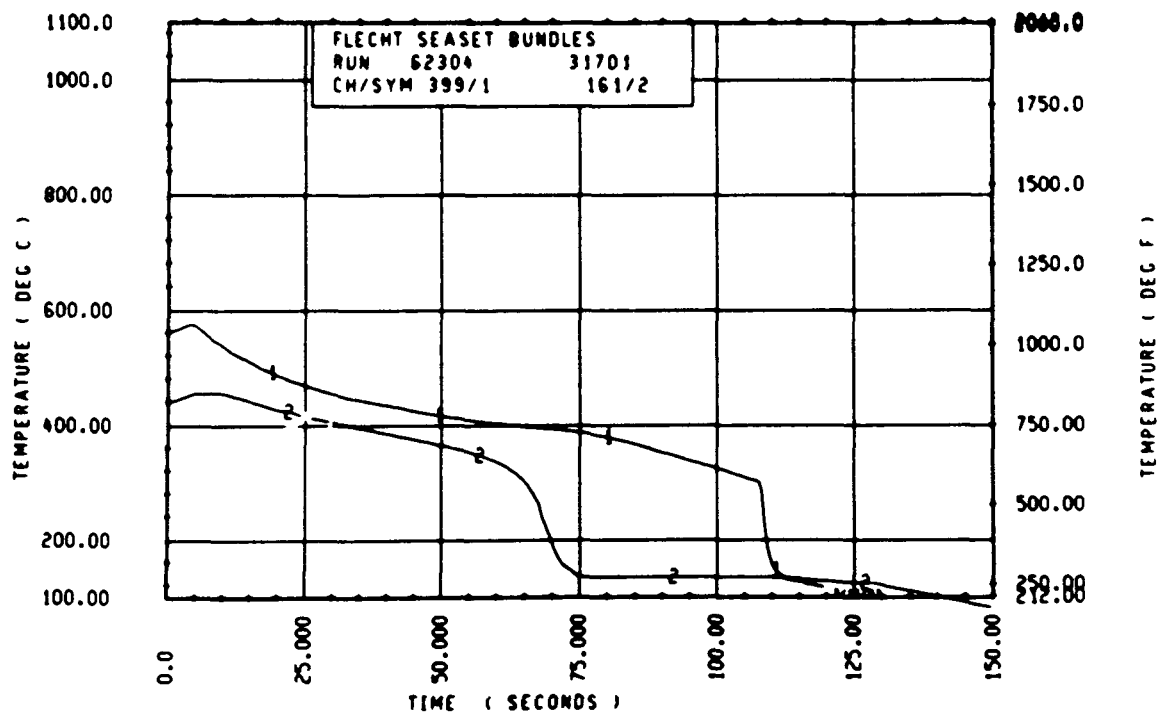
Rod 13G, 1.98 m (78 in.)



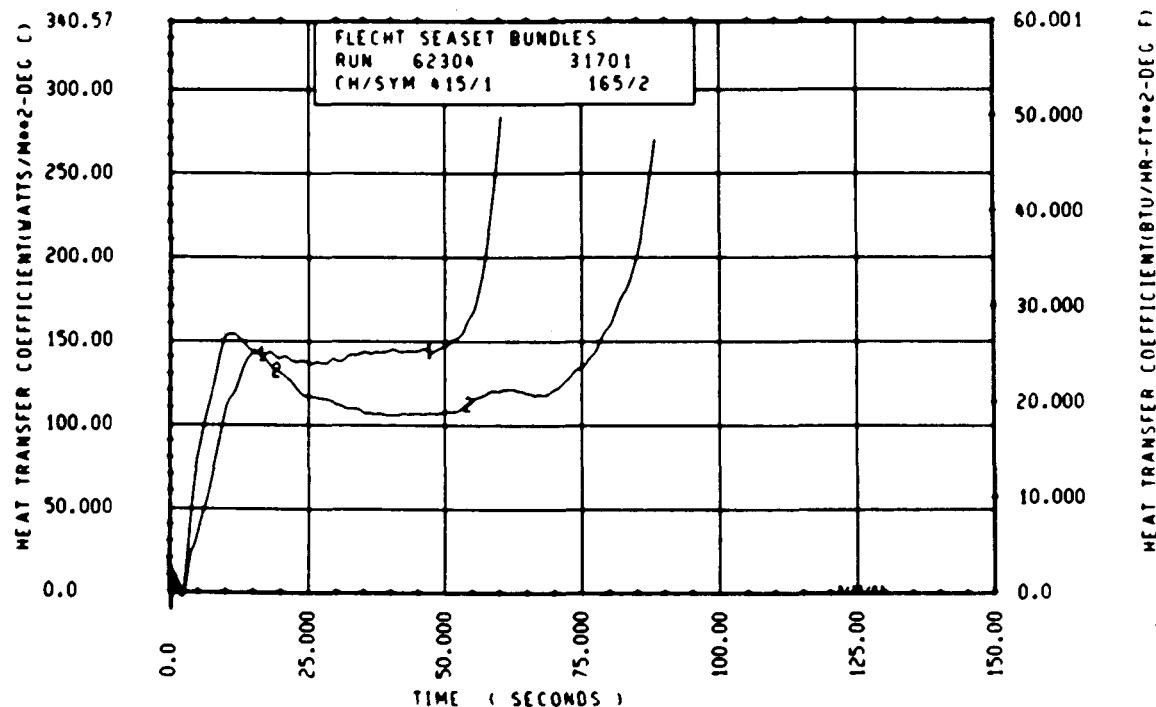
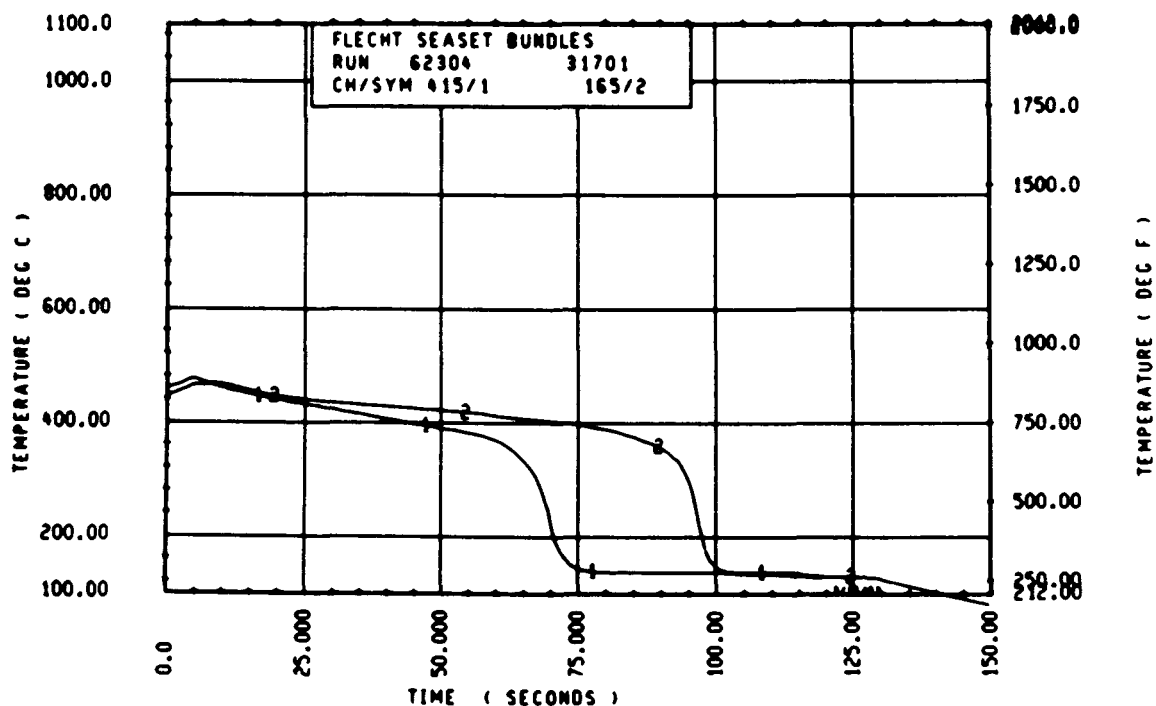
Rod 7E, 2.13 m (84 in.)



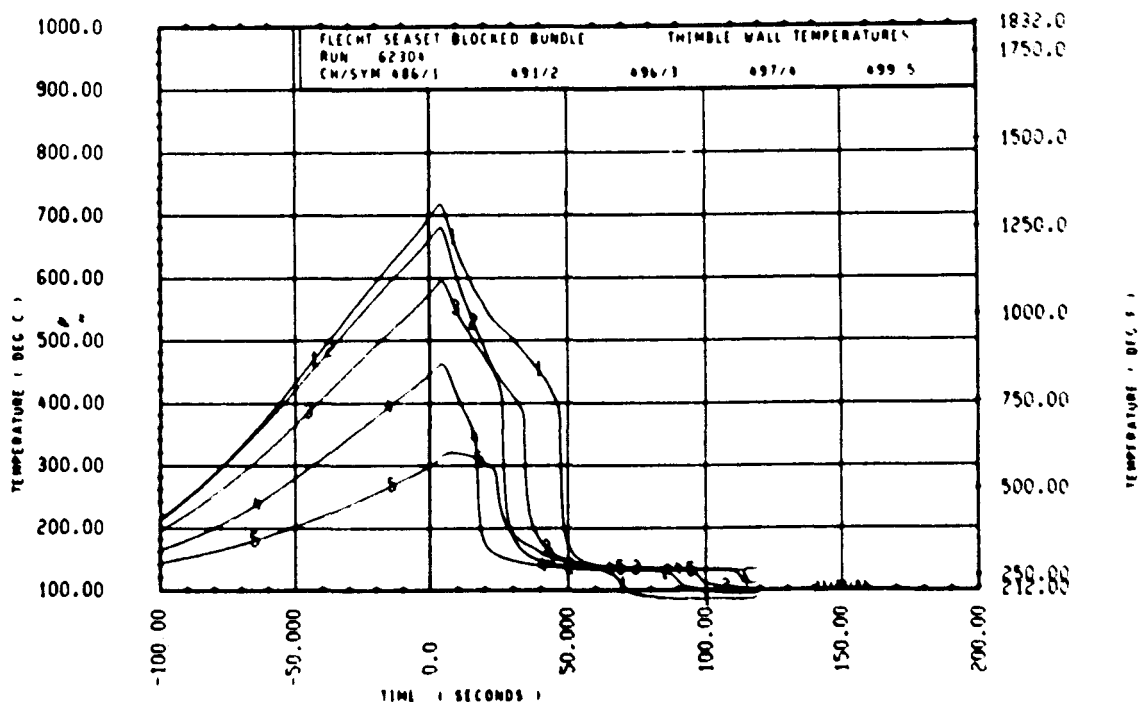
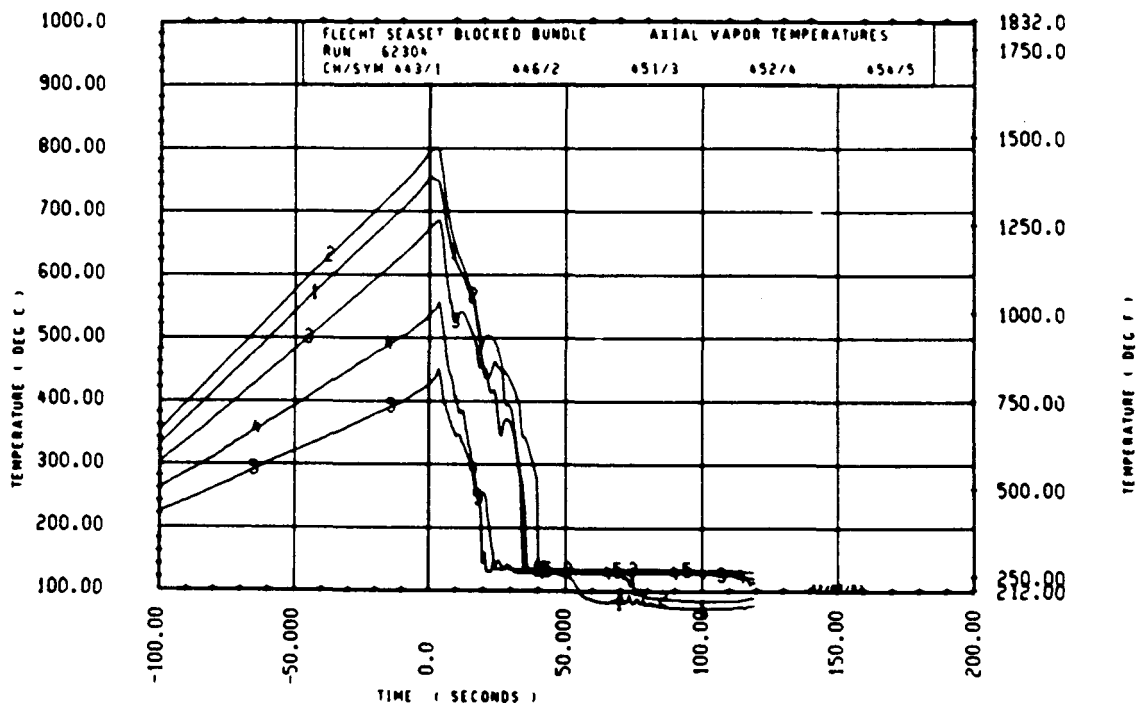
Rod 9C, 2.29 m (90 in.)

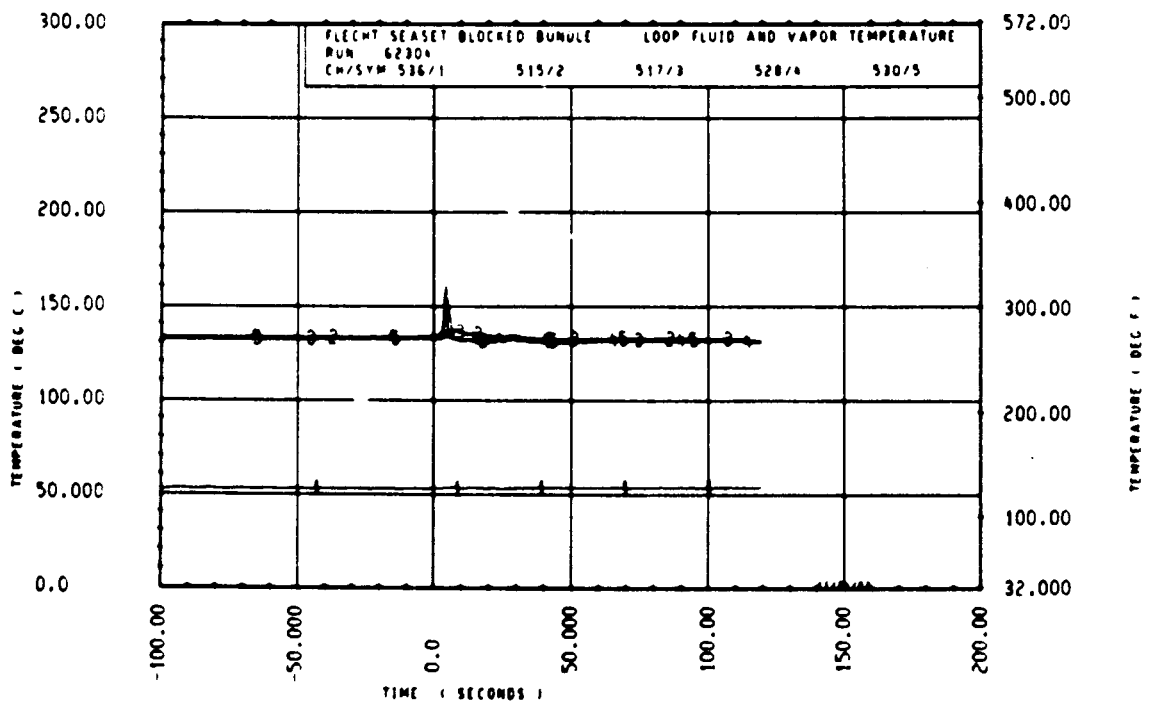
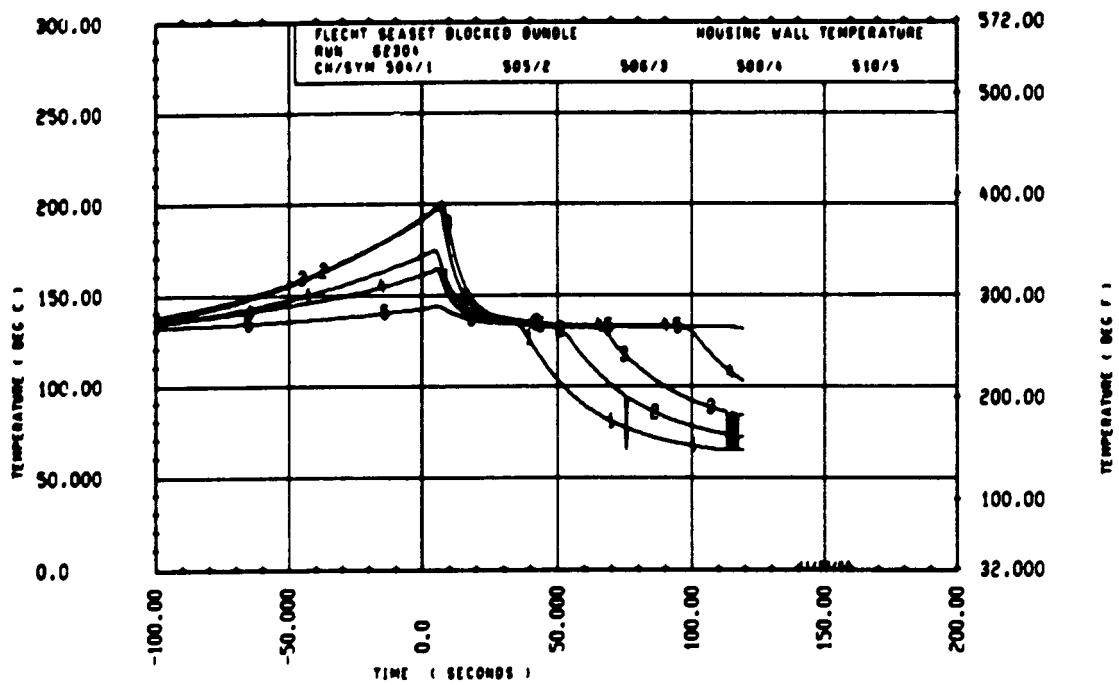


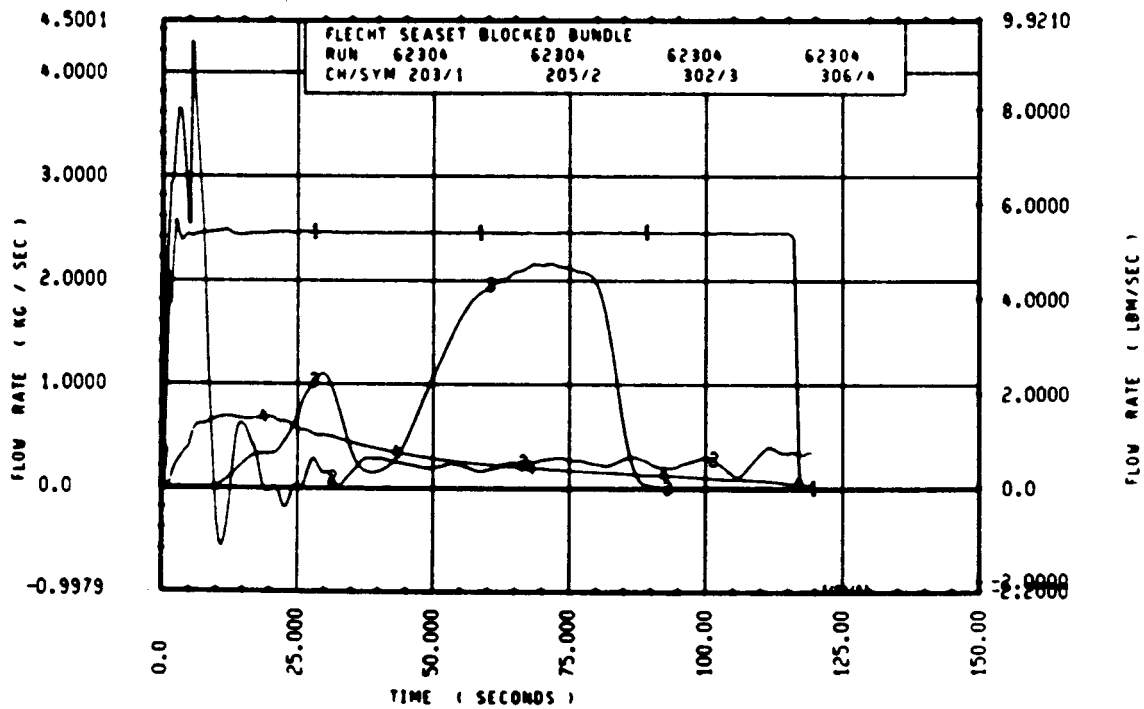
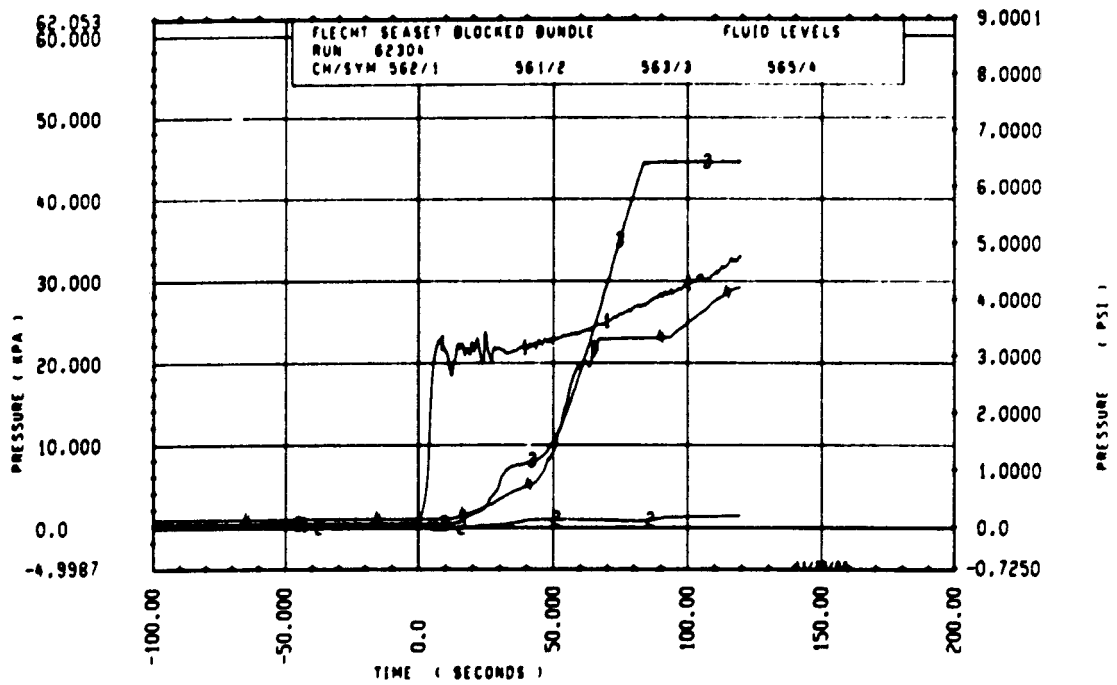
Rod 13G, 2.82 m (111 in.)

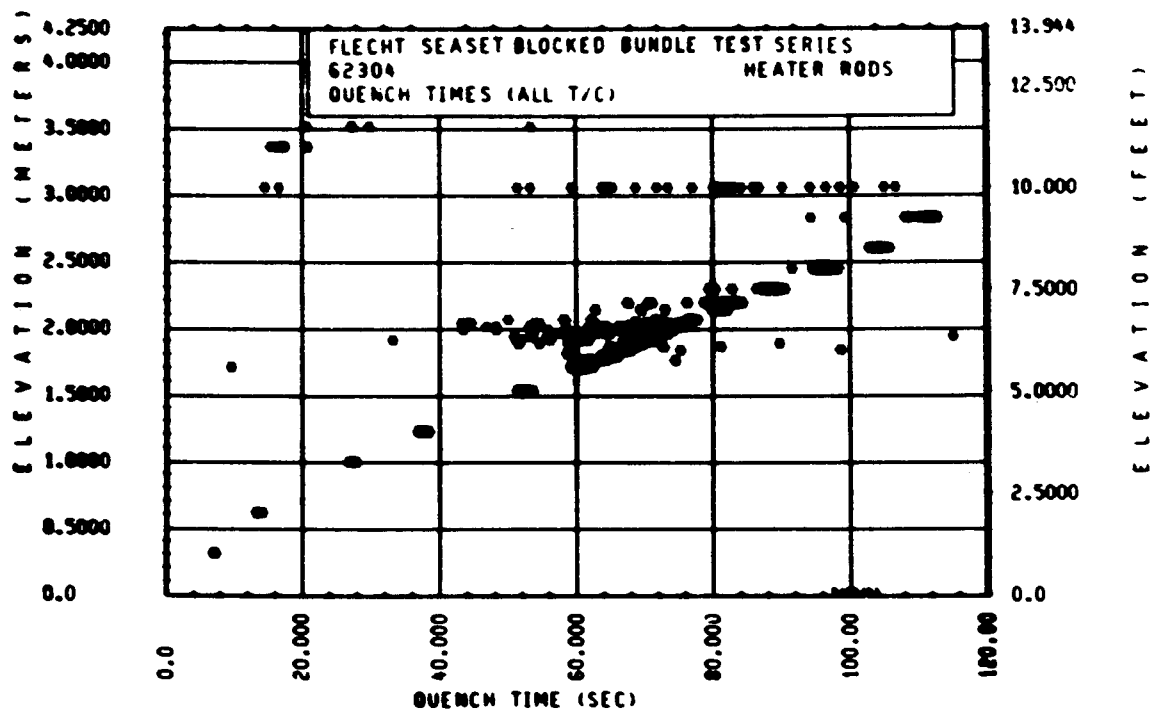
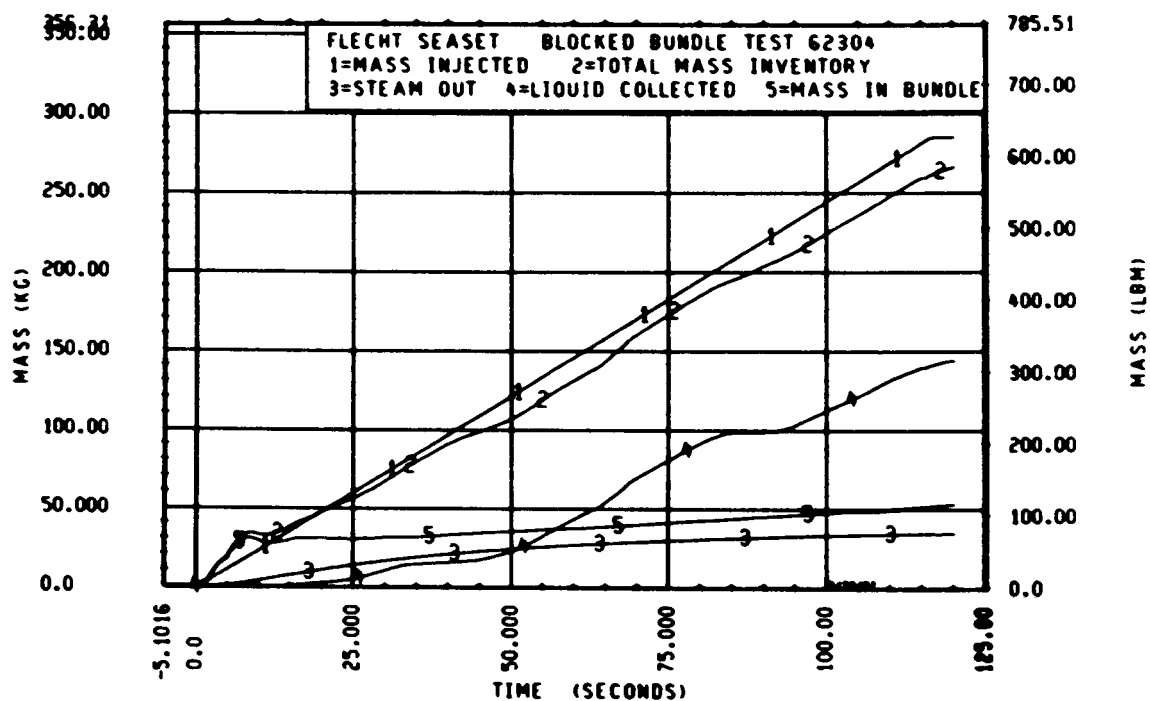


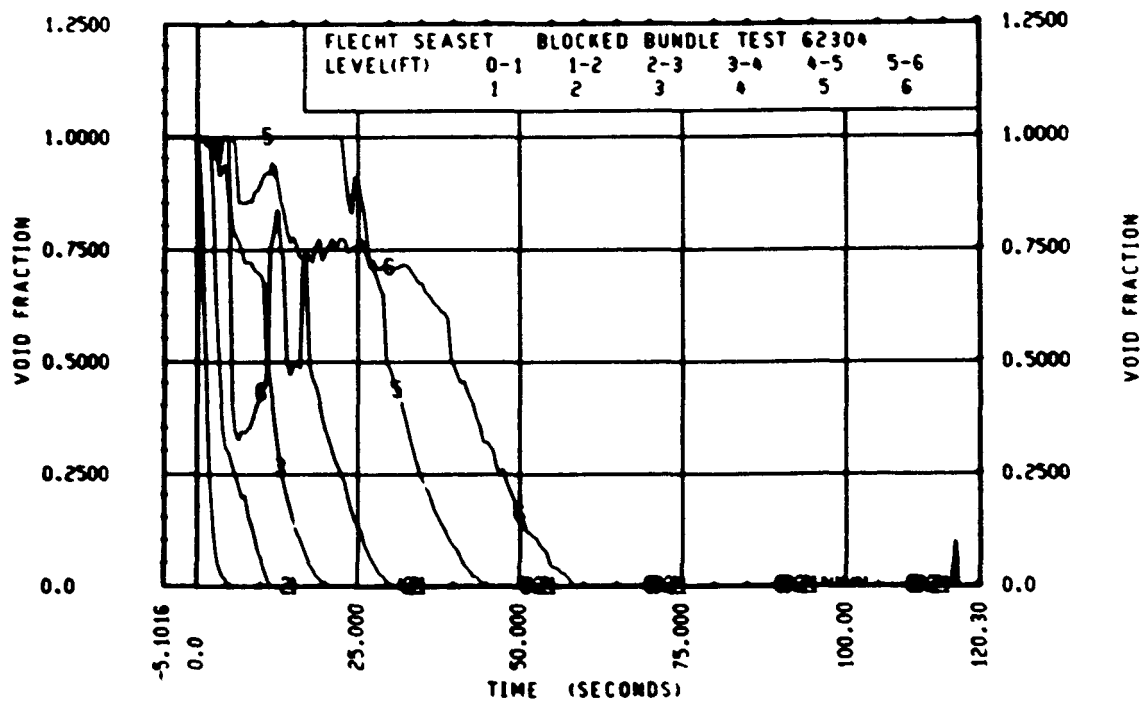
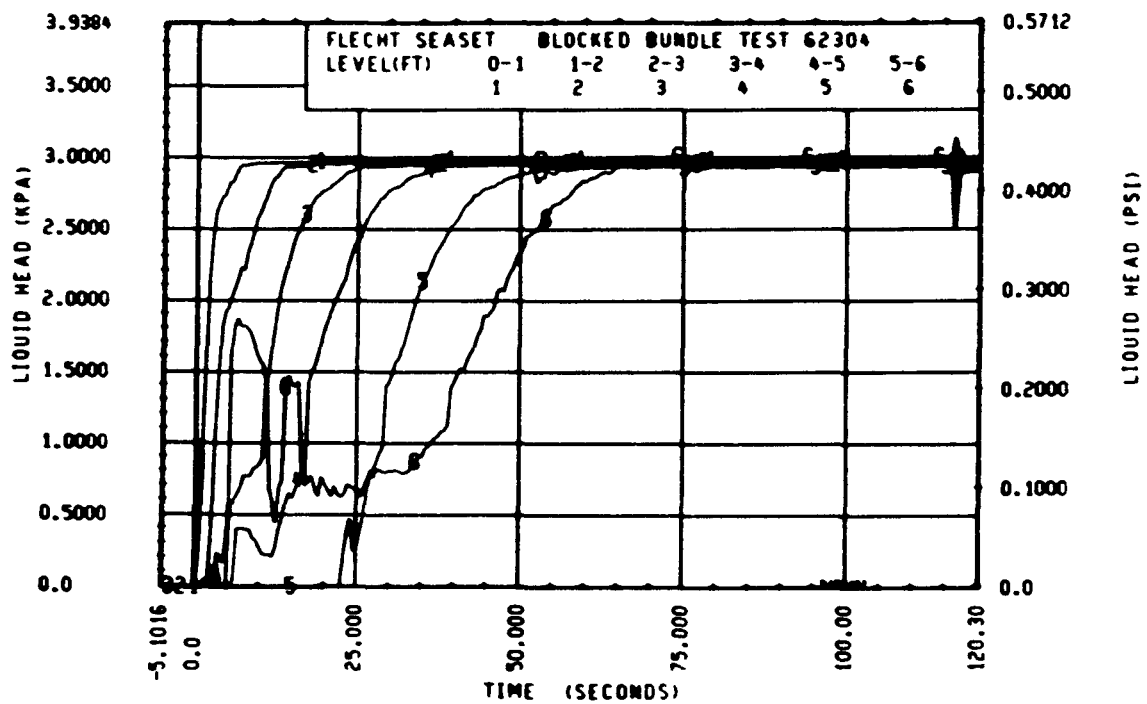
Rod 8H, 3.05 m (120 in.)

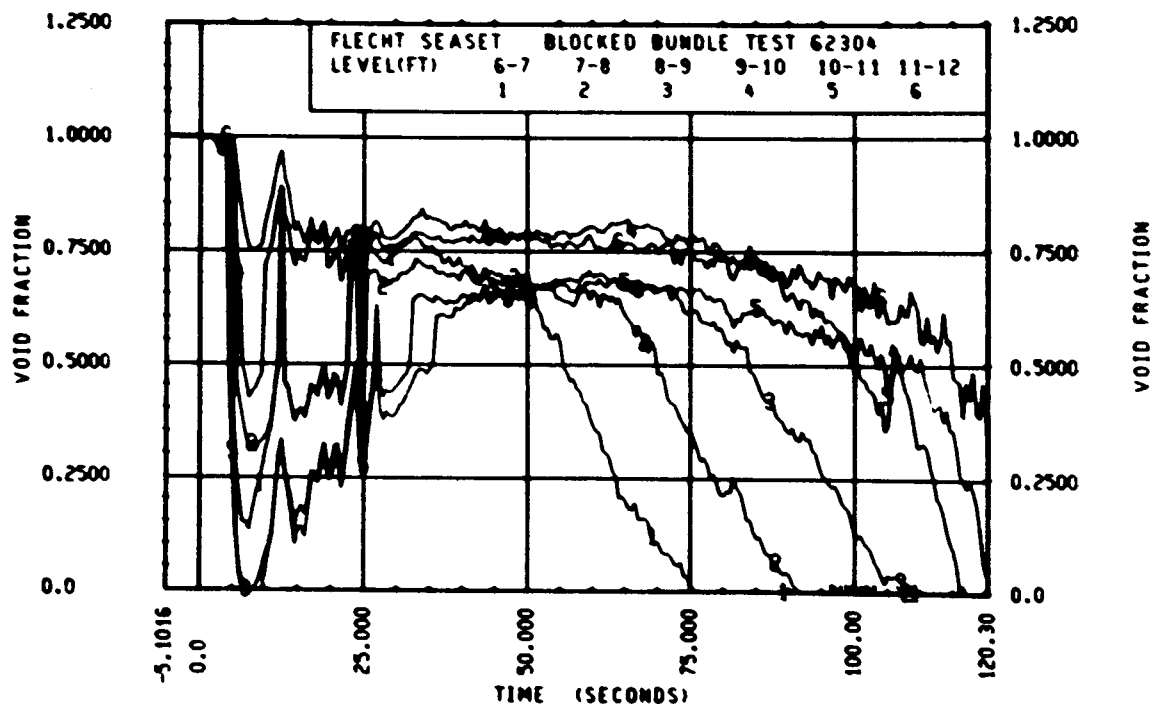
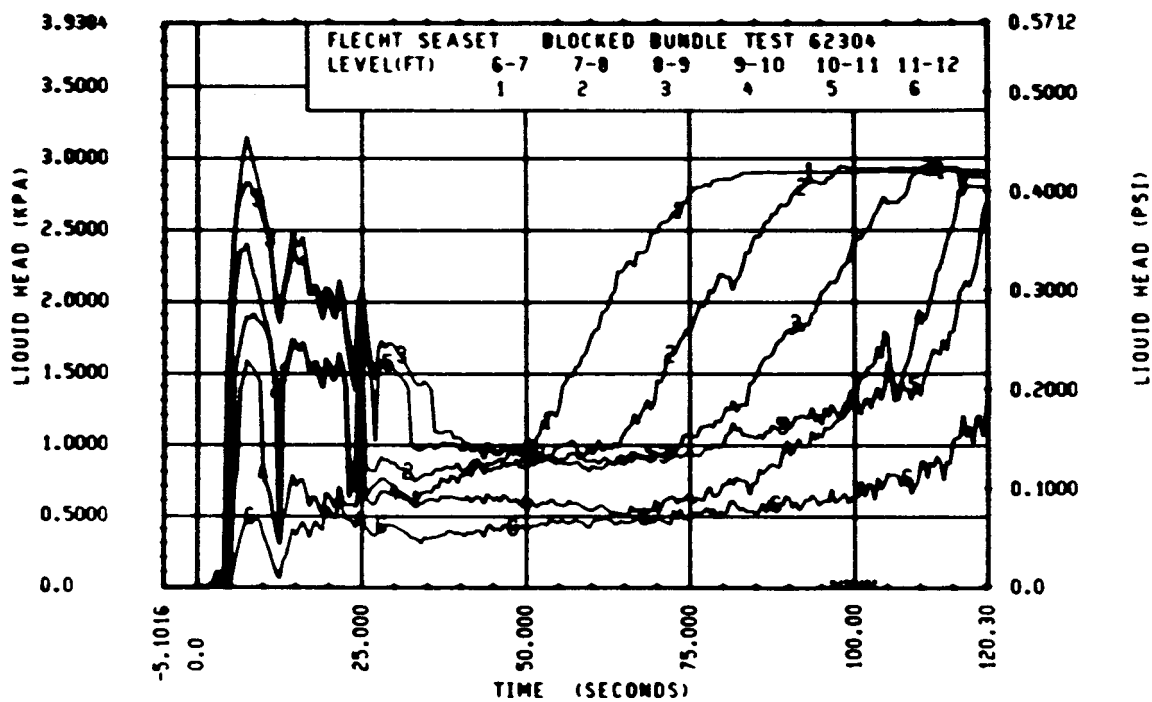












FLECHT SEASET 163-ROD BUNDLE FLOW BLOCKAGE TASK
SUMMARY AND COMMENT SHEET

Run: 62413
Test date: 9/27/82
Test type: Forced reflood
Parameter: Peak power effect

AS-RUN TEST CONDITIONS:

Upper plenum pressure	0.276 MPa (40.0 psia)
Initial peak clad temperature and location	875.9°C (1608.6°F), 8N-1.98 m (78 in.)
Initial peak rod power:	
Peripheral rods	3.284 kw/m (1.001 kw/ft)
Bypass rods	3.28 kw/m (0.999 kw/ft)
Blockage island rods	3.27 kw/m (0.997 kw/ft)
Flooding rate	38.1 mm/sec (1.50 in./sec)
Coolant temperature	53.8°C (129°F)
Initial bundle water level	-5.6 mm (-0.22 in.)

COMMENTS:

With the increase in the peak power to 3.3 kw/m (1 kw/ft), the power supplies were reconfigured with 54 rods in each so as not to exceed the power limitations. Rods G-15, H-15, I-15, and J-15 were moved from the peripheral rod supply to the blockage island rod supply, and rods I-6, J-6, C-8, C-9, D-9, D-10, E-10, C-11, D-11, and C-12 were moved from the bypass rod supply to the blockage island rod supply.

Carryover tank filled up at approximately 460 seconds.

Inlet mass flow:⁽¹⁾ -6.6% linearly decreasing to -2.6% by 500 seconds

Power decay:⁽¹⁾ peripheral rods, 0% linearly increasing to +1.5% by 400 seconds
bypass rods, 0% exponentially increasing to -2.5% by 400 seconds
blockage rods, 0% linearly increasing to -1% by 400 seconds

No heat transfer plots are included.

1. Relative to run 34524

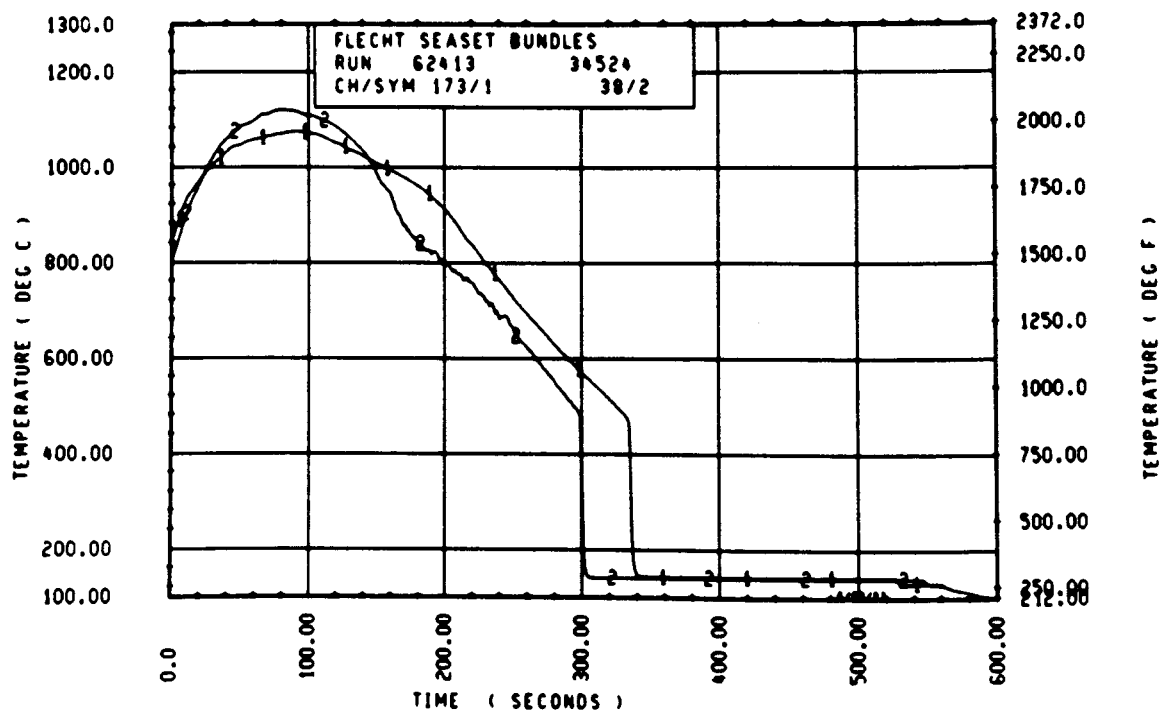
FLECHT SEASET 163 ROD BUNDLE TEST SERIES							
RUN NUMBER 62413							
ROD/ELEV	CHAN. NO	INITIAL AT FLOOD (DEG F)	MAXIMUM TEMPERATURE (DEG F)	TEMPERATURE RISE (DEG F)	TURNAROUND TIME (SECONDS)	QUENCH TEMPERATURE (DEG F)	QUENCH TIME (SECONDS)
9G 1- 0	3	685.	712.	27.	5.5	594.	22.8
10H 2- 0	6	698.	957.	59.	8.0	694.	49.0
9G 3- 3	9	1225.	1362.	136.	25.5	822.	96.3
3J 4- 0	11	1354.	1564.	210.	42.0	838.	143.9
7H 4- 0	12	1337.	1550.	213.	41.5	774.	147.9
8K 4- 0	13	1359.	1580.	222.	42.0	795.	151.8
8M 4- 0	14	1360.	1558.	198.	40.0	839.	141.9
12D 4- 0	17	1343.	1540.	198.	41.0	839.	140.9
5E 5- 0	20	1493.	1856.	363.	66.5	992.	214.4
7G 5- 0	21	1549.	1914.	365.	56.5	963.	212.9
9G 5- 0	24	1540.	1894.	354.	57.5	949.	218.1
5E 5- 7	33	1524.	1858.	334.	69.0	915.	262.7
8G 5- 7	45	1546.	1903.	358.	70.0	965.	266.0
9H 5- 9	52	1500.	1801.	301.	60.0	822.	268.0
7G 5-10	59	1561.	1866.	365.	80.5	879.	287.9
7F 5-11	62	1442.	1736.	293.	55.5	1182.	205.7
4G 5-11	64	1527.	1911.	384.	69.0	886.	296.6
2I 6- 0	67	1579.	1994.	415.	82.5	1007.	294.9
5D 6- 0	70	1464.	1848.	364.	92.5	873.	296.0
6J 6- 0	74	1517.	1893.	376.	80.0	694.	305.4
7M 6- 0	66	1538.	1942.	404.	71.5	930.	292.2
11E 6- 0	80	1545.	1936.	391.	81.0	914.	296.7
8H 6- 2	97	1367.	1723.	356.	60.0	867.	269.0
5H 6- 2	99	1530.	1955.	425.	81.5	886.	314.1
9E 6- 2	105	1337.	1898.	560.	111.5	1344.	232.8
8H 6- 3	111	1412.	1765.	352.	61.5	909.	274.0
4G 6- 3	124	1545.	1953.	408.	81.0	912.	321.9
11H 6- 4	134	1487.	1889.	401.	70.0	770.	264.3
9D 6- 4	143	1533.	1995.	463.	99.0	847.	323.0
9J 6- 5	165	1530.	1880.	349.	60.0	916.	309.9
9M 6- 5	166	1579.	1996.	417.	79.0	967.	325.4
8J 6- 6	192	1575.	1952.	377.	62.0	1045.	299.9
9U 6- 6	193	1543.	2017.	474.	99.0	882.	335.0
11F 6- 6	173	1552.	1967.	414.	89.0	869.	334.6
4G 7- 0	261	1476.	1769.	293.	44.5	621.	378.9
7U 7- 6	309	1462.	1827.	366.	86.0	905.	388.7
7G 7- 6	312	1566.	1831.	325.	55.5	1006.	345.0
11E 7- 6	325	1477.	1876.	399.	99.0	890.	410.7
5L 8- 0	337	1298.	1756.	457.	99.0	824.	457.9
7H 8- 0	345	1345.	1808.	463.	99.5	830.	429.1
7K 8- 0	346	1347.	1797.	450.	96.0	820.	447.1
5J 8- 6	366	1135.	1478.	343.	85.5	705.	493.0
7B 8- 6	368	1106.	1455.	347.	95.5	696.	498.7
7E 9- 3	383	1086.	1525.	439.	236.1	727.	483.1
8H 9- 3	387	1046.	1457.	411.	239.1	745.	483.0
9C 9- 3	389	1033.	1421.	388.	111.5	713.	511.0
11F 9- 3	394	1036.	1391.	355.	82.5	826.	448.7
7B10- 0	408	843.	1297.	454.	139.5	655.	564.0
8H10- 0	415	858.	1398.	539.	241.1	662.	519.1
6K10- 0	417	854.	1303.	443.	153.5	642.	564.0
8H10- 0	418	874.	1404.	530.	146.5	761.	564.0
6H11- 0	429	692.	937.	245.	106.0	559.	564.0
9G11- 0	431	692.	1096.	404.	248.1	716.	380.7
11E11- 0	432	688.	987.	300.	131.5	671.	387.0
5J11- 6	436	672.	889.	217.	98.0	571.	564.0
7B11- 6	437	644.	993.	349.	159.5	589.	564.0
8J11- 6	438	692.	934.	242.	153.5	631.	564.0

RUN 62413 HEATER ROD STATISTICAL DATA

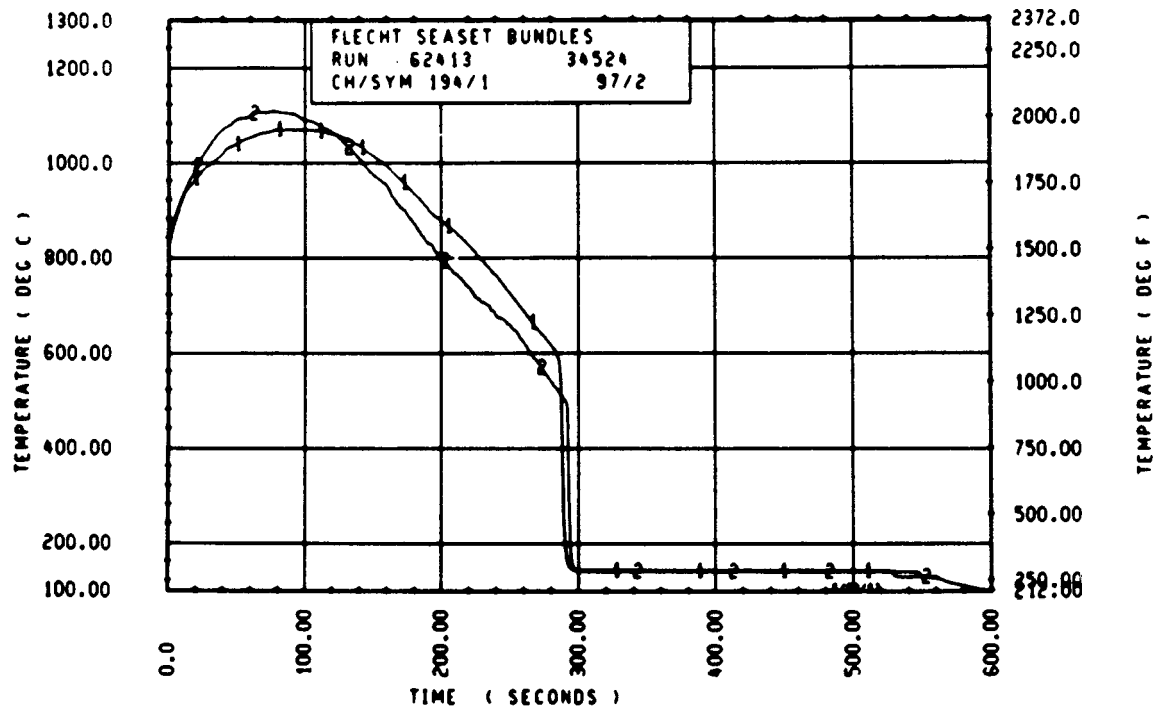
ELEV	INITIAL TEMP (DEG F)			MAX TEMP (DEG F)			TURNAROUND TIME (SEC)		
	MAX	MIN	MEAN	MAX	MIN	MEAN	MAX	MIN	MEAN
12	684.8	674.3	679.2	712.0	701.6	706.1	5.5	5.0	5.2
24	897.7	857.4	872.6	956.5	913.2	929.0	8.0	8.0	8.0
39	1225.4	1167.2	1187.4	1361.7	1303.6	1323.2	27.0	25.0	25.9
48	1364.8	1337.4	1352.1	1590.1	1540.2	1565.3	43.0	30.0	40.1
60	1574.9	1426.4	1512.7	1965.4	1684.5	1854.3	78.0	54.5	60.7
67	1587.9	1493.7	1547.5	1944.7	1809.3	1884.7	79.0	55.0	65.6
69	1520.7	1496.9	1504.0	1878.4	1782.4	1843.3	84.5	60.0	75.5
70	1596.6	1441.4	1511.6	1945.8	1816.1	1880.3	90.0	62.0	77.6
71	1527.2	1442.4	1477.6	1911.4	1735.5	1850.6	79.5	55.5	68.9
72	1581.4	1446.8	1532.7	1994.1	1847.8	1928.8	95.5	65.5	80.6
73	1585.8	1458.5	1516.9	2003.4	1851.2	1909.9	102.0	66.0	83.6
74	1578.2	1367.6	1498.2	1974.6	1723.3	1904.2	99.0	57.0	79.2
75	1584.7	1412.5	1509.8	1972.3	1764.6	1906.9	100.0	61.5	80.6
76	1607.5	1441.4	1538.4	2044.3	1870.5	1951.8	99.0	61.5	82.7
77	1579.3	1478.8	1555.4	2013.9	1791.3	1933.1	100.5	55.0	78.7
78	1608.6	1507.7	1553.8	2078.2	1817.3	1952.7	99.0	44.0	76.3
79	1605.3	1489.5	1554.1	2002.2	1873.8	1950.8	96.5	44.5	75.6
80	1570.6	1500.1	1540.5	2042.0	1868.2	1973.1	101.5	43.5	77.6
81	1584.7	1459.5	1526.3	2063.0	1852.3	1947.2	97.0	44.0	72.9
84	1524.0	1420.6	1487.1	1808.2	1657.0	1742.1	94.0	42.5	50.9
86	1593.3	1449.5	1527.4	1922.9	1762.3	1815.1	80.5	27.0	57.3
90	1527.2	1417.8	1479.6	1916.0	1803.7	1859.8	99.0	55.5	74.2
96	1391.2	1251.5	1341.9	1897.6	1755.6	1821.5	137.5	88.0	101.5
102	1199.3	1010.1	1143.4	1578.1	1455.2	1513.6	202.1	68.0	117.6
111	1099.8	1029.7	1057.4	1525.0	1382.8	1451.3	243.1	82.5	136.0
120	913.2	815.0	861.6	1430.6	1192.0	1345.3	253.1	89.0	184.7
132	700.5	662.7	691.2	1095.7	908.0	997.2	248.1	96.5	172.3
138	692.1	643.8	665.0	995.7	889.4	955.3	264.1	98.0	163.3

RUN 62413 HEATER ROD STATISTICAL DATA

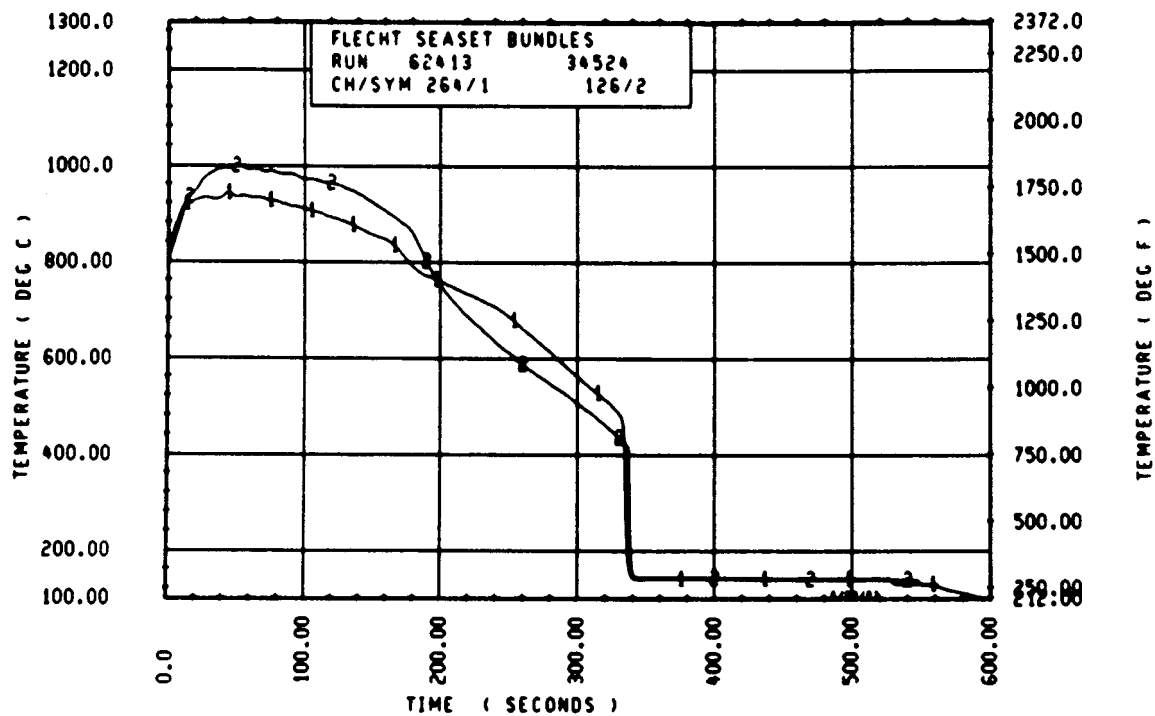
ELEV	TEMP RISE (DEG F)			QUENCH TEMP (DEG F)			QUENCH TIME (SEC)		
	MAX	MIN	MEAN	MAX	MIN	MEAN	MAX	MIN	MEAN
12	27.3	26.2	26.9	594.5	588.1	591.3	24.0	22.8	23.6
24	58.8	54.6	56.4	694.4	662.7	678.5	49.0	46.5	47.4
39	142.8	127.4	135.7	834.9	817.4	825.7	99.9	95.4	97.6
48	237.9	197.5	213.2	845.8	778.5	822.1	151.8	140.8	144.5
60	390.5	258.1	341.6	1043.4	948.8	977.3	225.9	210.5	217.1
67	362.4	306.7	337.2	996.8	795.3	921.7	272.8	256.8	264.4
69	363.5	285.5	334.3	933.0	821.7	899.6	286.5	268.0	278.1
70	387.5	349.3	368.7	1009.3	879.5	945.5	292.0	276.7	283.7
71	414.2	293.1	372.6	1182.4	828.4	955.4	296.6	205.7	269.8
72	430.8	363.7	396.1	1006.5	817.2	917.7	305.4	292.2	298.7
73	417.6	371.5	393.0	994.8	829.9	910.7	309.4	293.7	303.1
74	439.3	356.3	406.0	954.1	748.8	886.9	320.0	262.0	303.7
75	457.3	350.5	397.1	1085.9	539.4	899.6	321.9	207.9	295.9
76	462.6	359.1	413.4	993.2	769.7	910.0	334.3	264.3	312.2
77	461.8	312.6	397.8	1060.2	850.0	957.7	335.0	243.5	295.6
78	473.9	268.3	399.0	1323.4	735.0	953.8	345.8	155.7	304.1
79	481.7	289.2	396.7	1209.3	724.2	979.7	344.5	166.2	293.2
80	513.2	298.7	432.6	1450.9	767.9	1008.9	359.9	128.3	306.2
81	524.9	316.4	420.9	1450.8	907.7	1042.0	358.9	143.3	298.6
84	298.3	206.2	255.0	1029.9	815.2	864.6	385.4	261.9	355.2
86	378.3	195.8	287.7	1399.6	818.6	948.8	391.0	196.4	346.8
90	422.1	325.3	380.2	1429.1	844.4	953.9	424.9	231.9	381.1
96	535.9	435.6	479.6	1334.6	785.6	903.8	460.3	285.0	420.7
102	491.1	306.9	370.2	887.8	663.8	763.7	498.7	380.6	455.9
111	469.4	344.3	393.9	1006.0	483.3	750.1	564.0	360.4	486.6
120	582.1	377.0	463.5	884.3	470.3	690.3	564.0	391.8	520.9
132	403.6	225.3	305.9	715.6	559.2	626.7	564.0	380.7	474.4
136	348.8	217.3	296.2	814.1	546.6	630.4	564.0	330.1	510.6



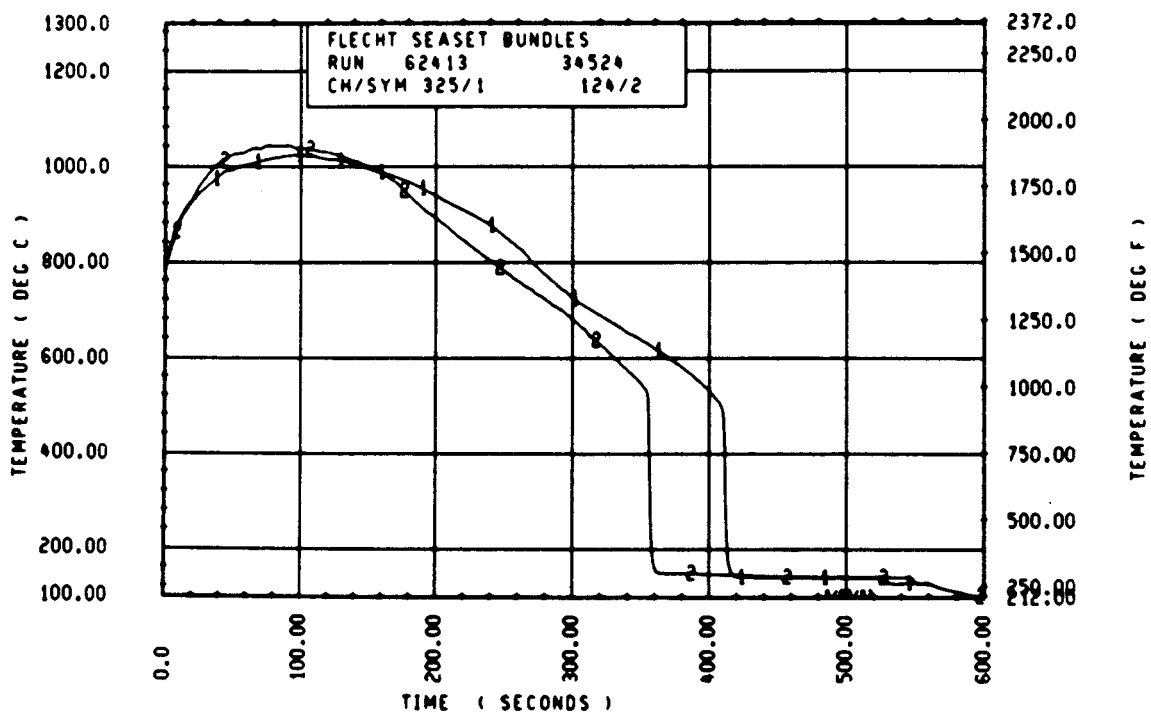
Rod 11F, 1.98 m (78 in.)



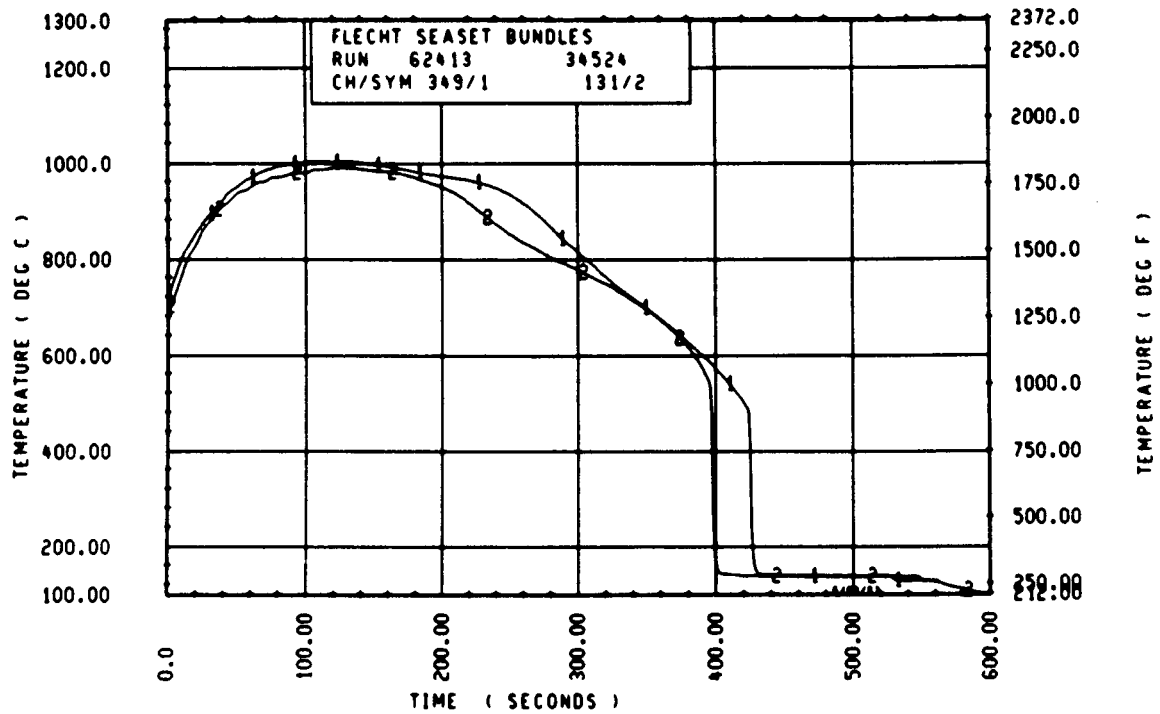
Rod 9E, 1.98 m (78 in.)



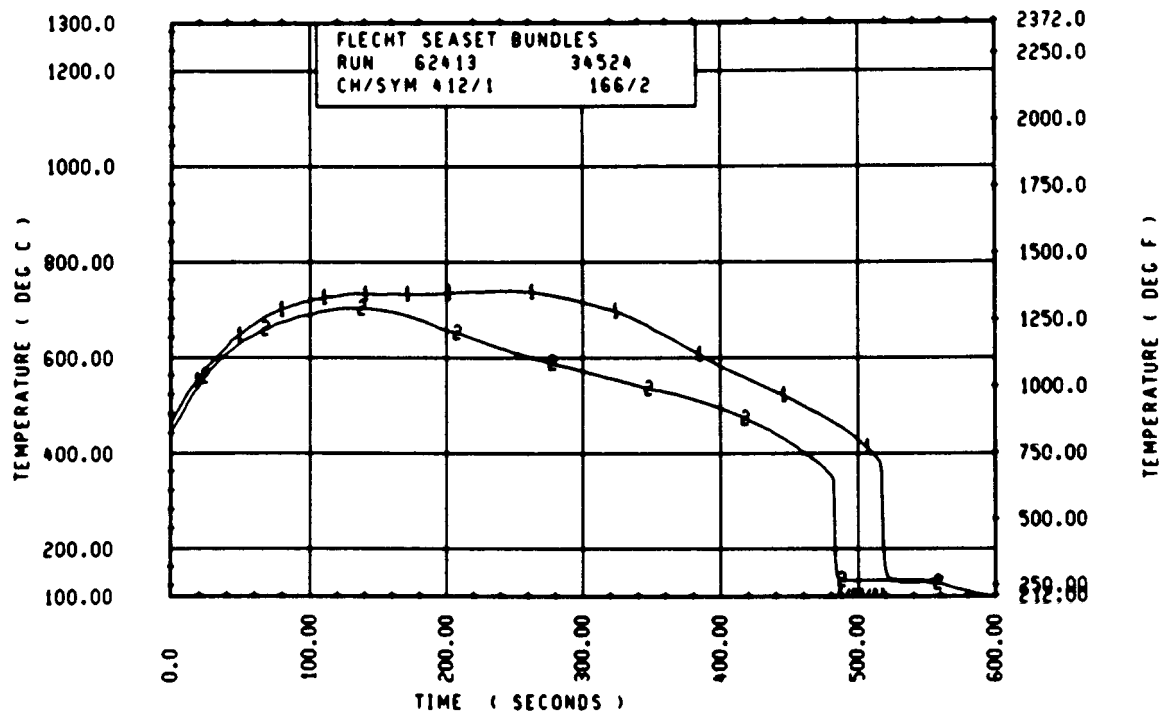
Rod 7E, 2.13 m (84 in.)



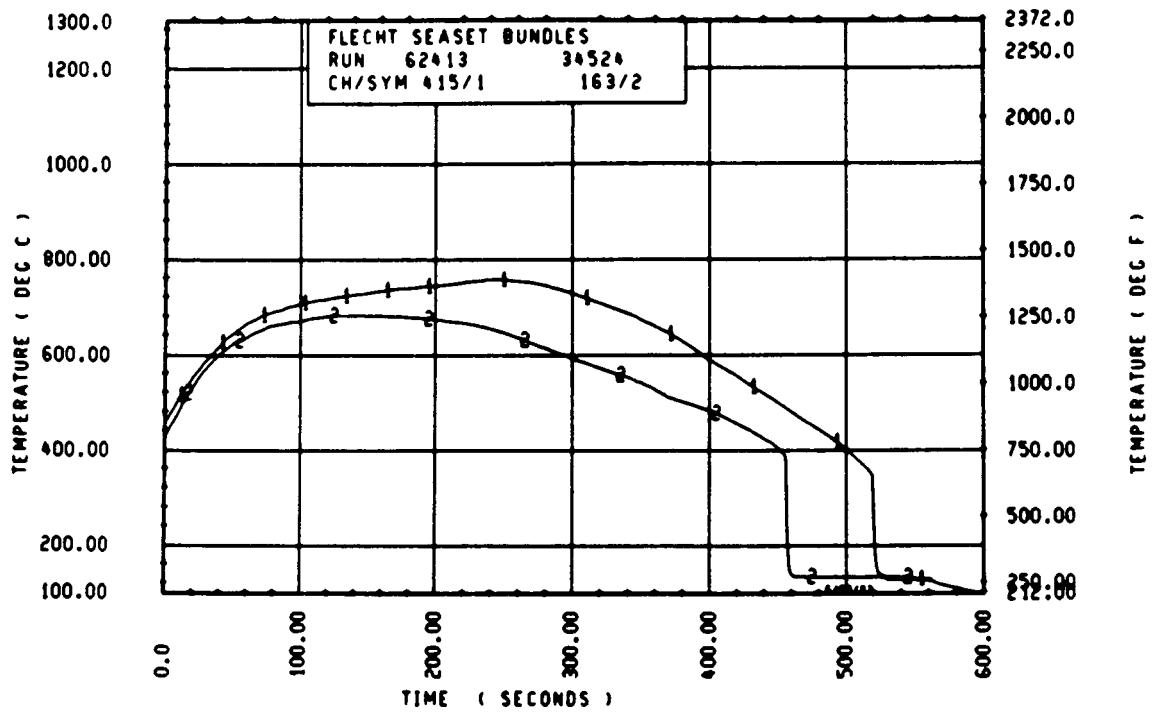
Rod 11E, 2.29 m (90 in.)



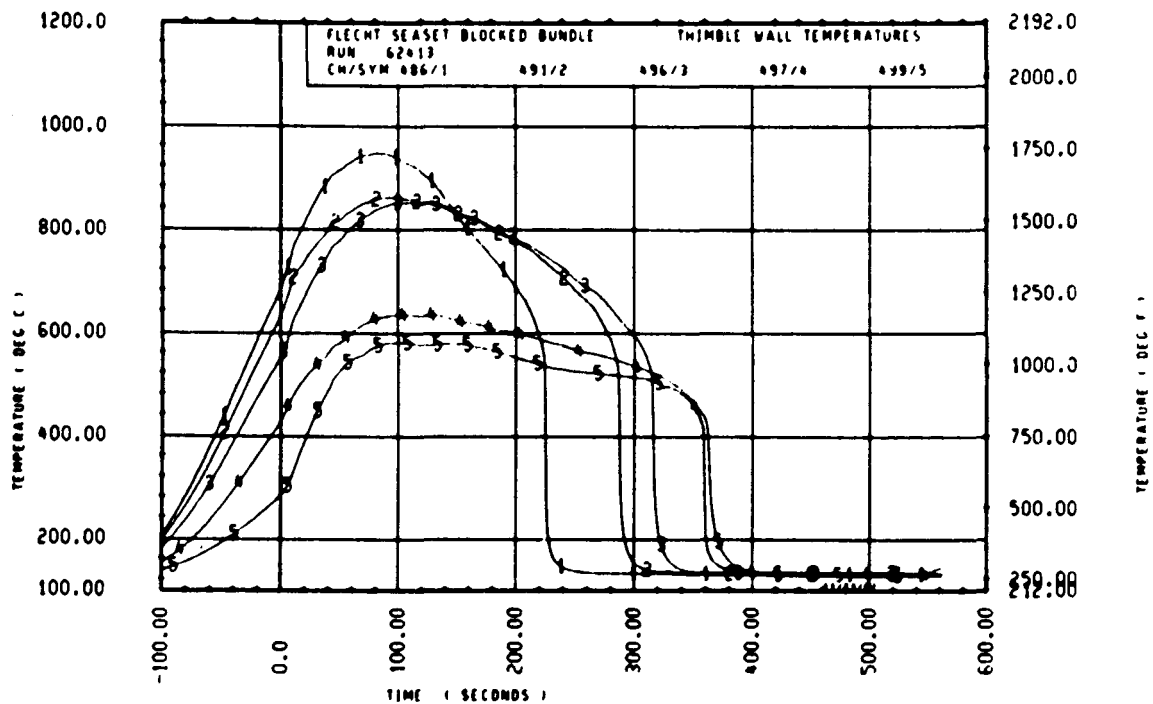
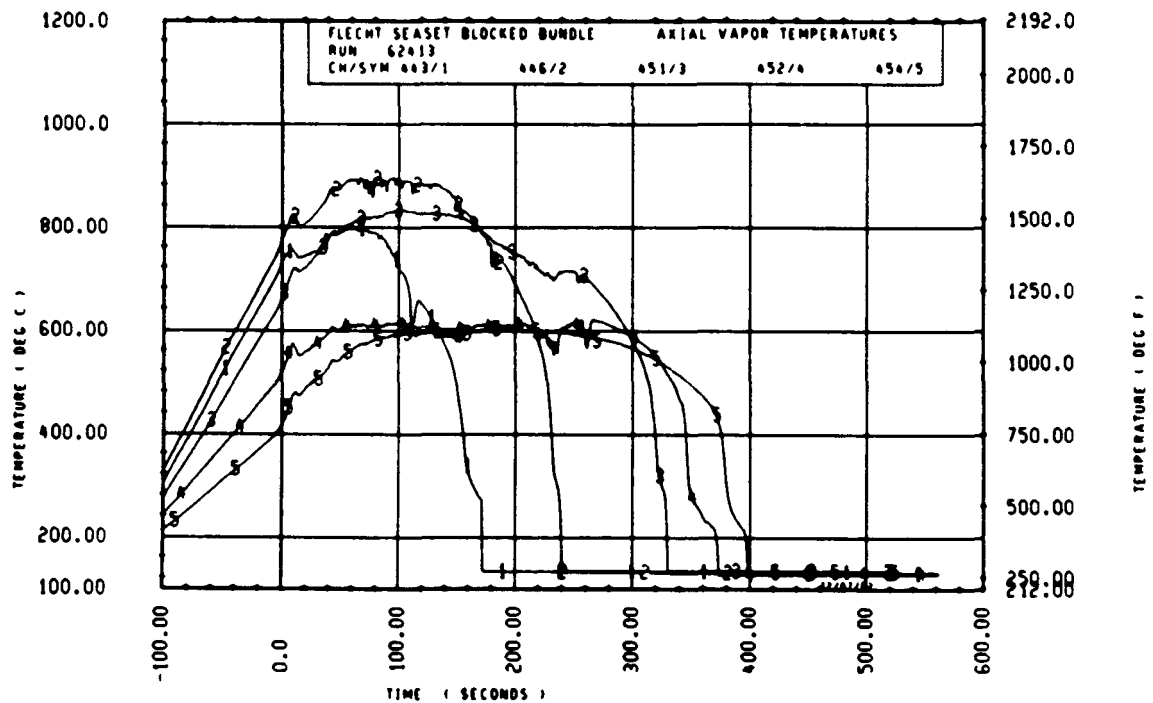
Rod 8E, 2.44 m (96 in.)

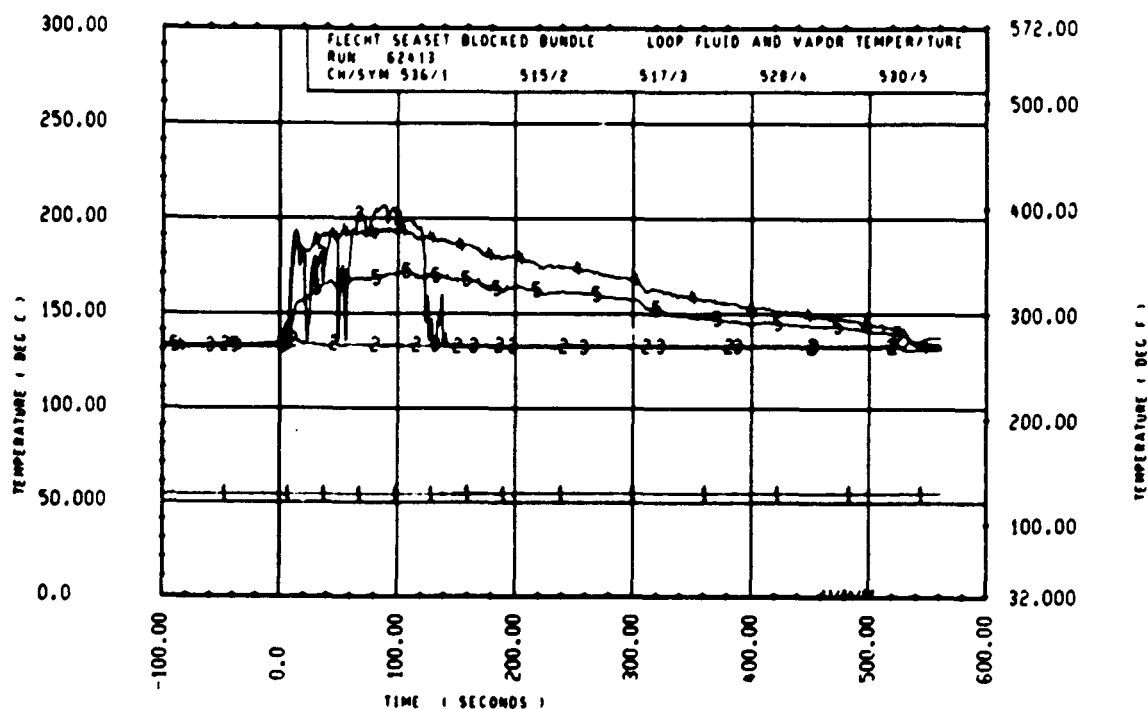
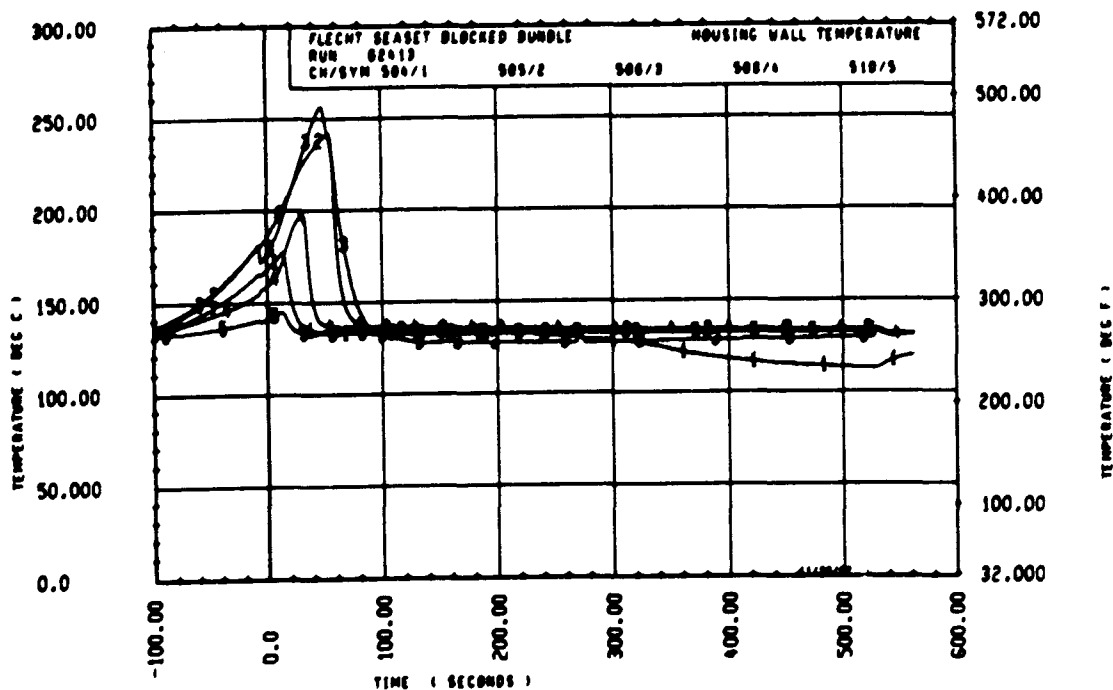


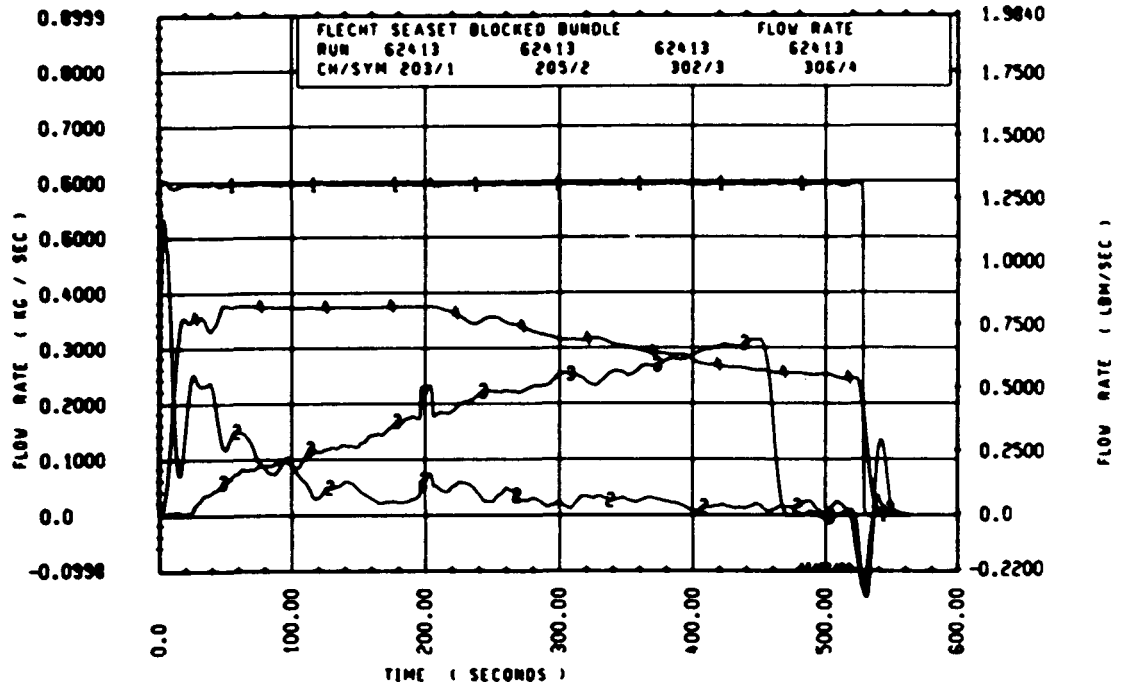
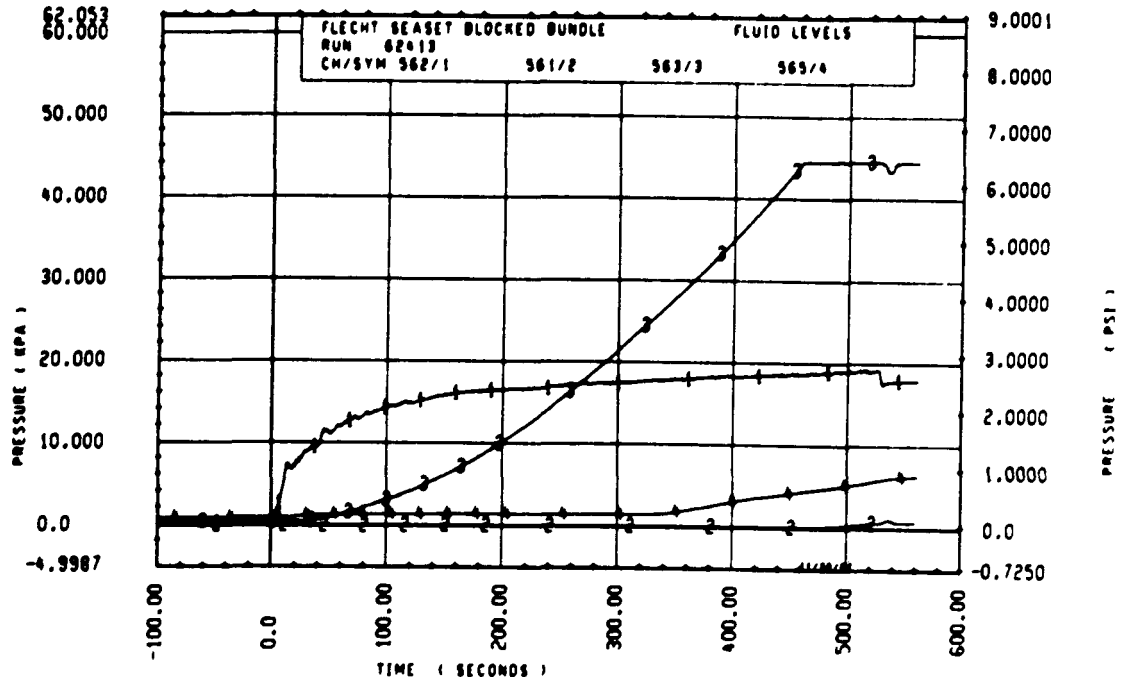
Rod 8D, 3.05 m (120 in.)

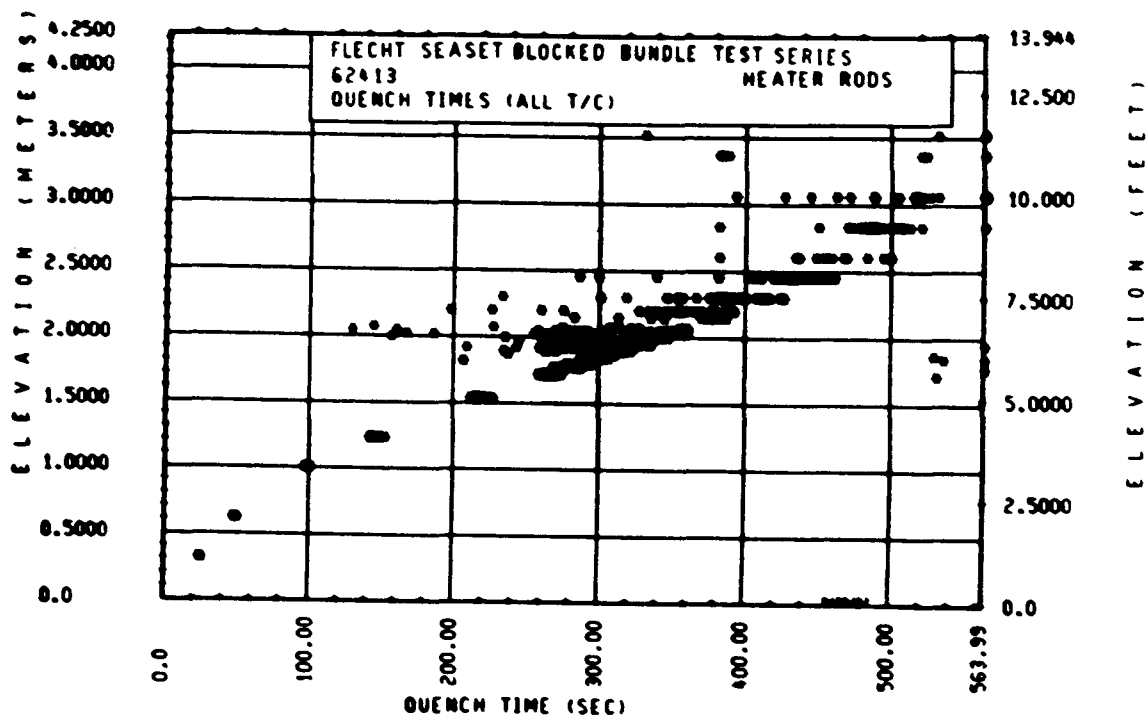
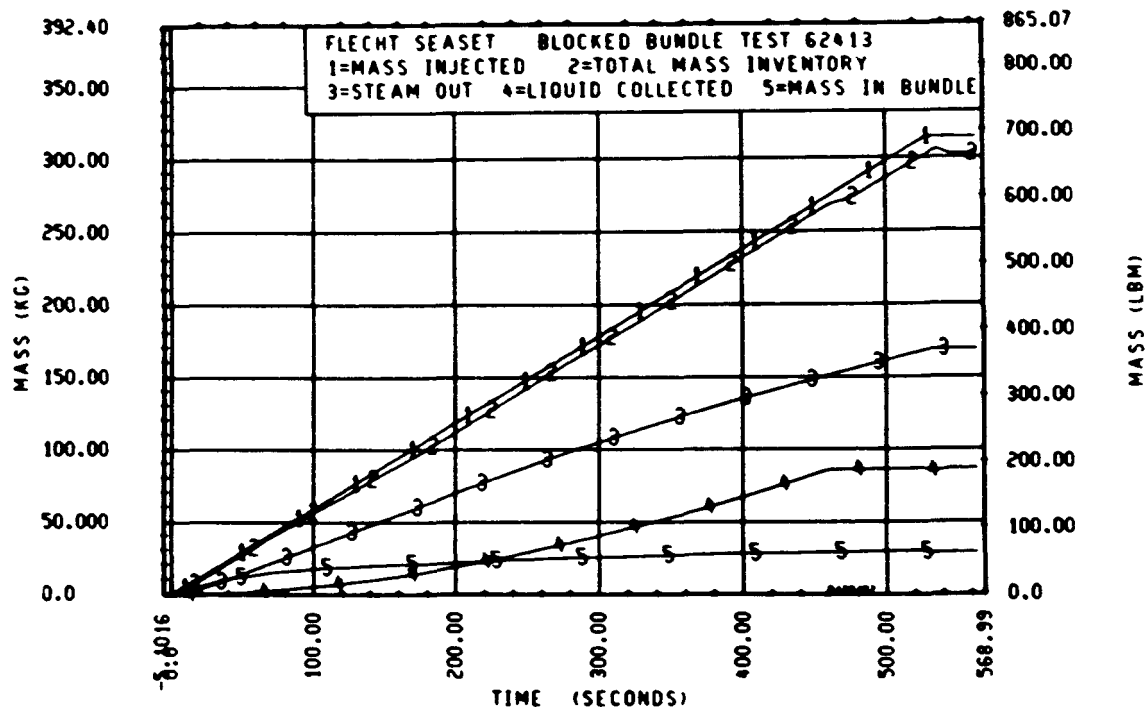


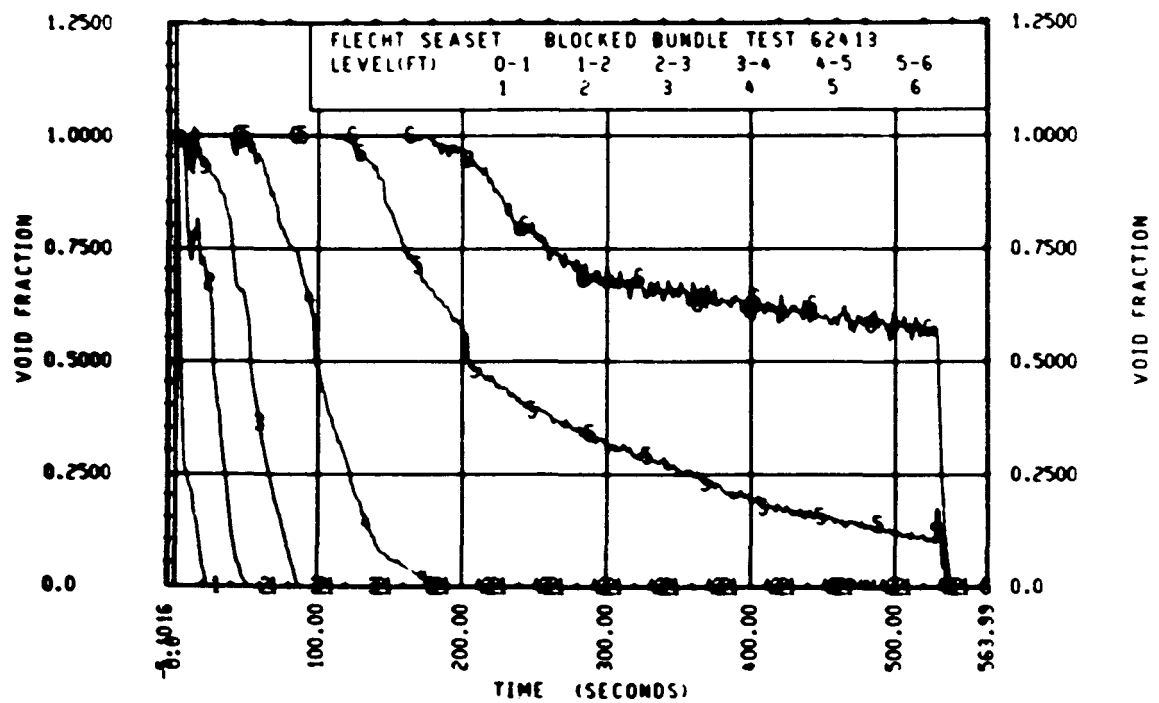
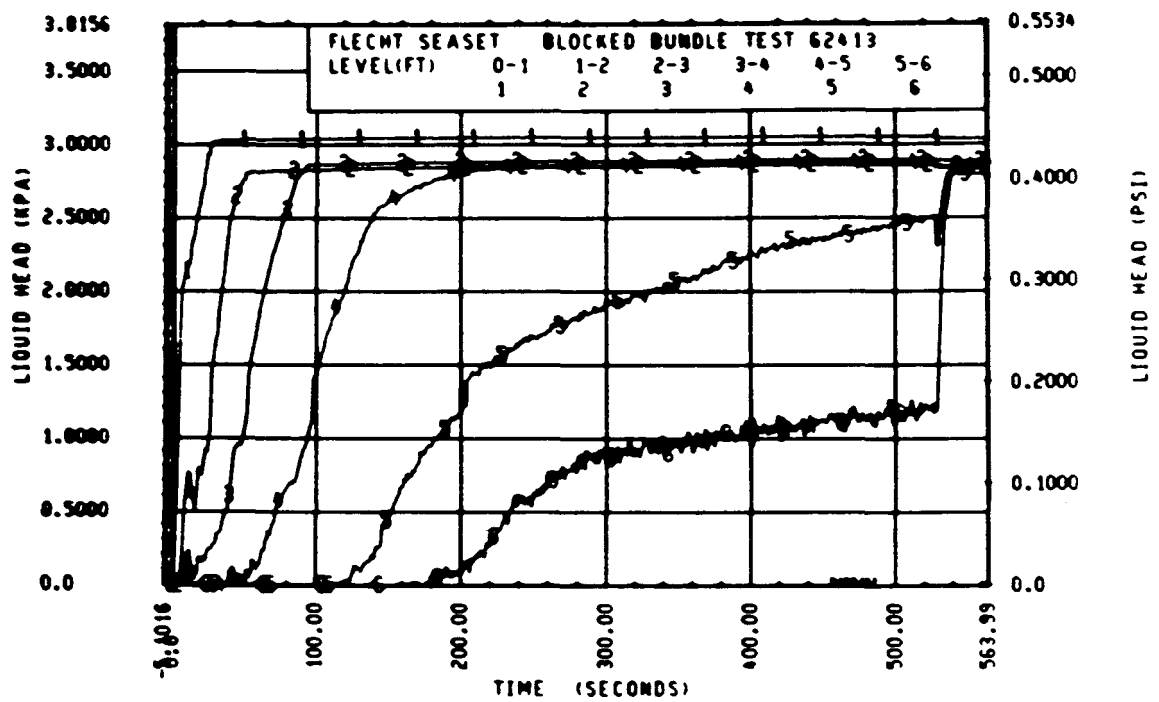
Rod 8H, 3.05 m (120 in.)

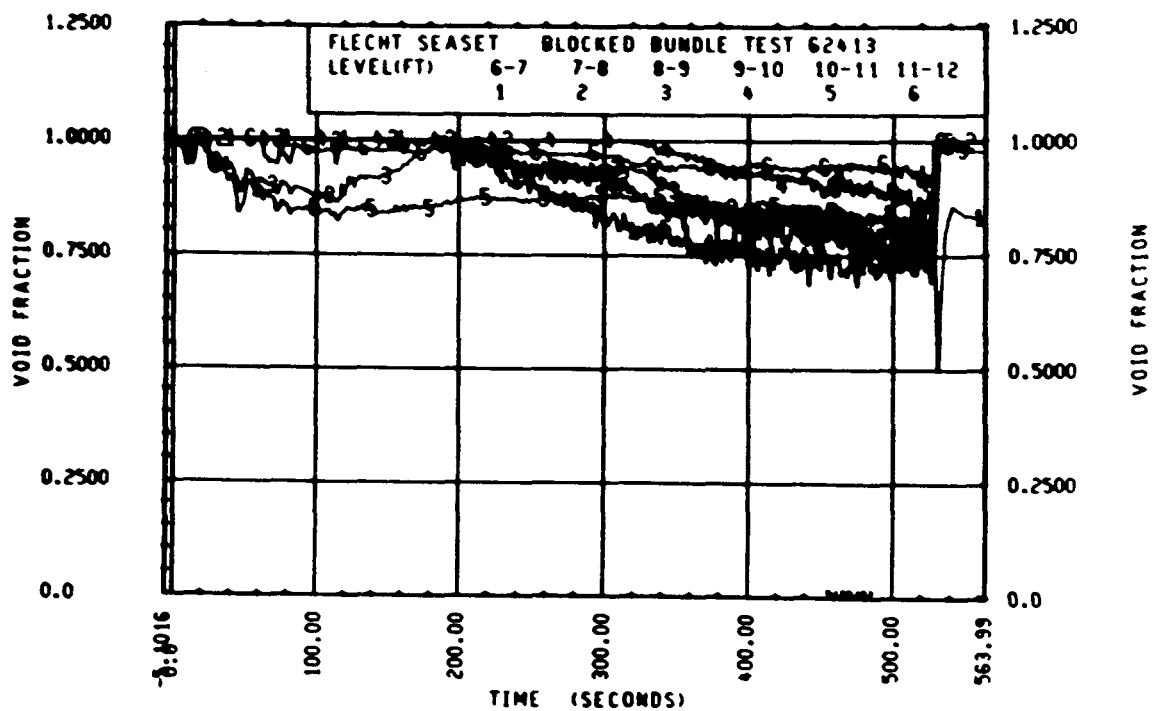
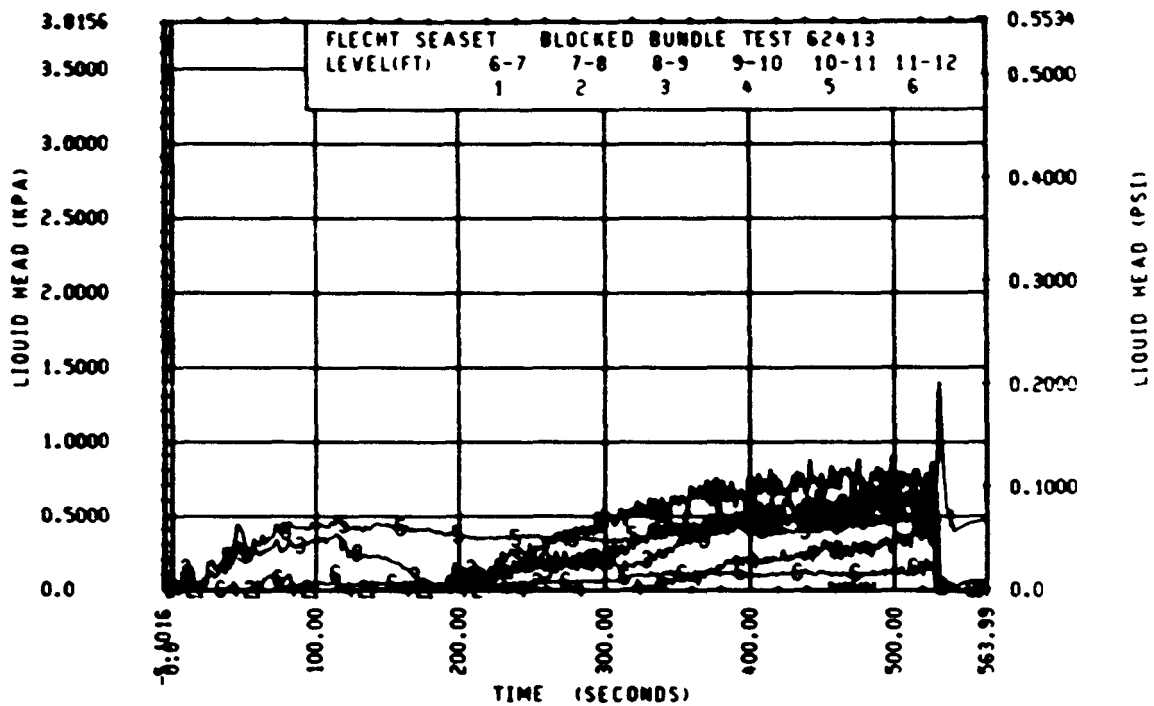












FLECHT SEASET 163-ROD BUNDLE FLOW BLOCKAGE TASK
SUMMARY AND COMMENT SHEET

Run: 62503
Test date: 9/28/82
Test type: Forced reflood
Parameter: Variable flow effect

AS-RUN TEST CONDITIONS:

Upper plenum pressure	0.274 MPa (39.7 psia)
Initial peak clad temperature and location	871.6°C (1600.9°F), 8N-1.93 m (76 in.)
Initial peak rod power:	
Peripheral rods	2.30 kw/m (0.700 kw/ft)
Bypass rods	2.29 kw/m (0.699 kw/ft)
Blockage island rods	2.29 kw/m (0.699 kw/ft)
Flooding rate	Variable (see page 62503-18)
Coolant temperature	52.8°C (127°F)
Initial bundle water level	+2.8 mm (+0.11 in.)

COMMENTS:

None

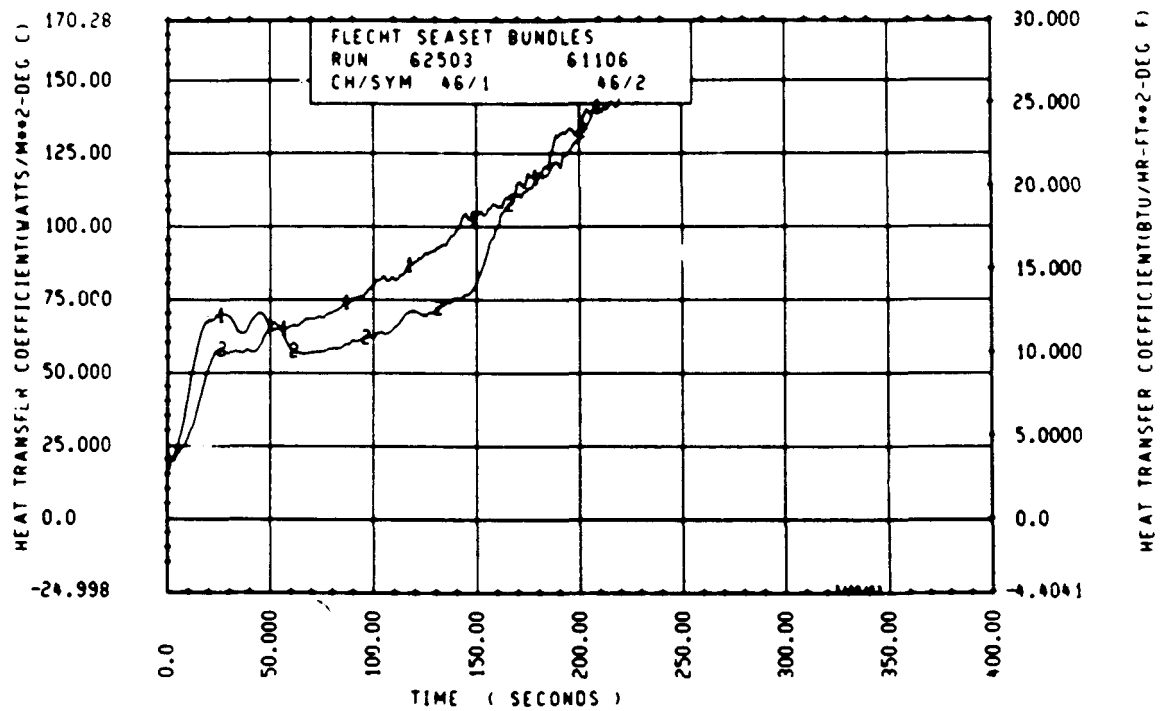
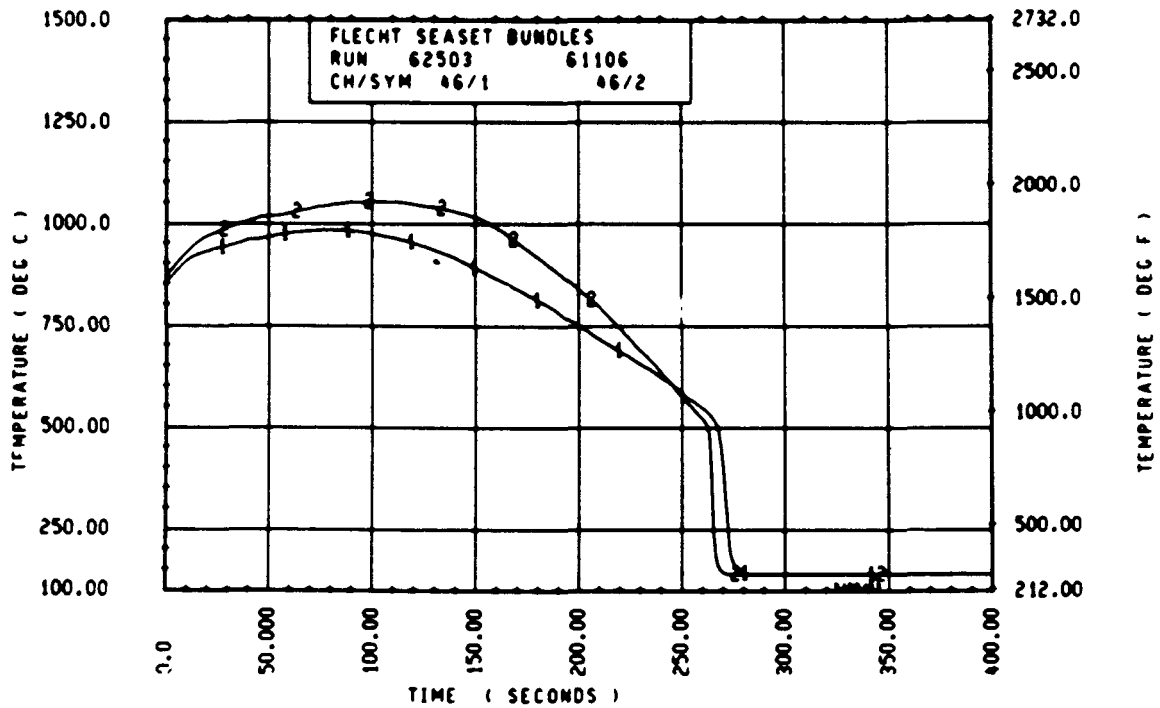
FLECHT SEASET 163 ROD BUNDLE TEST SERIES							
RUN NUMBER 62503							
ROD/ELEV	CHAN. NO	INITIAL AT FLOOD (DEG F)	MAXIMUM TEMPERATURE (DEG F)	TEMPERATURE RISE (DEG F)	TURNAROUND TIME (SECONDS)	QUENCH TEMPERATURE (DEG F)	QUENCH TIME (SECONDS)
96 1- 0	3	677.	695.	18.	5.0	564.	21.9
10H 2- 0	6	886.	925.	38.	8.0	644.	46.0
96 3- 3	9	1213.	1282.	69.	12.0	776.	88.7
3J 4- 0	11	1350.	1473.	123.	38.0	773.	129.9
7H 4- 0	12	1340.	1471.	132.	37.5	771.	132.9
8K 4- 0	13	1355.	1488.	133.	39.0	751.	137.7
8M 4- 0	14	1344.	1460.	110.	38.0	809.	126.4
12D 4- 0	17	1341.	1443.	103.	29.5	834.	125.9
5E 5- 0	20	1488.	1728.	239.	65.5	985.	203.9
76 5- 0	21	1544.	1769.	220.	55.0	961.	201.6
96 5- 0	24	1523.	1751.	228.	78.0	923.	206.7
5E 5- 7	33	1524.	1803.	279.	89.0	937.	265.6
66 5- 7	45	1543.	1807.	264.	83.0	927.	273.3
9H 5- 9	52	1483.	1803.	319.	98.5	826.	284.6
76 5-10	59	1502.	1798.	295.	88.0	760.	307.9
7F 5-11	62	1445.	1747.	302.	99.0	856.	307.9
46 5-11	64	1530.	1850.	320.	98.0	855.	325.6
21 6- 0	67	1577.	1886.	309.	95.5	944.	327.9
5D 6- 0	70	1461.	1805.	324.	102.0	806.	324.7
6J 6- 10	74	1519.	1785.	266.	95.0	893.	338.5
7H 6- 0	66	1537.	1864.	327.	99.0	804.	324.8
11E 6- 0	80	1538.	1838.	300.	91.0	891.	328.7
8H 6- 2	97	1364.	1757.	393.	121.0	857.	345.9
5H 6- 2	99	1528.	1873.	344.	101.5	864.	363.7
9E 6- 2	105	1330.	1821.	491.	117.5	282.	781.1
6H 6- 3	111	1406.	1771.	365.	123.5	912.	356.3
46 6- 3	124	1546.	1896.	351.	99.5	863.	376.8
11H 6- 4	134	1469.	1784.	314.	84.5	692.	377.4
9D 6- 4	143	1532.	1934.	403.	118.5	900.	383.9
9J 6- 5	165	1511.	1824.	313.	191.0	855.	400.6
9M 6- 5	166	1580.	1919.	339.	102.5	921.	383.8
8J 6- 6	192	1560.	1891.	331.	109.0	890.	402.5
9D 6- 6	193	1545.	1947.	402.	117.5	839.	410.9
11F 6- 6	173	1548.	1899.	351.	102.0	886.	397.7
46 7- 0	261	1469.	1800.	331.	101.5	694.	469.4
7D 7- 6	309	1468.	1904.	436.	194.0	814.	547.7
76 7- 6	312	1510.	1976.	466.	213.1	876.	529.8
11E 7- 6	325	1464.	1880.	416.	166.5	783.	539.8
5L 8- 0	337	1298.	1840.	541.	173.5	746.	612.5
7H 8- 0	345	1348.	1979.	631.	250.1	798.	611.9
7K 8- 0	346	1349.	1898.	549.	215.1	750.	604.6
5J 8- 6	366	1130.	1711.	581.	280.1	646.	656.9
76 8- 6	368	1117.	1662.	545.	250.1	646.	655.7
7E 9- 3	383	1092.	1818.	727.	310.1	732.	640.5
8H 9- 3	387	1044.	1634.	590.	194.0	701.	693.4
9C 9- 3	389	1036.	1642.	606.	311.1	701.	694.7
11F 9- 3	394	1032.	1709.	677.	313.1	672.	696.1
7810- 0	408	846.	1571.	725.	346.1	614.	734.1
8H10- 0	415	854.	1548.	694.	398.1	633.	732.1
6K10- 0	417	856.	1433.	576.	385.1	624.	731.1
6N10- 0	418	871.	1480.	609.	209.1	660.	731.1
6H11- 0	429	691.	1109.	418.	415.1	608.	740.9
9611- 0	431	680.	1422.	736.	378.1	838.	617.7
11E11- 0	432	679.	1416.	740.	377.1	610.	742.1
5J11- 6	436	686.	917.	231.	163.5	616.	726.1
7811- 6	437	645.	1328.	683.	412.1	574.	782.7
8J11- 6	438	688.	1054.	367.	449.1	591.	748.9

RUN 62503 HEATER ROD STATISTICAL DATA

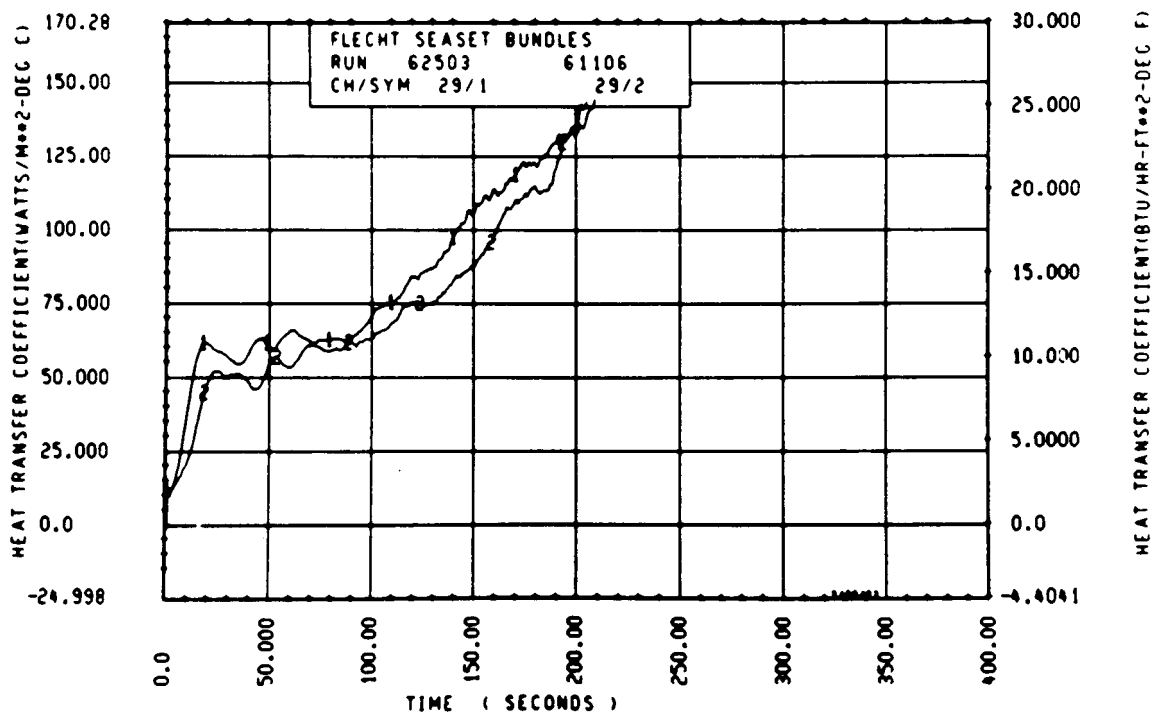
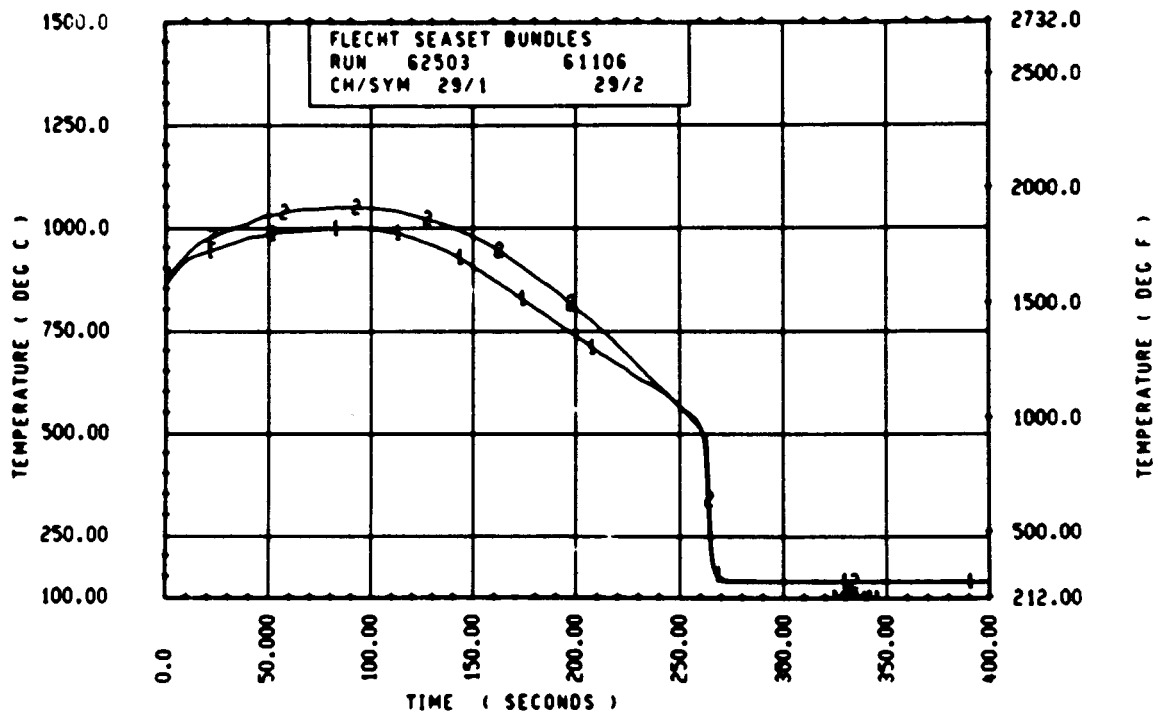
ELEV	INITIAL TEMP (DEG F)			MAX TEMP (DEG F)			TURNAROUND TIME (SEC)		
	MAX	MIN	PEAK	MAX	MIN	MEAN	MAX	MIN	MEAN
12	679.5	677.4	678.8	697.4	695.3	696.7	5.0	5.0	5.0
24	886.4	880.5	884.8	924.5	896.7	906.7	8.0	8.0	8.0
39	1212.6	1163.0	1162.0	1281.7	1236.8	1254.0	17.0	12.0	15.4
46	1367.0	1339.5	1350.2	1488.4	1443.5	1472.3	39.0	27.0	35.4
60	1548.9	1407.2	1502.5	1766.9	1531.5	1707.6	78.0	32.0	56.6
67	1587.9	1495.9	1544.6	1835.4	1715.5	1784.3	96.5	61.0	84.8
69	1517.5	1483.0	1503.6	1802.5	1716.6	1769.2	98.5	61.0	90.7
70	1591.2	1431.7	1512.5	1836.5	1781.3	1799.9	102.5	72.0	89.0
71	1530.5	1440.3	1474.1	1850.1	1746.7	1795.7	99.0	79.0	93.7
72	1580.3	1447.6	1531.2	1896.5	1784.6	1843.6	126.0	86.0	98.6
73	1573.6	1457.4	1517.1	1903.3	1781.3	1826.5	102.5	84.0	95.7
74	1576.0	1363.6	1494.3	1892.0	1723.3	1846.2	121.0	92.5	102.5
75	1581.4	1406.1	1507.6	1896.5	1771.3	1843.2	138.0	90.5	104.3
76	1600.9	1443.5	1533.6	1945.8	1783.5	1879.6	122.5	84.5	103.6
77	1580.3	1475.6	1530.7	1961.9	1792.5	1877.6	191.0	97.0	120.1
78	1599.8	1507.7	1547.5	1967.7	1734.4	1889.7	169.0	74.0	111.9
79	1590.1	1495.9	1544.6	1972.3	1762.3	1897.6	168.0	78.0	116.7
80	1568.4	1491.6	1537.5	1984.9	1753.4	1919.0	199.0	95.5	126.4
81	1565.2	1457.4	1520.5	1961.9	1845.5	1915.8	193.0	100.5	140.6
84	1525.1	1413.6	1480.6	1846.7	1732.2	1793.0	206.1	100.5	152.8
86	1573.6	1460.6	1522.0	1942.4	1757.9	1855.2	229.1	99.5	176.6
90	1516.4	1396.6	1473.9	2015.1	1812.7	1919.6	231.1	102.5	167.0
96	1390.2	1250.4	1338.4	2029.1	1794.7	1929.2	251.1	161.5	219.5
102	1183.6	1017.4	1139.0	1858.0	1662.5	1780.0	280.1	229.1	251.6
111	1091.6	1024.7	1055.8	1818.4	1553.2	1716.5	347.1	194.0	303.1
120	913.2	810.8	850.7	1732.2	1283.8	1574.8	433.1	192.5	323.7
132	691.1	675.3	683.3	1434.9	915.3	1294.3	415.1	326.1	378.5
136	667.6	629.1	655.4	1334.2	917.3	1191.3	445.1	163.5	355.6

RUN 62503 HEATER ROD STATISTICAL DATA

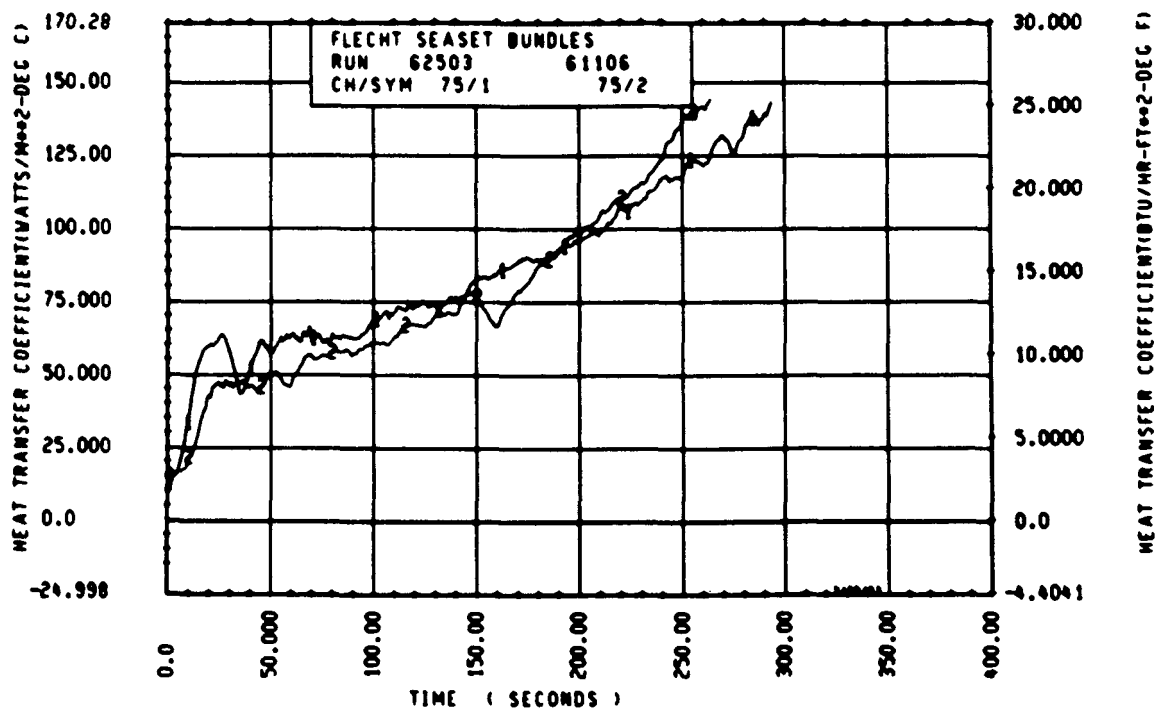
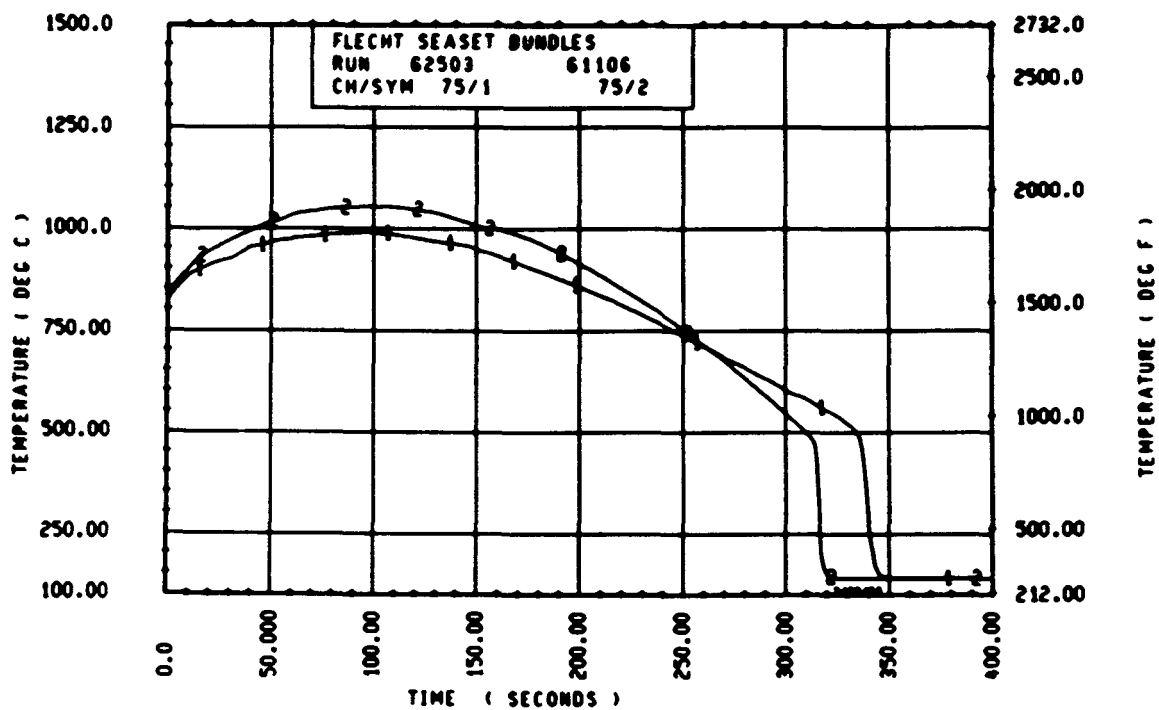
ELEV	TEMP RISE (DEG F)			QUENCH TEMP (DEG F)			QUENCH TIME (SEC)		
	MAX	MIN	PEAK	MAX	MIN	MEAN	MAX	MIN	MEAN
12	17.6	17.6	17.8	576.4	566.6	570.6	23.0	21.9	22.6
24	38.2	36.2	38.9	646.0	628.2	639.4	46.0	43.5	44.6
39	78.0	67.7	72.1	800.1	770.6	782.8	91.1	66.4	88.5
46	136.1	102.5	122.1	833.9	750.6	789.5	137.7	125.9	130.0
60	242.3	124.4	215.0	1003.6	839.4	935.5	213.8	199.7	206.0
67	282.2	211.0	239.7	954.6	752.1	883.1	276.8	255.8	266.0
69	319.5	223.9	265.6	919.0	825.4	858.3	303.8	278.5	289.7
70	364.1	245.3	287.4	966.3	760.0	866.7	313.6	289.9	301.7
71	361.1	283.4	310.6	877.5	786.8	843.7	325.8	307.9	314.5
72	376.3	266.1	312.5	943.5	803.8	863.4	343.8	323.8	331.0
73	352.1	273.6	306.3	934.0	844.1	875.3	354.7	323.6	339.6
74	424.9	295.6	351.9	920.1	721.2	863.9	366.5	345.9	355.6
75	391.6	284.9	335.4	911.8	478.2	819.9	376.8	347.6	365.4
76	414.5	289.8	346.0	952.4	691.7	880.1	390.8	360.6	378.0
77	440.1	306.8	346.9	958.5	786.1	884.6	417.5	376.8	390.9
78	419.8	181.2	342.2	962.5	614.0	864.2	431.6	366.5	401.6
79	407.6	196.1	348.0	1009.5	613.9	879.4	423.7	387.9	410.4
80	457.7	202.3	381.4	945.7	717.3	865.2	441.4	411.9	428.9
81	459.7	280.4	345.3	902.8	806.2	862.5	449.7	431.5	439.1
84	336.5	299.1	312.3	853.4	689.3	751.3	481.1	446.6	468.9
86	385.5	149.6	333.2	903.6	747.9	820.7	508.9	455.0	485.9
90	525.6	342.6	445.7	926.7	755.5	831.1	565.9	524.6	541.5
96	667.2	450.0	540.8	865.0	723.5	803.7	624.8	586.4	604.0
102	728.8	545.0	641.0	741.5	619.7	672.4	657.1	636.6	649.6
111	742.1	440.5	660.8	803.2	665.8	720.1	702.7	677.0	690.6
120	866.5	435.7	718.1	1005.3	529.0	656.0	738.7	577.7	721.2
132	757.5	234.7	611.0	838.0	542.8	614.5	751.0	617.7	726.5
136	705.1	231.5	535.9	1044.7	579.5	684.5	782.7	421.6	665.2



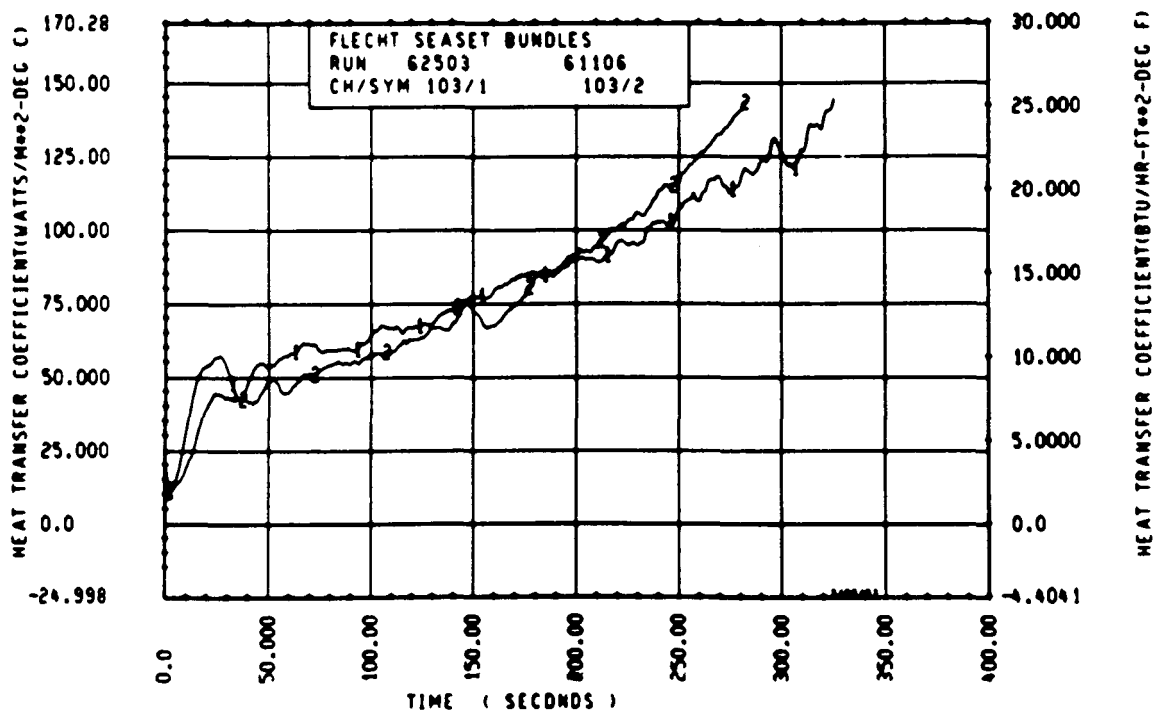
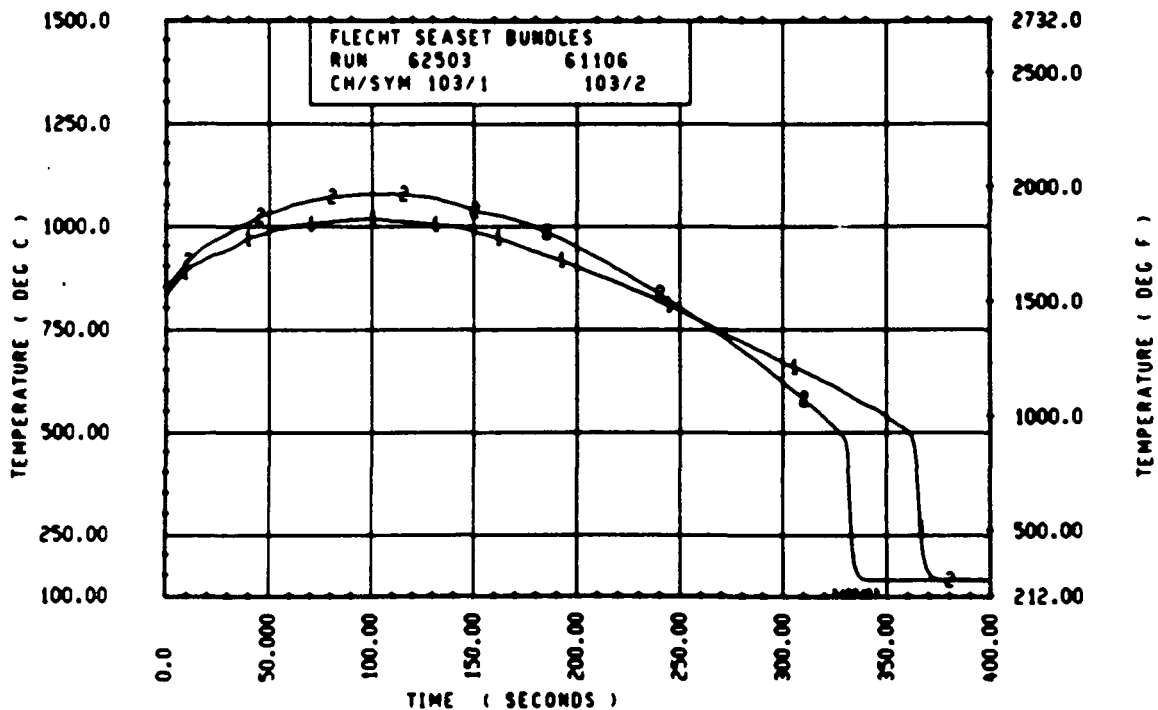
Rod 9G, 1.70 m (67 in.)



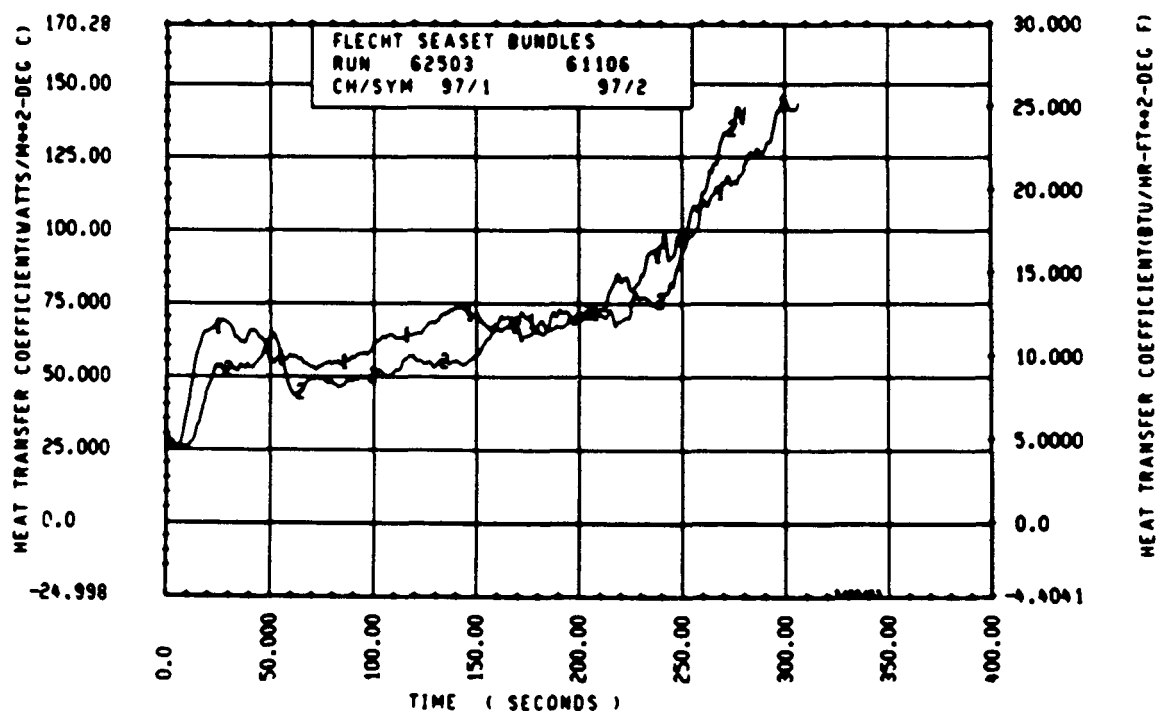
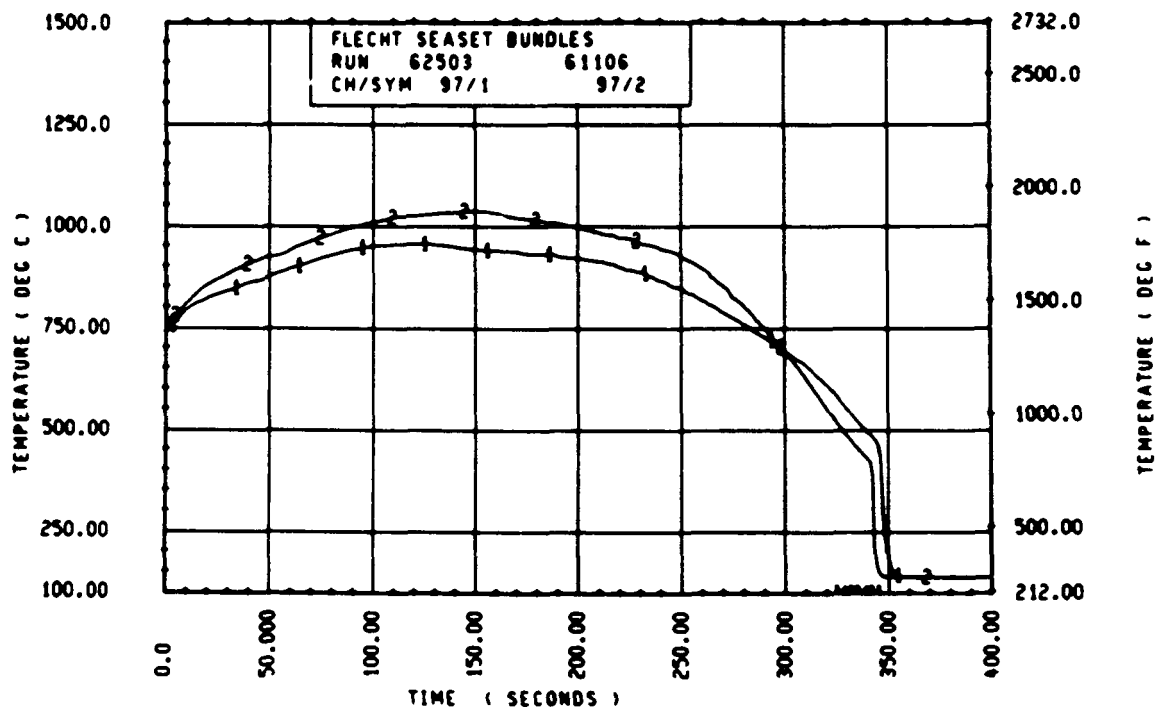
Rod 3H, 1.70 m (67 in.)



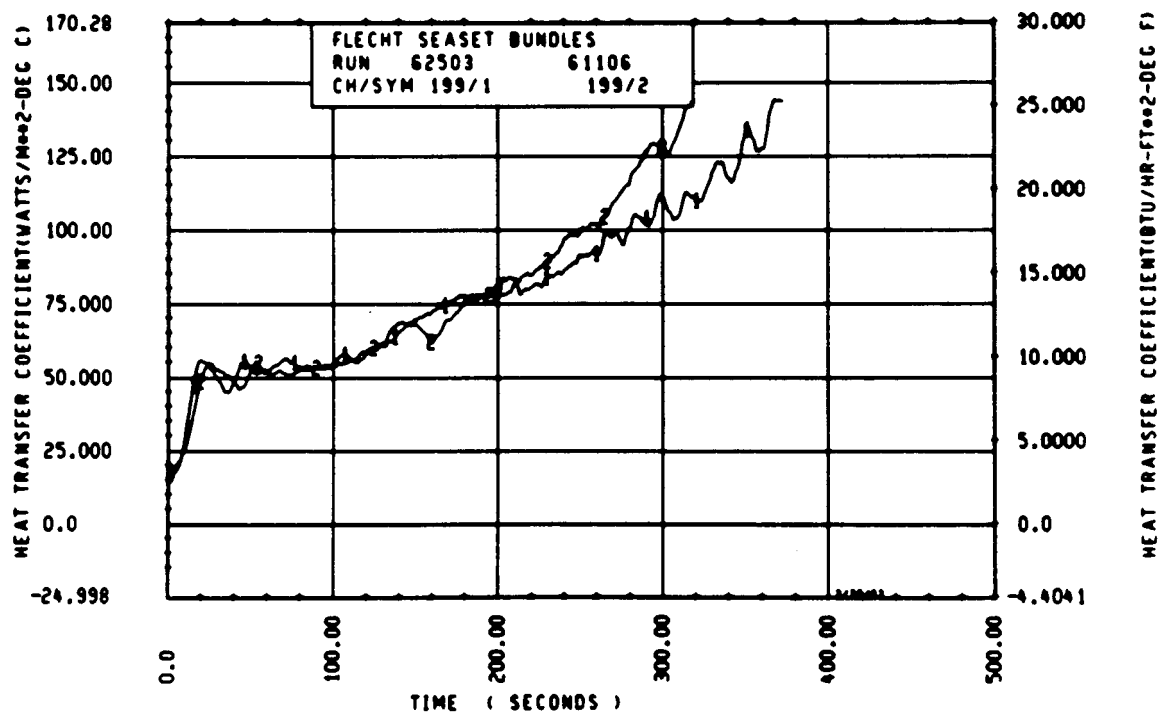
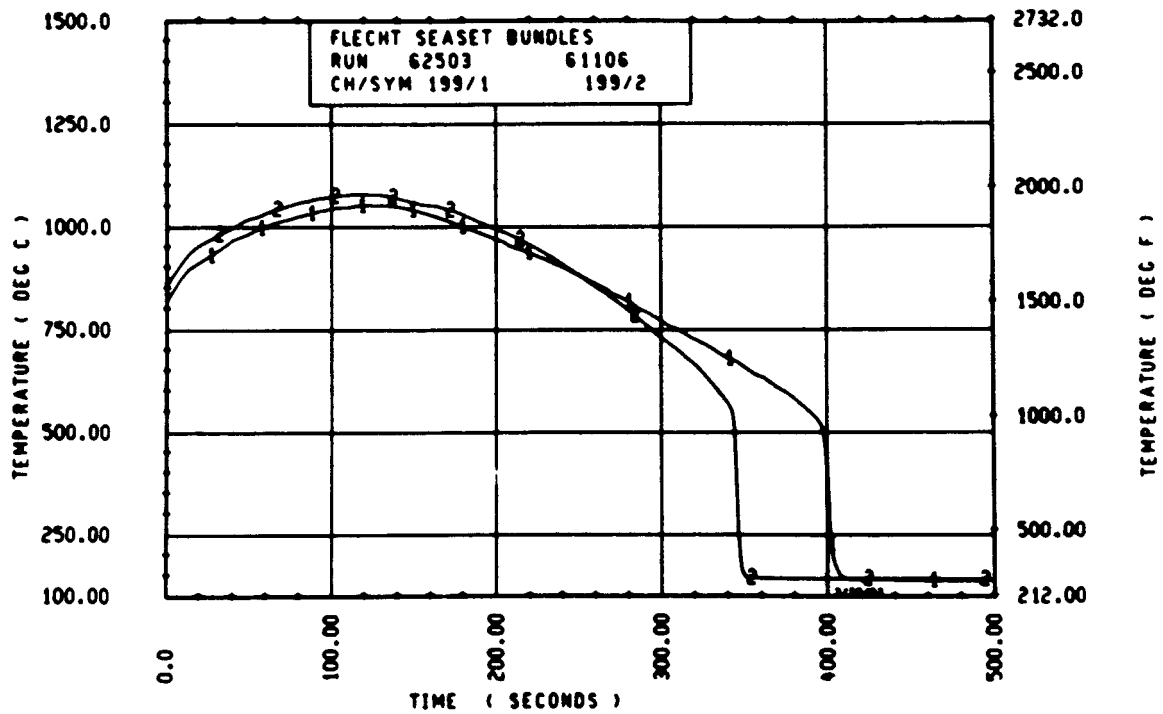
Rod 6L, 1.83 m (72 in.)



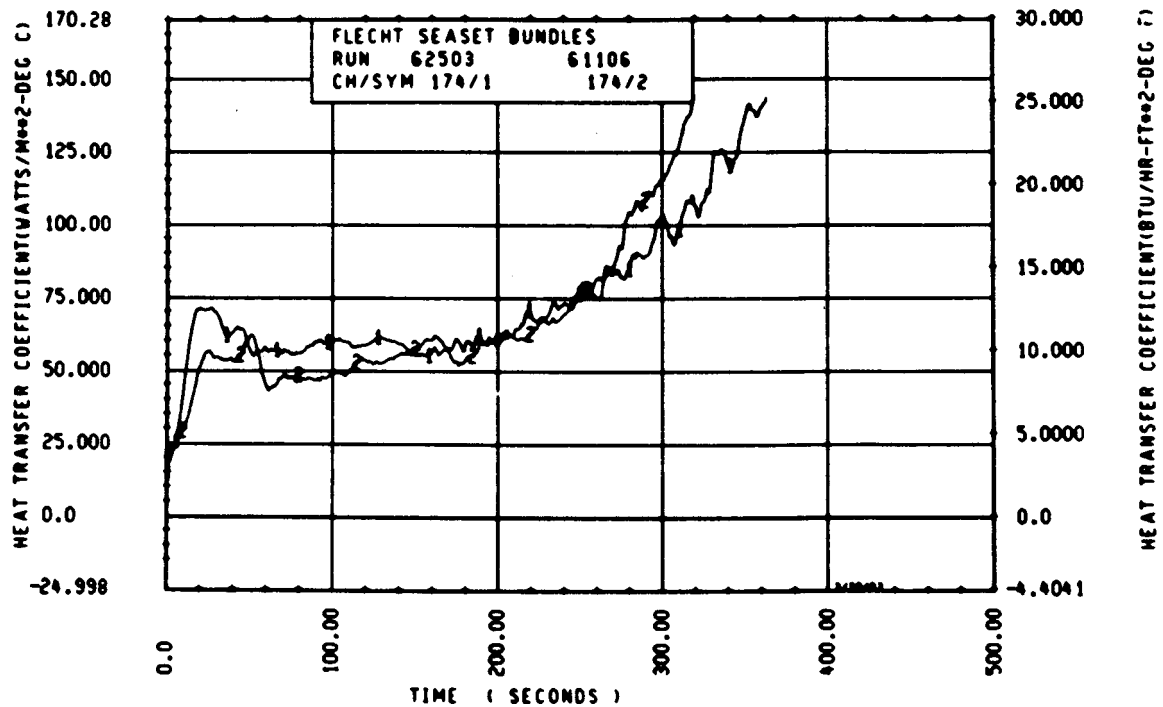
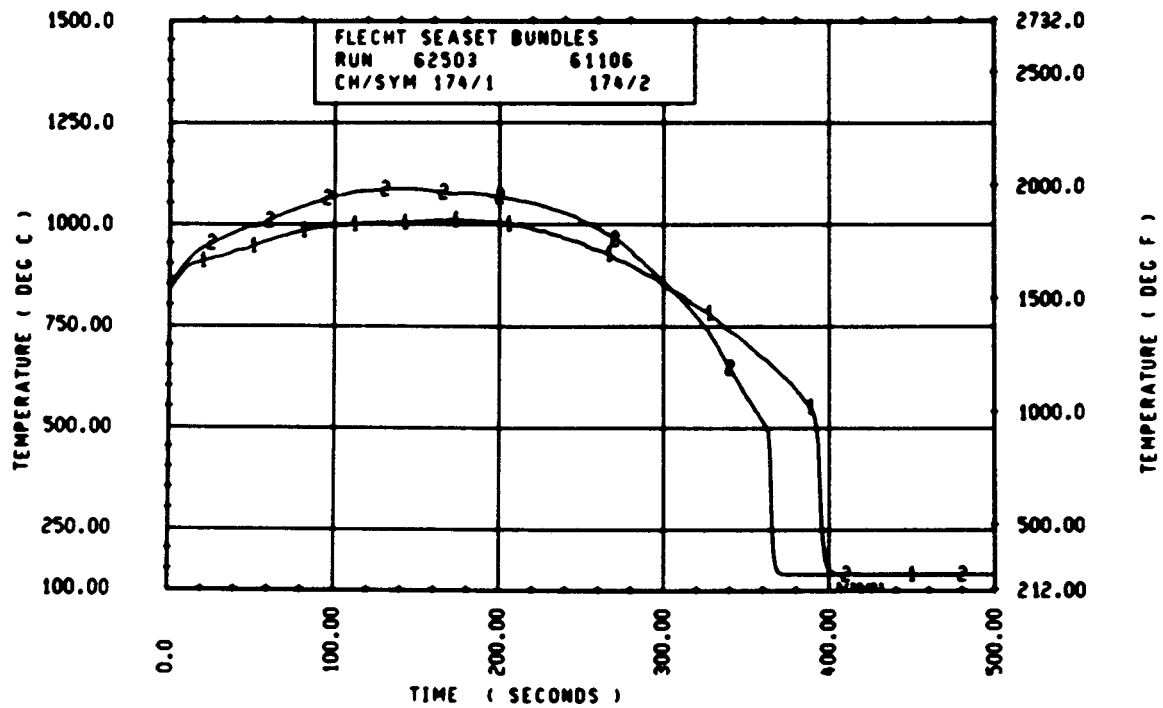
Rod 6L, 1.88 m (74 in.)



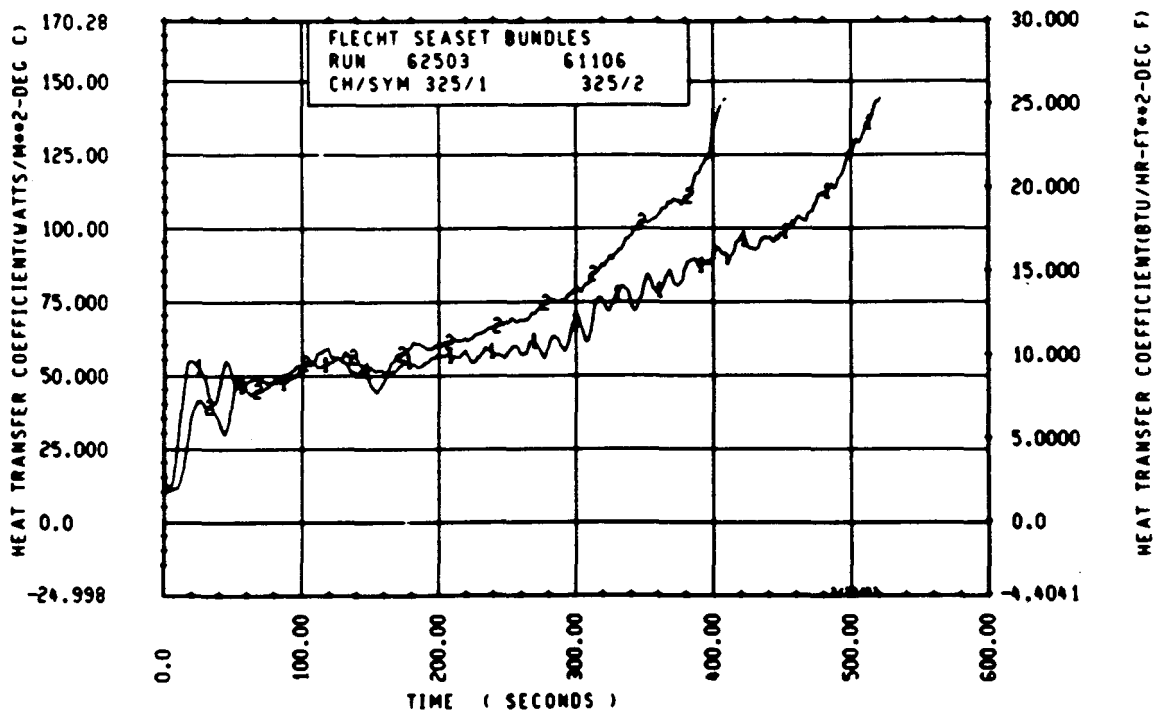
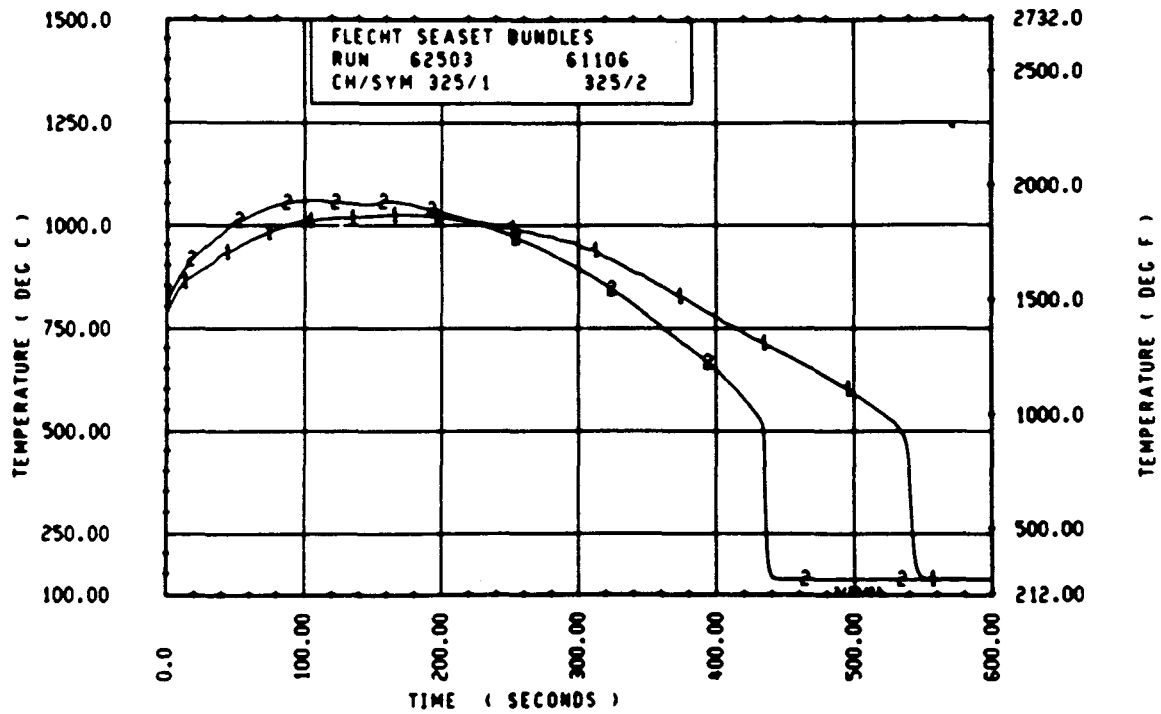
Rod 8H, 1.98 m (78 in.)



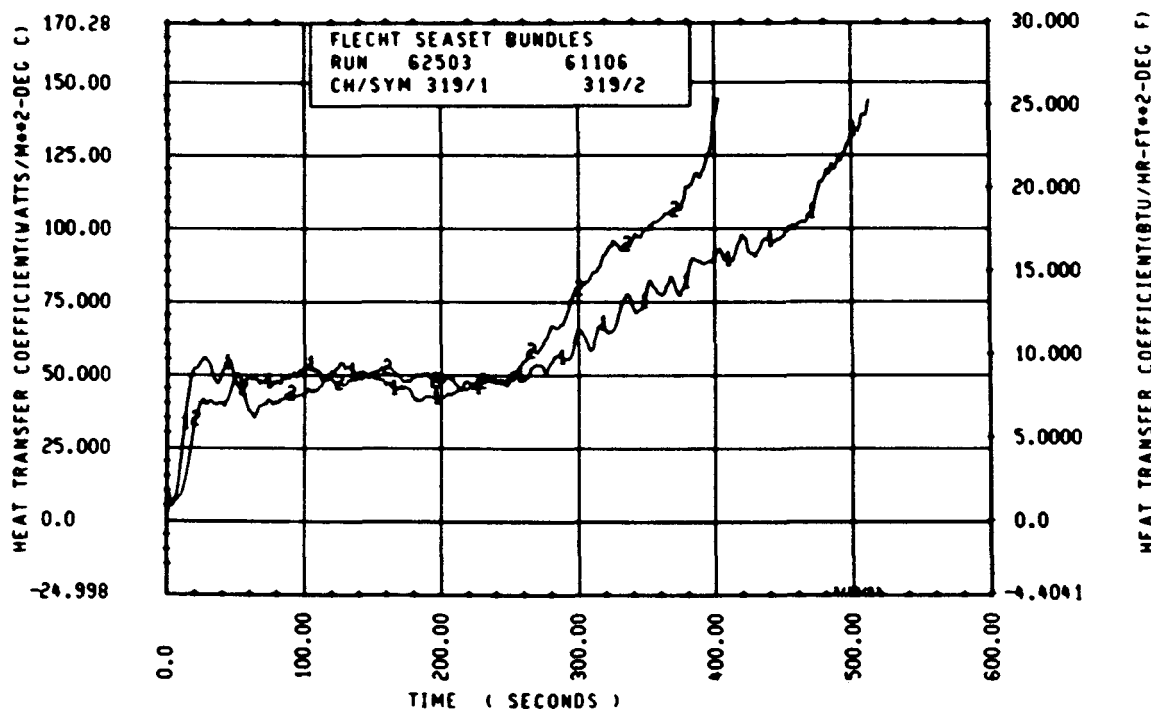
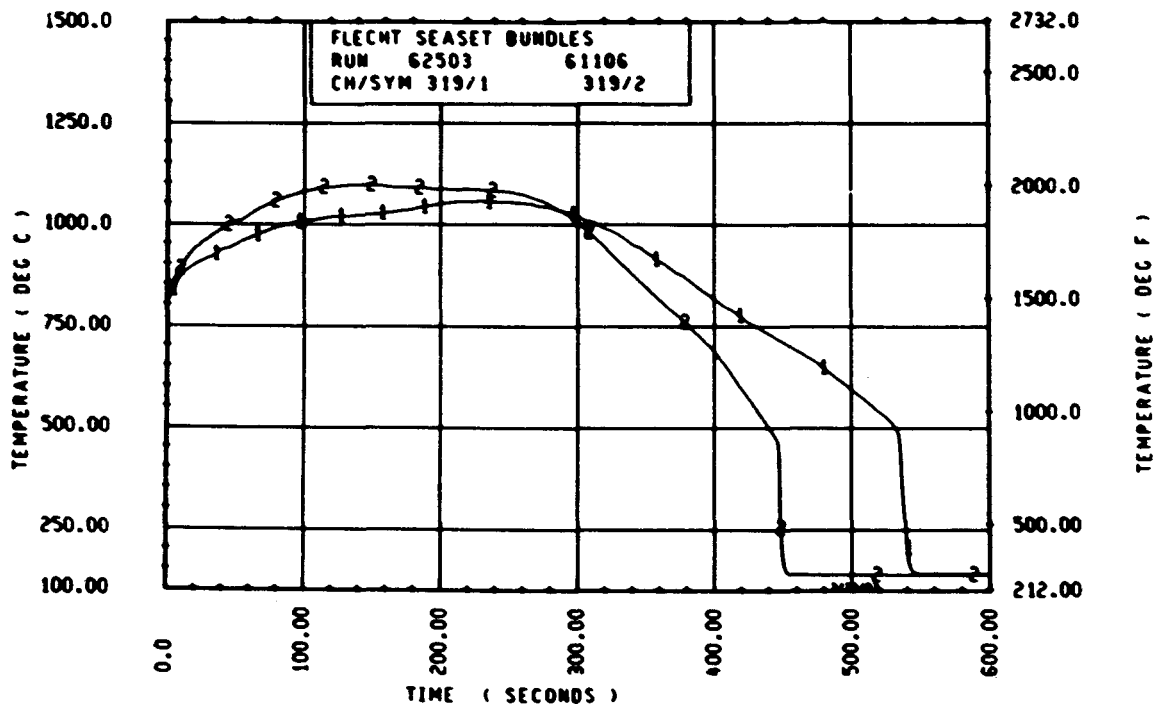
Rod 13G, 1.98 m (78 in.)



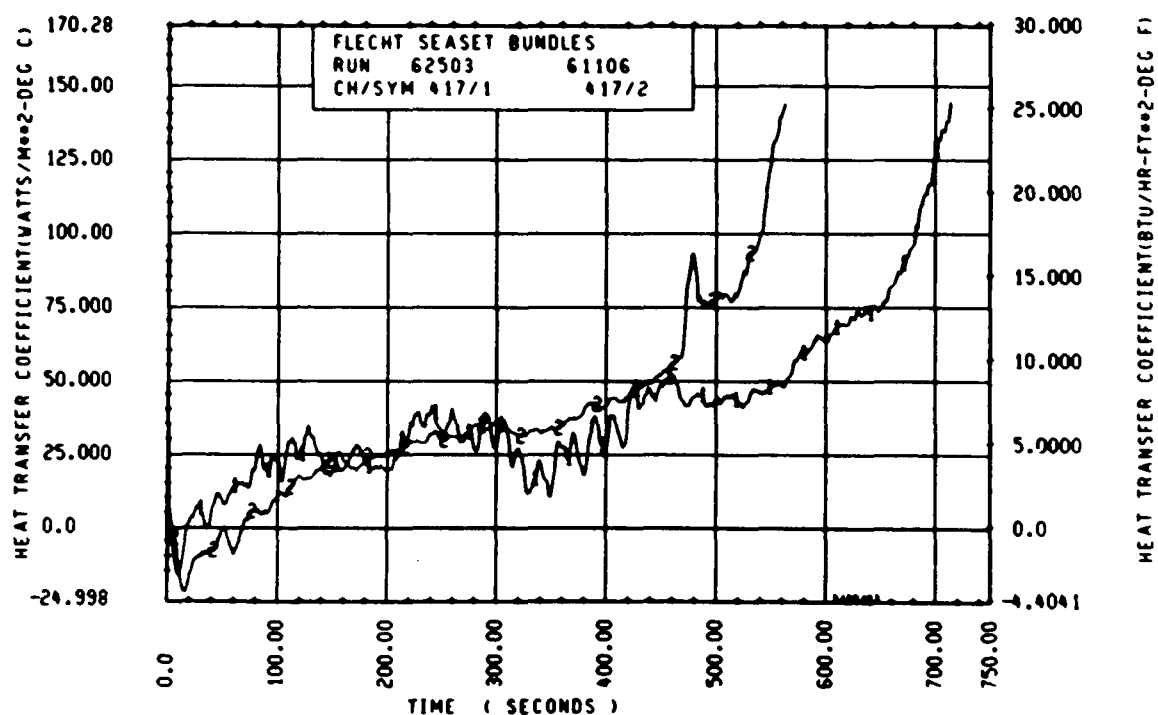
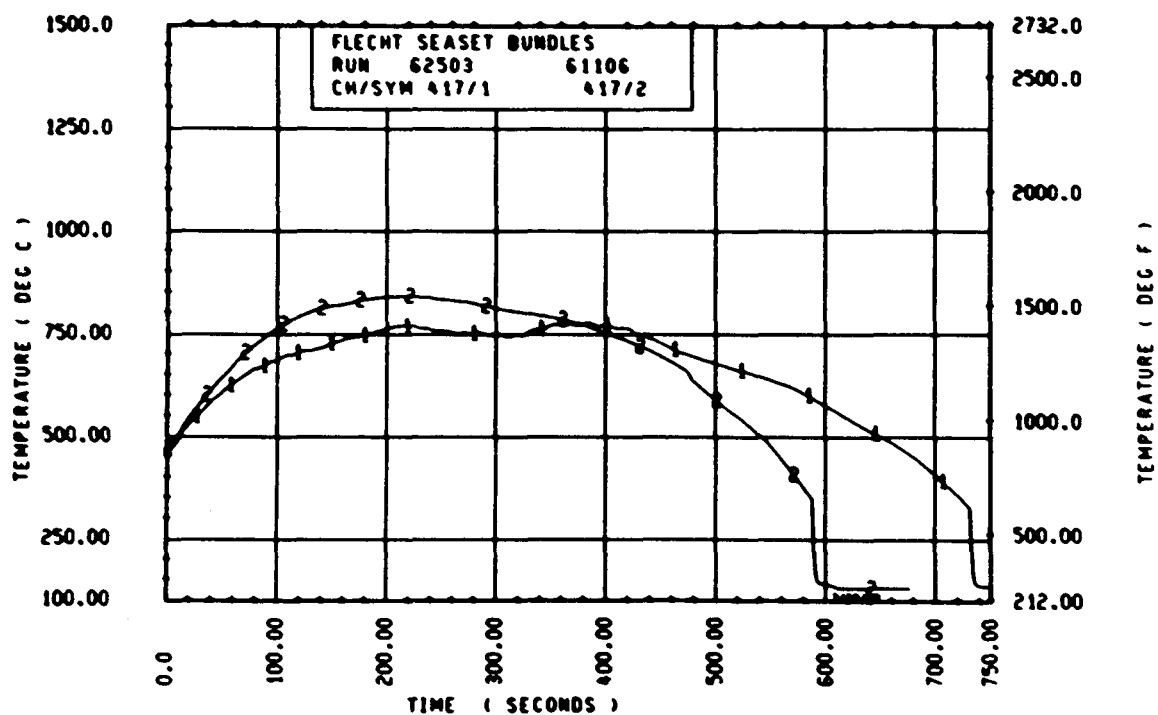
Rod 8H, 1.98 m (78 in.)



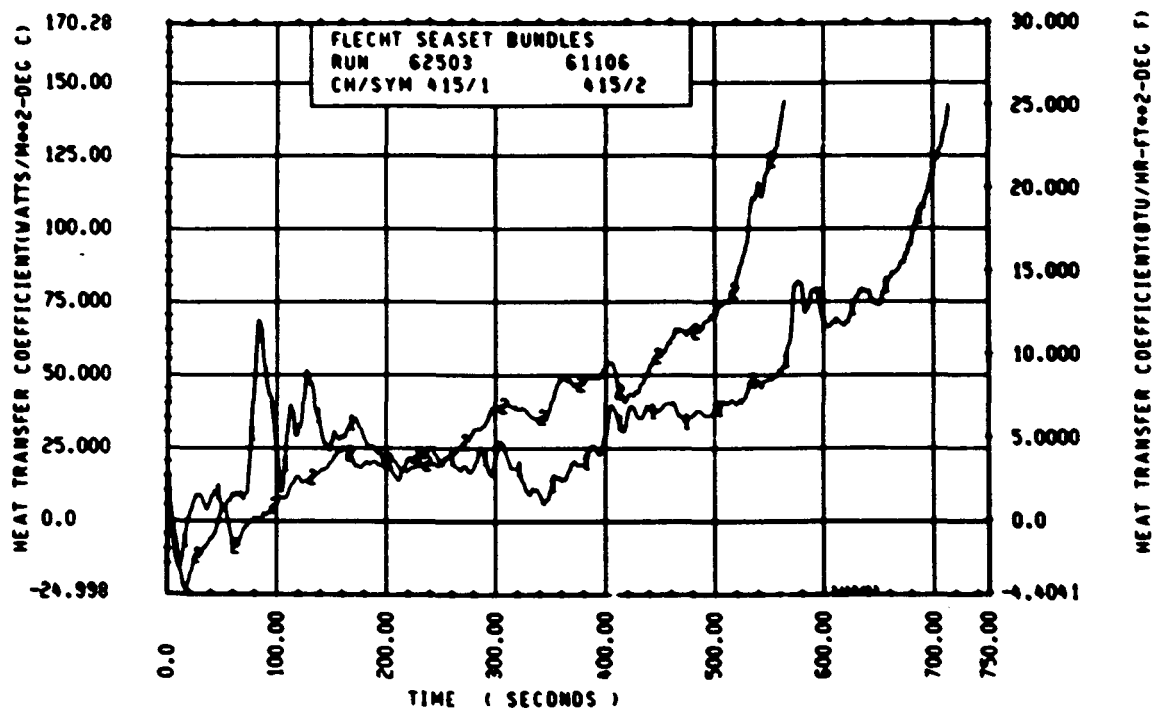
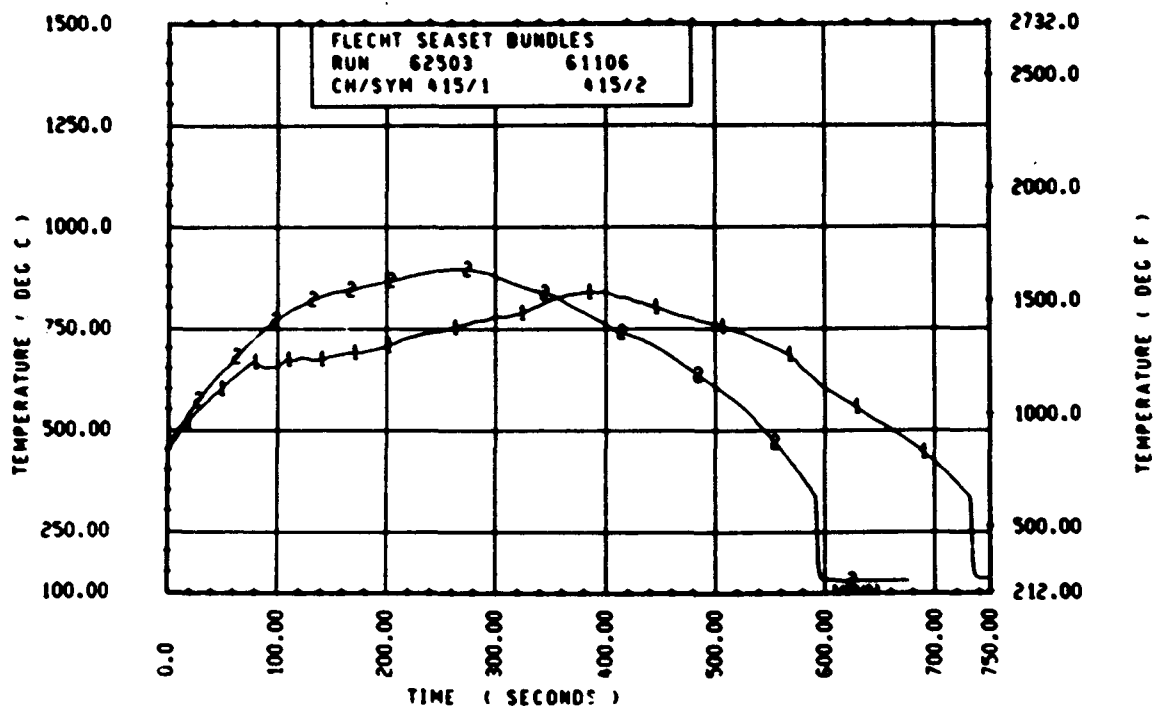
Rod 11E, 2.29 m (90 in.)



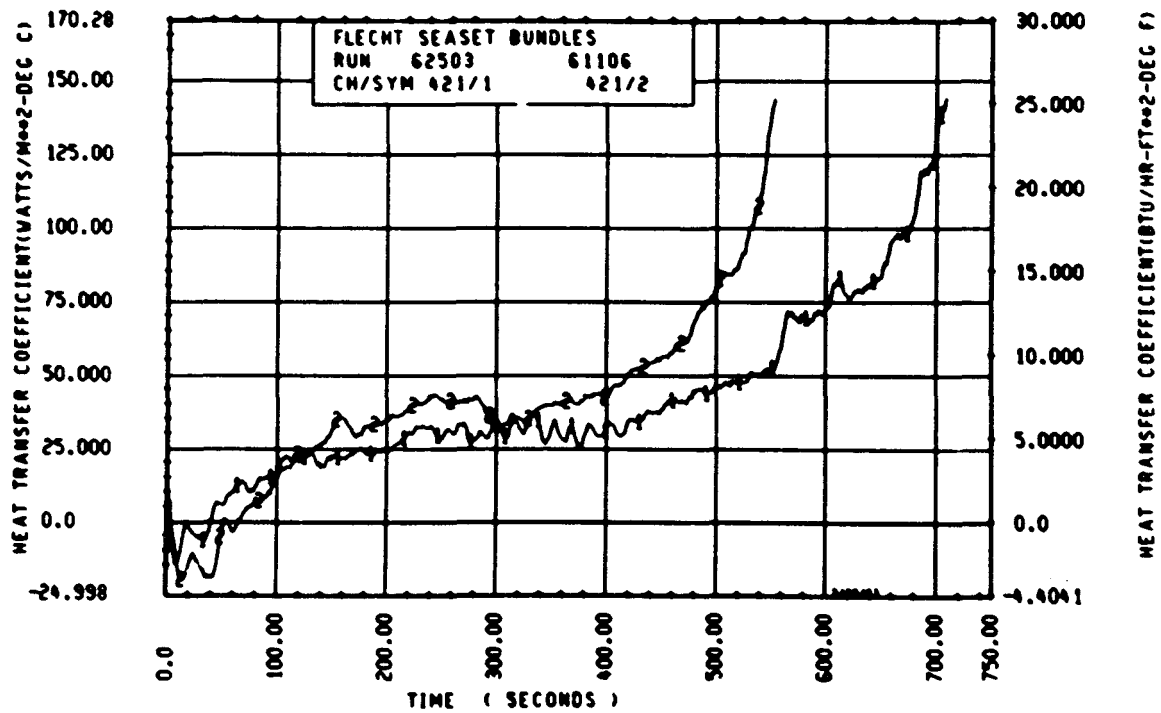
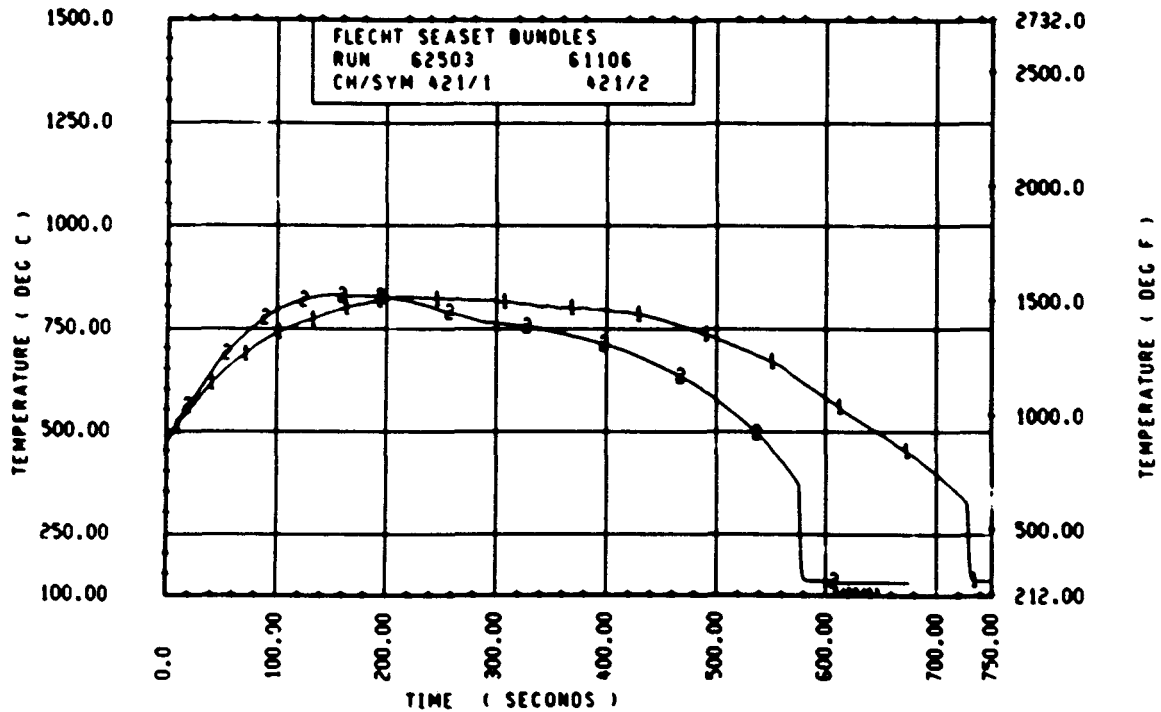
Rod 9G, 2.29 m (90 in.)



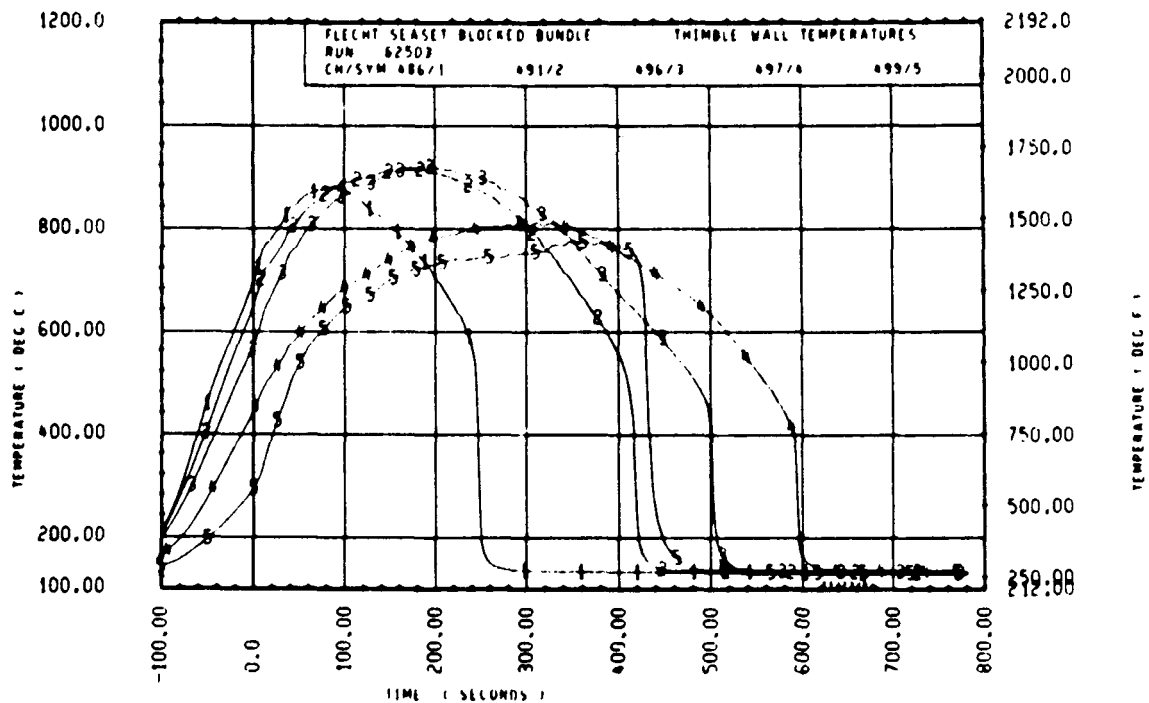
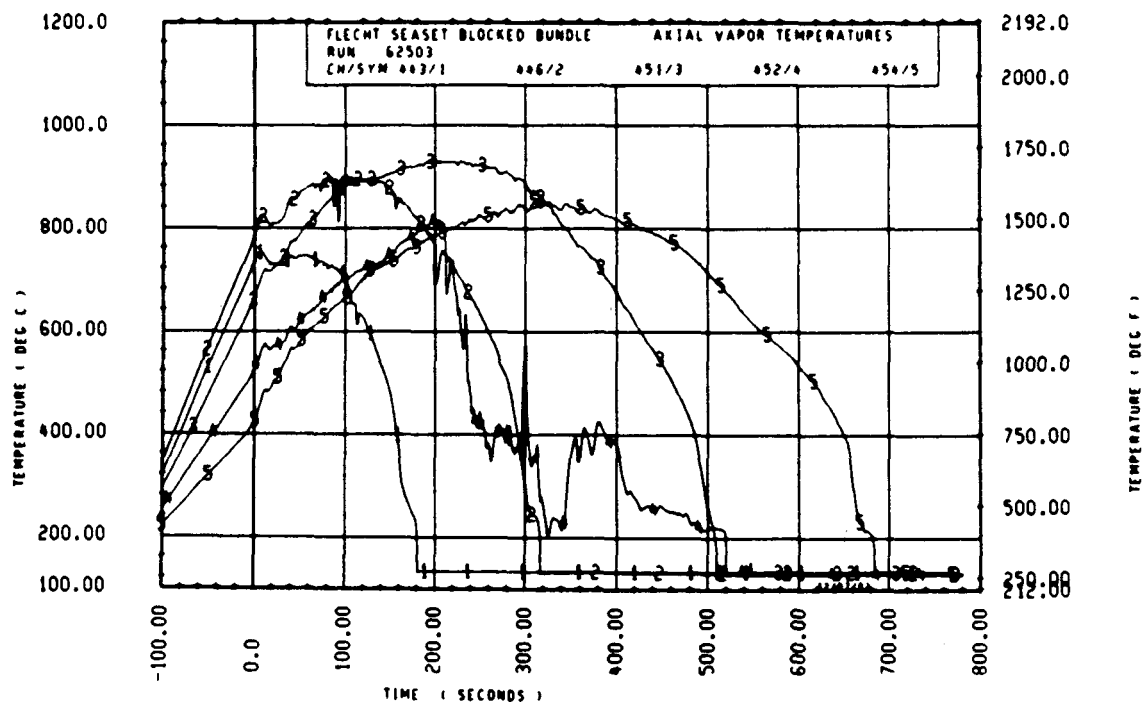
Rod 8K, 3.05 m (120 in.)

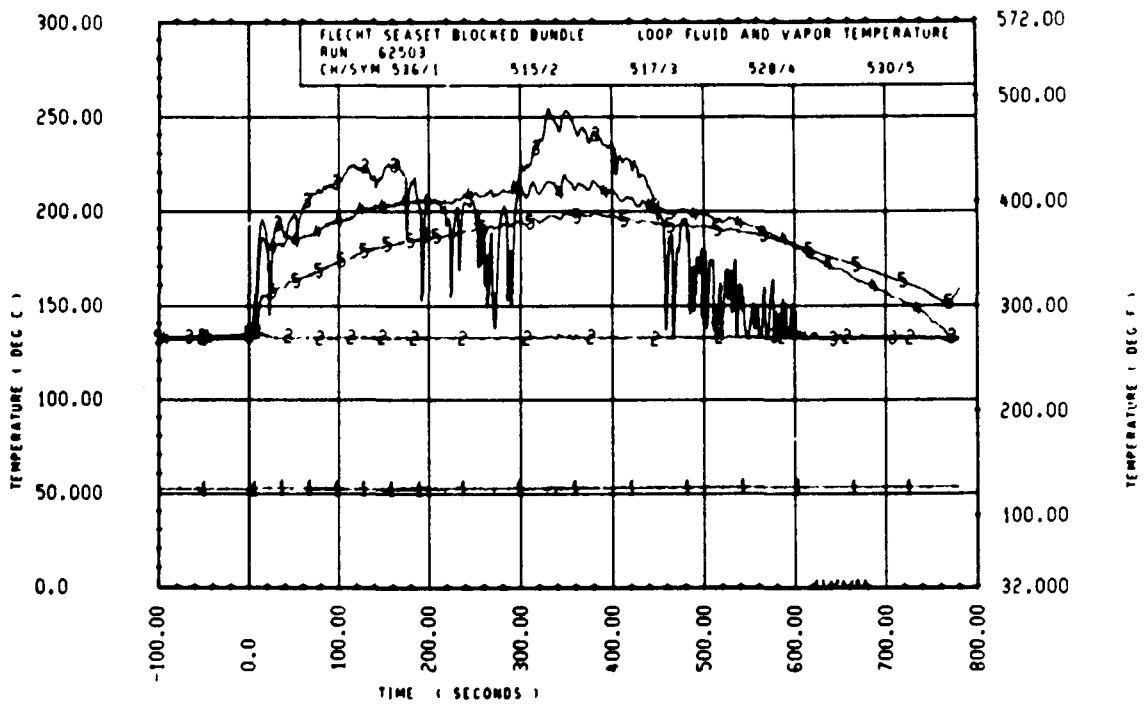
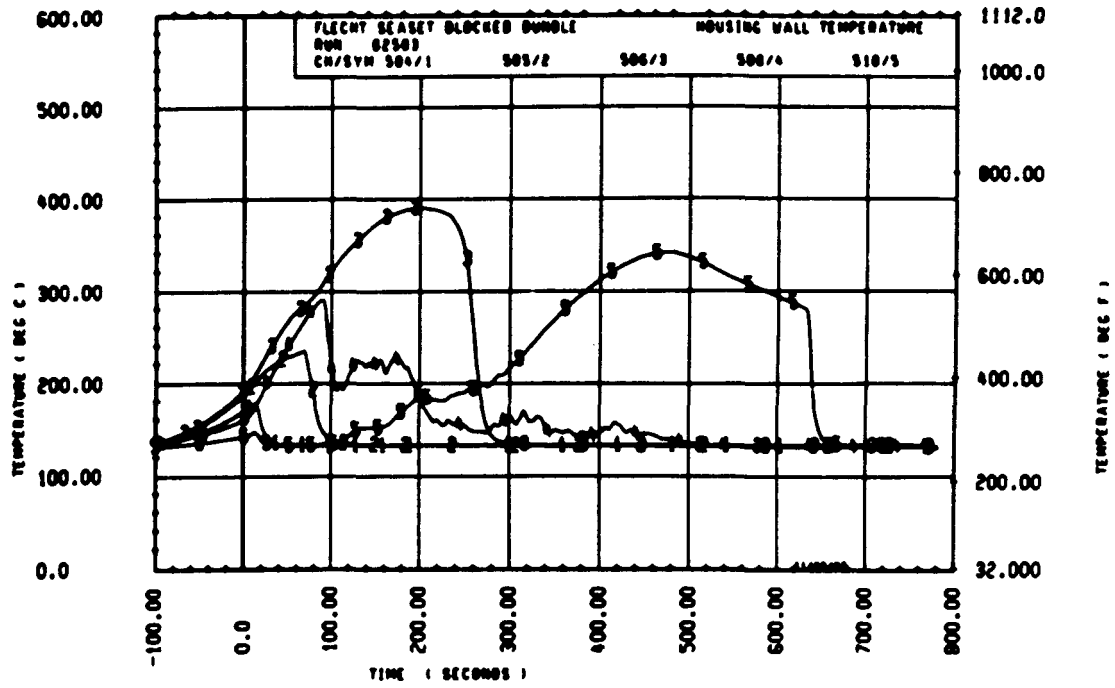


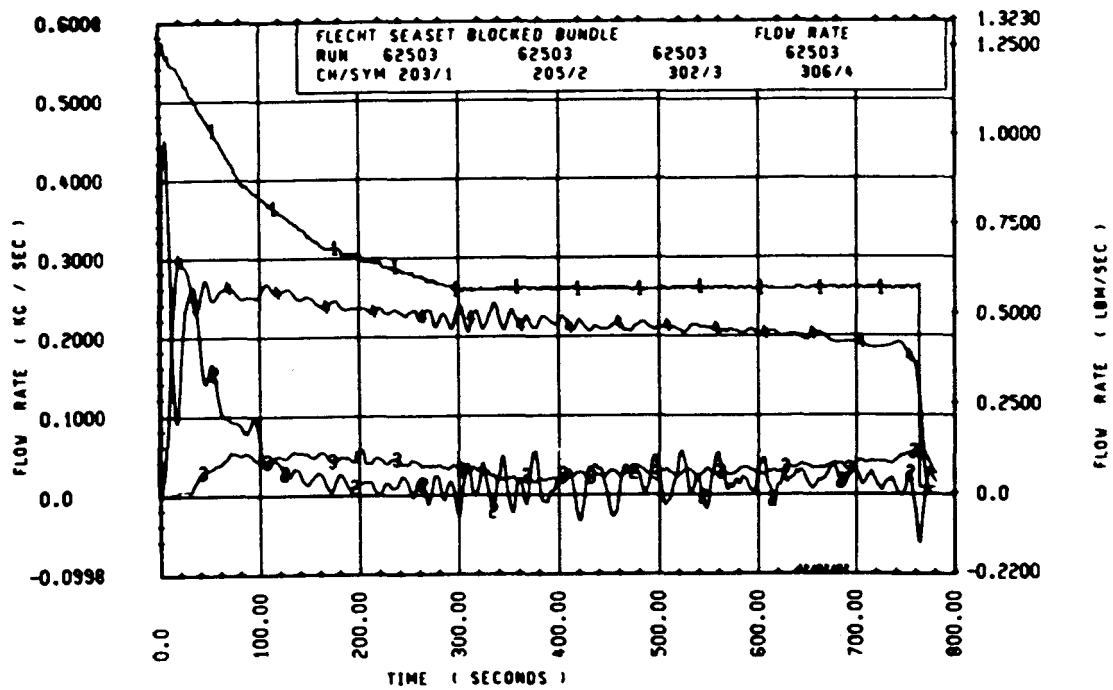
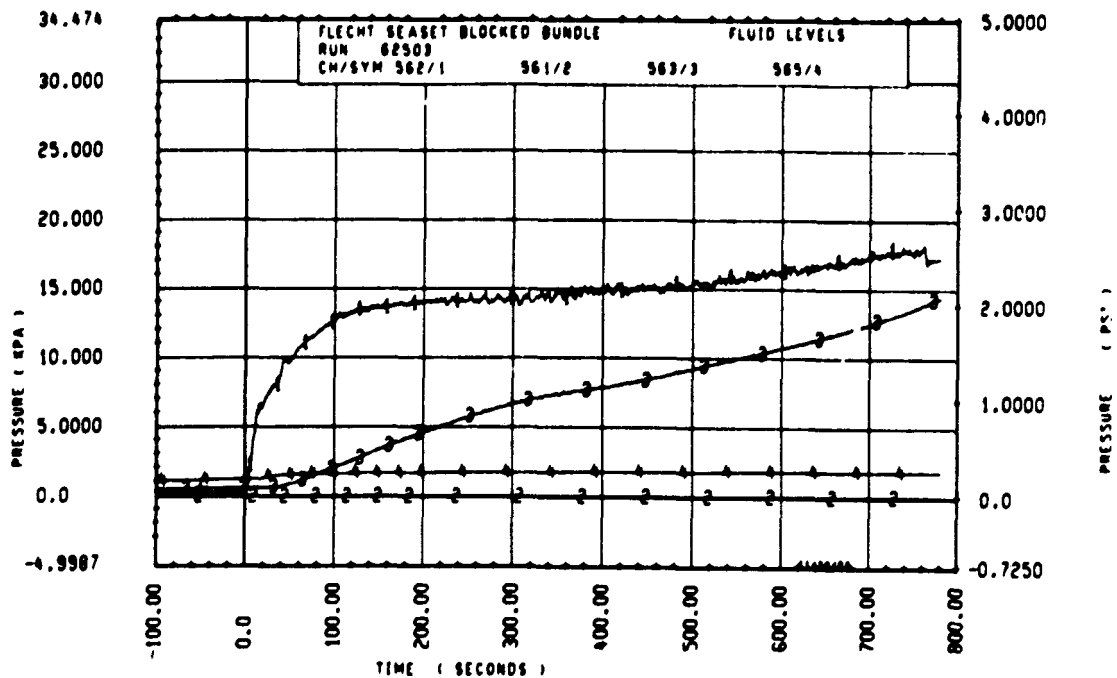
Rod 8H, 3.05 m (120 in.)

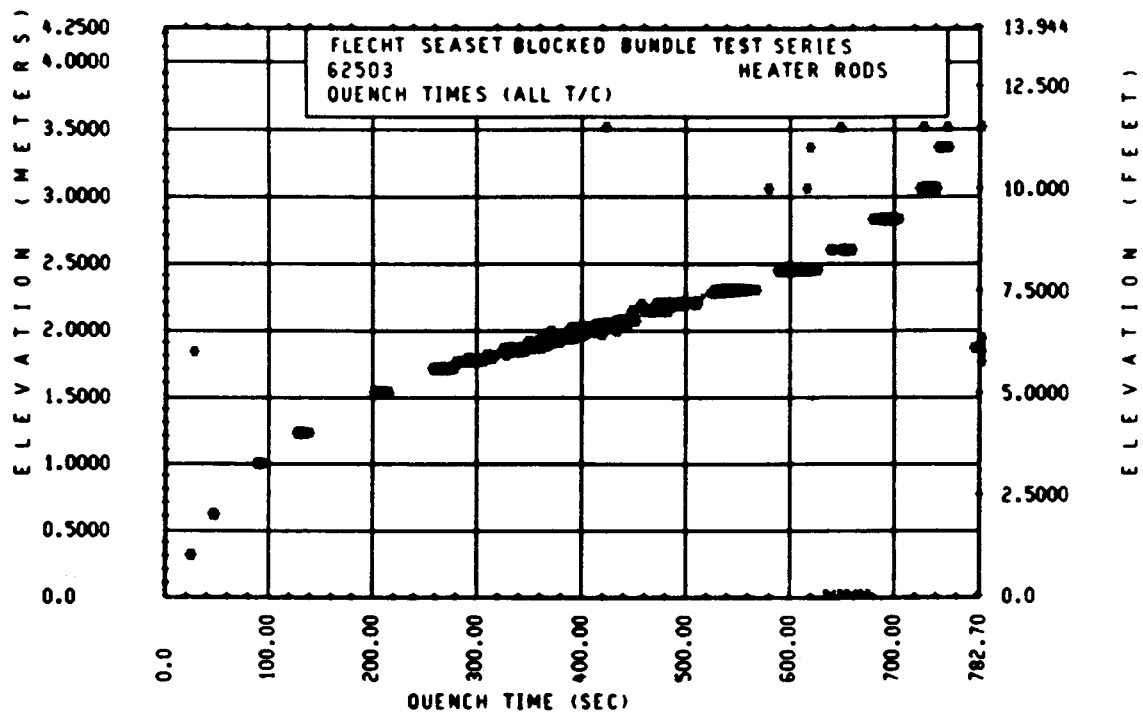
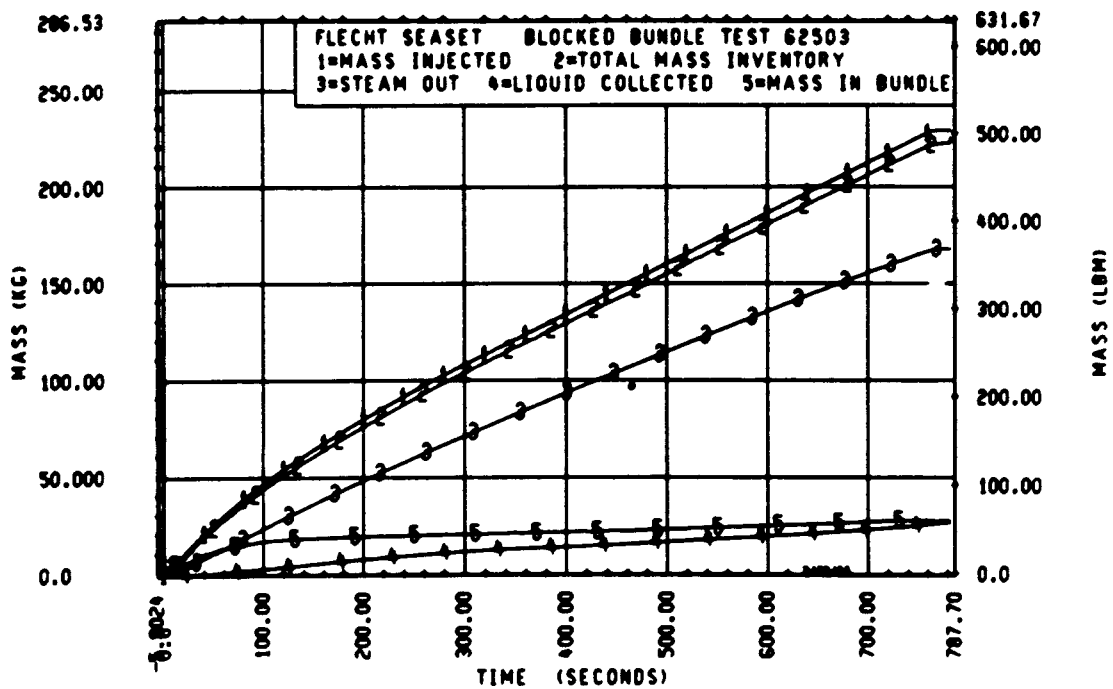


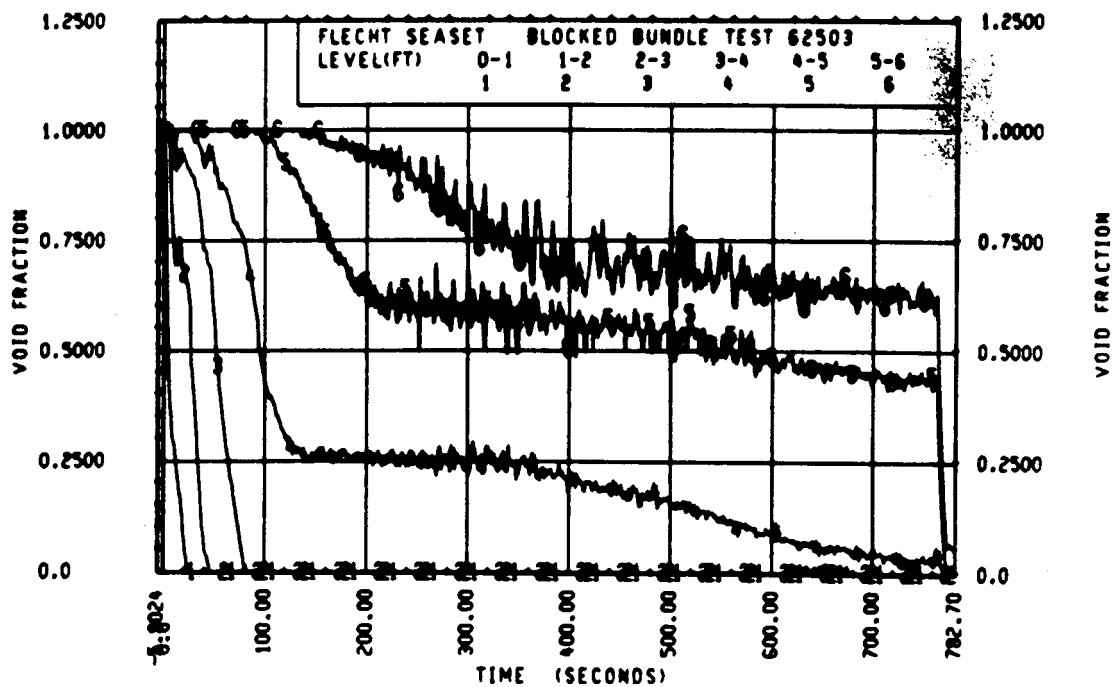
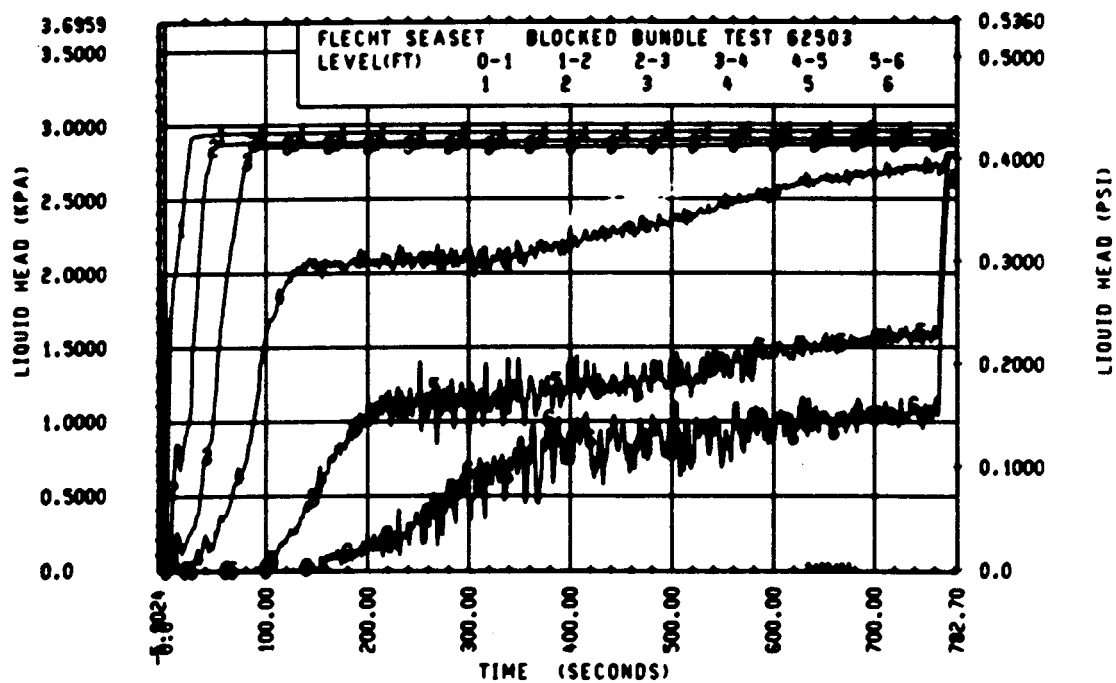
Rod 9M, 3.05 m (120 in.)

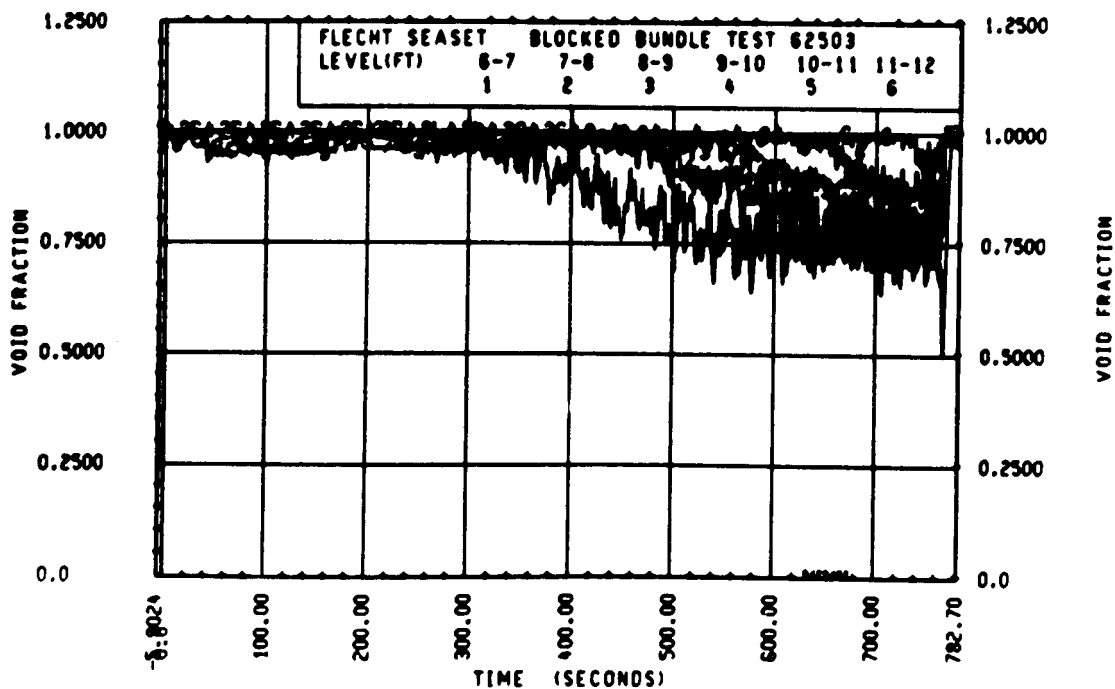
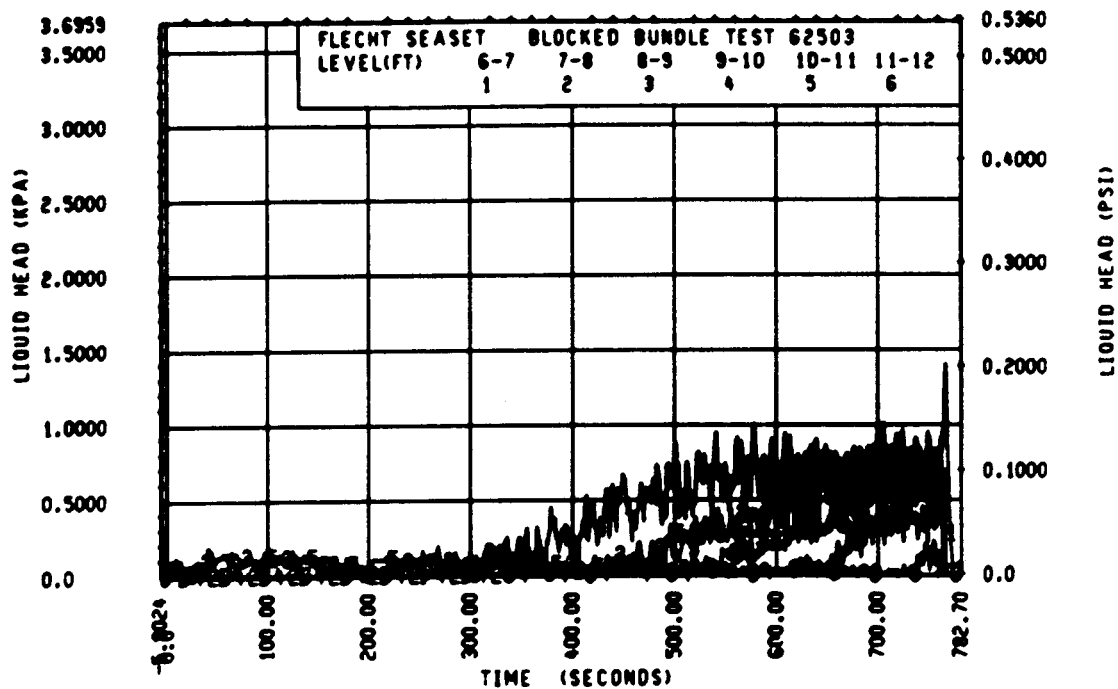












FLECHT SEASET 163-ROD BUNDLE FLOW BLOCKAGE TASK
SUMMARY AND COMMENT SHEET

Run: 62605
Test date: 9/29/82
Test type: Forced reflood
Parameter: Data repeatability (second)

AS-RUN TEST CONDITIONS:

Upper plenum pressure	0.272 MPa (39.5 psia)
Initial peak clad temperature and location	872.7°C (1602.0°F), 7G-1.70 m (67 in.)
Initial peak rod power:	
Peripheral rods	2.29 kw/m (0.698 kw/ft)
Bypass rods	2.29 kw/m (0.699 kw/ft)
Blockage island rods	2.29 kw/m (0.699 kw/ft)
Flooding rate	38.6 mm/sec (1.52 in./sec)
Coolant temperature	52.2°C (126°F)
Initial bundle water level	+5.6 mm (+0.22 in.)

COMMENTS:

Carryover tank filled up at approximately 375 seconds.

Inlet mass flow: ⁽¹⁾ -0.4% constant

Power decay: ⁽¹⁾ peripheral rods, -0.5% linearly increasing to -1% by 400 seconds
bypass rods, +0.5% linearly changing to -0.5% by 400 seconds
blockage rods, 0% constant

1. Relative to run 61005

FLECHT SEASET 163 ROD BUNDLE TEST SERIES
RUN NUMBER 62605

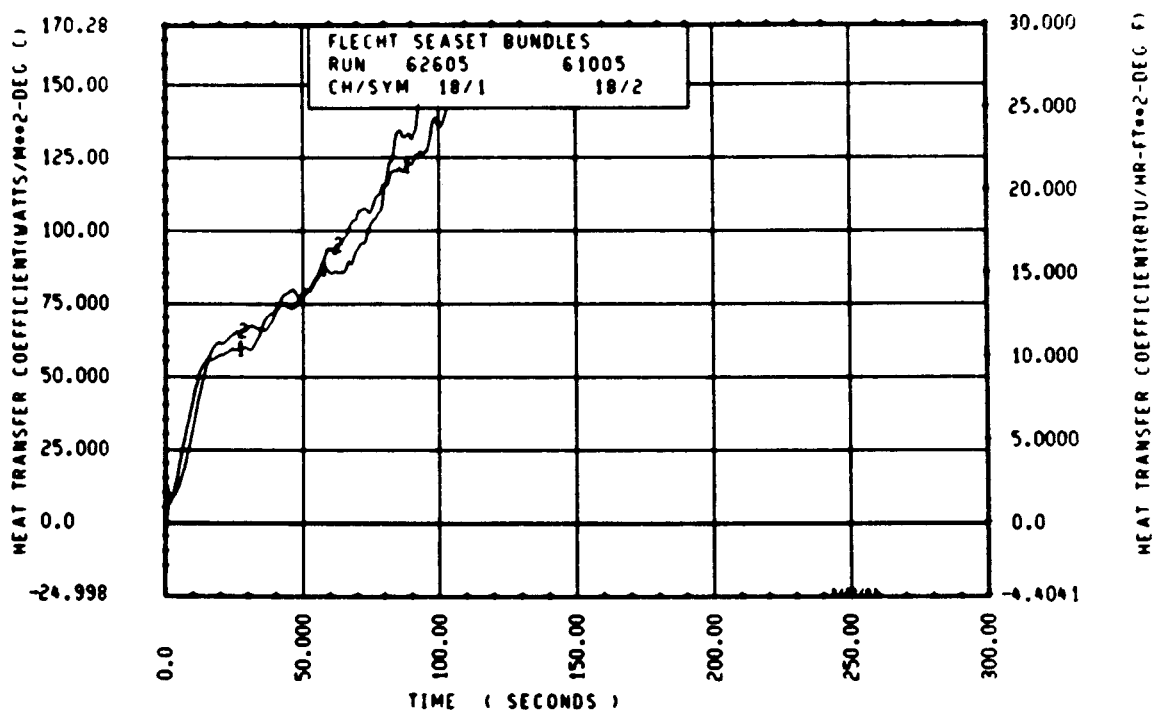
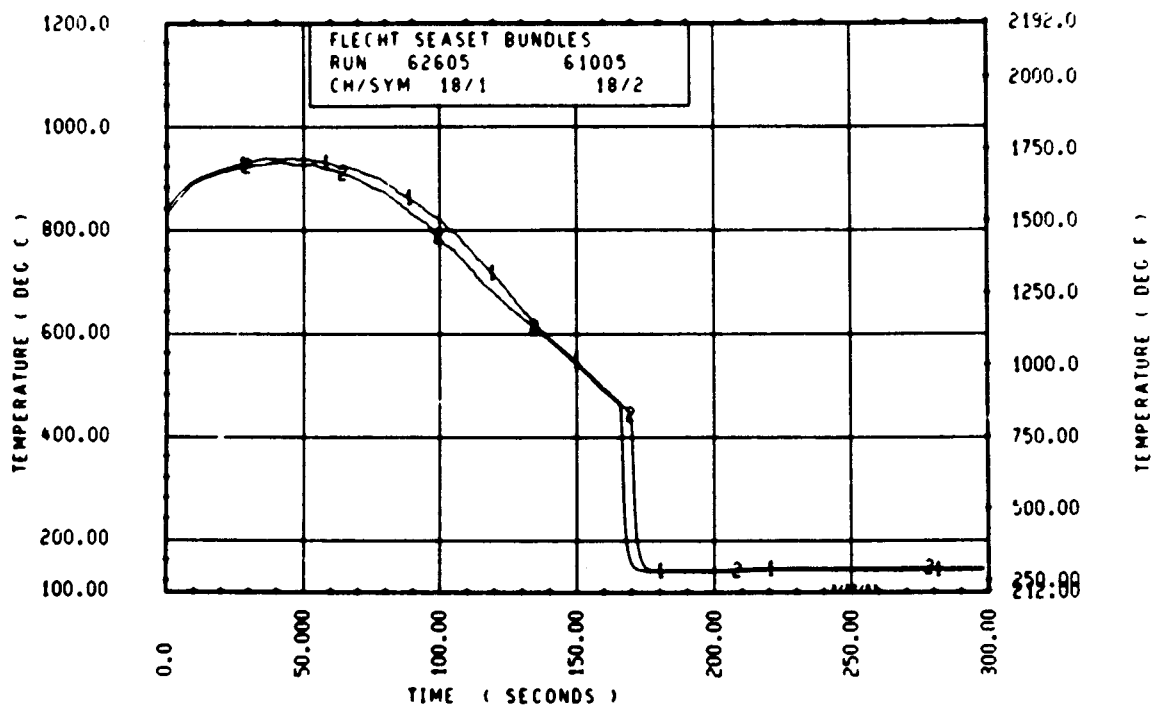
ROD/ELEV	CHAN. NO	INITIAL AT FLUCC (DEG F)	MAXIMUM TEMPERATURE (DEG F)	TEMPERATURE RISE (DEG F)	TURNAROUND TIME (SECONDS)	QUENCH TEMPERATURE (DEG F)	QUENCH TIME (SECONDS)
96 1- 0	3	674.	689.	15.	4.5	585.	18.0
10H 2- 0	6	897.	929.	32.	7.0	654.	42.2
96 3- 3	9	1220.	1289.	61.	14.0	771.	82.0
3J 4- C	11	1357.	1461.	103.	22.0	764.	115.3
7H 4- C	12	1373.	1482.	109.	23.5	746.	119.4
8K 4- C	13	1385.	1500.	115.	26.5	736.	120.0
8H 4- C	14	1347.	1450.	103.	21.0	764.	114.9
12D 4- C	17	1342.	1432.	90.	22.5	769.	113.8
5E 5- C	20	1514.	1699.	180.	47.5	887.	166.9
76 5- C	21	1577.	1746.	169.	36.5	850.	168.4
96 5- 0	24	1554.	1718.	163.	34.5	865.	170.4
5E 5- 7	33	1547.	1730.	183.	55.5	819.	197.8
86 5- 7	45	1562.	1739.	177.	35.5	831.	199.4
9H 5- 9	52	1511.	1671.	160.	23.5	710.	201.2
76 5-10	59	1532.	1722.	191.	36.5	793.	220.1
7F 5-11	62	1478.	1656.	178.	37.0	876.	178.8
46 5-11	64	1561.	1750.	189.	47.5	818.	221.3
2I 6- C	67	1566.	1795.	229.	51.5	906.	221.2
5D 6- 0	70	1504.	1707.	202.	55.5	815.	220.2
6J 6- C	74	1554.	1731.	177.	46.5	851.	225.2
7H 6- C	66	1552.	1766.	214.	55.0	840.	219.1
11E 6- C	80	1548.	1757.	209.	67.0	848.	222.2
8H 6- 2	97	1416.	1602.	186.	62.0	834.	198.2
5H 6- 2	99	1560.	1766.	206.	64.5	811.	233.1
9E 6- 2	105	1369.	1726.	336.	84.5	1376.	161.8
8H 6- 3	111	1450.	1622.	172.	57.0	894.	203.0
46 6- 3	124	1572.	1779.	207.	55.0	848.	240.2
11H 6- 4	134	1501.	1721.	220.	57.5	761.	215.0
9D 6- 4	143	1550.	1825.	275.	76.5	813.	238.9
9J 6- 5	165	1542.	1713.	171.	51.5	892.	227.3
9H 6- 5	166	1588.	1803.	215.	97.5	882.	244.0
8J 6- 6	192	1582.	1785.	202.	73.5	950.	232.9
9D 6- 6	193	1561.	1840.	279.	73.5	881.	248.7
11F 6- 6	173	1560.	1807.	247.	70.0	815.	249.0
46 7- 0	261	1510.	1651.	142.	36.0	767.	282.1
7D 7- 6	309	1456.	1709.	213.	62.0	857.	305.1
76 7- 6	312	1548.	1756.	208.	64.0	927.	291.1
11E 7- 6	325	1476.	1723.	248.	78.5	822.	311.1
5L 8- 0	337	1321.	1626.	306.	104.0	796.	336.2
7H 8- 0	345	1366.	1661.	295.	82.0	790.	335.2
7K 8- C	346	1384.	1654.	270.	88.5	794.	330.7
5J 8- 6	366	1171.	1388.	217.	53.5	886.	363.6
78 8- 6	368	1141.	1380.	238.	58.5	882.	361.3
7E 9- 3	383	1113.	1452.	339.	176.0	682.	381.7
8H 9- 3	387	1075.	1346.	271.	172.0	626.	380.1
9C 9- 3	389	1050.	1317.	267.	82.5	654.	379.0
11F 9- 3	394	1061.	1299.	239.	81.0	924.	257.8
7810- 0	408	813.	1172.	359.	159.0	607.	402.2
8H10- C	415	866.	1210.	344.	130.5	607.	394.1
8K10- C	417	872.	1195.	323.	166.0	617.	402.9
8H10- C	418	877.	1246.	369.	114.5	662.	399.2
6H11- C	429	687.	860.	174.	165.5	536.	383.2
9611- 0	431	676.	833.	154.	54.5	694.	87.7
11E11- 0	432	689.	862.	173.	53.5	386.	240.5
5J11- 6	436	645.	824.	179.	109.0	510.	397.2
7811- 6	437	558.	863.	304.	148.0	560.	359.3
8J11- 6	438	666.	833.	167.	81.5	514.	396.0

RUN 62605 HEATER ROD STATISTICAL DATA

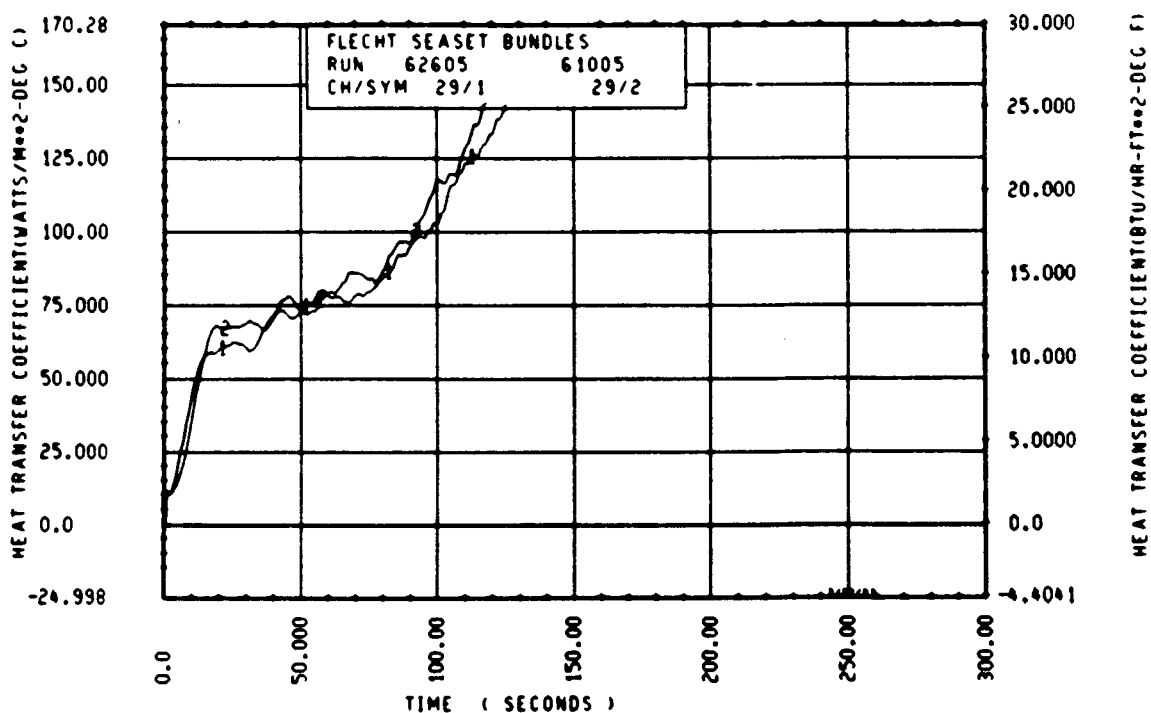
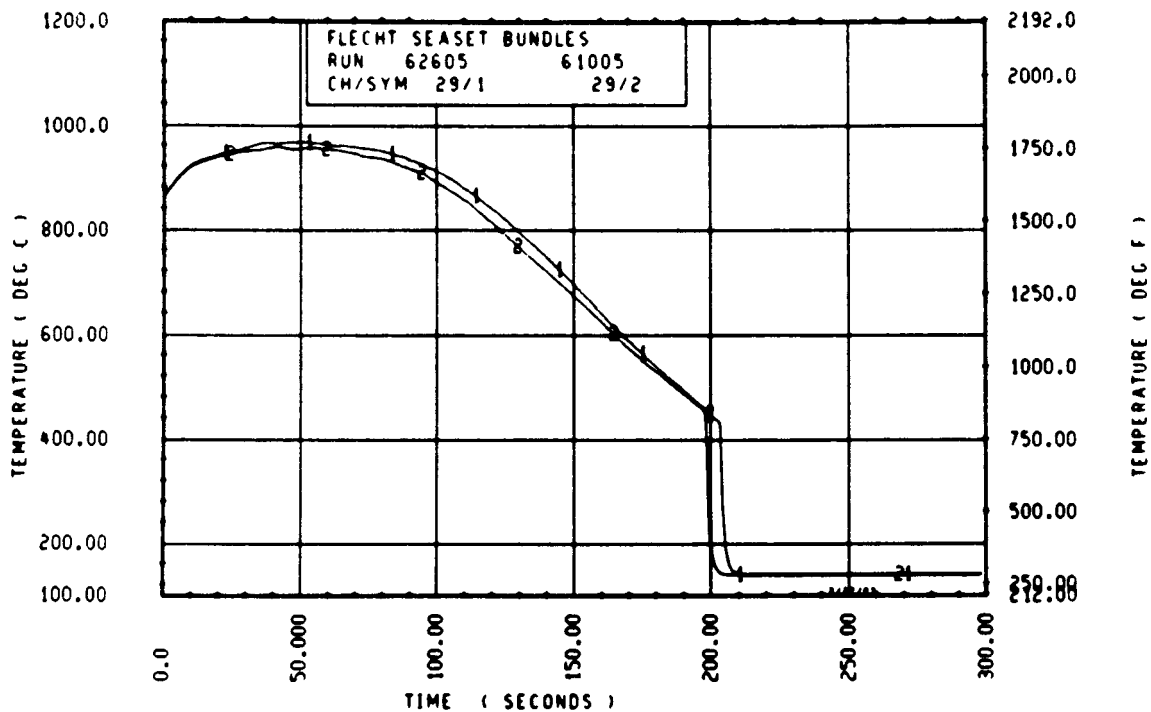
ELEV	INITIAL TEMP (DEG F)			MAX TEMP (DEG F)			TURNAROUND TIME (SEC)		
	MAX	MIN	MEAN	MAX	MIN	MEAN	MAX	MIN	MEAN
12	674.3	671.1	673.2	689.0	685.8	687.9	4.5	4.0	4.3
24	896.7	860.5	875.3	928.7	891.5	906.3	7.0	6.5	6.7
39	1228.5	1185.8	1201.1	1289.0	1253.5	1262.9	16.5	12.5	14.1
48	1389.1	1341.6	1368.3	1500.1	1431.7	1474.6	26.5	21.0	23.1
60	1577.1	1413.5	1524.9	1748.9	1531.5	1688.6	47.5	34.5	37.5
67	1602.0	1499.0	1559.5	1775.7	1691.0	1734.8	55.5	35.0	41.7
69	1550.0	1511.0	1529.2	1730.0	1671.3	1711.6	61.5	23.5	44.5
70	1585.7	1491.6	1530.7	1776.8	1718.8	1738.7	64.0	36.5	49.2
71	1560.8	1477.7	1501.9	1750.1	1655.9	1702.0	63.0	37.0	51.5
72	1597.7	1482.0	1550.3	1808.2	1706.5	1759.2	67.0	37.5	51.6
73	1576.0	1485.2	1532.1	1790.2	1692.2	1742.7	63.5	39.5	53.7
74	1573.8	1415.7	1525.5	1796.9	1602.0	1746.5	74.5	49.0	60.1
75	1581.4	1449.9	1526.9	1794.7	1621.8	1742.9	78.5	47.0	62.0
76	1593.3	1492.6	1553.8	1829.7	1721.0	1782.3	76.5	49.0	60.9
77	1587.9	1505.5	1550.3	1833.1	1651.5	1767.3	83.5	34.5	63.6
78	1590.1	1513.1	1564.6	1845.5	1696.5	1785.4	90.0	35.5	63.1
79	1598.7	1484.1	1562.6	1830.8	1732.2	1788.7	81.5	35.5	64.0
80	1585.7	1495.8	1551.3	1850.1	1735.5	1802.5	81.5	36.5	68.3
81	1574.9	1499.0	1543.2	1834.2	1714.3	1788.7	92.5	49.5	69.1
84	1564.1	1471.3	1516.7	1687.8	1598.7	1654.2	58.5	22.5	33.6
86	1593.3	1454.2	1530.0	1751.2	1641.6	1698.6	64.5	22.5	42.1
90	1547.8	1437.1	1498.7	1782.4	1643.8	1720.5	81.0	46.0	62.2
96	1420.0	1293.2	1364.3	1744.5	1617.4	1670.6	108.0	67.0	86.3
102	1220.1	1141.3	1187.5	1494.8	1379.6	1431.3	167.0	53.5	105.6
111	1113.3	1046.2	1078.6	1452.0	1272.3	1350.9	176.0	70.5	133.2
120	915.3	812.9	866.7	1274.4	1072.0	1205.0	174.0	75.0	127.3
132	702.6	676.5	688.4	911.1	822.2	859.7	165.5	47.5	91.5
138	665.9	558.2	623.5	862.5	719.3	803.2	148.0	29.0	82.8

RUN 62605 HEATER ROD STATISTICAL DATA

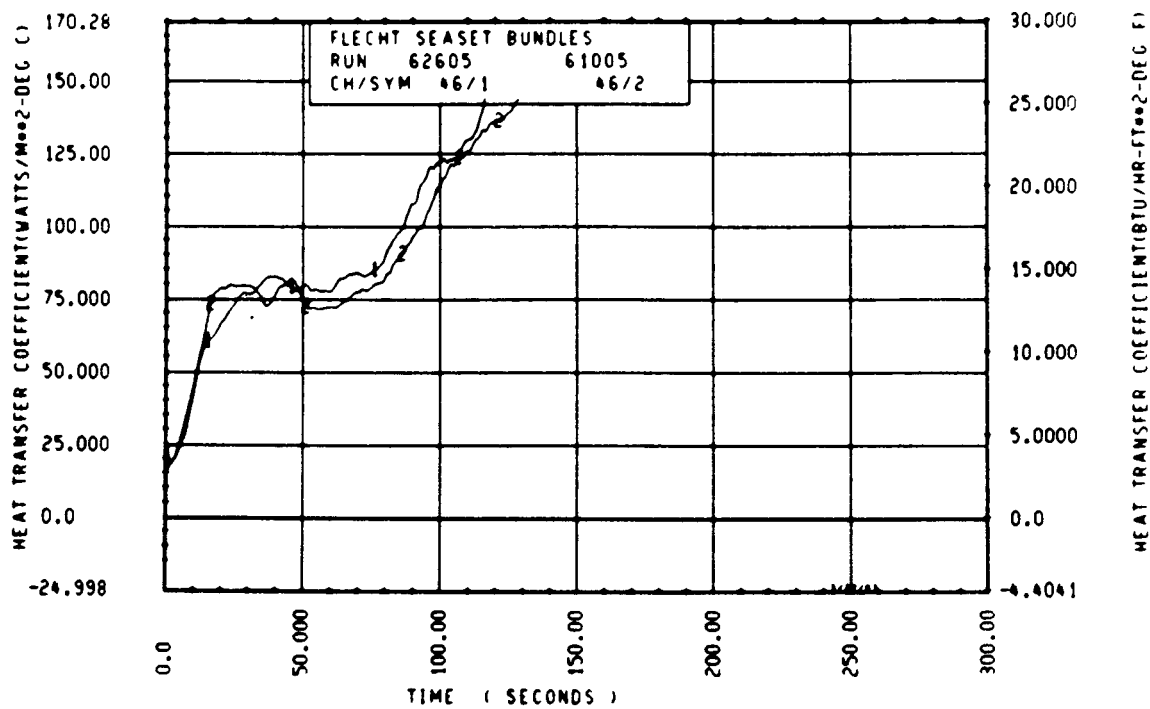
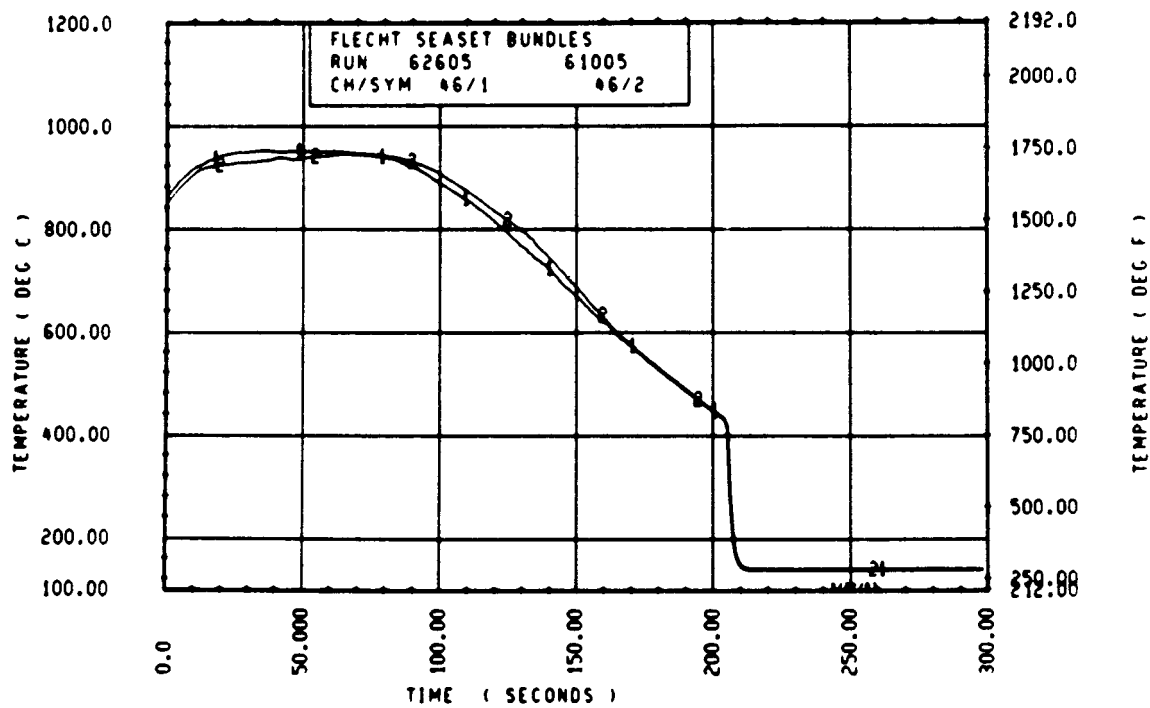
ELEV	TEMP RISE (DEG F)			QUENCH TEMP (DEG F)			QUENCH TIME (SEC)		
	MAX	MIN	MEAN	MAX	MIN	MEAN	MAX	MIN	MEAN
12	14.7	14.7	14.7	588.0	580.2	584.3	19.3	18.0	18.6
24	32.0	30.0	31.0	653.8	638.0	646.0	42.2	40.3	41.0
39	68.8	55.3	61.8	770.7	753.6	764.5	83.6	80.1	81.7
48	115.3	90.1	106.3	774.5	736.2	759.9	120.0	113.8	116.4
60	180.2	118.0	163.7	886.7	848.2	859.8	173.4	164.8	168.3
67	214.2	158.1	175.3	881.4	897.5	814.6	205.1	193.8	199.4
69	203.8	160.3	182.4	854.6	709.7	817.6	212.2	194.7	205.3
70	258.5	183.1	208.0	910.2	792.9	849.3	220.1	207.7	212.2
71	226.0	178.2	200.1	876.1	735.5	820.8	221.3	178.8	207.7
72	249.1	176.8	208.6	906.2	789.4	846.6	225.2	219.1	222.3
73	233.3	170.4	210.6	905.0	784.4	844.8	230.0	220.1	225.1
74	266.2	180.5	221.0	868.4	783.1	829.5	235.2	195.9	224.6
75	258.3	166.0	216.0	1212.6	699.9	873.6	240.2	198.1	224.0
76	275.2	193.3	228.4	943.5	760.8	852.4	245.2	204.0	234.1
77	288.5	145.9	217.0	1017.8	830.0	917.5	250.1	212.0	228.0
78	279.1	140.3	220.6	1148.4	729.3	907.6	254.2	181.3	234.4
79	288.3	153.0	226.0	1178.6	726.3	941.0	252.4	206.0	235.5
80	314.1	162.8	251.2	1187.9	830.9	939.5	264.4	202.0	245.8
81	304.8	185.1	245.5	1095.2	852.2	958.2	265.1	230.0	248.0
84	159.3	115.3	137.4	1010.5	737.1	798.3	284.2	226.0	272.2
86	220.5	112.1	160.6	1028.1	767.7	842.9	289.8	255.1	277.4
90	263.9	178.3	221.7	1025.0	764.9	870.7	319.0	291.1	301.7
96	348.6	269.8	306.3	902.6	726.1	828.2	344.1	318.7	331.3
102	284.0	206.8	243.7	754.8	633.4	697.4	363.6	346.0	357.1
111	353.5	204.4	272.3	1002.2	626.3	710.4	384.3	214.9	359.3
120	381.8	230.1	338.3	923.3	504.4	638.7	402.9	127.8	361.2
132	214.8	139.5	171.4	699.3	385.5	525.1	409.2	87.7	301.5
138	304.4	114.3	179.7	683.8	501.8	554.0	397.2	35.0	313.9



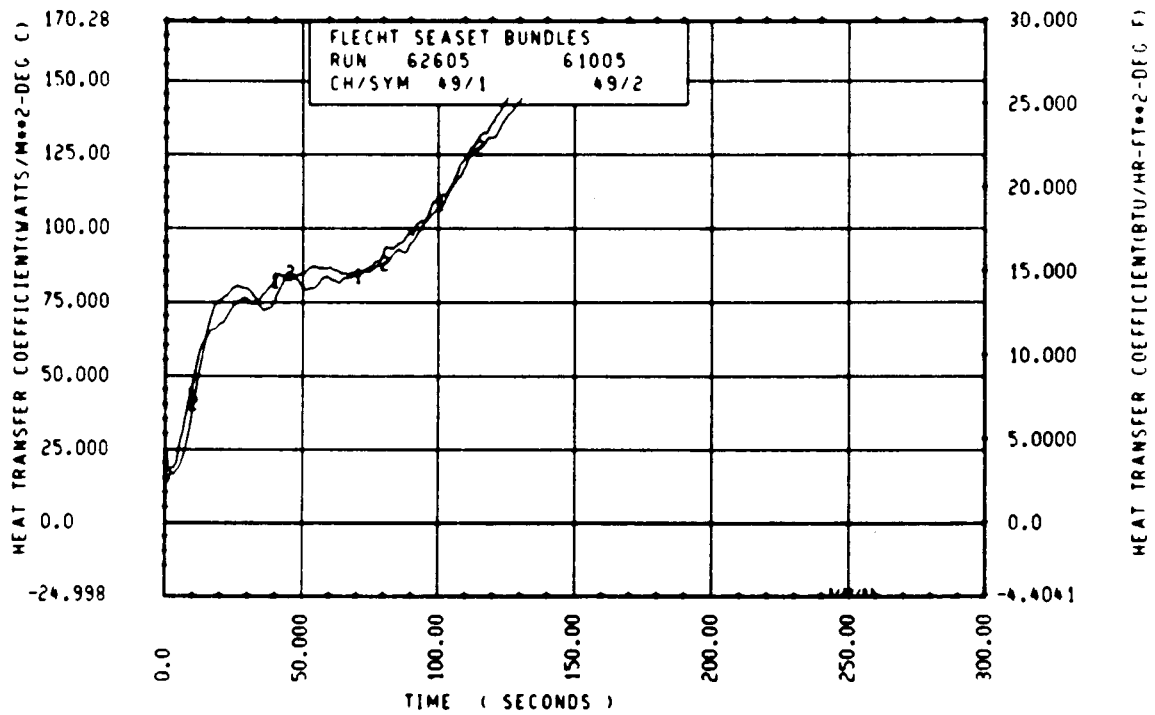
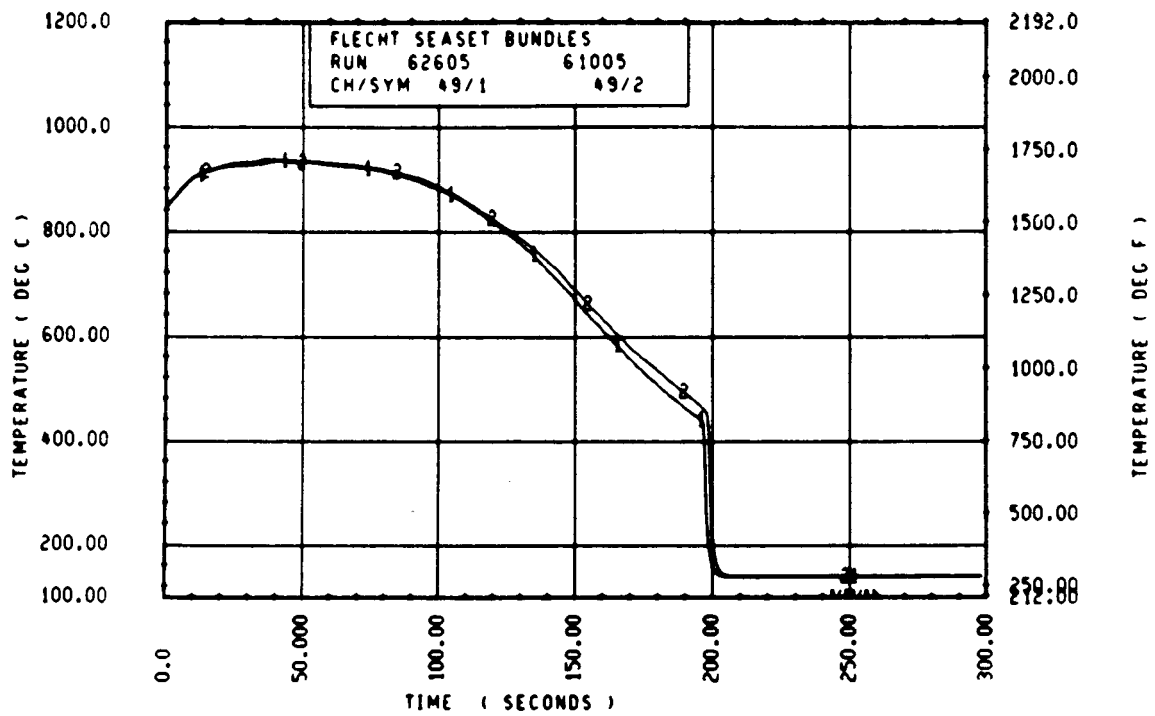
Rod 3H, 1.52 m (60 in.)



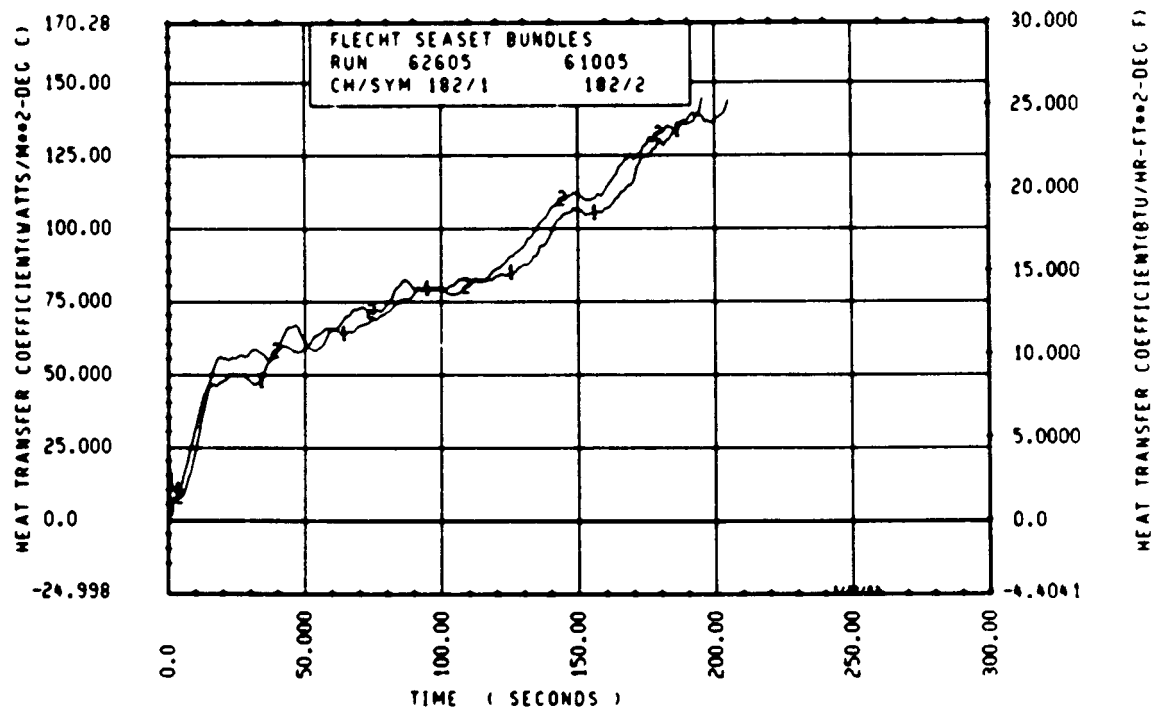
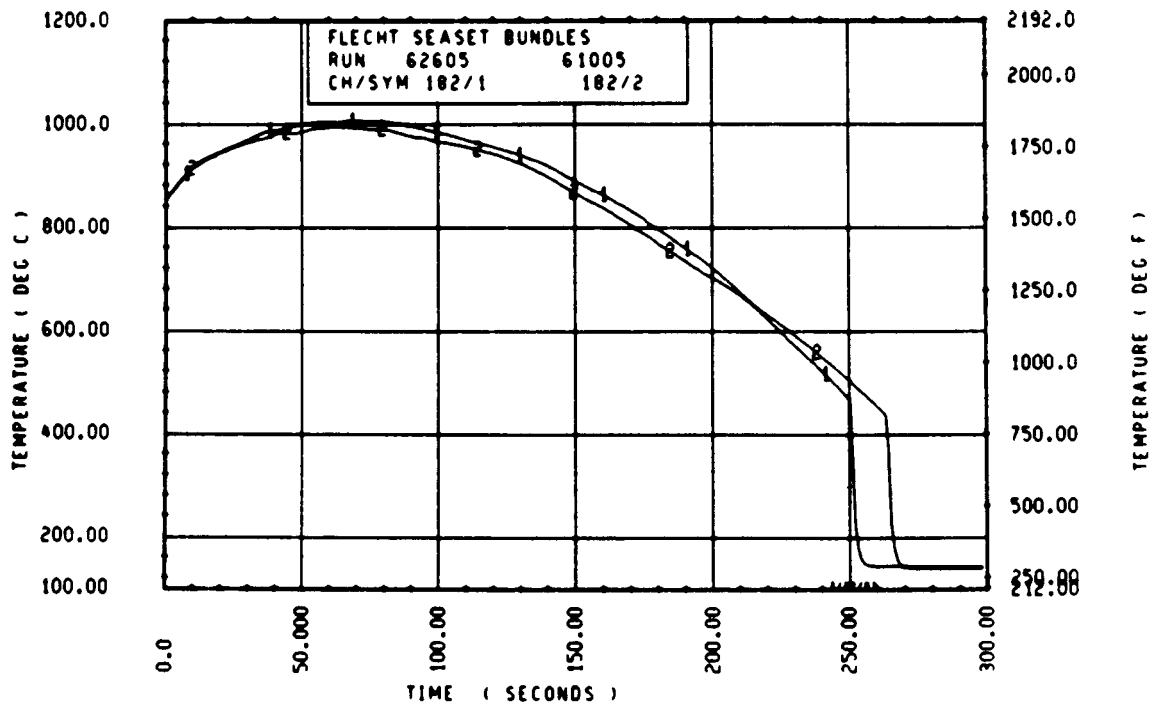
Rod 3H, 1.70 m (67 in.)



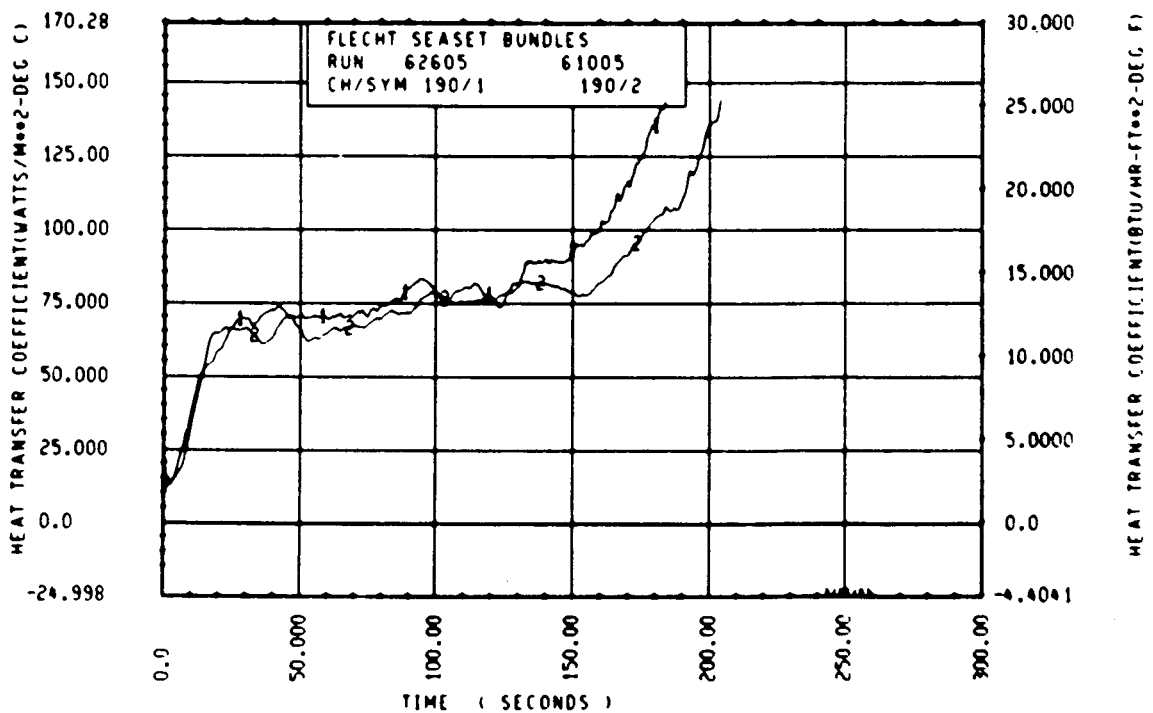
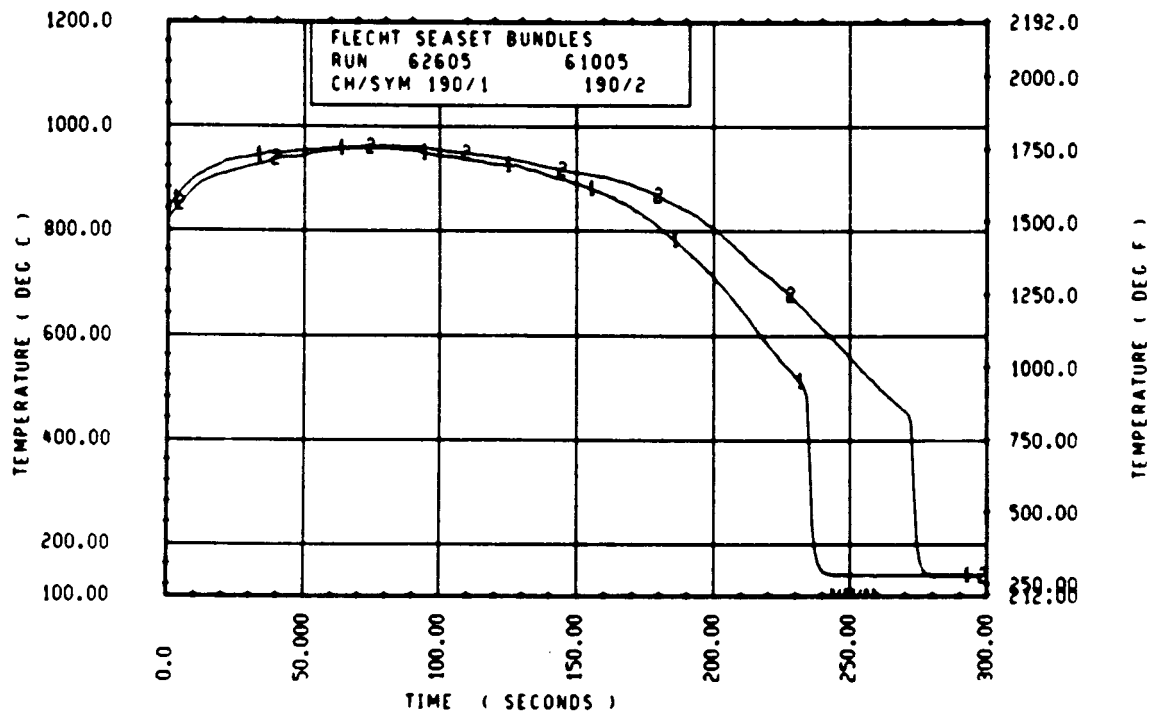
Rod 9G, 1.70 m (67 in.)



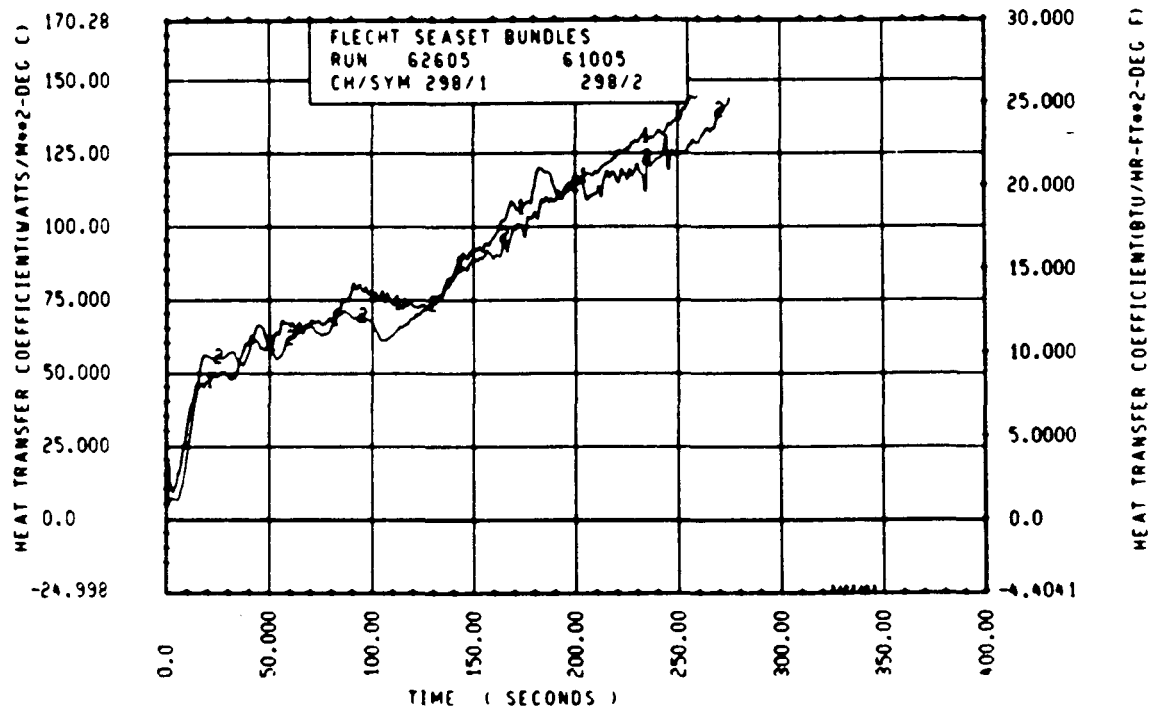
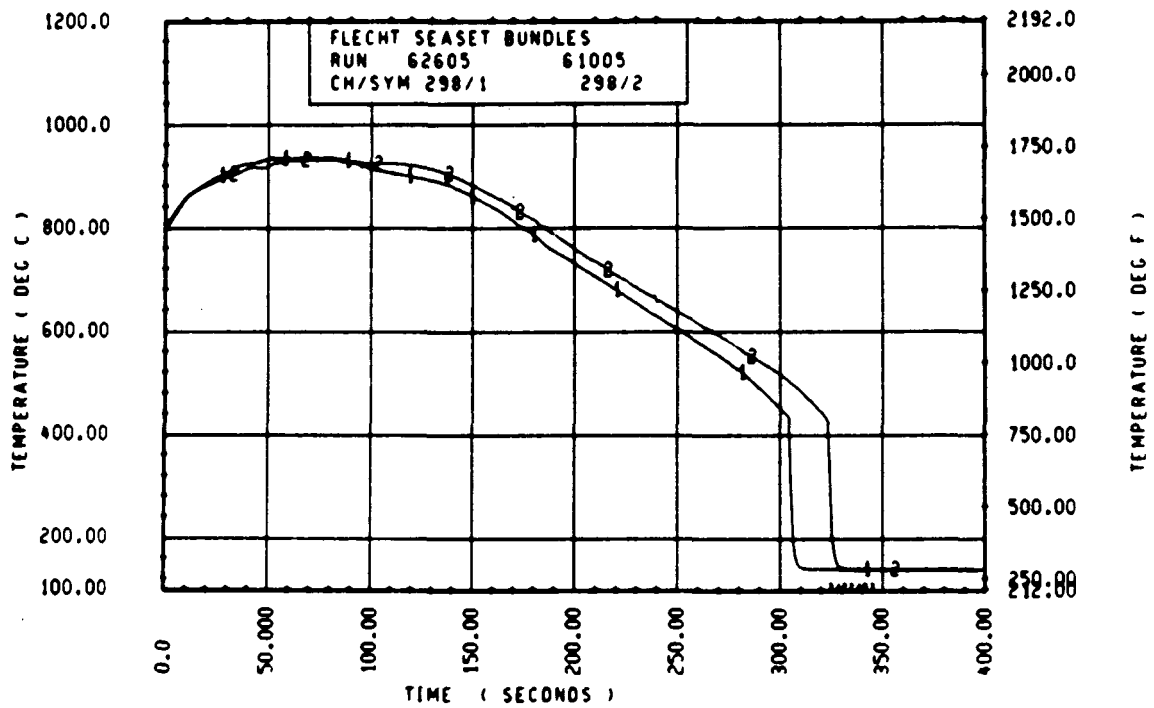
Rod 11K, 1.70 m (67 in.)



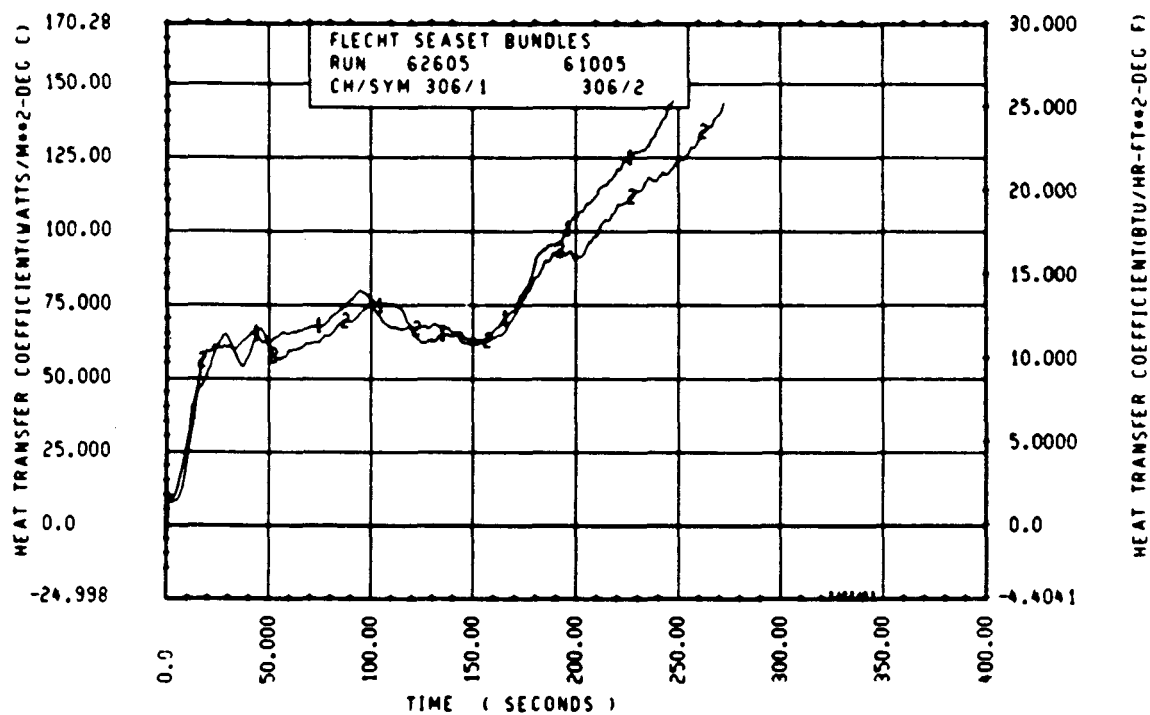
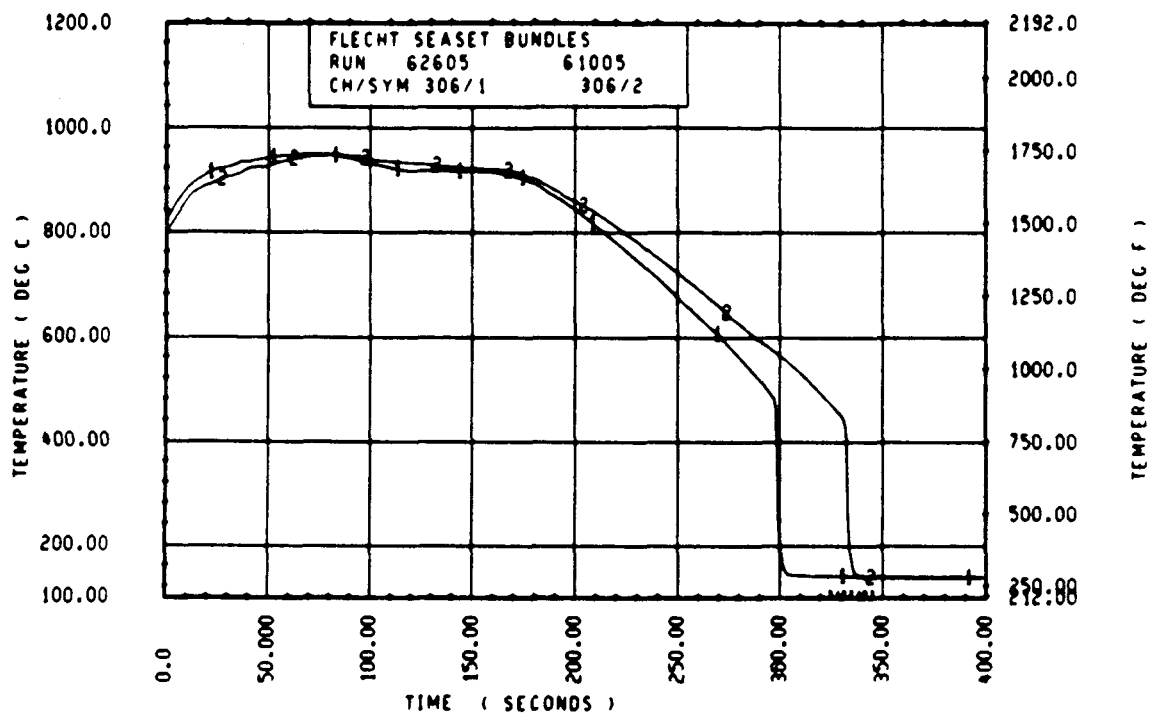
Rod 3H, 1.98 m (78 in.)



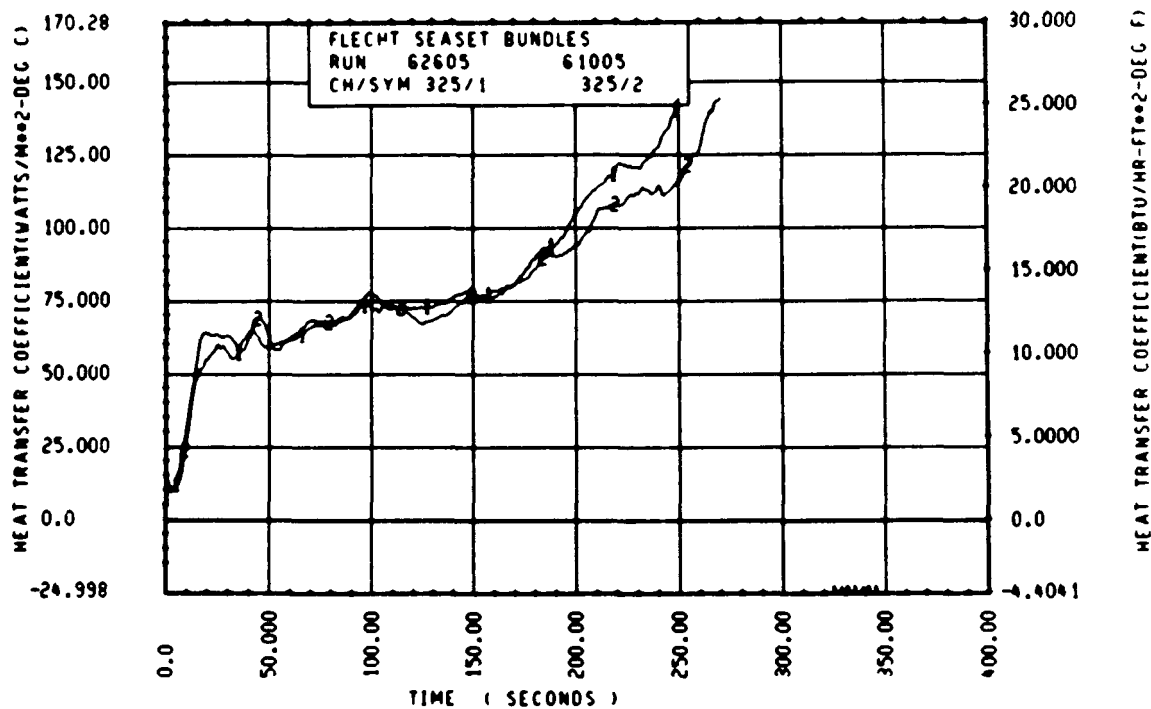
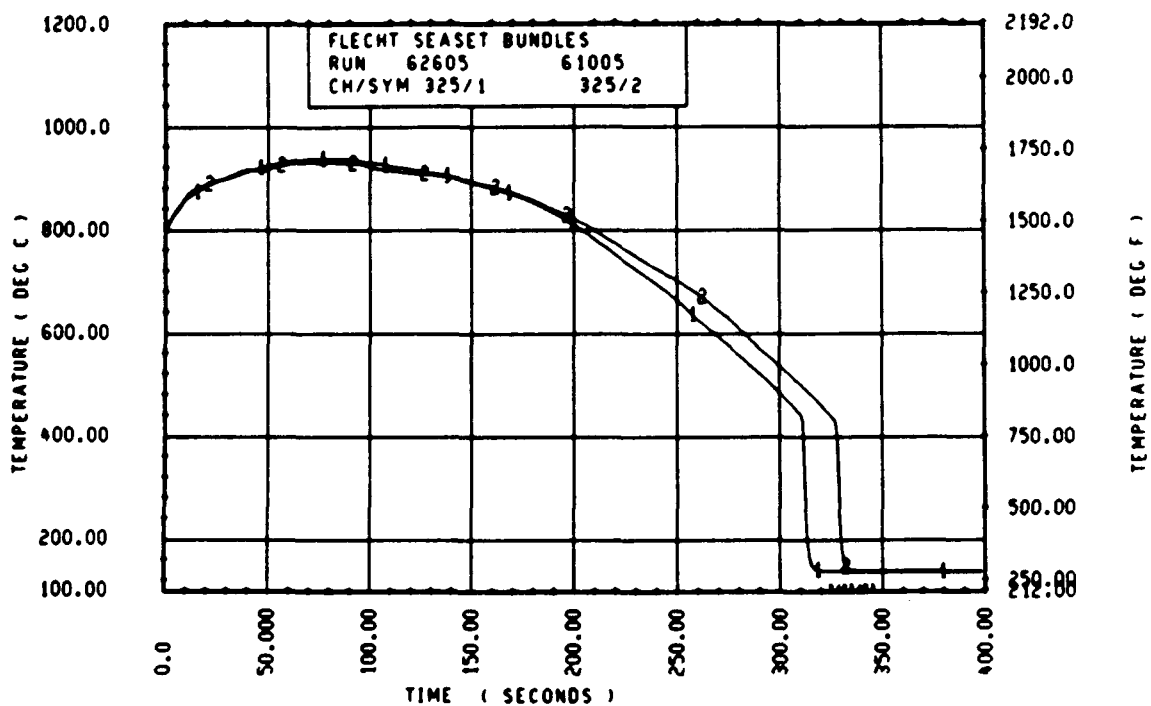
Rod 7H, 1.98 m (78 in.)



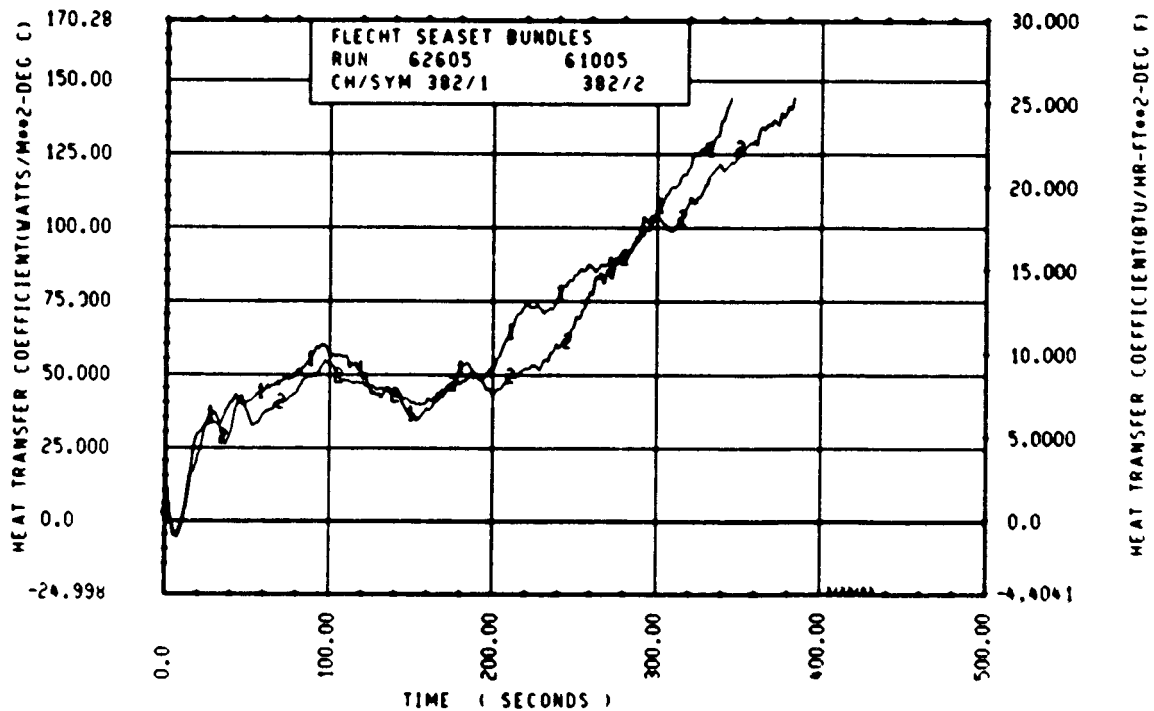
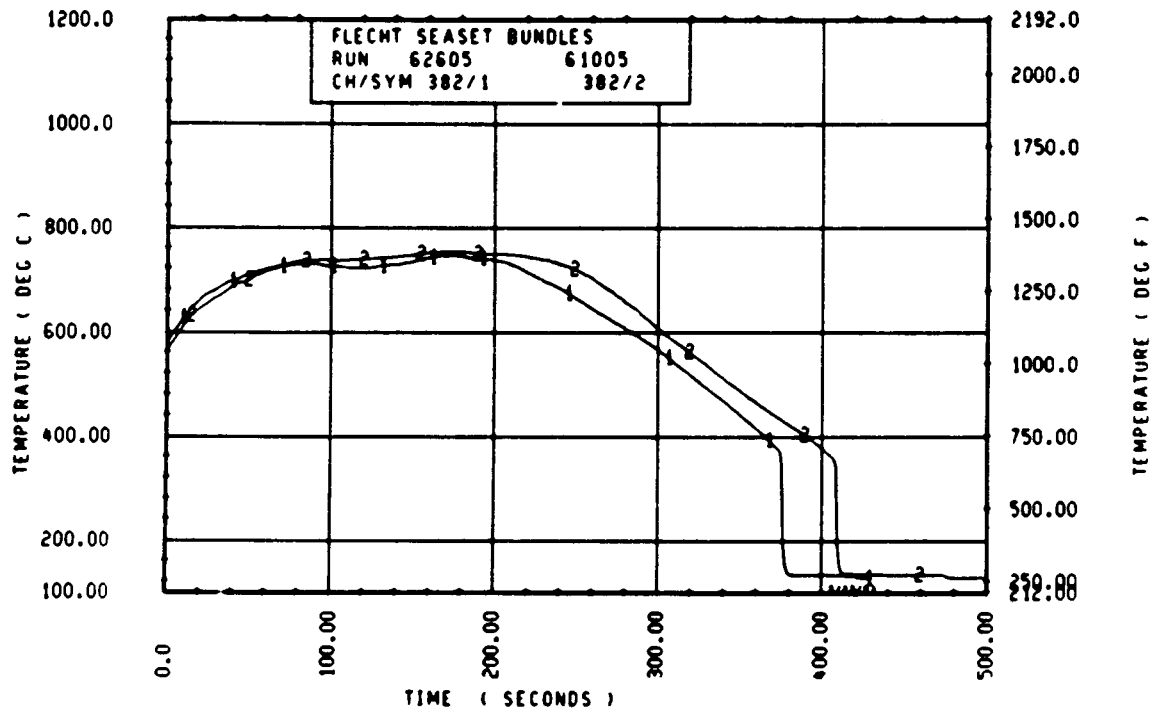
Rod 3H, 2.29 m (90 in.)



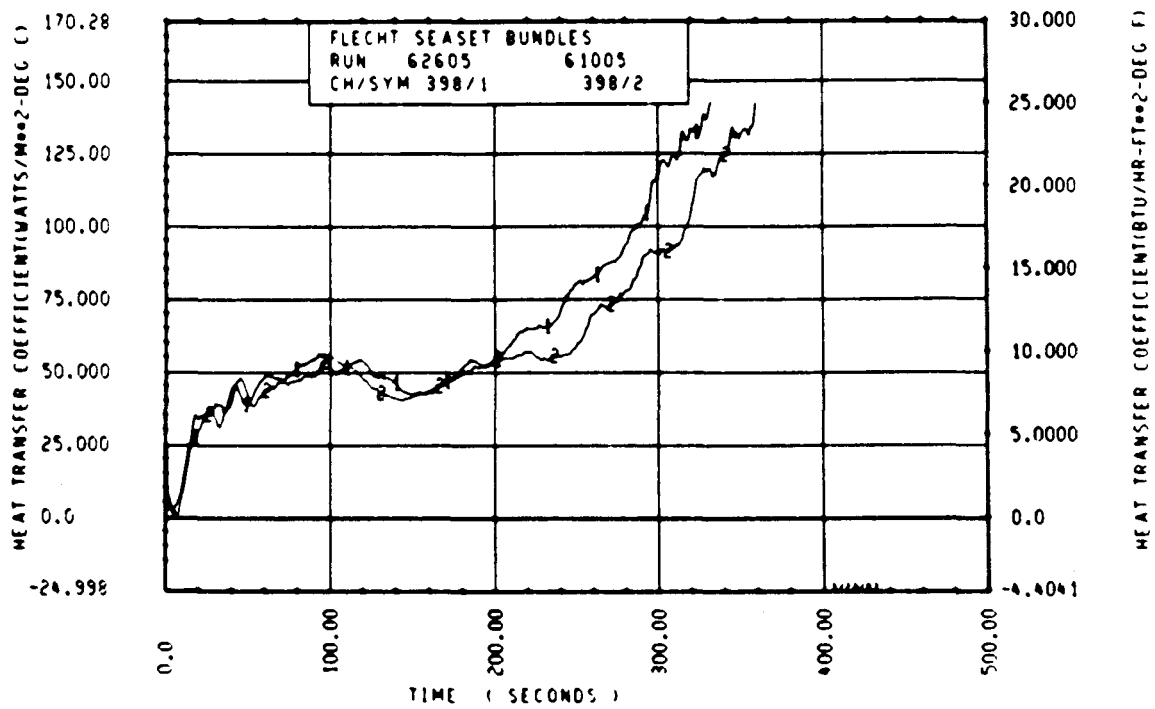
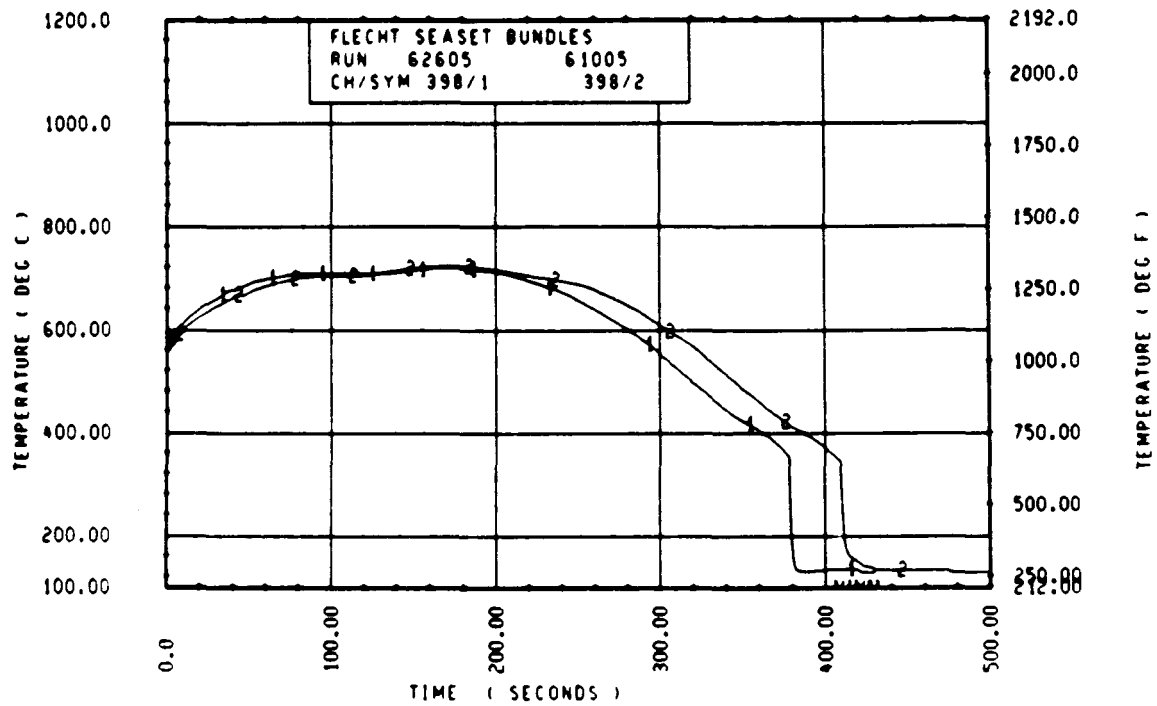
Rod 6G, 2.29 m (90 in.)



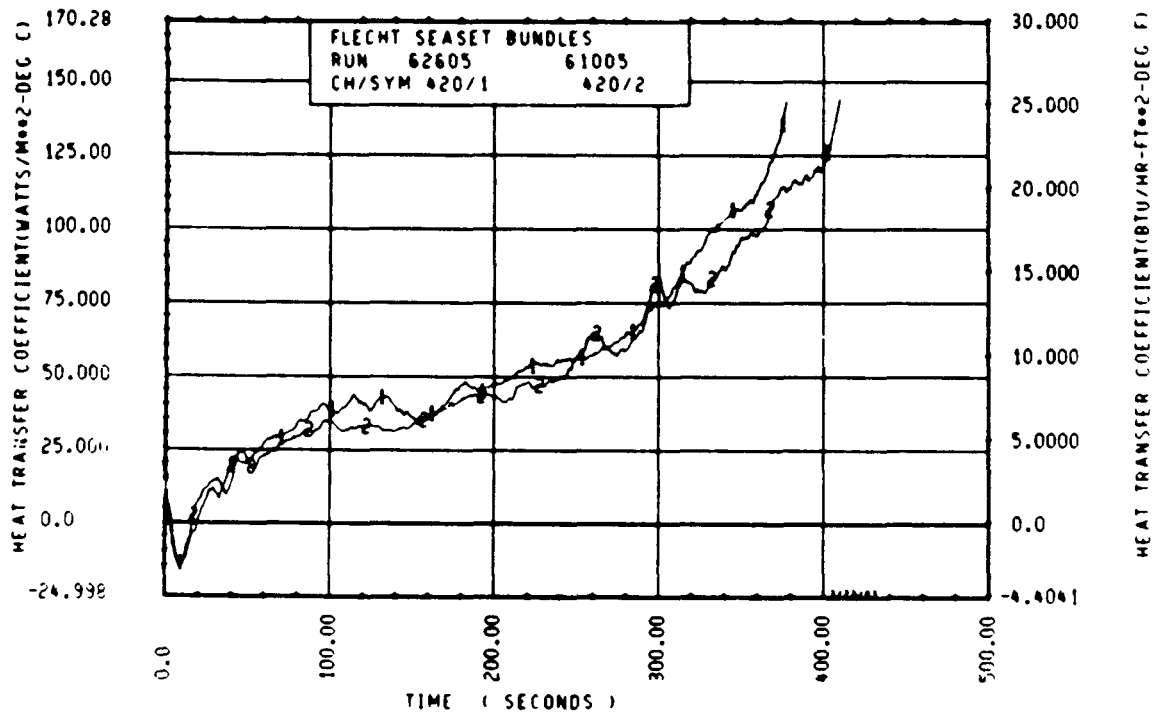
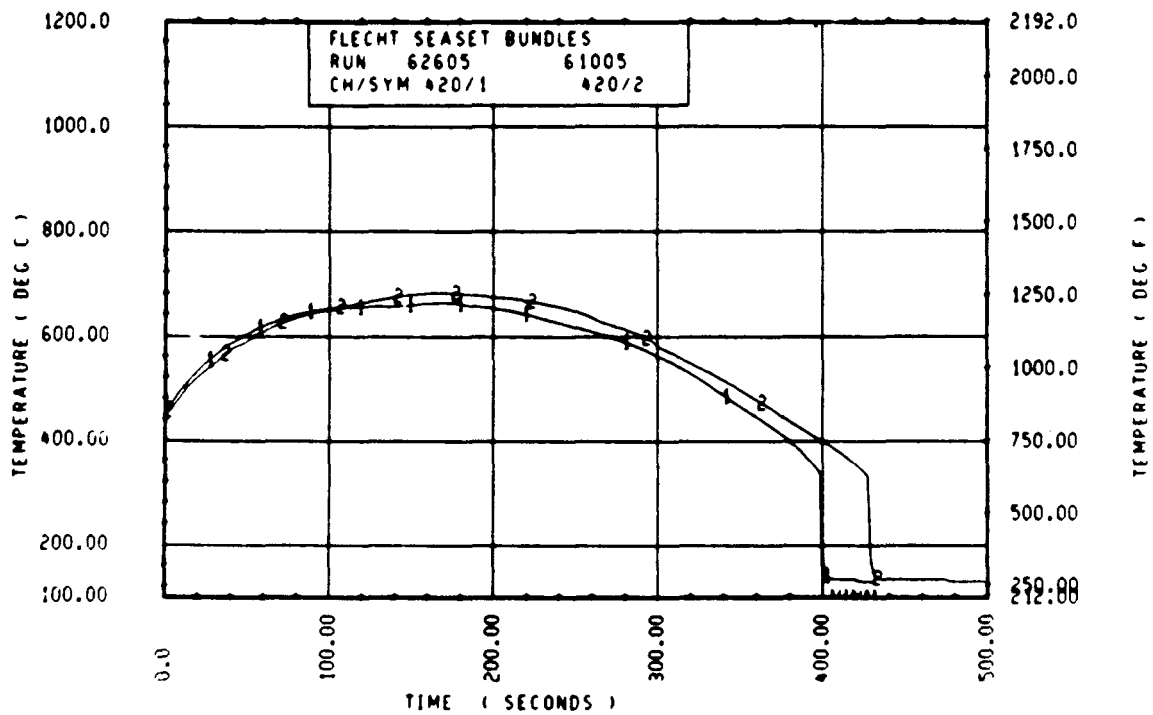
Rod 11E, 2.29 m (90 in.)



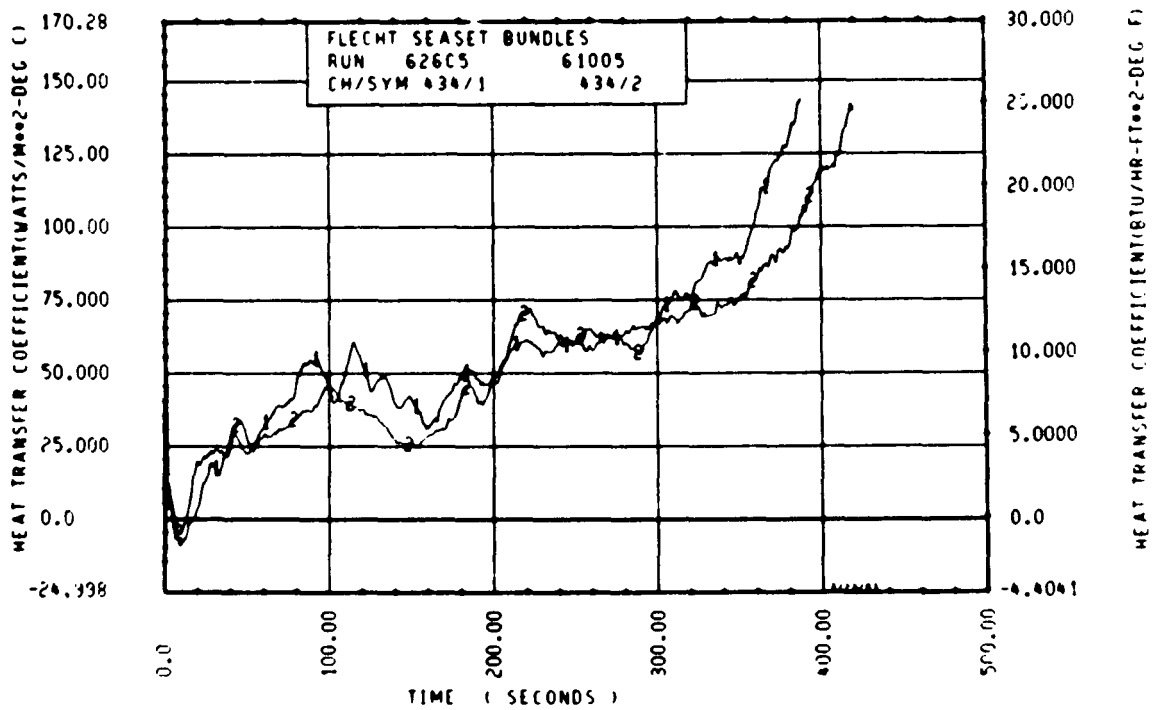
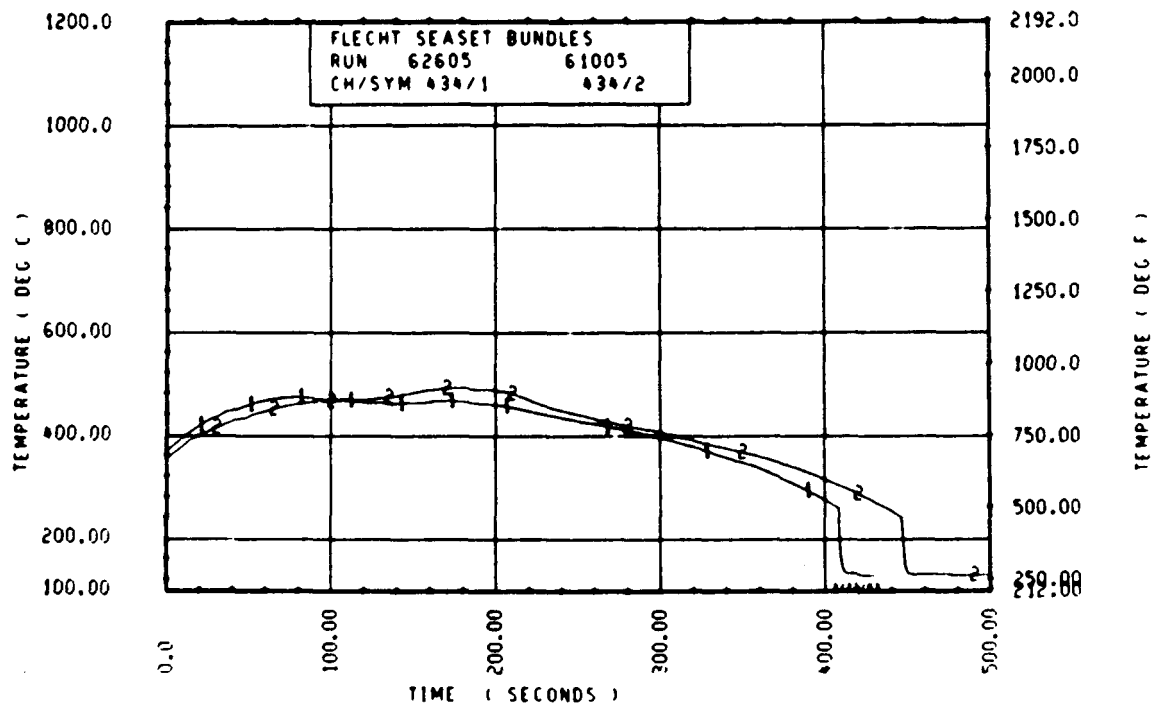
Rod 6G, 2.82 m (111 in.)



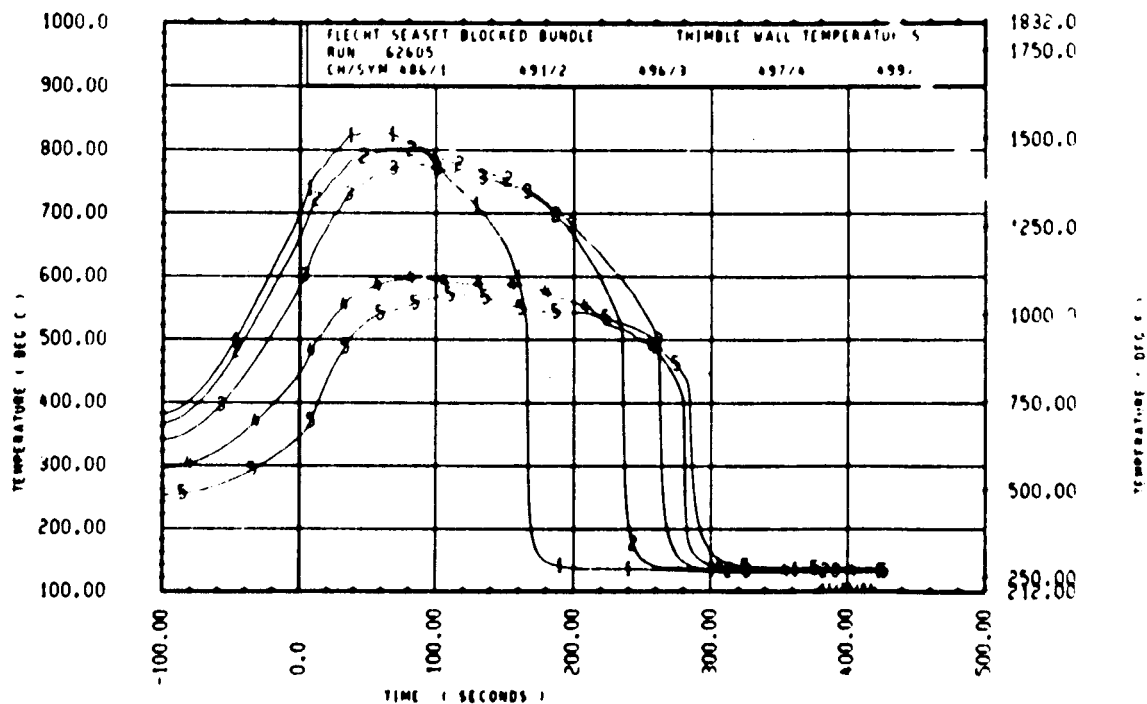
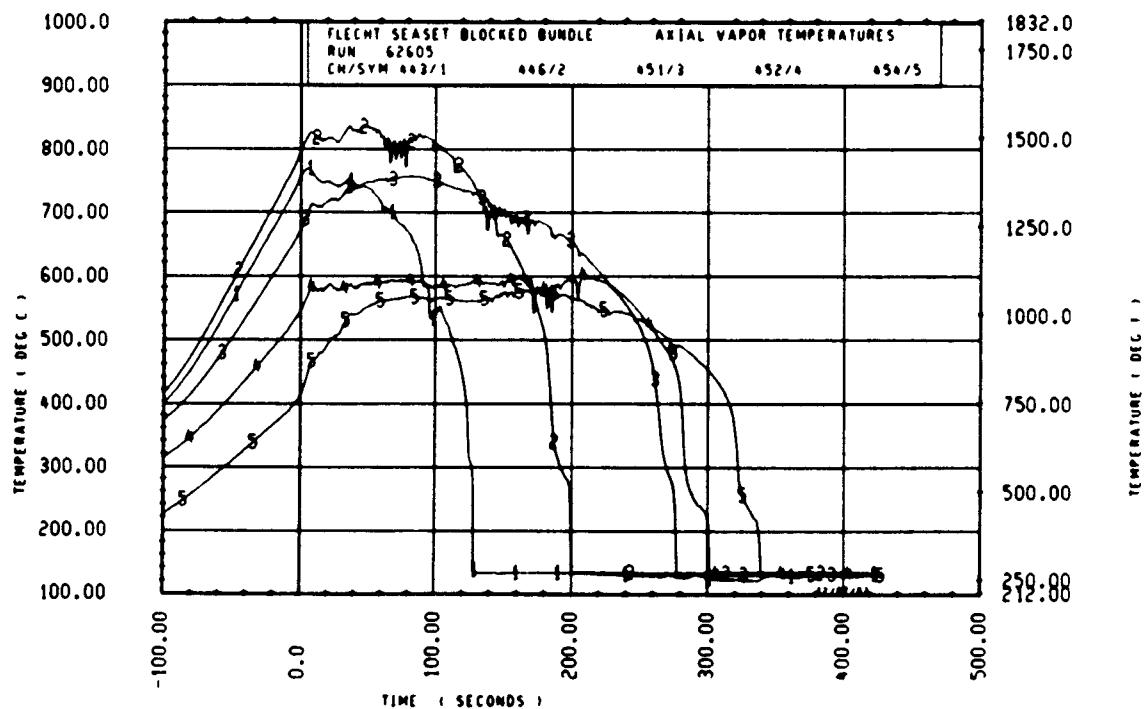
Rod 121, 2.82 m (111 in.)

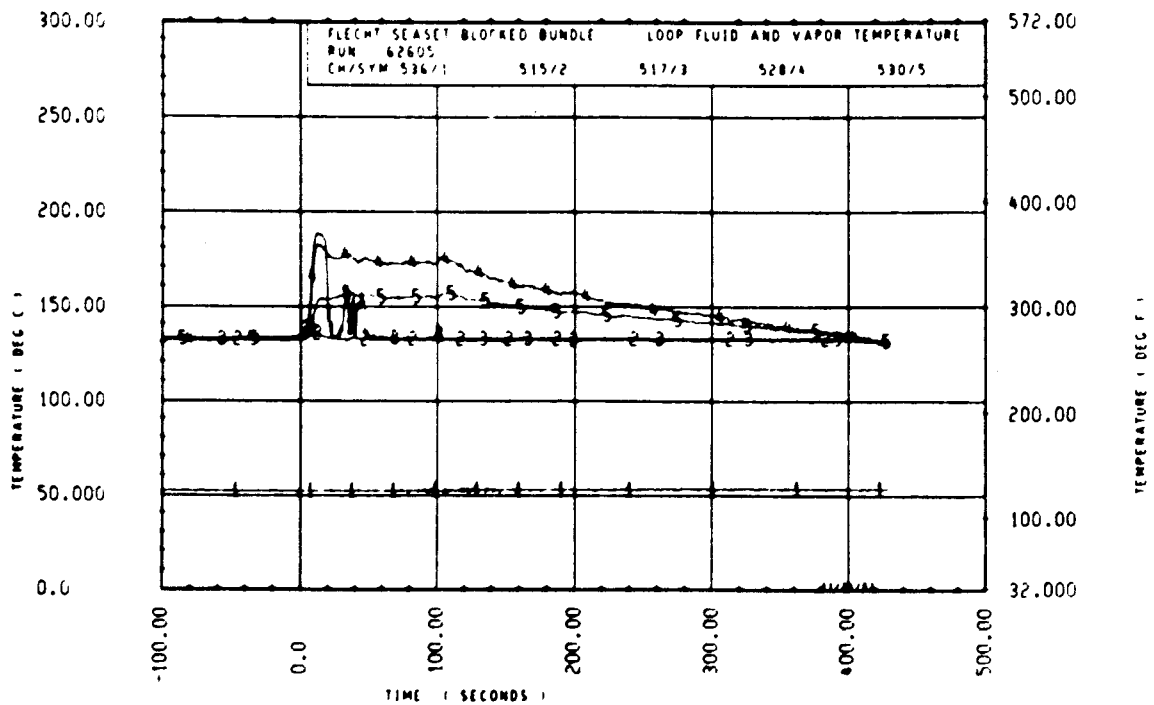
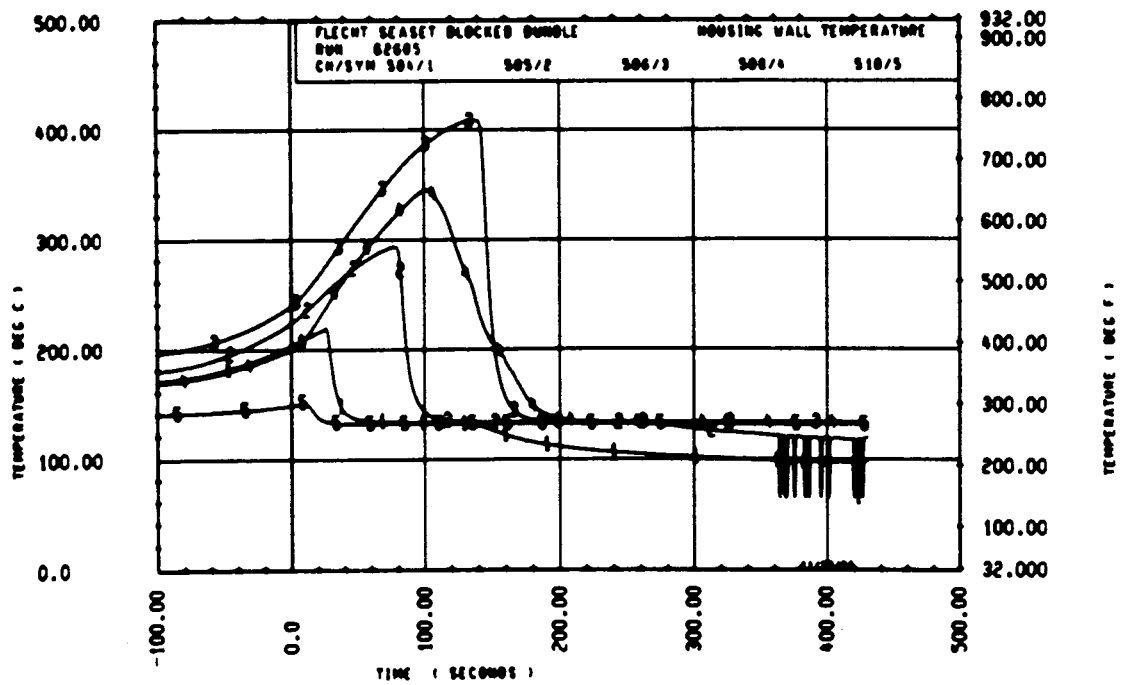


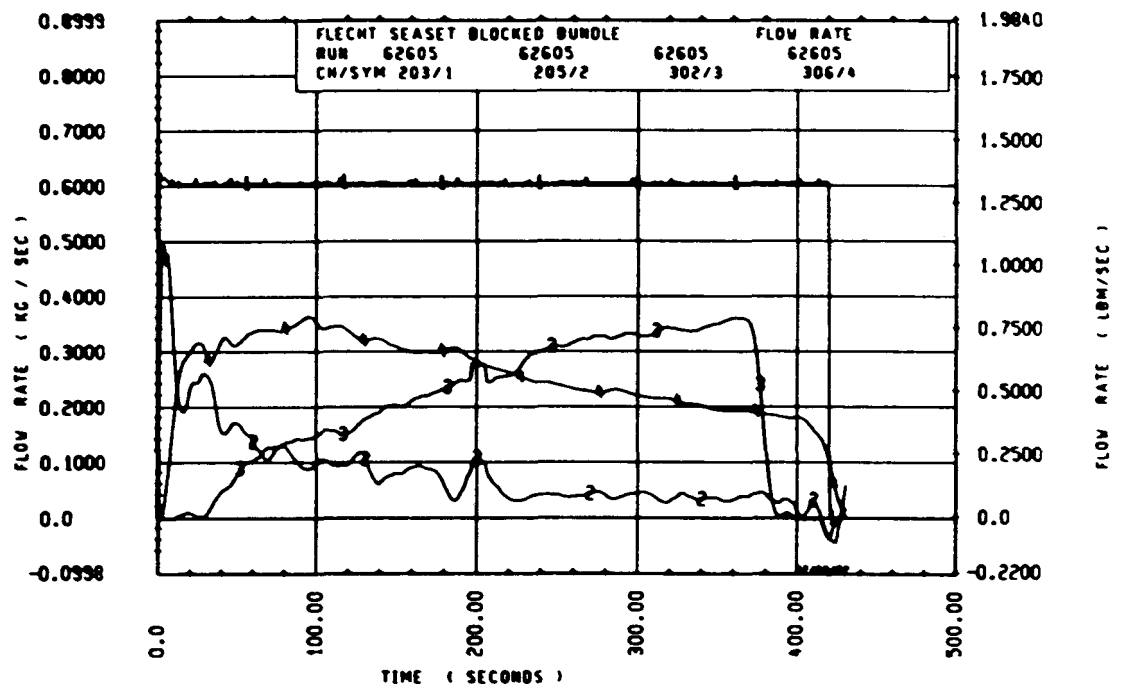
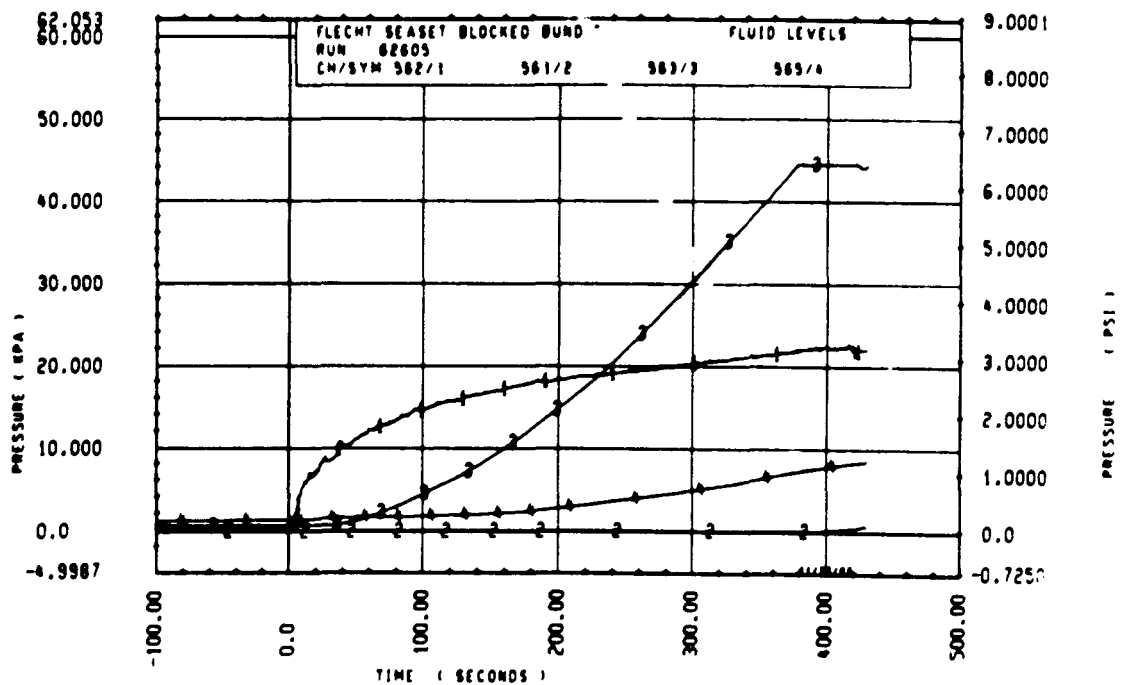
Rod 9K, 3.05 m (120 in.)

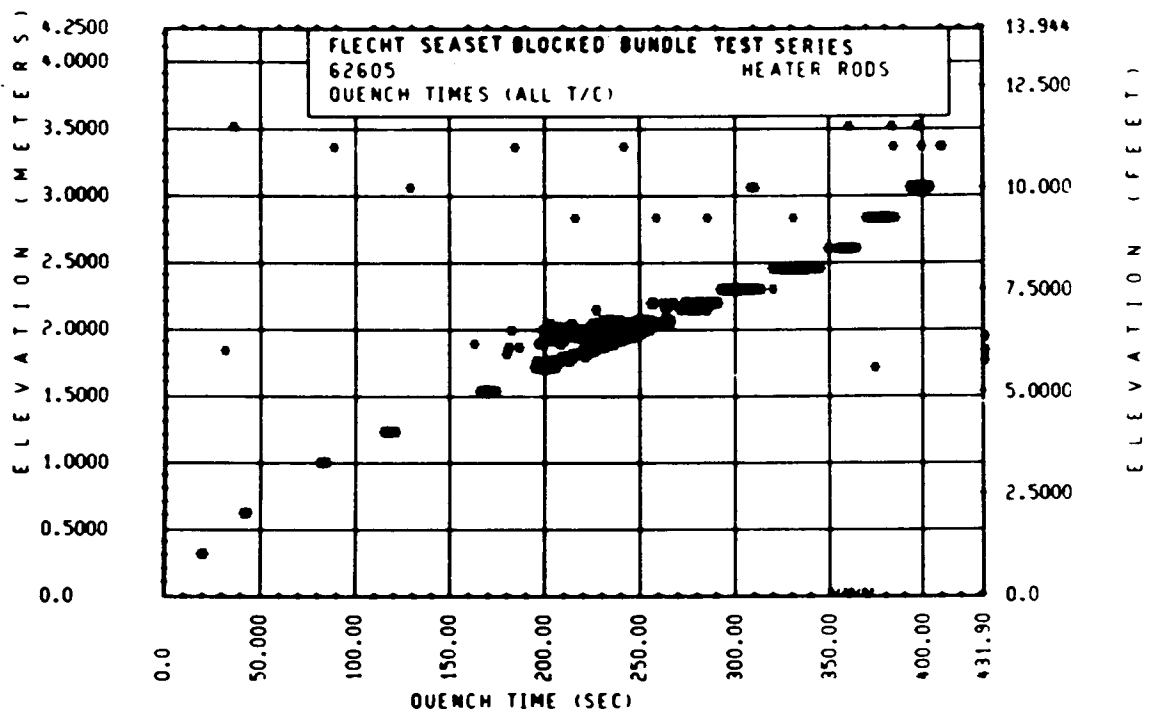
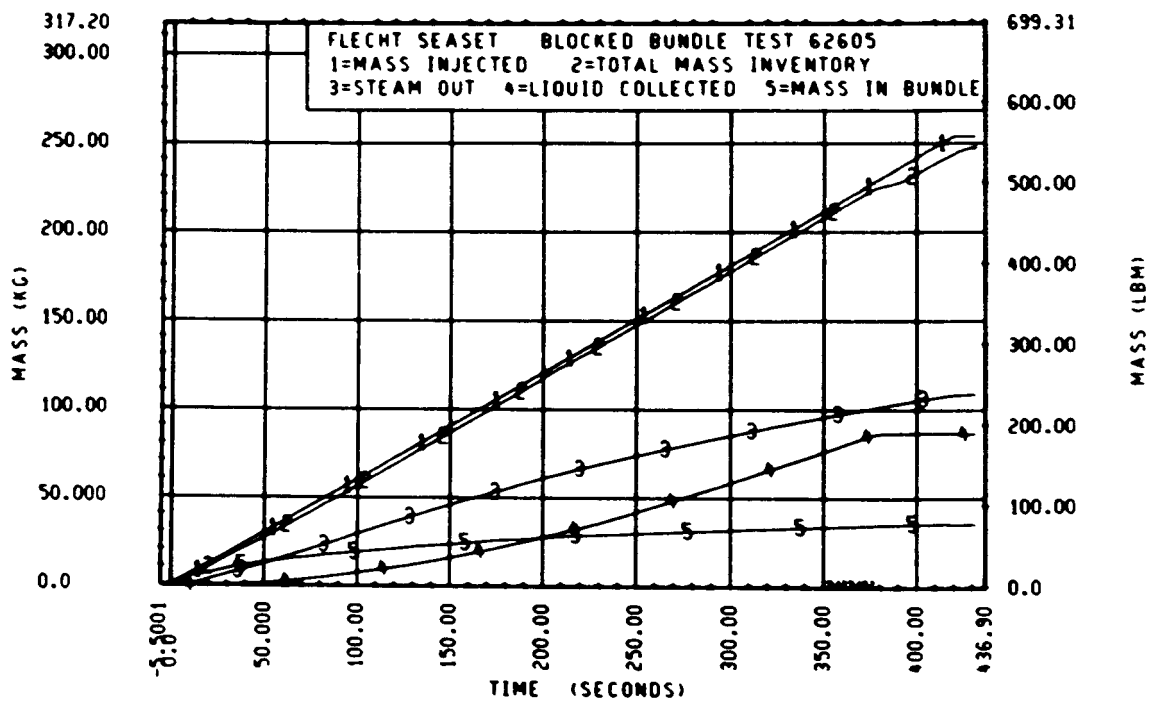


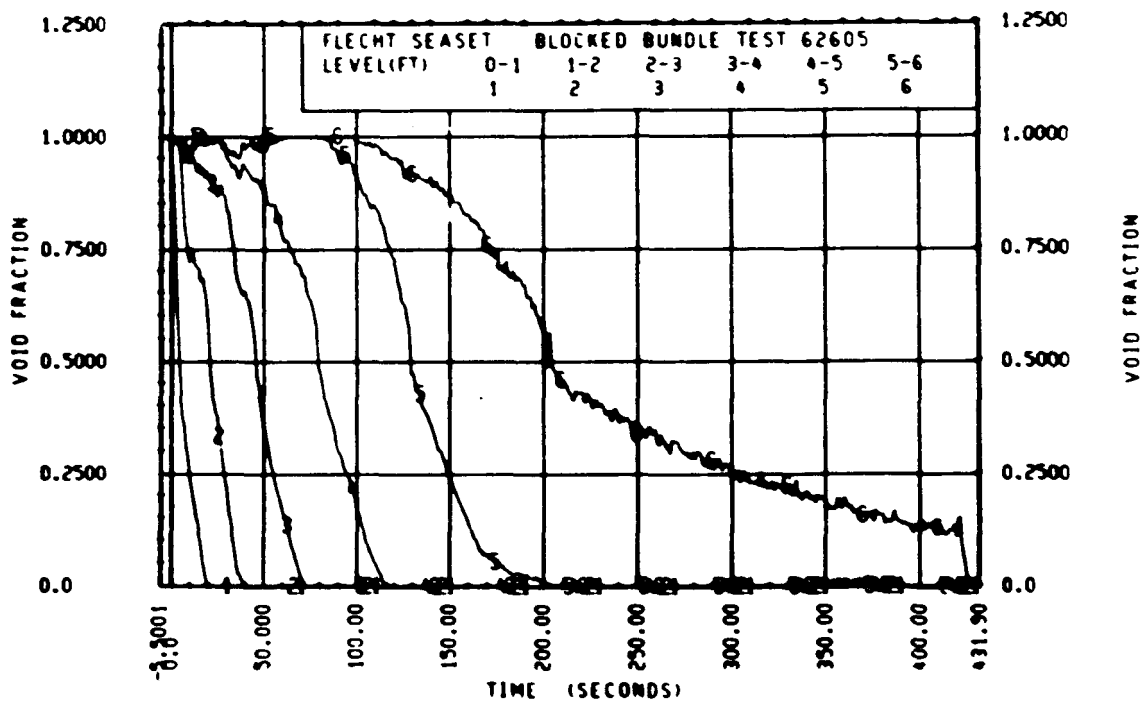
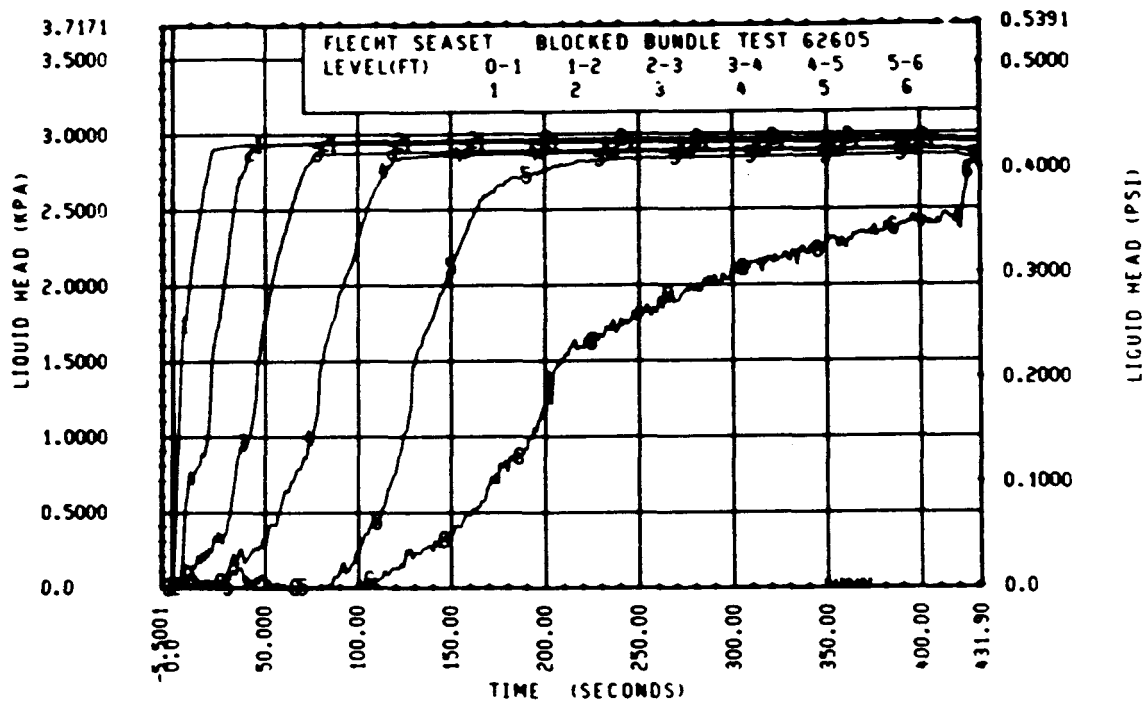
Rod 111, 3.35 m (132 in.)

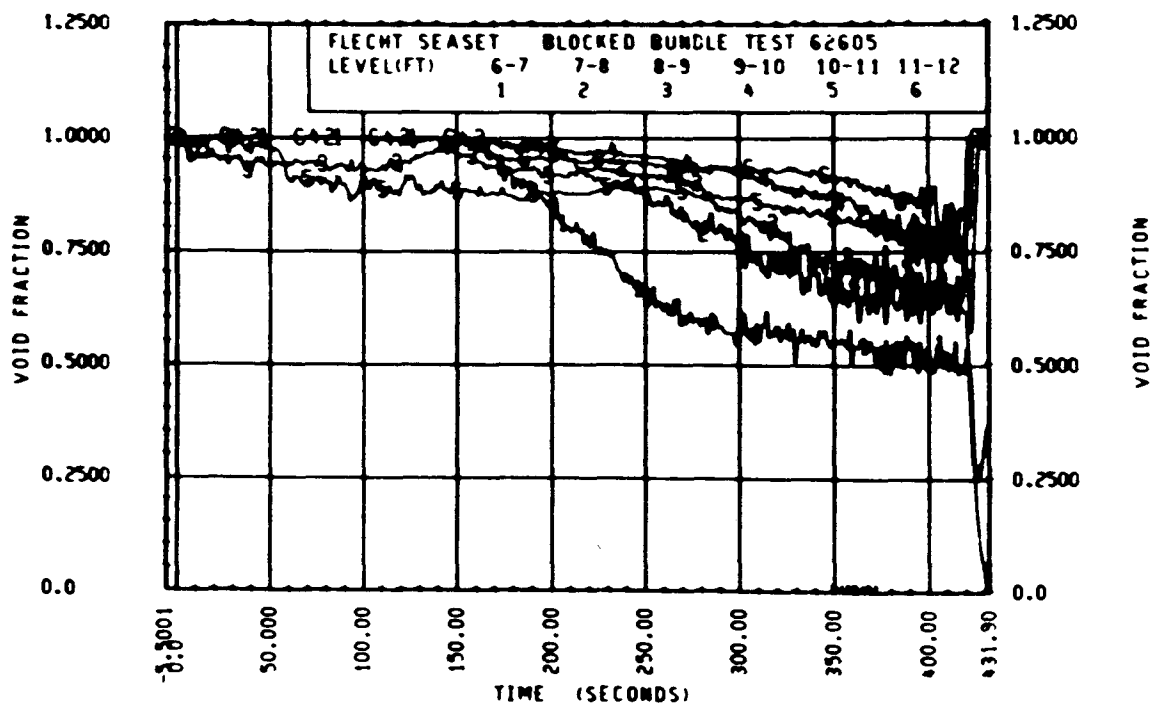
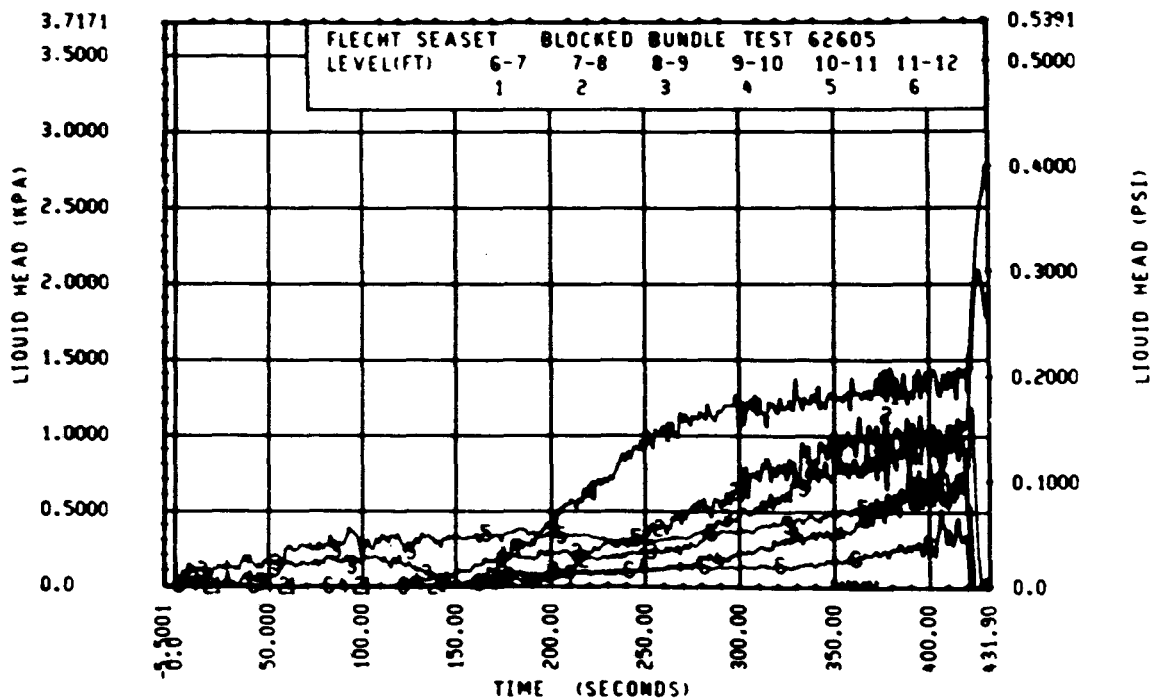












FLECHT SEASET 163-ROD BUNDLE FLOW BLOCKAGE TASK
SUMMARY AND COMMENT SHEET

Run: 62819
Test date: 10/7/82
Test type: Gravity reflood
Parameter: Pressure effect

AS-RUN TEST CONDITIONS:

Upper plenum pressure	0.141 MPa (20.3 psia)
Initial peak clad temperature and location	871.6°C (1600.9°F), 8N-1.93 m (76 in.)
Initial peak rod power:	
Peripheral rods	2.30 kW/m (0.701 kW/ft)
Bypass rods	2.29 kW/m (0.699 kW/ft)
Blockage island rods	2.30 kW/m (0.701 kW/ft)
Injection rate	5.76 kg/sec (12.7 lb/sec) for 14 sec 0.780 kg/sec (1.72 lb/sec) onward
Coolant temperature	73.2°C (91°F)
Initial bundle water level	+0.51 mm (+0.02 in.)

COMMENTS:

Downcomer filled up by approximately 20 seconds and remained filled up to 220 seconds. Carryover tank filled up by 250 seconds and upper plenum filled up at 290 seconds.

There was no corresponding test conducted in the 161-rod unblocked bundle; however, rod temperatures were compared to those of run 63018, which was conducted at the same conditions but at 0.274 MPa (40 psia) pressure.

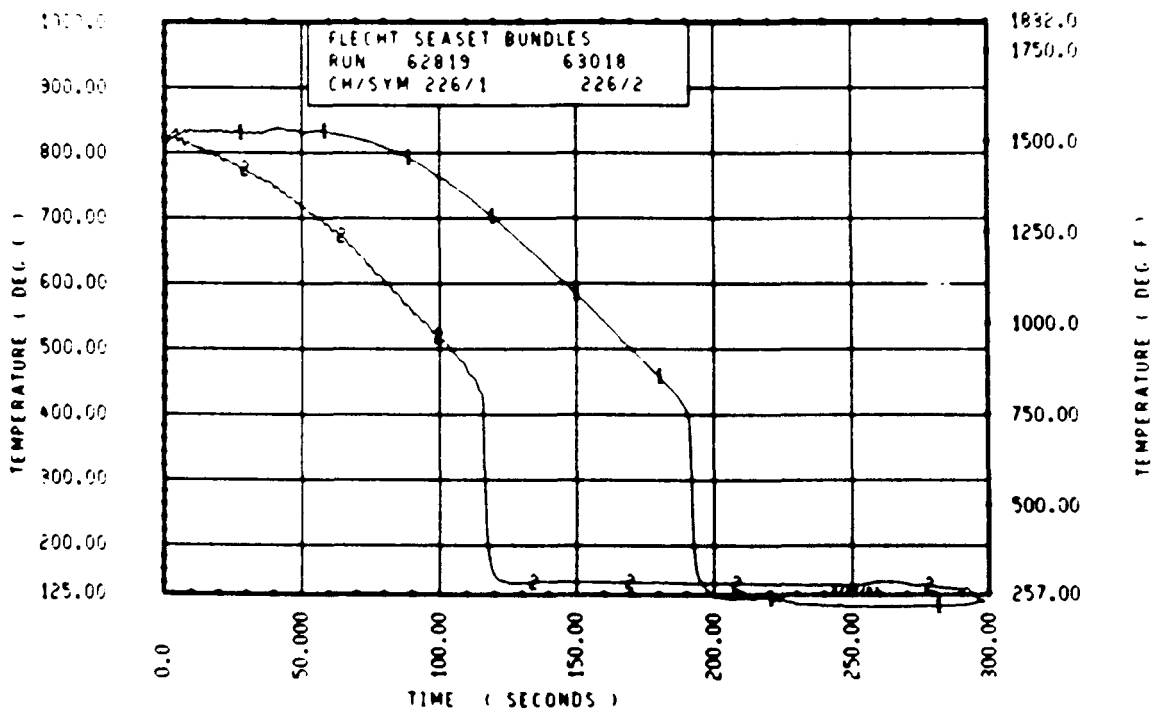
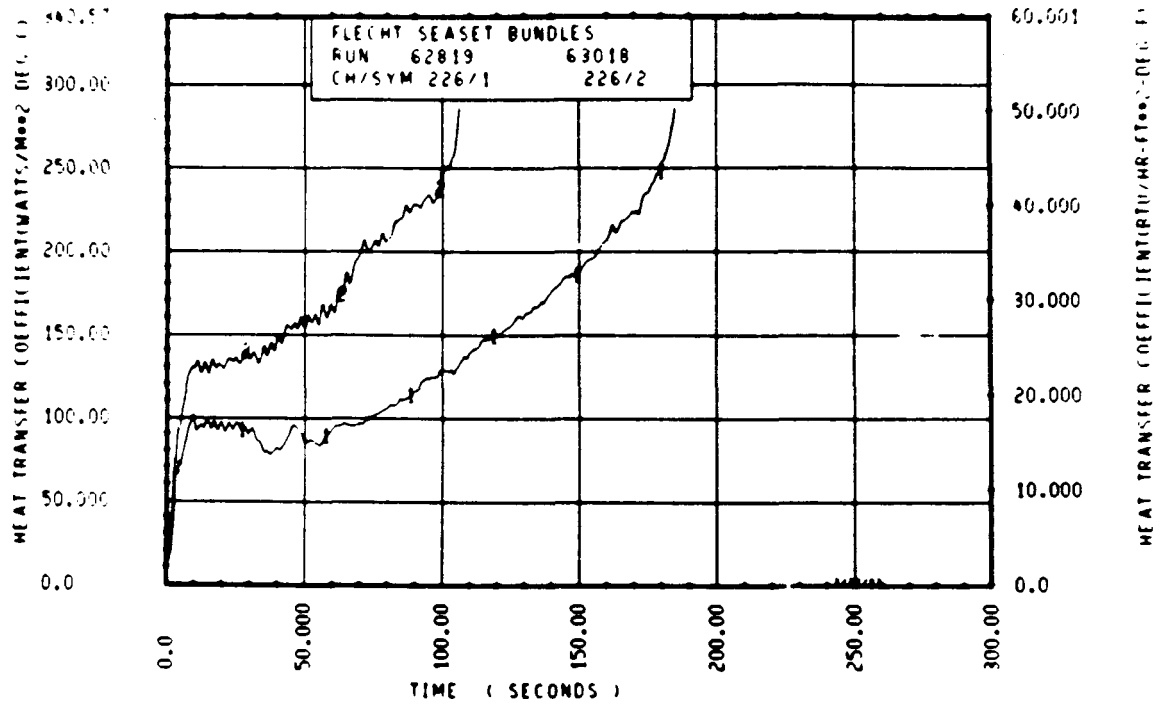
FLECHT SEASET 163 ROD BUNDLE TEST SERIES								
RUN NUMBER 62819								
ROD/ELEV	CHAN.	NO	TINITIAL AT FLOOD (DEG F)	MAXIMUM TEMPERATURE (DEG F)	TEMPERATURE RISE (DEG F)	TURNAROUND TIME (SECONDS)	QUENCH TEMPERATURE (DEG F)	QUENCH TIME (SECONDS)
96 1- 0		3	652.	657.	5.	1.5	644.	3.5
10M 2- 0		6	870.	881.	11.	4.0	772.	14.4
96 3- 3		9	1198.	1222.	24.	4.0	709.	75.4
3J 4- 0		11	1342.	1372.	31.	4.5	663.	124.4
7M 4- 0		12	1334.	1368.	34.	4.5	664.	127.9
8K 4- 0		13	1352.	1367.	35.	4.5	672.	127.4
8M 4- 0		14	1341.	1370.	30.	4.5	661.	124.3
120 4- 0		17	1329.	1359.	30.	4.5	690.	122.4
5E 5- 0		20	1479.	1553.	74.	42.0	763.	188.8
76 5- 0		21	1543.	1613.	70.	43.5	749.	186.4
96 5- 0		24	1517.	1590.	73.	41.5	736.	187.9
5E 5- 7		33	1517.	1571.	53.	42.0	739.	209.8
86 5- 7		43	1535.	1597.	62.	42.0	723.	225.1
9M 5- 9		52	1473.	1523.	49.	9.5	618.	225.1
76 5-10		59	1500.	1551.	51.	9.5	752.	222.9
7F 5-11		62	1443.	1491.	47.	9.5	1034.	118.3
46 5-11		64	1524.	1586.	62.	42.0	737.	232.1
21 6- 0		67	1574.	1630.	77.	42.0	782.	235.1
50 6- 0		70	1484.	1533.	49.	9.5	699.	234.0
6J 6- 0		74	1517.	1576.	59.	42.0	724.	236.2
7M 6- 0		66	1535.	1597.	62.	42.0	739.	233.8
11E 6- 0		80	1510.	1588.	78.	42.0	739.	234.9
8M 6- 2		97	1363.	1409.	47.	9.5	785.	160.4
5M 6- 2		99	1520.	1592.	73.	42.0	717.	240.7
9E 6- 2		105	1330.	1516.	186.	57.0	238.	444.2
8M 6- 3		111	1483.	1448.	45.	9.5	837.	166.4
46 6- 3		124	1539.	1610.	71.	42.0	752.	247.1
11M 6- 4		134	1465.	1525.	60.	41.0	741.	125.8
90 6- 4		143	1532.	1644.	112.	42.5	702.	245.2
9J 6- 5		165	1508.	1558.	50.	9.5	1117.	140.8
9M 6- 5		166	1573.	1659.	86.	57.0	765.	250.1
8J 6- 6		192	1556.	1626.	70.	40.5	944.	207.9
90 6- 6		193	1543.	1679.	136.	57.5	758.	251.6
11F 6- 6		173	1537.	1625.	88.	57.0	717.	252.2
46 7- 0		261	1481.	1517.	37.	4.5	735.	284.0
70 7- 6		309	1469.	1536.	67.	42.0	814.	276.1
76 7- 6		312	1514.	1563.	49.	9.5	872.	265.2
11E 7- 6		325	1462.	1577.	115.	77.5	746.	304.2
5L 8- 0		337	1290.	1470.	180.	192.5	725.	328.2
7M 8- 0		345	1330.	1492.	162.	88.5	813.	301.2
7K 8- 0		346	1343.	1506.	163.	198.0	726.	319.4
5J 8- 6		366	1126.	1162.	36.	4.5	674.	353.1
78 8- 6		368	1137.	1167.	30.	4.5	645.	366.1
7E 9- 3		383	1088.	1204.	116.	151.0	656.	374.6
8M 9- 3		387	1030.	1139.	109.	139.5	643.	372.2
9C 9- 3		389	1037.	1083.	46.	73.5	612.	379.9
11F 9- 3		394	1033.	1099.	66.	101.5	690.	337.1
7810- 0		408	837.	951.	115.	58.0	550.	413.2
8M10- 0		415	842.	1044.	202.	142.0	596.	400.2
8K10- 0		417	851.	983.	132.	112.5	540.	409.6
8M10- 0		418	864.	1053.	190.	193.5	612.	406.5
6M11- 0		429	670.	723.	53.	131.0	469.	340.2
9611- 0		431	662.	777.	115.	157.5	454.	329.3
11E11- 0		432	666.	709.	43.	85.5	522.	290.2
5J11- 6		436	646.	663.	17.	4.5	428.	228.0
7811- 6		437	611.	678.	67.	83.0	247.	265.2
8J11- 6		438	657.	714.	57.	112.5	247.	333.2

RUN 62819 HEATER ROD STATISTICAL DATA

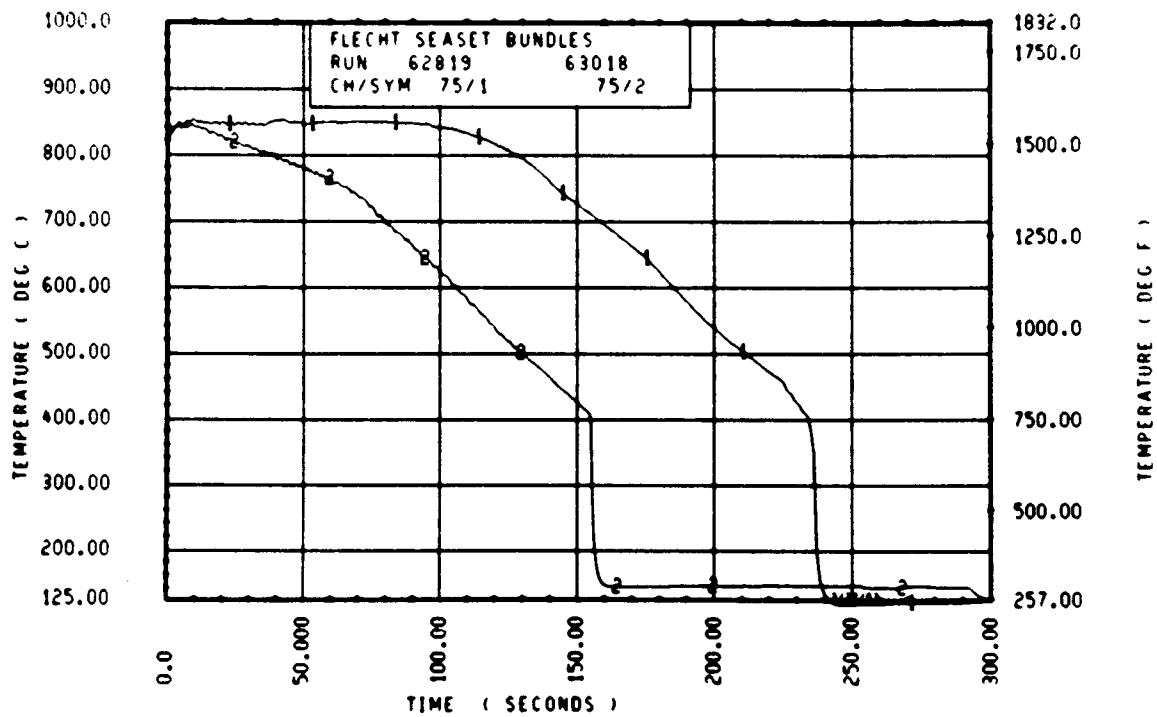
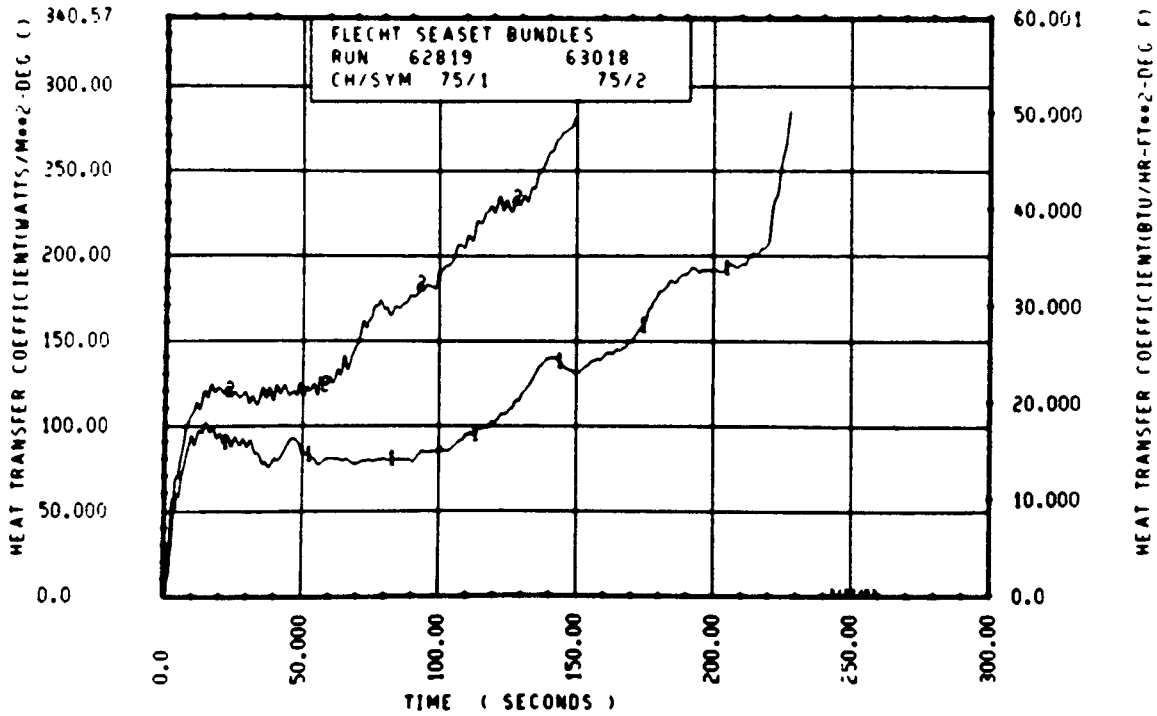
ELEV	INITIAL TEMP (DEG F)			MAX TEMP (DEG F)			TURNAROUND TIME (SEC)		
	MAX	MIN	MEAN	MAX	MIN	MEAN	MAX	MIN	MEAN
12	655.4	651.2	652.9	660.6	655.4	657.6	1.5	1.5	1.5
24	869.8	843.9	853.6	881.2	855.3	864.6	4.0	4.0	4.0
39	1198.2	1142.3	1165.9	1222.2	1166.1	1189.0	4.0	4.0	4.0
48	1361.7	1329.0	1343.7	1391.2	1358.5	1374.7	4.5	4.0	4.4
60	1543.5	1389.1	1492.2	1614.1	1422.1	1547.1	43.5	4.5	32.2
67	1599.8	1489.4	1539.0	1628.4	1535.9	1588.8	42.5	7.0	23.8
69	1512.0	1473.4	1495.0	1568.4	1516.4	1547.3	41.5	7.0	24.8
70	1586.8	1405.9	1505.2	1630.6	1490.5	1562.9	56.5	9.5	25.3
71	1524.0	1431.7	1477.3	1585.7	1490.5	1548.9	57.5	9.5	41.4
72	1578.1	1453.1	1528.1	1655.9	1514.2	1592.7	59.0	9.5	35.5
73	1572.7	1460.6	1515.3	1653.7	1515.3	1585.2	73.0	9.5	46.1
74	1576.0	1362.7	1491.0	1632.8	1409.3	1557.8	80.5	7.0	36.2
75	1576.0	1402.9	1503.7	1631.7	1447.8	1574.9	72.0	9.5	37.0
76	1600.9	1440.3	1524.7	1688.9	1495.8	1609.4	71.0	9.5	48.6
77	1572.7	1467.0	1523.9	1676.8	1506.6	1601.5	90.0	9.5	41.7
78	1596.6	1496.9	1538.2	1713.2	1561.9	1623.1	91.0	7.0	49.0
79	1577.1	1485.2	1538.7	1670.2	1558.6	1619.0	87.5	7.0	42.3
80	1558.6	1483.0	1526.4	1705.4	1584.6	1634.0	89.5	9.5	49.3
81	1551.1	1457.4	1512.3	1707.7	1537.6	1615.1	91.0	9.5	43.3
84	1537.0	1422.1	1484.9	1574.9	1458.4	1520.2	4.5	4.0	4.5
86	1572.7	1463.8	1518.6	1609.7	1506.1	1559.9	89.0	4.5	9.5
90	1516.4	1399.7	1471.2	1594.4	1490.5	1550.5	103.0	9.5	65.8
96	1383.8	1250.4	1331.4	1581.4	1466.1	1518.0	116.0	84.5	101.3
102	1178.5	1042.1	1146.1	1258.7	1124.7	1200.1	128.5	4.5	52.1
111	1088.5	1015.3	1048.4	1205.5	1050.3	1128.5	151.0	9.5	104.8
120	902.9	805.6	855.3	1109.2	845.0	995.4	157.5	41.5	117.6
132	670.1	656.4	663.5	776.5	683.7	722.1	157.5	85.5	125.1
138	657.5	611.2	633.7	714.1	641.7	670.7	112.5	4.5	58.6

RUN 62819 HEATER ROD STATISTICAL DATA

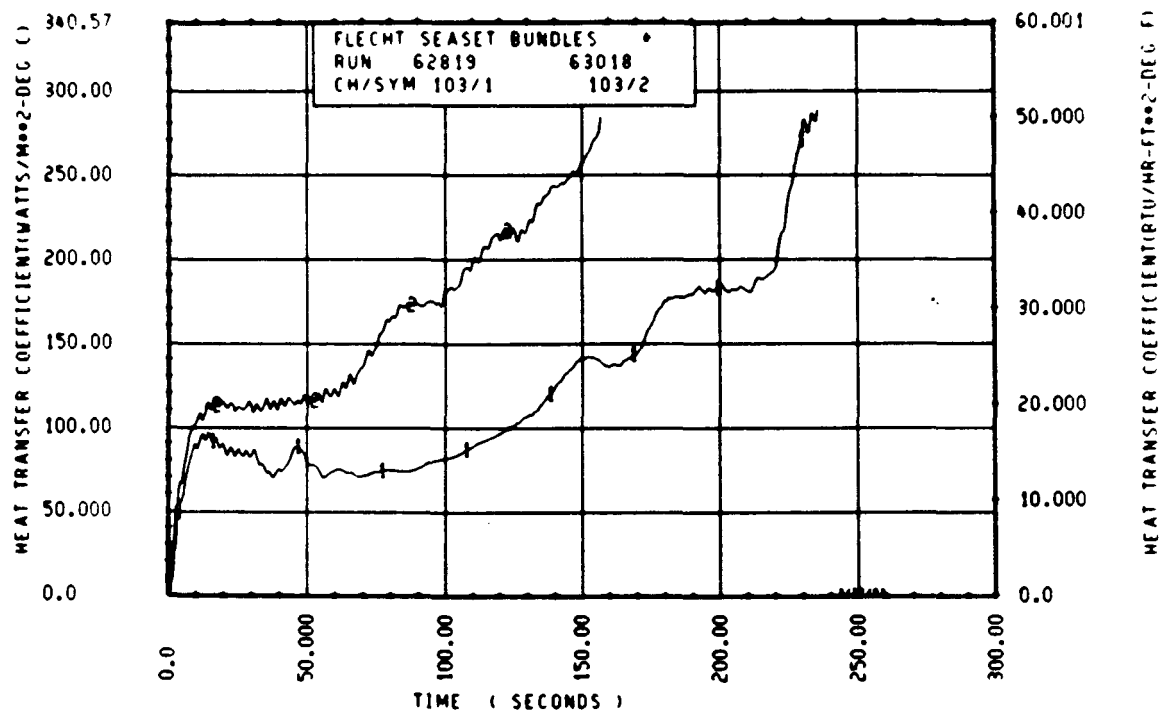
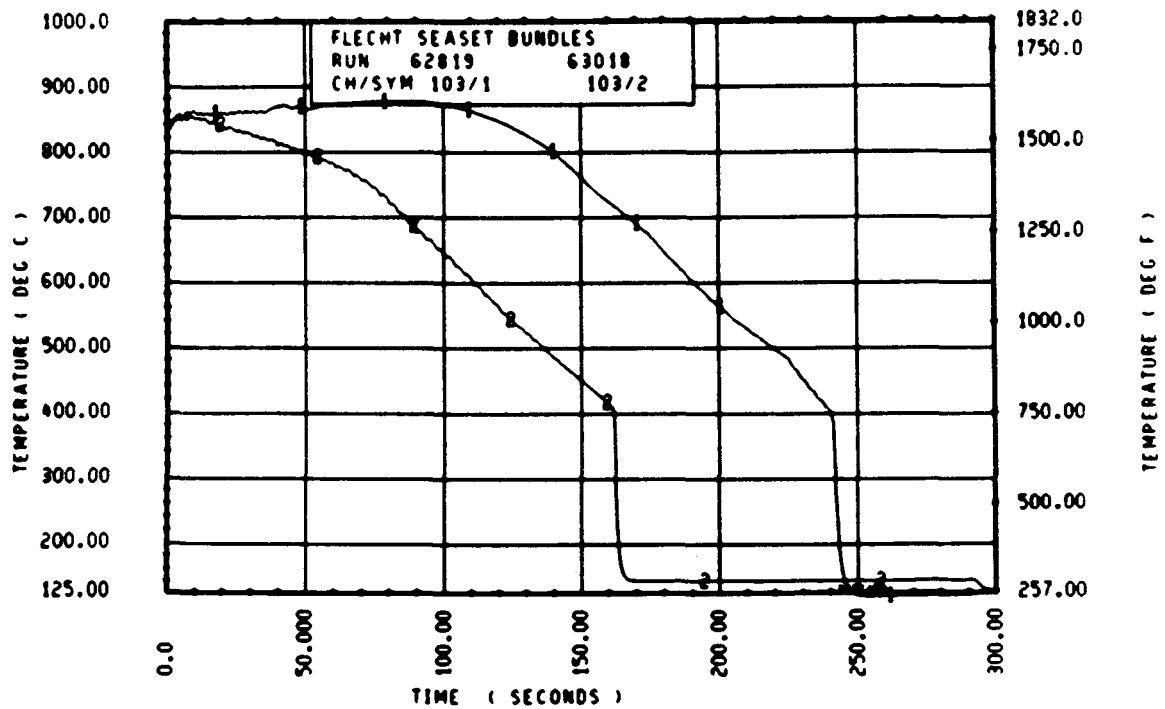
ELEV	TEMP RISE (DEG F)			QUENCH TEMP (DEG F)			QUENCH TIME (SEC)		
	MAX	MIN	MEAN	MAX	MIN	MEAN	MAX	MIN	MEAN
12	5.3	4.2	4.9	648.0	231.9	507.9	7.2	3.5	4.8
24	11.4	10.3	11.0	771.8	737.1	749.3	14.8	14.4	14.6
39	24.0	20.7	23.1	716.1	696.2	706.9	79.4	75.4	76.6
48	34.8	29.5	31.0	704.0	660.6	676.2	127.9	120.4	124.3
60	79.3	33.0	54.9	795.1	721.9	751.1	194.9	186.4	189.4
67	81.3	28.6	49.8	860.3	618.0	719.1	225.2	209.8	220.1
69	68.1	39.8	52.2	759.3	617.9	716.8	228.1	225.1	226.3
70	85.5	43.8	57.7	773.2	723.9	749.7	231.1	222.9	228.2
71	106.3	47.0	71.7	1034.4	626.1	777.8	233.2	118.3	202.9
72	85.6	44.7	64.5	781.8	616.2	726.0	236.3	233.6	234.9
73	97.5	53.4	69.9	768.4	680.6	730.5	240.1	234.2	237.1
74	95.0	46.5	66.8	814.3	665.5	745.6	242.5	113.7	217.4
75	108.8	44.9	71.2	871.0	487.6	742.9	247.1	133.8	216.5
76	112.2	49.5	79.7	934.3	702.5	759.6	249.2	125.8	226.3
77	130.8	39.6	77.6	1116.7	706.5	891.9	255.0	112.4	193.4
78	146.3	39.0	84.8	1128.2	678.7	864.4	257.2	113.7	206.6
79	161.9	41.2	80.3	1135.1	613.0	876.3	263.1	130.3	202.8
80	185.8	47.7	107.6	1228.1	698.9	885.5	264.2	121.3	220.2
81	190.2	47.7	102.8	1074.9	751.8	942.8	270.1	177.8	212.3
84	41.0	26.7	35.3	1004.0	688.0	774.5	287.2	178.9	257.5
86	70.4	34.7	41.3	1109.8	664.6	819.0	291.2	178.3	255.1
90	137.3	42.8	79.4	1000.1	699.5	819.4	308.1	241.2	282.5
96	241.6	127.5	186.6	965.2	686.2	781.2	334.1	272.8	315.2
102	84.0	30.0	54.0	771.8	614.4	691.4	366.1	326.1	344.5
111	161.4	34.0	85.1	690.5	584.9	639.5	388.2	337.1	369.5
120	232.1	39.3	145.1	668.4	247.0	565.7	413.2	301.9	386.1
132	114.9	22.1	58.6	521.9	245.9	429.2	408.2	290.2	337.8
138	67.2	16.8	37.0	560.7	247.6	373.9	333.2	220.1	258.4



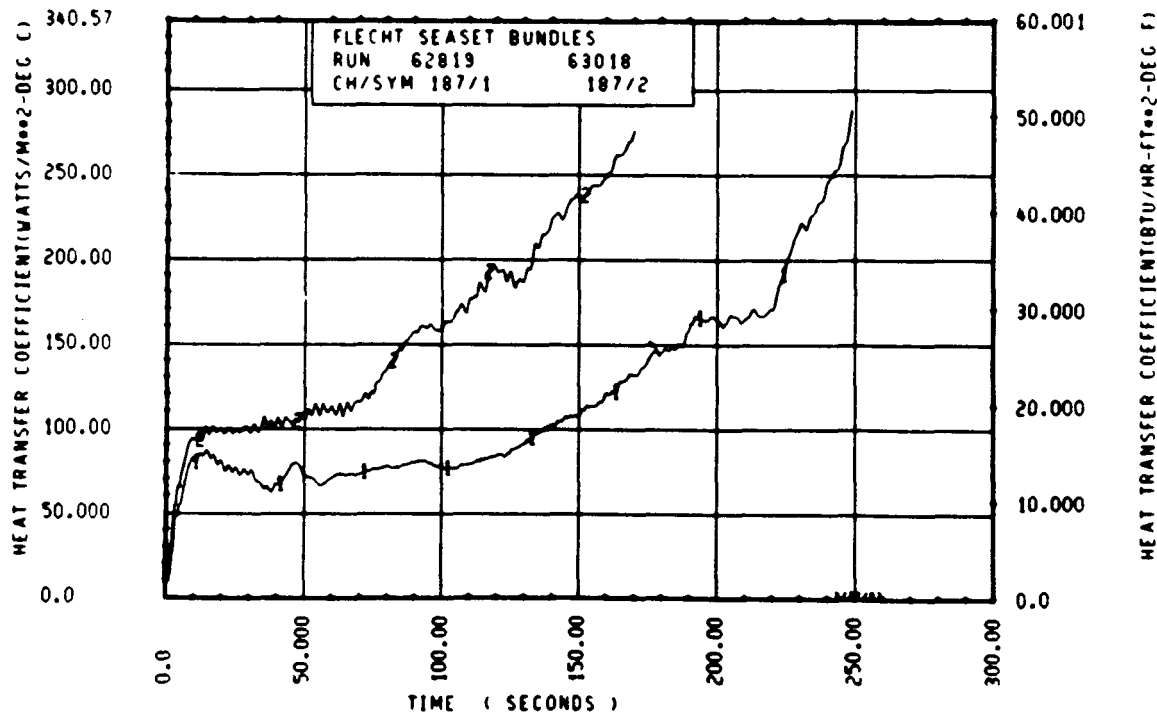
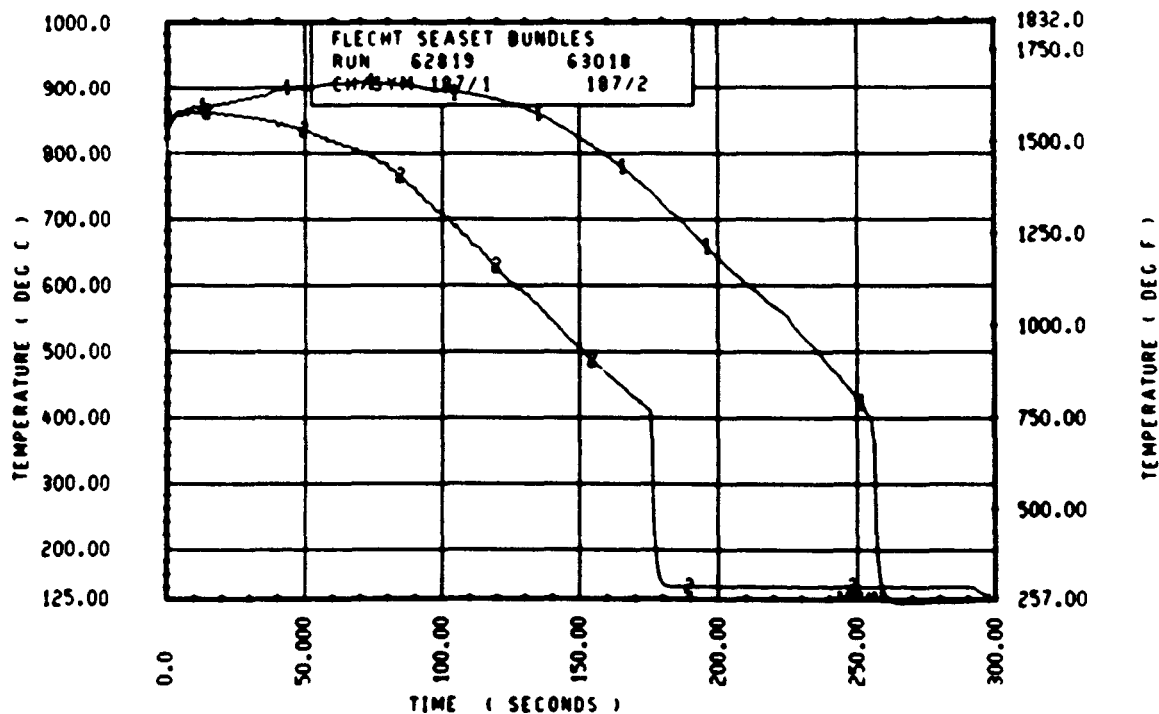
Rod 11E, 1.52 m (60 in.)



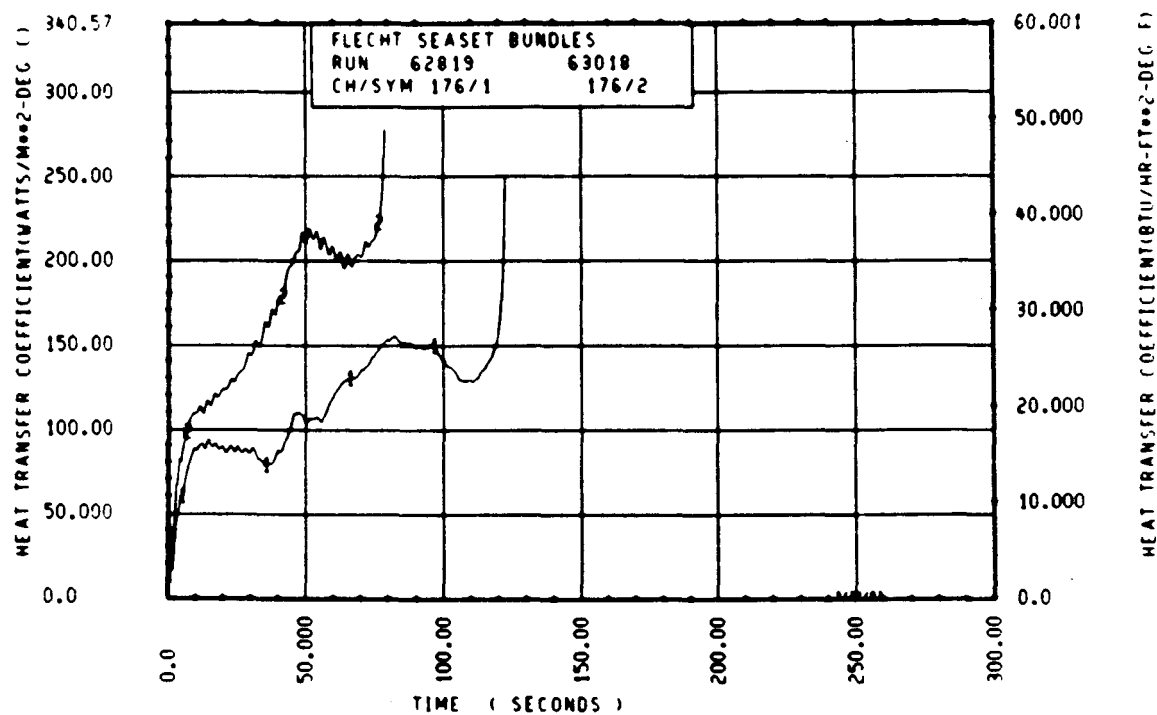
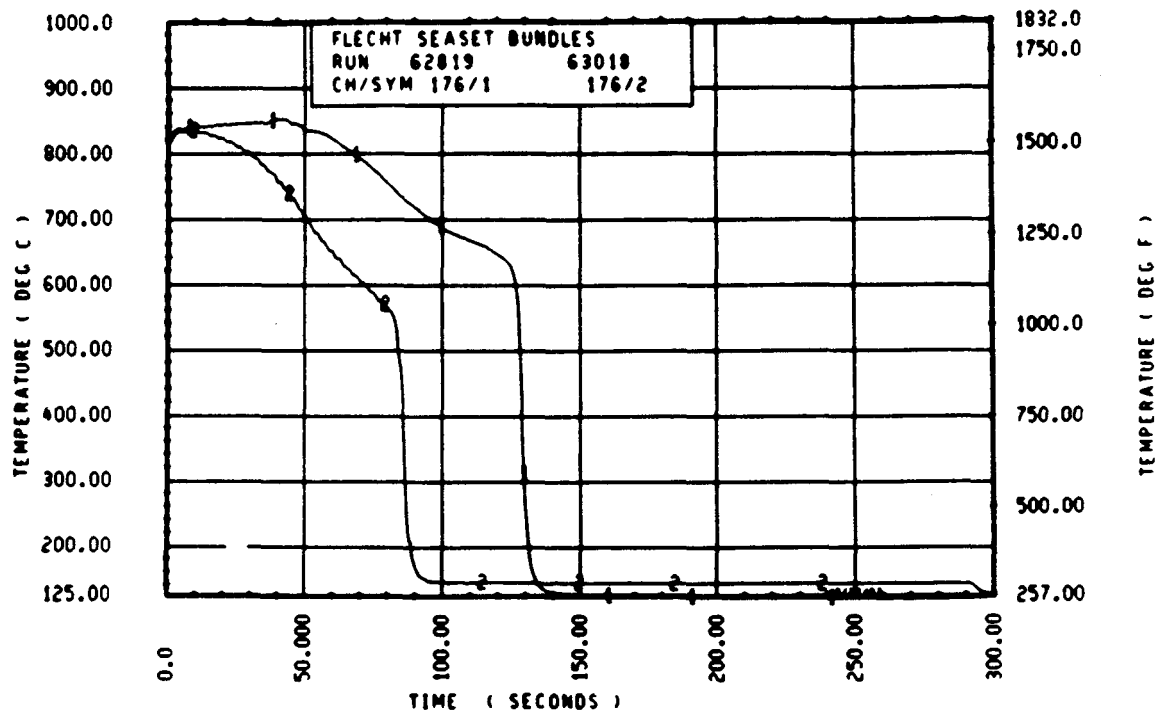
Rod 6L, 1.83 m (72 in.)



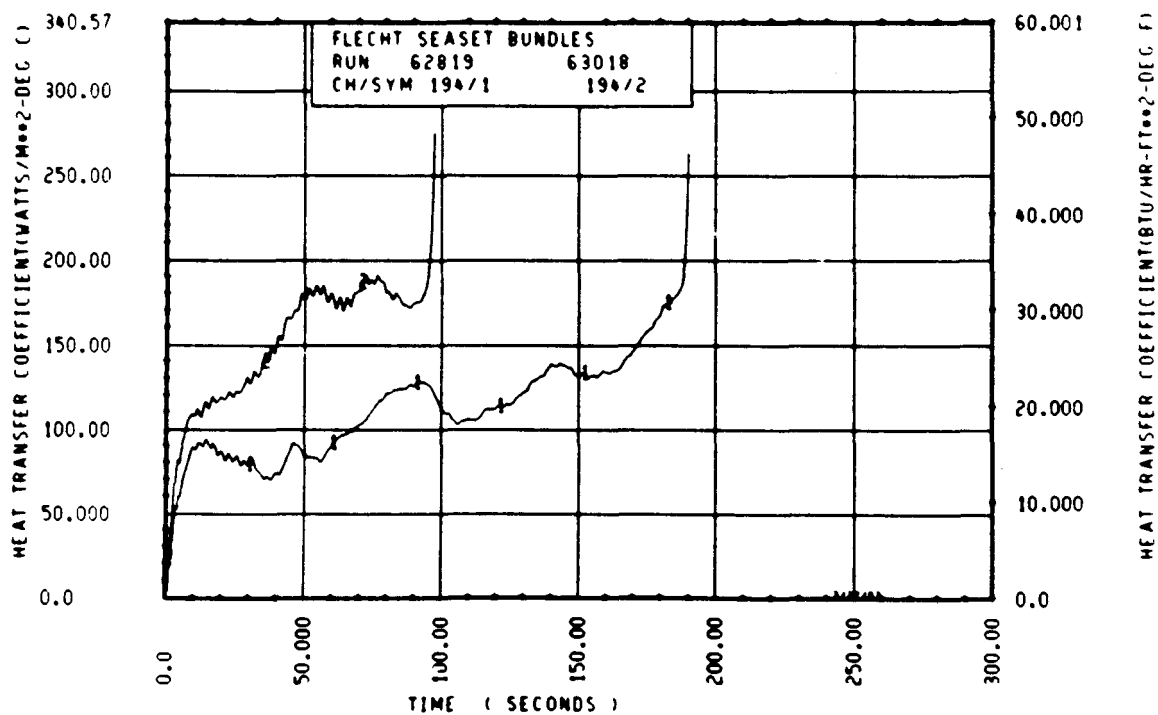
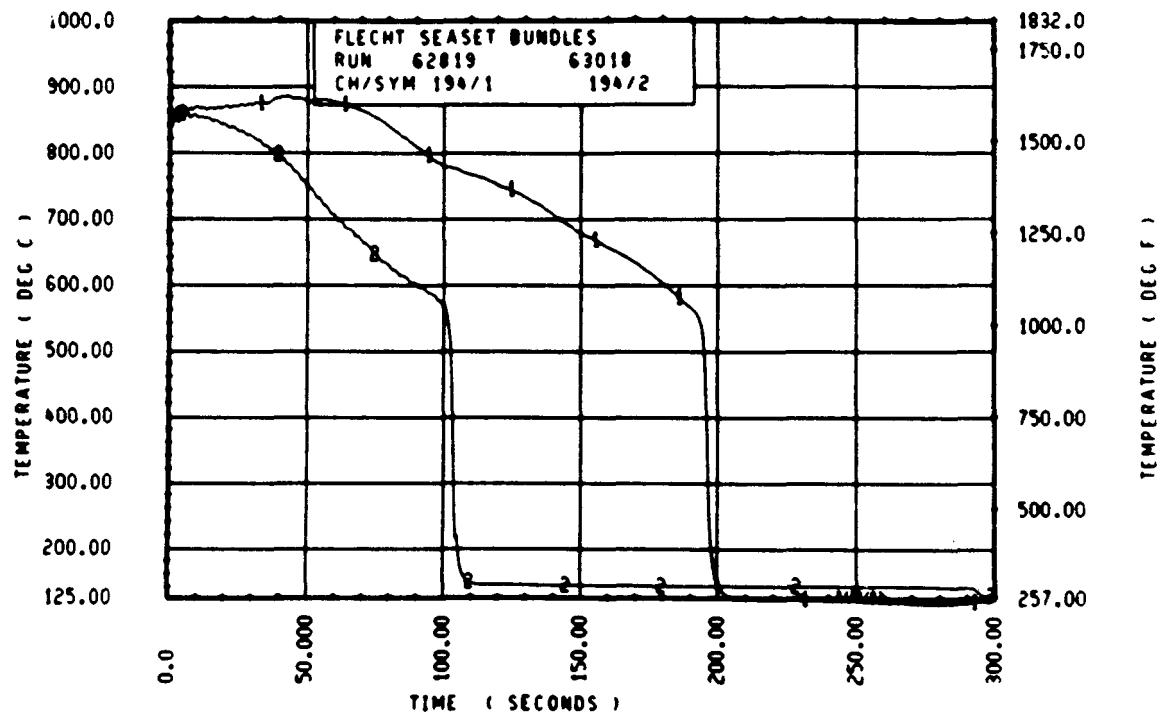
Rod 6L, 1.88 m (74 in.)



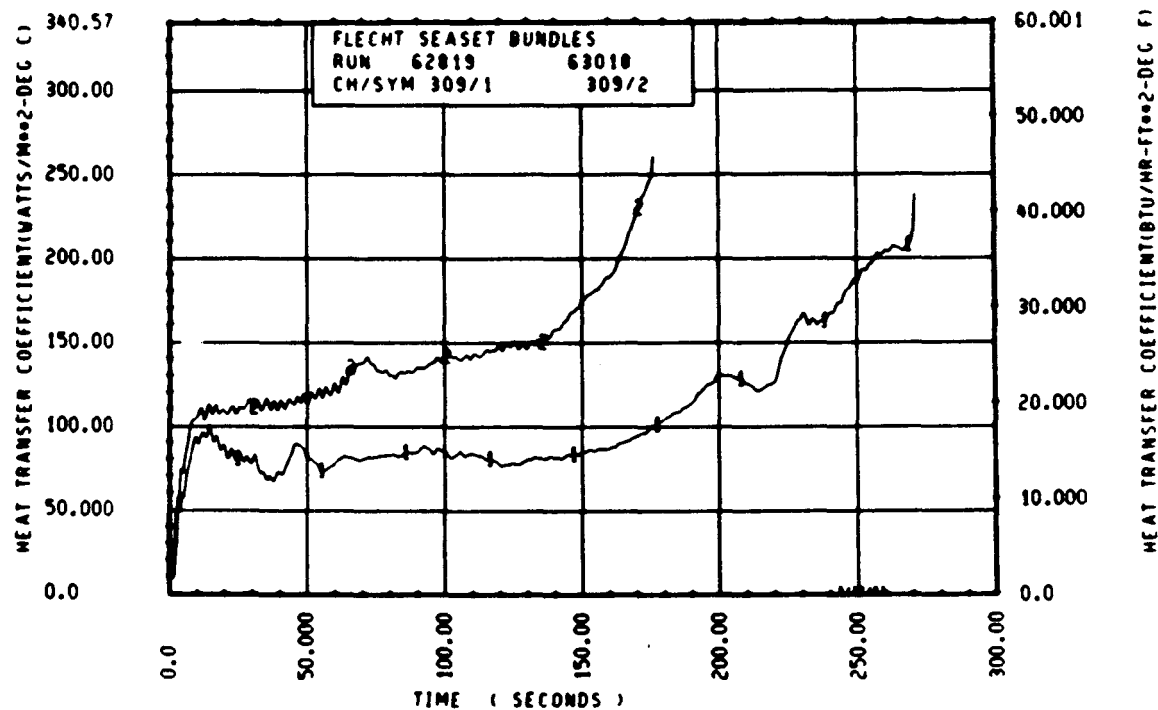
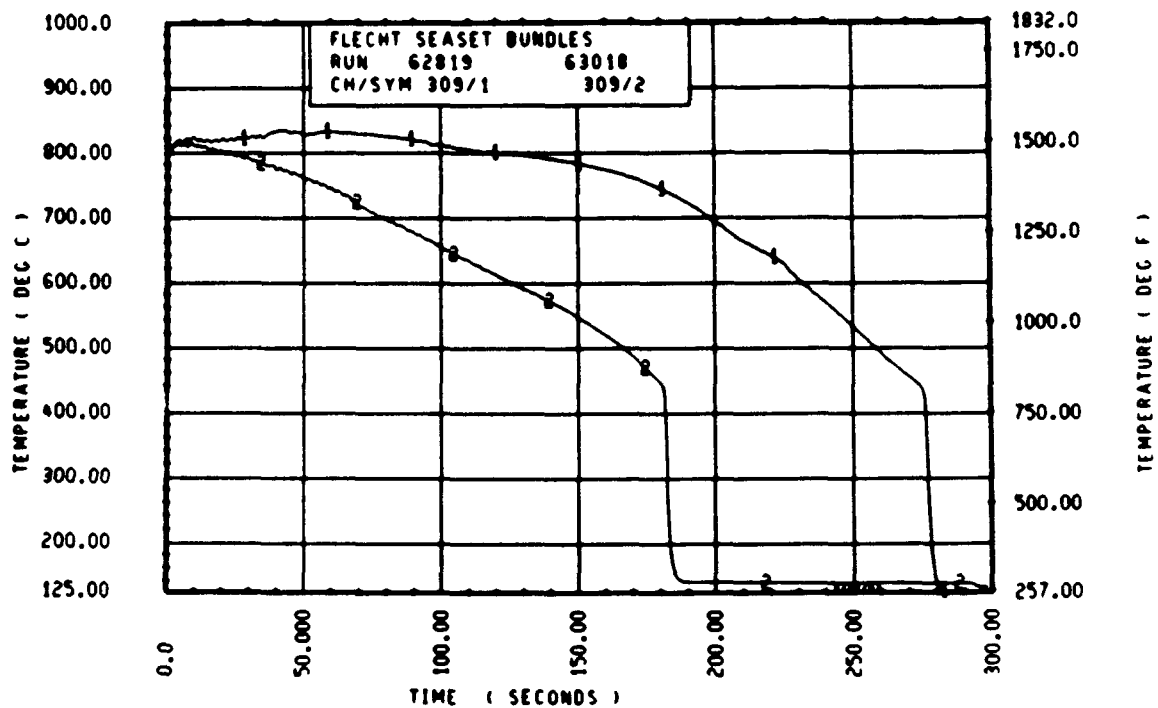
Rod 6J, 1.98 m (78 in.)



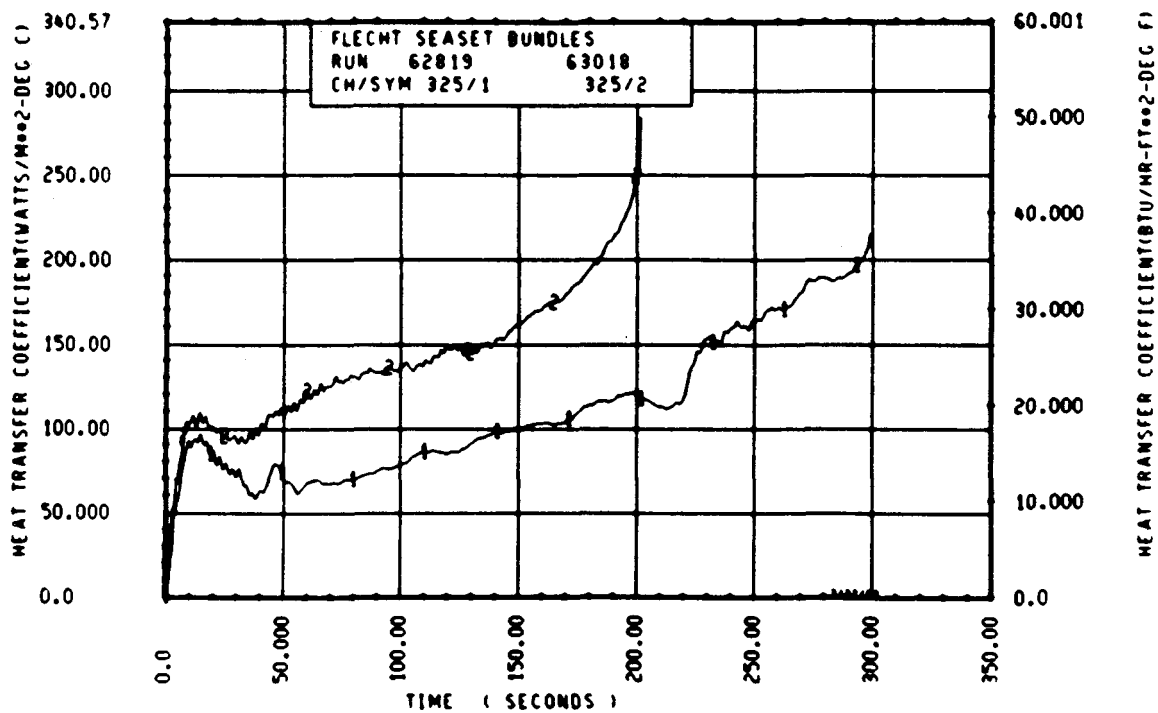
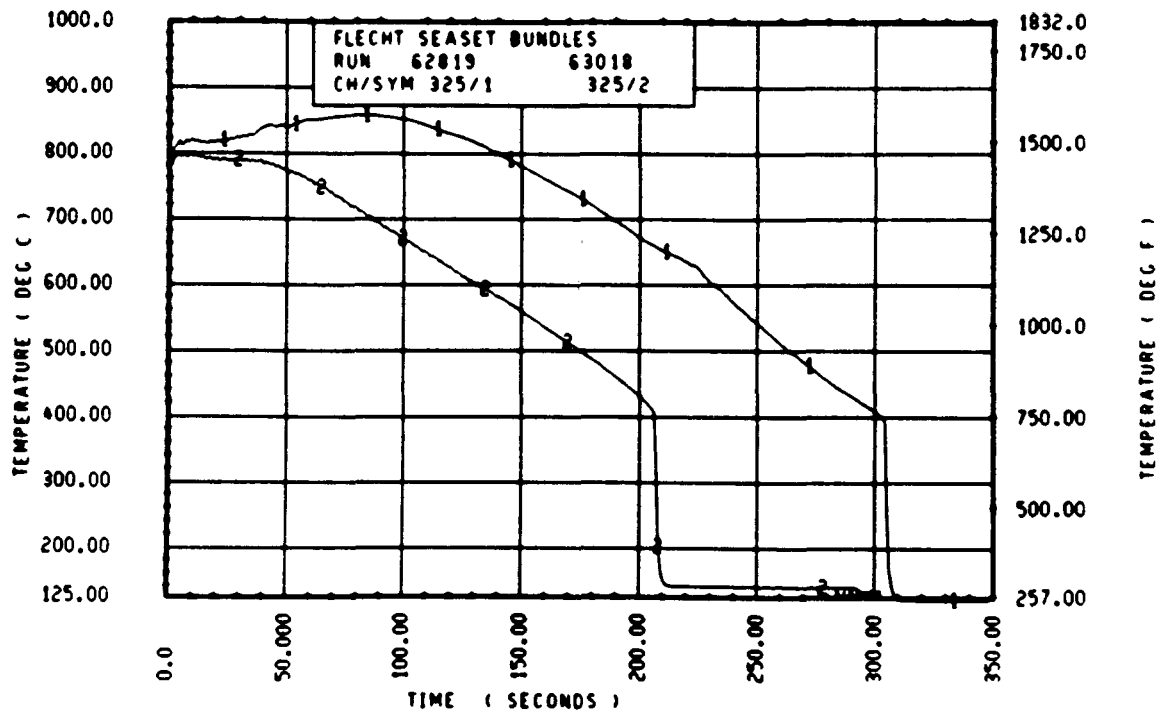
Rod 9F, 1.98 m (78 in.)



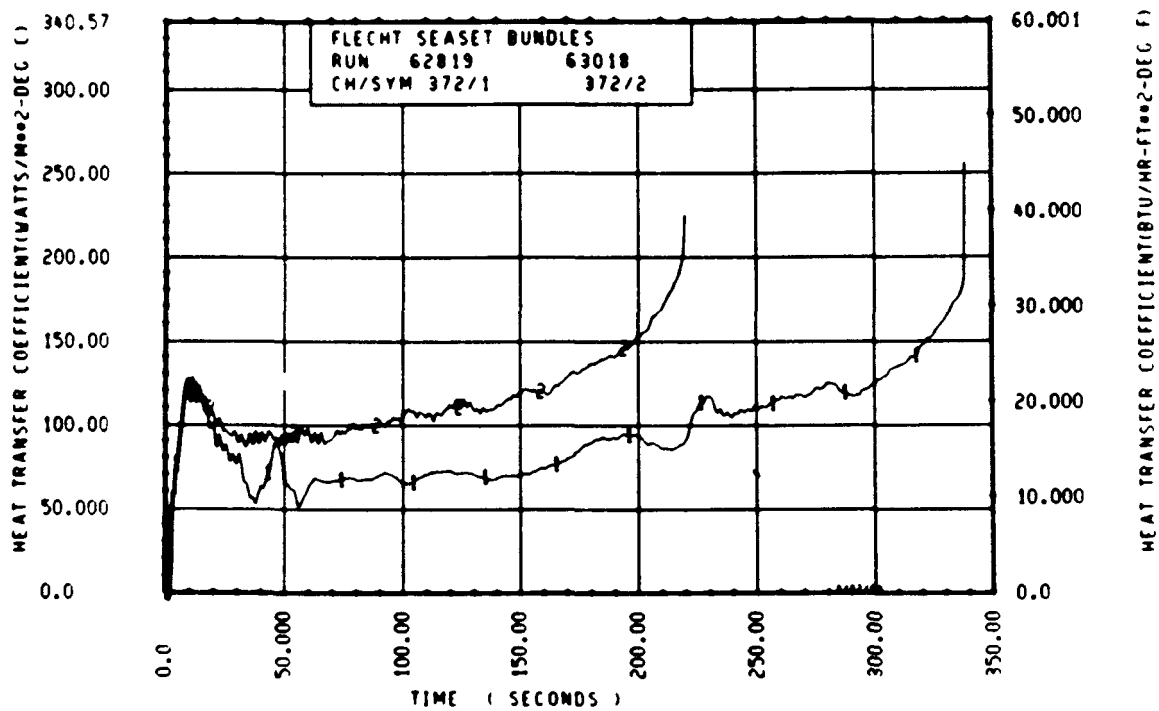
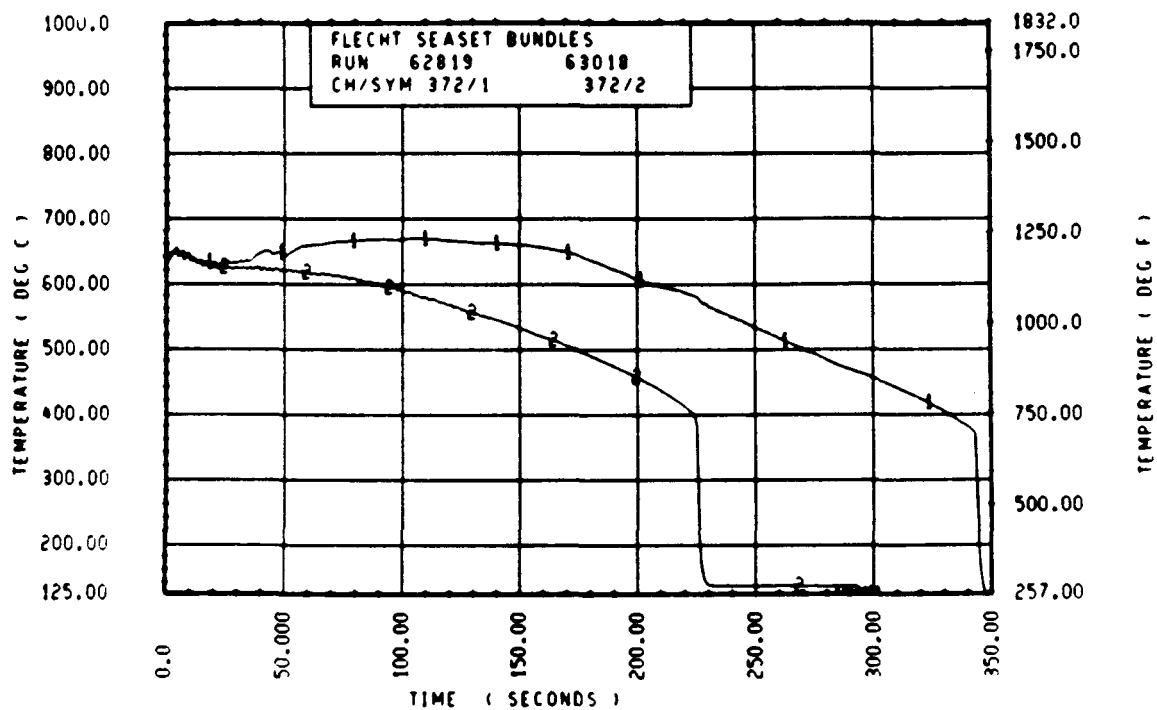
Rod 9E, 1.98 m (78 in.)



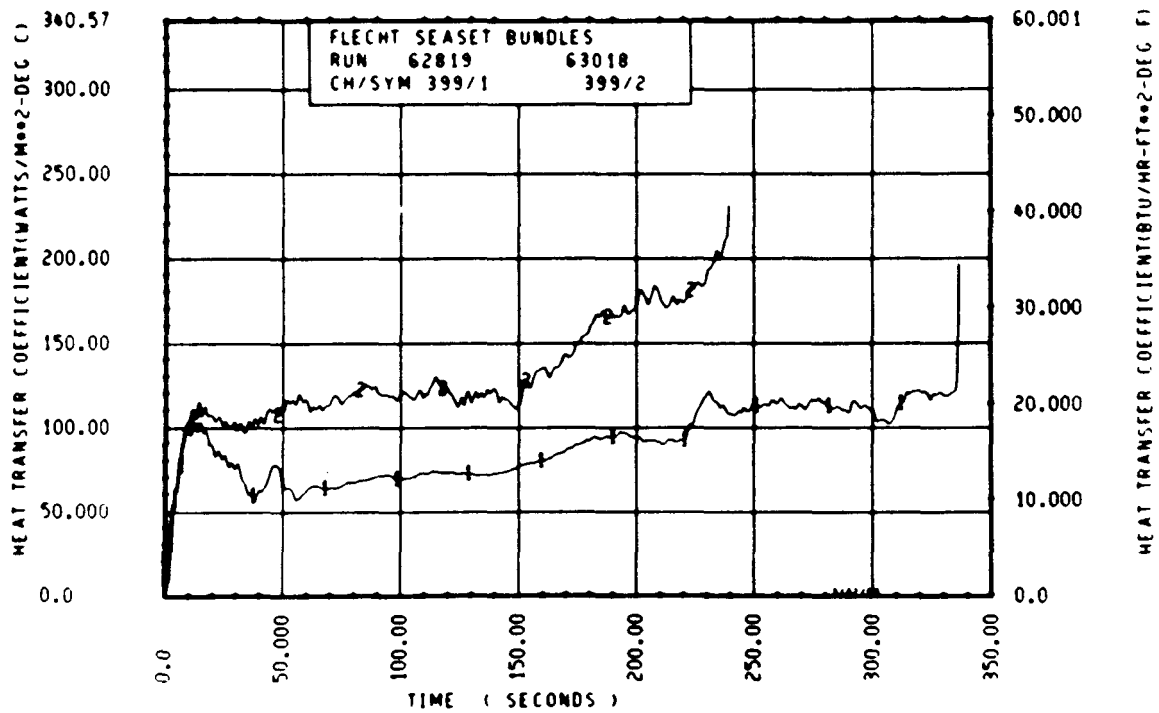
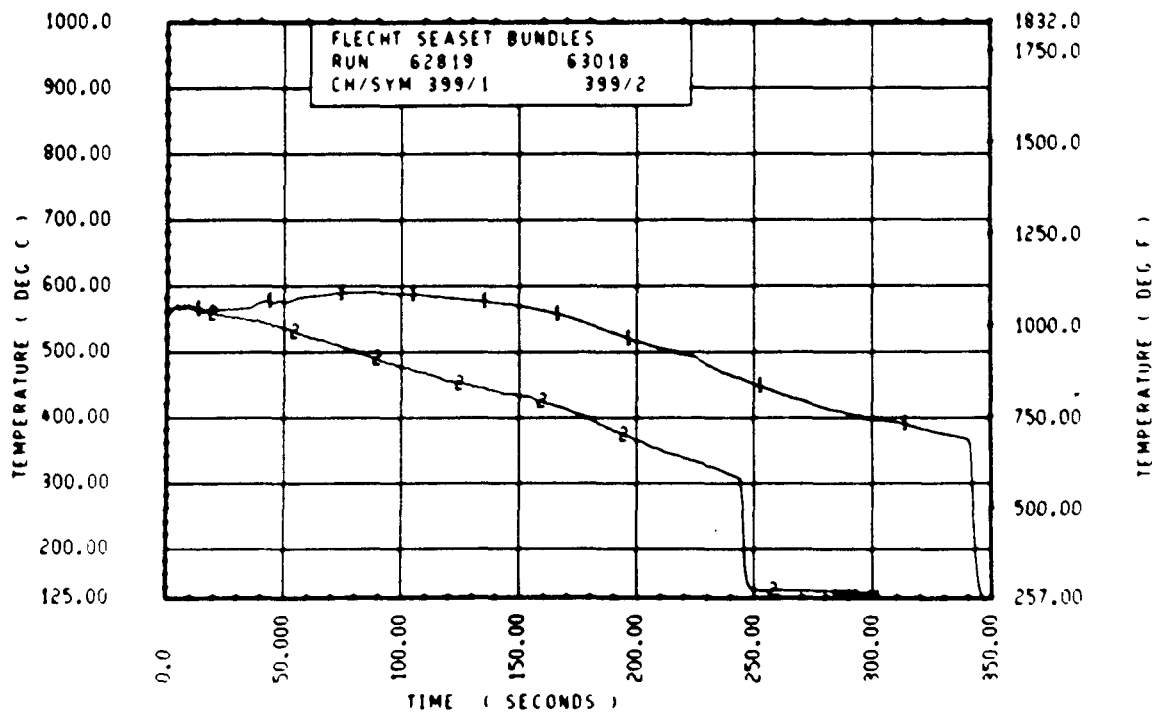
Rod 7D, 2.29 m (90 in.)



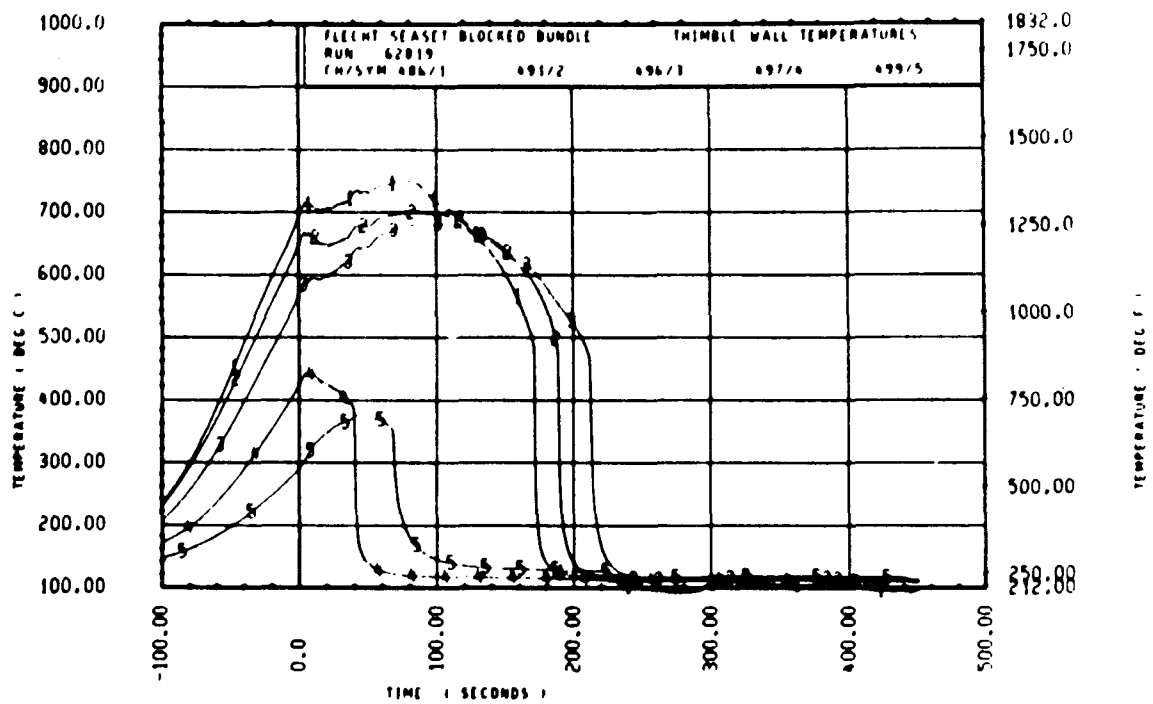
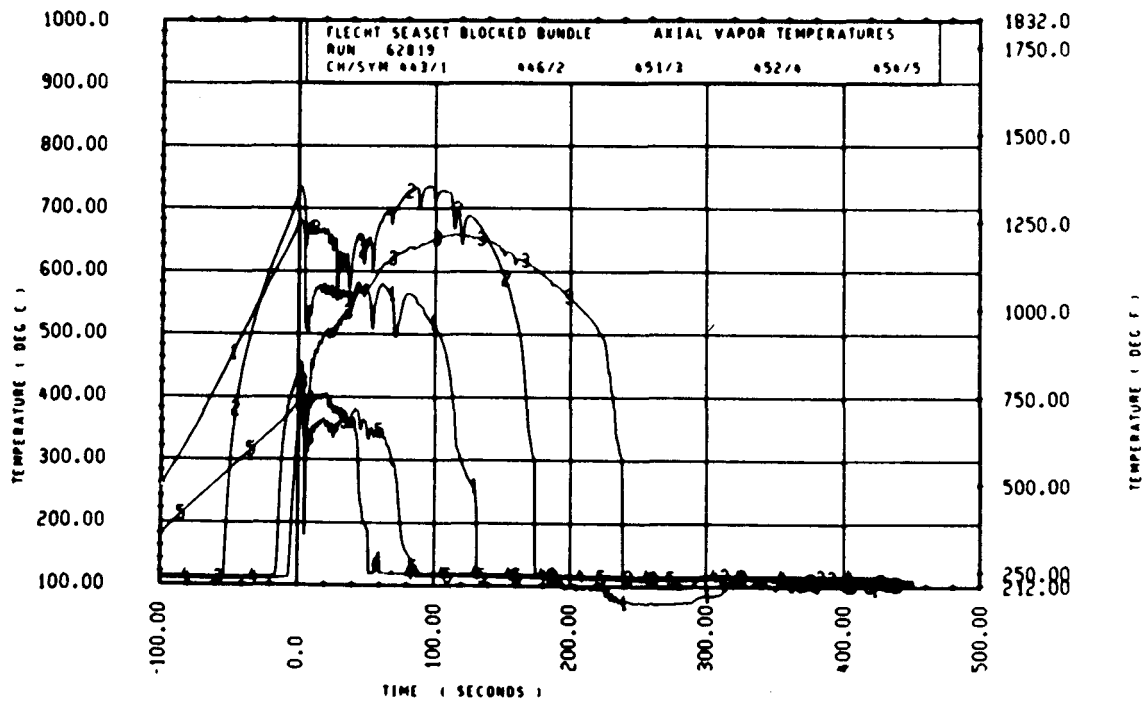
Rod 11E, 2.29 m (90 in.)

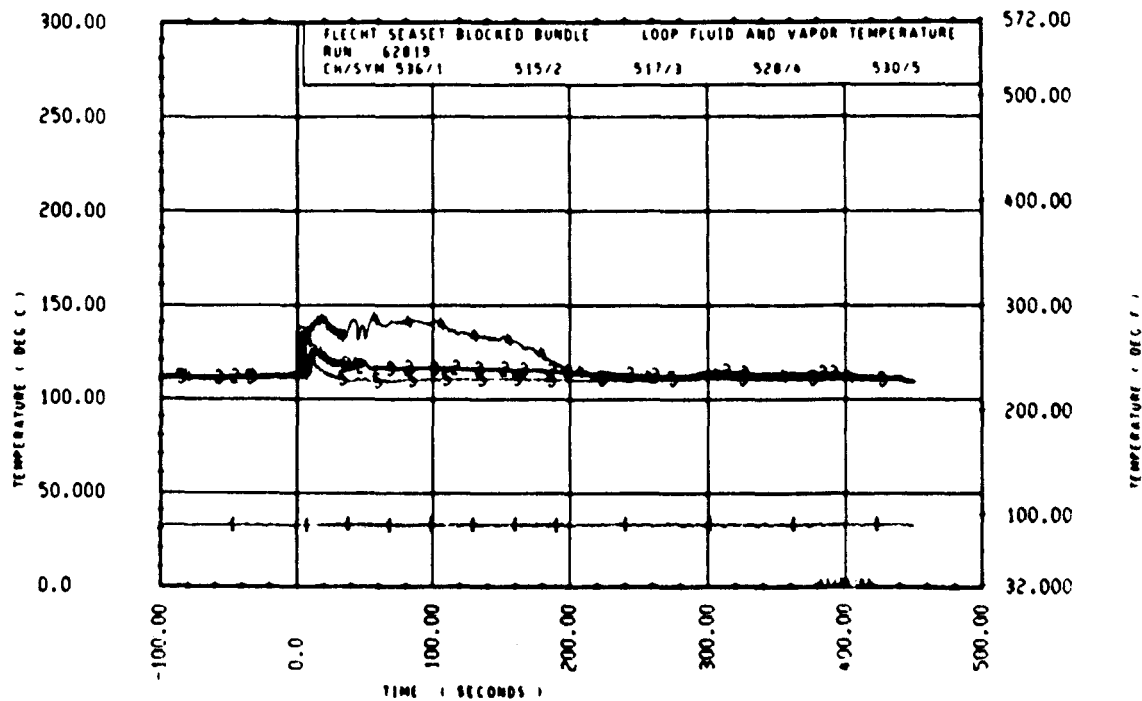
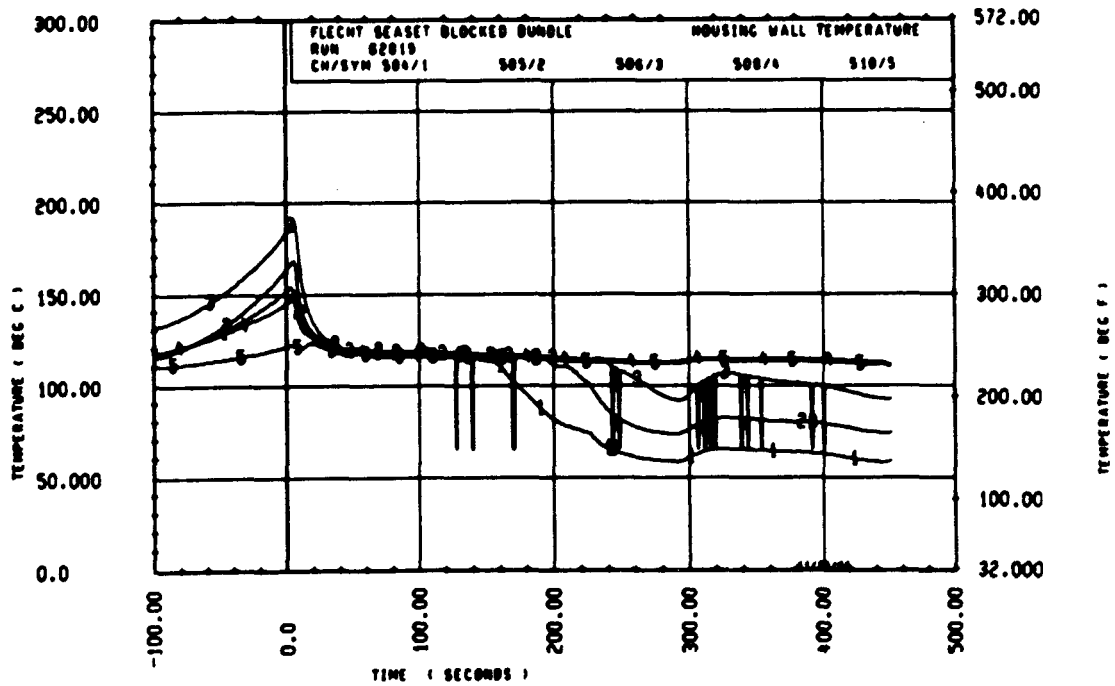


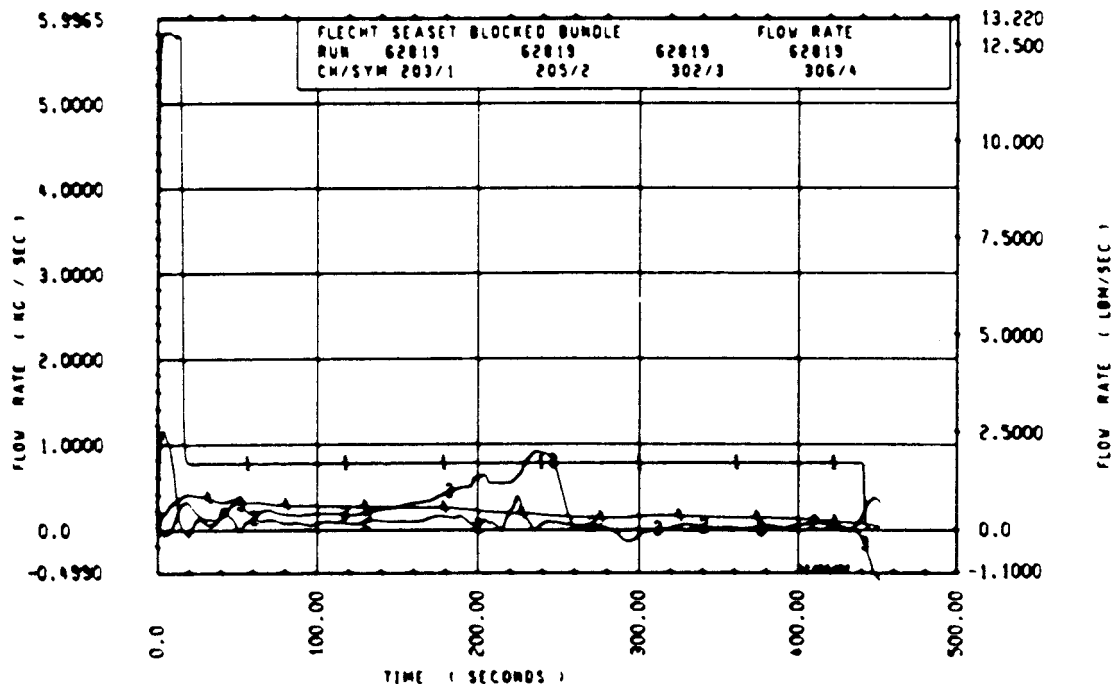
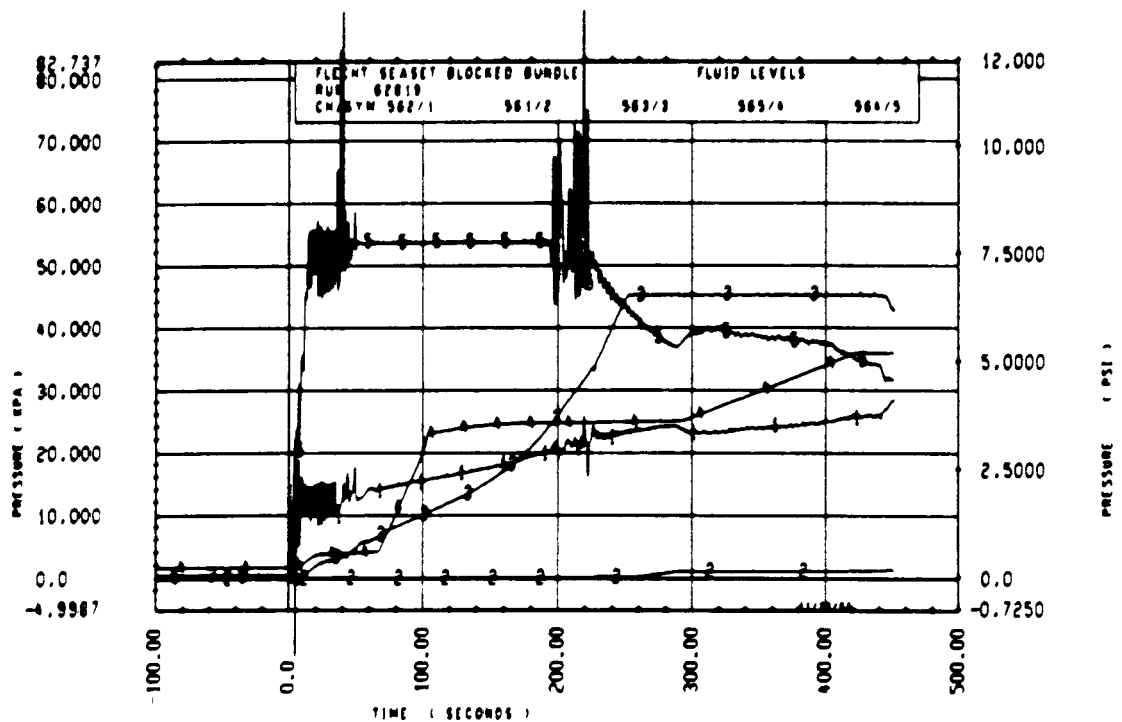
Rod 8J, 2.59 m (102 in.)

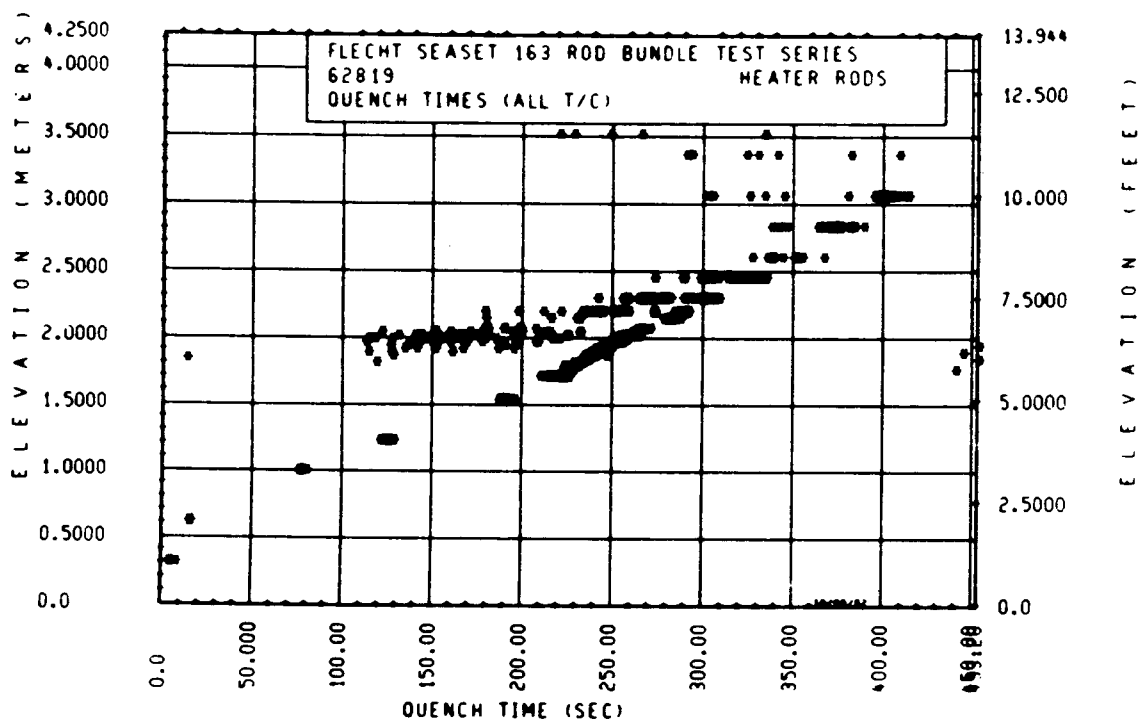
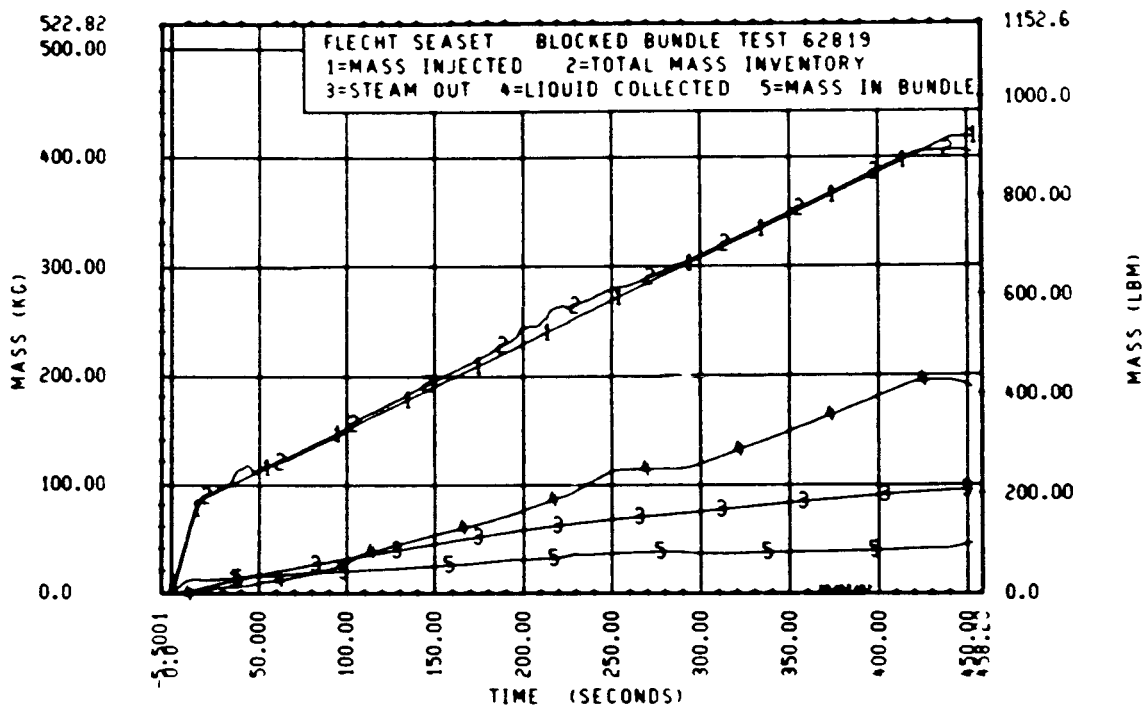


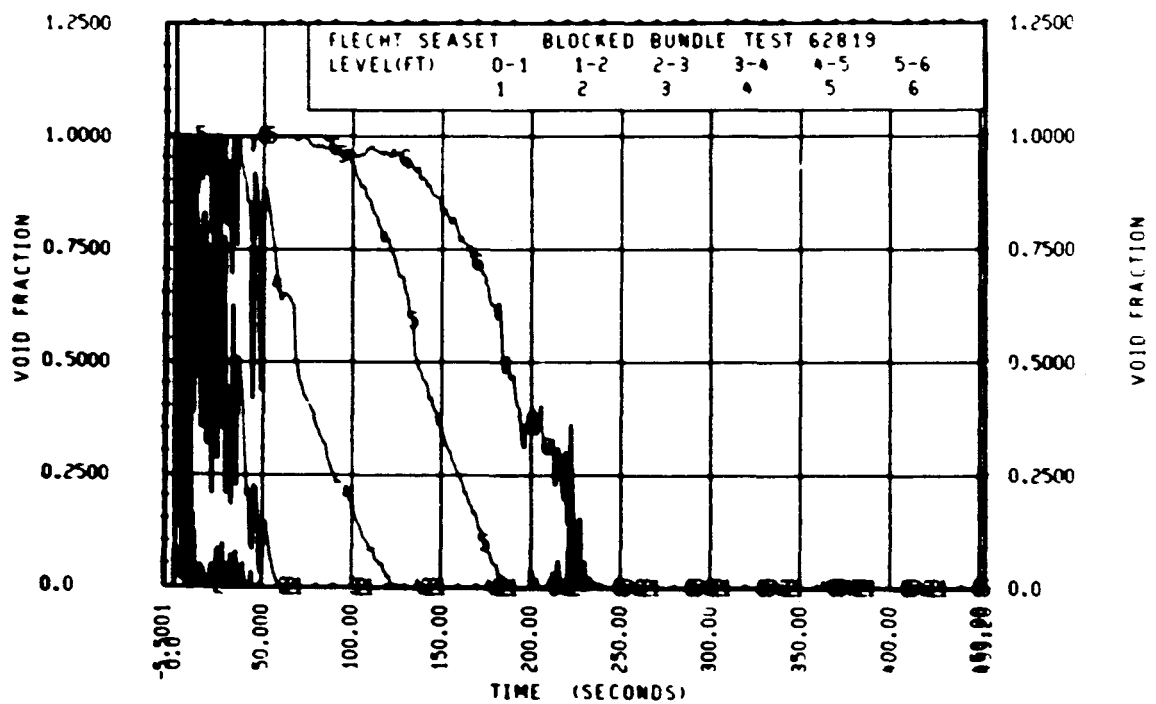
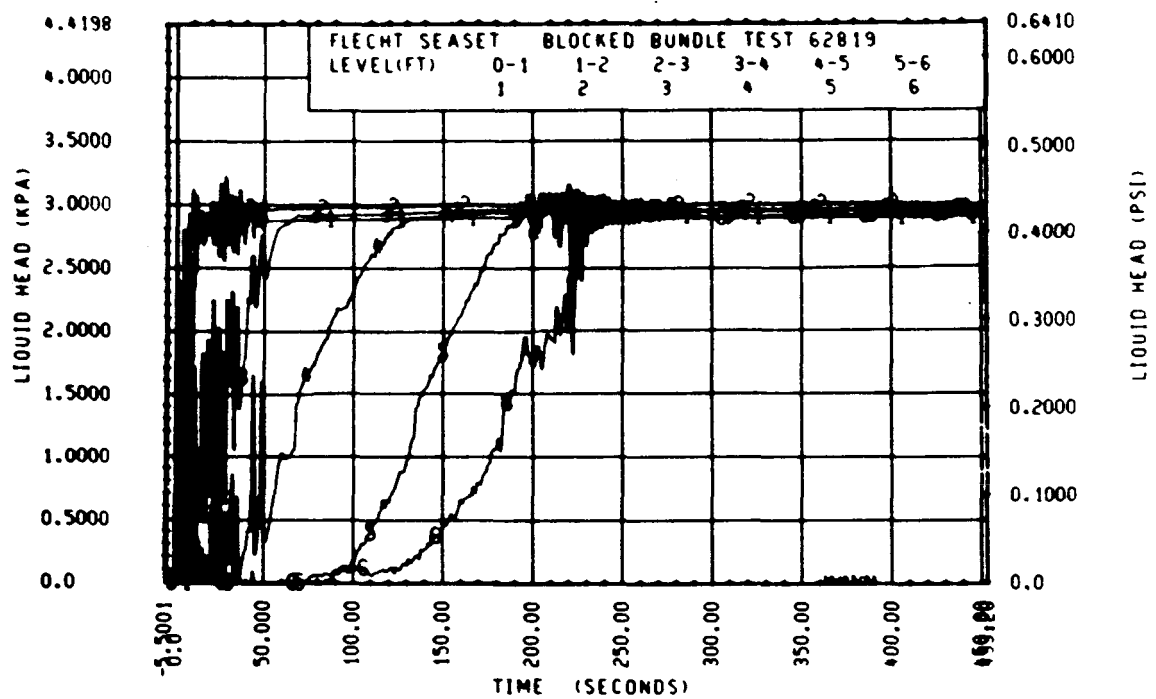
Rod 13G, 2.82 m (111 in.)

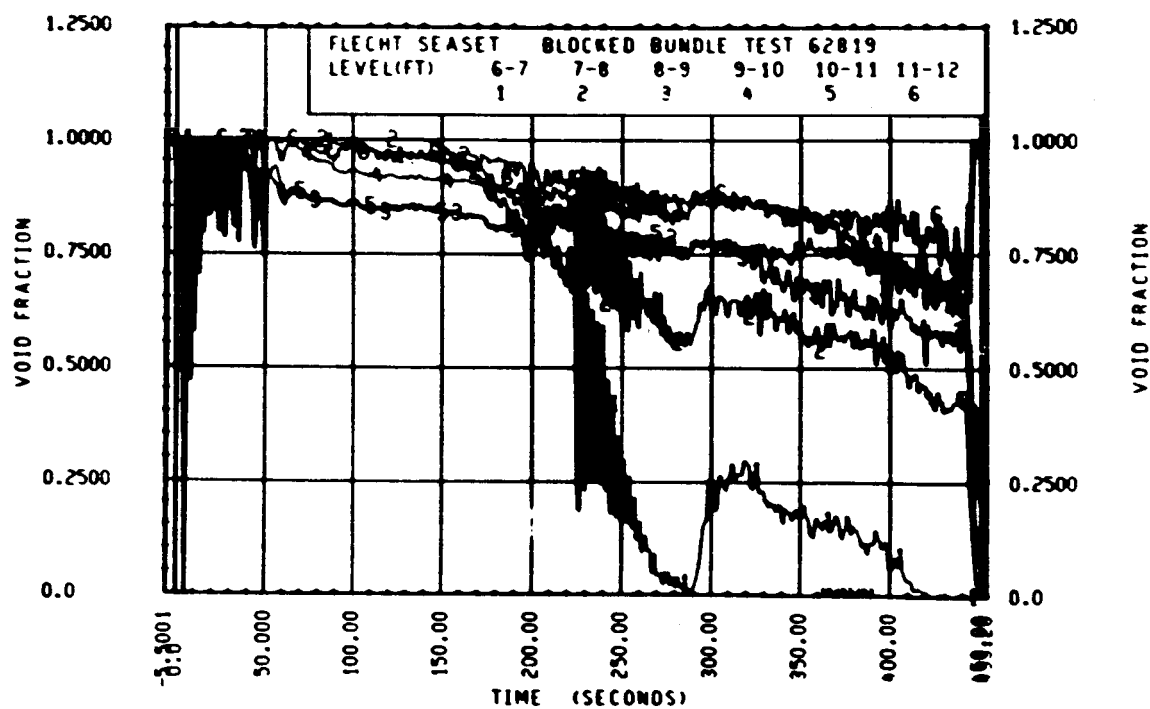
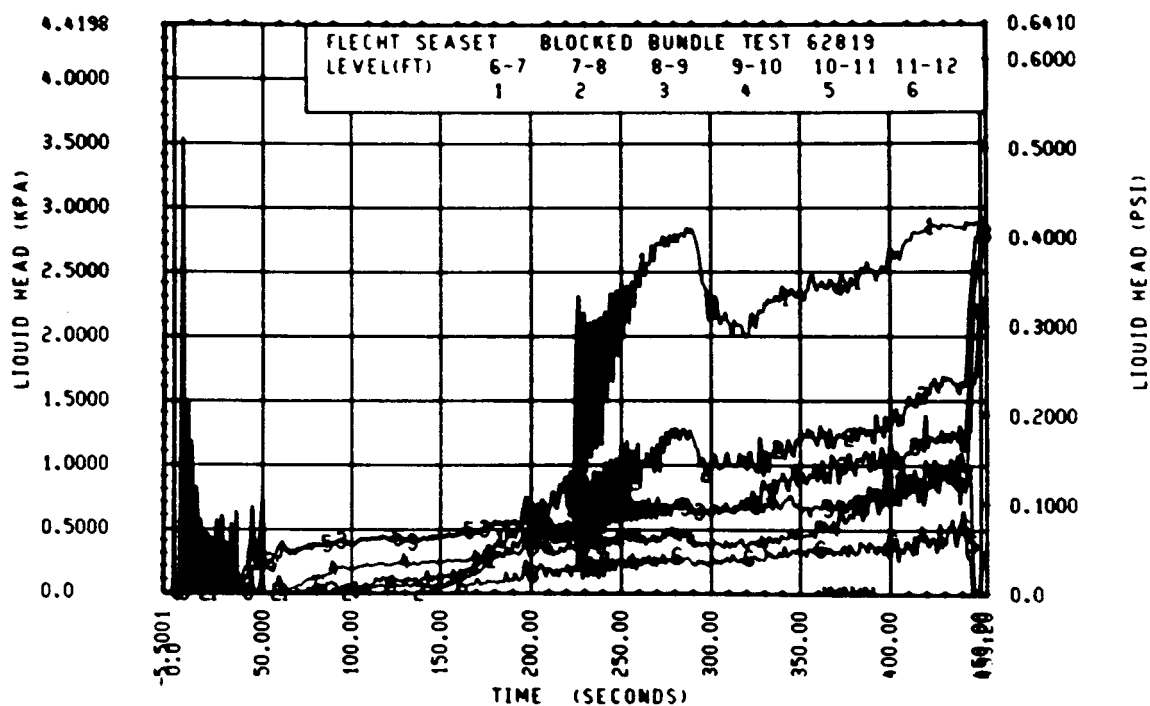












FLECHT SEASET 163-ROD BUNDLE FLOW BLOCKAGE TASK
SUMMARY AND COMMENT SHEET

Run: 62919
Test date: 10/8/82
Test type: Gravity reflood
Parameter: Mass injection rate

AS-RUN TEST CONDITIONS:

Upper plenum pressure	0.139 MPa (20.1 psia)
Initial peak clad temperature and location	871.6°C (1600.9°F), 8N-1.93 m (76 in.)
Initial peak rod power:	
Peripheral rods	2.30 kW/m (0.700 kW/ft)
Bypass rods	2.30 kW/m (0.700 kW/ft)
Blockage island rods	2.30 kW/m (0.700 kW/ft)
Injection rate	5.62 kg/sec (12.4 lb/sec) for 4.5 sec 0.594 kg/sec (1.31 lb/sec) onward
Coolant temperature	32.2°C (90°F)
Initial bundle water level	+5.6 m (+0.22 in.)

COMMENTS:

The injection flow was reduced in this test so that the downcomer would not fill up during the test.

Carryover tank filled up at approximately 380 seconds.

There was no corresponding test conducted in the 161-rod unblocked bundle; however, rod temperatures were compared to those of run 62819, which was conducted at the same conditions but at reduced time for high flow injection.

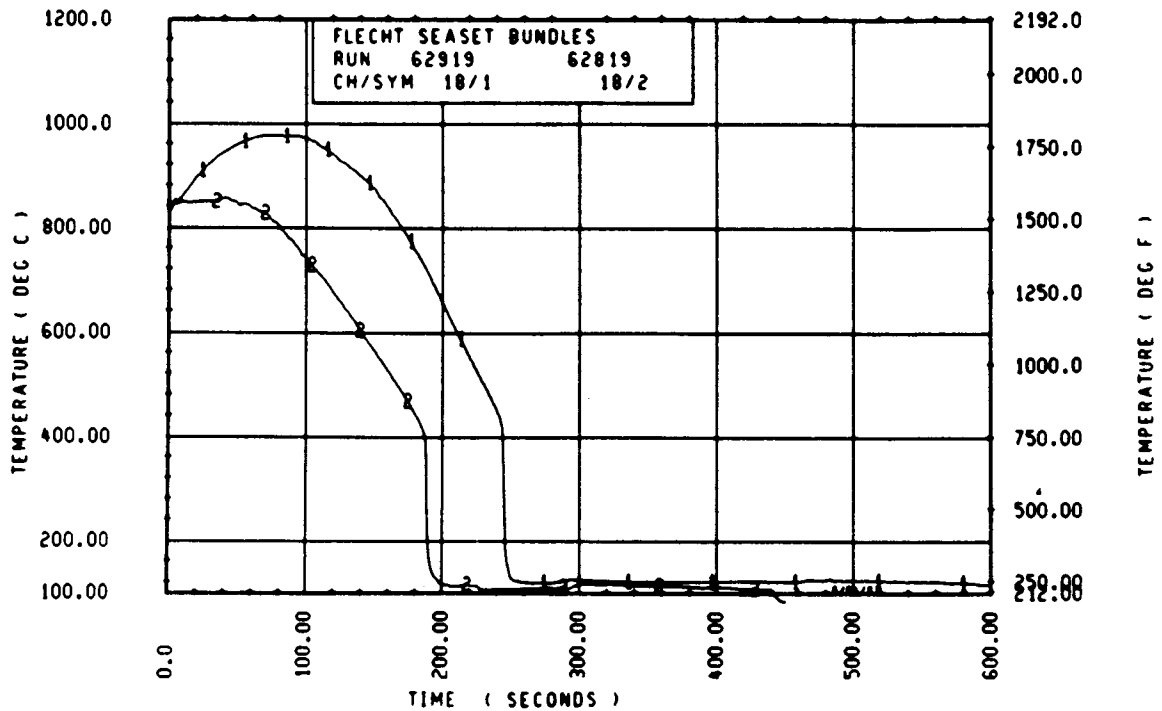
FLECHT SEASET 163 ROD BUNDLE TEST SERIES							
RUN NUMBER 62919							
ROD/CLV	CHAN. NO.	INITIAL AT FLECHT (DEG F)	MAXIMUM TEMPERATURE (DEG F)	TEMPERATURE RISE (DEG F)	TURNAROUND TIME (SECONDS)	QUENCH TEMPERATURE (DEG F)	QUENCH TIME (SECONDS)
90 1- C	3	652.	657.	5.	1.5	244.	7.5
104 2- C	6	670.	882.	-12.	4.0	626.	38.8
90 3- C	9	1195.	1233.	38.	22.5	732.	111.5
30 4- C	11	1341.	1456.	116.	37.0	702.	173.8
70 4- C	12	1331.	1454.	123.	47.5	711.	172.6
6K 4- C	13	1245.	1486.	137.	51.5	711.	179.4
6N 4- C	14	1341.	1451.	110.	47.5	745.	188.4
120 4- C	17	1333.	1436.	103.	43.0	755.	185.6
5E 5- C	20	1461.	1769.	308.	86.5	616.	247.0
76 5- C	21	1535.	1859.	324.	96.0	744.	243.7
90 5- C	24	1503.	1824.	321.	105.5	622.	244.6
5E 5- 7	32	1515.	1867.	352.	111.0	746.	291.1
60 5- 7	45	1537.	1947.	410.	111.5	745.	300.6
40 5- 4	52	1476.	1873.	395.	108.5	762.	303.1
76 5-10	56	1490.	1932.	436.	111.0	745.	311.8
7F 5-11	62	1440.	1868.	428.	111.5	690.	318.8
46 5-11	64	1520.	1909.	389.	107.5	764.	321.5
21 6- C	67	1571.	1939.	368.	100.0	664.	321.6
50 6- C	70	1470.	1856.	376.	111.0	726.	320.6
60 6- C	74	1513.	1885.	372.	96.5	777.	326.8
70 6- C	86	1536.	1921.	385.	93.5	782.	314.6
11E 6- C	80	1474.	1976.	497.	115.5	771.	323.4
60 6- 2	97	1351.	1824.	473.	133.5	757.	322.6
50 6- 2	99	1516.	1940.	428.	129.0	745.	334.0
9E 6- 2	105	1314.	1913.	598.	139.0	1330.	287.5
60 6- 3	111	1345.	1842.	447.	119.5	626.	329.0
46 6- 3	124	1535.	1953.	418.	113.5	775.	350.8
110 6- 4	134	1461.	1945.	484.	112.5	661.	331.1
90 6- 4	143	1525.	2035.	510.	125.0	776.	351.7
9J 6- 5	165	1506.	1896.	392.	102.5	652.	336.6
90 6- 5	166	1575.	1977.	402.	101.5	779.	355.3
60 6- 6	192	1556.	1968.	411.	110.0	652.	344.8
90 6- 6	195	1540.	2041.	501.	121.5	605.	365.0
11F 6- 6	173	1537.	1921.	384.	143.0	752.	359.0
46 7- C	261	1482.	1796.	314.	109.0	745.	405.0
70 7- 6	306	1464.	1883.	419.	116.0	634.	433.8
76 7- 6	312	1504.	1916.	411.	111.0	632.	430.0
11E 7- 6	325	1471.	1853.	382.	111.0	755.	436.4
5L 8- C	337	1244.	1756.	461.	96.5	747.	464.6
70 8- C	345	1337.	1639.	501.	119.5	606.	464.0
7K 8- C	346	1342.	1804.	462.	115.0	725.	473.7
50 8- 6	366	1120.	1495.	375.	90.0	666.	517.4
70 8- 6	386	1127.	1476.	349.	85.0	657.	525.6
7E 9- 3	383	1674.	1521.	441.	122.5	654.	549.1
60 9- 3	387	1633.	1437.	404.	121.0	627.	547.1
9L 9- 3	389	1631.	1422.	391.	126.0	627.	545.8
11F 9- 3	394	1629.	1411.	383.	118.5	694.	460.3
7010- C	406	642.	1250.	409.	140.5	551.	567.3
6010- C	415	647.	1246.	449.	142.5	531.	572.5
6010- C	417	655.	1269.	414.	143.0	566.	583.1
6010- 6	418	660.	1356.	491.	159.5	633.	584.1
6011- C	424	671.	875.	204.	131.0	522.	502.7
4611- C	431	666.	936.	272.	136.0	615.	346.6
11E11- C	432	667.	943.	276.	141.0	474.	476.2
5011- 6	436	654.	806.	151.	125.0	560.	401.8
7011- 6	437	620.	847.	219.	128.5	444.	513.1
6011- 6	438	663.	866.	203.	135.0	247.	555.1

KUN 62919 HEATER ROD STATISTICAL DATA

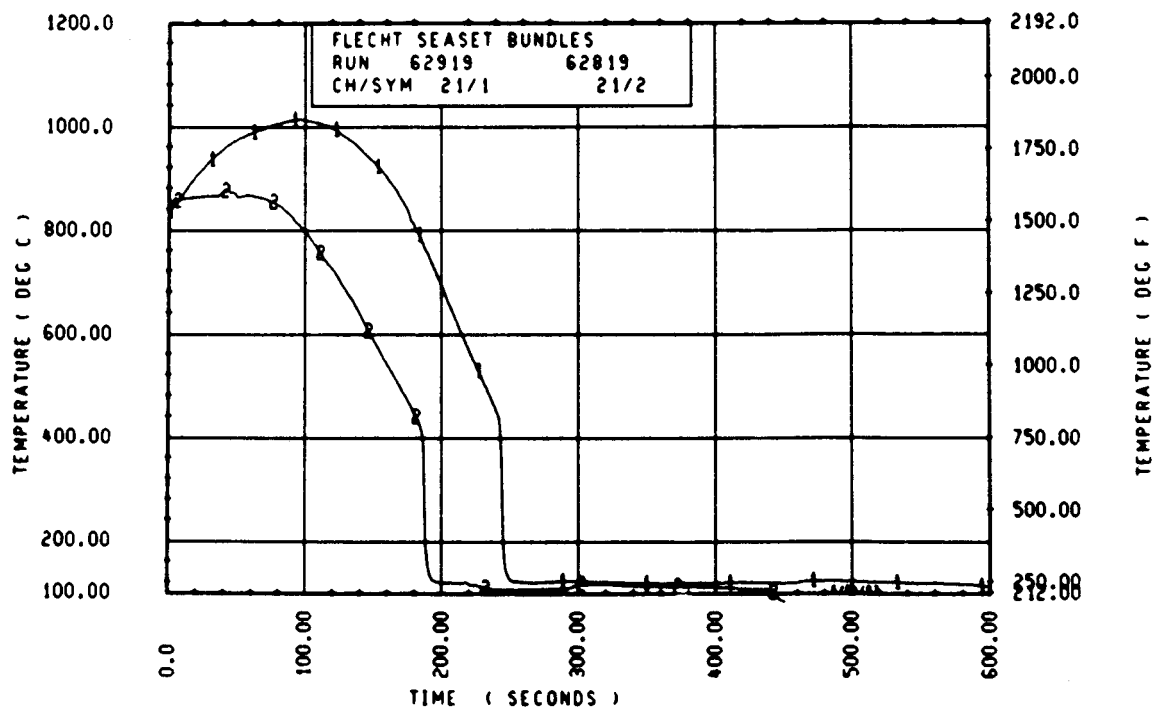
ELEV	IN-TIAL TEMP (DEG F)			MAX TEMP (DEG F)			TURNAROUND TIME (SEC)		
	MAX	MIN	PEAK	MAX	MIN	MEAN	MAX	MIN	PEAK
12	655.4	652.2	654.3	661.7	657.5	659.9	1.5	1.5	1.5
24	664.6	660.0	664.3	662.2	657.4	665.6	4.0	2.0	3.5
36	1195.1	1135.1	1154.7	1232.7	1165.1	1193.6	23.5	20.5	22.0
48	1359.5	1351.1	1342.3	1486.2	1436.0	1462.8	56.5	37.0	46.6
60	1534.8	1364.4	1470.4	1867.0	1459.5	1748.7	100.5	20.5	76.6
72	1578.2	1464.5	1535.0	1949.3	1803.7	1864.5	120.0	74.0	96.1
84	1511.0	1477.7	1445.6	1881.8	1782.4	1847.7	111.5	62.5	101.6
96	1580.6	1367.0	1447.1	1932.1	1830.8	1874.4	118.5	81.5	99.1
108	1519.7	1422.1	1472.2	1905.1	1868.2	1898.0	117.0	64.5	106.4
120	1572.6	1434.2	1521.0	1975.7	1855.7	1918.4	125.5	76.5	103.0
132	1571.7	1444.4	1511.6	1951.6	1852.3	1905.7	118.0	87.0	101.7
144	1570.0	1351.1	1463.6	2017.4	1816.1	1917.9	133.5	64.0	111.4
156	1581.4	1345.4	1500.0	1982.6	1842.2	1919.7	133.0	63.5	112.6
168	1600.4	1429.6	1526.6	2046.6	1903.3	1963.8	132.5	64.0	113.4
180	1574.9	1467.0	1525.7	2023.3	1854.6	1948.3	141.5	66.5	116.4
192	1598.6	1506.7	1540.4	2040.8	1822.9	1956.4	144.0	88.0	114.6
204	1582.5	1441.6	1543.6	2019.8	1836.5	1961.5	142.5	86.5	116.7
216	1561.4	1446.5	1530.6	2040.6	1837.6	1970.2	140.0	81.0	117.2
228	1558.7	1440.7	1511.0	2031.0	1807.1	1952.6	158.0	90.5	120.0
240	1533.7	1417.6	1484.1	1812.7	1647.1	1772.6	111.5	76.0	93.5
252	1573.6	1462.7	1514.4	1916.6	1746.7	1829.7	108.5	56.5	94.4
264	1504.4	1376.5	1467.7	1975.7	1803.7	1890.3	124.0	63.5	109.6
276	1380.7	1246.0	1332.3	1939.0	1755.6	1832.1	141.0	64.5	121.2
288	1173.4	1024.6	1137.6	1611.4	1457.4	1538.2	117.0	65.0	101.6
300	1074.2	1010.1	1044.0	1520.7	1353.2	1444.4	127.0	105.5	114.1
312	907.0	802.5	852.3	1374.3	1109.2	1289.6	170.5	116.5	136.6
324	671.1	657.5	664.4	993.6	840.8	925.5	141.0	117.0	129.4
336	662.7	626.1	646.0	924.5	805.6	861.3	139.0	125.0	132.0

KUN 62919 HEATER ROD STATISTICAL DATA

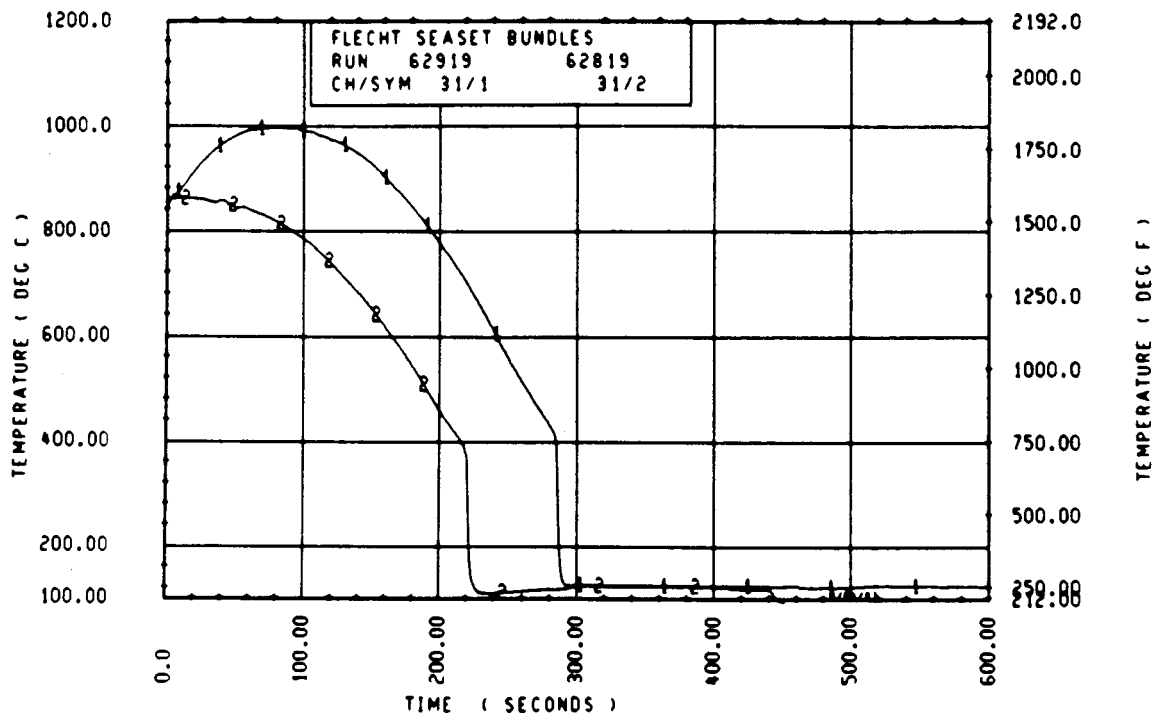
ELEV	TEMP RISE (DEG F)			QUENCH TEMP (DEG F)			QUENCH TIME (SEC)		
	MAX	MIN	PEAK	MAX	MIN	MEAN	MAX	MIN	MEAN
12	6.3	5.2	5.6	646.5	235.2	374.8	8.0	4.1	6.1
24	12.4	10.3	11.4	671.9	625.6	646.4	36.8	27.6	33.2
36	41.4	26.4	34.0	734.5	704.0	721.5	117.9	106.6	112.6
48	141.4	102.6	120.5	787.2	698.8	729.4	179.4	162.3	170.5
60	347.4	74.6	270.3	822.7	743.2	792.1	253.5	243.7	246.6
72	410.0	272.1	344.5	773.5	633.5	747.0	300.9	262.4	289.7
84	395.0	303.6	352.1	763.1	701.7	749.0	308.1	297.0	302.4
96	463.4	301.7	377.2	784.6	743.3	768.2	313.9	302.4	306.3
108	464.2	361.4	415.0	769.0	690.1	737.1	321.9	310.6	317.6
120	497.0	323.7	347.4	804.0	744.2	768.9	329.9	314.4	323.5
132	478.0	344.6	344.5	819.4	744.5	771.1	339.9	323.0	329.5
144	526.1	344.1	434.1	742.4	731.4	767.8	343.0	316.0	333.0
156	443.2	334.1	414.1	859.5	476.6	766.9	350.8	314.4	336.1
168	511.6	395.5	437.2	864.7	660.9	782.8	354.9	325.9	345.4
180	512.3	387.6	424.6	863.0	744.7	816.7	363.9	334.0	345.2
192	500.6	243.1	415.4	1069.4	650.5	815.1	369.9	296.7	351.4
204	466.4	277.6	417.7	1085.2	663.3	842.7	372.7	311.7	353.5
216	514.0	240.4	434.6	1064.3	692.3	830.6	384.6	320.4	367.4
228	503.6	320.1	442.6	926.1	770.3	853.6	387.6	351.0	364.5
240	320.6	266.6	266.5	402.0	700.8	755.7	413.0	355.1	390.4
252	361.4	185.1	310.3	911.3	696.9	775.5	417.1	365.1	404.0
264	476.6	335.6	442.5	472.6	731.6	817.7	448.4	411.4	433.5
276	574.4	410.3	444.6	854.6	706.6	787.3	498.6	448.6	474.4
288	450.3	348.7	400.5	746.5	620.7	679.2	526.1	485.1	510.3
300	470.0	325.6	440.3	694.4	601.8	646.1	563.1	466.5	540.7
312	502.7	366.6	437.3	832.3	391.3	604.2	588.1	365.7	560.2
324	328.6	181.2	261.2	615.3	371.5	472.4	593.1	340.6	467.7
336	272.3	151.3	213.3	645.4	247.0	470.6	555.1	246.4	460.1



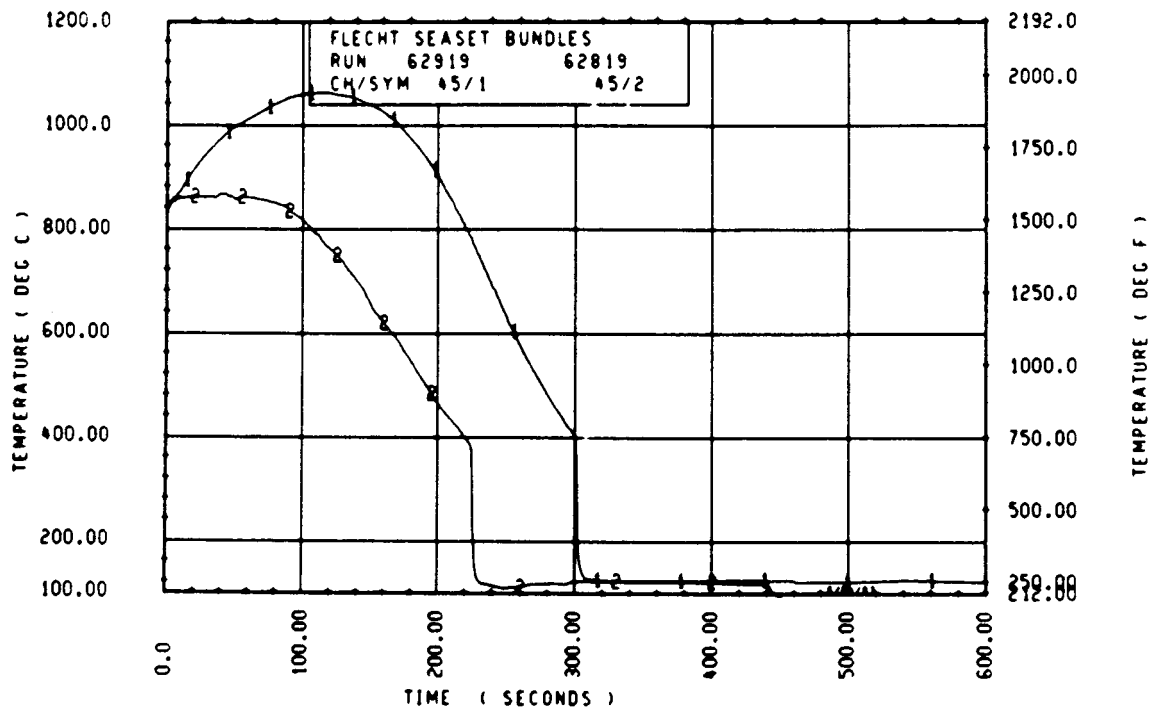
Rod 3H, 1.52 m (60 in.)



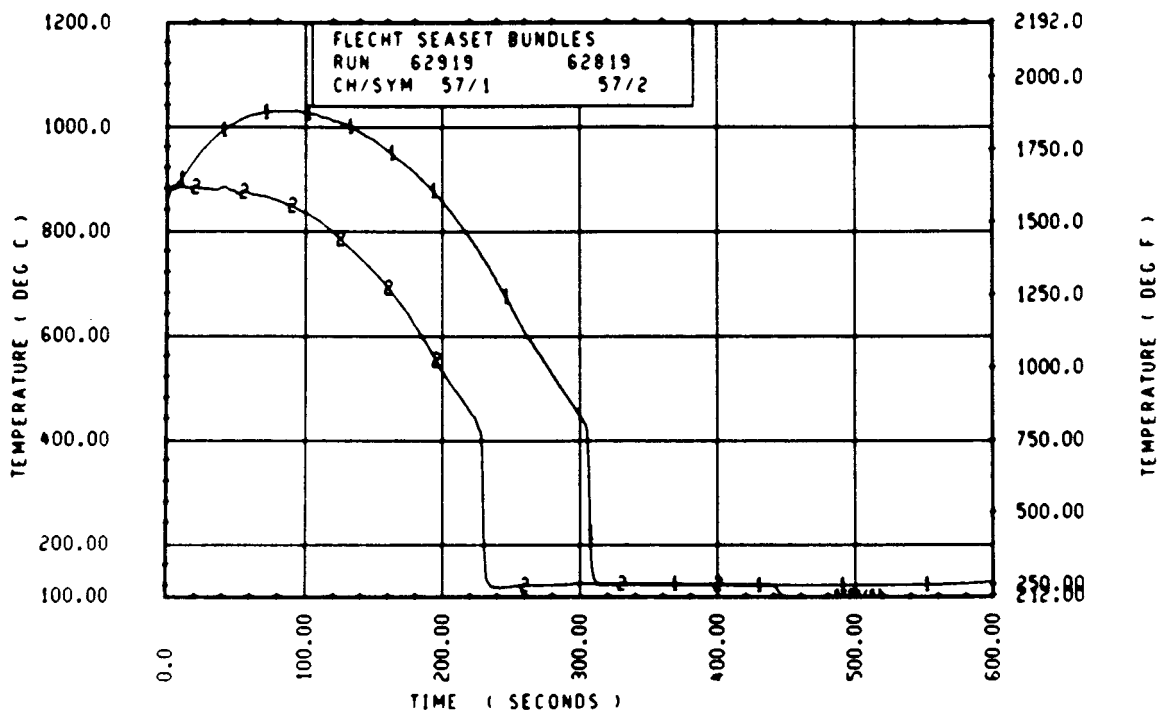
Rod 7G, 1.52 m (60 in.)



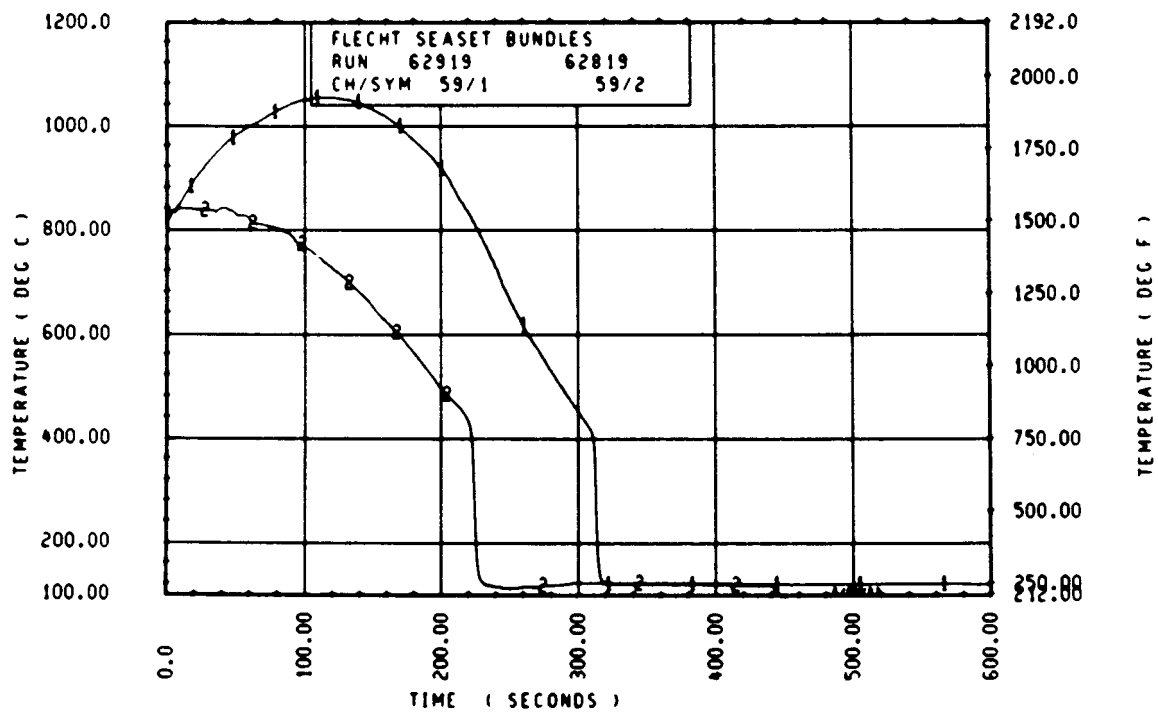
Rod 3K, 1.70 m (67 in.)



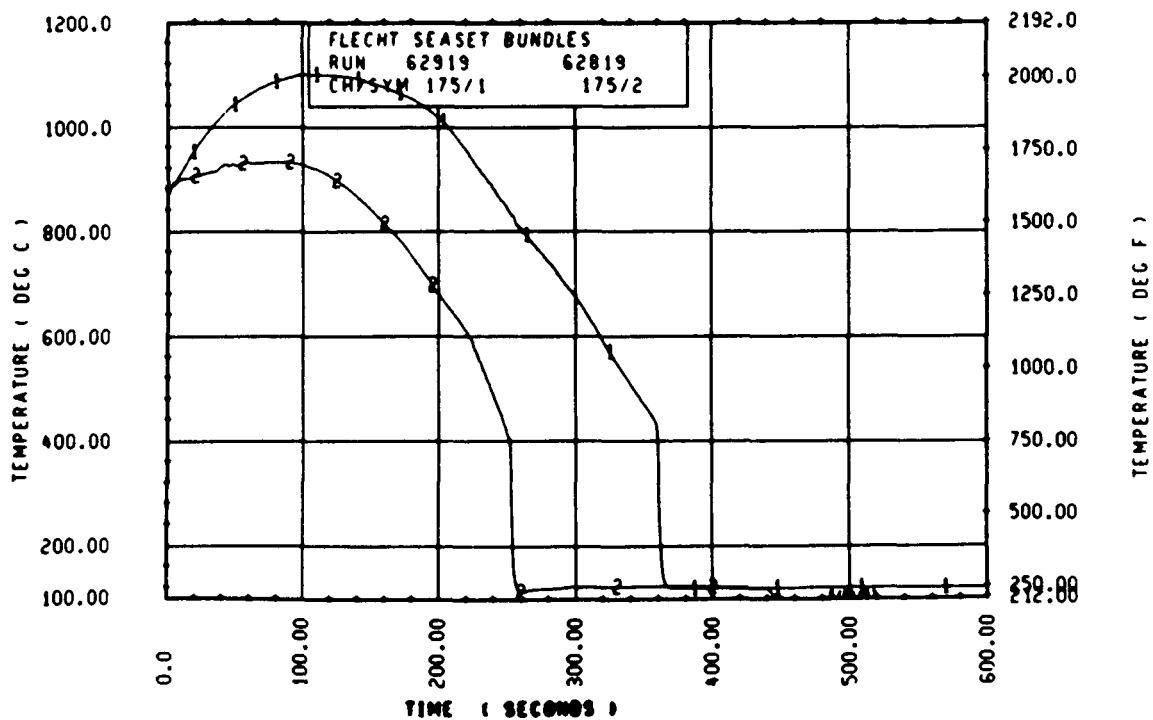
Rod 8G, 1.70 m (67 in.)



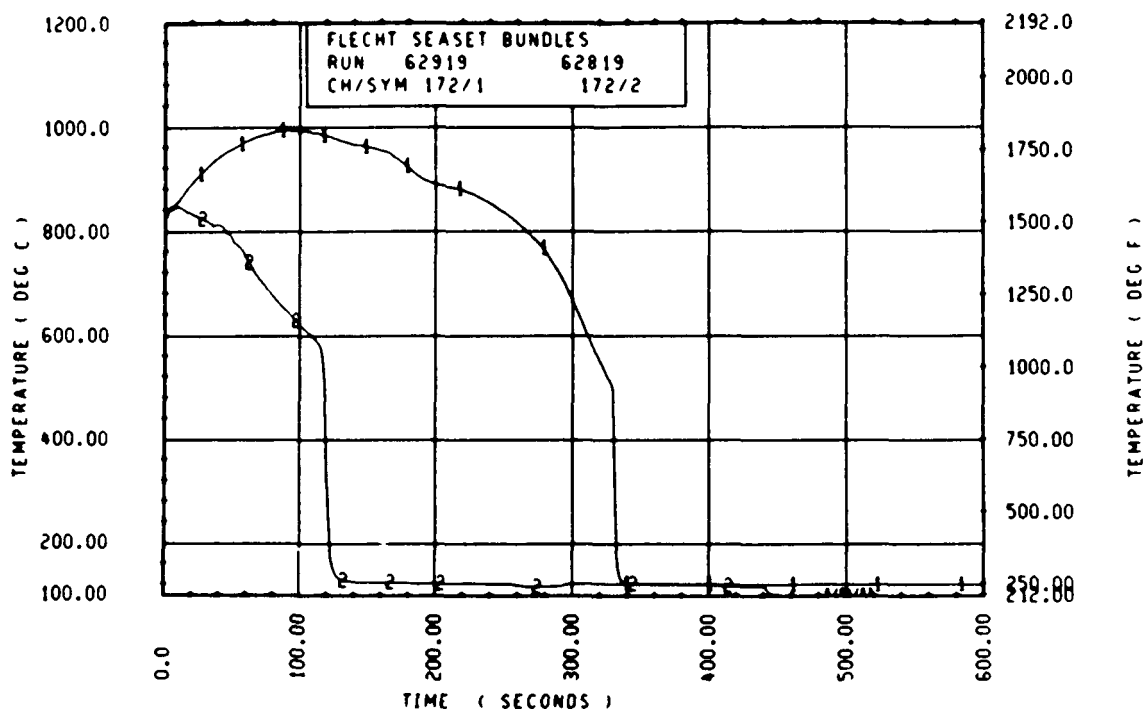
Rod 3K, 1.78 m (70 in.)



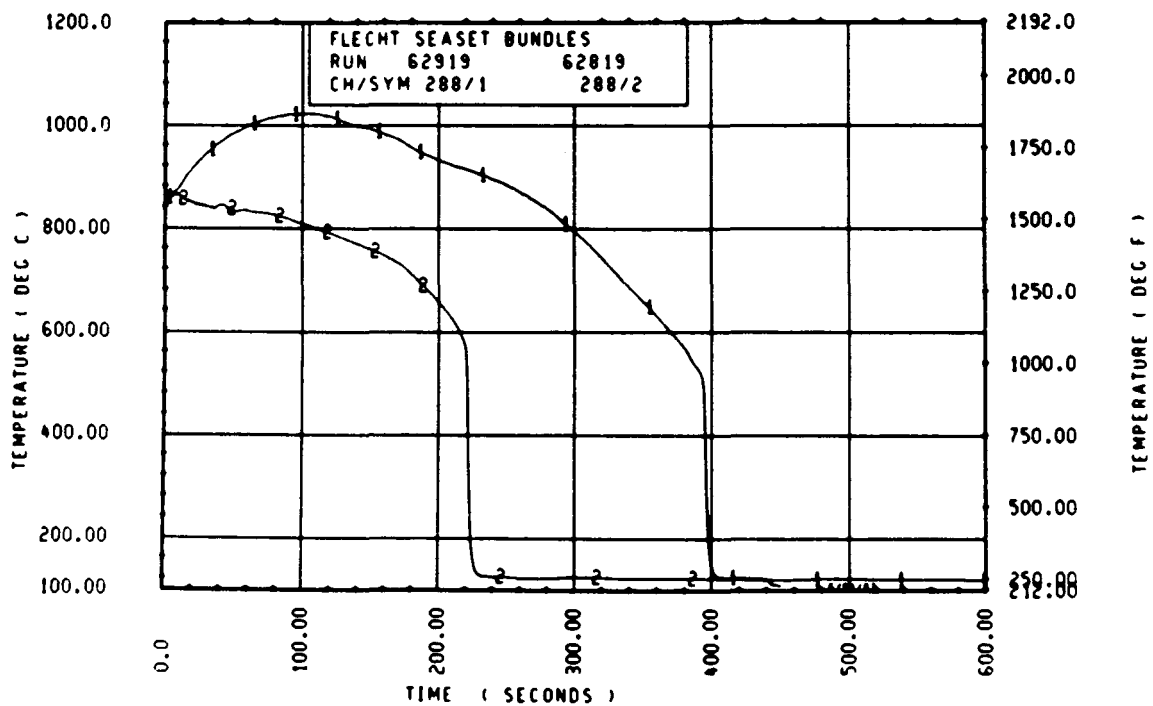
Rod 7G, 1.78 m (70 in.)



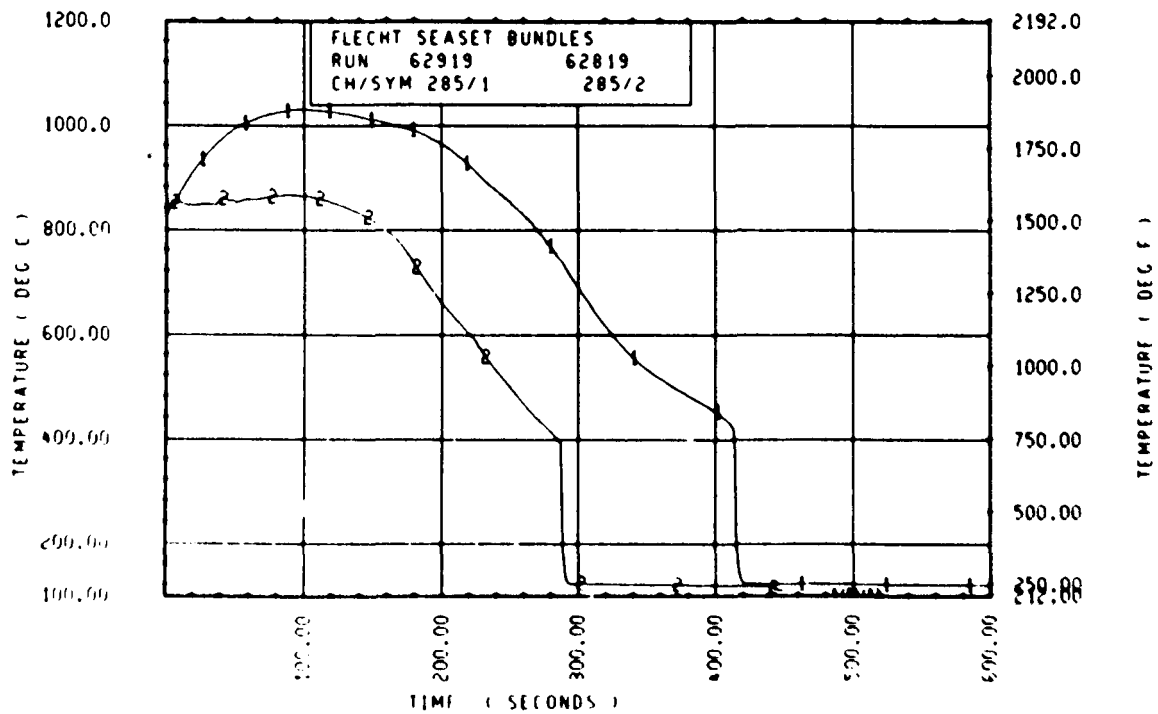
Rod 8N, 1.98 m (78 in.)



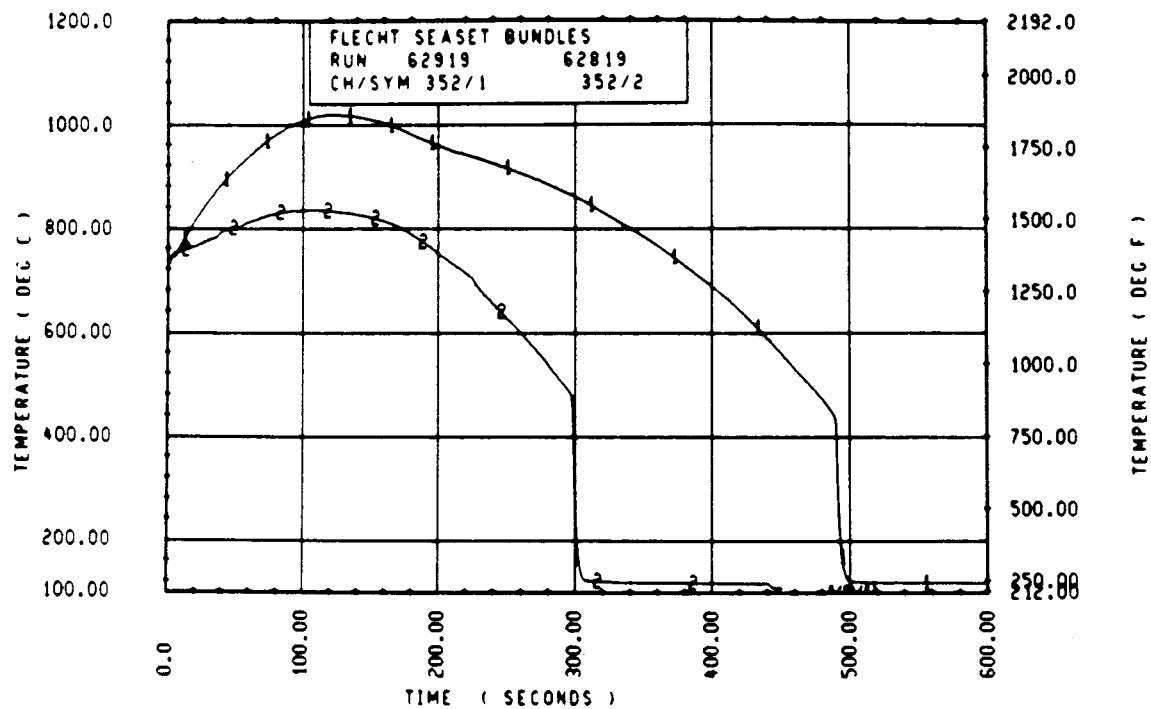
Rod 9H, 1.98 m (78 in.)



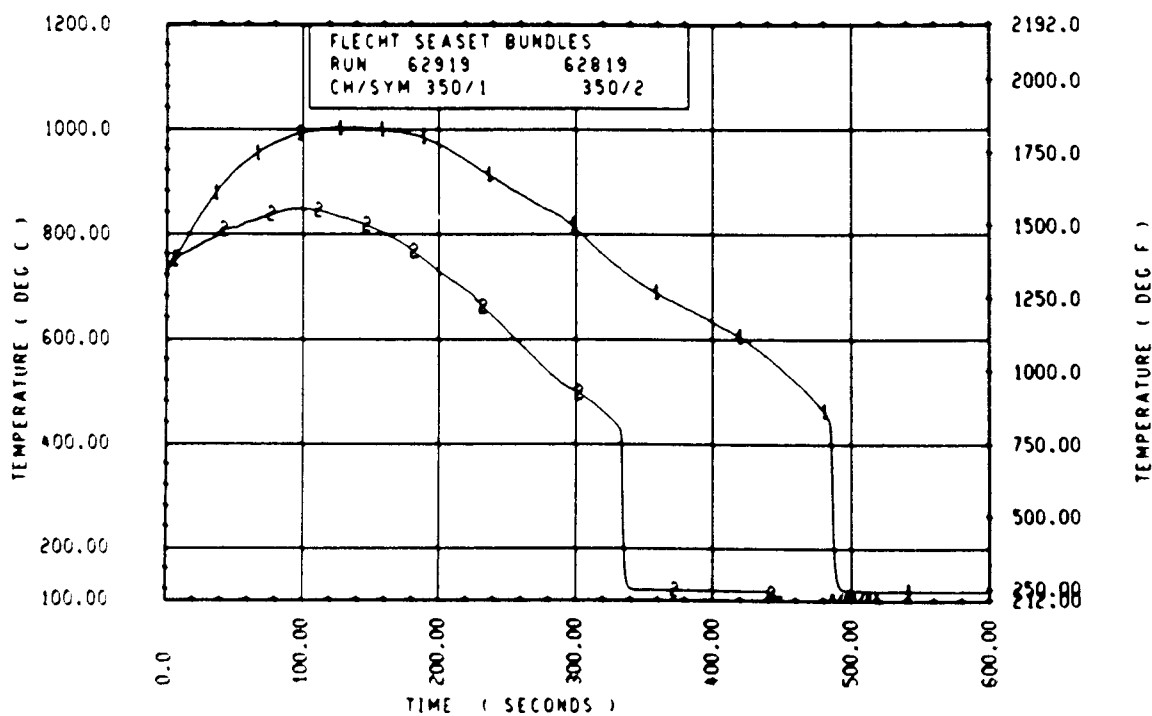
Rod 9H, 2.18 m (86 in.)



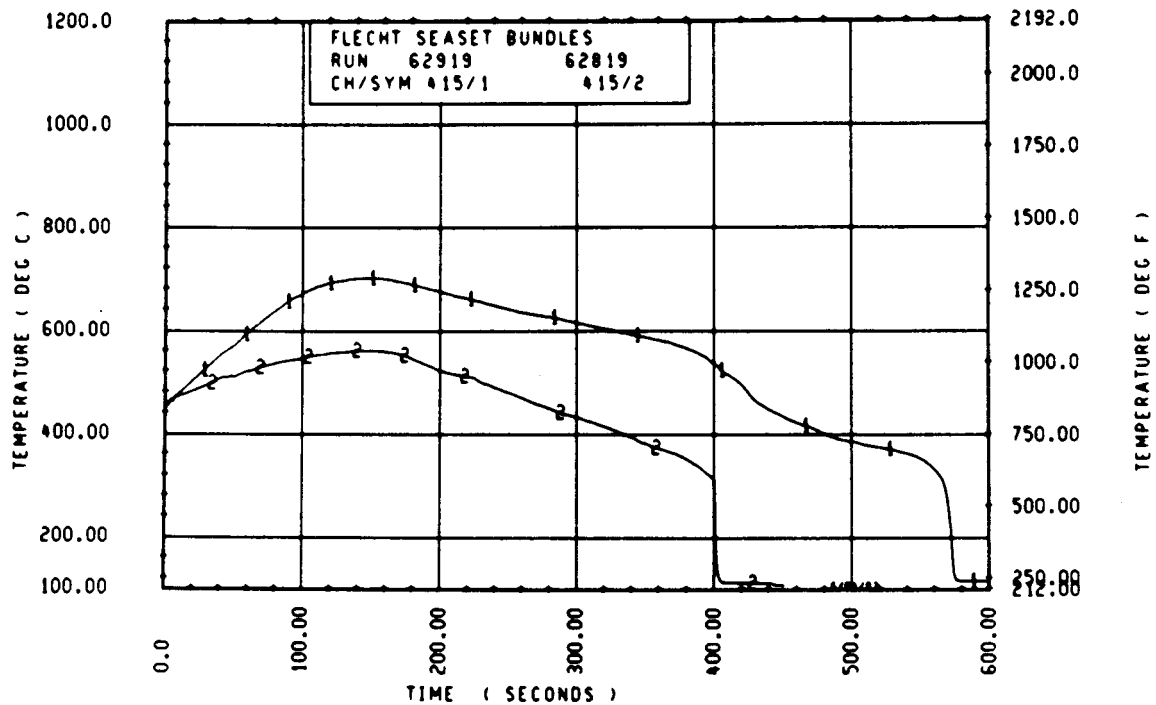
Rod 8N, 2.18 m (86 in.)



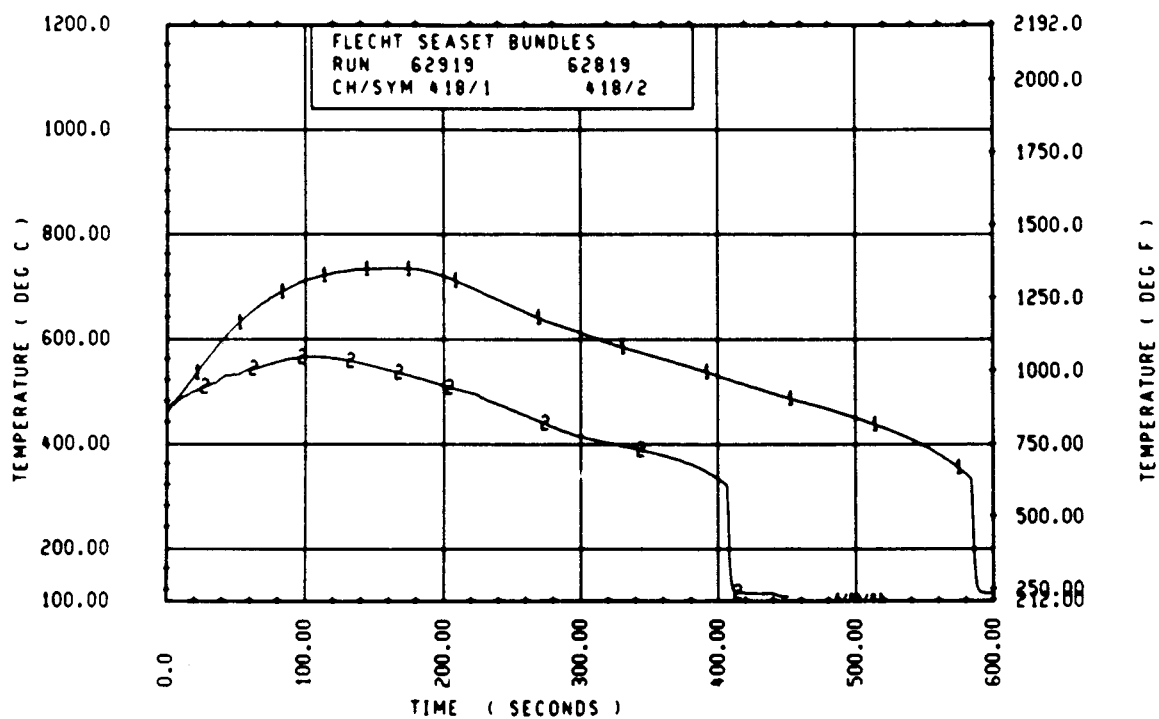
Rod 9H, 2.44 m (96 in.)



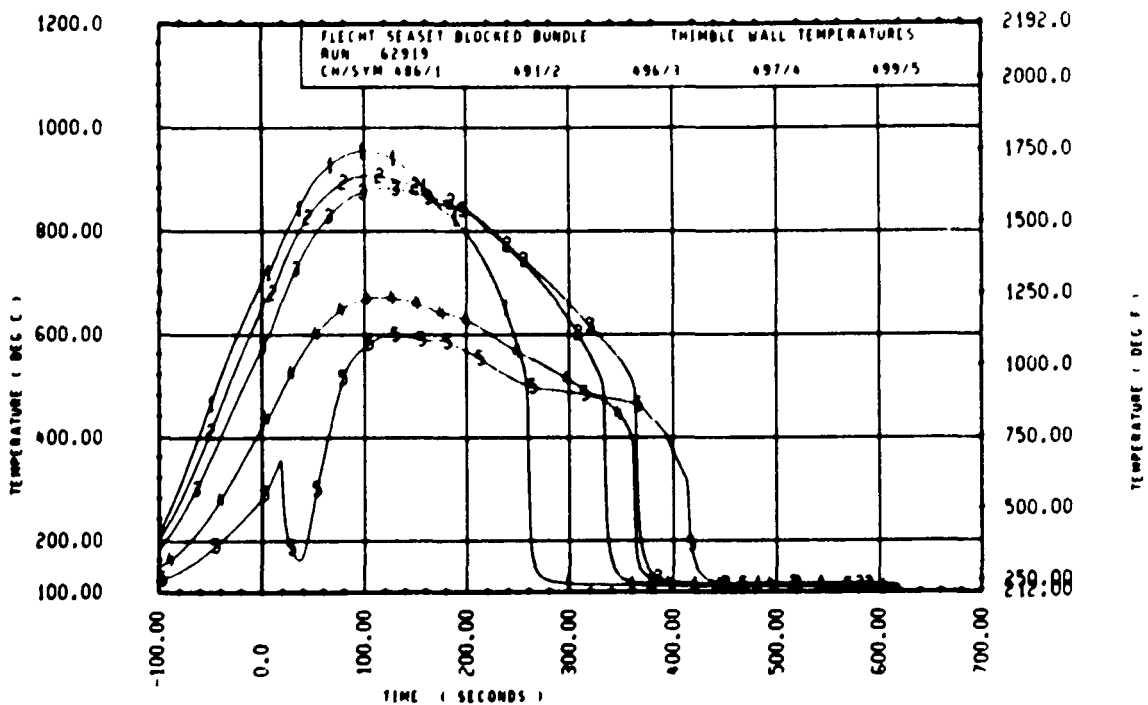
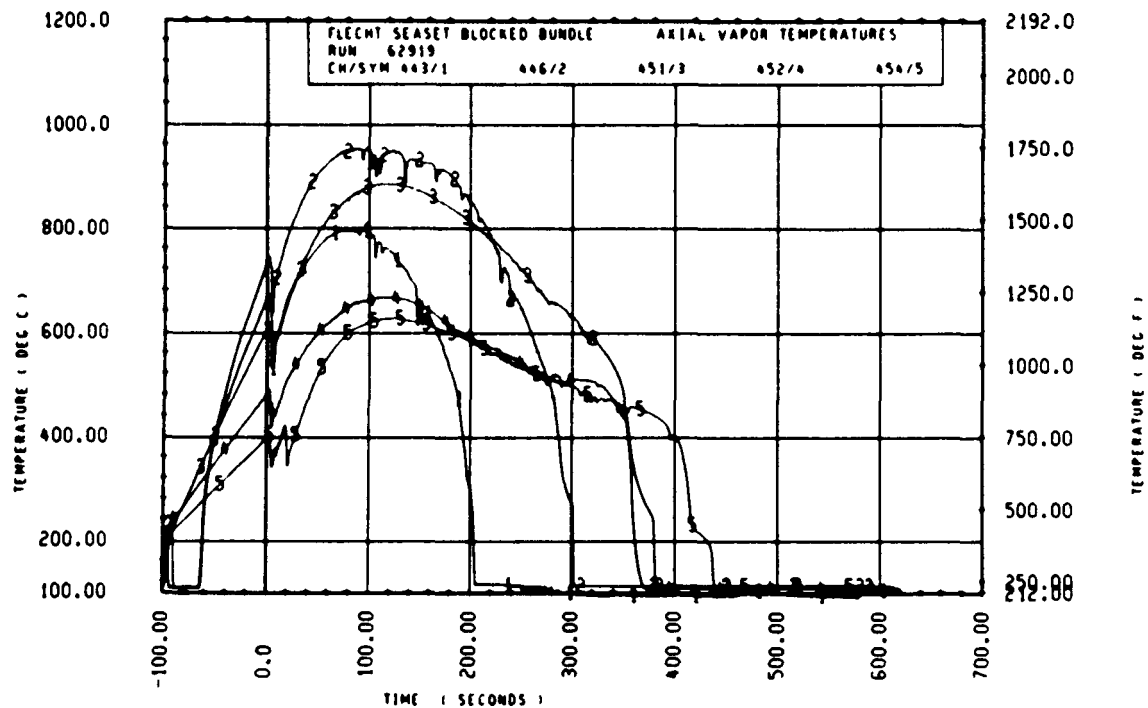
Rod 8H, 2.44 m (96 in.)

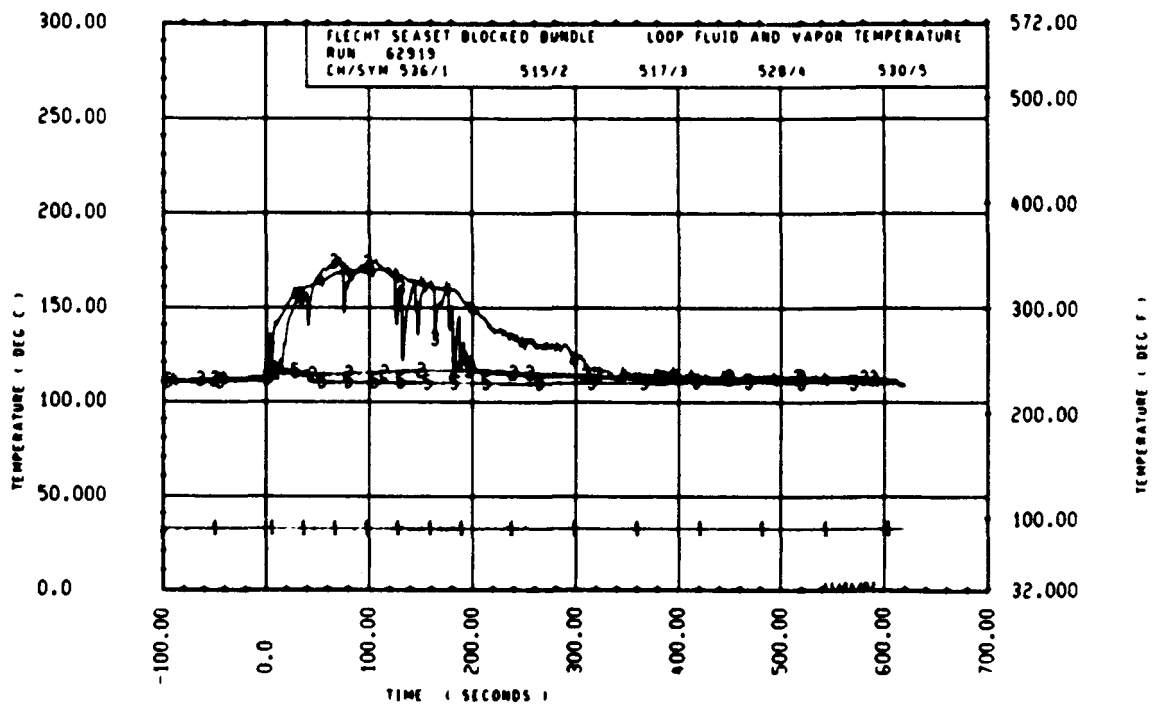
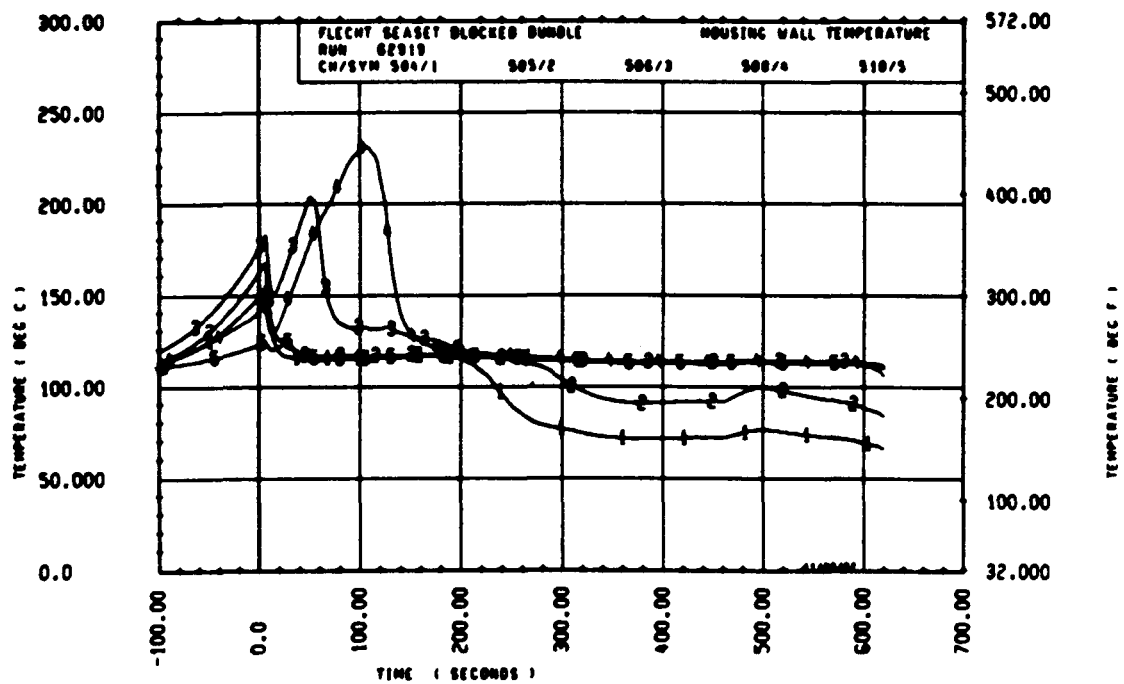


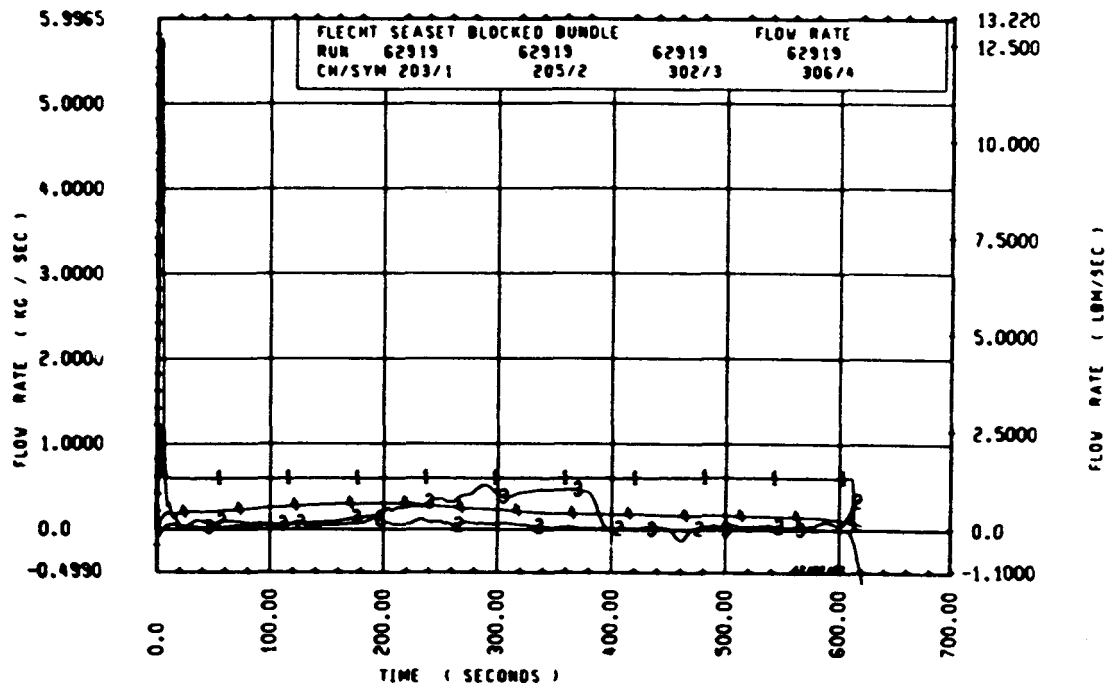
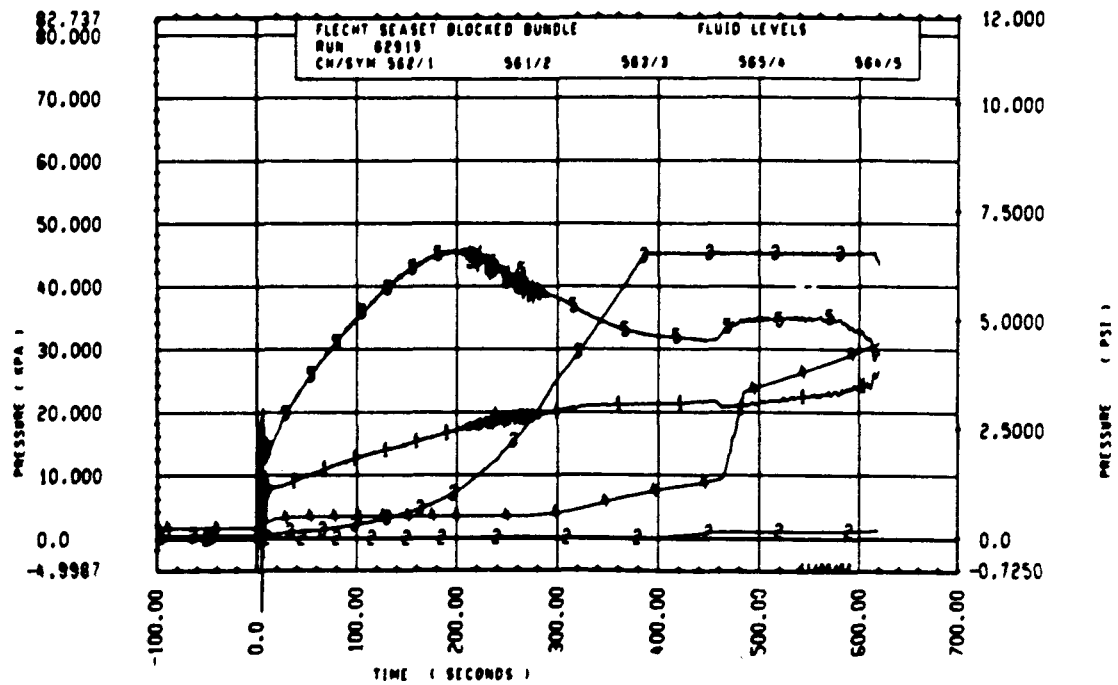
Rod 8H, 3.05 m (120 in.)

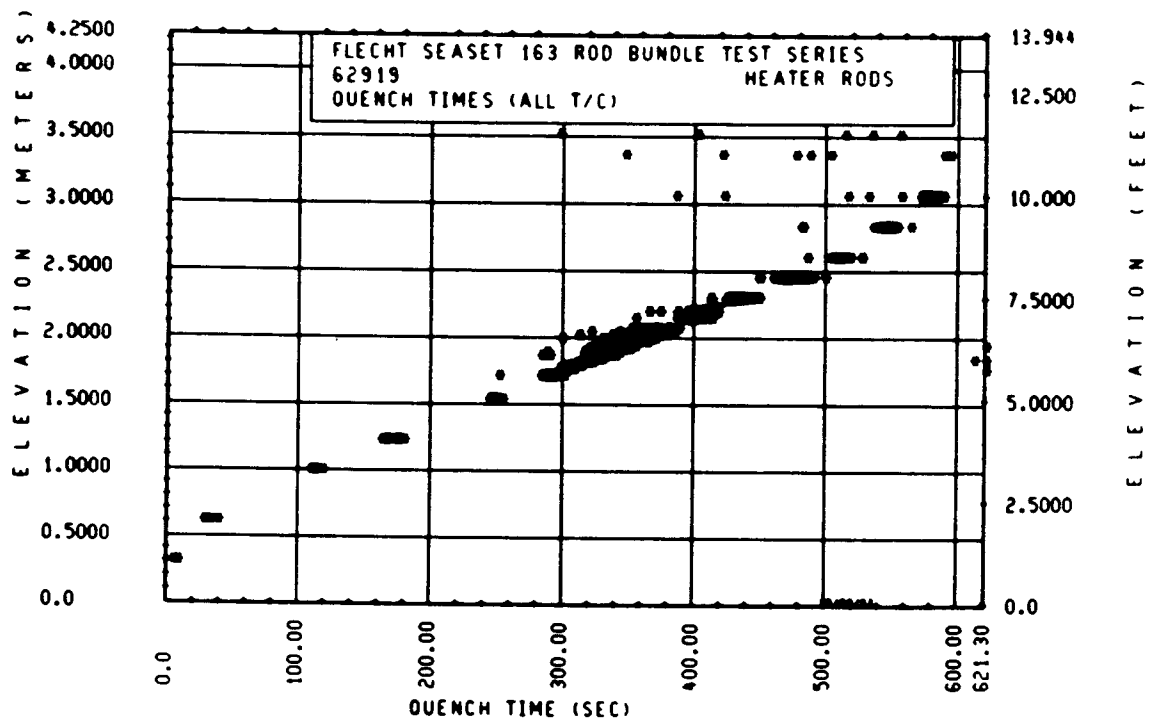
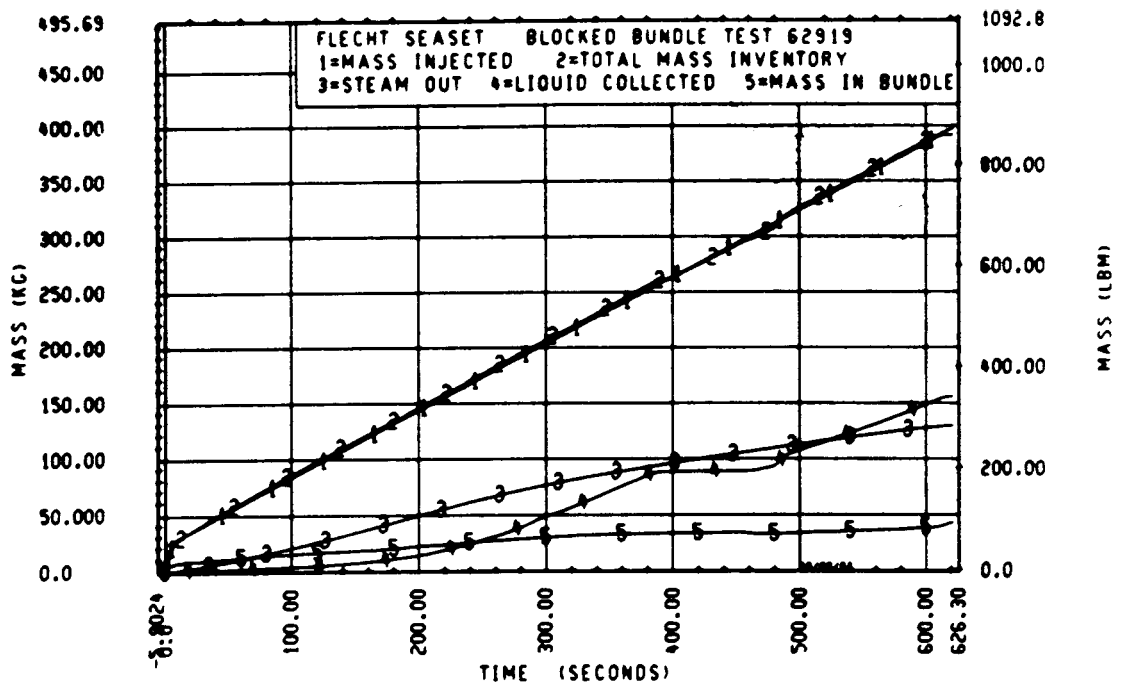


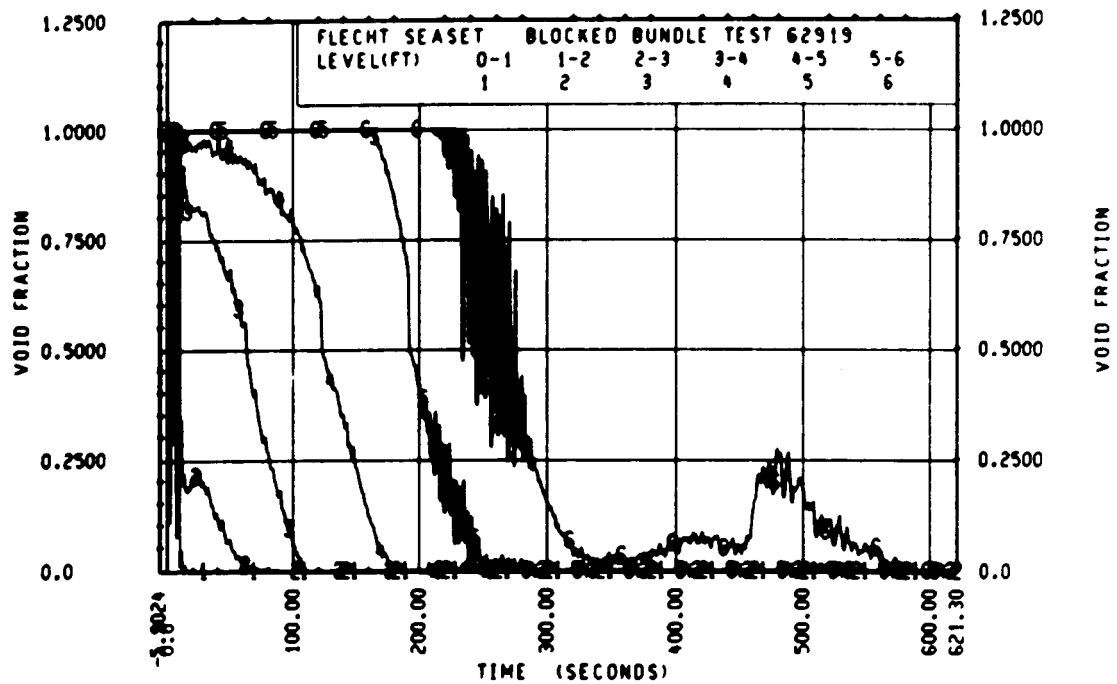
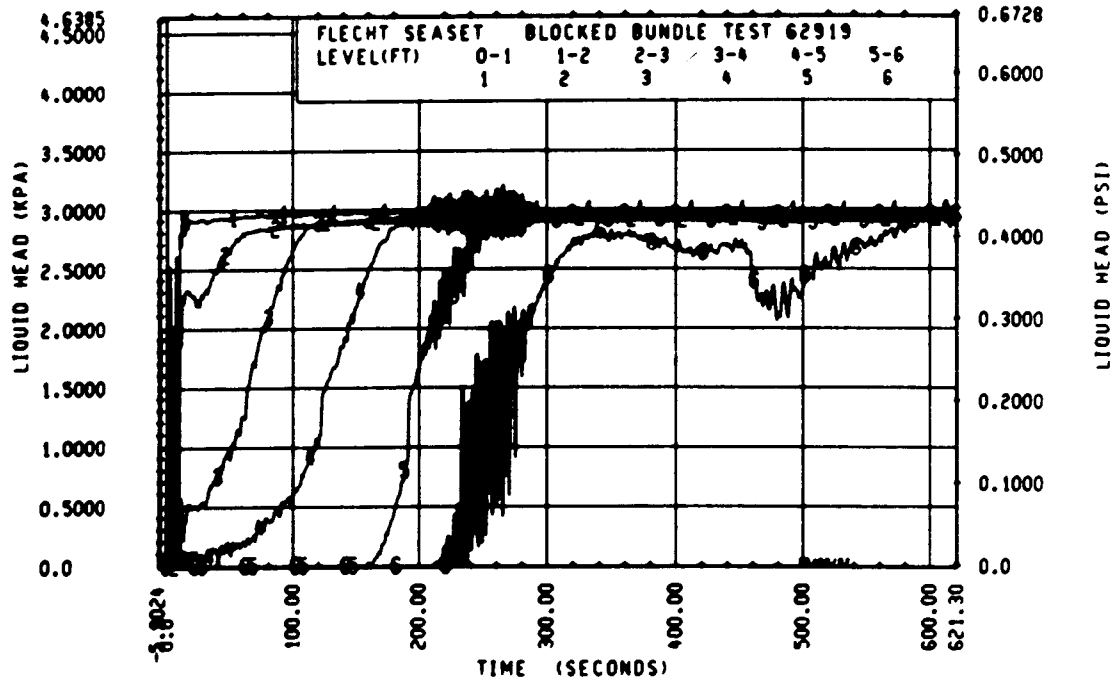
Rod 8N, 3.05 m (120 in.)

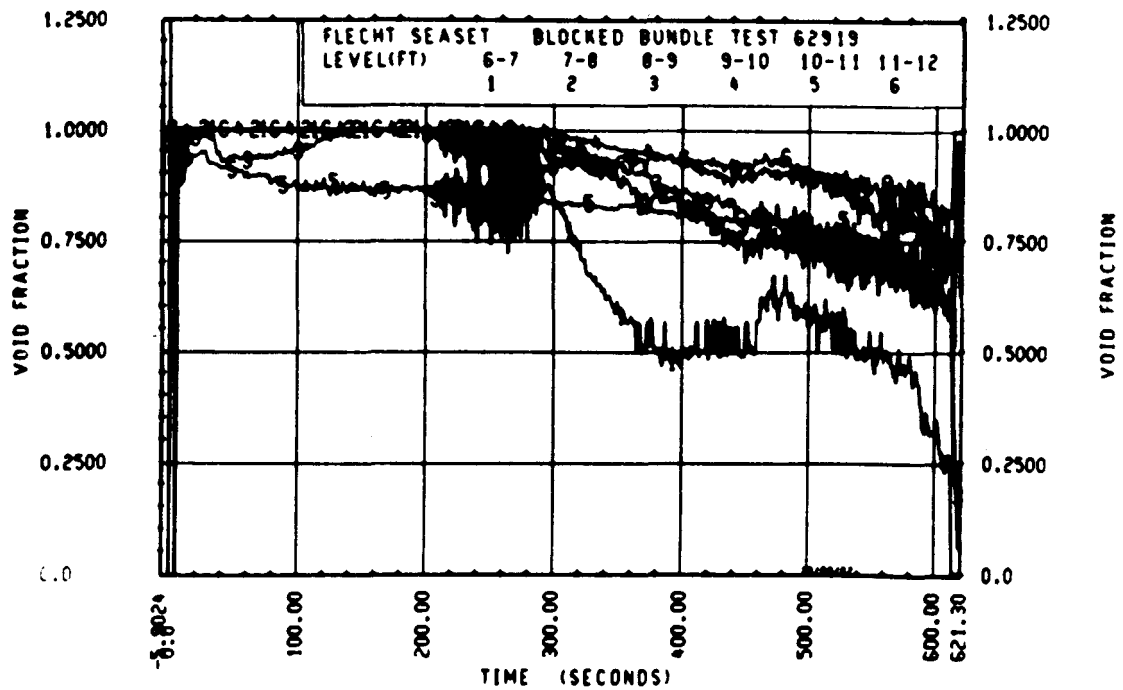
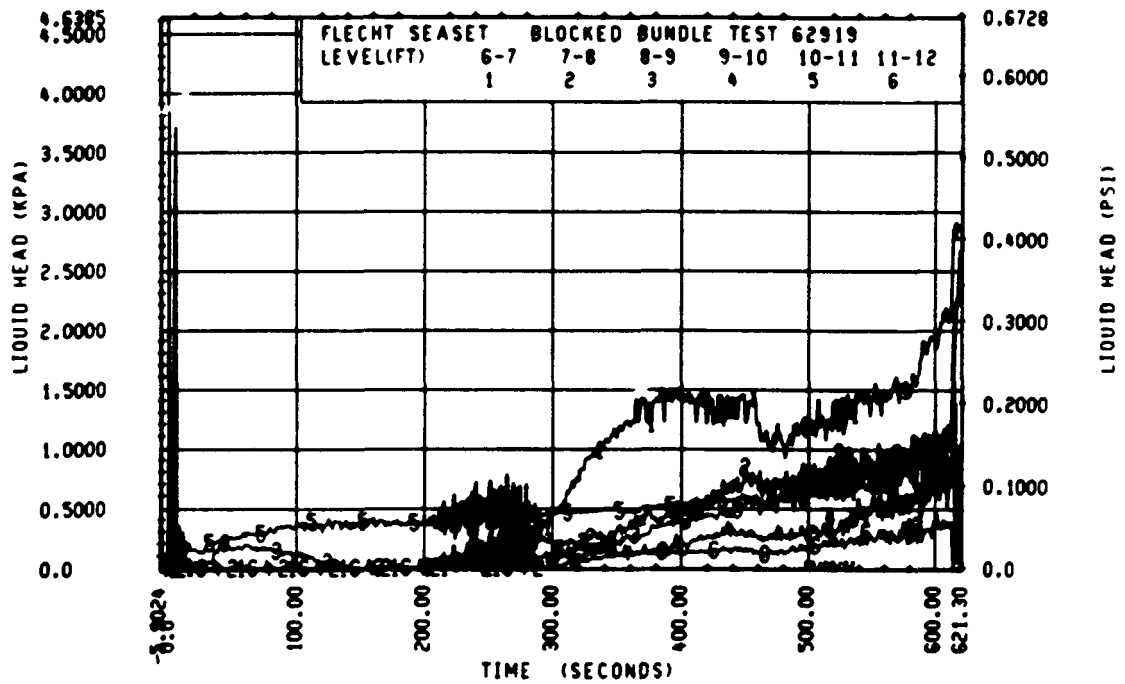












FLECHT SEASET 163-ROD BUNDLE FLOW BLOCKAGE TASK
SUMMARY AND COMMENT SHEET

Run: 63018
Test date: 10/11/82
Test type: Gravity reflood
Parameter: Pressure effect

AS-RUN TEST CONDITIONS:

Upper plenum pressure	0.276 MPa (40.0 psia)
Initial peak clad temperature and location	871.7°C (1601.0°F), 8N-1.93 m (76 in.)
Initial peak rod power:	
Peripheral rods	2.29 kW/m (0.699 kW/ft)
Bypass rods	2.30 kW/m (0.700 kW/ft)
Blockage island rods	2.29 kW/m (0.699 kW/ft)
Injection rate	5.76 kg/sec (12.7 lb/sec) for 14 sec 0.780 kg/sec (1.72 lb/sec) onward
Coolant temperature	52.2°C (126°F)
Initial bundle water level	-9.4 mm (-0.37 in.)

COMMENTS:

Carryover tank filled up at approximately 200 seconds.

Inlet mass flow: ⁽¹⁾ +7% after flow step decreasing to -1% by 40 seconds

Power decay: ⁽¹⁾ peripheral rods, 0% constant
bypass rods, -0.5% constant
blockage rods, 0% linearly increasing to +2.5% by 270
seconds

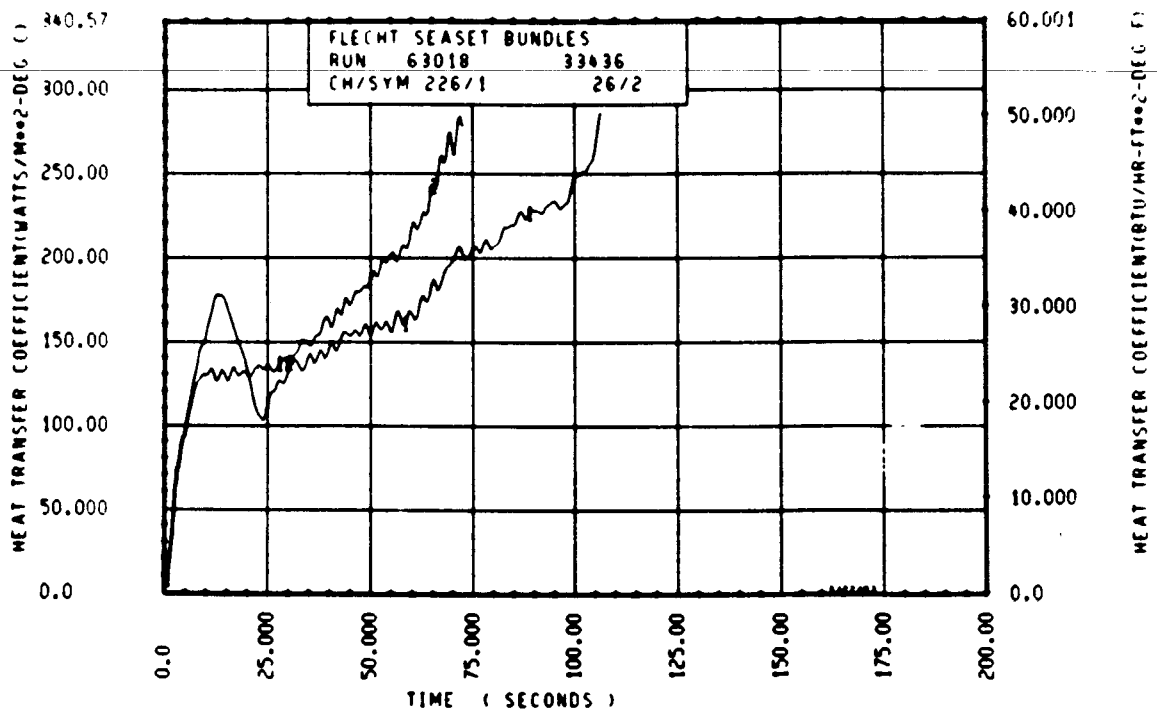
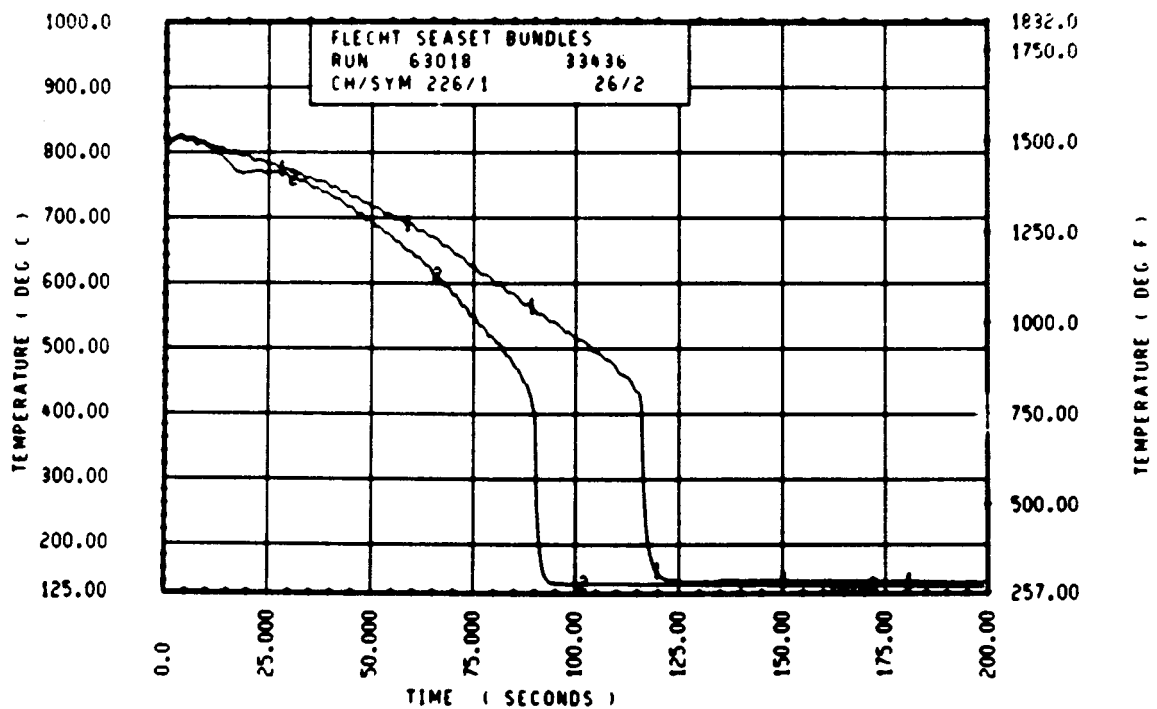
FLECHT SEASET 163 ROD BUNDLE TEST SERIES							
RUN NUMBER 63018							
ROD/LEVEL	CHAN. NO	INITIAL AT FLUCL (DEG F)	MAXIMUM TEMPERATURE (DEG F)	TEMPERATURE RISE (DEG F)	TURNAROUND TIME (SECONDS)	QUENCH TEMPERATURE (DEG F)	QUENCH TIME (SECONDS)
96 1- 0	3	669.	673.	4.	1.0	659.	3.7
10H 2- C	6	667.	898.	10.	2.0	762.	14.3
96 3- 3	9	1203.	1223.	20.	4.0	769.	51.4
3J 4- C	11	1349.	1374.	25.	4.0	754.	75.5
7H 4- C	12	1340.	1366.	26.	4.0	714.	78.6
8K 4- C	13	1350.	1386.	30.	4.0	736.	78.9
8N 4- C	14	1347.	1373.	26.	4.0	714.	76.6
12D 4- 0	17	1340.	1363.	23.	4.0	731.	78.4
5E 5- C	20	1466.	1501.	35.	4.0	846.	113.1
76 5- C	21	1537.	1574.	37.	6.5	863.	110.9
96 5- C	24	1507.	1542.	36.	6.5	862.	113.0
5E 5- 7	33	1522.	1558.	36.	4.0	825.	128.2
86 5- 7	45	1540.	1578.	38.	6.5	723.	142.3
9H 5- 9	52	1464.	1524.	40.	4.0	716.	127.3
76 5-10	59	1502.	1545.	42.	6.5	873.	117.2
7F 5-11	62	1444.	1480.	36.	4.0	902.	83.9
46 5-11	64	1526.	1562.	36.	4.0	758.	153.9
21 6- C	67	1573.	1612.	39.	6.5	812.	153.9
5D 6- 0	70	1483.	1516.	33.	4.0	735.	152.7
6J 6- C	74	1514.	1553.	35.	4.0	776.	154.9
7M 6- C	66	1536.	1576.	38.	9.0	783.	149.7
11E 6- C	80	1496.	1534.	36.	9.0	763.	153.1
8H 6- 2	97	1365.	1399.	34.	4.0	830.	92.6
5H 6- 2	99	1525.	1560.	35.	4.0	755.	160.0
9E 6- 2	105	1323.	1418.	95.	19.0	1276.	46.3
8M 6- 3	111	1404.	1443.	34.	4.0	854.	97.7
46 6- 3	124	1542.	1580.	38.	6.5	757.	166.1
11H 6- 4	134	1477.	1515.	39.	6.5	783.	82.4
9D 6- 4	143	1532.	1574.	42.	6.5	728.	164.0
9J 6- 5	165	1510.	1543.	34.	4.0	862.	110.4
9M 6- 5	166	1577.	1615.	38.	6.5	792.	167.4
8J 6- 6	192	1557.	1590.	34.	4.0	1014.	102.9
9D 6- 6	193	1534.	1587.	48.	14.0	762.	169.0
11F 6- 6	173	1533.	1565.	32.	4.0	765.	166.4
46 7- C	261	1484.	1516.	32.	4.0	730.	198.9
7D 7- 6	309	1464.	1504.	35.	4.0	806.	161.6
76 7- 6	312	1507.	1542.	36.	4.0	962.	146.7
11E 7- 6	325	1434.	1471.	37.	6.5	763.	206.5
5L 8- 0	337	1248.	1351.	53.	23.5	706.	226.9
7H 8- C	345	1343.	1389.	46.	23.0	811.	198.9
7K 8- C	346	1346.	1389.	43.	9.0	704.	221.1
5J 8- 6	366	1127.	1160.	33.	4.0	731.	221.7
78 8- 6	368	1133.	1163.	30.	4.0	660.	243.1
7E 9- 3	383	1066.	1124.	37.	9.0	672.	247.0
8H 9- 3	387	1044.	1078.	34.	9.0	621.	248.1
9C 9- 3	389	1040.	1071.	31.	9.0	607.	252.1
11F 9- 3	394	1037.	1069.	32.	9.0	725.	186.3
7M10- C	408	846.	925.	79.	35.0	557.	270.1
6M10- C	415	853.	960.	106.	66.0	605.	264.1
8K10- C	417	856.	929.	72.	60.0	564.	267.1
8N10- C	418	871.	974.	103.	44.0	603.	277.1
6M11- C	429	691.	707.	16.	4.0	519.	178.1
9611- C	431	685.	704.	19.	6.5	676.	32.6
11E11- 0	432	688.	705.	17.	4.0	550.	164.6
5J11- 6	436	671.	686.	15.	4.0	603.	103.0
7811- 6	437	634.	669.	30.	39.0	267.	173.0
6J11- 6	438	683.	698.	16.	6.5	513.	233.9

RUN 63018 HEATER ROD STATISTICAL DATA

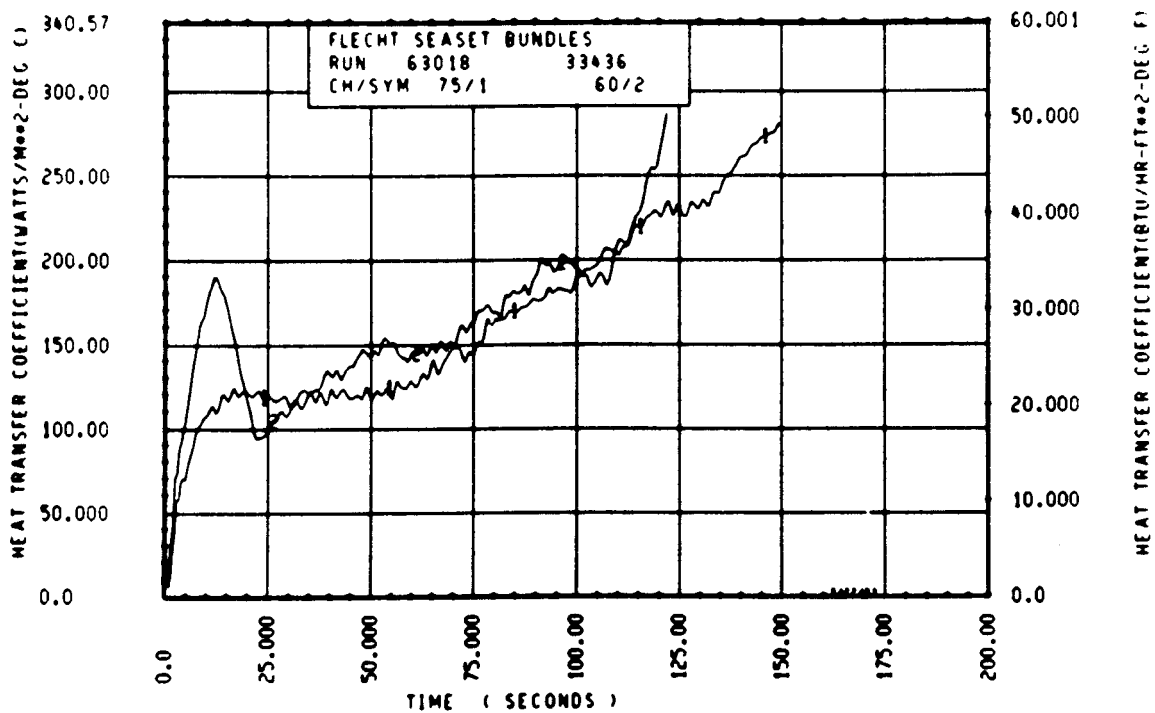
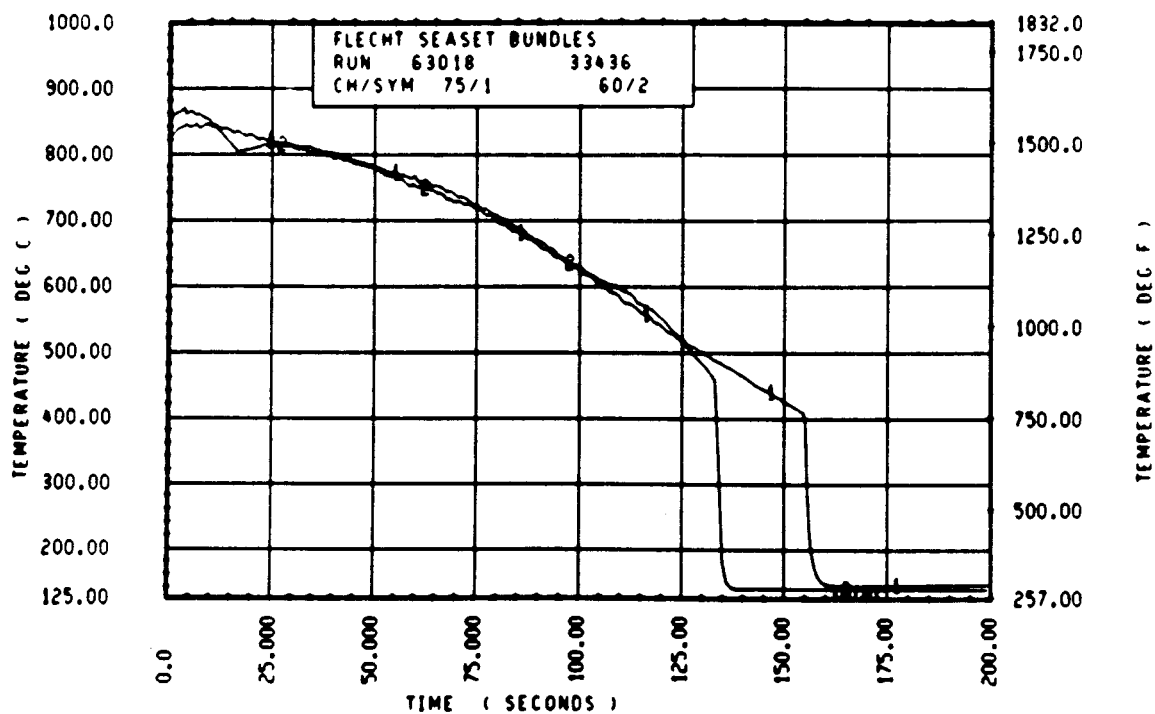
ELEV	INITIAL TEMP (DEG F)			MAX TEMP (DEG F)			TURNAROUND TIME (SEC)		
	MAX	MIN	MEAN	MAX	MIN	MEAN	MAX	MIN	MEAN
12	673.2	664.0	671.5	677.4	673.2	675.7	1.5	1.0	1.2
24	887.4	861.5	871.2	897.7	871.9	881.5	2.0	2.0	2.0
39	1203.5	1145.4	1164.0	1223.3	1166.1	1189.0	4.0	4.0	4.0
48	1365.9	1339.5	1344.7	1388.0	1362.7	1375.3	4.0	4.0	4.0
60	1537.6	1366.1	1483.7	1573.8	1414.6	1517.7	6.5	4.0	5.0
67	1581.4	1440.5	1530.4	1622.9	1524.4	1578.8	9.0	4.0	5.0
69	1519.7	1464.1	1504.7	1557.6	1524.0	1541.8	9.0	4.0	6.4
70	1590.1	1454.5	1517.0	1626.2	1502.3	1556.5	9.0	4.0	6.5
71	1520.2	1431.7	1473.5	1561.9	1477.7	1513.5	9.0	4.0	6.5
72	1574.9	1456.3	1526.2	1611.9	1493.7	1565.0	9.5	4.0	6.2
73	1572.6	1463.6	1516.7	1609.7	1501.2	1552.7	9.0	4.0	6.1
74	1577.1	1364.9	1492.1	1610.8	1398.6	1532.2	9.0	4.0	6.1
75	1582.5	1409.3	1500.5	1616.3	1443.5	1543.2	13.0	4.0	5.0
76	1601.0	1440.5	1522.3	1637.2	1480.9	1570.1	9.0	4.0	6.0
77	1577.1	1477.7	1526.5	1615.2	1509.9	1564.7	13.0	4.0	5.6
78	1597.7	1500.2	1544.3	1639.4	1537.0	1581.0	17.0	4.0	6.3
79	1581.4	1492.7	1545.1	1615.2	1533.7	1582.8	23.0	4.0	6.5
80	1556.7	1440.5	1500.0	1593.3	1532.6	1573.2	26.5	4.0	10.0
81	1556.5	1444.4	1500.0	1590.1	1512.0	1557.2	26.5	4.0	10.3
84	1534.6	1425.3	1480.0	1566.2	1452.0	1518.4	4.0	2.5	3.5
86	1576.0	1466.1	1521.0	1606.4	1500.1	1554.2	6.5	4.0	4.1
90	1511.0	1373.3	1467.0	1548.9	1412.5	1504.4	9.0	4.0	5.2
96	1384.9	1267.1	1336.0	1447.8	1324.7	1395.2	41.5	6.5	26.4
102	1181.7	1039.0	1144.4	1211.8	1067.9	1177.6	6.5	4.0	4.2
111	1087.5	1022.5	1054.0	1123.7	1054.5	1087.5	11.5	6.5	8.6
120	913.2	813.4	857.0	997.8	842.9	934.3	79.5	6.5	46.1
132	691.1	676.5	685.5	715.1	695.3	703.9	66.0	4.0	14.3
138	682.7	636.6	660.0	698.4	668.0	680.4	39.0	4.0	13.0

RUN 63018 HEATER ROD STATISTICAL DATA

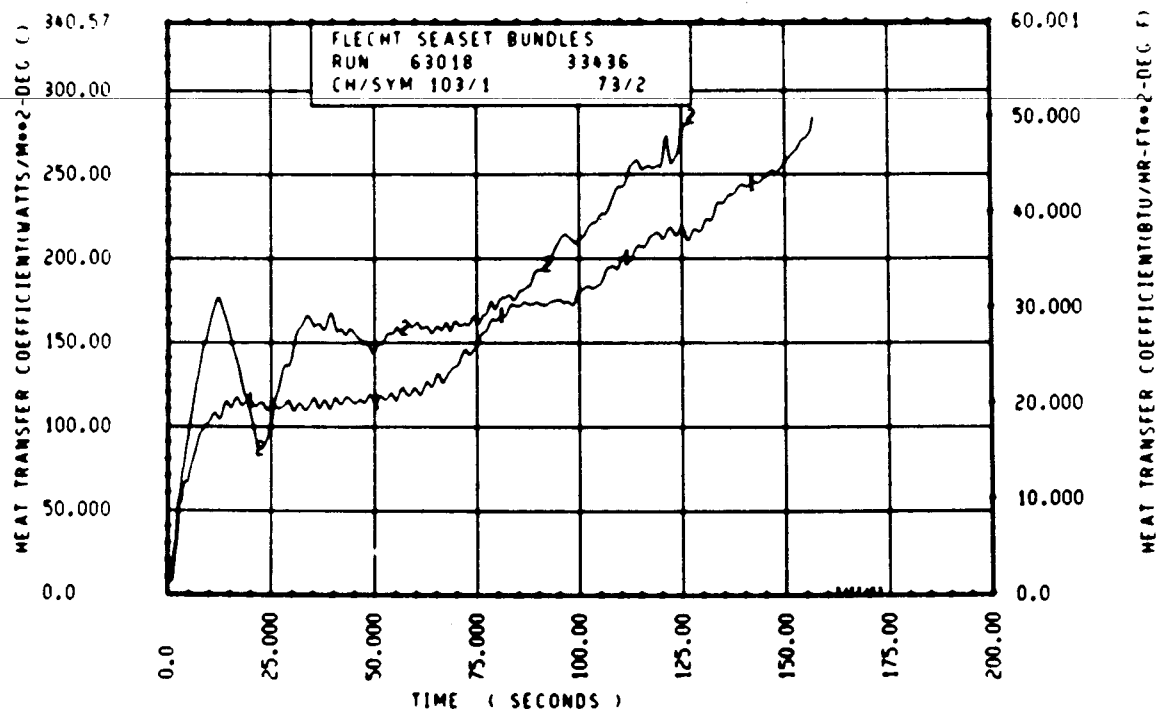
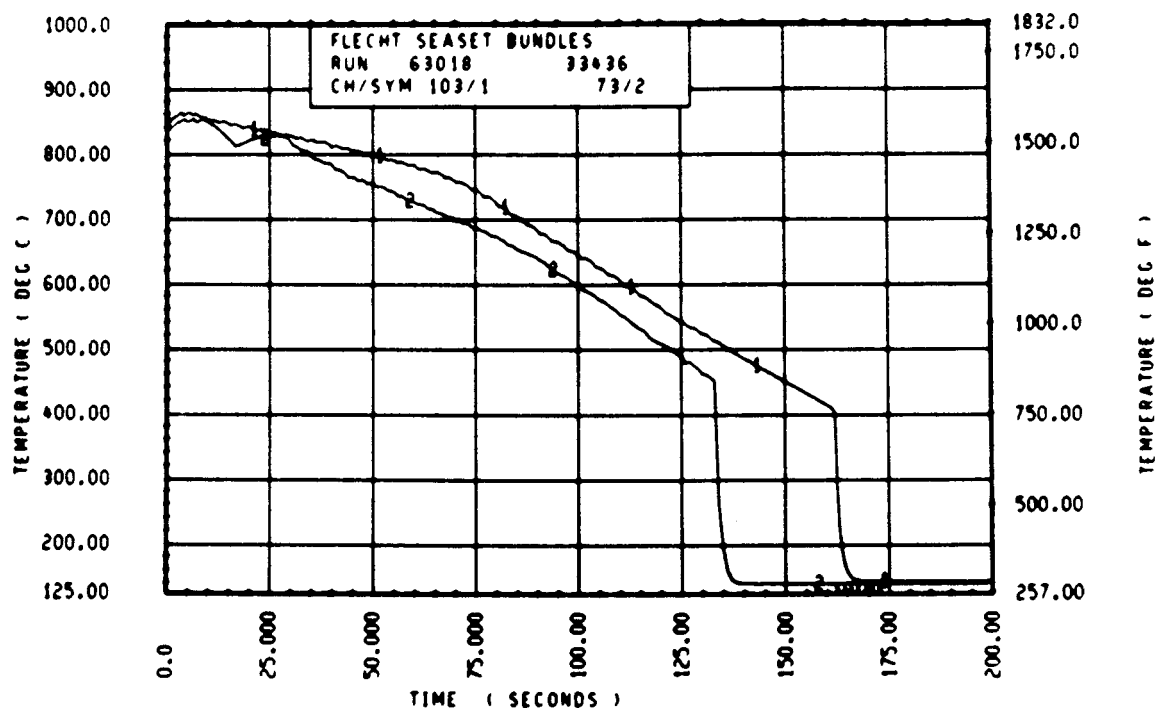
ELEV	TEMP RISE (DEG F)			QUENCH TEMP (DEG F)			QUENCH TIME (SEC)		
	MAX	MIN	MEAN	MAX	MIN	MEAN	MAX	MIN	MEAN
12	4.2	4.2	4.2	664.8	659.0	662.1	3.9	3.7	3.6
24	10.3	10.3	10.3	762.5	742.9	750.5	14.3	14.1	14.2
39	20.7	16.6	14.2	768.7	706.7	738.3	52.5	51.4	51.5
48	24.5	22.1	25.6	753.9	713.6	733.2	78.9	75.4	77.3
60	34.0	26.5	34.0	863.8	779.0	836.1	120.0	110.9	114.3
67	132.4	31.4	40.0	855.4	712.7	779.5	142.3	105.9	133.6
69	41.0	33.6	37.1	845.1	718.1	780.8	146.9	121.5	137.5
70	42.6	36.1	34.6	872.9	767.2	804.9	148.3	117.3	140.6
71	45.9	35.7	40.0	961.9	685.0	801.8	153.9	83.4	133.1
72	34.1	33.3	36.6	812.4	702.8	769.7	157.0	144.7	153.5
73	41.1	31.5	36.0	823.5	721.5	767.0	161.4	152.6	156.0
74	44.7	33.7	37.1	876.5	711.4	774.8	164.0	70.9	144.4
75	47.0	30.3	36.7	937.3	535.1	776.2	168.1	74.6	138.1
76	42.2	33.5	37.6	1031.3	724.6	799.9	170.3	78.4	148.5
77	45.5	32.2	36.2	1056.1	740.2	902.1	175.2	73.4	119.7
78	47.6	30.3	36.7	1073.5	728.3	876.7	175.9	67.6	124.8
79	59.5	31.4	37.6	1052.0	749.2	895.9	180.3	72.4	126.7
80	58.5	31.4	42.6	1106.6	263.5	876.6	293.1	76.4	146.9
81	68.6	33.3	46.3	1065.0	772.5	933.6	186.0	103.4	133.7
84	38.7	26.7	31.5	961.2	695.9	778.8	200.1	104.3	169.3
86	35.7	24.2	33.2	999.3	666.9	809.1	203.1	120.6	166.6
90	42.1	34.2	36.6	994.3	694.3	823.6	214.1	146.7	184.2
96	94.6	42.2	57.2	931.7	681.6	790.6	232.9	177.2	210.4
102	36.3	26.8	33.2	771.4	613.4	699.0	243.1	214.1	228.1
111	36.1	26.8	33.6	765.0	586.3	660.1	256.1	172.7	236.0
120	122.9	27.9	77.4	754.9	535.6	626.4	277.1	137.7	245.3
132	27.2	15.7	16.4	676.3	485.1	534.7	266.1	32.6	160.2
138	30.5	14.7	14.7	603.1	286.8	447.6	233.9	54.5	146.4



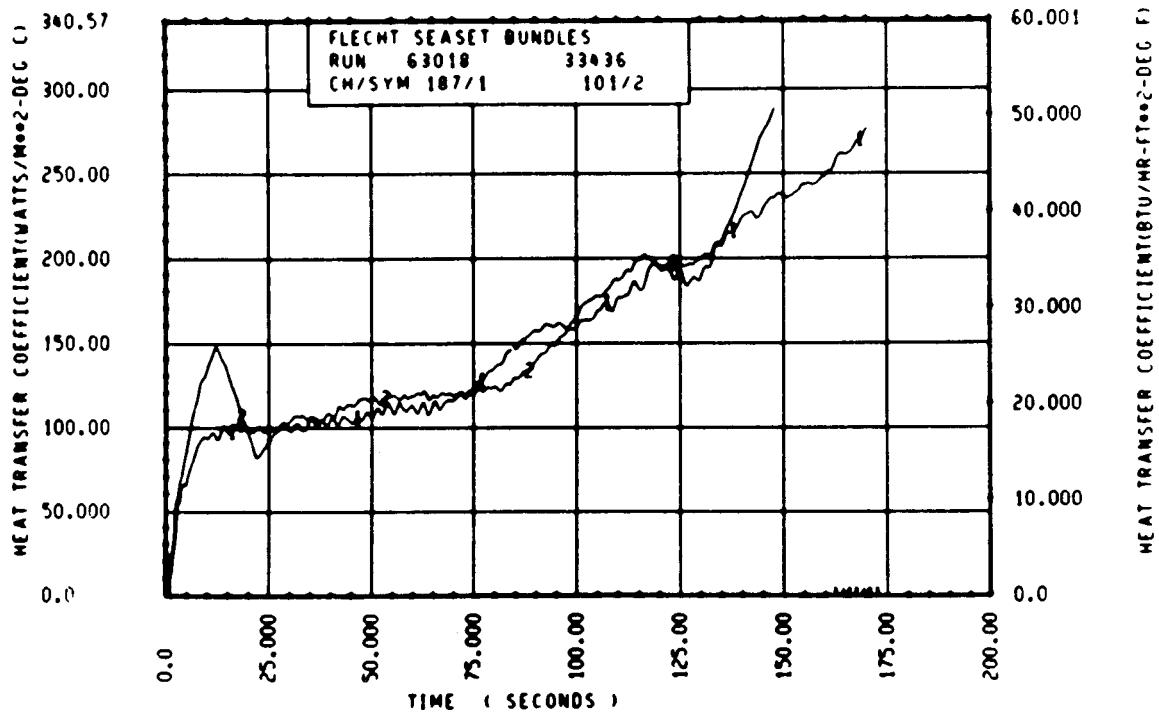
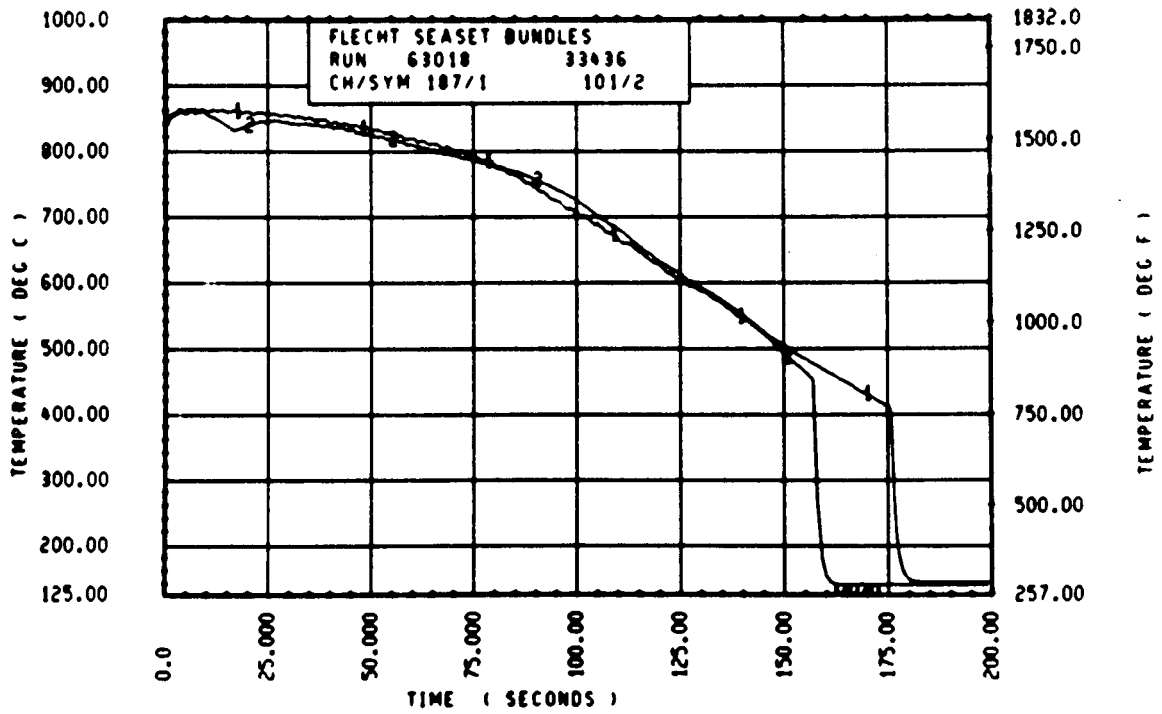
Rod 11E, 1.52 m (60 in.)



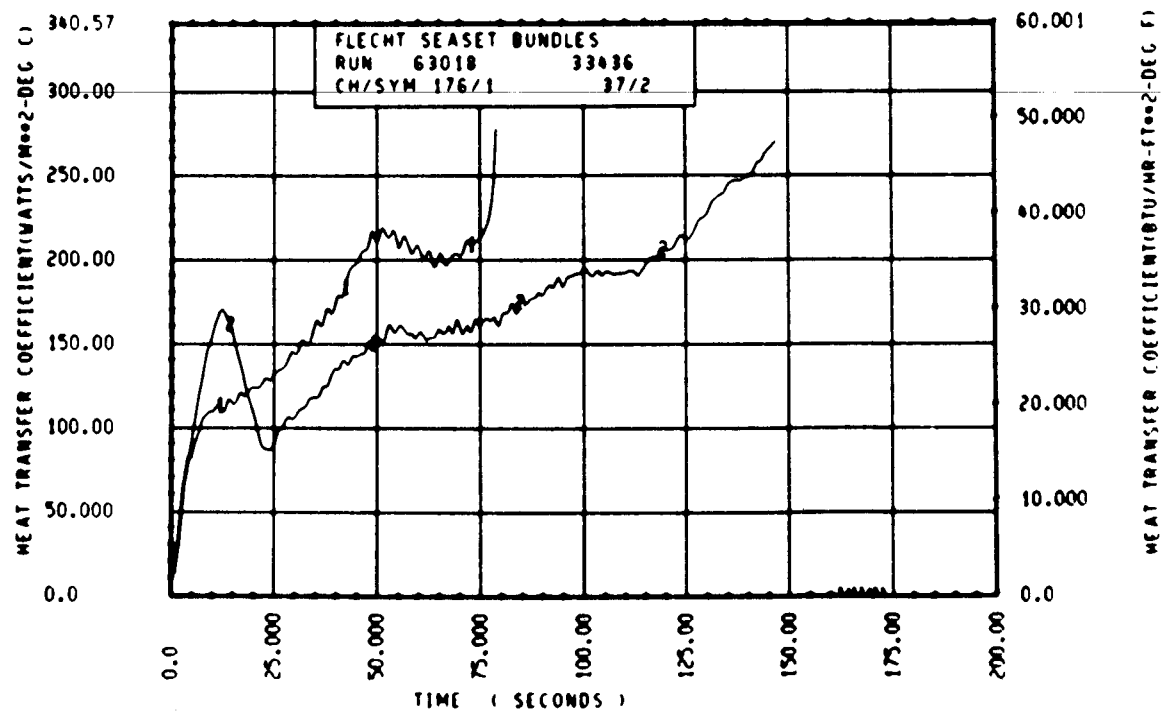
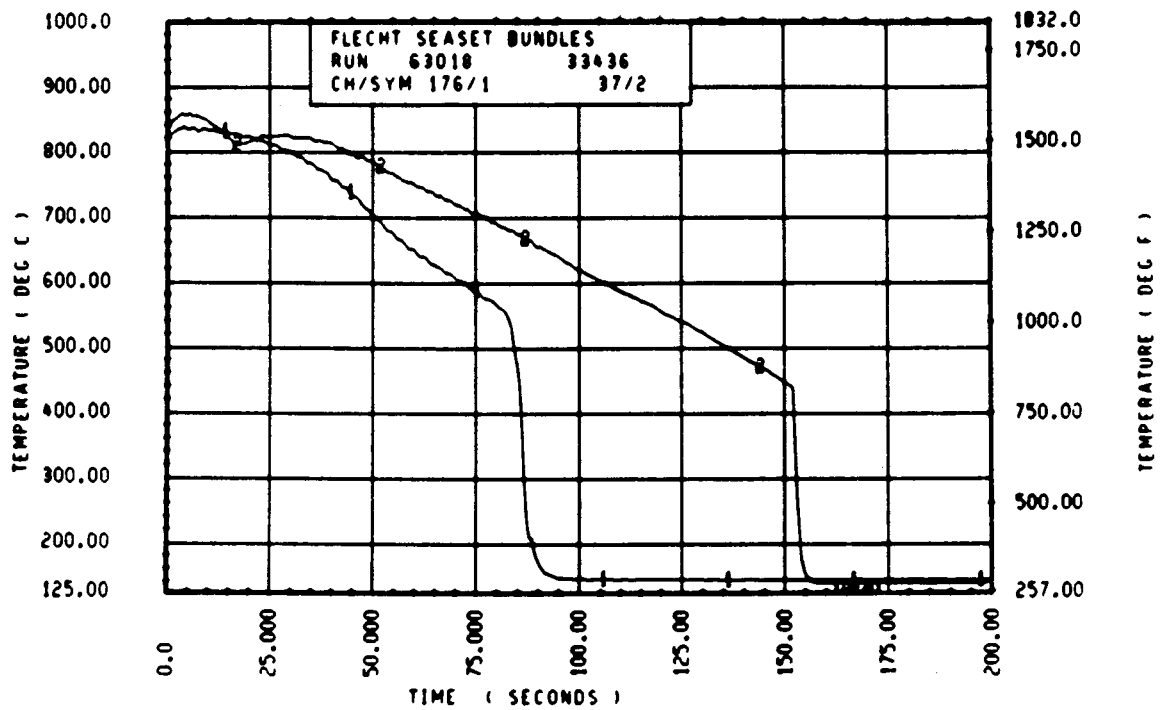
Rod 6L, 1.83 m (72 in.)



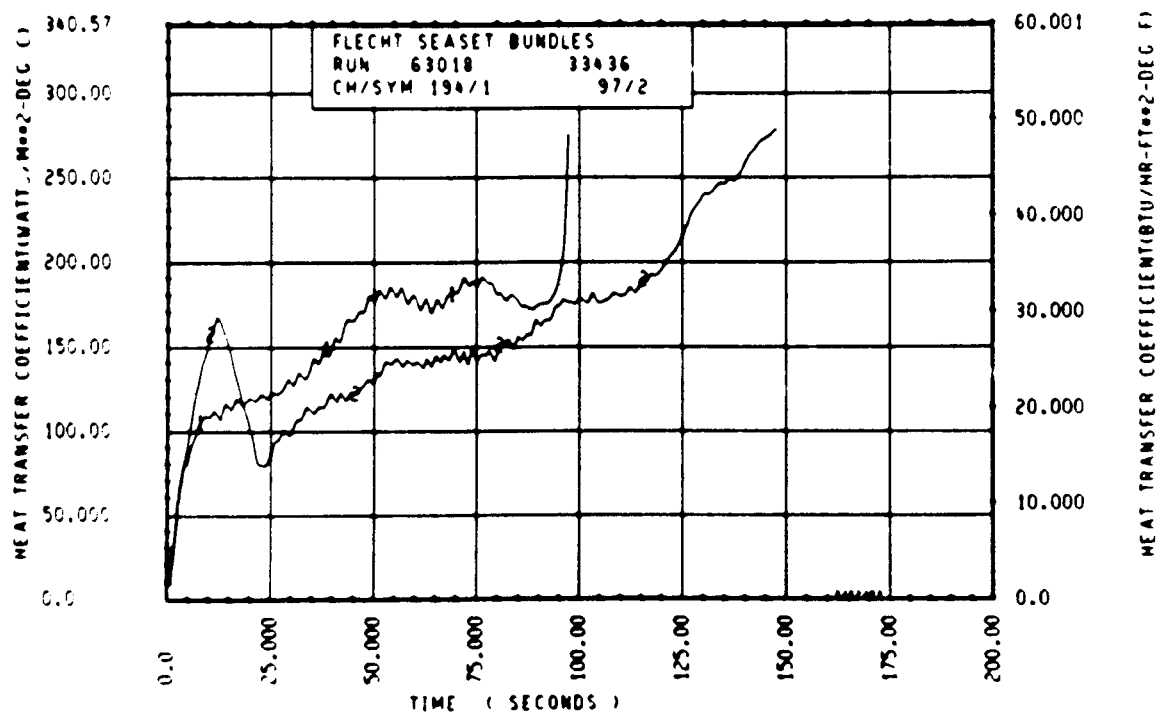
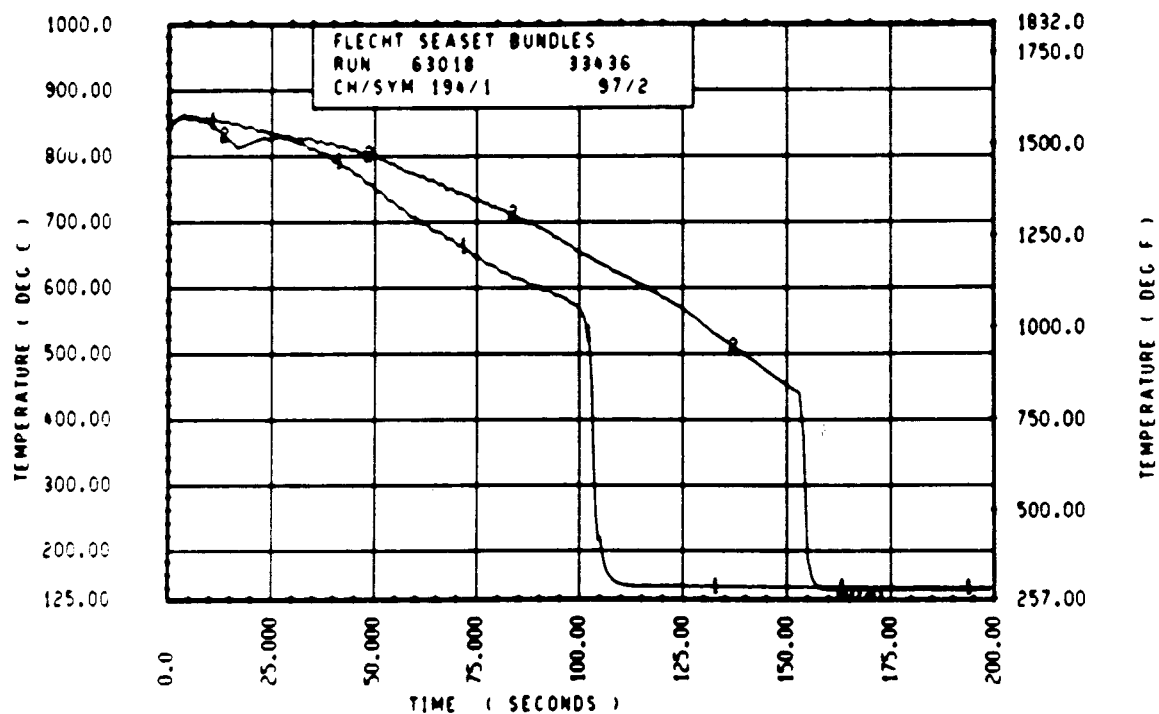
Rod 6L, 1.88 m (74 in.)



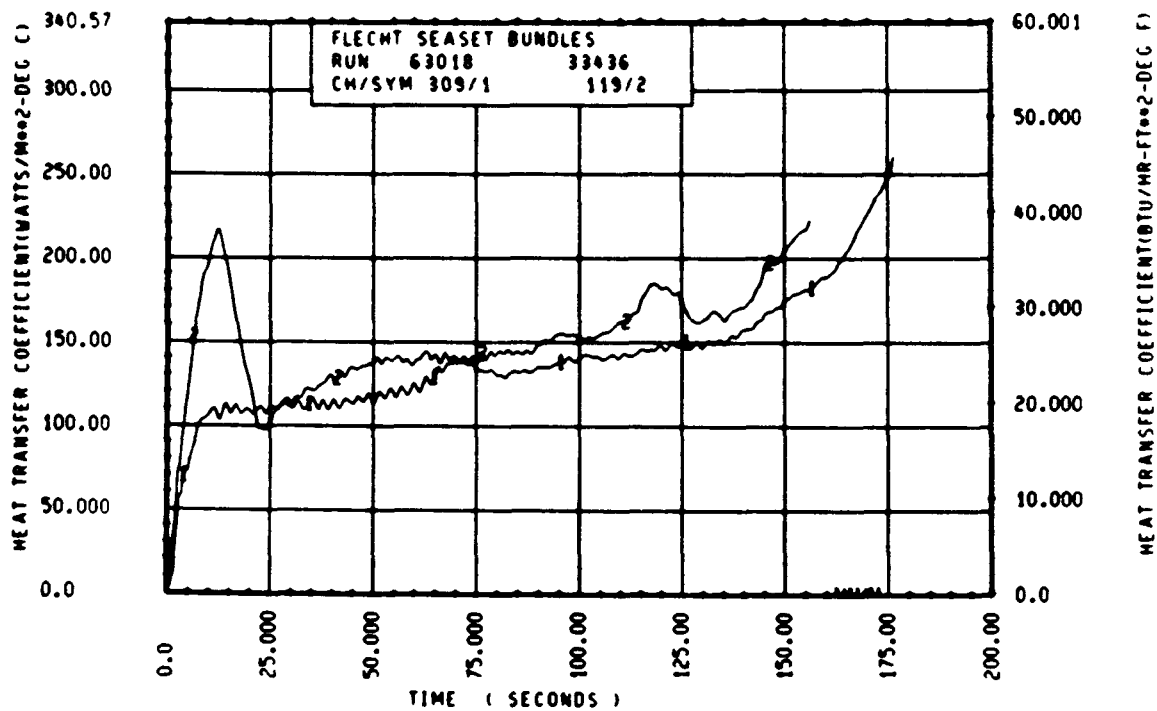
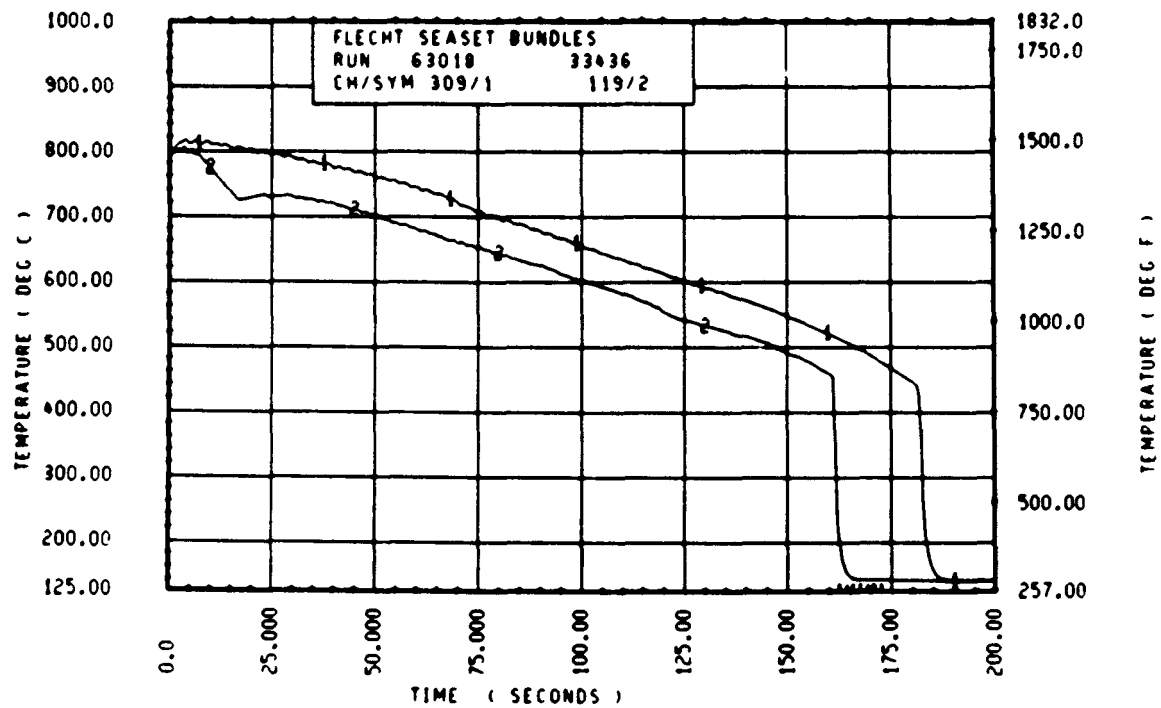
Rod 6J, 1.98 m (78 in.)



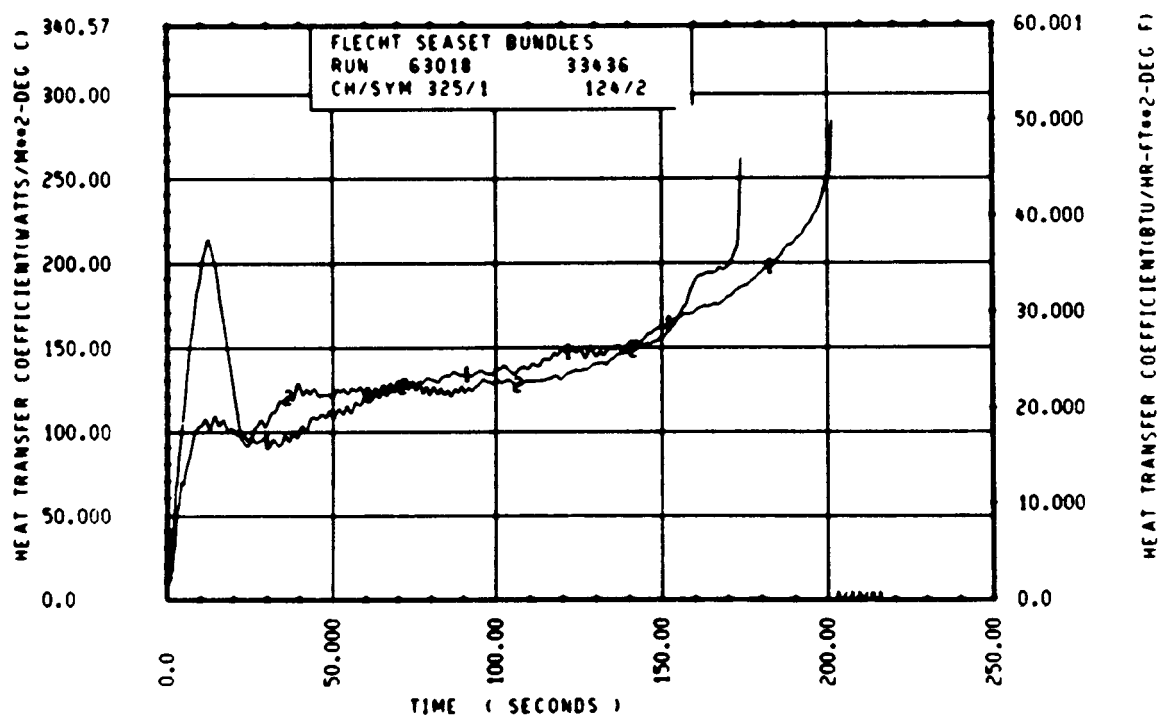
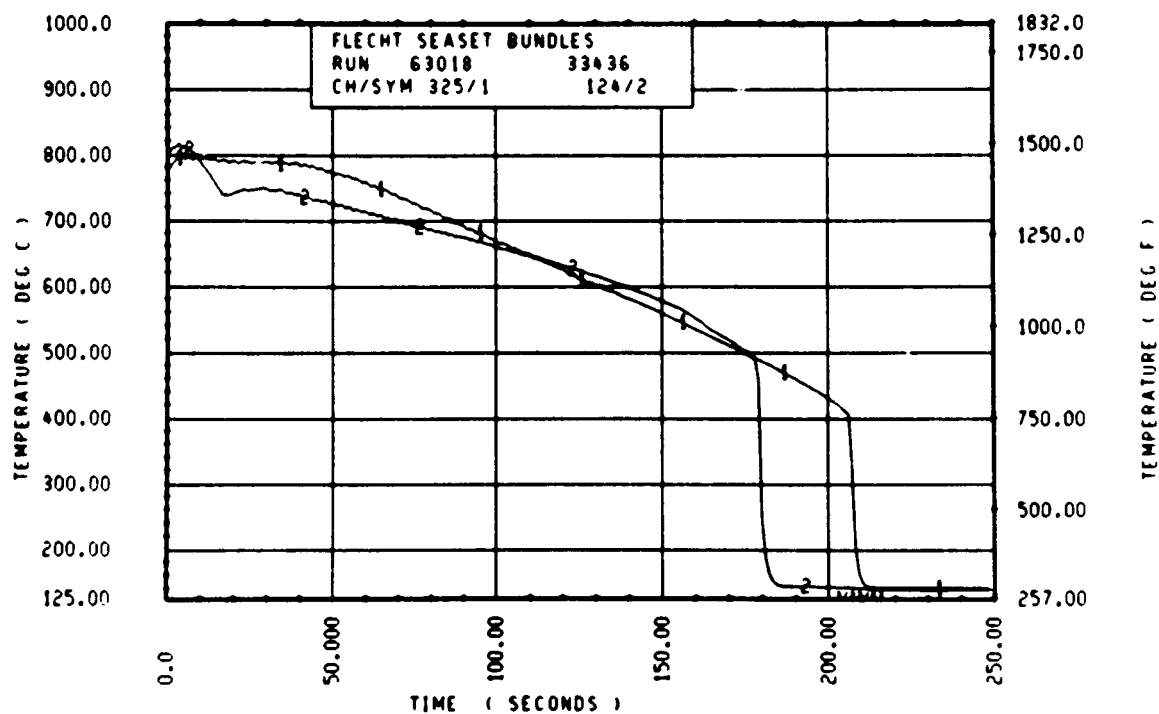
Rod 9f, 1.98 m (78 in.)



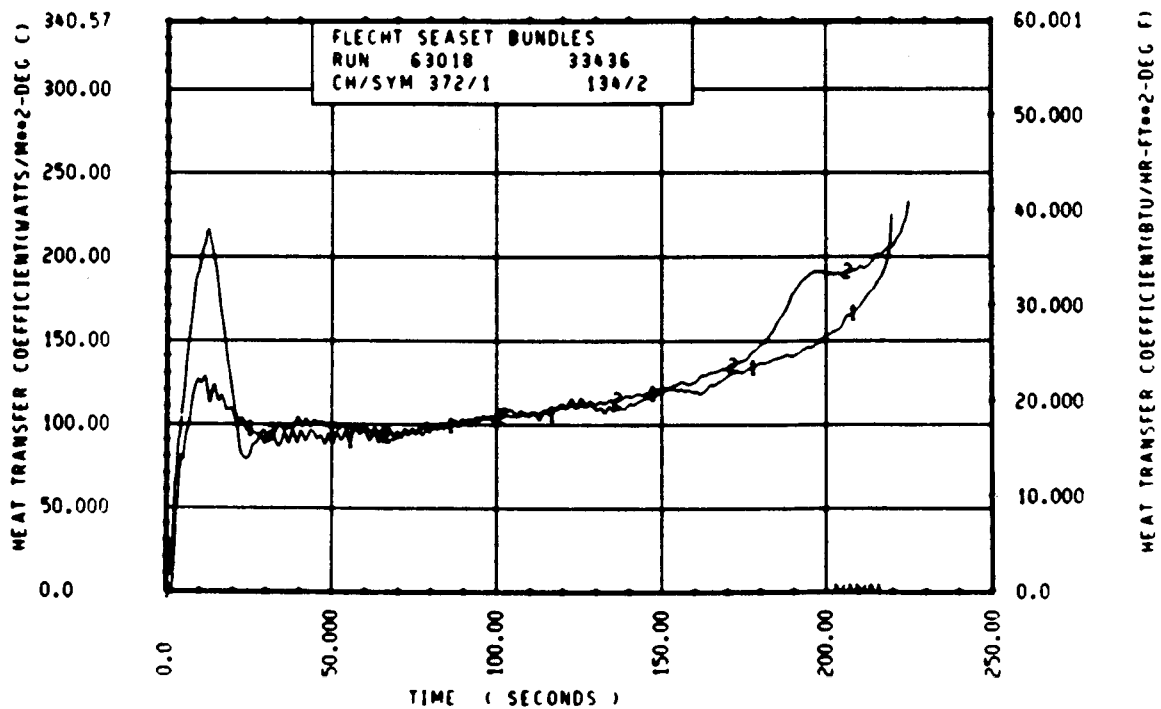
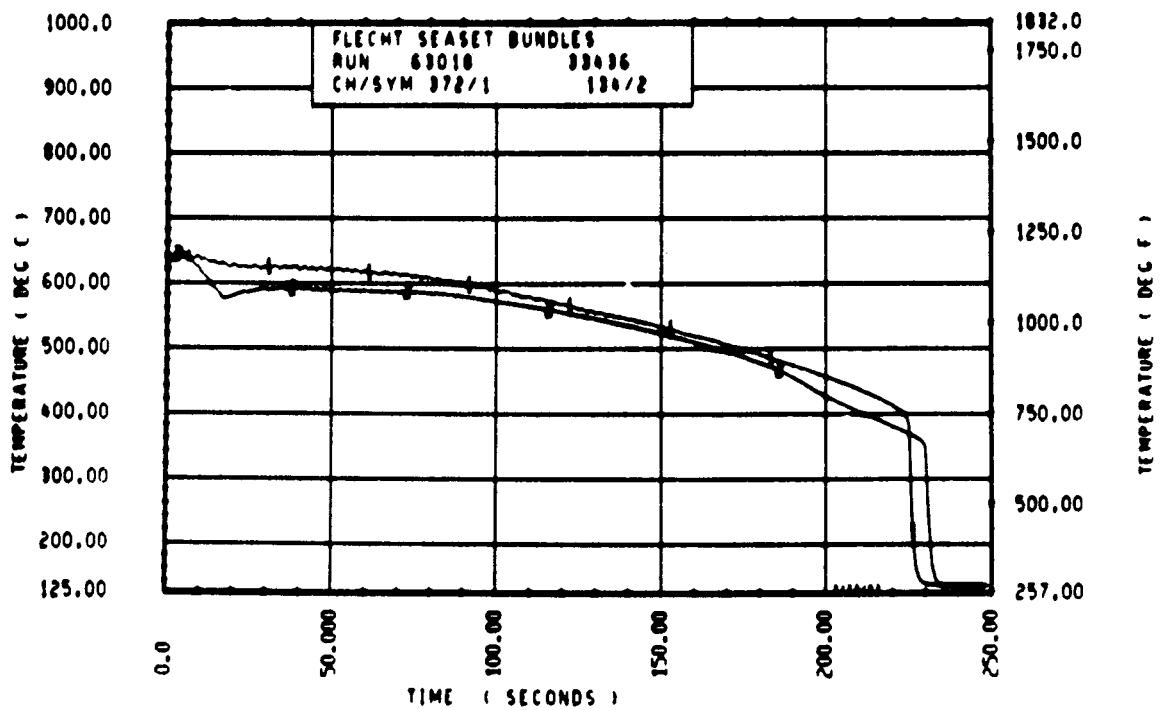
Rod 9E, 1.98 m (78 in.)



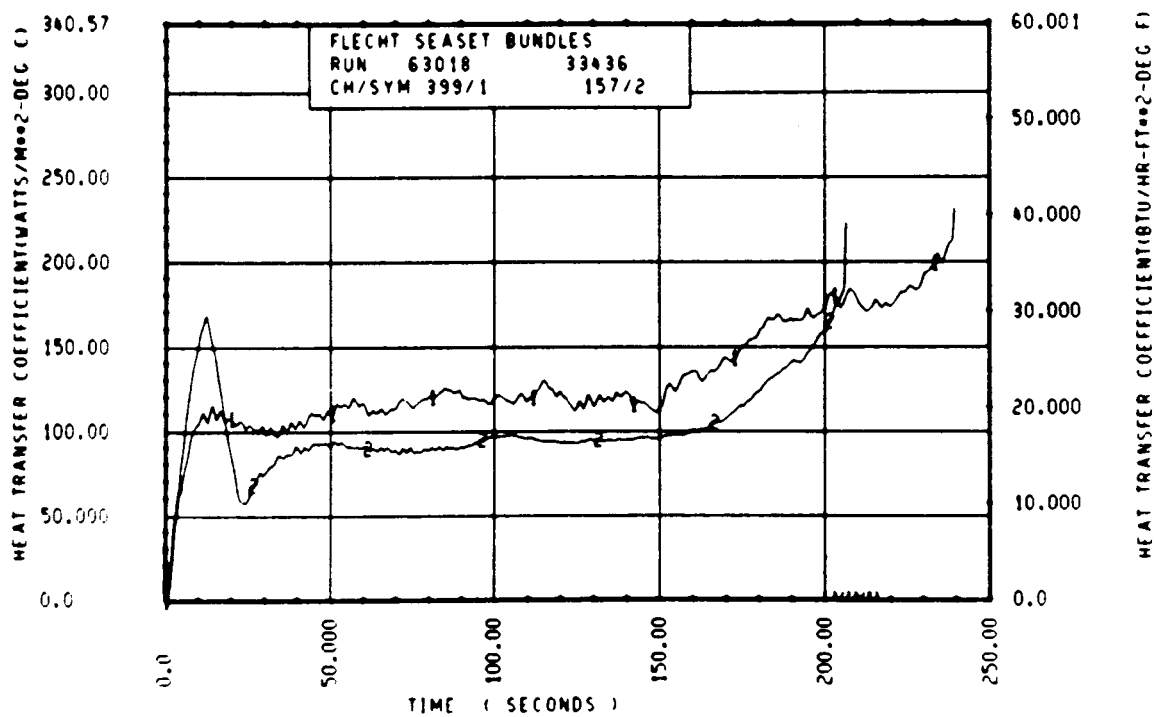
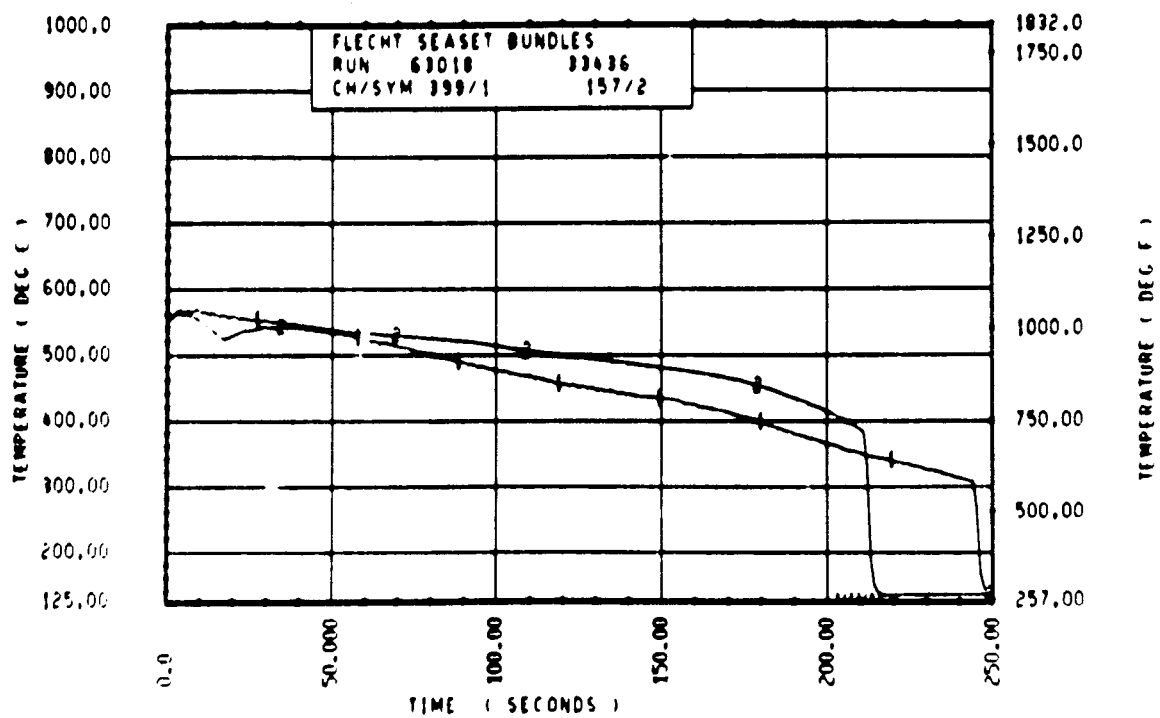
Rod 7D, 2.29 m (90 in.)



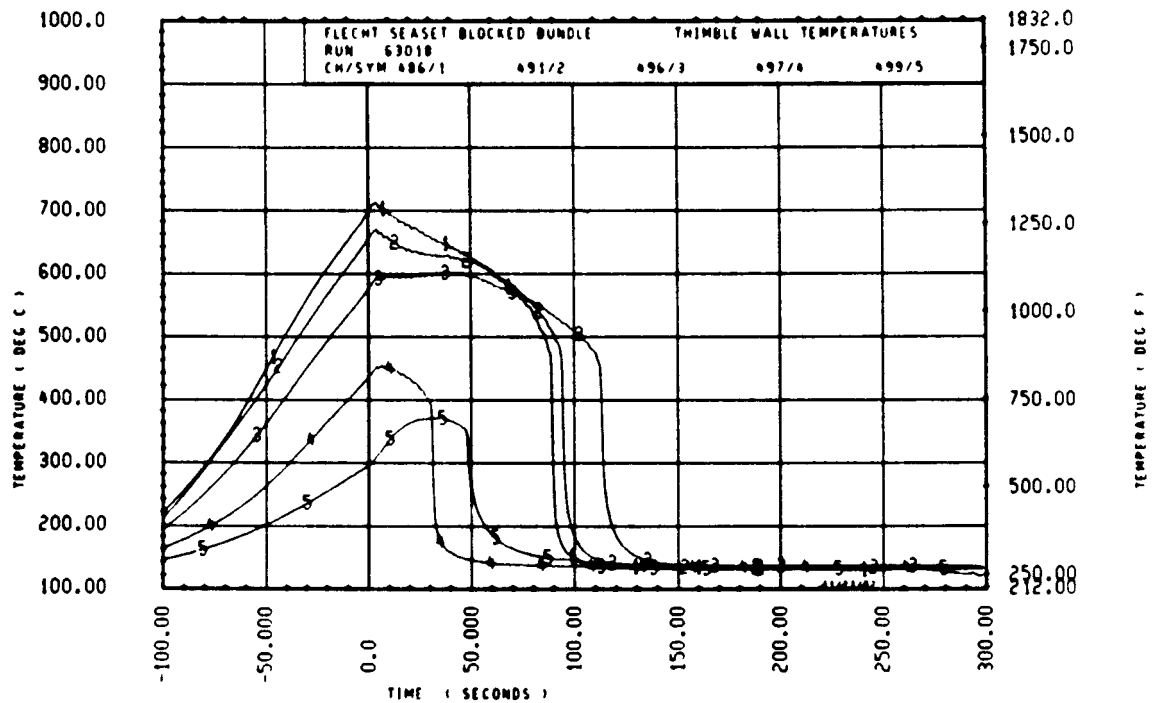
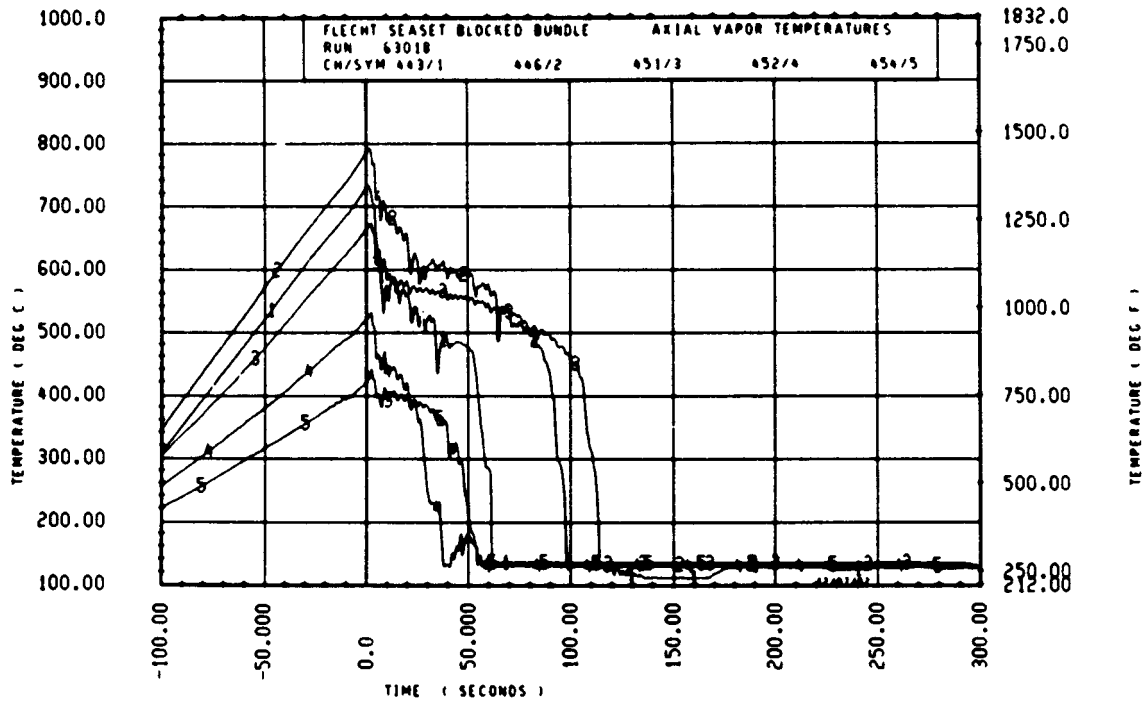
Rod 11E, 2.29 m (90 in.)

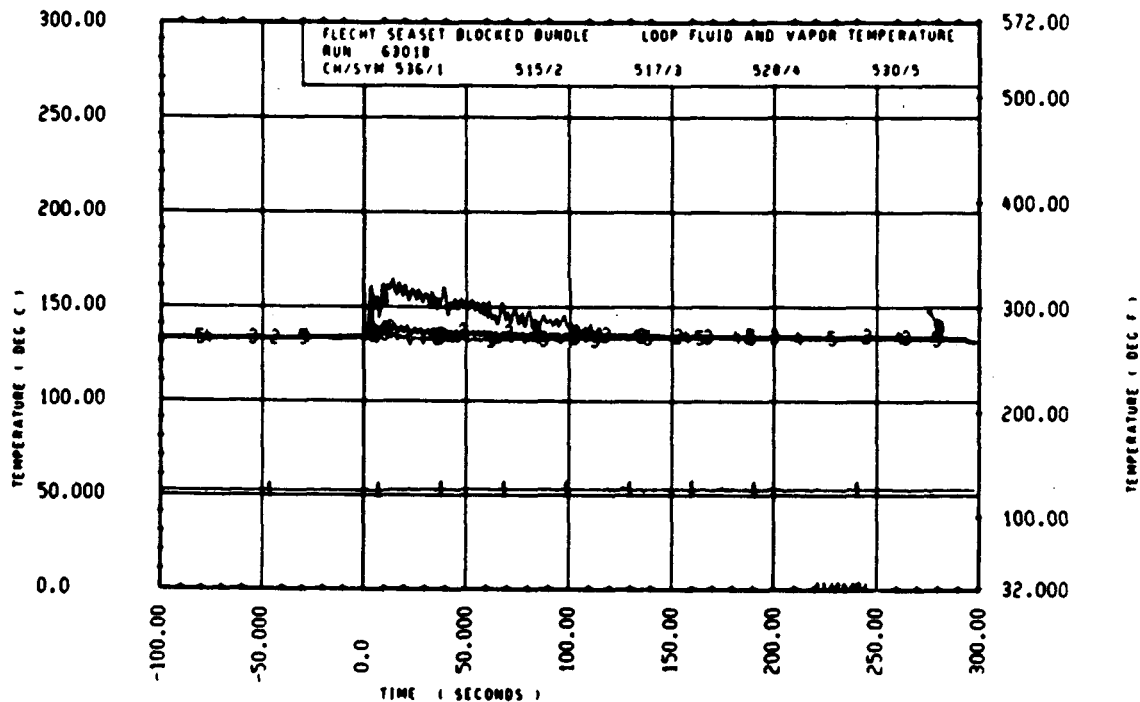
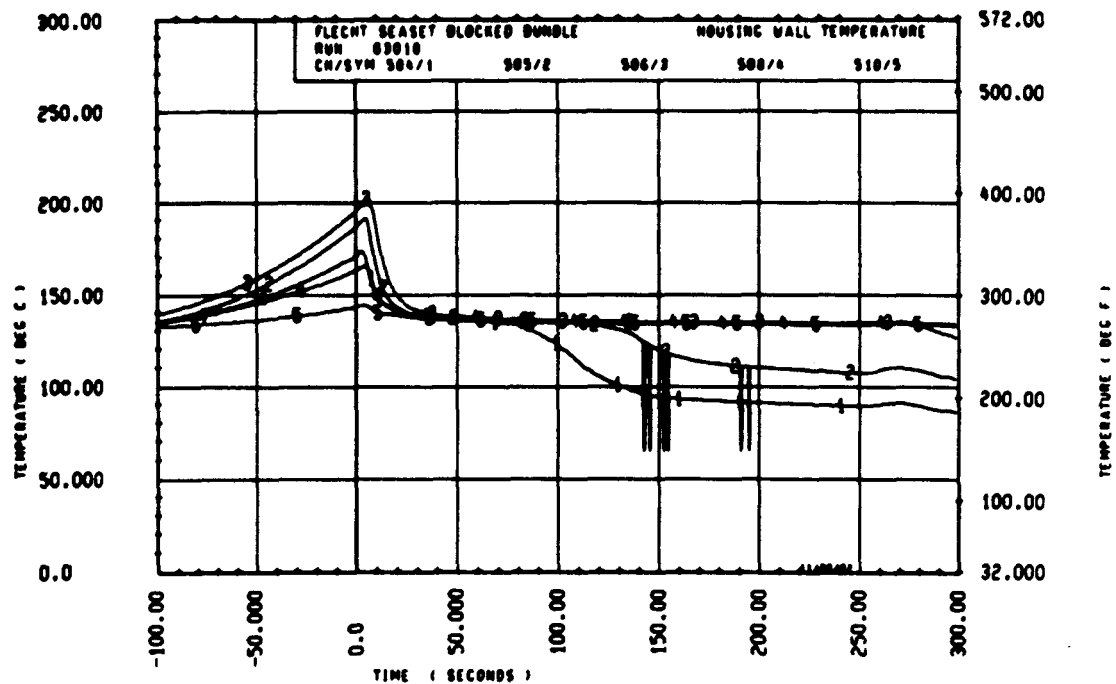


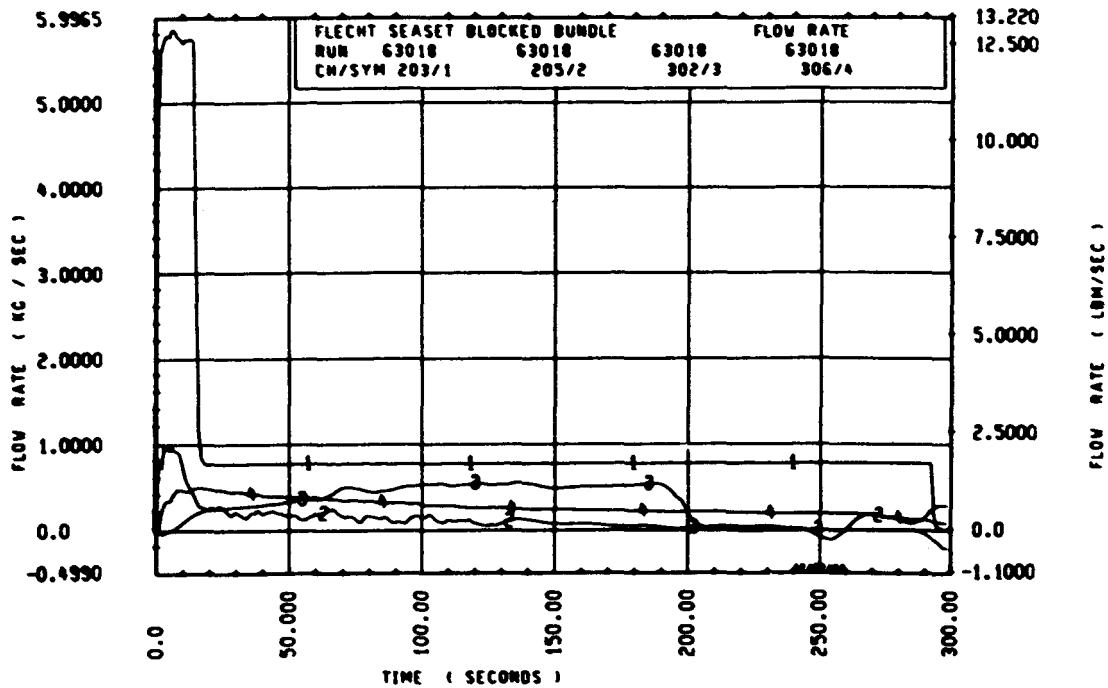
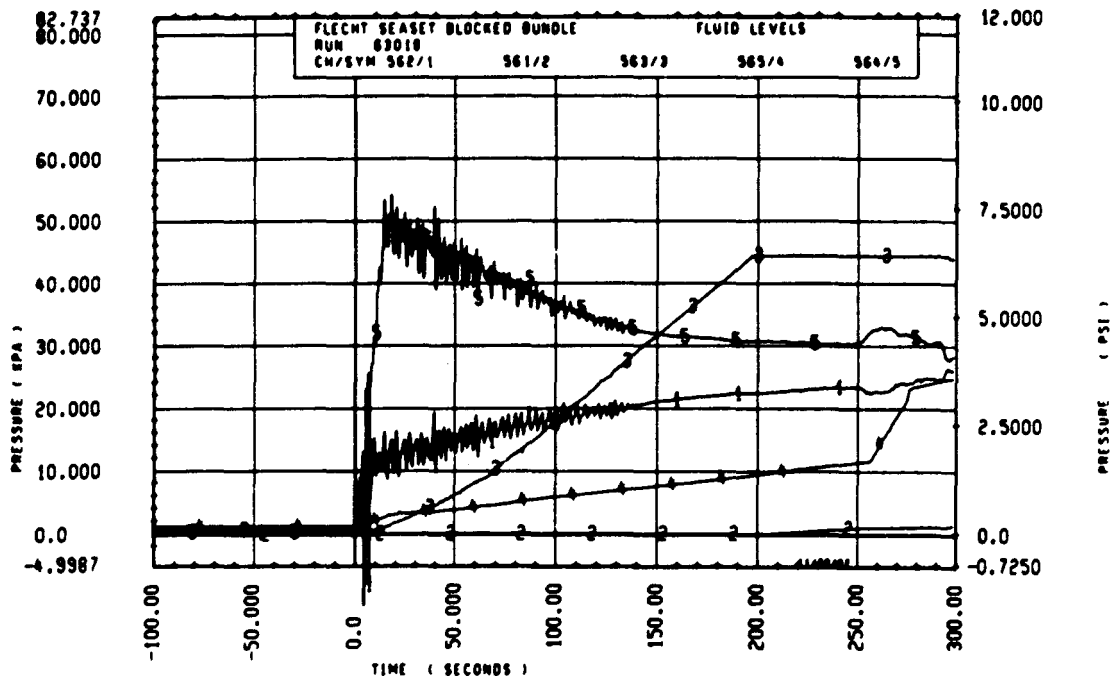
Rod 8J, 2.59 m (102 in.)

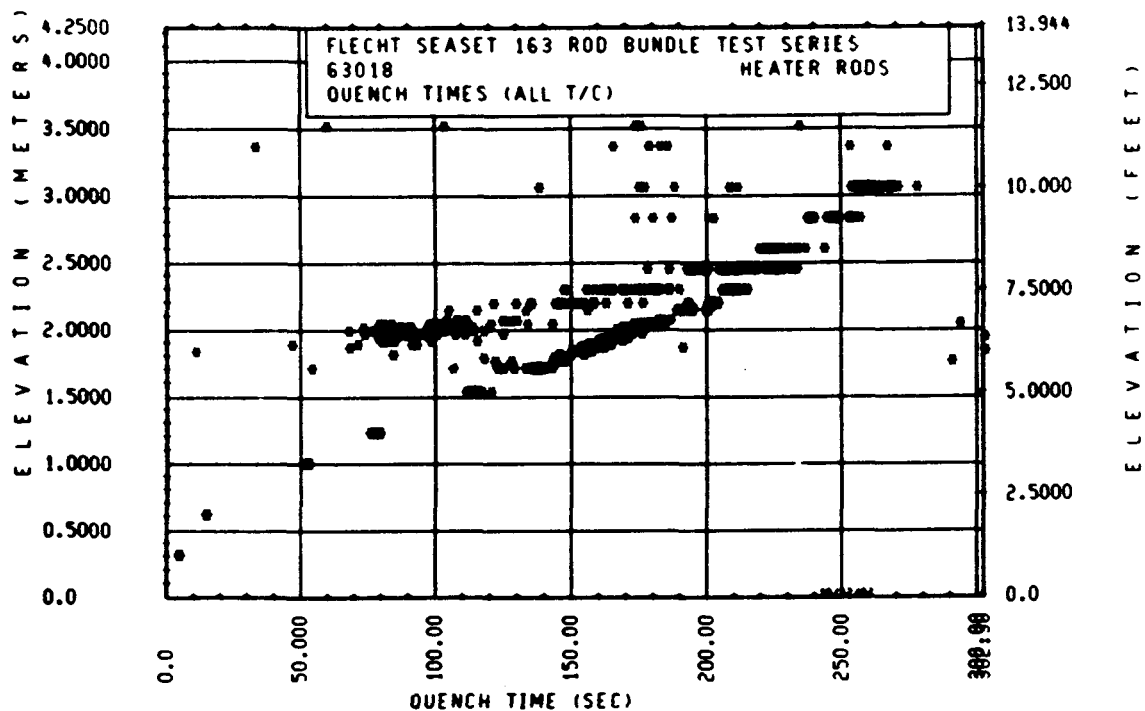
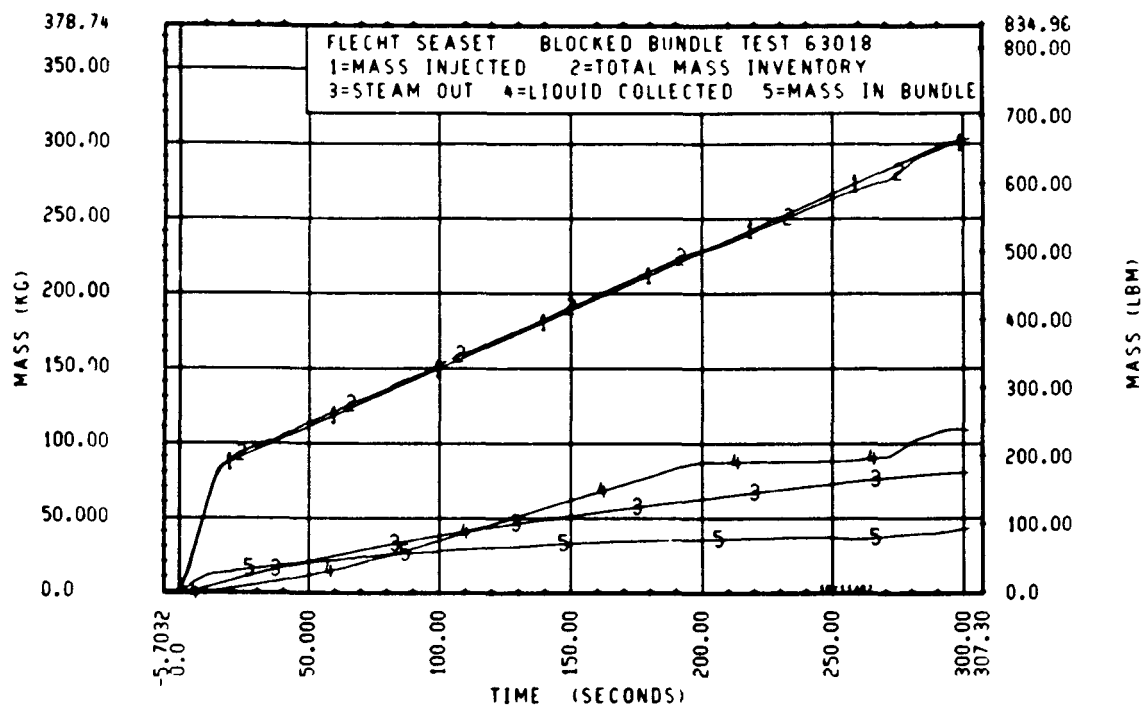


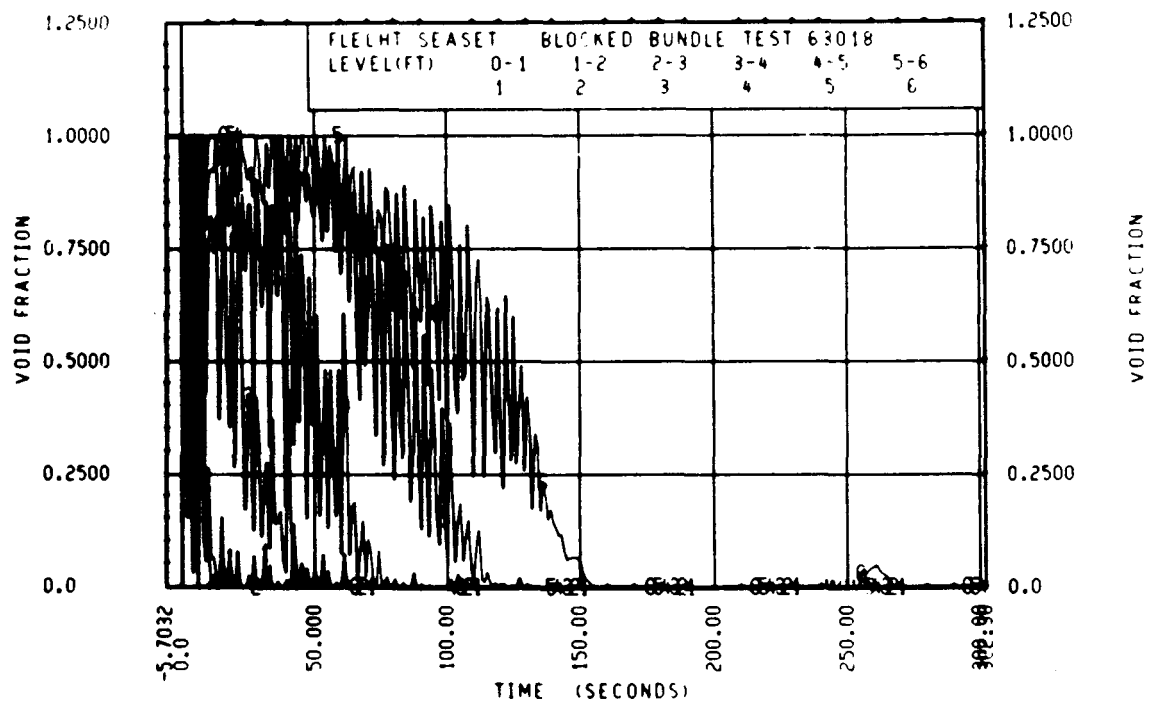
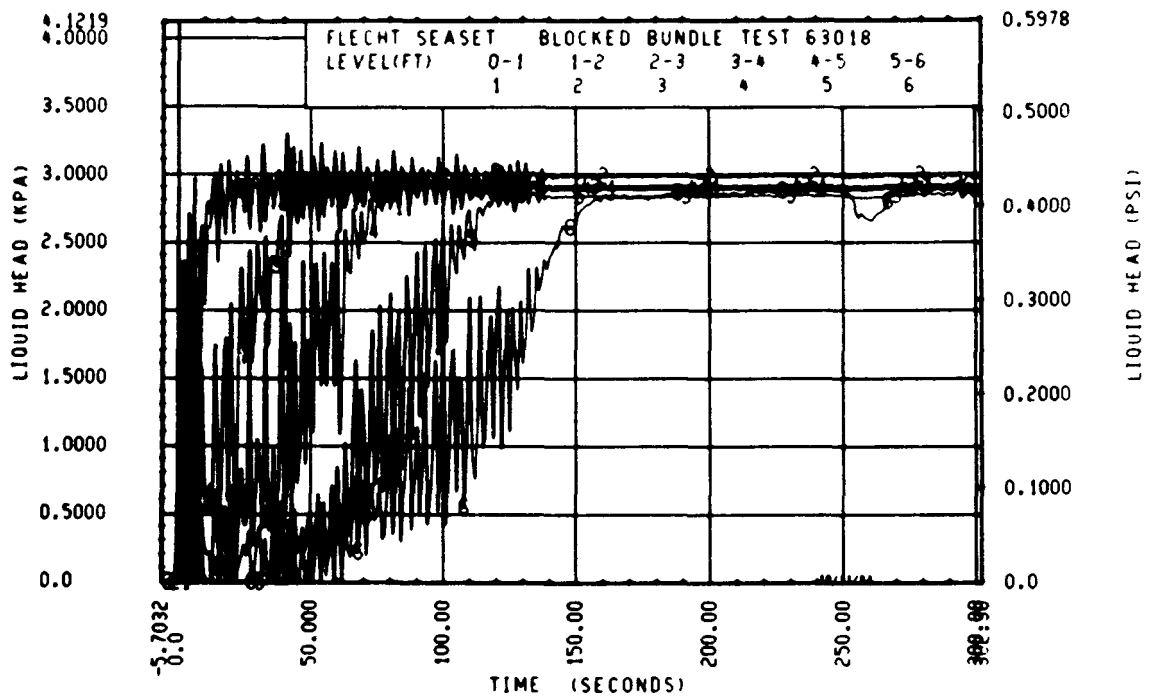
Rod 13G, 2.82 m (111 in.)

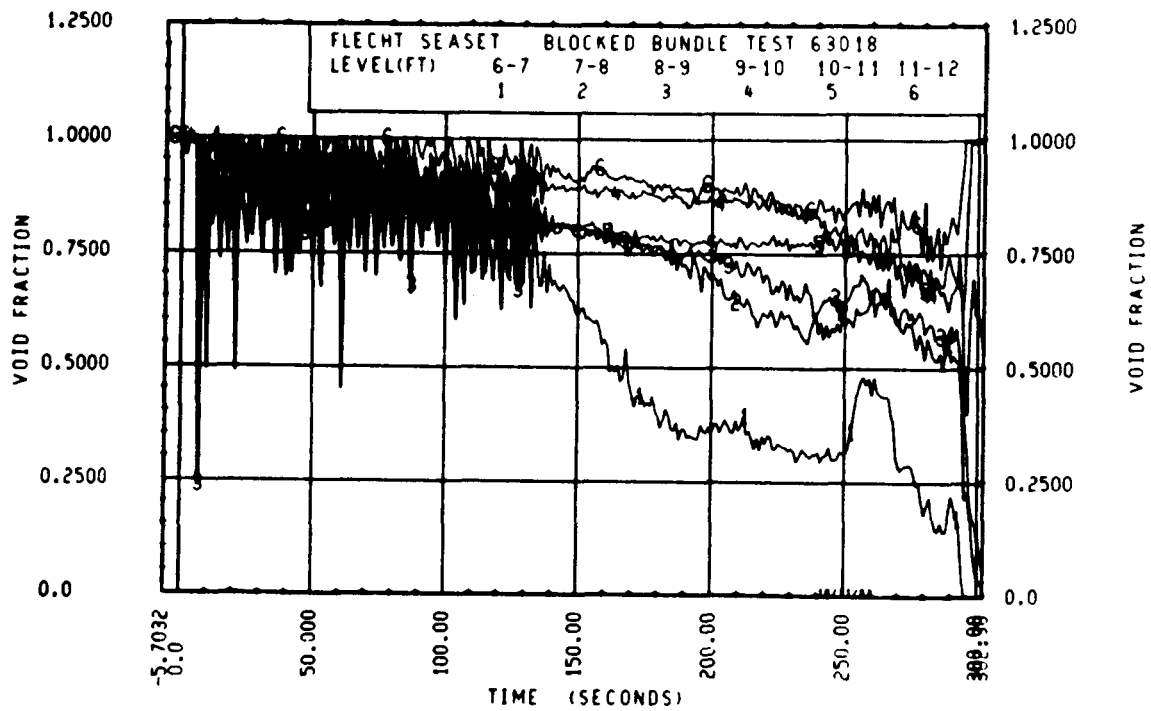
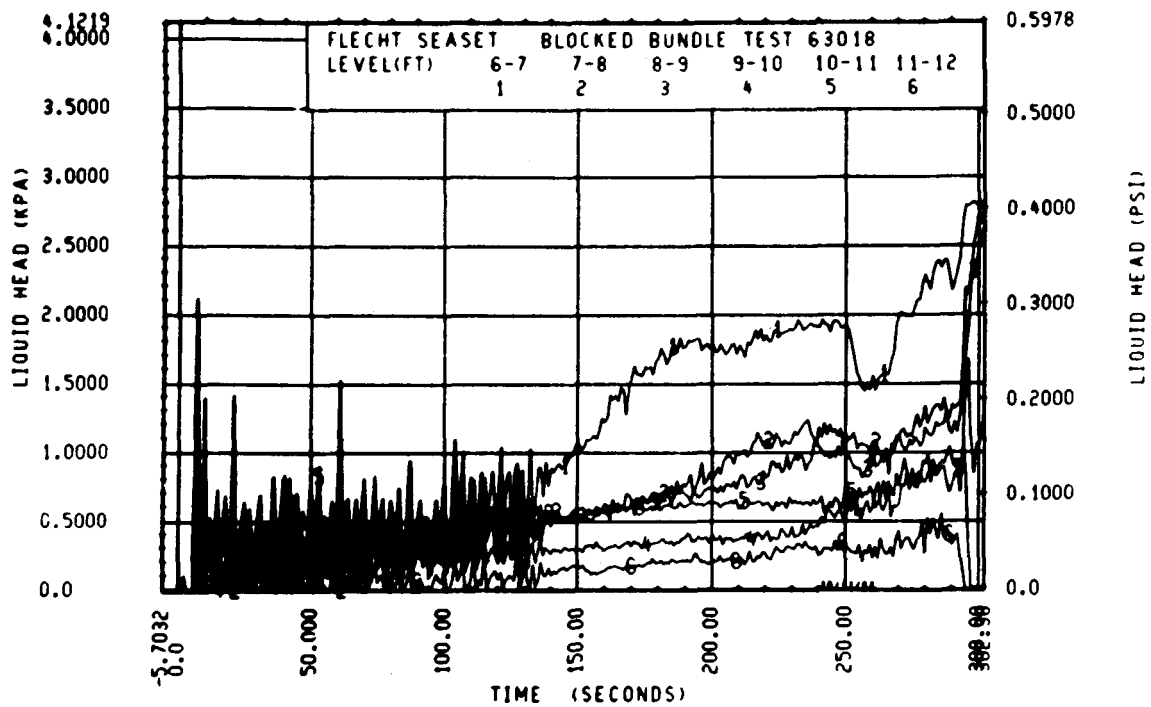












APPENDIX I

INSTRUMENTATION ERROR ANALYSIS

I-1. INTRODUCTION

The error associated with the measured data from the FLECHT SEASET 163-rod blocked bundle test series was derived from either equipment manufacturer specifications or system calibration data. Component calibrations were performed to verify that the manufacturers' specifications were met, and these manufacturers' specifications were used to compute the error estimate for the data path. System calibrations were performed when component calibrations were not expedient or when an accuracy improvement could be accomplished with a system calibration. The system calibration data were used to compute an estimate of error for the system response, and calibration standard equipment specifications were used to compute the error of the calibration data points. The total system error from a system calibration is a function of both equipment response error and calibration data error.

In all cases of error estimate, the standard deviation was computed and presented as the most probable error. The derivation of this error analysis technique was presented in paragraph D-7 of the 161-rod unblocked bundle data report.⁽¹⁾ The manufacturer-specified error is the maximum possible error for the respective component. The standard deviation of the error was calculated from the maximum error by the following, based on a uniform distribution over the error range:

$$\sigma^2 = \sum_{i=1}^n \frac{E_i^2}{3} \quad (I-1)$$

where

σ = data path standard deviation

E_i = component i maximum error

n = number of sources of error

1. Loftus, M. J., et al., "PWR FLECHT SEASET 161-Rod Unblocked Bundle, Forced and Gravity Reflood Task Data Report," NRC/EPRI/Westinghouse-7, June 1980.

When a system calibration was performed, the standard deviations from the calibration data and the calibration equipment were combined by the following equation to produce the best estimate of error:

$$\sigma = \sqrt{E_d^2 + E_c^2} \quad (I-2)$$

where

σ = data path standard deviation

E_d = calibration data standard deviation

E_c = calibration equipment standard deviation

The calibration data standard deviation is a measure of the error involved in fitting the calibration data. That is,

$$E_d = \left[\frac{\sum_{i=1}^n (Y_i - Y_f)^2}{n - 2} \right]^{1/2} \quad (I-3)$$

where

Y_i = calibration point

Y_f = predicted output from the calibration curve

n = number of calibration points

The calibration equipment standard deviation is a measure of the absolute error of the calibration point. If the calibration point in the above equation is calculated from an equation of the form

$$Y = x_1^{r_1} \cdot x_2^{r_2} \cdot x_3^{r_3} \quad (I-4)$$

then

$$\frac{\sigma_y^2}{y^2} = \sum_{i=1}^n \left(r_i \cdot \frac{\sigma_{x_i}}{x_i} \right)^2 \quad (I-5)$$

and

$$E_c = \sqrt{\sigma_y^2} \quad (I-6)$$

The standard deviations of best-estimate errors, statistically the most practical estimate of error, are presented in tables I-1 through I-4. The maximum possible errors, which are the sum of all the possible component errors and constitute the upper bound of error, are also presented in these tables.

Tables I-1 through I-4 provide a detailed listing of the errors by data channel. (Table 4-3 identifies channel locations and functions.) Application of the information in table I-1 to the recorded data requires an explanation of the analysis.

The data path is broken down into three parts: sensor, conditioner, and readout. The sensor is the device whose electrical output is proportional to a physical quantity (temperature, pressure, flow, power). The conditioner is a device which matches the electrical output of the sensor to the input requirements of the readout device. The readout device measures and records the electrical value of the signal from the conditioner. This recorded electrical value is subsequently used to compute the physical quantity it represents. The errors due to the transmission wires between the elements are not included in this analysis. Transmission wire errors were very small (± 0.001 percent) in comparison to the element errors, and were considered to be negligible.

The error values listed for sensor, conditioner, and readout are the manufacturers' specifications in engineering units. These numbers were used to compute the most probable and maximum error, as previously described. Where system calibrations were performed, the equipment calibration data list the standard deviation and maximum error as computed from the calibration data points in fitting the points to a first-order polynomial. The calibration point standard deviation is computed using the method described above. The calibration point maximum error was computed from the calibration equation by assuming that the maximum error occurs simultaneously in each component of the calibration equation.

The overall system standard deviation is calculated using the method described earlier for combining standard deviations (equation I-2).

TABLE I-1
INSTRUMENTATION ERRORS

Computer	Sensor Type	Error [$^{\circ}\text{C}$ ($^{\circ}\text{F}$)]				
		Sensor	Conditioner	Readout	Data Path	
					Most Probable	Maximum
1-502	Heater rod bundle thermocouples	± 1 (± 2) at -17.8°C to 277°C (0°F to 530°F); $+0.3775$ at 277°C to 1316°C (530°F to 2400°F); use $\pm 5^{\circ}\text{C}$ ($\pm 9^{\circ}\text{F}$)	± 0.3 (0.5)	± 2.03 (± 3.66)	± 1.32 (± 2.42)	± 3.33 (± 6.16)
503-539	Loop thermocouples	maximum	± 0.3 (± 0.5)	± 2.03 (± 3.66)	± 3.12 (± 5.62)	± 7.310 (± 13.16)
		± 2 (± 4) at -17.8°C to 277°C (0°F to 530°F); ± 0.75 at 277°C to 1316°C (530°F to 2400°F); use $\pm 10^{\circ}\text{C}$ ($\pm 18^{\circ}\text{F}$) maximum	± 0.3 (0.5)	± 2.03 (± 3.66)	± 1.74 (± 3.14) ± 5.894 (± 10.61)	± 4.53 (± 8.16) ± 12.3 (± 22.2)

TABLE I-2
POWER INSTRUMENTATION ERRORS^(a)

Computer Channel	Bundle Power	Error					
		Equipment Response (kw)		Calibration Standard (kw)		System Results(kw)	
		Most Probable	Maximum	Most Probable	Maximum	Most Probable	Maximum
540	Primary (400 kw)	± 3.27	± 5.38	± 0.515	± 0.515	± 3.31	± 5.43
541	Secondary (400 kw)	± 0.213	± 0.280	± 0.515	± 0.515	± 0.557	± 0.586
542	Primary (400 kw)	± 3.32	± 5.9	± 0.515	± 0.515	± 3.36	± 5.92
543	Secondary (400 kw)	± 0.170	± 0.235	± 0.515	± 0.515	± 0.542	± 0.566
544	Primary (400 kw)	± 4.25	± 8.25	± 0.515	± 0.515	± 4.28	± 8.26
545	Secondary (400 kw)	± 0.045	± 0.103	± 0.515	± 0.515	± 0.517	$\pm .525$

- a. The above errors were calculated for test run 62413 (1.0 kw/ft rod peak power). The three heater rod zones were reconfigured so that each zone contained 54 rods.

TABLE I-3
POWER INSTRUMENTATION ERRORS^(a)

Computer Channel	Bundle Power	Error					
		Equipment Response (kw)		Calibration Standard (kw)		System Results (kw)	
		Most Probable	Maximum	Most Probable	Maximum	Most Probable	Maximum
540	Primary (298 kw)	± 0.820	± 0.892	± 0.337	± 0.337	± 0.887	± 0.953
541	Secondary (298 kw)	± 0.087	± 0.173	± 0.337	± 0.337	± 0.348	± 0.379
542	Primary (323 kw)	± 1.583	± 2.54	± 0.439	± 0.439	± 1.643	± 2.577
543	Secondary (323 kw)	± 0.103	± 0.178	± 0.439	± 0.439	± 0.451	± 0.474
544	Primary (202 kw)	± 2.289	± 3.068	± 0.279	± 0.279	± 2.31	± 3.1
545	Secondary (202 kw)	± 0.068	± 0.113	± 0.279	± 0.279	± 0.287	± 0.301

- a. The above errors apply to all test runs except run 62413. Heater rod zone configuration was as follows: zone A - 58 rods; zone B - 64 rods; zone C - 40 rods.

TABLE I-4
FLOW AND PRESSURE MEASUREMENT INSTRUMENTATION ERRORS

Computer Channel	Sensor Type	Sensor Error	Conditioner Error	Readout Error	Data Path Error	
					Most Probable	Maximum
546	Flowmeter [3.8×10^{-3} m ³ /sec (60 gal/min)]	1.88×10^{-5} m ³ /sec (0.298 gal/min)	9.5×10^{-4} m ³ /sec (0.15 gal/min) 4×10^{-4} m ³ /sec (0.06 gal/min)	5.45×10^{-4} m ³ /sec (0.0864 gal/min)	1.27×10^{-5} m ³ /sec (0.202 gal/min)	3.75×10^{-5} m ³ /sec (0.594 gal/min)
547	Flowmeter [9.46×10^{-3} m ³ /sec (200 gal/min)]	1.31×10^{-5} m ³ /sec (0.207 gal/min)	9.5×10^{-4} m ³ /sec (0.15 gal/min)	1.36×10^{-5} m ³ /sec (0.216 gal/min)	1.22×10^{-5} m ³ /sec (0.193 gal/min)	3.61×10^{-5} m ³ /sec (0.573 gal/min)
548(a)	Flowmeter [$\pm 1.26 \times 10^3$ m ³ /sec (± 200 gal/min)]	--	--	--	--	--
549- 561	D/P cell [7.45 kPa (1.08 psi)]	0.01 kPa (0.002psi)	0.01 kPa (0.002psi)	0.01 kPa (0.002psi)	0.012kPa (0.002psi)	0.037kPa (0.006psi)
562	D/P cell [74.74 kPa (10.84 psi)]	0.15 kPa (0.022 psi)	0.11 kPa (0.016 psi)	0.11 kPa (0.016 psi)	0.124kPa (0.018psi)	0.370kpa (0.054psi)
563	D/P cell [99.63 kPa (14.45 psi)]	0.20 kPa (0.029 psi)	0.15 kPa (0.022 psi)	0.14 kPa (0.021 psi)	0.17 kPa (0.024 psi)	0.50 kpa (0.072 psi)

a. Flowmeter not utilized; calibration errors exceeded manufacturer's specifications

TABLE I-4 (cont)
FLOW AND PRESSURE MEASUREMENT INSTRUMENTATION ERRORS

Computer Channel	Sensor Type	Sensor Error	Conditioner Error	Readout Error	Data Path Error	
					Most Probable	Maximum
564	D/P cell [114.6 kPa (16.62 psi)]	0.23 (0.033)	0.17 (0.025)	0.17 (0.024)	0.19 (0.028)	0.57 (0.082)
565	D/P cell [79.71 kPa (11.56 psi)]	0.16 (0.023)	0.12 (0.017)	0.12 (0.017)	0.13 (0.019)	0.39 (0.057)
566	D/P cell [59.8 kPa (8.67 psi)]	0.12 (0.017)	0.090 (0.013)	0.090 (0.013)	0.097 (0.014)	0.30 (0.043)
567	D/P cell [74.74 kPa (10.84 psi)]	0.15 (0.022)	0.11 (0.016)	0.11 (0.016)	0.12 (0.018)	0.37 (0.054)
568	D/P cell [276 kPa (40psi)]	0.6 (0.08)	0.4 (0.06)	0.40 (0.058)	0.46 (0.067)	1.37 (0.198)
569	D/P cell [103 kPa (15 psi)]	0.21 (0.030)	0.15 (0.022)	0.15 (0.022)	0.17 (0.025)	0.51 (0.074)
570	D/P cell [34 kPa (5 psi)]	0.07 (0.01)	0.06 (0.008)	0.05 (0.007)	0.06 (0.008)	0.17 (0.025)
571	D/P cell [207 kPa (30 psi)]	0.4 (0.06)	0.31 (0.045)	0.30 (0.043)	0.34 (0.050)	1.02 (0.148)

TABLE I-4 (cont)
FLOW AND PRESSURE MEASUREMENT INSTRUMENTATION ERRORS

Computer Channel	Sensor Type	Sensor Error	Conditioner Error	Readout Error	Data Path Error	
					Most Probable	Maximum
572-573	D/P cell [87.01 kPa (12.62 psi)]	0.17 (0.025)	0.13 (0.019)	0.12 (0.018)	0.14 (0.021)	0.43 (0.062)
574-575	PT cell [690 kPa (100 psi)]	1.72 (0.250)	1.03 (0.150)	0.992 (0.144)	1.30 (0.188)	3.75 (0.544)
576	PT cell [3.45 MPa (500 psi)]	8.62 (1.25)	5.2 (0.75)	5.0 (0.72)	6.47 (0.939)	18.8 (2.72)

I-2. TEMPERATURE MEASUREMENTS

The errors for temperature channels 1 through 539 using type K thermocouples for the sensor, a 65°C (150°F) reference junction for signal conditioning, and the computer for readout are presented in table I-1. In the range of temperatures from 277°C to 1316°C (530°F to 2400°F), the sensor error is a percentage of the magnitude of the temperature. For temperatures below 277°C (530°F), the sensor error is constant.

I-3. POWER MEASUREMENTS

Computer channels 540, 542, 544 and 541, 543, 545 were, respectively, the primary and secondary power measuring channels used for the forced and gravity reflood tests. Three SCR (silicon-controlled rectifier) units regulated the amount of power to the test bundle to a maximum of 1.3 megawatts. Watt transducers, utilizing the Hall-effect method, were used to record the power delivered to the test bundle. Calibrations were performed on the watt transducers at periodic intervals to meet the manufacturer's specifications. A system calibration was performed on the power recording systems during the test series, and the combined data were used to compute the equipment response calibration data most probable and maximum errors. The calibration standard data values were derived from the calibration standard (YEW meter) component error. The system results were derived from the system calibration data and the calibration standard error estimates. The errors for the power measurement channels are presented in tables I-2 and I-3.

I-4. FLOW MEASUREMENTS

Channels 546 through 548 were the injection line turbine meter computer channels. The turbine meters were calibrated by the manufacturer; these data were used to determine the maximum sensor error. Manufacturer-specified errors were used for the signal conditioning and readout. These errors were then combined using equation (I-1) to provide the most probable error. The errors for the flow measurement channels are presented in table I-4.

I-5. PRESSURE

Channels 549 through 576 were the loop pressure measurements channels; the respective errors are presented in table I-4. Manufacturer-specified errors were used for the data path component errors. These were combined using equation (I-1) to determine the most probable errors associated with these channels.

APPENDIX J

CALCULATION TECHNIQUES

J-1. DATAR PROGRAM

The purpose of the DATAR model is to calculate the heat transfer coefficient for heater rods in the experimental facility. It accomplishes this by using available experimental data (as read from data tapes) and as-built heater rod dimensions, coupled with a mathematical model (paragraph J-2).

The DATAR code consists of 13 overlays, to reduce the computer field length required for code execution. These overlays consist of the following:

- o The main program overlay, together with those subroutines necessary to calculate film coefficients
- o The overlay which controls the reading and checking of input data, from both cards and tape
- o The overlay which checks for restart and, if present, properly positions input and output files and sets internal values
- o The overlay which reads input information from the main data tape header and calculates several internal values based on this information
- o The overlay which checks card input consistency and echoes the information to printed output
- o The overlay which echoes data tape header information to printed output
- o The overlay which reads input from cards and performs miscellaneous operations on the data

The program provides its own dynamic field length management, resulting in minimum operating expense.

The main program generally controls the flow of most input and output data read and generated by the program. A typical run is conducted using the following steps:

- (1) Radial node positions are calculated based on built-in radii and interval information. It should be noted that the code performs its calculations in the radial direction only. Axial conduction is ignored.
- (2) The appropriate time values are calculated for each data point produced.
- (3) Header information (run number, number of data scans, and the like) is written to the output tape, data tapes are read and correctly positioned, and the bundle power is calculated. The sink temperature is assumed to be the saturation temperature corresponding to the specified pressure for the test.
- (4) The temperature data for a rod thermocouple are read from the main data tape; miscellaneous information for that thermocouple, such as bundle position and axial and radial power factors, is read from a secondary data tape.
- (5) The thermocouple is considered good if the channel is not included in the bad channel list and the first temperature is greater than 66°C (150°F). If these two criteria are not met, a short entry is made on the output tape and data from the next channel are read.
- (6) Rod temperature profiles, surface heat flux, and heat transfer coefficients are calculated by successively calling subroutines containing the model described in paragraph J-2.
- (7) The data and results of calculations performed in step (6) are written to output.
- (8) Steps (4) through (7) are repeated for all bundle thermocouple channels; the run is then terminated.

DATAR uses three principal subroutines. Their functions are as follows:

- o To calculate the coefficient matrix
- o To calculate the temperatures and surface heat flux given the coefficient matrix
- o To invert the tridiagonal coefficient matrix

Several other subroutines perform miscellaneous calculations, such as material property evaluation and data interpolation.

J-2. Calculation Method

A heat conduction problem is termed an "inverse heat conduction problem" if at least one spatial condition is specified at an interior point of a heat-conducting body. Because of this unorthodox condition, the solution to an inverse problem is very complicated. Even if the governing equations are linear, classical methods such as Fourier analysis and Laplace transformation fail to yield a solution. For the Fourier method, the eigenvalues are not readily obtainable from the resulting Sturm-Liouville system of equations; hence, a Fourier series representation of the solution cannot be determined. Transformation techniques lead to a solution in Laplace variable space, which defies an inverse transform into the real time space. Although the numerical method is not without difficulty, meaningful results can be obtained if due care is exercised.

The mathematical formulations and methods used in DATAR to solve the inverse heat conduction problem are described in the following paragraphs. The governing partial differential equation and the associated difference approximation are outlined below. The key assumption used in the development of the approximation is that the nonlinear coefficients are slowly varying functions of the temperature of the system and may therefore be treated as constants. The validity of this assumption is addressed in paragraph J-10. When the difference approximation has been obtained, the solution method is described in considerable detail.

J-3. Basic Equations and Geometry

Let $T(r,t)$ denote the temperature at position r and time t in the ranges $0 < r \leq b$, $t \geq 0$. The applicable partial differential equation is

$$\frac{\partial}{\partial r} \left(k \frac{\partial T}{\partial r} \right) + \frac{k}{r} \frac{\partial T}{\partial r} + q''' = \rho c \frac{\partial T}{\partial t} \quad (J-1)$$

where k and c depend on T and are thermal conductivity and specific heat, respectively, and ρ is density. Axial heat conduction is neglected, since calculations have shown an insignificant effect unless within approximately 25 mm (1 in.) of the quench front.

The following boundary and initial conditions are given:

$$\frac{\partial T(0,t)}{\partial r} = 0 \quad (J-2)$$

$$T(a,t) = T_D(t) \quad 0 < a < b \quad (J-3)$$

$$\frac{\partial T(b,t)}{\partial r} = -\phi/k \quad (J-4)$$

$T(r,0)$, the initial temperature distribution, is also given.

Equation (J-2) assures symmetry at $r = 0$. Equation (J-3) represents the measured temperature at an internal point a . Equation (J-4) introduces another unknown, ϕ , the flux to be determined.

Since the measured temperature is given at discrete times, the partial differential equation may be viewed as a system of ordinary differential equations, one equation for each temperature measurement. The factor ϕ could then be computed at each time step so that the measured temperature is obtained; this approach is not used in DATAR. There are two primary reasons for considering the transient behavior of the system: first, the experimental error in the data, and second, the propagation time effects in the system. As shown below, if ϕ is computed at each time step using only the measured temperature at that time step, then the flux and external temperature will behave erratically. The second reason, the propagation effect, occurs because the flux ϕ reflects the behavior of the rod at the boundary, and the temperature is measured at an internal point of the rod. The temperature propagation time of the rod must be accounted for, since the measured temperature reflects changes in the boundary temperature that have occurred earlier. If the propagation time is greater than 0.5 second, then this transport effect must be allowed for by adjusting ϕ at one time step, given the temperature measurements at future times. A representative propagation time is not known, but rough estimates indicate that it is greater than 0.5 second. A detailed analysis of this phenomenon should prove useful in any future modifications of DATAR.

The spatial aspects of the problem are now considered. The physical region under consideration ($0 \leq r \leq b$) is composed of n radial regions, each with

potentially different physical properties. The result is a set of n partial differential equations, one equation for each region. At the interface points of the regions, temperature and heat transfer are required to be continuous. Let d be an interface point between regions R_{i-1} and R_i ; then,

$$\lim_{r \in R_{i-1}} T(r, t) = \lim_{r \in R_i} T(r, t) \quad (J-5)$$

$$\begin{array}{ll} r \in R_{i-1} & r \in R_i \\ r \rightarrow d & r \rightarrow d \end{array}$$

$$\lim_{r \in R_{i-1}} \frac{\partial T(r, t)}{\partial r} = \lim_{r \in R_i} \frac{\partial T(r, t)}{\partial r} \quad k(T) \quad (J-6)$$

$$\begin{array}{ll} r \in R_{i-1} & r \in R_i \\ r \rightarrow d & r \rightarrow d \end{array}$$

Given equations (J-1) through (J-6), the appropriate difference equation is first derived for each region separately using equation (J-1); then the regions are coupled by imposing equations (J-5) and (J-6). Equations (J-2) and (J-4) supply the boundary values, and equation (J-3) and the initial temperature distribution are used to develop the solution for $t \geq 0$.

J-4. Difference Equations

The following approximations are used for the partial derivatives in equation (J-1):

$$\frac{\partial}{\partial r} \quad k \frac{\partial T}{\partial r} \approx \frac{k}{(\Delta r)^2} \left[T(r + \Delta r, t) - 2T(r, t) + T(r - \Delta r, t) \right] \quad (J-7)$$

$$\frac{k}{r} \frac{\partial T}{\partial r} \approx \frac{k}{r} \left[\frac{T(r + \Delta r, t) - T(r - \Delta r, t)}{2\Delta r} \right] \quad (J-8)$$

$$\rho c \frac{\partial T}{\partial t} \approx \rho c \left[\frac{T(r, t) - T(r, t - \Delta t)}{\Delta t} \right] \quad (J-9)$$

The approximation of equation (J-7) neglects the term $(\partial k / \partial r) (\partial T / \partial r)$. The justification for this omission follows from the fact that $(\partial k / \partial r) (\partial T / \partial r)$ is much smaller than $k/r (\partial T / \partial r)$, the term in equation (J-8).

Since $\frac{\partial k}{\partial r} = \frac{\partial k}{\partial T} \frac{\partial T}{\partial r}$,

$$\frac{\frac{\partial k}{\partial r} \frac{\partial T}{\partial r}}{\frac{k}{r} \frac{\partial T}{\partial r}}$$

may be written as

$$\frac{r}{k} \frac{\partial k}{\partial r} \frac{\partial T}{\partial r}$$

Now r is small, less than 0.1. It is shown in paragraph J-10 that, for each material, $(1/k) (\partial k / \partial r)$ is less than 0.01. In fact, it is less than 0.001 for almost all materials. Finally, $\partial T / \partial r$ is a well-behaved function of r . Therefore the term omitted from equation (J-7) is less than 0.1 percent of the term in equation (J-8).

The approximations of equations (J-7), (J-8), and (J-9) also make use of the fact that k and c are slowly varying functions of T . In paragraph J-10, these assumptions are justified by showing that $\partial k / \partial T$ and $\partial c / \partial T$ are small.

Other approximations that could be used instead of equation (J-7) have been tested; no appreciable difference can be seen between the schemes which keep k constant and those which do not.

Note that k and c are evaluated at $T(r, t - \Delta t)$. Here the assumption is made that T is given at time $t - \Delta t$, and the procedure is advancing to time t . Since t is given at time $t = 0$, the required initial condition is supplied.

Equations (J-7), (J-8), and (J-9) are only used inside each region; the interface between regions is covered in paragraph J-5.

The approximations in equations (J-7), (J-8), and (J-9) are substituted into equation (J-1). Letting r_1, \dots, r_k denote the points in a region R and letting $\Delta r_1 = r_{1+1} - r_1$ and $T_1 = T(r_1, t)$, equation (J-1) may be rewritten as follows:

$$B_1 T_{1-1} + A_1 T_1 + C_1 T_{1+1} = D_1 \quad (J-10)$$

where the coefficients are given by

$$B_1 = 1 - (\Delta r)_1 / (2r_1) \quad (J-11)$$

$$A_1 = -2 - (\rho_1 c_1 / k_1) (\Delta r_1)^2 / \Delta t \quad (J-12)$$

$$C_1 = 1 + (\Delta r)_1 / (2r_1) \quad (J-13)$$

$$D_1 = -q_1''' - (\rho_1 c_1 / k_1) (\Delta r_1)^2 T_1^{\text{old}} / \Delta t \quad (J-14)$$

In equations (J-11) through (J-14), ρ_1 , c_1 , k_1 , and q_1 denote the value at the point r_1 , and T_1^{old} is given by $T(r_1, t - \Delta t)$. Note that c_1 and k_1 are evaluated using the previous temperature T_1^{old} . This assumption is related to the assumption used in deriving equations (J-7), (J-8), and (J-9).

In equations (J-10) through (J-14), the two points r_0 and r_{k+1} were used; these points reside at a distance Δr from the region r . The use of interface and boundary conditions eliminates these fictitious points.

J-5. Interface Conditions

Equations (J-10) through (J-14) hold for each region. The interface conditions in equations (J-5) and (J-6) are now applied and the redundant temperatures are eliminated. Ignoring for a moment the left-hand boundary of region 1 (the origin) and the right-hand boundary of region n (the external surface), equation (J-10) can be written for each of the internal interface points.

For region R_1 , the equation for the right-hand boundary may be written

$$B_k T_{k-1} + A_k T_k + C_k T_{k+1} = D_k \quad (J-15)$$

Here k denotes the right-hand end point of R_1 .

For region R_{i+1} , the equation for the left-hand boundary may be written

$$B_1' T_0' + A_1' T_1' + C_1' T_2' = D_1' \quad (J-16)$$

Here 1 denotes the left-hand end point of R_{i+1} , and primes are used on the coefficients and temperatures.

Because of the overlap of the regions, the temperatures T_{k-1} , T_k , and T_{k+1} refer to the same spatial points as do T_0' , T_1' , and T_2' , respectively.

The interface conditions, equations (J-5) and (J-6), then lead to the following equations:

$$T_k = T_1' \quad (J-17)$$

$$k_i \left[\frac{T_{k+1} - T_{k-1}}{2(\Delta r)_i} \right] = k_{i+1} \left[\frac{T_2 - T_0}{2(\Delta r)_{i+1}} \right] \quad (J-18)$$

Equation (J-17) requires that the temperatures are in agreement at the interface point. Equation (J-18) is a difference approximation to equation (J-6), which requires that the heat transfer out of region R_i is the same as the heat transfer into region R_{i+1} .

Equations (J-15) through (J-18) are a set of four equations in six unknowns that may be reduced to one equation in three unknowns: the temperatures at the interface and at the adjacent points on either side. Using T_{k-1} , T_k , and T_{k+1} for these temperatures, and letting

$$\sigma = \frac{k_{i+1} (\Delta r)_i}{k_i (\Delta r)_{i+1}}$$

equations (J-8) through (J-15) may be combined to obtain

$$B_k' T_{k-1} + A_k' T_k + C_k' T_{k+1} = D_k' \quad (J-19)$$

where the primed coefficients are given by

$$B'_k = B'_1(B_k + C_k) \quad (J-20)$$

$$A'_k = B'_1 A_k + \sigma A'_1 C_k \quad (J-21)$$

$$C'_k = \sigma C_k (B'_1 + C'_1) \quad (J-22)$$

$$D'_k = B'_1 D_k + \sigma D'_1 C_k \quad (J-23)$$

Equations (J-10) and (J-19) now provide a tridiagonal system for the temperatures internal to the total region under consideration, $0 \leq r \leq b$. For a point internal to a region R_1 , equation (J-10) is used, and for interface points, equation (J-19) is used.

J-6. Boundary Conditions

Derivation of boundary condition equations is given in the following paragraphs.

J-7. External Surface Boundary -- Letting T_N represent the temperature at the external boundary, equation (J-10) may be written

$$B_N T_{N-1} + A_N T_N + C_N T_{N+1} = D_N \quad (J-24)$$

Further, equation (J-4) may be written in difference form as

$$\frac{T_{N+1} - T_{N-1}}{2\Delta r_{N-1}} = - \frac{\phi}{k_N} \quad (J-25)$$

Combining these two equations yields

$$(B_N + C_N) T_{N-1} + A_N T_N = D_N + \frac{2C_N \Delta r_{N-1}}{k_N} \phi \quad (J-26)$$

J-8. Internal Boundary -- For $r = 0$, equation (J-1) and the condition in equation (J-2) may be used to derive the appropriate equation for T_0 . Rewriting equation (J-1) yields

$$\frac{\partial k}{\partial r} \frac{\partial T}{\partial r} + k \frac{\partial^2 T}{\partial r^2} + \frac{k}{r} \frac{\partial T}{\partial r} = \rho c \frac{\partial T}{\partial t} - q'''' \quad (J-27)$$

At $r = 0$, $\partial T / \partial r = 0$; moreover the term $(1/r) (\partial T / \partial r)$ may be replaced by $\partial^2 T / \partial r^2$ at $r = 0$, by using L'Hospital's rule, since $\partial T / \partial r = 0$. Using these expressions, equation (J-27) may be rewritten as

$$2 \frac{\partial^2 T}{\partial r^2} = \frac{\rho c}{k} \frac{\partial T}{\partial t} - \frac{q''''}{k} \quad (J-28)$$

The term $\partial^2 T / \partial r^2$ in equation (J-28) is approximated using $(2T_1 - 2T_0) / (\Delta r_0)^2$. This expression is the standard three-point difference approximation to the second derivative with the symmetry condition $T_{-1} = T_1$ being used, since $\partial T / \partial r = 0$.

The difference equation may be written

$$A_0 T_0 + C_0 T_1 = D_0 \quad (J-29)$$

where the coefficients are given by

$$A_0 = -4 - \frac{\rho_0 c_0}{k_0} \frac{(\Delta r_0)^2}{\Delta t} \quad (J-30)$$

$$C_0 = 4 \quad (J-31)$$

$$D_0 = \frac{-\rho_0 c_0}{k_0} \frac{(\Delta r_0)^2}{(\Delta t)} T(0, t - \Delta t) - q_0'''' \frac{(\Delta r_0)^2}{k_0 (\Delta t)} \quad (J-32)$$

Equations (J-10), (J-19), (J-26), and (J-29) form a linear tridiagonal set of $N+1$ equations in the $N+1$ unknowns T_0, \dots, T_N . However, equation (J-26) introduced another unknown, ϕ , but equation (J-3) leads to one of the T 's. As a result, there remain $N+1$ equations in $N+1$ unknowns. Let T_M denote the given internal temperature. Since k and c depend on the temperature at time $t - \Delta t$, ϕ is not brought over to the left-hand side of the equations nor is T_M moved to the right-hand side. Instead, ϕ is estimated using the values of T_M at future times. T_M is treated as an unknown, thus keeping the tridiagonal structure of the equations.

J-9. Method of Solution

Let $\underline{T}^t = (T_0, \dots, T_N)$; T_i is at time t . \underline{T}^{t-1} is a similar vector at time $t - \Delta t$. Now let A be the tridiagonal matrix:

$$\begin{bmatrix} A_0 & C_0 & & & \\ B_1 & A_1 & C_1 & & \\ & B_2 & A_2 & C_2 & \\ & & \ddots & \ddots & \ddots \\ & & & B_{N-1} & A_{N-1} & C_{N-1} \\ & & & & B_N & A_N \end{bmatrix}$$

Let S be a diagonal matrix with the i -th element given by

$$\frac{\rho_i c_i}{k_i} \frac{(\Delta r_i)^2}{\Delta t}$$

Here c_i and k_i are evaluated at $T_i^{t-\Delta t}$.

Let \underline{q} be the vector with the i -th component given by

$$-q_i''' = \frac{(\Delta r_i)^2}{k_i(\Delta t)}$$

Finally, let $\underline{\delta}$ be a vector with $\delta_i = 0$; $i = 0, \dots, N-1$; and $\delta_N = \Delta r_{N-1}/C_N k_N$.

Equations (J-10), (J-19), (J-26), and (J-29) may be abbreviated as

$$A\underline{I}^i = D\underline{I}^i = \underline{q} + \phi^i \underline{\delta} \quad (J-33)$$

Again, ϕ^i is unknown, but T_M^i is known.

For simplicity, assume $i = 1$; that is, the initial data for time = 0 are given, and the calculation is proceeding to time Δt .

Let \underline{p}^k denote a particular solution of the following equation:

$$A\underline{p}^k = D\underline{p}^{k-1} + \underline{q} \quad (J-34)$$

with \underline{p}^{k-1} given. Similarly, let \underline{h}^k denote a homogeneous solution of the following:

$$A\underline{h}^k = D\underline{h}^{k-1} \quad (J-35)$$

with \underline{h}^{k-1} given. Begin these sequences as follows:

$$\underline{p}^0 = \underline{I}^0 \quad (J-36)$$

and

$$A\underline{h}^1 = \underline{\delta} \quad (J-37)$$

Define \underline{I}^1 by $\underline{I}^1 = \underline{p}^1 + \phi^1 \underline{h}^1$; then \underline{I}^1 satisfies equation (J-33) in the form

$$A\underline{I}^1 = D\underline{I}^0 + \underline{q} + \phi^1 \underline{\delta}$$

This may be proved as follows. Multiplying the equation defining \underline{T}^1 by A yields

$$\begin{aligned} A\underline{T}^1 &= A(\underline{p}^1 + \phi^1 \underline{H}^1) \\ &= A\underline{p}^1 + \phi^1 A\underline{H}^1 \\ &= D\underline{p}^0 + \underline{q} + \phi^1 \delta \end{aligned}$$

using equations (J-34) and (J-37). Notice, however, that $\underline{p}^0 = T^0$ from equation (J-36); the proof is complete.

Moreover, if

$$\underline{T}^k = \underline{p}^k + \phi^k \underline{H}^1 + \phi^{k-1} \underline{H}^2 + \dots + \phi^1 \underline{H}^k \quad (\text{J-38})$$

then \underline{T}^k satisfies equation (J-33) for all $\phi^1, \phi^2, \dots, \phi^k$. The proof of this result is easily given by induction.

Therefore, given \underline{T}^0 , future temperatures may be approximated by $\underline{T}^1, \underline{T}^2, \dots, \underline{T}^k$, as far as necessary.

Note that the computation of \underline{p}^1 and \underline{H}^1 requires only the solving of a tri-diagonal system with the same matrix A [see equations (J-34), (J-35), and (J-37)].

Given that T^1, T^2, \dots, T^k have been computed, the values of ϕ^1 are chosen so that T_m^1 agrees with T_{data}^1 . Since there are k conditions and k unknowns, the values of ϕ may be obtained exactly. However, the experimental error in T_{data} causes ϕ to behave erratically if this procedure is followed.

It is more reasonable to derive a relationship between the ϕ^1 values, and then to obtain k equations in the one unknown, ϕ^1 . In other implementations, it is assumed that either ϕ is constant (that is, $\phi^1 = \phi^2 = \dots = \phi^k$) or that ϕ^{i+1} is a prescribed linear or quadratic function of ϕ^1 .

The approach in this study was to use the measured temperature profile to derive a relationship between ϕ^i and ϕ^{i+1} . First, the heat balance for the whole rod may be written as follows:

$$q''''V - \phi A = \frac{\partial T}{\partial t} \times \text{constant} \quad (\text{J-39})$$

where

V = volume of heated region

A = rod surface area

The $\partial T / \partial t$ term in equation (J-39) cannot be computed before ϕ is calculated; however, it may be estimated by

$$\left(\frac{\partial T}{\partial t} \right)^i \approx \frac{T_D^i - T_D^{i-1}}{\Delta t}$$

Here T_D^i is the measured temperature T_{data} . Therefore equation (J-39) may be approximated, yielding

$$q''''V - \phi^i A = \frac{T_D^i - T_D^{i-1}}{\Delta t^i} \times \text{constant} \quad (\text{J-40})$$

Assuming that the constant is independent of time, and writing equation (J-40) for both i and $i+1$, the constant may be eliminated. Solve for ϕ^{i+1} in terms of ϕ^i to obtain

$$\phi^{i+1} = E^{i+1} \phi^i + F^{i+1} \quad (\text{J-41})$$

where E^{i+1} and F^{i+1} are given by

$$E^{i+1} = \frac{(T_D^{i+1} - T_D^i) / (\Delta t)^{i+1}}{(T_D^i - T_D^{i-1}) / (\Delta t)^i}$$

$$F^{i+1} = \left[(q^{i+1})^{i+1} \times V - E^{i+1} \times (q^{i+1})^i \times V \right] / A$$

This relationship predicts the future behavior of ϕ^i more accurately than any of the aforementioned methods.

Moreover, a similar relationship may be derived for ϕ^{i+2} , ϕ^{i+3} , ... in terms of ϕ^i . If these expressions for future ϕ values are substituted into equation (J-38), there results the following expression for \underline{T}^k in terms of \underline{H}^1 , \underline{H}^2 , ... \underline{H}^k , \underline{p}^k and ϕ^1 :

$$\underline{T}^k = \underline{\alpha}^k + \phi^1 \beta^k$$

where $\underline{\alpha}^k$ and β^k are given by

$$\underline{\alpha}^k = \underline{p}^k + \sum_{j=1}^{k-1} F^{k+1-j} \underline{H}^j$$

$$\beta^k = \underline{H}^k \sum_{j=1}^{i-1} E^{k+1-j} \underline{H}^j$$

Now choose ϕ^1 by the standard least-squares procedure so that T_m^1, \dots, T_m^k best fits $T_{data}^1, \dots, T_{data}^k$. Thus,

$$\phi^1 = \frac{\sum_{i=1}^k (T_{data}^i - \alpha_m^i) \times \beta_m^i}{\sum_{i=1}^k (\beta_m^i \times \beta_m^i)}$$

where α_m^i and β_m^i represent the m-th components of the temperature vectors $\underline{\alpha}^i$ and $\underline{\beta}^i$. Therefore ϕ^1 is chosen so that the computed temperatures for the next k time steps best fit the measured temperatures for those k time steps.

Experience with this method suggests that $k = 3$ is an appropriate number of time steps.

J-10. Variation of k and c With Respect to T

In deriving the difference approximations for equations (J-1) and (J-4), it has been assumed that k and c are constants and that they may be evaluated using the temperature of the previous time step. Moreover, it has been assumed that $(1/k \, dk/dT)$ is less than 0.01. These assumptions are justified by considering the following expressions. For each material, dk/dT , $(1/k \, dk/dT)$, and dc/dT are listed. The expressions are obtained from the formulas in paragraph J-11. For materials in which $c(T)$ is a linear interpolate of a table, dc/dT has been estimated by computing the maximum $\Delta c/\Delta T$ value, as follows:⁽¹⁾

o Boron nitride

$$\frac{dk}{dT} = -8.8889 \times 10^{-4} \text{ Btu/hr-ft-}^\circ\text{F}^2$$

$$\frac{1}{k} \frac{dk}{dT} = \frac{-8.8889 \times 10^{-4}}{14.778 - 8.8889 \times 10^{-4} T} \, ^\circ\text{F}^{-1}$$

$$\frac{dc}{dT} = (0.333492) 1.3611 \times 10^{-3} e - (1.3611 \times 10^{-3} T) \text{ Btu/lbm-}^\circ\text{F}^2$$

o Kanthal

$$\frac{dk}{dT} = 4.3 \times 10^{-3} \text{ Btu/hr-ft-}^\circ\text{F}^2$$

$$\frac{1}{k} \frac{dk}{dT} = \frac{4.3 \times 10^{-3}}{9.7 + 4.3 \times 10^{-3} T} \, ^\circ\text{F}^{-1}$$

$$\frac{dc}{dT} = 0.0003 \text{ Btu/lbm-}^\circ\text{F}^2$$

1. The results of these computations are given in English engineering units, the form in which the data are analyzed by the code.

o Magnesium oxide

$$\frac{dk}{dT} = (121.814) - 0.010722 e^{-0.010722T} - \frac{2 (7015.835)}{T^2} \text{ Btu/hr-ft-}^\circ\text{F}^2$$

$$\frac{1}{k} \frac{dk}{dT} = \frac{121.814 - 0.010722 e^{-0.010722T} - \frac{2 (7015.835)}{T^2}}{0.2529 - 121.814 e^{-0.010722T} + \frac{7015.835}{T}} \text{ }^\circ\text{F}^{-1}$$

$$\frac{dc}{dT} = (0.111256) - 1.33715 \times 10^{-3} e^{-1.33715 \times 10^{-3} T} \text{ Btu/lbm-}^\circ\text{F}^2$$

o Nichrome V

$$\frac{dk}{dT} = 5.75 \times 10^{-3} \text{ Btu/hr-ft-}^\circ\text{F}^2$$

$$\frac{1}{k} \frac{dk}{dT} = \frac{5.75 \times 10^{-3}}{5.2 + 5.75 \times 10^{-3} T} \text{ }^\circ\text{F}^{-1}$$

$$\frac{dc}{dT} = 0.0002 \text{ Btu/lbm-}^\circ\text{F}^2$$

o Stainless steel 304

$$\frac{dk}{dT} = 4.2 \times 10^{-3} \text{ Btu/hr-ft-}^\circ\text{F}^2$$

$$\frac{1}{k} \frac{dk}{dT} = \frac{4.2 \times 10^{-3}}{8.4 + 4.2 \times 10^{-3} T} \text{ }^\circ\text{F}^{-1}$$

$$\frac{dc}{dT} = 0.001 \text{ Btu/lbm-}^\circ\text{F}^2$$

o Stainless steel 316

$$\frac{dk}{dT} = 4.3 \times 10^{-3} \text{ Btu/hr-ft-}^{\circ}\text{F}^2$$

$$\frac{1}{k} \frac{dk}{dT} = \frac{4.3 \times 10^{-3}}{7.5 + 4.3 \times 10^{-3} T} \text{ }^{\circ}\text{F}^{-1}$$

$$\frac{dc}{dT} = 0.001 \text{ Btu/lbm-}^{\circ}\text{F}^2$$

o Stainless steel 347

$$\frac{dk}{dT} = 4.2 \times 10^{-3} \text{ Btu/hr-ft-}^{\circ}\text{F}^2$$

$$\frac{1}{k} \frac{dk}{dT} = \frac{4.2 \times 10^{-3}}{8.3 + 4.2 \times 10^{-3} T} \text{ }^{\circ}\text{F}^{-1}$$

$$\frac{dc}{dT} = 2.8 \times 10^{-5} \text{ Btu/lbm-}^{\circ}\text{F}^2$$

For each material, excluding dk/dT and $(1/k) (dk/dT)$ for magnesium oxide, it is clear that temperature derivatives and the $(1/k) (dk/dT)$ term are appropriately small. Because of the special form of $k(T)$ for magnesium oxide, the analysis of dk/dT and $(1/k) (dk/dT)$ is more complicated. The interaction of the negative exponential term and the $1/T$ term makes precise estimates difficult. An alternative approach is to consider the original data. The $k(T)$ functions fit the following table:

$T [^{\circ}\text{C} (^{\circ}\text{F})]$	$k [\text{W/m}^2\text{-K} (\text{Btu/hr-ft-}^{\circ}\text{F})]$
212	20.8
392	16.33
752	9.53
1112	6.65
1472	4.91
1832	4.04
2192	3.53

The maximum $\Delta k/\Delta T$ for this table is 0.02 in the interval between 100°C and 200°C (212°F and 392°F).

The corresponding $(1/k) (\Delta k/\Delta T)$ value is 0.001, as required.

J-11. Material Properties

DATAR contains a built-in library of pertinent material properties which are unalterable by the user, to avoid potential errors and inconsistencies. Thermal conductivity and specific heat versus temperature curves are built in for each of the materials shown in table J-1. A constant density is built in for each of the materials, with the exception of magnesium oxide and boron nitride. In these two cases, the user must supply the density for the appropriate material. The thermal conductivity and specific heat of boron nitride are not a function of the density, since the heater rods are highly swaged, which provides for approximately 95-percent theoretical density. Note that the thermal conductivity of magnesium oxide depends on the density.

Each thermal conductivity or specific heat is calculated by either a least-squares fit to available data or a linear interpolation from a table of available data. Table J-1 gives the source of the data for each material. A summary of the methods used for each material follows:

o Boron nitride

$$k = 25.571 - 0.00276 T \text{ W/m-}^\circ\text{C} \\ (14.778 - 8.8889 \times 10^{-4} T \text{ Btu/hr-ft-}^\circ\text{F})$$

$$C_p = 2017.74 - 1396.26e^{-0.00295T} \text{ J/kg-}^\circ\text{C} \\ (0.48193 - 0.333492e^{-1.3611 \times 10^{-3}T} \text{ Btu/lb-}^\circ\text{F})$$

$$\rho = \text{input quantity [kg/m}^3 \text{ (lb/ft}^3\text{)]}$$

o Kanthal

$$k = 16.789 + 0.0134 T \text{ W/m-}^\circ\text{C} (9.7 + 4.3 \times 10^{-3} T \text{ Btu-hr-ft-}^\circ\text{F})$$

TABLE J-1
MATERIAL PROPERTY DATA SOURCES

Material	Property	Source of Data
Boron nitride	K	(a)
	Cp	Touloukian(b)
Kanthal	ρ	Supplied by user
	K	(c)
Magnesium oxide	Cp	(c)
	ρ	Supplier(d)
Nichrome V	K	Kingery, et al.(e)
	Cp	Touloukian(b)
Stainless steel 304	ρ	Supplied by user
	K	Touloukian(b)
Stainless steel 316	Cp	Touloukian(b)
	ρ	Touloukian(b)
Stainless steel 347	K	WCAP-2808(f)
	Cp	Touloukian(b)
Air	ρ	Touloukian(b)
	K	WCAP-2808(f)
	Cp	Touloukian(b)
	ρ	Touloukian(b)
	K	Baumeister(g)
	Cp	Baumeister(g)
	ρ	Baumeister(g)

- a. The thermal conductivity of powdered boron nitride is dependent on several factors. The formula used for this quantity reflects an engineering judgment which considers those factors pertinent to the Westinghouse use of this material.
- b. Touloukian, Y. S., Thermophysical Properties of High Temperature Solid Materials, Macmillan, New York, 1967.
- c. This quantity has been derived as a function of temperature from data obtained on materials of similar composition.
- d. "Physical Properties of Kanthal Alloys," G-45-07, The Kanthal Corporation, Bethel, CT.
- e. Kingery, W. D., et al., "Thermal Conductivity X. Data for Pure Oxide Materials Corrected to Zero Porosity," J. Am. Ceram. Soc. 37, 107-110 (1954).
- f. Marti Balaguer, L., "MPD Materials Design Manual," WCAP-2808, July 1966.
- g. Baumeister, T., Mechanical Engineers Handbook, 6th edition, McGraw-Hill, New York, 1958.

Cp = linear interpolation from the following:

T [°C (°F)]		Cp [J/kg-°C (Btu/lb-°F)]	
-32	(0)	456.4	(0.109)
648	(1200)	753.6	(0.180)
760	(1400)	1172.3	(0.280)
871	(1600)	745.2	(0.178)
1204	(2200)	779.6	(0.185)

$$\rho = 7144.2 \text{ kg/m}^3 \text{ (446.0 lb/ft}^3\text{)}$$

o Magnesium oxide

$$k = \rho_{\text{MgO}} (0.0273 - 13.15e^{-0.0192T} + 420.9/T)/223 \text{ w/m-°C}$$

$$[\rho_{\text{MgO}} (0.2529 - 121.814e^{-0.010722T} + 7015.835/T)/223 \text{ Btu/hr-ft-°F}]$$

$$Cp = 1377.353 - 465.805e^{-0.002406T} \text{ J/kg-°C}$$

$$(0.328976 - 0.111256e^{-1.33715 \times 10^{-3}T} \text{ Btu/lb-°F})$$

$$\rho = \text{input quantity [kg/m}^3 \text{ (lb/ft}^3\text{)]}$$

o Nichrome V

$$k = 8.997 + 0.0179 T \text{ w/m-°C (5.2 + 5.75} \times 10^{-3} T \text{ Btu/hr-ft-°F)}$$

Cp = linear interpolation from the following:

T [°C (°F)]		Cp [J/Kg-°C (Btu/lb-°F)]	
-32	(0)	427.1	(0.102)
260	(500)	502.4	(0.120)
482	(900)	535.9	(0.128)
593	(1100)	577.8	(0.138)
704	(1300)	623.8	(0.149)
816	(1500)	653.1	(0.156)
871	(1600)	661.5	(0.158)
982	(1800)	653.1	(0.156)

$$\rho = 8361.63 \text{ kg/m}^3 \text{ (522.0 lb/ft}^3\text{)}$$

o Stainless steel 304

$$k = 14.535 + 0.01308 T \text{ w/m-}^\circ\text{C} \text{ (8.4 + 4.2 x 10}^{-3} T \text{ Btu/hr-ft-}^\circ\text{F)}$$

Cp = linear interpolation from the following:

T [°C (°F)]		Cp [J/kg-°C (Btu/lb-°F)]	
-32	0	372.6	(0.089)
149	(300)	372.6	(0.089)
260	(500)	378.9	(0.0905)
371	(700)	389.4	(0.093)
482	(900)	404.0	(0.0965)
593	(1100)	420.8	(0.1005)
816	(1500)	458.4	(0.1095)
926	(1700)	475.2	(0.1135)
1038	(1900)	483.6	(0.1155)
1093	(2000)	485.7	(0.116)

$$\rho = 8025.2 \text{ kg/m}^3 \text{ (501.3 lb/ft}^3\text{)}$$

o Stainless steel 316

$$k = 12.978 + 0.01339 T \text{ w/m-}^\circ\text{C} \text{ (7.5 + 4.3 x 10}^{-3} T \text{ Btu/hr-ft-}^\circ\text{F)}$$

Cp = linear interpolation from the following:

T [°C (°F)]		Cp [J/kg-°C (Btu/lb-°F)]	
-32	(0)	439.6	(0.105)
204	(400)	510.8	(0.122)
315	(600)	540.1	(0.129)
427	(800)	561.0	(0.134)
871	(1600)	619.6	(0.148)
1038	(1900)	659.4	(0.1575)
1204	(2200)	703.4	(0.168)

$$\rho = 7949.96 \text{ kg/m}^3 (496.3 \text{ lb/ft}^3)$$

o Stainless steel 347

$$k = 13.064 + 0.0143 T \text{ w/m-}^\circ\text{C} (7.55 + 4.58 \times 10^{-3} T \text{ Btu/hr-ft-}^\circ\text{F})$$

$$Cp = 447.99 + 0.211 T \text{ J/kg-}^\circ\text{C} (0.107 + 2.8 \times 10^{-5} T \text{ Btu/lb-}^\circ\text{F})$$

$$\rho = 7905.1 \text{ kg/m}^3 (493.5 \text{ lb/ft}^3)$$

o Air

$$k = 20.91 \times 10^{-5} (T + 273)^{0.846} \text{ w/m-}^\circ\text{C} \\ [7.35 \times 10^{-5} (T + 460)^{0.846} \text{ Btu/hr-ft-}^\circ\text{F}]$$

$$Cp = 1009.02 \text{ J/kg-}^\circ\text{C} (0.241 \text{ Btu/lb-}^\circ\text{F})$$

$$\rho = 1.201 \text{ kg/m}^3 (0.075 \text{ lb/ft}^3)$$

Although the option is generally only used in the heater region, DATAR permits a mixture of any two materials to exist in any radial region. In this instance, the properties at each node in the region must be adjusted to account for the effect of the mixture. This is accomplished as follows:

Let

x	= volume fraction of material A
ρ_A, K_A, C_A	= properties of material A
ρ_B, K_B, C_B	= properties of material B
$\bar{\rho}, \bar{K}, \bar{C}$	= mixture properties

Then

$$\rho = x\rho_A + (1 - x)\rho_B$$

$$K = xK_A + (1 - x)K_B$$

$$\bar{C} = \frac{x\rho_A C_A}{\bar{\rho}} + \frac{(1 - x)\rho_B C_B}{\bar{\rho}}$$

This formulation provides an exact accounting of the mixture heat capacity and a parallel conduction path approximation for the effective thermal conductivity. The approximation to the mixture thermal conductivity is not expected to introduce any significant error, however, since the only mixed region for a normal case is the second radial region, which conducts less heat than any of the more exterior regions.

J-12. EFFECT OF POWER STEP ON HEAT TRANSFER COEFFICIENT

During the self-aspirating steam probe shakedown tests prior to the 21-rod bundle testing, it was learned that the thermal response could be improved by drying out the steam probe prior to flood. Therefore, the 21-rod bundle was heated up to a rod temperature of 871°C (1600°F) at a slow rate [1.3 kw/m (0.4 kw/ft) peak] to evaporate water trapped within the steam probe. The power was subsequently stepped up to the specified value at time of flood. However, approximately 2 seconds after flood was required for the power to achieve the specified value. After achieving the specified value, the power was decayed according to the ANS + 20 percent curve. This rapid power increase during flood initiation caused the DATAR code-calculated heat transfer to initially decrease, turn around, and then increase as flooding continued.

Although it was concluded in the 21-rod bundle program that the power step at flood initiation had a negligible effect on the reflood heat transfer data, the computer software was changed in the 163-rod bundle to allow this power step prior to flood, as shown in figure J-1. The corresponding effects on the measured rod temperature and calculated heat transfer coefficient are shown in figure J-2.

J-13. QUENCH PROGRAM

The QUENCH program was utilized for reduction of heater rod and housing thermocouple data. This program was designed to determine the following quantities:

- o Initial temperature
- o Maximum temperature
- o Turnaround time
- o Quench time
- o Quench temperature

The initial temperature or temperature at flood time was determined by interpolating between the temperature recorded at the last negative time (preflood) and the temperature recorded at the first positive time (postreflood). The maximum temperature was determined by simply searching for that temperature, and the turnaround time was the time at which the maximum temperature occurred.

To determine the quench time and temperature, the following method was used.

The program advances sequentially through all the data for each thermocouple channel, looking at five points at a time [$T(t)$ at 1 through $1 + 4$, figure J-3]. The first criterion applied is that the temperature, $T(t)$, must be greater than 149°C (300°F) to qualify as a potential quench condition. If it is not, the remaining criteria are skipped.

The second criterion checks whether the slope of the temperature-time curve between the third and fourth points is greater than 28°C (50°F) per second, that is, whether

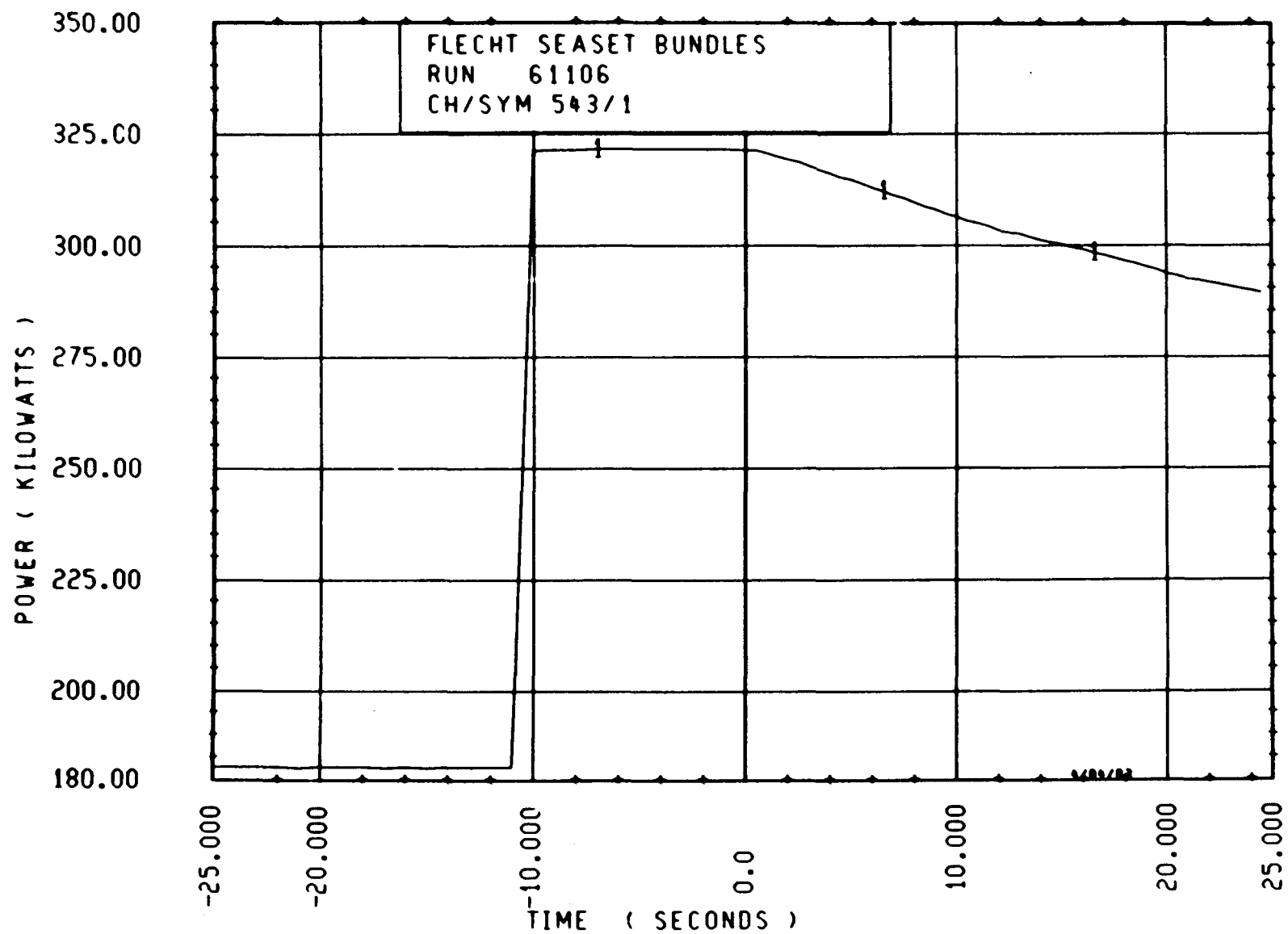


Figure J-1. Power Step Prior to Flood

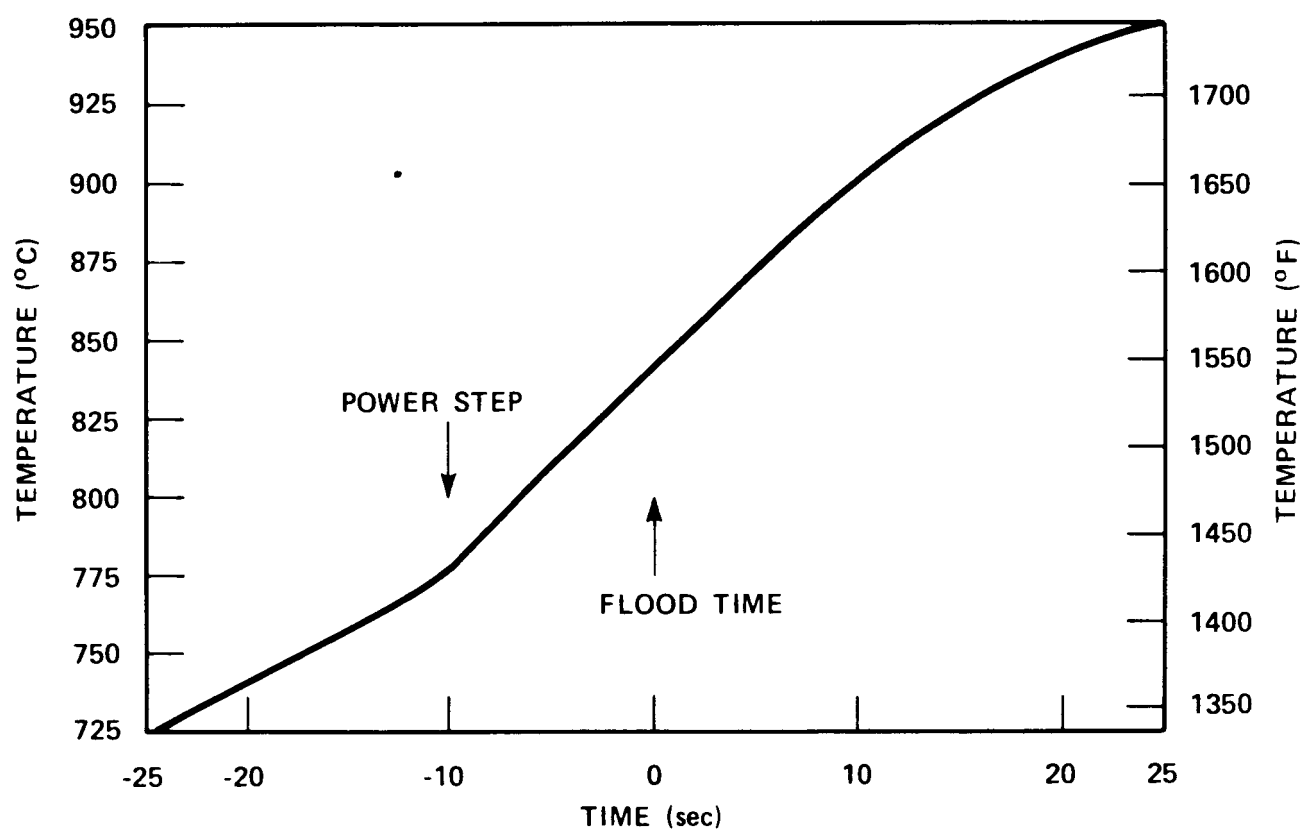


Figure J-2. Clad Temperature as a function of Time

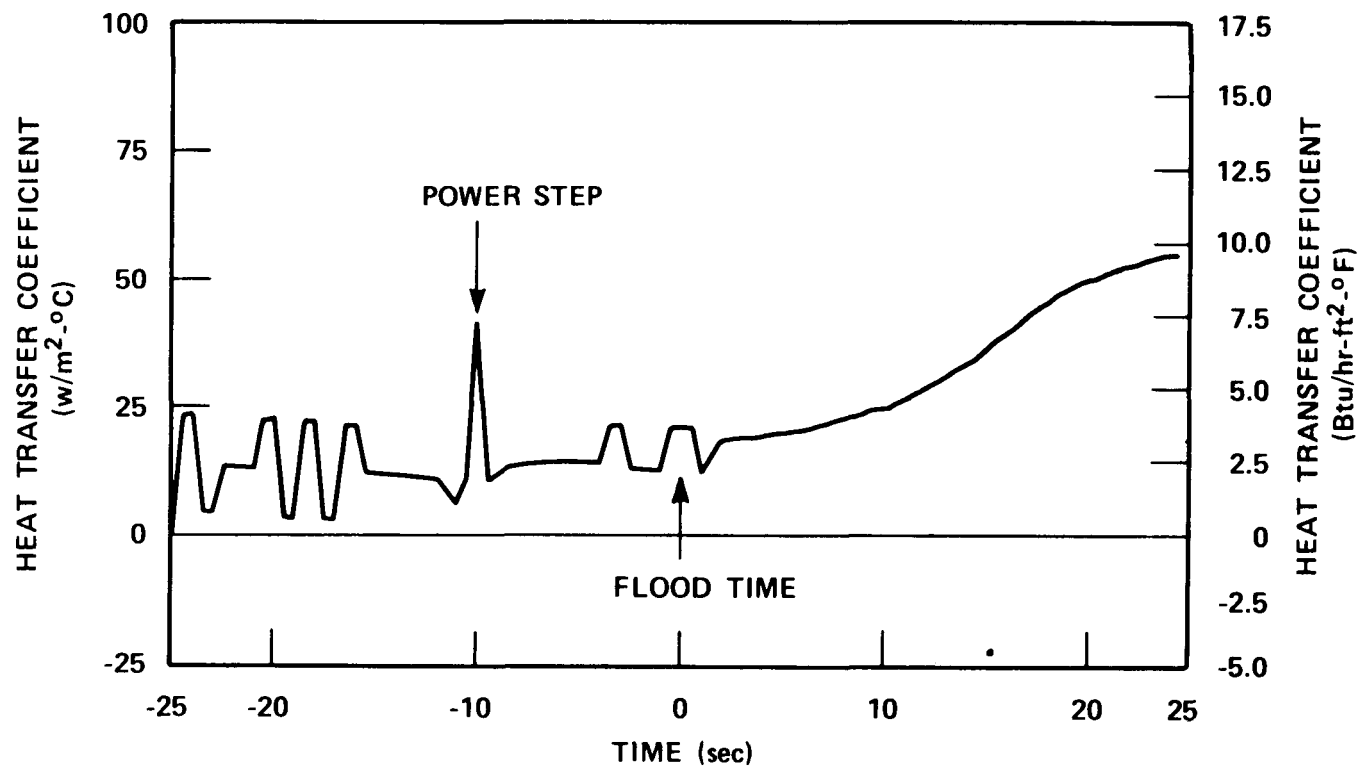


Figure J-3. Heat Transfer Coefficient as a Function of Time

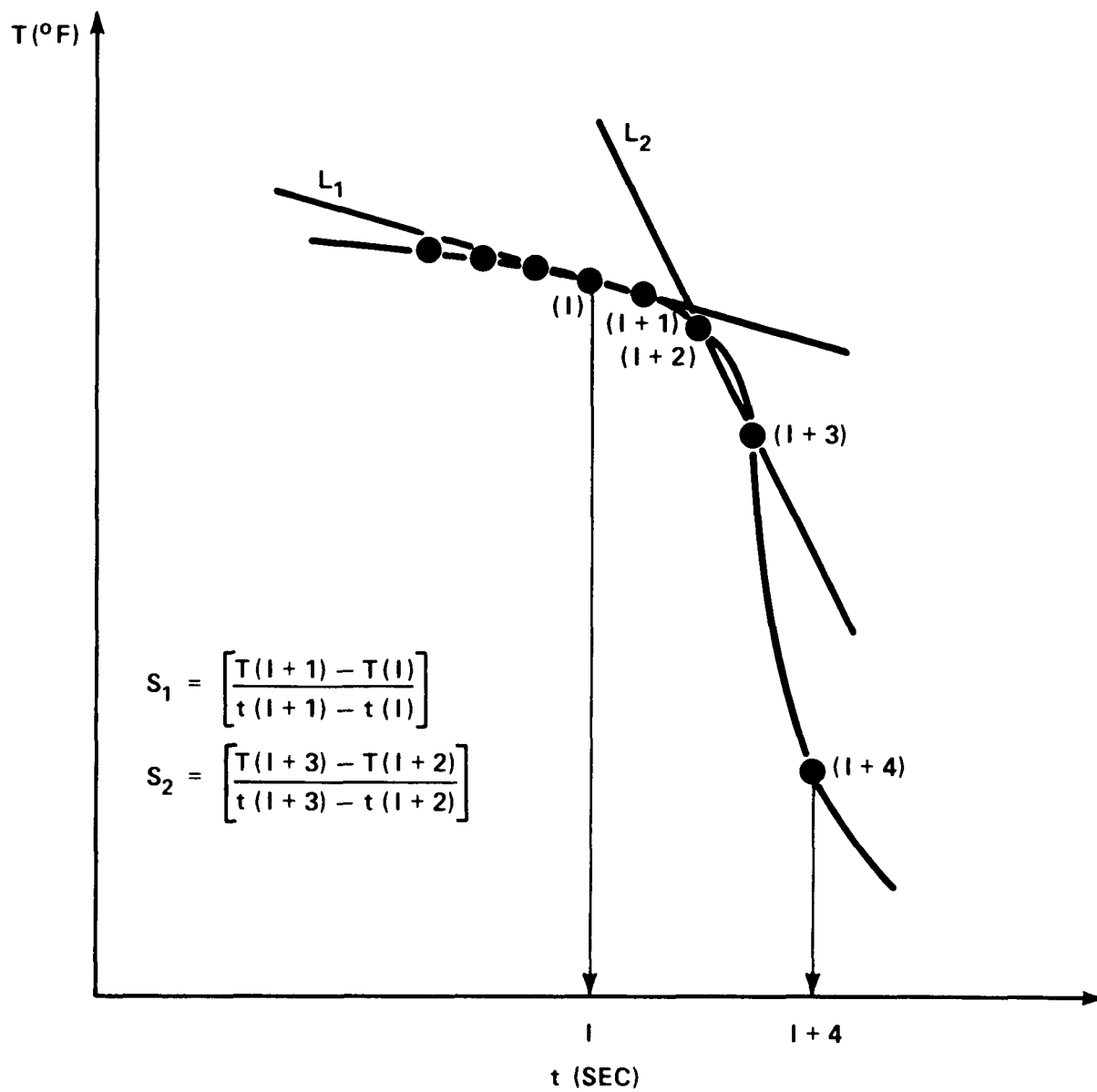


Figure J-4. Determination of Quench Time and Temperature (sheet 1 of 2)

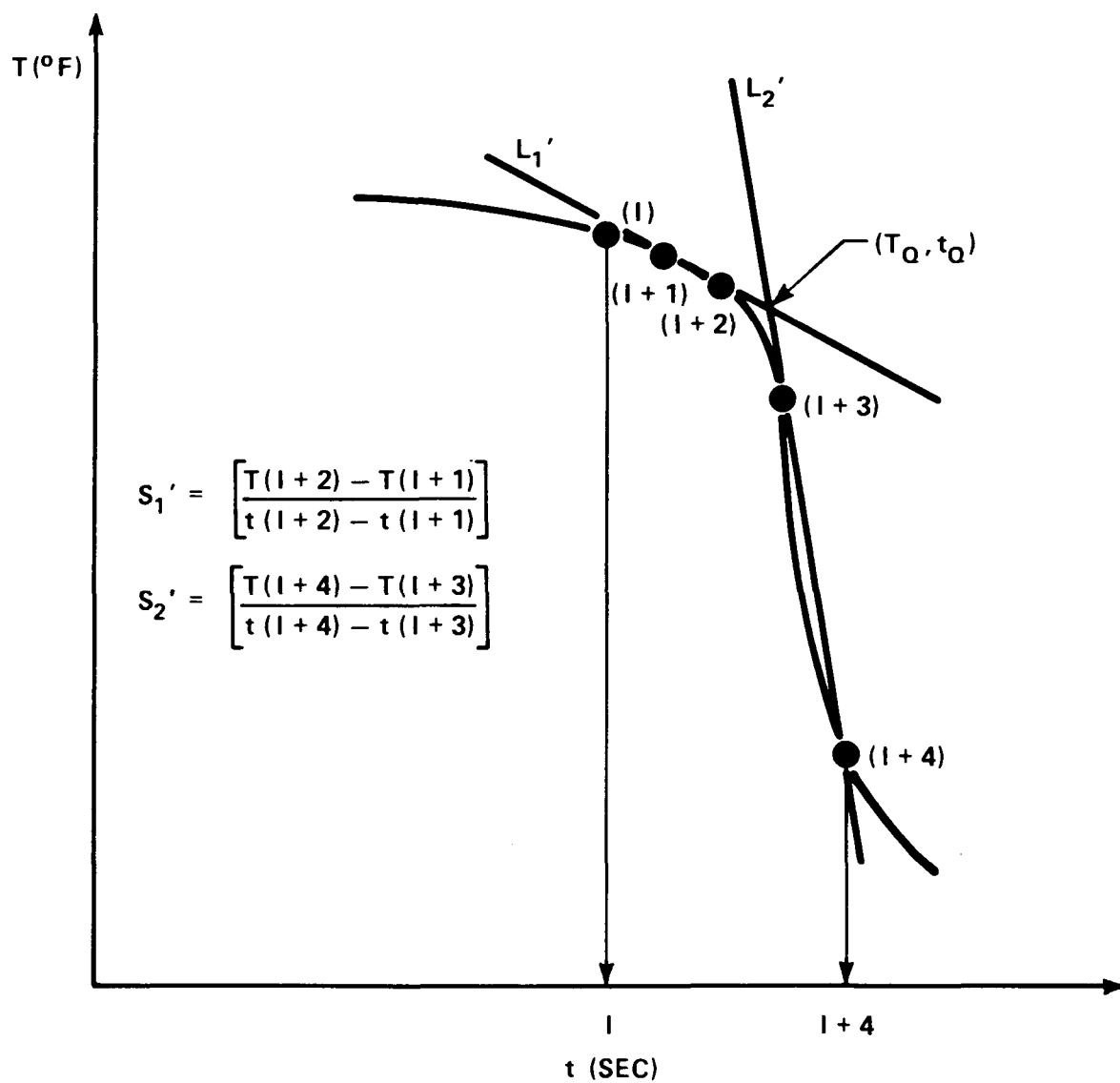


Figure J-4. Determination of Quench Time and Temperature (sheet 2 of 2)

$$\frac{T(1 + 3) - T(1 + 2)}{t(1 + 3) - t(1 + 2)} < -28^{\circ}\text{C/sec } (-50^{\circ}\text{F/sec})$$

The decision whether a quench exists or not is made on this basis. If not, the remaining criteria are skipped and the program advances to the next data point.

The third criterion checks whether the absolute value of the slope between the third and fourth points is two times greater than the absolute value of the slope between the first and second points, that is, whether $S_2 > 2S_1$. If so, a quench condition exists. If not, the program skips out of the search and advances to the next set of data points.

Finally, the program checks the absolute value of the slope between the fourth and fifth data points (S'_2) and compares it to the absolute value of the slope between the third and fourth points (S_2).

If $S'_2 > S_2$, then the quench time and temperature is defined to be the intersection of L'_1 and L'_2 (figure J-4).

The QUENCH program also calculates a quench front curve based upon a curve fit of the average quench time for each elevation. This quench front curve is subsequently differentiated with respect to time in order to obtain a quench front velocity.

J-14. FFLOWS PROGRAM

The FFLOWS program was utilized to calculate mass balance and void fraction for each reflood test. This program is a modification of the mass balance program used in the FLECHT SEASET 21-rod bundle test series.⁽¹⁾

The following calculations were performed:

- o The injected mass was calculated from the inlet turbine meter.
- o The liquid collected was calculated from the differential pressure cells on the carryover tank, upper plenum, and steam separator tanks, assuming all differential pressure was elevation head with water at the saturation temperature.

- o The steam flow was calculated from the orifice plate differential pressure cell using the measured steam temperature and local pressure to obtain the steam density.
- o The mass storage in the test bundle was calculated using the 0 to 3.56 m (0 to 140 in.) differential pressure cell reading (corrected for frictional pressure drop).
- o The mass storage in the downcomer was calculated from the differential pressure transmitter for the gravity reflood tests.

Between 0.494 and 3.41 kg (1.09 and 7.52 lb) of water collected in the aspirating steam probe collection tanks during a reflood test. This mass represents approximately 0.17 to 1.44 percent of the injected mass. When this mass was added to the total mass flow out of the system and the mass collection in the test system, the forced reflood test mass balance was usually within plus or minus 4 percent, with an average of 2.6 percent, and the gravity reflood test mass balance was within 1 percent, with an average of 0.4 percent. The percent mass aspirated through the 17 bundle thimble tube steam probes for each test is shown in figure J-5 as well as the total aspirated mass (17 bundle steam probes and 3 upper plenum and exhaust line steam probes).

In addition to calculation of the mass flows through the test system, the space-averaged void fraction was calculated from the measured pressure drop over each of the 0.30 m (12 in.) sections of the bundle. The measured pressure drop consists of three effects: elevation head, frictional pressure drop, and acceleration pressure drop due to liquid vaporization:

$$\begin{array}{ccccccc} \Delta P & & = & \Delta P & & + & \Delta P & & + & \Delta P \\ \text{measured} & & & \text{elevation} & & & \text{acceleration} & & & \text{friction} \end{array}$$

The relative magnitude of each of these components was examined in the FLECHT-SET Phase A report.⁽¹⁾ It was concluded that the vapor elevation head and the acceleration pressure drop were completely negligible and that the frictional pressure drop was a second-order effect compared to the liquid elevation head. The small frictional pressure drop for a gravity reflooding situation is attributed to the high injection rate, which quickly absorbs the bundle

1. Blaisdel, J. A., et al., "PWR FLECHT-SET Phase A Report," WCAP-8238, December 1973.

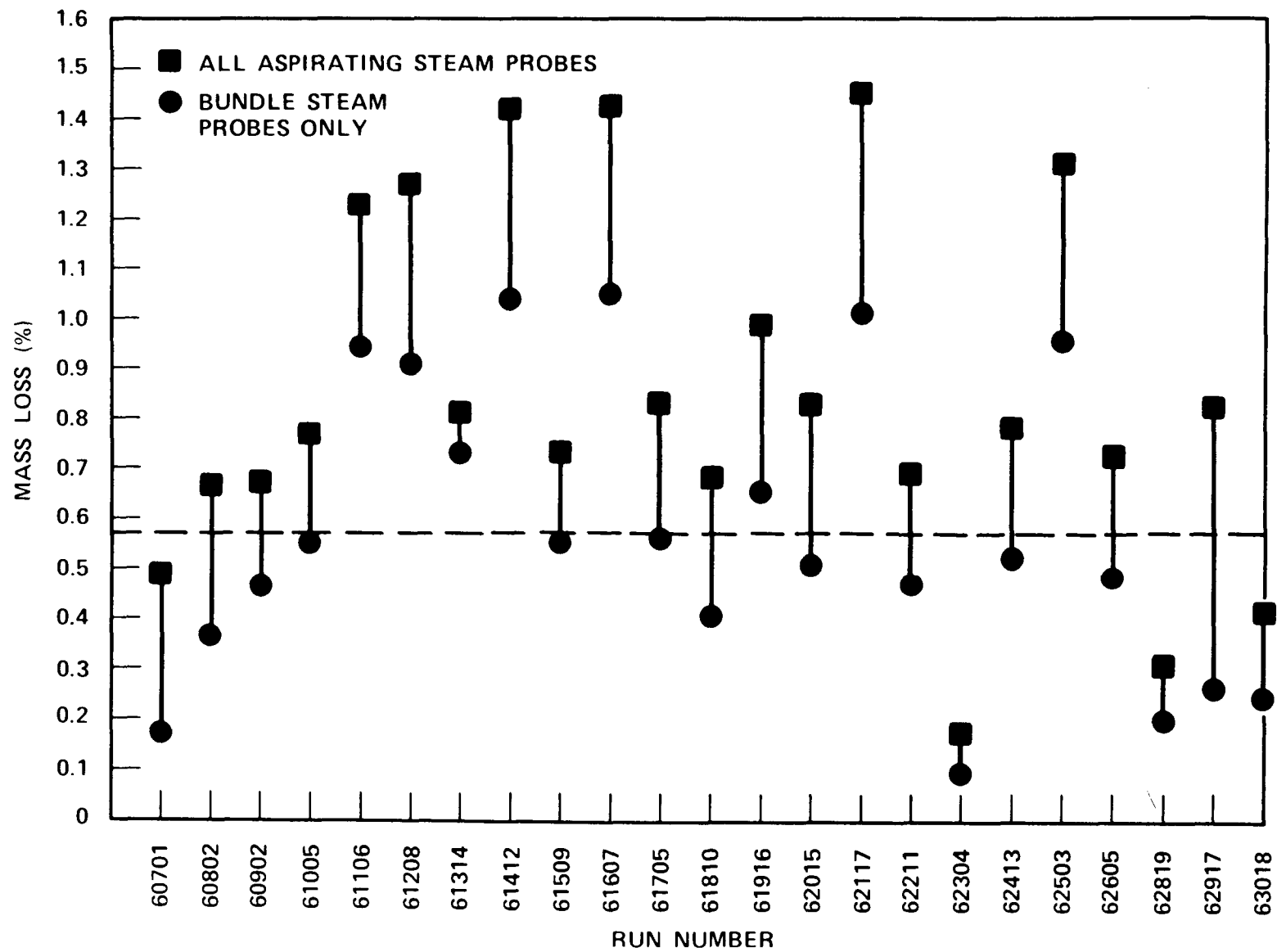


Figure J-5. Percentage of Mass Aspirated Through Steam Probes

energy. Therefore, the steam generation rate is small during the transient. It was felt that forced low flooding rate tests would result in such substantial evaporation of the injected flow that frictional pressure drop could be important during the transient. Because the 12 axial differential pressure cells on the test bundle were plus or minus 3.7×10^3 Pa (± 15 in. wg) pressure transmitters, the frictional pressure drop could be accurately accounted for in the tests. In this fashion, if the frictional pressure drop was calculated for a test, this value could be subtracted from the measured pressure drop to obtain the liquid elevation head, and therefore, the space-averaged void fraction.

The frictional pressure drop was calculated as

$$\Delta P_{\text{friction}} = \left(\frac{fL}{D_e} + K_g \right) \frac{\rho_b V_b^2}{2g_c}$$

where

L = length = 0.30 m (12 in.)

ρ_b = bundle steam density evaluated from the average of 26 bundle steam probe readings at respective elevations and test section pressure

D_e = bundle hydraulic diameter = 4 (flow area)/wetted perimeter

V_b = bundle steam velocity obtained from the mass flow rate through the exhaust orifice-plate = $M/(\rho_b \times \text{bundle flow area})$

f = friction factor

= $64/Re$ for $Re < 2000$

= $5.5 \times 10^{-3} \left[1.0 + \left(20000 \frac{D_e}{Re} + \frac{10^6}{Re} \right)^{1/3} \right]$ (1) for $Re > 2000$

K_g = grid pressure loss coefficient

= $C_v \xi^2$ (2)

-
1. Flow of Fluids Through Valves, Fittings, and Pipes, Crane Co., New York, 1979.
 2. Rehme, K., "Pressure Drop Correlation for Fuel Element Spacers," Nucl. Technol. 17, 15-23 (1973).

$$\begin{aligned}
C_v &= 6.5 \text{ for } Re > 30,000 \\
&= 196 Re^{-0.33} \text{ for } Re < 30,000 \\
E &= A_{grid}/A_{bundle}
\end{aligned}$$

In calculating the frictional pressure drop, the criterion used to determine when the frictional pressure drop was important relative to the elevation head within a 0.30 m (12 in.) span was whether the measured axial differential pressure for that span was 0.014 MPa (0.21 psid) or greater ($\alpha \sim 50$ percent). The span was considered to be full of water or two-phase mixture. In this case, no frictional pressure drop was calculated for that span. It should be noted that the pressure drop across a totally full 0.30 m (12 in.) span is 0.0029 MPa (0.42 psid) for saturated water at 0.38 MPa (40 psia). If the measured differential pressure was less than 0.0014 MPa (0.21 psid) for a given span, then the frictional pressure drop was calculated for the entire span and its value was subtracted from the measured pressure drop to obtain the elevation pressure drop component. The calculated elevation pressure drop was then used to calculate the mass storage and the void fraction within the 0.30 m (12 in.) span.

That is,

$$a = 1 - \frac{(\Delta P_{\text{measured}} - \Delta P_{\text{friction}})}{\rho_{\text{sat liquid}} g L}$$

where L = the distance between the differential pressure cells [0.30 m (12 in.)].

Examples of the calculated frictional pressure drop for the entire bundle for three tests are shown in figures J-6 through J-8. These frictional pressure drop values represent the summation of all the individual 0.30 m (12 in.) span frictional pressure drops for the bundle in which the measured pressure drop was less than 0.0014 MPa (0.21 psid) in each span. As these figures show, the calculated frictional pressure drop was less than 10 percent of elevation head for runs 61106 and 61509, averaging approximately 0.00007 to 0.00029 MPa (0.01

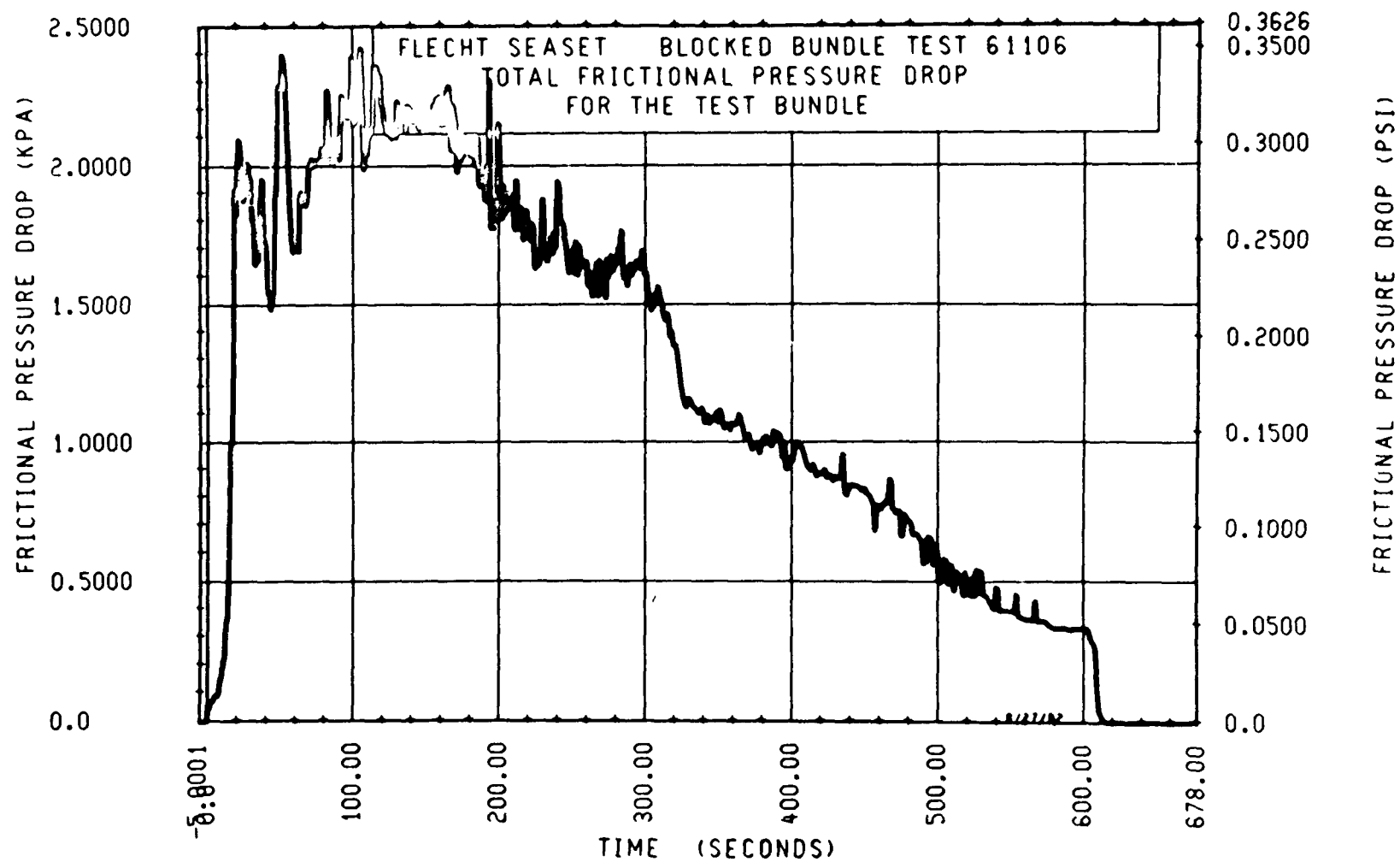


Figure J-6. Total Bundle Frictional Pressure Drop, Run 61106

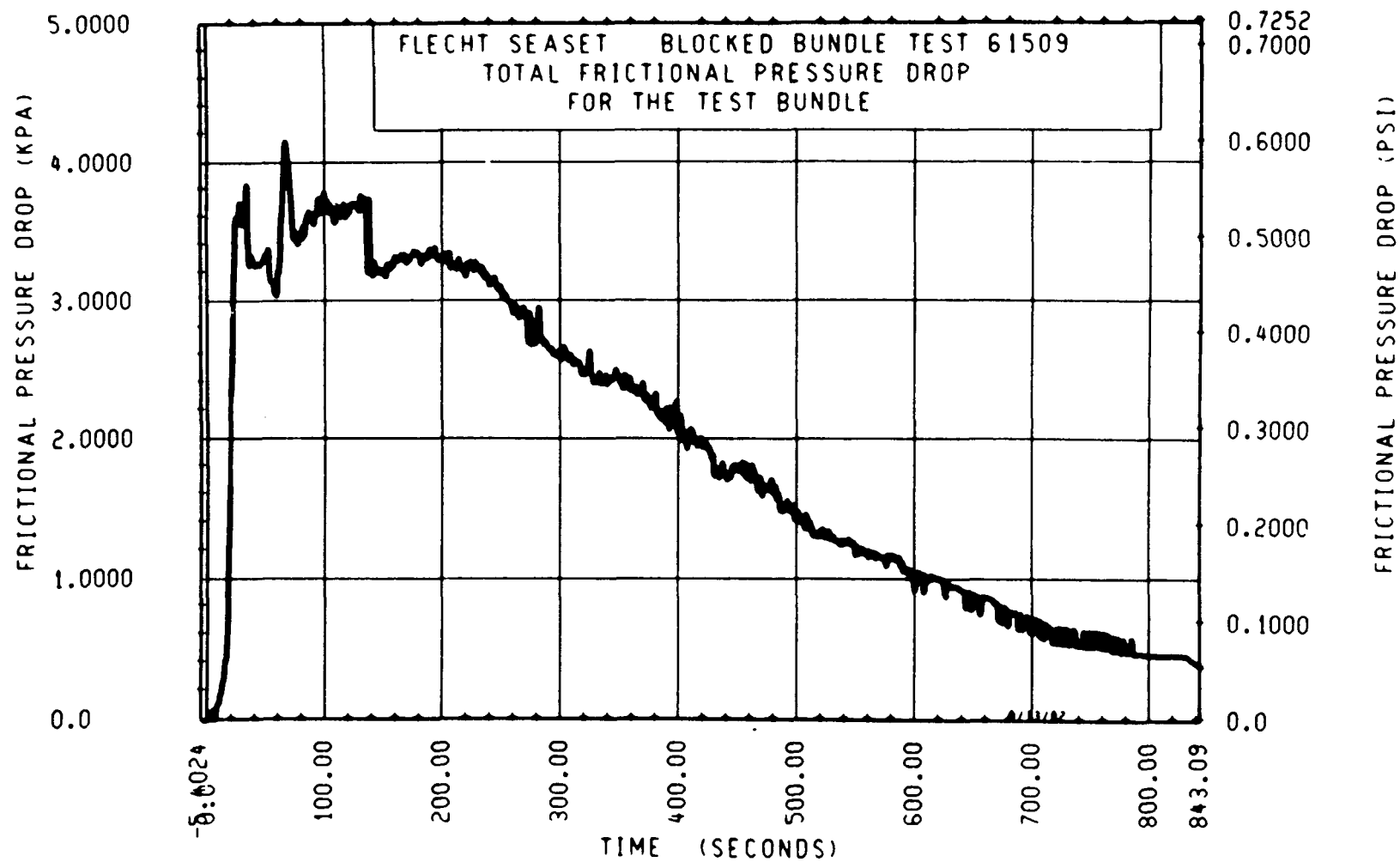


Figure J-7. Total Bundle Frictional Pressure Drop, Run 61509

J-38

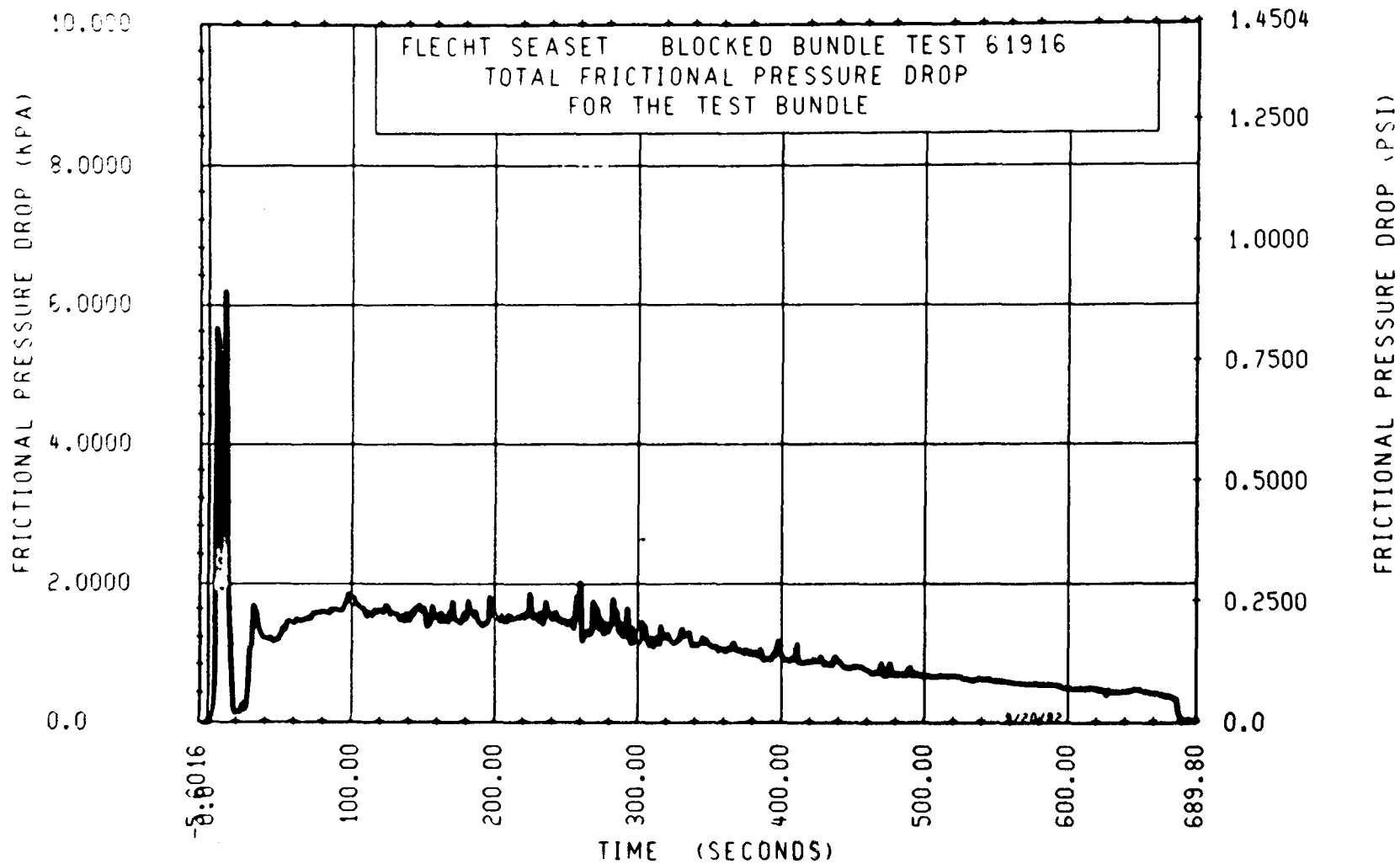


Figure J-8. Total Bundle Frictional Pressure Drop, Run 61916

to 0.042 psid) for each 0.30 m (12 in.) span. The calculated frictional pressure drop decreased with time approximately the same as the steam flow history from the rod bundle. The oscillations in the calculated frictional pressure drop were due to steam flow oscillations caused by the pressure control valve variations during the test. The maximum calculated frictional pressure drop per 0.30 m (12 in.) span of only 10 percent of the elevation pressure drop for a 50-percent void fraction mixture in that span was considered a small correction to the measured pressure drop.

When the stepped flooding rate test (run 61916) was conducted, a different trend was observed in the frictional pressure drop, as shown in figure J-8. Initially, the calculated frictional pressure drop was greater than 20 percent of the elevation head, because of the large burst of steam flow generated by the high flooding rate. The steam flow stayed high for an additional 10 seconds after the high injection period ended. The large steam flow was due to the boiloff of the high injected mass. Once this mass had been boiled and entrained out of the bundle, the steam flow and resulting frictional pressure drop decreased significantly, and was quite small to the end of the test. Therefore, the void fractions calculated at early times in variable flooding rate tests must be evaluated carefully, since the frictional pressure drop is large.

In general, it can be concluded that the frictional pressure drop is small relative to the water elevation head and can be accounted for by the method outlined above. The only case in which the frictional pressure drop becomes large compared to elevation head pressure drop is the very early period of forced stepped injection tests, in which a large amount of boiloff occurs.

In the FFLOWS code, a comparison between the two methods of measuring the mass stored in the bundle was performed. The two methods include the 0 to 3.66 m (0 to 144 in.) differential pressure cell and the sum of the 12 0.30 m (12 in.) differential pressure cells. As shown in figure J-9 for run 61106, good agreement was achieved for the two measurement methods.

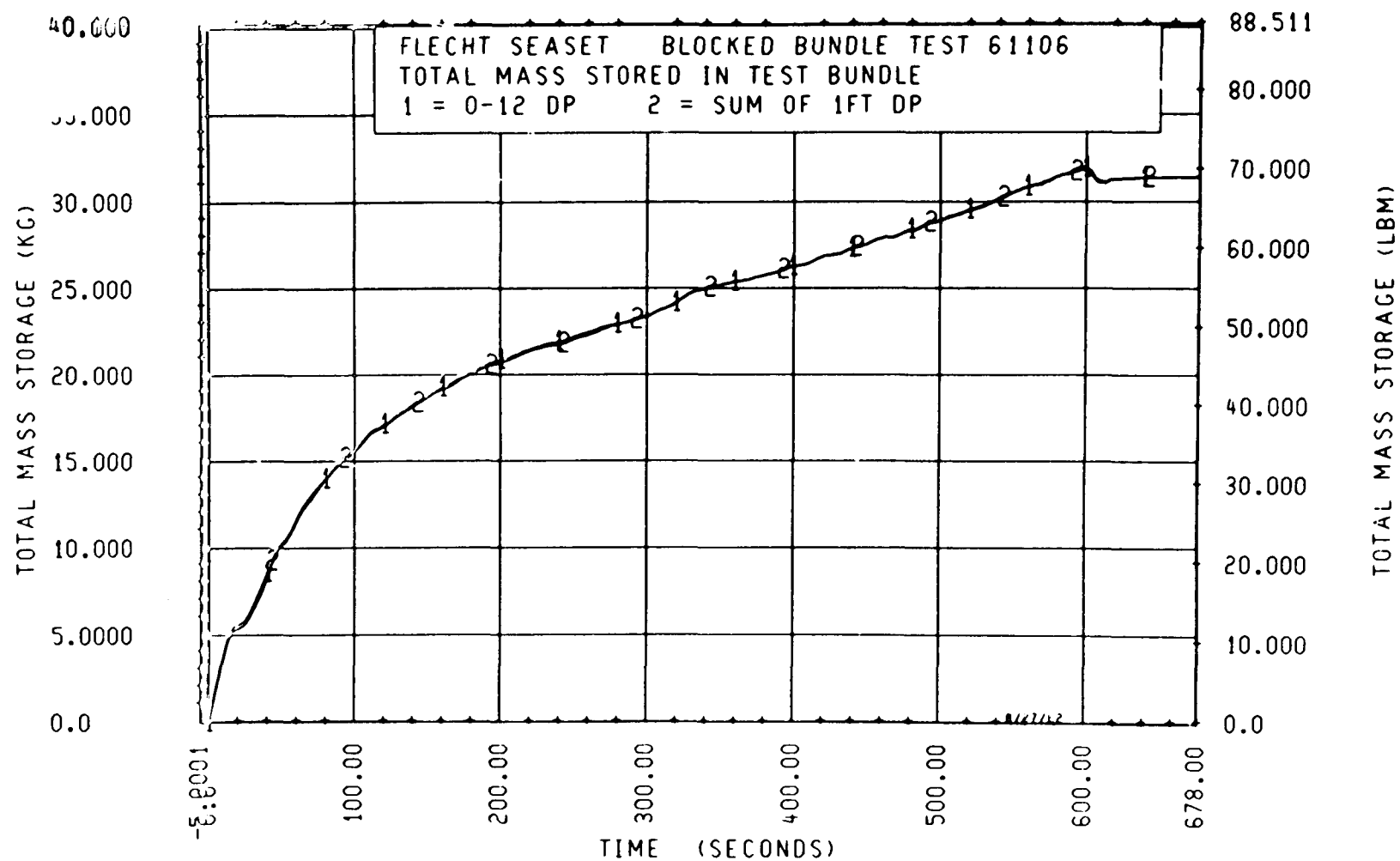


Figure J-9. Comparison of Measurement Methods for Mass Stored in Bundle

In the gravity reflood tests, a mass balance calculation was performed around the downcomer. The flooding rate into the bundle was calculated using the following equation:

$$M_{\text{input}} = \int_0^t \dot{m}_{\text{input}} dt = \int_0^t \dot{m}_{\text{inj}} dt - M_D(t)$$

where

$$\begin{aligned} M_{\text{input}} &= \text{mass of water in the bundle} \\ \dot{m}_{\text{input}} &= \text{mass flooding rate into the bundle} \\ \dot{m}_{\text{inj}} &= \text{mass injection rate into the downcomer} \\ M_D &= \text{mass of water in the downcomer} \end{aligned}$$

The flooding rate into the bundle, \dot{m}_{input} , was obtained from the time rate of change of mass put into the test section, M_{input} . The injection rate into the downcomer was measured by the turbine meter. The mass stored in the downcomer was calculated using the output of the differential pressure transducer which measured the liquid level in the downcomer. Bundle flooding rates calculated with this technique are shown in figure J-10, along with the downcomer injection rate.

J-15. DATA AVERAGING

A simple averaging technique was used for reducing much of the data presented in this report. This was done to clarify graphic presentation of results and to obtain average values of oscillating quantities where use of the instantaneous values could result in large errors. The technique used consisted of replacing each data point with the mean value of the original data point and a specified number of points before and after the time of interest. This process is defined by the following equation:

$$x(i) = \frac{1}{t(i + \Delta - 1) - t(i - \Delta)} \sum_{n=i - \Delta}^{i + \Delta - 1} \frac{x(n) + x(n+1)}{2}$$

J-42

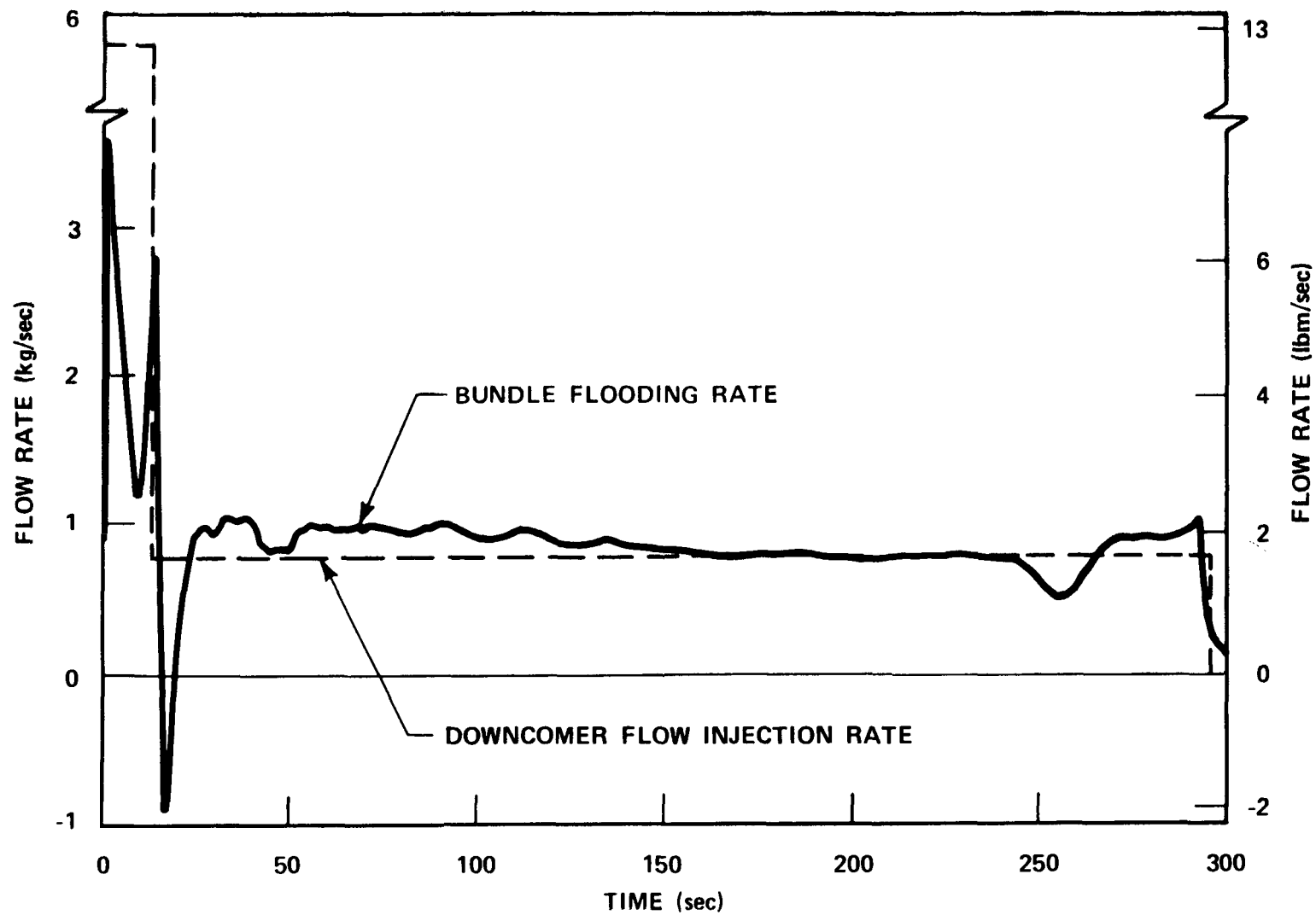


Figure J-10. Bundle Flooding Rate for Run 63018 Calculated From Time Rate of Change of Mass Put Into Test Section

where

$$x(n) = f(t)$$

$$\Delta t = \text{interval between data points}$$

$$\Delta i = n \times \Delta t$$

$$n = \text{integer}$$

APPENDIX K

BUNDLE GEOMETRY ANALYSIS

The posttest examination of the 163-rod blocked bundle revealed that the pin connecting the filler rods broke at the midplane elevation [1.83 m (72 in.)], as had previously been observed in the 21-rod bundle tests. The filler rods were found to be slightly bowed into the bundle; this subsequently caused some heater rod bow on the periphery of the bundle. As observed through the 1.83 m (72 in.) window prior to bundle removal, there was minimal separation between the lower grid assembly and the upper grid assembly, which is attached to the upper seal plate. However, in removal of the bundle from the housing, the lower grid assembly moved down approximately 0.46 m (18 in.), as shown in figure K-1, a posttest photograph of the entire bundle. There was also some filler rod bow in the grid span just above the midplane [2.10-2.62 m (83-103 in.)], as shown in figure K-2. The remainder of the bundle was observed to be essentially unchanged from its nominal pretest geometry, except for heater rod, filler rod, and blockage sleeve surface oxidation.

The heater rod bundle was disassembled row by row starting from row 0, and photographs were taken of the grid span for each row with the blockage sleeves. The relationship of the blockage islands to the photographs is shown in figure K-3. The pretest and posttest photographs for the eight rows with blockage sleeves (rows D through K) are shown in figures K-4 through K-19. These figures show that the interior of the bundle was unaffected by the filler rod and heater rod bow on the periphery of the bundle. However, it was found that 7 of the 42 blockage sleeves had rotated. As shown in figure K-3, six of the seven blockage sleeves rotated only approximately 30 degrees, but one sleeve (on rod 6D) rotated approximately 90 degrees.

From the disassembly and inspection of the bundle, it has been concluded that the geometry of the heater rod bundle did not significantly affect the test data.

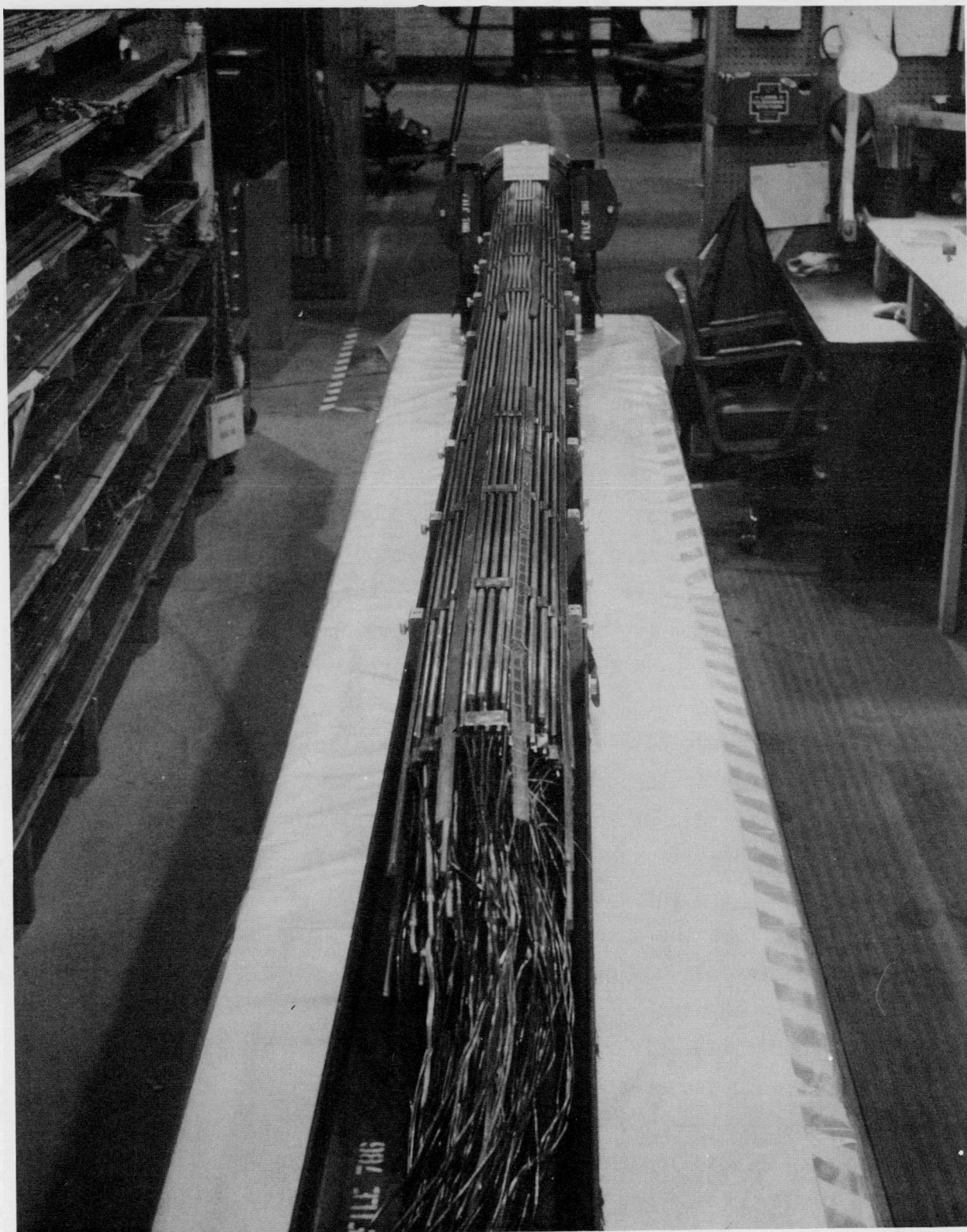


Figure K-1. 163-Rod Blocked Bundle, Posttest

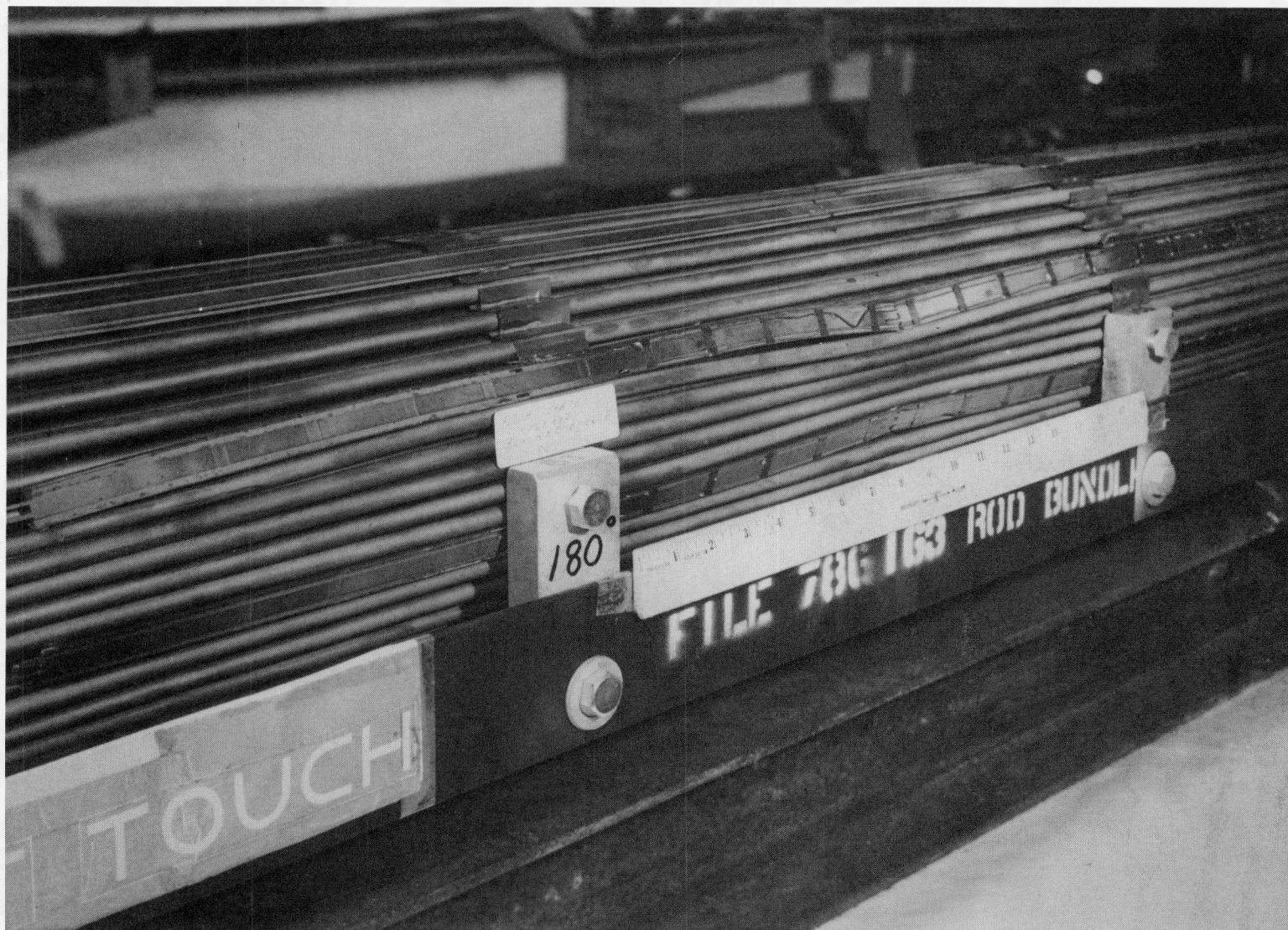


Figure K-2. Filler Rod Bow in 163-Rod Blocked Bundle
[2.10-2.62 m (83-103 in.) Grid Span]

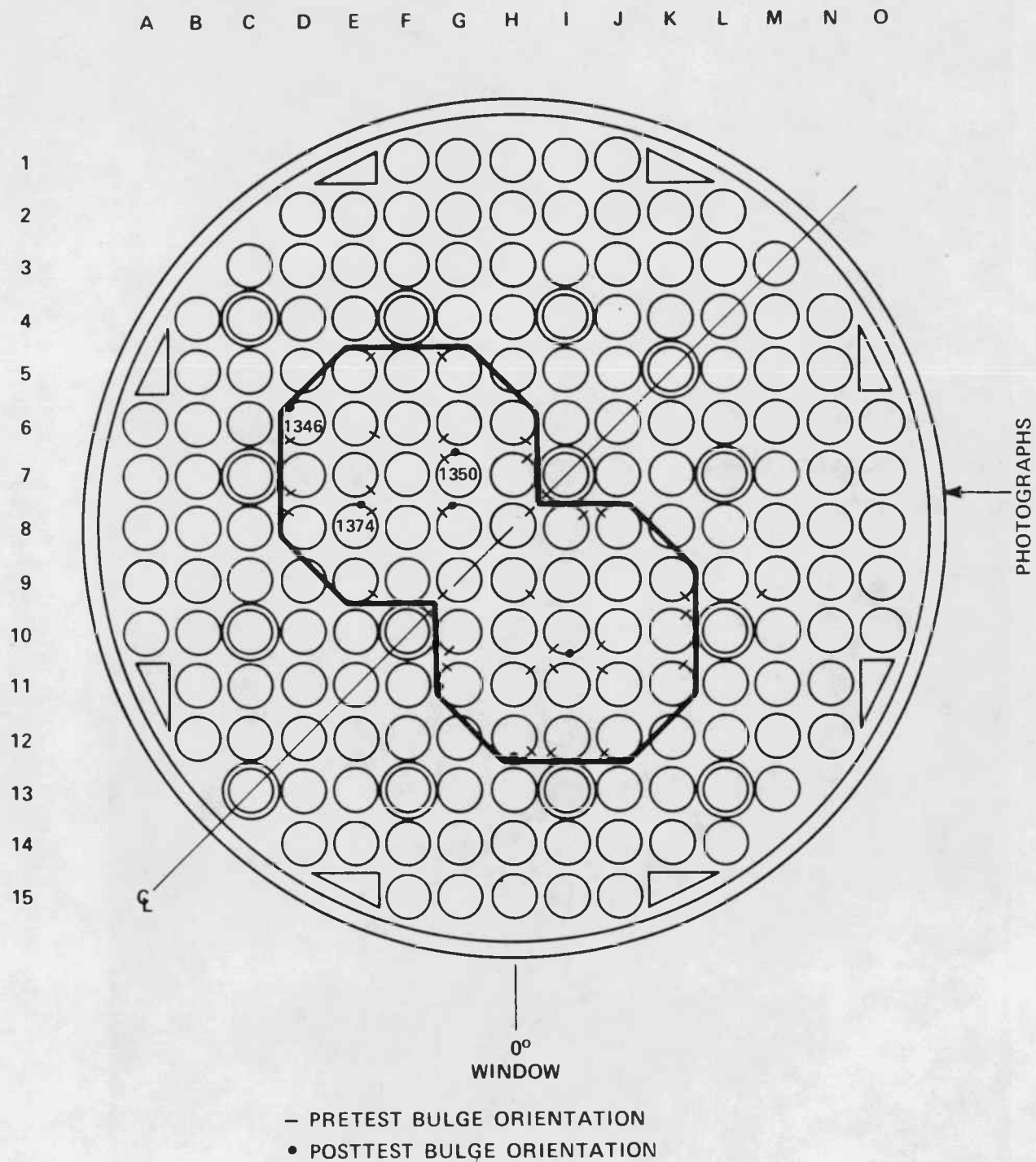


Figure K-3. Pretest and Posttest Bulge Orientation Diagram

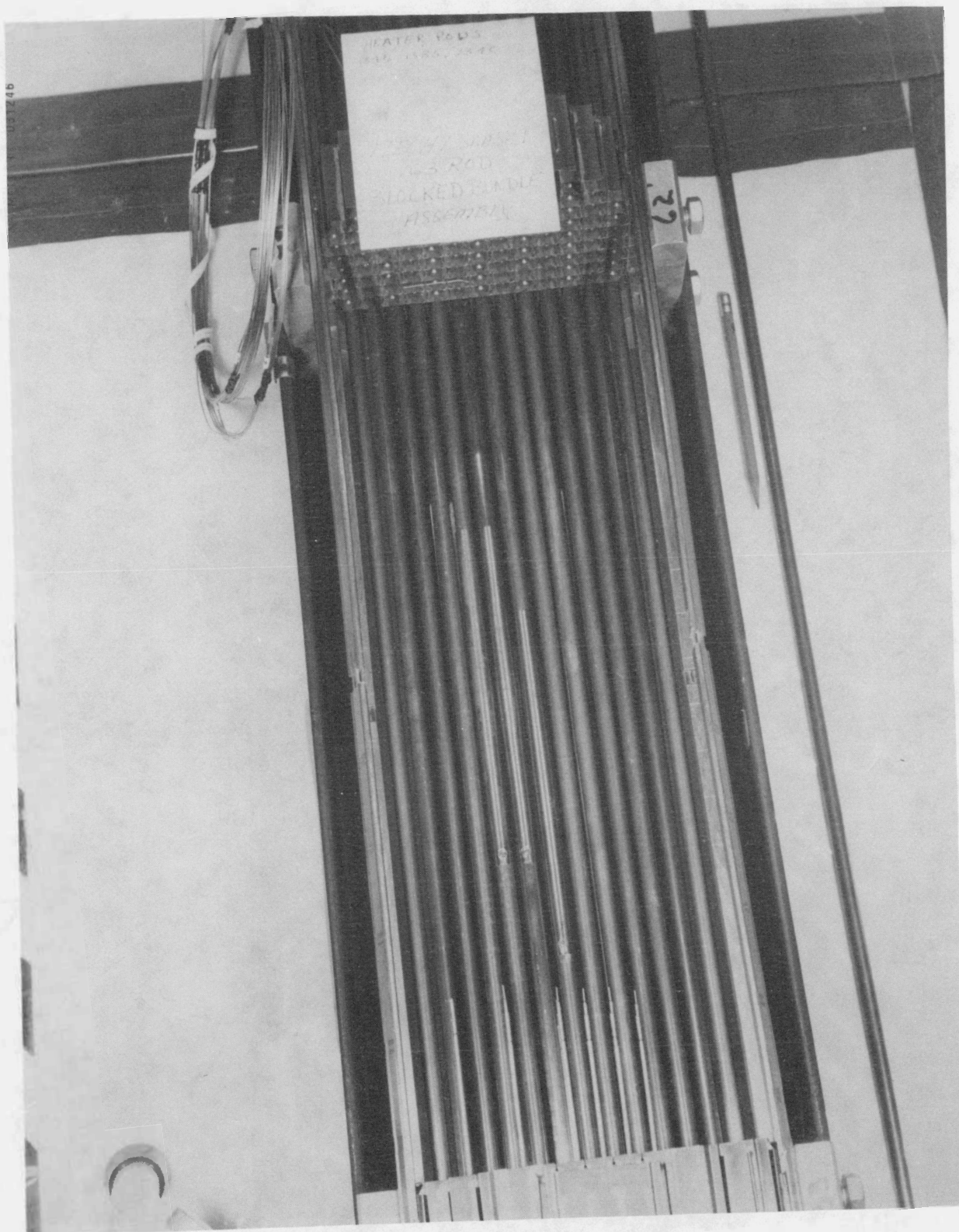


Figure K-4. Row D Heater Rods, Pretest, 1.57-2.11 m (62-83 in.)
Grid Span

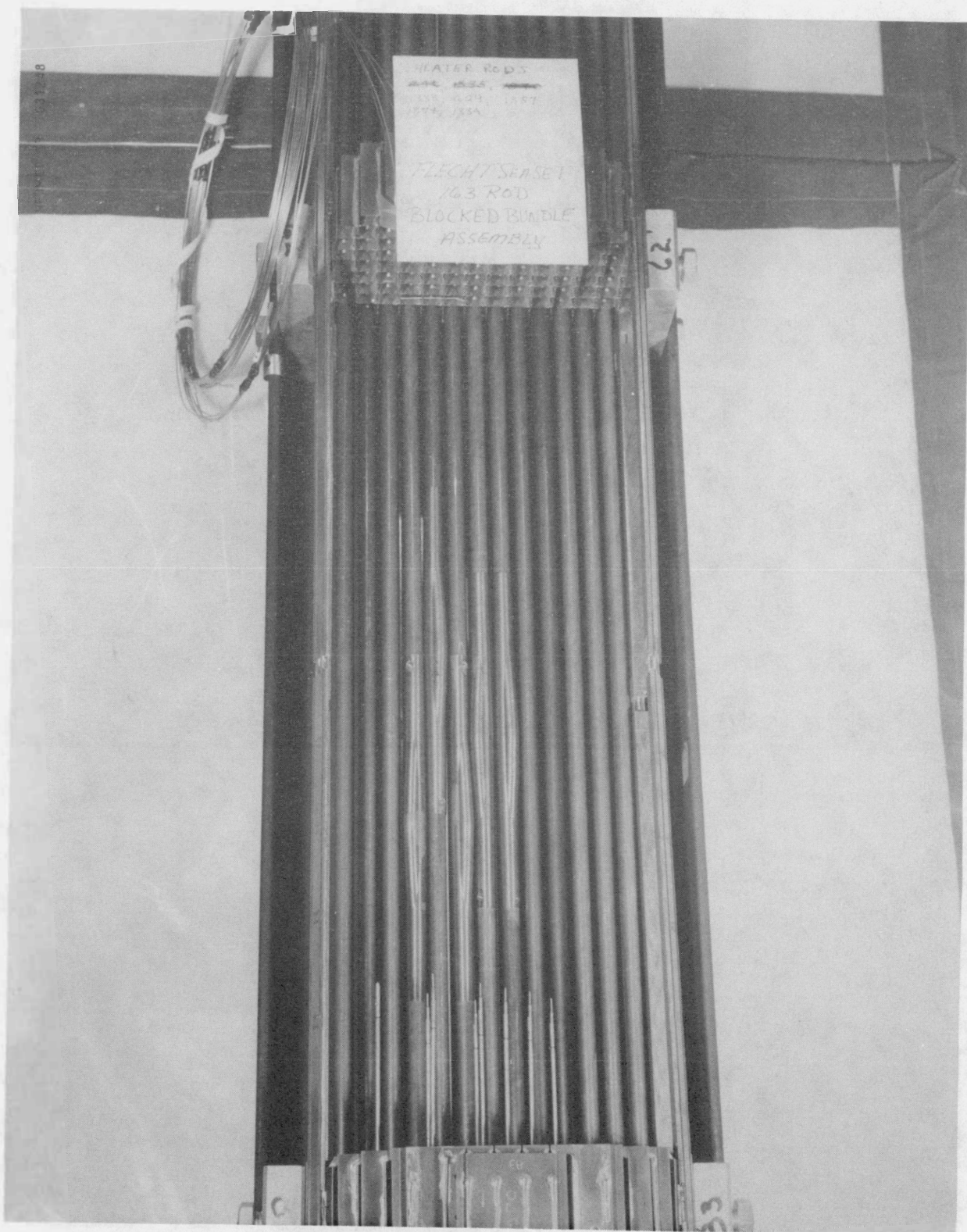


Figure K-6. Row E Heater Rods, Pretest, 1.57-2.11 m (62-83 in.)
Grid Span

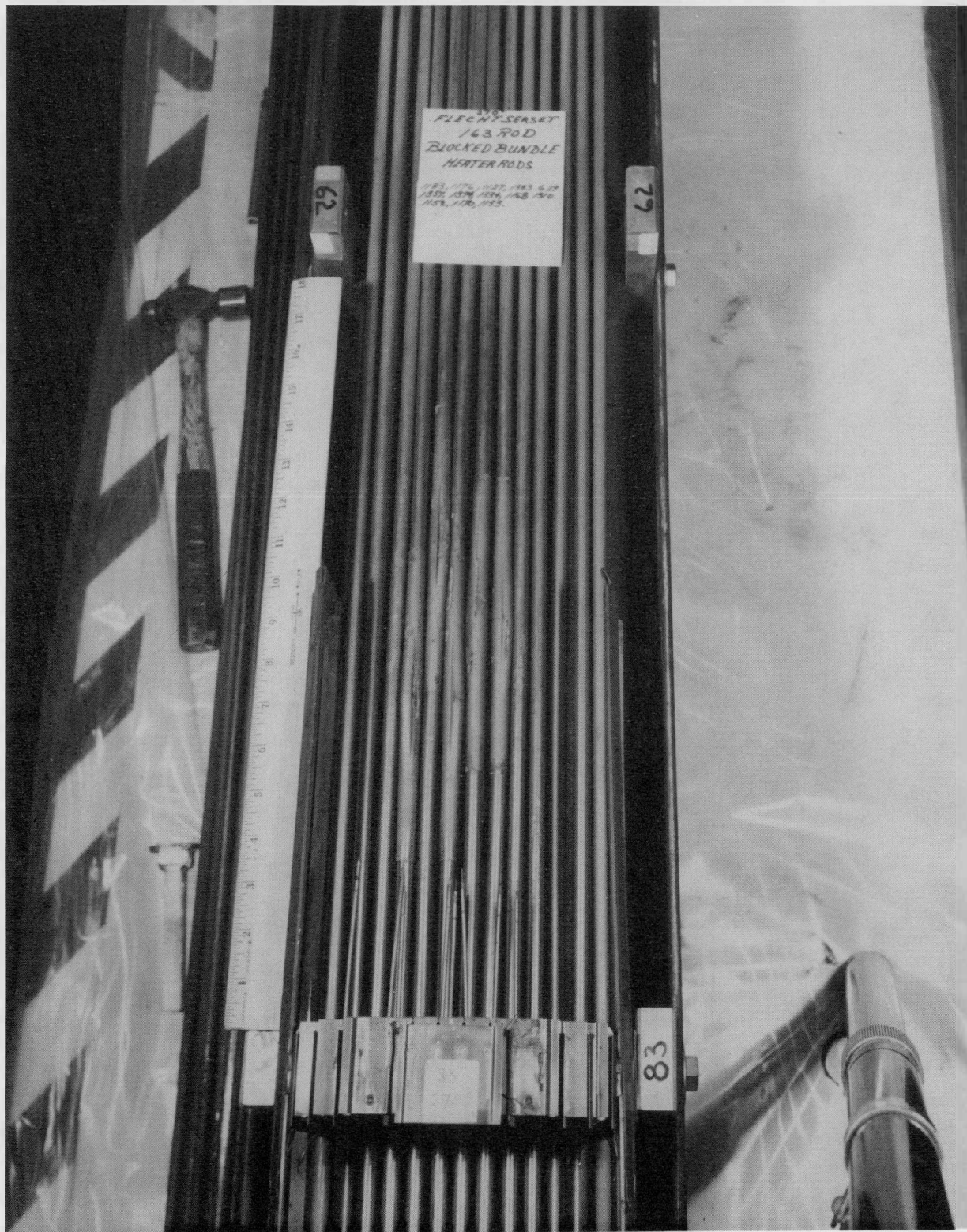


Figure K-7. Row E Heater Rods, Posttest, 1.57-2.11 m (62-83 in.)
Grid Span

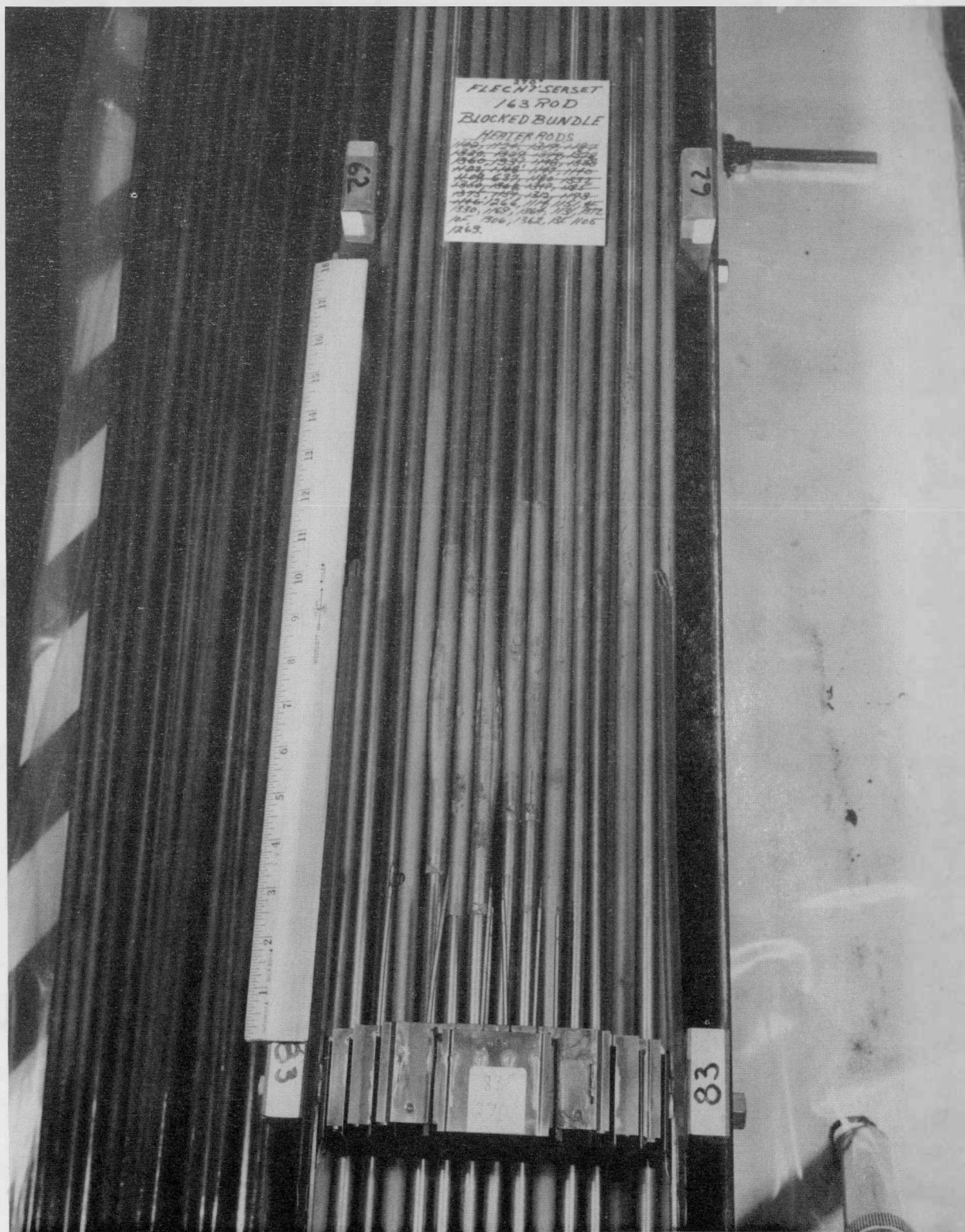
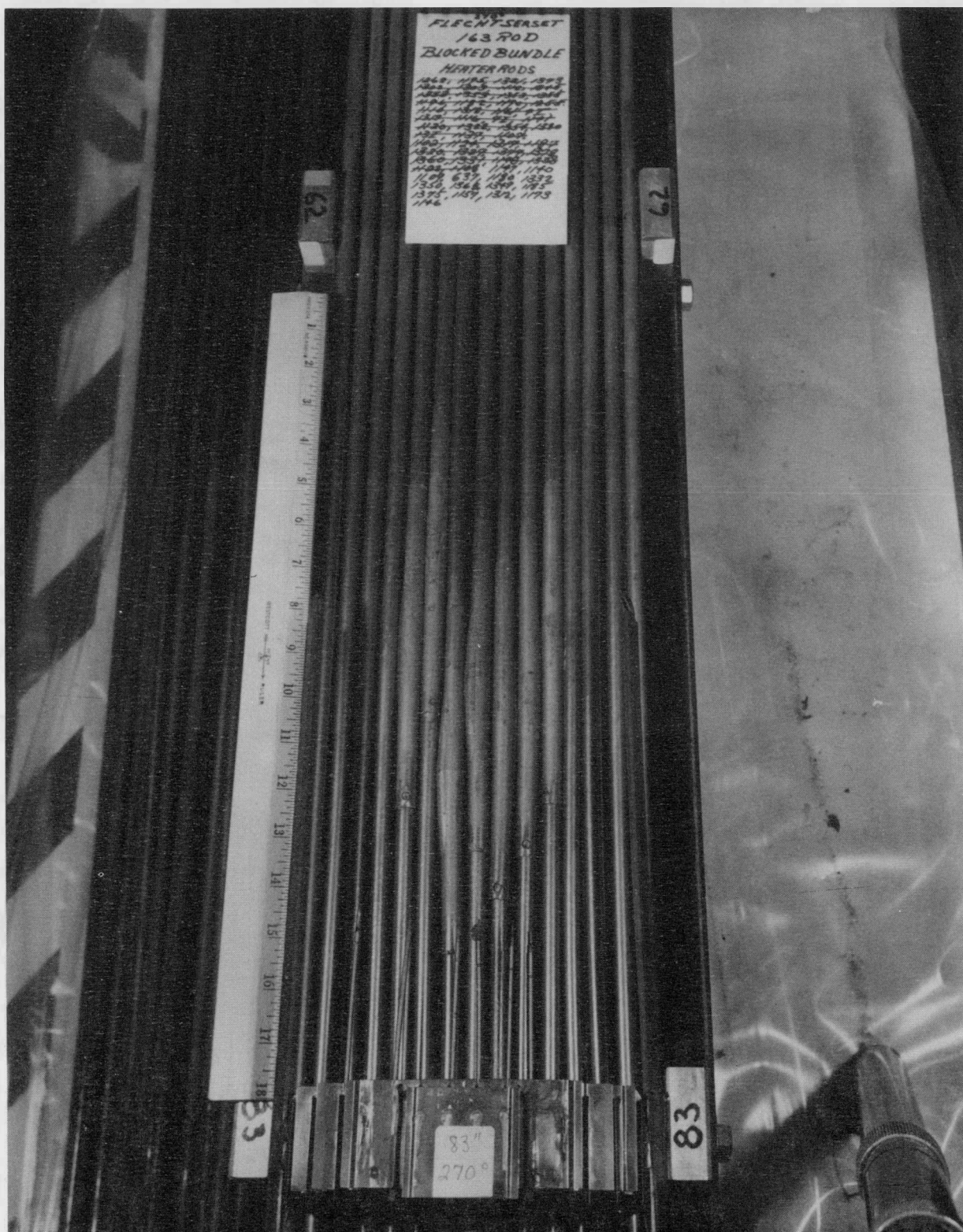


Figure K-9. Row F Heater Rods, Posttest, 1.57-2.11 m (62-83 in.) Grid Span



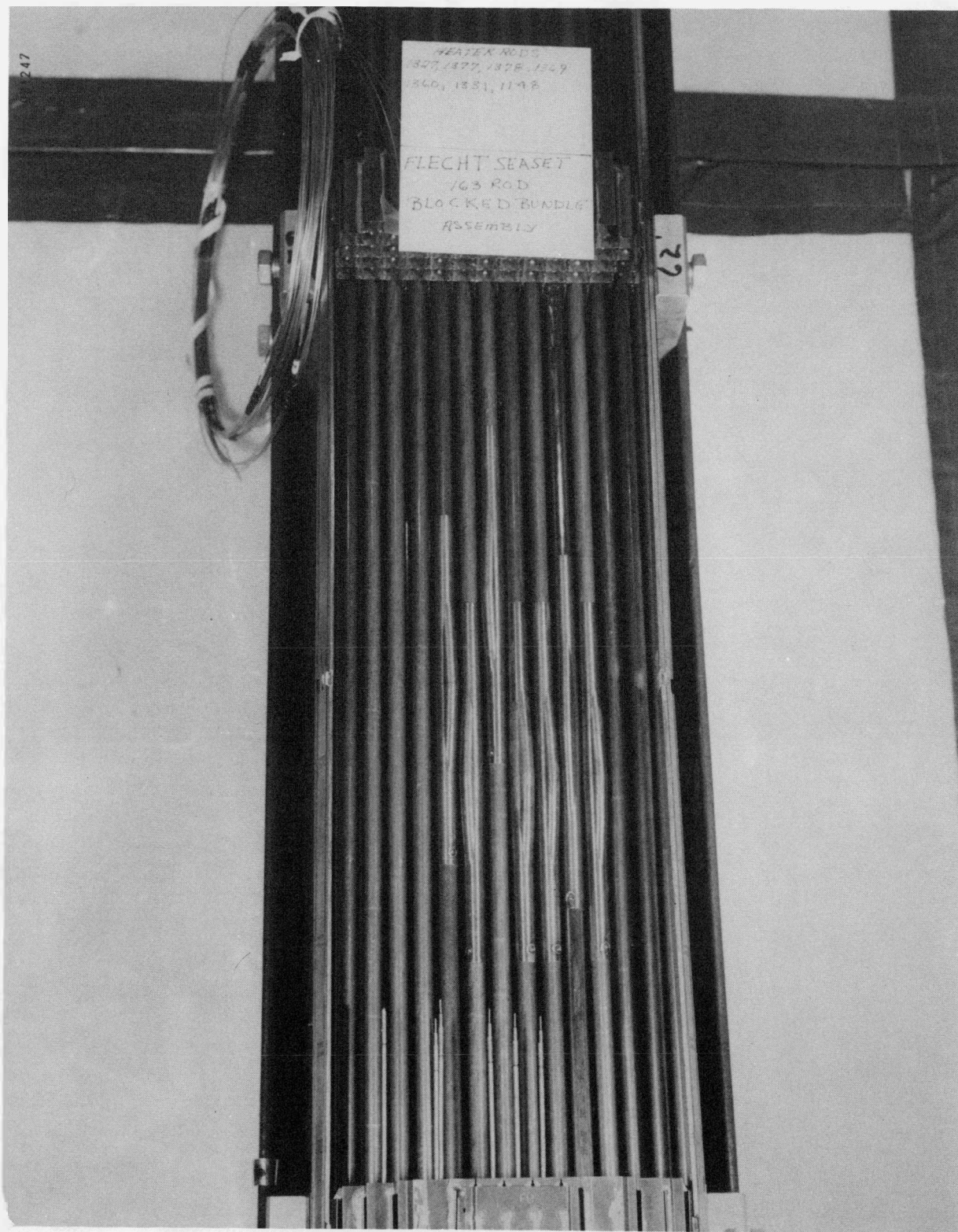


Figure K-12. Row H Heater Rods, Pretest, 1.57-2.11 m (62-83 in.)
Grid Span

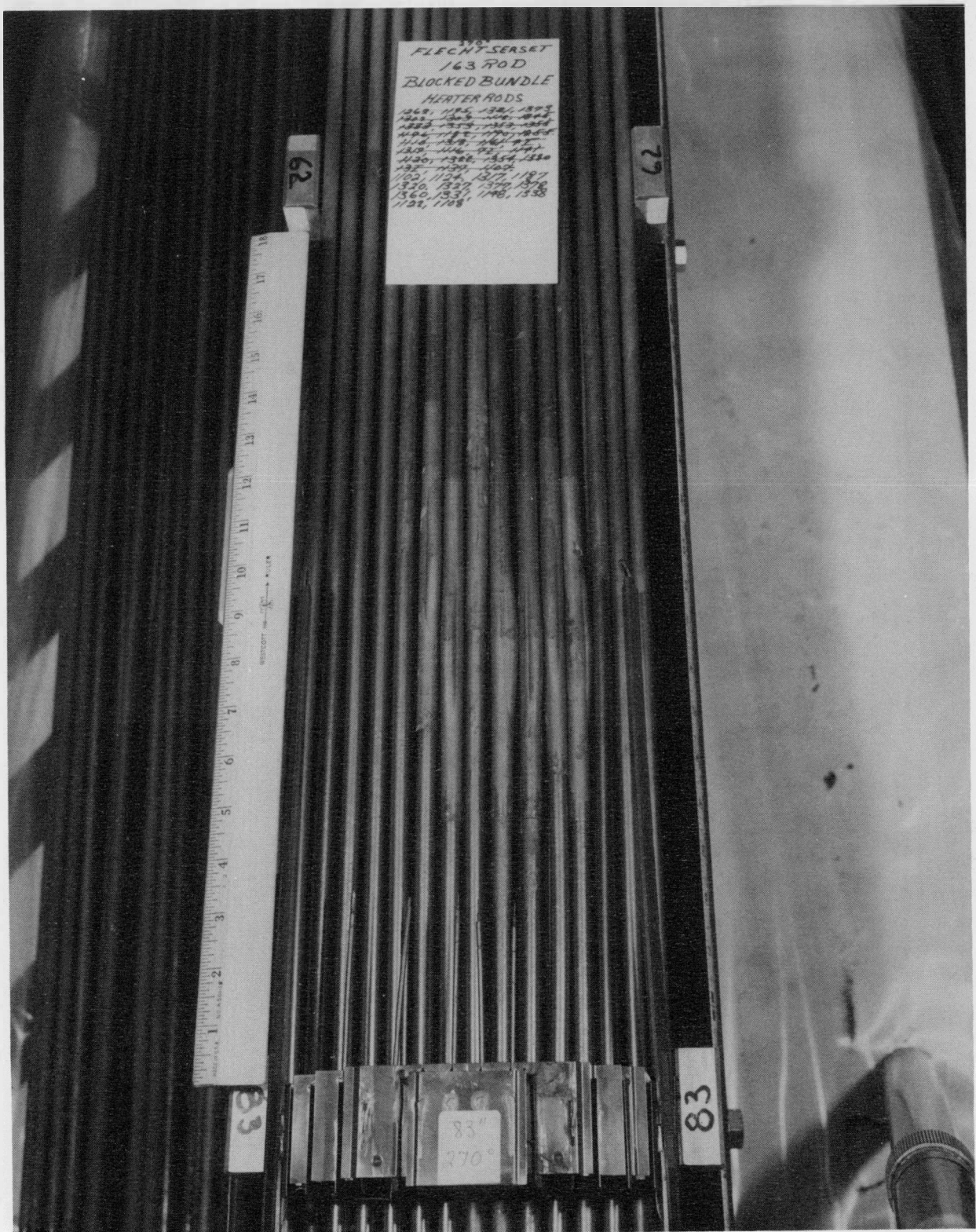


Figure K-13. Row H Heater Rods, Posttest, 1.57-2.11 m (62-83 in.) Grid Span

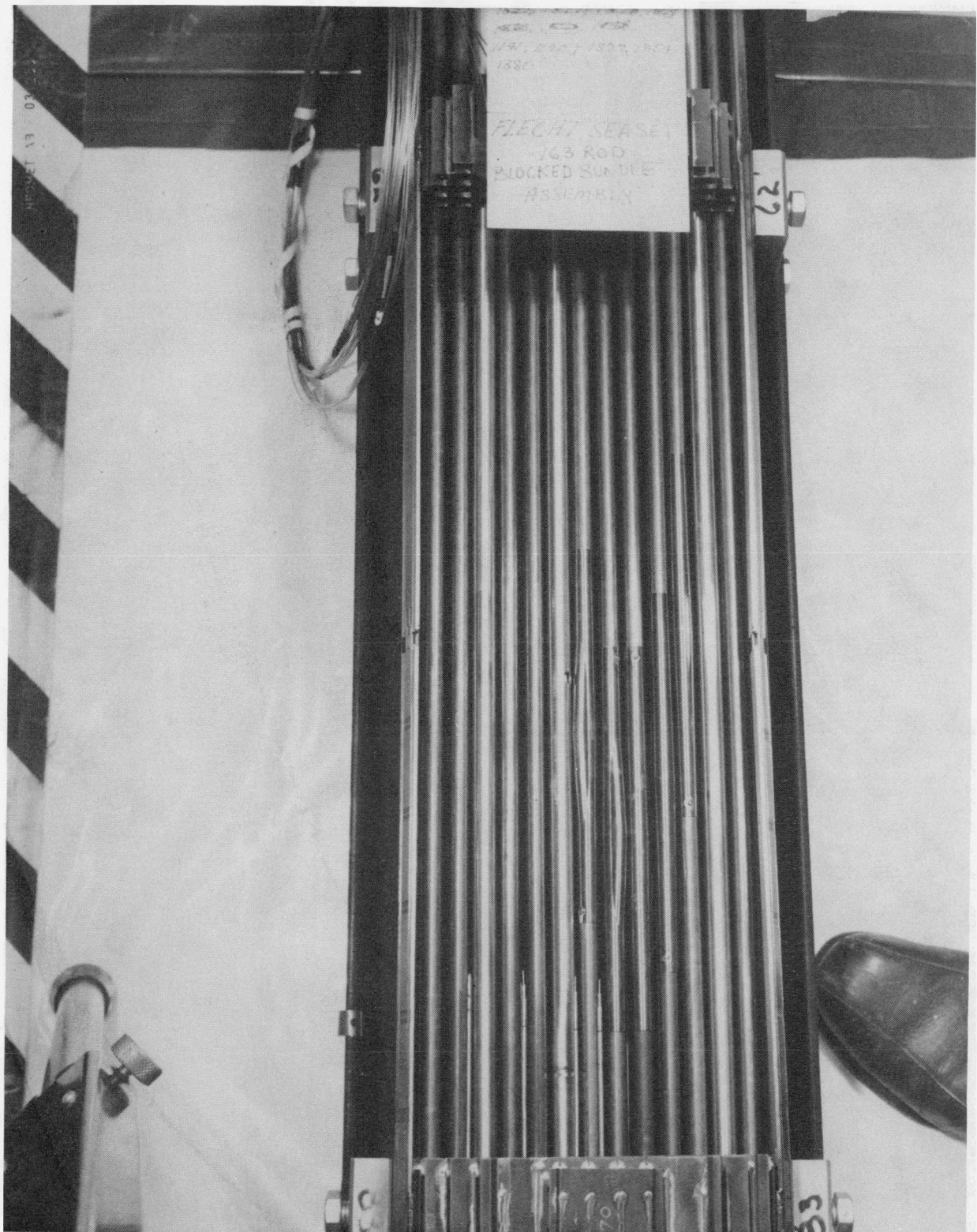


Figure K-14. Row I Heater Rods, Pretest, 1.57-2.11 m (62-83 in.)
Grid Span

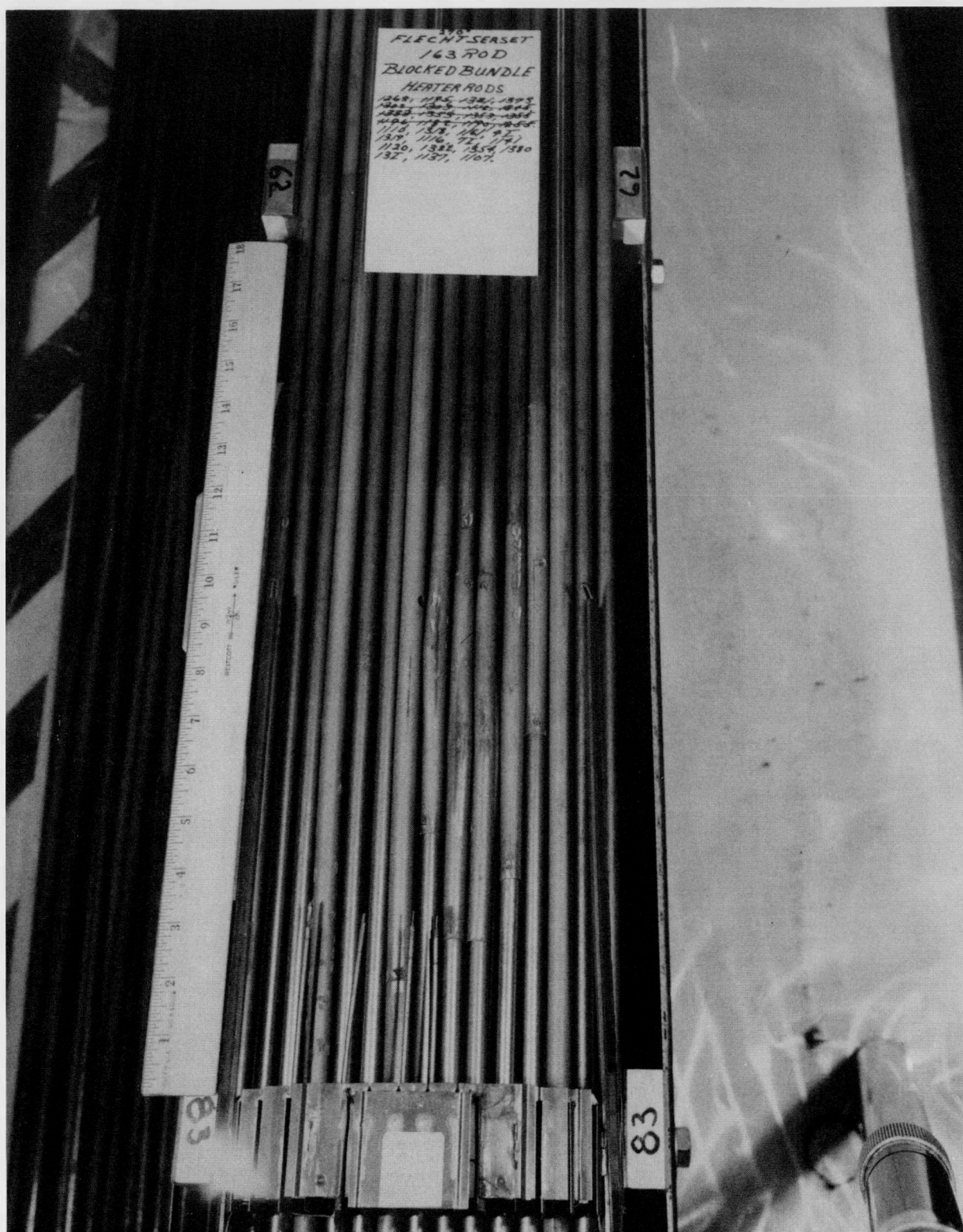


Figure K-15. Row I Heater Rods, Posttest, 1.57-2.11 m (62-83 in.)
Grid Span



Figure K-16. Row J Heater Rods, Pretest, 1.57-2.11 m (62-83 in.) Grid Span

